uOttawa

L'Université canadienne
Canada's university

FACULTÉ DES ÉTUDES SUPÉRIEURES ET POSTDOCTORALES

u Ottawa

L'Université canadienne
Canada's university

FACULTY OF GRADUATE AND POSTDOCTORAL STUDIES

Elizabeth Garven
AUTEUR DE LA THÈSE / AUTHOR OF THESIS

M.A.Sc. (Civil Engineering)
GRADE / DEGREE

Engineering
FACULTÉ, ÉCOLE, DÉPARTEMENT / FACULTY, SCHOOL, DEPARTMENT

Review of the Empirical Equations for Predicting the Shear Strength of Unsaturated Soils

TITRE DE LA THÈSE / TITLE OF THESIS

S. Vanapalli
DIRECTEUR (DIRECTRICE) DE LA THÈSE / THESIS SUPERVISOR

CO-DIRECTEUR (CO-DIRECTRICE) DE LA THÈSE / THESIS CO-SUPERVISOR

EXAMINATEURS (EXAMINATRICES) DE LA THÈSE / THESIS EXAMINERS

M. Fall

P. Simms

Gary W. Slater
Le Doyen de la Faculté des études supérieures et postdoctorales / Dean of the Faculty of Graduate and Postdoctoral Studies

Review of the Empirical Equations for Predicting the Shear Strength of Unsaturated Soils

Elizabeth A. Garven

Thesis submitted to the
Faculty of Graduate and Postdoctoral Studies
In partial fulfillment of the requirements
For the MASc degree in Civil Engineering

Civil Engineering
Faculty of Engineering
University of Ottawa

Your file Votre référence
ISBN: 978-0-494-61212-5
Our file Notre référence
ISBN: 978-0-494-61212-5

ABSTRACT

Shear strength is a key engineering property required in the design of several geotechnical structures that include earth dams, pavements, slopes, retaining walls and foundations. In many situations these structures are constructed with unsaturated soils or in soils that are placed in a state of unsaturated condition. The designs of these structures are based on conventional soil mechanics assuming that the soil is in a state saturated condition resulting in conservative estimations.

Several experimental techniques are presently available and more are evolving for determining the shear strength of unsaturated soils in the laboratory environment in this emerging research area that is of significant practical interest. However, these experimental techniques are expensive, time consuming and need elaborate testing equipment. In addition, qualified and trained personnel are required for reliably determining the shear strength behaviour of unsaturated soils. Due to these reasons, the focus of investigations in recent years has been directed towards predicting the shear strength of unsaturated soils. There are several techniques that include semi-empirical, empirical and mathematical fitting relationships that can be used in the prediction or estimation of the variation of shear strength of unsaturated soils with respect to suction. Such techniques are encouraging towards extending the mechanics of unsaturated soils into engineering practice.

In spite of recent advances in the field of unsaturated soils, few practitioners have background with respect to the shear strength behaviour and the mechanics of unsaturated soils. This thesis provides a historical background of the development of concepts related to our present understanding of the shear strength behaviour of unsaturated soils. The techniques of interpreting the shear strength behaviour proposed by various investigators are also summarized. The details presented in the thesis also include the state-of-the-art testing procedures for determining the shear strength behaviour. In addition, a wealth of 130 soils data published in the literature from various conferences and journals from all over the world are summarized.

There are twenty-five different equations that are available in the literature to predict the variation of shear strength with respect to suction using different techniques. All these techniques are summarized providing details of the philosophies used in the

development of these equations. Thirteen of the above equations use the soil-water characteristic curve (SWCC) and the saturated shear strength parameters (c' and ϕ') for predicting the shear strength of unsaturated soils. Other techniques that include mathematical fitting models and empirical relationships for estimating the shear strength of unsaturated soils are also summarized.

Seven prediction equations commonly used in the literature are chosen from the available 25 equations in the literature to predict the variation of shear strength with respect to suction using 130 data sets of published experimental results from the literature. A quantitative assessment method is used in comparing the predicted and measured shear strength results of the 130 sets. Each of the seven prediction equations is able to successfully predict the variation of shear strength with respect to suction for some of the soils; however, approximately 8% of the soils were not able to be successfully predicted by any of the 7 equations.

The shear strength behaviour of unsaturated soils is a complex relationship which is dependent on many factors including stress history, density, soil structure or fabric, water content, volume change behaviour during shearing state and testing techniques. For example, recent developments in shear strength testing techniques show that previously measured water content in samples may not be representative of the actual water content due to diffused air, condensation and evaporation in the system. In other words, the simple prediction procedures that are available in the literature are not capable of taking into account many complex parameters that influence the shear strength behaviour of unsaturated soils. Therefore, the available techniques or procedures have to be used in practice with engineering judgment while predicting the shear strength of unsaturated soils. Some guidelines and recommendations are provided with respect to the available prediction procedures such that practicing engineers and other investigators can use them understanding the strengths and weaknesses. Finally, the research work summarized in this thesis is also useful for other investigators to undertake future work in the area of shear strength of unsaturated soils to better understand its behaviour.

ACKNOWLEDGEMENTS

I would like to thank many people for their support and patience while I pursued this endeavor. I am grateful to my thesis Supervisor, Dr. Sai Vanapalli for guidance and mentorship. A special thank you goes out to Dr. Infante Sedano (Jules) – a good friend, supporter and mentor for this work. I am grateful to Fred Griffiths, Tammy Carter, Timo Tikka, Bobbi Beheil, Paul Walkington and my parents for their support and encouragement.

I communicated with Dr. Ian Donald regarding some of his earlier work in the field of shear strength of unsaturated soils. He sent me his copy of his Masters thesis – a thesis that I was unable to acquire through the library system. I enjoyed reading this 1956 document that was produced with a typewriter and hand prepared figures. The larger drawings were prepared with an ammonium solution and the charts prepared by hand. I traveled to Australia to meet with him at Monash University in Melbourne while I was on vacation. This thesis made a deep impression on me. It was fifty years old and I was reading concepts that were directly related to current unsaturated soil theory. The effort that went into producing such a document was impressive and I grew a greater appreciation for the use of one's mind and a pencil over the "advanced" technology of computers and calculators.

While gathering data for this thesis, I was unable to obtain the thesis of Dr. Rohm. I emailed him and his supervisor, Dr. Vilar to inquire if a copy could be obtained. I received an email from Dr. Vilar that he did not have a digital copy of the thesis, but he would send me a paper copy of one of the final drafts. It came in the mail several weeks later and was a contribution to my thesis.

In addition, emails exchanged with Dr. Lytton, Dr. Nishimura Dr. I-M. Lee and Dr. Medjo Eko were all important in the development of this thesis. The interaction with these authors enhanced my thesis and this experience immensely.

This thesis is about evolution and limitations of unsaturated shear strength concepts and it became a time for my evolution and for me to discover limitations of myself as a person and an engineer. I am grateful for everything and I have been blessed with the people that surround me.

Table of Contents

List of Figures

List of Tables

SYMBOLS AND TERMS

α Fitting parameter (Eqn. 3-3); the rate of suction change per unit of shear strength contributed by the suction (Figure 3.18, Eqn. 3-24); contact angle (in reference to the contact angle made between water and a solid surface).

α' Angle of shearing resistance determined from regression to experimental data. (Eqn. 3-12).

α_1 Fitting parameter that corresponds to the soil's effective cohesion (Eqn. 3-27).

β Fitting parameter (Eqn. 3-3); the theoretical maximum shear strength contribution due to suction of a soil (Eqn. 3-24; 3-47); angle illustrated in Figure 3.41.

β_1 Fitting parameter (Eqn. 3-28).

χ Bishop's variable. A parameter related to the degree of saturation that is used to proportion the amount of effective stress acting on the system.

ϕ' Effective angle of internal friction.

ϕ^b Angle of shear relative to the suction.

γ Fitting parameter (Eqn. 3-28).

η Fitting parameter equal to -0.55 determined by regression (Eqn. 3-25).

φ Fitting parameter defined in terms of net normal stress (Eqn. 3-29).

κ Fitting parameter (Eqn. 3-13) defined by Equation 3-16.

λ Fitting parameter (Eqn. 3-28); the slope of the line of A_i vs r from a mercury intrusion test of a soil. (Figure 3.26); fitting parameter (Eqn. 3-67).

μ Coefficient related to susceptibility of strength reduction (Eqn. 3-69).

π Osmotic suction.

Θ Normalized volumetric water content defined by $\Theta = \frac{\theta}{\theta_s}$ (Eqn. 3-13).

θ Volumetric water content.

θ_a The contact angle between the water and soil. Can be determined from a reference manual.

θ_w Volumetric water content .

θ_r Volumetric water content at residual suction.

θ_s Volumetric water content at saturation.

ρ_w Density of water (1000 kg/m^3).

σ Stress.

σ_1 Primary stress.

σ_3 Confining stress.

σ_n Net normal stress.

τ Shear strength.

τ_b The difference between maximum shear, τ_m, and the total height of the ellipse, b, that has been fit to experimental points (Eqn. 3-2).

τ_m Maximum shear strength in Equation 3-2.

τ_o Shear strength when suction = 0 kPa in Equation 3-2.

τ_{sr} Shear strength at the residual suction (Eqn. 3-46).

τ_{us} Shear strength contribution due to suction.

τ_{us-max} Maximum shear strength contribution due to suction within a data set.

ω Gravimetric water content.

ψ Total suction.

ψ_m Maximum suction.

ς Intermediate variable.

ζ_2 Fractal dimension in the shear plane.

A_i The surface area which could be measured by using a gauge of size r. The interface area between mercury and water in a mercury intrusion test.

AEV_I The air-entry value at 0 net normal stress determined from Figure 3.23.

AEV_S The change in air-entry value with respect to net normal stress. Shown in Figure 3.23.

A_{tot} Total area of voids.

A_w Area of water.

a Fitting parameter, bubbling pressure (Eqn. 2-5); fitting parameter (Eqn. 2-6); fitting parameter (Eqn. 2-7); fitting parameter (Eqn. 2-8); fitting parameter (Eqn. 2-9); fitting parameters to fit the Equation 3-50 to experimental data, illustrated on Figure 3.35; fitting parameter (Eqn. 3-51).

a_w Area of water.

a_2 Fitting parameter (Eqn. 3-53).

b Fitting parameter (Eqn. 2-5); fitting parameter (Eqn. 2-8).

c_1 Cohesion of the saturated soil (Eqn. 3-9).

c_2 Cohesion of the soil at a lower water content (Eqn. 3-9).

b Fitting parameters to fit the Equation 3-50 to experimental data. They are illustrated on Figure 3.35; fitting parameter (Eqn. 3-72).

b_2 Fitting parameter (Eqn. 3-53).

b_b Pore size index.

C The mean radius of the interface between mercury and water in a mercury porosimetry intrusion test; theoretical maximum cohesion (Eqn. 3-68).

c' Effective cohesion of the soil.

c'' The relative cohesion dependent upon the change in suction and net normal stress. Determined by regression to experimental data (Eqn. 3-12).

C_A Apparent cohesion.

C_{max} Maximum apparent cohesion (Figure 3.35).

c_{ult} Ultimate apparent cohesion (Eqn. 3-71).

c_m Maximum apparent cohesion (Eqn. 3-72).

D The fractal dimension of a pore-ball distribution of a three dimensional. Known as the fractal dimension and ranges from 2.0 to 3.0 (Eqn. 3-31); the surface tension of the interface between water and mercury (375 mN/m) or between air and mercury (485 mN/m). Can be determined from a physics reference manual.

d Fitting parameter (Eqn. 3-18).

d' The ordinate intercept for a stress-point envelope at a saturated condition when the mean net normal stress (p') is equal to 0.

f A parameter related to the degree of saturation and expansive structure of the soil. Related to the degree of saturation.

f_1 A fitting parameter to account for the change in area that is affected by water at different degrees of saturation (Eqn. 3-49).

$F1$ Intermediate term representing the AEV.

$F2$ Intermediate term representing the soil's shear strength under saturated conditions.

$F3$ Intermediate term representing the correction term for the shear strength of a soil under unsaturated conditions.

g Acceleration due to gravity.

h Fitting parameter (Eqn. 2-8).

h_c Capillary height.

I_p Plasticity index.

m Fitting parameter (Eqn. 2-6); fitting parameter (Eqn. 2-7); fitting parameter (Eqn. 2-9); intermediate variables known as the soil-water characteristics (Eqn. 3-33).

n Fitting parameter (Eqn. 2-6); fitting parameter (Eqn. 2-7); fitting parameter (Eqn. 2-9); intermediate variables known as the soil-water characteristics (Eqn. 3-33).

p Mean net stress in a stress point envelope; Variable that represents the slope of the linear part of the SWRC (Eqn. 3-19).

p_{at} Atmospheric pressure (101.3 kPa).

P_s Swelling pressure of the soil.

q Mean peak stress in a stress point envelope; Variable that represents the intercept of the linear part of the SWRC (Eqn. 3-20).

r_1 The radius of the micropores of soil.

r Radius of the capillary tube.

R Maximum radius of macropore, whose surface can be described as fractal. Can be measured by mercury intrusion porosimetry (Eqn. 3-34).

R_S Radius of curvature of meniscus (i.e., $r/\cos\alpha$).

S Degree of saturation.

S_e Effective degree of saturation. Defined by equation 2-4.

S_r Residual degree of saturation.

T_s The surface tension of the interface between water and mercury (375 mN/m) or between air and mercury (485 mN/m). Can be determined from a physics reference manual.

u_a Pore-air pressure.

u_w Pore-water pressure.

w_L Liquid limit.

$(u_a\text{-}u_w)_r$ Suction at the residual water content.

$(u_a\text{-}u_w)_b$ Suction at the air-entry value.

$(u_a\text{-}u_w)_{max}$ Maximum suction in a data set.

CHAPTER 1 INTRODUCTION

1.1 Background

Terzaghi's effective stress principle has a profound influence in geotechnical engineering practice all around the world since early 1930's. Significant geotechnical and geo-environmental applications were extended in engineering practice for saturated soils using the effective stress principle as a tool. The effective stress, $(\sigma\text{-}u_w)$ equation was used in Mohr-Coulomb equation for interpreting the shear strength behaviour of saturated soils. This approach was found to be useful in explaining the shear strength of all soils such as gravels, sands, silts, clays, including normally and over consolidated clays. Shear strength is a key engineering property required in the design of several geotechnical structures such as foundations, retaining walls and to assess the stability of slopes assuming fully saturated condition in soils.

The successful implementation of the single stress state variable, $(\sigma\text{-}u_w)$ in the interpretation of shear strength for the saturated soils encouraged Bishop (1959) to extend the same approach for unsaturated soils. Many investigators during the same period have made an attempt to interpret the shear strength behaviour of unsaturated in terms of a single stress state variable, $(\sigma\text{-}u_w)$ (Aitchison and Donald, 1956; Bishop and Donald, 1961; Bishop and Blight; 1963; Burland, 1965).

In many regions of the world, the annual rate of evaporation from soils is higher than the rate of infiltration. These regions are typically classified as semi-arid or arid and constitute about a third of the earth's surface (Dregne, 1976). The natural groundwater table typically is at a greater depth in these regions and the soil above the groundwater table is in a state of unsaturated condition. The stresses associated with the construction of geotechnical or other structures in these regions are distributed above the groundwater table (Oh et al, 2008).

The variation of pore-water pressure, u_w with respect to depth below the groundwater table is positive and linearly increases with the depth. However, the pore-water pressures above the groundwater table are negative. The pore-air pressure, u_a above the groundwater table is typically equal to the atmospheric pressure and the pore-water pressure, u_w, with respect to atmospheric pressure, u_a is called the matric suction, $(u_a-$

u_w). The engineering properties such as the shear strength, volume change and the coefficient of permeability are significantly influenced by matric suction, (u_a–u_w) which is also a stress state variable (Fredlund and Rahardjo, 1993). Therefore, the engineering behaviour of unsaturated soils cannot be interpreted using a single stress state variable, effective stress, (σ-u_w) extending the conventional concepts used in the geotechnical engineering practice that are valid for saturated soils.

There are several reasons for using the principles of saturated soils in conventional engineering practice for unsaturated soils:

(i) availability of a well established framework for interpreting the engineering behaviour of saturated soils;

(ii) lack of a simple framework for interpreting the engineering behaviour of unsaturated soils;

(iii) it is conservative to interpret the engineering behaviour of unsaturated soils using the mechanics of unsaturated soils.

The influence of pore water pressure, u_w, is over the entire inter particle contact cross-sectional area of the soil particles and hence a single stress state variable, (σ-u_w), which is the net stress or effective stress can be used as a tool to interpret the engineering behaviour of saturated soils. The soil in a state of unsaturated condition is influenced both by the pore air pressure, u_a, and the pore water pressure, u_w. Both pore air pressure, u_a, and the pore water pressure, u_w will have an influence on the cross sectional area of soil particles (Jennings and Burland, 1962). Therefore, the influence of the stress state variables, net normal stress (σ-u_a) and matric suction, (u_a–u_w) should be taken into account in the interpretation of the engineering behaviour of unsaturated soils. The stress state variables net normal stress, (σ-u_a) and matric suction, (u_a–u_w) are suitable in engineering practice as changing of the variables, total stress, σ or pore-water pressure, u_w will not influence the stress state of the other stress variable. In other words, both net normal stress (σ-u_a) and matric suction (u_a–u_w) perform as independent stress state variables.

The validity of stress state variables, net normal (σ-u_a) and matric suction, (u_a–u_w), as stress state variables was verified from triaxial test results performed by Bishop and Donald (1961) on an unsaturated silt varying the values of σ, u_a, and u_w keeping the

stress state variables (σ-u_a) or (u_a–u_w) constant. The resulting stress-strain curves showed monotonic stress-strain curve behaviour providing validity for the use of stress state variables (σ-u_a) and matric suction, (u_a–u_w) in the interpretation of unsaturated soils.

Several authors also supported the use of two stress state variables to map volume change behaviour in an unsaturated soil (Bishop and Blight, 1963; Burland, 1965; Aitchison, 1967; Matyas and Radhakrishna, 1968; Aitchison and Woodburn, 1969; Brackley, 1971; Aitchison and Martin, 1973). Studies by Fredlund and Morgenstern (1977) with respect to the volume change behaviour (i.e., null tests) further established the use of two stress state variables. A comprehensive framework is now available for interpreting the engineering behaviour of unsaturated soils extending the multiphase continuum mechanics approach in terms of two independent stress state variables (σ-u_a) or (u_a–u_w) (Fredlund and Morgenstern, 1977; Fredlund and Rahardjo, 1993).

However, later rigorous studies have shown that there were limitations in using the single stress state variable in the interpretation of the shear strength of unsaturated soils (Jennings and Burland, 1962, Bishop and Blight, 1963; Burland 1964; Fredlund and Morgenstern, 1977; Fredlund et al., 1978).

Fredlund et al. (1978) proposed an equation for interpreting the strength behaviour of unsaturated soils in terms of two stress state variables; net normal stress, (σ-u_a) and matric suction, (u_a–u_w).

$$\tau = c' + (\sigma - u_a)\tan\phi' + (u_a - u_w)\tan\phi^b \qquad [1\text{-}1]$$

where c is the effective cohesion, ϕ is the effective angle of internal friction, σ-u_a is the net normal stress, (u_a–u_w) is suction and ϕ^b is the angle of shear relative to the suction.

During the past three decades, the Fredlund et al. (1978) equation has been widely used for interpreting the shear strength of unsaturated soils.

1.2 Identification of Research Need

The shear strength of unsaturated soils can be determined by modifying the conventional testing equipment such as direct shear, triaxial shear or ring shear tests to facilitate testing under unsaturated conditions extending axis translation technique (Hilf,

1956). Such equipment is referred in the literature as modified direct shear, modified triaxial shear, or modified ring shear testing equipment (Fredlund and Rahardjo, 1993). However, determination of the shear strength of unsaturated soil using the modified equipments is time consuming, costly and requires specialized equipment and personnel. Typically more than two weeks to a month is required to conduct a series of tests to determine the variation of shear strength with respect to matric suction in the range of 0 to 500 kPa under a net normal stress value of interest. As a result, the applications of the shear strength concepts into engineering practice remain limited.

Due to this reason, several researchers in recent years have developed empirical or semi-empirical procedures for predicting the shear strength of unsaturated soils (Abramento and Carvalho, 1989; Öberg and Sallfors, 1995; Vanapalli et al, 1996; Fredlund et al. 1996; Khalili and Khabbaz, 1998; Bao et al, 1998, Vilar, 2006) using simple techniques. Most of these procedures use the soil-water characteristic curve (SWCC) as a tool in the prediction of the shear strength of unsaturated soils. The ability to predict the shear strength would alleviate the need for the costly and time-consuming testing. Such investigations would also encourage implementing the mechanics of unsaturated soils in engineering practice.

1.3 Objectives and Scope of the Study

The two key objectives of the present study are:

•The primary objective of the thesis is to synthesize all the research undertaken in the area of shear strength of unsaturated soils. This objective includes collection and summarizing all the published data of shear strength in the literature.

•The secondary objective is to examine all the empirical and semi-empirical techniques available for predicting the shear strength of unsaturated soils. The focus of this objective is to understand the strengths and as well as the limitations of each of these proposed prediction procedures and also to provide guidelines for the practicing engineers.

1.4 Thesis Organization

This thesis is organized into seven chapters. An introduction and justification for this thesis is presented here in Chapter 1.

Chapter 2 entitled, background provides the terminology associated with the mechanics of unsaturated soils including the basic information about the shear strength behaviour of unsaturated soils. In addition, the relationship between the soil-water characteristic curve (SWCC) and the shear strength of unsaturated soils as discussed by several investigators is summarized. This chapter also highlights the philosophy used by various investigators in the development of the equations or techniques that they proposed towards developing the empirical or semi-empirical equations.

Extensive literature review has been undertaken through this thesis and summarized in Chapters 3. The historical background of the development of our present understanding with respect to the shear strength of unsaturated soils is presented.

One of the key objectives of this thesis is to examine the strengths and limitations of the proposed empirical and semi-empirical equations available in the literature for predicting the shear strength of unsaturated soils. Chapter 4 summarizes the shear strength prediction equation of various investigators and provides guidelines for the definition of a "successful prediction" to evaluate the various prediction procedures. The advantages and limitations of the available semi-empirical and empirical predictive equations are also discussed.

Chapter 5 summarizes the data of all published shear strength tests in the testing performed on soils. Information related to sample preparation and testing methods is described in order to aid in the understanding and interpreting the shear strength of behaviour of the soil with engineering judgement.

Chapter 6 provides the test results from the application of the predictive equations to the soils outlined in Chapter 5. The test results will verify the applicability of the equations for use on various soils and will add to the database previously given by the founding author to refine the predictive equations for use.

Chapter 7 provides an interpretation of all the summarized shear strength results in the using the predictive equations. The chapter will include some final notes and discussions to explain miscellaneous concepts that have emerged through the research study and propose future work in this area.

CHAPTER 2 BACKGROUND

2.1 Introduction

In conventional geotechnical engineering practice, it is always assumed that the soil is in a state of saturated condition. In other words, the influence of suction is not taken into consideration even for soils that are not in a state of saturated condition. This assumption is conservative and has been extended in engineering practice. However, in recent years, the mechanics of unsaturated soils has been applied both in geotechnical and geo-environmental engineering practice (Fredlund and Rahardjo, 1993; Lu and Likos, 2004; Tindall and Kunkel, 1999). For example, the design of soil covers and soil liners are based on the mechanics of unsaturated soils. While the principles of unsaturated soil mechanics are familiar to geotechnical and geo-environmental engineers, the field is still regarded as an emerging research area.

This chapter has two sections; the first section present basic concepts of the mechanics of unsaturated soils to acquaint the reader with terminology used in the thesis. The focus of second section is aimed at introducing the testing procedures utilized to determine the shear strength behaviour of unsaturated soils. These details are required in the interpretation of the shear strength of unsaturated soils. In addition, the relationship between SWCC and the shear strength of unsaturated soils is summarized. This chapter also highlights the philosophy used by various investigators to develop the empirical or semi-empirical equations or techniques that they proposed.

2.2 What is an Unsaturated Soil?

There are two key differences between an unsaturated and a saturated soil. They are summarized below:

1. An unsaturated soil has four phases, while a saturated soil only has two.
2. An unsaturated soil has typically negative pore water pressures, while a saturated soil can have either positive or negative pore water pressure or no pore water pressure. The pore-air pressure, u_a in the unsaturated zone is typically equal to the atmospheric pressure and the pore-water pressure, u_w, with respect to atmospheric pressure, u_a is called the matric suction, (u_a-u_w).

A saturated soil has two phases, namely; solid (i.e. soil) and liquid phase (i.e. water). All the voids in a saturated soil are filled with water and the engineering behaviour of a saturated soil can be described in terms of a single stress state variable, effective stress, $(\sigma - u_w)$ (Terzaghi, 1943). An unsaturated soil has both the solid and liquid phases along with a gaseous phase (i.e., air). In addition to these three phases, there is a fourth phase which is referred to as the contractile skin (Fredlund and Rahardjo, 1993). The contractile skin is at the air-water interface. The contractile phase can be considered a separate phase as the properties of the contractile skin (eg. density and heat conductance) is different from the properties of the contiguous water phase (Davies and Rideal, 1963; Fredlund and Rahardjo, 1993).

2.3 The Concept of Suction

Soil suction can be defined as the free energy state of soil water that can be measured in terms of the partial vapour pressure of the pore water vapour (Edelfson and Anderson, 1943; Richards, 1965). This is most commonly referred to as total suction. It can be influenced by both temperature and pressure (Fredlund and Rahardjo, 1993). The total suction constitutes of two key components: matric suction and osmotic suction (Aitchison, 1965). In conventional geotechnical and soil science literature, total suction is expressed as $\psi = (u_a - u_w) + \pi$, where ψ is total suction, $(u_a - u_w)$ is matric suction and π is osmotic suction.

2.3.1 Matric and Osmotic Suction

The changes in suction due to the movement of the water in the liquid phase is termed as matric suction, $(u_a - u_w)$, while the osmotic suction, π, is related to the changes in water content that arise due to movement of water in the vapor phase.

From a practical perspective, the changes in water content that arise in unsaturated soils with higher suction values can be associated predominantly with total suction. In other words, at high suctions (i.e. typically greater than 1,500 kPa), the changes in water content due to matric suction can be neglected (Krahn & Fredlund 1972).

2.3.2 Physical Representation of Matric Suction

The structure of an unsaturated soil is formed by several pores which could be filled with air and water. Inside the soil pore structure, at air-water interface, a meniscus is formed in a similar manner to water in a capillary tube.

Consider a small glass tube inserted into water under atmospheric conditions (Fig. 2.1). The water rises up as a result of the surface tension and the tendency of water to wet the surface of the glass tube (i.e., hygroscopic properties).

Figure 2.1 presents a sketch of the capillary phenomenon. The downward forces must be equal to the upward forces at the air-water interface to achieve equilibrium conditions. A mathematical relationship that satisfies the criteria is given below:

$$2\pi \cdot r \cdot T_s \cdot \cos\alpha = \pi \cdot r^2 \cdot h_c \cdot \rho_w \cdot g \qquad [2\text{-}1]$$

where r = radius of the capillary tube; T_s = surface tension of water; α= contact angle; h_c = capillary height; ρ_w = density of water and g = acceleration due to gravity.

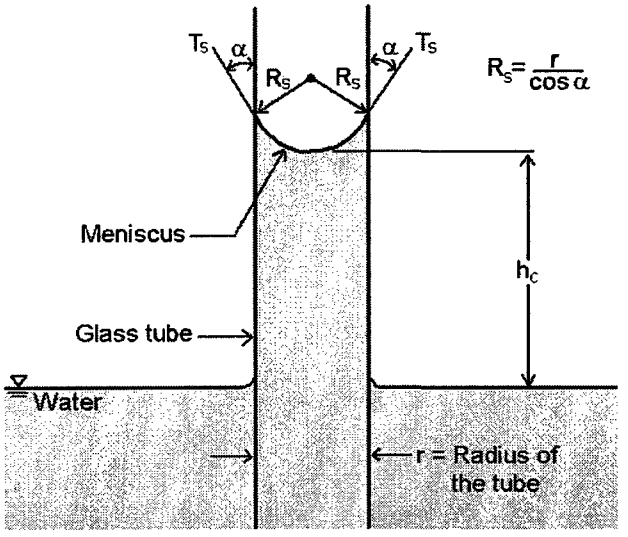

Figure 2.1. Capillary phenomenon.

Equation 2-1 can be rearranged to give the maximum height of water in the capillary tube:

$$h_c = \frac{2T_s}{\rho_w \cdot g \cdot R_s} \qquad [2\text{-}2]$$

where R_s = radius of curvature of meniscus (i.e., $r / \cos\alpha$).

The air pressure is atmospheric at the air-water interface (i.e., u_a = 0) and the water pressure is negative (i.e., $-\rho_w \cdot g \cdot h$). Equation 2-3 shows that the matric suction is a function of the surface tension and the capillary tube (i.e., soil pore radius).

$$(u_a - u_w) = \frac{2T_s}{R_s} \qquad [2\text{-}3]$$

where u_a = pore-air pressure; u_w = pore-water pressure; and R_s = radius of curvature of meniscus.

2.4 Measuring Suction

There are seven general methods for measuring suction of a soil (Fredlund and Rahardjo, 1993; Muñoz-Carpena, 2004):

1. Axis translation technique (pressure plate, Tempe cell)
2. Psychrometry (soil psychrometer)
3. Nuclear method (neutron moderation)
4. Dielectric methods (TDR, TDT, FDC, ADR, pore fluid squeezer)
5. Tensiometry (tensiometer, osmotic tensiometer, gypsum block, granular matrix sensor)
6. Heat dissipation (thermal conductivity sensor)
7. Moisture mass (filter paper)

Some methods are suitable only in the laboratory while others are used in situ. A summary of the different methods can be found in Table 2.1.

Table 2.1. Devices to measure suction. (modified from Fredlund and Rahardjo, 1993; modified from Muñoz-Carpena, 2004)

Method	Device	Type of Suction (matric, osmotic, total)	Lab/Field	Effective Range (suction or volumetric water content)
Axis translation	Pressure plate/ Tempe cell	Matric	Lab	0 -1500 kPa
Psychrometry	Soil psychrometer	Total	Lab, Field	100 – 8000 kPa 50 – 3000 kPa
Nuclear Method	Neutron moderation	Total	Lab, Field	0 – 0.60 ft^3 ft^{-3}
Dielectric Methods	Time Domain Reflecto-metry (TDR)	Matric	Field	0.05 – 0.50 ft^3 ft^{-3} or 0.05 to saturation (with specific soil calibration)
	Time Domain Transmis-sion (TDT)	Matric	Field	0.05 – 0.50 ft^3 ft^{-3} up to 0.70 ft^3 ft^{-3}
	Frequency Domain Ca-pacitance (FDC)	Matric	Field	Entire Range
	Frequency Domain Re-flectometry (FDR)	Matric	Field	Entire Range
	Amplitude Domain Re-flectometry (ADR)	Matric	Field	Entire Range
	Pore fluid squeezer	Osmotic	Lab	Entire Range
Tensiometry	Tensiometer	Matric or negative pore water pres-sures	Lab, Field	0 – 80 kPa
	Osmotic Tensiometer	Matric	Lab, Field	0 – 1500 kPa
	Miniature Tensiometer	Matric	Lab, Field	0 – 1500 kPa
	Gypsum block	Matric	Field	30 – 200 kPa
	Granular matrix sensor	Matric	Field	10 – 1000 kPa
Heat Dissipation	Thermal Conductivity Sensor	Matric	Field	0 – 400 kPa 10 – 1000 kPa
Moisture Mass	Filter Paper	Matric, Total	Lab	Entire Range

2.4.1 Axis Translation Techniques

The axis translation technique uses the difference between the pore-air pressure and the pore-water pressure to measure the suction in a soil. Water will cavitate at a water pressure of about -1 atm, limiting the ability to measure the suction in a soil. The axis translation technique translates the pore water pressure to a value greater than -1 atm by increasing the air pressure (Hilf, 1956) thus avoiding cavitation through the use of a semi-permeable membrane in the measuring system (Figure 2.2). The pressure plate uses a porous high air-entry ceramic stone as the semi-permeable membrane. The pressure plate apparatus can be used to test multiple samples at the same time. The high air-entry stone is saturated prior to testing and its saturated condition will prevent air from passing through the stone but will allow water from the sample to pass and drain away as the samples desaturate. The suction is controlled and water is allowed to drain from the soil sample. The pressure plate allows the testing of multiple samples which allows the experimentalist to accurately determine the moisture content of the sample at a known suction.

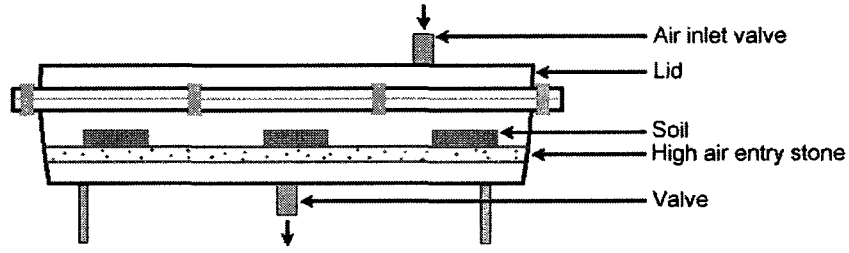

Figure 2.2. Schematic of the pressure plate apparatus.

The Tempe cell and the pressure plate apparatus also use axis translation technique to determine the SWCC. The Tempe cell also uses the high air-entry disk as a semi-permeable membrane but it may only test one sample at a time. Multiple points (ie. variation of water content with respect to suction) of the SWCC are determined from the same specimen. The water content is determined by measuring the water that has drained from the sample. It has the disadvantage of not measuring the gravimetric water content at each suction value; however, the water contents are determined on the same specimens. It is similar to using 'identical samples'. 'Identical samples' are samples that have the same density and soil fabric. The pressure plate apparatus uses multiple samples which may not be 'identical'.

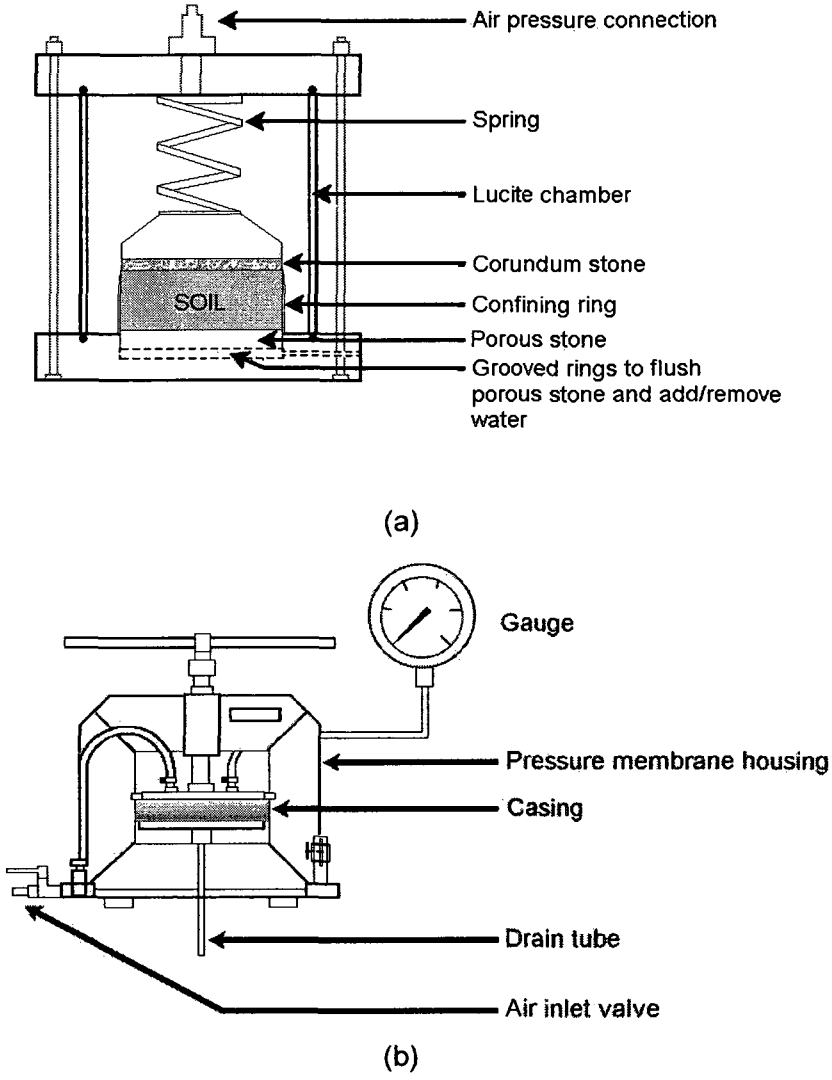

Figure 2.3. Schematic of (a) the Tempe cell and (b) pressure membrane apparatus. (from eijkelkamp.com).

The pressure plate apparatus and the Tempe cell (Figure 2.3 a and b) are similar in that both systems determine the SWCC by testing one sample at different suction values. The pressure membrane apparatus (Figure 2.3b) uses a cellulose membrane rather than a ceramic stone. The pressure plate apparatus also has a diaphragm built into the lid to ensure that the flexible cellulose membrane remains in contact with the soil sample. Axis translation methods are the most commonly used methods for determining SWCC in the laboratory.

The axis translation technique is also conventionally used during the determination shear strength using different types testing equipment. A high air-entry ceramic stone is a part of the modified direct shear or modified triaxial cell to control the suction of the sample. Once the sample has come into equilibrium, the shear strength of the soil is measured.

2.4.2 Moisture Mass Method: Filter Paper

The filter paper method indirectly measures either total or matric suction (Gardner, 1937; Fawcett and Collis-George, 1967; McQueen and Miller, 1968; Al-Khafaf and Hanks, 1974). Whatman generally used model no. 42, placed in direct contact to measure the matric suction while filter papers in a sealed container but not in direct contact with the soil sample can be used to measure the total suction (matric + osmotic). (Figure 2.4)

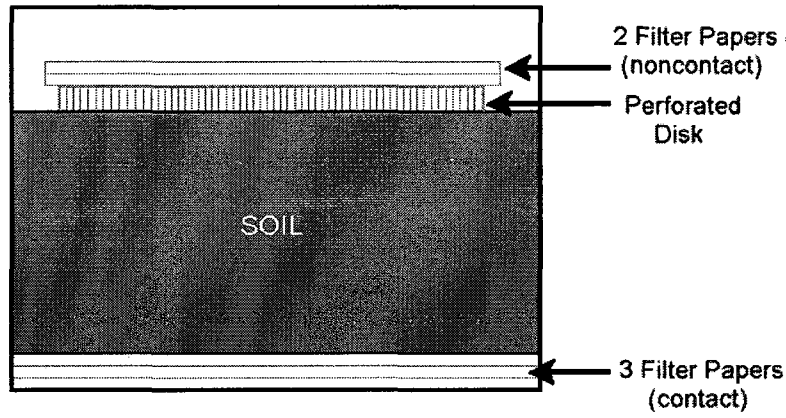

Figure 2.4. Schematic of filter paper used to measure total suction (non-contact) and matric suction (contact) (from Al-Khafaf and Hanks, 1974)

2.5 The Soil-Water Characteristic Curve (SWCC)

The relationship between the water content of a soil and the corresponding suction is defined as the soil-water characteristic curve (SWCC) (Buckingham, 1907; Haines, 1925; Williams, 1982). There are many terms to describe this relationship including pressure deficiency curve (Haines, 1927), pF curve (Donald, 1957), soil-moisture curve (SMC) (Aitchison and Donald, 1956; Donald, 1957; Aitchison, 1960) or soil –water retention curve (SWCC).

A SWRC is illustrated in Figure 2.5. The curve is divided into three main segments and a representation of the soil-air-water condition is shown above each segment. The three segments are the boundary effect zone, the transition zone and the residual zone of unsaturation (White et al, 1970). The suction will increase in the boundary effect zone, and there will be tension exerted on the water, but the soil remains saturated. There is a continuous water phase connecting all pores in this zone. When the suction increases to the value that will cause the largest pore in the soil matrix to drain, the value of suction is known as the air-entry value (AEV).

Beyond the AEV, the soil is said to be unsaturated. In the transition zone, a small change in the suction will cause a significant decrease in water content. In the soil matrix, the pores drain sequentially from the largest size to smallest size. During this phase, air enters into the pores, replacing water. At the lower suctions in the transition phase, water is still continuous throughout the soil voids. At larger suction values, the increase in percentage of air, decreases the amount of continuous water connecting the soil voids.

Eventually, the increase in suction will reach a point when a change in suction will cause little change in the water content. (White et al, 1970) This value of suction is known as the residual saturation and the corresponding water content is the residual water content. (Fredlund and Xing, 1994; Vanapalli et al, 1996; Sillers, 1997) The air content in the voids is significant and the amount of continuous water is minimal. The result is an inability to drain water in the soil. The soil is said to be dry at a value of 10^6 kPa. (Russam, 1958; Croney and Coleman, 1961; Fredlund et al, 1994)

The area of water in soil is equivalent to the relative saturation in the soil (Vanapalli, 1994). The relative saturation is also called the saturation index or equivalent saturation and can be defined by equation 2-4 which is a proportion of the saturation from saturation to the residual degree of saturation S_r.

$$S_e = \frac{S - S_r}{100 - S_r} \qquad [2\text{-}4]$$

Suction can be matric suction or osmotic suction or a combination of the two suctions acting within a soil. It is widely accepted that the mechanical behaviour of the soil is significantly influenced by matric suction.

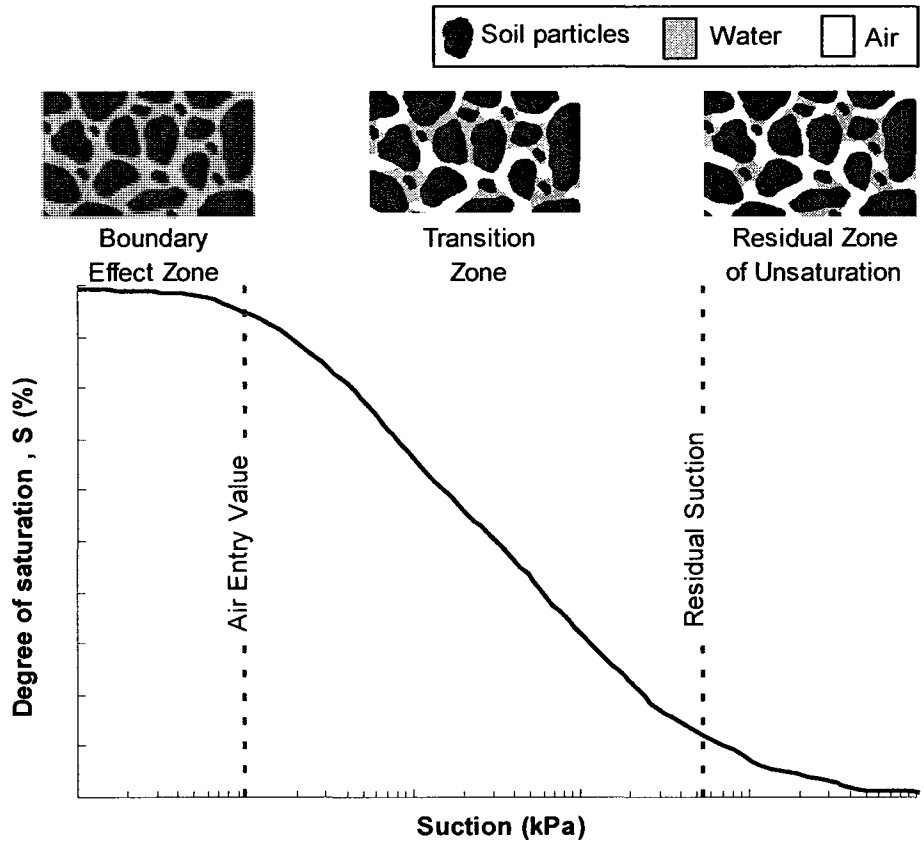

Figure 2.5. SWCC and schematic of water content changes. (modified from Vanapalli, 1994)

The SWCC of different materials will have different shapes. Sand has a larger maximum pore size and will have a lower AEV and begin to drain at lower suction. Alternately, clay has a smaller maximum pore size have a larger AEV which means that it can remain saturated under higher suction values. The rate of desaturation that occurs in the transition zone is dependent upon the distribution of the pore sizes in the soil matrix. The rate of desaturation is related to the distribution of pore sizes while the magnitude of the suction is related to the pore size. The residual suction values of different materials can vary depending on the percentage of fines within the soil and the orientation of the particles (Figure 2.6). The orientation of the particles, also known as the soil fabric will affect the size of the small pores in a soil sample.

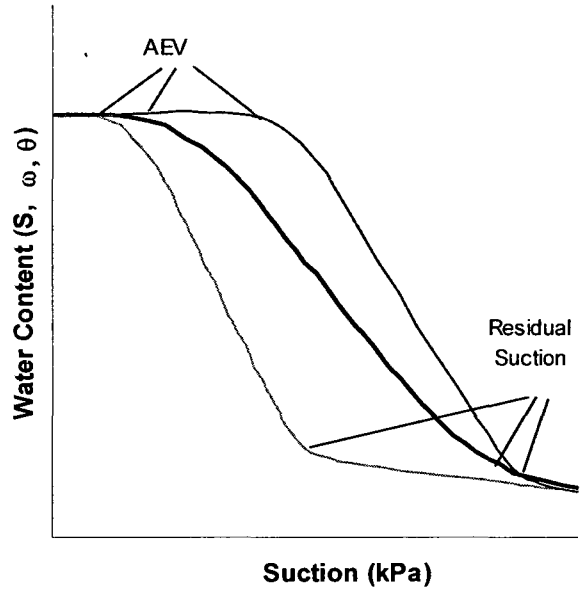

Figure 2.6. AEV and Residual Suction for several materials.

2.5.1 Measure of SWCC with applied Net Normal Stress

The shear strength of unsaturated soils are typically measured with net normal stresses ranging from 25 to 500 kPa. It is difficult to apply such large net normal stresses during the determination of the SWCC. The porous stones are unable to withstand such pressures. In 1994, Vanapalli proposed a technique to simulate pseudo net normal stress which is similar to using preconsolidated samples of the soil. The technique used by Vanapalli (1994) for measuring the SWCC is shown in Figure 2.7. The curve is loaded to a pressure greater than the intended loading pressure (A) and then left with a nominal

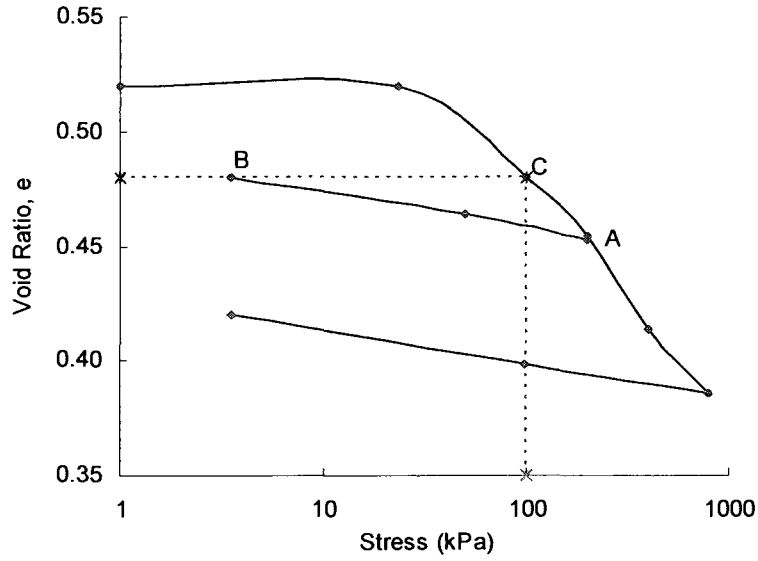

Figure 2.7. Consolidation curve for creating pseudo net normal stress. (modified from Vanapalli, 1994)

mass to allow the soil to rebound to the void ratio that a soil would have if it were loaded to 100 kPa (BC).

The SWCC is commonly determined without the application of a load or measuring the change in volume of the sample during testing. The volume change is neglected as it is assumed to be minimal. Realistically, the soil will be subjected to some loading and there will be volume change both during the loading and as well as the shearing stage.

2.5.2 Equations to Fit a Curve to the SWCC

The data of a measured SWCC can be represented by a mathematical equation can be used to fit a curve. Several equations are available in the literature to fit SWCC. Five equations (Eqns. 2-5 to 2-9) that readily approximate the shape of the SWCC through the use of different parameters are summarized below.

Brooks and Corey (1964):

$$\theta_w = \theta_r + (\theta_s - \theta_r)\left[\frac{a}{\psi}\right]^b \qquad [2\text{-}5]$$

where a = bubbling pressure; b = pore size index.

Brutsaert (1966):

$$\theta_w = \theta_r + \frac{(\theta_s - \theta_r)}{\left[1 + \left[\frac{a_b}{\psi}\right]^{n_b}\right]} \qquad [2\text{-}6]$$

van Genuchten (1980)

$$\theta_w = \theta_r + \frac{(\theta_s - \theta_r)}{\left[1 + \left[\frac{\psi}{a}\right]^{n}\right]^{m}} \qquad [2\text{-}7]$$

McKee and Bumb (1987)

$$\theta_w = \theta_r + \frac{(\theta_s - \theta_r)}{1 + e^{\left[\frac{h-a}{b}\right]}} \qquad [2\text{-}8]$$

Fredlund and Xing (1994):

$$\theta_w = \theta_r + \frac{(\theta_s - \theta_r)}{ln\left(e + \left(\frac{\psi}{a}\right)^n\right)^m} \quad [2\text{-}9]$$

where θ_w = water content; θ_r = residual water content; θ_s = saturated water content; ψ = suction;; and a, b, h, n, m = fitting parameters.

The fitting parameters for the above equations have meaning with regard to the shape of the SWCC. More details are available in various papers (Brooks and Corey, 1964; Brutsaert, 1966; van Genuchten, 1980; McKee and Bumb, 1987; Fredlund and Xing, 1994; Sillers, 1997). In this thesis, Equation 2-9 is used to fit the measured points of the SWCC does not but the curve is merely used to fit the data in order to interpolate between the measured points and obtain the required water content values (S, ω, θ) to use in the predictive equations.

2.5.3 Determination of AEV and Residual Suction

The AEV and residual water content is well-defined in coarse-grained soils. However, determination of the AEV and the residual suction of fine-grained soils can be challenging. A curve with a smoothed round shape makes the determination subject to interpretation. (Figure 2.8) The suction value, which is typically on a logarithmic scale, can influence the determination of the residual suction value. The range of error associated with estimation AEV, as a result, is reasonably narrow as the AEV is at lower suction values (~1-1000 kPa). Differences in choosing an AEV may vary from 5-20 kPa. The value of residual suction is at higher values of suction (~1,000-

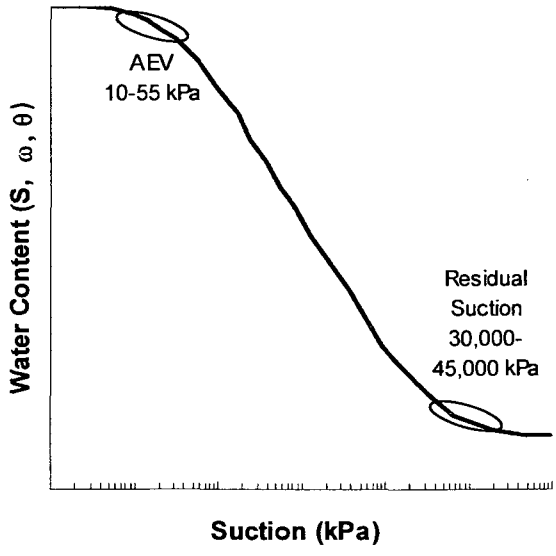

Figure 2.8. Possible range of AEV and residual suction for one soil.

200,000 kPa). Estimation of the value of residual suction may significantly vary (ie. 500 to 10,000 kPa).

2.6 Shear Strength

Earlier sections (2.1 to 2.5) provide a brief summary related to key concepts related to unsaturated soils and the SWCC which is used as a tool to predict the shear strength. The focus of this section is to provide background information for the shear strength behaviour of soils.

Shear strength of a saturated soil can be interpreted extending the effective stress concept by Terzaghi (1936) to the Mohr-Coulomb failure criterion as shown in equation 2-10.

$$\tau = c' + (\sigma - u_w) \cdot \tan \phi' \qquad [2\text{-}10]$$

where τ is the shear strength; c' is the effective cohesion of the soil; ϕ' is the effective angle of internal friction; and σ-u_w is the effective stress

There are two equations used in the interpretation of the shear strength behaviour of unsaturated soils. The first equation originates from the paper by Bishop from Imperial College in 1959 and the second from a paper by Fredlund, Morgenstern and Widger in 1978 (presented in section 2.5.1 and 2.5.2, respectively). These equations provide the foundation for many of the prediction equations presented in this thesis.

2.6.1 Bishop (1959)

In 1959, Bishop's paper on effective stresses in soil resulted in one of the fundamental equations of shear strength of unsaturated soils. Bishop proposed the variable, χ, which is a parameter related to the degree of saturation that is used to proportion the amount of effective stress acting on the system. Theoretically, χ will be equal to unity for saturated soils and decreasing to zero for a dry soil. In other words, χ varies as the degree of saturation changes from a saturated state to a total dry condition.

Bishop defined the equation for effective stress by dividing the type of soil into 4 different conditions: 1) fully saturated; 2) higher degrees of saturation; 3) lower degrees of saturation; and 4) fully dry. The equation representing the net effective stress of a soil that

has a high degree of saturation uses the pore water pressure, u_w (Eqn. 2-11). Alternately, the equation defining the net effective stress of a soil with a lower degree of saturation is uses the pore air pressure, u_a (Eqn. 2-12). The theoretical values of χ for the 4 different soil conditions are outlined below:

<table>
<tr><th colspan="2">Soil Condition</th><th>Value of χ</th><th colspan="2">Equation</th></tr>
<tr><td colspan="2">Saturated Soil</td><td>$\chi = 1$</td><td rowspan="2">$\sigma' = (\sigma - u_w) + \chi(u_a - u_w)$</td><td rowspan="2">[2-11]</td></tr>
<tr><td rowspan="2">Partially Saturated</td><td>High Degree</td><td>$\chi \approx 1$ (near unity)</td></tr>
<tr><td>Low Degree</td><td>$1 > \chi > 0$</td><td rowspan="2">$\sigma' = (\sigma - u_a) + \chi(u_a - u_w)$</td><td rowspan="2">[2-12]</td></tr>
<tr><td colspan="2">Dry Soil</td><td>$\chi = 0$</td></tr>
</table>

Bishop stated that for coarser grained soils, the suction *(u_a-u_w)* is less significant than the net normal stress. He concluded that the effective stress equation is not valid for fine-grained soils at low degrees of saturation. Substituting the effective stress equation (Eqn. 2-12) into the extended Mohr-Coulomb equation (Eqn. 2-10) results in Bishop's equation (Eqn. 2-13). Bishop concluded that this equation would not be effective for very fine-grained soils at lower degrees of saturation as the change in both shear strength and volume would be large when the water content is increased.

$$\tau = c' + (\sigma - u_a) \cdot \tan\phi' + \chi(u_a - u_w) \qquad [2\text{-}13]$$

As χ is related to the degree of saturation, it is related to the condition of the soil rather than a parameter of the soil. Thus, the equation is said to be constitutive in nature. Researchers have found limitations with respect to the quantification of χ both theoretically and experimentally (Jennings and Burland, 1962).

The net normal stress is expressed in terms of the pore air value, u_a, as unsaturated soil has both air and water in its pores and the pressure exerted by the liquid phase is less than the pressure exerted by the gaseous phase (Bishop, 1959). In addition, the area that is affected by the pore water pressure is reduced as the suction increases, owing to

the increase in the volume of air within the pores. In a generalized form, the shear strength of an unsaturated soil can be is expressed as below.

$$\tau = c' + (\sigma - u_a) \cdot \tan\phi' + \tau_{us} \qquad [2\text{-}14]$$

Where τ is the shear strength; c' is the effective cohesion of the soil; τ_{us} is the shear strength contribution due to suction; ϕ' is the effective angle of internal friction; σ-u_a is the effective stress; u_a-u_w is the suction.

2.6.2 Fredlund, Morgenstern & Widger (1978)

Several investigators described the behaviour of unsaturated soil using stress state variables which are comprised of various combinations of independent stress variables (Bishop and Blight, 1963; Aitchison, 1967; Matyas and Radharkrishna, 1968; Fredlund and Morgenstern, 1977).

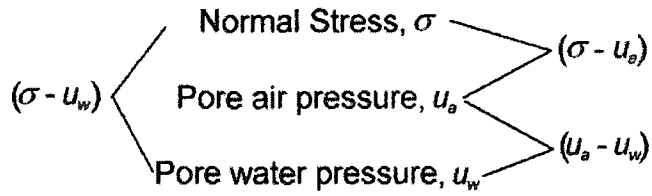

These variables can be combined into three separate stress state variables: $(\sigma - u_a)$, $(\sigma - u_w)$ and $(u_a - u_w)$. Ideally, the stress state variables would be independent if one variable could be altered without altering the other. Therefore, there are only two sets of independent stress state variables: $(\sigma - u_w)$, $(u_a - u_w)$ and $(\sigma - u_a)$, $(u_a - u_w)$. The use of independent stress state variables allows one variable to change and to understand the behaviour of the system due to that change (Fredlund and Morgenstern, 1977). Fredlund et al (1978) proposed an equation to describe shear strength behaviour of an unsaturated soil in terms of these stress state variables.

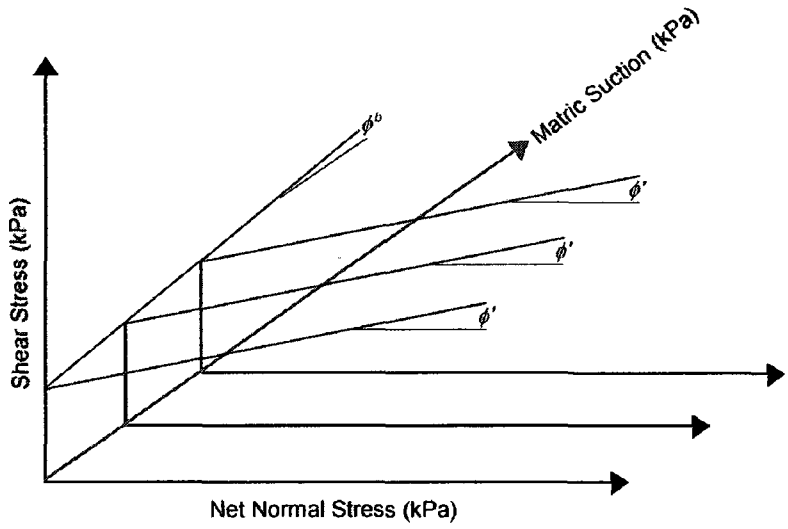

Figure 2.9. Three dimensional surface from Fredlund et al, 1978. (modified from Fredlund et al, 1993)

The authors defined the change in shear strength with respect to suction using the variable, *tan* ϕ^b (Eqn. 1-1). The angle, ϕ^b, (illustrated in Figure 2.9) was initially assumed to be linear based on the analysis of limited published results.

$$\tau = c' + (\sigma - u_a)tan\phi' + (u_a - u_w)tan\phi^b \qquad [1\text{-}1]$$

where ϕ^b is the friction angle with respect to the change in suction while the net normal stress is held constant.

The authors used three sets of data to examine the validity of the equation: compacted shale, Boulder clay and Potters flint/Peerless clay. The soils had 22%, 18% and 20% clay, respectively (Table 2.2). These sets of data were used as the results were expressed in terms of the stress state variables.

Subsequent experimental studies performed over a larger range of suction values have shown that the variation shear-strength with respect to soil suction is non-linear (Escario and Saez, 1986; Fredlund et al, 1987; Gan et al, 1988; Escario and Juca, 1989; Abramento and Carvalho, 1989).

Table 2.2. Soils used by Fredlund et al (1978) to test Equation 1-1.

	Compacted Shale	Boulder Clay	Potters flint/ Peerless clay
Authors	Bishop, Alpan, Blight and Donald, 1960		MIT, 1963
Range of Suction (kPa)	0 – 132	0 – 179	0 – 130
% Clay	22%	18%	20%
ϕ'	24.8°	27.3°	35.6°
ϕ^b	20.9°	24.0°	37.8°

The angle ϕ^b, was determined for each soil using Equation 1-1. Compacted shale and Boulder clay (Bishop et al, 1960) had an angle, *tan* ϕ^b, consistent with the anticipated result which is less than the effective angle of internal friction. The Potters flint/Peerless clay, however, resulted in an angle greater than the effective angle of internal friction (Table 2.2). However, the differences between ϕ' and ϕ^b were between 2.2° to 4.9° and as fine-grained soils were tested over a limited range of suction.

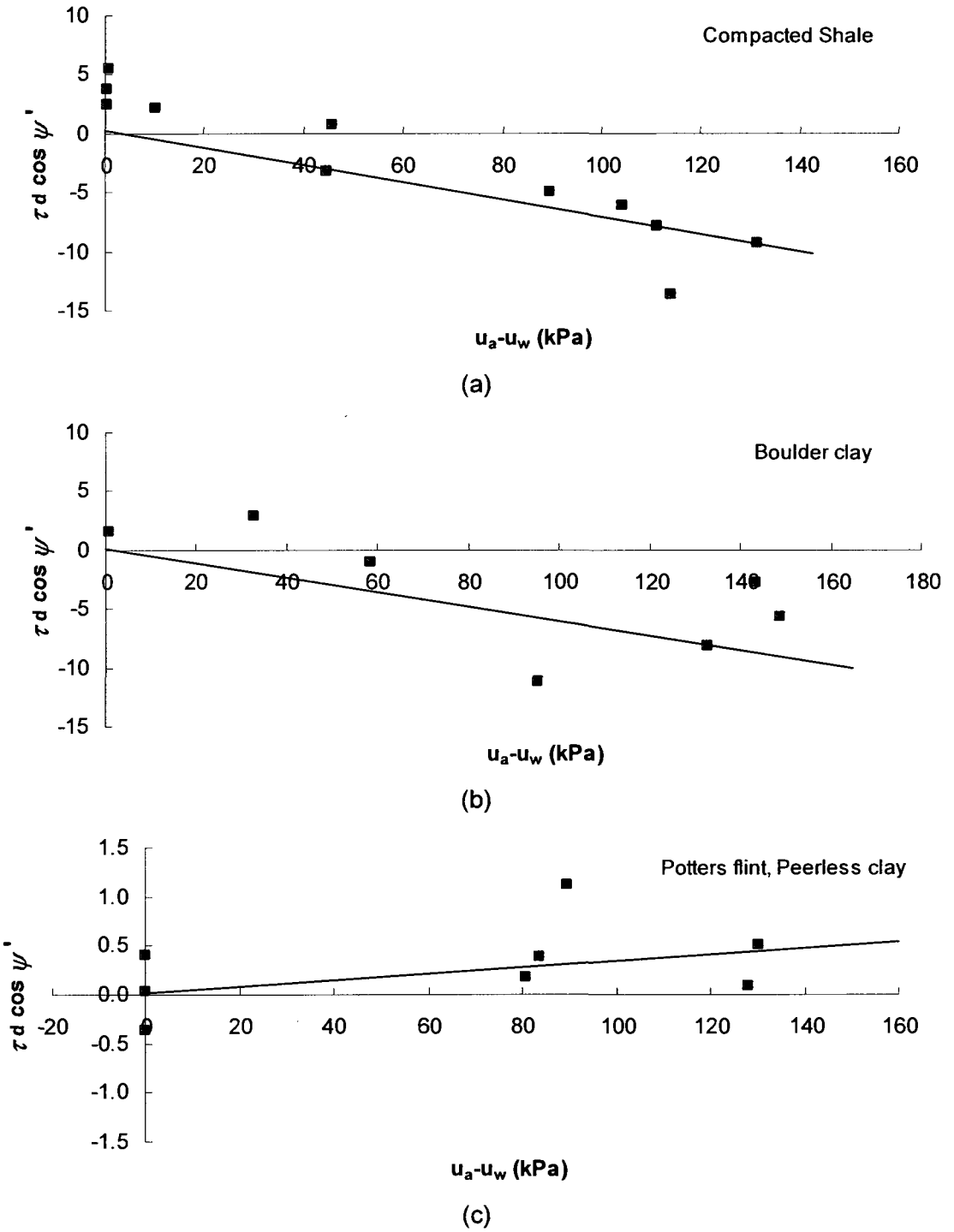

Figure 2.10. Change in shear strength from saturated strength plane for (a) compacted shale, (b) Boulder clay and (c) Potter's flint, Peerless clay. (modified from Fredlund et al, 1978)

2.6.3 Terminology

The shear strength is interpreted differently by various investigators in different papers. Some authors use the term deviator stress (Lee, Sung and Cho, 2006), the shear point strength (Fredlund et al, 1978; Röhm and Vilar, 1995) or conventional shear strength. The concept of these terms is illustrated in Figure 2.11 and defined in Equations 2-15 to 2-18, below. The normal stress for the deviator stress and stress point strength is different from the normal stress for the shear strength.

Table 2.3. Equations representing strength of the soil.

Equation		Net Normal Stress	
$(\sigma_1 - \sigma_3)$	Deviator Stress	$\left(\frac{\sigma_1 + \sigma_3}{2}\right)$	[2-15]
$\left(\frac{\sigma_1 - \sigma_3}{2}\right)$	Stress Point Strength	$\left(\frac{\sigma_1 + \sigma_3}{2}\right)$	[2-16]
$\left(\frac{\sigma_1 - \sigma_3}{2}\right) \cdot \cos\phi'$	Shear Strength, τ (2 dimensions)	$\left(\frac{\sigma_1 + \sigma_3}{2}\right)(1 - \sin\phi')$	[2-17]
$\left(\frac{\sigma_1 + 2\sigma_3}{3}\right) \cdot \cos\phi'$	Shear Strength, τ (3 dimensions)	$\left(\frac{\sigma_1 + 2\sigma_3}{3}\right)(1 - \sin\phi')$	[2-18]

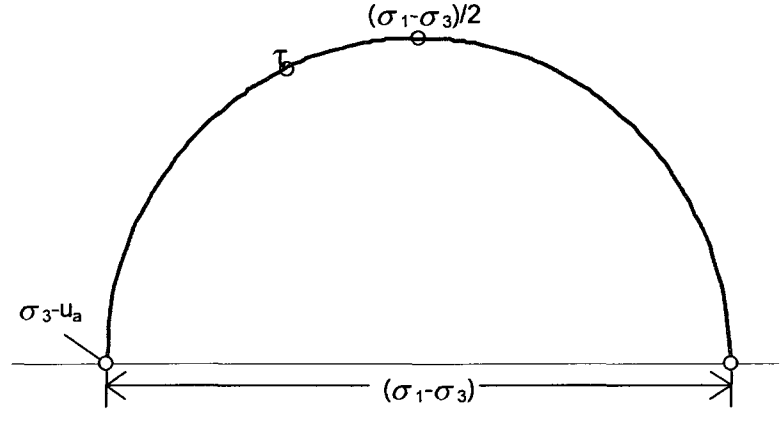

Figure 2.11. Mohr's circle illustrating the relationship between the strength equations.

The other technique used for interpreting the shear strength are based on apparent cohesion and total cohesion concepts. These terms have the same meaning and can be defined as the sum shear strength contribution due to suction and the effective cohesion (Eqn. 2-19).

$$apparent\ cohesion = C_A = c' + \tau_{us} \qquad [2\text{-}19]$$

Where τ_{us} is the shear strength contribution due to suction; C_A is the apparent cohesion.

2.6.4 Effective Strength Parameters

The effective strength parameters are a part of the unsaturated shear strength equation (ie. the effective cohesion, c', and the effective angle of internal friction, ϕ'). These parameters are specific to the soil and determined on the saturated soil specimens. They are conventionally determined using either the direct shear test, or the triaxial shear equipment.

The shear parameters are determined extending the concepts introduced by Mohr. Shear strength determined by the shear point envelope has different values of the shear strength parameters.

These parameters are labelled as the effective cohesion, d' and the effective angle of internal friction, ϕ^b, respectively. The differences in the shear strength parameters are illustrated in Figure 2.12. The conventional shear strength parameters are determined using a line tangent to the circles while the stress point envelope determines the parameters using a line connecting the apex of the circles.

The shear strength parameters from the two lines are related by the following equations (from Fredlund and Rahardjo, 1993):

$$\frac{c'}{\sin\phi'} = \frac{d'}{\tan\phi'} \qquad [2\text{-}20]$$

$$c' = d' \cdot \frac{\sin\phi'}{\tan\phi'} = \frac{d'}{\cos\phi'} \qquad [2\text{-}21]$$

Where c' is the effective angle of internal friction, d' is the ordinate intercept when the mean net normal stress (p') equals zero for a stress point envelope (Figure 2.12).

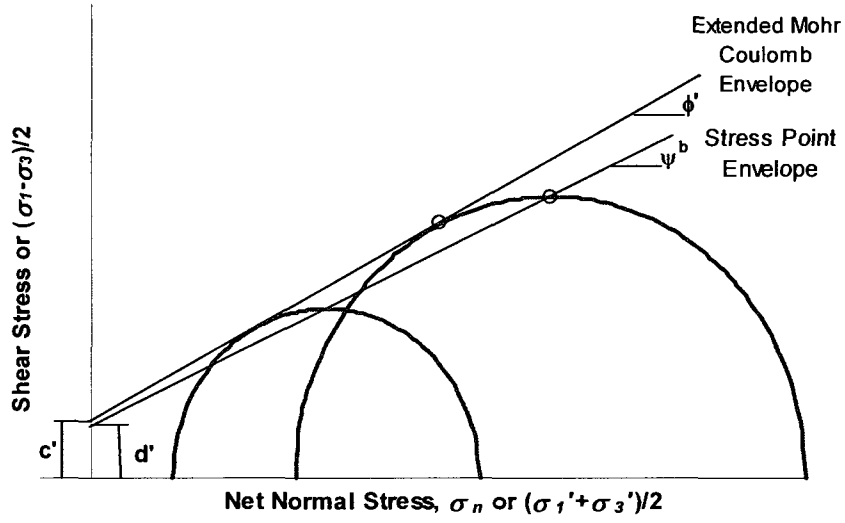

Figure 2.12. Soil parameters analyzed by extended Mohr-Coulomb envelope and extended envelope. (from Fredlund and Rahardjo, 1993)

2.7 General Notes on Shear Strength Testing

Shear strength testing is complex and has many small details to be aware of. The following section mentions and illustrates some of these details in order to provide insight into the complexity of the testing procedure.

2.7.1 Typical Shear Strength Envelope of an Unsaturated Soil

Figure 2-13 shows typical shear strength envelope which is plotted as the variation of shear strength with respect to suction and constitutes of two segments: a linear and a non-linear segment. The linear segment shows an increase in the shear strength contribution that occurs till the water in the soil pores begins to drain (ie. the air-entry value, AEV of the unsaturated soil). The shear strength in this region which constitutes the boundary effect zone increases at an angle approximately equal to the effective angle of internal friction, ϕ' for most of the soils. Beyond the AEV, the shear strength is non-linear. The non-linear behaviour can be attributed to the desaturation that occurs as the suction increases and the rate of desaturation has been related to the fabric of the soil (Vanapalli et al, 1996). When the soil is saturated, the increase in the net normal stress increase is equivalent to the increase in the matric suction. Beyond the AEV, the soil begins to desaturate and the result is the matric suction will be acting on less area of wa-

ter. (Vanapalli, 1994) The result is a non-linear relationship as the matric suction will have less effect than the net normal stress. (Vanapalli et al, 1996)

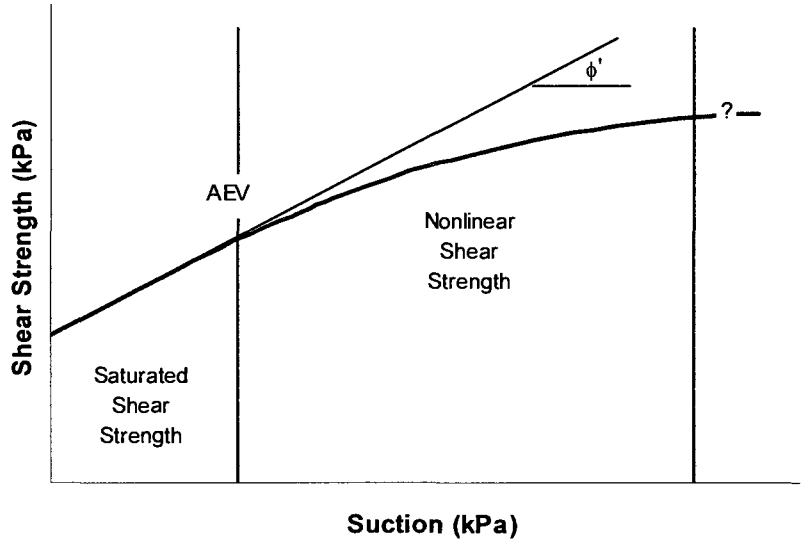

Figure 2.13. Schematic of shear strength curve.

2.7.2 Shear Strength Contribution Due to Suction

The shear strength results are presented by removing the saturated shear strength. The saturated shear strength is different for a soil tested in a direct shear apparatus as opposed to a soil tested using a direct shear apparatus. The confining pressure of the direct shear test is applied perpendicular to the failure plane and therefore, the confining pressure is equal to the net normal pressure. The net normal pressure of soils tested in a triaxial cell is composed of the confining pressure and the pressure applied in the axial direction (Figure 2.14; Equation 2-22). The saturated shear strength of soils tested by direct shear does not change with an increase in

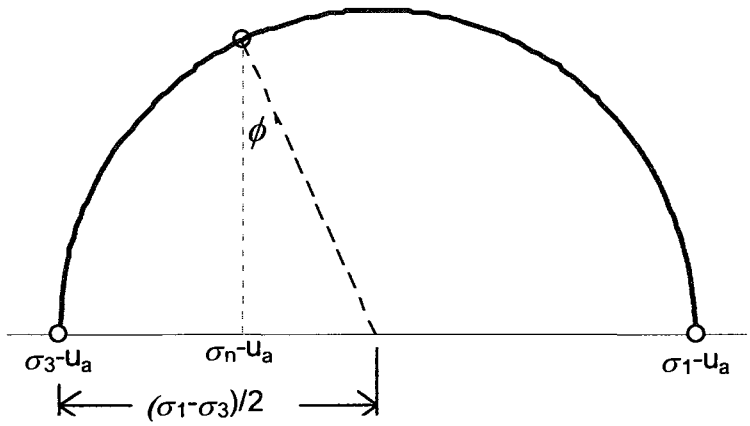

Figure 2.14. Determining net normal stress from triaxial test results.

suction (Figure 2.15a). The saturated shear strength of a triaxial soil sample increases with suction as a greater axial load is required to induce failure of the sample. (Figure 2.15b) Removing the saturated shear strength leaves the shear strength contribution due to suction. The resulting shear strength will allow the comparison of the test results of samples tested using the two testing apparatuses.

$$\sigma_n = \sigma_3 + \left(\frac{\sigma_1 - \sigma_3}{2}\right) \cdot (1 - \sin\phi') \qquad [2\text{-}22]$$

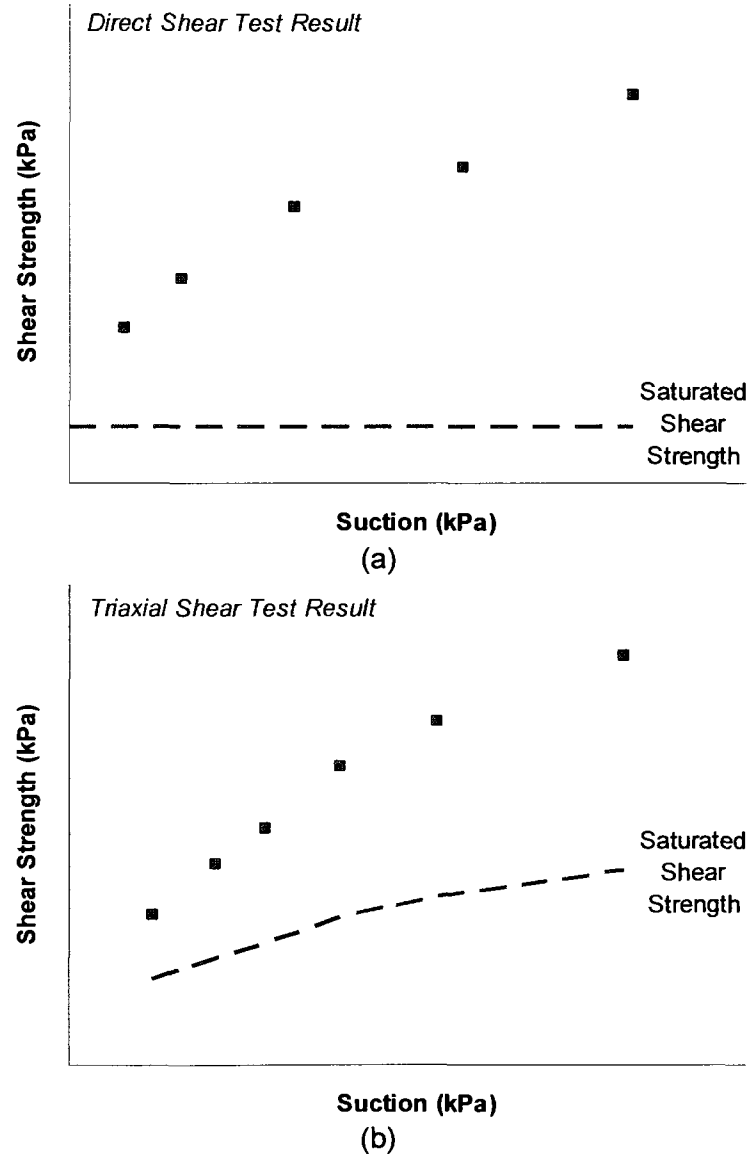

Figure 2.15. Difference in saturated shear strength component in (a) direct shear tests and (b) triaxial tests.

Two soils were tested using both a modified direct shear and a modified triaxial test: Soil 25, AV colluvium (Feuerharmel et al, 2006) and Soil 45, Ashikaga silt (Nishimura et al, 1999). The results can be compared although attention has to be paid to the differences in net normal pressures applied to the failure plane.

The AV colluvium (Soil 25) tested in direct shear apparatuses using similar confining stresses produced very different results. Plotting the results of the soil on one graph illustrates the difference (Figure 2.16a). The difference is seen by comparing shear tests performed at net normal stress of 100 kPa at a suction of 200 kPa. The shear strength contribution due to suction is 39 kPa vs. the other set where the shear strength contribution due to suction was 144 kPa. This is a significant difference in the shear strength which may be the result of a difference during testing.

Triaxial testing was performed on two samples the same material and were presented under a separate cover (Figure 2.17). The shape of the curve was different in that there is a peak in the soil subjected to a higher confining pressure. For the soil tested at a confining pressure of 100 kPa, when the net normal stress is 225 kPa or greater, the soil shows greater influence to the confining stress. The increase in net normal stress may cause a greater deformation. The greater deformation may correlate to the preconsolidation pressure of the soil, thereby increasing the rate of deformation. When the net normal stress is less than 225 kPa, the soil shows greater influence from suction.

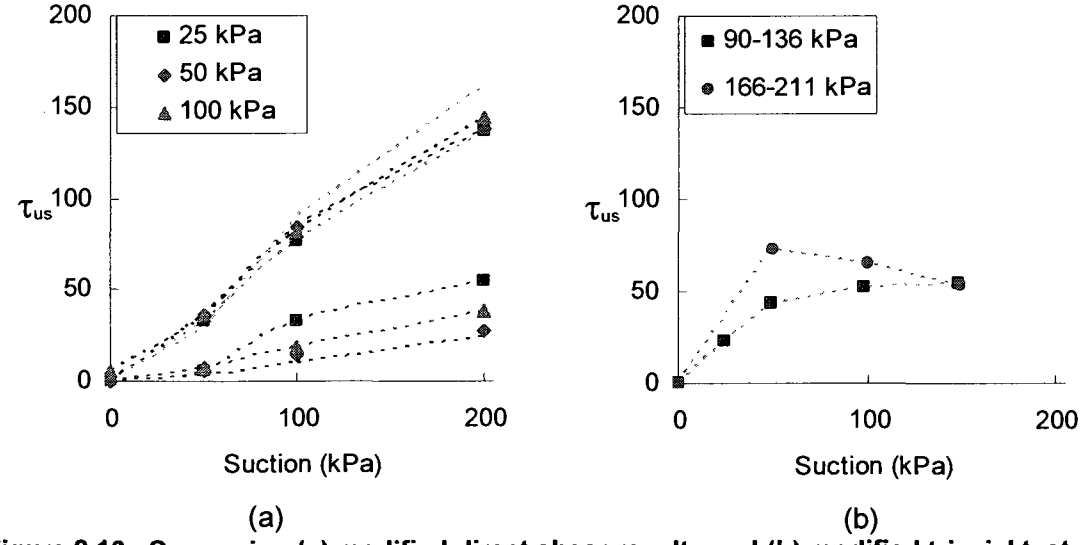

Figure 2.16. Comparing (a) modified direct shear results and (b) modified triaxial test results for Soil 25, AV Colluvium. (Feuerharmel et al, 2006)

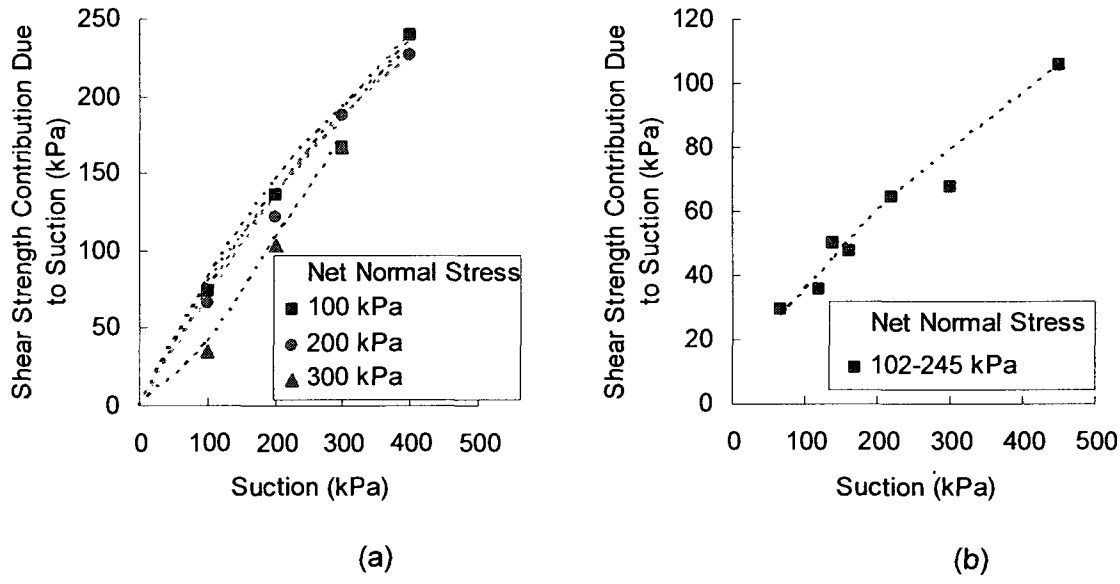

Figure 2.17. Comparing (a) modified direct shear results and (b) modified triaxial test results for Soil 45, Ashikaga silt. (Nishimura et al, 1999)

Ashikaga silt (Soil 44) was also tested by a modified direct shear test and a modified triaxial test apparatus. The results are presented below. The modified direct shear test was performed using net normal stresses ranging from 30 kPa to 300 kPa and the net normal stresses during the triaxial tests ranged from 102 kPa – 245 kPa. The shear strength contribution due to suction for the modified direct shear tests resulted in a narrow band of results up to confining stresses of 200 kPa. The test with a net normal stress of 300 kPa produced a similar result; however, the net result was a lower shear strength contribution due to suction. The high level of confinement may have allowed the particles in the soil to shear more readily. The triaxial test had a net confining pressure of 30 kPa and net normal stresses much higher, yet resulted in lower shear strength.

Differences in shear strength contribution due to suction performed using different testing apparatuses produces different results. In addition, testing the same soil in different batches or at different times appears to occasionally create different results. The complex nature of testing can create differences in testing.

2.7.3 Single Stage vs. Multi-Stage Testing

Single stage testing (Figure 2.18a) uses one sample and tests it only once. Multi-stage testing (Figure 2.18b) uses only one sample, but tests the sample to near failure,

changes the condition and tests the sample again to near failure. This pattern repeats until the desired testing sequence has been completed.

There are advantages and disadvantages to each of the test types. A single stage test has a definitive result and the sample can be tested to failure without stopping. It allows the change in suction to occur on samples of the same size. Multi-stage testing ensures that the testing occurs on an identical sample and minimizes cost and effort to prepare and test samples. It can be challenging to terminate the test prior to permanent deformation. Unsaturated soil testing is expensive and time consuming. Multi-stage testing eliminates the need for excess soil and reduces the time and cost to set up the test.

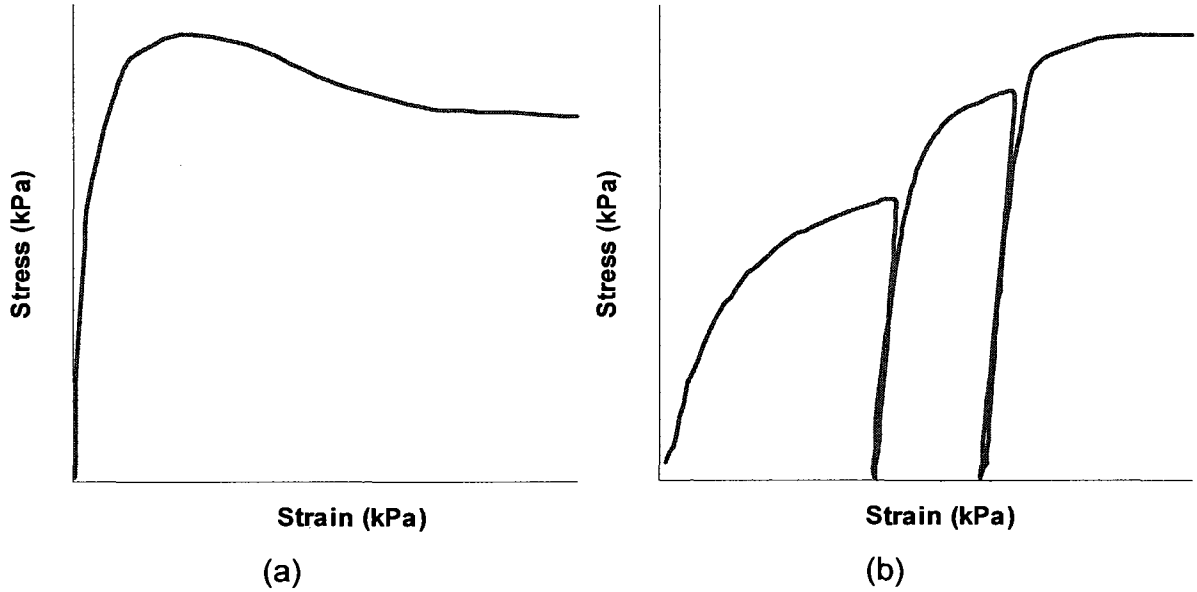

Figure 2.18. Shear strength testing results from (a) single-stage test; (b) multi-stage test with constant confining pressure and different suctions. (from Fredlund and Rahardjo, 1993)

2.7.4 Types of Shear Strength Tests for Unsaturated Soils

Shear strength tests for unsaturated soils are performed using the same means as the most common shear strength tests. It is important to be able to control or measure suction and confining conditions and, therefore, the testing apparatuses are modified. The modifications make the apparatus expensive and complex. Therefore, the tests for unsaturated soils are time consuming and require specialized personnel.

Modified Direct Shear Apparatus

The modified direct shear is one of the simplest shear tests to perform. The sample is sheared along a directed plane and the confining pressure is equal to the net normal pressure.

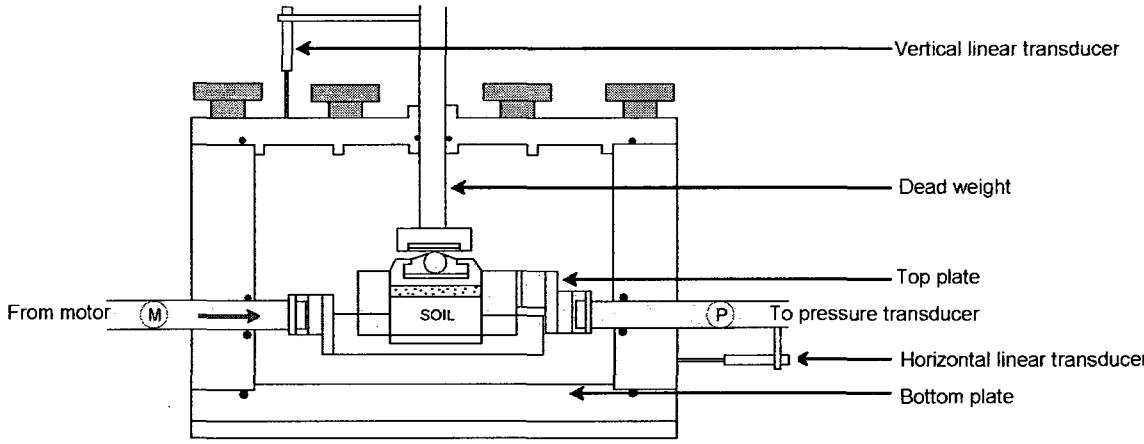

Figure 2.19. Schematic of modified direct shear testing. (from Gan et al, 1988)

Recently, a newer version of the modified shear box has been developed. This shear box does not use the axis translation technique as others to measure the suction, but rather it uses high-suction tensiometers. This eliminates the large pressurized chamber used in the original modified direct shear test. (Caruso and Tarantino, 2004)

Modified Triaxial Shear Apparatus

The modified triaxial test is a more complex test with a larger sample encased in a membrane. The apparatus allows the confining pressure to be applied to the sample prior to and during shearing. There is no directed shear plane so the sample will fail at an angle approximately equal to the angle of internal friction. The net normal stress is perpendicular to the failure plane in the sample.

The unconfined compression test is a special type of triaxial test where the confining pressure is equal to zero. The suction is commonly measured prior to and after testing but it can be difficult to measure in the apparatus.

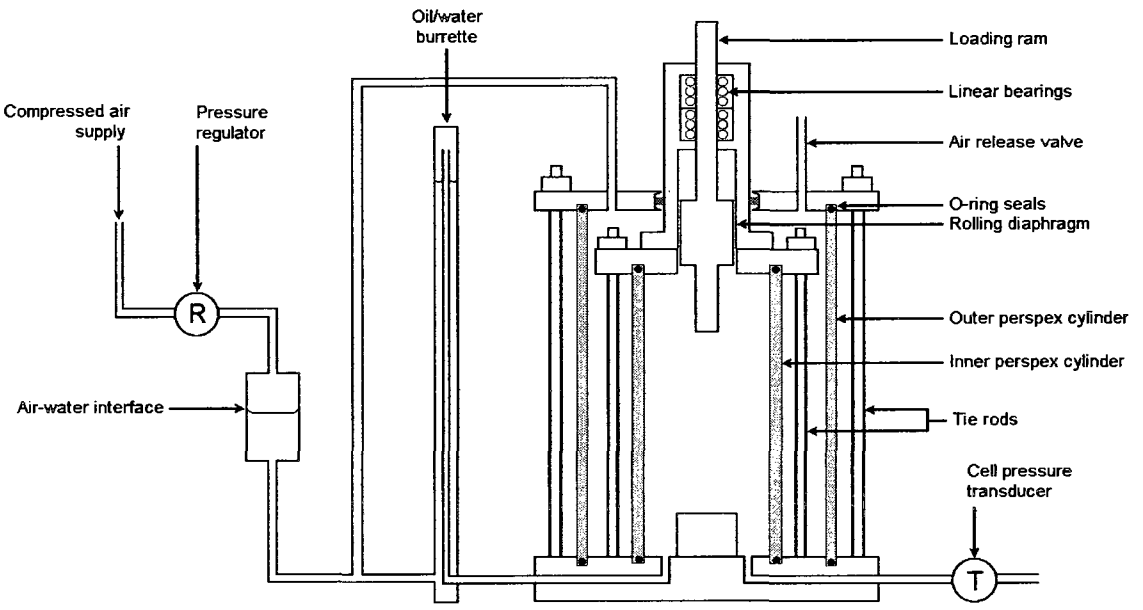

(a)

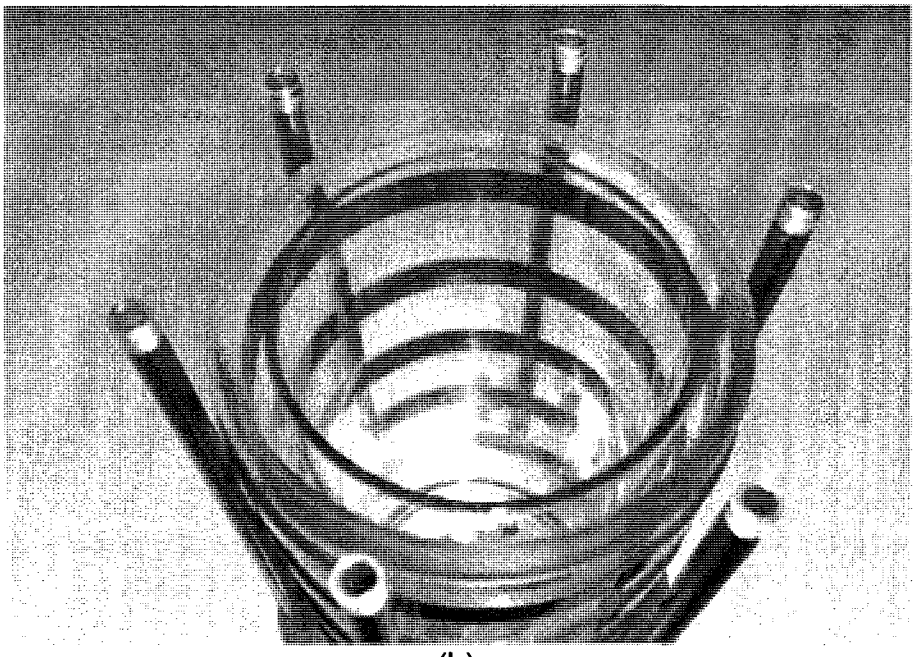

(b)

Figure 2.20. (a) Schematic of direct shear apparatus (from Wheeler, 1988) (b) a type of triaxial cell used in the modified apparatus – a double walled triaxial cell. (from Wfi.co.uk)

Modified True Triaxial Test

The modified true triaxial test is a test that tests cubic soil specimens measuring 80 mm x 80mm by 80mm. The apparatus isotropically loads the sample on three faces. Although it has been used, it is not a common test.

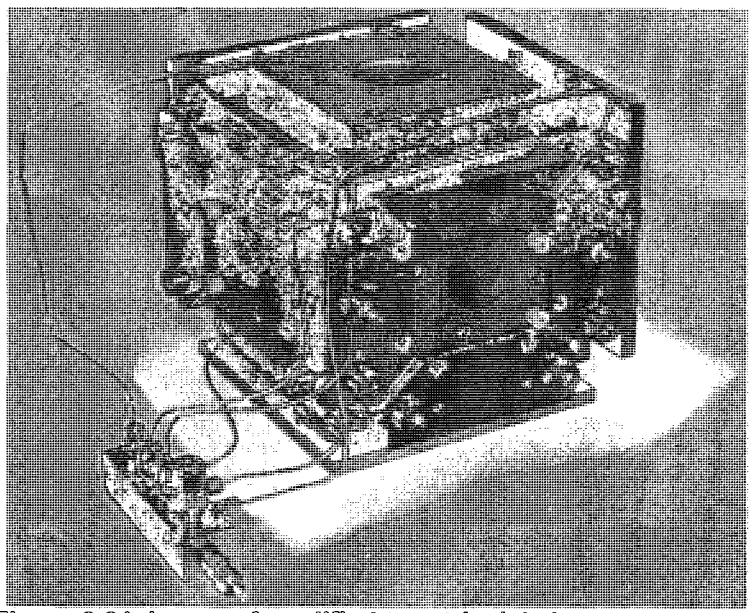

Figure 2.21. Image of modified true triaxial shear apparatus. (from ergotech.co.uk)

Modified Ring Shear Apparatus

The modified ring shear is less common and newly modified apparatus used to test unsaturated soils.

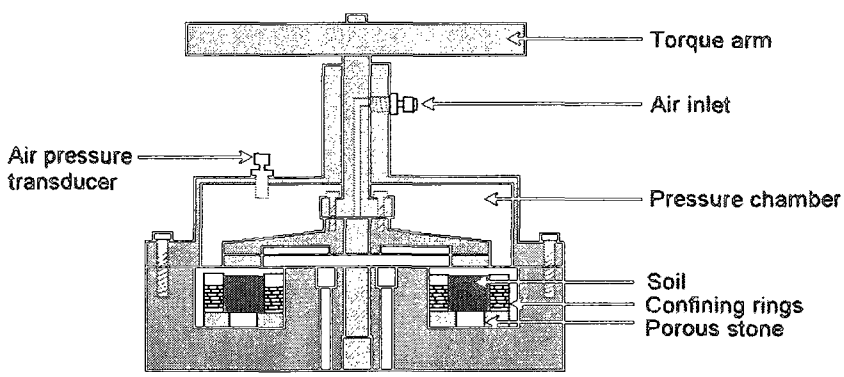

Figure 2.22. Schematic of direct shear apparatus. (from Infante Sedano, 2006)

In-situ Testing

There is an in situ test that has been developed to determine the shear strength of soil. The iswest, or in situ wedge test, was developed to test soils in place to get a true representation of shear strength of the soil. (Mirata, 1974; Mirata, 1998). Later, two other apparatus' were developed to test the soil almost immediately after it was removed from the borehole: the cylwest or cylindrical wedge test (Mirata, 1991) which later evolved into a larger version, the priswest, or prismatic wedge test (Mirata, 1998). These tests measure the total stress or the undrained shear strength of the soil.

The apparatus' have been tested on undisturbed clays and gravely sands (Mirata, 1991). Cylwest and iswest were found to produce comparable results when compared to shear box tests. (Mirata, 1991).

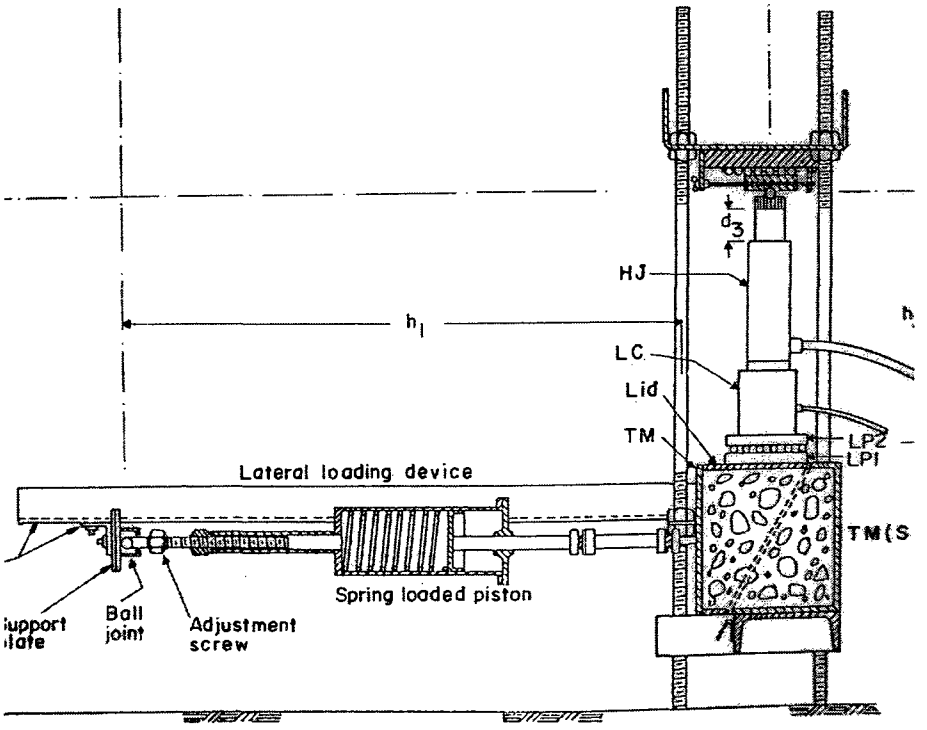

Figure 2.23. Schematic of in situ wedge shear apparatus. (from Mirata, 1998)

The most common tests are summarized in Figure 2.24.

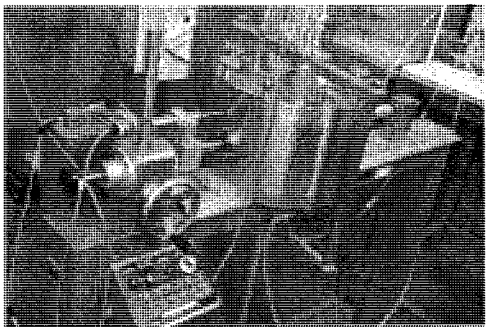

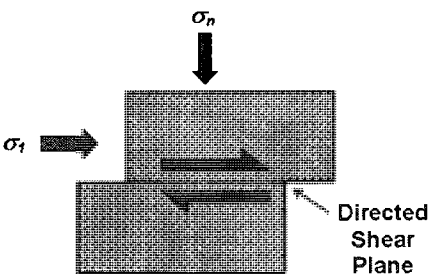

(a)

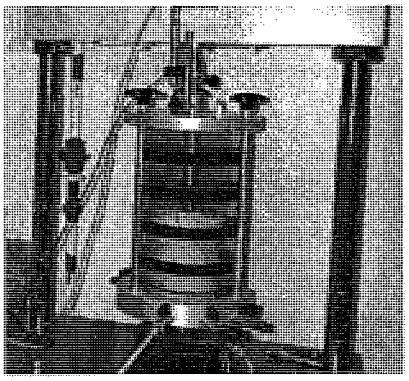

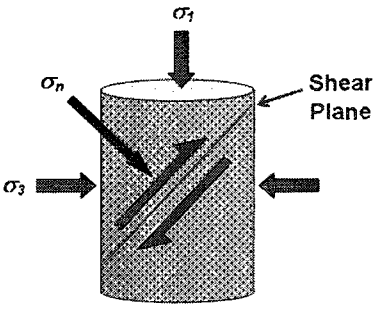

(b)

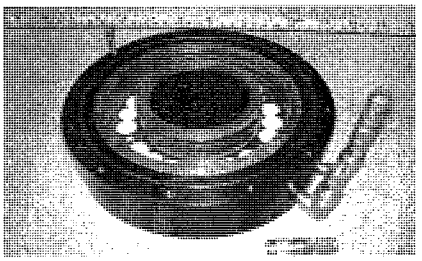

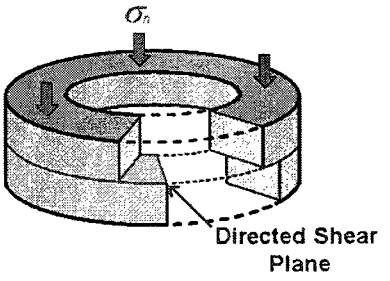

(c)

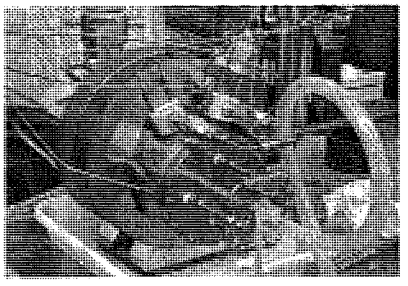

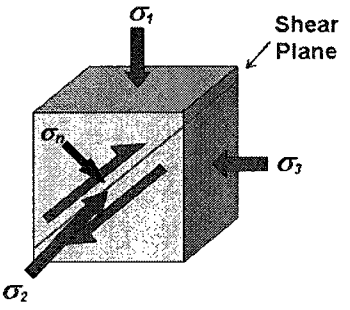

(d)

Figure 2.24. More common shear strength testing apparatus' for unsaturated soils: (a) modified direct shear (b) modified triaxial shear (c) modified ring shear (from Infante Sedano, 2006; environment.uwe.ac.uk); (d) modified true triaxial test (netl.doe.gov).

2.7.5 Analyzing Shear Strengths from Different Tests

Equations use the value of the net normal stress to determine the shear strength of the soil. In the case of direct shear test, the net confining pressure (σ_3-u_a) is the same as the net normal pressure (σ_n-u_a) because the shear plane is a directed shear plane. This is not the case for the triaxial test. Figure 2.24 (b) illustrates the failure plane in the triaxial test at an angle approximately equal to the angle of internal friction. The net normal stress is perpendicular to this failure plane and it is influenced by the axial stress as well as the confining pressure. The net normal stresses on four triaxial tests with a constant confining pressure are shown in Figure 2.25. Not only is the net normal stress larger than the net confining pressure, the net normal stresses are different for each sample.

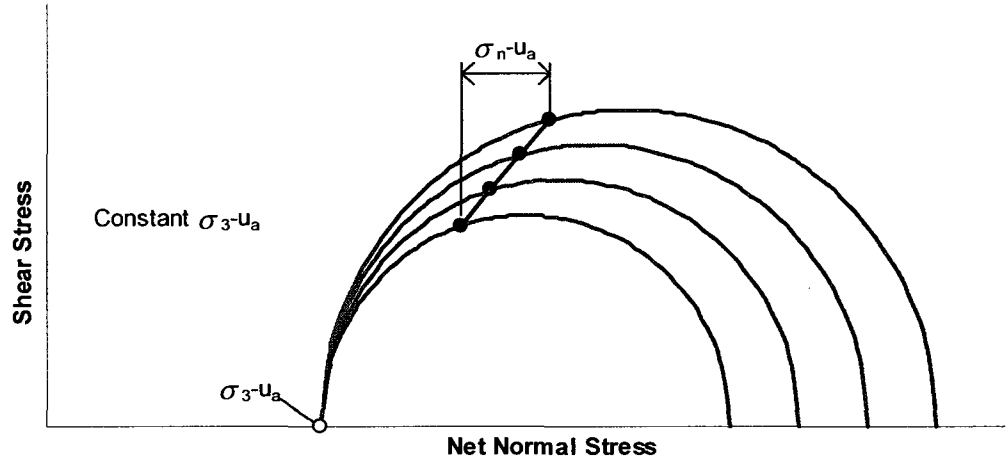

Figure 2.25. Constant confining pressure illustrating variation in net normal strength for triaxial testing.

2.7.6 Hysteresis

Hysteresis can be generally defined as a path-dependent situation. In the case of unsaturated soils, hysteresis refers to the difference between the drying curve SWCC and the wetting curve SWCC. The drying curve is measured by saturating a specimen with backpressure and starting at saturation, measuring the water content at different suction increments. The wetting curve can then be measured by measuring the water content at different suction increments as the suction is decreased again. An illustrative example is shown in Figure 2.26. The drying curve and wetting curve are different in that the wetting curve has lower water content for the same value of suction (degree of saturation at

A > degree of saturation at B). The difference between the drying curve and the wetting curve is known as hysteresis.

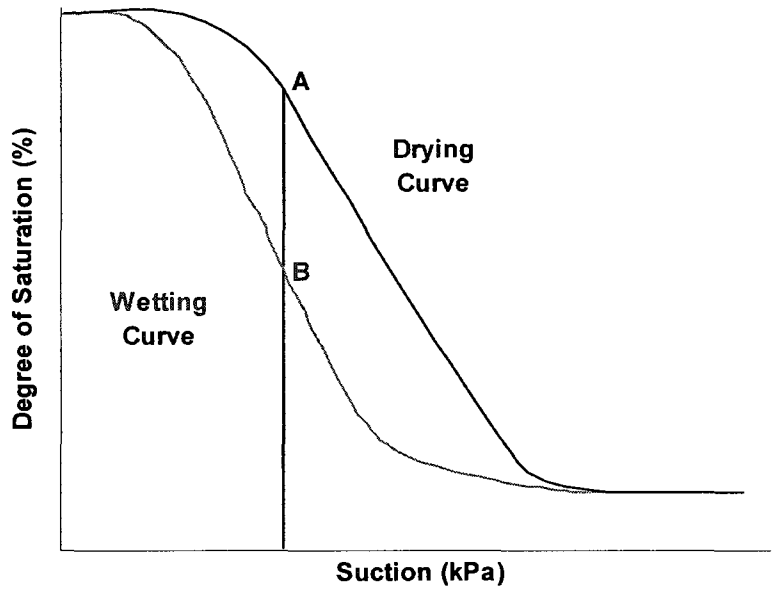

Figure 2.26. Illustration of hysteresis.

2.7.7 Specialized Accessories

Measurement of suction and unsaturated shear strength are complex tests and require specialized equipment, personnel and training. The testing procedure may require additional methods to measure the change in volume of water, measure the change in sample volume and to measure and flush the diffused air from the system.

Measuring Volume of Water

The twin burette system is one modification that can be used to measure the volume of water leaving the system. (Figure 2.27) The twin burette system is advantageous in that the configuration of valves running from the shearing system to the twin burettes can be configured such that the volume change can be measured in one burette and when it has reached its capacity, the valves can be altered to measure the other burette. (Infante Sedano, 2006) The standard burette system is modified for unsaturated soils by decreasing the diameter of the burette to increase precision (Fredlund and Rahardjo, 1993).

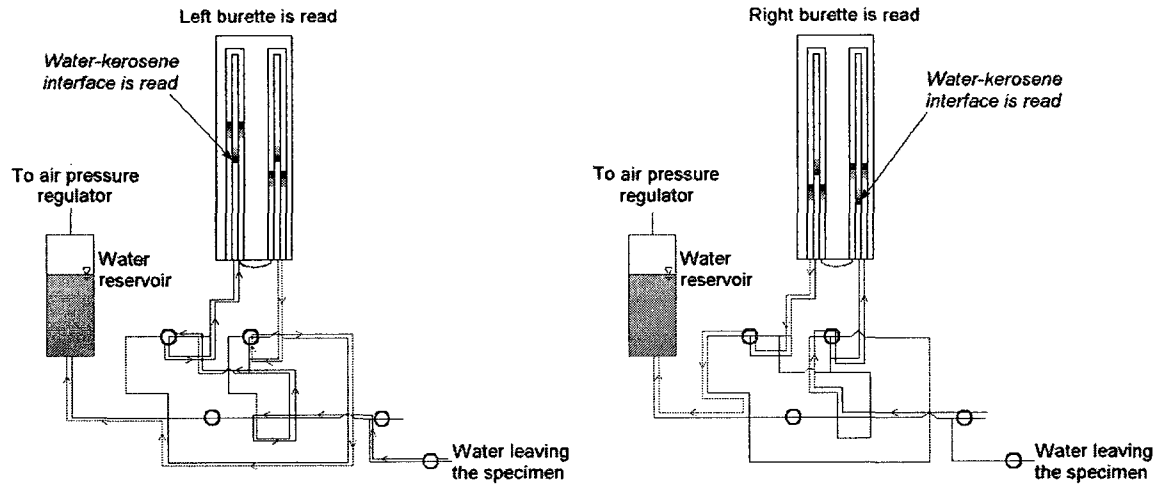

Figure 2.27. Schematic of twin burette system to measure volume change. (modified from Fredlund and Rahardjo, 1993).

Diffused Air

High air-entry disks are used as a semi-permeable membrane to separate the air and water in the system and to resist the flow of air when the pressure is increased. Diffusion of air across this membrane still occurs (Bishop and Donald, 1961). When air bubbles become trapped adjacent to the semi-permeable membrane, it interrupts the flow of water across the disk, to and from the sample. In addition, the air bubbles will displace water in the grooves beneath the disk and influence the displaced water volume measurement. Air bubbles displacing the water will make the soil specimen appear to be draining a greater volume of water ie. The specimen will appear to have a lower degree of saturation.

The diffused air can be removed by flushing the system regularly during testing. The system should be designed with smaller tubes and grooves to ensure that air bubbles are removed during flushing. The air trap is the area where the tubing widens and allows the air to rise out of the water. The released air can be measured and accounted for. (Infante Sedano, 2006)

Bishop and Donald (1961) designed a system with an air trap to measure the diffused air and later correct the volume of water displaced. (Figure 2.28) The air trap is a part of the volume measurement system.

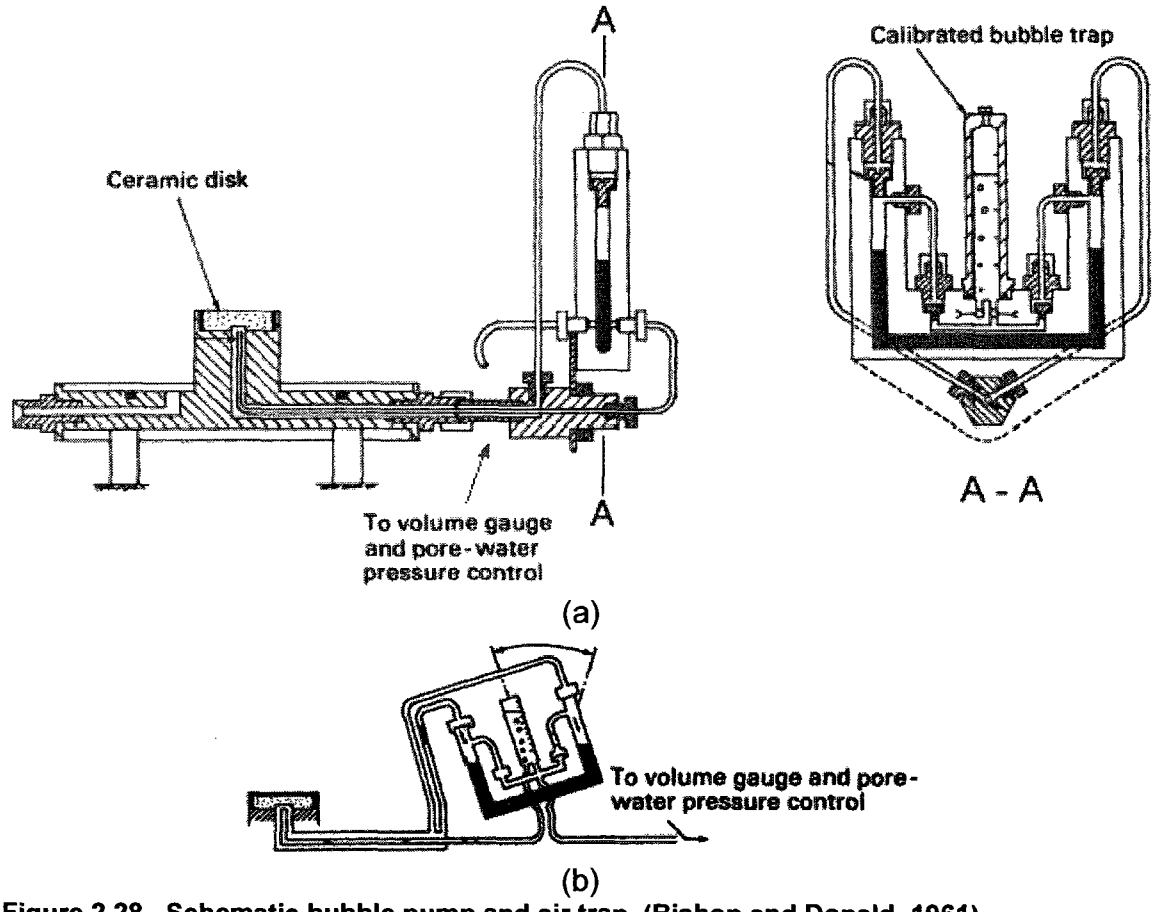

Figure 2.28. Schematic bubble pump and air trap. (Bishop and Donald, 1961)

Later a diffused air volume indicator (DAVI) was developed by Fredlund (1975) where the diffused air was separated from the volume measurement system. The burette and an adjacent exit tube is contained within a sealed cylinder (Figure 2.29). The air pressure in the cylinder is controlled to create a gradient similar to that at the below the high air-entry disk and this pressure is used to determine the volume of diffused air. (Infante Sedano, 2006)

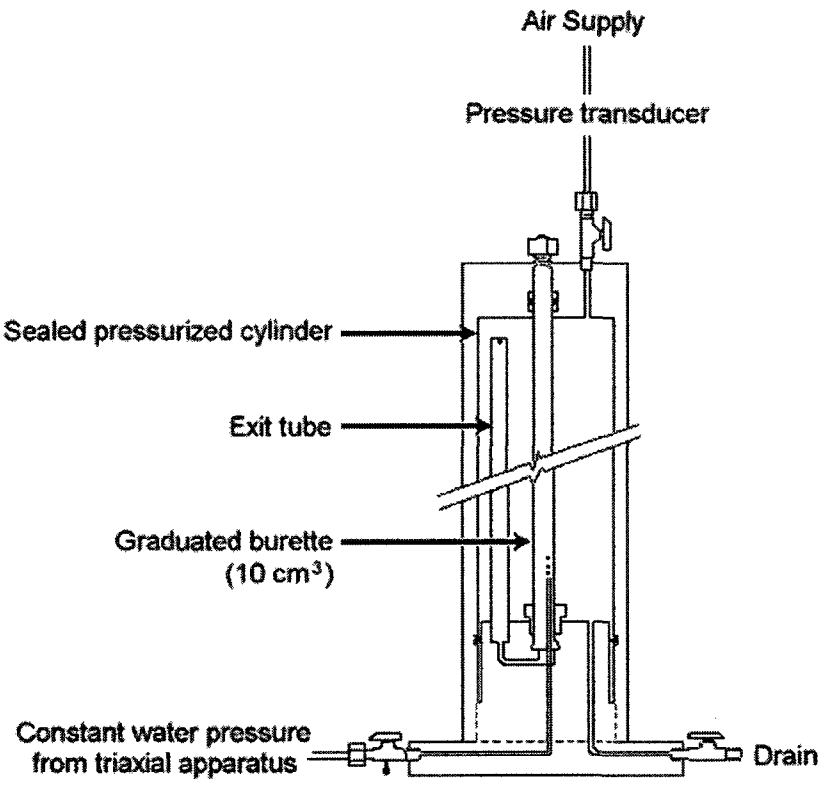

Figure 2.29. Diffused air volume indicator. (modified from Fredlund 1975)

Integrated Volume Gauge and Air Trap

Volume change indicator, a flushing system with an air trap and a diffused air volume indicator are common additions to more modern apparatus to measure the volume change and correct the degree of saturation of the tested specimens and ensure proper drainage during testing. An advanced piece of equipment was developed at the University of Ottawa that incorporated the volume change indicator and the DAVI into one system (Infante Sedano, 2006). The apparatus is elegant in its simplicity and by integrating the two functions into one piece of equipment, it helps to simplify an already complex apparatus.

The equipment consists of a small tube within a larger tube backed by a mirror for parallax conversion. (Figure 2.30)

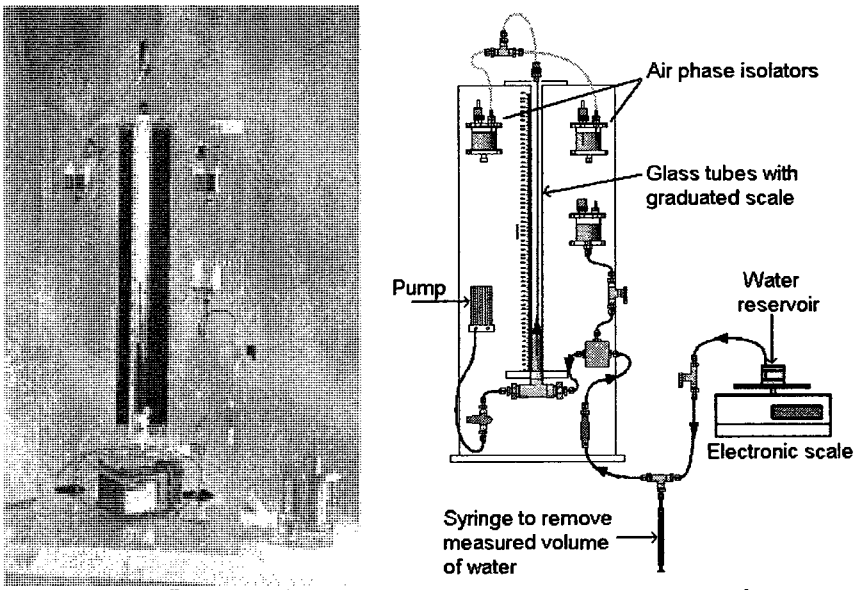

Figure 2.30. Design of a volume measurement system and pressure reading gauge. (from Infante Sedano, 2006)

The air phase isolation system is a series of two bottles: one that is for air and the other is partially filled with water. The bottles were used as an air reservoir to collect air from the system and return air to the system if needed. The system is not directly opened to the atmosphere as the vast change in humidity may cause a significant change in the system. The air phase isolator bottles allow air to enter and leave the system without exposing the system to a drier air. (Infante Sedano, 2006)

The inner burette system is used for precision measurement in the system. Illustrated in Figure 2.31a, the inner burette is lifted during flushing and as the water moves through the valves at the bottom, bubbles from the water rise into the outer tube. After flushing is complete, the inner burette is lowered and water will move up into the inner tube allowing a measurement to be taken. A one millimetre change in the inner tube was equal to 0.07 mL volume change. (Infante Sedano, 2006)

The various equipment and techniques designed by various authors illustrate the complex nature of testing unsaturated soils. Advances and designs emerge as researchers learn about unsaturated soil behaviour and testing and the limitations on the systems.

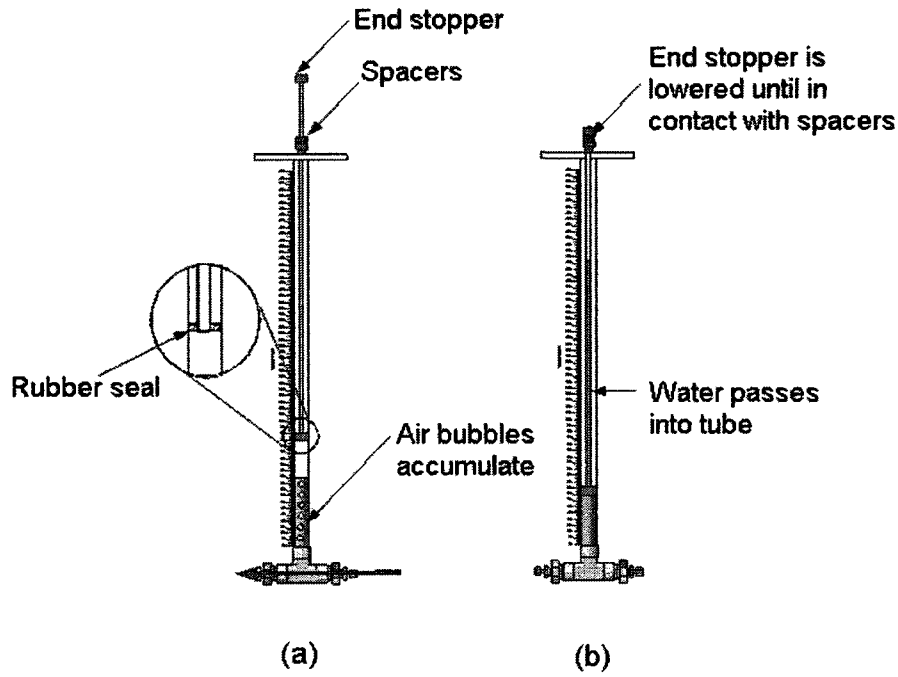

Figure 2.31. Illustration of the two tube system. (from Infante Sedano, 2006)

Air can be removed using a 1 mL syringe at the top of the air trap when setting the water in the system to its reference level (details on procedures can be found in the 2006 thesis by Infante Sedano). Water displaced from the sample during testing will move into the air trap apparatus and is expelled through the overflow tube. The volume of the water is measured by a high accuracy scale (Figure 2.32). The scale permits measurements of ±0.001g and can be automated to record changes during testing. The sensitivity of the scale and the movement of water resulted in constant fluctuation of the scale readings. This problem was overcome by fixing the tube securely to the measurement jar and by attaching a damper mass to the overflow tube at the lowest point prior to entering the measurement jar. This simple solution resulted in stabilizing the balance to the movement of air and water in the system and allowed the accurate measurement of overflow water from the system.

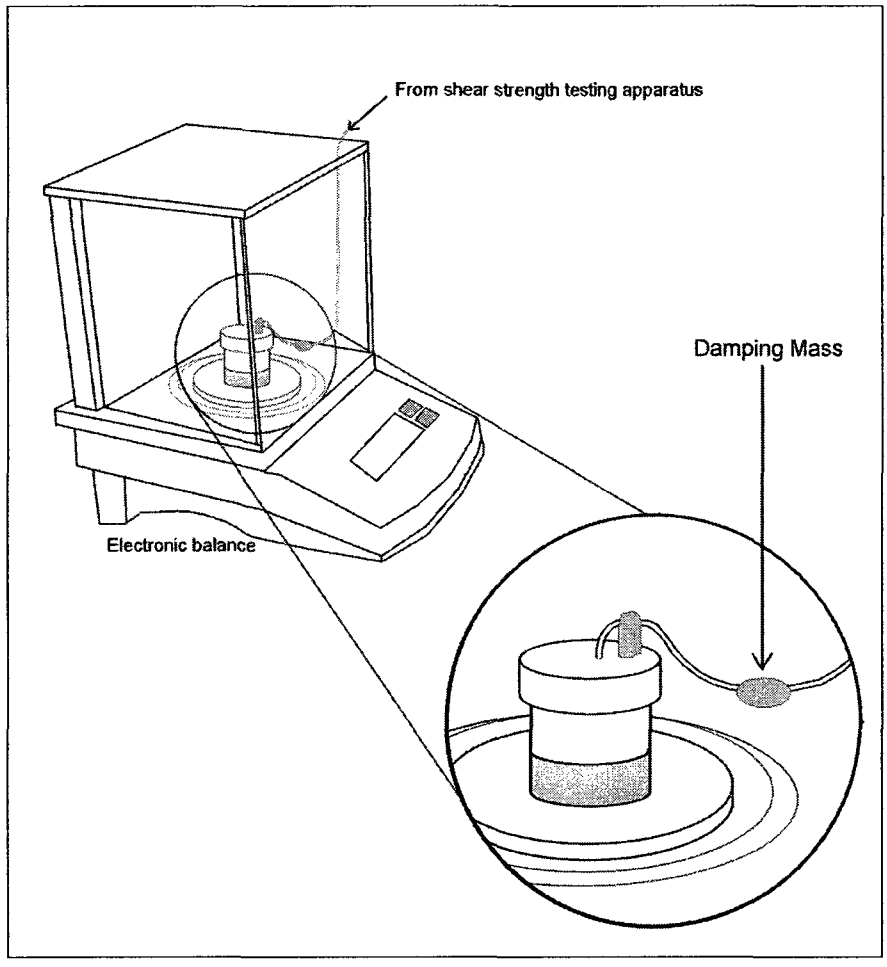

Figure 2.32. Design of a pressure reading gauge. (from Infante Sedano, 2006)

2.7.8 Considerations During Shear Strength Testing

The description of shear strength testing does not always fully convey the complexity of the test and the details that must be considered to ensure that the test produces an accurate result. Such details include volume change of water during flushing, measurement of diffused air, corrections for condensation and evaporation in the test system.

Several authors have discussed the problem of diffused air in the system. Diffused air accumulates with time and can emerge from the water with the change in pressure over the time taken to perform the test. Diffused air or any air in the system can interfere with the performance of the ceramic disc used in axis translation. The presence of water reduces or prevents water from moving across the disc, preventing the free drainage of

water from the sample. Diffused air can also influence the measured water content of the sample. A diffused air volume indicator, or DAVI, was developed (Fredlund, 1975) to measure the volume of air that accumulates in the system. The DAVI was isolated from the volume change measurement system.

In 2006, Infante Sedano developed a new method for measuring the water mass change that integrates the measurement of diffused air. Water expelled from the sample is collected in an overflow jar that is sitting on an automated, extremely sensitive scale. Flushing in the system occurs regularly and the circulating water passes by a wider chamber or air trap that allows air bubbles to rise so that the air can be removed. A syringe is used to measure and empty the air from the trap. When air is removed from the system, water is taken into the system and the volume of water in the overflow jar appears to decrease (Figure 2.33). These readings can be corrected to reflect the cumulative mass of water and the change in volume during the process of emptying the air trap can be used to measure the volume of diffused air. This calculation is only accurate when the laboratory Temperature is maintained at a constant value.

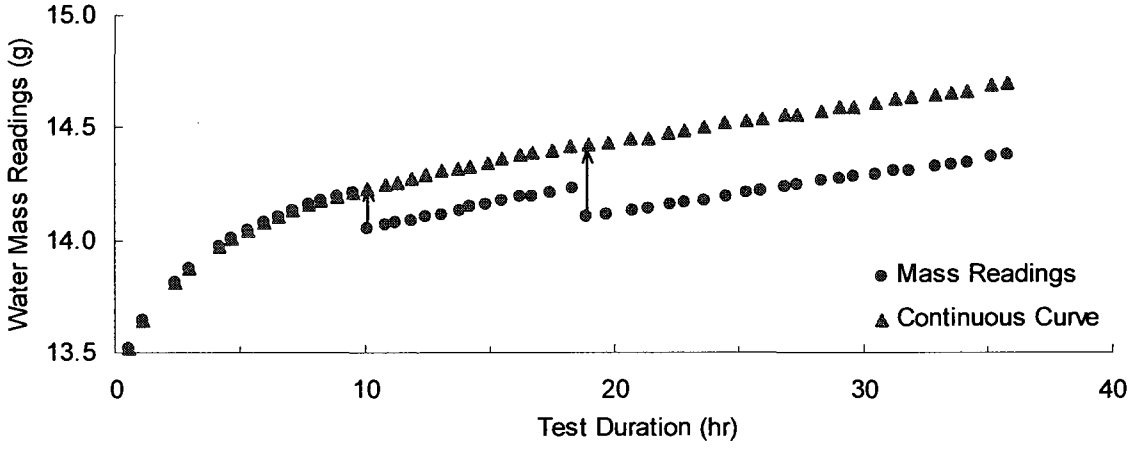

Figure 2.33. Water mass readings corrected for de-airing. (from Infante Sedano, 2006)

Measuring diffused air is interesting, but also essential. The infiltrating air is subtracted from the continuous reading curve and results in an alteration of the water mass curve. When the curve is corrected for air diffusion, the rate of change in the volume of water drained from the soil slows to a decreased rate and may even become constant.

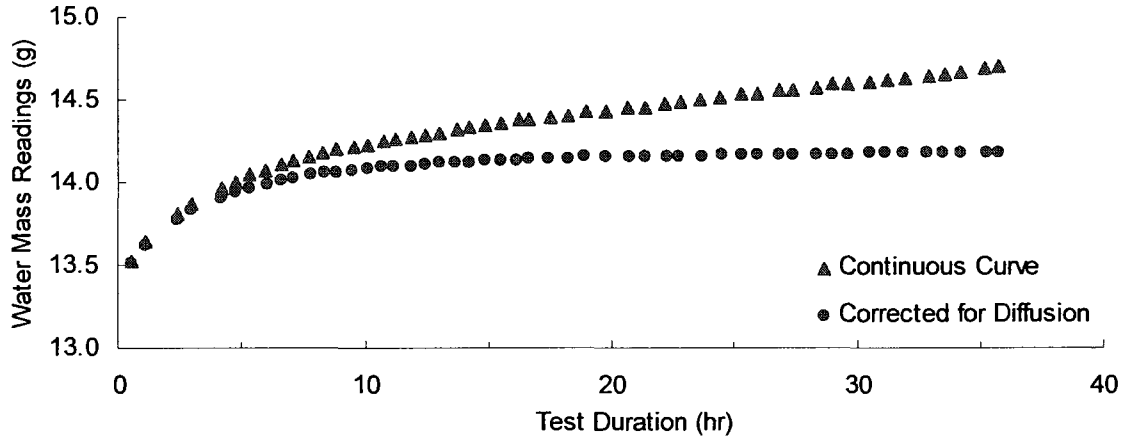

Figure 2.34. Water mass readings showing correction for air diffusion. (from Infante Sedano, 2006)

After the water mass reading is corrected for air diffusion, it may or may not have reached a constant mass. Infante Sedano (2006) discussed the reasons for this which includes evaporation and/or condensation in the system. A downward slope in the water mass plot indicates that water appears to be removed from the system (evaporation) while an upward slope indicates that excess water appears to be in the system (condensation). (Figure 2.35) Once the corrections have been applied for these factors a constant mass of water can be attained with time.

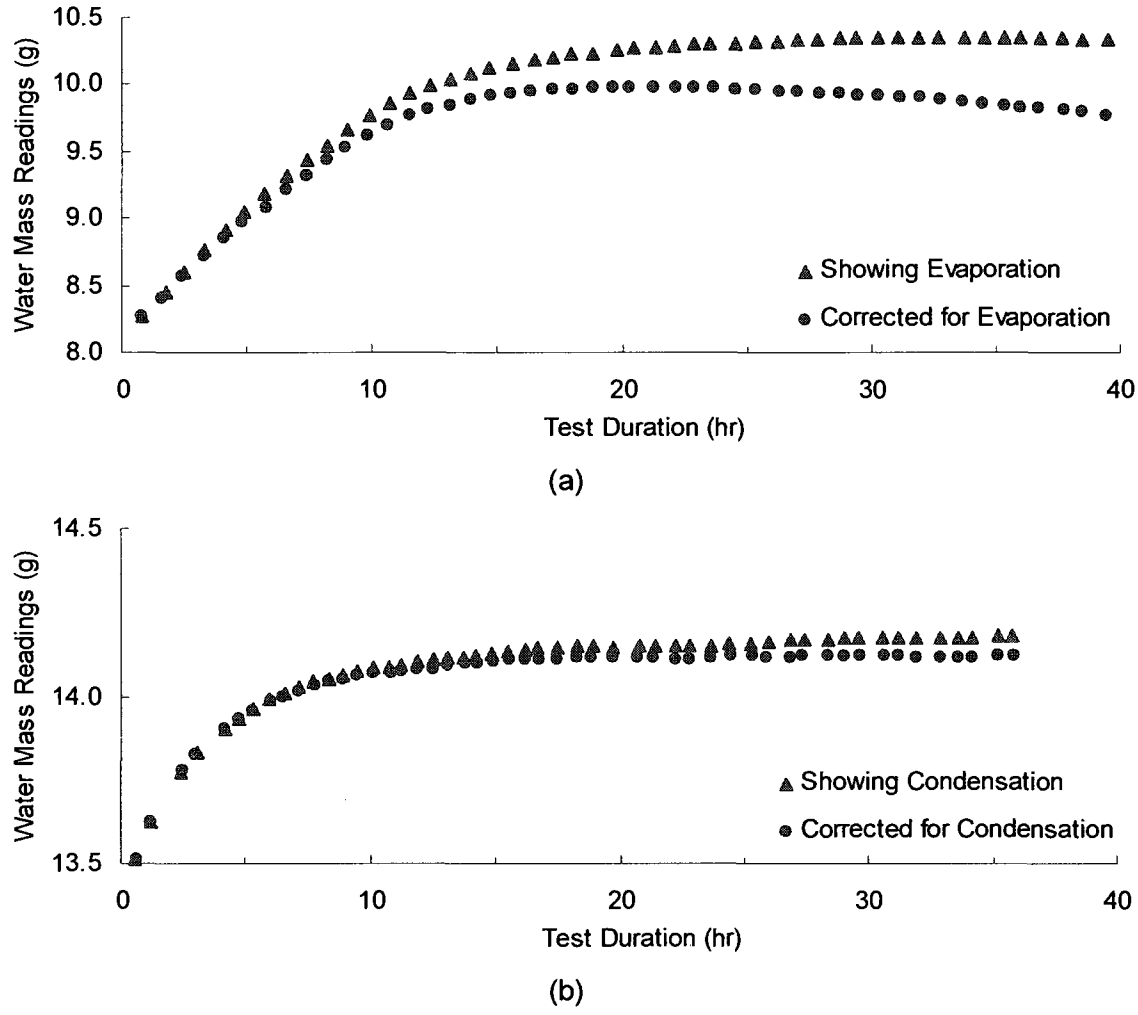

Figure 2.35. Water mass readings showing corrections for (a) evaporation; (b) condensation. (from Infante Sedano, 2006)

2.8 Factors Influencing the Shear Strength of Soils

Comparing shear strength results from fifty-two soils is useful for testing the proposed predictive equations. However, differences in results can be explained by difference in factors that affect shear strength. Shear strength is affected by the method of compaction, soil fabric, density and type of soil.

2.8.1 Soils Tested at Different Net Normal Stresses

Many soils presented in this thesis have been tested at two or more net confining pressures. This provides an opportunity to investigate the influence of net normal stress on the unsaturated shear strength of soil. As discussed in section 6.3 of this chapter, the AV colluvium (Figure 2.36) was influenced more by net normal stresses than the suction applied to the sample. The soil was tested using a modified triaxial test and the increase in net normal stress with the simultaneous increase in suction, allowed the influences of the two factors to be seen.

Soils tested using a modified direct shear test, however, have a constant net normal pressure and the change in shear strength can be attributed to other factors. Unsaturated shear test results are shown for two soils below. Soil 1, red silty clay is lean clay while Soil 3, Madrid clay sand is a clayey sand. The two soils were tested by the same authors in the same apparatus (Escario and Saez, 1986; Escario and Juca, 1989). Both soils were statically compacted and tested at the same net normal stresses. Red silty clay is influenced by net normal stress (Figure 2.36) while the Madrid clay sand shows little effect to the change in net normal stress (Figure 2.37)

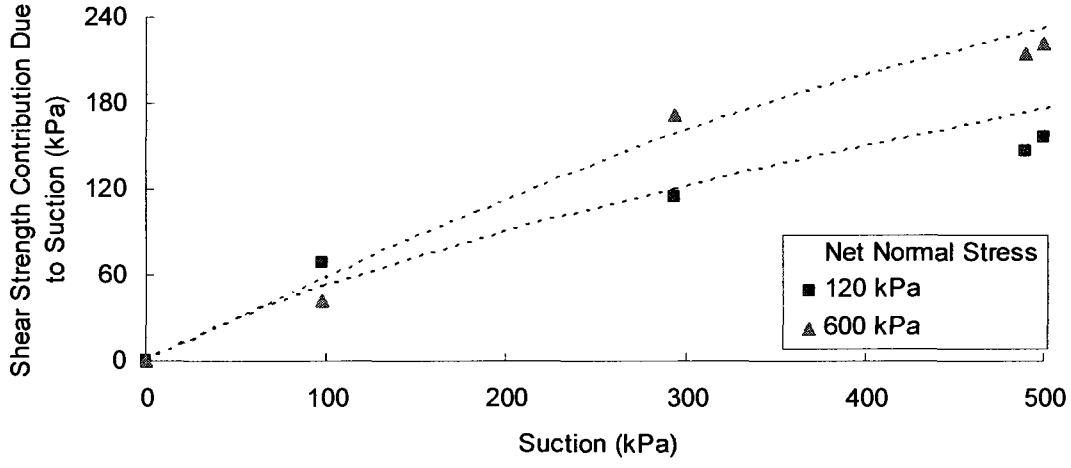

Figure 2.36. Results of red silty clay (Escario and Saez, 1986; Escario and Juca, 1989) tested at different confining pressures.

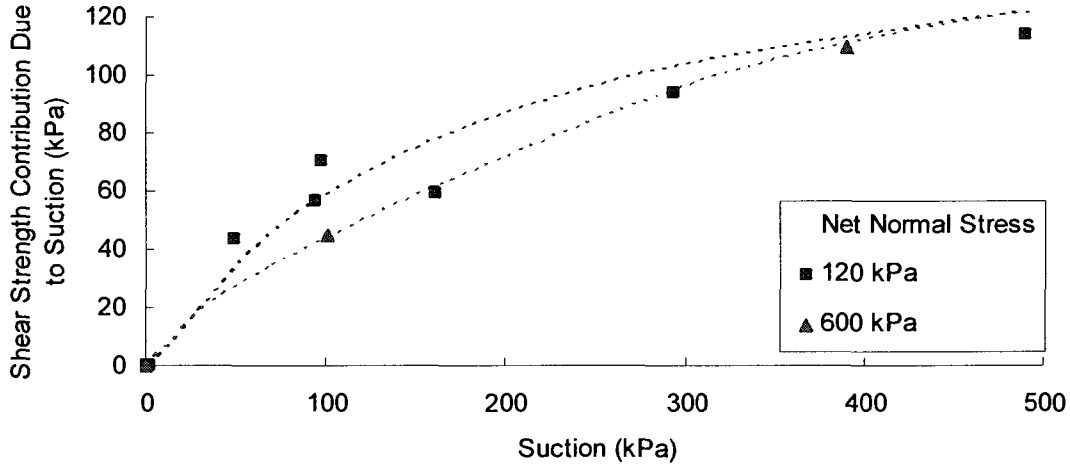

Figure 2.37. Results of Madrid clay sand (Escario and Saez, 1986; Escario and Juca, 1989) tested at different confining pressures.

2.8.2 Differences in Shear Strength Behaviour Due to Differences in Density

Testing done by Satija (1978) illustrates changes in unsaturated shear strength with density. The author used Dhanauri clay (Soil 6) tested in a modified triaxial test. (Figure 2.38) The results have been separated out into lower density and higher density samples tested at the same confining pressures. The high density material has a tighter soil structure, lower quantity of voids and greater contact area between the soil particles. The higher density material results in a greater shear strength.

At low suction, there is little difference between the shear strength values at different confining pressures. At higher values, there are larger differences in shear strength values measured at different confining pressures (Figure 2.38). Scatter in the shear strength points for each condition precludes any other conclusions about the effects of density.

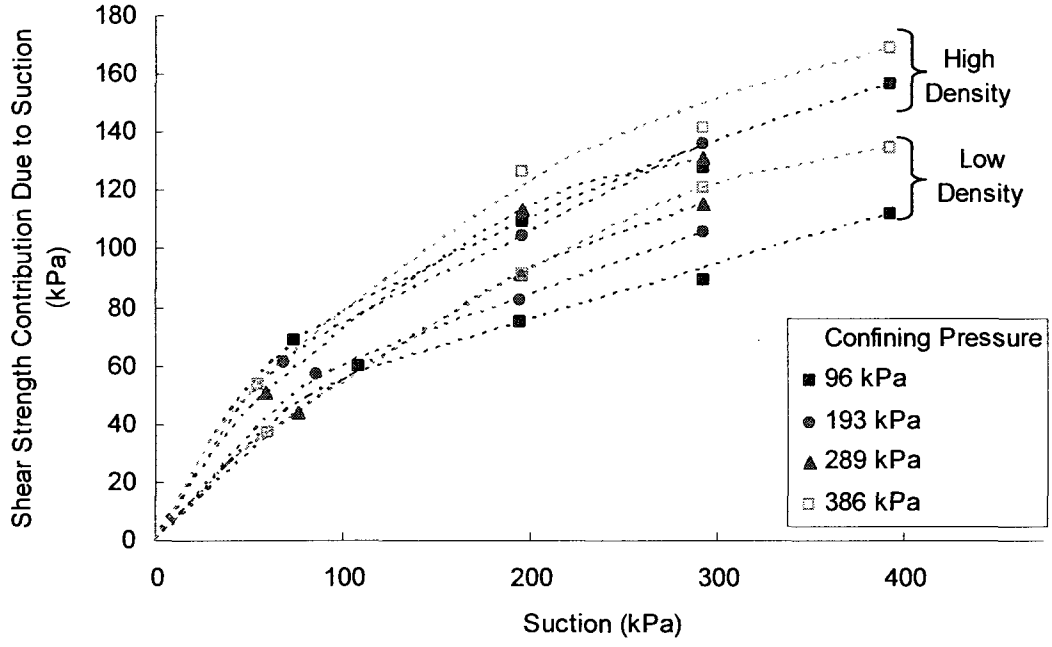

Figure 2.38. Comparison in shear strength due to differences in density of Dhanauri clay. (Gulhati and Satija, 1981)

2.8.3 Influence of Stress History

Stress history is the influence of the pressure that has been exerted on it in the past. Stress history is extremely important as it influences the settlement or consolidation of the soil. The potential of a soil to change volume or undergo settlement is estimated using a consolidation (void ratio versus pressure) curve. The preconsolidation pressure is the maximum pressure that the soil has had to bear in the past. If the soil is loaded with a pressure greater than the preconsolidation pressure, the rate of volume change or settlement is much greater.

Soils that are tested over a wide range of net normal pressures may be influenced by the stress history when the net normal pressure is in excess of the preconsolidation pressure of the soil. One soil illustrates the influence of net normal pressures (Feuerharmel et al, 2006).

AV colluvium (Feuerharmel et al, 2006) was portrayed in Figure 2.39. An undisturbed specimen was extracted from a depth of 5 m which implies an overburden pressure (p'_o)

of approximately 90 kPa. The preconsolidation pressure will likely be slightly higher than the overburden pressure unless an earth force such as a glacier or iceberg has influenced the soil. The sample has a low strength when the confining pressures are below the primary overburden pressure. When the net normal pressure is greater than the overburden pressure, the value the sample will shear at strengths that increase with the increasing confining pressure.

Influence of stress history may not be apparent when analyzing unsaturated shear strength data as there may be other factors present that make it difficult to distinguish the influence of stress history.

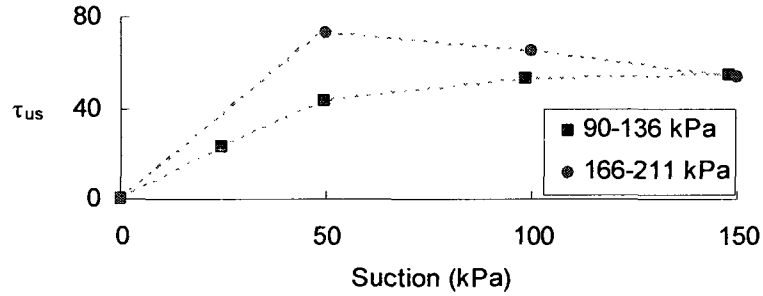

Figure 2.39. Influence of stress history from of AV colluvium. (Feuerharmel et al, 2006)

2.8.4 Influence of Soil Fabric

The soil fabric is the orientation of particles within a fine-grained soil (Fredlund and Rahardjo, 1993; Vanapalli et al, 1996). The fabric is created as the soil is compacted. A soil compacted at a water content less than the optimum water content results in a flocculated structure. A soil compacted at optimum water content results in a very organized, tight structure. Optimum water content is used to compact soil to its maximum density. Soil compacted at greater than optimum water content have a dispersed structure.

Unsaturated shear tests were performed on Indian Head till. (Vanapalli et al, 1996) The soil was compacted at dry of optimum water content, optimum water content and greater than optimum water content. Shear strength testing was performed using a modified direct shear apparatus. The soil was also tested at different confining pressures. The

tests are plotted together and a trend line applied for each preparation condition (Figure 2.40).

The till compacted at dry of optimum with the flocculated structure has fewer contact points between soil particles and results in the lowest general shear strength. The very dispersed, soil fabric of glacial till compacted wet of optimum has the greatest area of contact between particles and subsequently, the greatest general shear strength.

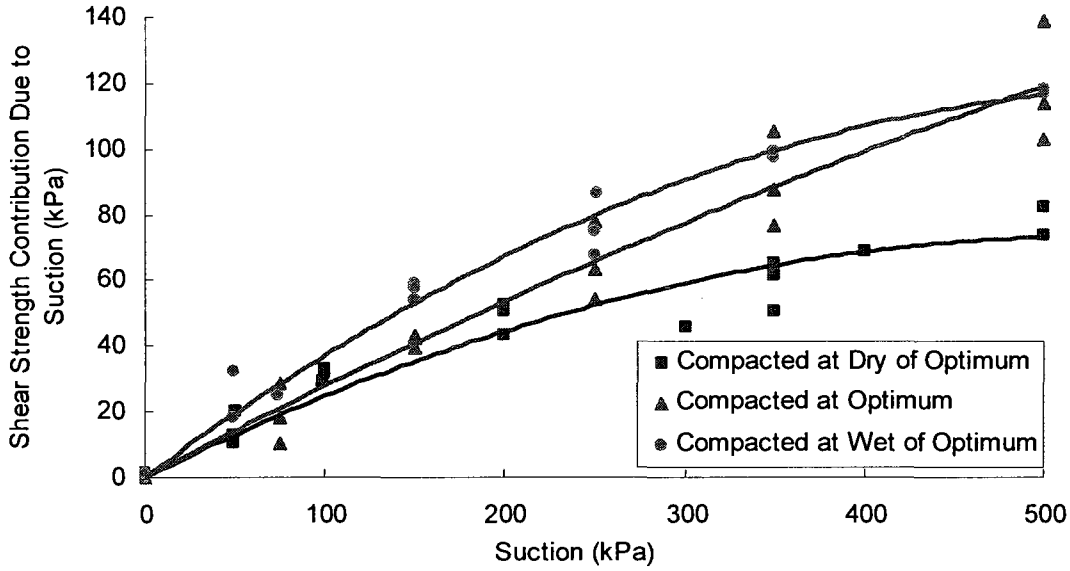

Figure 2.40. Shear strength curves of glacial till compacted at different water contents: dry of optimum, optimum and wet of optimum. (modified from Vanapalli et al, 1996)

2.9 Summary

Empirical equations for predicting the shear strength of unsaturated soils requires an understanding of several concepts: suction, measuring suction and SWCC, shear strength testing and how to analyze it and the accessories needed to measure volume change and diffused air. Testing is expensive, time consuming and requires specialized equipment and personnel. Empirical equations that could predict shear strength of unsaturated soils would be beneficial.

CHAPTER 3 EQUATIONS TO DESCRIBE THE SHEAR STRENGTH BEHAVIOUR OF UNSATURATED SOILS

3.1 Introduction

Significant research work has been undertaken during the last fifty years for both interpreting and predicting the shear strength behaviour of unsaturated soils (Bishop, 1959; Fredlund et al, 1978; Escario and Juca, 1978; Satija, 1978, Gan et al, 1988; Vanapalli et al, 1996; Bao et al, 1998; Rassam and Williams, 1999; Rassam and Cook, 1992; Tekinsoy et al, 2004; Xu, 2004; Lee et al, 2005). However, during the last fifteen years several investigators have proposed simple techniques for estimating or predicting shear strength of unsaturated soils as experimental procedures are difficult, time consuming and also need elaborate testing equipment (Lytton, 1995; Vanapalli et al, 1996, Öberg and Sallfors, 1997; Khalili and Khabbaz, 1998; Xu and Sun, 2001; Xu, 2004; Tekinsoy et al, 2006). There are twenty-five equations presently available in the literature to predict or estimate the shear strength of unsaturated soils. These equations have been developed based on different philosophies and can be subdivided into three major categories:

i. Semi-empirical equations that use SWCC as a tool

Some investigators have proposed empirical or semi-empirical equations based on the suction affecting the cross-sectional area of water present along with interparticle contact points of a soil in unsaturated condition providing approximate estimates from the water content information derived from the soil-water characteristic curve (SWCC) (Vanapalli et al, 1996; Fredlund et al. 1996; Öberg and Sallfors, 1997)

The equation proposed by Vanapalli et al. (1996) and Fredlund et al. (1996) are consistent with the continuum mechanics principles. The form of the proposed equation is in the same form as Fredlund et al. (1978) equation for interpreting the shear strength behaviour of unsaturated soil in terms of two stress state variables; namely, net normal stress, $(\sigma-u_a)$ and matric suction, (u_a-u_w). The equation proposed by Öberg and Sallfors (1997) is consistent with the equation proposed by Bishop (1959).

Other investigators also developed equations using the water content as a tool; however, the theory was based on reversible thermodynamics (Lytton, 1995, Aubeny and

Lytton, 2003). The information of water content in all the above equations is derived from the SWCC. In other words, all these equations use SWCC as a tool in the prediction of the shear strength of unsaturated soils.

Some investigators have proposed a set of equations to explain the behaviour of the relationship up to the AEV and another equation to explain the relationship between the shear strength and suction beyond the AEV (Rassam and Williams, 1999; Rassam and Cook, 2002; Tekinsoy et al, 2006).

ii. Equations based on Mathematical Fitting Methods

These equations encompass the largest number of equations. Many authors have proposed equations to fit the measured shear strength data based on several mathematical equations: logarithmic equation (Lu, 1992), exponential equations (Escario and Juca, 1989), hyperbolic relationships (Rohm and Vilar, 1995; Shen, 1996; Yu et al, 1998; Miao et al, 2002; Schick, 2004), and elliptical relationship (Abramento and Carvalho, 1989). These mathematical equations use one or more fitting parameters to provide a reasonable fit to the measured experimental data. In many cases, the physical meaning of the fitting parameters has not been provided. Due to this reason, the approach presented in these methods can be considered as purely empirical.

iii. Other Equations

Normalization Methods

Several investigators have developed equations or functions that use normalization techniques to one of key properties that influence the shear strength behaviour. The most common method is to normalize the volumetric water content by dividing it by the saturated volumetric water content of the soil (Vanapalli et al, 1996; Tekinsoy et al, 2006) which is equivalent to the degree of saturation in the soil. Some authors normalize measured data with respect to air-entry value or AEV (Khalili and Khabbaz, 1998). Other investigators normalize the measured water content data by dividing it by the range of water content from saturation to residual suction (Vanapalli et al, 1996). Rather than normalizing the water content, Bao et al, (1998) normalize the suction over the range of suction extending from saturation to residual suction.

Fractal Dimension Methods

The fractal can be defined as a geometric shape that can be split into parts where the parts are a reduced version of the whole, also called self-similarity (Xu and Sun, 2001) Fractal dimension can be calculated by taking the limit of the quotient of the log change in object size and the log change in measurement scale, as the measurement scale approaches zero. Fractal dimensions quantify the static geometry of an object. (www.learnthat.com). Fractal dimension has been used a tool to estimate the surface area of the pores on the surface of a soil. Xu and Sun, 2001 and Xu, 2004 have extended this approach to predict the shear strength of unsaturated soils.

The evolution of all the above prediction equations and interpretation for shear strength are discussed and summarized in this chapter in a chronological order starting with the shear strength behaviour of saturated soil.

3.2 Shear Strength

Shear strength is the maximum shearing resistance offered by a soil on its failure plane. The shear strength of a saturated soil is interpreted in conventional engineering practice extending Terzaghi's effective stress concept to the Mohr-Coulomb failure criterion using the equation below.

$$\tau = c' + (\sigma - u_w) \cdot \tan\phi' \qquad [2\text{-}1]$$

However, there are two equations available in the literature to interpret shear strength behaviour of unsaturated soils (Bishop, 1959; Fredlund et al, 1978). While both the equations use the stress state variables, $(\sigma - u_a)$ and $(u_a - u_w)$; the philosophy associated with each of the equations is different.

Bishop (1959) proposed an equation extending the principle of effective stress of saturated soils to unsaturated soils. He incorporated the variable, χ, which is related to the degree of saturation (Eqn. 2-13). The term χ varies between 0 for a dry soil and 1 for a saturated soil. This equation was found to have limitations for use beneath the critical degree of saturation (Jennings and Burland, 1962). Bishop and Blight in a later study (1963) noted that a change in matric suction didn't cause the same change in effective stress as a change in the net normal stress.

$$\tau = c' + [(\sigma - u_a) + \chi(u_a - u_w)] \cdot \tan\phi' \qquad [2\text{-}13]$$

Later, authors discussed the shear strength relationship in terms of independent stress state variables (Fredlund and Morgenstern, 1977). Fredlund, Morgenstern and Widger (1978) proposed Equation. 1-1 to describe the shear strength relationship with respect to suction.

$$\tau = c' + (\sigma - u_a)\tan\phi' + (u_a - u_w)\tan\phi^b \qquad [1\text{-}1]$$

For simplification purposes, the shear strength equation unsaturated soil can be visualized as having two components; namely, saturated shear strength, τ and the shear strength contribution due to suction, τ_{us} as given below:

$$\tau = c' + (\sigma - u_a) \cdot \tan\phi' + \tau_{us} \qquad [2\text{-}14]$$

where τ_{us} is the shear strength contribution due to suction.

3.3 Relationship between the Soil-Water Characteristic Curve and the Shear Strength of Unsaturated Soils

Donald (1956) was one of the earliest investigators who from experimental studies have shown the change in shear strength with respect to pressure deficiency or suction was a non-linear relationship. Some studies prior to Donald (1956) work and later works however visualized the shear strength contribution due to suction to be a linear relationship based on limited number of experimental studies that were undertaken (Fredlund et al, 1978).

Gan and Fredlund (1988) and Escario and Juca (1989) experimental studies show that the strength of unsaturated soils is non-linear. The modified direct shear test equipment was used in both these investigations. The typical results of these studies will be as shown in Figure 3.1. As discussed earlier, the shear strength can be visualized as the two components, which is, the saturated shear strength, τ, and the shear strength contribution due to suction, τ_{us}.

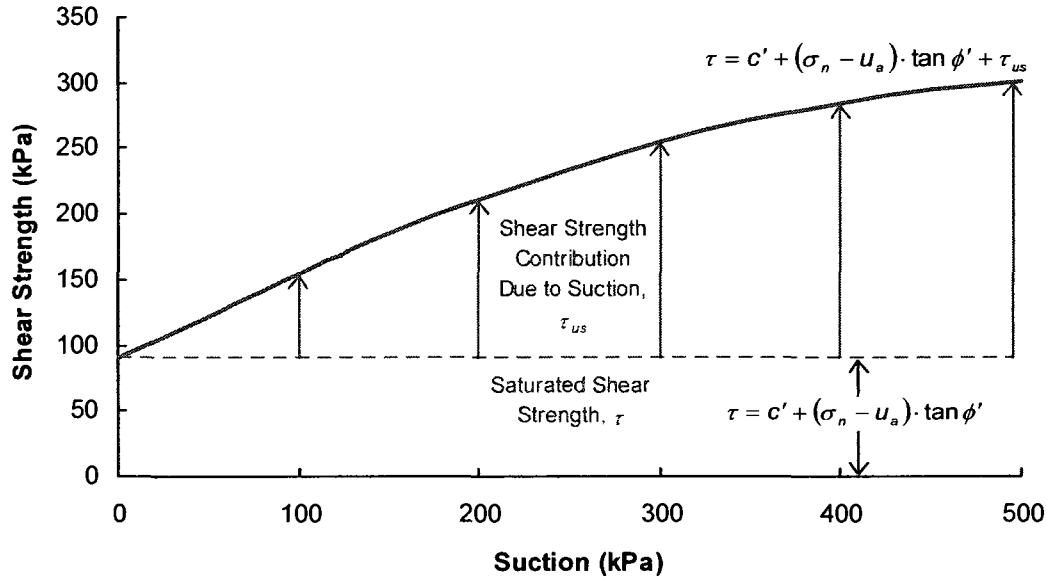

Figure 3.1. Illustration of the influence of shear strength on suction.

Figure 3.2 shows the relationship between the measured SWCC and shear strength of an unsaturated soil (modified from Garven and Vanapalli, 2006). There is initially little or no change in the water content of the SWCC in spite of increase suction up to the air-entry value of the soil (Figure 3.2). During this phase, the soil is essentially saturated, although the suction within the sample is greater than zero. During this phase, the increase in shear strength is approximately equal to effective angle of internal friction of the soil, ϕ' (Vanapalli et al, 1996 and Fredlund et al, 1996). In other words, the shear strength contribution due to suction, ϕ^b is equal to ϕ'.

Beyond the AEV, a change in suction will cause a significant change in the water content and the relationship between the shear strength and suction becomes non-linear (Vanapalli et al, 1996). The shear strength contribution due to suction ϕ^b starts reducing (Fredlund et al, 1996, Vanapalli et al, 1996).

After reaching a certain value of suction, there is very little change in the water content due an increase in suction. The suction at this point is referred as the residual suction. (Vanapalli et al, 1996; Sillers, 1997) Beyond the residual suction, the relationship between shear strength and suction is not well defined. The shear strength may increase,

decrease, or remain the same depending on the type of saturation (Vanapalli et al, 1996).

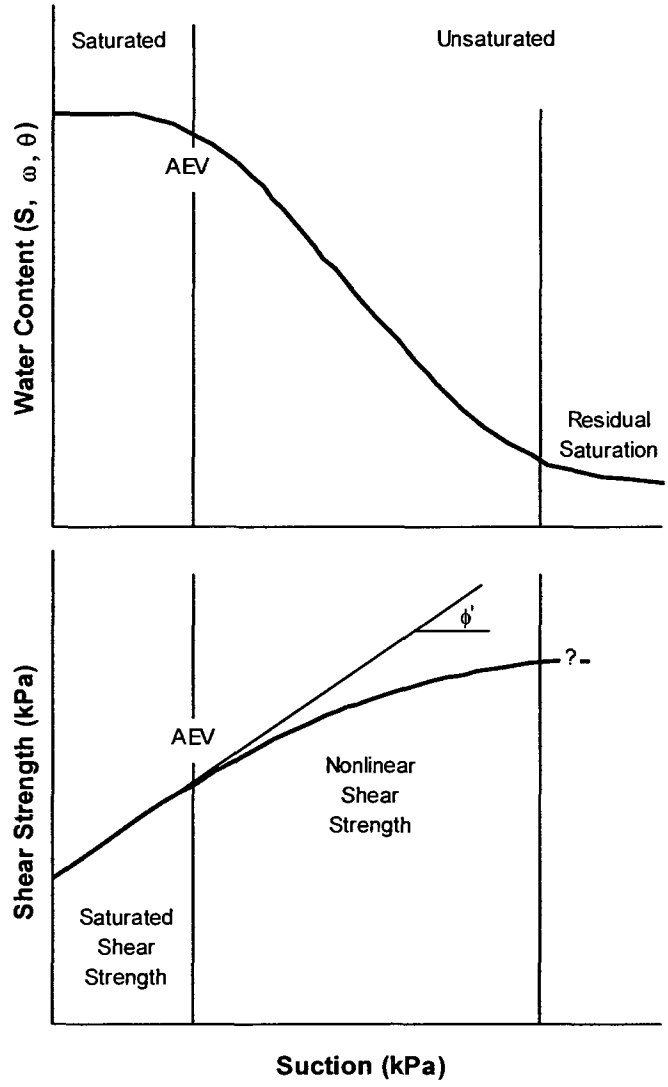

Figure 3.2. Changes in shear strength varying with changes in suction. (modified from Garven and Vanapalli, 2006)

3.4 Shear Strength Equations

Bishop's equation (1959) (i.e., Eqn. 2-13) and Fredlund et al (1978) (i.e., Eqn. 1-1) are commonly used in the interpretation of the shear strength of unsaturated soils. More details of these equations are already presented in section 3.3.1 and 3.3.2. These equations provide the foundation for many of the other equations presented by other investigators in the literature.

3.4.1 Escario and Juca (1989)

Escario and Juca presented the shear strength behaviour of three unsaturated soils: Madrid grey clay, Madrid clay sand and red silty clay. In addition to presenting the modified direct shear test results they have also provided the SWCC for all the three soils. The shear strength of all the three soils was tested over such a large range of suction. The red silty clay and the Madrid grey clay were tested over a range of suction from 0 kPa to 14,500 kPa. The Madrid clay sand was tested over a range from 0 kPa to 4000 kPa. The red silty clay is lean clay with a liquid limit of 33 and a plasticity index of 13. The Madrid grey clay is heavy silt with a liquid limit of 71 and a plasticity index of 35. The Madrid clay sand is lean clayey sand with a liquid limit of 32 and a plasticity index of 15. All the experimental results show the non-linear relationship between shear strength and suction.

These authors have found that the data for all the three followed a 2.5° elliptical pattern (Eqns. 3-1, 3-2).

$$\tan\phi' \cdot \left(\frac{\tau_o + \tau_b}{(u_a - u_w)_m}\right)^{1.5} \left((u_a - u_w)_m - (u_a - u_w)\right)^{2.5} + (\tau + \tau_b)^{2.5} = (\tau_m + \tau_b)^{2.5} \quad [3\text{-}1]$$

$$(\tau_m + \tau_b)^{2.5} - (\tau_o + \tau_b)^{2.5} = (\tau_o + \tau_b)^{1.5} \cdot (u_a - u_w)_m \cdot \tan\phi' \quad [3\text{-}2]$$

where

$(u_a - u_w)_m$ is the suction at maximum shear strength

τ_o is shear strength when suction = 0 kPa

τ_m is the maximum shear strength

is the difference between maximum shear, τ_m, and the total height of the ellipse, b, that has been fit to experimental points.

The pattern of shear strength envelope generated from the following equation and the terms are defined and presented in Figure 3.3.

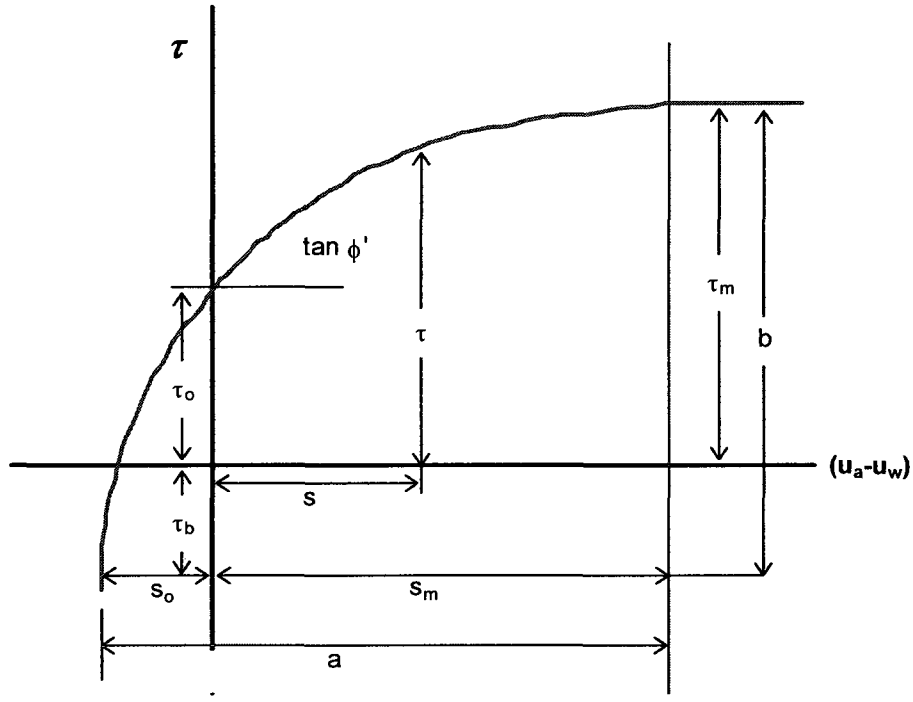

Figure 3.3. Graphical representation of symbols derived for ellipses of degree 2.5. (modified from Escario and Juca, 1989)

3.4.2 Abramento & Carvalho (1989)

Abramento and Carvalho (1989) have undertaken studies on sandy residual soil slope that experienced a landslide in Brazil. The pore-water pressure and soil suction of the soil slope were measured in situ using piezometers and tensiometers. Several laboratory tests that include grain size analysis, Atterberg limits and modified direct shear tests were measured in the laboratory. The Serra do Mar soil is a lean clayey sand borderline lean silty sand. The effective angle of internal friction, ϕ' of the soil was measured using CU tests in a triaxial shear testing apparatus. The angle of internal friction, ϕ' was measured to be 38 and 40 degrees with cohesion intercept value equal to 0 kPa. The values of 38 and 40 degrees were used to test the equation.

The authors note that the relationship between the shear strength contribution due to suction and the suction was non-linear. The paper proposes an exponential relationship (Eqn. 3-3) for fitting the non-linear shear strength data using two fitting parameters. The value of the fitting parameters was determined based on the experimental results. How-

ever, the fitting parameters were not correlated to soil parameters. For the Serra do Mar soil, the fitting parameter, β, was estimated to be 0.5. This value may be soil specific and can be defined as a relationship shown in Eqn. 3-4.

$$\tau_{us} = \alpha \cdot (u_a - u_w)^{\beta} \quad [3\text{-}3]$$

where

β is a fitting parameter

α is fitting parameter that can be generally defined as Eqn. 3-4

$$\alpha = \frac{tan\phi^b}{(u_a - u_w)^{1-\beta}} \quad [3\text{-}4]$$

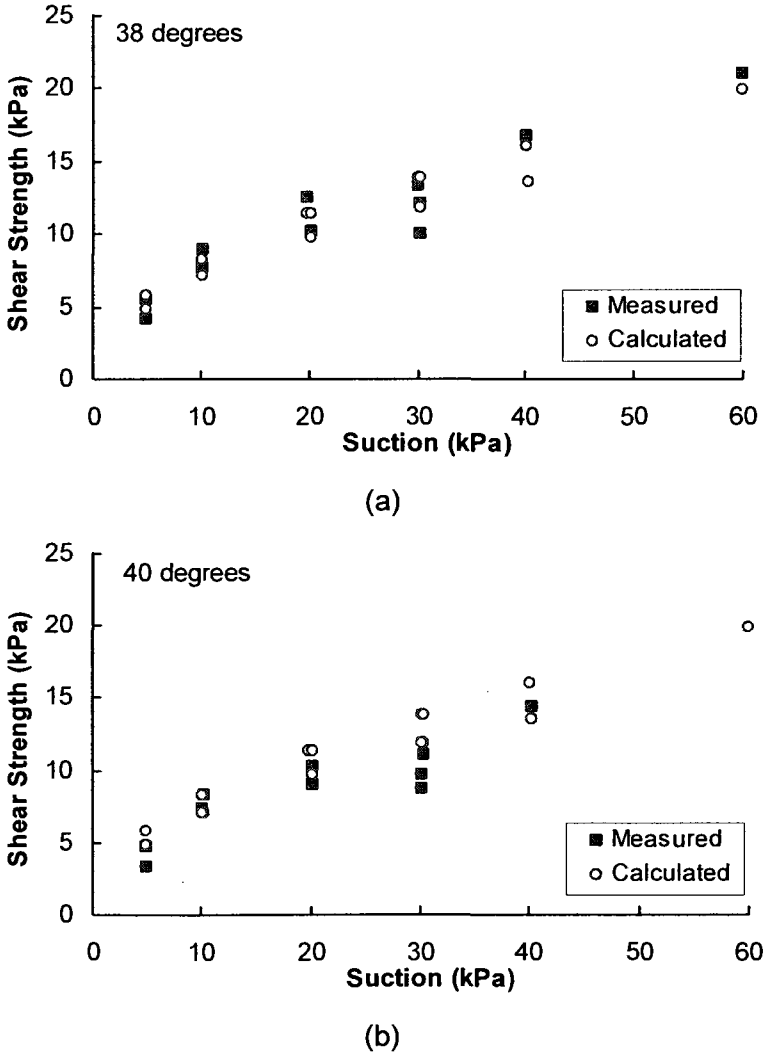

Figure 3.4. Experimental values and calculated values using (a) 38 degrees and (b) 40 degrees.

The equation was applied to the measured data using both measured angles of internal friction (38° and 40°). The results are shown in Figure 3.4. The equation matches the shape of the measured shear strength experimental data reasonably well.

3.4.3 Lu, Zhang, Chen and Feng (1992)

Lu et al (1992) investigations focused on the relationship between the following:

1. The angle of internal friction and plasticity index
2. Suction strength and swelling pressure.
3. Suction strength and swelling force.

The author proposed a relationship between the I_p and angle of internal friction ϕ as follows:

$$\phi = 37.4 - 0.49 \cdot I_p \qquad If\ 7 \le I_p \le 55 \qquad [3\text{-}5]$$

$$\phi = 12.4 - 0.427 \cdot I_p \qquad If\ I_p > 55 \qquad [3\text{-}6]$$

Lu et al (1992) proposed an equation (Eqn. 3-7) for estimating the shear strength of expansive soils using the information of swelling pressure. The equation was tested using four different soils which are designated as Lu A, Lu B, Lu C, and Lu D in this thesis. The four soils are: illite, montmorillonite, kaolin and 'powdered soil', respectively, and their properties are summarized in Table 3.1 below.

Table 3.1. Soils tested by Lu et al (1992).

Soil		w_L	I_p	Classification
A	Illite	45	21	Lean silt
B	Montmorillonite	82	31	Heavy silt
C	Kaolin	72	34	Heavy silt
D	Powdered soil	31	18	Lean clay

This investigators proposed that the unsaturated shear strength of an expansive soil is directly related to the swelling pressure, P_s, of the soil. (Eqn. 3-7). Lu et al (1992) further relates the proposed equation to Bishop's equation (Eqn. 2-13).

$$\tau_{us} = P_s \cdot \tan\phi' \quad [3\text{-}7]$$

$$P_s = (u_a - u_w) \cdot \chi \quad [3\text{-}8]$$

$$c_1 - c_2 = P_s \cdot \tan\phi' \quad [3\text{-}9]$$

where

P_s is the swelling pressure of the soil

c_1 is the cohesion of the saturated soil

c_2 is the cohesion of the soil at a lower water content

The results are presented in Table 3.2 (copied from Lu et al, 1992, Table 2) and are illustrated in Figure 3.5 below. The table does not contain any information about the suction of the soil. Figure 3.5 presents the data in terms of the shear strength with respect to the water content.

Table 3.2. Summary of Results (Table 2 from Lu et al, 1992).

Soil	Water Content (%)	Soil Density (g/cm^3)	c_1 (kPa)	ϕ_1 (°)	c_2 (kPa)	ϕ_2 (°)	P_s (kPa)	c_1-c_2 (kPa)	$P_s \tan\phi_1$ (kPa)
Lu A	16.0	1.62	139	25.4	23	22	242	116	115
	19.5	1.72	134	27.9	17	25.8	245	117	129
	20.5	1.70	112	26.2	25	23.9	235	87	116
	21.5	1.66	89	25.2	26	23.5	167	63	78
	23.0	1.64	68	22.7	31	31.6	105	37	44
	26.0	1.55	40	19.1	25	18.1	39	15	14
	34.0	1.34	74	15.1	40	14.8	78	34	22
Lu B	27.0	1.39	102	16.1	49	13.3	216	53	62
	34.0	1.34	74	15.1	40	14.8	78	34	22
Lu C	25.6	1.53	55	25.5	30	22.5	55	25	26
	30.2	1.46	41	22.3	28	22.3	19	13	8
Lu D	18.3	1.77	73	28.8	33	30.7	53	40	30

The graphical results illustrated in Figure 3-5 indicates that this is a reasonable correlation using this method for expansive soils.

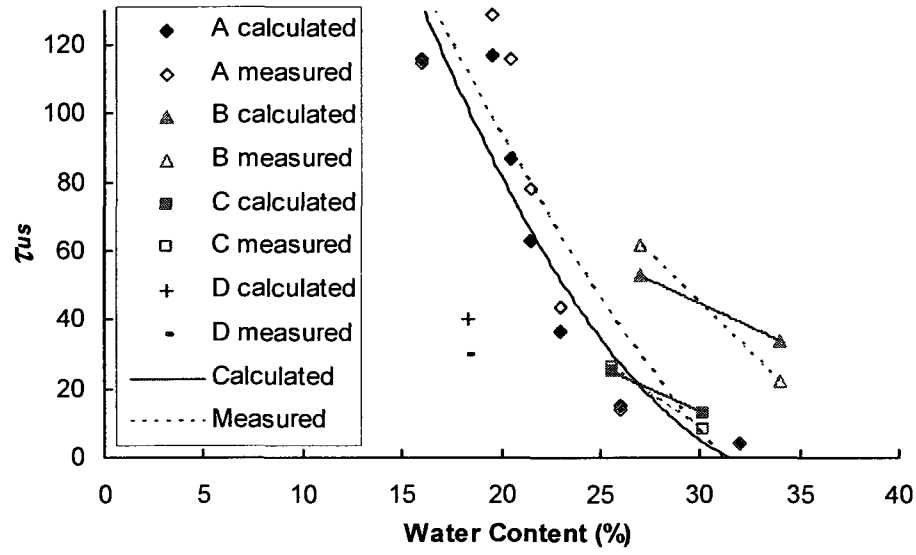

Figure 3.5. Summary of results. (created from Table 2 from Lu et al 1992)

3.4.4 Lytton (1995)

Lytton presented a keynote presentation at the Unsaturated Soils Conference in Brazil where he outlined an equation developed by Lamborn in 1986 (Eqn. 3-10). Lamborn proposed an equation for predicting the shear strength of unsaturated soils which are relatively "moist" and where the air is continuous using reversible thermodynamics. The key assumption in this approach is that the water tension creating stress acts on the soil skeleton.

$$\tau_{us} = (u_a - u_w) \cdot \theta_w \cdot \tan\phi' \qquad [3\text{-}10]$$

where
θ_w is the volumetric water content

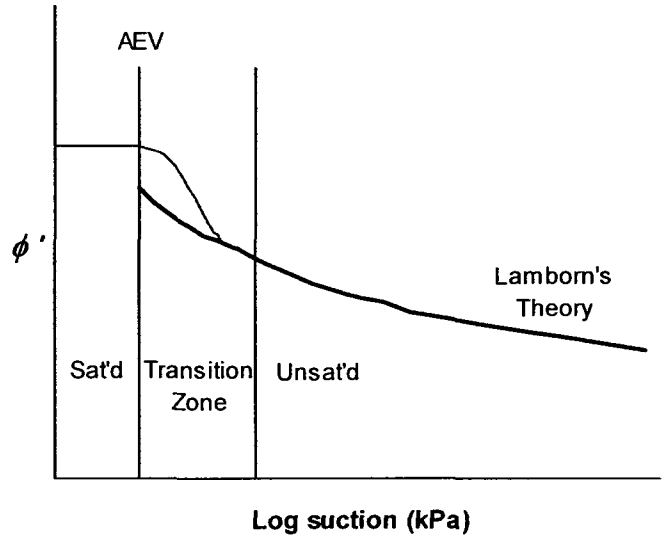

Figure 3.6. Change in friction angle due to the increase in suction. (from Lytton, 1995)

Lytton cites that data from Lam (1980) and Peterson (1992) to validate Lamborn's equation.

Peterson (1992) test Buckshot clay which is lean clay with a liquid limit, w_L of 56 and a plasticity index, I_p of 35. The saturated shear strength parameters were determined by a conventional triaxial shear testing apparatus and the unsaturated shear strength properties were measured using a modified triaxial test.

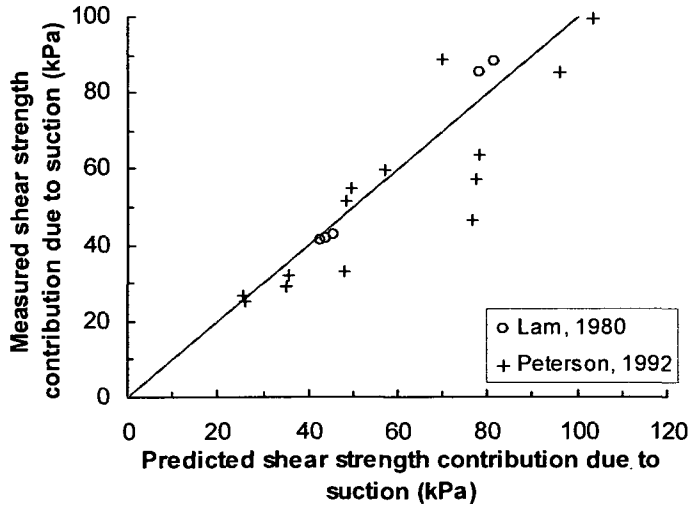

Figure 3.7. Comparison of measured values to predicted values from Lam, 1980. (from Lytton, 1995)

Lam (1980) tested a decomposed rhyolite (from Peterson, 1992). The unsaturated shear strength was measured using unconfined compression test results. He only publishes the plot of the measured values of the shear strength contribution due

to suction versus the predicted values for Lam's data (Figure 3.7). A correlation is seen although some points show a significant deviation.

3.4.5 Öberg and Sallfors (1997)

Öberg and Sallfors (1997) proposed an equation for non-clay soils such as sands or silts. The parameter χ used in Bishops equation is replaced with degree of saturation, S in this equation. Öberg and Sallfors suggest that Bishops χ variable is approximately the same as the degree of saturation for sands and silts. Similar aberrations were reported earlier in the literature.

While Bishop et al (1960) stated that there is no unique relationship between saturation and χ due to differences in the water content during wetting and drying (i.e. hysteresis); Donald (1960) studies show a relationship between χ and the degree of saturation that was almost unique. The variable, χ, was defined as the effective stress divided by the pressure and efficiency or suction. Jennings and Burland (1962) compared the values of χ and degree is saturation was soils presented by Bishop et al (1960) and Bishop and Donald (1961). Donald's theoretical relationship was valid for silty soils down to a degree of saturation between 40 and 60%. Clayey soils created a curved relationship which is different from the one developed by Donald. In their 1962 paper, Jennings and Burland felt that there was a critical degree of saturation where the effective stress was valid at higher degrees of saturation.

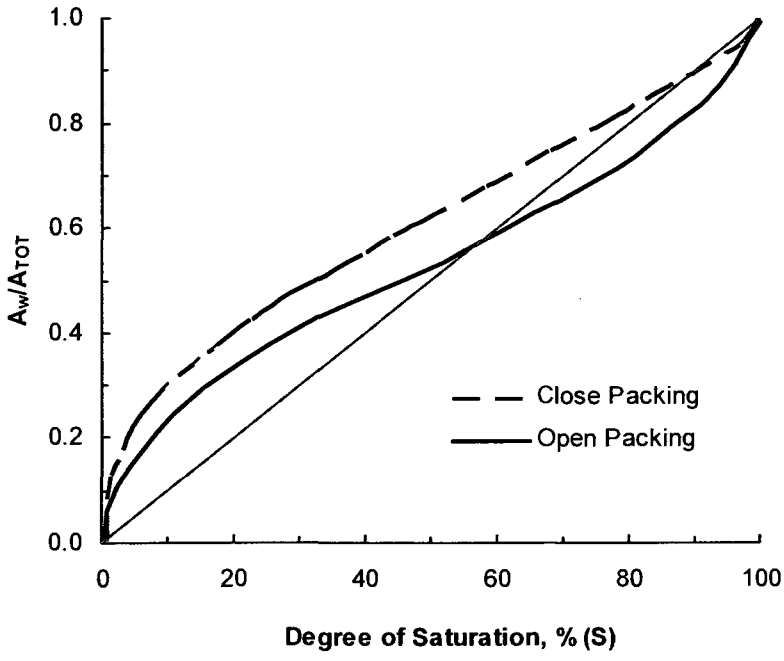

Figure 3.8. Change in friction angle. (modified from Öberg and Sallfors, 1997)

Bishop and Blight (1963) concluded that effective stress principles could be used in unsaturated soils equations by taking account of the influence of the net normal stress and the suction. The authors consider the χ parameter as the fraction of pore area occupied by water also known as saturation. The authors used ideal two and three dimensional soils and examine the relationship between χ and degree of saturation prepared from Sparks (1963).

Öberg (1995) prepared as sample with a soil skeleton comprised of an 'ideal soil' using spheres that could be organized with a deliberate placement. They set up two scenarios: a closed packing arrangement and an open packing arrangement. A series of tests was used to determine the relationship between A_w/A_{tot} versus the degree of saturation. This graph correlated with an earlier experiment conducted by Sparks (1963).

The results (Figure 3.8) show that the relationship between the two variables (A_w/A_{tot} and S) is non-linear. However, larger variation was observed when the degree of saturation was less than 60%. At higher degrees of saturation, the relationship between the two variables is not 1:1. In other words, the values deviate from a 1:1 relationship by less than 10% when the degree of saturation is greater than 60%.

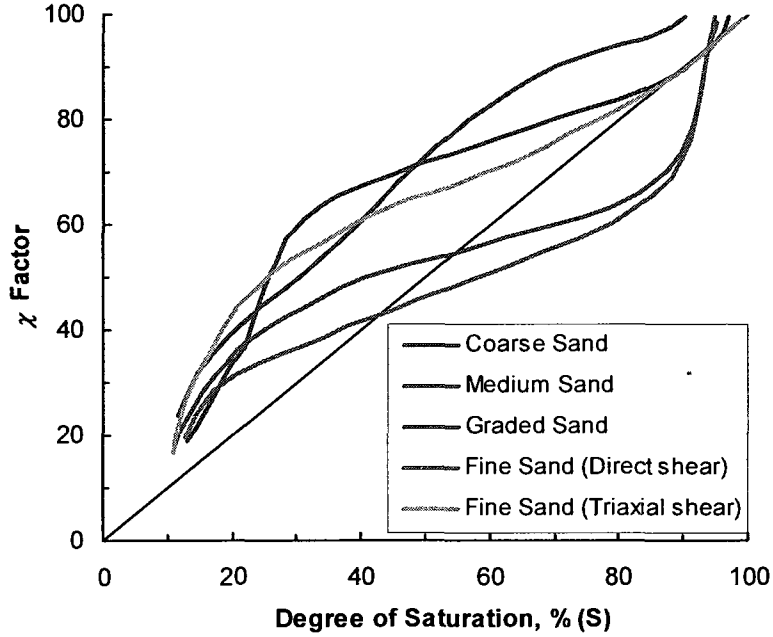

Figure 3.9. Relationship between χ and the degree of saturation. (modified from Donald, 1960)

This pattern of correlation is supported by a work done on four sands by Donald (1961) in Figure 3.9. Donald correlated χ, which is related to the A_w/A_{tot} and found that the variation of χ with degree of saturation has the same correlation as was seen in Figure 3.9.

The authors concluded from their observations that this correlation supports the development of the equation (Eqn. 3-11) at high degrees of saturation and predicted values should correlate within 20% of the measured values.

$$\tau = c' + (\sigma - u_a) \cdot tan\phi' + S \cdot (u_a - u_w) \cdot tan\phi' \qquad [3\text{-}11]$$

Table 3.3. Summary of soils used by Öberg and Sallfors (1995, 1997).

		Soils (Authors)	Sand + Silt (%)	w_L	I_p	Classification
Öberg and Sallfors, 1995	Öberg and Sallfors, 1997	Red silty clay (Escario and Saez, 1986)	>1	33	13	Lean clay
		Madrid grey clay (Escario and Saez, 1986)	>13.5	71	35	Heavy silt
		Notch Hill silt (Krahn et al, 1989)	90	43[(1)]	26[(1)]	Lean clay
		Glacial till (Fredlund et al, 1987)	70	36	19	Lean clay with sand
		Serra do Mar soil (Abramento Carvalho, 1989)	87	38	14	Lean clayey sand, borderline silty sand
		Mangle shale (Bishop and Blight, 1963)	79	36	16	Lean clay with sand
		Selset clay (Bishop and Blight, 1963)	80	33	18	Sandy lean clay
		Dhanauri clay (Gulhati and Satija, 1981)	73	49	24	Lean clay, borderline heavy clay
		Madrid clay sand (Escario and Saez, 1986)	>83	32	15	Lean clayey sand
		Jurong residual soil (Rahardjo et al, 1995)	58	36	15	Sandy lean clay

[(1)]Estimated from range and soil properties

Equation 3-11 was used on using four different soils: red silty clay and Madrid grey clay (Escario and Saez, 1986), Notch Hill silts (Krahn et al, 1989) and glacial till (Fredlund at al, 1987). The soil-water characteristic curve for each soil was not directly measured but rather approximated from SWCC with a similar gradation presented in Andersson and Wiklert (1972). The authors presented the equation in a second paper in 1997 but this

time they used the equation on ten different soils, including the four soils used in the 1995 paper.

The authors state that the equation can be used on sands and silts. However, the ten soils that were used in the published work are mostly fine-grained soils with varying plasticity values. The soil properties are summarized in Table 3.3. The soils are also characterized by the percentage of sand + silt in the specimen.

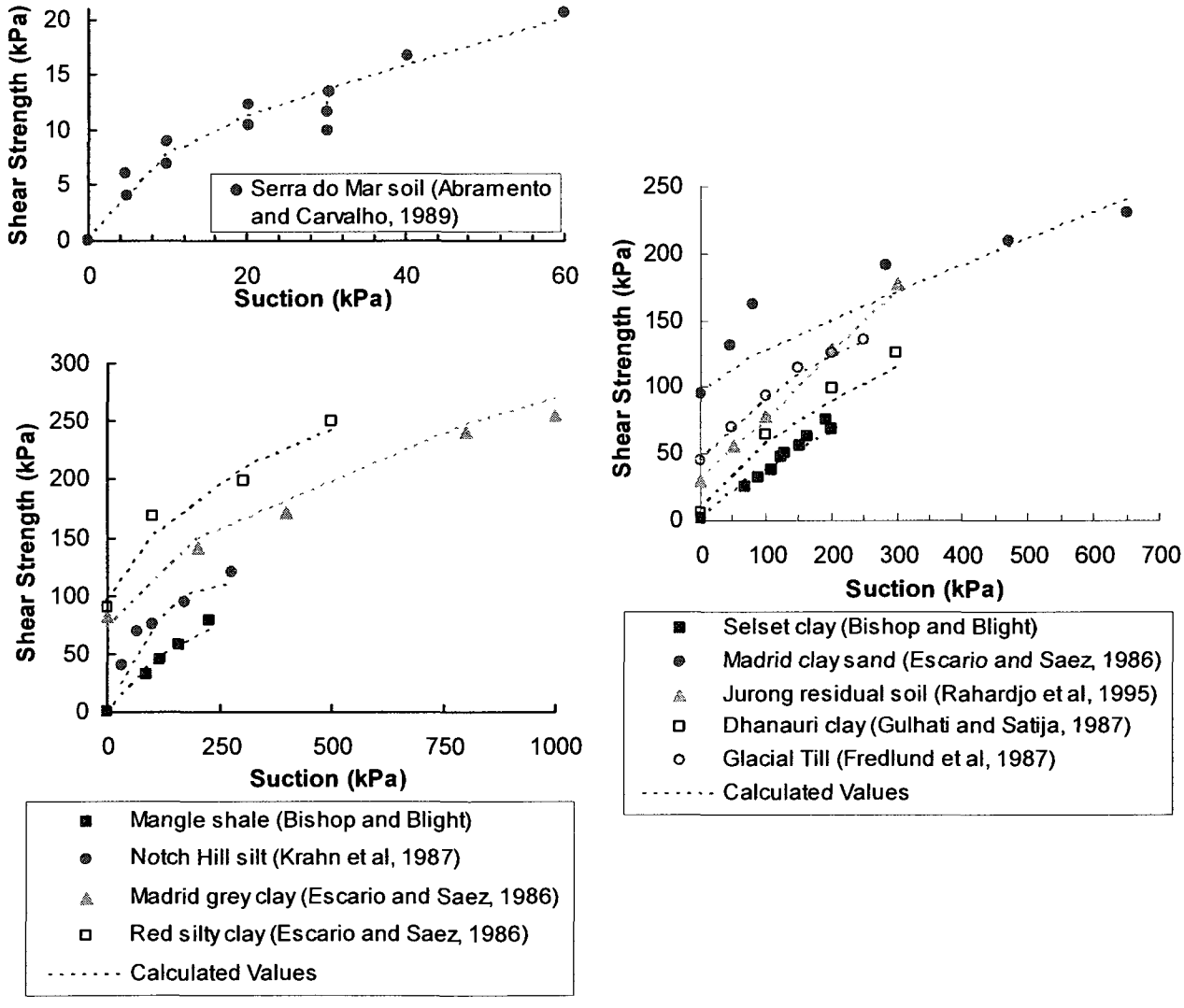

Figure 3.10. Measured versus calculated values using Equation 3-11 for ten soils clay. (modified from Öberg and Sallfors, 1995; Öberg and Sallfors, 1997)

3.4.6 Röhm and Vilar (1995)

Röhm and Vilar (1995) studied the shear strength of an unsaturated lateritic soil. Lateritic soil is sandy lean clay, borderline sandy lean silt. It has a liquid limit of 38 and a plasticity index of 14. The study focuses on the testing of the lateritic soil and developing a relationship between suction (u_a-u_w) and strength, where the strength, q, is defined as half the deviator stress. The equation (Eqn. 3-12) is determined based on the author's relationship for strength when the net normal stress is held constant. The variables were only displayed numerically and were assigned a variable designation for the purpose of description in this thesis.

$$q = c'' + (p - u_a) \cdot \tan\alpha' \qquad [3\text{-}12]$$

where

q is the strength defined as $\frac{(\sigma_1 - \sigma_3)}{2}$

c'' is the relative cohesion dependent upon the change in suction and net normal stress. Determined by regression to experimental data.

$(p - u_a)$ is the net normal stress defined by $\frac{(\sigma_1 + \sigma_3)}{2}$

$\tan\alpha'$ is the angle of shearing resistance determined from regression to experimental data.

Both the relative cohesion and the shearing angle increases as the suction increases. The equation was not intended to predict the relationship between strength and suction, but serve only to numerically describe the relationship between the two.

3.4.7 Vanapalli, Fredlund, Pufahl and Clifton (1996); Fredlund, Xing, Fredlund and Barbour (1996): The Kappa (κ) Equation

The Kappa equation [3-13) is a general, non-linear function that uses the relationship between the water content or degree of saturation and suction over the entire range of suction. (i.e., 0 to 1,000,000 kPa). A fitting parameter, κ, is used for providing close comparisons with the measured shear strength values.

$$a_w = \Theta^{\kappa}$$
$$\tau_{us} = (u_a - u_w)(\Theta^{\kappa})(\tan\phi') \qquad [3\text{-}13]$$

where
a_w is the area of water

Θ is the normalized volumetric water content defined by $\Theta = \frac{\theta}{\theta_s}$

κ is the fitting parameter

Up to the AEV, the normalized water content, which can be presented as degree of saturation, is equal to unity and there is no change in the normalized area of contact, a_w. Beyond the AEV, the change in normalized water content, $d\Theta^{\kappa} / d(u_a - u_w)$, is negative however the shear strength still increases. Although the area of water is decreasing, the shear strength contribution due to suction still increases. This equation proportions the effect of suction on net pressure by relating it to the normalized area of water which can, in turn be related to the volumetric water content.

The fitting parameter is a tool to provide reasonable comparisons between the predicted and measured shear strength values. In 2000, the fitting parameter was correlated with

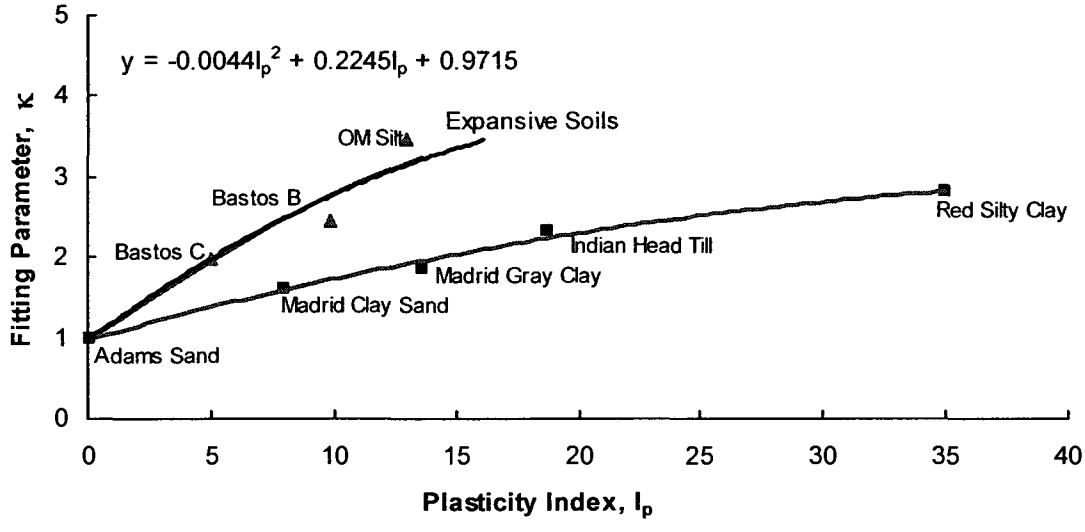

Adams sand	Adams , 1996
Madrid clay sand	Escario & Juca, 1989
Madrid gray clay	
Red silty clay	

Indian Head till	Vanapalli , 1996
Bastos B	Bastos , 2001
Bastos C	
OM silt	Oliviera & Marinho, 2001

Figure 3.11. Relationship between κ and plasticity index (modified from Oliveira & Marinho, 2003).

the plasticity index of the soil (Vanapalli and Fredlund, 2000). Subsequently, this relationship was expanded to include expansive soils (Oliveira and Marinho, 2001). Figure 3.11 shows the two curves developed by Oliveira and Marinho (2001). An equation

equation for the curve for compacted soils developed by Vanapalli et al (2000) is given as Equation 3-14. The curve specific for expansive soils is fit by Equation 3-15.

$$y = -0.0009 \cdot I_p^2 + 0.0833 \cdot I_p + 0.9848 \quad [3\text{-}14]$$

$$y = -0.0044 \cdot I_p^2 + 0.2245 \cdot I_p + 0.9715 \quad [3\text{-}15]$$

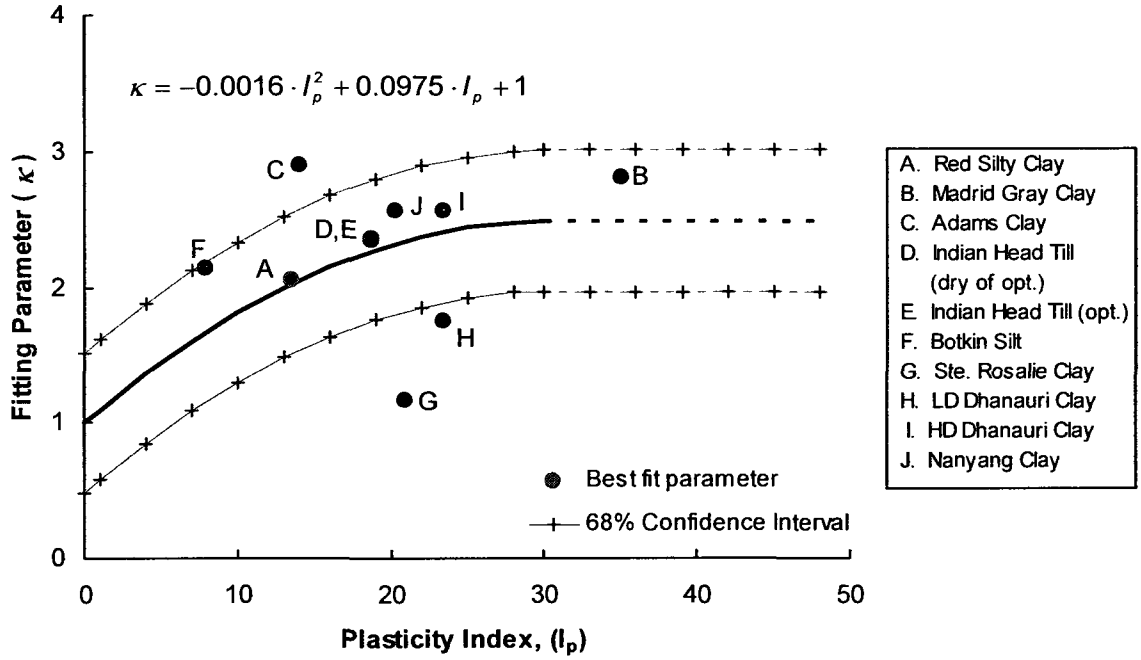

Figure 3.12. Relationship between κ and plasticity index. (modified from Garven & Vanapalli, 2006)

In 2006, Garven and Vanapalli expanded the original chart with a relationship for ten compacted clays. (Figure 3.12)

$$\kappa = -0.0016 \cdot I_p^2 + 0.0975 \cdot I_p + 1 \quad [3\text{-}16]$$

3.4.8 Vanapalli, Fredlund, Pufahl and Clifton (1996): General Equation

A general equation was proposed using the concept of normalization of the water content (gravimetric, volumetric water content or the degree of saturation), but without a fitting parameter (Eqn. 3-17). The range of normalized water content ranges from unity to zero from saturated to residual conditions.

This equation can be written in terms of degree of saturation or gravimetric water content as well as volumetric water content to predict the shear strength yielding similar results. The values of water content used in this equation are determined from soil-water characteristic curve. This equation is designed for prediction over range of suction from zero to 1,000,000 kPa.

$$\tau_{us} = (u_a - u_w)\left(\frac{\theta - \theta_r}{\theta_s - \theta_r}\right)(\tan\phi') \qquad [3\text{-}17]$$

Where
θ is the volumetric water content
θ_r is the volumetric water content at residual suction
θ_s is the volumetric water content at saturation

The shear strength contribution due to suction, τ_{us} decreases when the water content value is lower than the residual water content. Currently, there is limited information with regard to the shear strength beyond the residual water content. As the volumetric water content extends beyond the residual water content, the shear strength may decrease to where the total shear approaches zero and may even become negative, which is theoretically unsound.

3.4.9 Shen (1996, *from Bao et al, 1998*)

Shen (1996) proposed a hyperbolic relationship to predict the shear strength equation where the variable, *d*, is a fitting parameter (Eqn. 3-18). Limited information is available with regard to the development of the equation.

$$\tau_{us} = (u_a - u_w)\frac{1}{1 + d(u_a - u_w)} \cdot \tan\phi' \qquad [3\text{-}18]$$

where
d is a fitting parameter

3.4.10 Bao, Gong and Zhan (1998)

This equation originated from a keynote paper presented at the 1998 unsaturated soils conference. The authors stated that the characteristic of unsaturated soils relies on both the external stress and the soil suction there for a single stressed state variable is not sufficient for unsaturated soils. (Bao et al, 1998)

Bao et al develop an equation based on the linear portion of the SWCC because this is the portion of the shear strength curve that describes the behaviour of the unsaturated soil. The authors develop their equation (Eqn. 3-23) by defining the slope of the linear portion of the SWCC, p (Eqn. 3-19) and the y-intercept of the same line, q (Eqn. 3-20). The relationship between p and q with suction is equivalent to the General equation proposed by Vanapalli et al (1996) (Eqn. 3-17). One difference is that the volumetric water content at the air-entry value is approximately equal to the saturated volumetric water content whereas there can be several values of suction less than the suction of the air-entry value. Both Vanapalli et al's General Equation (Eqn. 3-17) and Bao et al's equation (Eqn. 3-23) are similar in that the shear strength will decrease beyond the residual suction/residual degree of saturation. In extreme cases, the shear strength will be calculated to be negative which is impossible.

$$p = \frac{log(u_a - u_w)_r}{log(u_a - u_w)_r - log(u_a - u_w)_b} \quad [3\text{-}19]$$

$$q = \frac{1}{log(u_a - u_w)_r - log(u_a - u_w)_b} \quad [3\text{-}20]$$

$$\frac{\theta - \theta_r}{\theta_s - \theta_r} = p - q \cdot log(u_a - u_w) \quad [3\text{-}21]$$

where
θ is the volumetric water content
θ_r is the volumetric water content at residual suction
θ_s is the volumetric water content at saturation
p is a variable that represents the slope of the linear part of the SWCC
q is a variable that represents the intercept of the linear part of the SWCC
$(u_a\text{-}u_w)_r$ is the suction at the residual water content
$(u_a\text{-}u_w)_b$ is the suction at the air-entry value

Substituting (3-18) and (3-19) into (3-20):

$$p - q \cdot log(u_a - u_w) = \frac{log(u_a - u_w)_r - log(u_a - u_w)}{log(u_a - u_w)_r - log(u_a - u_w)_b} \quad [3\text{-}22]$$

Resulting in:

$$\tau_{us} = (u_a - u_w)\left(\frac{log(u_a - u_w)_r - log(u_a - u_w)}{log(u_a - u_w)_r - log(u_a - u_w)_b}\right)(tan\,\phi') \quad [3\text{-}23]$$

The authors used three soils to test their own predictive equation as well as the general equation of Vanapalli et al (1996): glacial till (Vanapalli et al, 1996) and two Nanyang expansive soils (Bao et al, 1998). One sample of Nanyang soil was statically compacted while the other was tested in an undisturbed condition. The curves generated from Eqns. 3-17 and 3-23 are similar to each other for all three soils. The curves fit the experimental data from compacted glacial till and the undisturbed soils specimen reasonably well (Figure 3.13).

Table 3.4. Properties of soils used by Bao et al (1998).

Soil (Author)	w_L	I_p	Classification
Glacial Till (Vanapalli et al, 1996)	36	19	Lean clay
Nanyang undisturbed soil[(1)] (Bao et al, 1998)	60	32	Heavy clay
Nanyang compacted soil[(1)] (Bao et al, 1998)	37	14	Lean clay

[(1)]Classification is assumed based on assumption of gradation based on dry density of soils.

Bao et al (1998) suggest that the SWCC was measured in terms of the gravimetric water content and can result in a large change in volume. The authors comment that the residual water content was difficult to determine for expansive soils as the suction value is extremely high. The authors consider that the shrinkage limit may correlate with the residual water content as the amount of shrinkage at the residual water content and beyond will be minimal and the shrinkage is independent of the initial conditions of the soil.

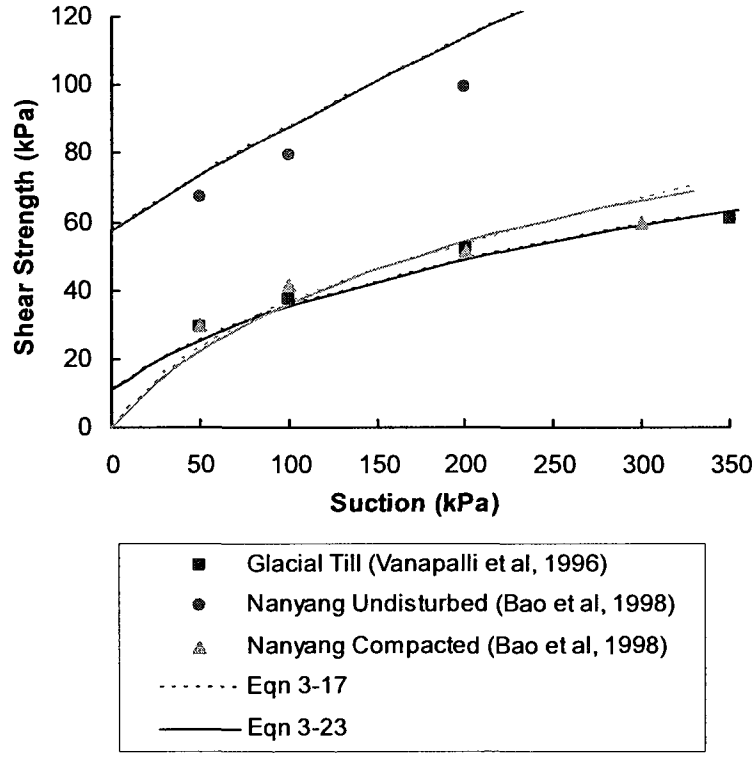

Figure 3.13. Comparing measured values with calculated values of Vanapalli et al General Equation (Eqn. 3-17) and Bao et al equation (Eqn. 3-23) for glacial till, Nanyang undisturbed soil and Nanyang compacted soil.

3.4.11 Yu, Ma and Wang (1998)

Performed with a modified true triaxial test on expansive soil, they fit a hyperbolic equation to the results to describe the change in shear strength with suction. A modified triaxial test is performed using a specimen which is a cube. The true triaxial test has moving platen on three sides that move simultaneously during the testing procedure. The apparatus is modified to include the ability to measure and control the suction and water control.

They analyze the difference in testing a compacted specimen against an undisturbed specimen using a multistage, true triaxial test. The authors noted the differences in deviator stress with confining pressure.

Compacted Soil

Yu et al (1998) found that with an increase in deviator stress (σ_1-σ_3), the suction decreases and attributes this occurrence to the specimen becoming denser. (Figure 3.14a) The degree of saturation increases contributing to a reduction in suction. They note that the deviator stress increases with further increase of strain. When the deviator stress is decreased, the authors hypothesized the development of a shear band in the center of the specimen. This band absorbs additional water from other areas of the sample. The measured suction reflects the suction occurring in the lower portion of the sample rather than in the area of the shear band. At a higher confining pressure, suction increases with a decrease in deviator stress but does not increase with a further increase in deviator stress (σ_1-σ_3) (Figure 3.14a).

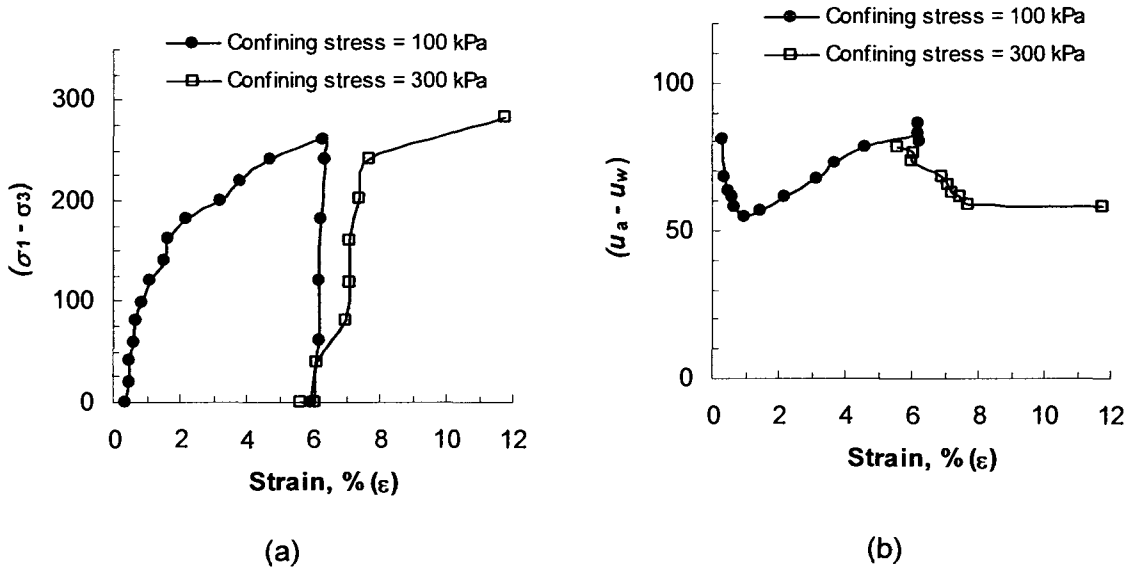

Figure 3.14. (a) Deviator stress vs. strain and (b) suction vs strain for a compacted soil specimen. (from Yu et al, 1998)

The variation detected in this sample seems to be along the failure plane. The minimal change in external water contents does not support the shear band theory and the increased water content near the center may simply be attributed to an increase in pores in the failure plane during rupture. (ie. in the bulge)

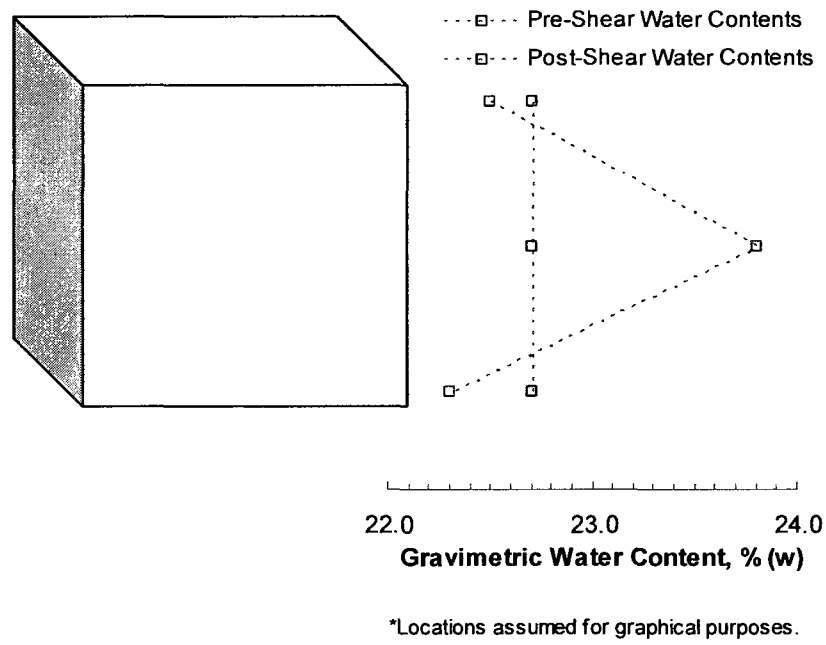

Figure 3.15. Change in water contents before and after shear test.

Undisturbed Specimen

The authors report that in the loading stress path, the sample is disturbed and becomes denser, decreasing the suction. (Figure 3.16) During unloading the sample is not disturbed and therefore, there is slight variation in the suction.

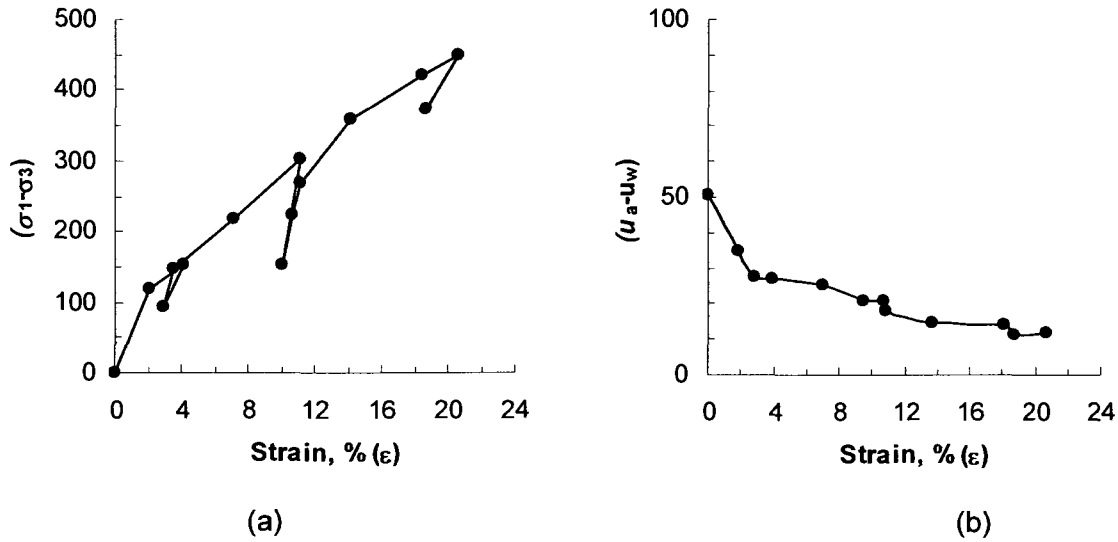

Figure 3.16. Deviator stress vs. strain and (b) Suction vs strain for an undisturbed specimen (from Yu et al, 1998).

It is noted that effective strength parameters are independent of the soil suction and that the effect of suction on shear strength has a limit (Drumright and Nelson, 1995; Röhm and Vilar, 1995; de Campos and Carrillo, 1995). A hyperbolic equation is used to define the relationship between suction and shear strength.

$$\tau_{us} = (u_a - u_w)\frac{1}{\frac{1}{\tan\alpha} + \frac{(u_a - u_w)}{\beta}} \qquad [3\text{-}24]$$

where

α is the rate of suction change per unit of shear strength contributed by the suction (Figure 3.17)

$$\alpha = \frac{(u_a - u_w)}{\tau_{us}}$$

β is the theoretical maximum shear strength contribution due to suction of a soil. Numerically, as the suction increases, β will approach the shear strength contribution due to suction.

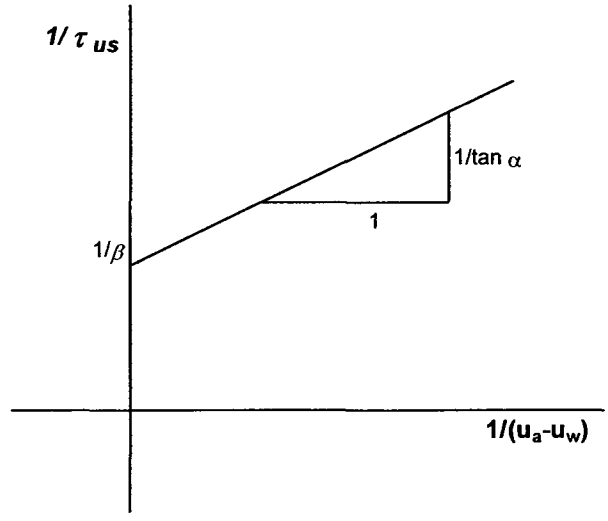

Figure 3.17. Graphical representation of variables of Equation 3-24. (Yu et al, 1998)

This diagram that α is equal to the angle of internal friction with respect to suction or ϕ^b. Using the equation, the authors equate β with the shear strength contribution due to suction. When suction is very large, τ_{us} is equal to β. To date, β cannot be related to soil properties and therefore, 3-24 cannot be used as a predictive equation.

3.4.12 Khalili and Khabbaz (1998)

The authors note that Bishop's effective stress equation (Eqn. 2-13) is a macroscopic relationship. This is because the effective stress acts on the particles of the soil and therefore, it is directly related to the structure of the soil. It is less effective to quantify the equation in terms of stresses at interparticle contact points (Khalili and Khabbaz, 1998). Macroscopic stresses include total stress, pore air pressure, pore water pressure while microscopic stresses are stresses exerted on the soil owing to capillary forces and physiochemical forces (Lu and Likos, 2006) Khalili and Khabbaz state that theoretical models at the microscopic level won't work. Therefore models that attempt to relate χ to the degree of saturation will be ineffective because the degree of saturation is not related to the soil structure. The authors present relationship between, χ and the suction ratio based on thirteen soils (Table 3.5). The suction ratio is defined as the ratio of suction over the air-entry value (Eqn. 3-25) and is presented to the power η which is a fitting parameter that is experimentally determined from thirteen soils data (Figure 3-19).

Based on Bishops equation, Khalili and Khabbaz generate an equation for the variable, χ. The equation is an empirical relationship using the stress state variable suction, and normalizing it by dividing it by the air-entry value for the soil. This relationship has an exponential η which is equal to a constant value of -0.55. This constant was determined experimentally using thirteen soils. Most of the soils are compacted samples and the soil properties are summarized in Table 3.5. Based on the soils used to determine the value of η the equation is designed for use on silts and sands.

Table 3.5. Samples used to create a relationship between χ and suction.

Soil (Authors)	Method of Compaction	w_L	I_p	Classification
Glacial till (Vanapalli et al, 1996)	C	36	19	Lean clay with sand
Notch Hill silt (Krahn et al, 1989)	C	57	32	Heavy clay
Dhanauri clay (Satija, 1978, taken from Fredlund et al, 1987)	C	49	24	Lean clay, borderline heavy clay
Copper mill tailings (Drumright, 1989)	C	NP	NP	Silty sand
Jossigny silt (Cui and Delage, 1993)	C	37	18	Lean clay
Vista Chinesa mature soil (De Campos and Carrillo, 1995)	U	51	18	Silty sand
Vista Chinesa yellow residual soil (De Campos and Carillo, 1995)	U	46	23	Lean clayey sand
Sand clay (Blight, 1967)	C	-	-	-
Glacial till (Fredlund et al, 1995)	C	36	19	Lean clay with sand
Speswhite kaolin (Wheeler and Sivakumar, 1995)	C	-	-	-
Madrid clayey sand (Escario and Saez, 1986)	C	32	15	Lean clayey sand
Sandy clay (Maswaswe, 1985)	-	-	-	-
Glacial till (Gan et al, 1988)	C	36	19	Lean clay with sand

(1) Estimated from range and soil properties C – compacted U - undisturbed

$$\chi = \left[\frac{(u_a - u_w)}{(u_a - u_w)_b}\right]^{\eta} \qquad [3\text{-}25]$$

Where $\eta = -0.55$ as determined from Figure 3.18.

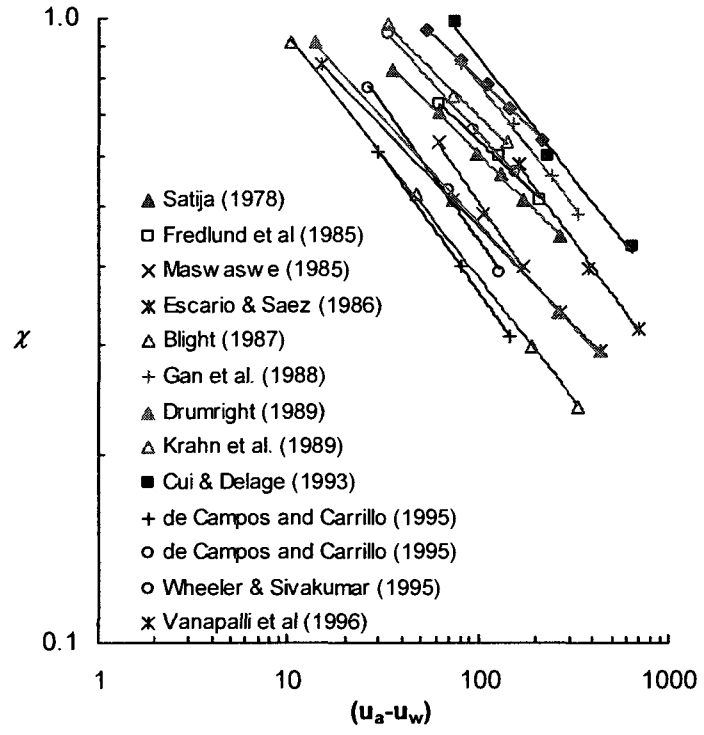

Figure 3.18. Graphical representation of the variable, χ, to suction. (from Khalili and Khabbaz, 1998)

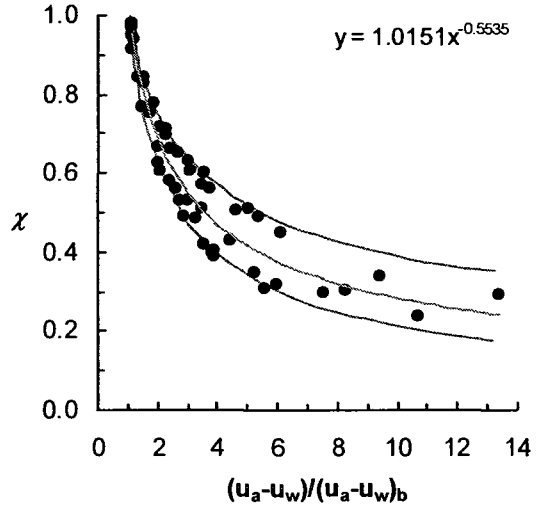

Figure 3.19. Relationship between effective stress parameter and suction ratio. (modified from Khalili and Khabbaz, 1998)

The resulting equation was tested using two soils: kaolin and a constructed soil comprised of kaolin and sand. The samples were compacted and tested using a modified Bishop-Wesley triaxial cell modified to allow control of pore air and pore water. The predicted shear strength was almost a perfect match to the measured values for both soils (Figures 3.20).

Table 3.6. Properties of soils used to test Equation 3-25.

Soil	w_L	I_p	Classification
Kaolin	63	33	Heavy clay
Sand-clay mix	63	33	Heavy clayey sand

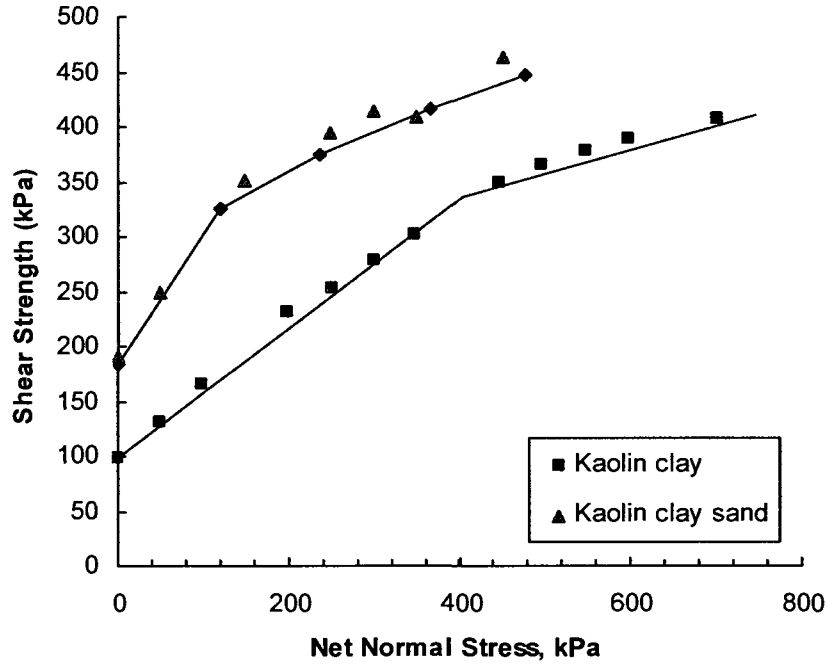

Figure 3.20. Measured versus predicted values for compacted kaolin clay and kaolin clay sand. (from Khalili and Khabbaz, 1998)

3.4.13 Rassam and Williams (1999)

Rassam and Williams attempted to quantify the shear strength of two unsaturated soils originating from mine tailings minds in Queensland, Australia. The first sample was taken at a distance of 50m from the discharge point, while the other was taken from a distance of 150m. The tailings nearest discharge point is 90% sand while the tailings sampled 150 m from the discharge point was 73.5% sand or a silty sand. Both samples were assumed to be non-plastic. The soils were tested under three confining pressures over range 0 to 100 kPa. The samples were prepared from slurried tailings and tested according to the procedure outlined in Ho and Fredlund (1982).

Rassam and Williams recognize the shape of the unsaturated soils curve which is a linear relationship up to and including the air-entry value, and non-linear beyond. The authors use the air-entry value in their prediction (Eqn. 3-29). They estimate this value from experimental data by plotting the air-entry value against normal stress (Figure 3.21).

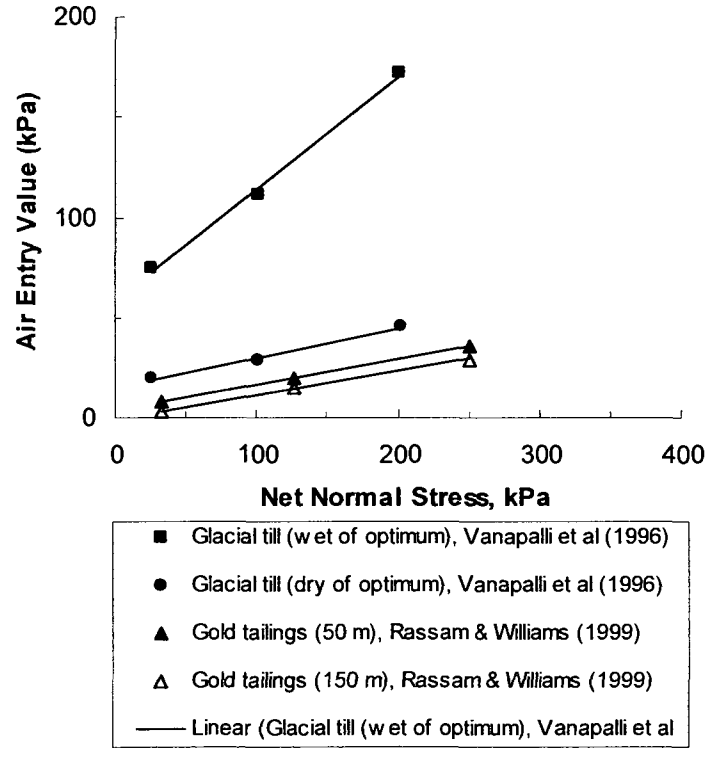

Figure 3.21. Linear relationship of air-entry value relative to the net normal stress illustrated using 2 soils. (Rassam and Cook, 2002)

The equation has three parts: *F1*, *F2*, and *F3*. F1 [Eqn. 3-29] estimates the air-entry value taking account of any normal stress. The authors comment that the confining pressure of the sample should extend to a value high enough to eliminate the dilation of the specimen during shearing because dilation disrupts the water base resulting in reduced strength. At lower levels of confining pressure the slope of the line representing the shear strength relationship due to suction will be negative due to the dilation.

The authors use an equation fitting program called Table Curve 3-D© to produce the 3-D surface to the experimental data. The second part of the equation [Eqn. 3-29] is similar to the equation for the saturated shear strength of soils with a variable, α, which corresponds to c'. The third equation, *F3* (Eqn. 3-28), uses 3 fitting parameters: β, γ, and λ. and describes the shape of the curve beyond the air-entry value. The authors comment that Abramento and Carvalho (1989) used a single term power function to describe the unsaturated shear strength of soils. However, their proposed equation takes into account the effects of normal stress on the contribution of matric suction to the shear strength and the fitting parameter β should always be less than unity.

The third term of equation Eqn. 3-29 is the hypothetical strength contribution due to suction. It is assumed to contribute to the shear strength at an angle equal to the effective angle of internal friction. The fourth term of this equation corrects for the decrease in the contribution of suction to strength caused by the desaturation of the soil (and it is coupled with net normal stress). The overall result of equations 3-26, 3-27 and 3-28 is combined in the overall Equation 3-29 (Rassam and Cook, 2002).

$$F1 = AEV_I + AEV_S(\sigma_3 - u_a) \qquad [3\text{-}26]$$

$$F2 = \alpha_1 + \tan\phi'[(\sigma_3 - u_a) + (u_a - u_w)] \qquad [3\text{-}27]$$

$$F3 = -[(u_a - u_w) - F1]^{\beta_1}[\gamma + \lambda(\sigma_3 - u_a)] \qquad [3\text{-}28]$$

$$\tau_s = \alpha + \sigma \cdot \tan\phi' + (u_a - u_w) \cdot \tan\phi' - \varphi[(u_a - u_w) - (u_a - u_w)_b]^{\beta} \qquad [3\text{-}29]$$

α_1 is a fitting parameter that corresponds to the soil's effective cohesion

β_1, γ and λ are fitting parameters

$F1$ represents the AEV

AEV_I is the air-entry value at 0 net normal stress determined from Figure 3.21.

AEV_S is the change in air-entry value with respect to net normal stress. Shown in Figure 3.21.

F2 represents the soil's shear strength under saturated conditions

F3 is a correction term for the shear strength of a soil under unsaturated conditions

$(u_a - u_w) - F1$ is the matric suction in excess of the AEV

$\varphi = (\gamma + \lambda\sigma)$ since σ is treated as a constant.

Equation 3-29 was used to predict the shear strength of two samples of tailings (Figure 3.22a and b). Each sample was tested at three different confining pressures: 30 kPa, 125 kPa and 250 kPa. The equation provides a good fit for both the samples. In addition, the authors used experimental data of glacial till compacted when the moisture content is wet of optimum (Vanapalli et al, 1996). The experimental data included testing using 3 confining pressures: 25 kPa, 100 kPa and 200 kPa. The curves generated with the Equation 3-29 provide a good fit for the experimental data (Figure 3.23). The curves are not smooth for any of the three data sets. The disjointed nature is for the till tested by Vanapalli et al (1996) may be attributed to the scale along the vertical axis. There is an obvious 'hinge' at the air-entry value as the equation changes from a linear relationship to a non-linear relationship.

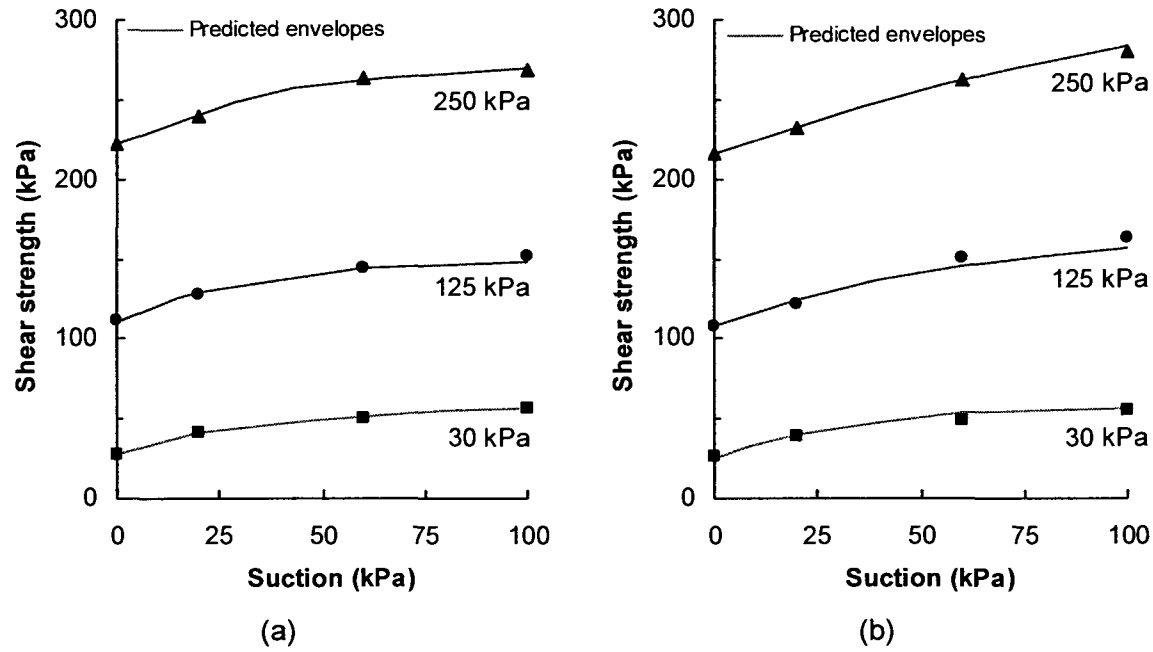

Figure 3.22. Predicted shear strength curves for soil (a) 50m from discharge and (b) 150 m from discharge. (from Rassam and Williams, 1999)

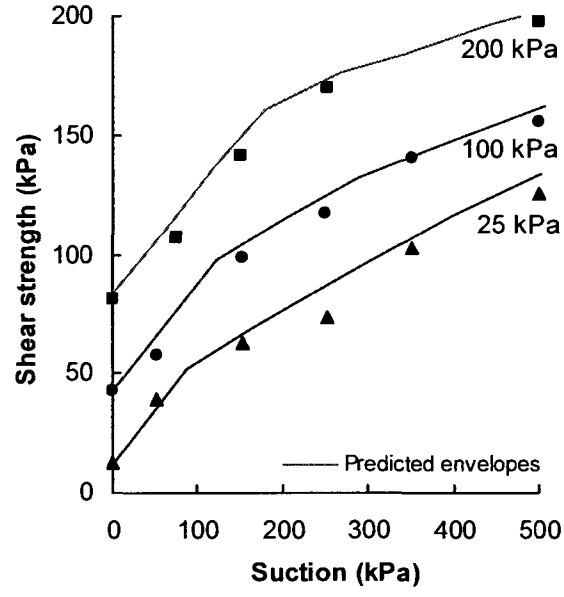

Figure 3.23. Calculated data compared to measured data from Vanapalli et al, 1996. Soil is prepared at a moisture content wet of optimum. (modified from Rassam and Williams, 1999)

3.4.14 Xu and Sun (2001)

Xu and Sun (2001) developed an empirical equation for predicting the shear strength of expansive soils based on the fractal dimension of soils. The fractal dimension in a statistical quantity to describe the ability of a fractal to fill a space by zooming to finer and finer scale. A fractal can be defined as a geometric shape that can be split into parts where the parts are a reduced version of the whole, also called self-similarity (Xu and Sun, 2001) Fractal dimension is used to estimate the surface area of the pores on the surface of a soil. Using the fractal dimension provides an accurate pore distribution on the surface of the soil and a better indication of the contact points of a soil (Xu and Sun, 2001).

Fractal properties have been used to estimate the density, porosity, the flow characteristics and the surface strength of the soil (Rieu and Sposito 1991a and b; Folorunso et al, 1994; Thevanayagam and Nesarajah, 1998). The fractal dimension can be determined from Eqn. 3-41.

$$A_i \sim r^{2-D} \qquad [3\text{-}30]$$

$$D = 2 - \lambda \qquad [3\text{-}31]$$

A_i The surface area which could be measured by using a gauge of size r. The interface area between mercury and water in a mercury intrusion test.

r_1 The radius of the micropores of soil.

D The fractal dimension of a pore-ball distribution. Known as the fractal dimension and ranges from 2.0 to 3.0.

λ The change in radius of the micropores per surface area. This variable can be determined by plotting and r_1 and A_i (Figure 3.24)

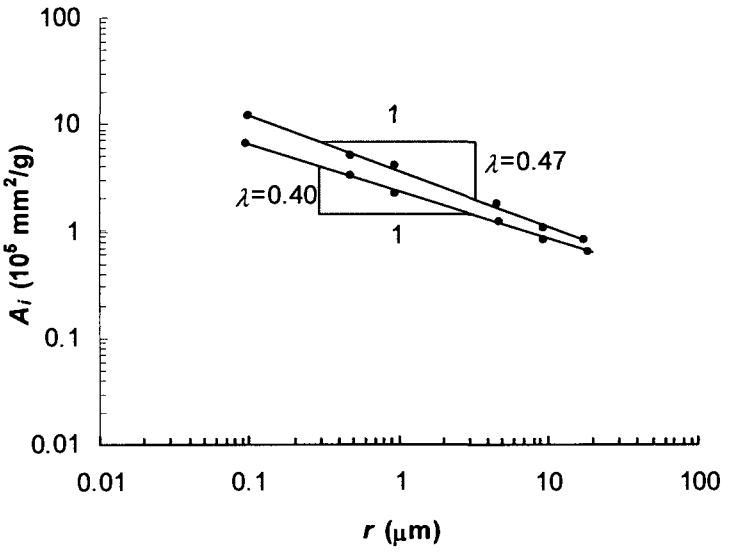

Figure 3.24. Results of mercury intrusion tests on Ningxia expansive soil. (from Xu and Sun, 2001)

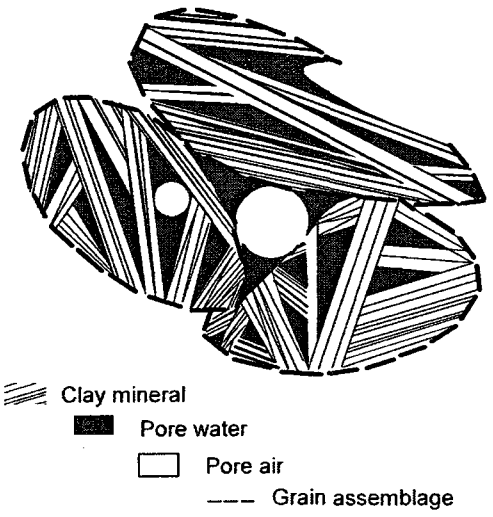

Figure 3.25. Skeleton chart of an expansive soil structure (modified from Xu and Sun, 2001)

The fractal model where a series of ball pores with radius, *r*, can be used as illustrated to approximate the micropore surface of an expansive soil. (Figure 3.26) The fractal dimension, *D*, is expressed as the distribution of the radii of the ball pores.

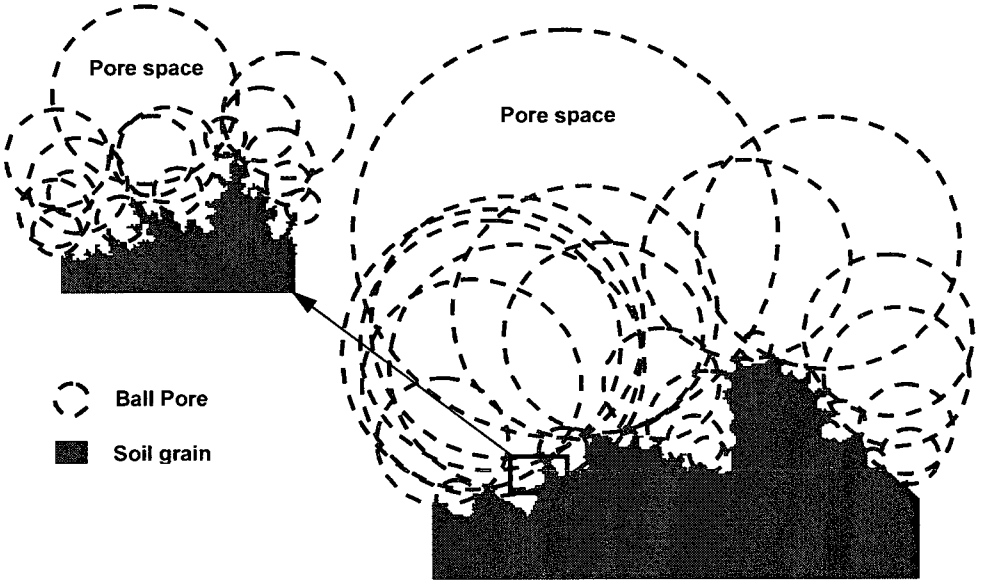

Figure 3.26. Illustration of ball-pore relative to micropores of soil (from Xu and Sun, 2001)

The matric suction and the radius of the micropores are inversely proportional and related by Eqn. 3-32. The soil-water characteristic curve (SWCC) can be determined from the fractal model using Eqn. 3-33. (Xu and Sun, 2001)

$$u_a - u_w = \frac{2T \cdot \cos\theta}{r_1} \qquad [3\text{-}32]$$

$$S = m^n \cdot (u_a - u_w)^{-n} \qquad [3\text{-}33]$$

$$m = \frac{2T \cdot \cos\theta_a}{R} \qquad [3\text{-}34]$$

$$n = 3 - D \qquad [3\text{-}35]$$

where

T	The surface tension of the interface between water and mercury (375 mN/m) or between air and mercury (485 mN/m). Can be determined from a physics reference manual. .
D	The fractal dimension of a pore-ball distribution. Known as the fractal dimension and ranges from 2.0 to 3.0. It can be calculated using Eqn. 3-35.
R	The maximum radius of macropore, whose surface can be described as fractal. Can be measured by mercury intrusion porosimetry.
θ_a	The contact angle between the water and soil. Can be determined from a reference manual.
m,n	Intermediate variables known as the soil-water characteristics.
α	Intermediate variable.
S	Degree of saturation.

Similar to Bishop's equation (Eqn. 2-13) the investigators propose an equation that is a function of the degree of saturation (Eqn. 3-40) where the variable, *f*, is proportional to the fraction of the area occupied by water (Eqn. 3-36). It is also related to the maximum macropore size and minimum pore size with the fractal dimension (Eqn. 3-39). Equation 3-41 represents the fractal dimension in a shear plane. The equation is developed by relating the circle pore distribution to the variable, *f*, and relating it to the equation for the SWCC (Eqn. 3-40). Combining Equation 3-37 and Equation 3-40 produces Equation 3-41. Combining the various equations sequentially resulted in the development of Equations 3-41 and 3-42 for the shear strength contribution due to suction of expansive soils. The variables, *m* and *S*, are determined through mercury porosimetry.

$$f = \frac{A_w}{A} \qquad [3\text{-}36]$$

$$\tau_{us} = (u_a - u_w) \cdot f \cdot \tan\phi' \qquad [3\text{-}37]$$

$$D_s = \frac{2}{3} D \qquad [3\text{-}38]$$

$$f = \left(\frac{r_1}{R}\right)^{2-D} \qquad [3\text{-}39]$$

$$f = S^{\frac{2-D_S}{3-D}} \quad [3\text{-}40]$$

$$\tau_{us} = m^{1-\varsigma} \cdot (u_a - u_w)^{\varsigma} \cdot \tan\phi' \quad [3\text{-}41]$$

$$\varsigma = \frac{2D}{3} - 1 \quad [3\text{-}42]$$

where

f	A parameter related to the degree of saturation and expansive structure of the soil.
D_s	The fractal dimension of the circle pore distribution in a shear plane.
D	The fractal dimension of a pore-ball distribution of a three dimensional. (the fractal dimension value typically ranges from 2.0 to 3.0)
c	The mean radius of the interface between mercury and water from a mercury intrusion test.
λ	The slope of the line of A_i vs r from a mercury intrusion test of a soil. (Figure 3.24)
T	The surface tension of the interface between water and mercury (375 mN/m) or between air and mercury (485 mN/m) (this value can be determined from a physics reference manual)
R	The maximum radius of macropore, whose surface can be described as fractal.
θ_a	The contact angle between the water and soil. Can be determined from a reference manual.
m, n	Intermediate variables known as the soil-water characteristics.
ς	Intermediate variable.

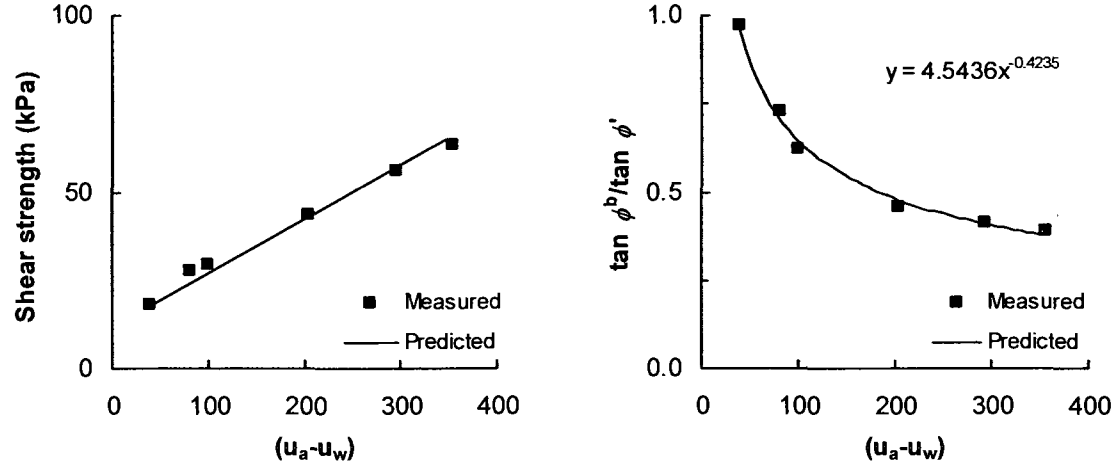

Figure 3.27. Comparing measured and predicted values for Ningxia expansive soil using (a) the shear strength versus suction plot and (b) the tan ϕ^b/tan ϕ' chart. (modified from Xu and Sun, 2001)

The equation was tested on Ningxia expansive soil presented in this paper. The predicted shear strength provides a reasonable fit to the measured points in Figures 3.27a and b. The predicted shear angle was compared to the measured shear angle (Figure 3.27b). The original data displayed on logarithmic scale is plotted on arithmetic scale.

The authors use two different scenarios to verify the theoretical validity of the equation:

1. When the soil is saturated, r goes to R and the tan ϕ^b/tan ϕ =1

2. When $r<R$, tan ϕ^b <tan ϕ which is consistent to experimental results from various authors.

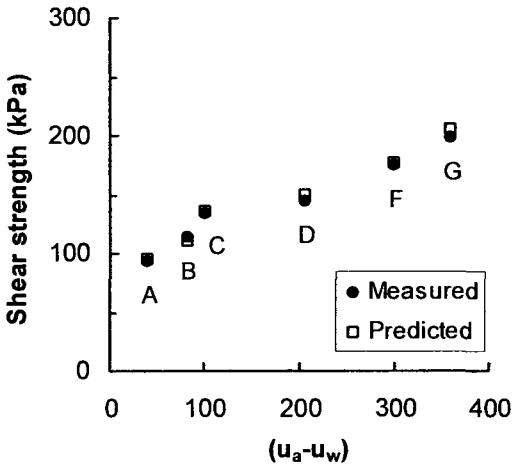

A σ_3-u_a = 84 kPa

B σ_3-u_a = 110 kPa

C σ_3-u_a = 142 kPa

D σ_3-u_a = ? kPa

E σ_3-u_a = 177 kPa

F σ_3-u_a = 220 kPa

Figure 3.28. Summary of measured and calculated values using Equation 3-41. (from Xu and Sun, 2001)

Xu and Sun (2001) compared the results in a detailed image (Figure 3.28) that included the different net normal stresses. They concluded that the equation was valid for more than expansive soils where the degree of saturation remains quite high. ie. where the micropores remain saturated.

3.4.15 Miao, Liu and Lai (2002)

Miao et al (2002) propose an equation for predicting the shear strength of unsaturated expansive soils based on the pore size and geometrical distribution. It is suggested to use the water content vs. suction relationship rather than the degree of saturation vs. suction to take account of shrinkage in expansive soils. The authors prepared specimens of the Nanyang expansive soil: one specimen was allowed volumetric change while the other was not (i.e. by subjecting a preload on the specimen). The sample that was prepared without preloading showed differences between each of the wet dry cycles, the difference between the wetting cycle and that drying cycle gets closer to each other in each increased cycle. The sample that has been exerted to a preload generated three stable repeatable wetting and drying curves. The authors suggest that the samples that were preloaded represented the realistic behaviour of the expansive soil.

The authors used the approximate linear relationship of the inverse of both the shear strength and the suction to develop their hyperbolic equation. Equation 3-43 is the line of this relationship which uses the parameters *a* and *b* to better fit the equation to the experimental data. At a saturated condition (ie. where the suction is 0 kPa), the inverse of the suction will be a singularity and thus, the atmospheric pressure can be introduced into the equation.

At a suction value of 0 kPa, the shear strength contribution due to suction is also 0 kPa. By substituting this boundary into Equation 3-43, the fitting parameter, b_2 can be estimated. Equation 3-44 can be substituting Equation 3-44 into the original equation to get Equation 3-45.

$$\frac{1}{\tau_{us} + p_{at}} = \frac{a_2}{u_s + p_{at}} + b_2 \qquad [3\text{-}43]$$

$$b_2 = \frac{1 - a_1}{p_{at}} \quad [3\text{-}44]$$

$$\tau_{us} = \frac{a_2 u_s}{1 + \frac{1 - a_2}{p_{at}} \cdot u_s} \quad [3\text{-}45]$$

where

p_{at} is the atmospheric pressure (101.3 kPa)

a_2, b_2 are fitting parameters to fit the Equation 3-45 to experimental data. They are illustrated on Figure 3.29.

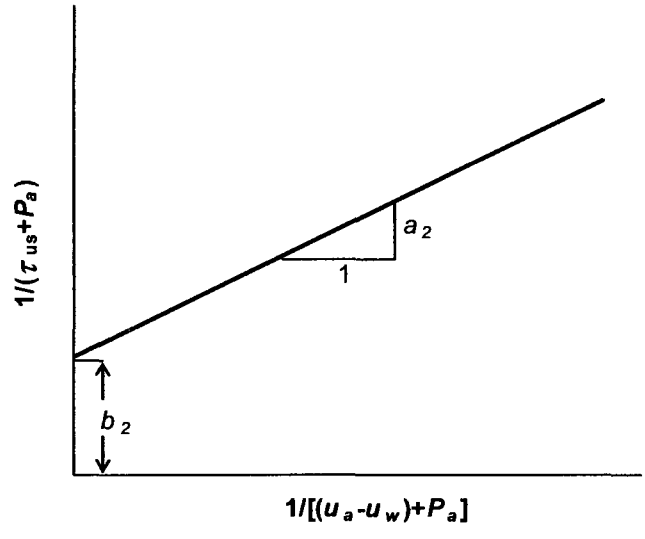

Figure 3.29. Schematic drawing showing the physical meanings of variables. (from Miao et al, 2002)

The shear strength of Nanyang expansive soil was tested by triaxial tests under three confining pressures by the authors. There is some variation between the confining pressures from test to test.

Test parameters, a_2 and b_2, were fitted through regression of experimental data. The resulting fit is shown in Figure 3.30 below. In addition, the authors used the Vanapalli general equation (Eqn. 3-17) to test the ability of the equation to predict the shear

strength data. Although the results from each equation were slightly different, both curves adequately match the measured data.

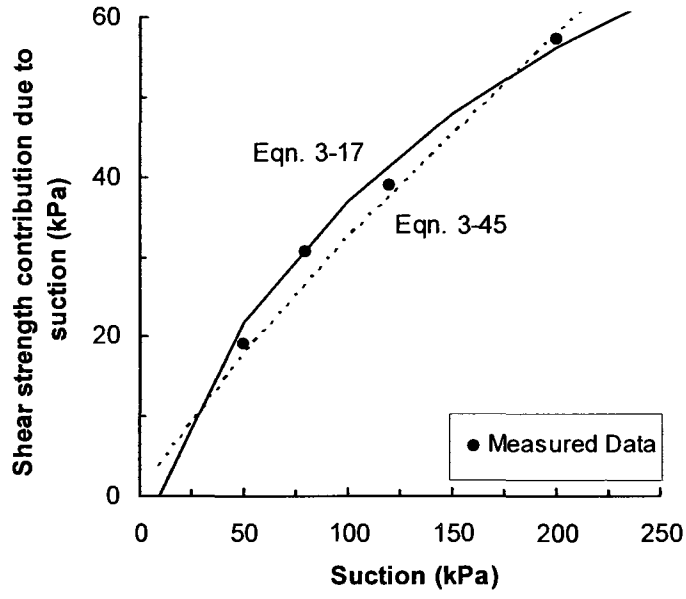

Figure 3.30. Comparing predicted data with measured data for Nanyang expansive soils. Curves were predicted using two formulae: Vanapalli et al general equation (3-17) and Miao et al equation (3-45). (generated from Miao et al, 2002)

3.4.16 Rassam and Cook (2002)

The authors develop a predictive equation that is an additive function from the knowledge of shear strength at residual suction. The additive function is an equation that is composed of several terms, each representing a part of the relationship, and when the parts are added together to represent the overall relationship.

The residual suction is difficult to determine from the SWCC of a clay soil as the changes in water content are gradual around the AEV and residual suction and a precise value is difficult to obtain. The residual suction is more easily determined for sands and silts. The authors define the concept of residual suction. There are several definitions of this concept but the authors acknowledge that there is a well defined definition given the graphical representation of this SWCC. The authors discussed the concept of critical threshold where the pressure applied during testing is less than the preconsolidation pressure. Dilation of the sample will occur and the slope of the shear strength line with relation to suction will be negative.

The boundary condition is applied whereby the angle ϕ^b=0 at residual suction. The contribution to the matric suction is determined experimentally. It requires knowledge of shear strength at residual suction and reduces the number of laboratory tests to only one. The equation can be used to predict shear strength over a wide range of suctions but it is most suited to coarse to medium grained soils where the residual suction can be easily obtained in the laboratory.

The Rassam and Cook paper enhances and expands the existing relationship of Rassam and Williams (1999).

$$\tau_s = \alpha + \sigma \cdot tan\phi' + (u_a - u_w) \cdot tan\phi' - \varphi[(u_a - u_w) - (u_a - u_w)_b]^\beta \quad [3\text{-}28]$$

Differentiating this equation with respect to suction gives (Eqn. 3-46) which is the relationship for $tan\phi^b$. When this equation is solved where $\psi = \psi_e$, the result is $tan\phi^b = tan\phi'$ which supports the theory of this equation. Equation 3-28 can be re-written to contain on the shear strength contribution due to suction (Eqn. 3.28a)

$$\tau_s = (u_a - u_w) \cdot tan\phi' - \varphi[(u_a - u_w) - (u_a - u_w)_b]^\beta \quad [3\text{-}28a]$$

$$\frac{d\tau_s}{d\psi} = tan\phi^b = tan\phi' - \varphi\beta(\psi - \psi_e)^{\beta-1} \quad [3\text{-}46]$$

The components of this equation are illustrated in Figure 3.31. Solving Equation 3-28a at residual suction gives Equation 3-46a.

$$\varphi = \frac{\psi_r \cdot tan\phi' - \tau_{Sr}}{(\psi_r - \psi_e)^\beta} \quad [3\text{-}46a]$$

Combining Equation 3-45 and 3-46a and solving for β yields:

$$\beta = \frac{tan\phi' \cdot (\psi_r - \psi_e)}{tan\phi' \cdot \psi_r - \tau_{Sr}} \quad [3\text{-}46b]$$

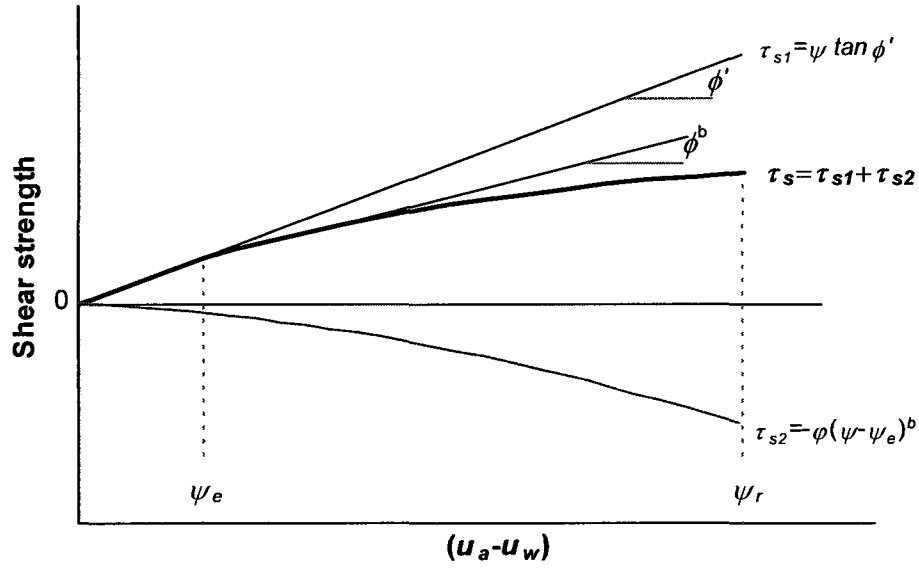

Figure 3.31. Graphical representation of the various components of Equation 3-28a. (from Rassam and Cook, 2002)

The numerator of Equation 3-46b represents the theoretical strength gain that would have occurred if the soil had not desaturated between the air-entry value and the residual suction. The denominator is the decrease in shear strength at the residual suction that can be attributed to the reduced saturation. The development of the equation follows logical theory based on saturated and unsaturated soil mechanics.

$$\tau_s = (u_a - u_w)\cdot \tan\phi' - \left[\frac{\psi_r \cdot \tan\phi' - \tau_{Sr}}{(\psi_r - \psi_e)^{\beta}}\right]\left[(u_a - u_w) - (u_a - u_w)_b\right]^{\frac{\tan\phi'\cdot(\psi_r-\psi_e)}{\tan\phi'\cdot\psi_r-\tau_{Sr}}} \qquad [3\text{-}47]$$

The authors use five soils to test the correlation: Kidston tailings (Rassam and Williams, 1999), decomposed fine ash tuff, glacial till (Gan and Fredlund, 1996; Gan at all 1988), Madrid clay sand and Madrid gray clay (Escario and Juca, 1989). Reasonable comparisons were observed between the measured and predicted points.

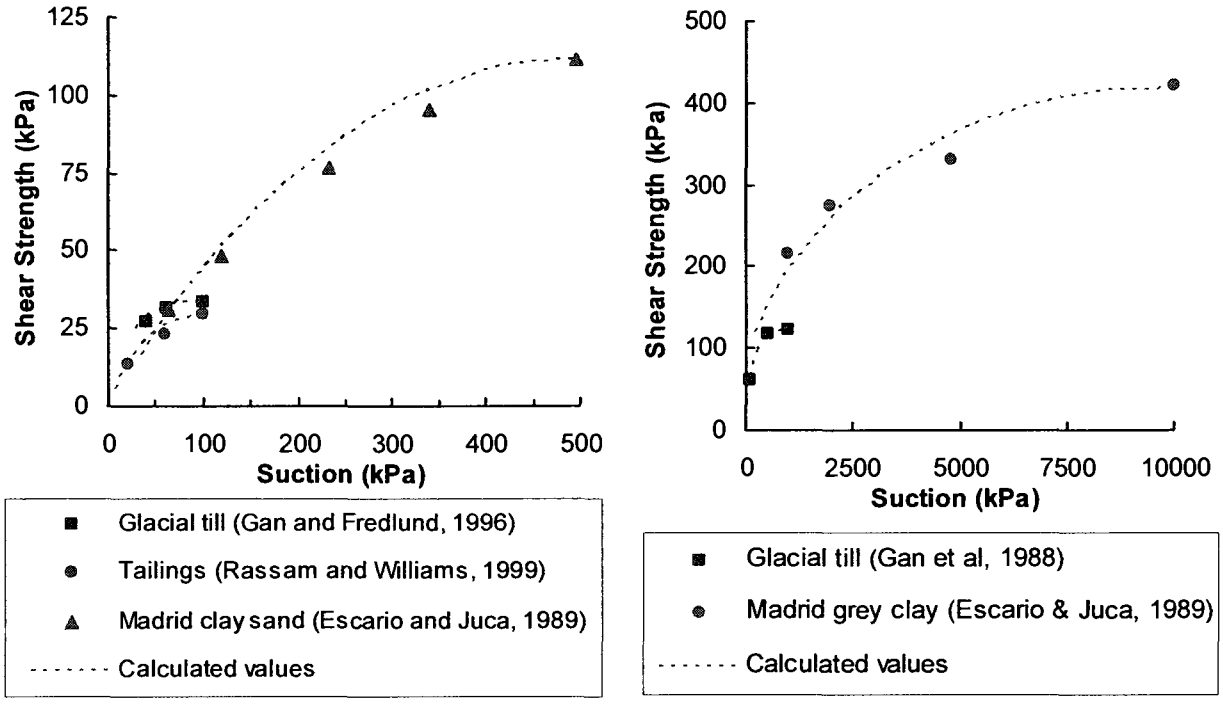

Figure 3.32. Measured values from five different soils over (a) lower suction range, (b) an intermediate suction range and (c) a higher suction range. (Rassam and Cook, 2002)

3.4.17 Aubeny and Lytton (2003)

The paper was to be considered as a companion paper to Lytton's (1995) research. The authors expand on the original equation (Eqn. 3-10) in this paper. They recognized that suction doesn't act over the entire surface of the particles and implemented the variable, f_1, to account for the change in area that is affected by water at different degrees of saturation. The factor was applied directly to Eqn. 3-10, resulting in Equation 3-48. In addition, the authors proposed a second equation (Eqn. 3-49) for interpreting unconfined compression test results. The unconfined compression test is a quick and simple, inexpensive tests that are well suited for practical use in industry.

$$\tau_{us} = f_1 \cdot (u_a - u_w) \cdot \theta \cdot \tan\phi' \qquad [3\text{-}48]$$

$$\tau_{us} = f_1 \cdot (u_a - u_w) \cdot \theta \cdot \frac{\sin\phi'}{1 - \sin\phi'} \qquad [3\text{-}49]$$

where

f_1 is a factor ranging from *1 to 1/θ* following the following guidelines:

If $S = 100\%$, $f_1 = 1/\theta$

If $85\% \le S \le 100\%$, $f_1 = 1 + \frac{S-85}{15}\left(\frac{1}{\theta} - 1\right)$

If $S \le 85\%$, $f_1 = 1$

The authors, however, do not provide accompanying data to test the validity of the proposed equations.

3.4.18 Lee, Lee and Kim (2003)

Lee, Lee and Kim proposed an equation to predict the shear strength of unsaturated soils using only one empirical soil parameters, C_{max}, or ultimate increment of apparent cohesion (Figure 3.33). The apparent cohesion (C_A) is the sum of the shear strength contribution due to suction and the effective cohesion. The shear strength contribution due to suction is represented by a hyperbolic equation to fit to the non-linear relationship between the shear strength and suction.

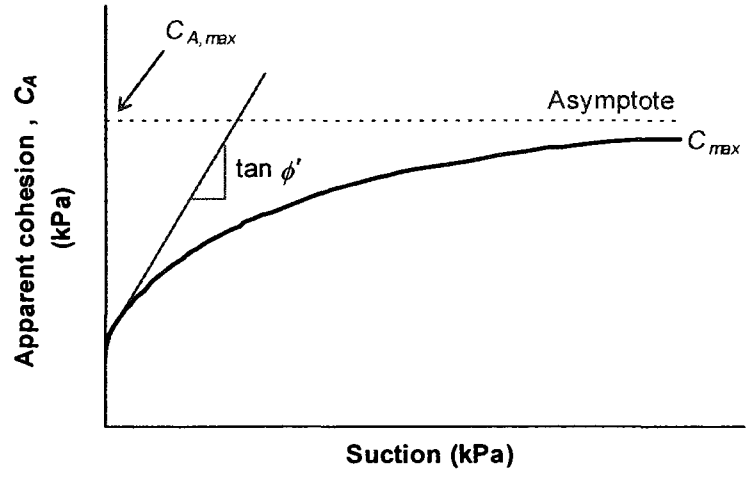

Figure 3.33. Schematic illustrating the variables of Equation 3-50. (modified from Lee et al, 2003)

The Equation 3-50 is a hyperbolic equation that is defined by 1/*a* (Eqn. 3-51) which is the initial slope and 1/*b* (Eqn. 3-52) which is the value related to the friction angle. The

variable, a, is the inverse of the angle of internal friction while the other fitting parameter, b is the maximum increment of strength.

$$C_A = c' + \frac{(u_a - u_w)}{a + b(u_a - u_w)} \quad [3\text{-}50]$$

$$a = \frac{1}{\tan\phi'} \quad [3\text{-}51]$$

$$b = \frac{1}{C_{max}} \quad [3\text{-}52]$$

The authors propose a method to predict the required parameter using an artificial neural network (ANN). They use Matlab to assist with the analysis of the ANN. The artificial neural network uses soil properties (sand fraction, silt and clay fraction, void ratio, compaction water percent, effective cohesion and effective angle of internal friction) to determine the ultimate increment of apparent cohesion (Figure 3.33) The goal of using the ANN is to increase ability to predict the strength of soil and minimize the number tests that have to be done to characterize the soils behaviour. The neural network is 'trained' to use the soil characteristics to predict the value of C_{max}. The authors reported that using this model, there is little influence of ϕ, void ratio and compacted water content on the determination of C_{max}.

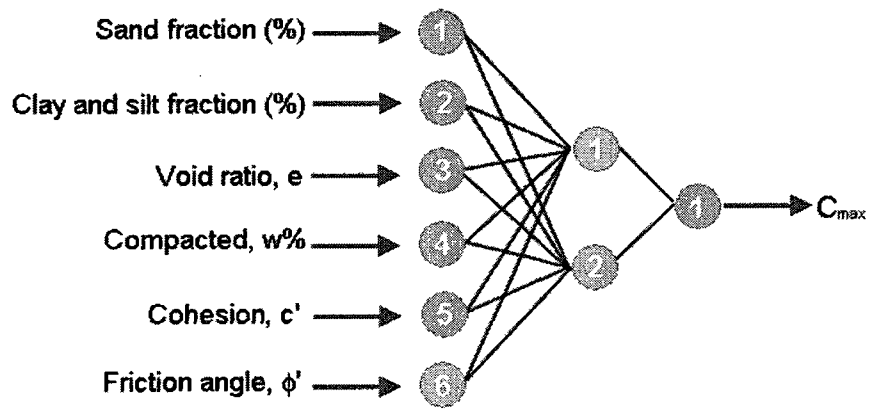

Figure 3.34. Schematic of classic 6-2-1 artificial neural network and the six parameters examined to explain variation in data. (from Lee et al, 2003)

Lee et al (2003) uses the relationship and applies it to twelve different soils. The results of the application are shown in Figure 3-35. The curves seemed to provide an adequate fit for all soils except the colluvium (de Campos and Carrillo, 1995).

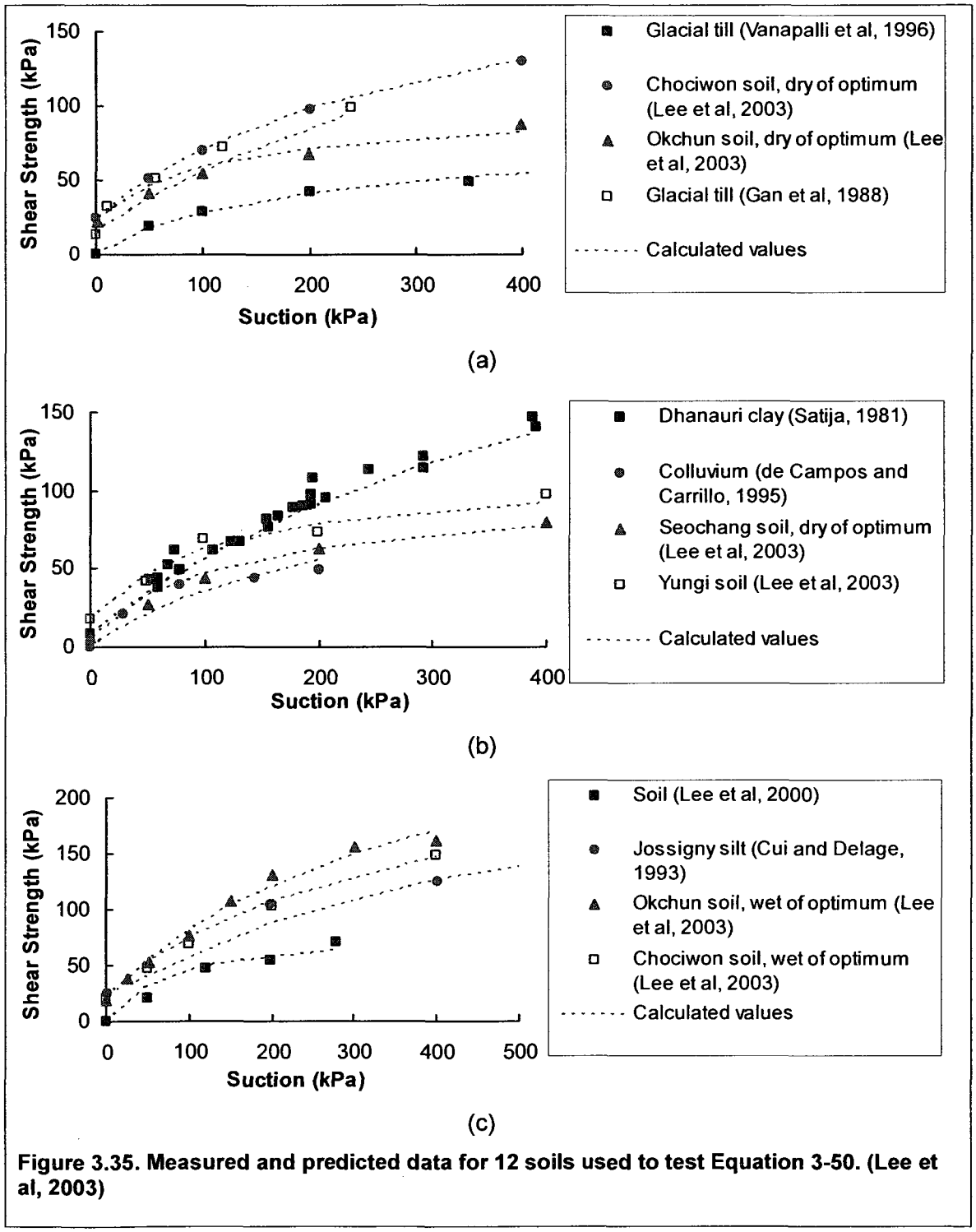

Figure 3.35. Measured and predicted data for 12 soils used to test Equation 3-50. (Lee et al, 2003)

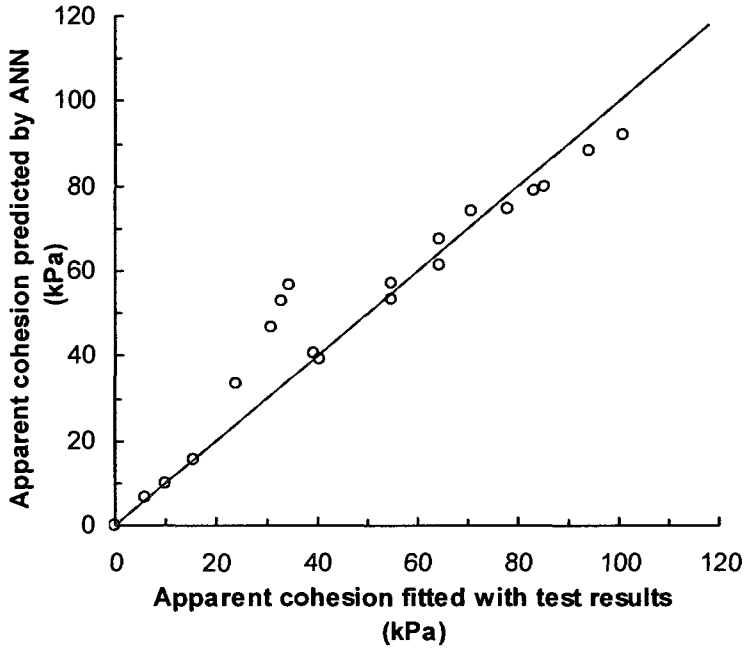

Figure 3.36. Comparison of predicted test results compared to test results for Model IV. (Lee et al, 2003)

The authors compared the ANN models by looking at the apparent cohesion and apparent cohesion fitted to test results. The four models presented in this paper seem to correlate with experimental data varying greatest with Model IV (Figure 3.36). The method proposed by the authors uses a knowledge-based and knowledge-calibrated method of analysis to predict shear strength of unsaturated soils.

3.4.19 Schick (2004)

Schick proposed an equation to predict the shear strength of unsaturated soils (Eqn. 3-53) originating from Miao et al (2001) original relationship. It's a hyperbolic relationship using two fitting parameters a_2 and b_2. (Eqn. 3-54 and 3-55, respectively) The fitting parameters are currently used to fit the equation to the experimental data (Figure 3.37.

$$\tau_{us} = \frac{(u_a - u_w)}{a_2 + b_2 \cdot (u_a - u_w)} \qquad [3\text{-}53]$$

$$a_2 = tan(\phi' - 90) \quad [3\text{-}54]$$

$$b_2 = tan\,\beta_2 = \frac{1}{\tau_{us}} \quad [3\text{-}55]$$

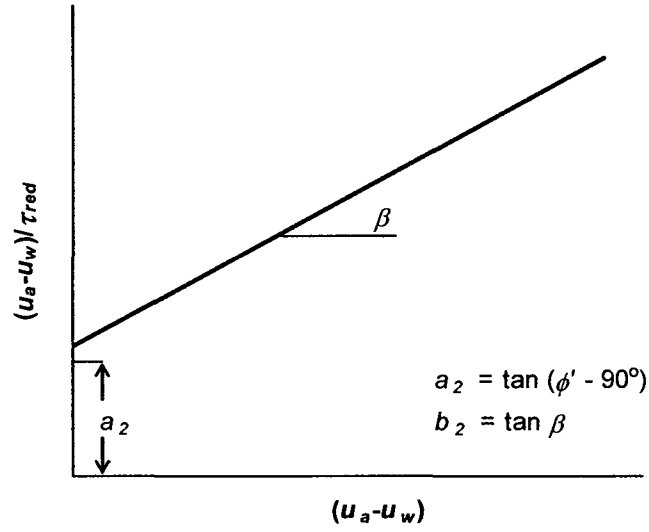

Figure 3.37. Illustration of fitting parameters *a* and *b* for Schick.

3.4.20 Xu (2004)

Several investigators have shown that the surface of soils is fractal (Avnir and Farin,1984; Vallejo, 1996; Xu and Sun, 2001) The concept of fractal dimension has been correlated to soil compression (McDowell et al, 1996), hydraulic conductivity (Thevanayagam and Nesarajah, 1998; Xu and Sun, 2002), soil cohesion (Bonala and Reddi, 1999) and swelling properties (Xu et al, 2003).

This author makes an amendment previously proposed with Xu and Sun in 2001 (Eqn. 3-41). The author utilizes the same base equation (Eqn. 3-57) but it is noted to be different from the original equation presented in Xu and Sun (2001). The difference between the two equations in that the intermediate soil water characteristics (m) from the 2001 paper is replaced with the air-entry value $(u_a\text{-}u_w)_b$. The fractal dimension in the shear plane was defined according to Mandelbrot's rule (Mandlebrot, 1982) and defined as D_s-1 whereas it was previously defined as $2/3D_s$ by Xu and Sun.

$$S_e = \left(\frac{u_{se}}{u_e}\right)^{3-D_S} \quad [3\text{-}56]$$

$$\tau_{us} = (u_a - u_w)_b^{1-\zeta_2} \cdot (u_a - u_w)^{\zeta_2} \cdot \tan\phi' \quad [3\text{-}57]$$

$$\zeta_2 = D_s - 2 \quad [3\text{-}58]$$

where

ζ_2 is the fractal dimension in the shear plane.

The fractal dimension of soil is commonly measured by using mercury intrusion porosimetry. In 2000, Watabe proposed a correlation between the SWCC and the fractal dimension. Xu used a Ningxia expansive soil tested by modified direct shear test as well as mercury intrusion. The author also uses five other soils (Table 3.7).

Table 3.7. Soils used to test Equation 3-57. (Xu, 2004)

Ningxia expansive soil	Xu, 2004
Glacial till	Vanapalli et al, 1996
Glacial till	Gan et al, 1988
Silt	Oloo and Fredlund, 1996
Silty soil	Nishimura and Fredlund, 2001
Gold tailings, 50 m	Rassam and Williams, 1999
Gold tailings, 150 m	

Good correlations were observed for most of the soils. The published results are however portrayed on a log-log scale. The published figures are reproduced here (Figures 3-42 to 3-47) on an arithmetic scale. The only soil that didn't appear to have a strong correlation was the Ashikaga silt.

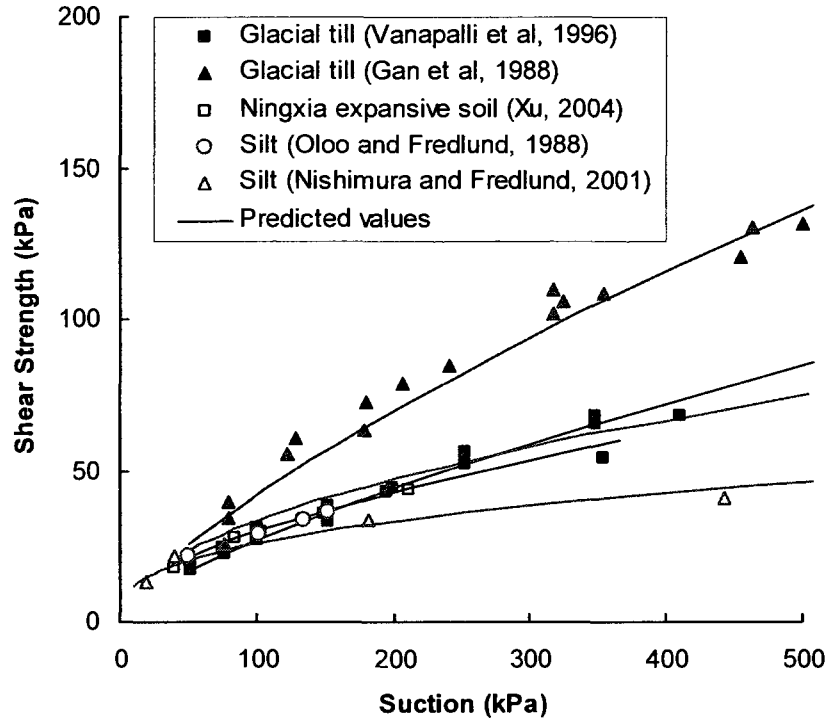

Figure 3.38. Predicted versus measured values 5 soils used by the investigators. (Xu, 2004)

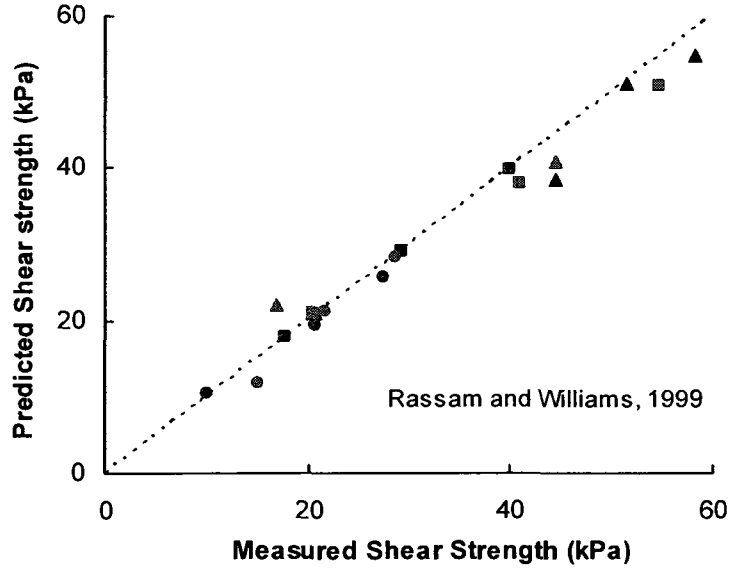

Figure 3.39. Predicted versus measured values for tailings. (Xu, 2004)

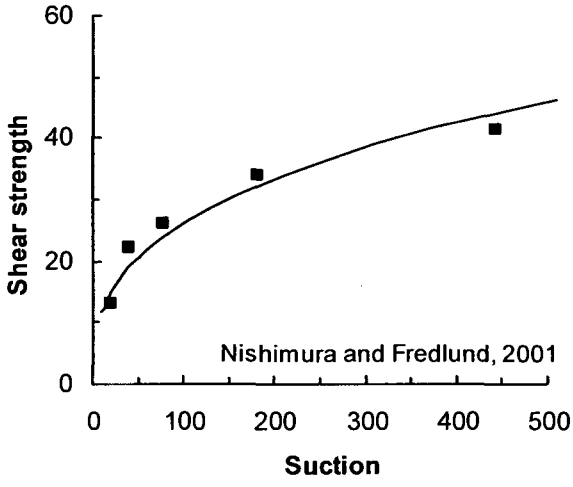

Figure 3.40. Predicted versus measured values for Nishimura and Fredlund silt. (Xu, 2004)

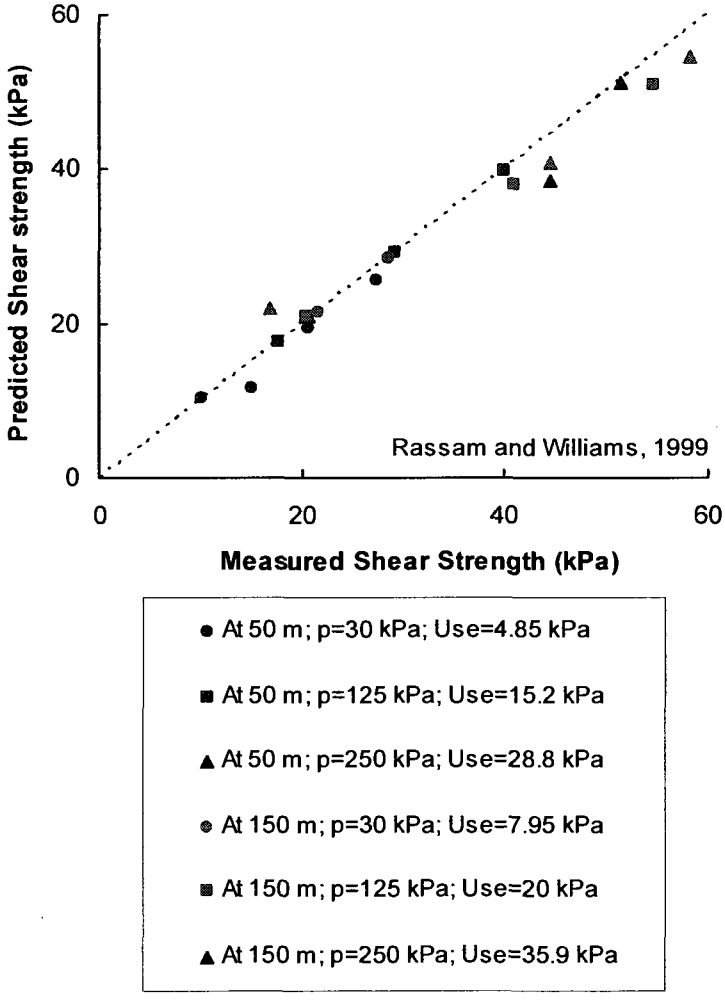

Figure 3.41. Predicted versus measured values for Rassam and Williams' Kidston tailings taken from both 50 m and 150 m. (Xu, 2004)

3.4.21 Tekinsoy, Kayadelen, Keskin and Söylemez (2004)

The authors proposed a logarithmic equation (Eqn. 3-64) with two fitting parameters, *m* and *n* to study the change in shear strength with an increase in suction. Two boundary equations were suggested to define the fitting parameters in terms of the known soil parameters. Firstly, they set the value of suction to 0 kPa and the value of *n* is defined in terms of *m* and P_{at} (Eqn. 3-60). Substituting back into the original equation produces Equation 3-61. The second boundary condition is obtained by differentiating the equation with respect to suction (Eqn. 3-62) which is equal to the change in shear strength with respect to suction, $tan\ \phi^b$. At the air-entry value (AEV), $tan\ \phi^b = tan\ \phi'$. The equation is then given in terms of the suction (at AEV) and the angle of internal friction of the soil and the atmospheric pressure. Substituting the value of *m* into the equation results in the predictive equation of Tekinsoy et al (Eqn. 3-64).

$$\tau_{us} = m \cdot ln[(u_a - u_w) + p_{at}] + n \quad [3\text{-}59]$$

$$n = m \cdot ln[p_{at}] \quad [3\text{-}60]$$

$$\tau_{us} = m \cdot ln\left[\frac{(u_a - u_w) + p_{at}}{p_{at}}\right] \quad [3\text{-}61]$$

$$\frac{d\tau_{us}}{d(u_a - u_w)} = \frac{m}{(u_a - u_w) + p_{at}} = tan\phi^b \quad [3\text{-}62]$$

$$m = tan\phi' \cdot (u_a - u_w)_b + p_{at} \quad [3\text{-}63]$$

$$\tau_{us} = tan\phi'[(u_a - u_w)_b + p_{at}] \cdot ln\left[\frac{(u_a - u_w) + p_{at}}{p_{at}}\right] \quad [3\text{-}64]$$

where p_{at} is the atmospheric pressure (101.3 kPa)

The authors utilized five sets of published data to test the equation (Table 3.8). Miao's equation (Eqn. 3-45) was used to for and Equation 3-64 was applied to Miao's Nanyang expansive soil (Figure 3-42). Both equations provide an adequate fit for the measured data. Miao's equation, Rassam and Cook's equation prediction equation was also plotted with Equation 3-64 and the measured data for Gan's glacial till (Figure 3.42). The

other three soils were compared to the prediction equation by Tekinsoy et al (Figure 3-42). For all five soils, the predictive equation was an adequate fit to the measured data.

Table 3.8. Published soils used to test Equation 3-64.

Nanyang expansive soil	Miao et al, 2002
Glacial till	Gan et al, 1988
Glacial till	Vanapalli et al, 1996
Dhanauri clay	Gulhati and Satija, 1981
Notch Hill silt	Krahn et al, 1989

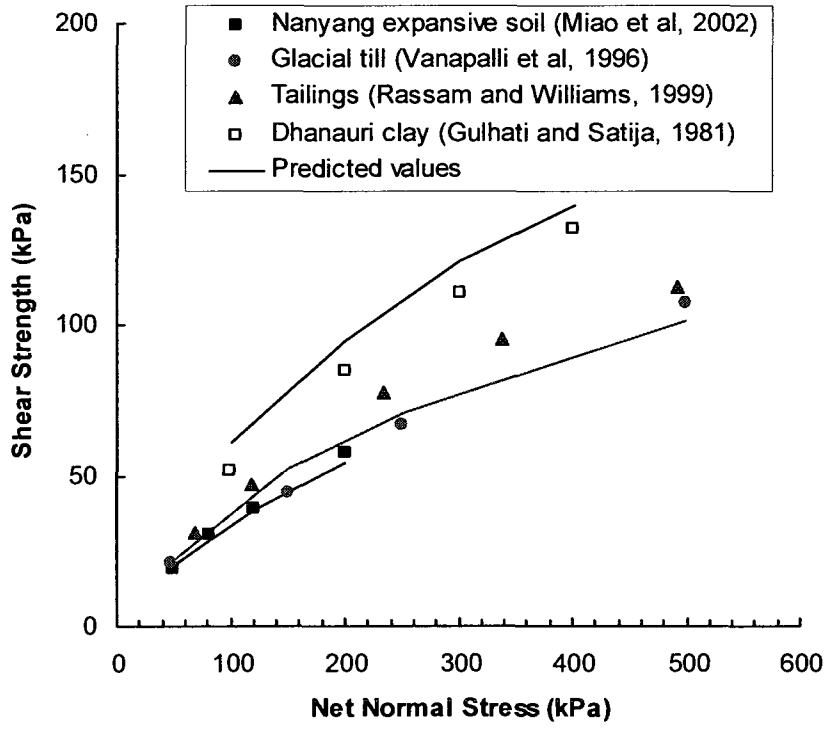

Figure 3.42. Published values used by the investigators to test Equation 3-64. (Tekinsoy et al, 2004)

3.4.22 Lee, Sung, Cho (2005)

The authors tested weathered Korean granite to examine the change in shear strength with an increase in suction. The study also included the examination of changes with respect to the net normal stress. Lee et al measured the SWCC was measured using a confining pressure controlled extractor (CPCE). The CPCE is a modified pressure plate extractor apparatus that resembles a small triaxial cell. The CPCE can test the soils under different isotropic confining stresses. Shear testing was performed by a typical modified triaxial compression test apparatus. The authors make note of the use of a diffused air volume indicator (DAVI) to remove the diffused air from the system during testing.

The authors propose an equation to fit the shear strength data. The equation recognizes the linear relationship between the shear strength and suction up to the AEV (Eqn. 3-65). The authors discuss the linear relationship between the AEV and the net normal stress (Figure 3.43) to determine the AEV at any confining pressure (Eqn. 3-65).

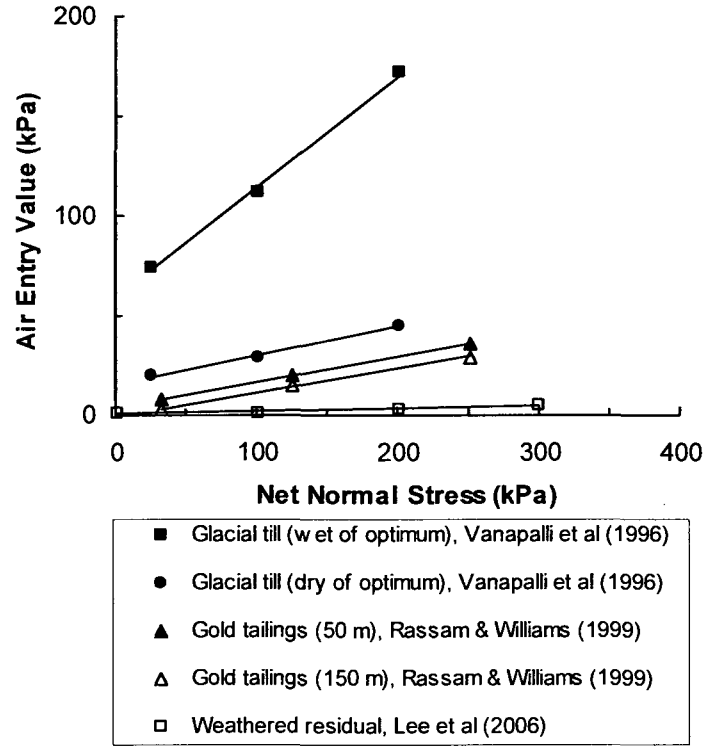

Figure 3.43. Relationship between the air-entry value and net normal stress for several soils. (Lee et al, 2005)

$$AEV = AEV_I + AEV_S(\sigma_s - u_a) \quad [3\text{-}65]$$

The equation to determine the unsaturated shear strength beyond the AEV uses two fitting parameters κ and λ (Eqn. 3-67). The fitting parameters were obtained by fitting the equation to experimental data. The authors used two method of fitting the equation:

1. Using the SWCC values when the net normal stress is 0 kPa.

2. Using the SWCC measured at the same net normal stress condition as the corresponding shear strength test.

if $(u_a - u_w) \leq AEV$:

$$\tau = c' + (\sigma_a - u_a) \cdot tan\phi' + (u_a - u_w) \cdot tan\phi' \quad [3\text{-}66]$$

if $(u_a - u_w) > AEV$:

$$\tau = c' + (\sigma_a - u_a) \cdot tan\phi' + AEV \cdot tan\phi' + [(u_a - u_w) - AEV]\theta^{\kappa}[1 + \lambda(\sigma_n - u_a)] \cdot tan\phi' \quad [3\text{-}67]$$

When data used from the SWCC measured with a net normal stress equal to that of the shear strength test condition, the resulting curve from Equations 3-66 and 3-67 (Figure 3.44) fit to the data very closely. Alternately, the curves generated from the SWCC measured a net normal stress equal to 0 kPa do not reasonably fit well, but still provide an adequate fit.

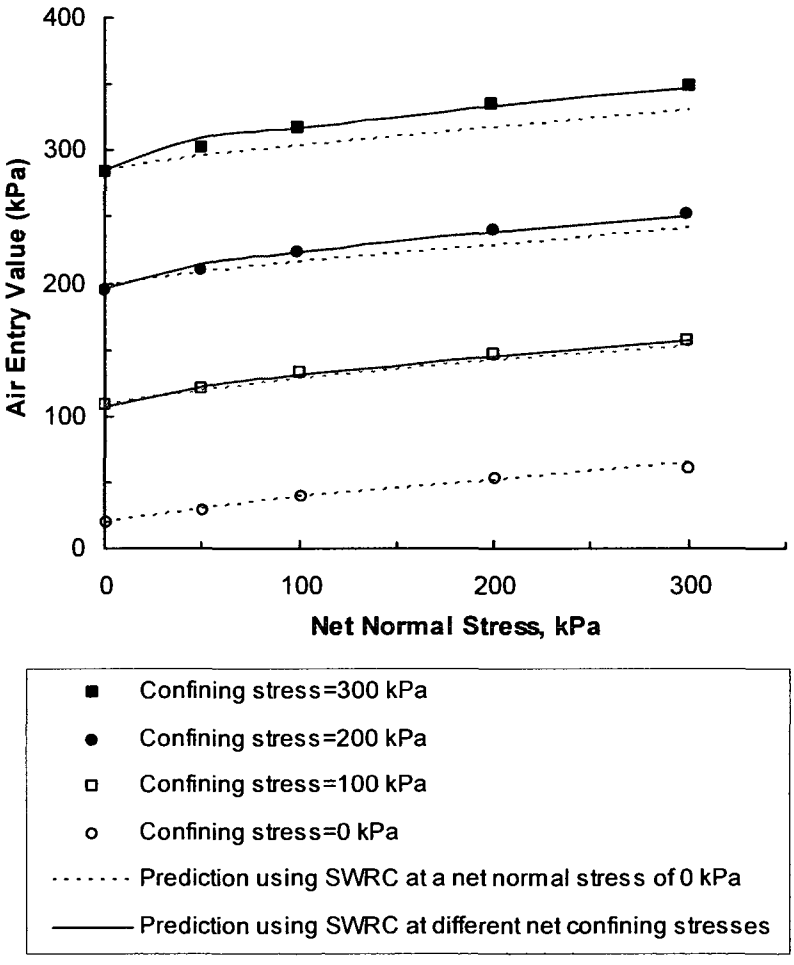

Figure 3.44. Measured and predicted relationships for weathered granite at different conditions. The data is presented with two separate prediction curves: one at a SWCC at 0 kPa confining stress and at varied confining stresses. (Lee et al, 2005)

3.4.23 Matsushi and Matsukura (2006)

Matsushi and Matsukura (2006) proposed an empirical equation for the prediction of shear strength of unsaturated soils. The authors express the opinion that there are no reliable values in matric suction available in practice. Instead, they propose predicting by using a hyperbolic equation to predict the change in apparent cohesion with respect to volumetric water content.

They use a shear box to test two undisturbed residual soils. The water contents were changed by drying in a low temperature oven and wetting to an appropriate moisture

content and allowing to come to equilibrium. Each soil was prepared in five different ways: ovendried, air-dried, natural water content, 5 ml water added and either 10 mL or13 mL water added. Each soil was subjected to different normal stresses of 10, 20, 30 and 40 kPa.

Using the five conditions (Table 3.9), the authors fit a curve to the data via regression (Eqn. 3-68). They make two assumptions:

1. The angle of shearing resistance, ϕ', remains constant.

2. An exponential function is appropriate to related apparent cohesion and volumetric water content.

Table 3.9. Summary of soil conditioning methods from Matsushi and Matsukura, 2006.

Sand-Soil		Silt-Soil	
A	Oven dried (40°C)	G	Oven dried (40°C)
B	Air dried (25°C)	H	Air dried (25°C)
C	Natural water content	I	Natural water content
D	Add 6 mL water	J	Add 5 mL water
E	Add 13 mL water	K	Add 10 mL water
F	Capillary saturation	L	Capillary saturation

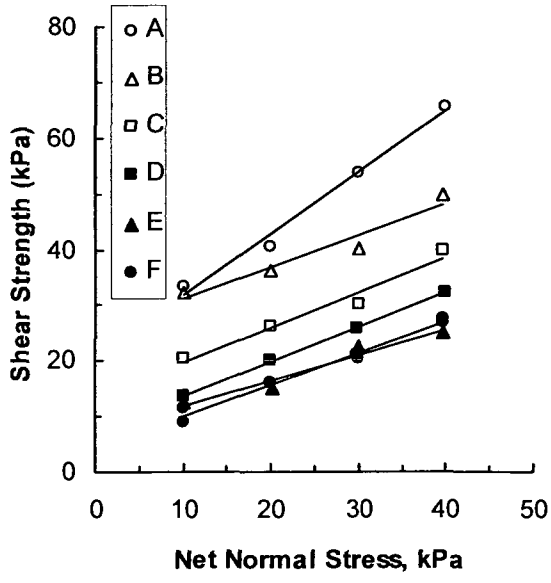

Figure 3.45. Relationship between the net normal stress and shear strength for a soil under 6 different moisture conditions for a sand soil. (Matsushi and Matsukura, 2006)

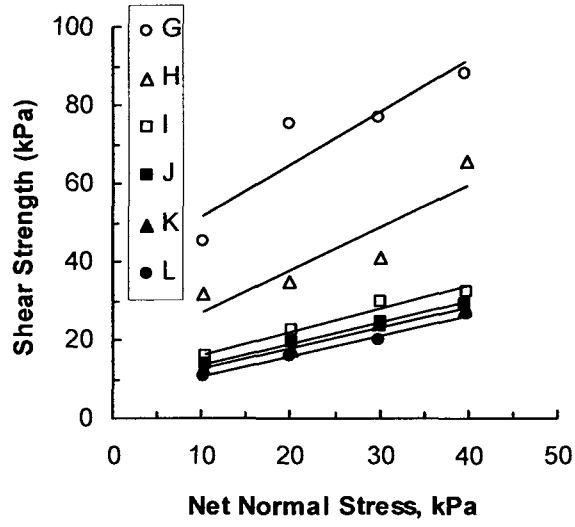

Figure 3.46. Relationship between the net normal stress and shear strength for a soil under 6 different moisture conditions for a silt soil. (Matsushi and Matsukura, 2006)

$$\tau = \sigma' \cdot tan\phi' + Ce^{-\mu\theta} \quad [3\text{-}68]$$

$$\ln[\tau - \sigma' \cdot \tan\phi'] = -\mu\theta + \ln C \quad [3\text{-}69]$$

1. Assign an arbitrary value to ϕ'.
2. Compute the term $\ln[\tau - \sigma' \cdot \tan\phi']$ for every data set of τ and σ'.
3. Conduct a simple linear-regression for the data sets of $\ln[\tau - \sigma' \cdot \tan\phi']$ and θ.
4. Repeat 1-3 to seek the most suitable value of ϕ'.
5. Determine the value of ϕ' which gives the highest correlation coefficient.
6. Determine the value of C and μ from the y-intercept (ln C) and inclination ($-\mu$) of the regression line.

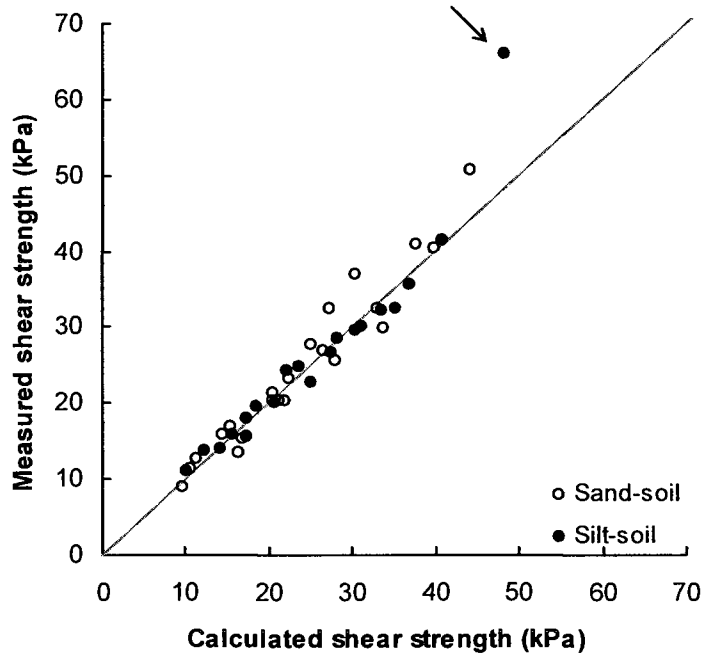

Figure 3.47. Comparison of calculated shear strength versus the measured shear strength. (Matsushi and Matsukura, 2006)

Determining the fitting parameters requires measured data. The ability of the equation to fit the curve is illustrated in Figure 3.47. The correlation seems acceptable with the exception of one point which was noted by the authors.

3.4.24 Vilar (2006)

The investigator proposed an enhancement to the equation proposed by Lee et al, 2003. (Eqn. 3-50). The equation uses this hyperbolic equation and applies two conditions to define the curve fitting variables (*a* and *b*): The condition of the soil when the suction is less than the air-entry value (AEV) is shown in Eqn. 3-51. As the suction approaches zero, the inverse of the variable *a* approaches the slope of the line tan ϕ'. The author assumes that the maximum cohesion occurs when the soil reaches the residual degree of saturation resulting in Eqn. 3-51, and is the same equation presented by Lee et al, 2003. The authors propose that the residual suction could be determined from air dried samples, thus determining *b* (Eqn. 3-71).

$$c = c' + \frac{\psi}{(a + b\psi)} \quad [3\text{-}50]$$

$$\left.\frac{dc}{d\psi}\right|_{\psi \to 0} = \frac{1}{a} = \tan\phi' \quad [3\text{-}51]$$

$$\lim_{\psi \to \infty} = c_{ult} = c' + 1/b \quad [3\text{-}70]$$

$$b = \frac{1}{(c_{ult} - c')} \quad [3\text{-}71]$$

The investigator used the equation on 12 different soils. The air dried or ultimate cohesion value of the published soils data was not determined so the maximum cohesion was used instead by altering Eqn. 3-71 to:

$$b = \frac{1}{(c_m - c')} - \frac{1}{(\psi_m \tan\phi')} \quad [3\text{-}72]$$

The air dried or ultimate cohesion value of the published soils data was not determined so the shear strength contribution due to suction at the largest suction was used instead. Only shear strength data within the range of 0~500 kPa was used in this thesis. The final resulting equation is given by:

$$\tau_{us} = \frac{(u_a - u_w)}{\frac{1}{\tan\phi'} + \left(\frac{1}{\tau_{us-max}} - \frac{1}{(u_a - u_w)_{max} \cdot \tan\phi'}\right)} \quad [3\text{-}73]$$

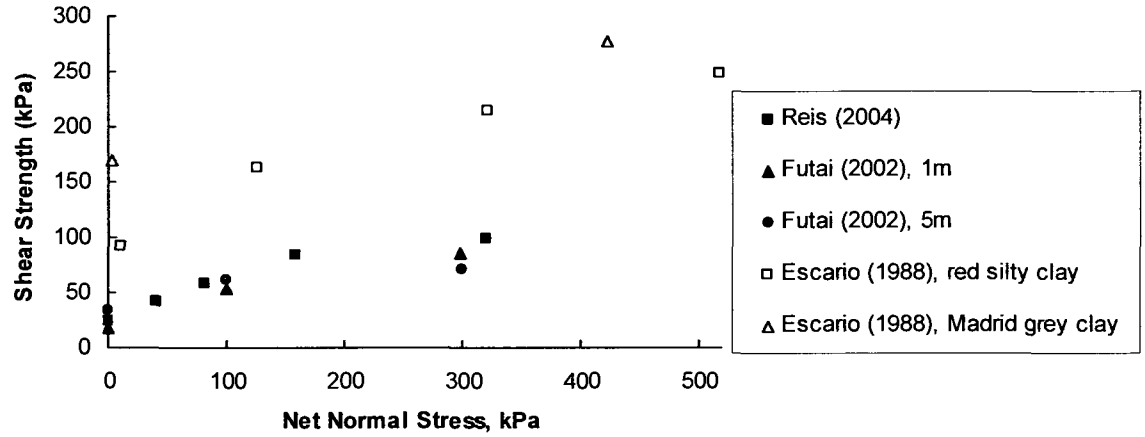

(a)

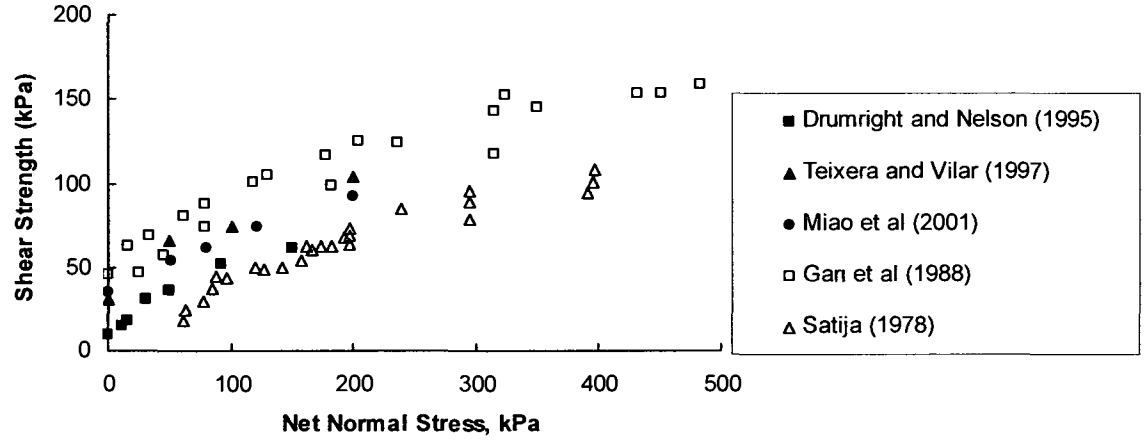

(b)

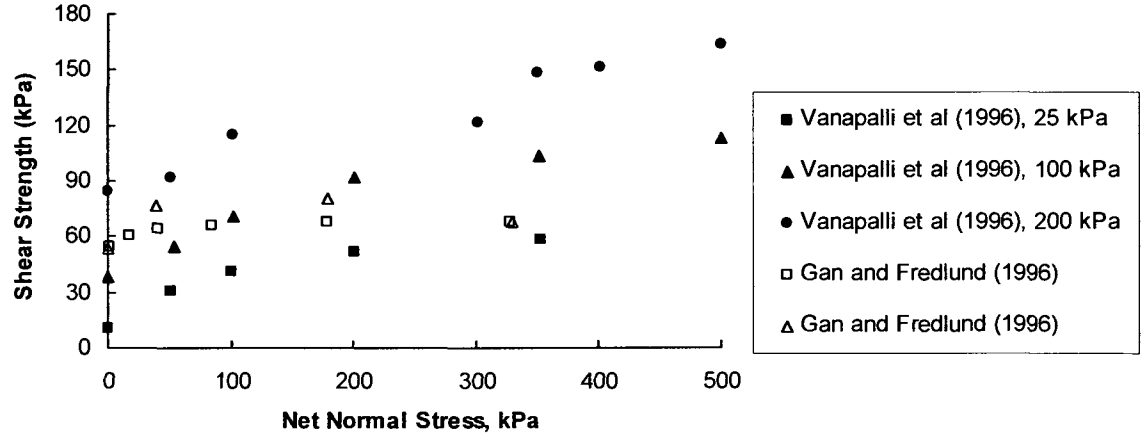

(c)

Figure 3.48. Shear strength data used to test the semi-empirical equation (Vilar, 2006).

3.5 Summary

Several investigators have contributed to better understand the shear strength behaviour of unsaturated soils. To date, there are twenty-five equations available in the literature to describe and predict shear strength of unsaturated soils to best of the knowledge of the author. Although most equations are related to the suction of the soil, two of these equations are formulated based on the water content. Only a few of the equations are truly predictive in nature and many of them are purely empirical. Most of the proposed equations were verified on using limited data. This is still an emerging field which requires more studies that need extensive testing under controlled conditions. Our present understanding is still at its infancy and needs more investigations.

The next chapter defines the guidelines for predicted data to provide an acceptable fit to measured data. The chapter also provides the validation for the equations that was published with the shear strength equations and revisits the validation with respect to the new guidelines for an acceptable fit.

CHAPTER 4 VALIDATION OF SHEAR STRENGTH EQUATIONS

4.1 Introduction

The two key equations; namely, Bishop's (1959) equation and Fredlund et al (1978) equation that are commonly used in the literature for interpreting the experimental results were briefly discussed in the earlier chapters.

Table 4.1. The two equations used for interpreting the shear strength of unsaturated soils.

$\tau = c' + (\sigma - u_w) \cdot tan\phi' + \chi(u_a - u_w) \cdot tan\phi'$ *Bishop, 1959*	[2-13]
$\tau = c' + (\sigma - u_a) \cdot \tan\phi' + (u_a - u_w) \cdot \tan\phi^b$ *Fredlund, Morgenstern and Widger, 1978*	[1-1]

The Bishop's (1959) equation extends the Terzaghi effective stress principle in the conventional Mohr-Coulomb approach through the use of a variable, χ, which is related to the degree of saturation in the soil. The Fredlund et al (1978) equation also uses Mohr-Coulomb approach, however, it is based on two independent stress state variables, $(\sigma - u_a)$ and matric suction, $(u_a - u_w)$. The prediction equations that are proposed in the literature are consistent with the Fredlund et al 1978 equation.

Twenty-five equations have evolved over the last fifty years to predict or estimate the shear strength of unsaturated soils. As the measurement of the shear strength of unsaturated soils is expensive, time-consuming and requires specialized equipment and personnel. Table 4.2 summarizes the shear strength equations that have been proposed for predicting the shear strength of unsaturated soils.

There is currently no set standard to determine if predicted shear strength values provide an 'acceptable fit' to measured data points. A visual assessment was often used to comment on the correlation of calculated and measured values. In this thesis, an acceptable fitting guide is established to quantify the ability of the soil to fit the data. This

chapter presents and discusses the data that has been published and quantifies the ability of an equation to provide and 'acceptable fit'.

Table 4.2a. Summary of equations that use the SWCC as a tool.

$\tau = c' + [(\sigma - u_a) + \chi(u_a - u_w)] \cdot \tan\phi'$ Bishop, 1959	2-13
$\tau = c' + (\sigma - u_a) \cdot \tan\phi' + (u_a - u_w) \cdot \theta_w \cdot \tan\phi'$ Lytton, 1995	3-10
$\tau = c' + (\sigma - u_a) \cdot \tan\phi' + S \cdot (u_a - u_w) \cdot \tan\phi'$ Öberg and Sallfors, 1995, 1997	3-11
$\tau = c' + (\sigma - u_a) \cdot \tan\phi' + (u_a - u_w)(\Theta^{\kappa})(\tan\phi')$ Vanapalli, Fredlund, Pufahl and Clifton, 1996 Fredlund, Xing, Fredlund and Barbour, 1996	3-13
$\tau_{us} = (u_a - u_w)\left(\frac{\theta - \theta_r}{\theta_s - \theta_r}\right)(\tan\phi')$ Vanapalli, Fredlund, Pufahl and Clifton, 1996	3-17
$\tau = c' + (\sigma - u_a) \cdot \tan\phi' + (u_a - u_w)\left(\frac{log(u_a - u_w)_r - log(u_a - u_w)}{log(u_a - u_w)_r - log(u_a - u_w)_b}\right)(\tan\phi')$ Bao, Gong and Zhan, 1998	3-23
$\tau = c' + \left[(\sigma - u_a) + \left[\frac{(u_a - u_w)}{(u_a - u_w)_b}\right]^{\eta}(u_a - u_w)\right] \cdot \tan\phi'$ Khalili and Khabbaz, 1998	3-25
$\tau = c' + (\sigma - u_a) \cdot \tan\phi' + f_1 \cdot (u_a - u_w) \cdot \theta \cdot \tan\phi'$ Aubeny and Lytton, 2003	3-48
$\tau = c' + (\sigma - u_a) \cdot \tan\phi' + \tan\phi'[(u_a - u_w)_b + p_{at}] \cdot ln\left[\frac{(u_a - u_w) + p_{at}}{p_{at}}\right]$ Tekinsoy, Kayadelen, Keskin and Soylemez, 2004	3-64

Table 4.2b. Summary of equations based on mathematical fitting methods.

$\tau = c' + (\sigma - u_a)tan\phi' + (u_a - u_w)tan\phi^b$ Fredlund, Morgenstern and Widger, 1978	1-1
$(\tau_m + \tau_b)^{2.5} - (\tau_o + \tau_b)^{2.5} = (\tau_o + \tau_b)^{1.5} \cdot (u_a - u_w)_m \cdot tan\phi'$ Escario and Juca, 1989	3-1
$\tau = c' + (\sigma - u_a) \cdot tan\phi' + \alpha \cdot (u_a - u_w)^{\beta}$ Abramento and Carvalho, 1989	3-3
$q = c'' + (p - u_a) \cdot tan\alpha'$ Rohm and Vilar, 1995	3-12
$\tau = c' + (\sigma - u_a) \cdot tan\phi' + (u_a - u_w)\frac{1}{1 + d(u_a - u_w)} \cdot tan\phi'$ Shen, 1996	3-18
$\tau = c' + (\sigma - u_a) \cdot tan\phi' + (u_a - u_w)\frac{1}{\frac{1}{tan\alpha} + \frac{(u_a - u_w)}{\beta}}$ Yu, Ma and Wang, 1998	3-24
$C_A = c' + \frac{(u_a - u_w)}{a + b(u_a - u_w)}$ Lee, Lee and Kim, 2003	3-50
$\tau = c' + (\sigma - u_a) \cdot tan\phi' + \frac{(u_a - u_w)}{a_2 + b_2 \cdot (u_a - u_w)}$ Schick, 2004	3-53
$\tau = c' + (\sigma - u_a) \cdot tan\phi' + \frac{(u_a - u_w)}{\frac{1}{tan\phi'} + \left(\frac{1}{\tau_{us-max}} - \frac{1}{(u_a - u_w)_{max} \cdot tan\phi'}\right)}$ Vilar, 2006	3-73

Table 4.2c. Summary of other equations.

$\tau = c' + (\sigma - u_a) \cdot \tan\phi' + P_s \cdot \tan\phi'$ Lu et al, 1992	3-7
$\tau = \alpha + \sigma \cdot \tan\phi' + (u_a - u_w) \cdot \tan\phi' - \varphi[(u_a - u_w) - (u_a - u_w)_b]^{\beta}$ Rassam and Williams, 1999	3-29
$\tau = c' + (\sigma - u_a) \cdot \tan\phi' + m^{1-\varsigma} \cdot (u_a - u_w)^{\varsigma} \cdot \tan\phi'$ Xu and Sun, 2001	3-41
$\tau = (u_a - u_w) \cdot \tan\phi' - \left[\frac{\psi_r \cdot \tan\phi' - \tau_{Sr}}{(\psi_r - \psi_e)^{\beta}}\right][(u_a - u_w) - (u_a - u_w)_b]^{\frac{\tan\phi' \cdot (\psi_r - \psi_e)}{\tan\phi' \cdot \psi_r - \tau_{Sr}}}$ Rassam and Cook, 2002	3-47
$\tau = c' + (\sigma - u_a) \cdot \tan\phi' + (u_a - u_w)_b^{1-\zeta_2} \cdot (u_a - u_w)^{\zeta_2} \cdot \tan\phi'$ Xu, 2004	3-57
$\tau = c' + (\sigma_a - u_a) \cdot \tan\phi' + AEV \cdot \tan\phi' + [(u_a - u_w) - AEV]\theta^{\kappa}[1 + \lambda(\sigma_n - u_a)] \cdot \tan\phi'$ Lee, Sung and Cho, 2005	3-67

4.2 An Acceptable Fit to Measured Data?

In this thesis, predicted shear strength is suggested to be acceptable value if it is within 10% of the measured value of the data set. A data set is defined to provide a successful or acceptable fit when 50% or more of the predicted shear strength values from the data set are within the 10% of the measured values.

The acceptable limit is applied as a percentage of the shear strength contribution due to suction. Compared to the total shear strength (which the sum of the shear strength of saturated soil and the shear strength contribution due to unsaturated condition), the shear strength contribution due to suction can be small. The analyses of an acceptable fit based on shear strength contribution as well as total shear strength will be presented and discussed.

Exceptions

Exceptions to the limit of an acceptable fit are necessary in certain cases when the predicted shear strength value deviates from the trends of the measured shear strength values due to reasons such as the experimental errors. In such a scenario, the data

point may be excluded from the data set using engineering judgement. The individual data point will not be included in the count of values for an acceptable fit; however, the value will be shown in the plots.

However, when the measured shear strength values are less than 50 kPa, a tolerance of ± 5 kPa will be considered acceptable instead of using the criteria defined.

4.3 Analysis of Published Results

A selected number of prediction equations are used to provide comparisons between the measured and predicted shear strength values. The reasons associated with why only certain prediction equations have been used in this study are discussed in a later section. This section discusses the ability of the equations to fit experimental data. The results from the published articles are shown in this chapter and also the data is summarized in the form of tables.

The table in which the data is summarized has four columns: number of data points, number of points with an acceptable fit, average deviation and acceptable fit. The number of data points is the total number of shear strength data points. The second column has the number of data points that provide an acceptable fit as per the introduced definition. This column compares the predicted values to the measured values using the following formula:

$$Deviation(\%) = \left| \frac{(\tau_{predicted} - \tau_{measured})}{\tau_{measured}} x100 \right| \qquad [4\text{-}1]$$

The average deviation is the average of the absolute value of all deviations for a data set:

$$Average\ Deviation = \frac{\sum |Deviation(\%)|}{n} \qquad [4\text{-}2]$$

In the above equation, n is the total number of points in a data set. Ideally, the average deviation should be 10% or less to be an acceptable fit. The column with the heading acceptable fit and a question mark is a column that can be used as a quick reference as to whether an equation meets the criteria.

The percent deviation was arbitrarily chosen by values that may be considered as an acceptable fit for practical applications. The ability to predict the unsaturated shear strength within 10% can be considered to be acceptable in geotechnical engineering practice. The average deviation value (Eqn. 4-2) can be used to indicate if there is large deviation occurring within a data set and indicate the ability for the equation to approximate the shape. If the average deviation for a set of shear strength data is within 10%, it may indicate that the calculated values will approximate the shape of the curve made by measured data points (Figure 4.1a). When the average deviation is greater than 10%, it indicates that the shape of a curve through calculated values is different from the curve of measured data points (Figure 4.1b). Alternately, a larger average deviation may indicate a variation within the measured data (Figure 4.1c).

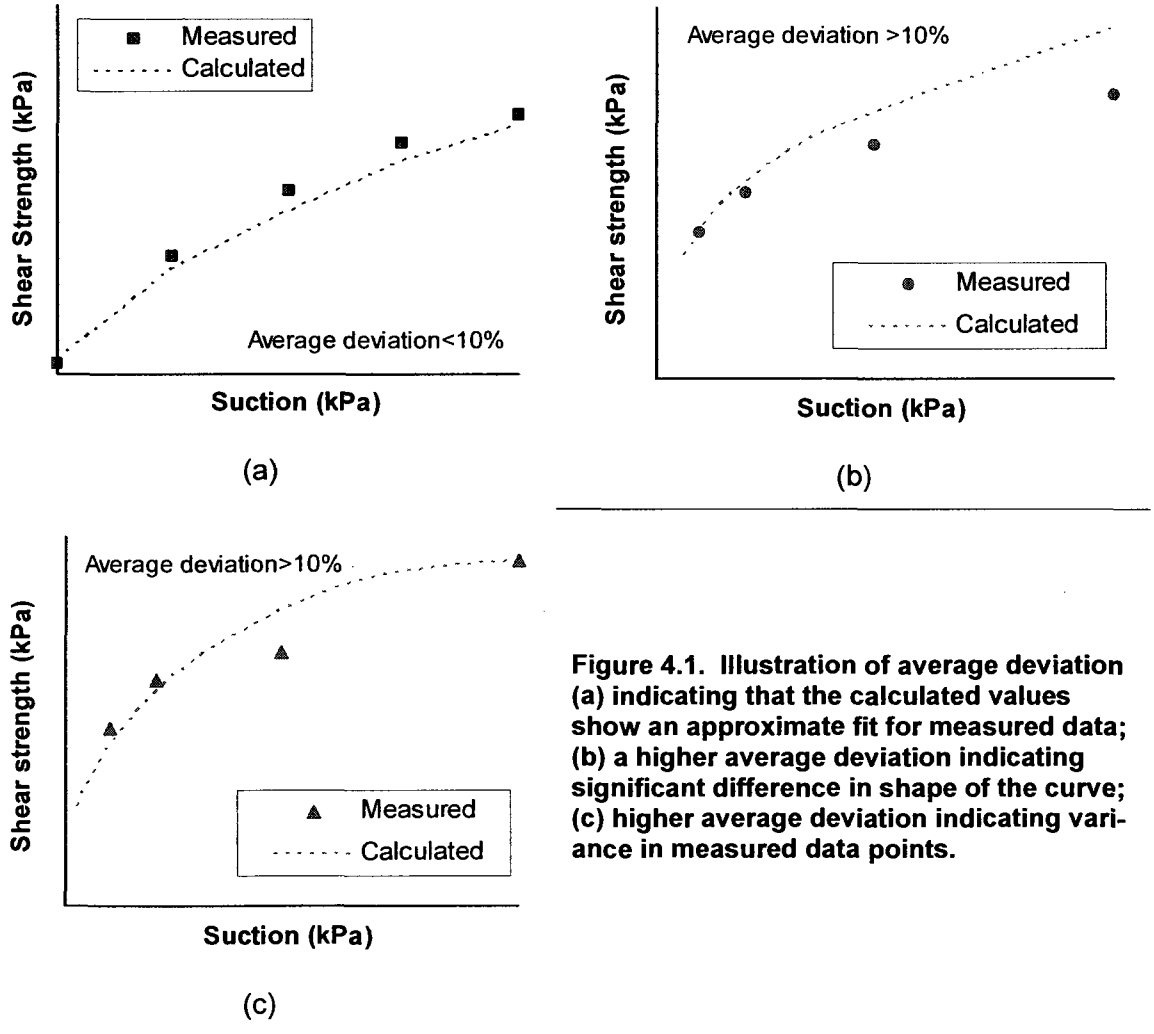

Figure 4.1. Illustration of average deviation (a) indicating that the calculated values show an approximate fit for measured data; (b) a higher average deviation indicating significant difference in shape of the curve; (c) higher average deviation indicating variance in measured data points.

4.3.1 Escario and Juca (1989)

The authors proposed a 2.5 degree elliptical equation, which is a mathematical fitting method to provide comparisons between the measured and estimated values of shear strength (Eqn. 3-1). The proposed equation was used on shear strength data measured on three different soils.

The soils include two clays; namely, Red silty clay and Madrid grey clay, and one sand, which is Madrid clay sand. The shear strength behaviour of these three compacted soils was measured using a modified direct shear apparatus. The Red silty clay was tested under three different net normal stresses of 120, 300 and 600 kPa over a range of suction from 0 to 14,000 kPa. The Madrid grey clay was tested only under a net normal stress of 300 kPa over a range of suction from 0 to 14,000 kPa. Finally, the Madrid clay sand was tested under two different net normal stresses of 120 and 600 kPa over a range of suction from 0 to 4,000 kPa and 0 to 2,000 kPa, respectively. The relationship provided an adequate fit to the each of the six sets of measured data (Table 4.3; Figure 4.2).

This equation cannot be used as an equation for predicting the variation of shear strength with respect to suction as this equation does not have any parameters or constants used which are related to other soil properties.

$$\tan\phi' \cdot \left(\frac{\tau_o + \tau_b}{(u_a - u_w)_m}\right)^{1.5} \left((u_a - u_w)_m - (u_a - u_w)\right)^{2.5} + (\tau + \tau_b)^{2.5} = (\tau_m + \tau_b)^{2.5} \qquad [3\text{-}1]$$

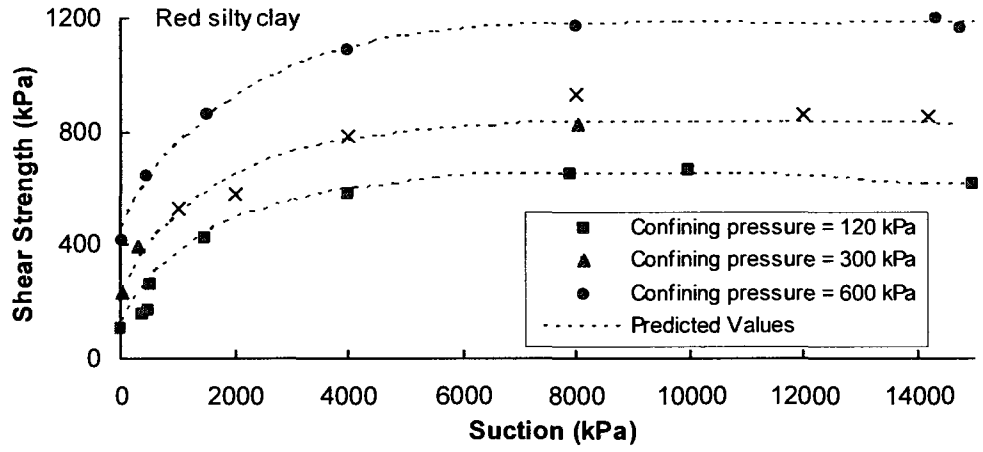

(a)

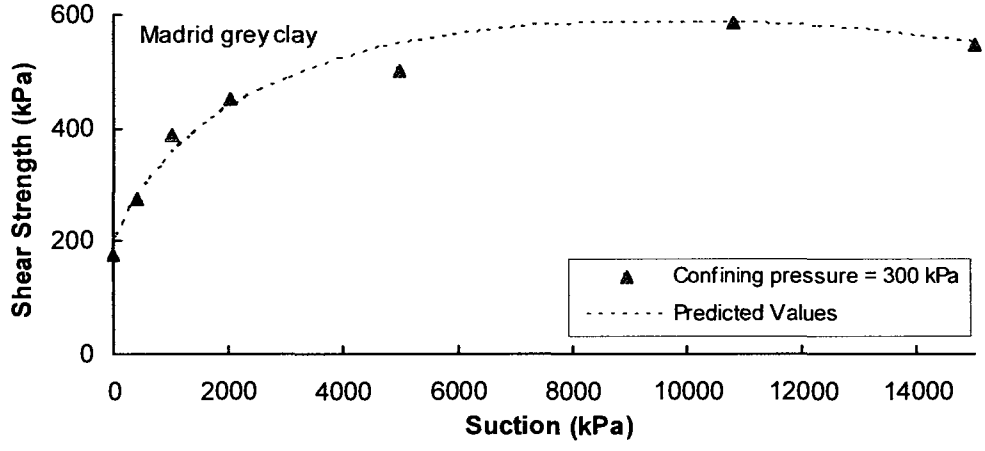

(b)

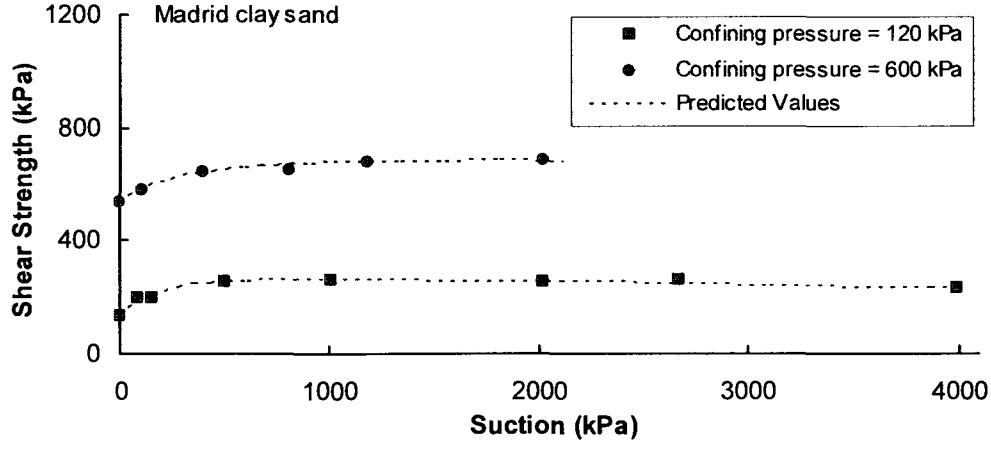

(c)

Figure 4.2. Illustration of predicted values to match measured values for (a) Red silty clay, (b) Madrid grey clay and (c) Madrid clay sand. (from Escario and Juca, 1989)

Table 4.3. Results of analysis of Equation 3-1 from Escario and Juca (1989)

Soil	No. of Data Points	No. of Points with an Acceptable Fit	Average Deviation (%)	Acceptable Fit? (Y/N)
Red Silty Clay (σ_n=120 kPa) *Escario and Juca (1989)*	9	6	6.9	Y
Red Silty Clay (σ_n=300 kPa) *Escario and Juca (1989)*	3	2	9.3	Y
Red Silty Clay (σ_n=600 kPa) *Escario and Juca (1989)*	7	7	2.3	Y
Madrid Grey Clay (σ_n=300 kPa) *Escario and Juca (1989)*	7	7	3.8	Y
Madrid Clay Sand (σ_n=120 kPa) *Escario and Juca (1989)*	8	8	1.9	Y
Madrid Clay Sand (σ_n=600 kPa) *Escario and Juca (1989)*	6	6	0.7	Y

4.3.2 Abramento & Carvalho (1989)

Abramento and Carvalho used the data measured from the Serra do Mar residual soil to test the fit of the proposed equation. The undisturbed samples were tested in a modified triaxial apparatus at a net confining pressure of approximately 10 kPa. The proposed equation adequately fits the measured data (Table 4.4; Figure 4.3). A total of 11 experiments were conducted using six different suction values. Several tests were conducted to check the repeatability of the results on specimens obtained from field to account for the possible differences in the soil conditions at the site.

$$\tau = c' + (\sigma - u_a) \cdot \tan\phi' \alpha \cdot (u_a - u_w)^{\beta} \qquad [3\text{-}3]$$

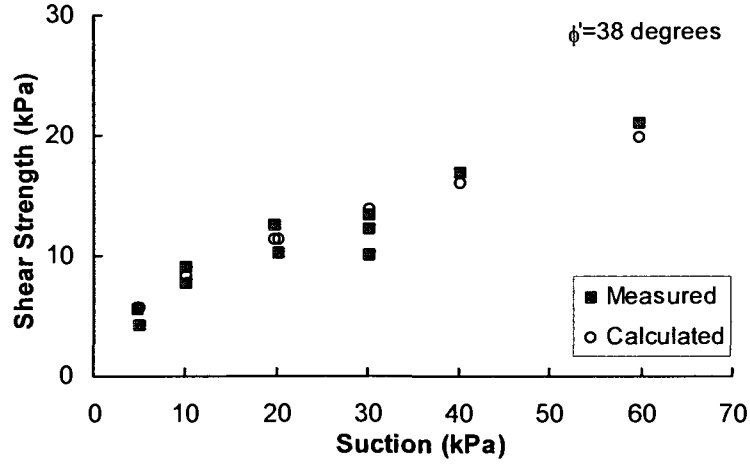

(a)

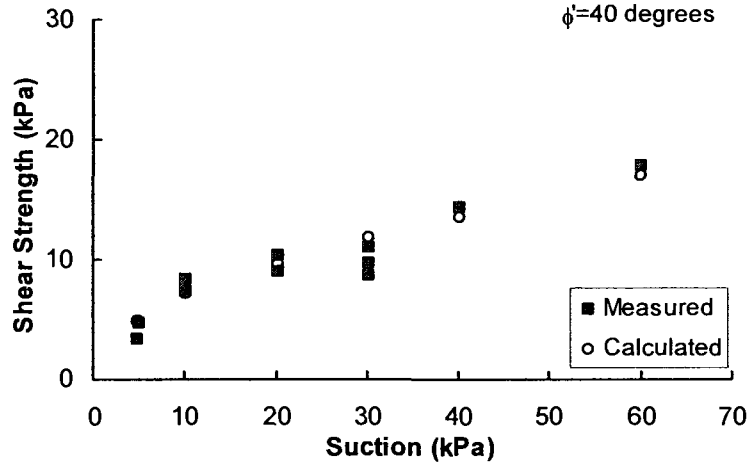

(b)

Figure 4.3. Experimental values and calculated values using Equation 3-3 based on two angles of internal friction: (a) 38 degrees and (b) 40 degrees. (from Abramento and Carvalho, 1989)

Table 4.4. Summary of analysis of Equation 3-3 from Abramento and Carvalho, 1989.

Soil	No. of Data Points	No. of Points with an Accept-able Fit	Average Deviation (%)	Acceptable Fit? (Y/N)
Serra do Mar Residual Soil (using $\phi = 38^{\circ}$)	11	8	9.6	Y
Serra do Mar Residual Soil (using $\phi = 40^{\circ}$)	11	8	11.0	Y

4.3.3 Lytton (1995)

Lytton presented Lamborn's equation (1986) and used the shear strength data of Lam (1980) and Peterson (1992) to test the ability to predict the shear strength of unsaturated soils. The correlation is marginally acceptable for the weathered rhyolite but provides a good fit for the Buckshot clay (Table 4.5; Figure 4.4). The weathered rhyolite is listed as acceptable as it meets the criteria for an acceptable fit. However, the average deviation of the set of points is greater than 10%. This can be explained by the marginal acceptability of the fit and the large deviation in the non-fitting points. Figure 4.4 shows the points for the given data and indeed supports the large deviation in the non-fitting points. There is a large distribution of the measured shear strength values for different samples tested at the same suction value.

$$\tau = c' + (\sigma - u_a) \cdot \tan\phi' + (u_a - u_w) \cdot \theta_w \cdot \tan\phi' \qquad [3\text{-}10]$$

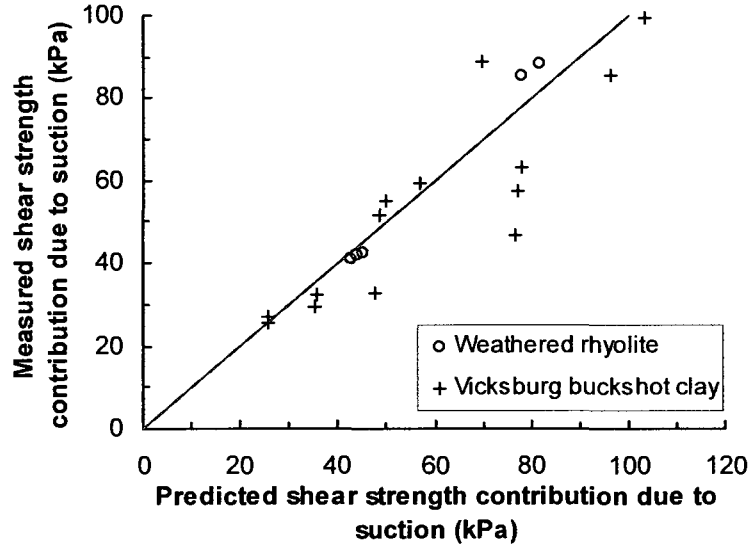

Figure 4.4. Comparison of measured values to predicted values from Lam, 1980. (from Lytton, 1995)

Table 4.5. Results of analysis of Equation 3-10 from Lytton (1995).

Soil	No. of Data Points	No. of Points with an Acceptable Fit	Average Deviation (%)	Acceptable Fit? (Y/N)
Weathered rhyolite *Lam (1980)*	15	8	17.4	Y
Vicksburg Buckshot clay *Peterson (1992)*	5	5	6.2	Y

4.3.4 Öberg and Sallfors (1997)

Öberg and Sallfors applied their equation (Eqn. 3-11) to eleven sets of shear strength data published in the literature (Table 4.6). The eleven soils were classified according to ASTM D-2487 as lean clays to heavy silt with varying degrees of sand. However, based on particle size analysis, the soils can be categorized as silts and sands. The Red silty clay and Madrid grey clay results of Escario and Saez (1986) had no particle size distribution to indicate the percentage of silt present in these soils.

The authors suggests to use the equation for predicting the shear strength behaviour of only silts and sands that have no plasticity. The resulting analysis shows that eight of the eleven soils show a reasonably good fit between the measured and predicted values of shear strength using Equation 3-11 (Table 4.6; Figures 4.5 and 4.6).

$$\tau = c' + (\sigma - u_a) + S \cdot (u_a - u_w) \cdot \tan\phi' \qquad [3\text{-}11]$$

Table. 4.6. Results of analysis on data presented for Equation 3-11 from Öberg and Sallfors (1997).

Soil ***(Authors)***	**No. of Data Points**	**No. of Points with an Acceptable Fit**	**Average Deviation (%)**	**Acceptable Fit? (Y/N)**
Glacial Till *Fredlund et al, 1987*	9	8	4.9	Y
Notch Hill Silt *Krahn 1989*	5	3	18.0	Y
Madrid Grey Clay *Escario and Saez (1986)*	5	4	6.1	Y
Red Silty Clay *Escario and Saez (1986)*	4	3	6.6	Y
Madrid Clay Sand *Escario and Saez (1986)*	5	2	11.7	N
Selset Clay *Bishop and Blight (1963)*	10	4	9.2	N
Mangle Shale *Bishop and Blight (1963)*	4	2	13.8	N
Serra do Mar Residual Soil (38°) *Abramento and Carvalho (1989)*	11	9	9.6	Y
Serra do Mar Residual Soil (40°) *Abramento and Carvalho (1989)*	11	9	9.2	Y
Dhanauri Clay *Gulhati and Satija (1981)*	5	3	11.0	Y
Jurong Residual Soil *Rahardjo et al (1995)*	6	6	5.0	Y

The SWCC is required for using the above equation. However, measured SWCC data was not available for all the soils tested. The SWCC of soils with similar properties from Andersson and Wiklert (1972) were used.

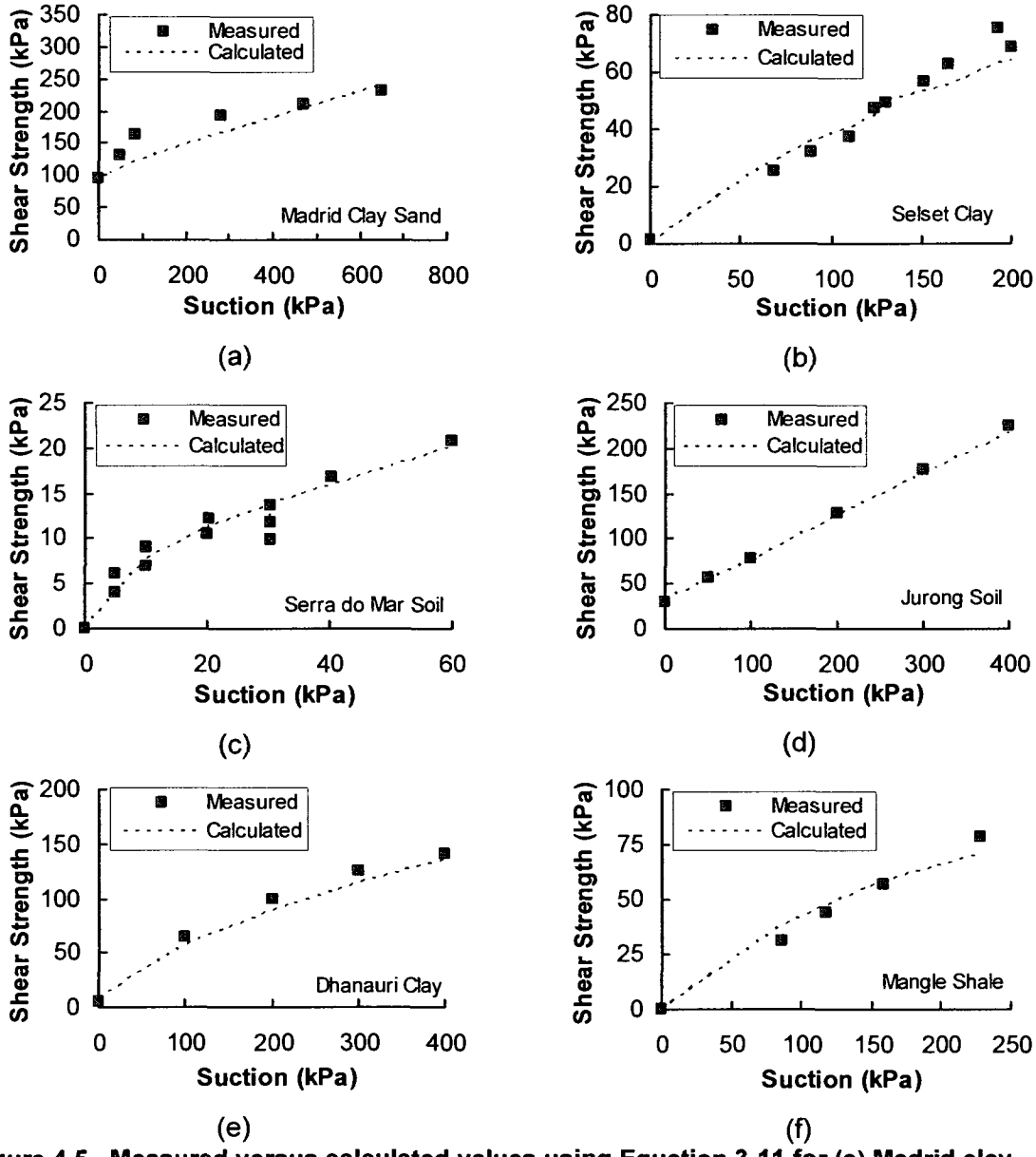

Figure 4.5. Measured versus calculated values using Equation 3-11 for (a) Madrid clay sand, (b) Selset clay, (c) Serra do Mar soil, (d) Jurong soil, (e) Dhanauri clay, and (f) Mangle shale. (modified from Öberg and Sallfors, 1995; Öberg and Sallfors, 1997)

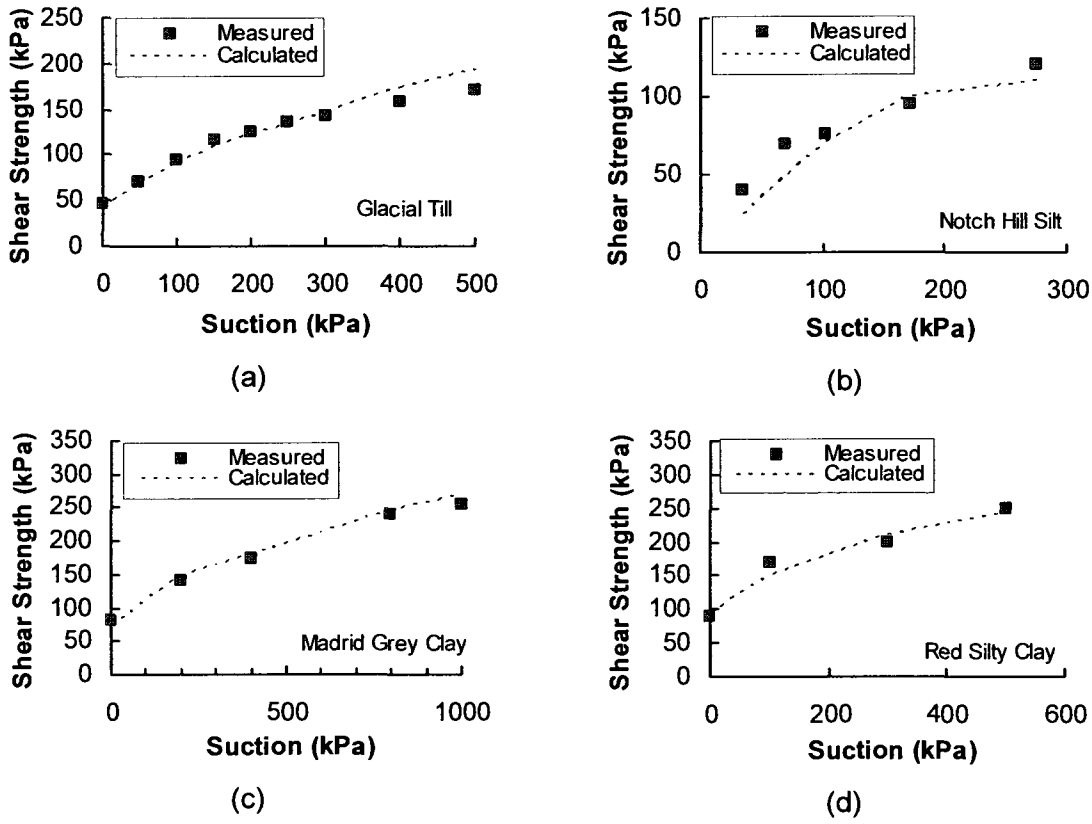

Figure 4.6. Measured versus calculated values using Equation 3-11 for (a) glacial till, (b) Notch Hill silt, (c) Madrid grey clay and (d) red silty clay. (modified from Öberg and Sallfors, 1995)

Vanapalli and Fredlund (2000) utilized the published data for red silty clay, Madrid grey clay and Madrid clay sand (Escario and Juca, 1989) to evaluate four equations. These authors evaluated the equations over the entire range of suction for each soil as well over a lower range of 0 to 1000 kPa.

The shear strength of Madrid clay sand was measured up to a suction of 8000 kPa while the clays were measured up to 14,500 kPa. The analysis of these soils was done in two stages: 1) the ability to fit over a range of suctions from 0 to 1000 kPa and then 2) the ability of the equation to fit the measured data over the entire range of suction (Table 4.7; Figure 4.7). Over a suction range of 0 to 1000 kPa, the equation provided an adequate fit only for the Madrid grey clay. When the data was examined over the entire range of suctions, both the Madrid gray clay and the Madrid clay sand provided an adequate fit using the predictive equation.

Table 4.7. Results of analysis of Equation 3-11 from Vanapalli and Fredlund (2000)

Soil	No. of Data Points	No. of Points with an Acceptable Fit	Average Deviation (%)	Acceptable Fit? (Y/N)
Up to suctions of 1000 kPa				
Madrid Clay Sand *Escario and Juca (1989)*	4	2	21.6	N
Madrid Grey Clay *Escario and Juca (1989)*	3	2	7.1	Y
Red Silty Clay *Escario and Juca (1989)*	4	1	26.2	N
Over the entire range of suction				
Madrid Clay Sand *Escario and Juca (1989)*	7	5	14.4	Y
Madrid Grey Clay *Escario and Juca (1989)*	7	4	10.2	Y
Red Silty Clay *Escario and Juca (1989)*	8	1	34.4	N

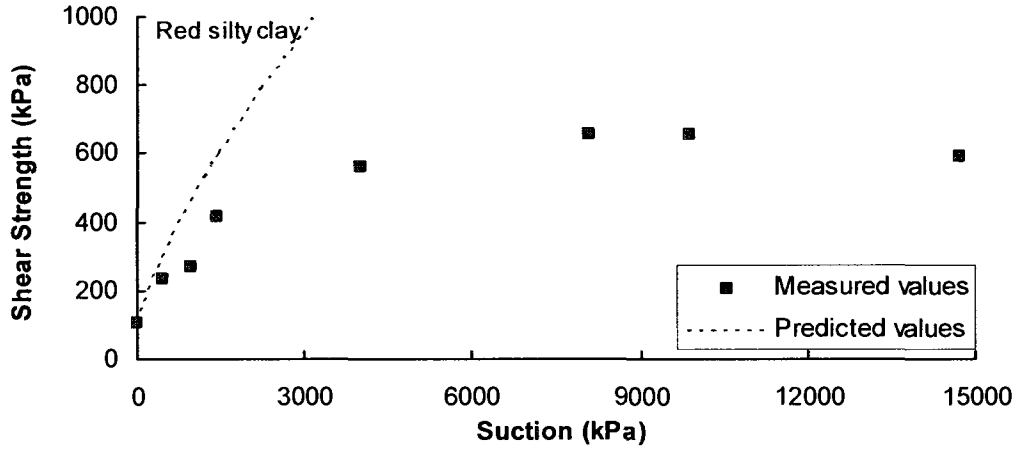

(a)

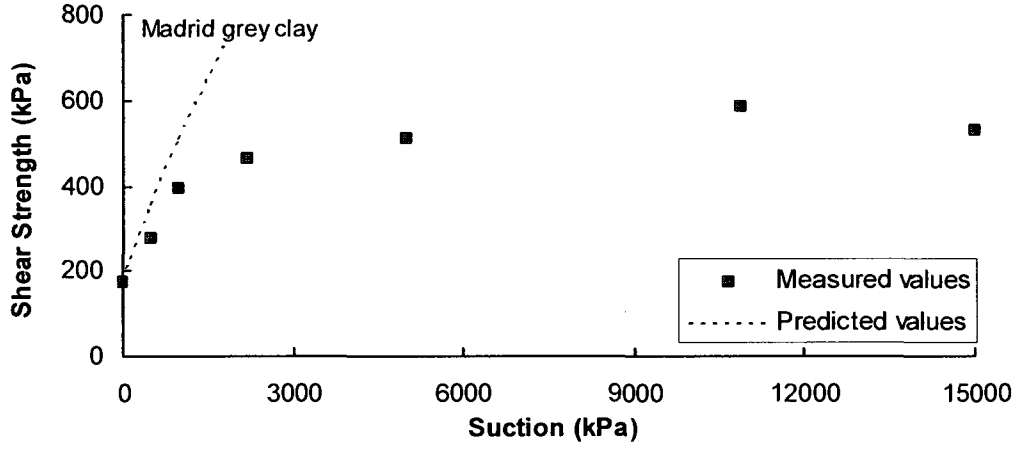

(b)

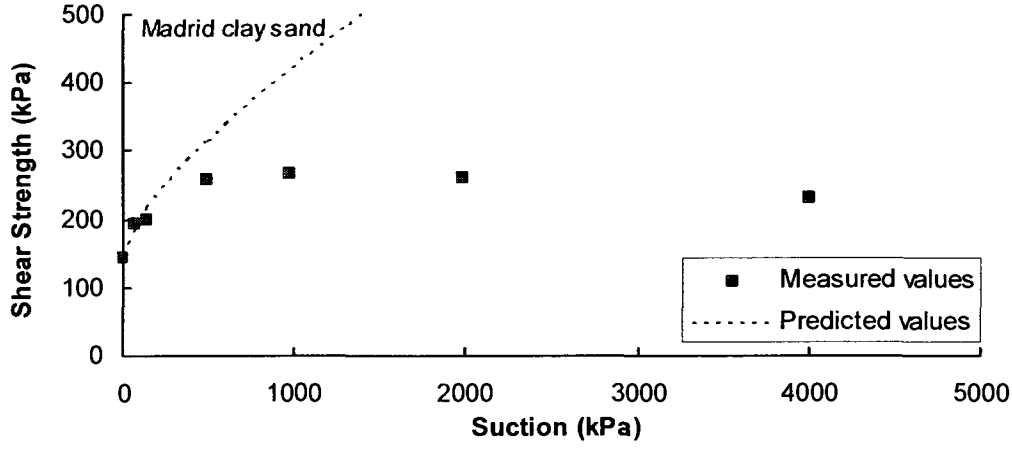

(c)

Figure 4.7. Measured and predicted values from Equation 3-11 on (a) red silty clay; (b) Madrid grey clay and (c) Madrid clay sand. (From Vanapalli and Fredlund, 2000)

Miao et al (2001) applied the Equation to Madrid grey clay tested by Escario and Saez (1986). The result is summarized in Table 4.8 and Figure 4.8. Half of the points were within ten percent of the measured values and therefore, considered acceptable.

Table 4.8. Results of analysis of Equation 3-11 from Miao et al (2001)

Soil	No. of Data Points	No. of Points with an Acceptable Fit	Average Deviation (%)	Acceptable Fit? (Y/N)
Madrid clayey sand *Escario and Saez (1986)*	6	3	9.0	Y

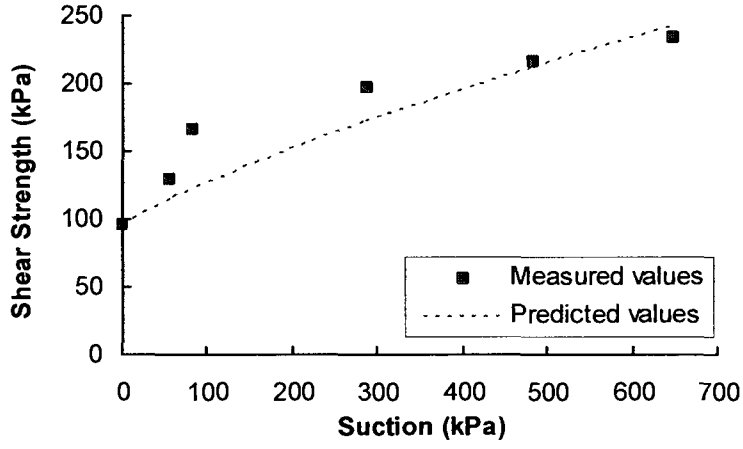

Figure 4.8. Measured and predicted values using Equation 3-11 on Madrid grey clay. (from Miao et al, 2001)

4.3.5 The Kappa (κ) Equation

Vanapalli et al 1996 and Fredlund et al 1996 proposed equation (3-13), which is sometimes referred in the literature as the κ (Kappa) equation. The proposed equation was tested by Vanapalli et al (1996) on glacial till that were compacted at three different water contents: dry of optimum, wet of optimum and at optimum moisture content conditions. In addition, the samples are tested at three different net normal stresses. The fitting parameter, κ, was varied until a reasonable fit was observed between the predicted

and measured shear strength values. The summary of the ability of the equation to fit the data is shown in Table 4.9 for each of the net normal stresses (Figure 4.9).

$$\tau = c' + (\sigma - u_a) \cdot \tan\phi' + (u_a - u_w)(\Theta^{\kappa})(\tan\phi') \qquad [3\text{-}13]$$

Table 4.9. Results of analysis glacial till prepared at different moisture content conditions and tested under different net normal stresses using Equation 3-13 from Vanapalli et al (1996)

Soil	No. of Data Points	No. of Points with an Acceptable Fit	Average Deviation (%)	Acceptable Fit? (Y/N)
Dry of Optimum Preparation				
σ_n = 25 kPa	5	4	5.9	Y
σ_n = 100 kPa	5	5	4.7	Y
σ_n = 200 kPa	7	6	7.4	Y
Optimum Moisture Content				
σ_n = 25 kPa	5	4	4.6	Y
σ_n = 75 kPa	7	5	8.4	Y
σ_n = 200 kPa	4	3	7.3	Y
Wet of Optimum Preparation				
σ_n = 25 kPa	5	4	8.9	Y
σ_n = 100 kPa	5	5	2.9	Y
σ_n = 200 kPa	4	4	3.7	Y

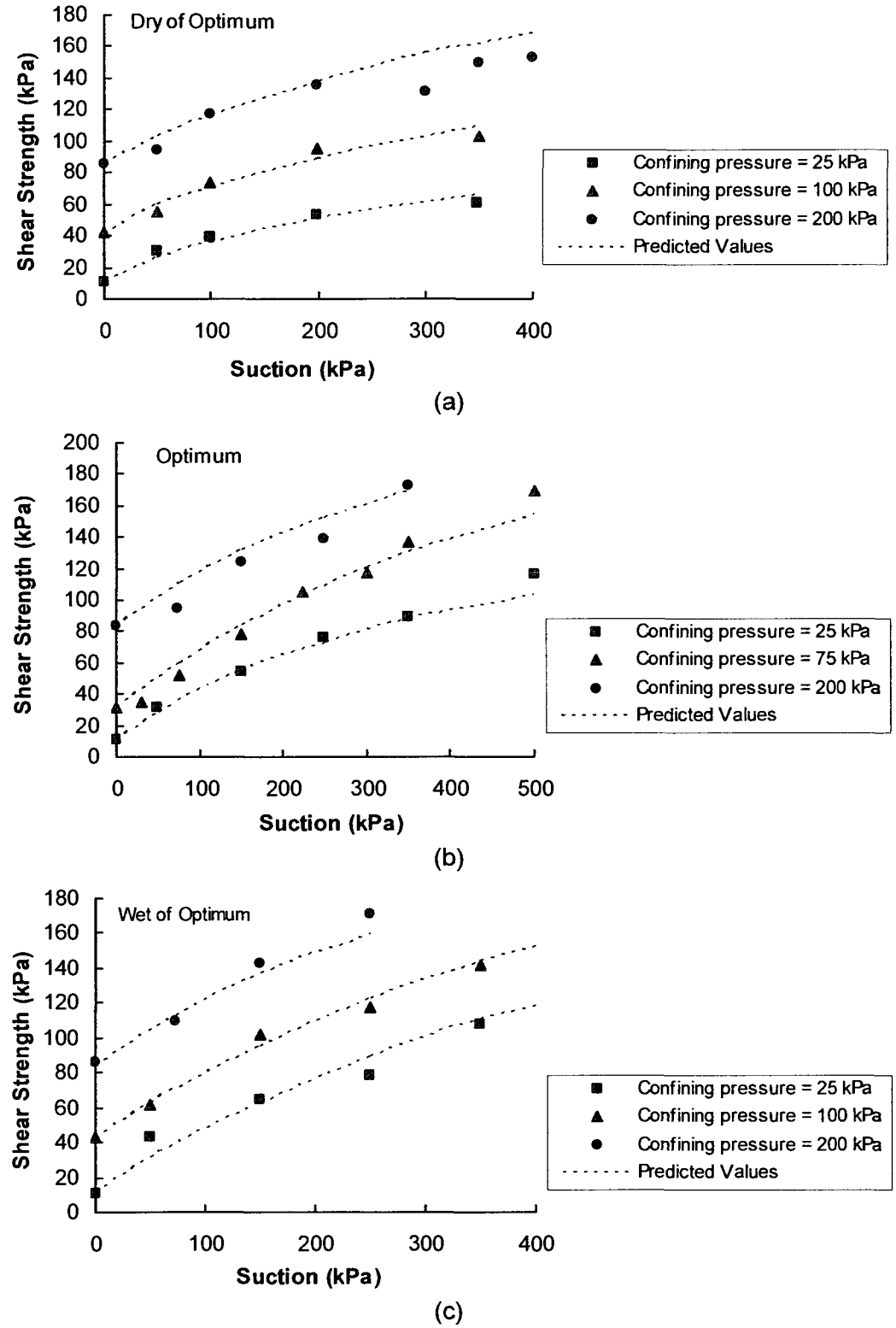

Figure 4.9. Measured and predicted values from Equation 3-13 on Indian Head glacial till prepared at (a) dry of optimum; (b) optimum and (c) wet of optimum moisture content. (from Vanapalli et al, 1996)

Vanapalli and Fredlund (2000) applied the equation to red silty clay, Madrid grey clay and Madrid clay sand using the published results of Escario and Juca (1989). The soils were analyzed over the range of 0 to 1000 kPa (referring it as low suction range) and also over a large of suctions measured (for suction range of 0 to 10,000 kPa or higher) (Table 4.10). The equation adequately fit the shear data for all three soils up to 1000 kPa and over the large range of suction measured from 0 to 14,000 kPa. The paper presents the relationship between κ and the plasticity index of the soil. This equation can be considered to be a predictive shear strength equation as the fitting parameter κ can be derived from a relationship proposed by Vanapalli and Fredlund (2000) between κ and plasticity index values.

Table 4.10. Analysis of data presented using Equation 3-13 from Vanapalli and Fredlund (2000)

Soil	No. of Data Points	No. of Points with an Acceptable Fit	Average Deviation (%)	Acceptable Fit? (Y/N)
Up to suctions of 1000 kPa				
Madrid Clay Sand *Escario and Juca (1989)*	4	4	5.7	Y
Madrid Grey Clay *Escario and Juca (1989)*	3	3	4.0	Y
Red Silty Clay *Escario and Juca (1989)*	4	3	8.1	Y
Over the entire range of suction				
Madrid Clay Sand *Escario and Juca (1989)*	7	5	22.3	Y
Madrid Grey Clay *Escario and Juca (1989)*	7	6	4.2	Y
Red Silty Clay *Escario and Juca (1989)*	8	6	6.5	Y

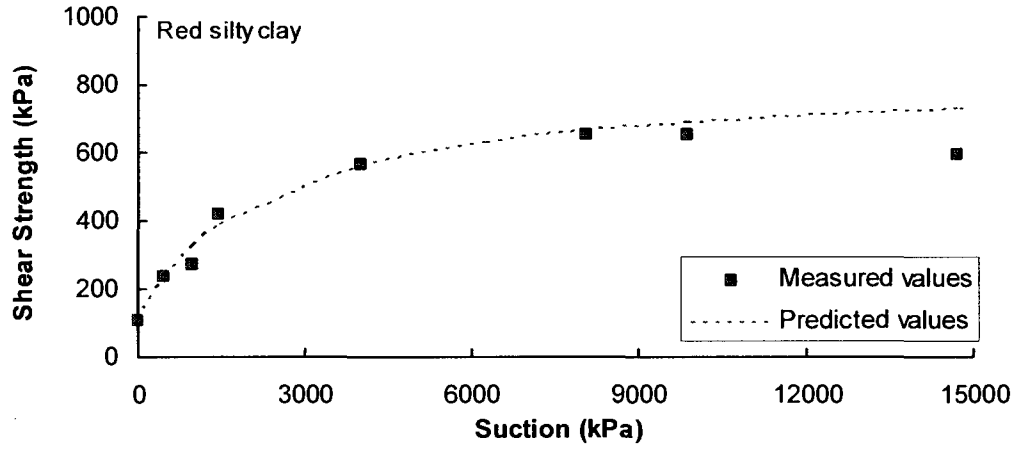

(a)

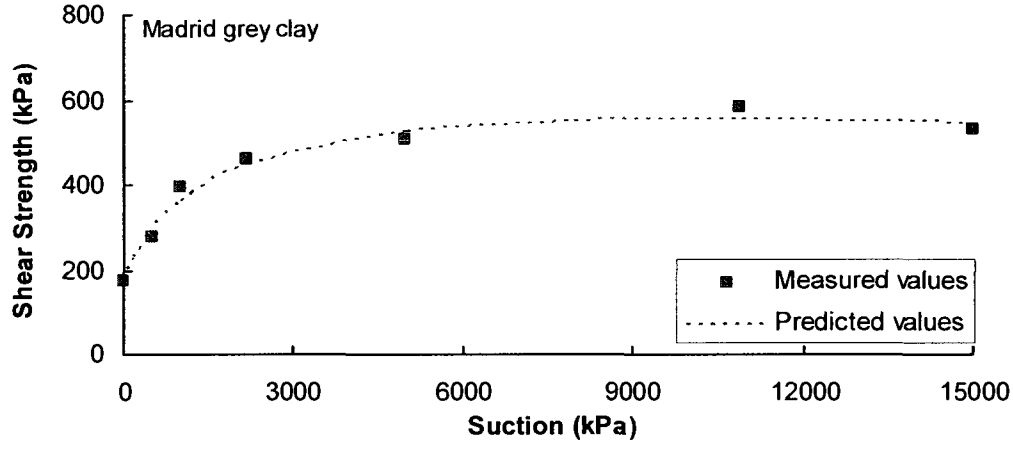

(b)

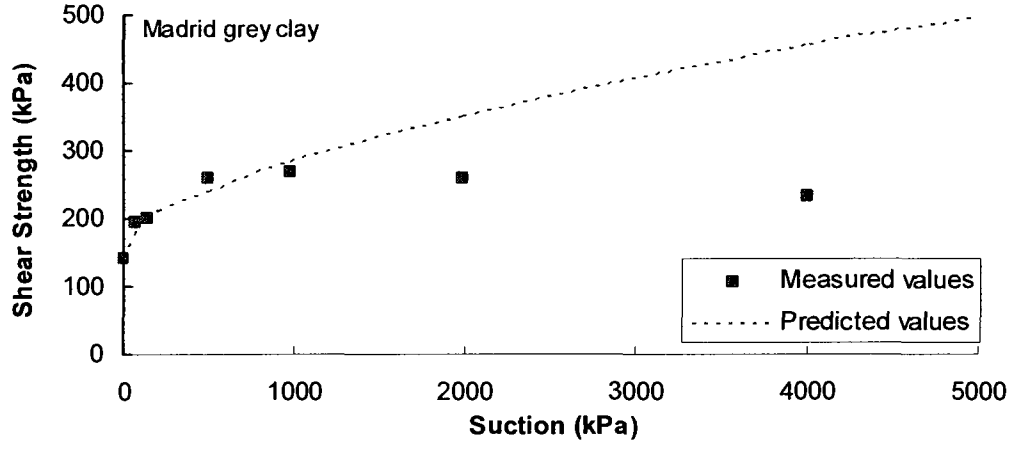

(c)

Figure 4.10. Measured and predicted values from Equation 3-13 on (a) red silty clay; (b) Madrid grey clay and (c) Madrid clay sand. (from Vanapalli and Fredlund, 2000)

4.3.6 Vanapalli, Fredlund, Pufahl and Clifton (1996): General Equation

The equation was used in a conference paper (Vanapalli and Fredlund, 2000) testing the equation against three sets of data published by Escario and Juca (1989). The same three soils that were used for the κ equation were used to test the general equation over a narrow range of suction and the entire range of suction. Equation 3-17 is different from other equations in that it utilizes both the AEV and the residual suction as a part of the equation. The values had to be determined from the measured SWCC for each soil. The results from the prediction are shown in Table 4.11. The equation provides an acceptable prediction for all three soils over the narrow range of suction as well as over the entire range of suctions.

$$\tau = c' + (\sigma - u_a) \cdot \tan\phi' + (u_a - u_w)\left(\frac{\theta - \theta_r}{\theta_s - \theta_r}\right)(\tan\phi') \qquad [3\text{-}17]$$

Table 4.11. Analysis of data using Equation 3-17 from Vanapalli and Fredlund (2000)

Soil	No. of Data Points	No. of Points with an Acceptable Fit	Average Deviation (%)	Acceptable Fit? (Y/N)
Up to suctions of 1000 kPa				
Madrid Clay Sand *Escario and Juca (1989)*	4	3	7.2	Y
Madrid Grey Clay *Escario and Juca (1989)*	3	3	4.0	Y
Madrid Grey Clay *Escario and Juca (1989)*	4	3	10.1	Y
Over the entire range of suction				
Madrid Clay Sand *Escario and Juca (1989)*	7	5	8.0	Y
Madrid Grey Clay *Escario and Juca (1989)*	7	5	9.9	Y
Red Silty Clay *Escario and Juca (1989)*	8	5	11.4	Y

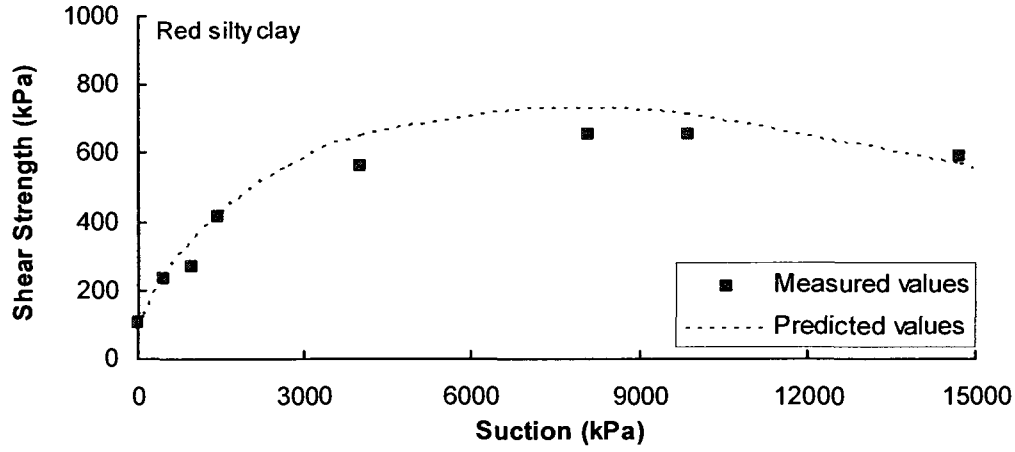

(a)

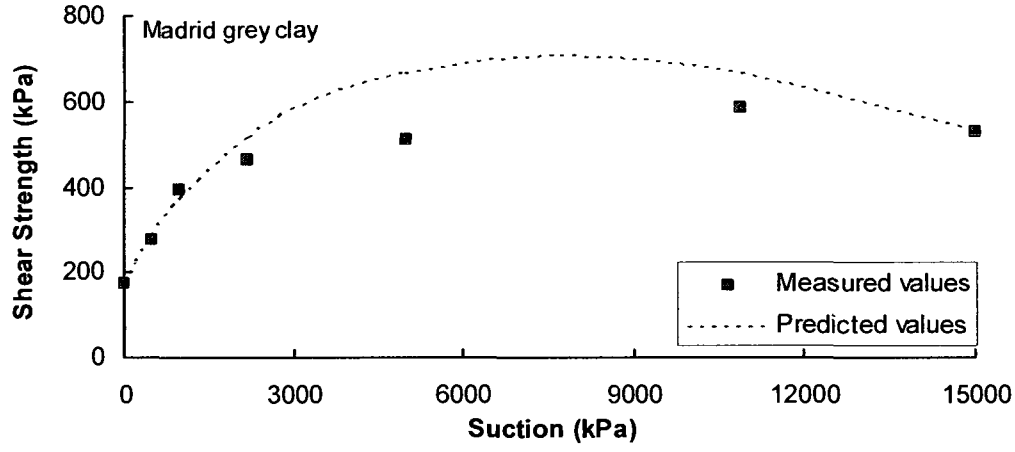

(b)

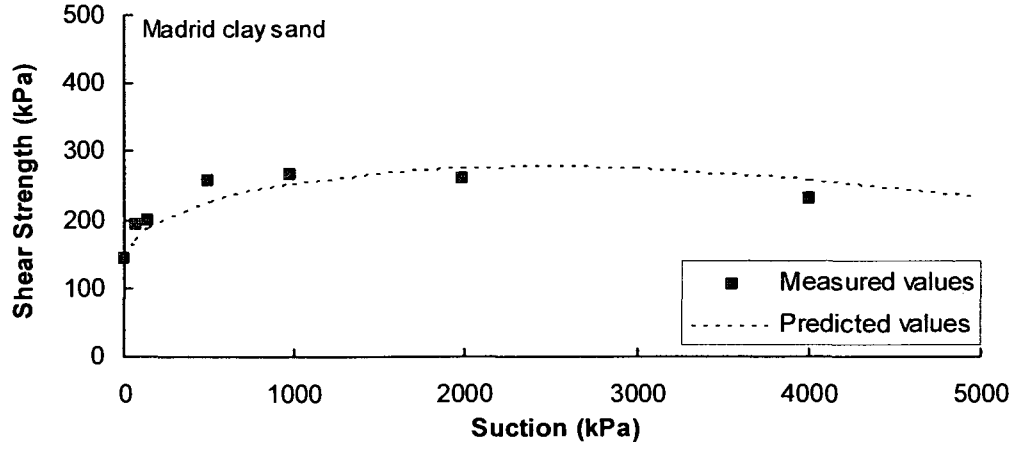

(c)

Figure 4.11. Measured and predicted values from Equation 3-17 on (a) Red silty clay; (b) Madrid grey clay and (c) Madrid clay sand. (From Vanapalli and Fredlund, 2000)

Bao et al (1998) used Equation 3-17 to predict the shear strength of three soils: glacial till (Vanapalli et al, 1996), undisturbed Nanyang expansive soil and compacted Nanyang soil (Bao et al, 1998). The predicted curves (Figure 4.12) appeared to be and adequate fit for the measured data, however a qualitative analysis indicates that the equation provides an adequate fit for the glacial till, but was not effective for the expansive soil in either the neither undisturbed nor compacted state. (Table 4.12)

Table 4.12. Results of analysis of three soils using Equation 3-17 from Bao et al, 1998.

Soil	No. of Data Points	No. of Points with an Acceptable Fit	Average Deviation (%)	Acceptable Fit? (Y/N)
Glacial Till *Vanapalli et al (1995)*	4	3	7.6	Y
Nanyang expansive soil: compacted *Bao et al (1998)*	4	1	12.6	N
Nanyang expansive soil: undisturbed *Bao et al (1998)*	3	1	11.5	N

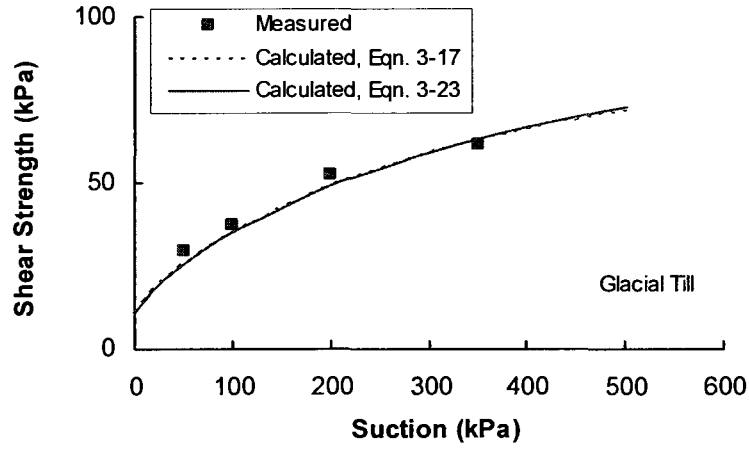

(a)

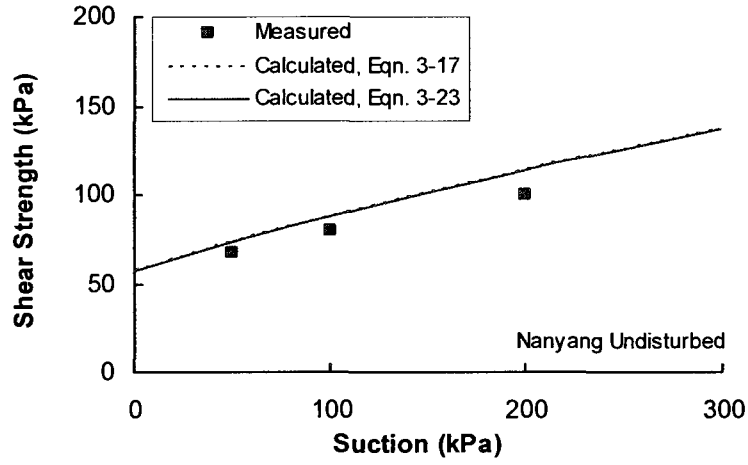

(b)

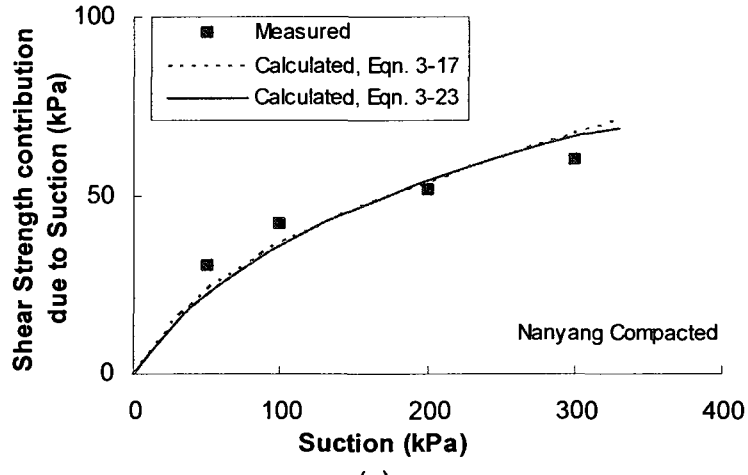

(c)

Figure 4.12. Comparing measured values with calculated values of Vanapalli et al General Equation (3-17) and Bao et al Equation (3-23) for (a) glacial till, (b) Nanyang undisturbed soil and (c) Nanyang compacted soil.

In a later study (Miao et al, 2001) the equation was tested against measured data from a compacted sample of Nanyang expansive soil. The Nanyang soil was tested in a modified triaxial test up to a suction of 200 kPa. The authors reported an adequate fit (Figure 4.13) which is supported by the numbers in Table 4.13.

Table. 4.13. Results of analysis on Nanyang expansive soil presented for Equation 3-17 from Miao et al (2001)

Soil	No. of Data Points	No. of Points with an Acceptable Fit	Average Deviation (%)	Acceptable Fit? (Y/N)
Nanyang expansive soil *Miao et al, 2002*	4	3	5.7	Y

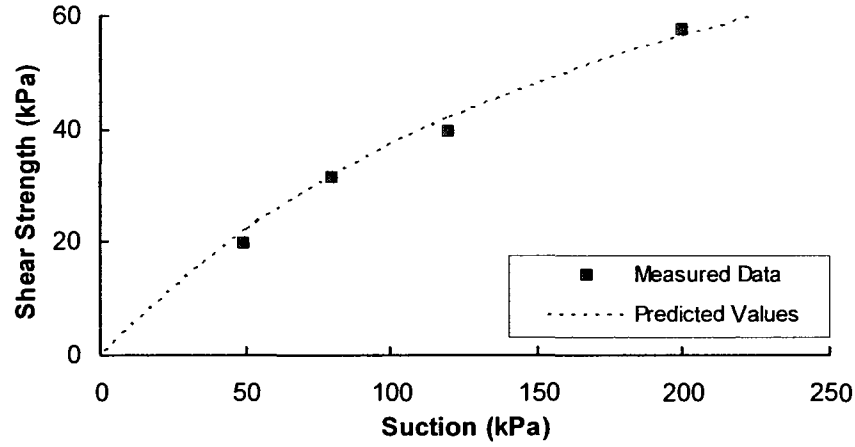

Figure 4.13. Measured and predicted values from Equation 3-17 on Nanyang expansive soil. (from Miao et al, 2001)

4.3.7 Bao, Gong and Zhan (1998)

As a part of a keynote paper, Bao et al (1998) proposed Equation 3-23 using an approach similar to Vanapalli et al (1996) general equation (Eqn. 3-23). The authors expanded the relationship by incorporating two boundary conditions: the air-entry value and the relationship between suction and water content. The proposed equation was tested on three soils: glacial till (Vanapalli et al, 1996), undisturbed Nanyang clay and compacted Nanyang clay (Bao et al, 1998). The graphical results from Equation 3-23 were presented in section 4.3.6. The ability to fit the measured data was similar for both

equations and therefore, the results were also similar. (Table 4.14; Figure 4.12) The equation seemed to provide an adequate fit for all three soils but quantitatively provided an adequate fit for only the glacial till. The equation did not provide an adequate fit for either the Nanyang compacted soil, nor the undisturbed Nanyang soil.

$$\tau = c' + (\sigma - u_a)\cdot \tan\phi' + (u_a - u_w)\left(\frac{log(u_a - u_w)_r - log(u_a - u_w)}{log(u_a - u_w)_r - log(u_a - u_w)_b}\right)(\tan\phi') \qquad [3\text{-}23]$$

Table 4.14. Results of analysis of three soils using Equation 3-23 from Bao et al, 1998.

Soil	No. of Data Points	No. of Points with an Acceptable Fit	Average Deviation (%)	Acceptable Fit? (Y/N)
Glacial Till *Vanapalli et al (1996)*	4	3	7.8	Y
Nanyang expansive soil: compacted *Bao et al (1998)*	4	1	12.7	N
Nanyang expansive soil: undisturbed *Bao et al (1998)*	3	1	11.5	N

4.3.8 Khalili and Khabbaz (1998)

The investigators proposed an equation (3-25) which was an extension by an equation proposed by Bishop in 1959. To test the equation, the authors used compacted specimens of kaolin and a man-made kaolin-sand mixture to test Equation 3-25. The shear strength of the prepared samples were measured in a modified triaxial testing apparatus at a confining pressure of 100 kPa. The kaolin was tested over a suction range of approximately 700 kPa and the sand–kaolin mix was tested up to 500 kPa. The equation provides a very close fit to both soils (Table 4.15; Figure 4.14).

$$\tau = c' + (\sigma - u_a)\cdot \tan\phi' + (u_a - u_w)\cdot \tan\phi' \cdot \left[\frac{(u_a - u_w)}{(u_a - u_w)_b}\right]^{\eta} \qquad [3\text{-}25]$$

Table 4.15. Results of analysis of two soils using Equation 3-25 from Khalili and Khabbaz (1998)

Soil	No. of Data Points	No. of Points with an Acceptable Fit	Average Deviation (%)	Acceptable Fit? (Y/N)
Kaolin	12	12	2.8	Y
Sand-clay mixture	7	7	3.6	Y

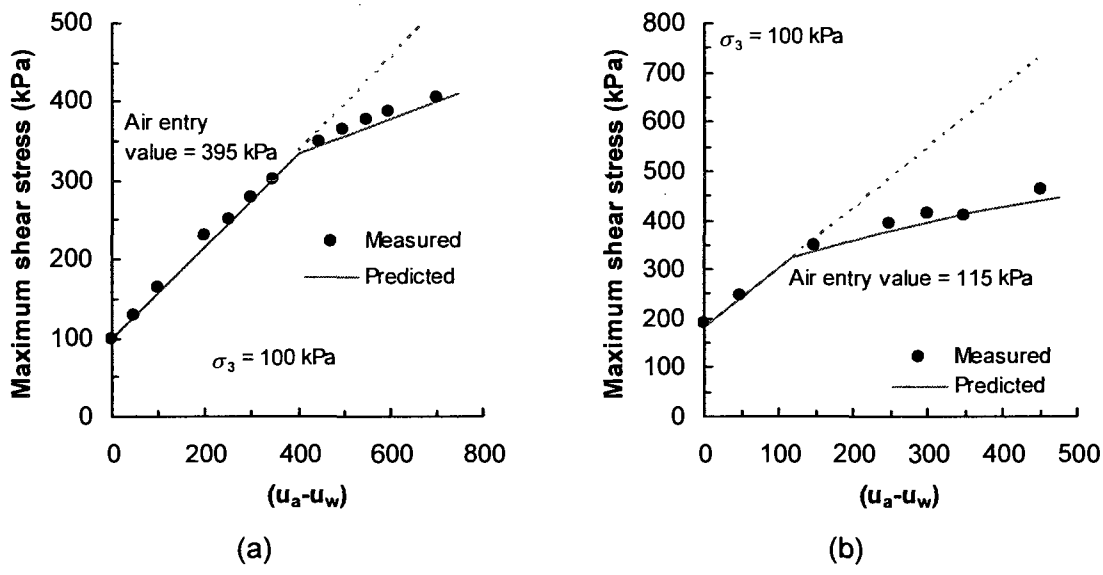

Figure 4.14. Measured versus predicted values for (a) compacted kaolin clay; (b) kaolin clay sand. (from Khalili and Khabbaz, 1998)

Vanapalli and Fredlund (2000) tested the Khalili and Khabbaz equation (Eqn. 3-25) using the shear strength data of three soils presented by Escario and Juca (1989). The equation provided an adequate fit for the Madrid clay sand over a range of suction from 0 to 1000 kPa; however, there were significant differences between the measured and predicted shear strength values when tested over a larger range of suction (Table 4.16). Similar observations were derived when the equation was tested on the data of Madrid grey clay and the red silty clay.

Table 4.16. Results of analysis of three soils using Equation 3-25 from Vanapalli and Fredlund (2000)

Soil	No. of Data Points	No. of Points with an Accept-able Fit	Average Deviation (%)	Acceptable Fit? (Y/N)
Up to suctions of 1000 kPa				
Madrid Clay Sand *Escario and Juca (1989)*	4	3	7.7	Y
Madrid Grey Clay *Escario and Juca (1989)*	3	1	20.4	N
Madrid Grey Clay *Escario and Juca (1989)*	4	1	38.7	N
Over the entire range of suction				
Madrid Clay Sand *Escario and Juca (1989)*	7	3	>10.0	N
Madrid Grey Clay *Escario and Juca (1989)*	7	1	>32.0	N
Red Silty Clay *Escario and Juca (1989)*	8	1	>36.6	N

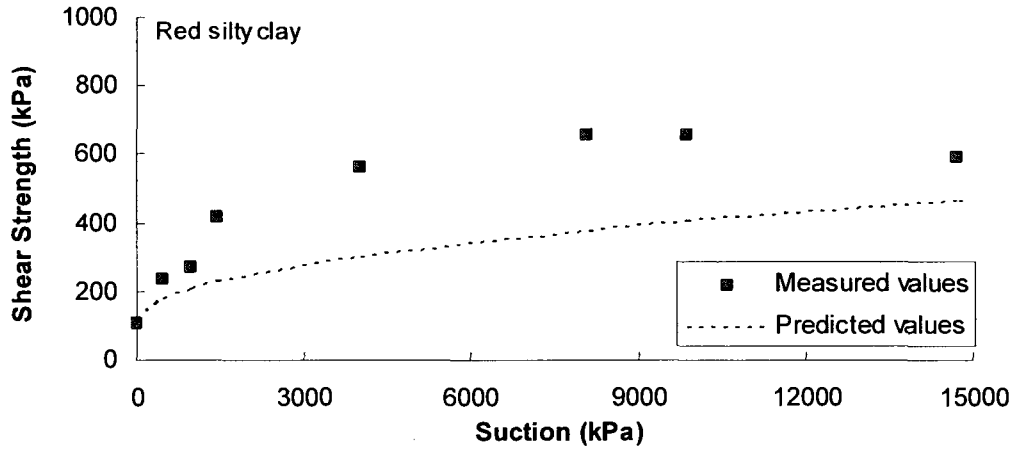

(a)

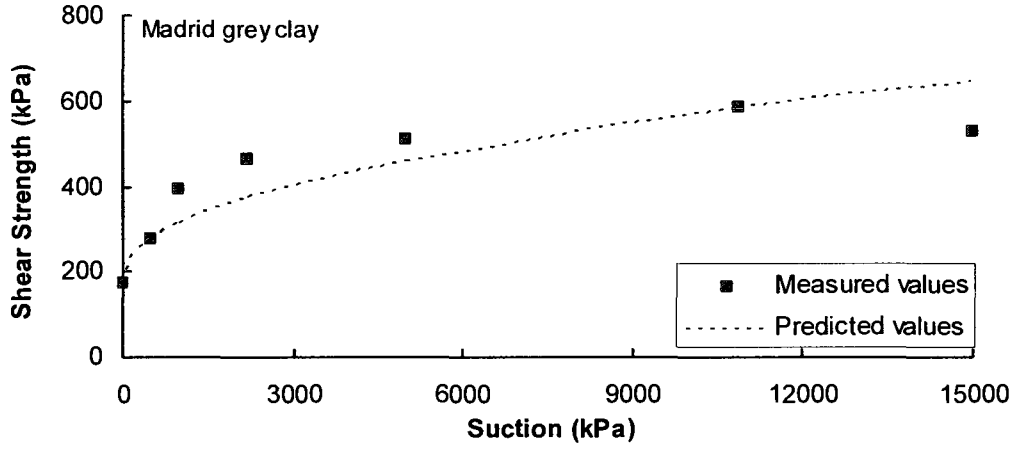

(b)

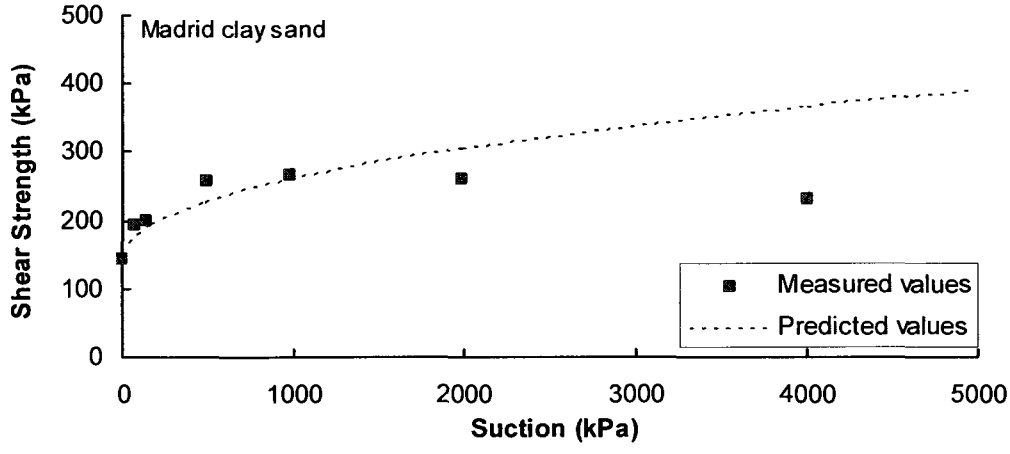

(c)

Figure 4.15. Measured and predicted values from Equation 3-25 on (a) red silty clay; (b) Madrid grey clay and (c) Madrid clay sand. (from Vanapalli and Fredlund, 2000)

4.3.9 Rassam and Williams (1999)

Rassam and Williams (1999) proposed an equation (Eqn. 3-29) that hinged around the air-entry value to accommodate linearity up to the AEV and the non-linearity of the shear strength data beyond the AEV. The investigators used a program, TableCurve 3D© to generate a surface for the relationship between shear strength, net normal stress and suction. The authors recognize a dual effect of effective stress:

1. An increase in effective stress will increase sample consolidation resulting in an increased slope in the linear portion of the SWCC.
2. The dilative effect during shearing attributed to disruption of water phase at lower confining pressures.

The investigators applied the technique (represented by Equation 3-29) to three different soils: glacial till (Vanapalli et al, 1996), tailings from a distance of 50 m from discharge point and tailings sampled at a distance of 150 m from the discharge point in the tailings pond (Rassam and Williams, 1999).

$$\tau = \alpha + \sigma \cdot tan\phi' + (u_a - u_w) \cdot tan\phi' - \varphi[(u_a - u_w) - (u_a - u_w)_b]^{\beta} \qquad [3\text{-}29]$$

The tailings were tested over a range of suction from 0 to 100 kPa with three different confining pressures (30, 125 and 200 kPa). The glacial till (Vanapalli et al, 1996) was tested over a range of suction from 0 to 500 kPa. Three different confining pressures (25, 100 and 200 kPa) were applied during testing.

Equation 3-29 provided a visual fit (Figures 4.16 and 4.17) for all three soils under all confining pressures. For the nine situations (Table 4.17) the equation provided a quantitative fit.

Table. 4.17. Results of analysis on data presented for Equation 3-29 from Rassam and Williams (1999)

Soil	No. of Data Points	No. of Points with an Acceptable Fit	Average Deviation (%)	Acceptable Fit? (Y/N)
Tailings, 50 m, σ_n = 30 kPa *Rassam and Williams, 1999*	4	4	2.1	Y
Tailings, 50 m, σ_n = 125 kPa *Rassam and Williams, 1999*	4	4	1.0	Y
Tailings, 50 m, σ_n = 250 kPa *Rassam and Williams, 1999*	4	4	0.4	Y
Tailings, 150 m, σ_n = 30 kPa *Rassam and Williams, 1999*	4	4	4.6	Y
Tailings, 150 m, σ_n = 125 kPa *Rassam and Williams, 1999*	4	4	2.8	Y
Tailings, 150 m, σ_n = 250 kPa *Rassam and Williams, 1999*	4	4	0.5	Y
Glacial Till, σ_n = 25 kPa *Vanapalli et al, 1996*	5	4	9.0	Y
Glacial Till, σ_n = 100 kPa *Vanapalli et al, 1996*	6	5	5.6	Y
Glacial Till, σ_n = 200 kPa *Vanapalli et al, 1996*	5	5	5.2	Y

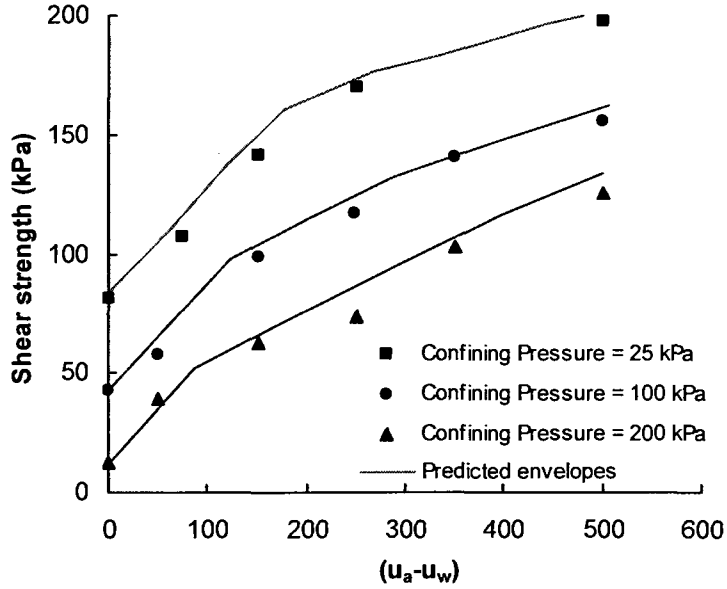

Figure 4.16. Calculated data compared to measured data from Vanapalli et al, 1996. Soil is prepared at a moisture content wet of optimum. (modified from Rassam and Williams, 1999)

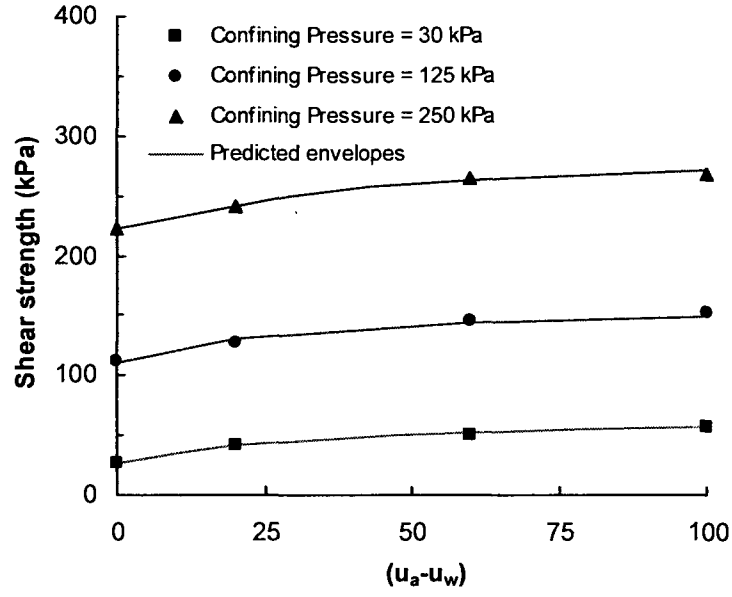

(a)

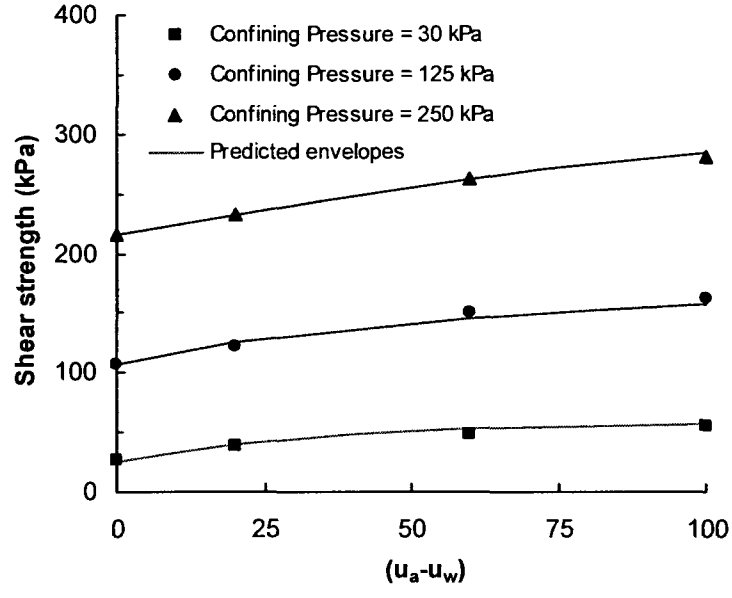

(b)

Figure 4.17. Predicted curves for soil (a) 50m from discharge and (b) 150 m from discharge. (from Rassam and Williams, 1999)

4.3.10 Xu and Sun (2001)

The investigators proposed an equation to predict the shear strength of unsaturated expansive soils based on the fractal dimension of the soil. The fractal geometry of the soil is used to define physical surface properties of the soil – namely the void spacing of the soil surface.

Xu and Sun performed triaxial tests on Ningxia triaxial soil over a range from 40 to 400 kPa. The confining pressure was not constant for each test performed, nor was the resulting normal stress. The equation was compared on measured pointes was compared on a point by point basis. The deviation for each point is less than 10 % for all values of suction. (Table 4.18)

$$\tau = c' + (\sigma - u_a) \cdot \tan\phi' + m^{(2/3D)} \cdot (u_a - u_w)^{(2/3D)} \cdot \tan\phi' \qquad [3\text{-}41]$$

Table 4.18. Results of analysis from Xu and Sun, 2001 using Equation 3-43.

σ_n (kPa)	Suction (kPa)	Deviation (%)
84 kPa	39.75	2.7
110 kPa	82.78	4.6
142 kPa	102.09	2.5
142 kPa	208.47	3.4
177 kPa	300.33	2.9
220 kPa	360.74	2.1

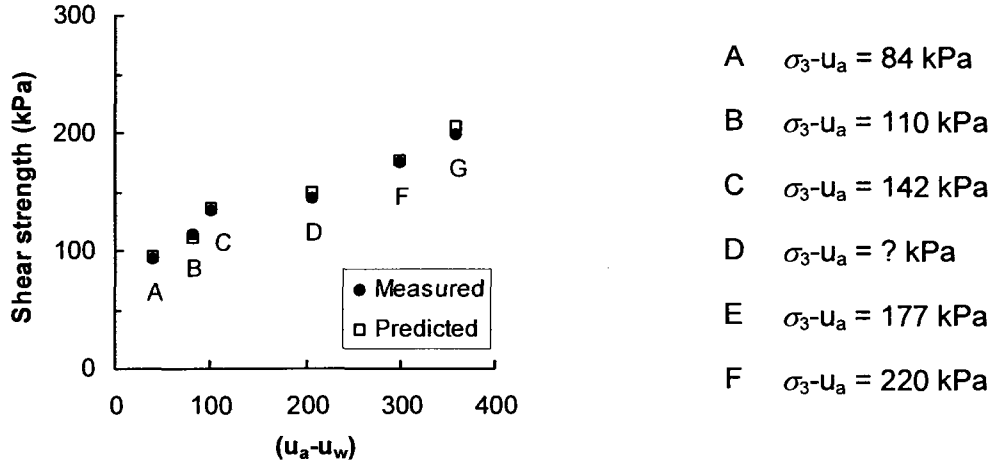

Figure 4.18. Summary of measured and calculated values using Equation 3-41. (from Xu and Sun, 2001)

4.3.11 Miao, Liu and Lai (2002)

Miao et al used the experimental data from Nanyang expansive soil to apply the equation (Eqn. 3-45). The equation uses a fitting parameter, a_1 that can be determined by fitting the data to experimental data. The resulting points provided an adequate fit (Table 4.19).

$$\tau = c' + (\sigma - u_a) \cdot \tan\phi' + \frac{a_1 (u_a - u_w)}{1 + \frac{1 - a_1}{p_a} \cdot (u_a - u_w)} \qquad [3\text{-}45]$$

Table. 4.19. Results of analysis on Nanyang expansive soil presented for Equation 3-45 from Miao et al (2001)

Soil	No. of Data Points	No. of Points with an Acceptable Fit	Average Deviation (%)	Acceptable Fit? (Y/N)
Nanyang expansive soil *Miao et al, 2002*	4	3	7.1	Y

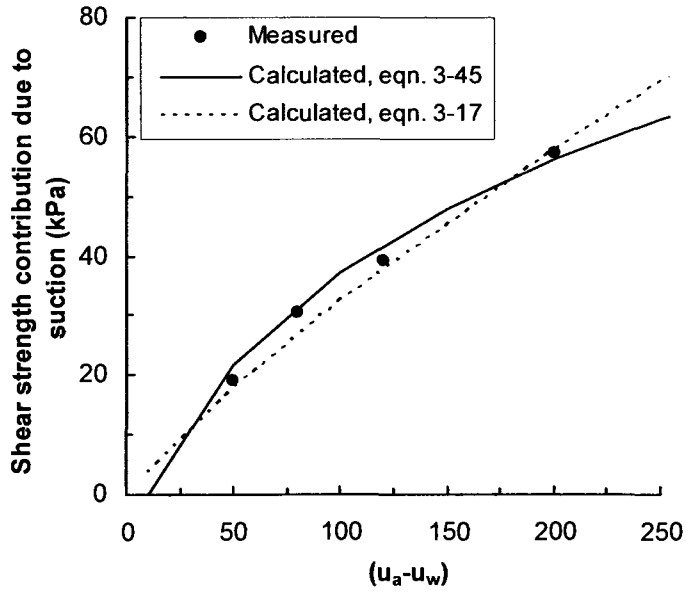

Figure 4.19. Comparing predicted data with measured data for Nanyang expansive soils. Curves were predicted using two formulae: Vanapalli et al general equation (3-17) and Miao et al equation (3-45). (generated from Miao et al, 2002)

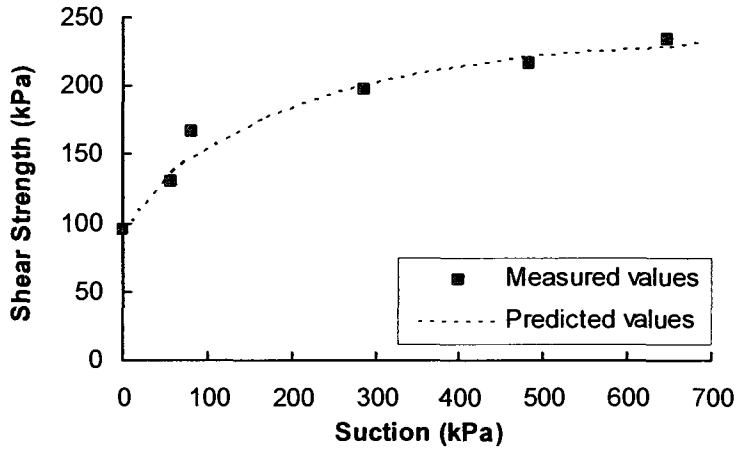

Figure 4.20. Measured vs predicted values from Equation 3-45 from Nanyang expansive soil. (from Miao et al, 2002).

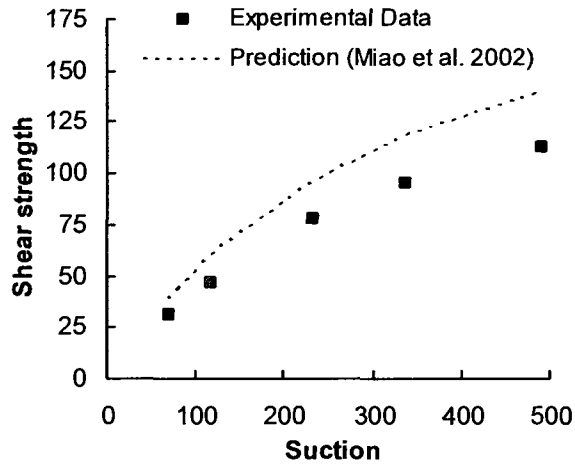

Figure 4.21. Measured and predicted equations on Gan et al glacial till. (Tekinsoy et al, 2004)

4.3.12 Rassam and Cook (2002)

Rassam and Cook provided an advanced version to the equation proposed by Rassam and Williams (1999). The resulting equation (Eqn. 3-47) was based on fitting the equation to experimental data. The authors tried the equation with five soils: tailings sampled at a depth of 50 m (Rassam and Williams, 1999), decomposed fine ash tuff (Gan and Fredlund, 1996), glacial till (Gan et al, 1988), Madrid grey clay and Madrid clay sand (Escario and Juca, 1989). There are two exceptions in the soil conditions tested. The decomposed fine ash tuff was tested at critical stress and the glacial till did not have an accompanying SWCC measured with a similar representative sample. The equation provides an adequate fit for the unsaturated shear strength data (Table 4.20).

$$\tau = (u_a - u_w)\cdot \tan\phi' - \left[\frac{(u_a - u_w)_r \cdot \tan\phi' - \tau_{Sr}}{[(u_a - u_w)_r - (u_a - u_w)_b]^{\beta}}\right][(u_a - u_w) - (u_a - u_w)_b]^{\frac{\tan\phi'\cdot[(u_a-u_w)_r-(u_a-u_w)_b]}{\tan\phi'\cdot(u_a-u_w)_r-\tau_{Sr}}} \quad [3\text{-}47]$$

Table 4.20. Results of analysis on data presented for Equation 3-47 from Rassam and Cook (2002)

Soil	No. of Data Points	No. of Points with an Acceptable Fit	Average Deviation (%)	Acceptable Fit? (Y/N)
Tailings, 50 m *Rassam and Williams, 1999*	3	3	2.2	Y
Decomposed fine ash tuff *Gan et al, 1996*	3	2	5.1	Y
Glacial till *Gan et al, 1988*	5	5	4.7	Y
Madrid grey clay *Escario and Juca, 1989*	4	4	6.0	Y
Madrid clay sand *Escario and Juca, 1989*	3	2	6.2	Y

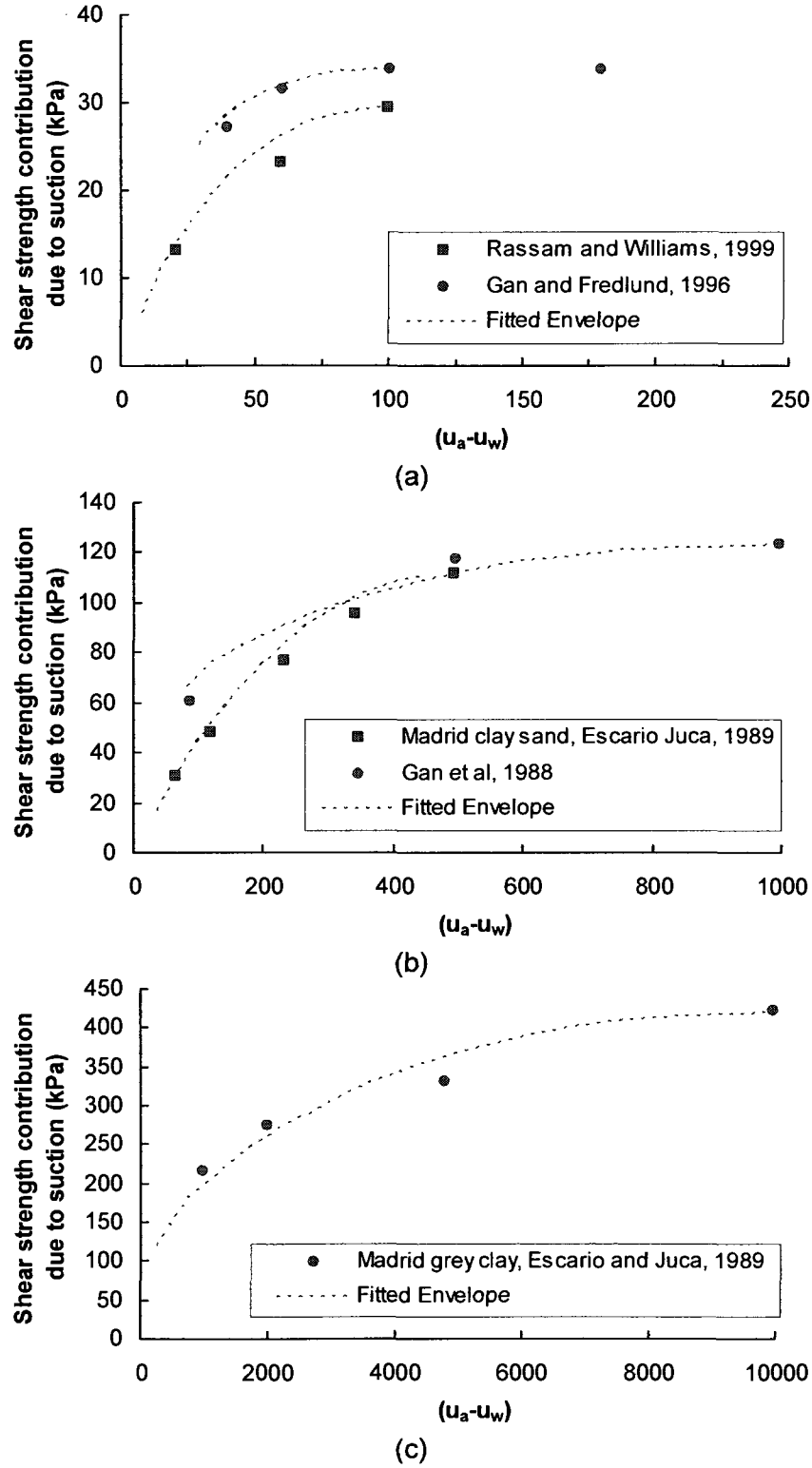

Figure 4.22. Measured values from five different soils over (a) lower suction range, (b) an intermediate suction range and (c) a higher suction range. (Rassam and Cook, 2002)

4.3.13 Lee, Lee and Kim (2003)

The authors used ten soils to test their hyperbolic equation (Eqn. 3-50). Six of the soils were previously published, while four of the soils were presented in this paper. The shear strength data is presented but the SWCC of the soils are not. Two of the soils; the Okchun soil and Chociwon soil are prepared at moisture contents wet of optimum and dry of optimum conditions. The shear strength for the wet and dry conditions is measured separately and the equation applied to each of the data sets.

The published results by Lee et al (2003) appear to provide an acceptable fit for all soils and compaction conditions (Figures 4.23 and 4.24). Of the six soils from other authors, four of the soils were adequately fit using the equation (Table 4.21). The colluvium and the Lee soil were not fit by the equation. The equation fit the four soils prepared and tested by the authors. The equation fits both soils prepared at both wet of optimum and dry of optimum conditions. Although the equation creates a result that is acceptable for most of the soils, the fitting parameters, *a* and *b*, are currently not related to soil parameters and therefore, the equation is still not truly predictive.

$$\tau = c' + (\sigma - u_a) \cdot \tan\phi' + \frac{(u_a - u_w)}{a_3 + b_3(u_a - u_w)} \qquad [3\text{-}50]$$

Table 4.21. Results of analysis on data presented for Equation 3-50 (from Lee et al, 2003).

Soil	No. of Data Points	No. of Points with an Acceptable Fit	Average Deviation (%)	Acceptable Fit? (Y/N)
Glacial till *Gan et al, 1988*	6	3	12.6	Y
Glacial till *Vanapalli et al, 1996*	5	5	4.5	Y
Dhanauri clay *Satija, 1981*	23	18	7.1	Y
Colluvium *De Campos and Carrillo, 1995*	4	1	15.0	N
Lee soil *Lee et al, 2000*	4	2	15.3	N
Jossigny silt *Cui and Delage, 1993*	4	3	4.0	Y
Okchun soil, wet of optimum *Lee, Lee and Kim, 2003*	8	8	5.0	Y
Okchun soil, dry of optimum *Lee, Lee and Kim, 2003*	5	4	8.4	Y
Chociwon soil, wet of optimum *Lee, Lee and Kim, 2003*	5	4	6.1	Y
Chociwon soil, dry of optimum *Lee, Lee and Kim, 2003*	5	5	1.7	Y
Yungi soil *Lee, Lee and Kim, 2003*	4	3	6.6	Y
Seochang soil, wet of optimum Lee, Lee and Kim, 2003	5	5	8.3	Y

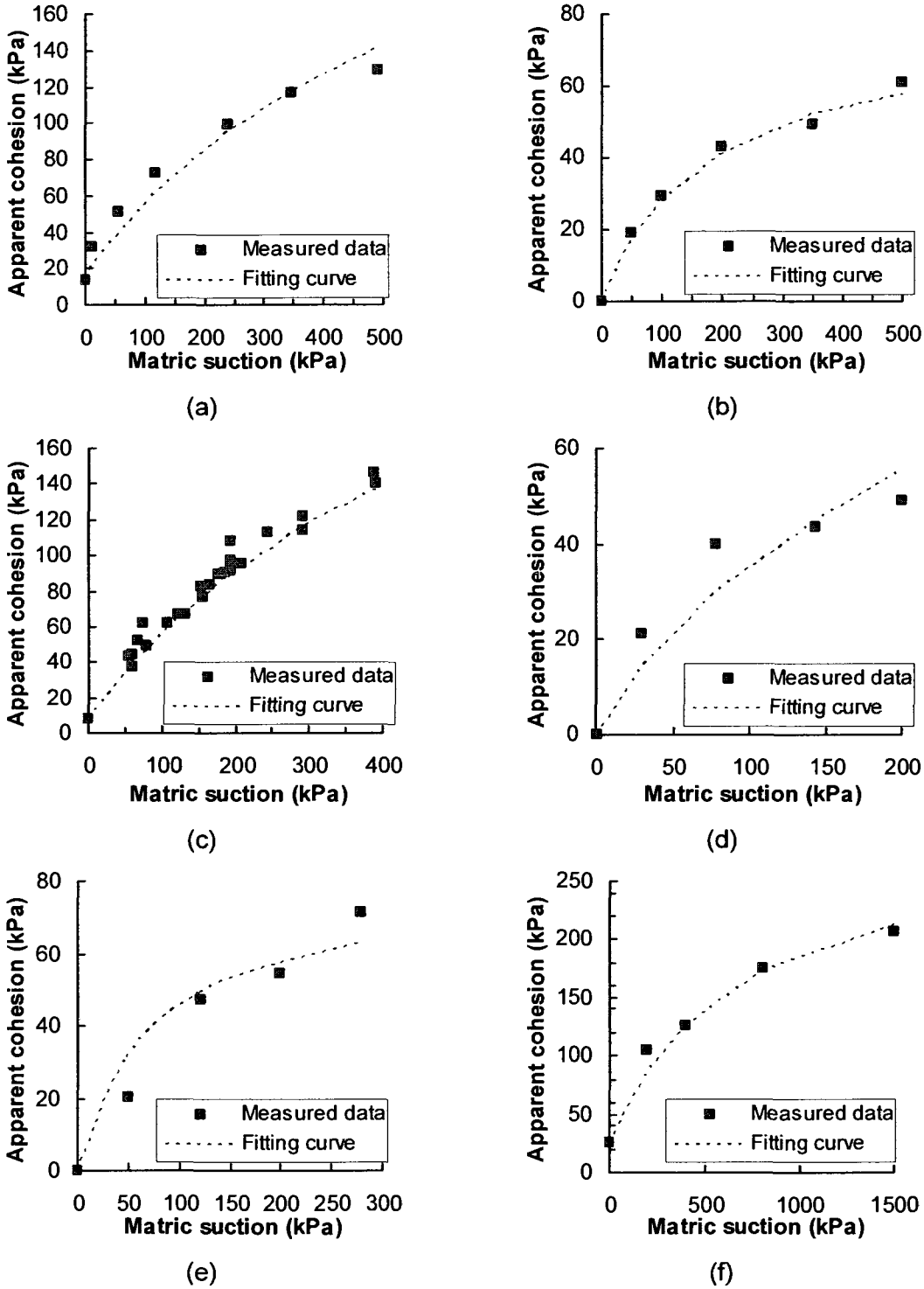

Figure 4.23. Fitting curve and predicted data applied to (a) glacial till (Gan et al, 1988); (b) glacial till (Vanapalli et al, 1996); (c) Dhanauri clay (Satija, 1981); (d) colluvium (de Campos and Carrillo, 1995); (e) soil (Lee et al, 2000); (f) Jossigny silt (Cui and Delage, 1993).

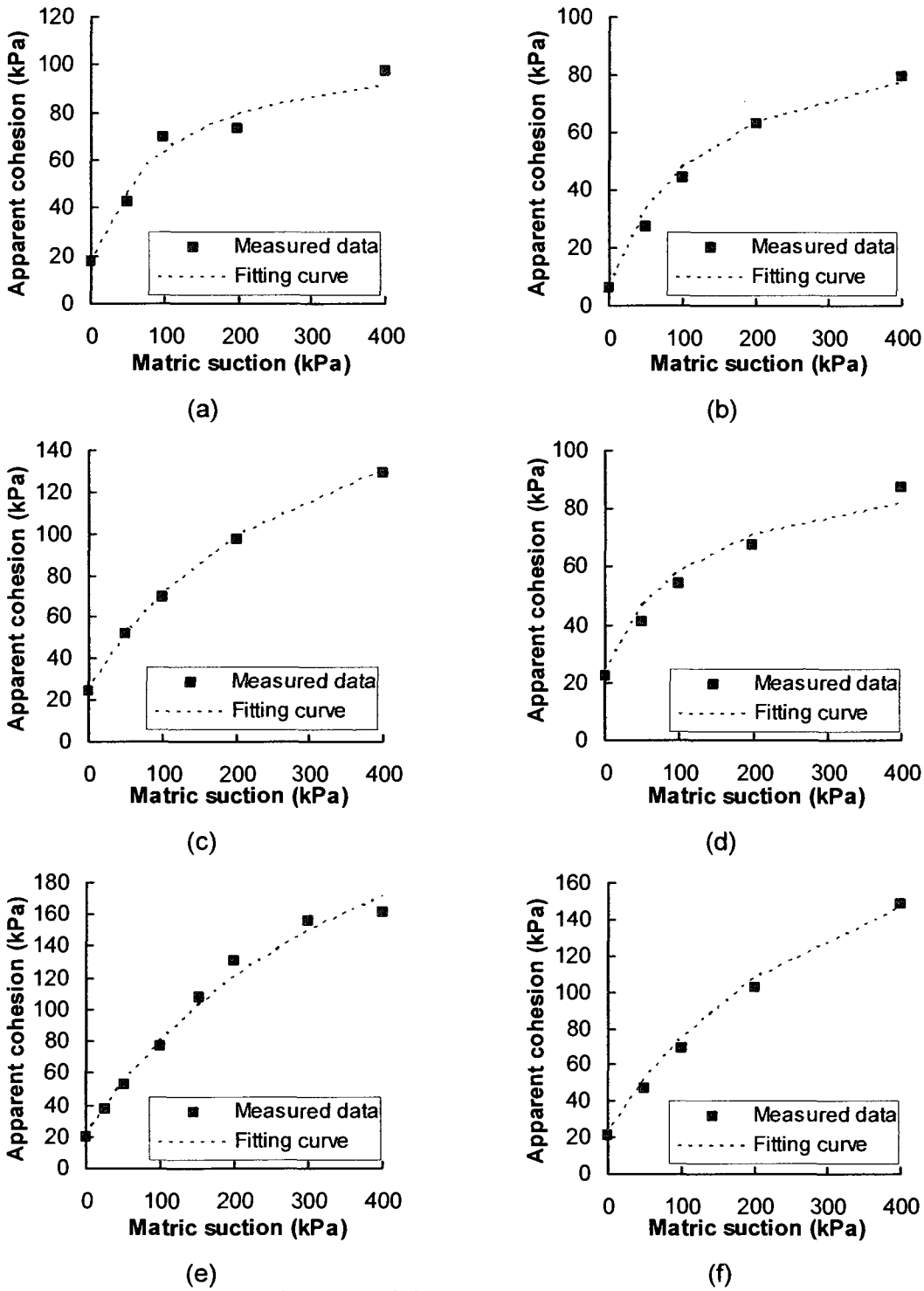

Figure 4.24. Fitting curve and predicted data applied to (a) Yungi soil (Lee et al, 2003); (b) Seochang soil, dry of optimum (Lee et al, 2003); (c) Chociwon soil, dry of optimum (Lee et al, 2003); (d) Okchun soil, dry of optimum (Lee et al, 2003); (e) Okchun soil, wet of optimum (Lee et al, 2003); (f) Chociwon soil, wet of optimum (Lee et al, 2003).

4.3.14 Xu (2004)

Xu proposed a variation to the Xu and Sun equation (2001). Xu tested the unsaturated shear strength of the Ningxia expansive soil in order to test the predictive ability of the equation (Eqn. 3-57). Xu used the concept of Watabe (2000) to predict the fractal dimension from the SWCC. He tested the equation using seven soils. Six of the soils were previously published soils from various authors. The tailings data (Rassam and Williams, 1999) was tested under three different confining stresses: 30, 125 and 250 kPa. The Botkin silt data (Oloo and Fredlund, 1996) is considered as one data set but the soil was tested with multiple net normal stresses. Of all the soils tested using Equation 3-57, the Botkin silt was the only soil that did not meet the requirements for an acceptable fit. (Table 4.22)

$$\tau = c' + (\sigma - u_a)\cdot \tan\phi' + (u_a - u_w)_b^{D-1}\cdot(u_a - u_w)^{D-2}\cdot \tan\phi' \qquad [3\text{-}57]$$

Table 4.22. Results of analysis on data presented for Equation 3-57 from Xu (2004).

Soil	No. of Data Points	No. of Points with an Acceptable Fit	Average Deviation (%)	Acceptable Fit? (Y/N)
Ningxia expansive soil *Xu, 2004*	6	6	3.5	Y
Glacial till *Vanapalli et al, 1996*	23	15	6.5	Y
Botkin silt *Oloo and Fredlund, 1996*	16	7	9.1	N
Glacial till *Gan et al, 1988*	15	10	10.3	Y
Ashikaga silt *Nishimura and Fredlund, 2001*	5	4	8.7	Y
Tailings, 50 m, σ_n = 30 kPa *Rassam and Williams, 1999*	3	3	5.6	Y
Tailings, 50 m, σ_n = 125 kPa *Rassam and Williams, 1999*	3	3	4.5	Y
Tailings, 50 m, σ_n = 250 kPa *Rassam and Williams, 1999*	3	2	5.4	Y
Tailings, 150 m, σ_n = 30 kPa *Rassam and Williams, 1999*	3	2	8.2	Y
Tailings, 150 m, σ_n = 125 kPa *Rassam and Williams, 1999*	3	3	4.9	Y
Tailings, 150 m, σ_n = 250 kPa *Rassam and Williams, 1999*	3	2	14.5	Y

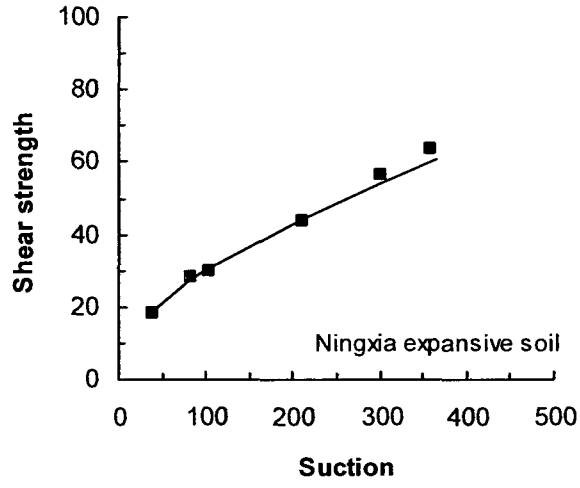

Figure 4.25. Predicted versus measured values for Ningxia expansive soil. (Xu, 2004)

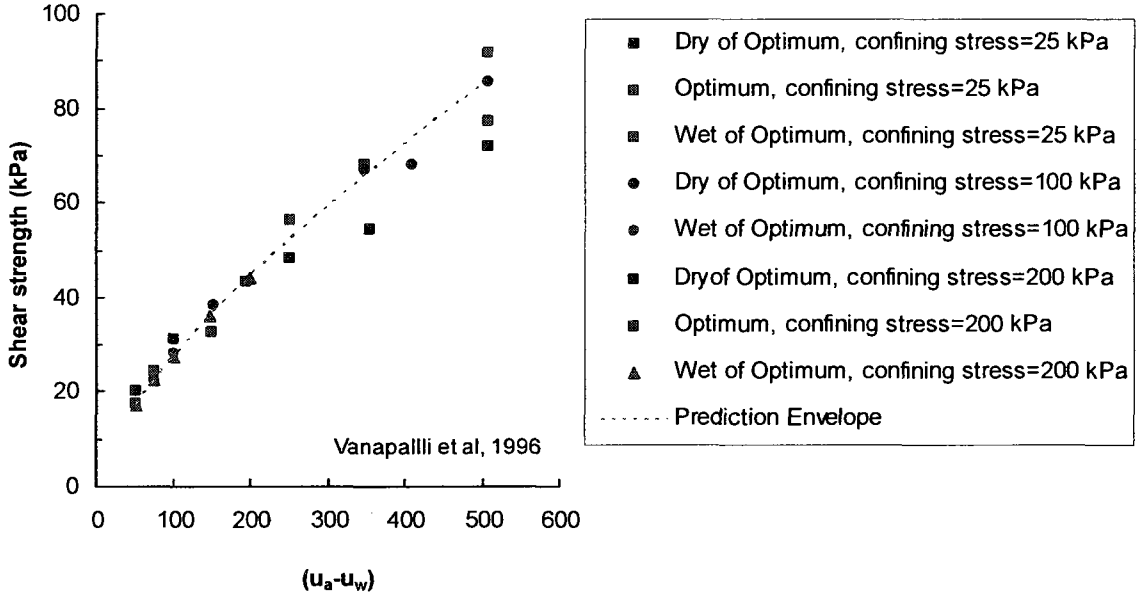

Figure 4.26. Predicted versus measured values for Vanapalli et al glacial till in its various conditions. (Xu, 2004)

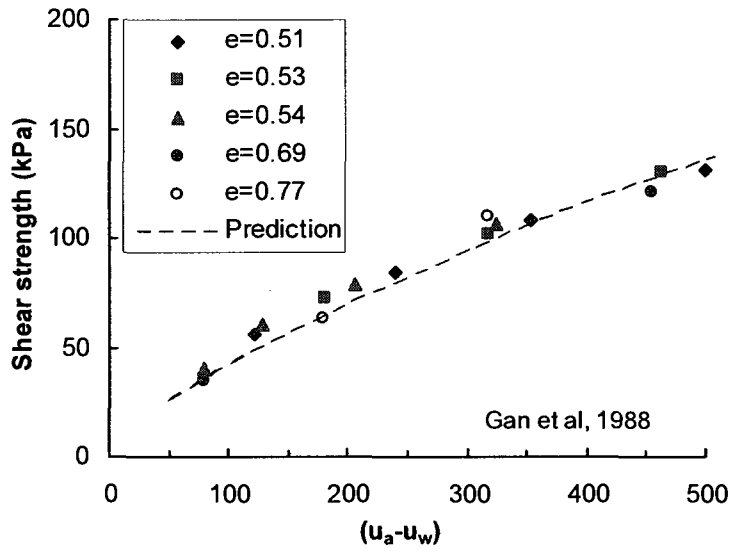

Figure 4.27. Predicted versus measured values for Gan glacial till in its various void ratios. (Xu, 2004)

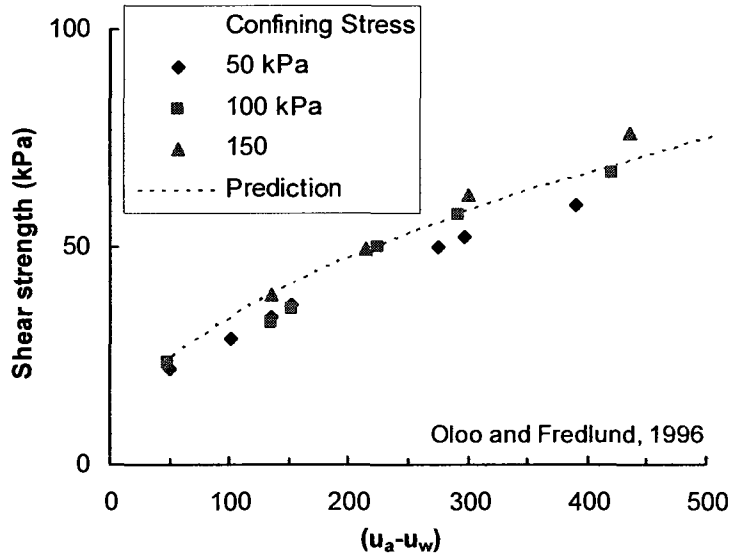

Figure 4.28. Predicted versus measured values for Botkin silt in its various conditions. (Xu, 2004)

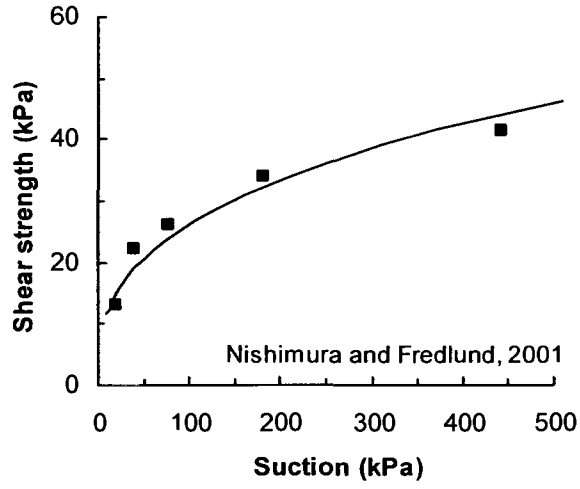

Figure 4.29. Predicted versus measured values for Nishimura and Fredlund's silt. (Xu, 2004)

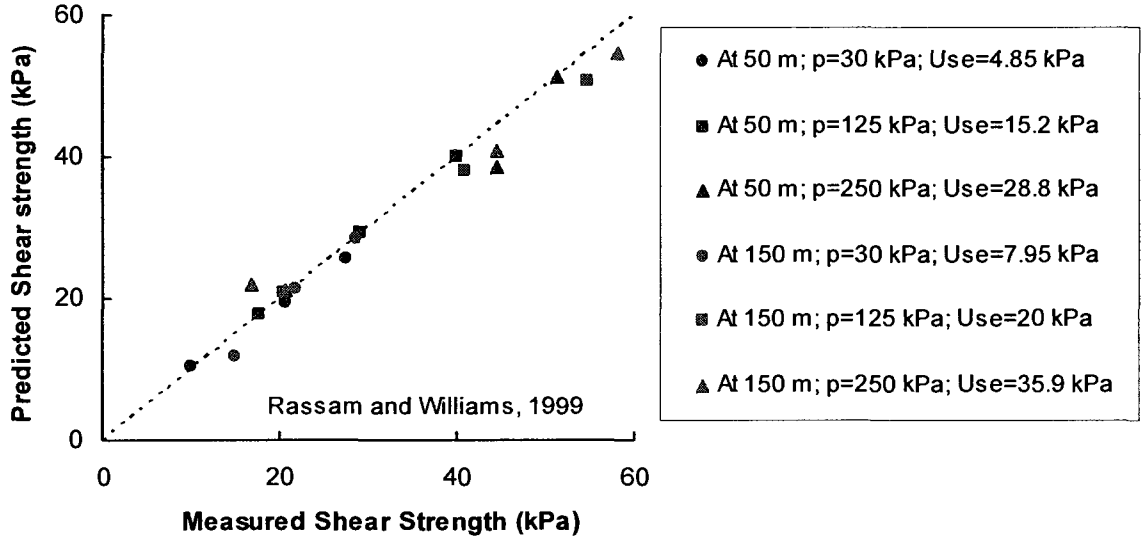

Figure 4.30. Predicted versus measured values for Rassam and Williams' Kidston tailings taken from both 50 m and 150 m (Xu, 2004).

4.3.15 Tekinsoy, Kayadelen, Keskin, Söylemez (2004)

The authors incorporate the atmospheric pressure into a logarithmic equation they proposed for predicting the shear strength of unsaturated soils (Eqn. 3-64). They tested their equation on Nanyang expansive soil and 4 other soils. The equation provided an acceptable fit for three of the soils including the Nanyang expansive soil (Table 4.23).

However, the fit for the Dhanauri clay and the Notch Hill silt was not acceptable although graphically, it appeared adequate.

$$\tau = c' + (\sigma - u_a) \cdot \tan\phi' + \tan\phi' [(u_a - u_w)_b + p_{at}] \cdot ln\left[\frac{(u_a - u_w) + p_{at}}{p_{at}}\right] \quad [3\text{-}64]$$

Table 4.23. Results of analysis on data presented for Equation 3-64 from Tekinsoy et al, 2006

Soil	No. of Data Points	No. of Points with an Acceptable Fit	Average Deviation (%)	Acceptable Fit? (Y/N)
Nanyang expansive soil *Tekinsoy et al, 2004*	4	4	4.4	Y
Glacial till *Vanapalli et al, 1996*	5	5	2.6	Y
Glacial till *Gan et al, 1988*	4	3	6.3	Y
Dhanauri clay *Gulhati and Satija, 1981*	4	2	11.1	N
Notch Hill silt *Krahn et al, 1989*	3	1	11.3	N

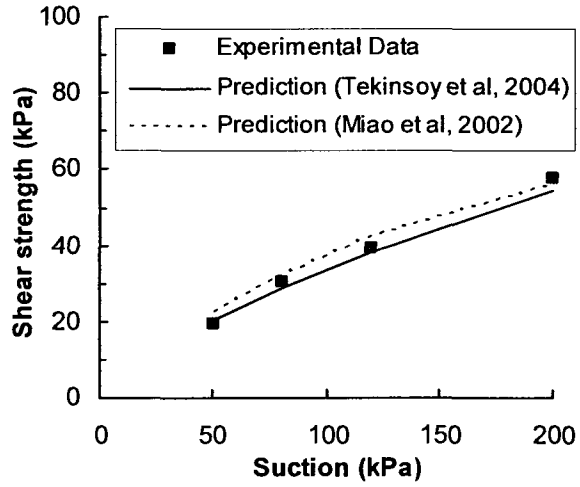

Figure 4.31. Prediction curves for Equation 3-64 and 3-45 against the measured data of Miao et al Nanyang expansive soil. (Tekinsoy et al, 2004)

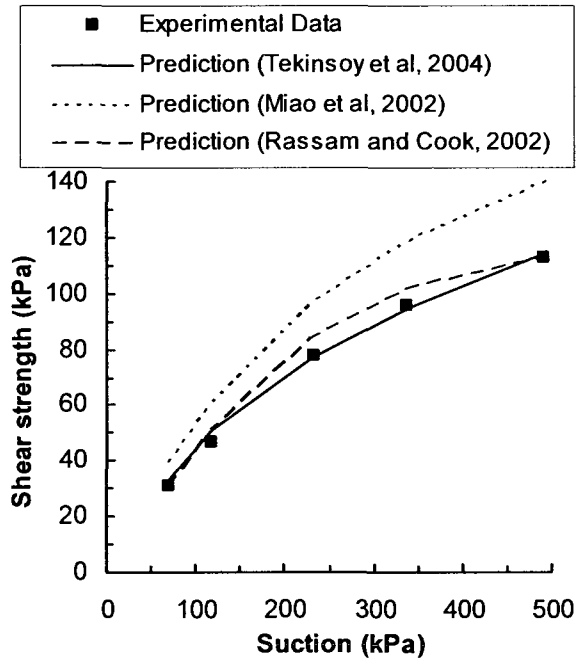

Figure 4.32. Application of three equations to Gan et al glacial till. (Tekinsoy et al, 2004)

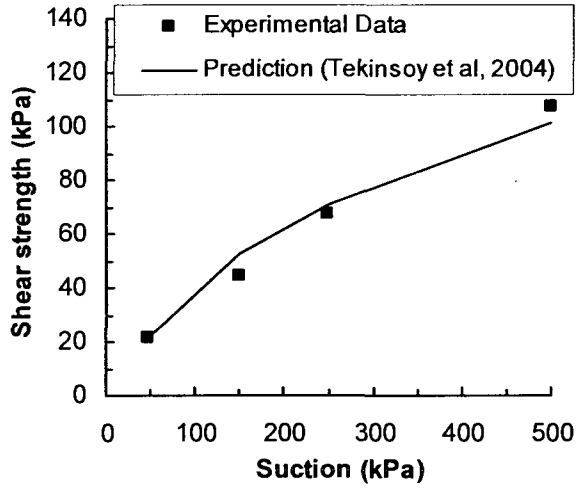

Figure 4.33. Application of Eqn. 3-64 to Vanapalli et al glacial till. (Tekinsoy et al, 2004)

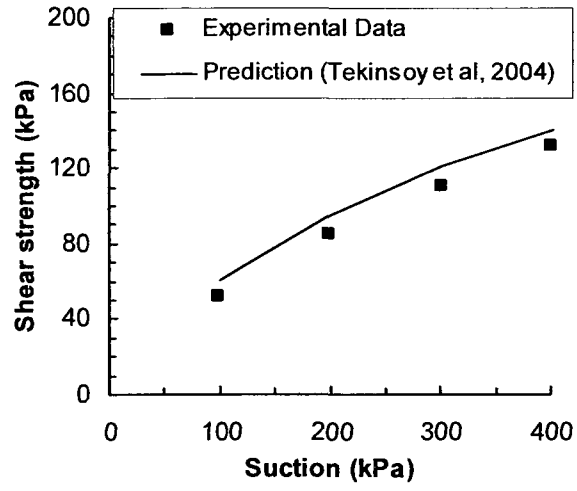

Figure 4.34. Prediction curve for Dhanauri clay. (Tekinsoy et al, 2004)

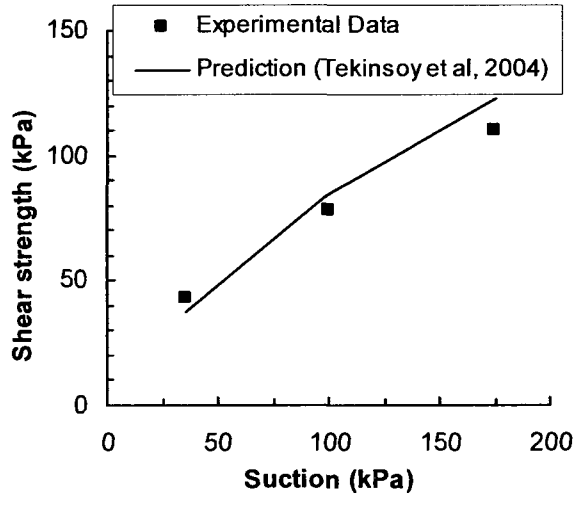

Figure 4.35. Prediction curve for Notch Hill silt. (Tekinsoy et al, 2004)

4.3.16 Lee, Sung, Cho (2005)

Lee, Sung and Cho proposed an equation (3-67) that recognized the change in shear strength behaviour before and after the AEV. They tested a weathered granite under different confining stresses. They also determined the SWCC of the granite under different confining stresses using a CPCE. They then proceeded to fit curves to the data (i) using the data from the SWCC measured with no confining pressure (Table 4.24) and (ii) also at a confining pressure equal to the confining pressure applied during shearing (Table 4.31). The resulting graphs illustrate the measured data and the two curves and although there is a difference in the graphs, qualitatively, there is little difference (Figure 4.36). The equation provides an acceptable fit using a 'confined' SWCC or the 'unconfined' SWCC.

$$\tau = c' + (\sigma_a - u_a)\cdot tan\phi' + (u_a - u_w)_b \cdot tan\phi' + \left[(u_a - u_w) - (u_a - u_w)_b\right]\cdot \theta^{\kappa}\left[1 + \lambda(\sigma_n - u_a)\right]\cdot tan\phi' \quad [3\text{-}67]$$

Table 4.24. Results of analysis on data presented for Equation 3-67 from Lee et al (2005) using a confining stress of 0 kPa when determining the SWCC of a weathered granite.

Net Normal Stress (kPa)	No. of Data Points	No. of Points with an Acceptable Fit	Average Deviation (%)	Acceptable Fit? (Y/N)
0	5	5	5.2	Y
100	5	5	0.9	Y
200	5	5	0.5	Y
300	5	5	0.6	Y

Table 4.25. Results of analysis on data presented for Equation 3-67 from Lee et al (2005) using different confining stresses to determine the SWCC of a weathered granite.

Net Normal Stress (kPa)	No. of Data Points	No. of Points with an Acceptable Fit	Average Deviation (%)	Acceptable Fit? (Y/N)
100	5	5	2.5	Y
200	5	5	2.9	Y
300	5	5	3.5	Y

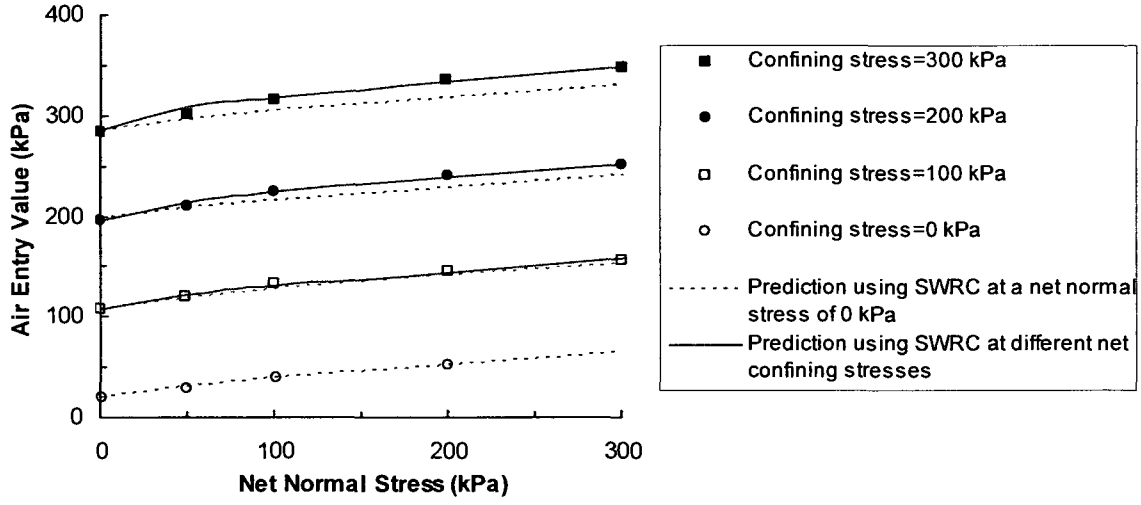

Figure 4.36. Measured and predicted relationships for weathered granite at different conditions. The data is presented with two separate prediction curves: one at a SWCC at 0 kPa confining stress and at varied confining stresses (Lee et al, 2005)

4.3.17 Matsushi and Matsukura (2006)

Matsushi and Matsukura proposed an equation (Eqn. 3-68) that uses the volumetric water content rather than the matric suction. The authors set up a testing programme for two soils; silt and sand. This testing programme differs from others in that there are more shear points recorded. For both soils, the equation provided an acceptable fit. (Table 4.26)

$$\tau = \sigma' \cdot \tan\phi' + Ce^{-\mu\theta} \qquad [3\text{-}68]$$

Table 4.26. Results of analysis on data presented for Equation 3-68 from Matsushi and Matsukura (2006)

Soil	No. of Data Points	No. of Points with an Acceptable Fit	Average Deviation (%)	Acceptable Fit? (Y/N)
Sand soil *Matsushi and Matsukura, 2006*	22	18	7.5	Y
Silt soil *Matsushi and Matsukura, 2006*	19	17	4.9	Y

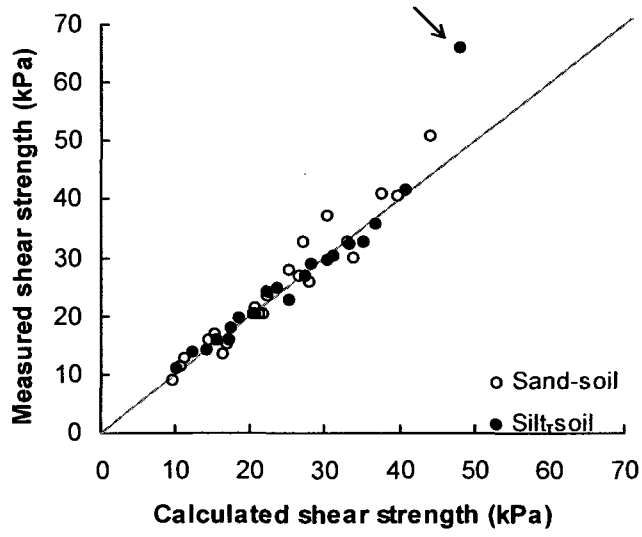

Figure 4.37. Comparison of calculated shear strength versus the measured shear strength. (Matsushi and Matsukura, 2006)

4.3.18 Vilar (2006)

The investigator proposed an enhancement to the equation proposed by Miao et al, 2002. (Eqn. 3-45). The equation uses the hyperbolic equation (3-45) and applies two conditions to define the curve fitting variables (*a* and *b*): The condition of the soil when the suction is less than the air-entry value (AEV) is shown in Eqn. 3-46. As the suction approaches zero, the inverse of the variable *a* approaches the slope of the line tan ϕ'. The author assumes that the maximum cohesion occurs when the soil reaches the residual degree of saturation resulting in Eqn. 3-46. The authors propose that the residual suction could be determined from air dried samples, thus determining *b*.

$$\tau_{us} = \frac{(u_a - u_w)}{\frac{1}{\tan\phi'} + \left(\frac{1}{\tau_{us-\max}} - \frac{1}{(u_a - u_w)_{\max} \cdot \tan\phi'}\right)} \qquad [3\text{-}73]$$

The investigator tried the equation on 12 different soils (Figure 4.38 to 4-40). The measured shear strength at or near 500 kPa (or the shear strength at the maximum suction measured) was used as $\tau_{us\text{-}max}$.

Of the twelve soils, two of them (glacial till and ash tuff) were tested at more than one net normal stress. The total number of data sets was 15 sets of data. Twelve of fifteen data sets had an acceptable fit with this technique (Table 4.27). Although this technique uses measured data, the relative amount of effort in comparison to a full unsaturated soils shear strength test is minimal. However, the modified technique varies slightly from the initially proposed technique for determining the curve fitting variable, c_{ult}. Further testing will be required to verify this equation.

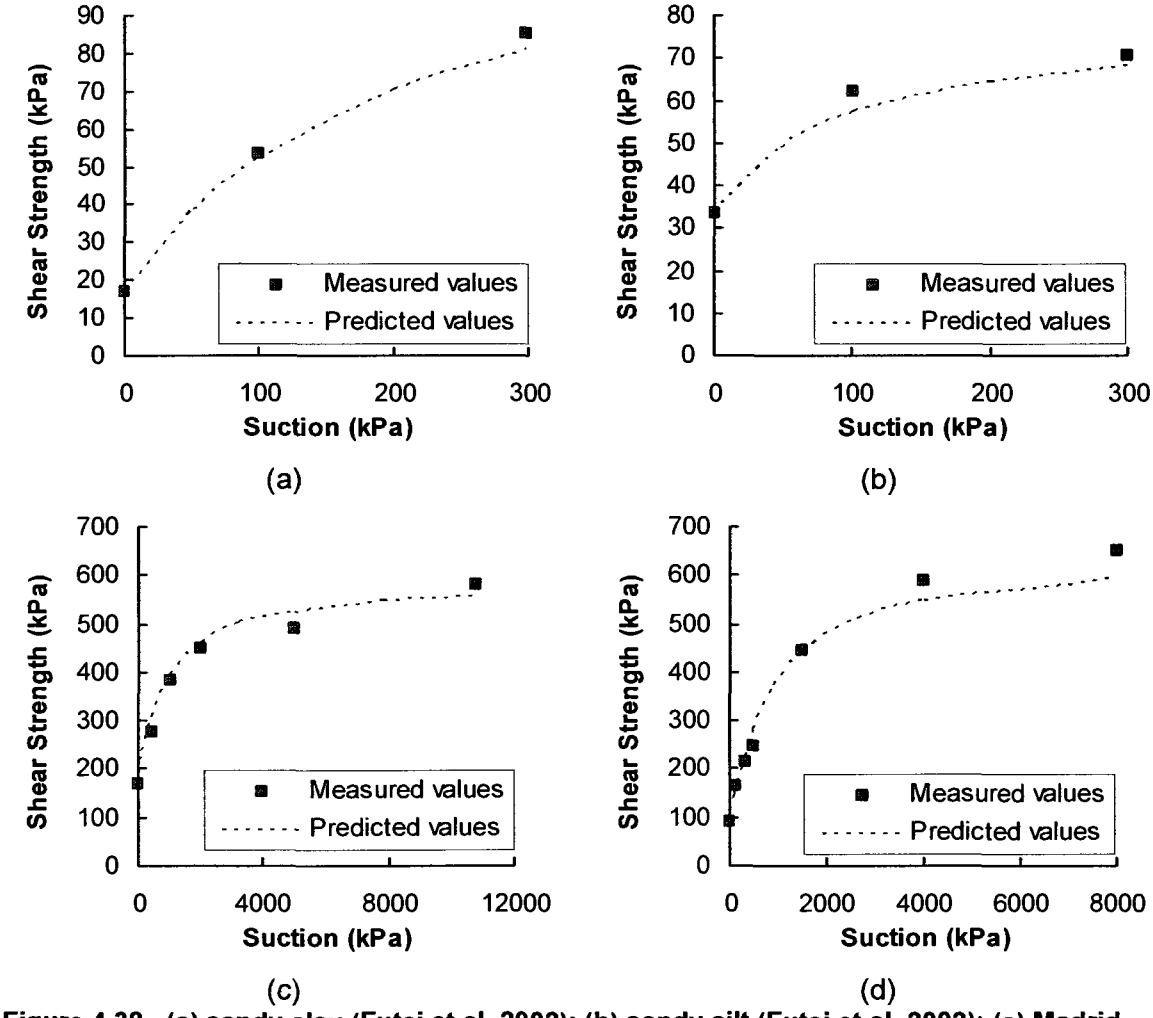

Figure 4.38. (a) sandy clay (Futai et al, 2002); (b) sandy silt (Futai et al, 2002); (c) Madrid grey clay; (d) red silty clay.

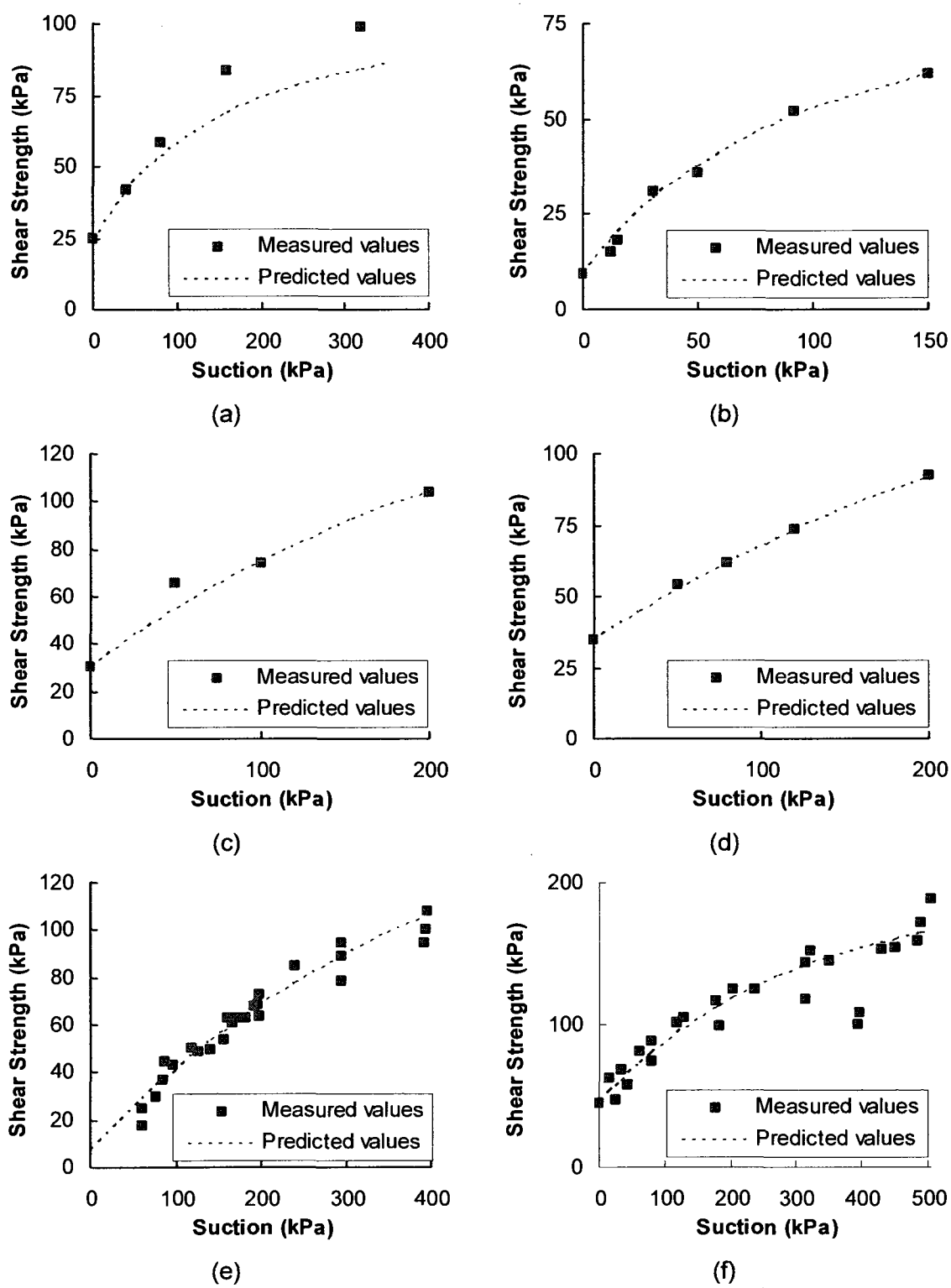

Figure 4.39. (a) silty sand (Reis, 2004); (b) copper tailings (Drumright and Nelson, 1995); (c) Sandy clay (Teixeira and Vilar, 1997); (d) Nanyang expansive (Miao et al, 2001); (e) Dhanauri clay (Satija, 1981); (f) glacial till (Fredlund et al, 1988).

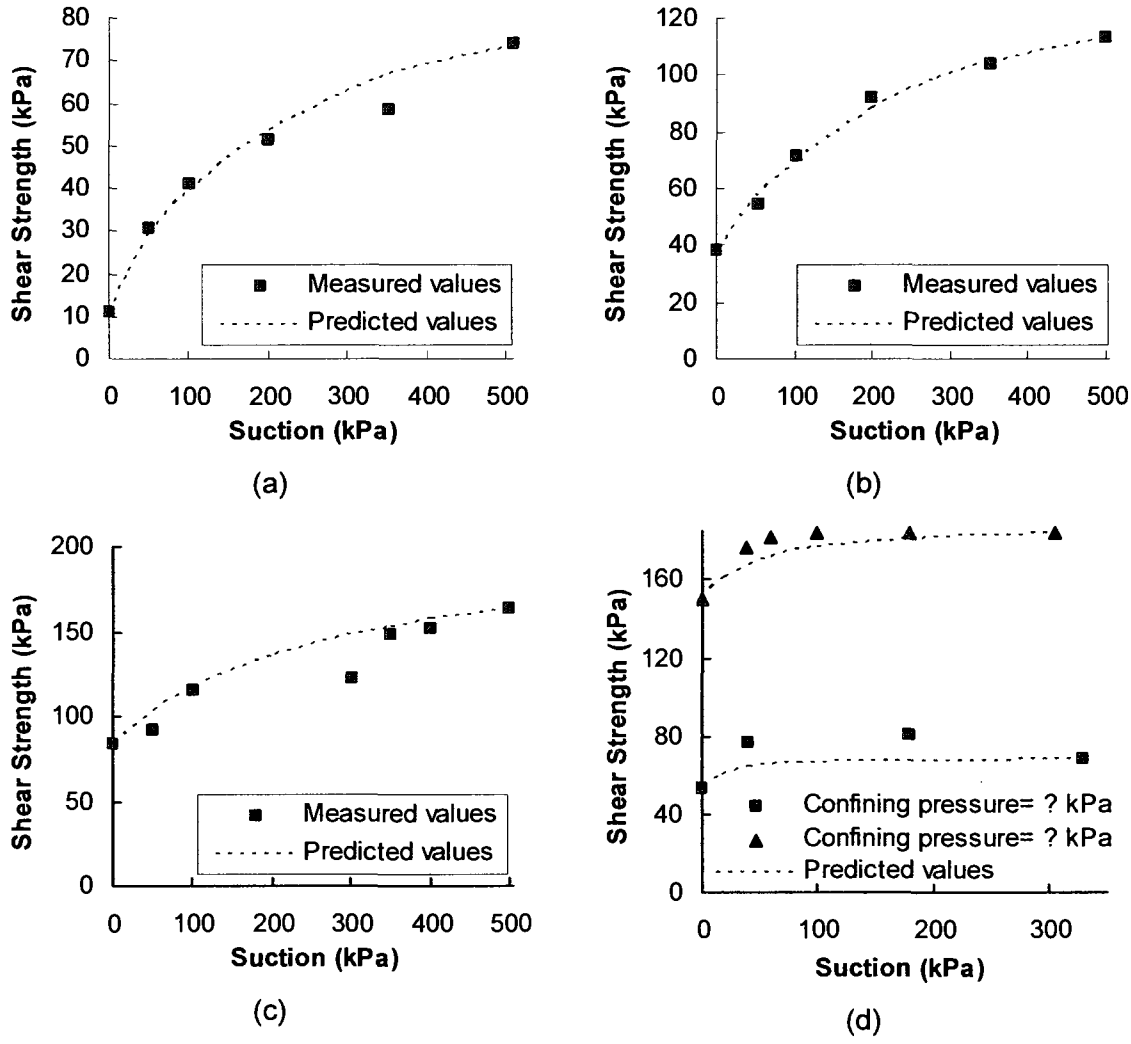

Figure 4.40. (a) ash tuff (Gan and Fredlund, 1996); (b) glacial till (Vanapalli et al, 1996); (c) glacial till (Vanapalli et al, 1996); (d) glacial till (Gan and Fredlund, 1996).

Table 4.27. Results of analysis on data presented for from Vilar (2006).

Soil	No. of Data Points	No. of Points with an Acceptable Fit	Average Deviation (%)	Acceptable Fit? (Y/N)
Sandy clay *Futai et al, 2002*	3	3	4.7	Y
Sandy silt *Futai et al, 2002*	3	2	7.5	Y
Silty sand *Reis, 2004*	5	2	16.8	N
Madrid grey clay *Escario, 1988*	6	5	9.6	Y
Red silty clay *Escario, 1988*	7	5	12.0	Y
Sandy clay *Teixeira and Vilar, 1997*	4	3	6.7	Y
Copper tailings *Drumright and Nelson, 1995*	7	7	2.8	Y
Nanyang clay *Miao et al, 2001*	5	5	5.3	Y
Dhanauri clay *Satija, 1981*	25	20	4.3	Y
Glacial till *Fredlund et al, 1988*	25	20	8.2	Y
Glacial till *Vanapalli et al, 1996*	8 6 6	5 5 5	9.6 7.9 3.7	Y Y Y
Ash tuff Gan and Fredlund, 1996	5 3	2 1	14.4 15.2	N N

4.4 Summary

Twenty-five equations have been proposed to predict or estimate the change in shear strength with respect to suction. Only eleven of the equations are truly predictive which is defined as relating the fitting parameters and equation variables to the properties of the soil. Only seven prediction equations which are more commonly used will be applied to a group of soils to examine their ability to predict the unsaturated shear strength. The strengths and limitations of each of the equations will be discussed in Chapter 6. The properties of the soils including the shear strength behaviour will be discussed in Chapter 5.

CHAPTER 5 SOIL INFORMATION

5.1 Introduction

The ability of the equation to predict the unsaturated shear strength of soils can only be tested using experimental data from numerous soils. In Chapter 4, published data from numerous authors was used to test equations. The testing is expensive and requires specialized equipment and therefore, is in short supply. Previously published data can be used for this purpose. This chapter presents shear strength of several investigators published work. In Chapter 6 comparisons will be provided between the measured data summarized in this chapter with predicted values.

5.2 Background of Soils Used in this Analysis

The shear strength behaviour of several types of soils was studied by various investigators over the past fifty years in various parts of the world. Summary of all the data provided in this chapter can be grouped into different categories: residual soils, laterites, colluvium, loess, expansive soils and glacial till.

A residual soil is a soil that remains after some or part of the natural soil has been dissolved by chemical weathering. The remainder of the soil properties are dependent upon the parent material of the soil. A laterized soil is residual soil formed by leaching silica and the addition of aluminium and iron oxides. Laterized soils form in humid, often tropical climates, and may be red to dark brown in colour. Stiffness may vary from soft to hard and the method of formation can be conducive to formation of concretions. Laterites are related to kaolin. Residual soils are found in areas with a tropical climate where the climate is conducive to the increased weathering of soils. In these areas, the soils remain unsaturated most of the time. Investigations into the shear strength behaviour of unsaturated soils improve understanding of these residual soils.

A colluvial soil is gravity-deposited soil that is found on slopes or at bottom of slopes. At the bottom of slopes the deposit can form into a fan-like formations (Madigan, 2007). A loess is a homogenous, often porous Aeolian soil that is wind deposited. Loess may be calcareous in composition. Non-glacial loess is usually silt-sized material deposited from desert or playa. Brazil is known to have tropical loess while China has thick deposits of

desert loess. Loess soils can stand in vertical cliffs for extended periods and often drains easily. Loess soils are known to be collapsible. However, in general, any soils that have a low dry unit weight, bulky particle shapes and water-sensitive cohesion are susceptible to collapse (Li, 1989)

Expansive soil is a soil with clay minerals that will take on large amounts of water and are susceptible to swelling. Expansive soils can undergo a large volume change but can also exert a large swelling pressure on adjacent structures with the ability to cause extensive damage.

5.3 Presentation of Results of the Shear Strength of Unsaturated Soils

Fifty-two sets of data were extracted from numerous published sources. The soils represent different types of soils with varying classifications. Soils were chosen that had accompanying soil water characteristic curves (SWCC) and preference was given to soils tested under effective conditions using consolidated drained (CD) test results. This chapter presents the soils and the properties including the method of testing. The soils were tested using multiple confining pressures and the results from all tests are presented. The shear strength graphs and respective SWCC for the soils are presented in Appendix A of this thesis.

Data has been digitized from published works using a program called DigNo created at the University of Ottawa (Infante Sedano, 2006). The plot of shear strength and the SWCC for each soil is presented in these pages as well as a summary of the soil-type and methods of testing. The shear strength is presented as the shear strength contribution due to suction (τ_{us}).

Soils tested using a modified direct shear apparatus has a net normal stress equal to the confining stress as the confining stress is applied perpendicular to the directed shear plane of the shear box. Triaxial tests fail along an angled plane at an angle specific to each soil. The net normal stress on samples tested in a triaxial cell varies from sample to sample as the net normal stress is a combination of the confining pressure and the axial loading applied to cause failure in the sample.

The shear strength values measured at 0 kPa suction allows the authors to verify that the soil parameters are correct. In some instances, the use of the data at 0 kPa suction

prompted a recalculation of the soil parameters presented in the published work. On occasion, the calculated soil effective stress parameters (c' and ϕ) were to be found to be different from the published values. When shear strength at 0 kPa suction is provided, the published soil parameters are assumed to be correct.

5.3.1 Escario and Juca (1989)

Three soils were tested by Escario and Juca in 1989 as a part of a study on unsaturated soils to test a range of soil types under unsaturated conditions and to examine the shape of the resulting curves. These soils (red silty clay, Madrid grey clay and Madrid clay sand) have been used to test various equations on the shear strength of unsaturated soils.

This paper provides more results on the three soils which were initially tested by Escario and Saez in 1986. In 1986, the soils over the range of 0 to 1000 kPa, but did not have data on the SWCC of the soils. The data from Escario and Saez (1986) was plotted with the data from Escario and Juca (1989).

The samples were prepared by static compaction. The pressure membrane apparatus was used to determine the SWCC. The SWCC data is shown as the water content versus the suction. The volume-mass properties are used to convert the gravimetric water content to the degree of saturation. The sample size was 70 mm diameter and 20 mm high. The shear strength was tested using a modified direct shear apparatus developed by Escario (1980). Shear testing occurred at a shear velocity of 2.4 mm/day.

Red Silty Clay

The tested red silty clay *(Soil 1)* was classified using the Unified soil classification system (ASTM D2487). The red silty clay is a lean clay whose properties are summarized in Table 5.1. The soil was tested at three net normal stresses: 120 kPa, 300 kPa and 600 kPa (Table 5.4).

Table 5.1. Properties of Soil No. 1, red silty clay (Escario and Saez, 1986; Escario and Juca, 1989).

ϕ'	c'	Sand (%)	Silt (%)	Clay (%)	w_L	I_p
32	37.8	14	86		33	13
USCS Classification: Lean clay (CL)						
Sample Preparation: Compacted			Shear Strength Test:		Modified direct shear test	

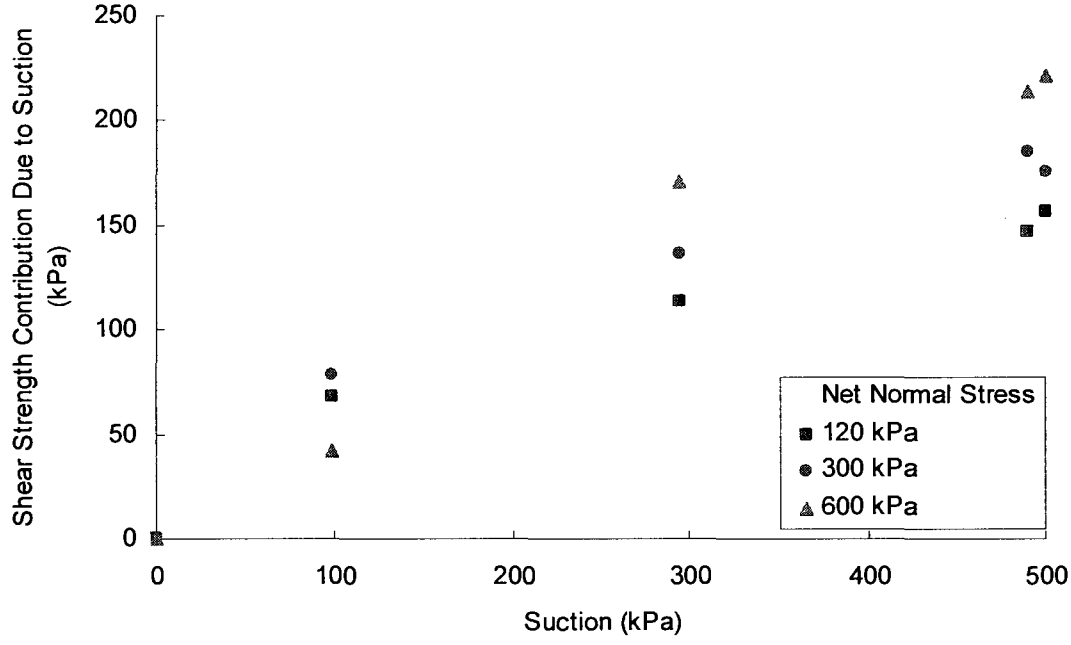

Figure 5.1. Shear strength contribution due to suction for red silty clay. (Escario and Saez, 1986; Escario and Juca, 1989)

Madrid Grey Clay

The tested Madrid grey clay *(Soil 2)* was a heavy silt with only 1% sand. The properties are summarized in Table 5.2. The soil was tested under a net normal stress of 300 kPa (Table 5.4).

Table 5.2. Properties of Soil No. 2, Madrid grey clay (Escario and Saez, 1986; Escario and Juca, 1989)

ϕ'	c'	Sand (%)	Silt (%)	Clay (%)	w_L	I_p
25.3	21	1	99		71	35
USCS Classification: Heavy silt (MH)						
Sample Preparation:	Compacted		Shear Strength Test:		Modified direct shear test	

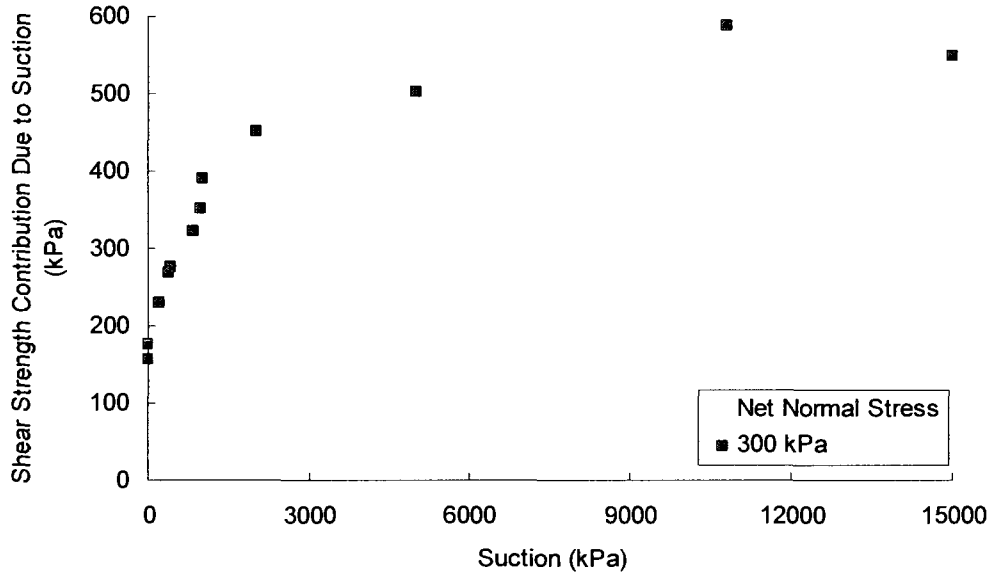

(a)

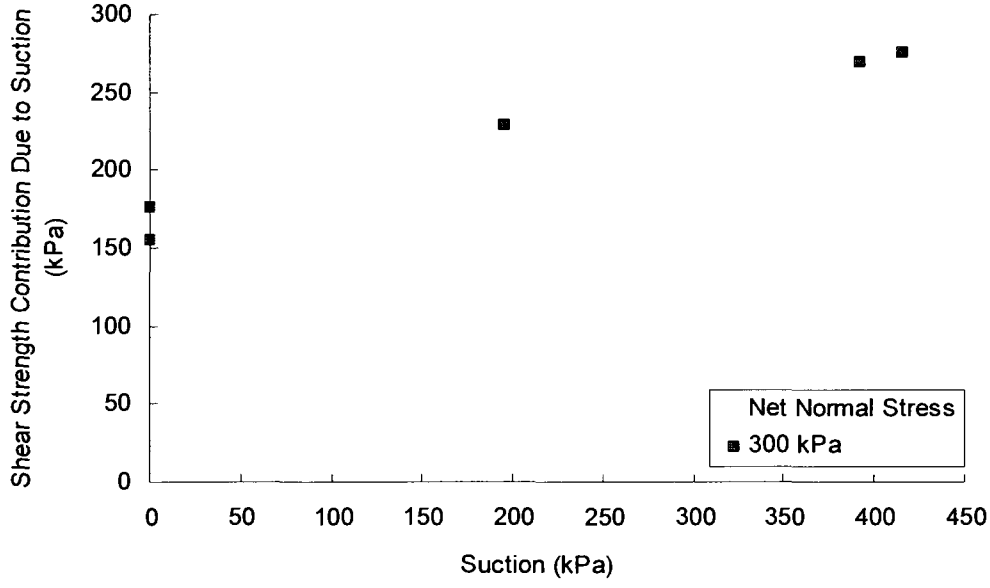

(b)

Figure 5.2. Shear strength contribution due to suction for Madrid grey clay. (Escario and Saez, 1986; Escario and Juca, 1989)

Madrid Clay Sand

The properties of Madrid clay sand (*Soil* 3) is defined in Table 5.3. The clay sand was tested using the net normal stresses of 120 kPa and 600 kPa (Table 5.4). Saturated shear strength parameters were determined from the unsaturated soil tests at 0 kPa suction.

Table 5.3. Properties of Soil No. 3, Madrid clay sand (Escario and Juca, 1989).

ϕ'	c'	Sand (%)	Silt (%)	Clay (%)	w_L	I_p
40	39.5	87	13		32	15
USCS Classification: Clayey sand (SC)						
Sample Preparation:	Compacted		Shear Strength Test:	Modified direct shear test		

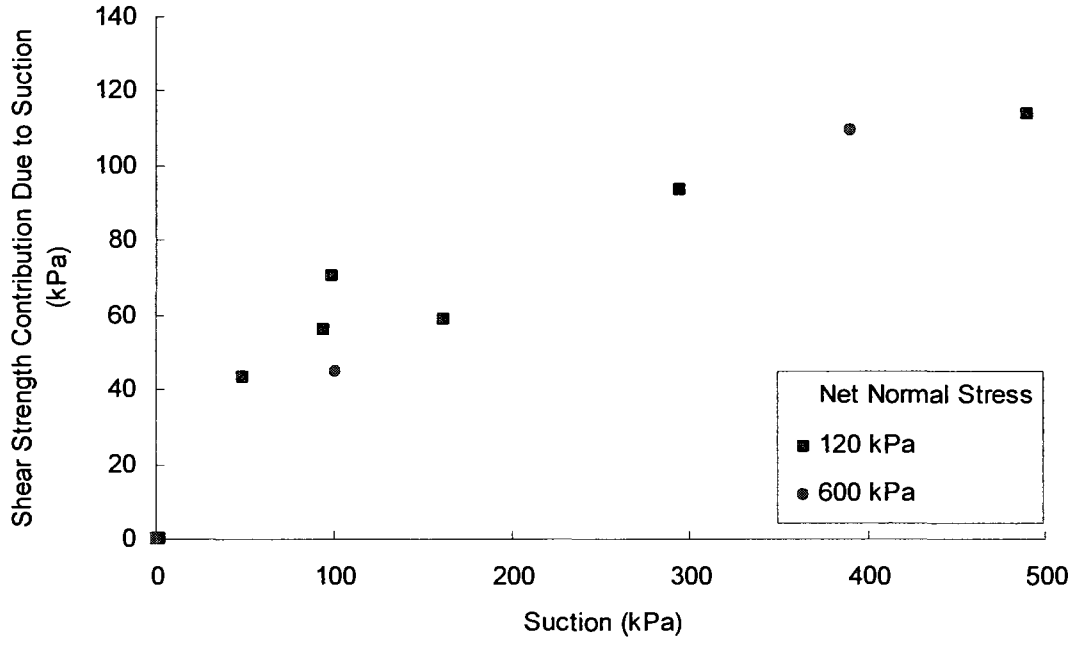

Figure 5.3. Shear strength contribution due to suction for Madrid clay sand. (Escario and Juca, 1989)

Table 5.4. Confining pressures and net normal stresses for red silty clay (Soil 1), Madrid grey clay (Soil 2) and Madrid clay sand (Soil 3) (Escario and Saez, 1986; Escario and Juca, 1989).

	Soil 1a	Soil 1b	Soil 1c	Soil 2	Soil 3a	Soil 3b
Confining Pressure, σ_3 (kPa)	120	300	600	300	120	600
Net normal stress, σ_n (kPa)	120	300	600	300	120	600

5.3.2 Vanapalli, Fredlund, Pufahl and Clifton (1996)

The data for Indian Head glacial till was presented in Vanapalli (1994) and later in several publications including Vanapalli et al in 1996 (Soil 4). The till was from Indian Head, Saskatchewan and was prepared by air-drying it and passing it through the 2 mm sieve. According the to the USCS classification system (ASTM D2487) the till is a lean clay with sand (Table 5.5).

The shear strength behaviour was tested at different water contents representing dry of optimum moisture conditions, optimum moisture conditions and wet of optimum moisture conditions. Only data from the samples prepared at optimum content data are summarized in this thesis. The samples were prepared using a constant volume mold to statically compact samples in a ring with a diameter of 100 mm and a height 20 mm. Both the specimens for the shear strength tests and the SWCC are obtained from such specimens.

The shear strength was measured using multistage testing equipment developed by Gan and Fredlund (1988). The SWCC was determined using a pressure plate apparatus over a range of 0 to 1500 kPa. The SWCC for higher suctions (4,500 to 300,000 kPa) was measured using osmotic desiccators with different saline solutions. The water content was determined after the sample was allowed to come into equilibrium.

Table 5.5. Properties of Soil No. 4, Indian Head till (Vanapalli et al, 1996b).

ϕ'	c'	Sand (%)	Silt (%)	Clay (%)	w_L	I_p
22.5	15	28.0	42.0	30.0	36	18
USCS Classification: Lean clay with sand (CL)						
Sample Preparation:	Compacted		Shear Strength Test:		Modified direct shear test	

Table 5.6. Confining pressures and net normal stresses for Soil no. 4, Indian Head till (Vanapalli et al, 1996b).

	Soil 4a	Soil 4b	Soil 4c
Confining Pressure, σ_3 (kPa)	25	100	200
Net normal stress, σ_n (kPa)	25	100	200

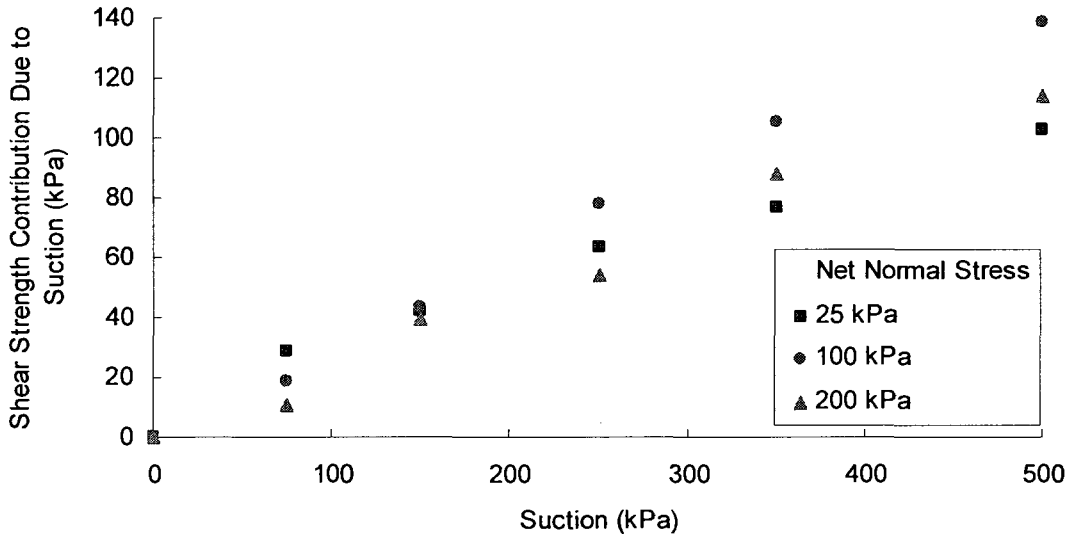

Figure 5.4. Shear strength contribution due to suction for Indian Head till prepared at (a) optimum moisture content. (Vanapalli et al, 1996b)

The gravimetric water content of samples compacted at optimum conditions equal to 16.3% and the dry density was 1.8 Mg/m^3. The strain rate for shear testing was 2.7 mm/day.

5.3.3 Vanapalli, Wright and Fredlund (2000)

Botkin silt (Soil 5) was presented in a paper by Vanapalli et al, 2000. The unsaturated shear strength behaviour of this soil was tested using a modified version of the Vanapalli κ equation for interpreting unconfined compressive strength over the entire range of suction (0 to 1,000,000 kPa). The soil is lean clay with sand. The soil was statically compacted to a density of 1.85 Mg/,m^3. The sample was prepared to have a 50 mm diameter and a height of 104 mm. The saturated specimens were air dried to different water contents and wrapped and stored for a period of four days to allow the specimen to achieve equilibrium. Air dried specimens allow water to evaporate from the surface. Wrapping the samples and allowing them to sit allows the water distribution to become constant throughout the specimen.

Table 5.7. Properties of Soil No. 5, Botkin silt (Vanapalli et al, 2000).

ϕ'	c'	Sand (%)	Silt (%)	Clay (%)	w_L	I_p
36.5	14.2	27.5	48.5	24.0	25	8
USCS Classification: Lean clay with sand (CL)						
Sample Preparation:	Compacted		Shear Strength Test:	Unconfined compression test		
Confining Pressure, σ_3 (kPa)	0		Net normal stress, σ_n (kPa)	6 - 802		

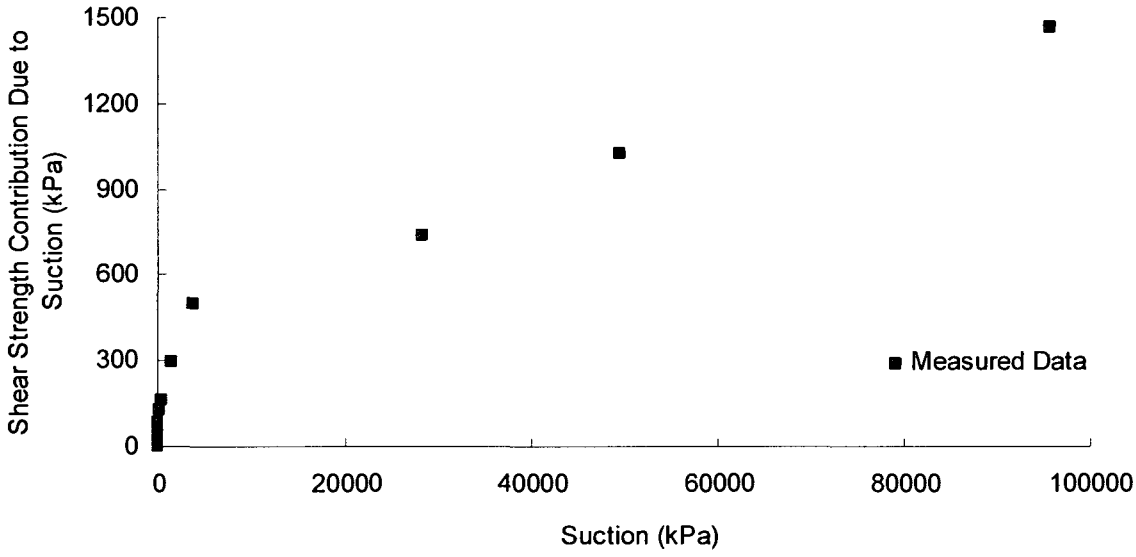

(a)

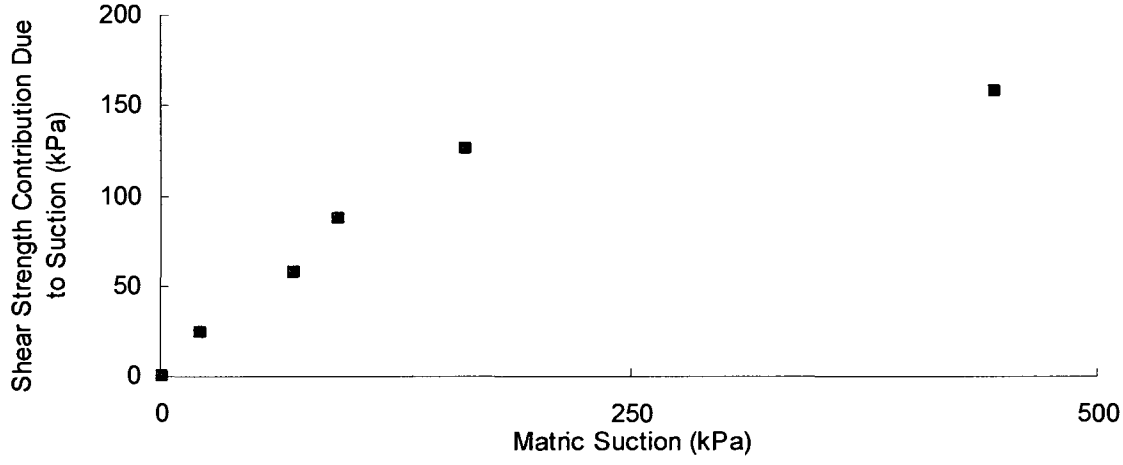

(b)

Figure 5.5. Shear strength contribution due to suction for Botkin silt over a range of suctions from (a) 0-95,600 kPa; (b) 0-500 kPa. (Vanapalli et al, 2000)

The data was interpreted assuming effective conditions for the unconfined compression test. Vanapalli et al examined the water content at three different levels of the unconfined specimen after testing. The water content through the profile was found to be constant and it was assumed that the suction was constant in the specimen. Therefore, the assumption of effective conditions used in the analysis of these results is reasonable.

The SWCC was measured testing the soil specimen in a Tempe cell over the suction range of 0 to 500 kPa. Small blocks were then cut from the specimen from the Tempe cell and placed in an osmotic desiccators to measure portion of the SWCC at high suction.

5.3.4 Gulhati and Satija (1981)

Gulhati and Satija presented an equation based on statistically analysis to interpret the shear strength of unsaturated soil. Soil 6 as used in this approach. The Dhanauri clay was prepared at a two different densities: one at low-density and the other at high-density. The conventional undrained triaxial tests were used to determine the effective strength parameters of the Dhanauri soil. The soil properties are summarized in Table 5.8 and can be classified as lean clay borderline to fat clay. The shear strength was measured using a modified triaxial test at a shear rate was 0.00001%/s.

The SWCC was generated using the degree of saturation values and the suction of the soil measured prior to testing. The authors note using a bubble pump during testing to remove air bubbles in the system.

Table 5.8. Properties of Soil No. 6, Dhanauri clay (Satija, 1978; Gulhati and Satija, 1981).

ϕ'	c'	Sand (%)	Silt (%)	Clay (%)	w_L	I_p
30	7.8	8	70	25	49	25
USCS Classification: Lean clay (CL) borderline to fat clay (CH)						
Sample Preparation:	Compacted		Shear Strength Test:	Modified triaxial test		

Table 5.9. Confining pressures and net normal stresses for soil no. 6, Dhanauri clay (Satija, 1978; Gulhati and Satija, 1981).

	Confining Pressure, σ_3 (kPa)	Net Normal Stress, σ_n (kPa)
Soil 6a	96.1	186-228
Soil 6b	193.3	325-364
Soil 6c	289.4	455-511
Soil 6d	386.5	590-667
Soil 6e	96.1	193-263
Soil 6f	193.3	328-388
Soil 6g	289.4	460-524
Soil 6h	386.5	604-694

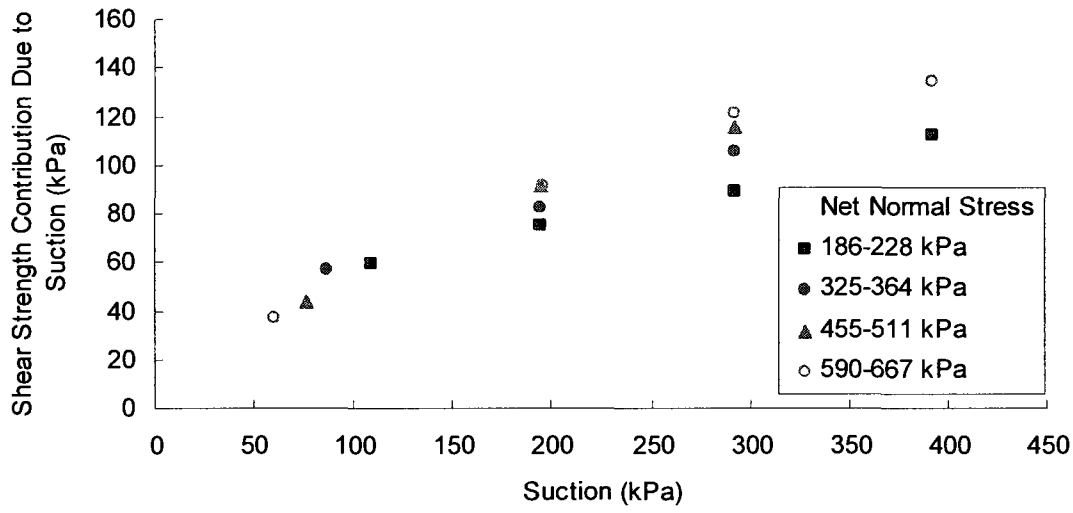

(a)

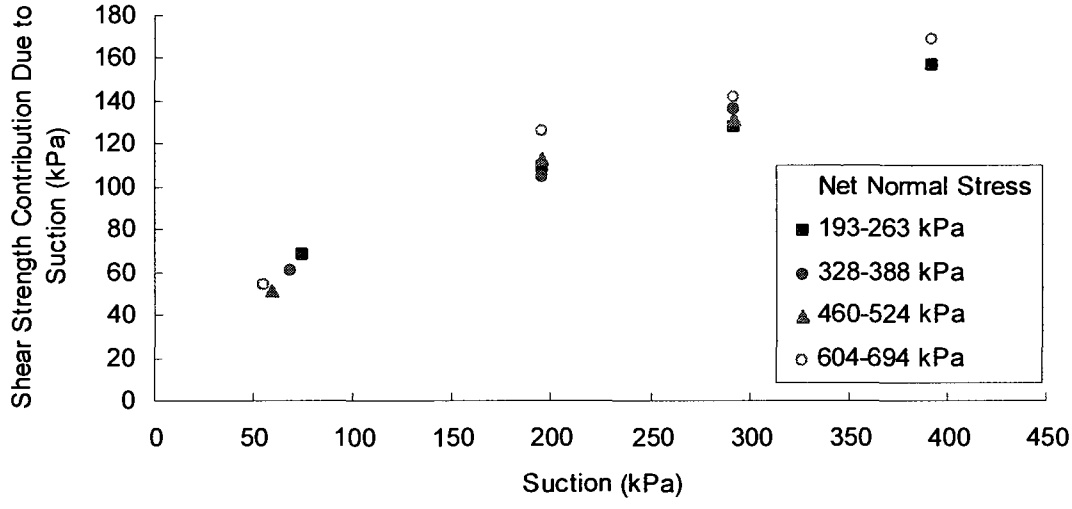

(b)

Figure 5.6. Shear strength contribution due to suction for Dhanauri clay compacted at (a) high density; and (b) at low density. (Satija, 1978; Gulhati and Satija, 1981)

The soils were tested at four different confining pressures: 96.1 kPa, 193.3 kPa, 289.4 kPa and 386.5 kPa. The net normal stresses for the samples ranged from 186 kPa at 100 kPa to 694 kPa at a suction of 400 kPa.

5.3.5 Lee, Sung and Cho (2005)

Lee et al (2005) presented a Korean weathered granite (Soil 7) in a paper discussing the effect of stress state on unsaturated soils. Weathered granite is a silty sand that was air-dried and sieved to remove particles greater than 2 mm. The soil was then re-wetted with distilled water to a gravimetric water content of 10%. The soil is silty sand. The material is non-plastic (Table 5.10). The effective shear strength parameters of the soil were determined using a conventional triaxial testing equipment.

Table 5.10. Properties of Soil No. 7, weathered granite (Lee et al, 2005).

ϕ'	c'	Sand (%)	Silt (%)	Clay (%)	w_L	I_p
30.4	13	87.6	12.4		NP	
USCS Classification: Silty sand (SM) [1]						
Sample Preparation:	Compacted		Shear Strength Test:		Modified triaxial test	

[1] classification is due to assumed non-plastic behaviour of the soil.

The SWCC was measured using three apparatuses: the confining pressure controlled extractor (CPCE), the Tempe cell and a pressure plate. The CPCE is a modified pressure plate that can confine the sample under isotropic stress while the SWCC was being measured. The authors measured the SWCC under a confining pressure equal to the confining pressure applied during testing under unconfined conditions. The SWCC measured with no confining pressure is closest to the SWCC developed for the other soils and, due to this reason, these SWCC were in this thesis.

The shear strength was tested using a modified triaxial apparatus. The confining pressures were 0, 100, 200 and 300 kPa although the net normal stresses varied from sample to sample. The ranges in net normal stresses corresponding to each confining pressure is summarized in Table 5.11. The determination of the angle of internal friction and the cohesion varies from the results presented. The authors determined an effective angle of internal friction, ϕ' of 41° and a cohesion of 19.5 kPa. Re-analyzing the data reveals the angle of internal friction to be 30.4° with an effective cohesion of 13 kPa.

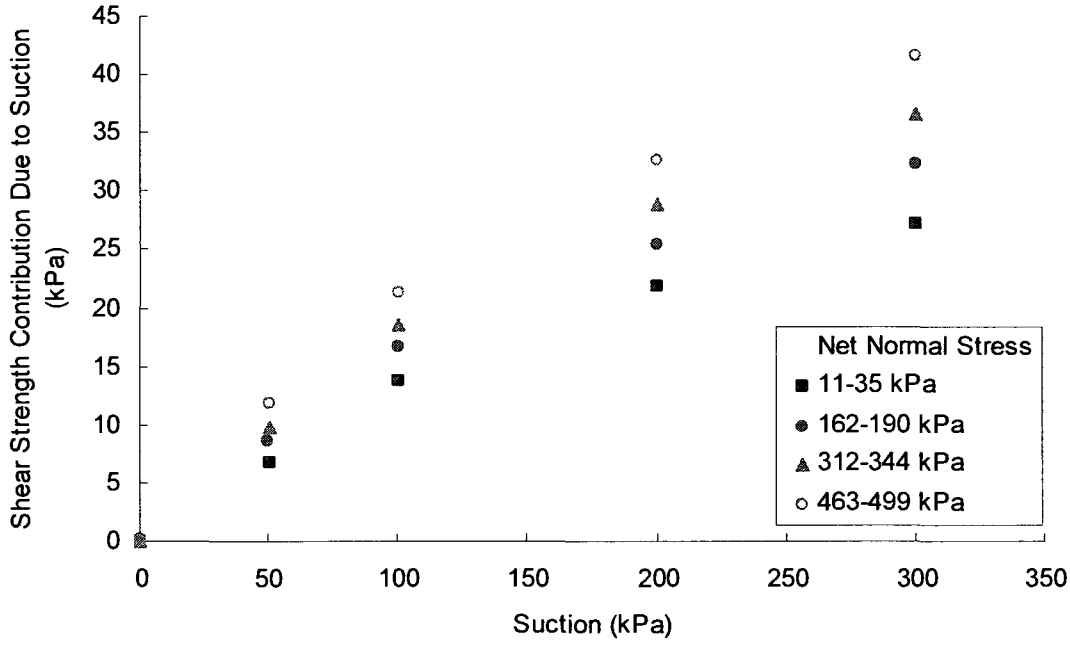

Figure 5.7. Shear strength contribution due to suction for weathered granite. (Lee et al, 2006)

Table 5.11. Confining pressures and net normal stresses for soil no. 7, weathered granite (Lee et al, 2005).

	Soil 7a	Soil 7b	Soil 7c	Soil 7d
Confining Pressure, σ_3 (kPa)	0	150	200	300
Net normal stress, σ_n (kPa)	11-35	162-190	312-344	463-499

5.3.6 Rahardjo, Heng and Choon (2004)

Rahardjo et al (2004) tested Jurong soil (Soil 8) to examine the change in shear strength in residual soils due to rainfall. (ie. Infiltration conditions) In other words, the focus of the study was to determine the shear strength behaviour due to wetting condition. The soil properties were determined for sandy lean clay (Table 5.12). The saturated shear strength parameters were measured using a conventional triaxial testing apparatus.

The soil specimens used for testing were prepared with a diameter of 50 mm. The height of the specimen was equal to 100 mm. The specimen was compacted in 10

equal layers. The soil was tested at three confining pressures (50, 100 and 150 kPa) using a modified triaxial test (Table 5.12). The consolidated drained (CD) results are presented in this thesis (Figure 5.8). The authors made certain that the equipment was flushed during testing to remove any diffused air.

The SWCC of the soil was determined using the pressure plate apparatus up to a suction of 500 kPa.

Table 5.12. Properties of Soil No. 8, Jurong soil (Rahardjo et al, 2004).

ϕ'	c'	Sand (%)	Silt (%)	Clay (%)	w_L	I_p
31	0	34	24	42	36	15
USCS Classification: Sandy lean clay (CL)						
Sample Preparation:	Compacted		Shear Strength Test:	Modified triaxial test		

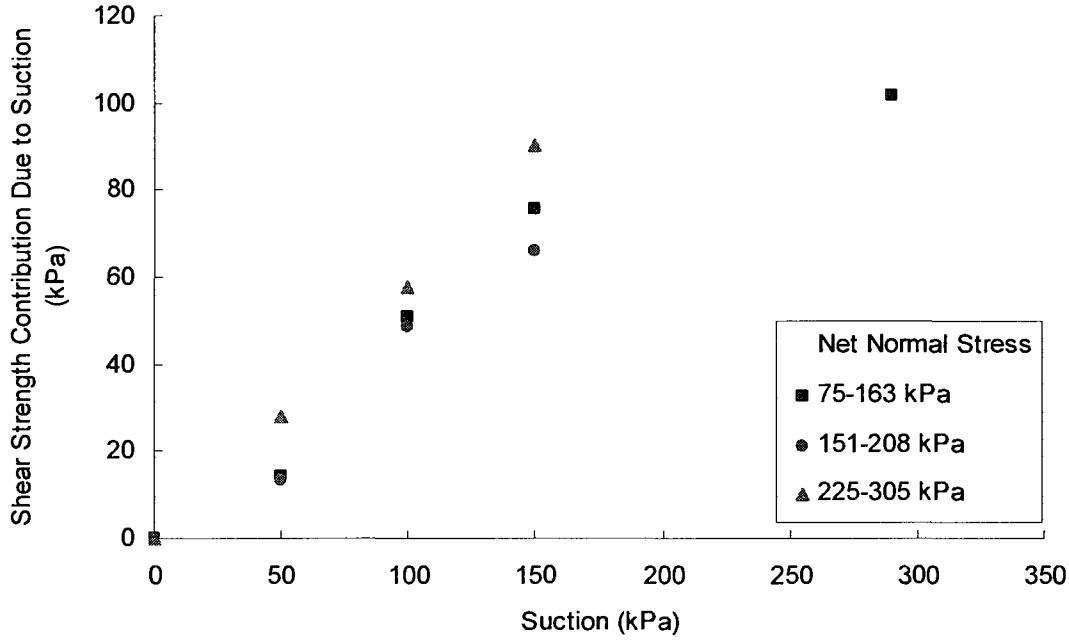

Figure 5.8. Shear strength contribution due to suction for Jurong soil. (Rahardjo et al, 2004).

Table 5.13. Confining pressures and net normal stresses for soil no. 8, Jurong soil (Rahardjo, 2004).

	Soil 8a	Soil 8b	Soil 8c
Confining Pressure, σ_3 (kPa)	50	100	150
Net normal stress, σ_n (kPa)	75-163	151-208	225-305

5.3.7 Bao, Gong and Zhan (1998)

Bao, Gong and Zhan (1998) presented shear strength data of two expansive clays in a keynote paper on properties of unsaturated soils and slope stability. They tested two Nanyang clays: a compacted specimen (Soil 9) and an undisturbed specimen (Soil 10). The effective strength parameters were measured using a conventional triaxial testing apparatus.

Nanyang Undisturbed Clay

The undisturbed sample (Soil 9) is heavy silt. The gradation of the soil is not known and this classification assumes that the soil is fine-grained, as described by the author. The shear strength is tested using a modified triaxial test under a confining pressure of 60 kPa with a range of net normal stress from 94 to 141 kPa. (Table 5.14)

The SWCC was measured using a pressure plate apparatus. The SWCC of the undisturbed sample is presented as normalized volumetric water content over the range of water contents bounding the transition zone, $(\theta-\theta_r)/(\theta_s-\theta_r)$. This relationship is also known as the effective degree of saturation. The data points were not visible on the graphs in the paper, but a best fit line is presented to represent the SWCC. The best fit line was generated using Fredlund and Xing (1994) equation, (Eqn. 2-9). Several points were picked off this line and taken to be the SWCC for the soil.

Table 5.14. Properties of Soil No. 9, Nanyang undisturbed clay (Bao et al, 1998).

ϕ'	c'	Sand (%)	Silt (%)	Clay (%)	w_L	I_p
19.7	21.8	unknown			60	33

USCS Classification: Heavy silt (MH)*			
Sample Preparation:	Undisturbed	Shear Strength Test:	Modified triaxial test
Confining Pressure, σ_3 (kPa)	60	Net normal stress, σ_n (kPa)	94-141

*Assumed from information provided – gradation unknown.

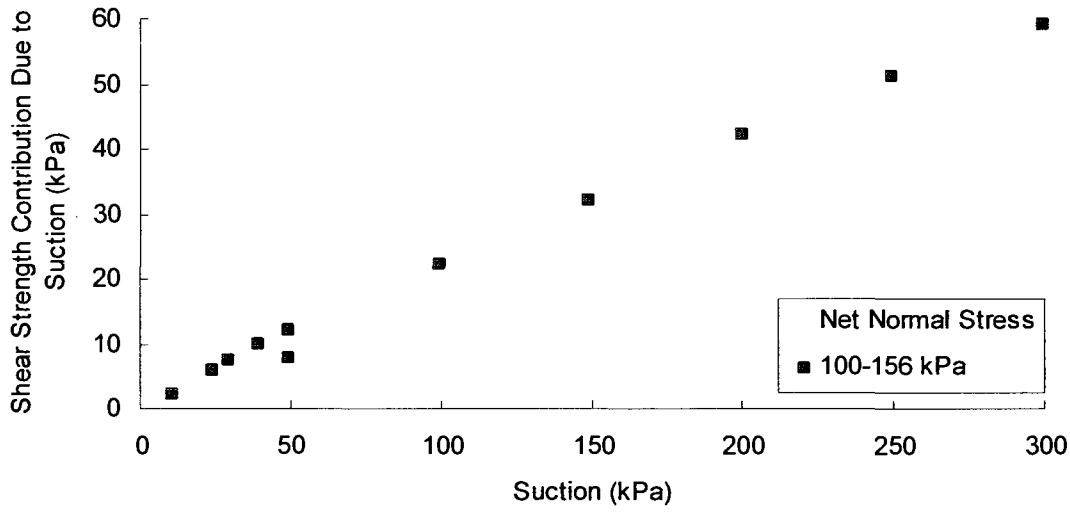

Figure 5.9. Shear strength contribution due to suction for Nanyang undisturbed clay. (Bao et al, 1998)

Nanyang Compacted Clay

The compacted sample (Soil 10) is lean clay. The gradation of the soil is not known but it is assumed to be a fine-grained soil as classified by the author. The effective strength parameters were measured on saturated soil using a triaxial cell (Table 5.15). The un-saturated shear strength is measured using a modified triaxial apparatus. Neither the confining pressure nor the net normal stress values were given for this soil.

The SWCC was measured using a pressure plate apparatus and presented in terms of the volumetric water content versus suction. Volume-mass properties of the soil are used to determine the SWCC in terms of the degree of saturation. Again, the data

points were not visible on the graphs in the paper, but a best fit line is presented to represent the SWCC. The best fit line was generated using Fredlund and Xing equation (1994). Several points were picked off this line and used as the SWCC for the soil.

Table 5.15. Properties of Soil No. 10, Nanyang compacted clay (Bao et al, 1998).

ϕ'	c'	Sand (%)	Silt (%)	Clay (%)	w_L	I_p
28.7	5.9	unknown			37	14
USCS Classification: Lean clay (CL)*						
Sample Preparation:	Compacted		Shear Strength Test:		Modified triaxial test	
Confining Pressure, σ_3 (kPa)	unknown		Net normal stress, σ_n (kPa)		Unknown	

*Assumed from information provided – gradation unknown.

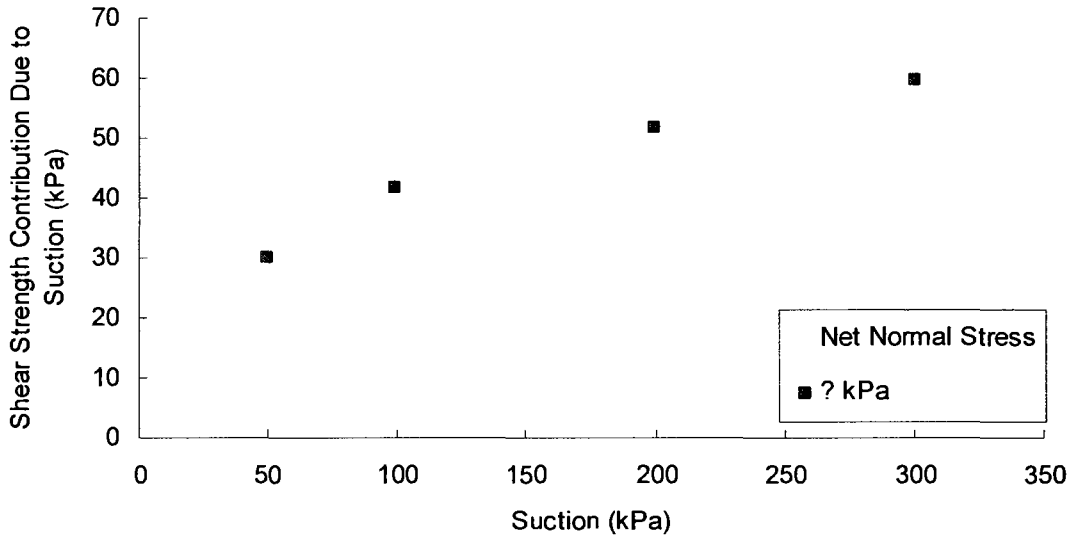

Figure 5.10. Shear strength contribution due to suction for Nanyang compacted clay. (Bao et al, 1998)

5.3.8 Tarantino and Tombolato (1995)

The investigators prepared a paper to investigate the shear strength of a non-active clay using a range of compaction pressures and confining pressures. They were interested in whether the shear strength of an unsaturated soil was influenced by compaction characteristics or on the microfibre (or soil structure) of the soil. The authors used high suction tensiometers The testing was performed on a Speswhite kaolin (Soil 11). The soil is

a heavy silt borderline to fat clay (Table 5.16). The soil was statically compacted to a sample measuring and tested in a modified direct shear apparatus. The saturated shear strength parameters were tested using a conventional direct shear box. The soil was prepared using different compaction pressures: 300 kPa, 600 kPa and 1200 kPa. The soil was tested at a three net normal stresses: 300, 600 and 900 kPa.

Table 5.16. Properties of Soil No. 11, Speswhite kaolin (Tarantino and Tombolato, 2005).

ϕ'	c'	Sand (%)	Silt (%)	Clay (%)	w_L	I_p
17.3	44.3	0	80	20	64	32
USCS Classification: Heavy silt (MH) borderline to fat clay (CL)						
Sample Preparation:	Compacted		Shear Strength Test:	Modified direct shear test		

Table 5.17.Confining pressures and net normal stresses for soil no. 11, Speswhite kaolin (Tarantino and Tombolato, 2005).

	Soil 11a	Soil 11b	Soil 11c	Soil 11d
Compaction Pressure, (kPa)	300	600	600	1200
Confining Pressure, σ_3-u_a (kPa)	300	300	600	900
Net normal stress, σ_n-u_a (kPa)	300	300	600	900

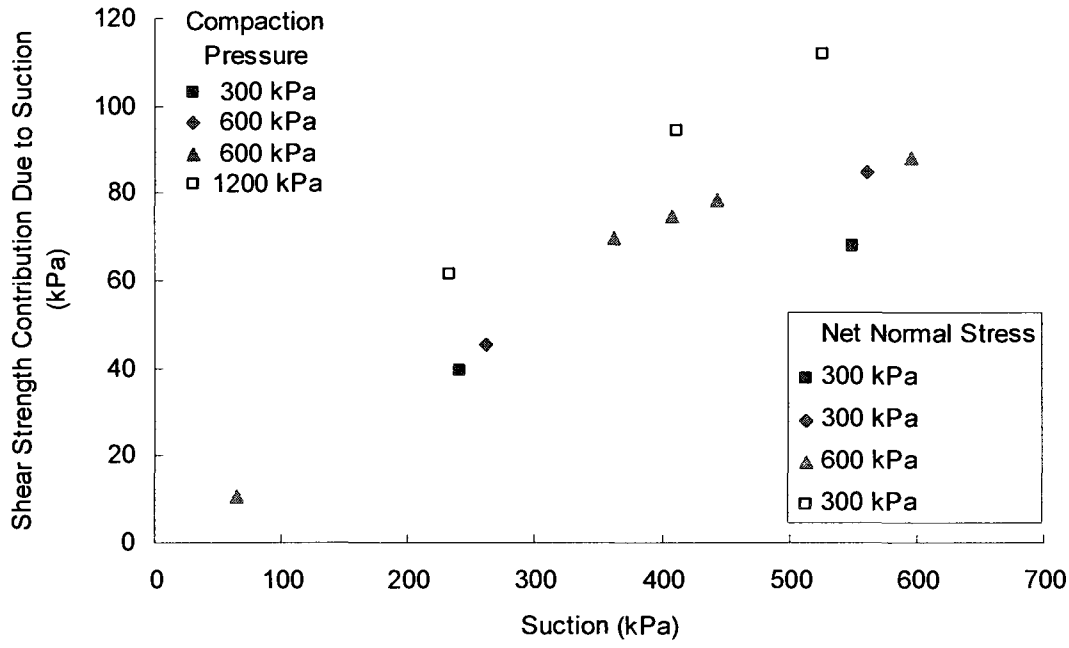

Figure 5.11. Shear strength contribution due to suction for Speswhite kaolin. (Tarantino and Tombolato, 1995)

5.3.9 Khalili, Geiser and Blight (2004)

Khalili et al (2004) wrote a paper to critically review the effective stress concept, particularly examining the Khalili and Khabbaz (1998) relationship. They used Hume Dam clay at three different depths to investigate the concept. The effective stress parameters were determined by multistage testing in a conventional triaxial shear strength apparatus.

The soils were tested using a modified Bishop-Wesley hydraulic triaxial cell and confining pressures of 200 kPa.

Soil SJ10a

The soil (Soil 12) is the sampled from a depth of 11.5-11.8 kPa and is sandy lean clay (Table 5.18). The undisturbed specimen was tested using a modified Bishop-Wesley hydraulic triaxial cell and confining pressure of 200 kPa. The samples were sheared at a rate of 0.003%/min. The net normal stress ranged from 301 to 361 kPa.

Table 5.18. Properties of Soil No. 12, SJ10a (Khalili et al, 2004).

ϕ'	c'	Sand (%)	Silt (%)	Clay (%)	w_L	I_p
29	5	33	67		39	21
USCS Classification: Sandy lean clay (CL)						
Sample Preparation:	Undisturbed		Shear Strength Test:		Modified triaxial test	
Confining Pressure, σ_3 (kPa)	200		Net normal stress, σ_n (kPa)		301-361	

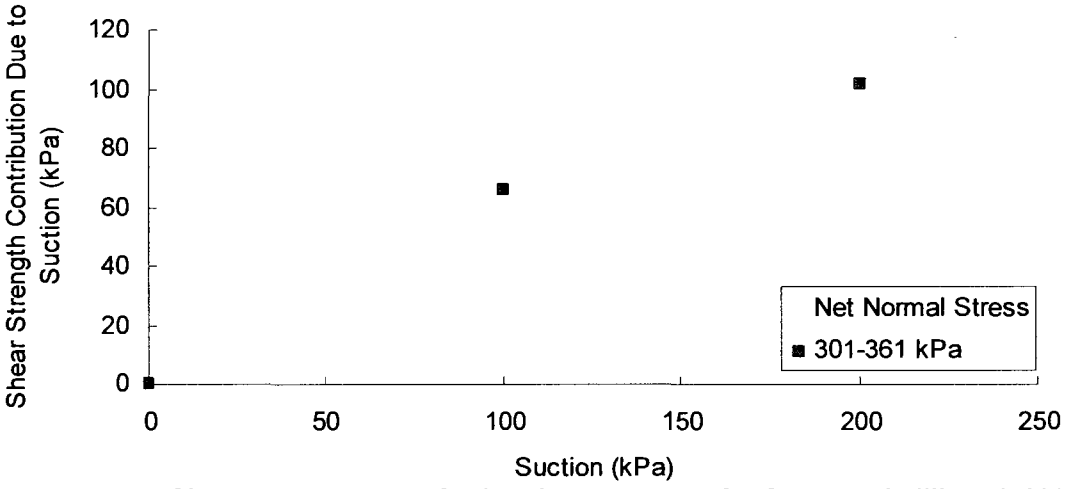

Figure 5.12. Shear strength contribution due to suction for SJ10a. (Khalili et al, 2004)

Soil SJ10b

The soil (Soil 13) is the sampled from a depth of 20.5-20.8 kPa and is sandy lean clay (Table 5.19). The undisturbed specimen was tested using a modified Bishop-Wesley hydraulic triaxial cell and confining pressure of 200 kPa. The samples were sheared at a rate of 0.003%/min. The net normal stress ranged from 313 to 420 kPa.

Table 5.19. Properties of Soil No. 12, SJ10b (Khalili et al, 2004).

ϕ'	c'	Sand (%)	Silt (%)	Clay (%)	w_L	I_p
29	19	26	74		33	12
USCS Classification: Lean clay with sand (CL)						
Sample Preparation:	Undisturbed		Shear Strength Test:		Modified triaxial test	
Confining Pressure, σ_3 (kPa)	200		Net normal stress, σ_n (kPa)		313-420	

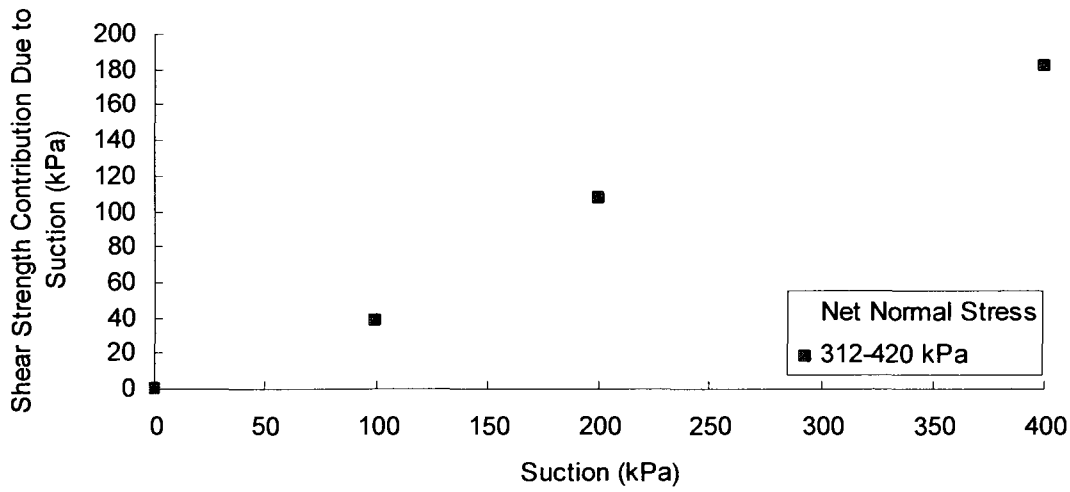

Figure 5.13. Shear strength contribution due to suction for SJ10b. (Khalili et al, 2004)

Soil SJ11

The soil (Soil 14) is the sampled from a depth of 23.5-23.8 kPa and is sandy silty clay (Table 5.20). The undisturbed specimen was tested using a modified Bishop-Wesley hydraulic triaxial cell and confining pressure of 200 kPa. The samples were sheared at a rate of 0.003%/min. The net normal stress ranged from 303 to 450 kPa.

Table 5.20. Properties of Soil No. 14, SJ11 (Khalili et al, 2004).

ϕ'	c'	Sand (%)	Silt (%)	Clay (%)	w_L	I_p
30	5	36	64		25	6
USCS Classification: Sandy silty clay (CL-ML)						
Sample Preparation:	Undisturbed		Shear Strength Test:	Modified triaxial test		
Confining Pressure, σ_3 (kPa)	200		Net normal stress, σ_n (kPa)	303-450		

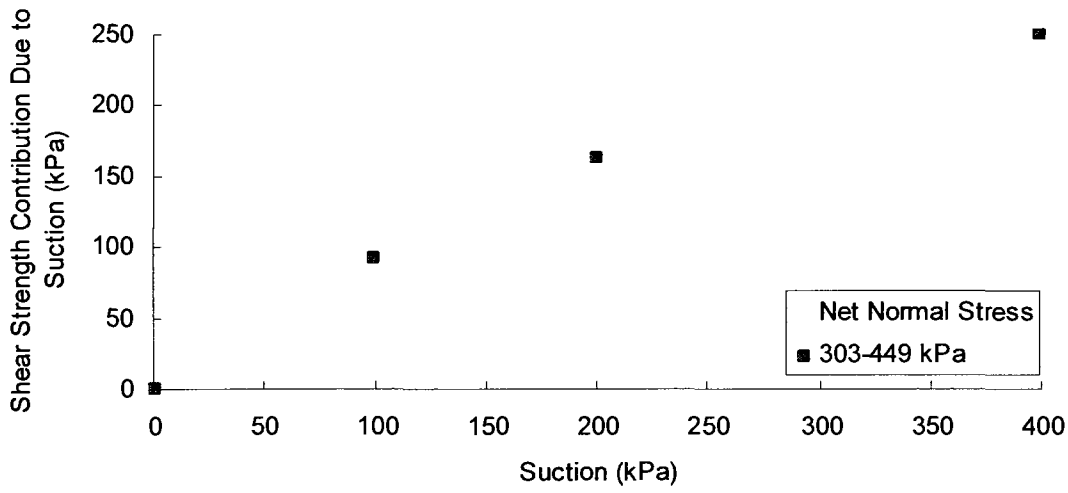

Figure 5.14. Shear strength contribution due to suction for SJ11. (Khalili et al, 2004)

5.3.10 Rassam and Williams (1999)

Rassam and Williams (1999) used tailings from the Kidston mine in Australia to examine the shear strength of a dessicating soil. They proposed an equation to try to predict the shear strength behaviour of tailings under unsaturated conditions. The tailings were sampled at two distances from the discharge outlet: 50 m (Soil 15) and 150 m (Soil 16). The particle size distribution curves for these soils are given in Appendix B.

The soils were prepared for shear strength testing from slurry mixture into a sample measuring 38 mm diameter by 75 mm height in a procedure defined by Head (1982). The size of the samples prepared to measure the SWCC were not available.

The SWCC for the soils were determined over a range of 0 – 500 kPa using a pressure plate apparatus. The AEV for soil 15 was reported to be 2.5 kPa and for 7 kPa for soil 16.

Tailings (50m)

The soil (Soil 15) sample 50m the discharge outlet at is poorly-graded silty sand. The soil properties are given in Table 5.21. The unsaturated shear strength testing was multistage testing under consolidated drained conditions (CD). The soil was tested at three confining pressures: 30, 125 and 250 kPa. A summary of the net normal stresses is provided in Table 5.23. The effective stress parameters were determined using the

modified triaxial apparatus at 0 kPa suction from the three confining pressures. The angle of internal friction for the soil 15 was re-analyzed and found to be 30.6° which differs from the reported angle of 41.7° reported by the authors. The soil has a cohesion value of 0 kPa.

Table 5.21. Properties of Soil No. 15, tailings (50m) (Rassam and Williams, 1999)

ϕ'	c'	Sand (%)	Silt (%)	Clay (%)	w_L	I_p
30.6	0	89.1	10.9	0	NP	
USCS Classification: Poorly-graded silty sand (SP-SM)						
Sample Preparation:	From slurry		Shear Strength Test:	Modified triaxial test		

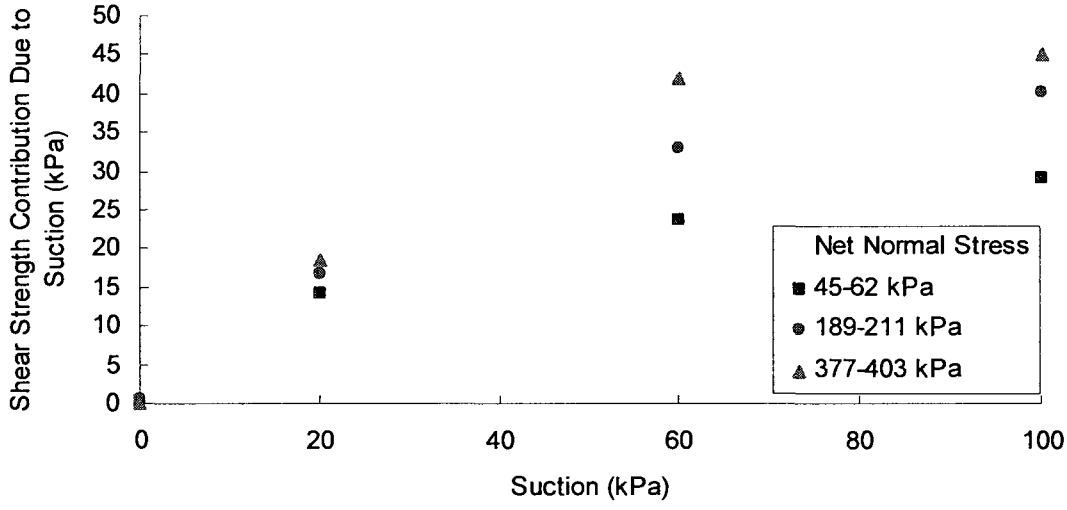

Figure 5.15. Shear strength contribution due to suction for tailings (50m). (Rassam and Williams, 1999)

Tailings (150m)

The soil (Soil 16) sampled 150m from the discharge outlet at is also silty sand. Soil 16 is finer than soil 15, as expected and contains a trace of clay. The soil properties are given in Table 5.22. The unsaturated shear strength testing was multistage testing under consolidated drained conditions. Soil 16 was tested at three confining pressures: 30, 125 and 250 kPa. A summary of the net normal stresses is provided in Table 5.23. The effective stress parameters were determined using the modified triaxial cell test at 0 kPa suction from the three confining pressures. The angle of internal friction for the soil 16

was re-analyzed and found to be 29.9° which differs from the reported angle of 40.7° reported by the authors. The soil has a cohesion value of 0 kPa.

Table 5.22. Properties of Soil No. 16, tailings (150m) (Rassam and Williams, 1999)

ϕ'	c'	Sand (%)	Silt (%)	Clay (%)	w_L	I_p
29.9	0	71.0	29.0	0	NP	
USCS Classification: Silty sand (SM)						
Sample Preparation:	From slurry		Shear Strength Test:	Modified triaxial test		

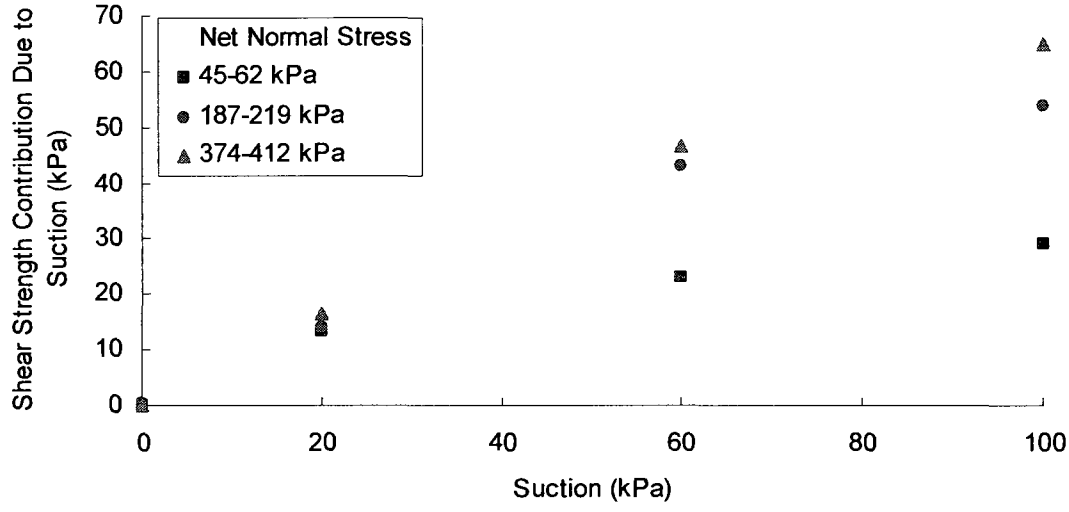

Figure 5.16. Shear strength contribution due to suction for tailings (150m). (Rassam and Williams, 1999)

Table 5.23. Confining pressures and net normal stresses for soil nos. 15 and 16 (Rassam and Williams, 1999)

	Soil 15a	Soil 15b	Soil 15c	Soil 16a	Soil 16b	Soil 16c
Confining Pressure, σ_3 (kPa)	30	125	250	30	125	250
Net normal stress, σ_n (kPa)	45-62	189-211	377-403	45-62	187-219	374-412

5.3.11 Röhm and Vilar (1995)

Röhm and Vilar published a paper to examine the influence of matric suction and effective stress on shear strength of unsaturated soil. The authors used the data from Röhm's thesis (1992) to examine these influences. The soil (Soil 17) is laterized sand from Brazil that is deposited as both alluvium and colluvium. The soil can be classified by the USCS as clayey sand borderline to silty sand. The soil properties are summarized in Table 5.24. The particle size distribution of the soil tested can be found in Appendix B of this thesis.

The saturated shear strength properties were determined by consolidated, undrained (CU) test in a modified triaxial test. The unsaturated shear strength behaviour was determined via multistage testing on a modified triaxial test on undisturbed samples of laterite. The results are presented in terms of stress point (q and p) and were translated into shear strength and net normal stress using the effective strength properties of the soil. Soil 17 was tested at 5 different confining stresses 50, 200, 300, 400 and 600 kPa. Tests at 300 kPa and 600 kPa have limited number of points and therefore, were not used in this thesis. The confining pressures and subsequent net normal stresses are summarized in Table 5.25 below.

The SWCC was measured using a pressure cell described by Klute (1986). The sample was determined over a range of 0 to 1500 kPa. The SWCC information can be found in Appendix A of this thesis. The shear strength was tested in multistage modified testing apparatus and plotted in terms of q and p. The authors applied 5 different confining pressures: 50, 200, 300, 400 and 600 kPa. Tests at 300 kPa and 600 kPa have limited number of points and therefore, are not used in this thesis.

Table 5.24. Properties of Soil No. 17, Brazilian laterite (Röhm and Vilar, 1995).

ϕ'	c'	Sand (%)	Silt (%)	Clay (%)	w_L	I_p
21.8	2.3	52	19	29	38	14
USCS Classification: Clayey sand (SC) borderline to silty sand (SM)						
Sample Preparation:	Undisturbed		Shear Strength Test:	Modified triaxial test		

Table 5.25. Confining pressures and net normal stresses for Brazilian laterite (Röhm and Vilar, 1995).

	Soil 17a	Soil 17b	Soil 17c
Confining Pressure, σ_3 (kPa)	50	200	400
Net normal stress, σ_n (kPa)	77-145	300-360	640-727

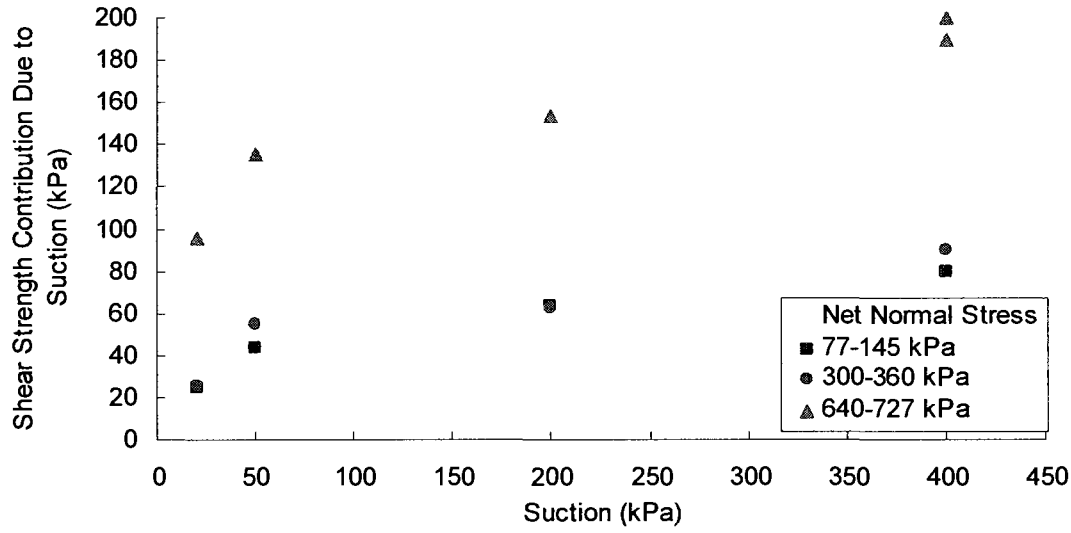

Figure 5.17. Shear strength contribution due to suction for Brazilian laterite. (Röhm and Vilar, 1995).

5.3.12 Abramento and Carvalho (1989)

Abramento and Carvalho researched soil at a location of a known landslide in Brazil (Soil 18). They performed tests on the soil both in the laboratory and in situ. Serra do Mar soil is a clayey sand borderline to silty sand (Table 5.26) They used the measured unsaturated shear strength data to propose an equation to fit the non-linear relationship. The saturated shear strength parameters were determined in a triaxial test apparatus under consolidated, undrained (CU) loading conditions. The effective strength parameters were measured to be 38° and 40°. The angle for the set of data is taken to be 38° and cohesion of 0 kPa.

The unsaturated shear strength was measured on undisturbed soil samples using multi-stage testing in a modified triaxial cell. The Serra do Mar soil was tested at a confining pressure of approximately 10 kPa which is a range of net normal stress from 20 to 28 kPa (Table 5.26) The SWCC was not directly measured, but created from the initial suctions and degree of saturation measurements of the samples prior to shear strength testing.

Table 5.26. Properties of Soil No. 18, Serra do Mar soil (Abramento and Carvalho, 1989).

ϕ'	c'	Sand (%)	Silt (%)	Clay (%)	w_L	I_p
38	0	74	13	13	39	14
USCS Classification: Clayey sand (SC) borderline to silty sand (SM)						
Sample Preparation:	Undisturbed		Shear Strength Test:	Modified triaxial test		
Confining Pressure, σ_3 (kPa)	10		Net normal stress, σ_n (kPa)	20-28		

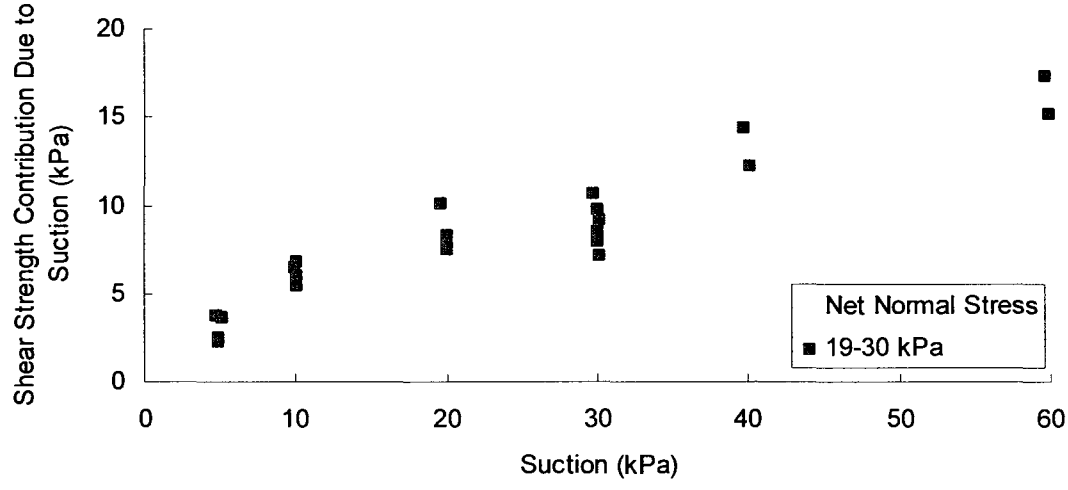

Figure 5.18. Shear strength contribution due to suction for Serra do Mar soil. (Abramento and Carvalho, 1989).

5.3.13 Adams (1996)

Adams performed tested on a agricultural soil and to examine the testing using a triaxial cell. The sandy clay loam (Soil 19) is classified as sandy clay. The properties of the soil are summarized in Table 5.27 below. The saturated soil parameters were determined using a triaxial test.

The soil was prepared by using a compact the soil in five layers into a split mold with dimensions of 70 mm diameter x 140 mm high. Unsaturated shear strength testing was performed using a modified triaxial cell similar to the stress-path Bishop and Wesley cell. The cell uses a null-type pressure plate to create and measure the suction in the sample. The author measures both volume change and diffused air in the system. The author performed limited consolidated, drained tests (CD). The testing was performed at a confining pressure of 25 kPa with a net normal stress of 43-59 kPa. The authors also tested the soil under constant water conditions which is not presented in this thesis.

The SWCC was measured by using a pressure plate apparatus. The range of the curve extended from a suction up to 800 kPa.

Table 5.27.Properties of Soil No. 19, Sandy clay loam (Adams, 1996).

ϕ'	c'	Sand (%)	Silt (%)	Clay (%)	w_L	I_p
33.1	10.2	48.1	23.6	28.3	33	14
USCS Classification: Sandy lean clay (CL)						
Sample Preparation:	Compacted		Shear Strength Test:	Modified triaxial test		
Confining Pressure, σ_3 (kPa)	25		Net normal stress, σ_n (kPa)	43-59		

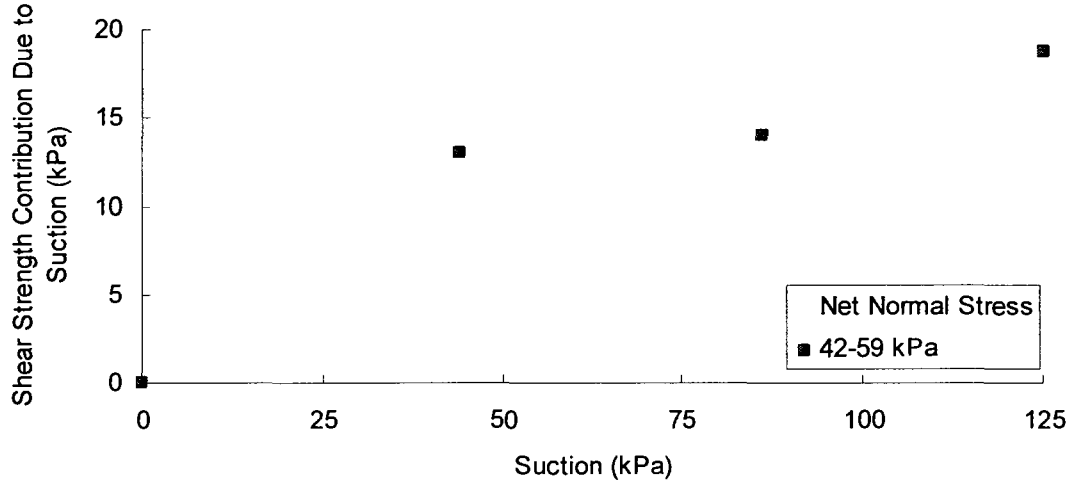

Figure 5.19. Shear strength contribution due to suction for sandy clay loam. (Adams, 1996).

5.3.14 Donald (1957)

Donald presented shear strength behaviour testing of four Frankston unsaturated sands in his 1957 Masters thesis. This work describes in detail some of the earliest modified direct shear equipment used. Donald used colloidal membranes in the apparatus as opposed to the more standard presently used ceramic stones. The sands are four man-made variations of the Frankston sand labeled as: Frankston fine (Soil 20), medium Frankston (Soil 21), graded Frankston (Soil 22) and brown sand (Soil 23).

The sand over a 325 mesh sieve and the material retained on the sieve was medium Frankston. The material that passed the 325 and was decanted from beaker to beaker till the particles settled in the beaker settled in about a minute. This material became Frankston fine. Graded Frankston was created from different gradations to make a well graded sand. Brown sand was created by sieving over a 100 mesh sieve, decanting the soil from beaker to beaker to remove excess fines and finally, the sand was boiled in hydrogen peroxide to remove organic material.

The SWCC of the samples was measured directly in the modified shear apparatus without applying any dead load. The shear strength was measured in the same apparatus with dead loads applied. A back calculation of the net normal stress indicates a net normal stress of approximately 2 kPa. In addition, some of the SWCC was measured in a pressure plate apparatus. Both sets of data are shown on the curves in Appendix A.

Frankston Fine

Frankston fine (Soil 20) is a lean silt. The soil properties are summarized in Table 5.28. The soil has minimal confinement and compacted specimens were tested under drained conditions in a modified direct shear test apparatus.

Table 5.28. Properties of Soil No. 20, Frankston Fine (Donald, 1957)

ϕ'	c'	Sand (%)	Silt (%)	Clay (%)	w_L	I_p
34	0	0	100	0	0	0
USCS Classification: Lean silt (ML)						
Sample Preparation:	Compacted		Shear Strength Test:	Modified direct shear test		
Confining Pressure, σ_3 (kPa)	2		Net normal stress, σ_n (kPa)	2		

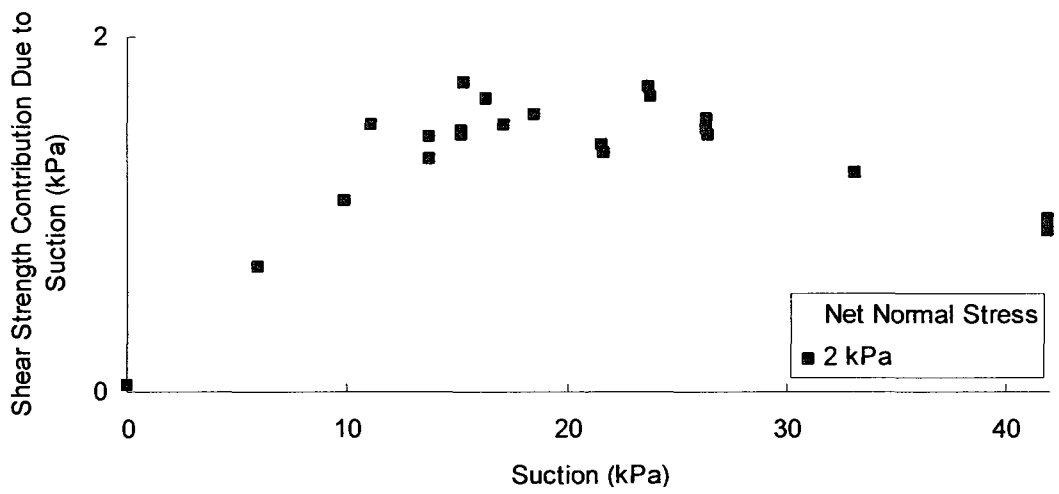

Figure 5.20. Shear strength contribution due to suction for red silty clay. (Escario and Saez, 1986; Escario and Juca, 1989)

Medium Frankston

Medium Frankston (Soil 21) is sandy lean silt. The soil properties are summarized in Table 5.29. The soil has minimal confinement and compacted specimens were tested under drained conditions in a modified direct shear test apparatus.

Table 5.29. Properties of Soil No. 21, Medium Frankston (Donald, 1957).

ϕ'	c'	Sand (%)	Silt (%)	Clay (%)	w_L	I_p
34	0	34.8	65.2	0	0	0
USCS Classification: Sandy lean silt (ML)						
Sample Preparation:	Compacted		Shear Strength Test:	Modified direct shear test		
Confining Pressure, σ_3 (kPa)	2		Net normal stress, σ_n (kPa)	2		

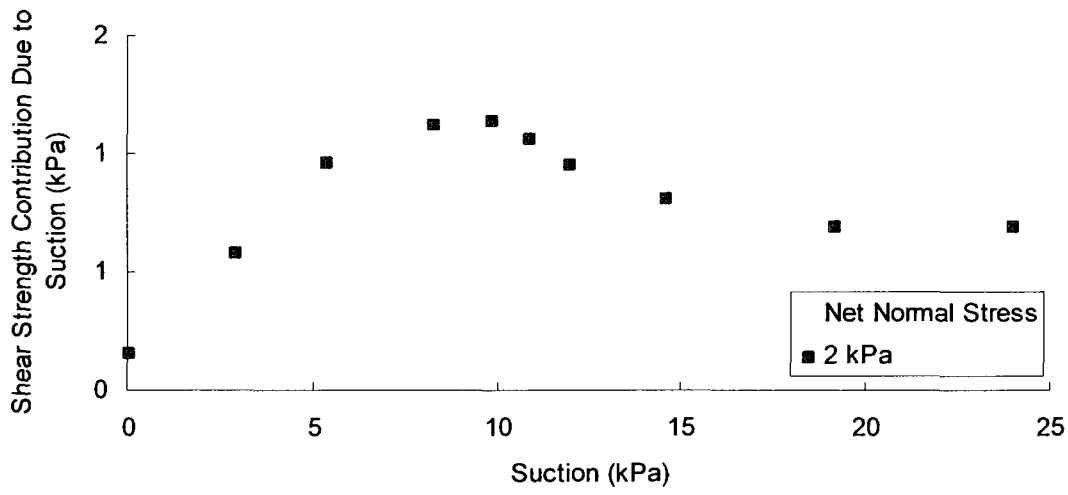

Figure 5.21. Shear strength contribution due to suction for Medium Frankston. (Donald, 1957)

Graded Frankston

Graded Frankston (Soil 22) is sandy lean silt. The soil properties are summarized in Table 5.30. The soil has minimal confinement and compacted specimens were tested under drained conditions in a modified direct shear test apparatus.

Table 5.30. Properties of Soil No. 22, Graded Frankston (Donald, 1957).

ϕ'	c'	Sand (%)	Silt (%)	Clay (%)	w_L	I_p
33	0	38.5	61.5	0	NP	
USCS Classification: Sandy lean silt (ML)						
Sample Preparation:	Compacted		Shear Strength Test:		Modified direct shear test	
Confining Pressure, σ_3 (kPa)		2	Net normal stress, σ_n (kPa)		2	

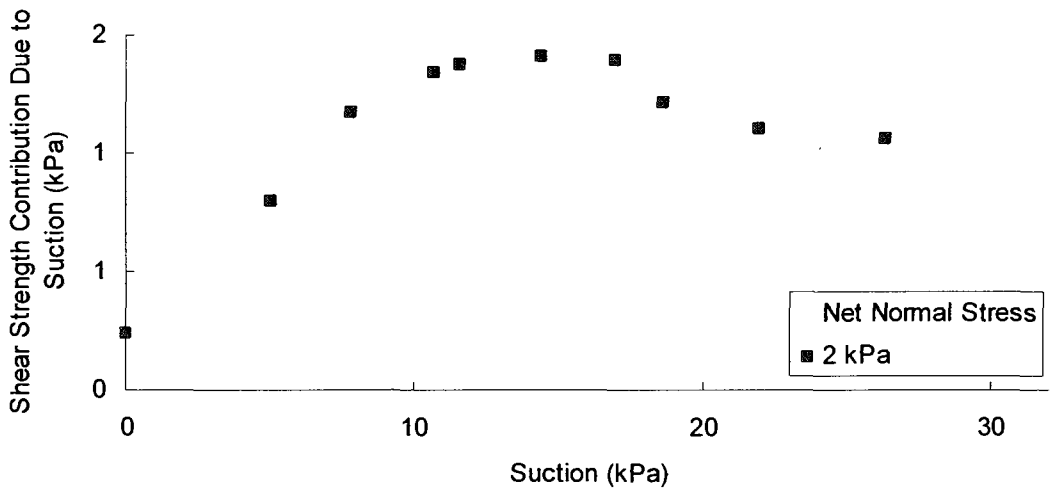

Figure 5.22. Shear strength contribution due to suction for Graded Frankston. (Donald, 1957)

Brown Sand

Brown sand (Soil 23) is silty sand. The soil properties are summarized in Table 5.31. The soil has minimal confinement and compacted specimens were tested under drained conditions in a modified direct shear test apparatus.

Table 5.31. Properties of Soil No. 23, Brown sand (Donald, 1957).

ϕ'	c'	Sand (%)	Silt (%)	Clay (%)	w_L	I_p
30	0	68.9	31.1	0	NP	
USCS Classification: Silty sand (SM)						
Sample Preparation:	Compacted		Shear Strength Test:		Modified direct shear test	
Confining Pressure, σ_3 (kPa)		2	Net normal stress, σ_n (kPa)		2	

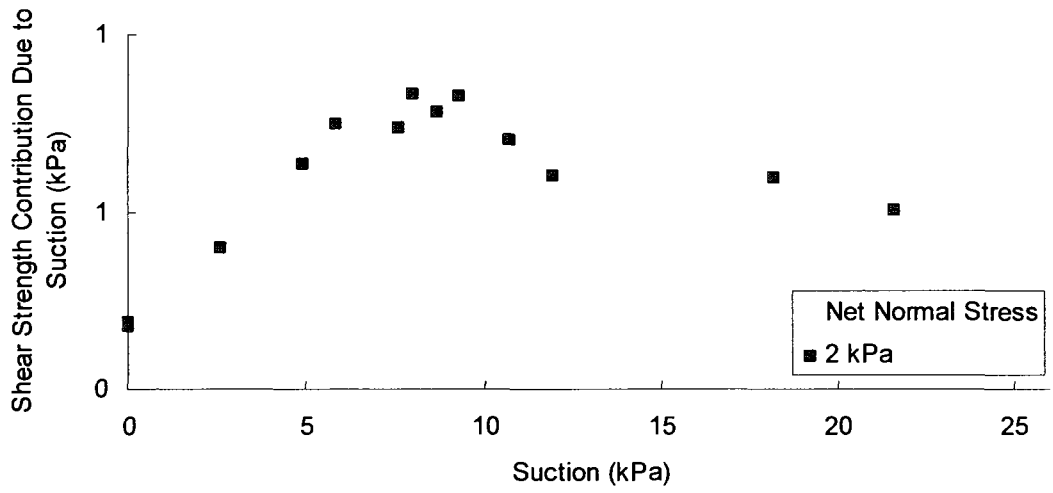

Figure 5.23. Shear strength contribution due to suction for brown sand. (Donald, 1957)

5.3.15 Drumright and Nelson (1995)

Drumright tested copper tailings (Soil 24) in both a drained condition and in a constant water condition. Specimens were prepared by compacting them into a Harvard mini mold using the "undercompaction" technique (Ladd, 1978). The effective strength parameters were measured using a multistage, consolidated drained test (CD) in a modified triaxial cell. Testing included both CD and CW tests although only the CD tests were used in this thesis. The system was flushed regularly to remove any air formation near the ceramic disk below the sample. In addition, the water change during testing was measured to determine the change in volume saturated specimens. Two non-contacting induction sensors were placed approximately mid-height of the specimens during unsaturated shear strength testing to measure lateral deformation. The author tested the strength of soil in a modified triaxial test at four confining conditions: 10 kPa, 48 kPa, 50 kPa and 150 kPa. Only three confining pressures were used in this thesis (Table 5.33).

The SWCC was measured over a range of 0 to 150 kPa using a pressure plate apparatus. The gravimetric water content presented was revised into degree of saturation using volume-mass properties given in the paper.

Table 5.32. Properties of Soil No. 24, Copper tailings (Drumright and Nelson, 1995).

ϕ'	c'	Sand (%)	Silt (%)	Clay (%)	w_L	I_p
38.3	13	59	32	9	NP	
USCS Classification: Silty sand (SM)						
Sample Preparation:	Slurry preparation		Shear Strength Test:	Modified triaxial test		

Table 5.33. Confining pressures and net normal stresses for Copper tailings (Drumright and Nelson, 1995).

	Soil 24a	Soil 24b	Soil 24c
Confining Pressure, σ_3 (kPa)	14	48	50
Net normal stress, σ_n (kPa)	31-78	87-141	91-147

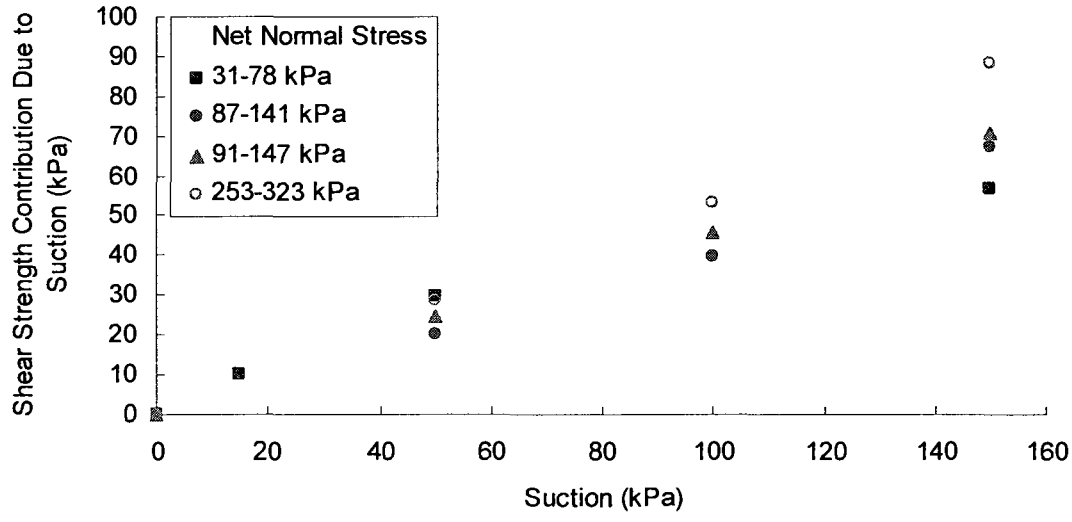

Figure 5.24. Shear strength contribution due to suction for Copper tailings. (Drumright and Nelson, 1995)

5.3.16 Feuerharmel, Bica, Gehling and Flores (2006)

Several authors presented shear strength data on the AV colluvium (Soil 25) and RO colluvium (Soil 26) soils from the slopes of Brazil. Three published papers presented unsaturated shear strength data of the AV colluvium while two of those papers also presented data on the RO colluvium.

The shear strength of the unsaturated soils was determined by modified direct shear test (Feuerharmel, Bica, Gehling and Flores, 2006; Feuerharmel, Pereira, Gehling and Bica, 2006) and by modified triaxial test (Pereira, Feuerharmel, Gehling and Bica, 2006). Both tests had multiple confining pressures. The modified direct shear specimen was 60 mm diameter x 20 mm height and the modified triaxial shear test sample measured 50 mm diameter x 100 mm height.

The SWCC was determined in one paper (Pereira, Feuerharmel, Gehling and Bica, 2006) and is used to accompany the data from all three papers. The soils are presented as the same soils across the three references. The SWCC was determined using a combination of pressure plate apparatus and filter paper. The SWCC was measured over a range of suction from 0 to 1500 kPa and is presented in Appendix A.

AV Colluvium

Samples of AV colluvium (Soil 25) were tested as undisturbed samples in modified direct shear test (Table 5.34 to 5.36) and using a modified triaxial shear test. (Table 5.31). According the USCS classification from ASTM D2487, AV colluvium is sandy heavy silt. The soil gradation and plasticity was the same across all three papers, however, there was a variation in the effective angle of internal friction and the effective cohesion values reported in these papers. Soil 25 was tested under 7 different confining pressures that are summarized with the accompanying net normal stresses in Table 5.37.The test results were published as q versus suction but were translated to values of shear strength using the effective stress soil parameters.

Table 5.34. Properties of Soil No. 25, AV colluvium (Feuerharmel, Bica, Gehling and Flores, 2006; Feuerharmel, Pereira, Gehling and Bica, 2006; Pereira, Feuerharmel, Gehling and Bica, 2006).

ϕ'	c'	Sand (%)	Silt (%)	Clay (%)	w_L	I_p
25.8	17.3	32	15	53	56	22
USCS Classification: Sandy heavy silt (MH)						
Sample Preparation:	Undisturbed		Shear Strength Test:		Modified direct shear test	

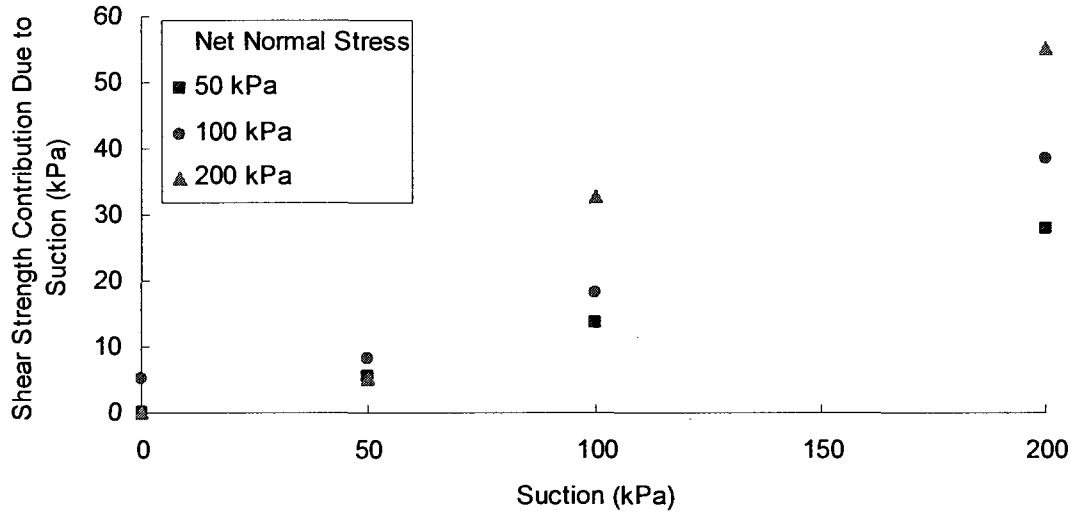

Figure 5.25. Shear strength contribution due to suction for AV colluvium. (Feuerharmel, Bica, Gehling and Flores, 2006)

Table 5.35. Properties of Soil No. 25, AV colluvium (Feuerharmel, Bica, Gehling and Flores, 2006).

ϕ'	c'	Sand (%)	Silt (%)	Clay (%)	w_L	I_p
21.1	14.0	32	15	53	56	22
USCS Classification: Sandy heavy silt (MH)						
Sample Preparation:	Undisturbed		Shear Strength Test:		Modified direct shear test	

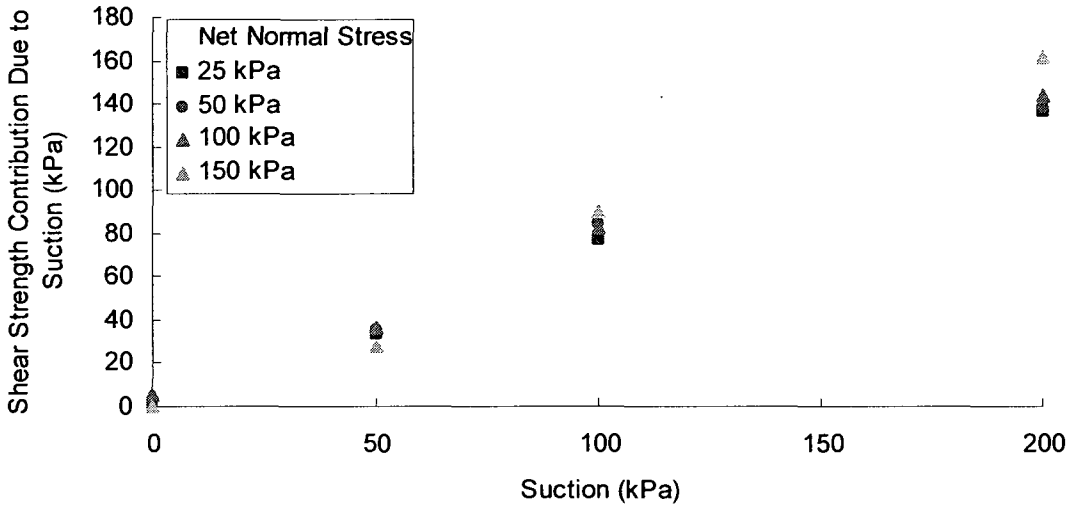

Figure 5.26. Shear strength contribution due to suction for AV colluvium. (Feuerharmel, Pereira, Gehling and Bica, 2006)

Table 5.36. Properties of Soil No. 25, AV colluvium (Feuerharmel, Pereira, Gehling and Bica, 2006).

ϕ'	c'	Sand (%)	Silt (%)	Clay (%)	w_L	I_p
27.6	12.4	32	15	53	56	22
USCS Classification: Sandy heavy silt (MH)						
Sample Preparation:	Undisturbed		Shear Strength Test:	Modified triaxial test		

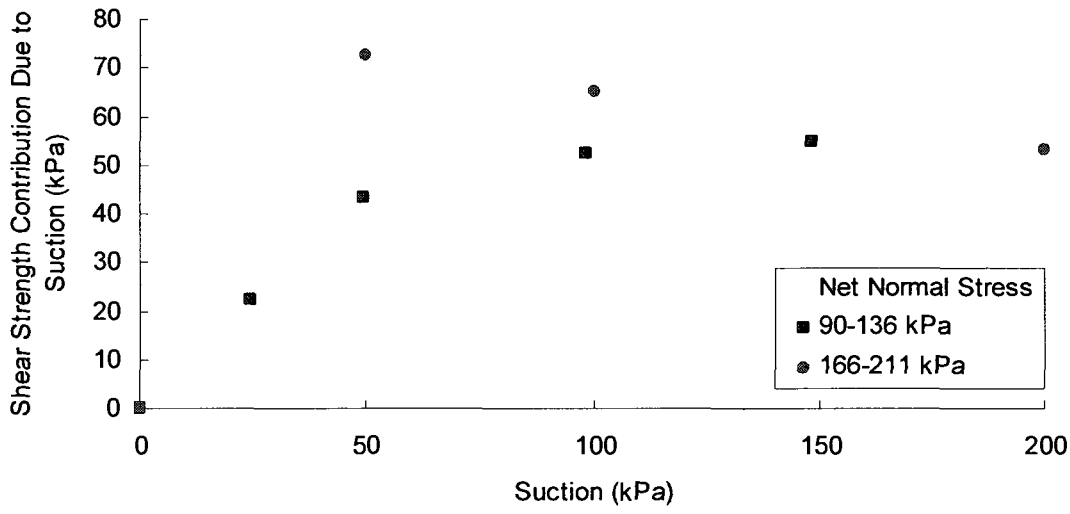

Figure 5.27. Shear strength contribution due to suction for AV colluvium. (Pereira, Feuerharmel, Gehling and Bica, 2006)

Table 5.37.Confining pressures and net normal stresses for soil no. 25, AV colluvium.

	Confining Pressure, σ_3 (kPa)	Net Normal Stress, σ_n (kPa)	Authors
Soil 25a	50	50	Feuerharmel, Bica, Gehling and Flores, 2006
Soil 25b	100	100	
Soil 25c	200	200	
Soil 25d	25	25	Feuerharmel, Pereira, Gehling and Bica, 2006;
Soil 25e	50	50	
Soil 25f	100	100	
Soil 25g	50	90-136	Pereira, Feuerharmel, Gehling and Bica, 2006
Soil 25h	100	166-211	

RO Colluvium

Undisturbed samples of RO colluvium (Soil 26) were tested as samples in modified direct shear test (Table 5.38 to 5.39). The RO colluvium is a heavy silt with trace sand. The soil gradation and plasticity was the same across all three papers. However, some variations were observed in the effective angle of internal friction values reported in these papers. The shear strength parameters were determined for the soils in each of the three references. Soil 26 was tested under 7 confining pressures that are summarized with the accompanying net normal stresses in Table 5.40.The test results were published as q versus suction but were translated to values of effective shear strength parameters.

Table 5.38. Properties of Soil No. 26, RO colluvium (Feuerharmel, Bica, Gehling and Flores, 2006).

ϕ'	c'	Sand (%)	Silt (%)	Clay (%)	w_L	I_p
27.4	13.2	13	34	53	74	17
USCS Classification: Heavy silt (MH)						
Sample Preparation:	Undisturbed		Shear Strength Test:	Modified direct shear		

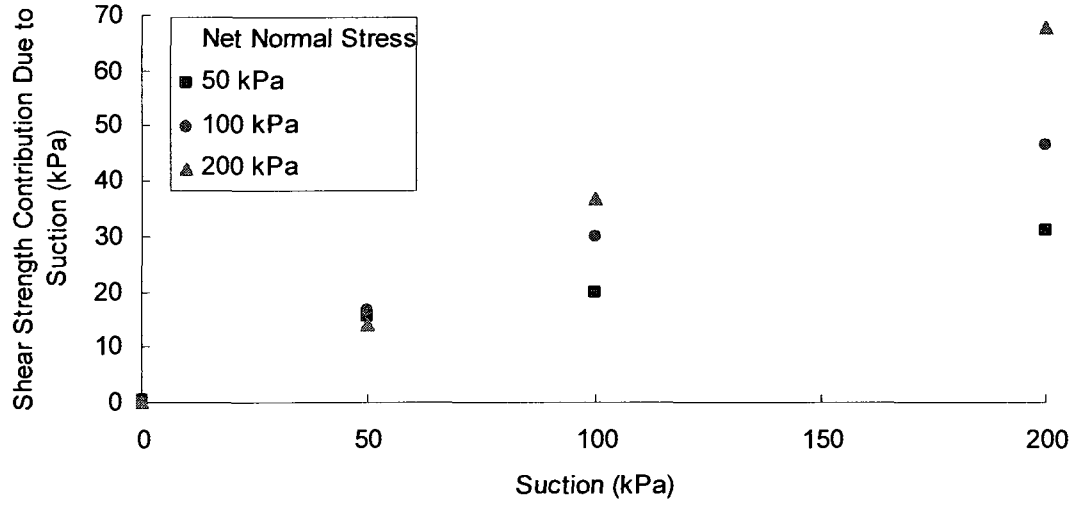

Figure 5.28. Shear strength contribution due to suction for RO colluvium. (Feuerharmel, Bica, Gehling and Flores, 2006)

Table 5.39. Properties of Soil No. 26, RO colluvium (Feuerharmel, Pereira, Gehling and Bica, 2006).

ϕ'	c'	Sand (%)	Silt (%)	Clay (%)	w_L	I_p
28	14.1	13	34	53	74	17
USCS Classification: Heavy silt (MH)						
Sample Preparation:	Undisturbed		Shear Strength Test:		Modified direct shear test, Modified triaxial test	

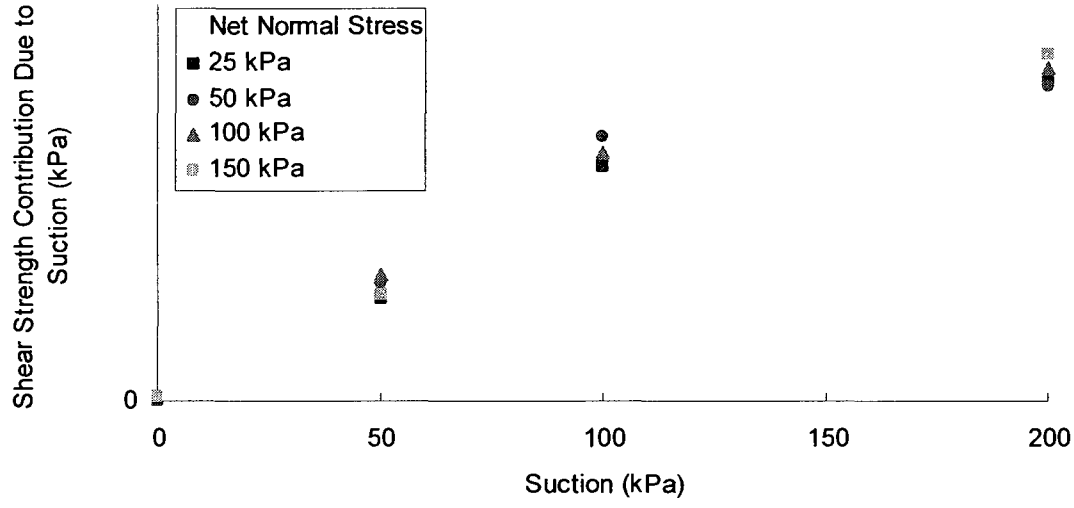

Figure 5.29. Shear strength contribution due to suction for RO colluvium. (Feuerharmel, Pereira, Gehling and Bica, 2006)

Table 5.40. Confining pressures and net normal stresses for soil no. 25, AV colluvium.

	Confining Pressure, σ_3 (kPa)	Net Normal Stress, σ_n (kPa)	Authors
Soil 26a	50	50	Feuerharmel, Bica, Gehling and Flores, 2006
Soil 26b	100	100	
Soil 26c	200	200	
Soil 26d	25	25	Feuerharmel, Pereira, Gehling and Bica, 2006
Soil 26e	50	50	
Soil 26f	100	100	
Soil 26g	150	150	

Table 5.41. Summary of strength parameters for AV colluvium and RO colluvium for three different published data sets.

		Published Values		Calculated Values	
Soil	**Authors**	c'	ϕ'	c'	ϕ'
AV Colluvium	Feuerharmel, Bica, Gehling and Flores, 2006	8.1	32.0	17.3	25.8
RO Colluvium		14.1	28.5	13.2	27.4
AV Colluvium	Feuerharmel, Pereira, Gehling and Bica, 2006	-	25.8	12.4	27.6
RO Colluvium		-	28.5	14.1	28.0
AV Colluvium	Pereira, Feuerharmel, Gehling and Bica, 2006	16.6	29.9	15.7	31.4

5.3.17 Cunningham, Ridley, Dineen and Burland (2003)

Cunningham, Ridley, Dineen and Burland (2003) prepared a paper to examine the behaviour of unsaturated silty clay. The authors used a man-made mixture comprised of 20% Speswhite kaolin, 10% London clay and 70% silica silt. The resulting mixture is a lean clay with sand and the properties of the soil are summarized in Table 5.42. Effective strength parameters were determined by consolidated, drained (CD) tests done at 0 kPa suction in the modified triaxial test. The angle of internal friction recorded as 31° and a cohesion of 20 kPa. The shear strength contribution due to suction at 0 kPa suction does not equal to 0 kPa. Re-examining the data presented in the paper revealed that the angle of internal friction is 35.3° with a cohesion of 10 kPa. When these numbers were used, the shear strength contribution due to suction is approximately 0 kPa at a 0 kPa suction condition with the exception of the unconfined condition which had a 7 kPa difference.

The samples were prepared by reconstituting the mixture from a slurried condition. The 204 mm diameter soil sample was loaded with 200 kPa of pressure by an oedometer, resulting in a firm cake-like sample. The samples were trimmed from the larger sample using a sample lathe. A Bishop-Wesley stress-path triaxial cell was modified to include an air circulation system that allowed the sample to be dried to various suctions using circulating air. The suction in the soil in the modified triaxial apparatus was measured using two miniature probes: one positioned at the top of the soil and one at the side of the soil. Samples were tested it in the modified triaxial test under a variety of confining conditions including an unconfined condition (Table 5.43).

Table 5.42. Properties of Soil No. 27, CRDB silt (Cunningham et al, 2003).

ϕ'	c'	Sand (%)	Silt (%)	Clay (%)	w_L	I_p
35.5	10	22	52	26	28	18
USCS Classification: Lean clay with sand (CL)						
Sample Preparation:	Reconstituted from slurry		Shear Strength Test:		Modified triaxial test	

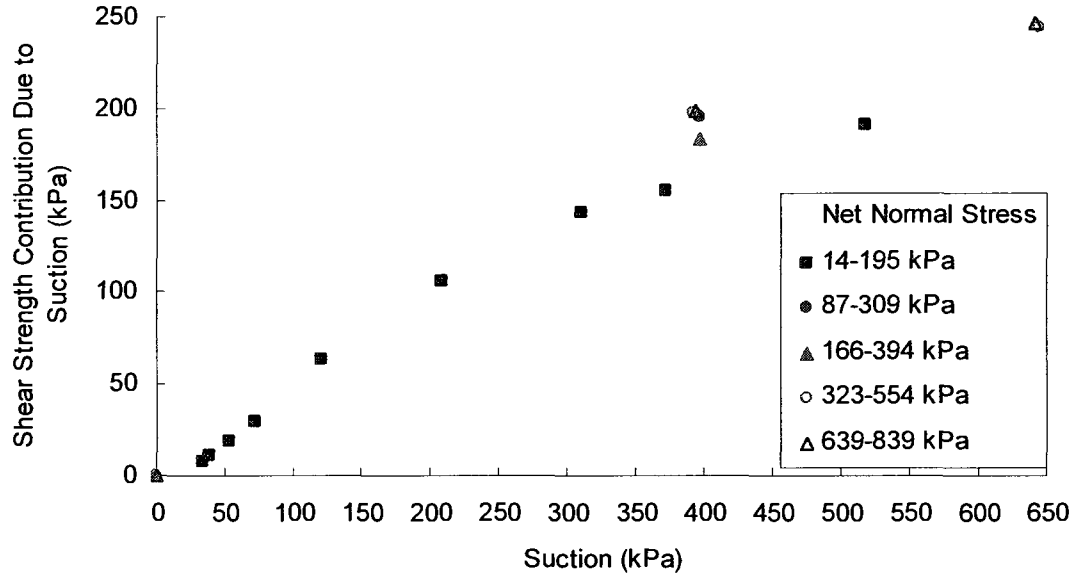

Figure 5.30. Shear strength contribution due to suction for CRDB silt. (Cunningham et al, 2003)

Table 5.43. Confining pressures and net normal stresses for CRDB silt (Cunningham et al, 2003).

	Soil 15a	Soil 15b	Soil 15c	Soil 16d	Soil 16e
Confining Pressure, σ_3 (kPa)	0	50	100	200	400
Net normal stress, σ_n (kPa)	14-195	87-309	166-394	323-554	639-839

5.3.18 Oloo and Fredlund (1996)

Oloo and Fredlund (1996) discussed the value of ϕ^b for statically compacted soils using Botkin silt (Soil 28) and Indian Head till (Soil 29) tested during a thesis program (Oloo, 1994).

The SWCC was measured using pressure plate apparatus over a limited range of suction. The SWCC for the Botkin silt was measured up to 150 kPa while the SWCC of the glacial till is measured up to a suction of 200 kPa. The water content for the SWCCs are presented as the volumetric water content. The volumetric water content is translated to the degree of saturation using volume mass properties supplied for the soils.

Botkin Silt

Botkin silt is a silty clayey sand from the Botkin pit. The soil properties are summarized in Table 5.44 and the particle size distribution curve is available in Appendix B. The sample is prepared as statically compacted specimens. The saturated soil parameters are tested by performing consolidated, drained (CD) tests in a direct shear test apparatus. Unsaturated shear strength testing was performed using a modified direct shear apparatus. The specimens were tested under three confining conditions: 50, 100 and 150 kPa (Table 5.45).

Table 5.44. Properties of Soil No. 28, Botkin silt (Oloo and Fredlund, 1996)

ϕ'	c'	Sand (%)	Silt (%)	Clay (%)	w_L	I_p
28	2.5	52.5	37.5	10	22	6
USCS Classification: Silty clayey sand (SC-SM)						
Sample Preparation:	Compacted		Shear Strength Test:		Modified direct shear test	

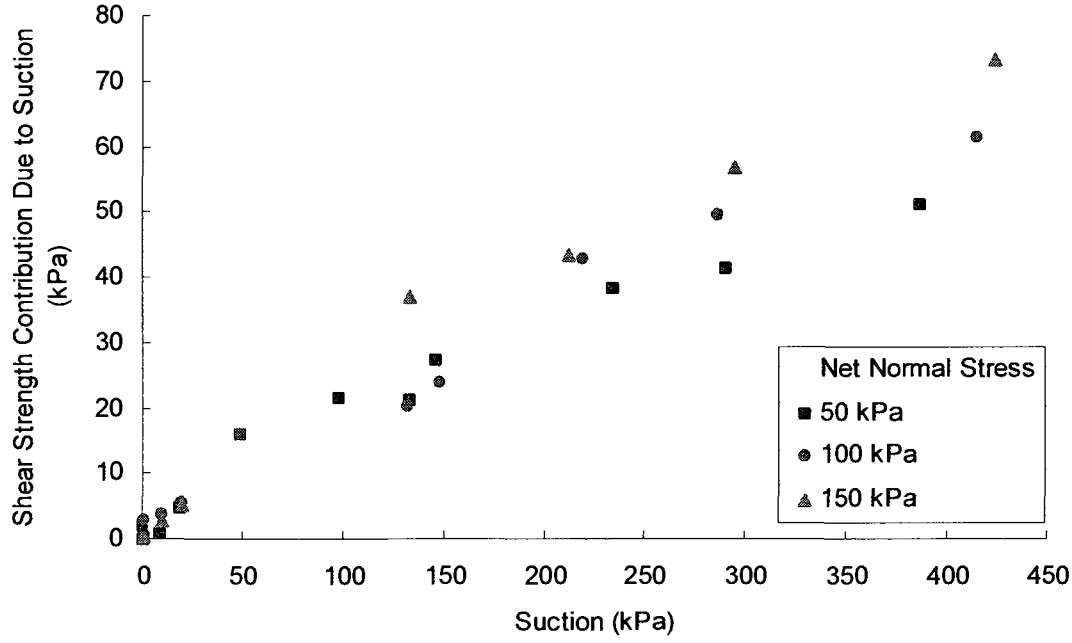

Figure 5.31. Shear strength contribution due to suction for Botkin silt. (Oloo and Fredlund, 1996)

Table 5.45. Confining pressures and net normal stresses for Botkin silt (Oloo and Fredlund, 1996).

	Soil 28a	Soil 28b	Soil 28c
Confining Pressure, σ_3 (kPa)	50	100	150
Net normal stress, σ_n (kPa)	50	100	150

Glacial Till

Glacial till is lean clay with sand taken sampled from an area near Indian Head, Saskatchewan. The soil properties are summarized in Table 5.46 and the particle size distribution curve is available in Appendix B. The angle of internal friction for the Indian Head till was taken as Vanapalli's values of 22° and an effective cohesion of 17 kPa. However, the shear contribution due to suction at 0 kPa suction is significantly different from the expected shear value of 0 kPa. Recalculating the angle and cohesion using the available published information reveals that the angle of internal friction for this soil is 23° with a cohesion value of 0 kPa.

Unsaturated shear strength testing was performed using a modified direct shear apparatus. The specimens were tested under three confining conditions: 50, 100 and 150 kPa (Table 5.47).

Table 5.46. Properties of Soil No. 29, glacial till (Oloo and Fredlund, 1996)

ϕ'	c'	Sand (%)	Silt (%)	Clay (%)	w_L	I_p
23	0	28	42	30	36	19
USCS Classification: Lean clay with sand (CL)						
Sample Preparation:	Compacted		Shear Strength Test:		Modified direct shear test	

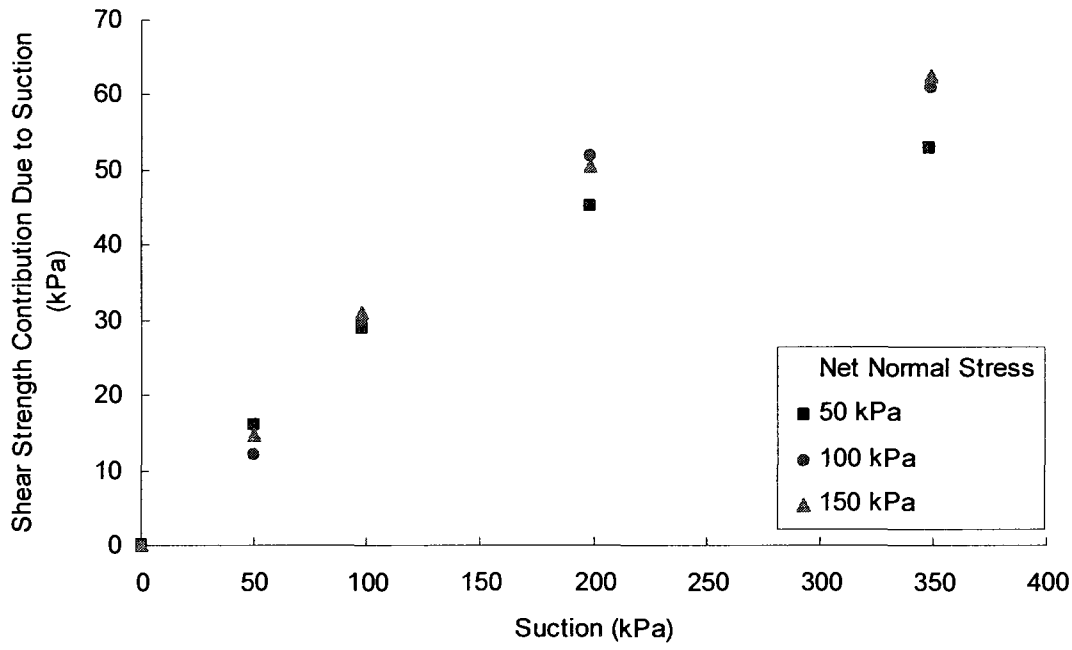

Figure 5.32. Shear strength contribution due to suction for glacial till. (Oloo and Fredlund, 1996)

Table 5.47. Confining pressures and net normal stresses for glacial till (Oloo and Fredlund, 1996).

	Soil 28a	Soil 28b	Soil 28c
Confining Pressure, σ_3 (kPa)	50	100	150
Net normal stress, σ_n (kPa)	50	100	150

5.3.19 Miao, Liu and Lai (2002)

Miao, Liu and Lai (2002) measured the unsaturated shear strength of Nanyang expansive clay (Soil 30) and to examine the hyperbolic relationship they proposed for estimating the shear strength. The Nanyang soil is an expansive soil that can be classified as fat clay (Table 5.48). The saturated soil parameters were determined in a triaxial test, but the authors do not specify if the test was performed under drained or undrained conditions. Reanalyzing the existing data revealed a cohesion of 38.3 kPa rather than the 32 kPa reported by the authors. The unsaturated shear strength testing was performed

using a modified triaxial apparatus at a confining pressure of 100 kPa with net normal stresses varying from 106-195 kPa.

The SWCC was determined using a pressure plate apparatus. Two different SWCC were determined: one with no pre-load applied to the sample and the second with a pre-load on the sample. However, the soils determined with no pre-load were used for the prediction of shear strength.

Table 5.48. Properties of Soil No. 30, Nanyang expansive soil (Miao et al, 2002).

ϕ'	c'	Sand (%)	Silt (%)	Clay (%)	w_L	I_p
21.5	38.3	6.7	68.5	24.8	58	32
USCS Classification: Fat clay (CH)						
Sample Preparation:	Compacted		Shear Strength Test:		Modified triaxial test	
Confining Pressure, σ_3 (kPa)		100	Net normal stress, σ_n (kPa)		106-195	

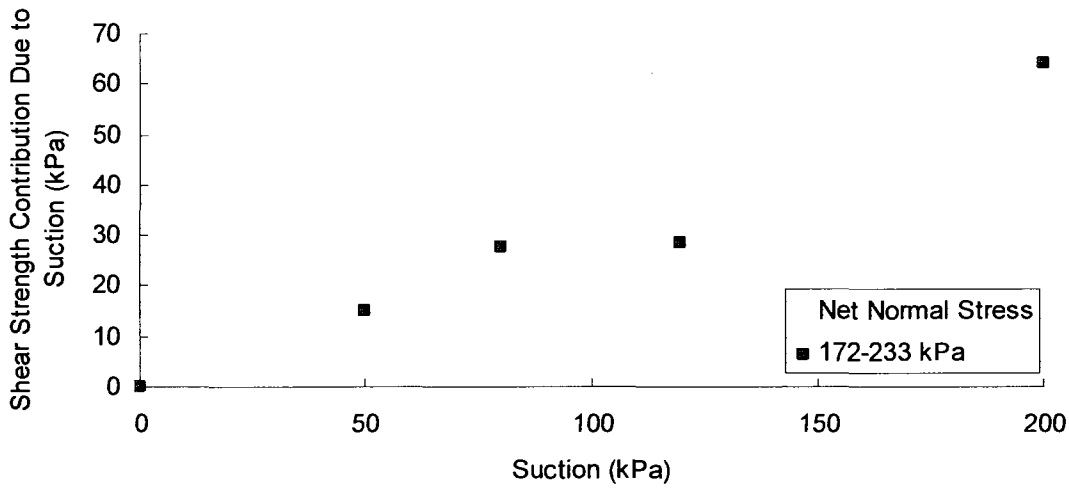

Figure 5.33. Shear strength contribution due to suction for Nanyang expansive soil. (Miao et al, 2002)

5.3.20 Futai, Almeida and Lacerda (2006)

Futai, Almeida and Lacerda (2006) examined the unsaturated shear characteristics of two soils from Brazil. These two tropical soils were undisturbed samples taken from depths of 1 m and 5 m, respectively. Both soils are from the same geological parent, but

the soil taken from 1 m is a lateritic soil, while the soil from 5 m is a saprolitic soil. The shear strength was determined using a stress path triaxial cell. The authors discuss changing the suction using axial translation techniques in a suction equilibrium chamber and transferring the sample to a modified triaxial testing apparatus. The strength was presented in terms of p and q and translated into shear strength and net normal stress using the effective shear strength parameters.

The SWCC was determined by pressure plate using the axis translation technique, over a range of 0 to 10,000 kPa. The test procedure of the SWCC was not reported in the paper.

Ouro Preto Tropical (1m)

The soil sampled at a depth of 1m (Soil 31) is a sandy fat clay. The properties of the soil are summarized in Table 5.49. The soil is tested in modified triaxial testing equipment with three different confining pressures: 25 kPa, 50 kPa and 100 kPa (Table 5.50).

Table 5.49. Properties of Soil No. 31, Ouro Preto tropical soil (1m) (Futai et al, 2006).

ϕ'	c'	Sand (%)	Silt (%)	Clay (%)	w_L	I_p
27.9	19	44	9	46	57	29
USCS Classification: Sandy fat clay (CH)						
Sample Preparation:	Undisturbed		Shear Strength Test:	Triaxial test		

Table 5.50. Confining pressures and net normal stresses for Ouro Preto tropical soil (1m) (Futai et al, 2006).

	Soil 31a	Soil 31b	Soil 31c
Confining Pressure, σ_3 (kPa)	25	50	100
Net normal stress, σ_n (kPa)	49-100	92-153	164-240

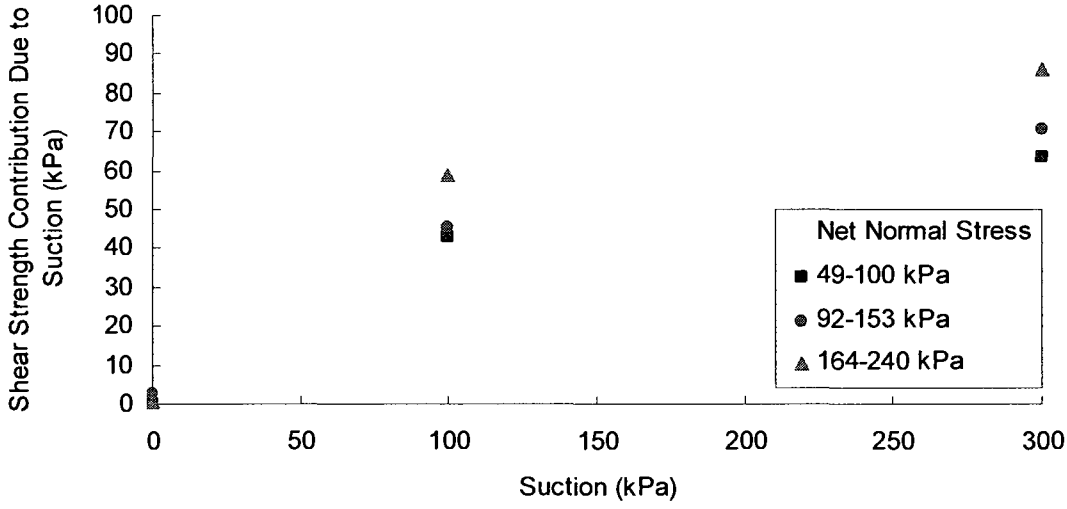

Figure 5.34. Shear strength contribution due to suction for Ouro Preto tropical soil (1m). (Futai et al, 2006)

Ouro Preto Tropical (5m)

The soil sampled at a depth of 5m (Soil 32) is a sandy lean clay saprolite. The properties of the soil are summarized in Table 5.51. The soil is tested in a triaxial with three different confining pressures: 25 kPa, 50 kPa and 100 kPa (Table 5.52).

Table 5.51. Properties of Soil No. 32, Ouro Preto tropical soil (5m) (Futai et al, 2006).

ϕ'	c'	Sand (%)	Silt (%)	Clay (%)	w_L	I_p
31.2	10.4	38	54	8	42	19
USCS Classification: Sandy lean clay (CL)						
Sample Preparation:	Undisturbed		Shear Strength Test:		Modified triaxial test	

Table 5.52. Confining pressures and net normal stresses for Ouro Preto tropical soil (5m) (Futai et al, 2006).

	Soil 32a	Soil 32b	Soil 32c
Confining Pressure, σ_3 (kPa)	25	50	100
Net normal stress, σ_n (kPa)	57-85	88-160	157-255

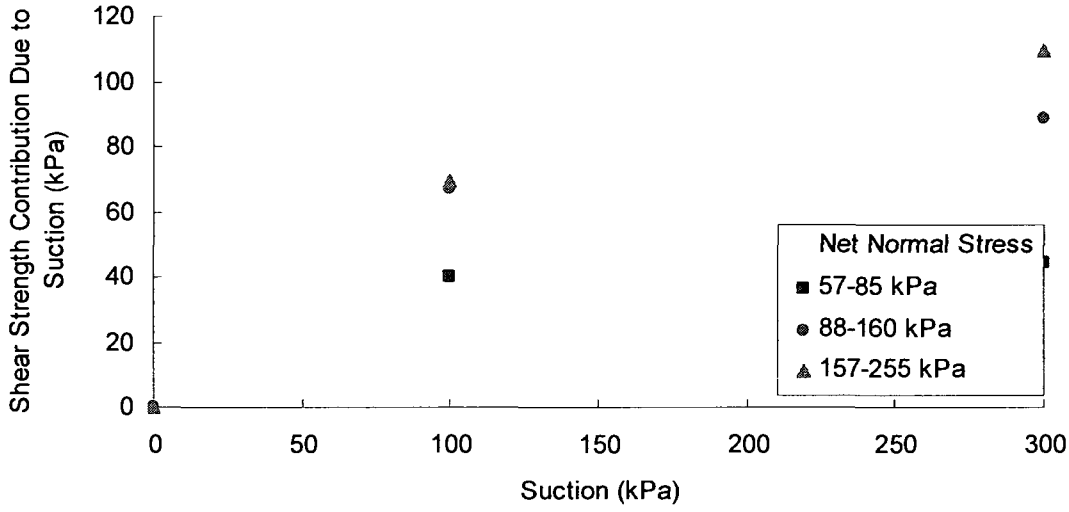

Figure 5.35. Shear strength contribution due to suction for Ouro Preto tropical soil (5m). (Futai et al, 2006)

5.3.21 Hardcastle, Li and Fragaszy (1992)

Hardcastle, Li and Fragaszy (1992) studied unsaturated properties of four Washington loess soils from a thesis prepared by Li (1989). The four soils are labelled by their clay content: C02 (Soil 33), C11 (Soil 34), C20 (Soil 35) and C30 (Soil 36). Loess soils are known for their potential collapsible behaviour. The saturated shear strength parameters were determined from triaxial tests on the samples. The reference does not specify if the test was a drained or undrained test.

The SWCC was determined using a pressure plate apparatus up to a suction of 500 kPa. The paper (Hardcastle et al, 1992) presents the SWCC as the saturation ratio versus suction, but the SWCC was presented as gravimetric water content versus suction in the 1989 thesis by Li.

C02

Soil 33 (C02) is a lean silt with sand with a very low plasticity index. The soil properties are summarized in Table 5.53. Undisturbed samples were tested in a modified triaxial test. The soil was tested using two confining pressures: 69 and 138 kPa. The equivalent resulting net normal stresses is summarized in Table 5.54.

Table 5.53. Properties of Soil No.33, C02 (Hardcastle, Li and Fragaszy, 1992).

ϕ'	c'	Sand (%)	Silt (%)	Clay (%)	w_L	I_p
35	1	20	78	2	22	2
USCS Classification: Lean silt with sand (ML)						
Sample Preparation:	Undisturbed		Shear Strength Test:		Modified triaxial test	

Table 5.54. Confining pressures and net normal stresses for C02 (Hardcastle, Li and Fragaszy, 1992).

	Soil 33a	Soil 33b
Confining Pressure, σ_3 (kPa)	69	138
Net normal stress, σ_n (kPa)	112-127	220-232

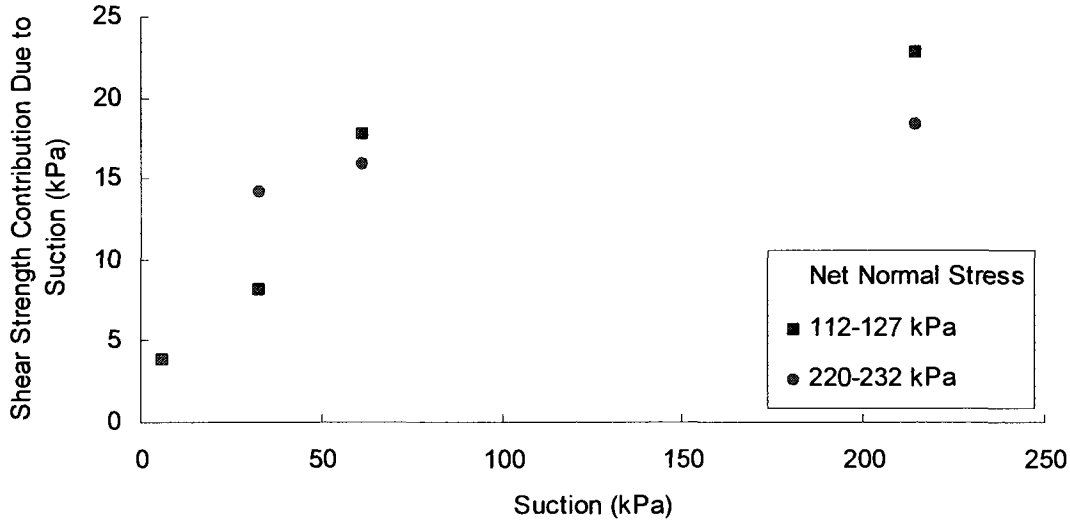

Figure 5.36. Shear strength contribution due to suction for C02. (Hardcastle, Li and Fragaszy, 1992)

C11

Soil 34 (C11) is a lean silt with a trace amount of sand. The soil properties are summarized in Table 5.55. Undisturbed samples were tested in a modified triaxial test. The soil was tested using two confining pressures: 69 and 138 kPa. The equivalent resulting net normal stresses is summarized in Table 5.56.

Table 5.55. Properties of Soil No.34, C11 (Hardcastle, Li and Fragaszy, 1992).

ϕ'	c'	Sand (%)	Silt (%)	Clay (%)	w_L	I_p
27.5	0	6	83	11	29	6
USCS Classification: Lean silt (ML)						
Sample Preparation:	Undisturbed		Shear Strength Test:		Modified triaxial test	

Table 5.56. Confining pressures and net normal stresses for C11 (Hardcastle, Li and Fragaszy, 1992).

	Soil 34a	Soil 34b
Confining Pressure, σ_3 (kPa)	69	138
Net normal stress, σ_n (kPa)	111-121	211-220

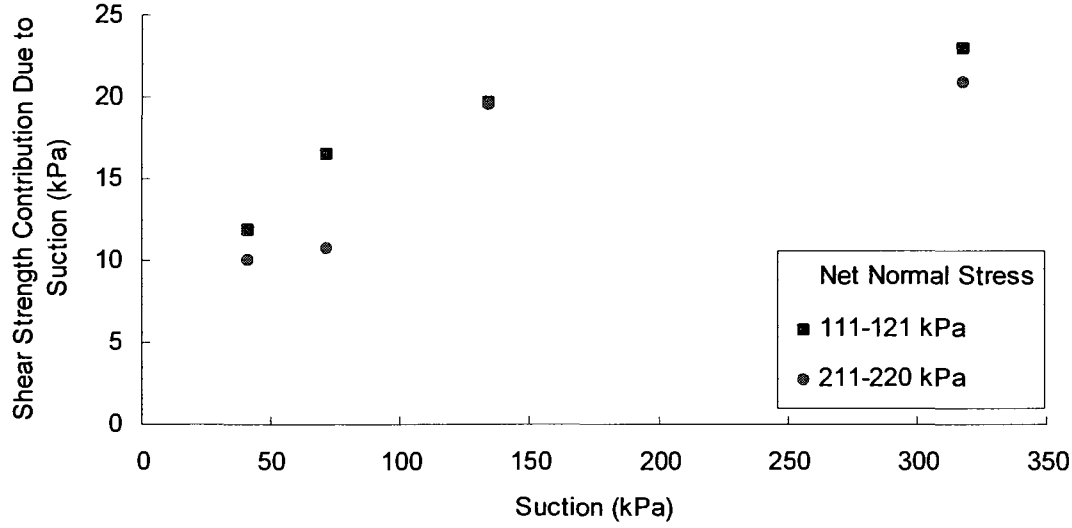

Figure 5.37. Shear strength contribution due to suction for C11. (Hardcastle, Li and Fragaszy, 1992)

C20

Soil 35 (C20) is a lean clay with minimal sand. The soil properties are summarized in Table 5.57. Undisturbed samples were tested in a modified triaxial test. The soil was tested using two confining pressures: 69 and 138 kPa. The equivalent resulting net normal stresses is summarized in Table 5.58.

Table 5.57.Properties of Soil No.35, C20 (Li and Fragaszy, 1992).

ϕ'	c'	Sand (%)	Silt (%)	Clay (%)	w_L	I_p
25.3	0	3.6	76.4	20	30	12
USCS Classification: Lean clay (CL)						
Sample Preparation:	Undisturbed		Shear Strength Test:		Modified triaxial test	

Table 5.58. Confining pressures and net normal stresses for C20 (Hardcastle, Li and Fragaszy, 1992).

	Soil 35a	Soil 35b
Confining Pressure, σ_3 (kPa)	69	138
Net normal stress, σ_n (kPa)	107-117	202-217

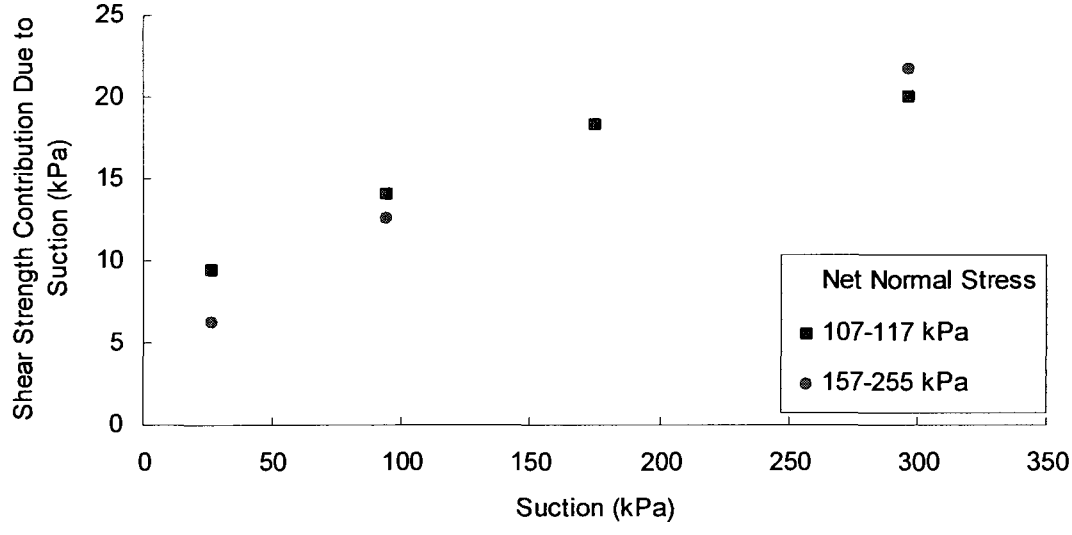

Figure 5.38. Shear strength contribution due to suction for C20. (Hardcastle, Li and Fragaszy, 1992)

C30

Soil 36 (C30) is a lean clay with minimal sand. The soil properties are summarized in Table 5.59. Undisturbed samples were tested in a modified triaxial test. The soil was tested using two confining pressures: 69 and 138 kPa. The equivalent resulting net normal stresses is summarized in Table 5.60.

Table 5.59. Properties of Soil No.36, C30 (Hardcastle, Li and Fragaszy, 1992).

ϕ'	c'	Sand (%)	Silt (%)	Clay (%)	w_L	I_p
29	0	2.2	67.8	30.0	38	17
USCS Classification: Lean clay (CL)						
Sample Preparation:	Undisturbed		Shear Strength Test:	Modified triaxial test		

Table 5.60. Confining pressures and net normal stresses for C30 (Hardcastle, Li and Fragaszy, 1992).

	Soil 36a	Soil 36b
Confining pressure, σ_3 (kPa)	69	138
Net normal stress, σ_n (kPa)	116-158	218-260

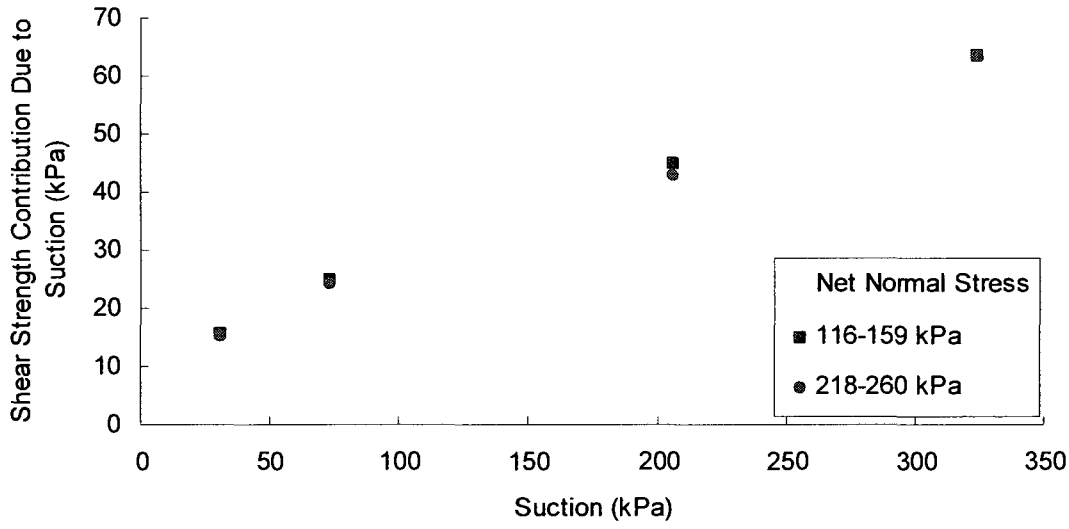

Figure 5.39. Shear strength contribution due to suction for C30. (Hardcastle, Li and Fragaszy, 1992)

5.3.22 Juca, Ferreira and Bastos (1997)

Juca, Ferreira and Bastos (1997) published a paper on volume change and shear strength of Recife clay (Soil 37) in unsaturated conditions. Recife clay is an expansive soil that is classified by USCS as heavy silt with sand. The properties of the soil are summarized in Table 5.61.

Unsaturated shear strength testing was performed using suction controlled direct shear apparatus based which is similar to the one developed by Escario (1989). The soil was subjected to three different confining pressures: 7, 50 and 80 kPa (Table 5.62). The filter paper method was used to measure suctions after shearing. Both Whatman No. 42 filter paper and Schleicher and Schuell No. 589 filter paper was used to measure the soil suction.

A pressure cell or Tempe cell apparatus was used to measure the SWCC up to a suction of 1000 kPa. Samples were molded into a ring measuring 50 mm in diameter and 20 mm in height.

Table 5.61. Properties of Soil No. 37, Recife clay (Juca et al,1997)

ϕ'	c'	Sand (%)	Silt (%)	Clay (%)	w_L	I_p
30	12	20	21	59	73	19
USCS Classification: Heavy silt with sand (MH)						
Sample Preparation:	Undisturbed		Shear Strength Test:		Modified direct shear test	

Table 5.62. Confining pressures and net normal stresses for Recife clay (Juca et al, 1997).

	Soil 37a	Soil 37b	Soil 37c
Confining Pressure, σ_3 (kPa)	7	50	80
Net normal stress, σ_n (kPa)	7	50	80

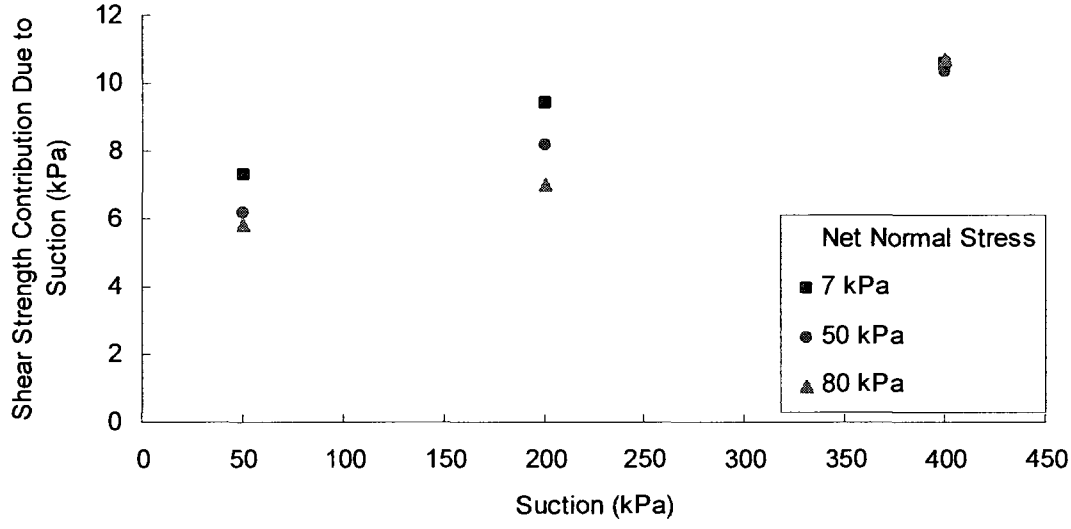

Figure 5.40. Shear strength contribution due to suction for Recife clay. (Juca et al, 1997)

5.3.23 Pereira and Fredlund (1999)

Pereira and Fredlund (1999) tested metastable structural gneiss sand (Soil 38) that is known to be a collapsible residual soil. They were testing to investigate both the shear strength and the volume change of the soil. The soil is modified by passing it over a 2 mm sieve and removing the material retained on the sieve. This material comprises about 2% of the entire sample. The remaining soil is a clayey sand with 48% fines of low plasticity. The saturated shear strength parameters were determined from a modified direct shear box and the angle of internal friction is seen to be very low. The properties of the soil are summarized in Table 5.63.

The shear strength of the soil was tested in a modified direct shear test. Specimens are statically compacted into a mold measuring 100 mm in diameter by 25 mm thick. Specimens measuring 51mm x 51 mm x 21 mm were extruded from this specimen for testing. The soil was tested using four different confining stresses: 25, 50, 100 and 200 kPa. Only two sets of data were used in this thesis (Table 5.64). The relationship is different than most unsaturated shear strength data as the shape of the curves are concave (Figure 5.41). This shape is unlike standard shear strength testing. The non-linear behaviour seen in the shear strength-suction relationship is normally convex downward.

The SWCC was determined using both pressure plate tests and Tempe cell tests. Both types of tests provided good correlation to each other. The SWCC was measured up to a suction of 500 kPa. Results are presented in Appendix A.

Table 5.63. Properties of Soil No. 38, Pacatuba residual sand (Pereira and Fredlund, 1999).

ϕ'	c'	Sand (%)	Silt (%)	Clay (%)	w_L	I_p
9	0	52	35	13	29	12
USCS Classification: Clayey Sand (SC)						
Sample Preparation:	Undisturbed		Shear Strength Test:	Modified direct shear test		

Table 5.64. Confining pressures and net normal stresses for soil Pacatuba residual sand (Pereira and Fredlund, 1999).

	Soil 38a	Soil 38b
Confining Pressure, σ_3 (kPa)	25	50
Net normal stress, σ_n (kPa)	25	50

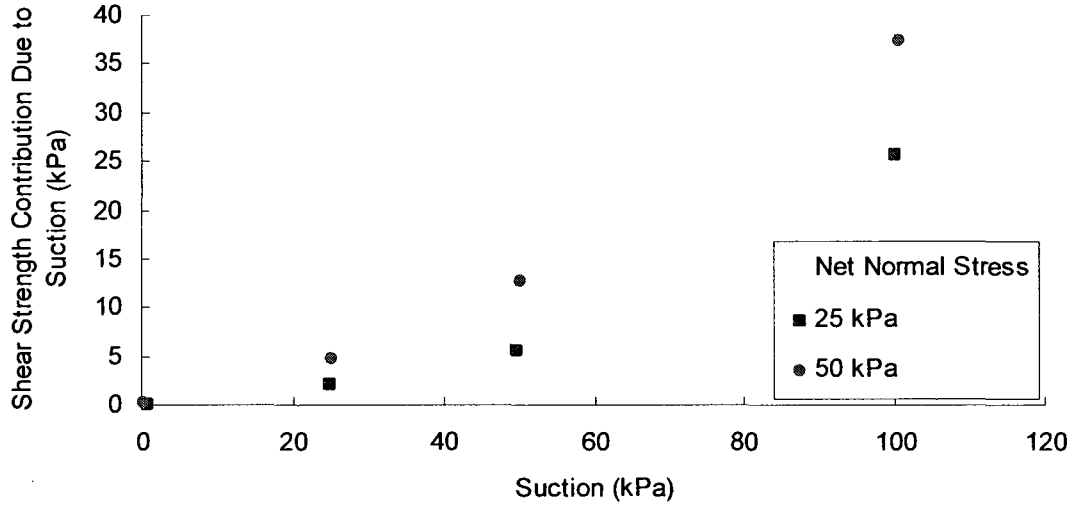

Figure 5.41. Shear strength contribution due to suction for Pacatuba residual sand. (Perreira and Fredlund, 1999)

5.3.24 Xu and Sun (2001)

Xu and Sun (2001) and Xu (2004) described shear strength of unsaturated soils in terms of the fractal dimension which infers the area of voids of the soil surface. They used Ningxia expansive soil (Soil 39) to test their equations. Ningxia soil is heavy silt with sand but is close to the borderline between clay and silt and near the borderline between heavy and lean. The saturated shear strength parameters were determined in the modified triaxial shear test apparatus under consolidated, undrained (CU) conditions. The soil properties are summarized in Table 5.65.

The shear strength specimens were compacted to a size of 25mm diameter by 80mm, height. Shear strength was measured using a modified triaxial test and sheared at a

rate of 1.5 x 10^{-4} mm/s. Unsaturated shear strength testing was performed under CU conditions at a net confining pressure of 400 kPa with net normal stresses ranging from 639-839 kPa (Table 5.65).

The SWCC was determined with both a pressure plate apparatus and a tensiometer, although the experimental use of the tensiometer is not described. The SWCC was given in terms of effective saturation, S_e= [(S-S_r)/(100-S_r)] where S_r is the residual degree of saturation. The residual degree of saturation was given as 18%, so the SWCC could be changed to be expressed as the degree of saturation and suction.

Table 5.65. Properties of Soil No. 39, Ningxia expansive soil (Xu and Sun, 2001; Xu, 2004).

ϕ'	c'	Sand (%)	Silt (%)	Clay (%)	w_L	I_p
24	27	25	57	18	51	22
USCS Classification: Heavy silt with sand (MH) borderline with fat clay with sand (CH) borderline to lean silt with sand (ML) borderline to lean clay with sand (CL)						
Sample Preparation:	Compacted		Shear Strength Test:		Modified triaxial test	
Confining Pressure, σ_3 (kPa)		400	Net normal stress, σ_n (kPa)		639-839	

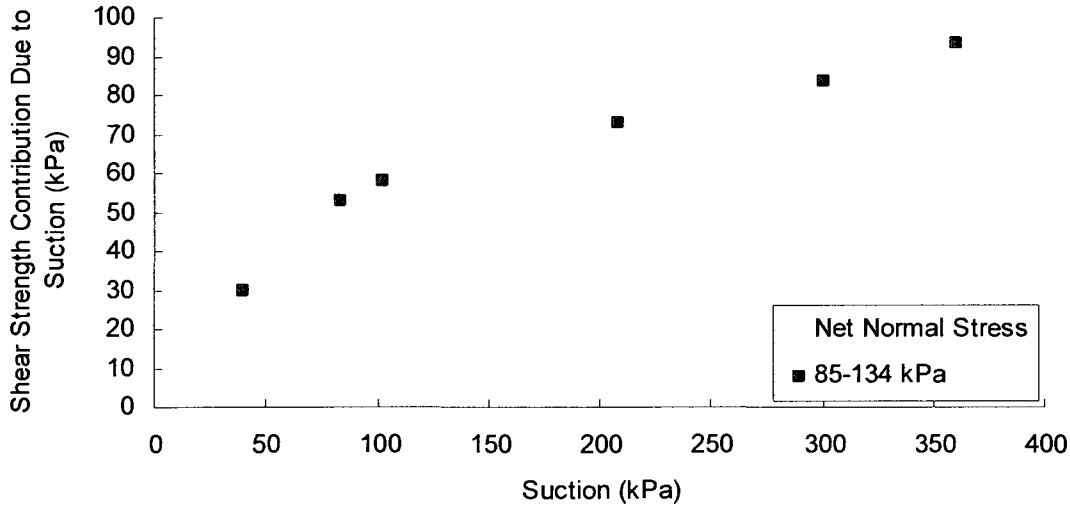

Figure 5.42. Shear strength contribution due to suction for Ningxia expansive soil. (Xu and Sun, 2001; Xu, 2004)

5.3.25 Zhan and Ng (2006)

Zhan and Ng (2006) tested Chinese expansive soil in a natural state (Soil 40) and compacted state (Soil 41) to examine the shear strength and volume change properties of the unsaturated soil. Samples were sheared under consolidated, drained conditions. The sample was sheared at a rate of 0.0019 mm/min until the horizontal displacement was 6 mm.

The SWCC was tested by pressure plate apparatus up to 500 kPa. The authors note a low air-entry value for the natural soil and explain the difference as the presence of cracks and fissures.

Hubei natural soil

The natural soil (Soil 40) is an expansive soil that is classified as heavy clay borderline to lean clay. The saturated soil parameters were determined using a conventional direct shear test. The soil properties are shown in Table 5.66.

Unsaturated shear testing was performed in a modified direct shear test apparatus under a net normal pressure of 50 kPa. A block of undisturbed soil was sampled from a depth of approximately 1 m below the surface. Undisturbed shear strength specimens were cut from the larger block using a sharp edged scalpel. The sample was cut to the dimensions of 50.8 x 50.8 x 21.4 mm to fit the modified shear strength apparatus.

Table 5.66. Properties of Soil No. 40, Hubei natural soil (Zhan and Ng, 2006).

ϕ'	c'	Sand (%)	Silt (%)	Clay (%)	w_L	I_p
28.7	16.2	3	48	39	51	31
USCS Classification: Heavy clay (CH) borderline to lean clay (CL)						
Sample Preparation:	Undisturbed		Shear Strength Test:		Modified direct shear test	
Confining Pressure, σ_3 (kPa)		50	Net normal stress, σ_n (kPa)		50	

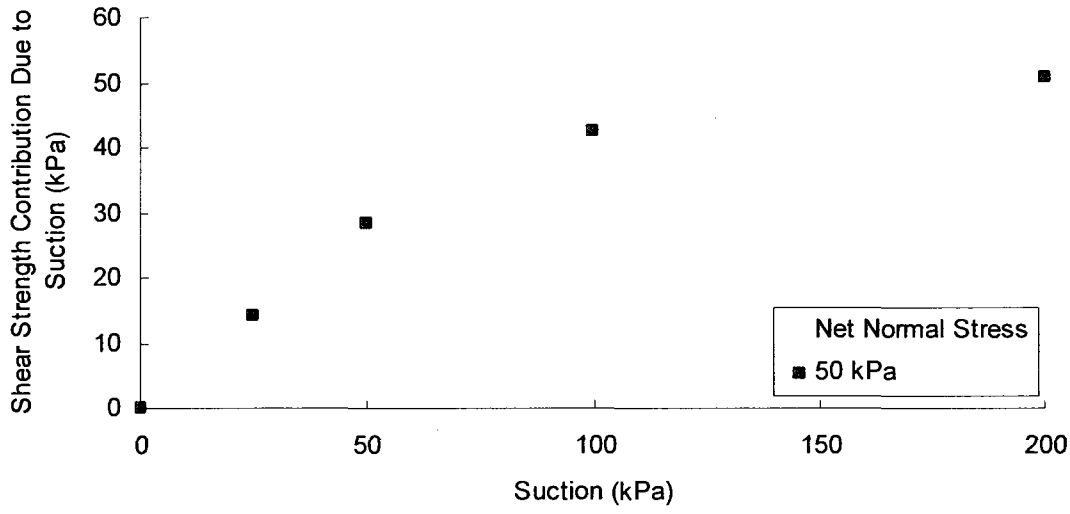

Figure 5.43. Shear strength contribution due to suction for Hubei natural soil. (Zhan and Ng, 2006)

Hubei compacted soil

The compacted soil (Soil 41) is an expansive soil that is classified as heavy clay borderline to lean clay. The saturated soil parameters were determined using a conventional direct shear test. The soil properties are shown in Table 5.67.

Unsaturated shear testing was performed in a modified direct shear test apparatus under a net normal pressure of 50 kPa. Unsaturated shear strength specimens were created by statically compacting the soil into a mold of dimensions of 50.8 x 50.8 x 21.4 mm. The soil was compacted in three layers at a moisture content dry of optimum.

Table 5.67. Properties of Soil No. 41, Hubei compacted soil (Zhan and Ng, 2006).

ϕ'	c'	Sand (%)	Silt (%)	Clay (%)	w_L	I_p
24	-	3	48	39	51	31
USCS Classification: Heavy silt (MH) borderline to lean silt (ML)						
Sample Preparation:	Compacted		Shear Strength Test:		Modified direct shear test	
Confining Pressure, σ_3 (kPa)		50	Net normal stress, σ_n (kPa)		50	

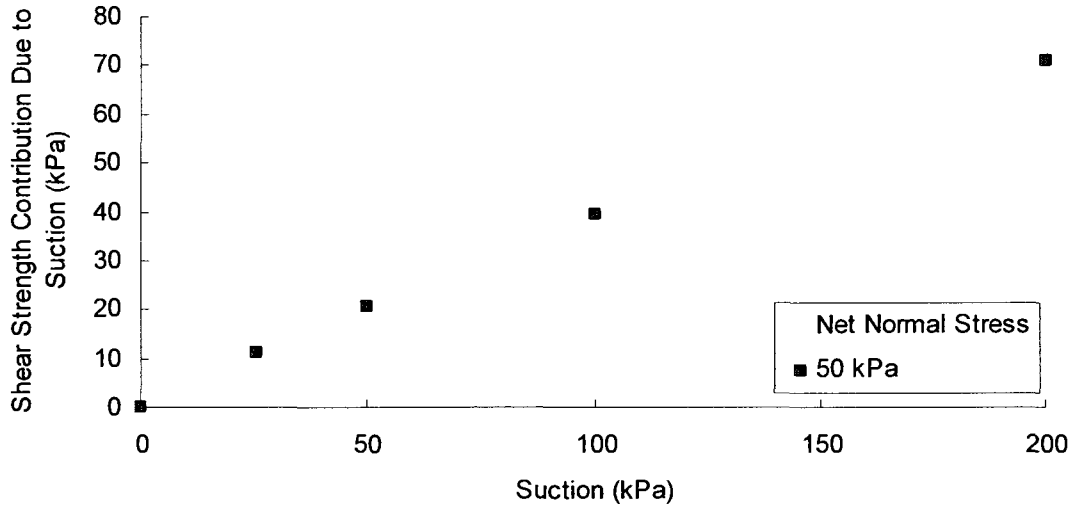

Figure 5.44. Shear strength contribution due to suction for Hubei compacted soil. (Zhan and Ng, 2006)

5.3.26 Huat, Ali and Hashim (2005)

Huat, Ali and Hashim (2005) published a paper on testing unsaturated residual soil (Soil 42). The soil is a tropical residual soil that can be classified as sandy heavy silt. The saturated shear strength were determined using a direct shear test. The published values were given as a range as pattern of shear strengths is not consistent. Recalculating these parameters reveals an effective angle of internal friction of 21.6° with cohesion of 11 kPa. The soil properties are summarized in Table 5.68.

Unsaturated shear strength values are determined using a modified shear box. The shear box has dimensions of 60 mm x 60 mm rather than the standard 50 mm x 50 mm to provide a better test for tropical residual soils which are known to be nonhomogenous and anisotropic (Huat et al, 2005). Blocks of soil were cut from a slope and shear samples were cut to size in the laboratory. The sample was tested at four net normal stresses (Table 5.69).

The SWCC was measured on a soil sample sampled from the same site but not taken from the same material tested for shear. The SWCC is measured using a pressure plate apparatus.

Table 5.68. Properties of Soil No. 42, KL residual (Huat et al, 2005).

ϕ'	c'	Sand (%)	Silt (%)	Clay (%)	w_L	I_p
unknown		43	9	48	95	50
USCS Classification: Sandy heavy silt (MH)						
Sample Preparation:	Undisturbed		Shear Strength Test:	Modified direct shear test		

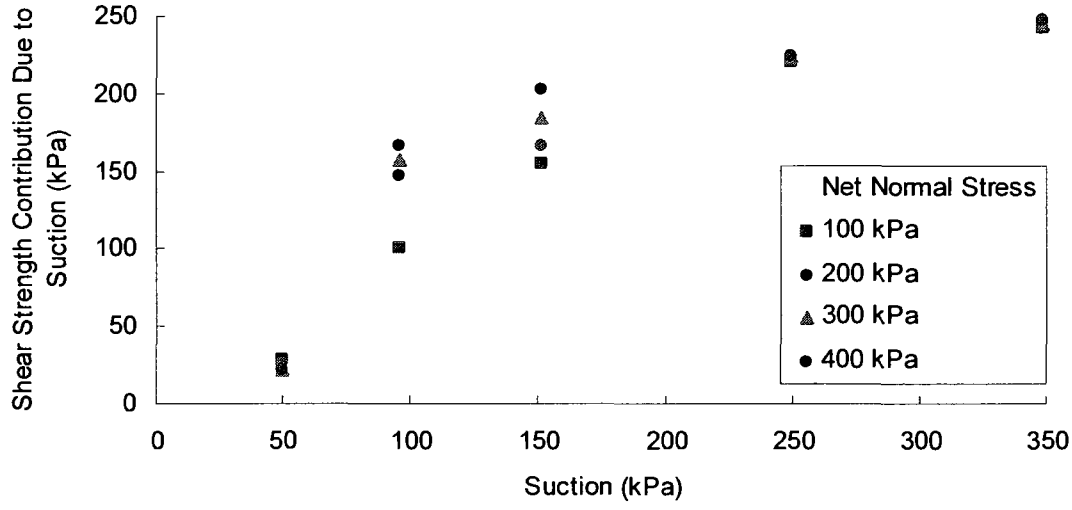

Figure 5.45. Shear strength contribution due to suction for KL residual. (Huat et al, 2005)

Table 5.69. Confining pressures and net normal stresses for KL residual (Huat et al, 2005).

	Soil 42a	Soil 42b	Soil 42c	Soil 42d
Confining Pressure, σ_3 (kPa)	100	200	300	400
Net normal stress, σ_n (kPa)	100	200	300	400

5.3.27 Reis and Vilar (2003)

The investigators prepared the paper specifically to examine the unsaturated shear strength of two undisturbed residual soils: one younger (Jovem, Soil 43) and the other a mature (Maturado, Soil 44) residual soil. The soils came from a gneiss rock but the mature soil is more weathered than the younger soil. Although they originated from the same parent material, the soils from the two horizons were very different (Table 5.70).

Table 5.70. Properties of two residual soils: Jovem and Maturado (Reis and Vilar, 2005).

Soils	Soil 43 Jovem Residual	Soil 44 Maturado Residual
ϕ'	27.1	31.3
c'	20.3	16.8
Sand (%)	50.0	27.0
Silt (%)	45.0	15.0
Clay (%)	5.0	43.0
w_L	38	68
I_p	27	29
USCS Classification:	Heavy silt (MH) borderline to silty sand (SM)	Heavy silt (MH)
Sample Preparation:	Undisturbed	
Shear Strength Test:	Modified direct shear test	

The soils were tested in a saturated and unsaturated condition using a modified triaxial test. The unsaturated soil was tested as consolidated drained test using different confining pressures. The confining pressures and the corresponding net normal stresses are summarized in the table below (Table 5.71).

Table 5.71. Confining pressures and net normal stresses for 2 residual soils (Reis and Vilar, 2003).

	Jovem			Maturado	
	Soil 43a	**Soil 43b**	**Soil 43c**	**Soil 44a**	**Soil 44b**
Confining Pressure, σ_3 (kPa)	50	100	200	50	200
Net normal stress, σ_n (kPa)	101-212	199-296	306-385	96-186	306-385

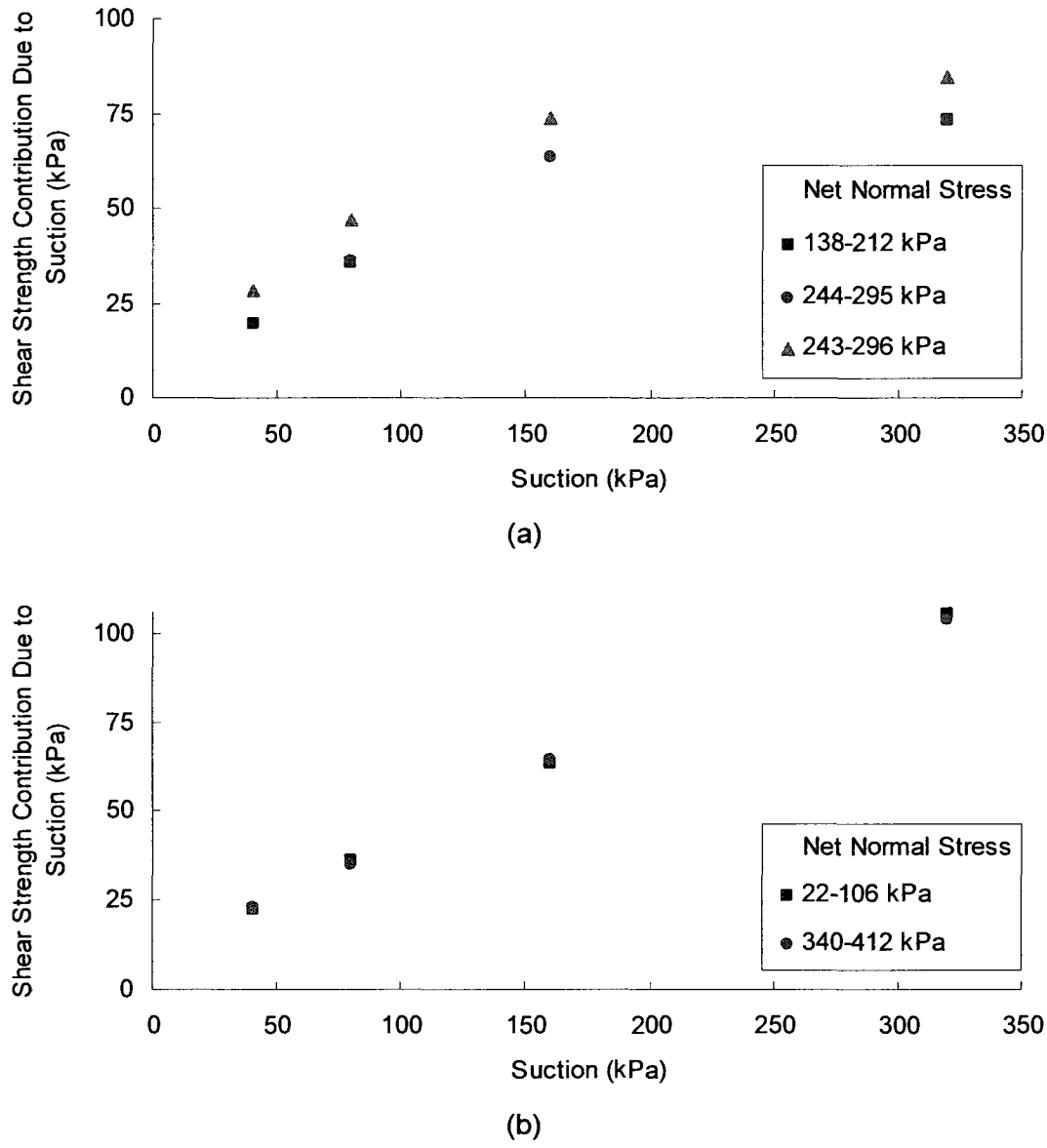

Figure 5.46. Shear strength contribution due to suction for: (a) Jovem residual and (b) Maturado residual. (from Reis and Vilar, 2003)

They fit the data points with a hyperbolic equation originally proposed by Miao et al (2001). The fitting parameters, *a* and *b*, for the Jovem soil was determined to be 1.86 and 0.0072, respectively. The fitting parameters, *a* and *b*, for the Maturado soil was determined to be 1.80 and 0.0039, respectively. The equation provided a line that fit the data although it is not a predictive equation.

$$c = c' + \frac{\psi}{(a + b\psi)} \qquad [3\text{-}50]$$

5.3.28 Nishimura Fredlund, Gan and Hirabayashi (1999)

Nishimura, Fredlund, Gan and Hirabayashi (1999) and Nishimura and Fredlund (1999) used tests done on lean silt (Soil 43) to examine and describe properties of unsaturated soils. The silt was used in numerous papers to explain and develop concepts. Properties of the soil are summarized in Table 5.72.The particle size distribution curve is located in Appendix B.

Specimens for testing were compacted under a pressure of 600 kPa. Unsaturated shear strength testing was performed using both a modified direct shear apparatus (Nishimura et al, 1999) and a modified triaxial test (Nishimura and Fredlund, 1999). The modified direct shear test was sheared at a rate of 0.05 mm/min until a horizontal displacement of 12 mm was attained. The triaxial shear test was sheared at a rate of 0.014 mm/min until shear strain exceeded 20%.

The SWCC was determined using a pressure plate apparatus up to 500 kPa and an osmotic dessicator for higher suctions. The portion of the SWCC coincident with shear strength testing was tested in the pressure plate apparatus.

Table 5.72. Properties of Soil No. 43, Ashikaga silt (Nishimura et al, 1999; Nishimura and Fredlund, 1999).

ϕ'	c'	Sand (%)	Silt (%)	Clay (%)	w_L	I_p
25	0	0	92	8	0	0
USCS Classification: Lean silt (ML)						
Sample Preparation:	Compacted		Shear Strength Test:		Modified direct shear, Modified triaxial test	

Table 5.73. Confining pressures and net normal stresses for Ashikaga silt (Nishimura et al, 1999; Nishimura and Fredlund, 1999).

	Soil 44a	Soil 44b	Soil 44c	Soil 44d	Soil 44e	Soil 44f
Confining Pressure, σ_3 (kPa)	30	60	100	200	300	25
Net normal stress, σ_n (kPa)	30	60	100	200	300	102-245

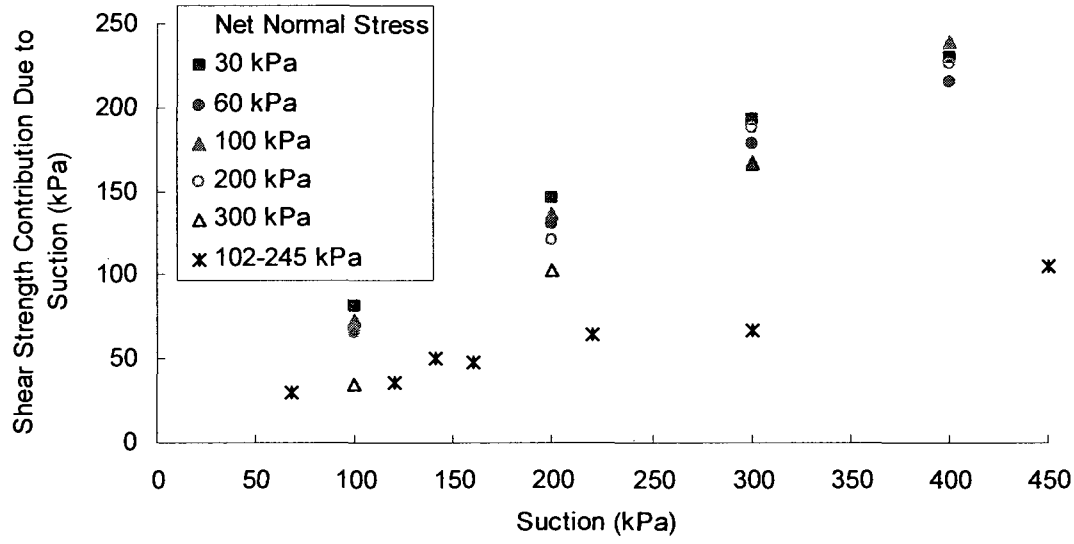

Figure 5.47. Shear strength contribution due to suction for Ashikaga silt. (Nishimura et al, 1999; Nishimura and Fredlund, 1999).

5.3.29 Toll, 1990

Kiunyu gravel is a lateritic material from the Kiunyu gravel pit. The soil was tested as a part of a thesis testing several lateritic soils (Toll, 1988). Kiunyu gravel is classified as a sandy clayey gravel according the the USCS. Saturated soil parameters were determined using a triaxial test apparatus and undrained conditions. The properties of the soil are summarized in Table 5.74. The particle size distribution is found is Appendix B.

The unsaturated shear strength was tested using a modified triaxial test under constant water (CW) conditions. Specimens were prepared by removing material greater than 9.5 mm and compacted into a split mold of a 100 mm diameter and 200 mm height. The material was placed in 50 mm lifts and statically compacted. The strain rates in some of the earlier tests were 0.08/min. However, in later tests, the rate was reduced to 0.016%/min and when left overnight, the rate was reduced to 0.003%/min to prevent maximum travel of the apparatus.

The SWCC was measured using a pressure plate apparatus up to a suction of 500 kPa. The water content is given as gravimetric water content and can be translated to degree of saturation by published mass-volume properties of the soil. In addition, Toll measured

the SWCC by air drying the sample. The curves beyond 100 kPa are similar, but show significant differences at suctions less than 100 kPa. The SWCC information can be found in Appendix A.

Table 5.74. Properties of Soil No. 45, Kiunyu gravel (Toll, 1990).

ϕ'	c'	Sand (%)	Silt (%)	Clay (%)	w_L	I_p
39.3	0	30	7	8	62	33
USCS Classification: Sandy clayey gravel (GC)						
Sample Preparation:	Compacted		Shear Strength Test:		Modified triaxial test	
Confining Pressure, σ_3 (kPa)		50	Net normal stress, σ_n (kPa)		87-177	

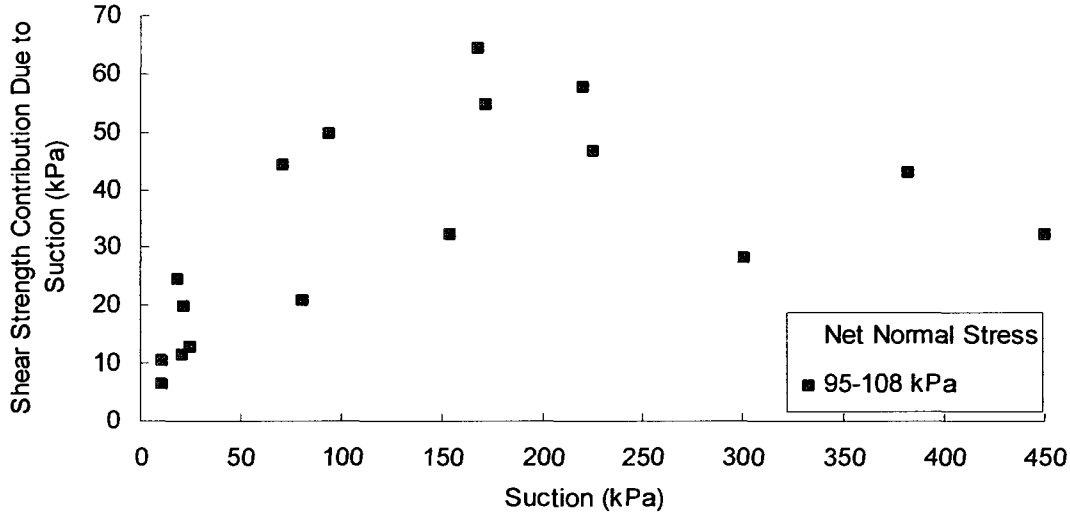

Figure 5.48. Shear strength contribution due to suction for Kiunyu gravel. (Toll, 1988; Toll, 1990)

5.3.30 Cui and Delage (1993)

The authors examined the yielding behaviour and volume of an aeolian silty material from the eastern Paris region. Jossigny silt (Soil 46) is classified by the USCS as lean clay. The saturated soil parameters were determined using a triaxial test. Soil properties are summarized in Table 5.75.

Soil specimens are prepared by statically compacting the soil in three layers into a 38 mm diameter mold using a double piston system. Unsaturated soil testing was undertaken using an osmotic triaxial apparatus (Delage et al, 1987) that uses different solutions of salt to alter the water content of the soil. The soil is wrapped in a cellulose membrane and placed in a triaxial cell. The solutions are circulated in the triaxial cell to allow a change in the water content within the sample. The temperature of the apparatus had to be maintained at a constant such that there will not be any change in the concentration of the sample. The soil was tested at four different confining pressures. The confining pressures and the corresponding net normal stresses are summarized in Table 5.76. The SWCC was generated using the suction values and the water contents prior to shear testing.

Table 5.75. Properties of Soil No. 46, Jossigny silt (Cui and Delage, 1993).

ϕ'	c'	Sand (%)	Silt (%)	Clay (%)	w_L	I_p
35.3	10	4	62	34	37	18
USCS Classification: Lean clay (CL)						
Sample Preparation:	Compacted		Shear Strength Test:		Modified triaxial test	

Table 5.76. Confining pressures and net normal stresses for Jossigny silt (Cui and Delage, 1993).

	Soil 46a	Soil 46b	Soil 46c	Soil 46c
Confining Pressure, σ_3 (kPa)	0	50	100	200
Net normal stress, σ_n (kPa)	136-267	215-350	330-665	514-665

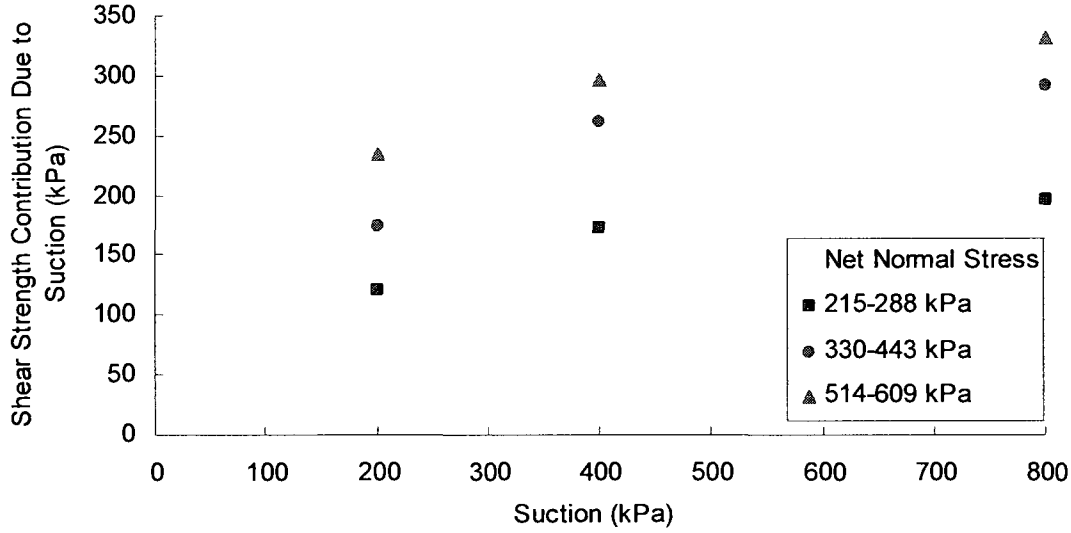

Figure 5.49. Shear strength contribution due to suction for Jossigny silt. (Cui and Delage, 1993)

5.3.31 De Campos and Carrillo (1995)

The authors prepared the paper to describe a modified direct shear test for residual soils and they used the device on four soils from a landslide in Brazil. Two soils were colluvium soils and two soils were colluviums. The colluvium soils have higher percentages of fines and only the yellow residual soil is non-plastic (Table 5.77). Conventional shear tests were performed to determine the effective shear strength parameters of the soils.

The investigators note that most of the unsaturated shear tests resulted in dilatory behaviour for the four soils. However, occasional strain softening was seen at higher suctions during testing performed on the young residual soil. All soils showed continuously contracting behaviour during soaked conditions. The authors note that there was not always a well defined peak during the shear testing of the soil. Failure was determined when the slope of the stress-strain curves became constant. The investigators note that fourth-order polynomial equations provide the best fit for these four soils.

Table 5.77. Properties of two residual soils and two colluvium soils: Soils 48-51 (de Campos and Carrillo, 1995; Carrillo and de Campos, 1997).

Soils	Soil 48 Yellow Colluvium	Soil 49 Red Colluvium	Soil 50 Yellow Residual	Soil 51 Mature Residual
ϕ'	26.4	26.8	26.7	30.4
c'	0.0	11.1	13.7	8.6
Sand (%)	50.3	44.5	71.7	60.0
Silt (%)	4.6	5.8	12.2	6.5
Clay (%)	42.5	43.2	7.6	24.4
w_L	46	60	30	51
I_p	23	17	NP	18
Net Normal Stress (kPa)	56	55	53	56
USCS Classification:	Clayey sand (SC) borderline to lean clay (CL)	Sandy heavy silt (MH)	Silty sand (SM)	Silty sand (SM)
Sample Preparation:	Undisturbed			
Shear Strength Test:	Modified direct shear test			

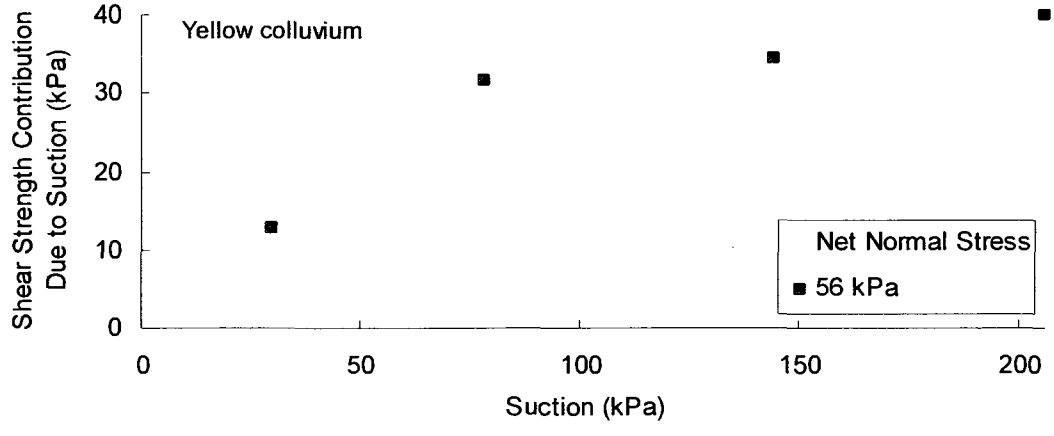

Figure 5.50. Shear strength of Brazilian colluviums and residual soils. (from de Campos and Carrillo, 1995)

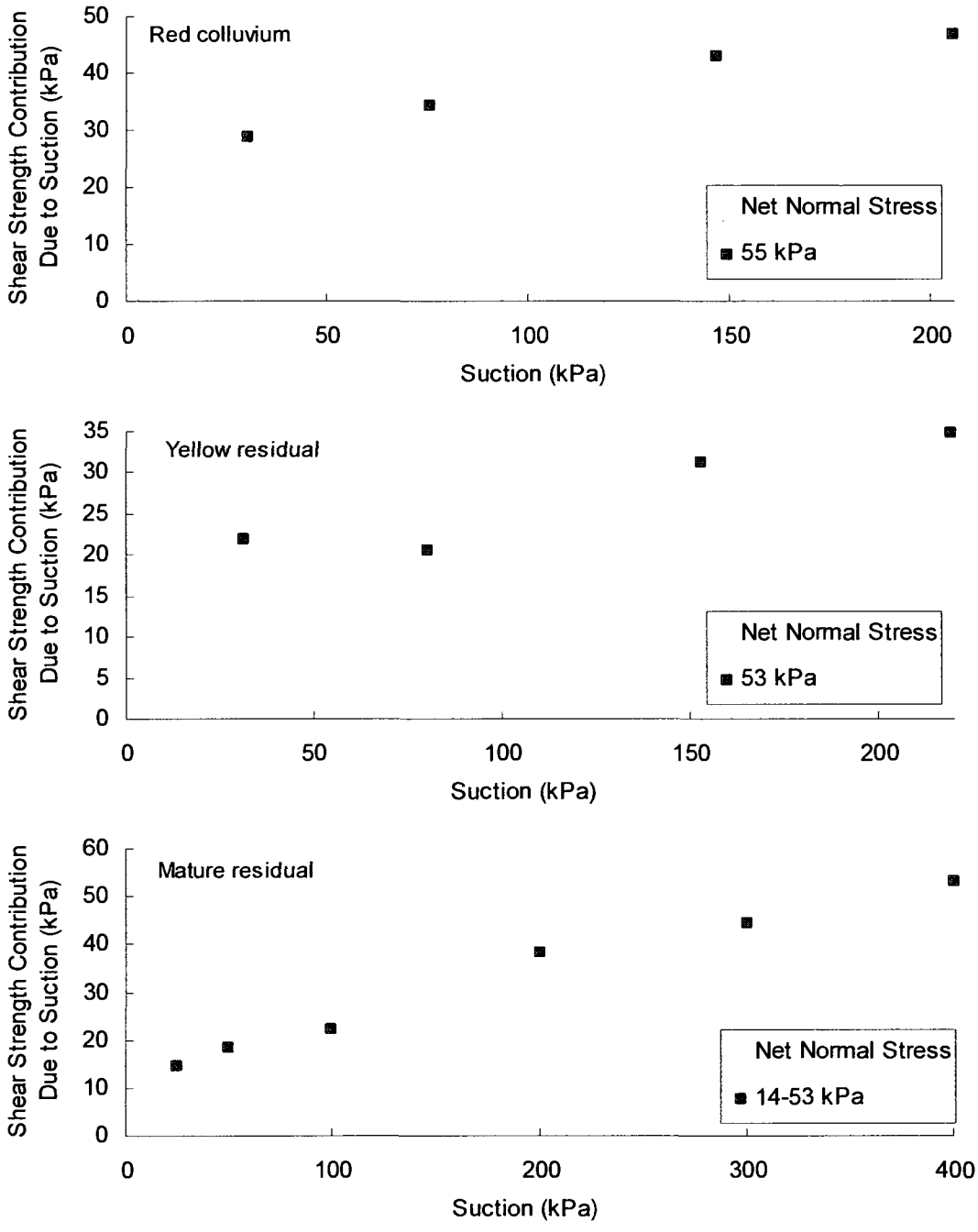

Figure 5.50. Shear strength of Brazilian colluviums and residual soils. (from de Campos and Carrillo, 1995)

5.3.32 Pineda and Colmenares (2005)

The investigation was performed to examine the shear strength contribution due to suction of commercial kaolin. The soil was prepared at a dry of optimum water content and statically compacted. The properties of the material are summarized in Table 5.78. The effective shear strength parameters were derived from the plot of kaolin (Wheeler and Sivakumar, 1999). The soil was tested in a conventional modified triaxial testing apparatus under unconfined compression conditions. The undrained test is run with 0 kPa confining pressure and a net normal stress of 12-46 kPa and the plot of the results shown in Figure 5.51 below.

Table 5.78. Properties of Soil No. 52, commercial kaolin. (Pineda and Colmenares, 2006)

ϕ'	c'	Sand (%)	Silt (%)	Clay (%)	w_L	I_p
33.0*	0.0*	unknown			84	38
USCS Classification: Heavy silt (MH)						
Sample Preparation:	Compacted		Shear Strength Test:		Unconfined compression test	
Confining Pressure, σ_3 (kPa)		0	Net normal stress, σ_n (kPa)		12-46	

* Effective stress parameters taken from Wheeler and Sivakumar (1999); data used in Pineda and Colmenares, 2006.

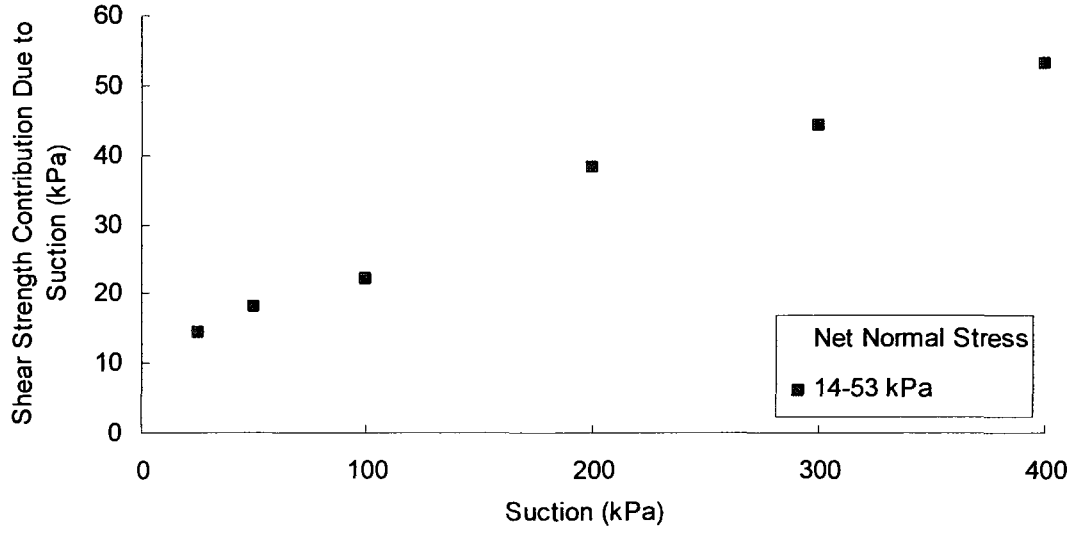

Figure 5.51. Shear strength of commercial kaolin (from Pineda and Colmenares, 2006).

5.4 Summary

In this chapter, the shear strength contribution due to suction is summarized for a 52 soils. They represent a wide variety of soils types sampled from numerous locations from around the world. The soils are prepared in different ways and tested using different apparatus. Many different soils are tested at different confining stresses and can be used to examine the effects of suction on the shear strength of soils. The wide range of soils will provide an excellent database to test the validity of the proposed predictive equations available in the literature for predicting the shear strength of unsaturated soils. The analyses of shear strength prediction using the data summarized in this chapter are available in Chapter 6.

CHAPTER 6 ANALYSIS OF SHEAR STRENGTH RELATIONSHIPS

6.1 Introduction

Shear strength data published in the literature was summarized in Chapter 5. A total of 52 soils data was summarized which included compacted soils, expansive soils, residual soils and loess. This data was collected from more than 50 publications from journals and conferences and theses. In most cases, the SWCC data was also summarized in addition to the laboratory shear strength test results. While most of these soil samples tested were prepared in the laboratory; a few natural samples were also tested. The summarized data, however, was not developed using consistent testing procedures by all the investigators as most of the shear strength testing procedures, techniques and equipment are still evolving during the last 50 years. In addition, unsaturated soils are complex to test and to analyze. For example, the specimens may be compacted at different water contents resulting in different soil structure and density. Soils compacted at lower water contents have an aggregated structure with larger pore spaces (macrostructure) and fewer interparticle contact points. The larger pores will drain readily when matric suction increases. Soils compacted at a moisture content greater than the optimum water content have a dispersed structure, which is very tight with small interpore spaces (microstructure) and more interparticle contact points. The soil will drain less quickly as the suction increases.

Typically, shear strength test results are plotted as the variation of shear strength with respect to suction. In this value, the shear strength contribution under saturated condition is also included. However, in this Chapter, the shear strength contribution only due to suction is presented. This data can be compared to see if there is any influence due to net normal stress, method of testing (ie. direct shear vs triaxial shear test), soil structure and density.

Finally, seven predictive equations (3-10, 3-11, 3-13, 3-25, 3-48, 3-64 and 3-73) are applied to the soils and the results presented and discussed in this chapter.

6.2 Predictive Equations

Seven equations were tested using the 52 sets of data from the literature to assess their ability to predict the shear strength contribution due to suction (3-10, 3-11, 3-13, 3-25, 3-48, 3-64 and 3-73). The prediction equations are summarized in Table 6.1 below. This data was summarized in the previous chapter.

Table 6.1. Summary of equations to describe the shear strength behaviour of unsaturated soils.

$\tau_{us} = (u_a - u_w) \cdot \theta_w \cdot \tan\phi'$ *Lytton, 1995*	Formulated for "moist" soils or soils beyond the range of saturation.	[3-10]
$\tau = c' + (\sigma - u_a) + S \cdot (u_a - u_w) \cdot \tan\phi'$ *Öberg and Sallfors, 1995*	Proposed for use on silts and sands.	[3-11]
$\tau_{us} = (u_a - u_w)(\Theta^{\kappa})(\tan\phi')$ *Vanapalli, Fredlund, Pufahl and Clifton, 1996* *Fredlund, Pufahl, Fredlund and Barbour, 1996*	Formulated for the entire range of suction.	[3-13]
$\chi = \left[\frac{(u_a - u_w)}{(u_a - u_w)_b}\right]^{\eta}$ *Khalili and Khabbaz, 1998*	Used for predicting the shear beyond the air-entry value.	[3-25]
$\tau_{us} = f_1 \cdot (u_a - u_w) \cdot \theta \cdot \tan\phi'$ *Aubeny and Lytton, 2003*	Formulated for "moist" soils or soils beyond the range of saturation.	[3-48]
$\tau_{us} = \tan\phi'[(u_a - u_w)_b + p_{at}] \cdot \ln\left[\frac{(u_a - u_w) + p_{at}}{p_{at}}\right]$ *Tekinsoy, Kayayadelen, Keskin and Söylemez, 2006*	Proposed model most suitable for fine-grained soils.	[3-64]
$\tau_{us} = \frac{(u_a - u_w)}{\frac{1}{\tan\phi'} + \left(\frac{1}{\tau_{us-max}} - \frac{1}{(u_a - u_w)_{max} \cdot \tan\phi'}\right)}$ *Vilar, 2006*	Uses one measured shear strength point in predicting the shear strength.	[3-73]

Several other equations (3-17, 3-23, 3-41, 3-57) are also predictive but are not addressed in this thesis. Equations 3-17 and 3-23 use the residual suction or degree of saturation as part of their equation. Equations 3-40 and 3-57 use the residual degree of

saturation to translate the degree of saturation of the SWCC into the effective degree of saturation, S_e. The fractal dimension is determined from the SWCC to use these equations are expressed in terms of effective saturation. The use of the residual suction or residual water content is not used in this thesis as the focus is to predict the shear strength in the suction range of 0 to 500 kPa.

Four of the equations use the SWCC to determine the shear strength contribution due to suction.The SWCC in this thesis was usually presented with either volumetric water content, gravimetric water content or the degree of saturation. However, it is seen in Table 6.1 that some formulae utilize the degree of saturation while others utilize the volumetric water content. The relationship between these variables was calculated for all data sets using their respective mass-volume properties. In some cases, the information was limited, so the resulting values were approximated using engineering judgement and other information from the published work.

The other two equations (Eqns. 3-31 and 3-64) do not require the measurement of the SWCC, but would require the determination of the AEV for a given soil. Equation 3-64 also uses the atmospheric pressure which is commonly expressed as 103.1 kPa. There is currently no method to predict the AEV of a given soil, so this parameter would have to be measured. Determination of this value is less time consuming in comparison to the determination of the SWCC.

6.2.1 Soils

The capability of successfully predicting the shear strength using the equations summarized in Table 6.1. Equations should be tested using the experimental data. Published data was extracted from numerous journals, conferences and theses using DiGno, a digitizing program developed at the University of Ottawa (Infante Sedano, 2006). This information was summarized in Chapter 5. Every effort has been made to extract the data so that it is as close to the original data presented by the authors. The documents were often digitally reproduced by photocopy or fax to be transmitted to the University of Ottawa and minor distortions may have occurred. The calibration of DiGno to a printed image minimizes the effect of distortions; however but there maybe some errors still exist.

Fifty-two individual soils data sets were summarized to test the equations. Many of the soils were tested at more than one confining pressures, resulting in 130 sets of unsatu-

rated shear strength data. Soils were chosen based on the presence of both shear strength data and a SWCC. Preference was given to tests performed in consolidated, drained condition (CD).

A suction range of 0 ~ 500 kPa represents a range of suction that is of interest in practice. In addition, when the suction is less than 500 kPa, it is matric suction acting on the system and there is little influence of osmotic suction. Therefore, data used in this thesis was limited to suction values up to 500 kPa.

The soils were grouped in two different ways to assist in the analysis. The first group of soils were classified using the soil using the Unified Soil Classification system (ASTM D2487) and summarized in Table 6.2. Most of the soils tested are classified as low plasticity clay. Nine of the soils are classified as silt and eleven soils are classified as sand. The gradation of two of the soils is not summarized. These soils were fine-grained soils and their classification based on relevant information.

Table 6.2. Summary of soils presented in the thesis classified using the Unified classification system.

Soil Type	No. of Soils	Sand (%)	Range of w_L	Range of I_p
Predominantly sandy soils	14	41 – 89	0 – 51	0 – 23
Low Plasticity Silts	7	0 – 39	0 – 84	0 – 38
High Plasticity Silts	10	0 – 45	51 – 95	17 – 50
Low Plasticity Clays	17	2 – 50	25 – 49	6 – 27
High Plasticity Clays	4	3 – 44	51 – 60	26 – 33

Öberg and Sallfors (1997) proposed an equation for sands and silts but the gradation of the soils was based on the particle size of the soil (Table 6.3). The soils summarized using this approach fall in the second group of the soils are sands and silts as per this classification. The definition of sand and silt is defined as percentage by mass greater than 50% of the entire sample specimen. Only five of the 52 soils were not sands and silts.

Table 6.3. Summary of soils grouped as particle size.

Soil	No. of Soils	Sand + Silt (%)	w_L
Sands and Silts	44	50 – 100	0 – 95
Clays	6	35 – 47	56 – 74
Unknown	2	Unknown	37 - 60

Differences in the type of shear strength testing techniques were highlighted in this thesis. The relative number of tests conducted also has a significant influence on the outcome of the analysis of the equations. In general, the number of soils tested using a modified direct shear apparatus and the modified triaxial test apparatus is almost equal. The number does not equal the number of soils tested. This is explained as one of the modified triaxial tests was performed under unconfined conditions and one soil was tested using both the modified triaxial test and the modified direct shear test. A minimal number of soils were tested under unconfined conditions. Both the range of the net confining pressures and the range of the net normal stresses are given for each apparatus.

Table 6.4. Summary of the breakdown of the number of soils tested using the various testing methods.

		Range of (σ_3-u_a)	Range of (σ_n-u_a)
Modified Direct Shear Test	24	2-300	2-300
Modified Triaxial Test	25	10-400	20-450
Unconfined Compression Test	4	0	6-195
Unknown	1		

The types of soils used for the research work is also of interest as the list of soil types (Table 6.5) includes problematic soils. Wind deposited soils (aeolian, loess), expansive soils and residual soils are some of the most common problematic soils. Commercially produced kaolin and tailings are soils that have been subjected to human processing and man-made soils include those soils that were created from two or more different soils, or soils that have had their gradation altered prior to testing. Other soils include a variety of tills, silts and clays that have not been labelled as remarkable in characteristic.

Table 6.5. Breakdown of soil types.

Aeolian	1
Loess	4
Commercial soil	1
Expansive	7
Man-made	4
Residual	17
Tailings	3
Other	15

The method of preparation of the soils is also a key parameter as it influences the structure of the soil. There was an almost equal number of soils that were statically compacted compared to the soils that were undisturbed (Table 6.6). Four of the soils were compared by placing the materials in a slurried condition and then compacting them to the appropriate density.

Table 6.6. Summary of methods of preparation.

Compacted	25
Undisturbed	23
Slurry compacted	4

6.2.2 Sample Size

The size of each data set is important when examining the fit as the low numbers can create a bias and an inability to determine any outliers within the set. Table 6.7 summarizes the number of points for each data set. The number of points in a set ranges from 1 to 22 points with an average number of points equal to 4.7. Comparatively, this is a small number and this must be considered while assessing the shear strength prediction equations. Most sets of data do not meet the minimum amount of points to show statistical significance and therefore, it is impossible to remove outliers.

Table 6.7. Summary of sample size for each data set.

Soil No.	Total
1a	4
1b	4
1c	4
2a	1
2b	2
3a	4
3b	2
4a	6
4b	6
4c	6
5	6
6a	4
6b	3
6c	3
6d	4
6e	4
6f	3
6g	3
6h	4
7a	5
7b	5
7c	5
7d	5
8a	5
8b	4
8c	3
9	12
10	4
11a	3
11b	2
11c	7
11d	4
12	3

Soil No.	Total
13	4
14	4
15a	4
15b	4
15c	4
16a	4
16b	4
16c	4
17a	5
17b	4
17c	5
18	22
19	3
20	21
21	9
22	12
23	12
24a	4
24b	4
24c	4
24d	4
25a	4
25b	4
25c	4
25d	4
25e	4
25f	4
25g	4
25h	5
25i	4
26a	4
26b	4
26c	4

Soil No.	Total
26d	4
26e	4
26f	4
26g	3
27a	9
27b	4
27c	4
27d	4
27e	4
28a	11
28b	10
28c	8
29a	5
29b	5
29c	4
30	5
31a	2
31b	2
31c	2
32a	2
32b	2
32c	2
32d	2
33a	4
33b	4
34a	4
34b	4
35a	4
35b	3
36a	4
36b	4
37a	3
37b	3

Soil No.	Total
37c	3
38a	4
38b	4
38c	4
39	6
40	4
41	4
42a	5
42b	5
42c	5
42d	5
43a	3
43b	3
43c	4
44a	4
44b	4
45a	4
45b	4
45c	4
45d	4
45e	3
45f	7
46	17
47a	3
47b	3
47c	3
48	4
49	4
50	4
51	4
52	6

6.2.3 Effective Angle of Internal Friction

The effective angle of internal friction, ϕ', is a key term in all of the equations as it is a component of saturated shear strength. In addition, it is used in many of the empirical equations to predict the shear strength contribution due to suction. The angle of internal friction can be determined by a triaxial test; however, it is important that the angle is determined by plotting the net normal stress versus the shear strength. Several authors used the net confining pressures versus shear strength, resulting in the appearance a significantly higher angle of internal friction, ϕ'.

The angle of internal friction, ϕ', can be determined in two ways:

i) using a conventional shear strength test apparatus (direct or triaxial)

ii) using a saturated test in a modified shear strength testing apparatus

Differences may be seen in the angle of internal friction, ϕ' in the order of 1-2° as shear stresses at failure are different. It is important to determine the angle of internal friction using the same testing method that will be used to determine the unsaturated shear strength.

6.2.4 Influence of Net Normal Stress

The net normal stress used has some influence on the shear strength behaviour. Some soils show some change in shear strength contribution due to suction under the influence of different net normal stresses. However, some do not.

The testing performed by Vanapalli (1994) with samples prepared at different water contents allows some discussion with this regard. Previously, this data had always been viewed as shear strength versus suction. The plots (Figure 6.1 and 6.2) present the data as the shear strength contribution due to suction versus suction.

Vanapalli prepared specimens of Indian Head till at different water contents: dry of optimum, optimum water content and wet of optimum water content. The soil was tested in a modified direct shear apparatus at different confining pressures. The results are presented in two different ways: soils prepared at the same water content (Figure 6.1) and soils tested at the same net normal stresses (Figure 6.1)

Dry of optimum water content will result in larger voids and clod formation in the sample. In Figure 6.1 the dry of optimum samples show a difference in shear strength between 5 and 20 kPa between the soils tested at 25 kPa and the soils tested at 200 kPa. The shear strength of the soil tested at 200 kPa is generally higher than the soil tested at 25 kPa. The soils prepared at optimum water content will have a more organized soil structure. The difference in shear strength between the soil tested at the 25 kPa and

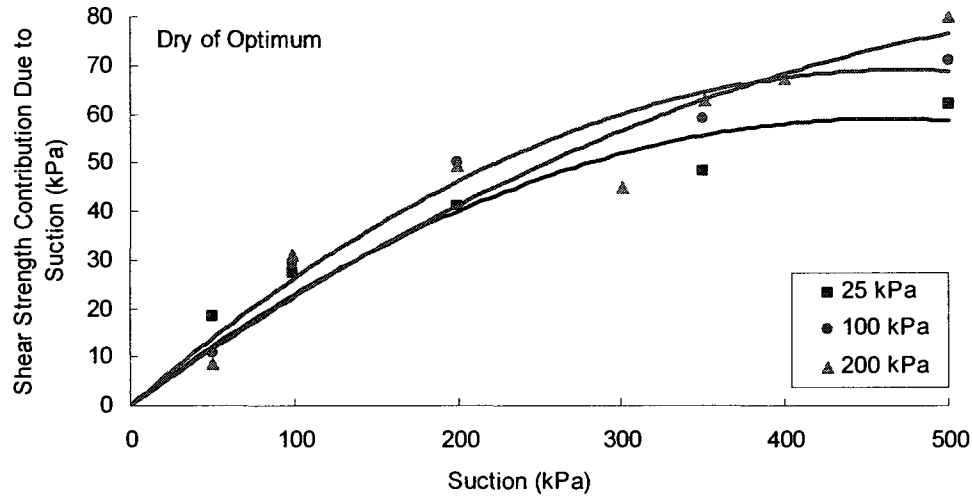

(a)

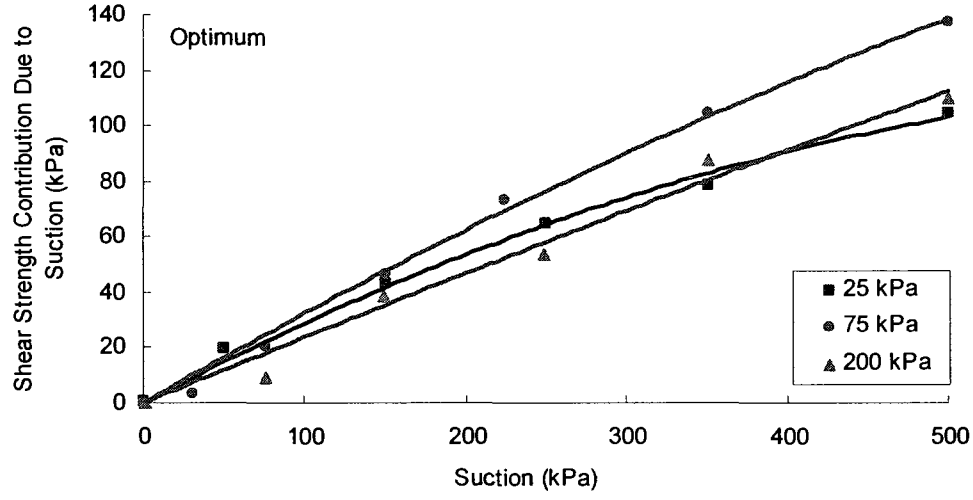

(b)

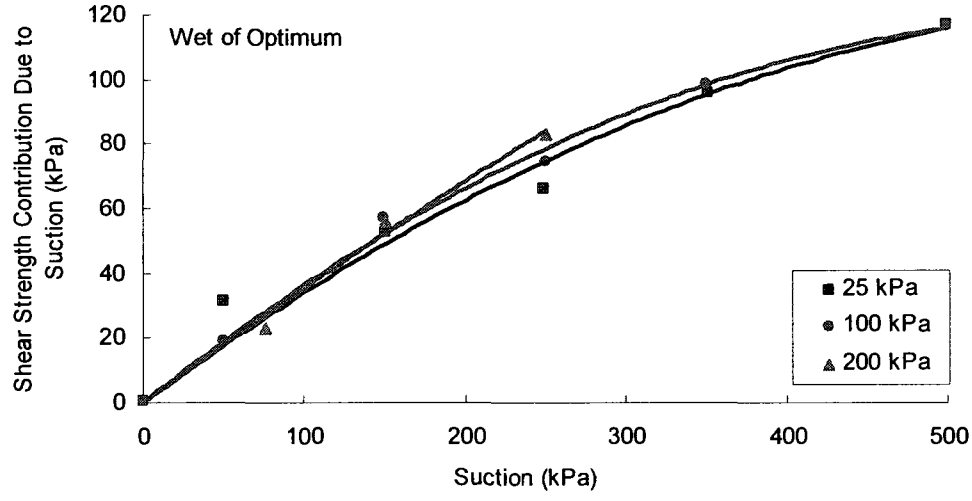

(c)

Figure 6.1. Influence of net normal stress on shear strength contribution due to suction for soils prepared at (a) dry of optimum water content, (b) optimum water content and (c) wet of optimum water content.

200 kPa varies from 5 to 15 kPa but the shear strength of the soil tested at 75 kPa is considerably higher (5-40 kPa difference). Soil prepared at wet of optimum condition will have a more dispersed structure with relatively smaller continuous voids. The resulting difference in shear strengths of the soils tested at 25, 100 and 200 kPa ranges from 5-15 kPa, although the general polynomial trend lines are much closer for samples prepared at wet of optimum. In general, specimens prepared at dry of optimum conditions have a lower shear strength contribution due to suction that could be attributed to the soil structure (Vanapalli et al, 1999).

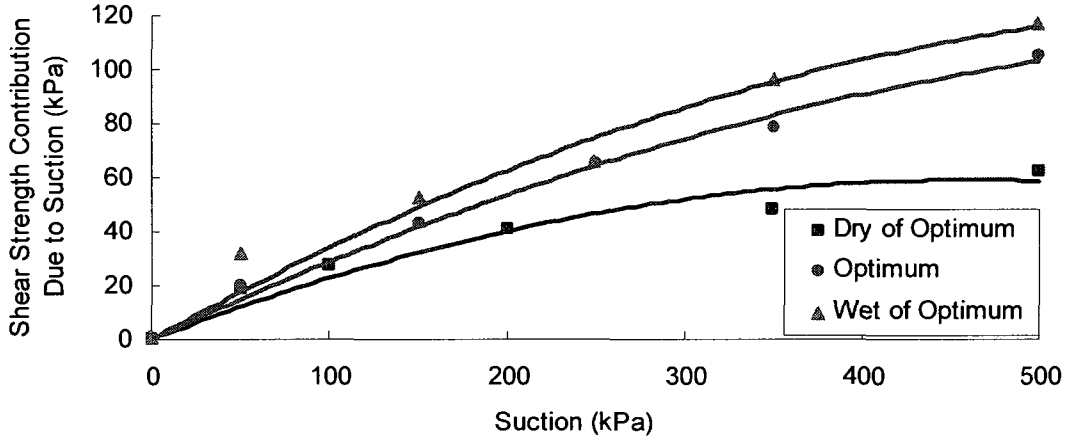

(a)

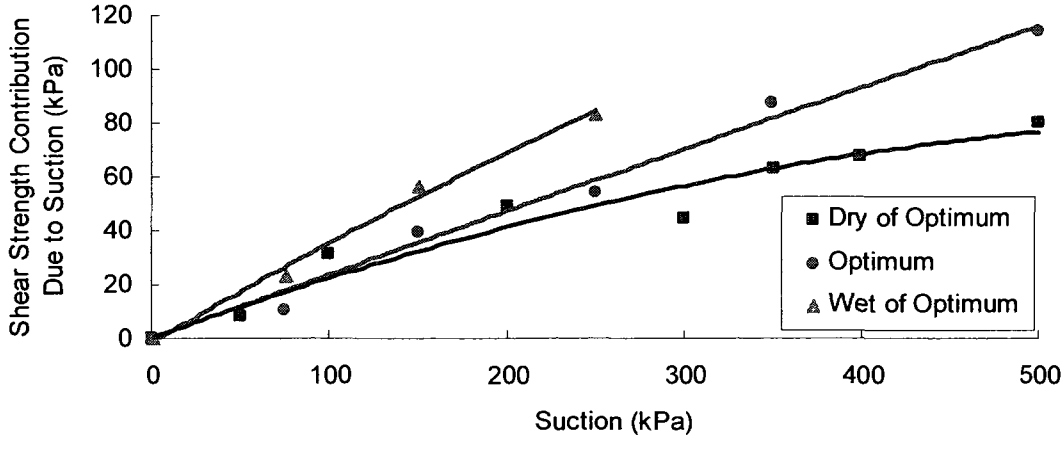

(b)

Figure 6.2. Influence of soil fabric on shear strength contribution due to suction for two confining pressures: (a) 50 kPa, and (b) 200 kPa.

In Figure 6.2, the soils are grouped according to the net normal stress for 25 and 200 kPa. For a net normal stress of 25 kPa, the shear strength of the soils prepared at optimum and wet of optimum water content varies by only 5-15 kPa while the shear strength of the soil prepared at dry of optimum is 5 to 50 kPa lower than the strength of the soil prepared at optimum conditions. For soils tested under a net normal stress of 200 kPa, there is a difference in shear strength for the soils prepared at dry, optimum and wet of optimum moisture content conditions.

6.2.5 Effect of Stress History

The effect of the stress history on the soil is also another factor that influences the shear strength contribution due to suction. Work done by Tarantino and Tombolato (2005) used Speswhite kaolin tested in a modified shearbox. The investigators used three different pressures (300 kPa, 600 kPa and 1200 kPa) and tested at three net normal stresses (300 kPa, 600 kPa and 900 kPa).

Figure 6.3 shows the results of the testing expressed as shear strength contribution due to suction. Figure 6.3a is the testing performed on overconsolidated samples, or samples that are tested at net normal stress less than or equal to the compaction stress. Two overconsolidated samples (compacted at 600 and 1200 kPa) show an increase in shear strength contribution due to suction even though testing occurred at the same net normal stress. The greater strength exhibited may be attributed to the greater density occurring from the larger load applied during compaction.

Figure 6.3b shows samples tested at normally consolidated conditions. The compaction stress equals the net normal stress applied during testing. The sample compacted and tested at a pressure of 900 kPa shows a much greater shear strength contribution due to suction. Comparing the two plots, two things become apparent: 1) the shear strength contribution due to suction is influenced by the greater density (due to the influence of higher compaction pressure) and the net normal stress; 2) the net normal stress has a greater influence on the shear strength contribution due to suction than the increase in density for Speswhite kaolin.

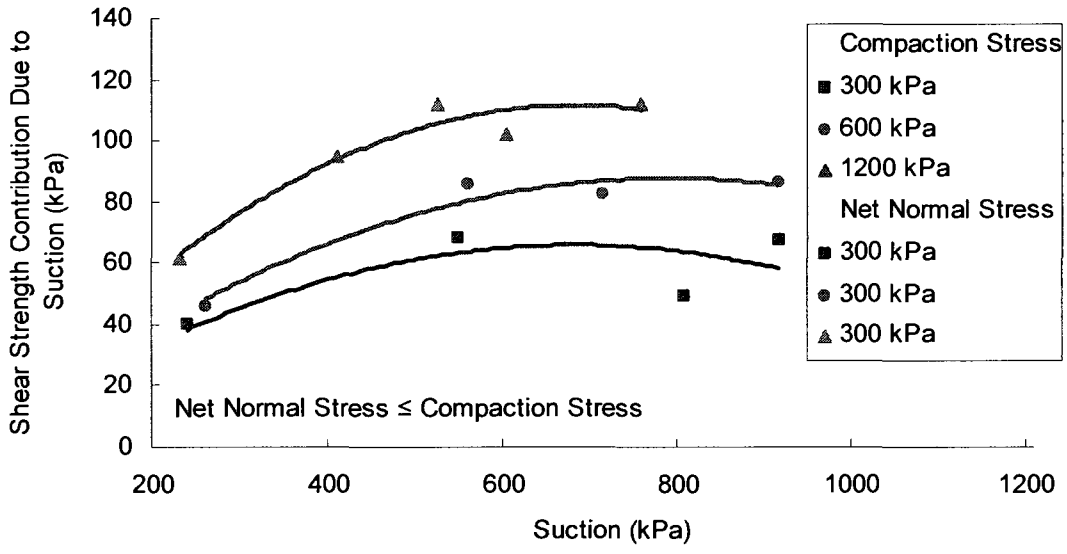

(a)

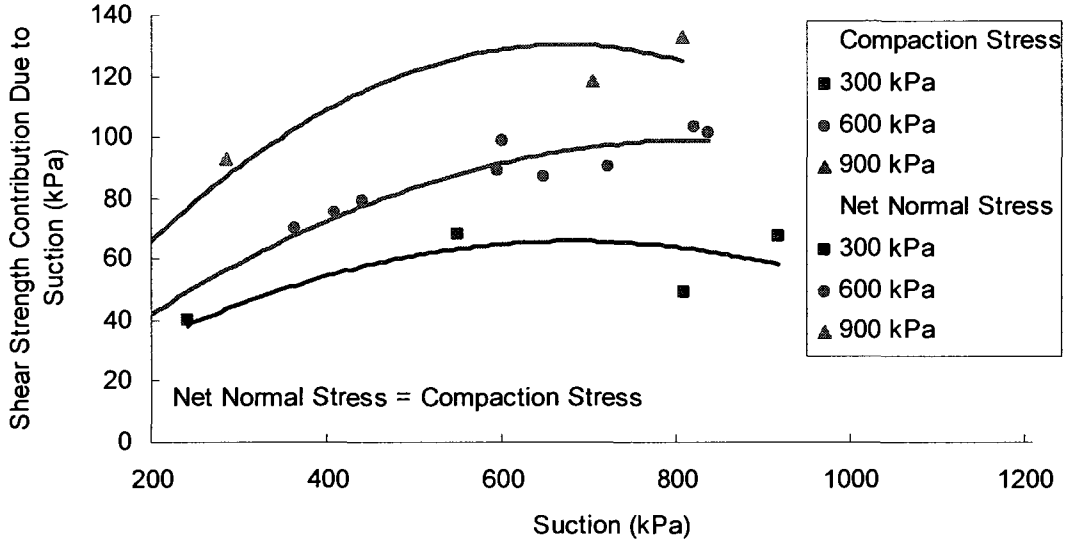

(b)

Figure 6.3. Influence of stress history on shear strength contribution due to suction for soils prepared when (a) net normal stress is less than the compaction stress, (b) net normal stress equals the compaction stress.

6.2.6 Soil-Water Characteristic Curve (SWCC)

The SWCC is used in as a tool in the shear strength prediction in all six prediction equation. All seven predictive equations currently utilize the SWCC or its components. Some equations use the air-entry value (AEV); information in the shear strength prediction equations of some models.

The SWCC information for every set of shear strength data is shown in Appendix A. The method of determination is listed with the corresponding curve and described with the soil summary in Chapter 5. A curve is fit to the data to allow interpolation between the measured data points. The Fredlund and Xing equation (1994) was chosen to generate a curve to best fit measured data. This equation uses three fitting parameters (*a, m and n*) and the residual suction. Microsoft solver was used to fit the equation to the measured data using the square of the difference. The fitting parameters for the equation have meaning with respect to different aspects of the curve. However, the fitting parameters are merely used to produce a best fit in this instance. The curve fit to the data is shown with the SWCC in Appendix A.

6.2.7 Air-Entry Value

The AEV can be determined from the shear strength data or the SWCC. In this thesis, the SWCC determined with minimal confining pressure was used for all soils. The AEV can be determined from the shear strength data as the interface between the linear and non-linear segments of the curve. In some instances, the collapsing phenomenon at high shear strength that was discussed in section 6.1 made the determination of the AEV challenging. A shortage of measured shear strength data points left large gaps where the shear strength could not be determined.

The AEV can also be determined from the SWCC where the soil begins to desaturate. However, it is not always possible to reliably measure. Clays that desaturate slowly pose a significant challenge as it is difficult to pinpoint when the soil begins to desaturate. The AEV is at the low end of the logarithmic scale (ie. 1-300 kPa) which makes a more exact value easier to find.

There is a difference in the AEV determined using the SWCC and the shear strength data. The variation is illustrated in Figure 6.4. Figure 6.4a shows the A strong correlation in the AEV determined from the shear data and the SWCC. This may be influenced by the lack of confining pressure on the shear strength samples. Alternately, the AEV in Figure 6.4b is 57 kPa when determined from the shear strength data compared to the 25 kPa when determined from the SWCC. The AEV has been found to be related to the net normal stress of a soil (Rassam and Williams, 1999; Lee et al, 2005). A summary of the AEV determined from the shear strength data and the respective SWCC is summarized in Table 6.8. When it was possible to use the AEV determined from the shear strength

data, that AEV was used. When it was not possible to determine the AEV from shear strength data, the AEV from the SWCC was used.

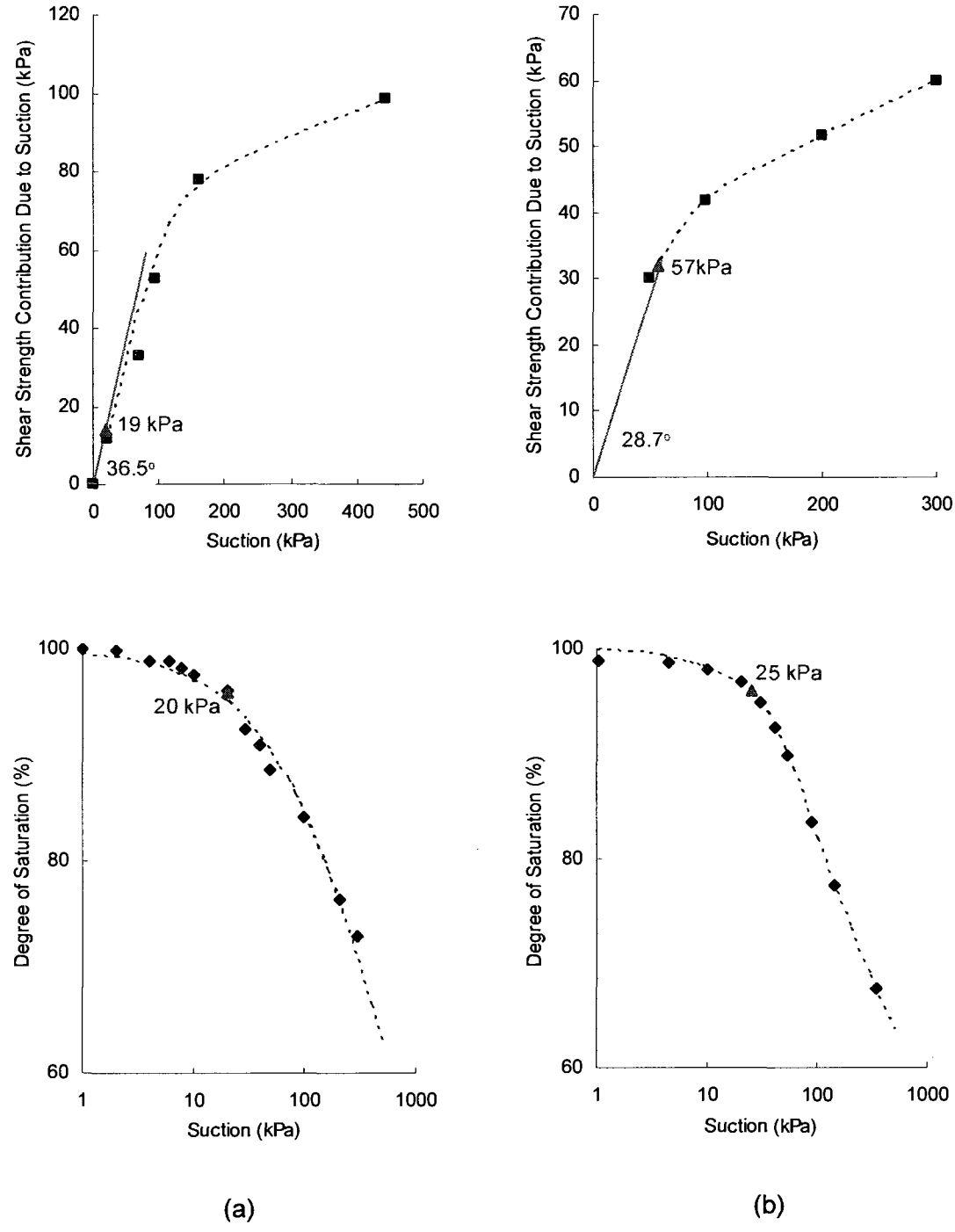

Figure 6.4. Differences between AEV determined from shear strength data and SWCC. (a) A similar value is determined from the two curves (from Vanapalli et al, 1999); (b) different values are determined from the shear strength curves and SWCC. (Bao et al, 1998)

Table 6.8. Summary of AEV determined from the shear strength data and the SWCC.

No.	Soil	Air Entry Value (AEV)	
		From shear strength data	From SWRC
1a	Red silty clay	100	100
1b		166	
1c		300	
2	Madrid gray clay	97	30
3	Madrid clay sand	47	100
3		40	
4a	Indian Head Till	76	40
4b		26	
4c		36	
5	Botkin Silt	19	20
6a	LD Dhanauri clay	61	70
6b		61	
6c		57	
6d		37	
6e	HD Dhaunari clay	26	5
6f		70	
6g		36	
6h		44	
7a	Weathered granite	6	3
7b		5	
7c		2	
7d		3	
8a	Jurong soil	65	100
8b		45	
8c		150	
9	Bao expansive undisturbed	16	30
10	Bao expansive natural	57	25
11	*Granitic soil*	-	-
12	SJ10a	*a*	80
13	SJ10b	150	50
14	SJ1	*a*	142
15a	Tailings (50 m)	*a*	3
15b		*a*	
15c		*a*	
16a	Tailings (150 m)	20	6
16b		20	
16c		20	6
17a	Röhm laterite	*a*	2
17b		*a*	
17c		*a*	
18	Serro do Mar soil	5	b
19	Adams soil	13	2
20	Frankston Fine	0	10
21	Medium Frankston	1	8
22	Graded Frankston	0	9
23	Brown sand	0	8
24a	Copper tailings	10	20
24b		12	
24c		13	
24d		15	
25a	AV colluvium	0	2
25b		0	
25c		11	
25d		*a*	
25e		*a*	
25f		*a*	
25g		*a*	
25h		*a*	
25i		*a*	
26a	RO colluvium	17	3
26b		22	
26c		23	
26d		*a*	
26e		*a*	
26f		*a*	
26g		*a*	
27a	CRDB silt	120	200
27b		20	
27c		37	
27d		16	
27e		20	

a Shear strength data exists above the ϕ' line

b Difficult to determine AEV from SWRC

c Shear data forms concave shape

Table 6.8. ***continued***

No.	Soil	Air Entry Value	
		From shear strength data	From SWRC
28a	Oloo Botkin silt	6	22
28b		13	
28c		8	
29a	Oloo Indian Head till	10	25
29b		30	
29c		30	
30	Nanyang expansive	64	50
31a	Futai tropical (1 m)	70	1
31b		*a*	
31c		*a*	
32a	Futai tropical (5 m)	*a*	300
32b		*a*	
32c		*a*	
32d		*a*	
33a	C02	7	20
33b		12	
34a	C11	16	10
34b		11	
35a	C20	18	3
35b		1	
36a	C30	28	5
36b		30	
37a	Recife clay	11	18
37b		11	
37c		13	
38a	Perreira sand	*c*	4
38b		*c*	
38c		*c*	
39	Ningxia soil	a	20
40	Zhan natural soil	52	*b*
41	Zhan compacted soi	47	25
42a	KL residual	*a*	50
42b		*a*	
42c		*a*	
42d		*a*	
43	Mature residual	-	-
44a	Nishimura silt	a	3
44b		a	
44c		a	
44d		a	
44e		c	
45	Kiunyu gravel	83	100
46a	Jossigny silt	*a*	10
46b		*a*	
46c		*a*	

a Shear strength data exists above the ϕ' line

b Difficult to determine AEV from SWRC

c Shear data forms concave shape

6.2.8 Volume Change

The current available empirical and semi-empirical shear strength equations do not address the influence of volume change of the sample. The influence of volume change is explained using the data collected from Tarantino and Tombolato (2005) (Figure 6.5). The figure illustrates the change in soil specimens when the water content is held constant and the normal stress is increased. Soil specimens of Speswhite kaolin were prepared to different void ratios: 1.4 and 1.2. The sample with a void ratio of 1.4 had an initial suction of 831 kPa. Increasing the net normal stress to 900 kPa resulted in the void ratio decreasing to 1.0 and the suction increasing to 700 kPa. A second specimen was prepared with a net normal stress of 0 kPa, a void ratio of 1.2 and an initial suction of

458 kPa. Applying a 900 kPa net normal stress resulted in a decrease in the void ratio to 0.8 and the suction increased to 340 kPa. The soils prepared to different initial void ratios but when the same net normal stress was applied to the sample, a significant change in void ratio occurred and a resulting change in suction. It is interesting to note that the magnitude of change of the void ratio for each of the two samples is the same.

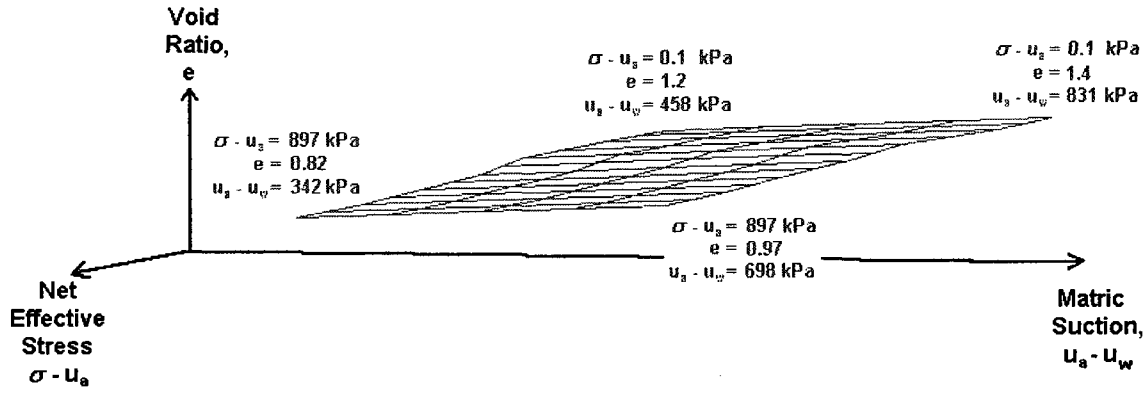

Figure 6.5. Relationship between effective stress, void ratio and matric suction under constant water content. (generated from data taken from Tarantino and Tombolato, 2005)

Volume change is considered negligible during the determination of the SWCC and it is not highlighted during the measurement of the shear strength, yet volume change influences the shear strength and suction of the unsaturated soils.

6.3 Analysis of Shear Strength Prediction Equations

The seven equations were used against the 130 data sets representing 52 different soils. The resulting fits are graphically illustrated in Appendix C. The percentage of acceptable fits ranged from 26.8% to 92.9% without using the average 10% deviation guideline. An acceptable fit was defined as having 50% or more of the data points falling within 10% of the shear strength (saturated + unsaturated). An exception to this limit was made when the shear strength was less than 50 kPa, then a flat value of ±5 kPa was applied. The average deviation of all points was used to indicate a similarity in shape to the measured data. The percentage of acceptable fits ranged from 26.0% to 81.9% when the average 10% deviation guideline is applied.

It is apparent that there is not one empirical equation that can be applied to fit all of the measured data. It is interesting to note that 7.7% of the data sets could not be fit by any one of the seven equations. Although the seven equations provide an acceptable fit for

79% of all data sets, there is no set pattern for any of the soils with respect to fitting different soil types.

The equations were examined with regard to the soils that were fit by the equations (Tables 6.11-6.16). The soils were summarized using the type of soil, method of compaction, method of testing, and soil properties. There was no discernable pattern emerged from the data.

The semi-empirical equation proposed by Vilar (2006) was to use the shear strength contribution due to suction of one air-dried sample as the sample to provide the ultimate cohesion value in the equation. Alternately, the investigator provided a theoretical basis to use one measured point at the maximum suction as the sample to provide the value of c_{ult}. The range of suctions used in this thesis was from 0~500 kPa. Hence the largest measured suction for the range from 0-500 kPa was used as the c_{ult} value to determine the fitting parameter, *b*. The result was a large number of fits to the measured data – more than any strictly empirical relationship. Moreover, even the soils that did not have an acceptable fit had a moderately conservative unsaturated shear strength curve.

Table 6.9. Summary of results of applying equations to data sets from the 52 soils (130 data sets).

	Limit based on shear strength contribution due to suction		Limit based on shear strength (saturated + unsaturated shear)	
Equation Number	**Number of Acceptable Fits**	**Percentage (%)**	**Number of Acceptable Fits**	**Percentage (%)**
Equation 3-10 *Lytton, 1995*	14	10.8	44	34.6
Equation 3-11 *Öberg and Sallfors, 1997*	32	24.6	66	52.0
Equation 3-13 *Vanapalli, Fredlund, Pufahl and Clifton, 1996*	27	20.8	61	48.0
Equation 3-25 *Khalili and Khabbaz, 1998*	34	26.2	70	55.1
Equation 3-49 *Aubeny and Lytton, 2003*	18	13.8	46	36.2
Equation 3-64 *Tekinsoy, Kayayadelen, Keskin and Söylemez, 2006*	14	10.8	51	40.2
Equation 3-73 *Vilar, 2006*	80	61.5	118	92.9
No Fit *(number of data sets that are not fit by any equation)*	64	49.2	10	7.7

Table 6.10. Summary of results of applying equations to data sets from the 52 soils Including the 10% deviation.

	Limit based on shear strength contribution due to suction		Limit based on shear strength (saturated + unsaturated shear)	
Equation Number	**Number of Acceptable Fits**	**Percentage (%)**	**Number of Acceptable Fits**	**Percentage (%)**
Equation 3-10 *Lytton, 1995*	12	9.2	33	26.0
Equation 3-11 *Öberg and Sallfors, 1995*	23	17.7	46	36.2
Equation 3-13 *Vanapalli, Fredlund, Pufahl and Clifton, 1996*	23	17.7	48	37.8
Equation 3-25 *Khalili and Khabbaz, 1998*	33	25.4	61	48.0
Equation 3-49 *Aubeny and Lytton, 2003*	15	11.5	33	26.0
Equation 3-64 *Tekinsoy, Kayayadelen, Keskin and Söylemez, 2006*	11	8.5	34	26.8
Equation 3-73 *Vilar, 2006*	74	56.9	104	80.0
No Fit *(number of data sets that are not fit by any equation)*	69	53.1	23	17.8

Table 6.11. Characteristics of soils that are fit by equation 3-10 (Total=33).

		Number of Soils	Percentage
Soil Type	Aeolian	0	0.0
	Loess	8	24.2
	Commercial soil	3	9.1
	Expansive	2	6.1
	Man-made	0	0.0
	Residual	11	33.3
	Tailings	2	6.1
	Other	9	27.3
Soil Classification	Lean clay (CL)	7	21.2
	Fat clay (CH)	1	3.0
	Lean silt (ML)	5	15.2
	Heavy silt (MH)	11	33.3
	Sand	9	27.3
Test Type	Modified direct shear test	14	42.4
	Modified triaxial test	19	57.6
	Unconfined compression test	0	0.0
Method of Compaction	Static compaction	17	51.5
	Undisturbed	14	42.4
	Slurry preparation	2	6.1
Soil Characteristics	Sand (%)	0-89	
	Clay (%)	0-58	
	Liquid limit, w_L	0-74	
	Plasticity index, I_p	0-33	

Table 6.12. Characteristics of soils that are fit by equation 3-11 (Total = 46).

		Number of Soils	Percentage
Soil Type	Aeolian	0	0.0
	Loess	7	15.2
	Commercial soil	2	4.3
	Expansive	2	4.3
	Man-made	3	6.5
	Residual	14	30.4
	Tailings	5	10.9
	Other	13	28.3
Soil Classification	Lean clay (CL)	23	50.0
	Fat clay (CH)	1	2.2
	Lean silt (ML)	4	8.7
	Heavy silt (MH)	8	17.4
	Sand	10	21.7
Test Type	Modified direct shear test	11	23.9
	Modified triaxial test	35	76.1
	Unconfined compression test	0	0.0
Method of Compaction	Static compaction	28	60.9
	Undisturbed	13	28.3
	Slurry preparation	5	10.9
Soil Characteristics	Sand (%)	0-89	
	Clay (%)	0-58	
	Liquid limit, w_L	0-74	
	Plasticity index, I_p	0-32	

Table 6.13. Characteristics of soils that are fit by equation 3-13 (Total =48).

		Number of Soils	Percentage
Soil Type	Aeolian	0	0.0
	Loess	7	14.6
	Commercial soil	1	2.1
	Expansive	2	4.2
	Man-made	5	10.4
	Residual	13	27.1
	Tailings	4	8.3
	Other	16	33.3
Soil Classification	Lean clay (CL)	18	37.5
	Fat clay (CH)	1	2.1
	Lean silt (ML)	4	8.3
	Heavy silt (MH)	11	22.9
	Sand	14	29.2
Test Type	Modified direct shear test	16	33.3
	Modified triaxial test	31	64.6
	Unconfined compression test	1	2.1
Method of Compaction	Static compaction	24	50.0
	Undisturbed	17	35.4
	Slurry preparation	7	14.6
Soil Characteristics	Sand (%)	1-89	
	Clay (%)	0-58	
	Liquid limit, w_L	0-74	
	Plasticity index, I_p	0-35	

Table 6.14. Characteristics of soils that are fit by equation 3-25 (Total = 61).

		Number of Soils	Percentage
Soil Type	Aeolian	0	0.0
	Loess	7	11.5
	Commercial soil	4	6.6
	Expansive	2	3.3
	Man-made	1	1.6
	Residual	19	31.1
	Tailings	7	11.5
	Other	21	34.4
Soil Classification	Lean clay (CL)	18	29.5
	Fat clay (CH)	1	1.6
	Lean silt (ML)	7	11.5
	Heavy silt (MH)	14	23.0
	Sand	18	29.5
Test Type	Modified direct shear test	23	37.7
	Modified triaxial test	37	60.7
	Unconfined compression test	1	1.6
Method of Compaction	Static compaction	36	59.0
	Undisturbed	18	29.5
	Slurry preparation	7	11.5
Soil Characteristics	Sand (%)	0-89	
	Clay (%)	0-58+	
	Liquid limit, w_L	0-84	
	Plasticity index, I_p	0-38	

Table 6.15. Characteristics of soils that are fit by equation 3-48 (Total=33).

		Number of Soils	Percentage
Soil Type	Aeolian	0	0.0
	Loess	6	18.2
	Commercial soil	3	9.1
	Expansive	2	6.1
	Man-made	0	0.0
	Residual	11	33.3
	Tailings	2	6.1
	Other	9	27.3
Soil Classification	Lean clay (CL)	8	24.2
	Fat clay (CH)	1	3.0
	Lean silt (ML)	5	15.2
	Heavy silt (MH)	11	33.3
	Sand	8	24.2
Test Type	Modified direct shear test	13	39.4
	Modified triaxial test	20	60.6
	Unconfined compression test	0	0.0
Method of Compaction	Static compaction	16	48.5
	Undisturbed	15	45.5
	Slurry preparation	2	6.1
Soil Characteristics	Sand (%)	0-89	
	Clay (%)	0-58	
	Liquid limit, w_L	0-74	
	Plasticity index, I_p	0-32	

Table 6.16. Characteristics of soils that are fit by equation 3-64 (Total=34).

		Number of Soils	Percentage
Soil Type	Aeolian	0	0.0
	Loess	0	0.0
	Commercial soil	0	0.0
	Expansive	2	5.9
	Man-made	4	11.8
	Residual	10	29.4
	Tailings	7	20.6
	Other	11	32.4
Soil Classification	Lean clay (CL)	16	47.1
	Fat clay (CH)	1	2.9
	Lean silt (ML)	0	0.0
	Heavy silt (MH)	6	17.6
	Sand	11	32.4
Test Type	Modified direct shear test	7	20.6
	Modified triaxial test	27	79.4
	Unconfined compression test	0	0.0
Method of Compaction	Static compaction	19	55.9
	Undisturbed	7	20.6
	Slurry preparation	8	23.5
Soil Characteristics	Sand (%)	5-88	
	Clay (%)	0-58	
	Liquid limit, w_L	0-74	
	Plasticity index, I_p	0-33	

Table 6.17. Characteristics of soils that are NOT fit by equation 3-73 (Total = 23).

		Number of Soils	Percentage
Soil Type	Aeolian	3	13.0
	Loess	0	0.0
	Commercial soil	0	0.0
	Expansive	0	0.0
	Man-made	1	4.3
	Residual	13	56.5
	Tailings	1	4.3
	Other	3	13.0
Soil Classification	Lean clay (CL)	9	39.1
	Fat clay (CH)	0	0.0
	Lean silt (ML)	1	4.3
	Heavy silt (MH)	7	30.4
	Sand	6	26.1
Test Type	Modified direct shear test	11	47.8
	Modified triaxial test	12	52.2
	Unconfined compression test	0	0.0
Method of Compaction	Static compaction	6	26.1
	Undisturbed	15	65.2
	Slurry preparation	2	8.7
Soil Characteristics	Sand (%)	0-59	
	Clay (%)	8-48	
	Liquid limit, w_L	0-95	
	Plasticity index, I_p	0-50	

6.4 Summary

The presently available empirical and semi-empirical shear strength equations are useful for implementing the mechanics of unsaturated soils into engineering practice. Most of the equations are able to reasonably predict the shear strength of unsaturated soils. However, none of the available equations is able to predict the shear strength of all the data available in the literature. This is because there are many parameters such as soil structure, density, stress history, compaction energy, and volume change behaviour influence the shear strength behaviour. The presently available prediction equations that use the SWCC do not take into account of all theses parameters. Also, there are still several limitations associated with the measurement techniques. Therefore, more research is necessary to further improve the presently available semi-empirical methods in the literature for predicting the shears strength of unsaturated soils.

CHAPTER 7 SUMMARY AND CONCLUSIONS

7.1 SUMMARY

Conventional soil mechanics principles are used in engineering practice assuming saturated conditions even for soils that are in anunsaturated condition. For example, several geotechnical structures such as earth dams including foundations are typically in a state of unsaturated condition in many arid and semi-arid regions for their entire design life. The use of conventional soil mechanics for soils that are in a state of unsaturated condition is not rational. There are several reasons associated with the use of conventional soil mechanics for unsaturated soils. The key reason for such a practice is the lack of a valid framework that is simple for the consulting engineers to implement the state-of-the-art understanding about the engineering behaviour of unsaturated soils into engineering practice.

Shear strength is one of the key unsaturated soil properties that are commonly used in the design of several structures such as earth dams, retaining walls, and foundations. Significant research has been undertaken during the last 20 years to better understand the shear strength behaviour of unsaturated soils. The focus of this research was mainly directed towards developing simple techniques for estimation or prediction of the shear strength of unsaturated soils.

The research field of unsaturated soils is considered as an emerging area as significant fundamental research is still in progress. This is true both with respect to understanding the concepts as well as the testing techniques. Due to this reason, some basic details related to the mechanics of unsaturated soils are provided for the reader to get acquainted with the terminology and concepts in the early chapters of the thesis. As the focus of the thesis is related to the shear strength behaviour of unsaturated soils, a detailed historical background is provided both with respect to theoretical aspects and as well as the testing procedures. The evolution of shear strength equations used for the interpretation is chronologically summarized collecting information from the literature. The proposed shear strength equations for interpretation were developed based on time consuming experimental studies. The determination of the shear strength of unsaturated soils using laboratory experiments needs highly technical personnel and also expensive testing equipment. Due to this reason, several empirical or semi-empirical relationships

have been proposed in the literature to predict the shear strength of unsaturated soils. To date, twenty-five equations have been proposed in the literature to interpret, estimate or predict the non-linear relationship between the shear strength and suction using different methods and philosophies. Thirteen of these equations use the soil-water characteristic curve (SWCC) as a tool in some form for the estimation or prediction of shear strength of unsaturated soil. Ten of the twenty five equations can be categorized as truly predictive equations of which six of the equations use the SWCC as a tool (Lytton, 1995; Fredlund et al, 1996; Vanapalli et al, 1996; Öberg and Sallfors, 1997; Khalili and Khabbaz, 1998; Aubeny and Lytton, 2003; Tekinsoy et al, 2004). One semi-empirical equation uses one measured point but does not rely on SWCC (Vilar, 2006). It is not a fully developed predictive equation (Eqn. 3-73) in the sense that the current equation uses one measured point to approximate the curve. However, measuring one point and approximating the shear strength curve over a range of suctions increases the likelihood that the unsaturated shear strength concepts may be adapted in industry. Measurement of one point is still a rigorous and time consuming endeavour. Most of the comparisons between the measured and predicted shear strength results are for a suction range from 0 to 500 kPa. This suction range is typically of interest for practicing engineers.

The ability of the equations to predict the shear strength of unsaturated soils was examined using the data summarized from the literature on 52 different soils. The soil properties of all these soils were also summarized in the thesis. The data set for each soil used in the analyses includes the saturated shear strength parameters (c' and ϕ') and the SWCC. Other information about the testing techniques, equipment used and the testing conditions were also summarized. Comparisons between the measured and predicted shear strength are also provided. These comparisons are provided as relationship between the shear strength contribution due to suction and suction. The shear strength contribution due to suction is calculated by removing the saturated shear strength from the measured shear strength of unsaturated soil.

The 52 soils used in the analyses were classified using the Unified Soil Classification system. The percentage of sand, liquid limit and plastic limit information is also summarized. The soils were also grouped by particle size using the methodology set out by Öberg and Sallfors (1995). A majority of the soils can be classified as silts and sands and only a handful of these soils tested were clay using this methodology.

All seven equations used for predicting the shear strength of unsaturated soils use the SWCC or some information derived from the SWCC. The Fredlund and Xing (1994) equation was used for providing a best-fit curve with the measured data points. The six predictive equations are applied to each of the 130 data sets and a successful prediction is quantitatively assessed. Each of the equations is able to successfully predict the unsaturated shear strength of some of the soils; however, approximately 56.5% of the soils were not able to be successfully predicted by using any of the seven prediction equations. The studies summarized in this thesis highlight some of the limitations of the presently available prediction equations in the literature.

7.2 CONCLUSIONS

Seven predictive equations were tested using data extracted from published works. The seven equations (Table 7.1) are summarized from chapter 3. Four equations (3-10, 3-11, 3-13, and 3-48) use the SWCC as a part of the prediction. Two equations function independently of the SWCC. In addition, one equation (3-13) uses a fitting parameter, κ, which is determined from a relationship based on the plasticity of the soil.

Table 7.1. Summary of equations to describe the shear strength behaviour of unsaturated soils.

$\tau_{us} = (u_a - u_w) \cdot \theta \cdot \tan\phi'$ *Lytton, 1995*	Formulated for "moist" soils or soils beyond the range of saturation.	3-10
$\tau_{us} = S \cdot (u_a - u_w) \cdot \tan\phi'$ *Öberg and Sallfors, 1995*	Proposed for use on silts and sands.	3-11
$\tau_{us} = (u_a - u_w)(\Theta^{\kappa})(\tan\phi')$ *Vanapalli, Fredlund, Pufahl and Clifton, 1996*	Formulated for the entire range of suction	3-13
$\tau_{us} = \chi \cdot (u_a - u_w) \cdot \tan\phi'$ $\chi = \left[\frac{(u_a - u_w)}{(u_a - u_w)_b}\right]^{\eta}$ *Khalili and Khabbaz, 1998*	Used for predicting the shear beyond the air-entry value.	3-25
$\tau_{us} = f_1 \cdot (u_a - u_w) \cdot \theta \cdot \tan\phi'$ *Aubeny and Lytton, 2003*	Formulated for "moist" soils or soils beyond the range of saturation.	3-48
$\tau_{us} = \tan\phi'[(u_a - u_w)_b + p_{at}] \cdot \ln\left[\frac{(u_a - u_w) + p_{at}}{p_{at}}\right]$ *Tekinsoy, Kayayadelen, Keskin and Söylemez, 2006*	Most suitable for fine-grained soils.	3-64
$\tau_{us} = \frac{(u_a - u_w)}{\frac{1}{\tan\phi'} + \left(\frac{1}{\tau_{us-max}} - \frac{1}{(u_a - u_w)_{max} \cdot \tan\phi'}\right)}$ *Vilar, 2006*	Uses one measured shear strength point in predicting the shear strength.	3-73

A total of 130 data sets of shear strength results measured on fifty-two different soils from the literature were examined in this thesis (Table 7.2). Predictive equationsEquation 3-25 (Khalili and Khabbaz, 1998) and Equation 3-11 (Oberg and Sallfors, 1997) provided the best results for all sets of data. Equation 3-12 (Fredlund et al, 1996 and Vanapalli et al, 1996) also had a similar result. These equations had success rates between 48% and 55%. The semi empirical equation (Eqn, 3-73) had an extremely high success rate with 93% success. However, it is important to note that the technique was fit based on one measured point. Almost 8% of the data sets could not be fit by any of the seven equations.

Table 7.2. Summary of equations limitations.

Equation Number	Percentage (%)
Equation 3-10 *Lytton, 1995*	34.6
Equation 3-11 *Öberg and Sallfors, 1995*	52.0
Equation 3-13 *Fredlund, Xing, Fredlund and Barbour, 1996* *Vanapalli, Fredlund, Pufahl and Clifton, 1996*	48.0
Equation 3-25 *Khalili and Khabbaz, 1998*	55.1
Equation 3-48 *Aubeny and Lytton, 2003*	36.2
Equation 3-64 *Tekinsoy, Kayayadelen, Keskin and Söylemez, 2006*	40.2
Equation 3-73 *Vilar, 2006*	92.9
No Fit (number of data sets that are not fit by any equation)	7.7

Equations 3-10 and Equations 3-48 are defined by the authors for use on soils in a moist condition and beyond the range of saturation (Table 7.1). The data used in this thesis to test these equations is up to and just beyond the saturation of the soil, so a low result for these equations is not unexpected. The materials that were successfully predicted by Equations 3-10 were sands, silts and a couple of lean clays with a plasticity index just above the borderline between sands and clays.

Equation 3-11 (Öberg and Sallfors, 1997) was proposed for use on sands and silts. The investigators define sands and silts according to the size of the particles. The equation predicted the unsaturated shear strength of the largest portion of the data sets. The data that had successful predictions had large percentages of silt and sand sized particles. The USCS Classification for most includes sands and silts and some clay. All

clays were classified as low plasticity clays and almost all of these clays (except soil 6) had large percentages of sand.

Equation 3-13 (Vanapalli et al, 1996) was also successfully predicted a higher number of unsaturated shear strengths of the data sets. The soils that were successfully predicted by this equation were sands and silts and some clays where the percentage of silts and sand sized particles is greater than 70%. Equation 3-25 (Khalili and Khabbaz, 1998) also predicted the data of sands and silts and clays with high percentages of silt and sand-sized particles. The particle sizes of one soils (Soil 1) is not known but it is likely to have high quantity of silt based on the liquid limit and plastic limit.

The measured data used in this thesis was published over a large range of years. Although valuable, there are limitations to the published data. Work presented by Infante Sedano (2006) highlighted some of the complex issues encountered during testing and emphasized the need for careful experimental work in the complex field of unsaturated soil. This thesis both explained and portrayed problems in measuring water content of the soil including regular flushing of the system, diffused air, condensation and evaporation in the testing system.

Limited data points and limited soils make further assessment of equations challenging. The data is valuable to examine the trends in unsaturated trends shear strength and to assess the different soils and preparation methods available. Recent developments emphasize the importance of accuracy during testing. It is important to assess the soils on their unsaturated shear strength behaviour and eliminate differences in testing method, preparation method and to measure the change in water content accurately.

7.3 SUGGESTION FOR FURTHER RESEARCH

The understanding of unsaturated soil behaviour using a wide range of soils, test methods and testing procedures is the basis for future work. Further research in this field should include testing a large range of soils with a range of plasticities under controlled sample preparation, measuring diffused air and volume change.

Testing using modified direct shear and modified triaxial shear test should be performed on the same material under the same sample preparation and compaction characteristics to examine the influence of net normal stress in soils. Careful correction for diffused air, evaporation, condensation as highlighted in earlier chapters will allow a careful examination of the influence of net normal stress.

Previous work by numerous authors highlights the challenges in both testing of unsaturated soils and in the development of empirical relationships to describe the behaviour. Summarizing this work and discussing differences will allow future work in shear strength to proceed in a consistent and knowledgeable manner.

CHAPTER 8 REFERENCES

Abramento, M., and Carvalho, C.S. (1989) Geotechnical parameters for the study of slopes instabilisation at Serra do Mar-Brazilian Southeast. Proceedings of the 12th International Conference on Soil Mechanics and Foundation Engineering, Rio de Janeiro, 3: 1599–1602.

Adams, B.A. (1996) Critical state behaviour of an agricultural soil. Ph.D. Thesis. University of Saskatchewan, Saskatoon, Saskatchewan.

Aitchison, G.D., and Donald, I.B. (1956) Effective stresses in unsaturated soils. Proceedings of the 2nd Australia-New Zealand Conference on Soil Mechanics and Foundation Engineering, Christchurch, New Zealand, 192-199.

Aitchison, G.D. (1957) The strength of quasi-saturated and unsaturated soils in relation to the pressure deficiency in the pore water. Proceedings of the 4th International Conference on Soil Mechanics and Foundation Engineering, 1: 135-139.

Aitchison, G.D. (1960) Relationship of moisture stress and effective stress functions in unsaturated soils. Pore-pressure and suction in soils, Soil Mechanics and Foundation Engineering. Butterworths, 47-52.

Aitchison, G.D., and Martin, R. (1973) Membrane oedometer for complex stress-path studies in expansive clays. Proceedings of the 3rd Cold Expansive Soils, Haifa, Israel, 2: 83-88.

Aitchison, G.D. (1965) Moisture equilibrium and moisture changes in soils beneath covered areas, A Symposium In Print, G.D. Aitchison, Ed. Australia: Butterworths, 1965, 278.

Aitchison, G.D. (1967) the separate roles of the site investigation, quantification of soil properties and selection of operational environment in the determination of foundation design on expansive soils. Proceedings of the 3rd Asian Reg. Conference on SMFE, 2: 72-77.

Aitchison, G.D., and Woodburn, J.A. (1969) Soil suction in foundation design. Proceedings of 7th ICSMFE, Mexico, 2: 1-8.

Al-Khafaf, S., and Hanks, R.J. (1974) Evaluation of the filter paper method for estimating soil water potential. Soil Science. 117:194–199.

Alikonis, A., Amsiejus, J., and Stragys, V. (1999) Improvement of shear box apparatus and methodology of test. Proceedings of the 12th European Conference on Soil Mechanics and Geotechnical Engineering, Amsterdam, 1053-1058.

Andersson, S. and Wiklert, P. (1972) Markfysikaliska undersökningar i odlad jord, XXIII. Om de vattenhållande egenskaperna hos svenska jordarter. Swedish University of Agricultural sciences, Uppsala, 53 p. [In Swedish]

American Society for Testing and Materials, ASTM (1997) Standard classification of soils for engineering purposes: Unified Soil Classification System (D2487-93). Annual Books of ASTM Standards. 04.08, 217–227.

Aubeny, C., and Lytton, R. (2003) Estimating strength versus location and time in high-plasticity clays. Texas Transportation Institute, College Station, Texas.

Avnir, D., and Farin, D. (1984) Molecular fractal surfaces. Nature (London), 308(15): 261–263.

Bao, C., Gong B., and Zhan, L. (1998) Properties of unsaturated soils and slope stability of expansive soils. Proceedings of the Second International Conference on Unsaturated Soils (UNSAT 98). Beijing, China. 1: 71-98.

Bishop, A.W. and Blight, G.E. (1963) Some aspects of effective stress in saturated and partly saturated soils. Géotechnique, 13(3): 177-197.

Bishop, A.W. and Donald, I.B. (1961) The experimental study of partly saturated soil in the triaxial apparatus. Proceedings of the Fifth Conference on Soil Mechanics, 1: 13-21.

Bishop, A.W., Alpan, I., Blight, G.E., and Donald, I.B. (1960) Factors controlling the strength of partly saturated cohesive soils. Proceedings of the ASCE Research Conference on Shear Strength of Cohesive Soils, Boulder, Colorado .503-532.

Bishop, A.W. (1959) The principle of effective stress. Teknick Ukeblad, 39: 859-863.

Blight, G.E. (1967) Effective stress evaluation for unsaturated soils. Journal of Soil Mechanics and Foundations Division, ASCE, No. SM2, 125-148.

Bonala, M.V.S., and Reddi, L.N. (1999) Fractal representation of soil cohesion. Journal of Geotechnical Geoenvironmental Engineering, 125(10): 901-904.

Brackley, I.J.A. (1975) Swell pressure and free swell in compacted clay. Proceedings of the 3rd I.C.E.S., Haifa, Israel, 1: 169-176.

Brooks, R. H., and Corey, A. T. (1964) Hydraulic properties of porous media. Hydrology paper number 3. Colorado State University, Fort Collins.

Brutsaert, W. (1966) Probability laws for pore size distributions. Journal of Soil Science, 101: 85-92.

Buckingham, E. (1907) Studies on the movement of soil moisture. U.S. Department of Agriculture Bureau of Soils, Bulletin 38.

Burland, J.B. (1964) Effective stresses in partly saturated soils. Discussion of 'Some aspects of effective stress in saturated and partly saturated soils' by Blight, G.E. and Bishop, A.W. Géotechnique, 14: 65–68.

Burland, J.B. (1965) Some aspects of the mechanical behaviour of partly saturated soils. In Moisture Equilibrium and Moisture Changes in Soils Beneath Covered Areas. Butterworths: Sydney; 270–278.

Caruso, M. and Tarantino, A. (2004) Technical Note: A shearbox for testing unsaturated soils at medium to high degrees of saturation. Géotechnique, 54(4): 281-284.

Croney, D., and Coleman, J. (1961) Pore pressure and suction in soil. Proceedings of the Conference on Pore Pressure and Suction in Soils, Butterworths, London. 31-37.

Croney, D., Coleman, J.D., and Black, W.P.M. (1958) Movement and distribution of water in relation to highway design and performance. Water and its conduction in soils. Highway Research Board Special Report 40, US Highway Reasearch Board. Washington, D.C. 226-252.

Cui, Y.J., and Delage, P. (1993) On the elasto-plastic behaviour of an unsaturated silt. Unsaturated Soils, ASCE Geotechnical Special Publication No 39, 115-126.

Cunningham, M.R., Ridley, A.M., Dineen, K., and Burland, J.B. (2003) The mechanical behaviour of a reconstituted silty clay. Géotechnique, 53(2): 183-194.

de Campos, T.M.P., and Carrillo, C.W. (1995) Direct shear testing on an unsaturated soil, Proceedings of the First International Conference on Unsaturated Soils (UNSAT 95), 1: 31-38.

Donald, I.B. (1956) Shear strength measurements in unsaturated non-cohesive soils with negative pore pressures. Proceedings of the 2nd Australia-New Zealand Conference on Soil Mechanics and Foundation Engineering, 200-207.

Donald, I.B. (1957) Effective stresses in unsaturated non-cohesive soils with controlled negative pore pressures. M.Eng.Sc. Thesis, University of Melbourne, Melbourne, Australia.

Donald, I.B. (1961) The mechanical properties of saturated and partly saturated soils with special reference to negative pore-water pressure, Ph.D. Thesis, Imperial College of Science and Technology, University of London, England.

Dregne, H.E. (1976) Soils of arid regions. International Centre for Arid and semi-arid Land Studies, Texas Technical University, Lubbock, Texas, USA. Elsevier Scientific Publishing Company, Amsterdam, The Netherlands.

Drumright, E.E., and Nelson, J.D. (1995) Shear strength of unsaturated tailings sand. Proceedings of the First International Conference on Unsaturated Soils, 45.

Drumright, E.E. (1989) The contribution of matric suction the shear strength of unsaturated soils, Ph.D.. Thesis. Colorado State University, Fort Collins, Colorado. 329 p.

Edelfson, D.H. and Anderson, A.B.C. (1943) Thermodynamics of soil moisture. Hilgardia, 15: 30-298.

eijkelkamp.com (2008) Schematic: tempe cell.

Environment.uwc.ac.uk (2008) Schematic: ring shear apparatus.

Ergotech.co.uk (2008) Image: true triaxial test.

Escario, V. (1980) Suction controlled penetration and shear tests. Proceedings of the 4th ASCE: International Conference on Expansive Soils, II, 781-797.

Escario, V., and Juca, J. (1989) Shear strength and deformation of partly saturated soils. Proceedings of the 12th International Conference on Soil Mechanics and Foundation Engineering, Rio de Janeiro, 2: 43-46.

Escario, V., and Saez, J. (1986) Discussion: Shear strength of soils under high suction values. Proceedings of the 9th European Conference SMFE, Dublin. 3: 1157.

Escario, V., and Saez, J. (1986) Shear strength of partly saturated soils. Géotechnique, 36(3): 452-456.

Fawcett, R.G., and Collis-George, N. (1967) A filter paper method for determining the moisture characteristic of soil. Australian Journal of Experimental Agriculture and Animal Husbandry. 7:162–167.

Feuerharmel, C, Bica, A.V.D., Gehling, W.Y.Y., and Flores, J.A. (2005) A study of the shear strength of two colluvium soils. International Symposium on Advanced Experimental Unsaturated Soil Mechanics (Experus 2005), Trento, Italy.

Feuerharmel, C., Pereira, A., Gehling, W.Y.Y., and Bica, A.V.D. (2006) Determination of the shear strength parameters of two unsaturated colluvium soils using direct shear test. Proceedings of the Fourth International Conference on Unsaturated Soils (UNSAT 06), Carefree, Arizona, 2: 1181-1190.

Folorunso, O.A., Puente, D.E., Rolston, D.E. and Pinzon, J.E. (1994) Statistical and fractal evaluation of the spacial characteristics of soil surface strength, Soil Science Society of America Journal, 58: 284-295.

Fredlund, D.G. (1975) A diffused air indicator for unsaturated soils. Canadian Geotechnical Journal. 12: 533-539.

Fredlund, D. G. (1987). Slope stability analysis incorporating the effect of soil suction. Geotechnical Engineering and Geomorphology, 113-144.

Fredlund D.G. (1995) The scope of unsaturated soil mechanics. Proceedings of the 1st International Conference on Unsaturated Soils (UNSAT 95), Paris, 3: 1155-1177.

Fredlund, D.G., and Morgenstern, N.R. (1977) Stress state variables for unsaturated soils. Journal of the Geotechnical Engineering Division, ASCE, 103(GT5): 447-466.

Fredlund, D.G., and Rahardjo, H. (1993) Soil mechanics for unsaturated soils, John Wiley & Sons, Inc., New York, 346-365.

Fredlund, D.G. and Xing, A. (1994) Equations for the soil-water characteristic curve, Canadian Geotechnical Journal, 31: 521 - 532.

Fredlund, D.G., Morgenstern, N. R., and Widger, R. A. (1978) Shear strength of unsaturated soils. Canadian Geotechnical Journal, 15(3): 313-321.

Fredlund, D.G., Rahardjo, H., and Gan, J.K. (1987) Non-linearity of strength envelope for unsaturated soils. Proceedings of 6th International Conference on Expansive Soils, New Delhi, 49-54.

Fredlund, D.G., Rahardjo, H., and Ng, T. (1993) Effect of pore-air and negative pore-water pressures on stability at the end-of-construction. Proceedings, International Conference on Dam Engineering, Johor Bahru, Malaysia, 43-51.

Fredlund, D.G., Xing, A., and Huang, S. (1994) Predicing the permeability function for unsaturated soils. Canadian Geotechncial Journal, 15(3): 313-321.

Fredlund, D.G., and Xing, A. (1994), Equations for the soil-water characteristic curve. Canadian Geotechnical Journal, 31: 521 - 532.

Fredlund, D.G., Vanapalli, S.K., Xing, A., and Pufahl, D.E. (1995) Predicting the shear strength function for unsaturated soils using the soil-water characteristic curve. Proceedings of the First International Conference on Unsaturated Soils (UNSAT 95), (1): 63.

Fredlund, D.G., Xing, A., Fredlund, M.D., and Barbour, S.L. (1996) Relationship of the unsaturated soil shear strength to the soil-water characteristic curve. Canadian Geotechnical Journal, 33(3): 440-448.

Fredlund, D.G. and Xing, A. (1994) Equations for the soil-water characteristic curve. Canadian Geotechnical Journal, 31: 521 - 532.

Fredlund, D.G., Morgenstern, N.R., and Widger, R.A. (1978) Shear strength of unsaturated soils. Canadian Geotechnical Journal, 15(3): 313-321.

Gan, J.K-M., and Fredlund, D.G. (1988) Multistage direct shear testing of unsaturated soils. Geotechnical Testing Journal, 11(2): 132-138.

Fredlund, D.G., Rahardjo, H., and Gan, J.K.-M. (1987) Non-linearity of shear strength envelope of unsaturated soils. Proceedings of 6th International Conference on Expansive Soils, New Delhi, 1: 49-54.

Futai, M.M., Almeida, M.S.S., and Lacerda, W.A. (2006) The shear strength of tropical soils in Ouro Preto, Brazil. Proceedings of the Fourth International Conference in Unsaturated Soils (UNSAT 2006), Carefree, Arizona, 2: 1200-1211.

Gan, K.J., and Fredlund, D.G. (1988) Multistage direct shear testing of unsaturated soils. Geotechnical Testing Journal, 11(2): 132-138.

Gan, J.K-M., and Fredlund, D.G. (1996) Shear strength characteristics of two saprolitic soils. Canadian Geotechnical Journal, 33: 595-609.

Gan, J.K.M., Fredlund, D.G., and Rahardjo, H. (1988) Determination of the shear strength parameters of an unsaturated soil using the direct shear test. Canadian Geotechnical Journal, 25: 500–510.

Gardner R. (1937) A method of measuring the capillary tension of the soil moisture over a wide moisture range. Soil Science, 43: 277-283

Garven, E., and Vanapalli, S.K. (2006) Evaluation of empirical procedures for predicting the shear strength of unsaturated soils. Proceedings of the Fourth International Conference on Unsaturated Soils (UNSAT 06). American Society of Civil Engineers Geotechnical Special Publication No. 147(2): 2570-2581.

Gulhati, S.K., and Satija, B.S. (1981) Shear strength of partially saturated soils. Proceedings of the 10th International Conference on Soil Mechanics and Foundation Engineering, Stockholm, 1: 609-612.

Haines, W.B. (1925) A note on the cohesion developed by capillary forces in an ideal soil. Journal of Agricultural Science, 15: 529-535.

Haines, W.B. (1927) Studies on the physical properties of soils. Journal of Agricultural Science. 17: 264-290.

Hamilton, L.W. (1939) The effects of internal hydrostatic pressure on the shearing strength of soils. Proceedings of the American Society for Testing Materials, 39: 1100-1121.

Hilf, J.W. (1956) An investigation for pore-water pressure in compacted cohesive soils. Technical Memorandum No 654, Bureau of Reclamation, US Department of the Interior, Denver, Colorado.

Ho, D.Y.F., and Fredlund, D.G. (1982) A multi-stage triaxial test for unsaturated soils. Geotechnical Testing Journal, ASTM 5(1/2): 18-25.

Ho, D.Y.F., and Fredlund, D.G. (1982) Increase in strength due to suction for two Hong Kong soils. ASCE, 263-295.

Ho, D.Y.F., and Fredlund, D.G. (1982) Strain rates for unsaturated soil shear strength testing, Proceedings fo the 7th Southeast Asian Geotechncial Conference, Hong Kong, 787-803.

Huat B. K., Ali, F.H. and Choong. F.H. (2006) Effects of loading rate on the volume change behaviour of unsaturated residual soil. The International Journal of Geotechnical and Geological Engineering, 24:1527-1544.

Infante Sedano, J.A. (2006) A modified ring shear test device for testing the hydro-mechanical behaviour of unsaturated soils. Ph.D. Thesis. University of Ottawa, Ottawa.

Jennings, J.E., and Burland, J.B. (1962) Limitations to the use of effective stresses in partially saturated soils. Géotechnique, 12(2): 125-144.

Jucá, J.F.T., Ferreira, R.N., and Bastos, E.G. (1997) Shear strength of an unsaturated expansive clay (NSAT 97). 145-150.

Khalili, N., Geiser, F., and Blight, G.E. (2004) Effective stress in unsaturated soils: Review with new evidence. International Journal of Geomechanics, 4(2): 15-26.

Khalili, N., and Khabbaz, M.H. (1998) Technical Note: A unique relationship for χ for the determination of the shear strength of unsaturated soils. Géotechnique, 48(5): 681-687.

Klute, A. (1986) Method of soil analysis, Part 1: physical and mineralogical method. Agronomy Monograph number 9, 2nd edition, 635-662.

Krahn, J. & Fredlund, D.G. (1972) On total, matric and osmotic suction. Journal of Soil Science, 114: 339-348.

Krahn, J., Fredlund, D.G., and Klassen, M.J. (1989) Effect of soil suction on slope stability at Notch Hill. Canadian Geotechnical Journal, 26(2): 103-110.

Ladd, R.S. (1978) Preparing test specimens using undercompaction. Geotechnical Testing Journal, 1(4): 16.

Lam, K.S. (1980) Strength and suction – Moisture retention of a compacted residual volcanic soil. Thesis Number GT-79-13, Asian Institute of Technology, Bangkok, Thailand.

Lee, S.J., Lee, S.R., and Kim, Y.S. (2003) An approach to estimate the unsaturated shear strength using artificial neural network and hyperbolic formulation. Computers and Geotechnics, 489-503.

Lee, I.-M., Sung, S.-G., and Cho, G.-C. (2005) Effect of stress state on the unsaturated shear strength of a weathered granite. Canadian Geotechnical Journal, 42(2): 624-631.

Likos, W. J., and Lu, N. (2004). Hysteresis of capillary stress in unsaturated granular soil. Journal of Engineering Mechanics, 130(6): 646–655.

Lu, N., and Likos, W. J. (2004) Unsaturated soil mechanics, Wiley: New York.

Lu, Z. (1992) The relationship of shear strength to swelling pressure for unsaturated soils. Chinese Journal of Geotechnical Engineering, 143: 1-8. [in Chinese].

Lytton (1995) Keynote Address: Foundations and Pavements on Unsaturated Soils, Proceedings of the First International Conference on Unsaturated Soils (UNSAT 95).

Madigan, T. (2007) The Geology of the MNRRA Corridor. The National Park Service Reference.

Mandlebrot, B.B. (1982) The fractal geometry of nature. New York: Freeman.

Maswoswe, J. (1985) Stress paths for a compacted soil during collapse due to wetting. Ph.D. Thesis. Imperial College, London, England.

Matsushi, Y., and Matsukura, Y. (2006) Cohesion of unsaturated residual soils as a function of volumetric water content. Bulletin of Engineering Geology Environment, 65: 449-455.

Matyas, E.L., and Radharkrishna, H.S. (1968) Volume change characteristics of partially saturated soils. Géotechnique, 18(4): 432-448.

MIT (1963) Engineering behaviour of partially saturated soils. Research Report, R: 63-26.

McKee, C. and Bumb, A. (1987) Flow-testing coal bed methane production wells in the presence of water and gas. SPE Formation Evaluation, December, 599-608.

McDowell, G. R., Bolton, M.D., and Robertson, D. (1996) The fractal crushing of granular materials. Journal of Methods Physical Solids, 44(12): 2079–2102.

McQueen, I.S. and Miller, R.F. (1968) Calibration and evaluation of a wide-range gravimetric method for measuring moisture stress. Soil Science, 106(3): 225-231.

Miao, L., Liu, S., and Lai, Y. (2002) Research of soil-water characteristics and shear strength features of Nanyang expansive soil. Engineering Geology, 65(4): 261-267.

Miao, L., Yin, Z., and Liu, S. (2001) Empirical function representing the shear strength of unsaturated soils. Geotechnical Testing Journal, 24(2): 220-223.

Miao, L., Liu, S., and Lai, Y. (2002) Research of soil-water characteristics and shear strength features of Nanyang expansive soil. Engineering Geology, 65(4): 261-267.

Mirata, T. (1974) The in situ wedge shear test - a new technique in soil testing. Géotechnique, 24(3), 311-332.

Mirata, T. (1991) Developments in wedge shear testing of unsaturated clays and gravels. Géotechnique , 41(1): 79-100.

Mirata, T. (1998). Manual for wedge shear testing of soils. Department of Civil Engineering, METU, 170pp.

Muñoz-Carpena, R. (2004) Field devices for monitoring soil water content. Publication #BUL343, Department of Agricultural and Biological Engineering, Florida Cooperative Extension Service, Institute of Food and Agricultural Sciences, University of Florida.

Nishimura, T., and Fredlund, D.G. (1999) Unconfined compression shear strength of an unsaturated silty soil subjected to high total suction. Proceedings of the International Symposium on Slope Stability Engineering- IS-Shikoku'99, Matsuyama, Shikoku, Japan. 757 -762.

Nishimura, T., and Fredlund, D.G. (2000) Relationship between shear strength and matric suction in an unsaturated silty soil. Asian Conference on Unsaturated Soils from Theory to Practice, Singapore. 563-568.

Nishimura, T., Fredlund, D.G., Hirabayashi, Y., and Gan, J.K.M. (1999) Total stress ratio and shear strength parameters for an unsaturated compacted soil. Proceedings of the 11th Asian Regional Conference, Seoul, Korea. 125-128.

Nishimura, T., Hirabayashi, Y., Fredlund, D.G., and Gan, J.K.M. (1999) Influence of stress history on the strength parameters of an unsaturated statically compacted soil. Canadian Geotechnical Journal, 36: 251- 261.

Öberg, A.-L. (1995) Stability of sand and silt slopes. Internal Report, Department of Geotechnical Engineering, Chalmers University of Technology, Gothenburg.

Öberg, A.L., and Sallfors, G. (1995) A rational approach to the determination of the shear strength parameters of unsaturated soils. Proceedings of the First International Conference on Unsaturated Soils (UNSAT 95), 151-158.

Öberg, A.L., and Sallfors, G. (1997) Determination of shear strength parameters of unsaturated silts and sands based on the water retention curve. Geotechnical Testing Journal, 20(1): 40-48.

Oliveira, O.M., and Marinho, F.A.M. (2003) Unsaturated shear strength behaviour of a compacted residual soil. Proceedings of the Asian Conference on Unsaturated Soils: Unsaturated Soil Geotechnical and Geoenvironmental Issues. Osaka, Japan. 237-242.

Oloo, S.Y., and Fredlund, D.G. (1996) A method for determination of *fb* for statically compacted soils. Canadian Geotechnical Journal, 33: 272-280.

Parashar, S.P., Wong, K.S, Choa, V., and Rahardjo, H. (1995) Shear strength, volume change and permeability characteristics of a compacted residual soil. Proceedings of the First International Conference on Unsaturated Soils (UNSAT 95). 165-170.

Pereira, A., Feuerharmel, C., Gehling, W.Y.Y., and Bica, A.V.D. (2005) A study on the shear strength envelope of an unsaturated colluvium soil. Proceedings of the Fourth International Conference on Unsaturated Soils (UNSAT 06), Carefree, Arizona, 2: 1191-1199.

Pereira, J.H.F., and Fredlund, D.G. (1999) Shear strength behaviour of a residual soil of gneiss compacted at metastable structure condition. Proceedings of the 11th Pan Am Conference on Soil Mechanics and Geotechnical Engineering, Iguanzu Falls, Brazil. 369-377.

Peterson, R.W. (1992) Shear strength of unsaturated soils. Proceedings of the 7th International Conference on Expansive Soils, Dallas, 2: 89-94.

Rassam, D.W., and Cook, F.J. (2002). Predicting the shear strength envelope of unsaturated soils. Geotechnical Testing Journal, 28: 215-220.

Rassam, D.W., and Williams, D.J. (1999) Bearing capacity of dessicated tailings. Journal of Geotechnical and Geoenvironmental Engineering, 125(7): 600-609.

Reis, R.M., and Vilar, O.M. (2005) Stress-strain behaviour of an unsaturated residual soil from gneiss. International Symposium on Advanced Experimental Unsaturated Soil Mechanics (Experus 2005), Trento, Italy.,423-432.

Richards, B.G. (1965) Measurement of free energy of soil moisture by the psychrometer technique using thermistors. Moisture Equilibria and Changes in Soils Beneath Covered Areas, A Symposium in Print, G.D. Aitchison, Ed., Butterworths, Australia, 39-46.

Rieu, M. and Sposito G. (1991a). Fractal fragmentation, soil porosity and soil water properties: I. Theory. Soil Science Society of America Journal, 55, 1231-1238.

Rieu, M., and Sposito, G. (1991b) Fractal fragmentation, soil porosity and soil water properties: II. Applications. Soil Science Society of America Journal, 55, 1239-1244.

Röhm, S.A, and Vilar, O.M. (1994) A influência da estruturia de um solo arenoso laterizado não saturado na sua resistência ao cisalhamento. 2^0 simpósio sobre solos não saturados, Recife, Brazil, 211-216. [in Portuguese]

Röhm, S.A., and Vilar, O.M. (1995) Shear strength of an unsaturated sandy soil. Proceedings of the First Conference on Unsaturated Soils (UNSAT 95), 1: 189-193.

Russam , K. (1958) An investigation into the soil moisture: conditions under roads in Trinidad. B.W.I Géotechnique, 8:55-71.

Satija, B.S. (1978) Shear behaviour of partly saturated soils, Ph.D. Thesis, Indian Institute of Technology, New Delhi, India.

Schick, P. (2004) Scherfestigkeit durch Kapillarität in unzementierten ungesättigten bindigen Böden, Bautechnik, 81(1): 31- 37. [in German]

Shen, Z. (1996). The problems in the present studies on mechanics for unsaturated soils. Proceedings of the Symposium on Geotechnical Aspects of Regional Soils, Nanjing. [in Chinese]

Sillers, W.S. (1997) The mathematical representation of the soil-water characteristic curve. MSc Thesis, University of Saskatchewan, Saskatoon Saskatchewan, Canada.

Sparks, A.D.W. (1963) Theoretical considerations of stress equations for partly saturated soils. Proceedings of the Third Regular Conference for Africa on Soil Mechanics, Salisbury, Rhodesia 1: 215-218.

Tarantino, A., and Tombolato, S. (2005) Coupling of hydraulic and mechanical behaviour in unsaturated compacted clay. Géotechnique, 55(4): 307-317.

Tekinsoy, M.A., Kayadelen, C., Keskin, M.S., and Soylemez, M. (2004) An equation for predicting shear strength envelope with respect to matric suction. Computers and Geotechnics, 31(7): 589-593.

Terzaghi, K (1936) The shearing resistance of saturated soils and the angle between planes of shear. Proceedings of the First International Conference on Soil Mechanics, 1: 54-56.

Terzaghi, K. (1943) Theoretical Soil Mechanics, John Wiley: New York, USA; 270–296.

Thevanayagam, S. and Nesarajah, S. (1998) Journal of Geotechnical and Geoenvironmental Engineering, 53-66.

Tindall, J.A., and Kunkel, J.R. (1999) Unsaturated Zone Hydrology for Scientists and Engineers. Prentice-Hall, Inc.:624 pp.

Toll, D.G. (1988) The behaviour of unsaturated compacted naturally occurring gravel, Ph.D. Thesis, Imperial College of Science and Technology, University of London, London, England.

Toll, D.G. (2000) Influence of fabric on the shear behaviour of unsaturated compacted soils. Advances in Unsaturated Soils: ASCE Geotechnical Special Publication No. 99: 222-234.

Toll, D.G. (1990) A framework for unsaturated soil behaviour. Géotechnique, 40(1): 31-44.

van Genuchten, M.Th., (1980) A closed-form equation for predicting the hydraulic conductivity of unsaturated soils. Soil Science Society of America Journal, 44: 892-898.

Vallejo, L.E. (1996) Fractal analysis of the fabric change in a consolidated clay. Engineering Geology (Amsterdam), 43: 281–290.

Vanapalli, S.K., and Fredlund, D.G. (2000) Comparison of different procedures to predict unsaturated soil shear strength. ASCE Geotechnical Special Publication No. 99: 195-209.

Vanapalli, S.K., Fredlund, D.G., and Pufahl, D.E. (1996a) Comparison of saturated-unsaturated shear strength and hydraulic conductivity behaviour of a compacted sandy-clay till.

Vanapalli, S.K., Fredlund, D.G., and Pufahl, D.E. (1996b) The relationship between the soil-water characteristic curve and the unsaturated shear strength of a compacted glacial till. Geotechnical Testing Journal, 19(3): 259-268.

Vanapalli, S.K., Wright, A., and Fredlund, D.G. (2000) Shear strength of two unsaturated silty soils over the suction range from 0 to 1,000,000 kPa. Proceedings of the 53rd Canadian Geotechnical Conference, Montreal, Quebec, 1161-1168.

Vanapalli, S.K. (1994) Simple test procedures and their interpretation in evaluating the shear strength of unsaturated soils. Ph.D. thesis, University of Saskatchewan, Saskatoon. 350p.

Vanapalli, S.K., Fredlund, D.G., Pufahl, D.E., and Clifton, A.W. (1996) Model for the prediction of shear strength with respect to soil suction. Canadian Geotechnical Journal, 33(3): 379-392.

Vilar, O.M. (2006) A simplified procedure to estimate the shear strength envelope of unsaturated soils. Canadian Geotechnical Journal, 43: 1088-1095.

Watabe, Y., Leroueil, S., and Le Bihan, J.-P. (2000). Influence of compaction

conditions on pore-size distribution and saturated hydraulic conductivity of a glacial till. Canadian Geotechnical Journal, 37: 1184-1194.

Wfi.co.uk (2008) Image: double-walled triaxial cell.

Williams, P.J. (1982) The surface of the Earth, an introduction to geotechnical science. Longman Inc., New York.

Wheeler S.J. (1988) The undrained shear strength of soils containing large gas bubbles. Géotechnique, 38: 399-413.

Wheeler, S.J. and Sivakumar, V. (1995). An elasto-plastic critical state framework for unsaturated soil. Géotechnique, 45(1): 35-53.

White, N.F., Duke, H.R., Sunada, D.K. and Corey, A.T. (1970) Physics of desaturation in porous materials. Journal of Irrigation and Drainage Division, ASCE, 96(IR2): 165-191.

Won, O.T., and Vanapalli, S.K. (2008) A simplified model for predicting the elasticity of unsaturated soils. Proceedings of the 8th International Congress on Advances in Civil Engineering, 15-17 September 2008, Eastern Mediterranean University, Famagusta, North Cyprus, 89-96.

Wulfsohn, D., Adams, B.A., and Fredlund, D.G. (1996) Application of unsaturated soil mechanics for agricultural conditions. Canadian Agricultural Engineering, 38(3), 173-181.

Xu, Y.F., and Sun, D.A. (2001) Determination of unsaturated shear strength using a fractal model. Fractals, 91: 51-60.

Xu, Y., and Sun, D. (2002) A fractal model for soil pores and its application to determination of water permeability, Physica A, 316 (1-4): 56-64.

Xu, Y. (1997) Mechanical properties of unsaturated expansive soils and its application in engineering, Ph. D. thesis, HoHai University, Nanjing. [in Chinese].

Xu, Y. (2004) Bearing capacity of unsaturated expansive soils. Geotechnical and Geological Engineering, 22: 611-625.

Xu, Y.F. (2004) Fractal approach to unsaturated shear strength. Journal of Geotechnical and Geoenvironmental Engineering, 130(3): 264-273.

Yu S., Ma, A., and Wang, Z. (1998) The feature of suction and hyperbola model for shear strength of unsaturated soil. Proceedings of the Second Technical Committee of International Conference on Unsaturated Soils, 1: 192-195.

Zhan, T.L.T., and Ng, C.W.W. (2006) Technical Note: Shear strength characteristics of an unsaturated expansive clay. Canadian Geotechnical Journal, 43: 751-763.

Index of Equations

APPENDICES

Review of the Empirical Equations for Predicting the Shear Strength of Unsaturated Soils

Elizabeth A. Garven

Thesis submitted to the
Faculty of Graduate and Postdoctoral Studies
In partial fulfillment of the requirements
For the MASc degree in Civil Engineering

Civil Engineering
Faculty of Engineering
University of Ottawa

APPENDICES

APPENDIX A: SOIL INFORMATION

APPENDIX B: PARTICLE SIZE DISTRIBUTIONS

APPENDIX C: MEASURED AND CALCULATED SHEAR STRENGTH VALUES

APPENDIX A

SOIL INFORMATION

Soil No. 1a

Red silty clay

Escario and Saez, 1986; Escario and Juca, 1989

Compacted Sample
Sand = 14%, Silt and Clay= 86%; Liquid Limit = 33, Plasticity Index = 13
Lean clay, CL

Shear Strength

Test Method: Modified direct shear

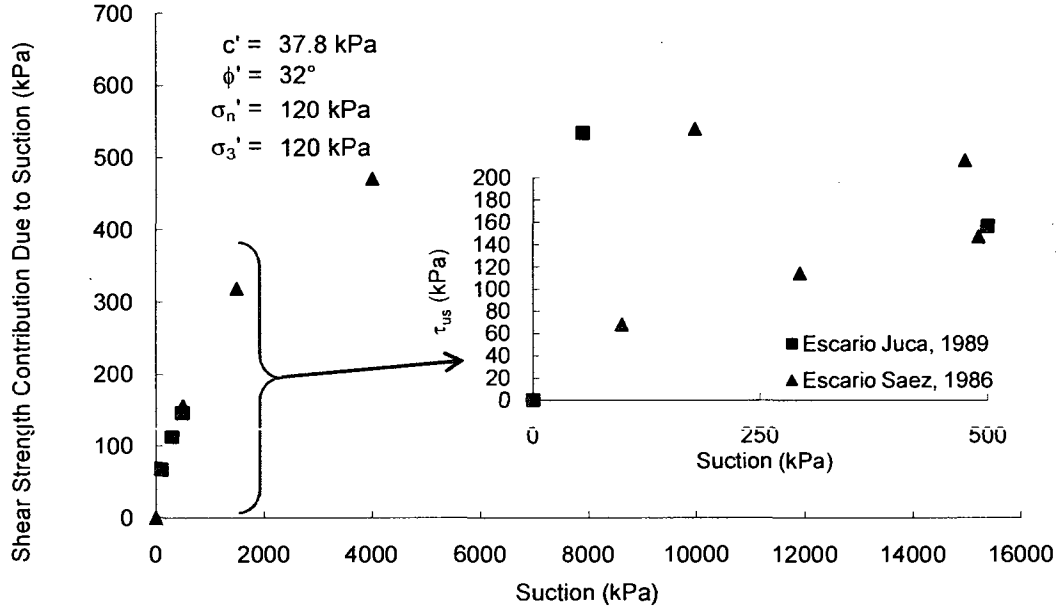

SWRC

Test Method: Pressure membrane apparatus

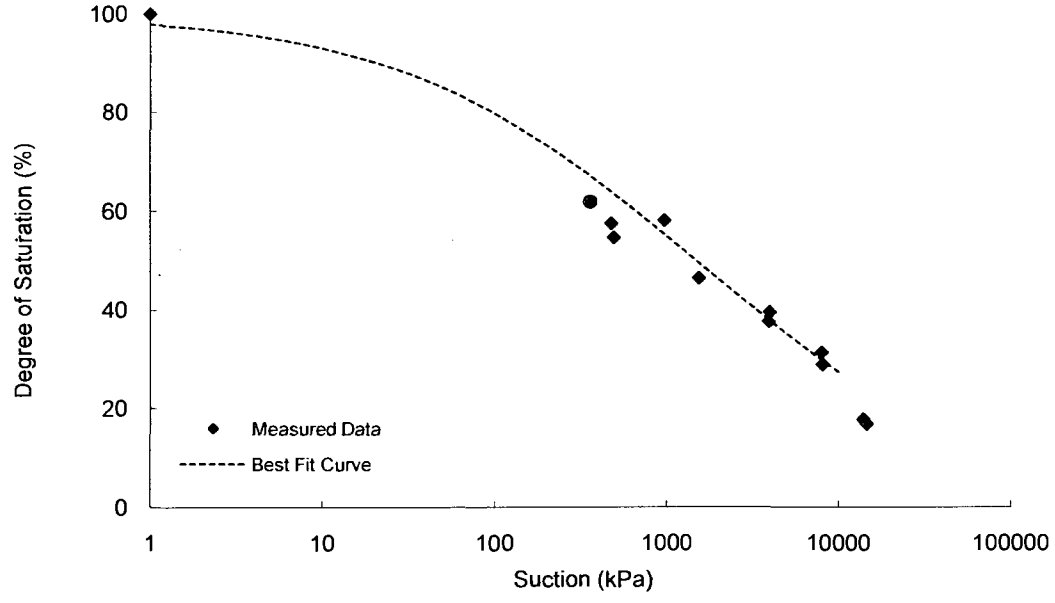

Soil No. 1b **Red silty clay**

Escario and Saez, 1986; Escario and Juca, 1989

Compacted Sample Sand = 14%, Silt and Clay= 86%; Liquid Limit = 33, Plasticity Index = 13 Lean clay, CL

Shear Strength Test Method: Modified direct shear

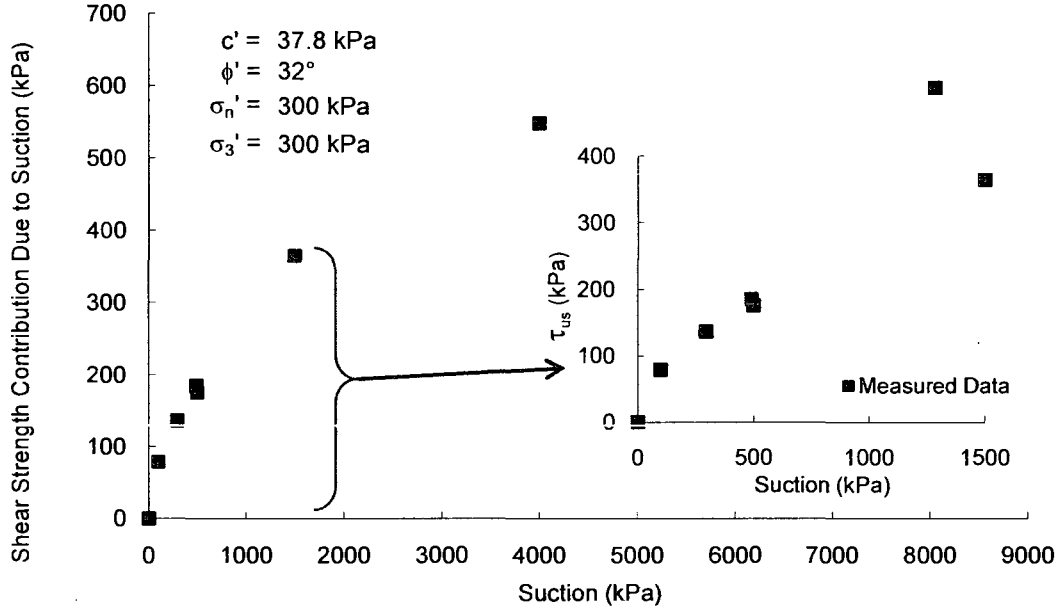

SWRC Test Method: Pressure membrane apparatus

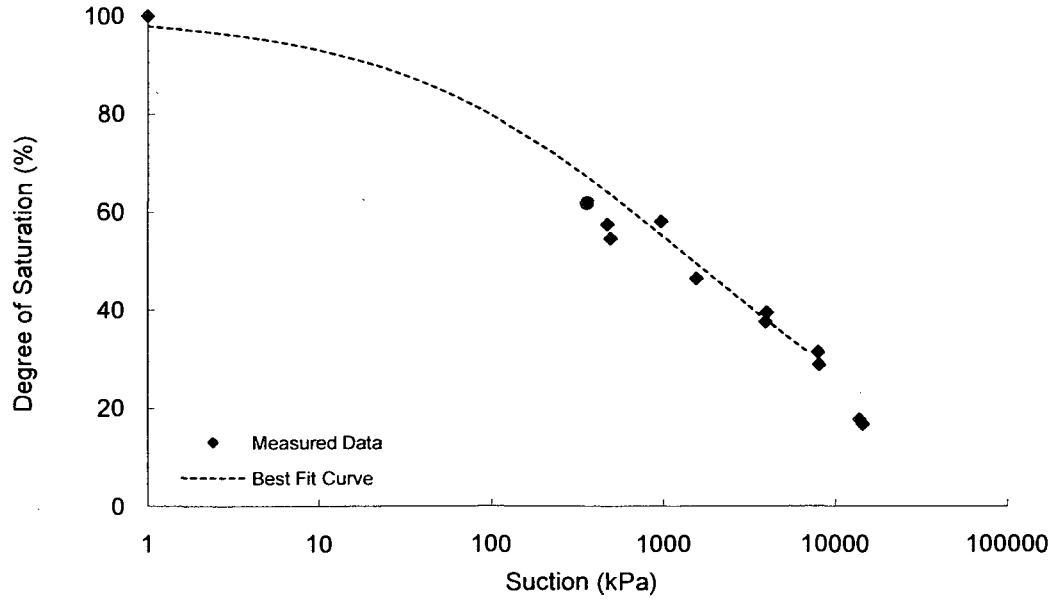

Soil No. 1c **Red silty clay**

Escario and Saez, 1986; Escario and Juca, 1989

Compacted Sample
Sand = 14%, Silt and Clay= 86%; Liquid Limit = 33, Plasticity Index = 13
Lean clay, CL

Shear Strength Test Method: Modified direct shear

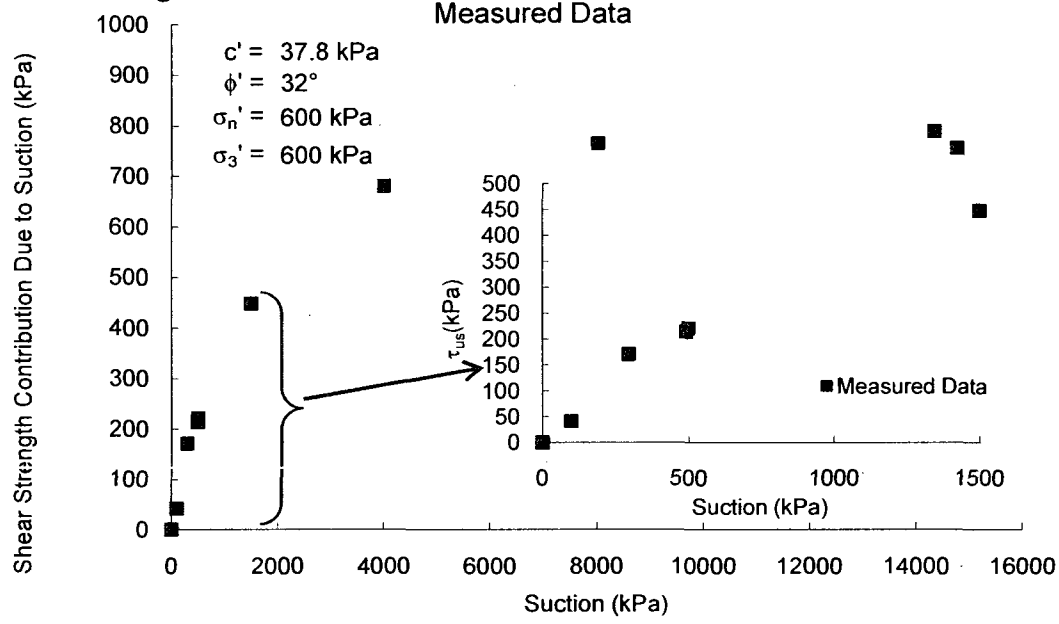

SWRC Test Method: Pressure membrane apparatus

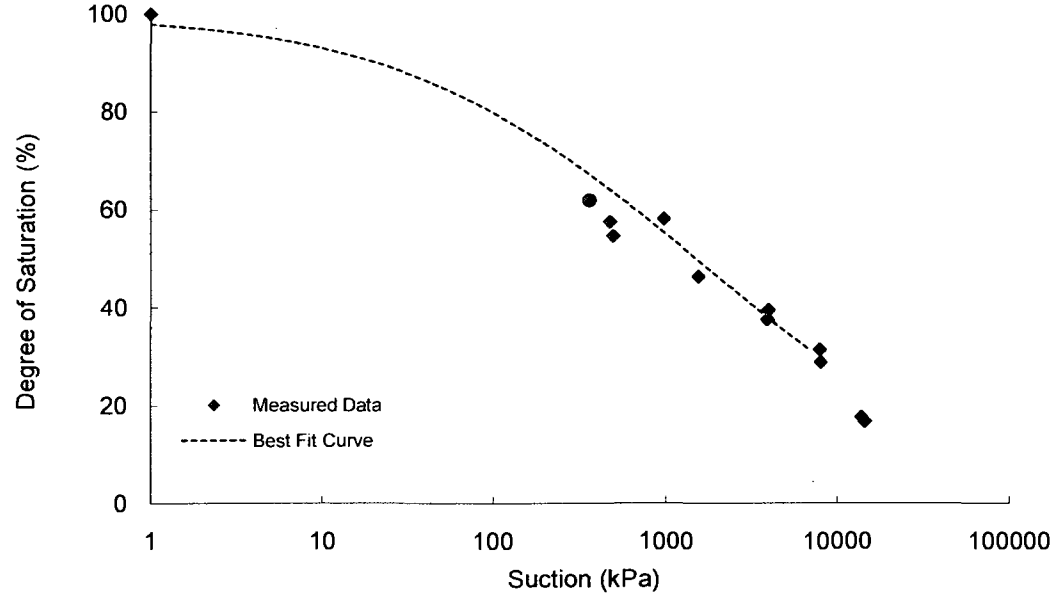

Soil No. 2

Madrid grey clay

Escario and Saez, 1986; Escario and Juca, 1989

Compacted Sample
Sand = 1%, Silt and Clay= 99%; Liquid Limit = 71, Plasticity Index = 35
Heavy silt, MH

Shear Strength

Test Method: Modified direct shear

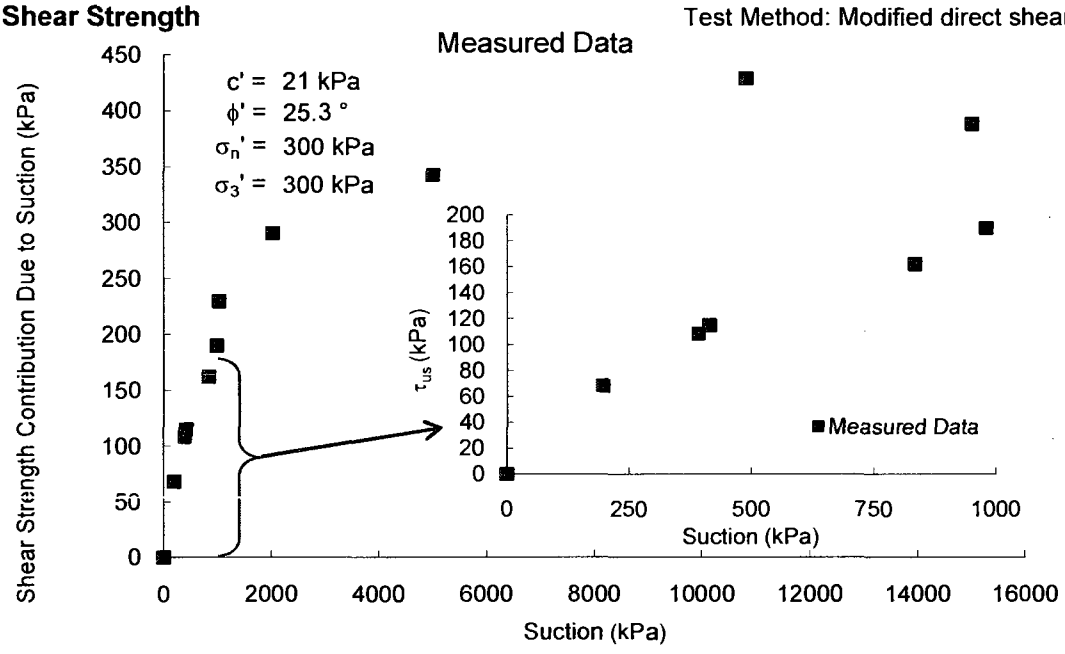

SWRC

Test Method: Pressure membrane apparatus

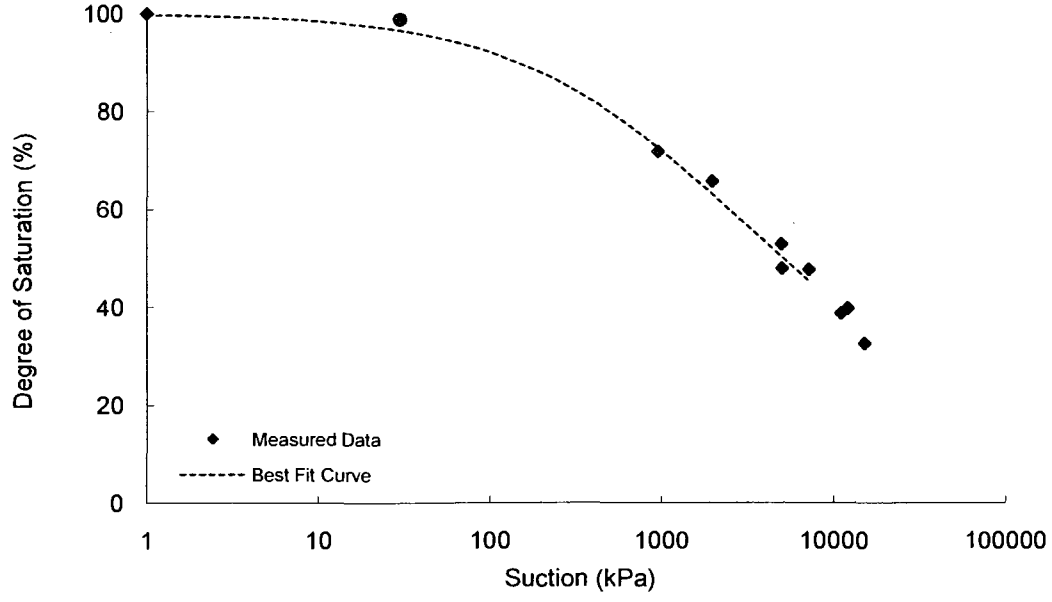

Soil No. 3a

Grey clay sand

Escario and Saez, 1986; Escario and Juca, 1989

Compacted Sample

Sand = 87%, Silt and Clay= 13%; Liquid Limit = 32, Plasticity Index = 15

Lean clay, CL

Shear Strength

Test Method: Modified direct shear

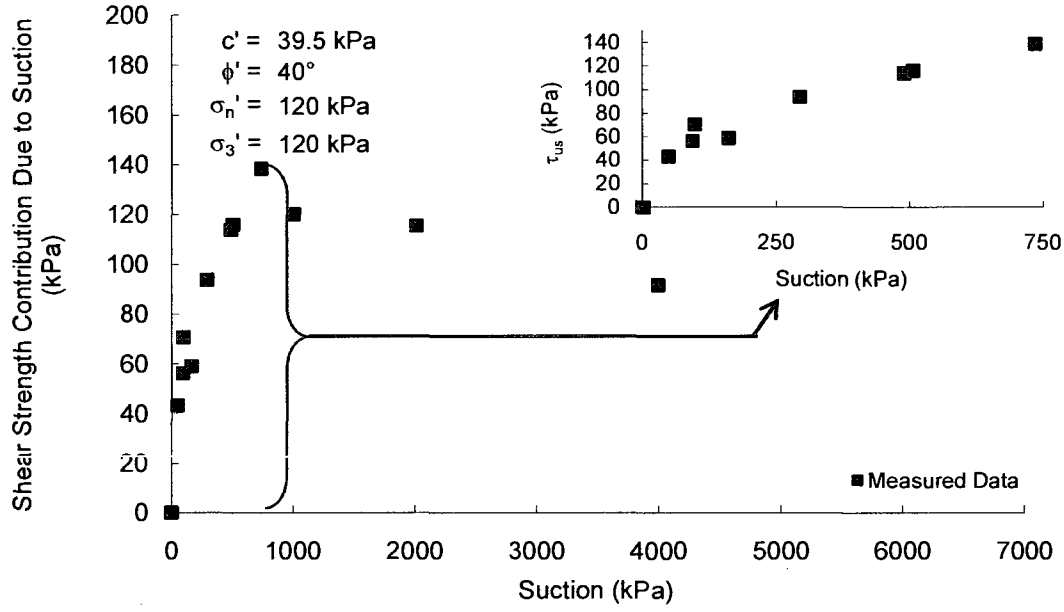

SWRC

Test Method: Pressure membrane apparatus

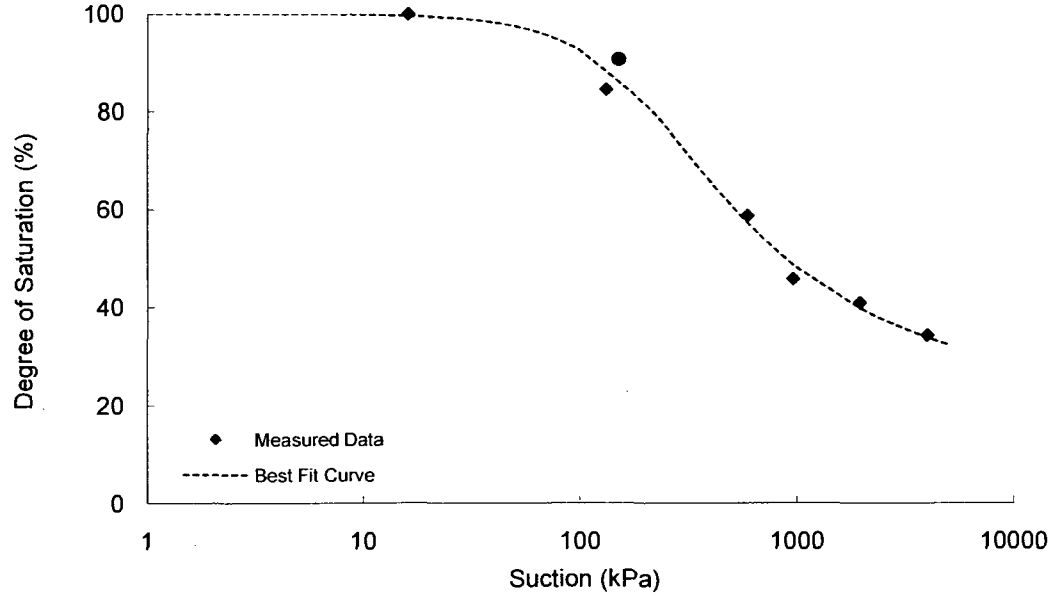

Soil No. 3b

Grey clayey sand

Escario and Saez, 1986; Escario and Juca, 1989

Compacted Sample
Sand = 87%, Silt and Clay= 13%; Liquid Limit = 32, Plasticity Index = 15
Lean clay, CL

Shear Strength

Test Method: Modified direct shear

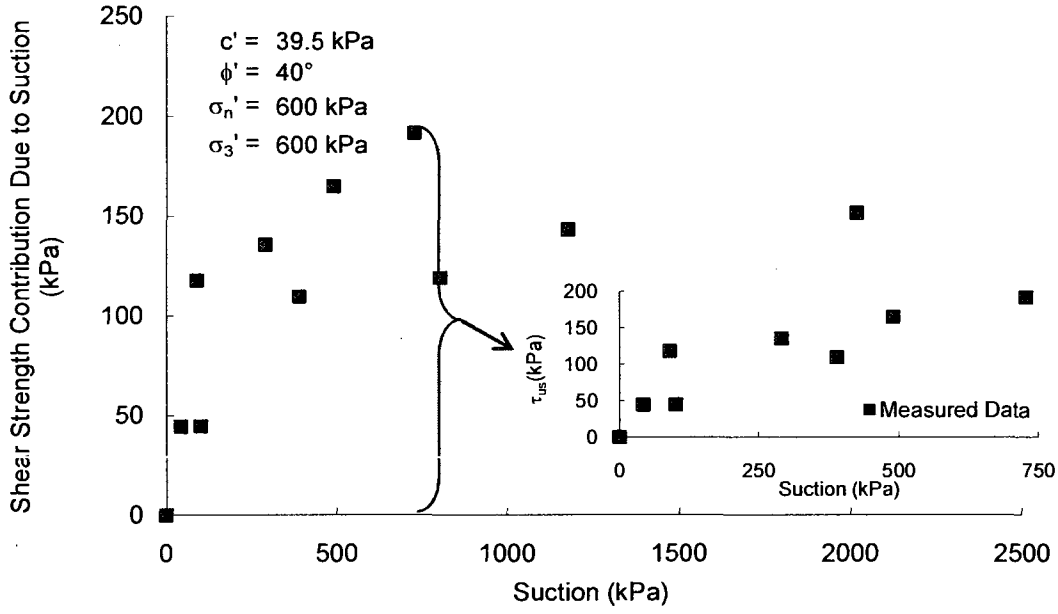

SWRC

Test Method: Pressure membrane apparatus

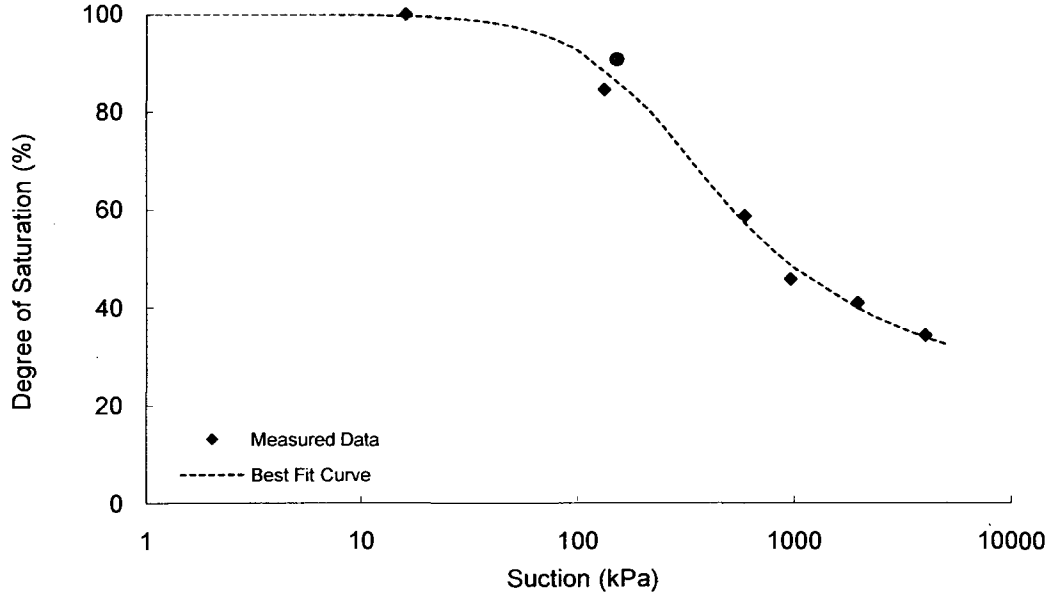

Soil No. 4a

Glacial till, optimum

Vanapalli, Fredlund, Pufahl and Clifton, 1996

Compacted Sample
Sand = 28%, Silt = 42%, Clay = 30%; Liquid Limit = 36, Plasticity Index = 19
Lean clay, CL

Shear Strength

Test Method: Modified direct shear

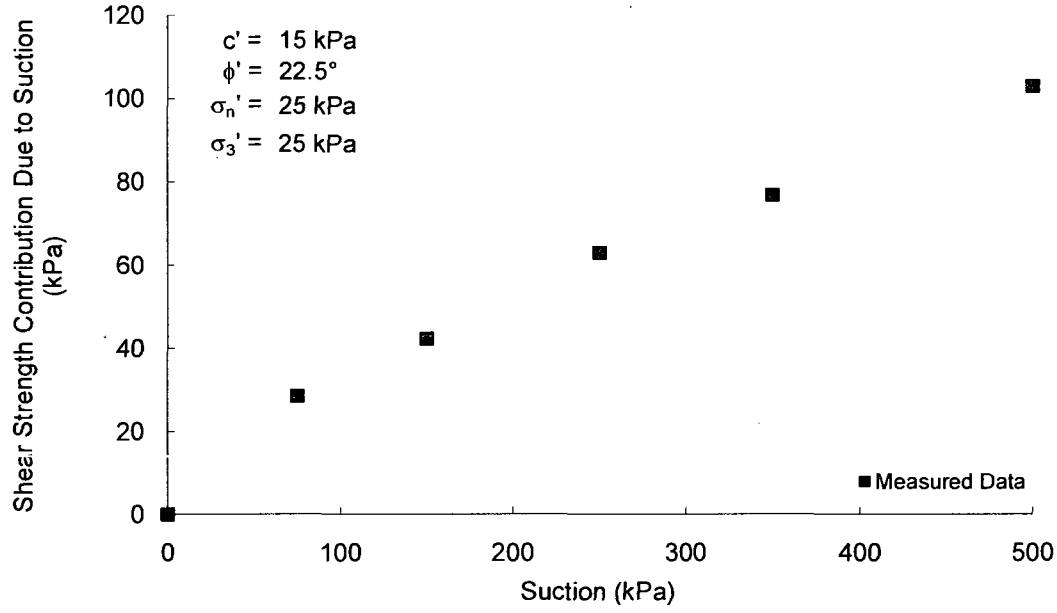

SWRC

Test Method: Pressure membrane apparatus

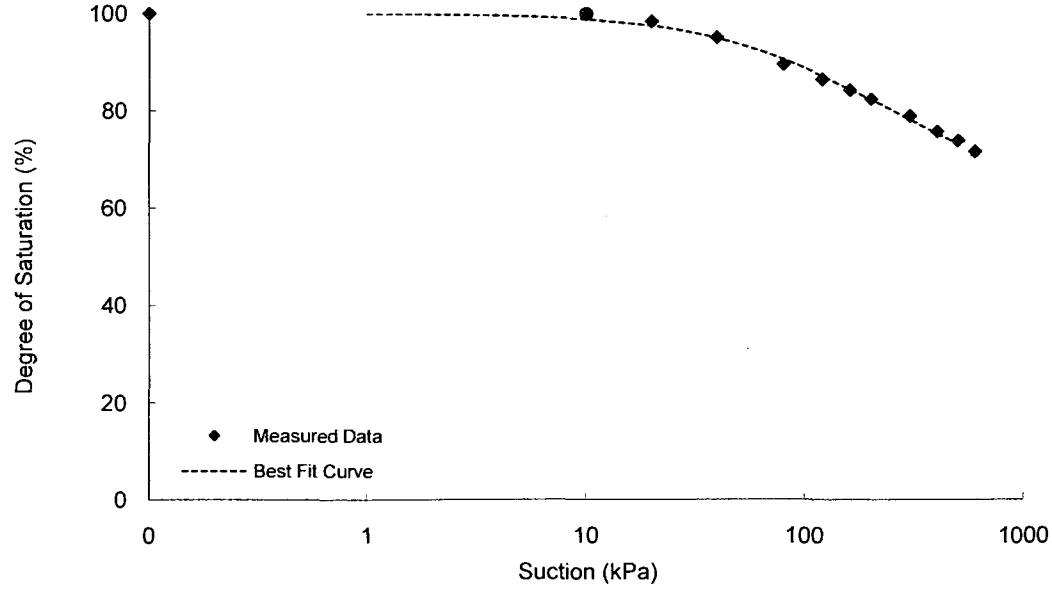

**Gradation curve available in Appendix B

Soil No. 4b

Glacial till, optimum

Vanapalli, Fredlund, Pufahl and Clifton, 1996

Compacted Sample
Sand = 28%, Silt = 42%, Clay = 30%; Liquid Limit = 36, Plasticity Index = 19
Lean clay, CL

Shear Strength

Test Method: Modified direct shear

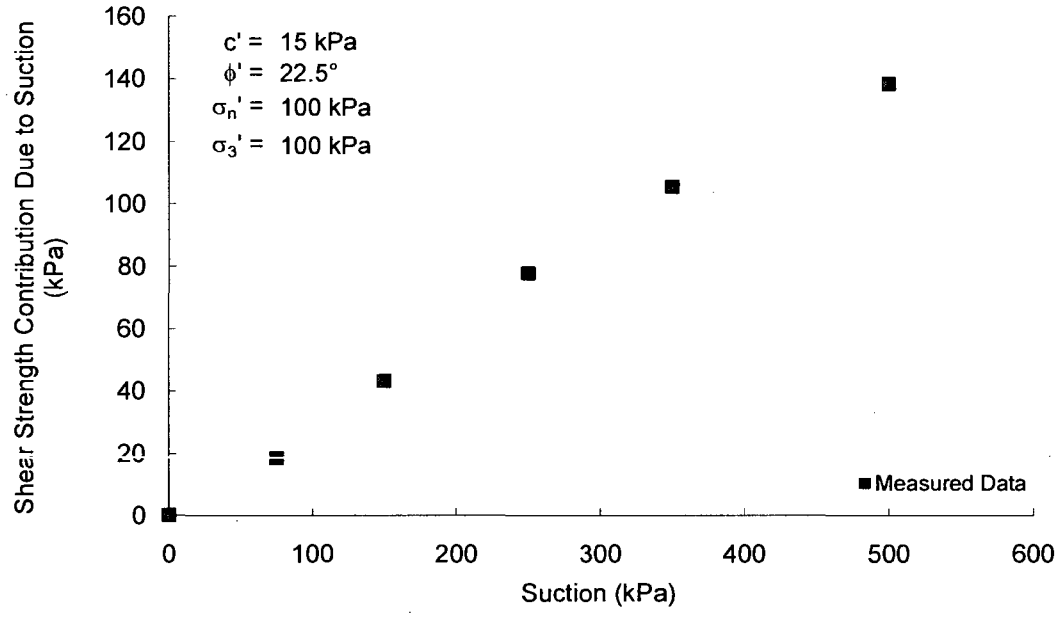

SWRC

Test Method: Pressure membrane apparatus

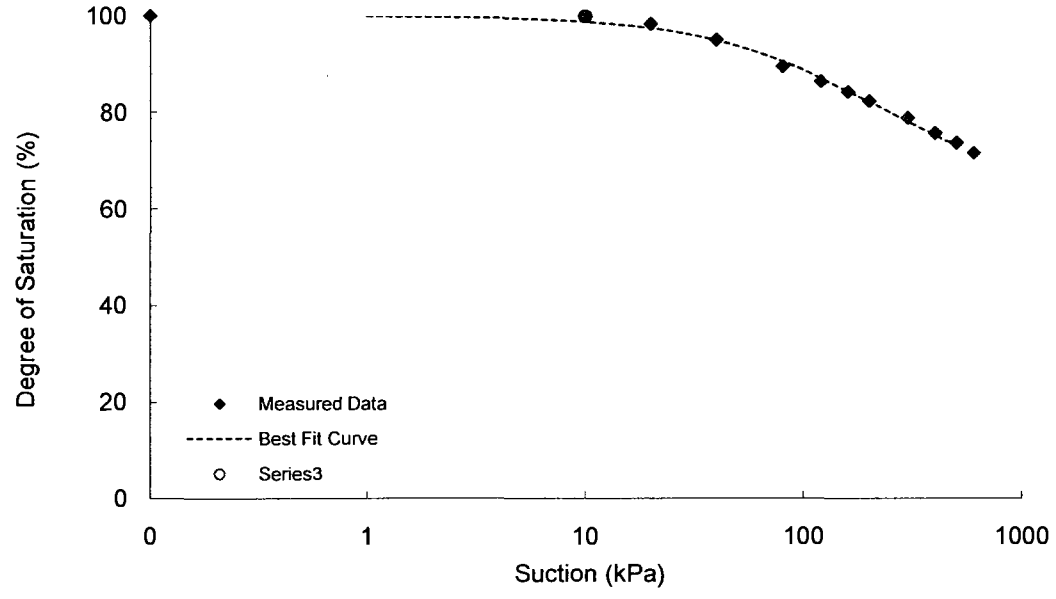

**Gradation curve available in Appendix B

Soil No. 4c

Glacial till, optimum

Vanapalli, Fredlund, Pufahl and Clifton, 1996

Compacted Sample

Sand = 28%, Silt = 42%, Clay = 30%; Liquid Limit = 36, Plasticity Index = 19

Lean clay, CL

Shear Strength

Test Method: Modified direct shear

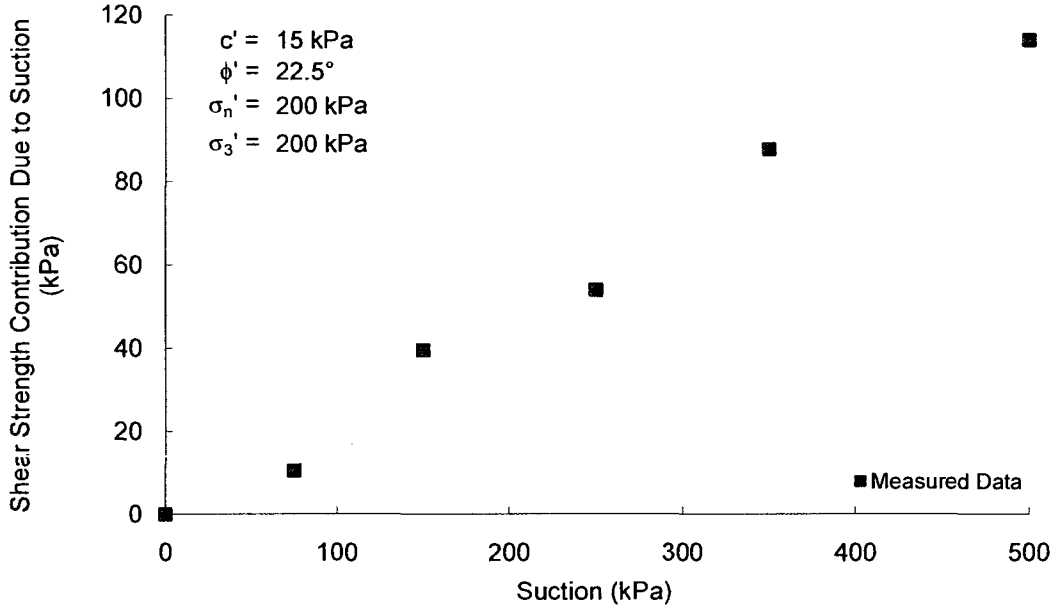

SWRC

Test Method: Pressure membrane apparatus

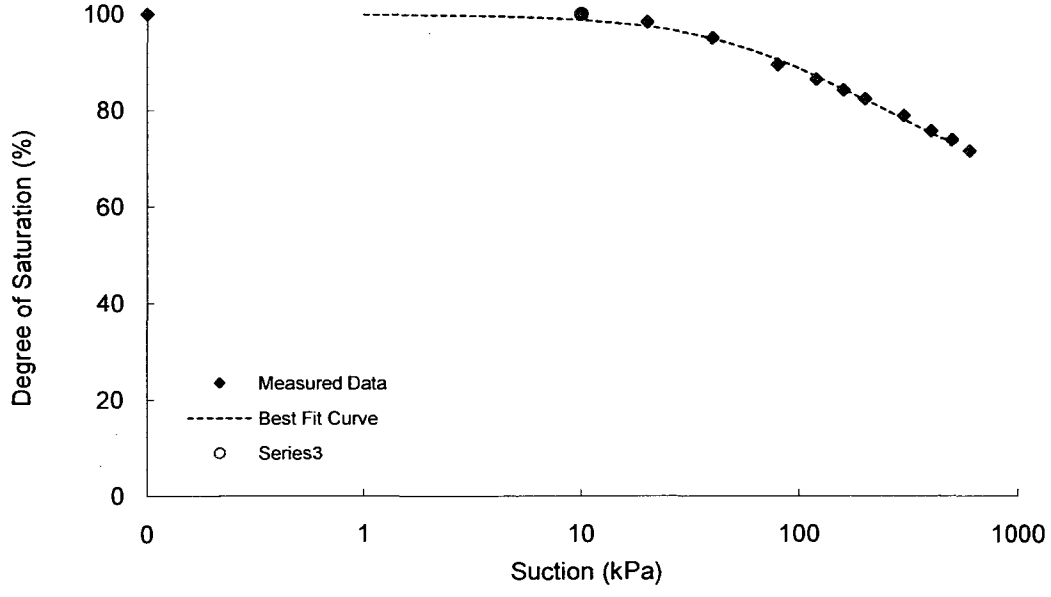

**Gradation curve available in Appendix B

Soil No. 5

Botkin Silt

Vanapalli, Wright and Fredlund, 1999

Compacted Sample
Sand = 27.5%, Silt = 48.5%, Clay = 24%; Liquid Limit = 25, Plasticity Index = 8
ML, Lean silt

Shear Strength

Test Method: Unconfined compression test

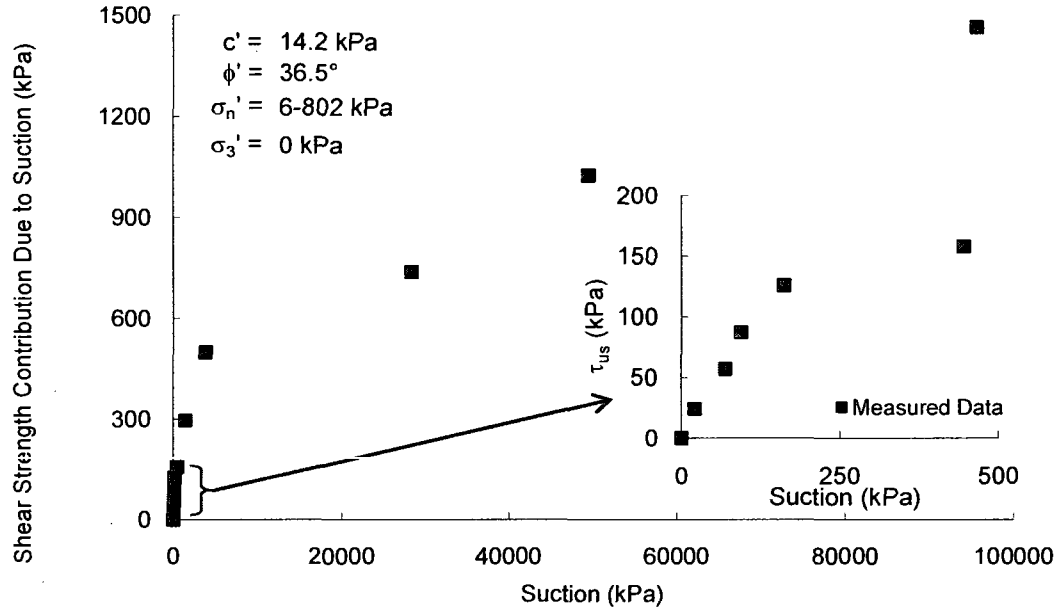

SWRC

Test Method: Tempe cell, osmotic dessicator

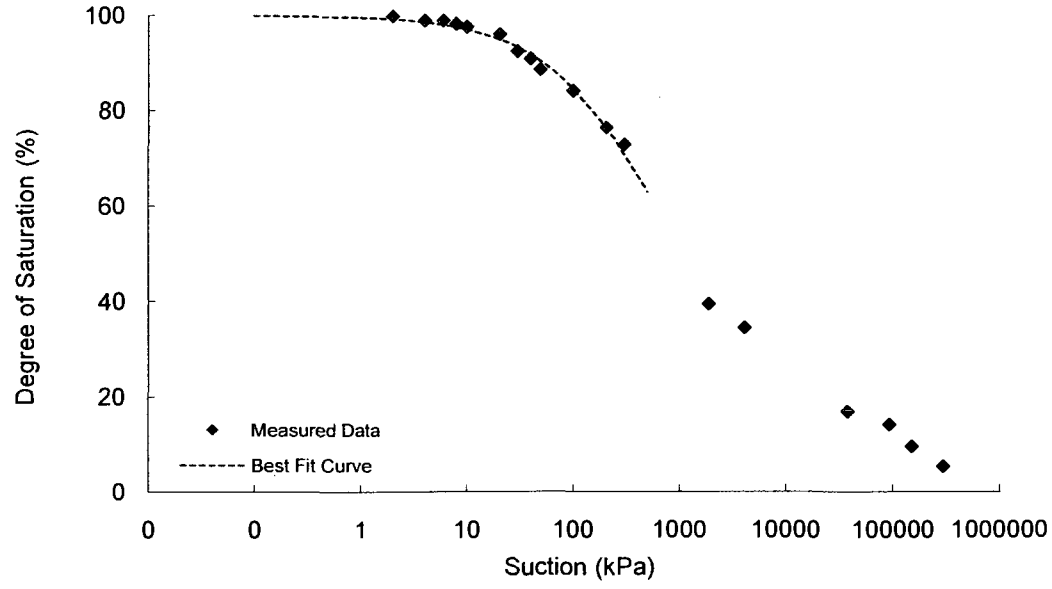

**Gradation curve available in Appendix B

Soil No. 6a

Low-density Dhanauri clay
Satija, 1978

Compacted Sample
Sand = 5%, Silt = 70%, Clay = 25%; Liquid Limit = 49, Plasticity Index = 24
Lean clay, CL

Shear Strength

Test Method: Modified triaxial test

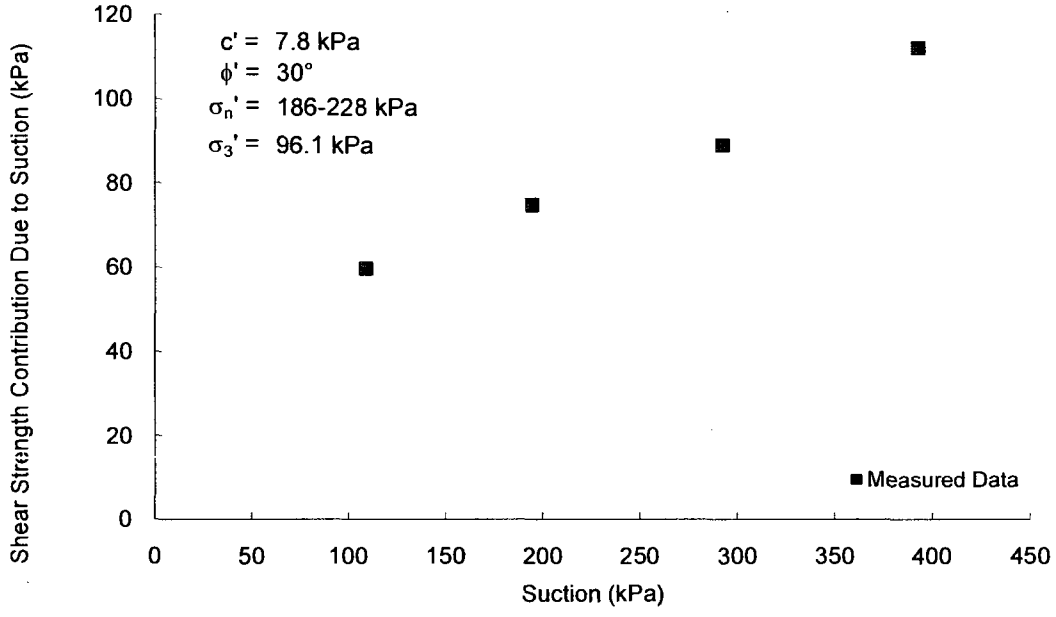

SWRC

Test Method: Pressure plate on triaxial base (determined during testing)

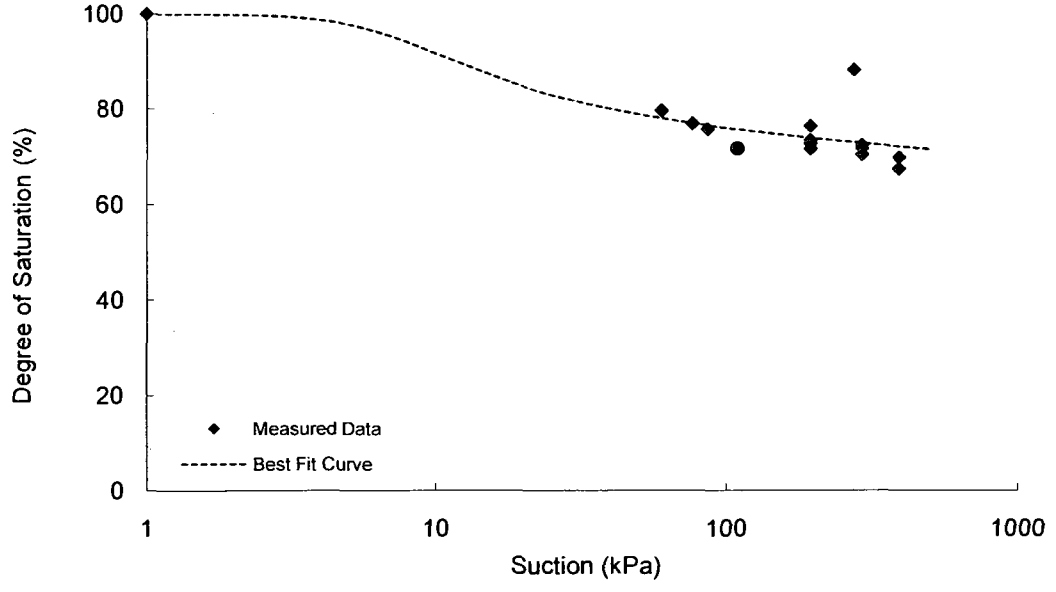

**Gradation curve available in Appendix B

Soil No. 6b

Low-density Dhanauri clay
Satija, 1978

Compacted Sample
Sand = 5%, Silt = 70%, Clay = 25%; Liquid Limit = 49, Plasticity Index = 24
Lean clay, CL

Shear Strength

Test Method: Modified triaxial test

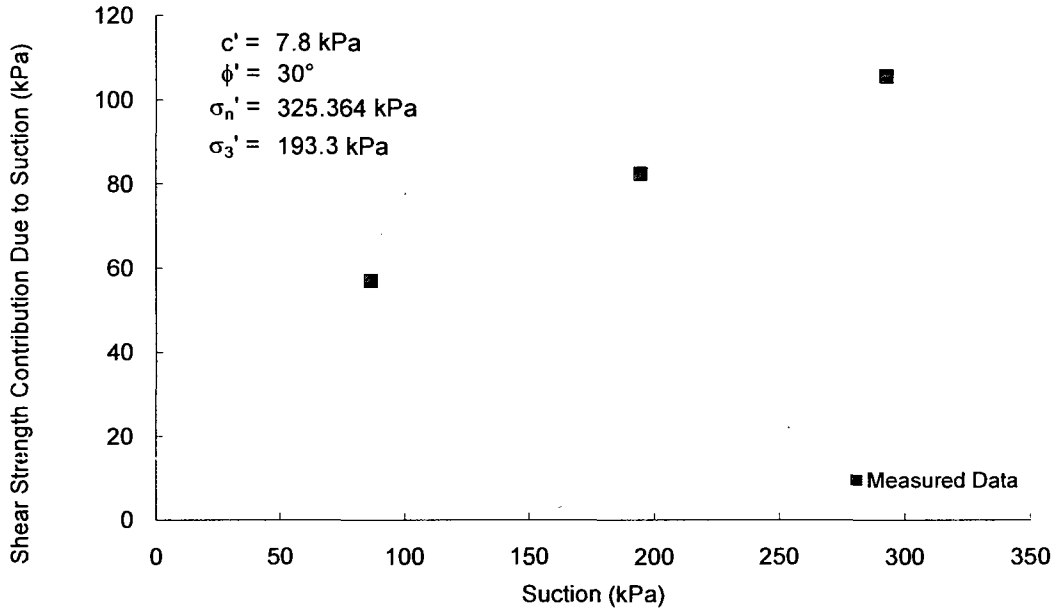

SWRC

Test Method: Pressure plate on triaxial base (determined during testing)

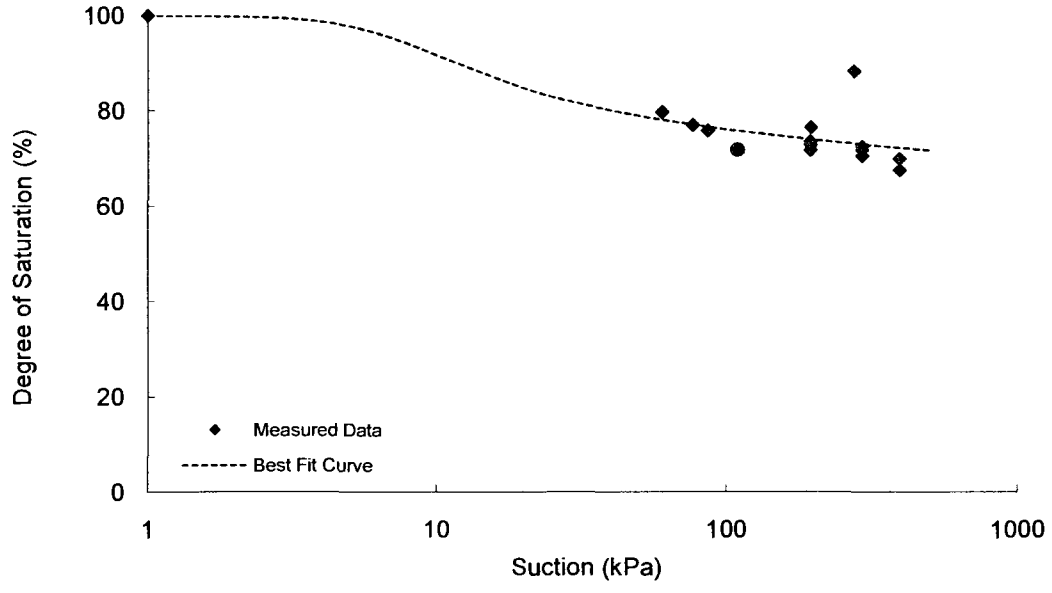

**Gradation curve available in Appendix B

Soil No. 6c

Low-density Dhanauri clay
Satija, 1978

Compacted Sample
Sand = 5%, Silt = 70%, Clay = 25%; Liquid Limit = 49, Plasticity Index = 24
Lean clay, CL

Shear Strength

Test Method: Modified triaxial test

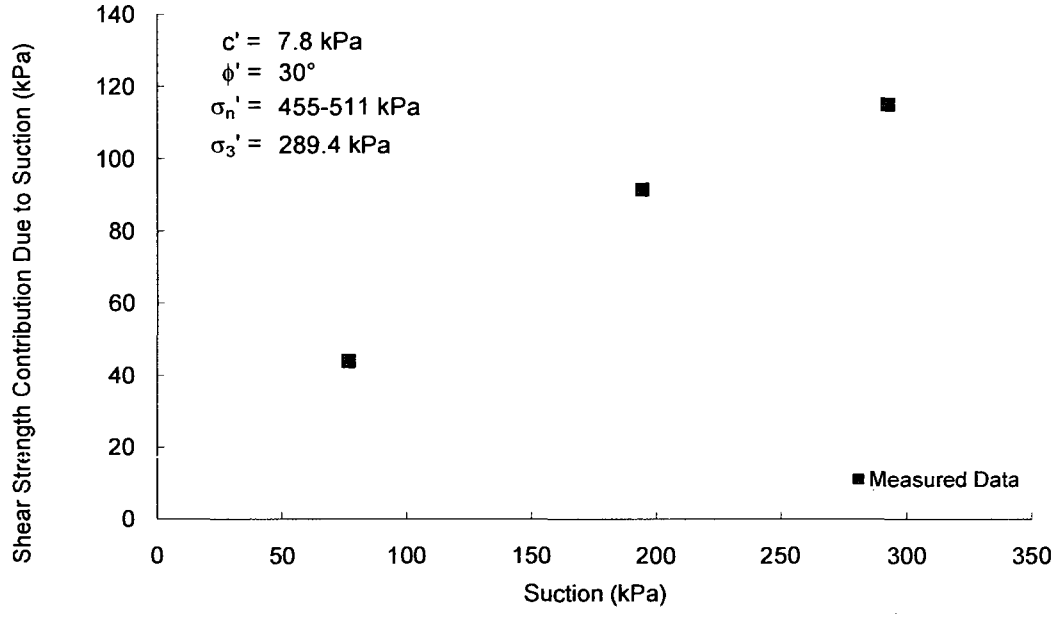

SWRC

Test Method: Pressure plate on triaxial base (determined during testing)

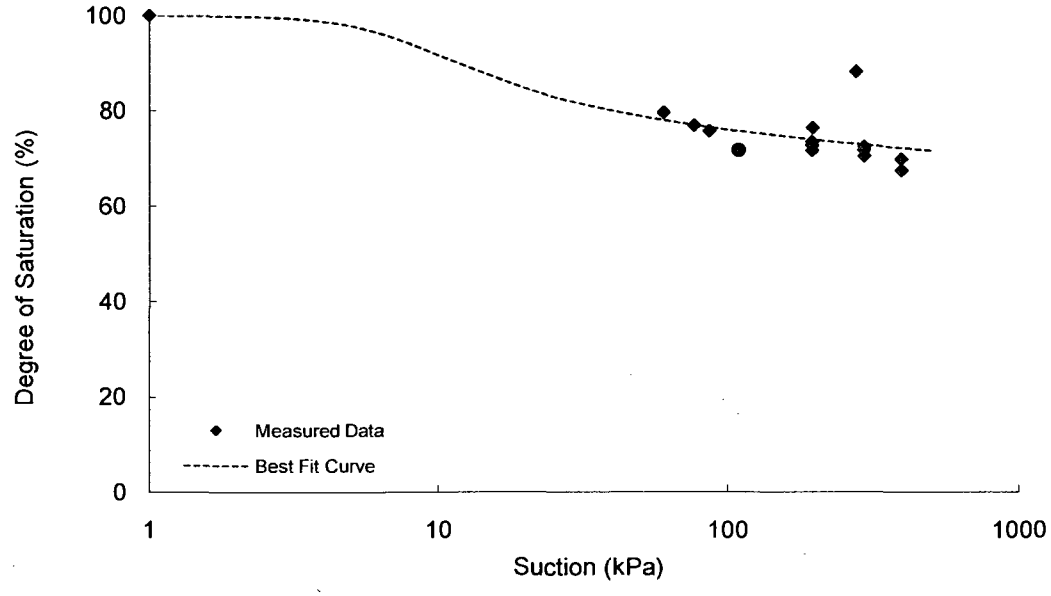

**Gradation curve available in Appendix B

Soil No. 6d

Low-density Dhanauri clay
Satija, 1978

Compacted Sample
Sand = 5%, Silt = 70%, Clay = 25%; Liquid Limit = 49, Plasticity Index = 24
Lean clay, CL

Shear Strength

Test Method: Modified triaxial test

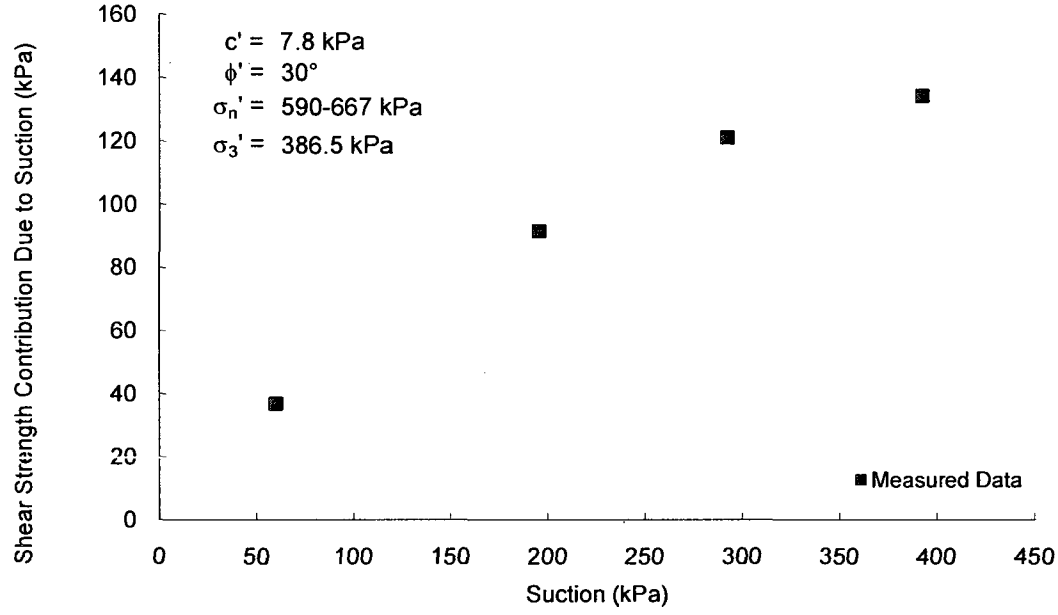

SWRC

Test Method: Pressure plate on triaxial base (determined during testing)

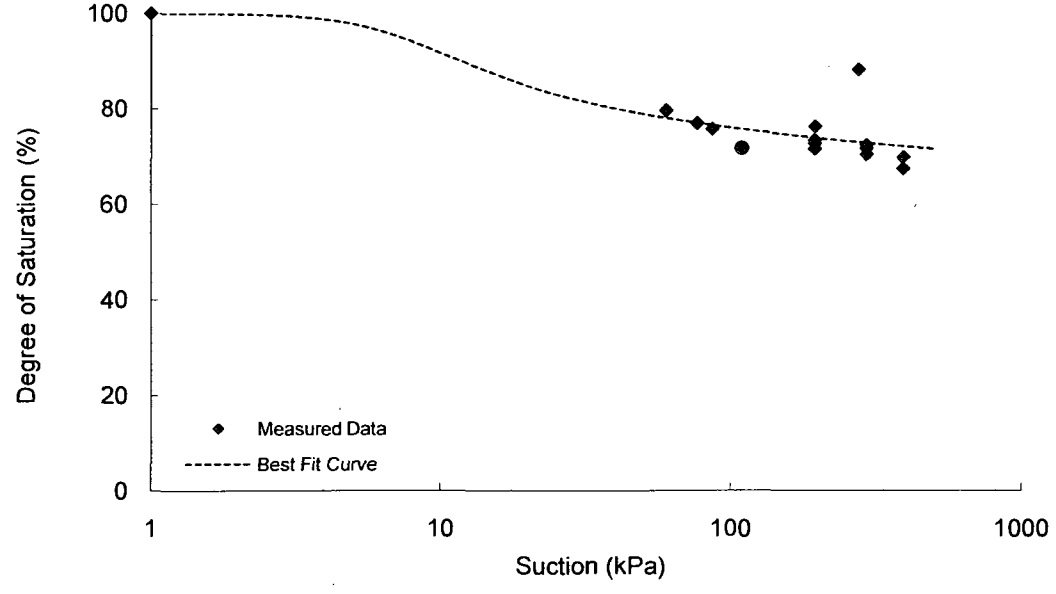

**Gradation curve available in Appendix B

Soil No. 6e

High-density Dhanauri clay
Satija, 1978

Compacted Sample
Sand = 5%, Silt = 70%, Clay = 25%; Liquid Limit = 49, Plasticity Index = 24
Lean clay, CL

Shear Strength

Test Method: Modified triaxial test

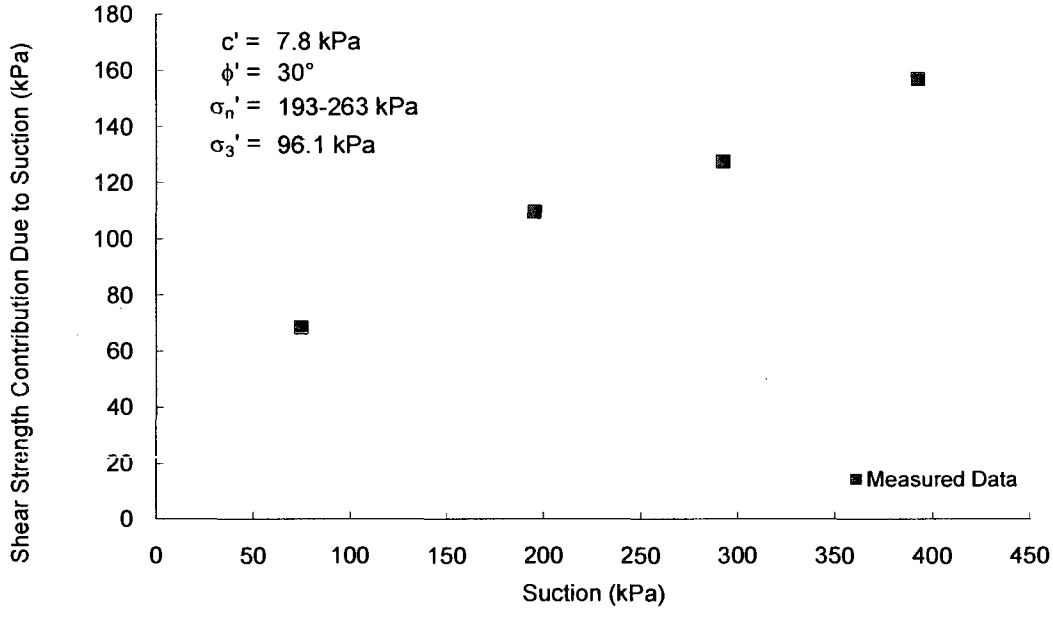

SWRC

Test Method: Pressure plate on triaxial base (determined during testing)

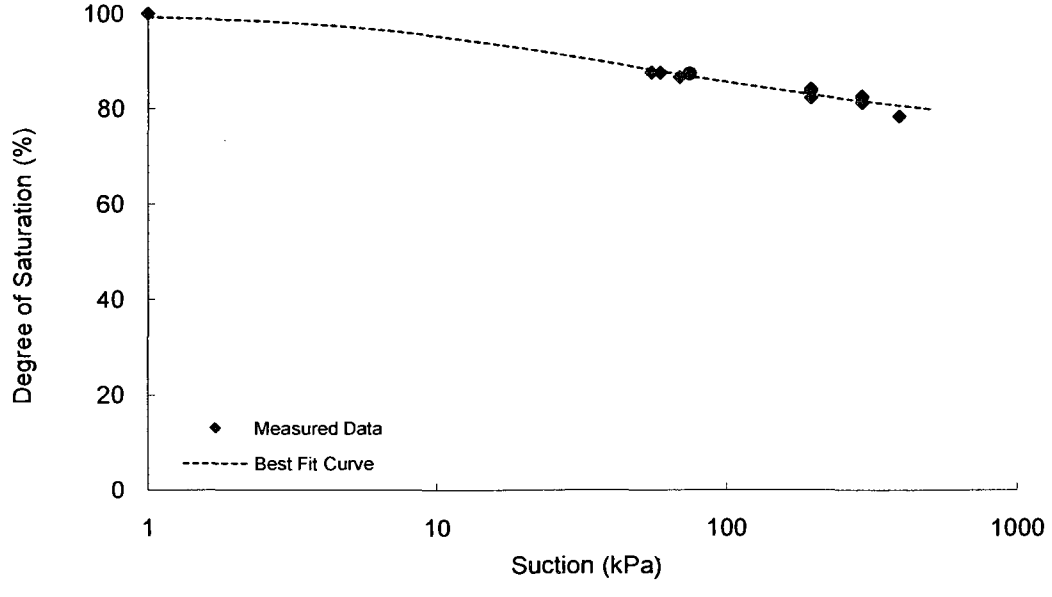

**Gradation curve available in Appendix B

Soil No. 6f

High-density Dhanauri clay
Satija, 1978

Compacted Sample
Sand = 5%, Silt = 70%, Clay = 25%; Liquid Limit = 49, Plasticity Index = 24
Lean clay, CL

Shear Strength

Test Method: Modified triaxial test

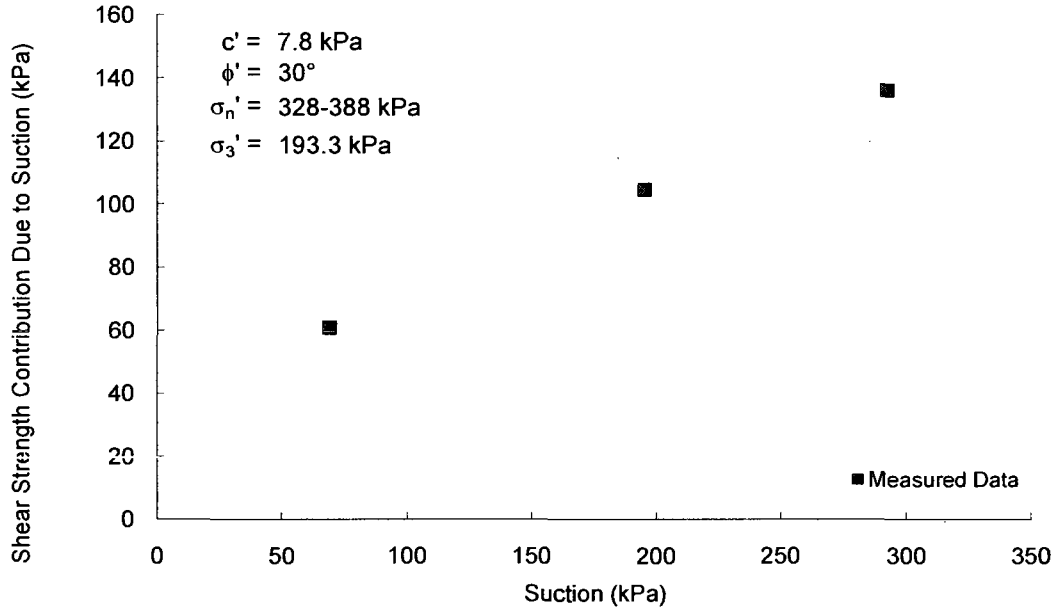

SWRC

Test Method: Pressure plate on triaxial base (determined during testing)

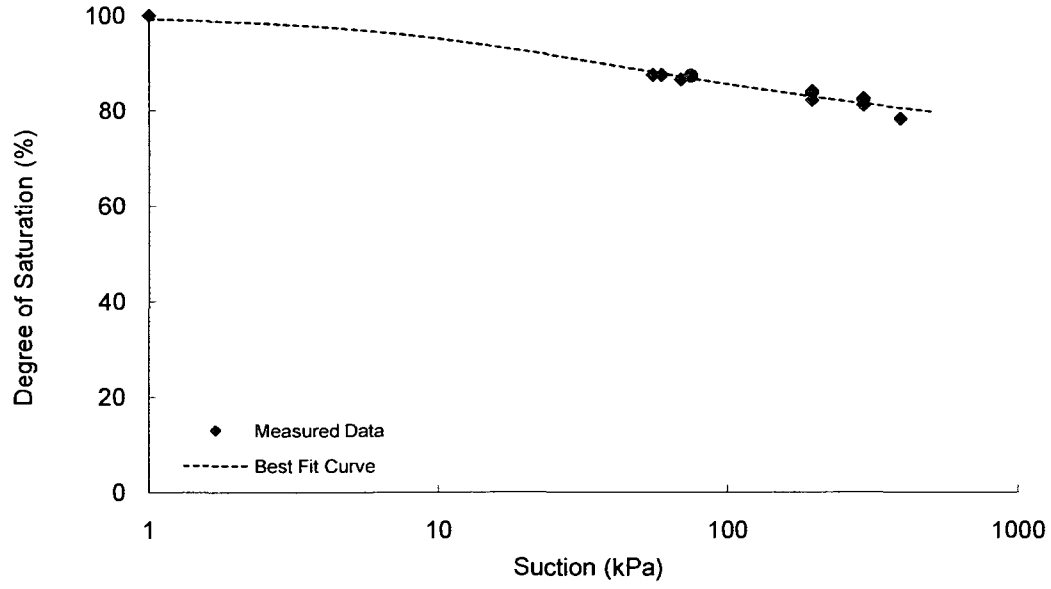

**Gradation curve available in Appendix B

Soil No. 6g

High-density Dhanauri clay
Satija, 1978

Compacted Sample
Sand = 5%, Silt = 70%, Clay = 25%; Liquid Limit = 49, Plasticity Index = 24
Lean clay, CL

Shear Strength

Test Method: Modified triaxial test

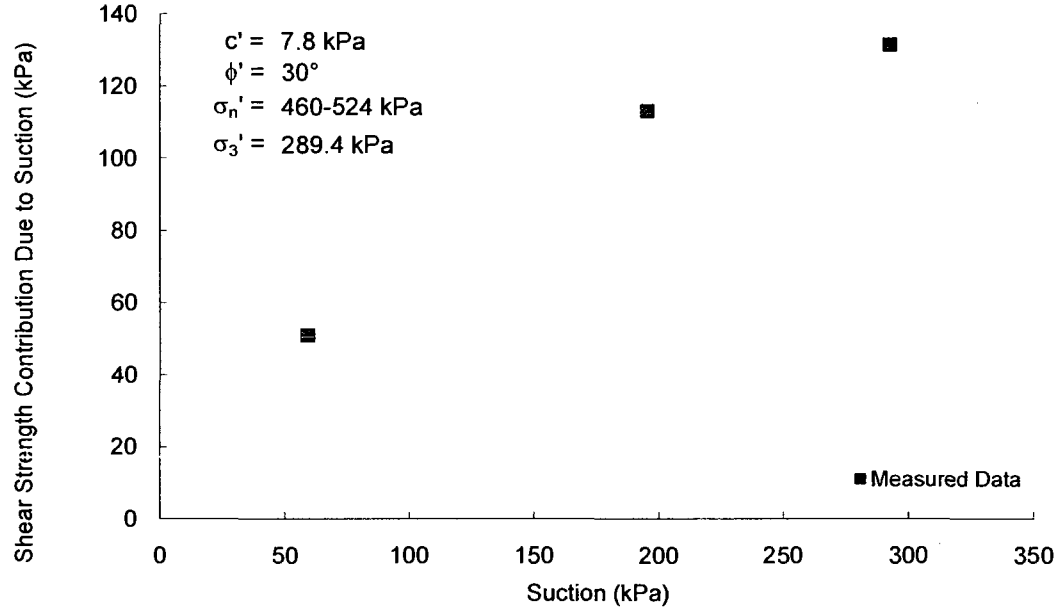

SWRC

Test Method: Pressure plate on triaxial base (determined during testing)

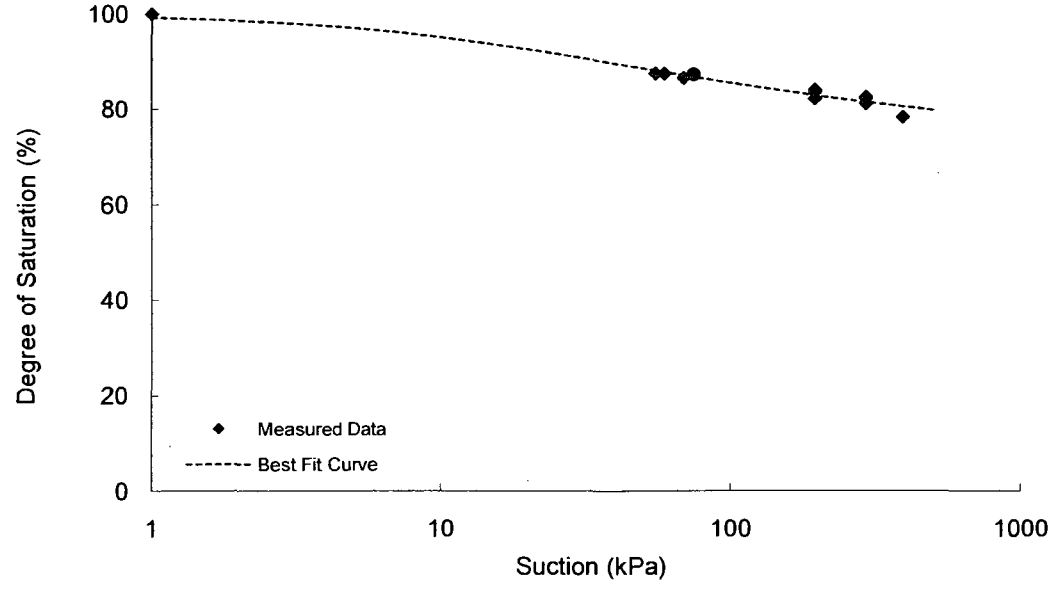

**Gradation curve available in Appendix B

Soil No. 6h

High-density Dhanauri clay
Satija, 1978

Compacted Sample
Sand = 5%, Silt = 70%, Clay = 25%; Liquid Limit = 49, Plasticity Index = 24
Lean clay, CL

Shear Strength

Test Method: Modified triaxial test

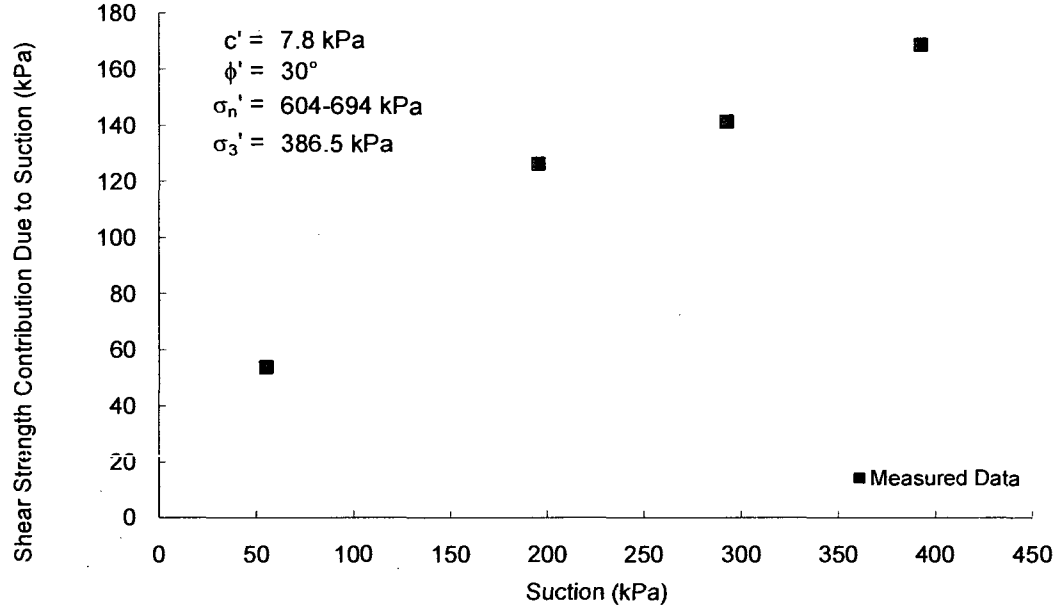

SWRC

Test Method: Pressure plate on triaxial base (determined during testing)

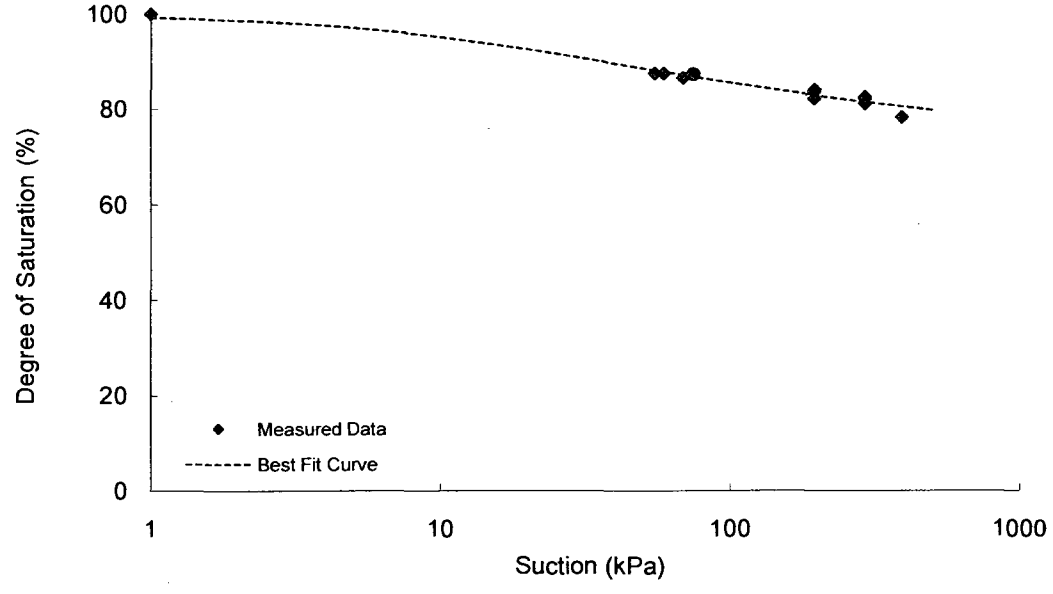

**Gradation curve available in Appendix B

Soil No. 7a

Weathered Granite
Lee, Sung and Cho, 2005

Compacted Sample
Sand = 87.6%, Silt and Clay= 12.4%; Liquid Limit = NP, Plasticity Index = NP
Silty sand, SM

Shear Strength

Test Method: Modified triaxial test

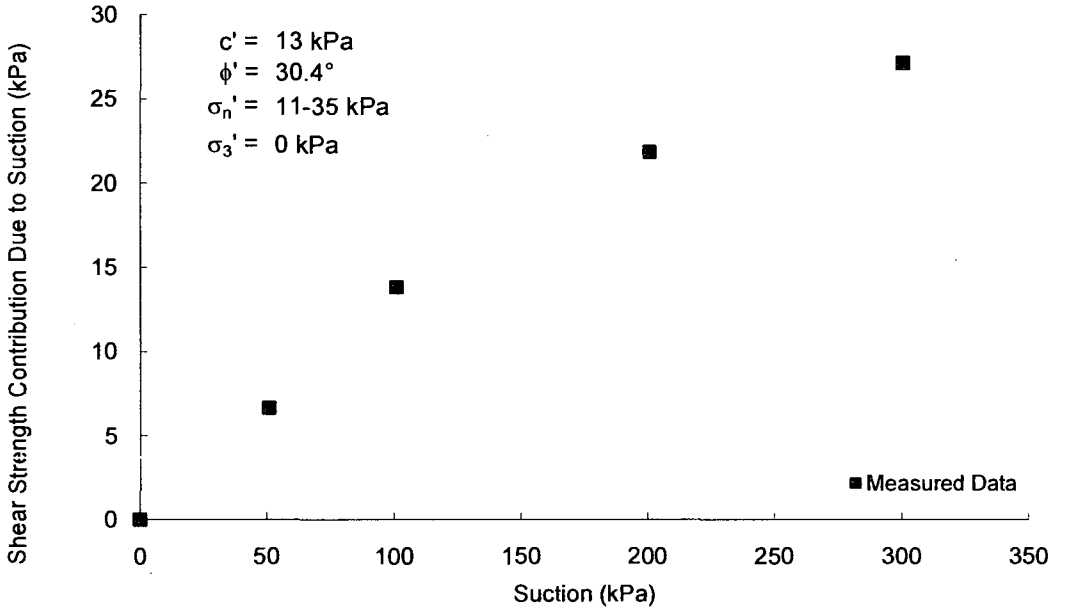

SWRC

Test Method: Pressure plate, tempe cell, CPCE

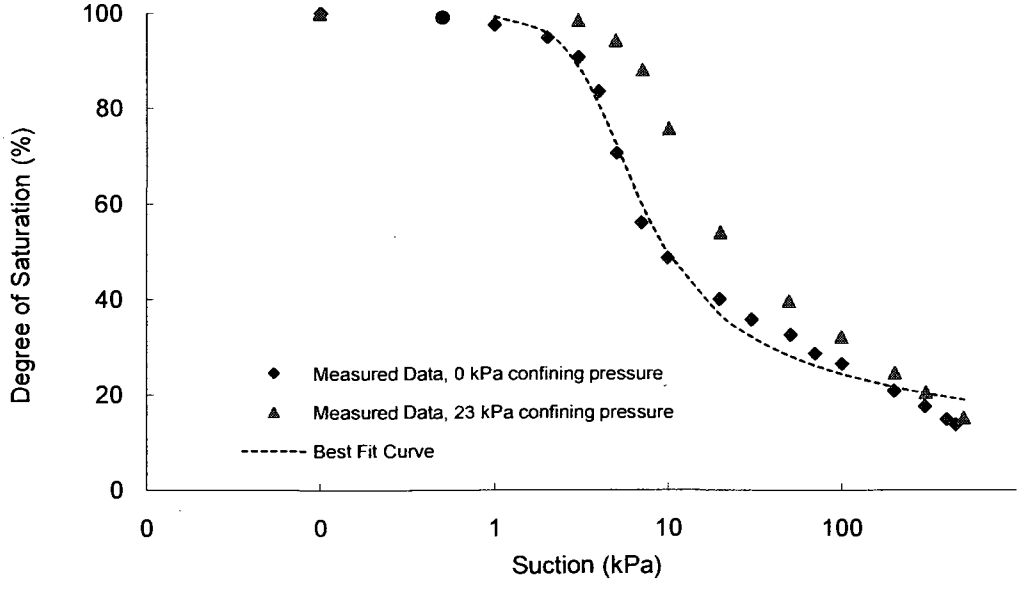

**Gradation curve available in Appendix B

Soil No. 7b

Weathered Granite
Lee, Sung and Cho, 2005

Compacted Sample
Sand = 87.6%, Silt and Clay= 12.4%; Liquid Limit = NP, Plasticity Index = NP
Silty sand, SM

Shear Strength

Test Method: Modified triaxial test

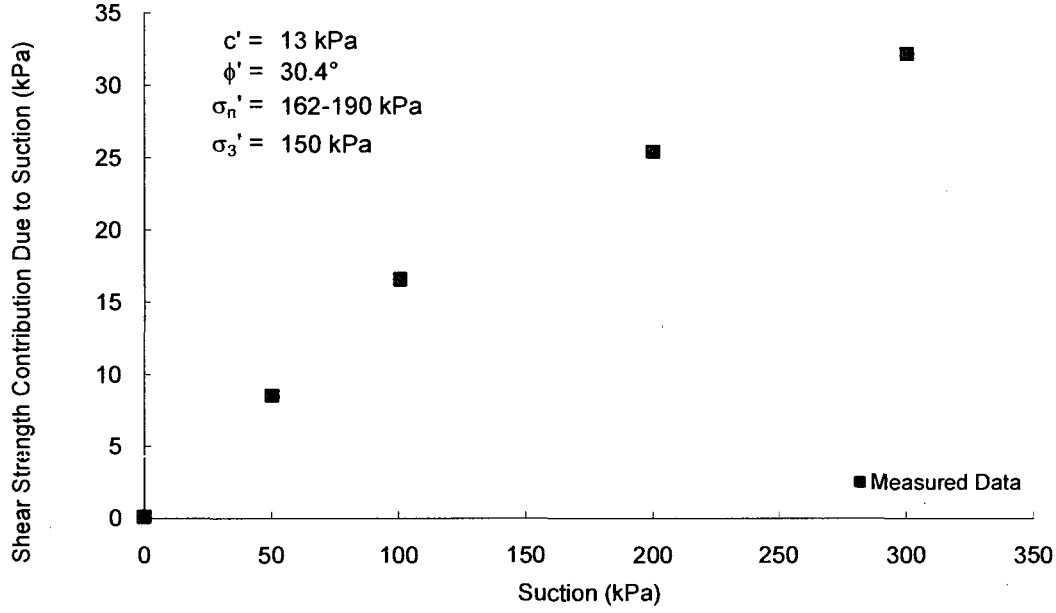

SWRC

Test Method: Pressure plate, tempe cell, CPCE

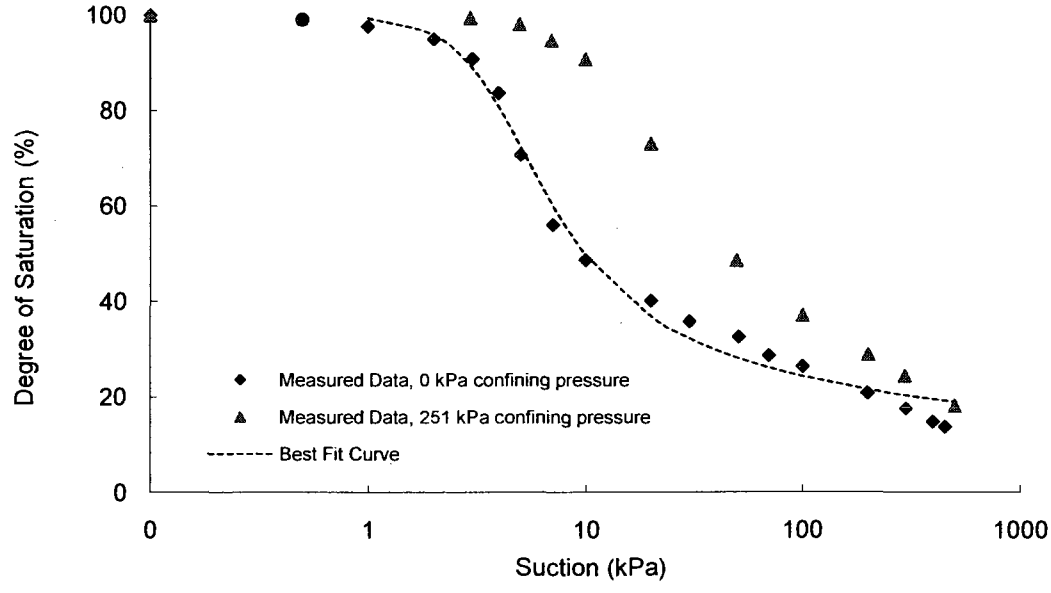

**Gradation curve available in Appendix B

Soil No. 7c

Weathered Granite
Lee, Sung and Cho, 2005

Compacted Sample
Sand = 87.6%, Silt and Clay= 12.4%; Liquid Limit = NP, Plasticity Index = NP
Silty sand, SM

Shear Strength

Test Method: Modified triaxial test

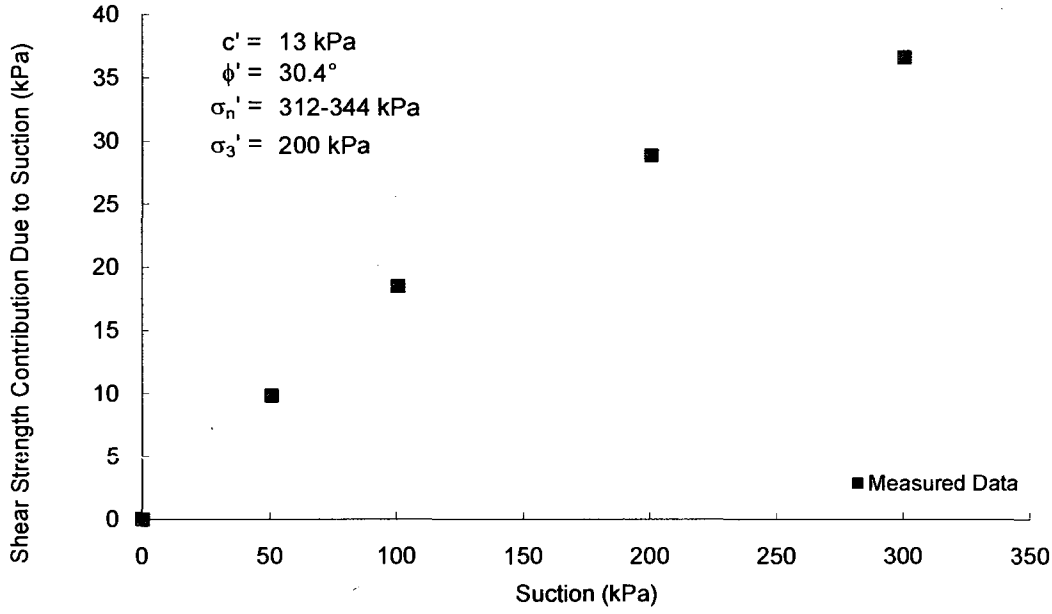

SWRC

Test Method: Pressure plate, tempe cell, CPCE

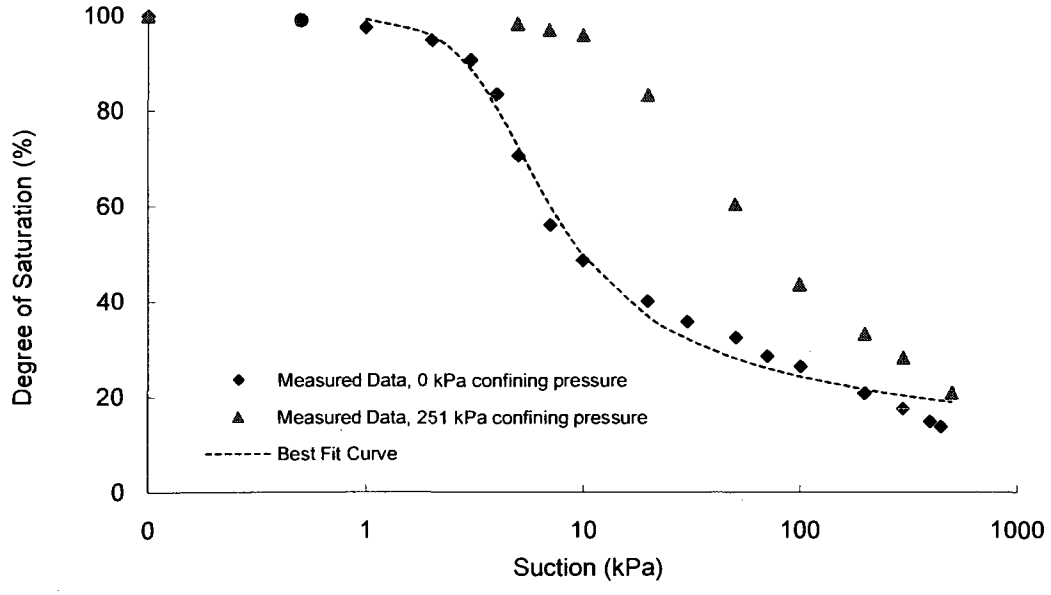

**Gradation curve available in Appendix B

Soil No. 7d

Weathered Granite
Lee, Sung and Cho, 2005

Compacted Sample
Sand = 87.6%, Silt and Clay= 12.4%; Liquid Limit = NP, Plasticity Index = NP
Silty sand, SM

Shear Strength

Test Method: Modified triaxial test

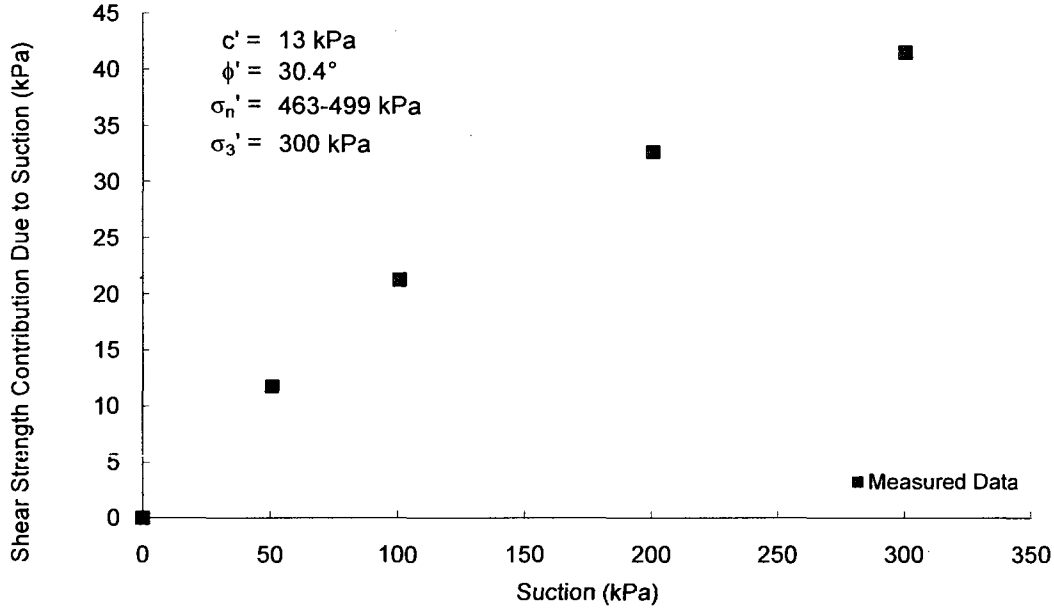

SWRC

Test Method: Pressure plate, tempe cell, CPCE

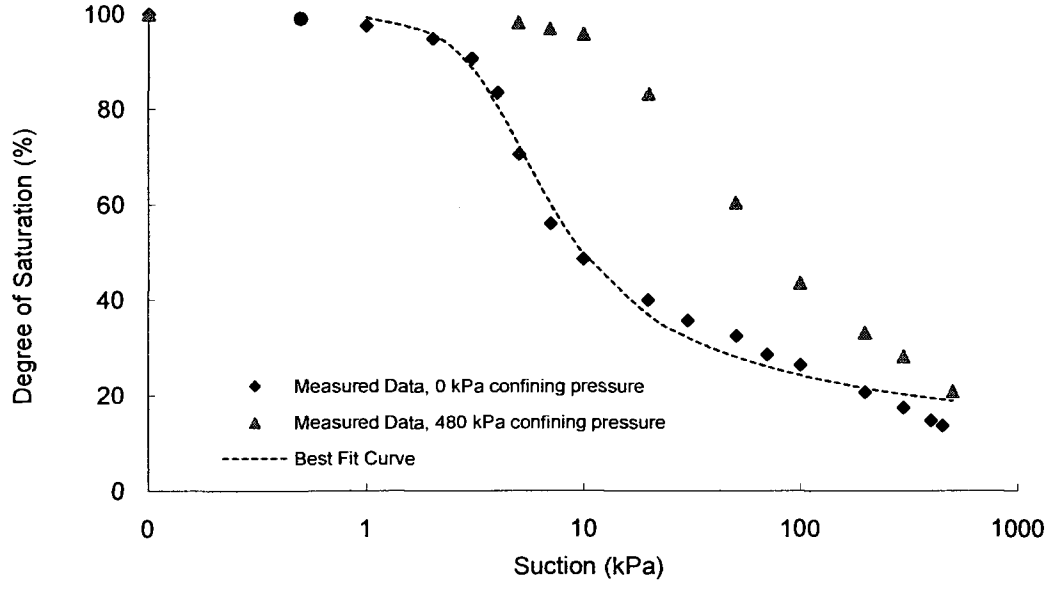

**Gradation curve available in Appendix B

Soil No. 8a

Jurong soil

Rahardjo, Heng and Choon, 2004

Compacted Sample
Sand = 34%, Silt = 24%, Clay = 42%; Liquid Limit = 36, Plasticity Index = 14
Lean clay, CL

Shear Strength

Test Method: Modified triaxial test

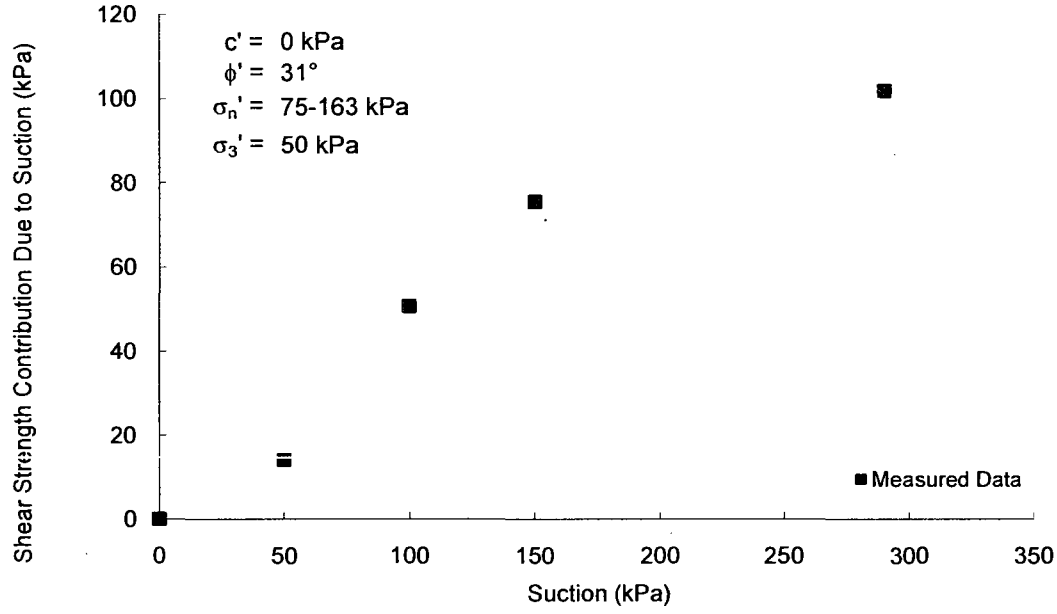

SWRC

Test Method: Pressure plate

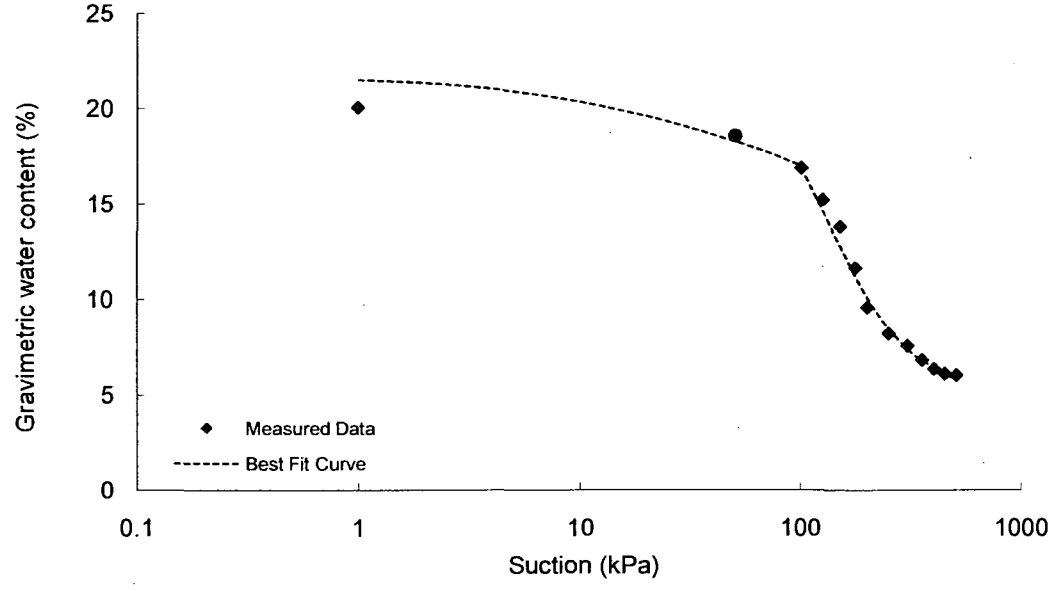

**Gradation curve available in Appendix B

Soil No. 8b

Jurong soil

Rahardjo, Heng and Choon, 2004

Compacted Sample
Sand = 34%, Silt = 24%, Clay = 42%; Liquid Limit = 36, Plasticity Index = 14
Lean clay, CL

Shear Strength

Test Method: Modified triaxial test

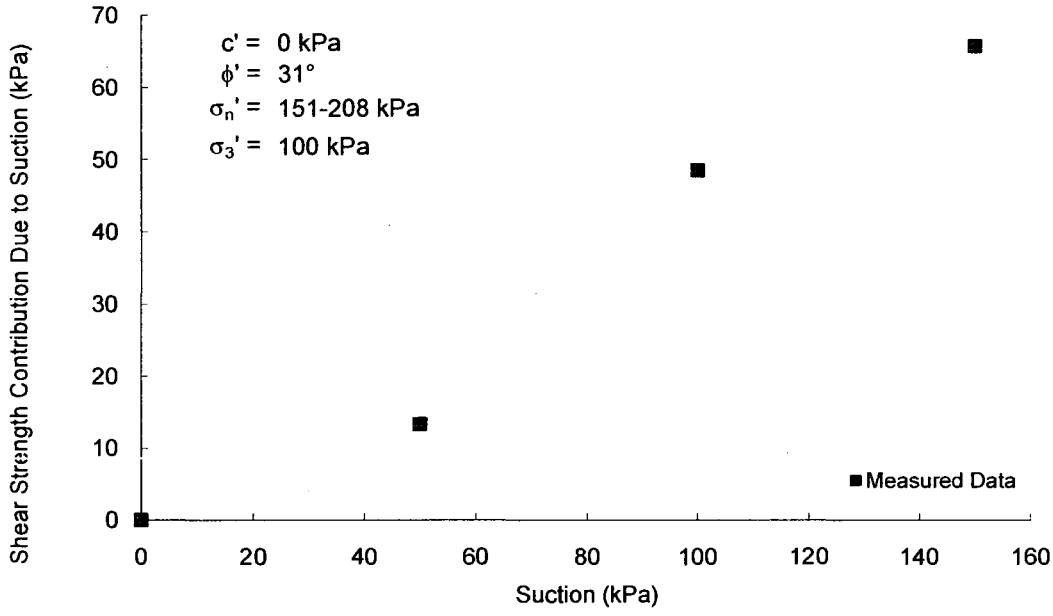

SWRC

Test Method: Pressure plate

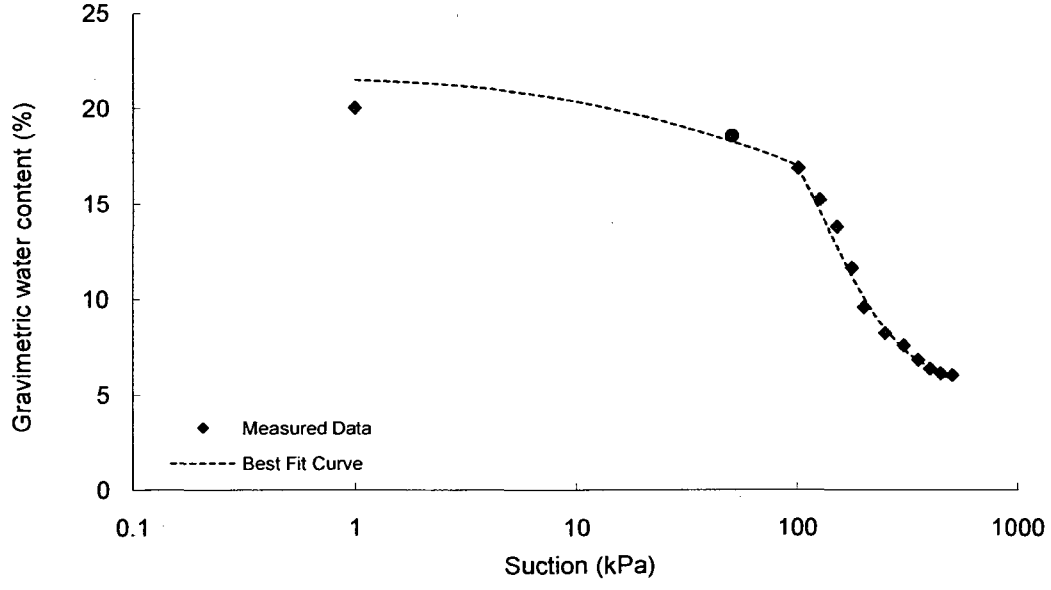

**Gradation curve available in Appendix B

Soil No. 8c

Jurong soil

Rahardjo, Heng and Choon, 2004

Compacted Sample
Sand = 34%, Silt = 24%, Clay = 42%; Liquid Limit = 36, Plasticity Index = 14
Lean clay, CL

Shear Strength

Test Method: Modified triaxial test

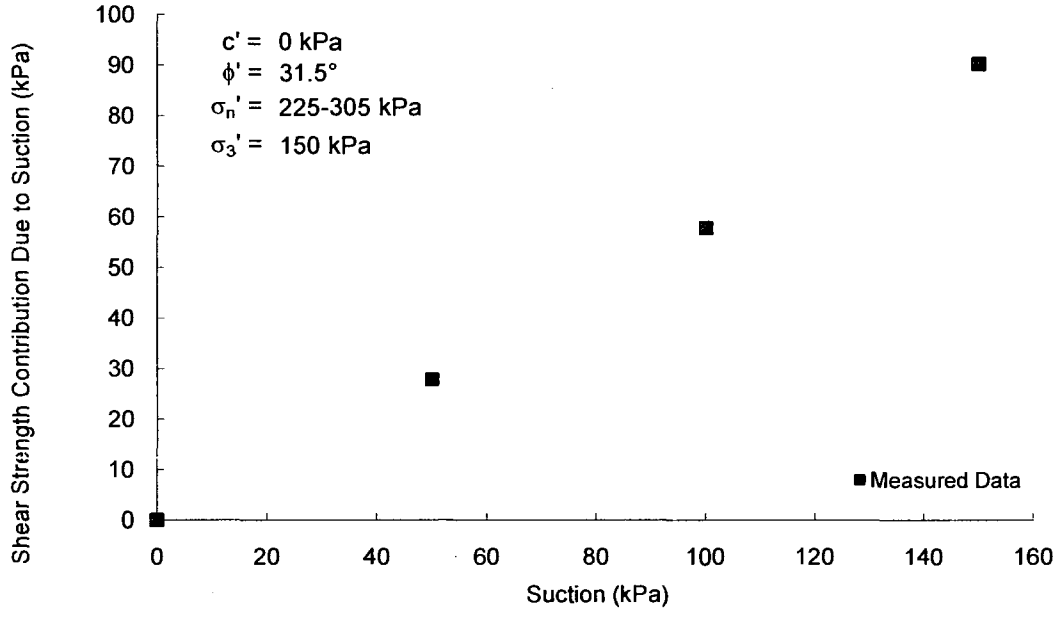

SWRC

Test Method: Pressure plate

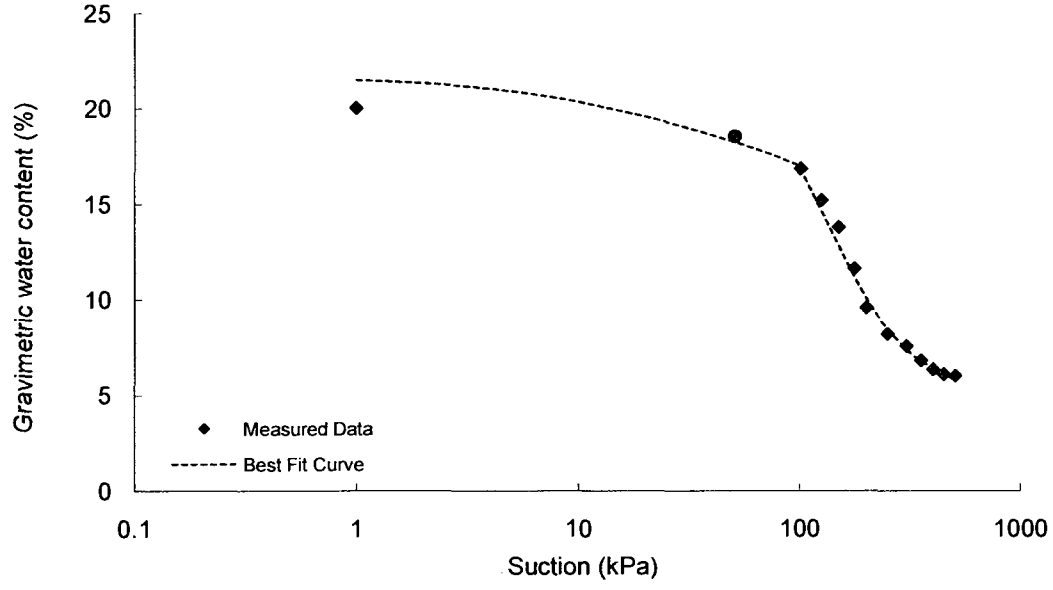

**Gradation curve available in Appendix B

Soil No. 9

Nanyang undisturbed clay
Bao, Gong and Zhan, 1998

Undisturbed Soil Specimens
Sand = ?%, Silt = ?%, Clay = ?%; Liquid Limit = 60, Plasticity Index = 33
Fat clay, CH

Shear Strength

Test Method: Modified triaxial test

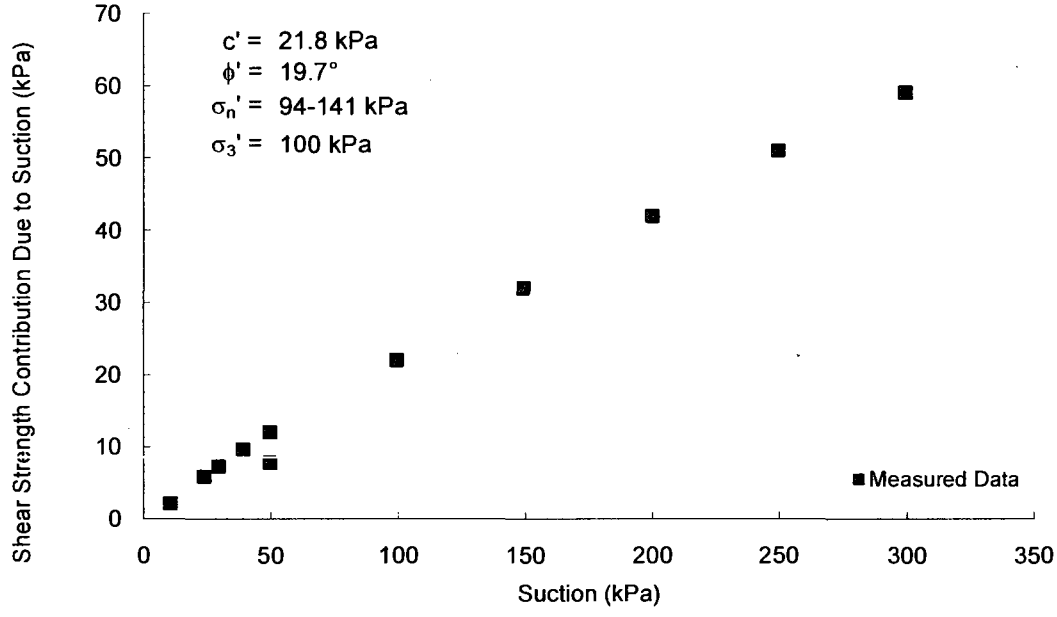

SWRC

Test Method: Pressure plate

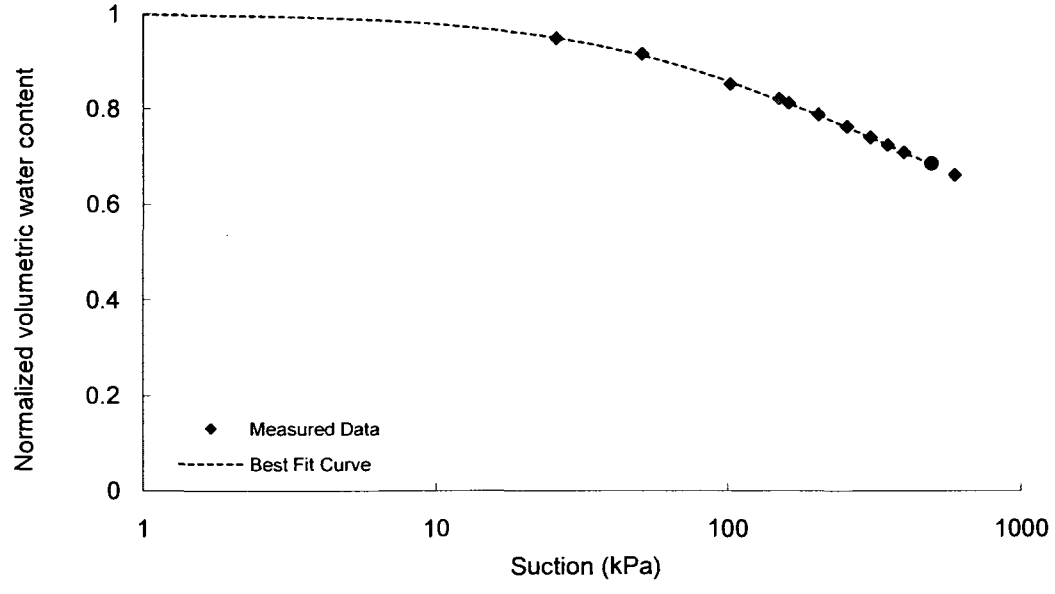

Soil No. 10

Nanyang compacted clay

Bao, Gong and Zhan, 1998

Undisturbed Soil Specimens

Sand = ?%, Silt = ?%, Clay = ?%; Liquid Limit = 37, Plasticity Index = 14

Lean clay, CL

Shear Strength

Test Method: Modified triaxial test

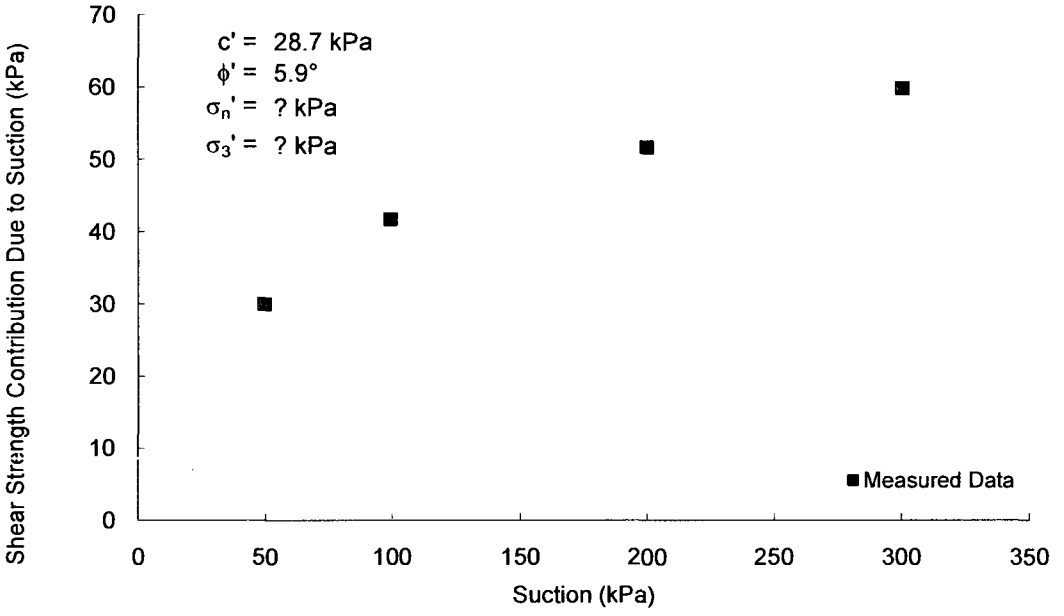

SWRC

Test Method: Pressure plate

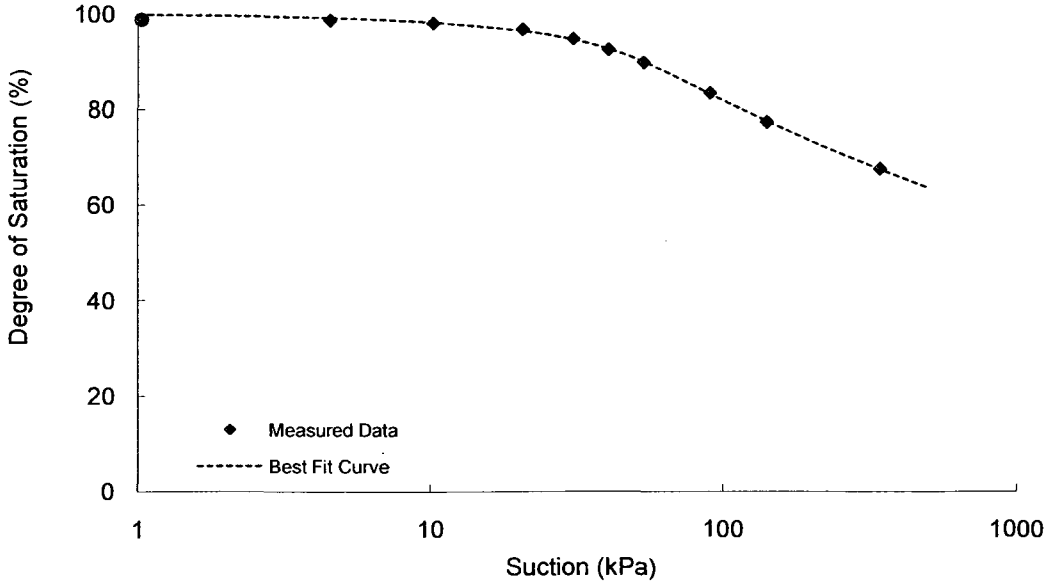

Soil No. 11a

Speswhite kaolin

Tarantino and Tombolato, 2005

Compacted Sample

Sand = 0%, Silt = 80%, Clay = 20%; Liquid Limit = 64, Plasticity Index = 32

Heavy silt, MH

Shear Strength

Test Method: Modified direct shear test

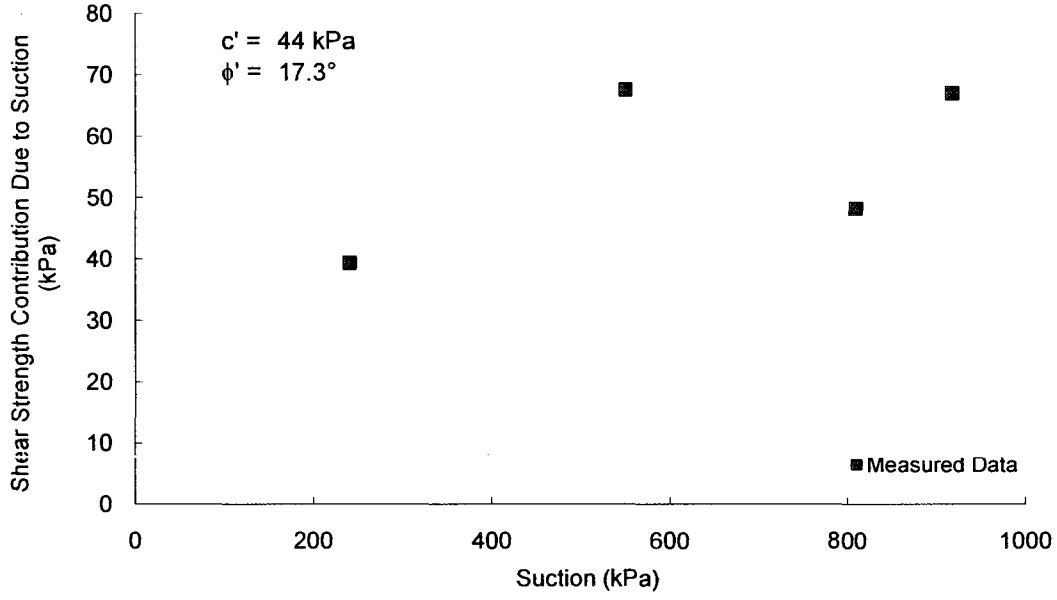

SWRC

Test Method: Axis translation

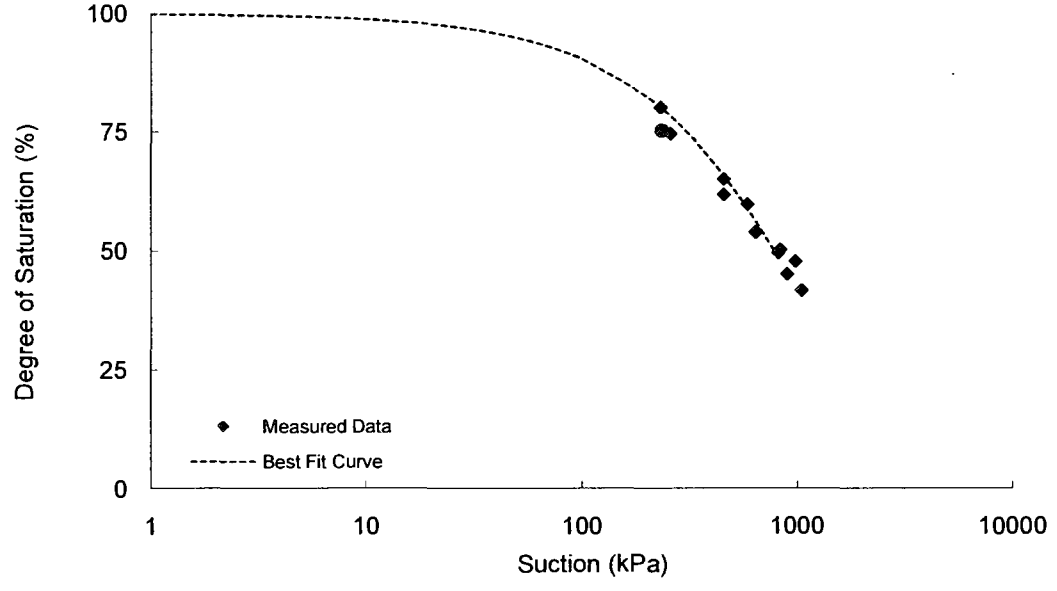

Soil No. 11b

Speswhite kaolin

Tarantino and Tombolato, 2005

Compacted Sample

Sand = 0%, Silt = 80%, Clay = 20%; Liquid Limit = 64, Plasticity Index = 32

Heavy silt, MH

Shear Strength

Test Method: Modified direct shear test

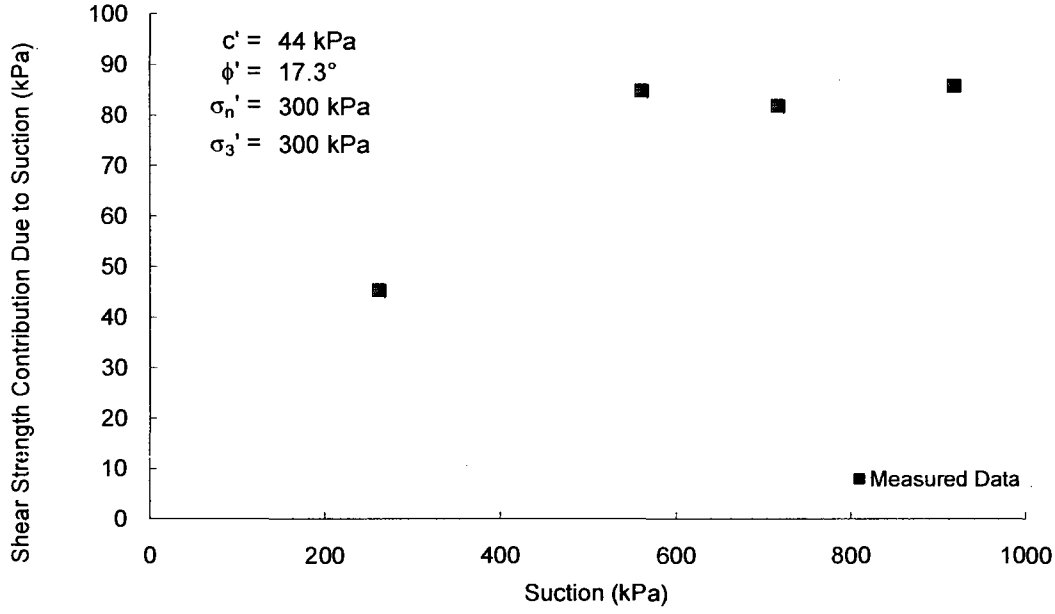

SWRC

Test Method: Axis translation

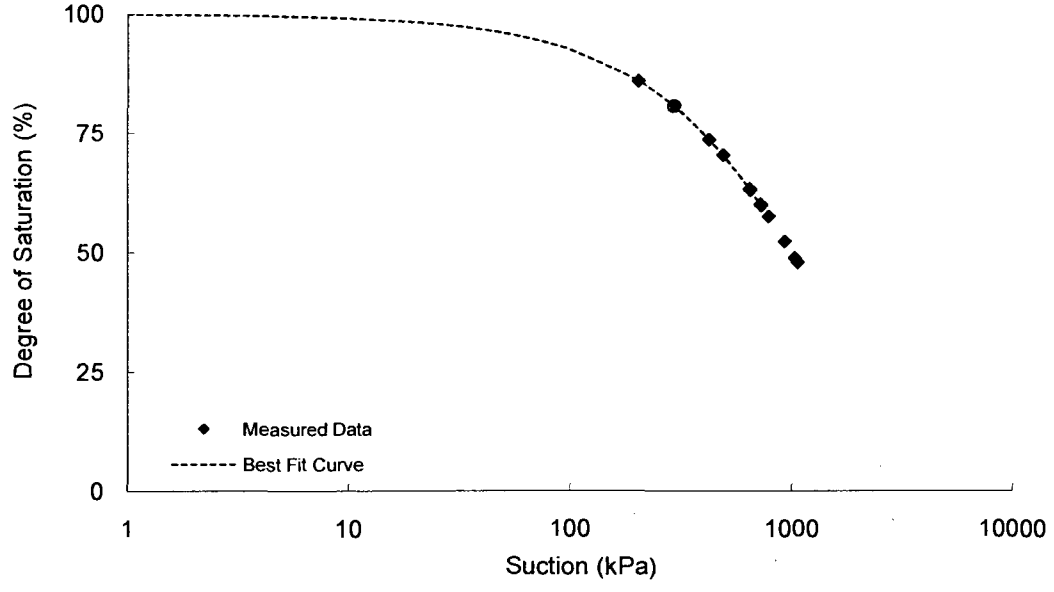

Soil No. 11c

Speswhite kaolin

Tarantino and Tombolato, 2005

Compacted Sample

Sand = 0%, Silt = 80%, Clay = 20%; Liquid Limit = 64, Plasticity Index = 32

Heavy silt, MH

Shear Strength

Test Method: Modified direct shear test

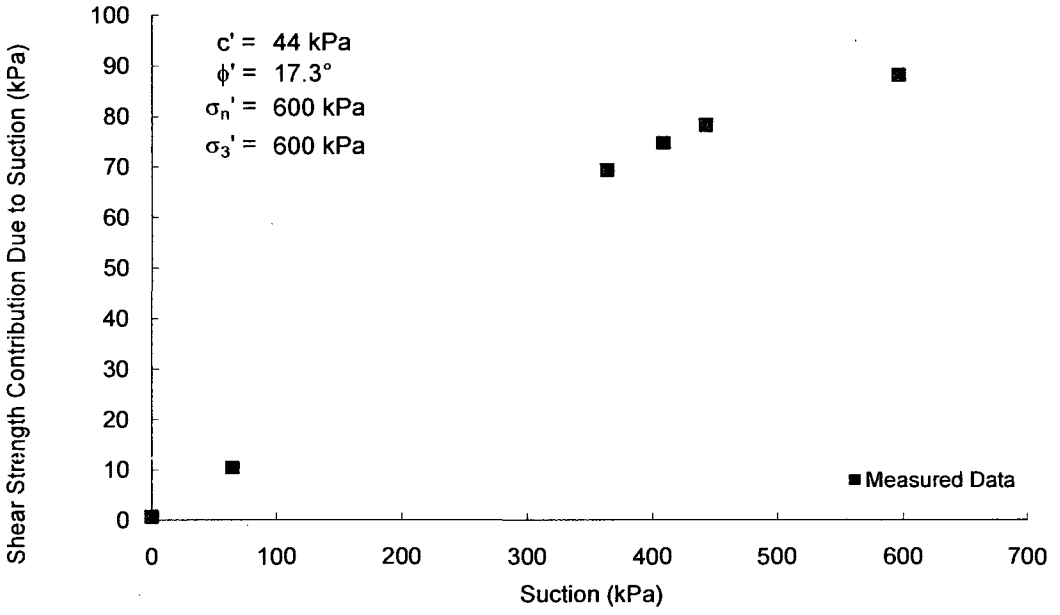

SWRC

Test Method: Axis translation

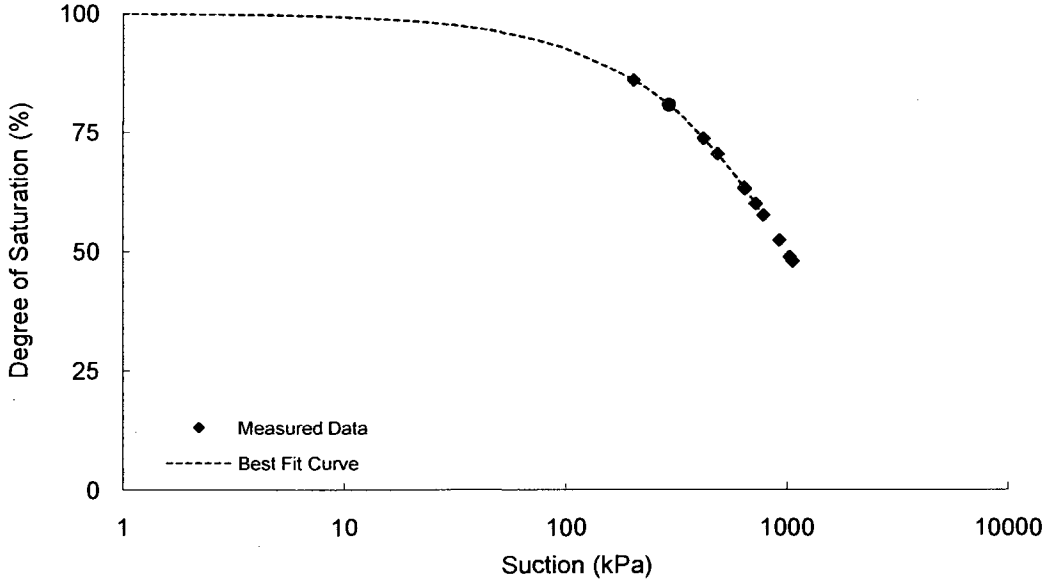

Soil No. 11d

Speswhite kaolin

Tarantino and Tombolato, 2005

Compacted Sample

Sand = 0%, Silt = 80%, Clay = 20%; Liquid Limit = 64, Plasticity Index = 32

Heavy silt, MH

Shear Strength

Test Method: Modified direct shear test

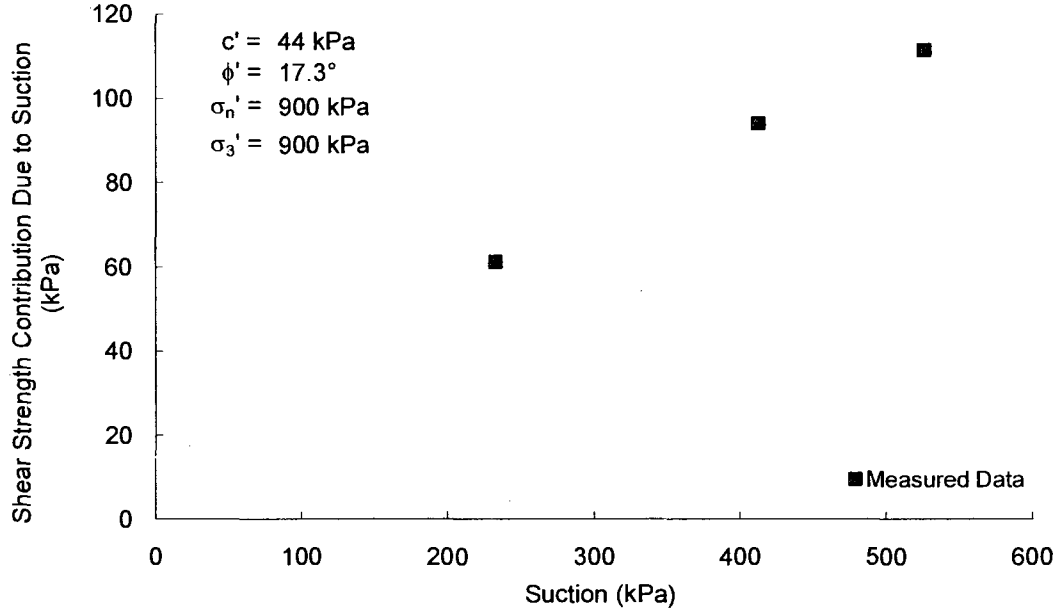

SWRC

Test Method: Axis translation

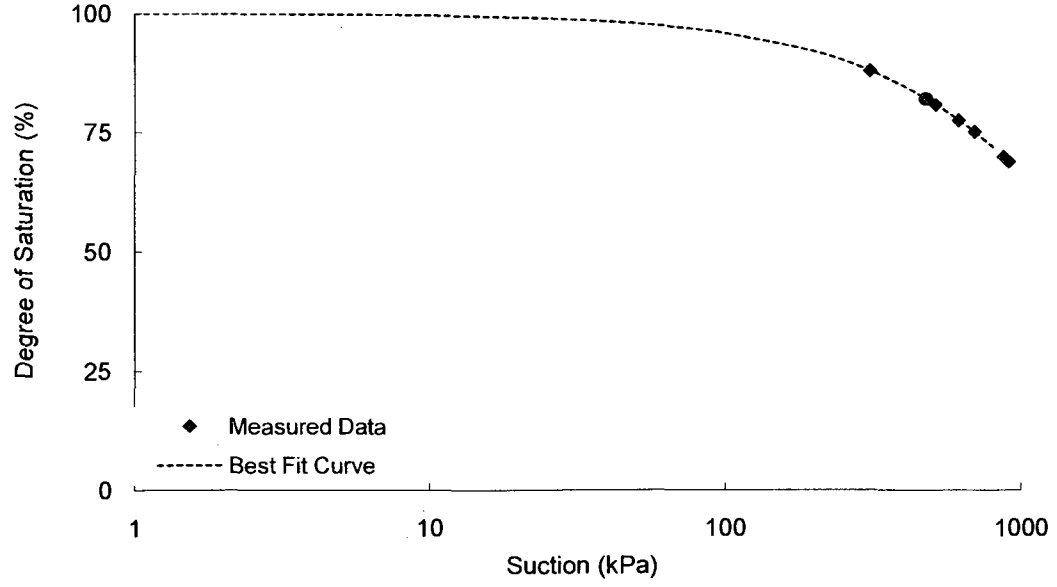

Soil No. 12 **SJ10a**

Khalili, Geiser and Blight, 2004

Undisturbed Soil Specimens

Sand = 33%, Silt and Clay= 67%; Liquid Limit = 39, Plasticity Index = 21

Lean clay, CL

Shear Strength

Test Method: Modified triaxial test

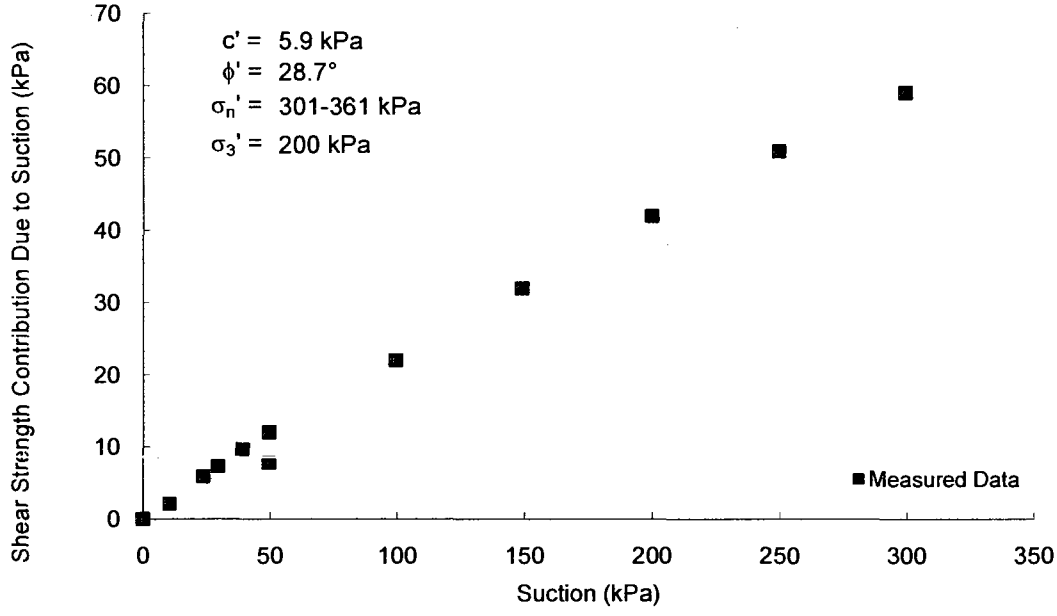

SWRC

Test Method: Pressure plate

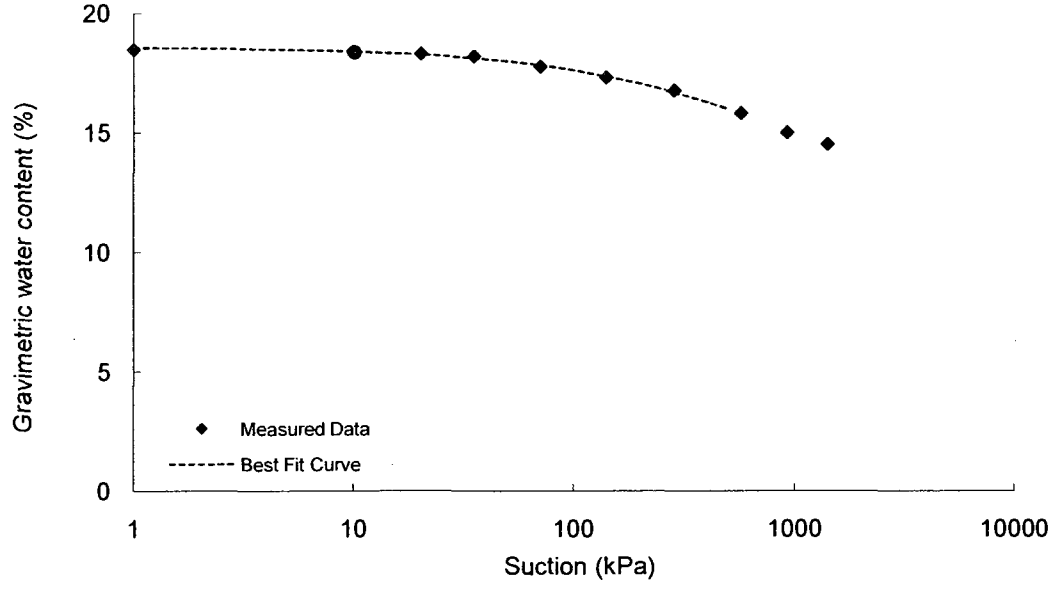

**Gradation curve available in Appendix B

Soil No. 13 **SJ10b**

Khalili, Geiser and Blight, 2004

Undisturbed Soil Specimens

Sand = 26%, Silt and Clay= 74%; Liquid Limit = 33, Plasticity Index = 12

Lean clay, CL

Shear Strength Test Method: Modified triaxial test

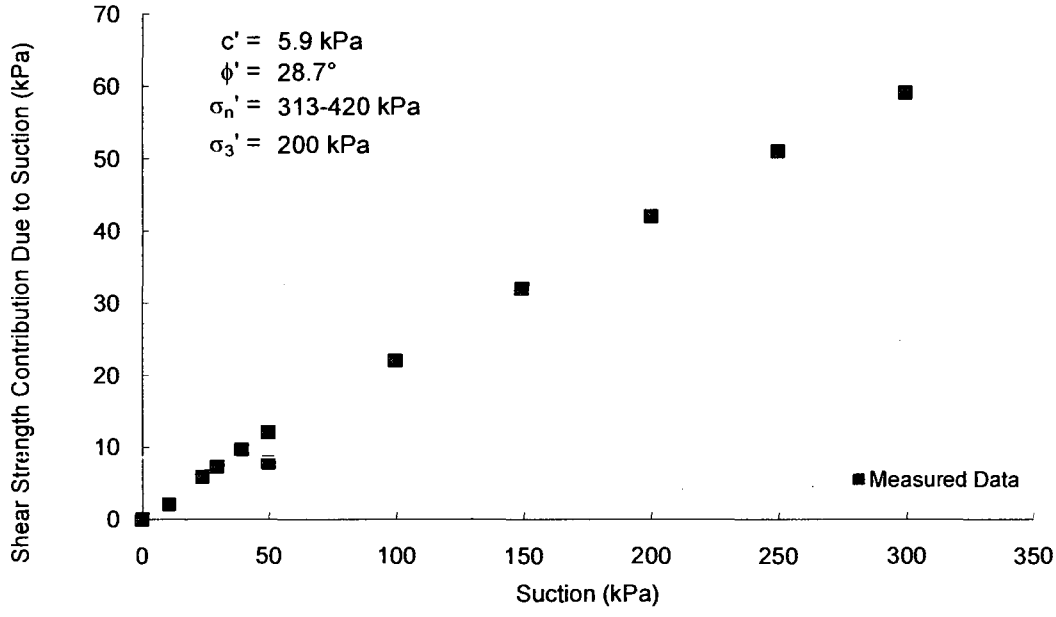

SWRC Test Method: Pressure plate

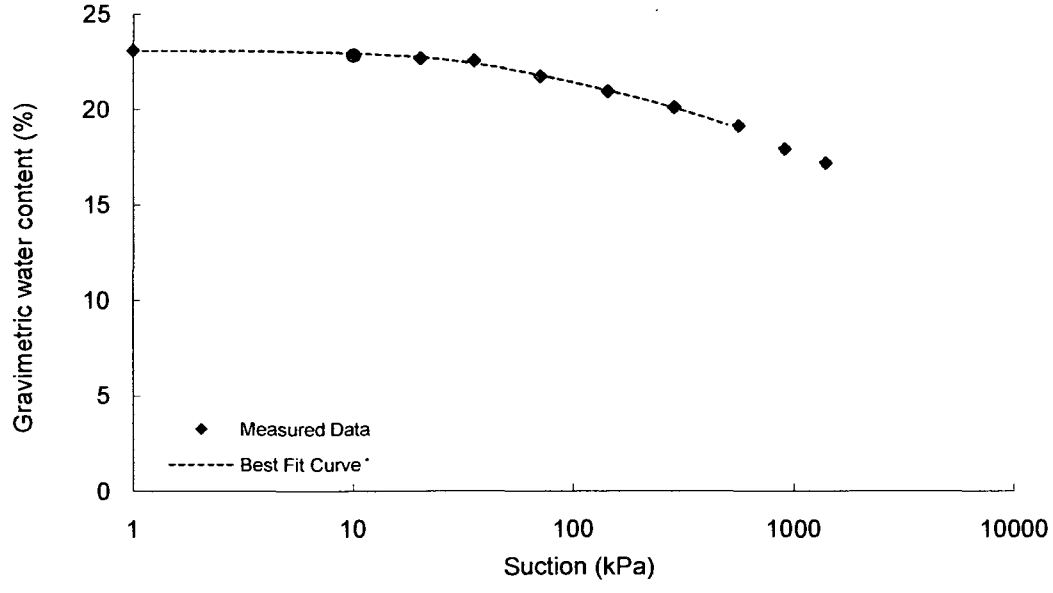

**Gradation curve available in Appendix B

Soil No. 14 **SJ11**

Khalili, Geiser and Blight, 2004

Undisturbed Soil Specimens Sand = 36%, Silt and Clay= 64%; Liquid Limit = 25, Plasticity Index = 6 Silty clay, CL-ML

Shear Strength Test Method: Modified triaxial test

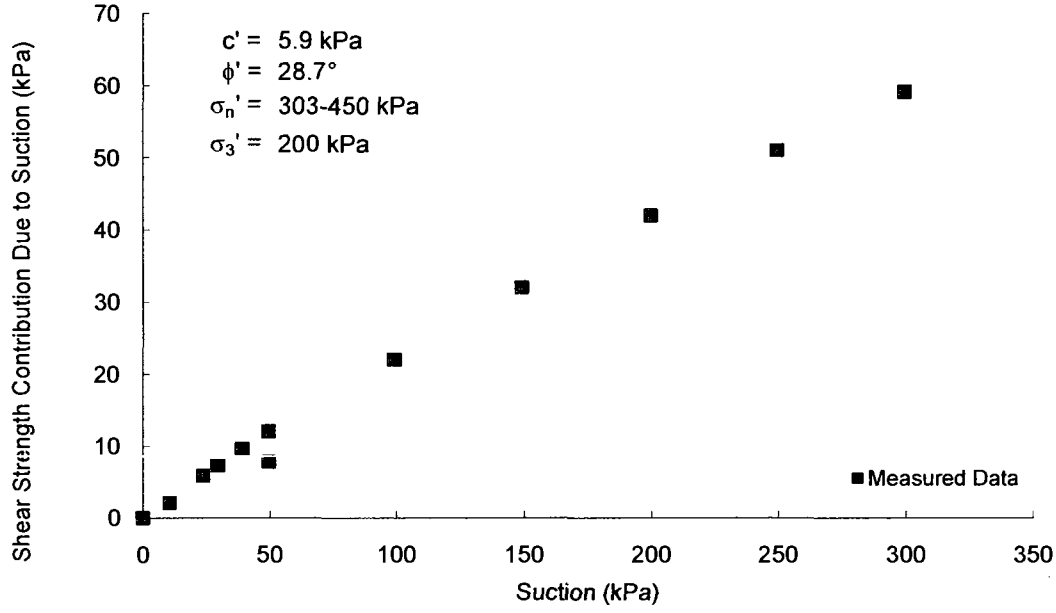

SWRC Test Method: Pressure plate

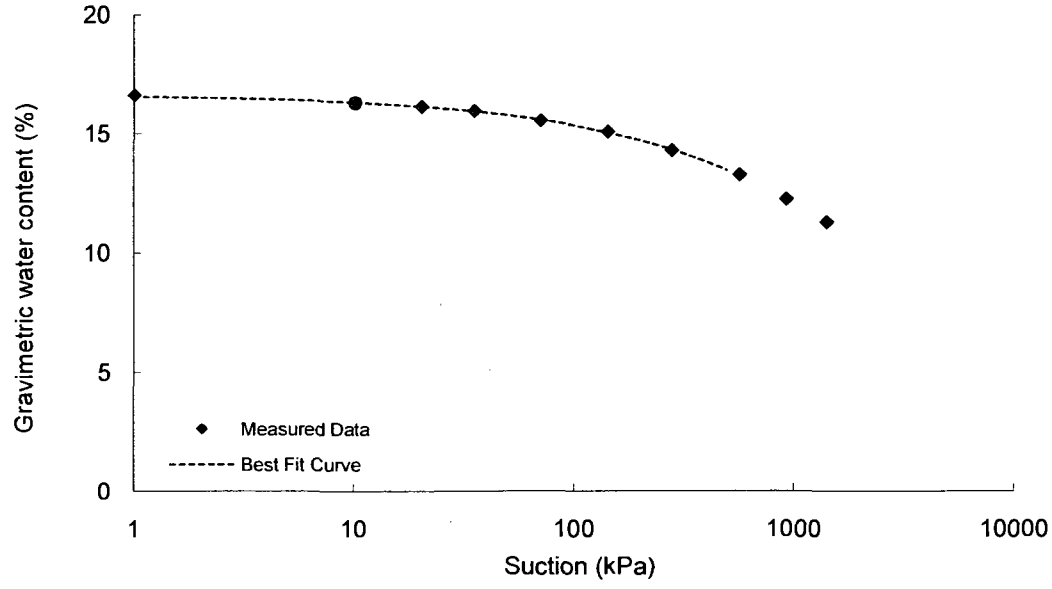

**Gradation curve available in Appendix B

Soil No. 15a

Tailings (50 m)
Rassam and Williams, 1999

Sample Prepared Using Reconstituted from slurry
Sand = 87.1%, Silt = 12.9%, Clay = 0%; Liquid Limit = NP, Plasticity Index = NP

Shear Strength

Test Method: Modified triaxial test

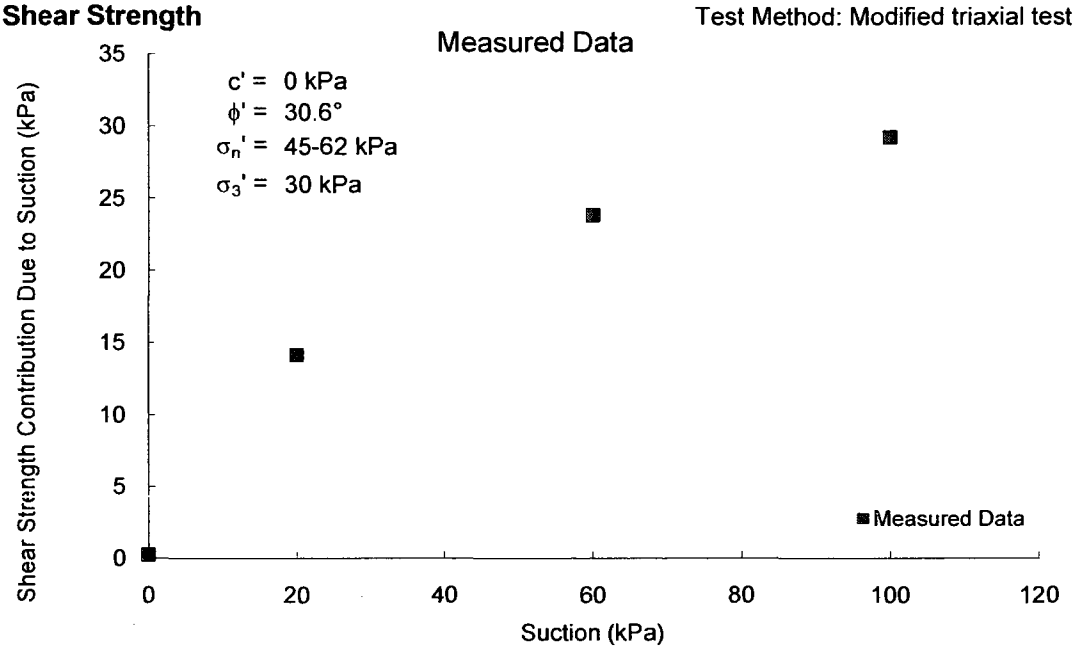

SWRC

Test Method: Pressure plate

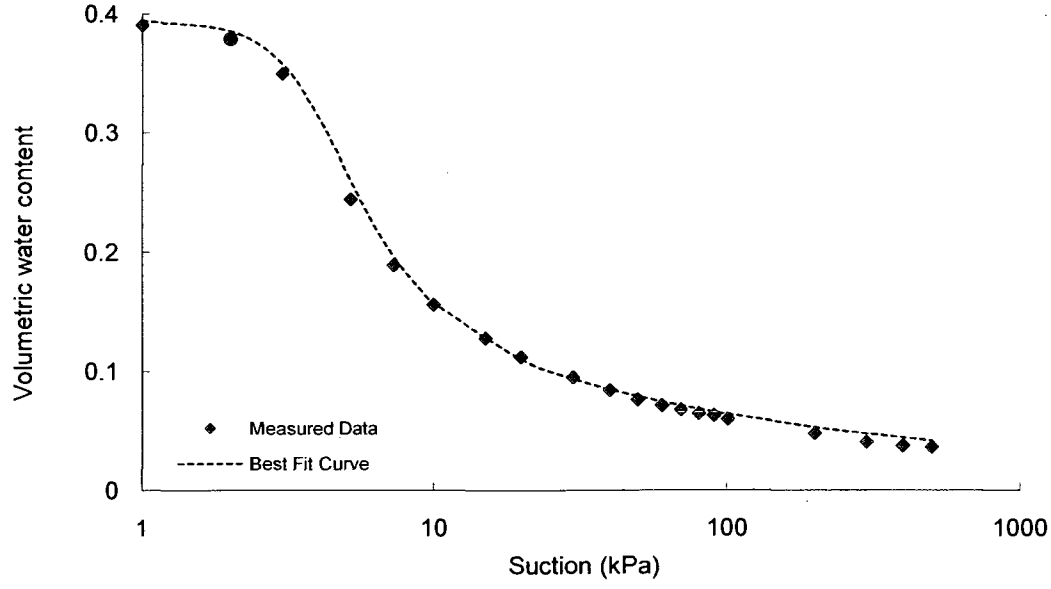

**Gradation curve available in Appendix B

Soil No. 15b

Tailings (50 m)
Rassam and Williams, 1999

Sample Prepared Using Reconstituted from slurry
Sand = 87.1%, Silt = 12.9%, Clay = 0%; Liquid Limit = NP, Plasticity Index = NP

Shear Strength

Test Method: Modified triaxial test

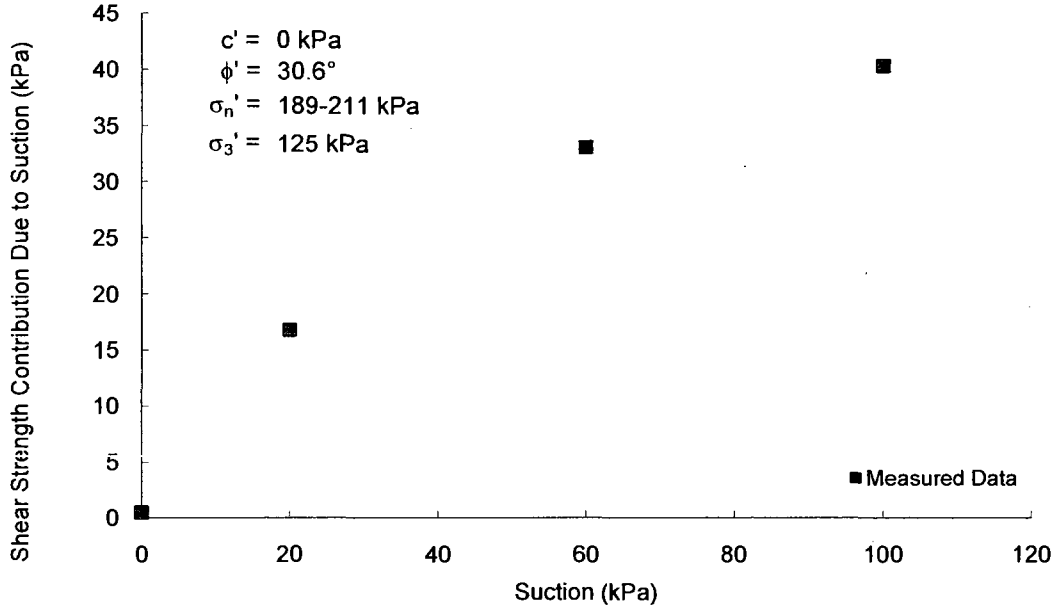

SWRC

Test Method: Pressure plate

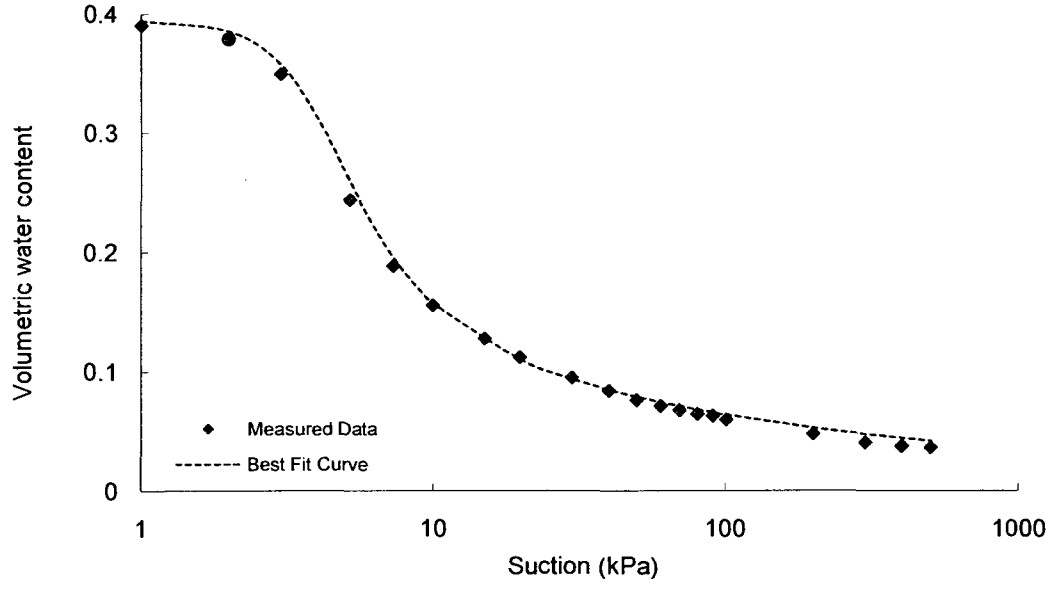

**Gradation curve available in Appendix B

Soil No. 15c

Tailings (50 m)
Rassam and Williams, 1999

Sample Prepared Using Reconstituted from slurry
Sand = 87.1%, Silt = 12.9%, Clay = 0%; Liquid Limit = NP, Plasticity Index = NP

Shear Strength

Test Method: Modified triaxial test

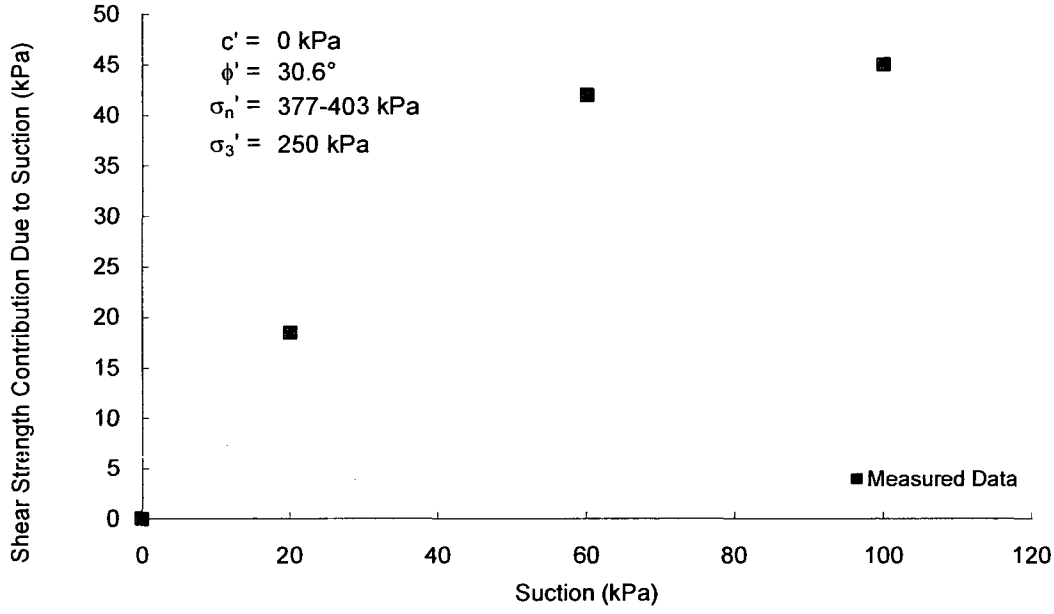

SWRC

Test Method: Pressure plate

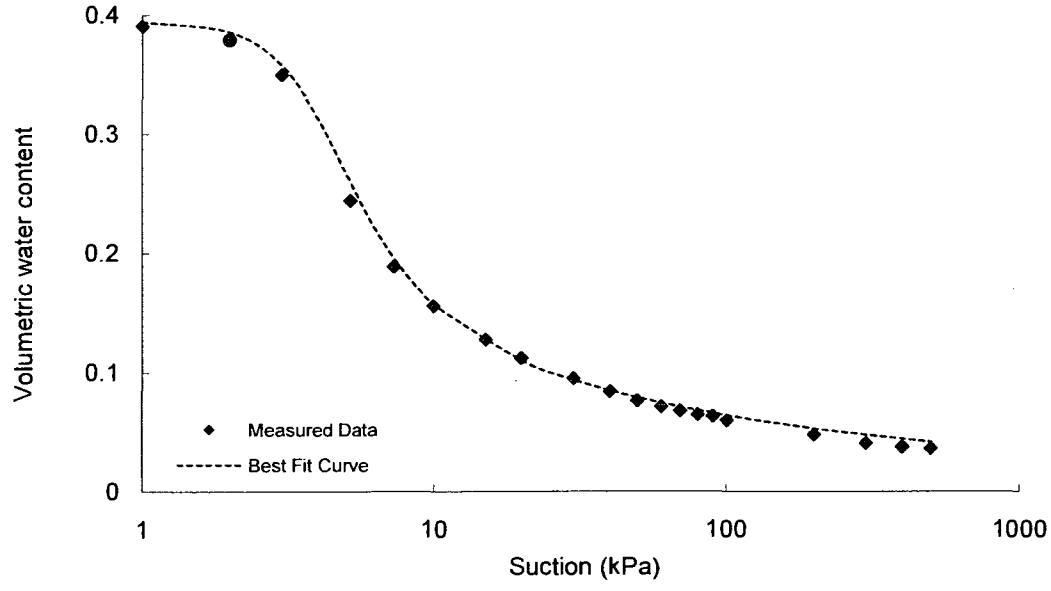

**Gradation curve available in Appendix B

Soil No. 16a

Tailings (150 m)
Rassam and Williams, 1999

Sample Prepared Using Reconstituted from slurry
Sand = 71%, Silt = 29%, Clay = 0%; Liquid Limit = NP, Plasticity Index = NP

Shear Strength

Test Method: Modified triaxial test

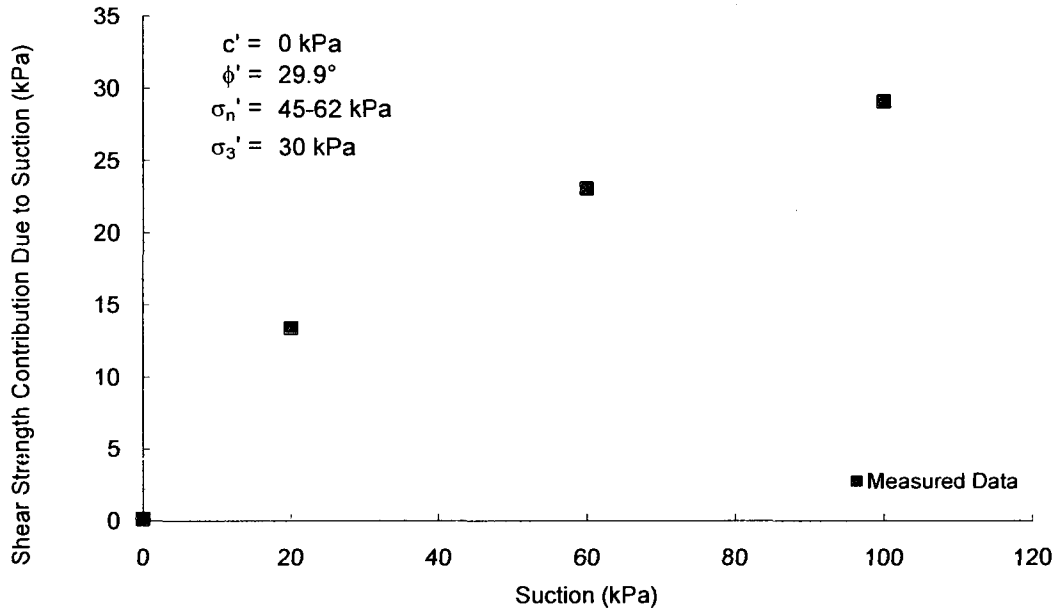

SWRC

Test Method: Pressure plate

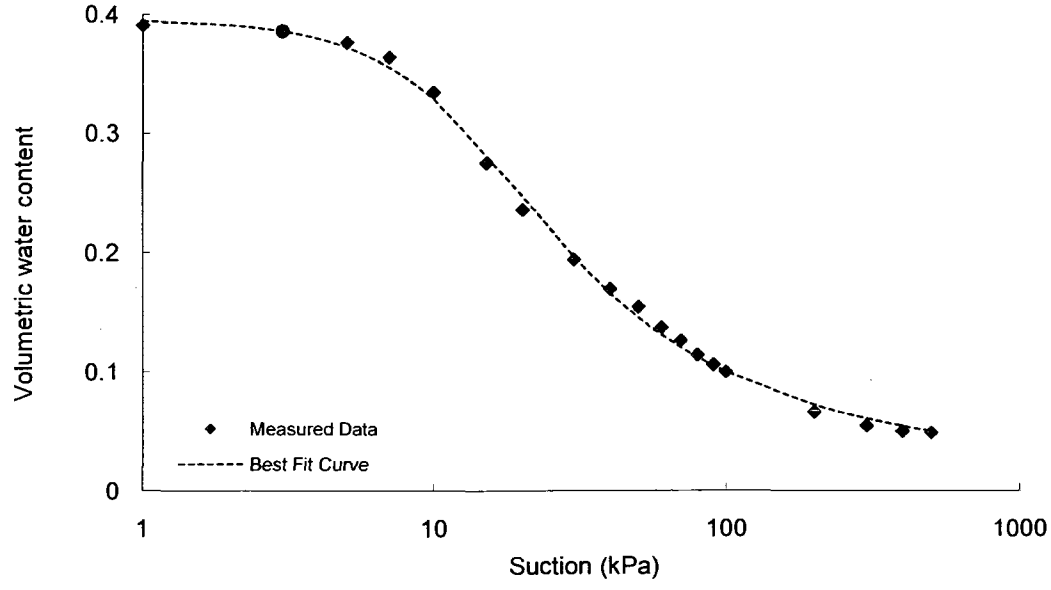

**Gradation curve available in Appendix B

Soil No. 16b

Tailings (150 m)
Rassam and Williams, 1999

Sample Prepared Using Reconstituted from slurry
Sand = 71%, Silt = 29%, Clay = 0%; Liquid Limit = NP, Plasticity Index = NP

Shear Strength

Test Method: Modified triaxial test

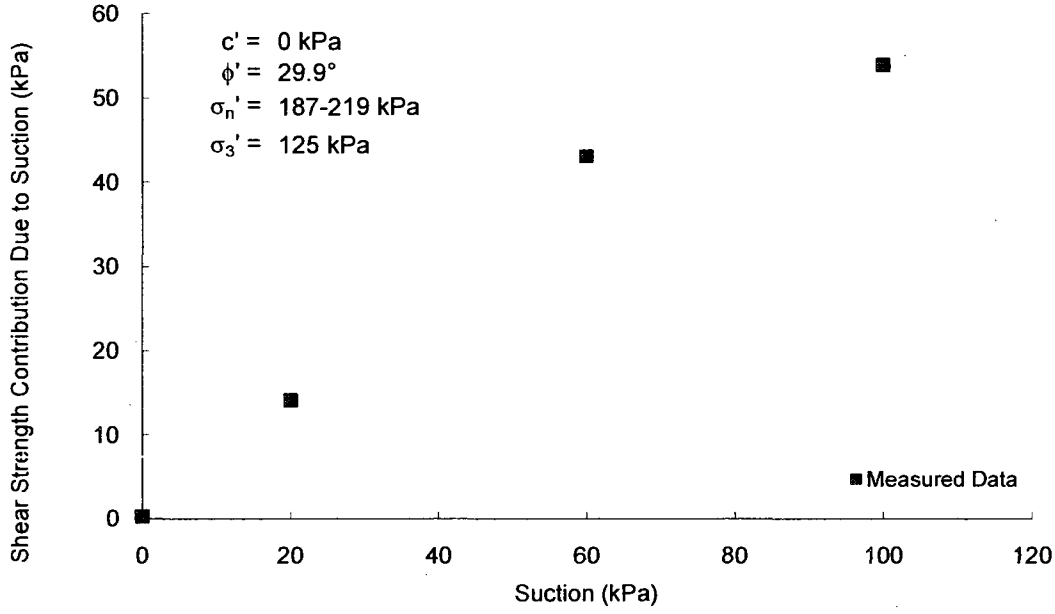

SWRC

Test Method: Pressure plate

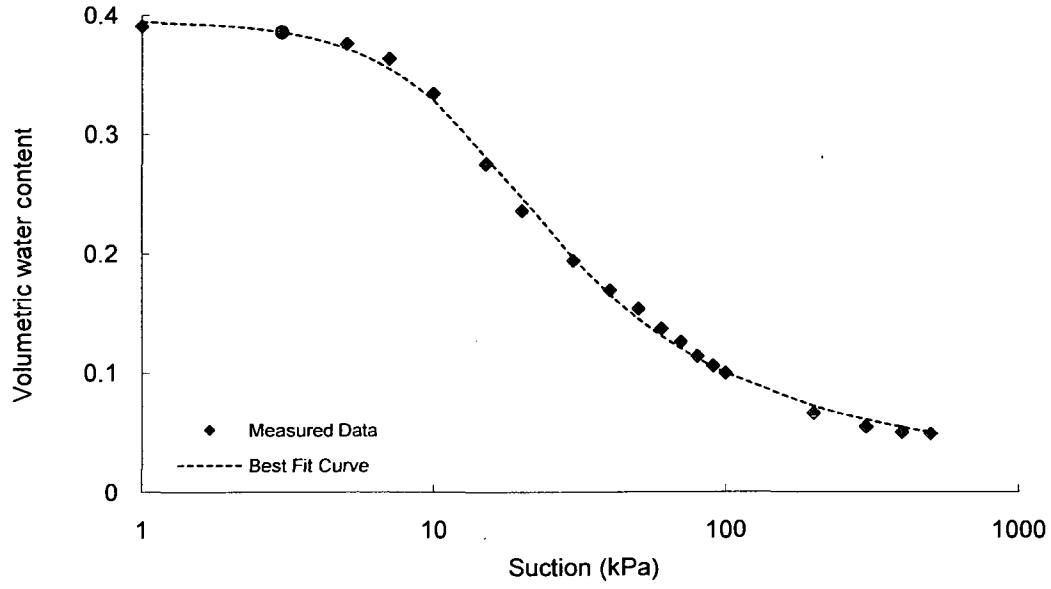

**Gradation curve available in Appendix B

Soil No. 16c

Tailings (150 m)
Rassam and Williams, 1999

Sample Prepared Using Reconstituted from slurry
Sand = 71%, Silt = 29%, Clay = 0%; Liquid Limit = NP, Plasticity Index = NP

Shear Strength

Test Method: Modified triaxial test

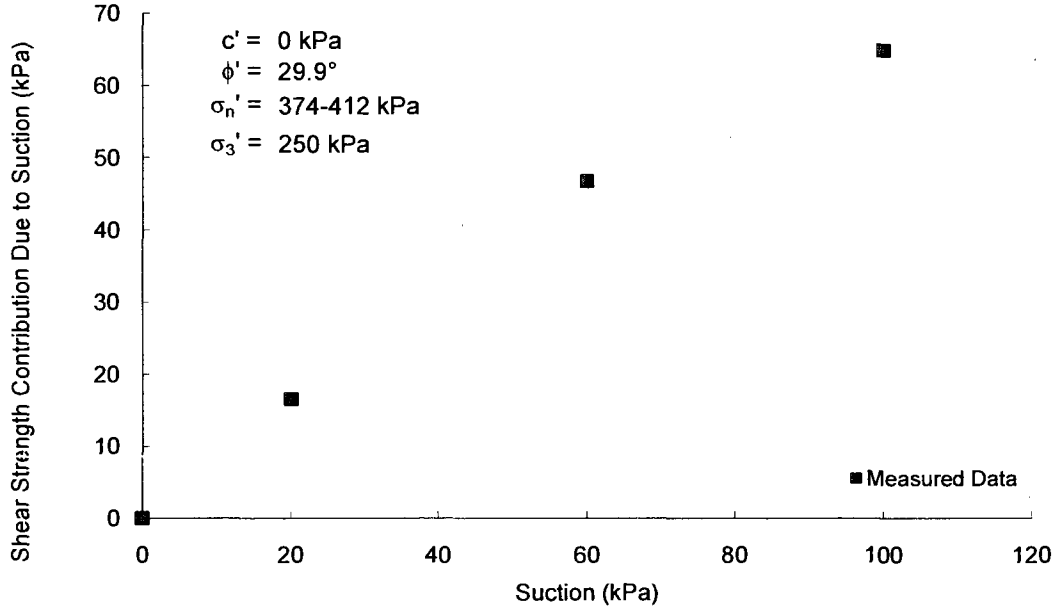

SWRC

Test Method: Pressure plate

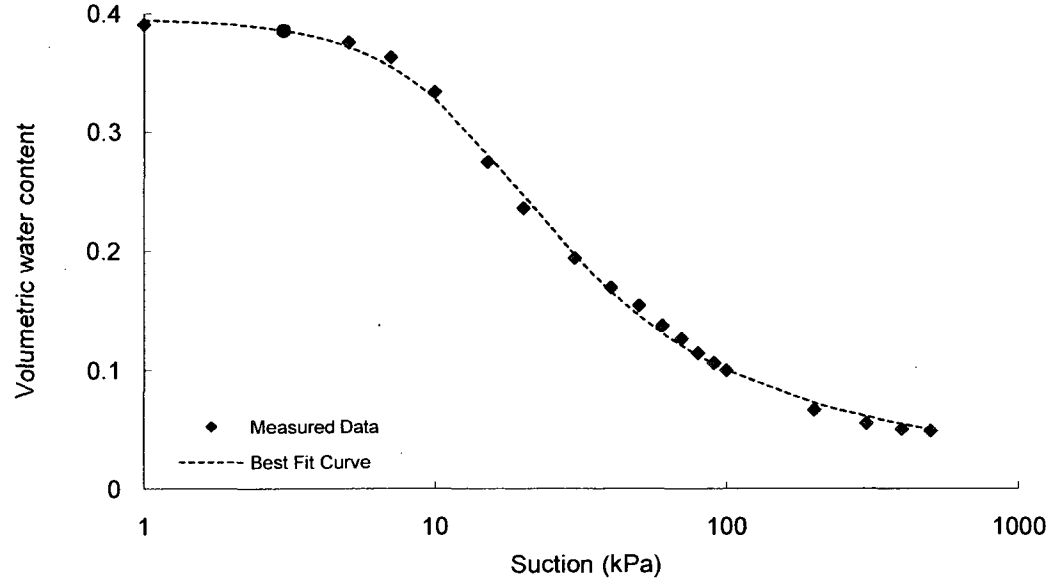

**Gradation curve available in Appendix B

Soil No. 17a

Brazilian laterite
Rohm and Vilar, 1995

Undisturbed Soil Specimens
Sand = 52%, Silt = 19%, Clay = 29%; Liquid Limit = 38, Plasticity Index = 14
Lean clay, CL

Shear Strength

Test Method: Modified triaxial test

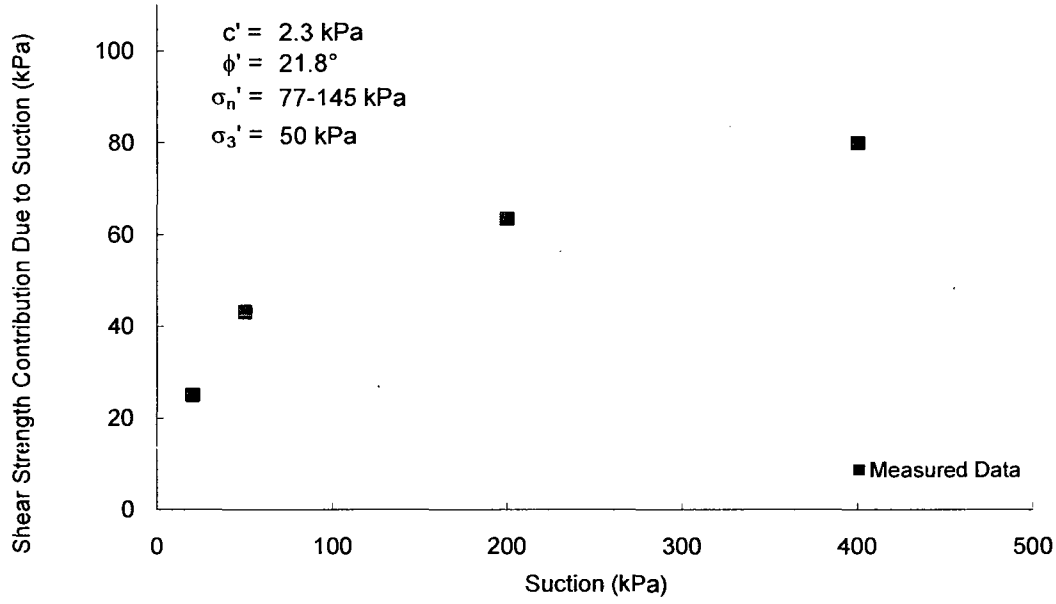

SWRC

Test Method: unknown

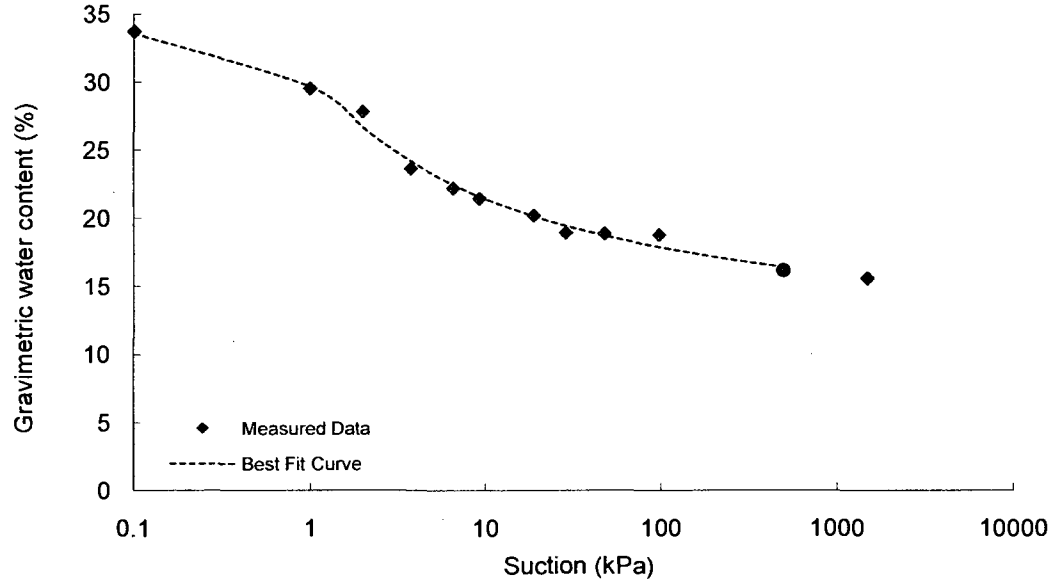

**Gradation curve available in Appendix B

Soil No. 17b

Brazilian laterite
Rohm and Vilar, 1995

Undisturbed Soil Specimens
Sand = 52%, Silt = 19%, Clay = 29%; Liquid Limit = 38, Plasticity Index = 14
Lean clay, CL

Shear Strength

Test Method: Modified triaxial test

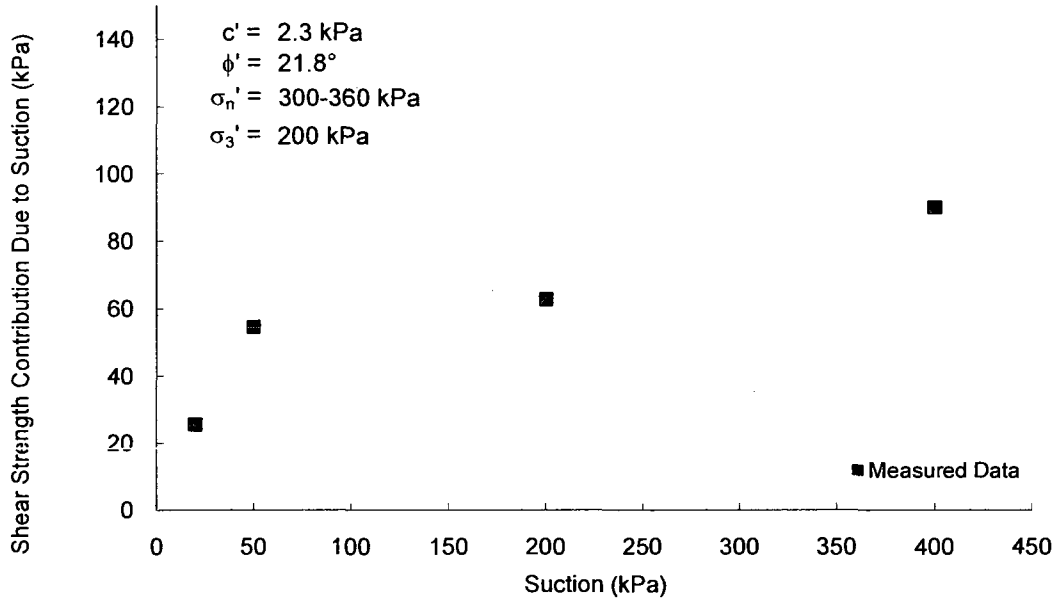

SWRC

Test Method: unknown

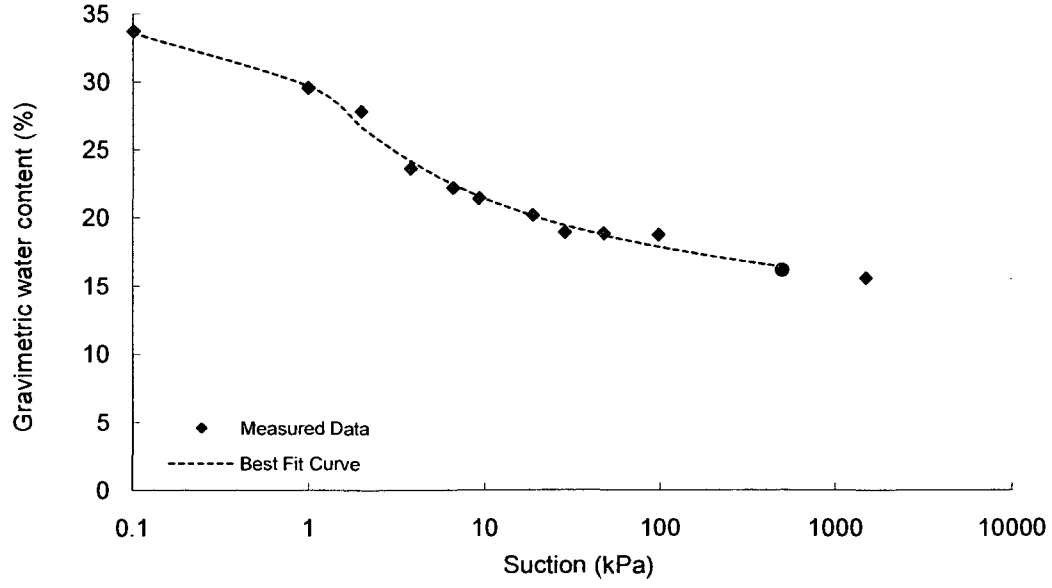

**Gradation curve available in Appendix B

Soil No. 17c

Brazilian laterite
Rohm and Vilar, 1995

Undisturbed Soil Specimens
Sand = 52%, Silt = 19%, Clay = 29%; Liquid Limit = 38, Plasticity Index = 14
Lean clay, CL

Shear Strength

Test Method: Modified triaxial test

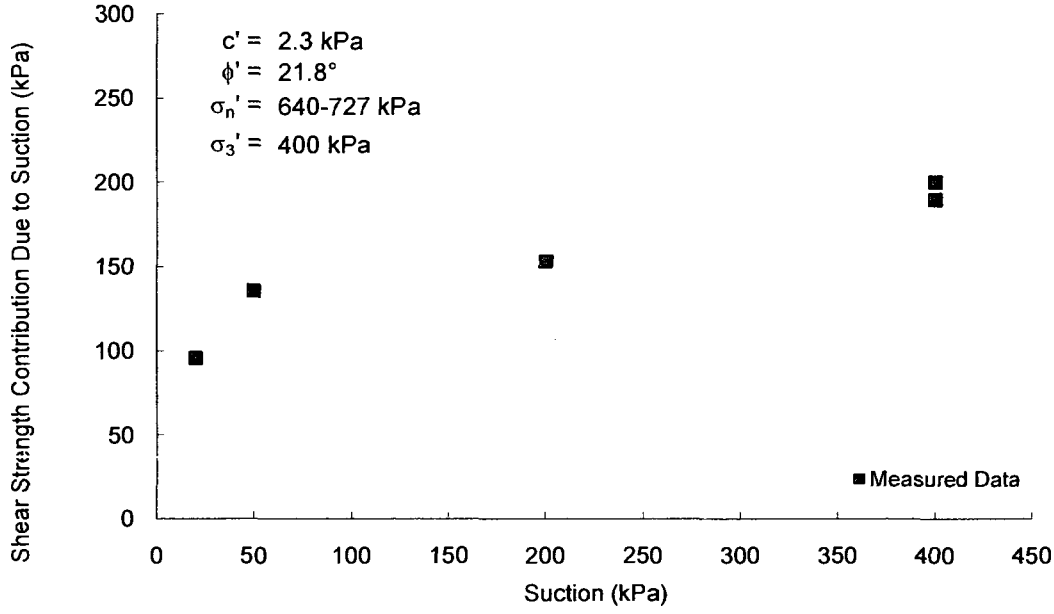

SWRC

Test Method: Pressure cell

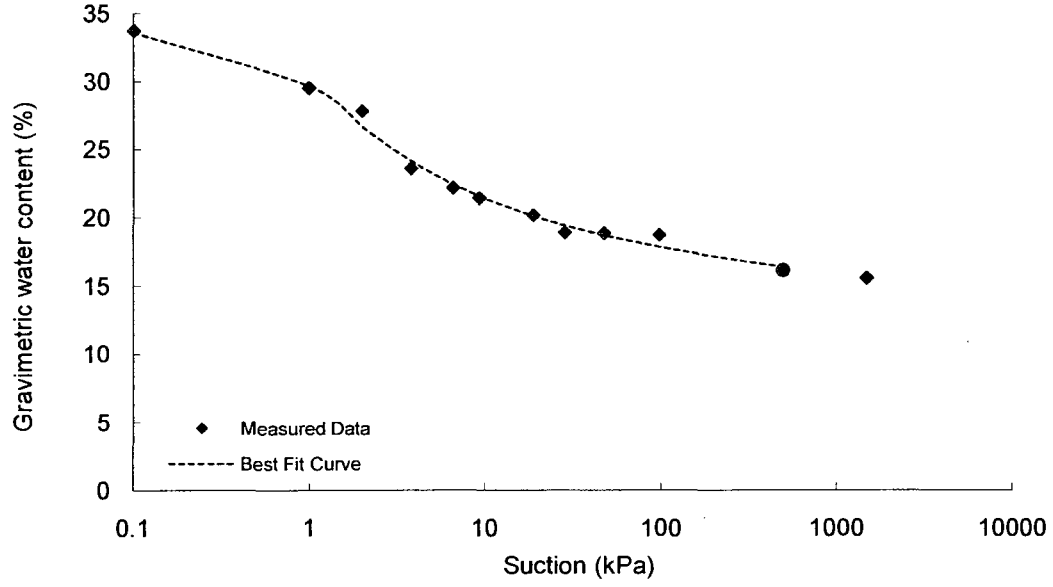

**Gradation curve available in Appendix B

Soil No. 18

Serro do Mar soil
Abramento and Carvalho, 1989

Undisturbed Soil Specimens
Sand = 74%, Silt = 13%, Clay = 13%; Liquid Limit = 39, Plasticity Index = 14
Lean clay, CL

Shear Strength

Test Method: Modified triaxial test

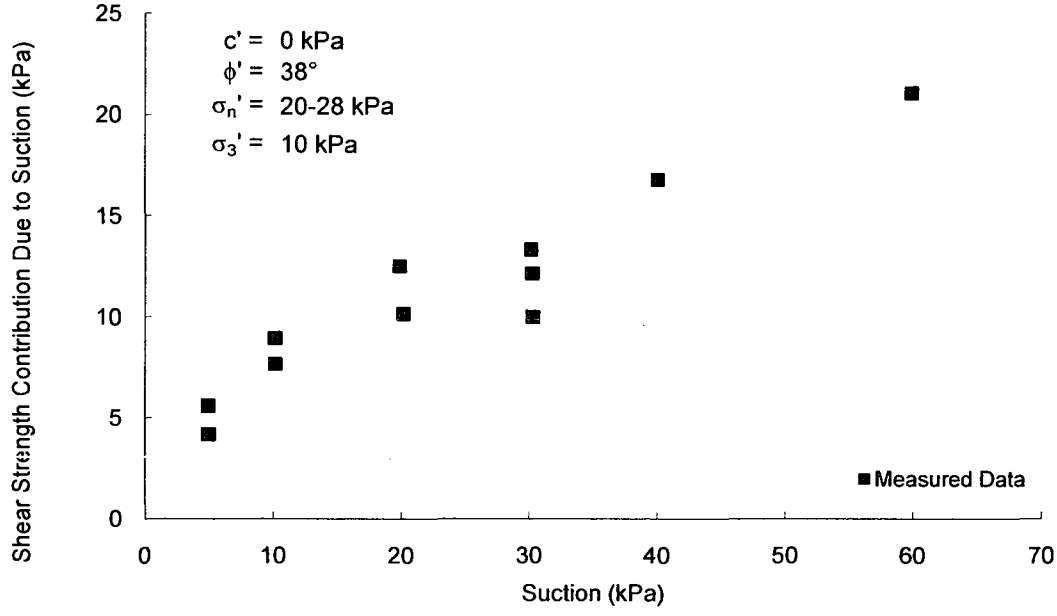

SWRC

Test Method: Indirect (created from pre-test information)

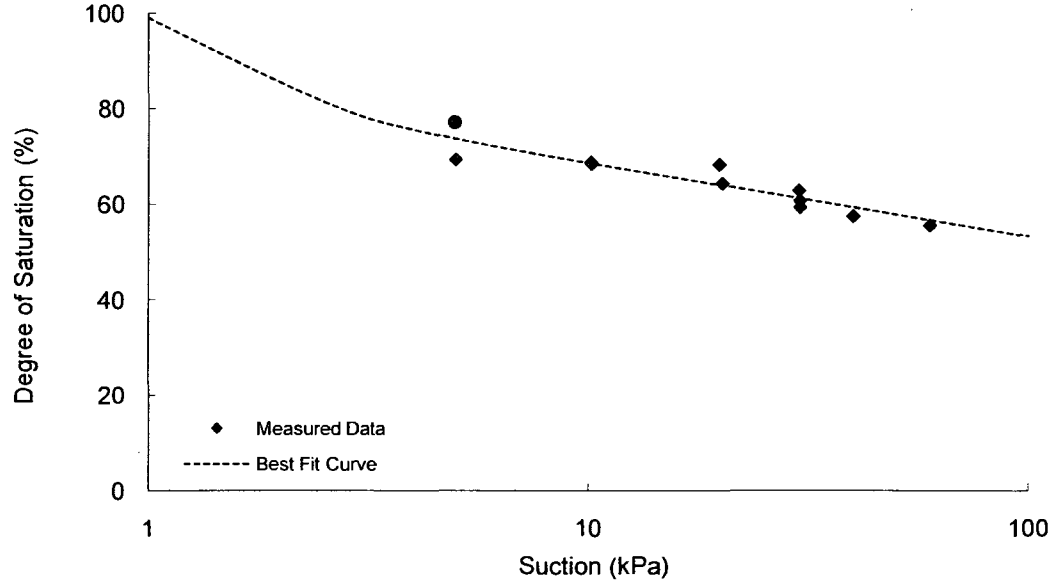

Soil No. 19

Sandy clay loam
Adams, 1996

Compacted Sample
Sand = 48.1%, Silt = 23.6%, Clay = 28.3%; Liquid Limit = 33, Plasticity Index = 14
Lean clay, CL

Shear Strength

Test Method: Modified triaxial test

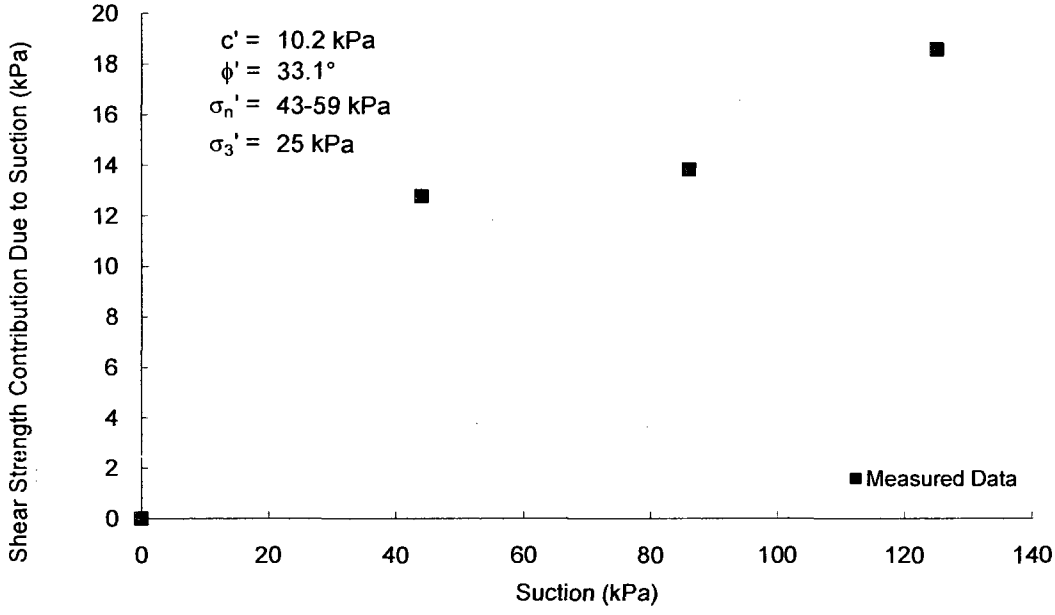

SWRC

Test Method: Pressure plate

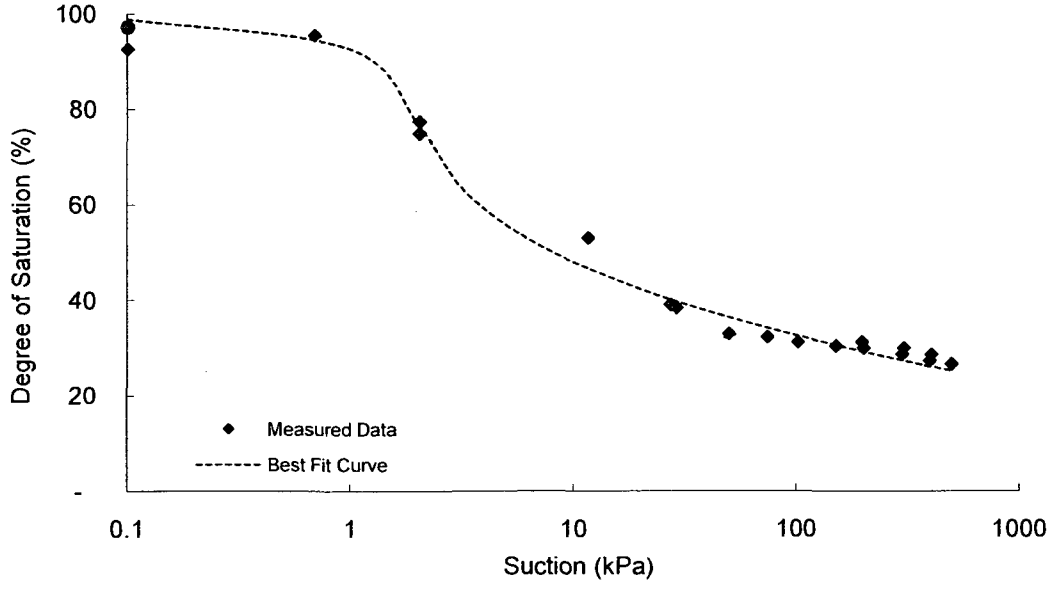

Soil No. 20

Frankston Fine
Donald, 1957

Compacted Sample
Sand = 0%, Silt = 100%, Clay = 0%
Lean silt, ML

Shear Strength

Test Method: Modified direct shear test

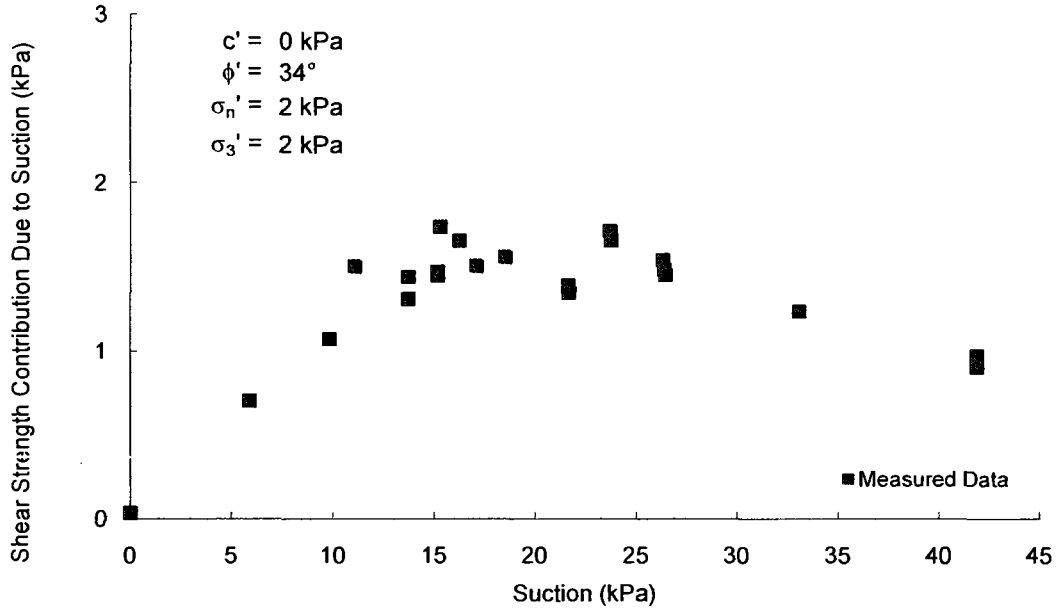

SWRC

Test Method: Pressure plate

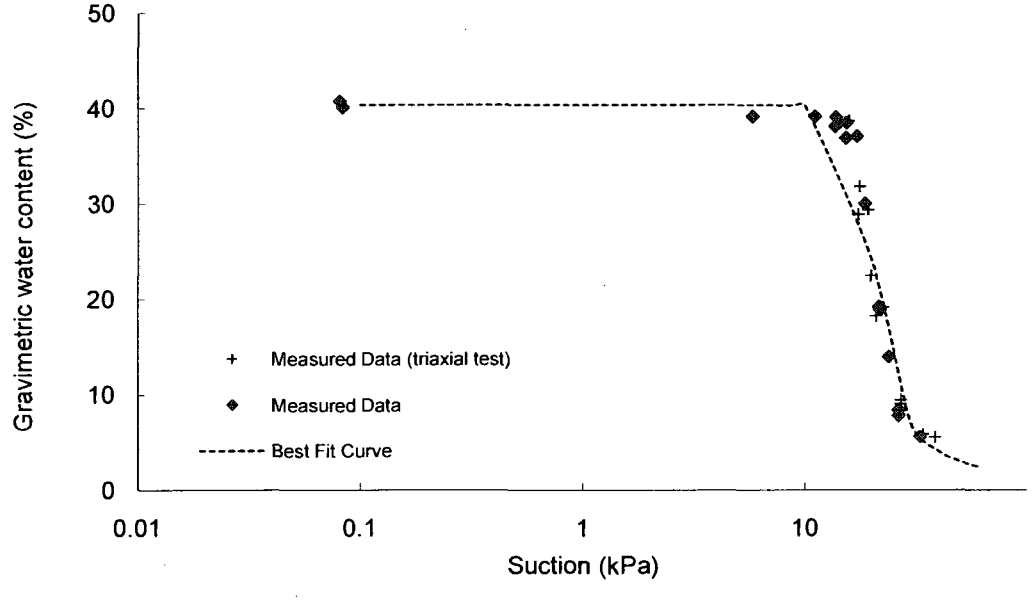

**Gradation curve available in Appendix B

Soil No. 21

Medium Frankston
Donald, 1957

Compacted Sample
Sand = 34.8%, Silt = 65.2%, Clay = 0%
Sandy lean silt (ML)

Shear Strength

Test Method: Modified direct shear test

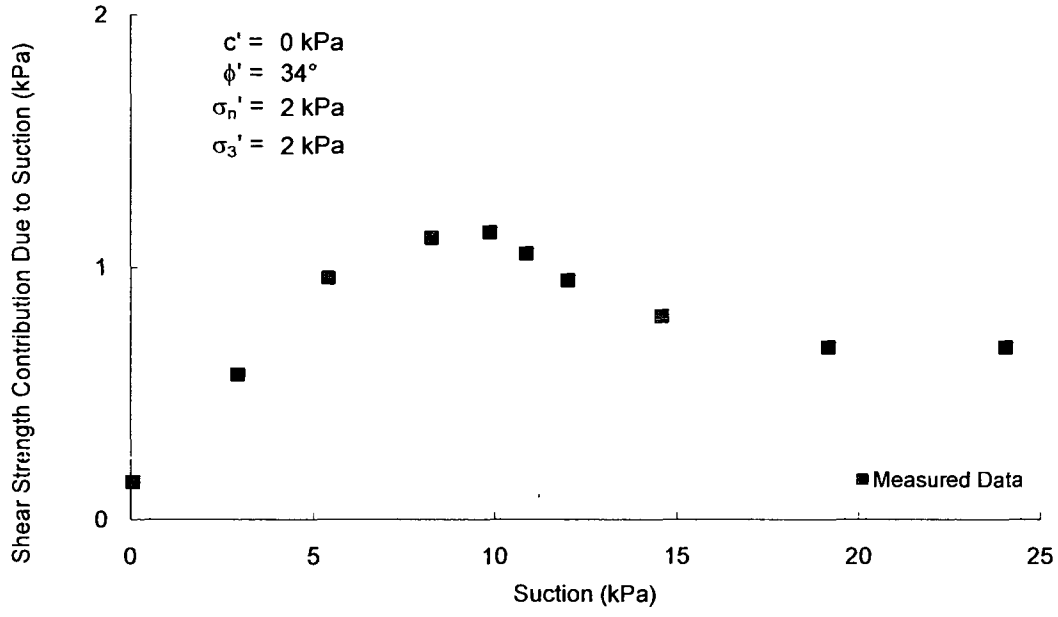

SWRC

Test Method: Pressure plate

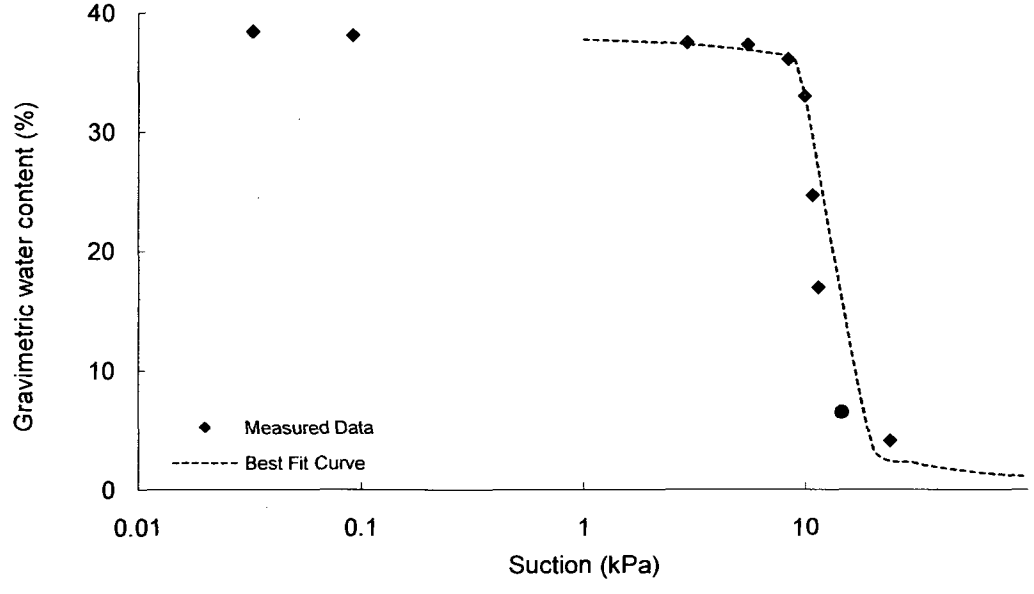

**Gradation curve available in Appendix B

Soil No. 22

Graded Frankston
Donald, 1957

Compacted Sample
Sand = 38.5%, Silt = 61.5%, Clay = 0%
Sandy lean silt (ML)

Shear Strength

Test Method: Modified triaxial test

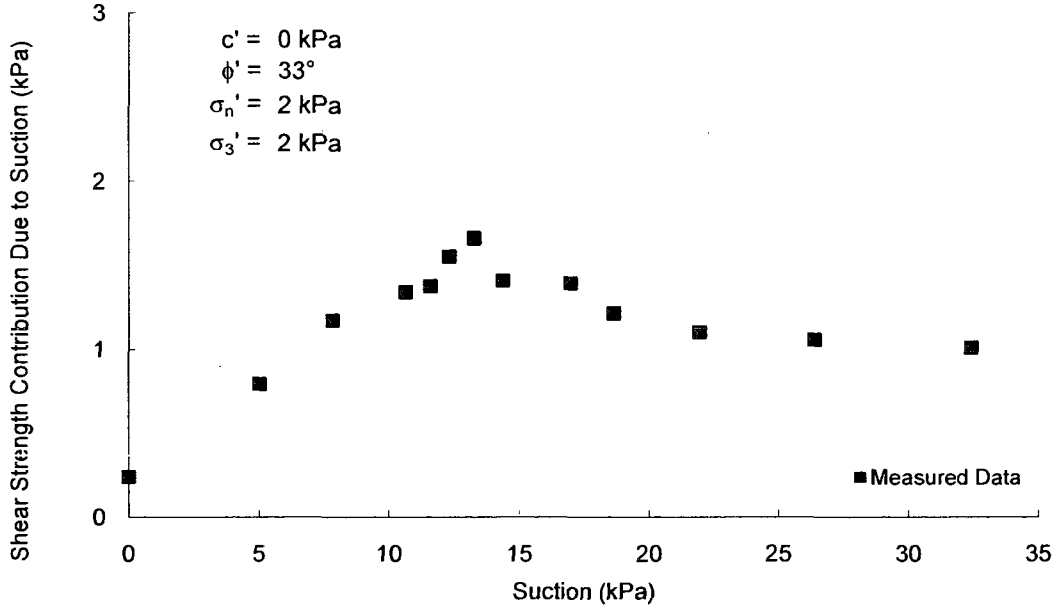

SWRC

Test Method: Pressure plate

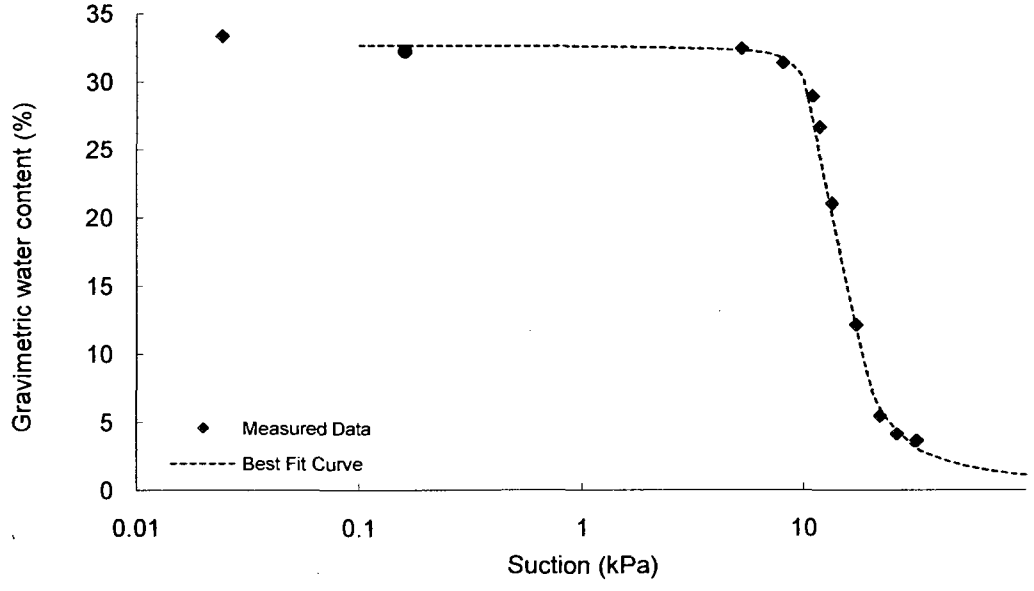

**Gradation curve available in Appendix B

Soil No. 23

Brown sand
Donald, 1957

Compacted Sample
Sand = 68.9%, Silt = 31.1%, Clay = 0%
Silty sand (SM)

Shear Strength

Test Method: Modified triaxial test

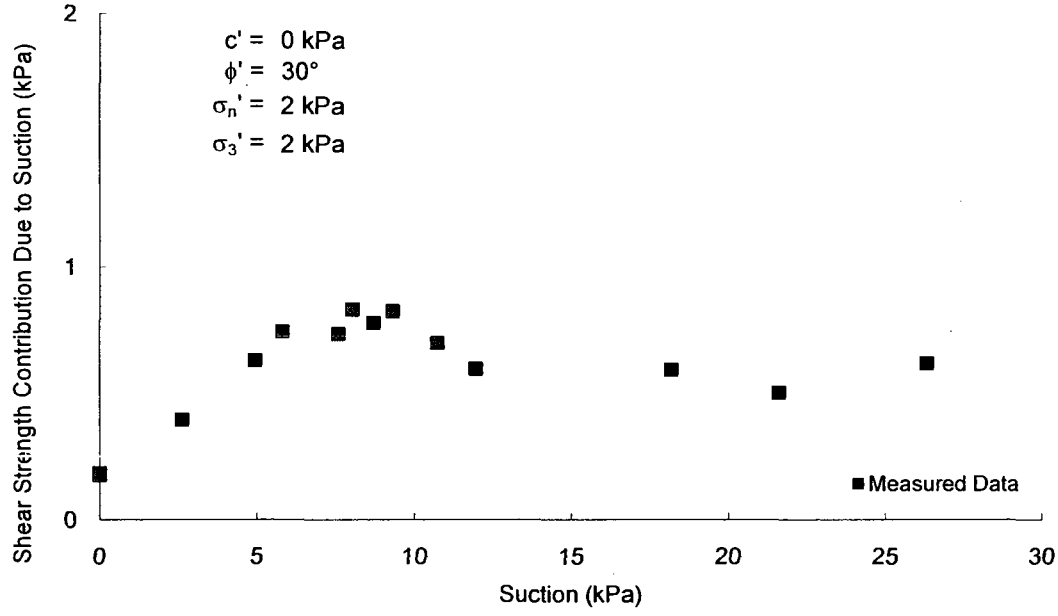

SWRC

Test Method: Pressure plate

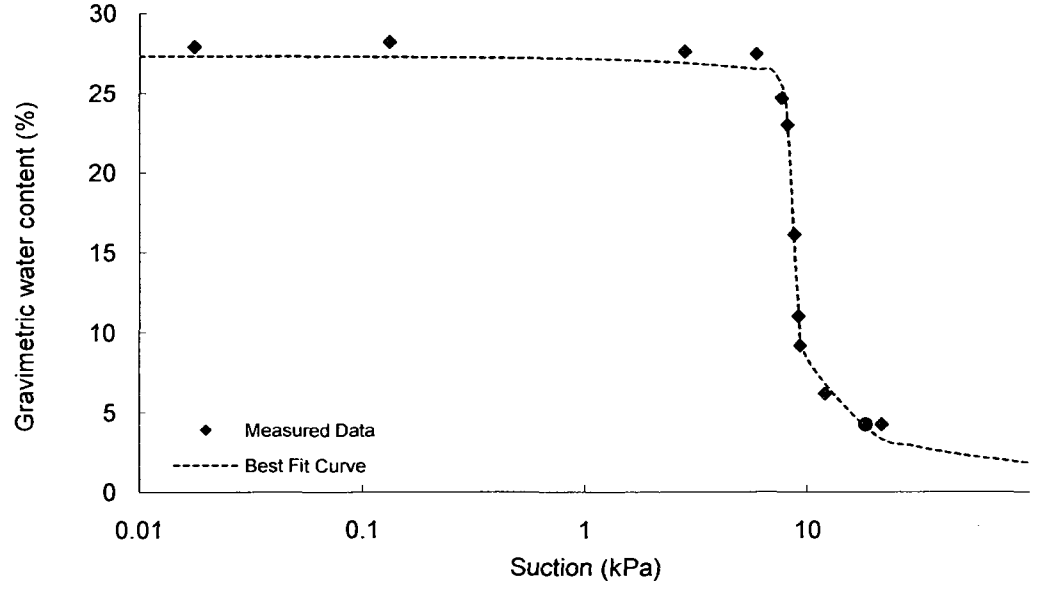

**Gradation curve available in Appendix B

Soil No. 24a

Copper tailings

Drumright and Nelson, 1995; Drumright, 1989

Sample Prepared Using i) static compact; ii) slurry preparation
Sand = 59%, Silt = 32%, Clay = 9%
Silty sand, SM

Shear Strength

Test Method: Modified triaxial test

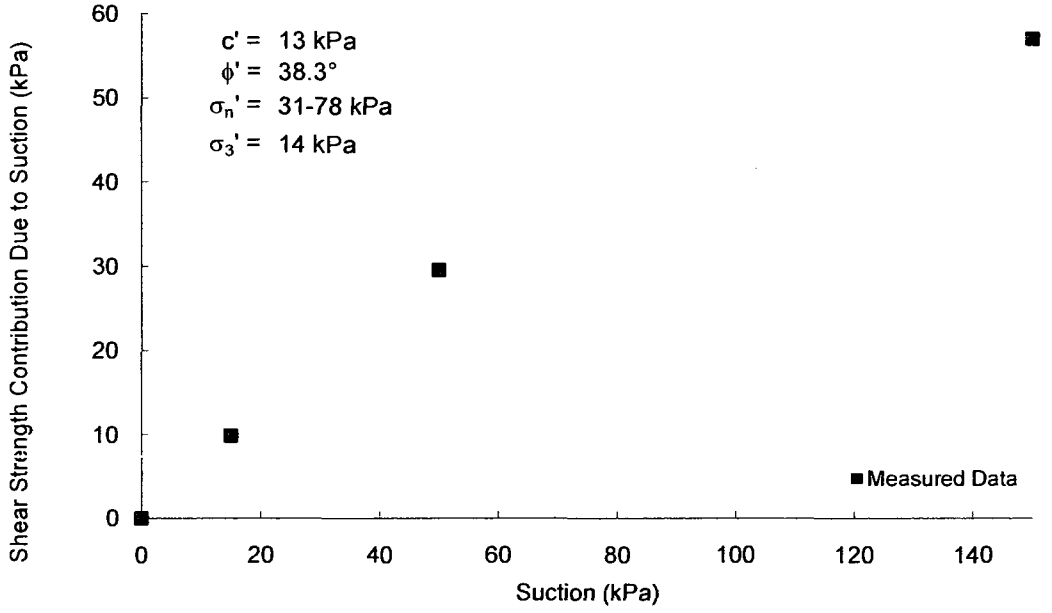

SWRC

Test Method: Pressure plate

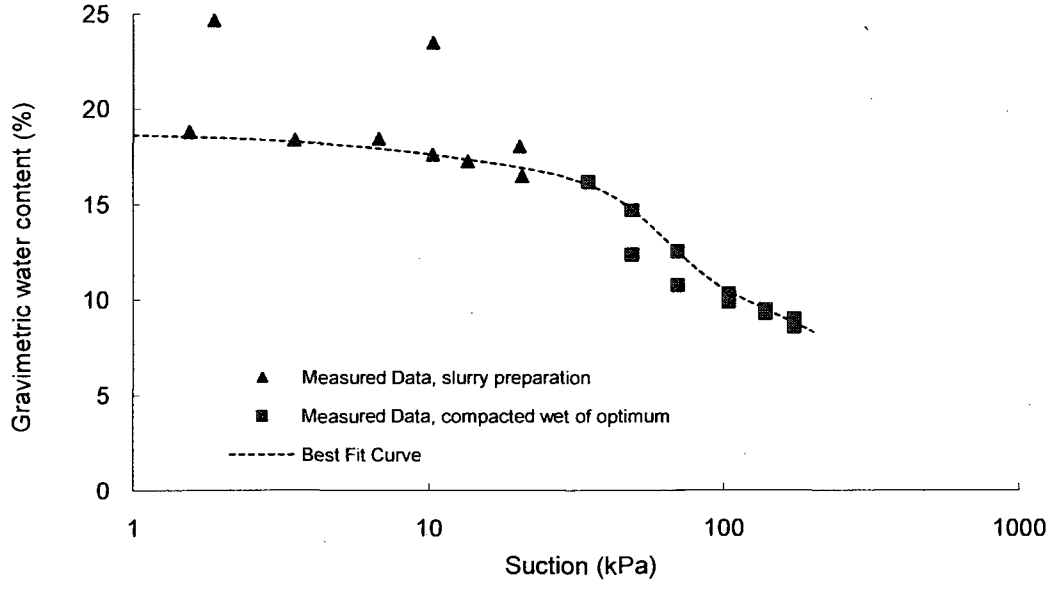

**Gradation curve available in Appendix B

Soil No. 24b

Copper tailings

Drumright and Nelson, 1995; Drumright, 1989

Sample Prepared Using i) static compact; ii) slurry preparation
Sand = 59%, Silt = 32%, Clay = 9%
Silty sand, SM

Shear Strength

Test Method: Modified triaxial test

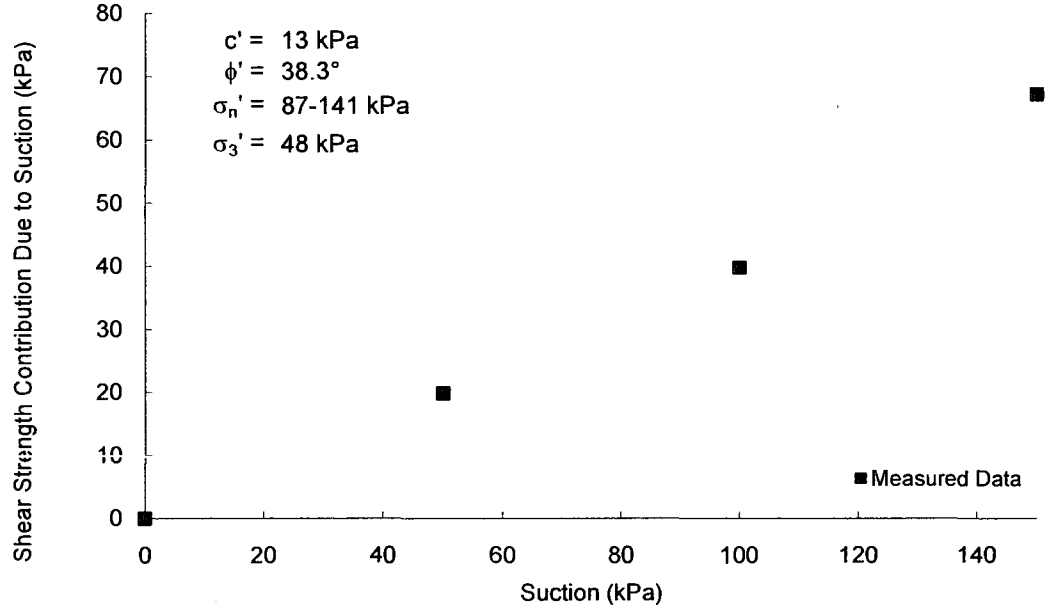

SWRC

Test Method: Pressure plate

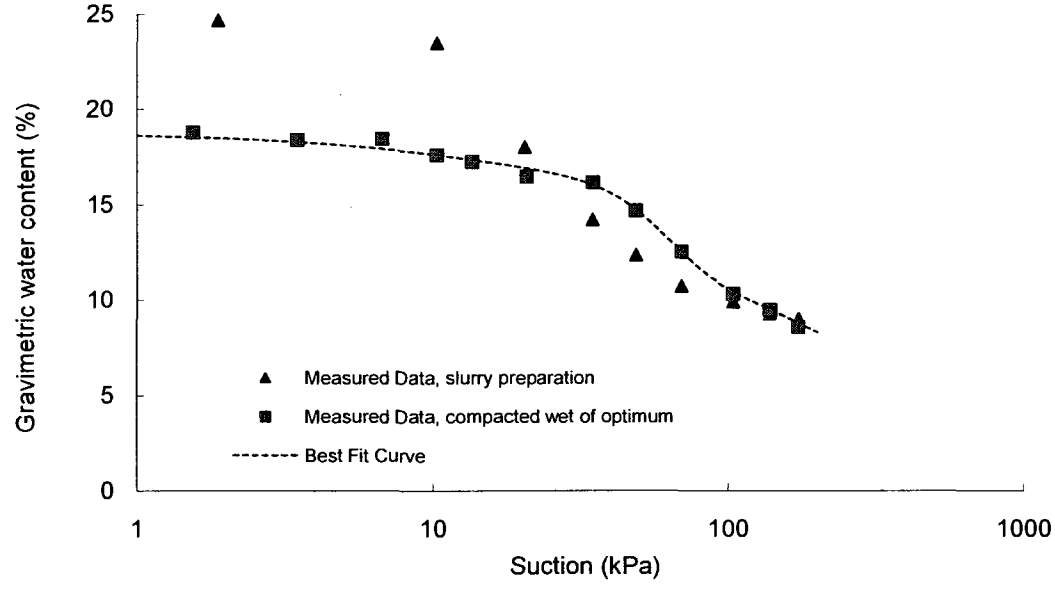

**Gradation curve available in Appendix B

Soil No. 24c

Copper tailings

Drumright and Nelson, 1995; Drumright, 1989

Sample Prepared Using i) static compact; ii) slurry preparation
Sand = 59%, Silt = 32%, Clay = 9%
Silty sand, SM

Shear Strength

Test Method: Modified triaxial test

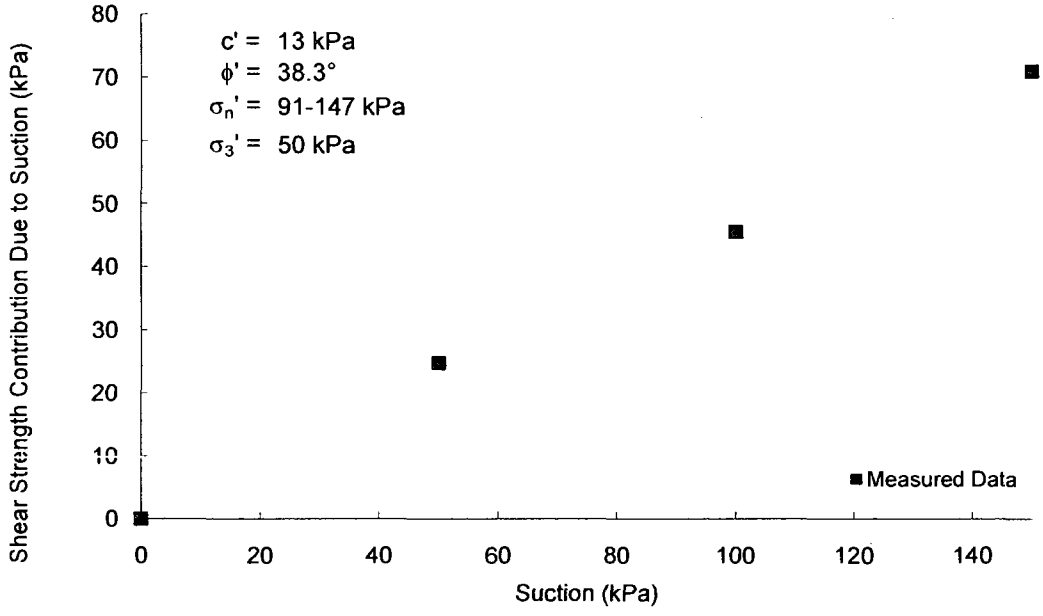

SWRC

Test Method: Pressure plate

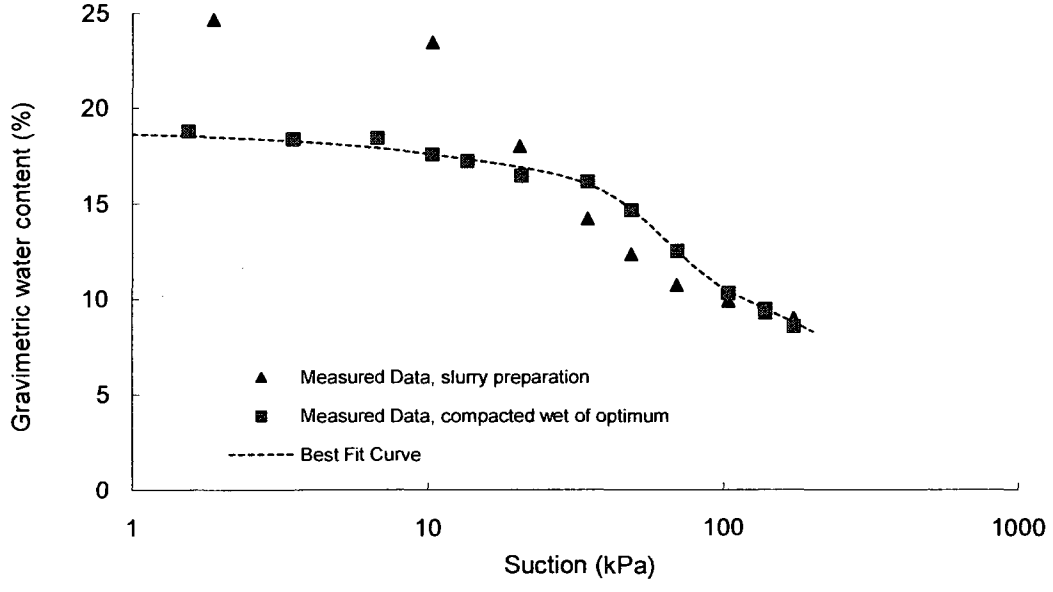

**Gradation curve available in Appendix B

Soil No. 24d

Copper tailings

Drumright and Nelson, 1995; Drumright, 1989

Sample Prepared Using i) static compact; ii) slurry preparation Sand = 59%, Silt = 32%, Clay = 9% Silty sand, SM

Shear Strength

Test Method: Modified triaxial test

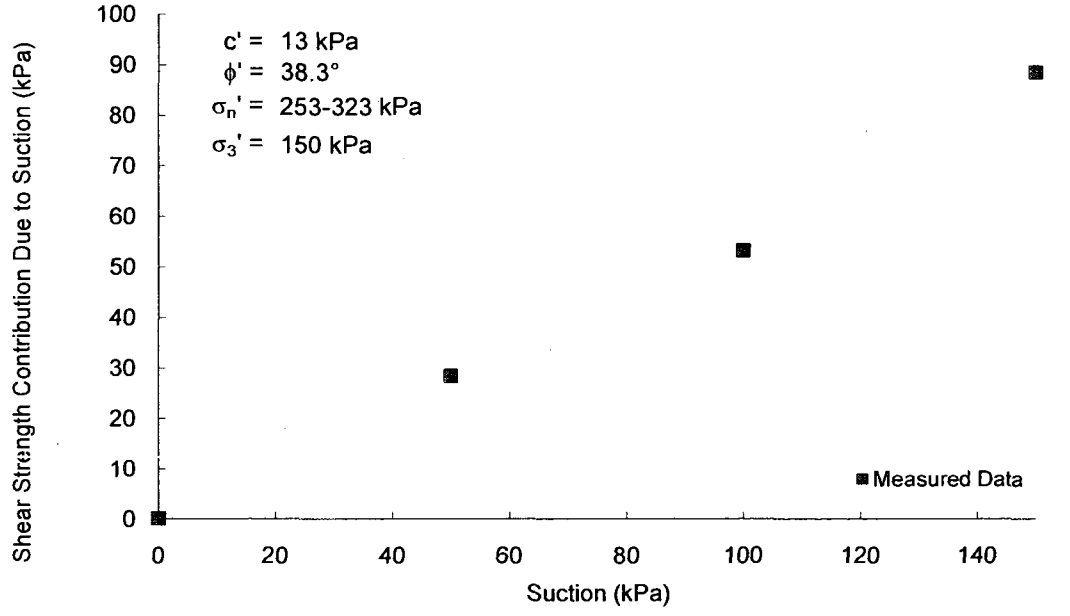

SWRC

Test Method: Pressure plate

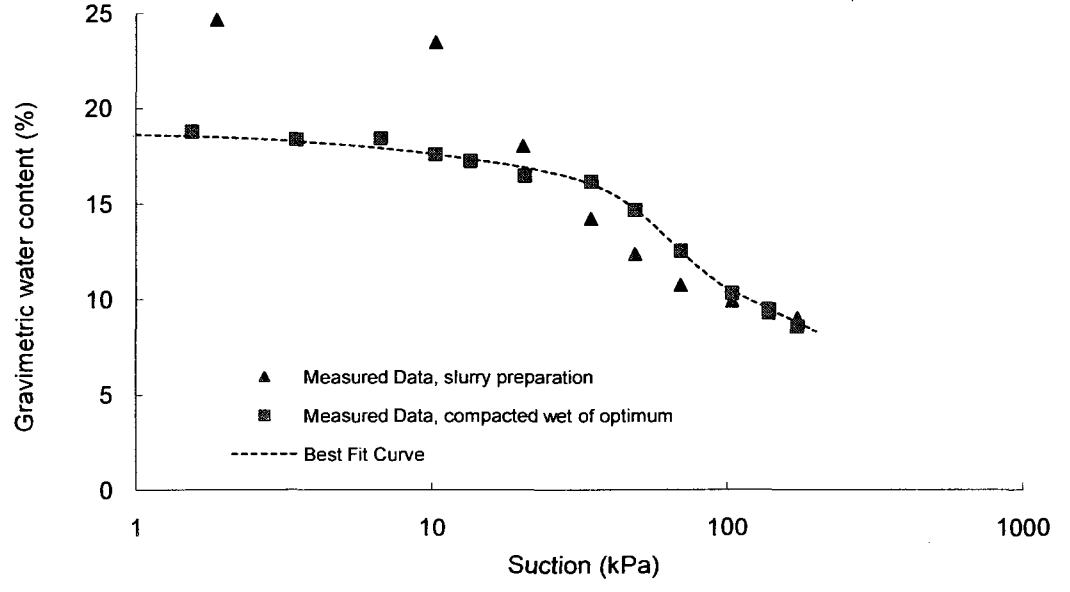

**Gradation curve available in Appendix B

Soil No. 25a **AV colluvium**

Feuerharmel, Bica, Gehling and Flores, 2006

Undisturbed Soil Specimens
Sand = 32%, Silt = 15%, Clay = 53%; Liquid Limit = 56, Plasticity Index = 22
Heavy silt, MH

Shear Strength

Test Method: Modified direct shear test

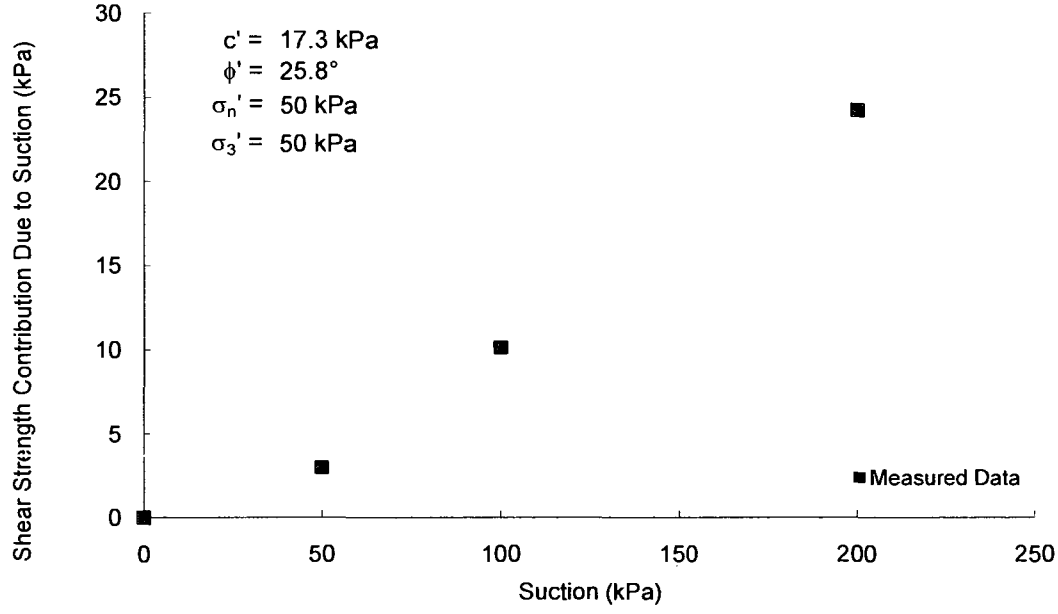

SWRC

Test Method: Pressure plate, filter paper

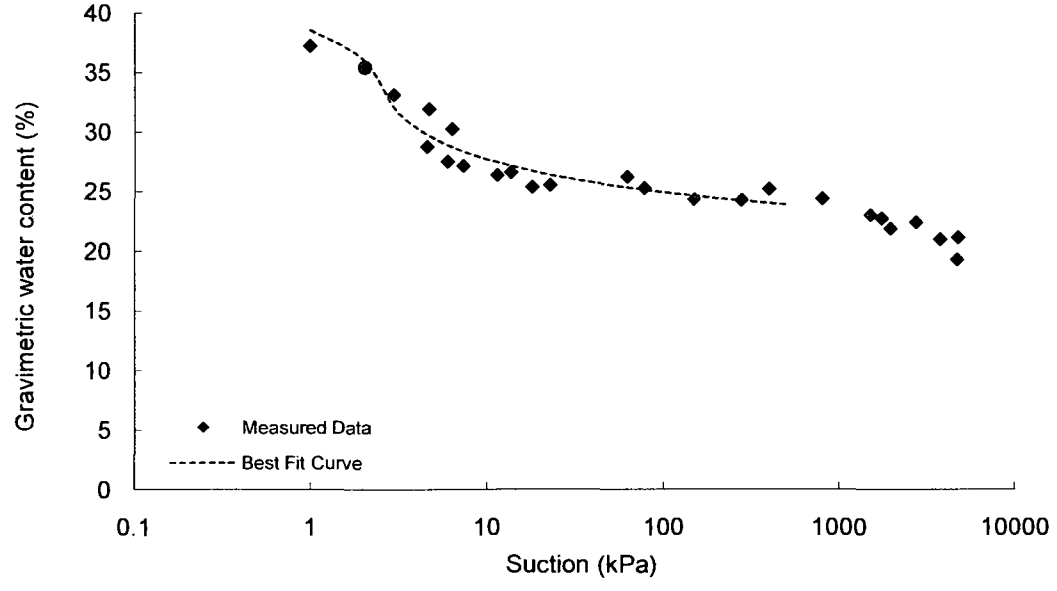

**Gradation curve available in Appendix B

Soil No. 25b

AV colluvium

Feuerharmel, Bica, Gehling and Flores, 2006

Undisturbed Soil Specimens

Sand = 32%, Silt = 15%, Clay = 53%; Liquid Limit = 56, Plasticity Index = 22

Heavy silt, MH

Shear Strength

Test Method: Modified direct shear test

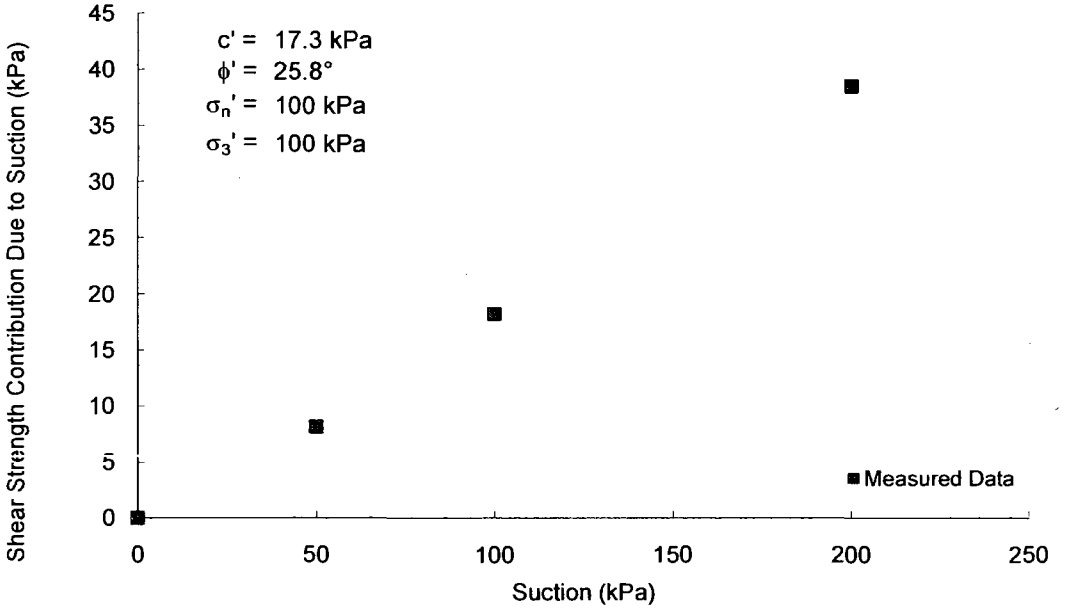

SWRC

Test Method: Pressure plate, filter paper

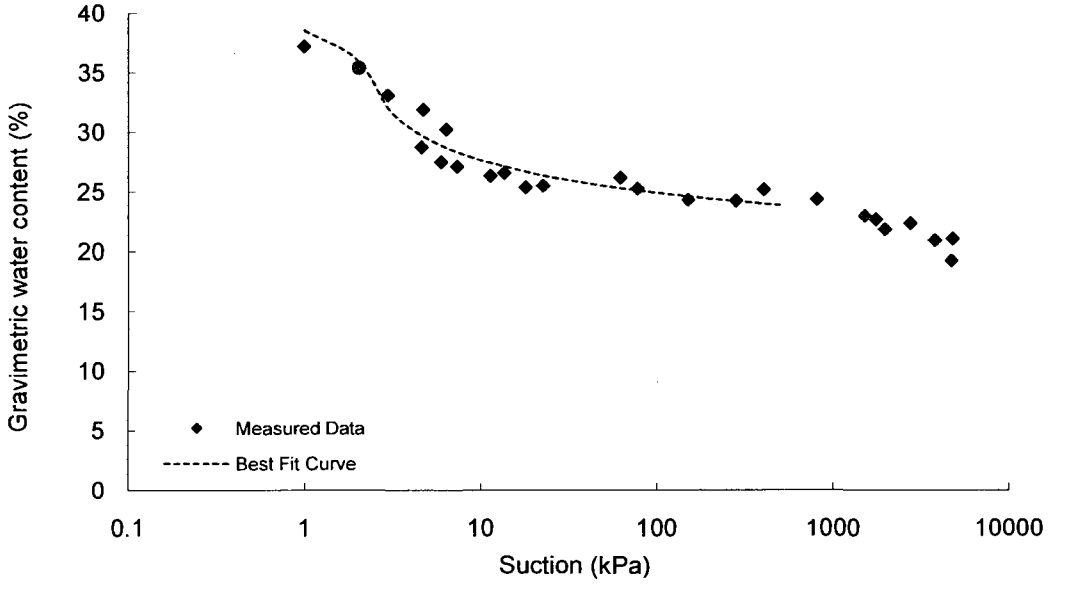

**Gradation curve available in Appendix B

Soil No. 25c

AV colluvium

Feuerharmel, Bica, Gehling and Flores, 2006

Undisturbed Soil Specimens
Sand = 32%, Silt = 15%, Clay = 53%; Liquid Limit = 56, Plasticity Index = 22
Heavy silt, MH

Shear Strength

Test Method: Modified direct shear test

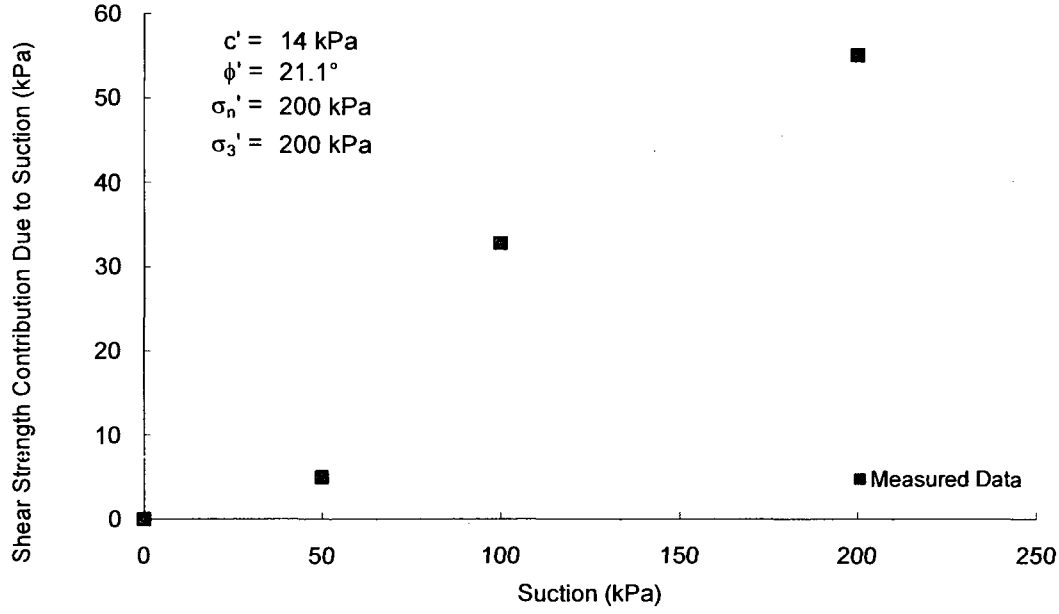

SWRC

Test Method: Pressure plate, filter paper

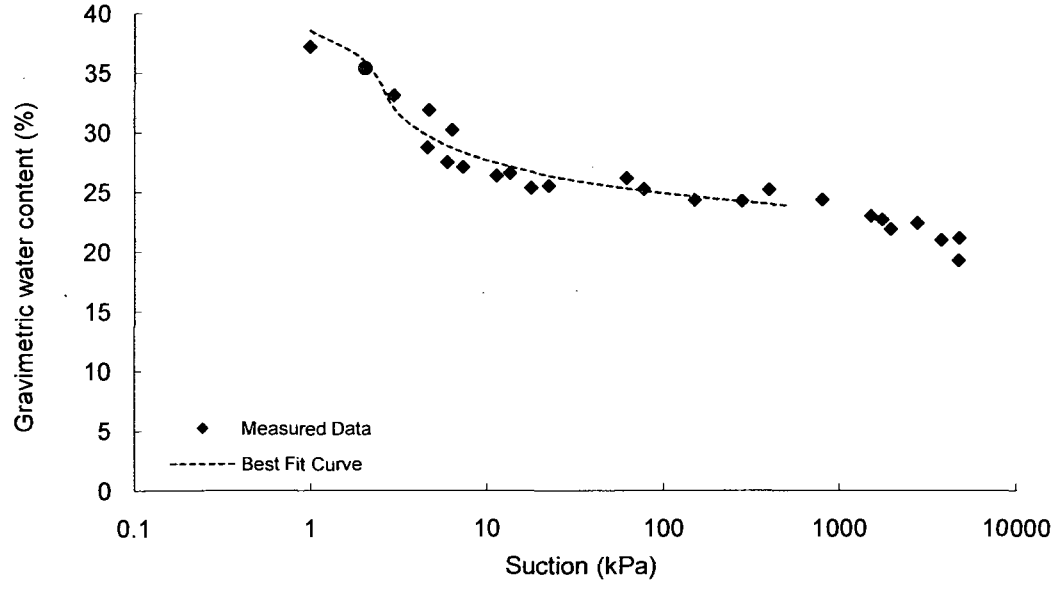

**Gradation curve available in Appendix B

Soil No. 25d **AV colluvium**

Feuerharmel, Pereira, Gehling and Bica, 2006

Undisturbed Soil Specimens
Sand = 32%, Silt = 15%, Clay = 53%; Liquid Limit = 56, Plasticity Index = 22
Heavy silt, MH

Shear Strength Test Method: Modified direct shear test

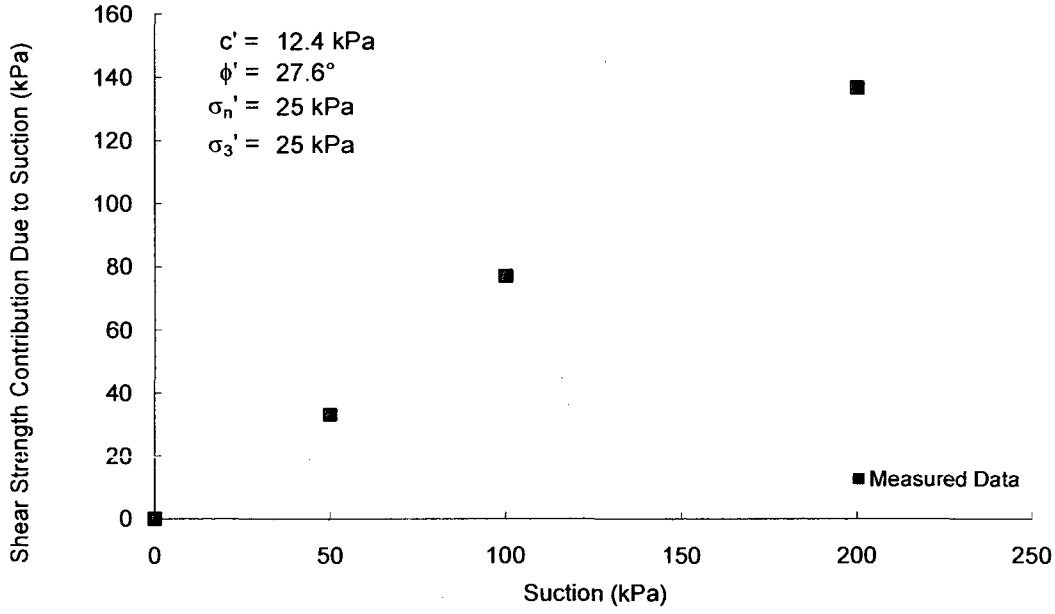

SWRC Test Method: Pressure plate, filter paper

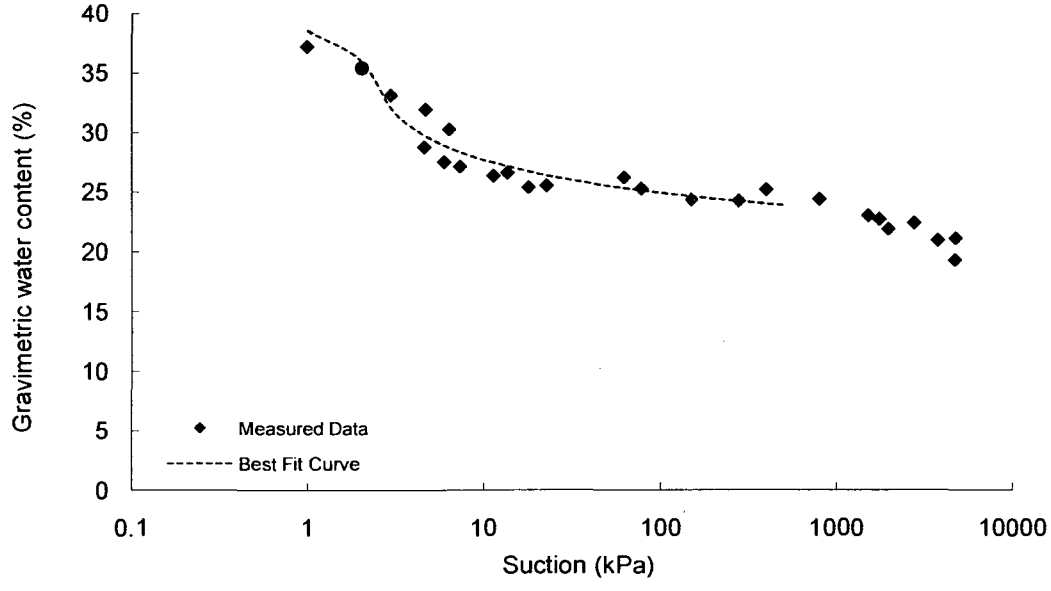

**Gradation curve available in Appendix B

Soil No. 25e

AV colluvium

Pereira, Feuerharmel, Gehling and Bica, 2006

Undisturbed Soil Specimens

Sand = 32%, Silt = 15%, Clay = 53%; Liquid Limit = 56, Plasticity Index = 22

Heavy silt, MH

Shear Strength

Test Method: Modified direct shear test

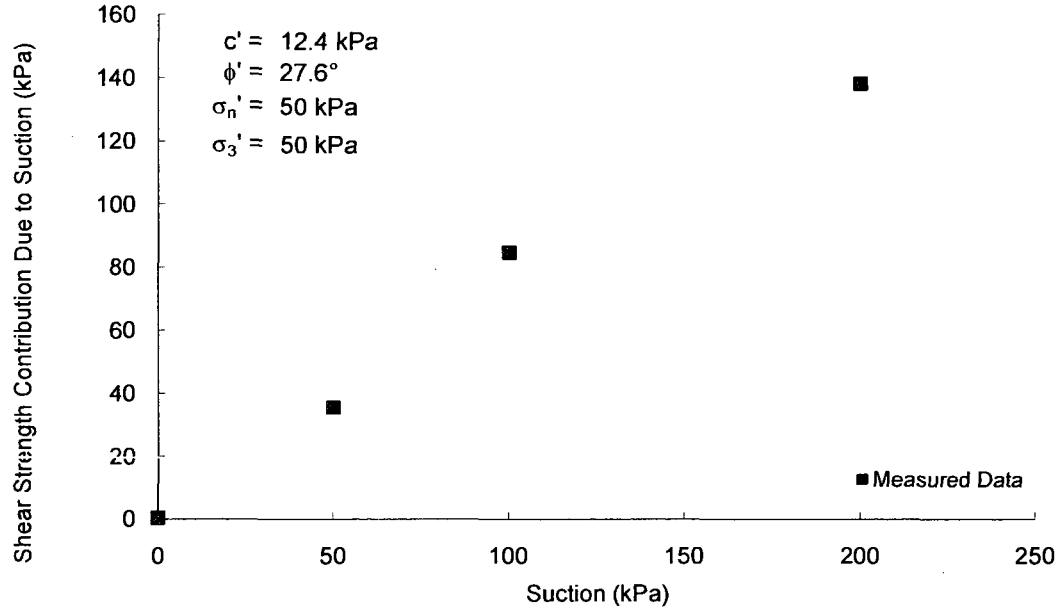

SWRC

Test Method: Pressure plate, filter paper

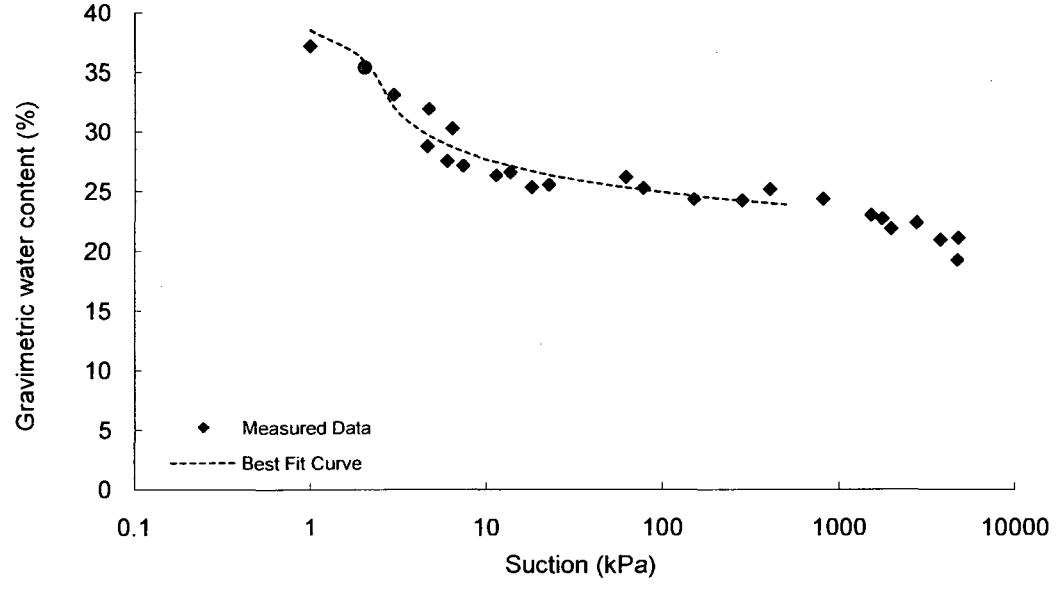

**Gradation curve available in Appendix B

Soil No. 25f **AV colluvium**

Pereira, Feuerharmel, Gehling and Bica, 2006

Undisturbed Soil Specimens Sand = 32%, Silt = 15%, Clay = 53%; Liquid Limit = 56, Plasticity Index = 22 Heavy silt, MH

Shear Strength Test Method: Modified direct shear test

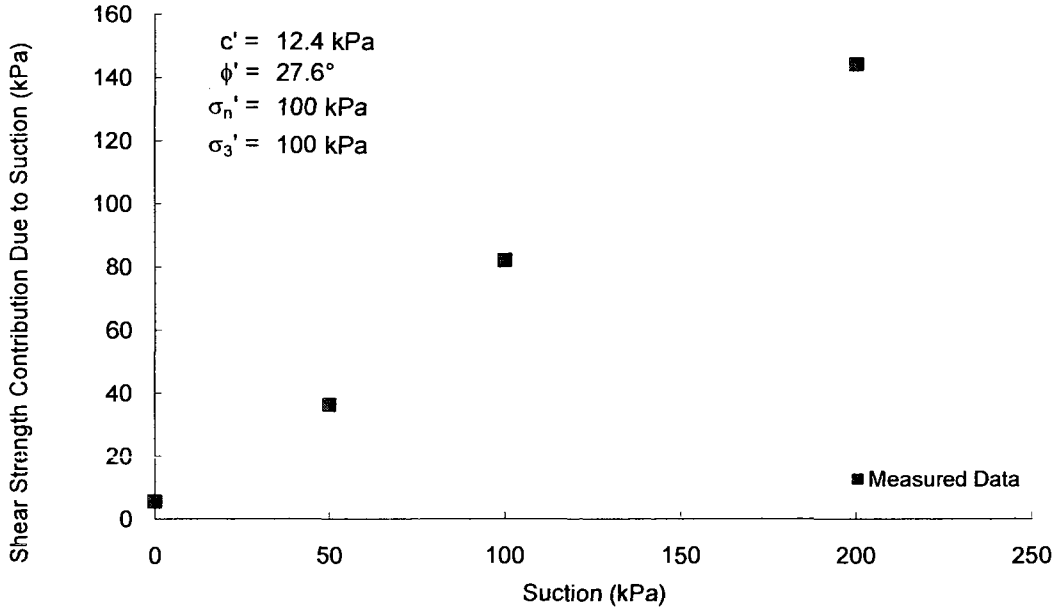

SWRC Test Method: Pressure plate, filter paper

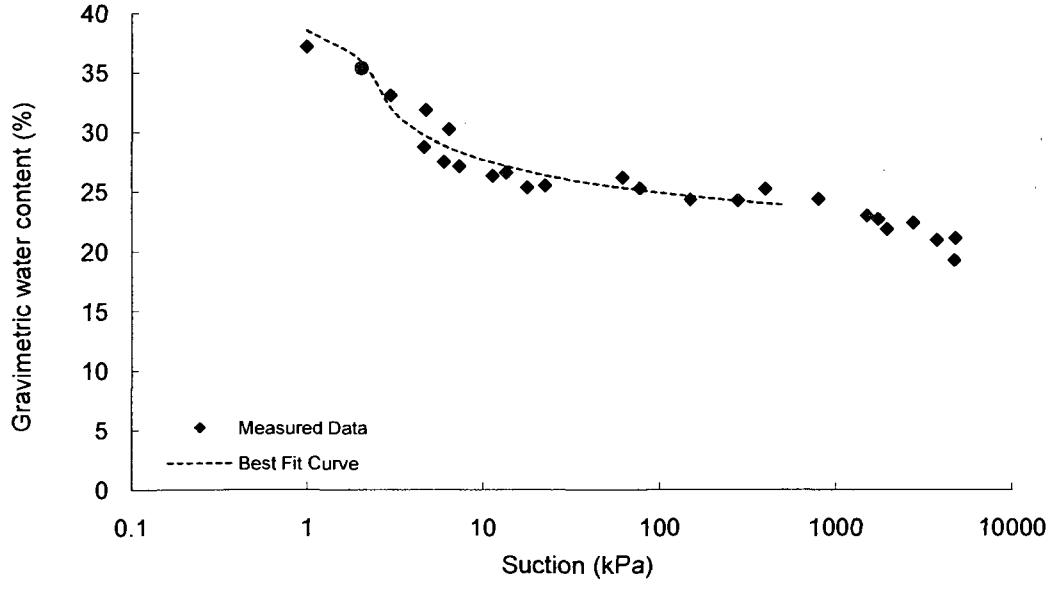

**Gradation curve available in Appendix B

Soil No. 25g **AV colluvium**

Pereira, Feuerharmel, Gehling and Bica, 2006

Undisturbed Soil Specimens
Sand = 32%, Silt = 15%, Clay = 53%; Liquid Limit = 56, Plasticity Index = 22
Heavy silt, MH

Shear Strength Test Method: Modified direct shear test

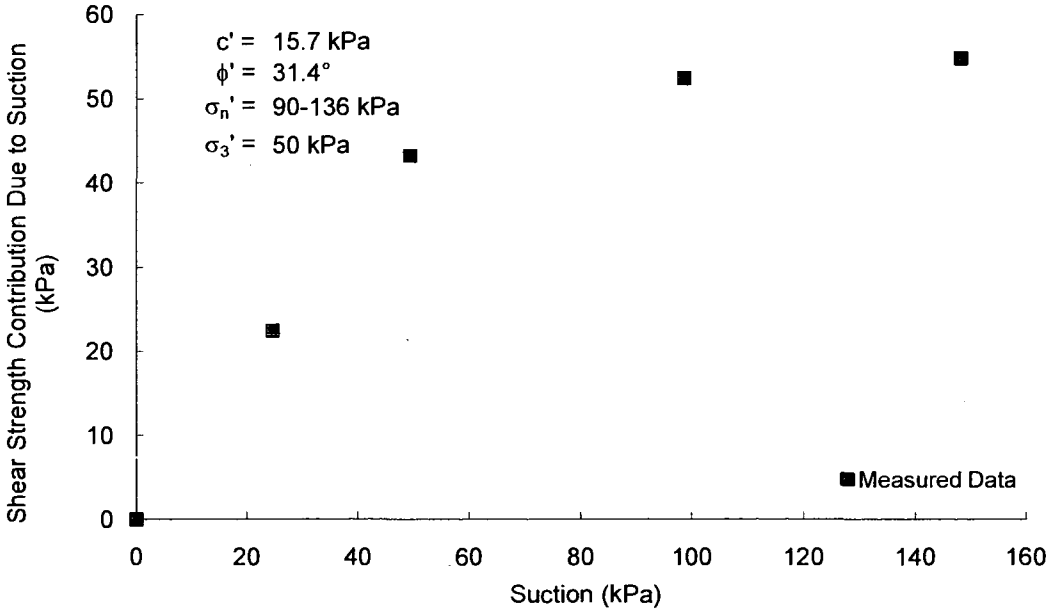

SWRC Test Method: Pressure plate, filter paper

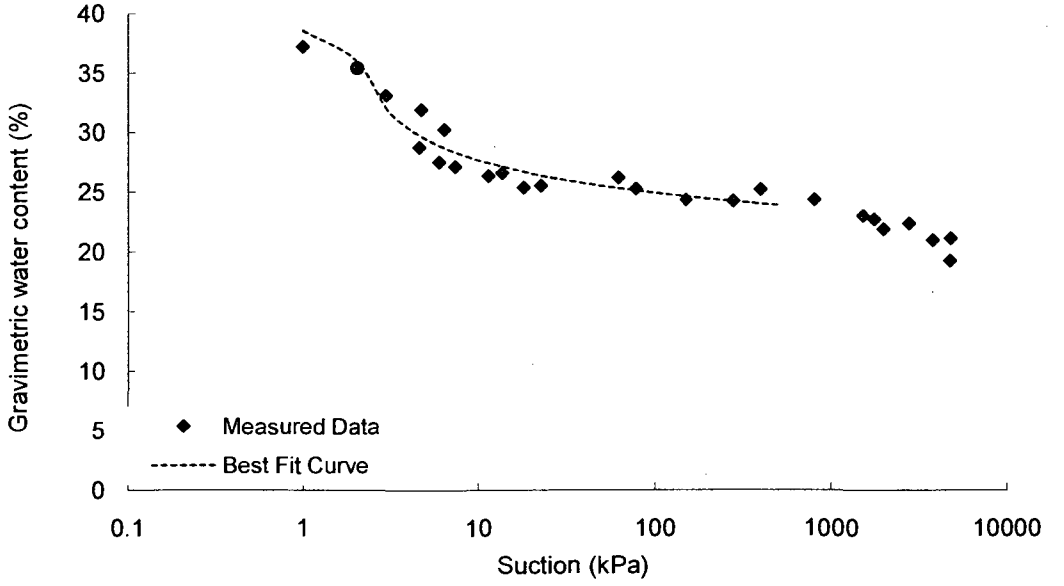

**Gradation curve available in Appendix B

Soil No. 26a **RO colluvium**

Feuerharmel, Bica, Gehling and Flores, 2006

Undisturbed Soil Specimens

Sand = 13%, Silt = 34%, Clay = 53%; Liquid Limit = 74, Plasticity Index = 17

Heavy silt, MH

Shear Strength

Test Method: Modified direct shear test

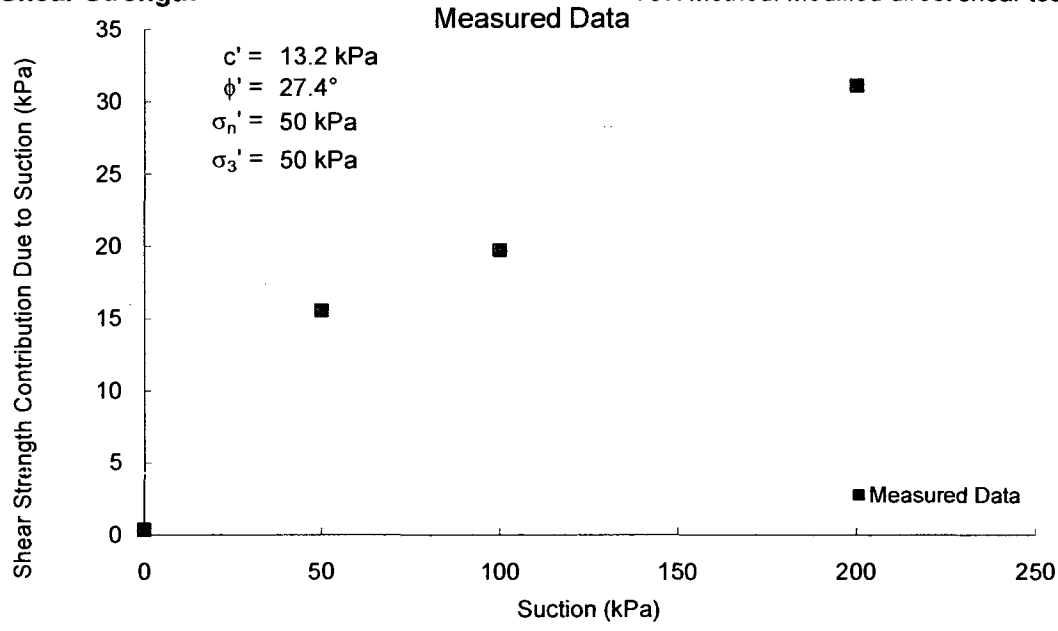

SWRC

Test Method: Pressure plate, filter paper

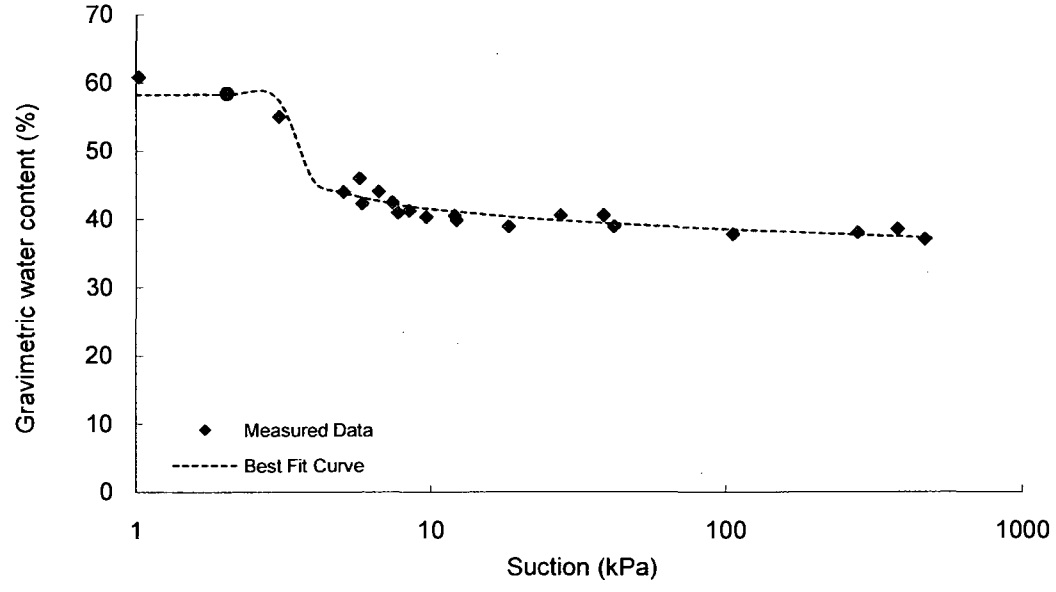

Soil No. 26b

RO colluvium

Feuerharmel, Bica, Gehling and Flores, 2006

Undisturbed Soil Specimens

Sand = 13%, Silt = 34%, Clay = 53%; Liquid Limit = 74, Plasticity Index = 17

Heavy silt, MH

Shear Strength

Test Method: Modified direct shear test

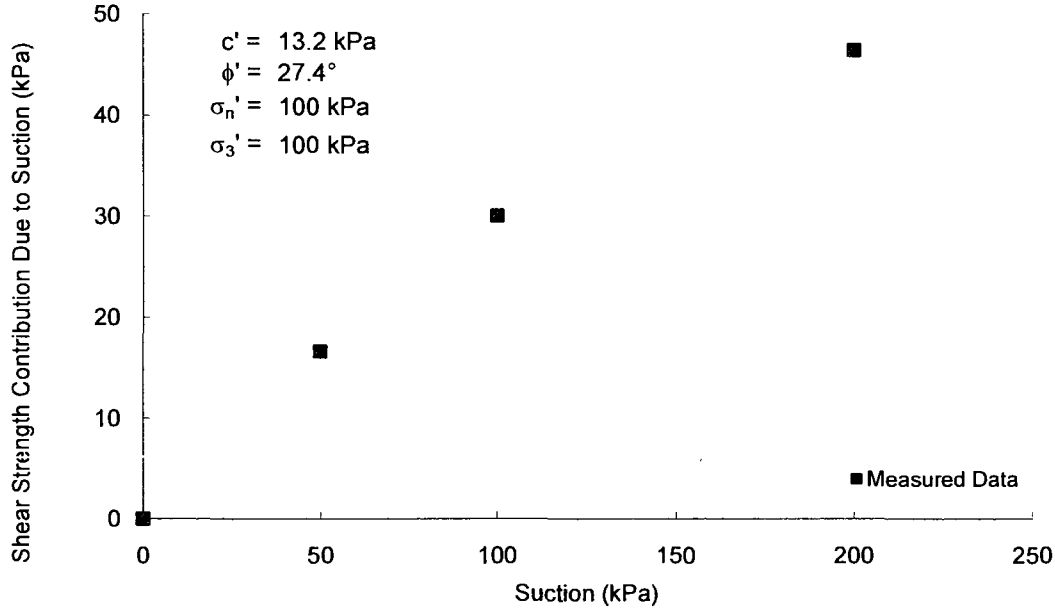

SWRC

Test Method: Pressure plate, filter paper

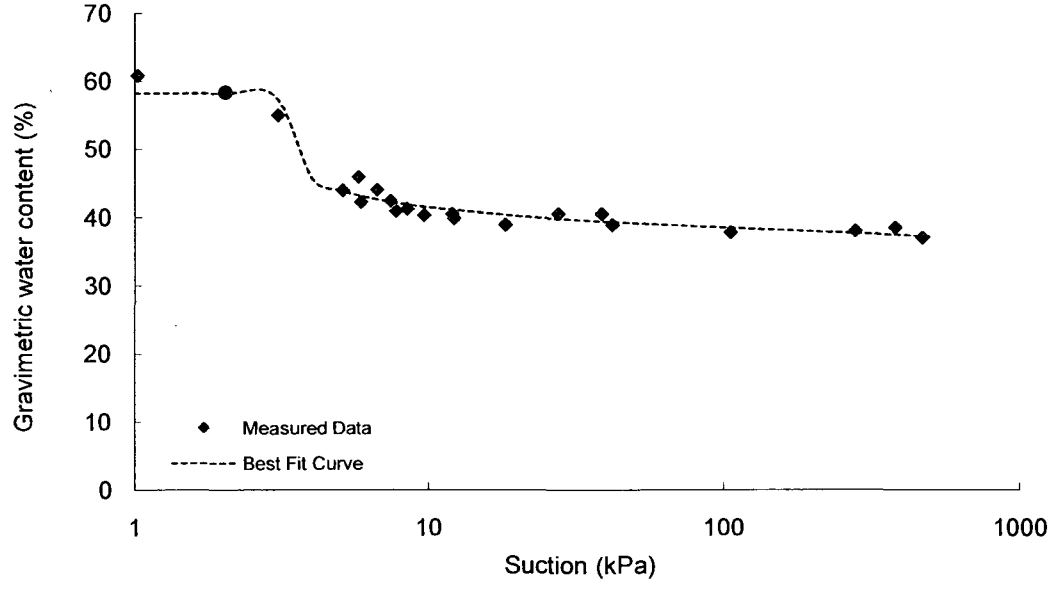

Soil No. 26c

RO colluvium

Feuerharmel, Bica, Gehling and Flores, 2006

Undisturbed Soil Specimens

Sand = 13%, Silt = 34%, Clay = 53%; Liquid Limit = 74, Plasticity Index = 17

Heavy silt, MH

Shear Strength

Test Method: Modified direct shear test

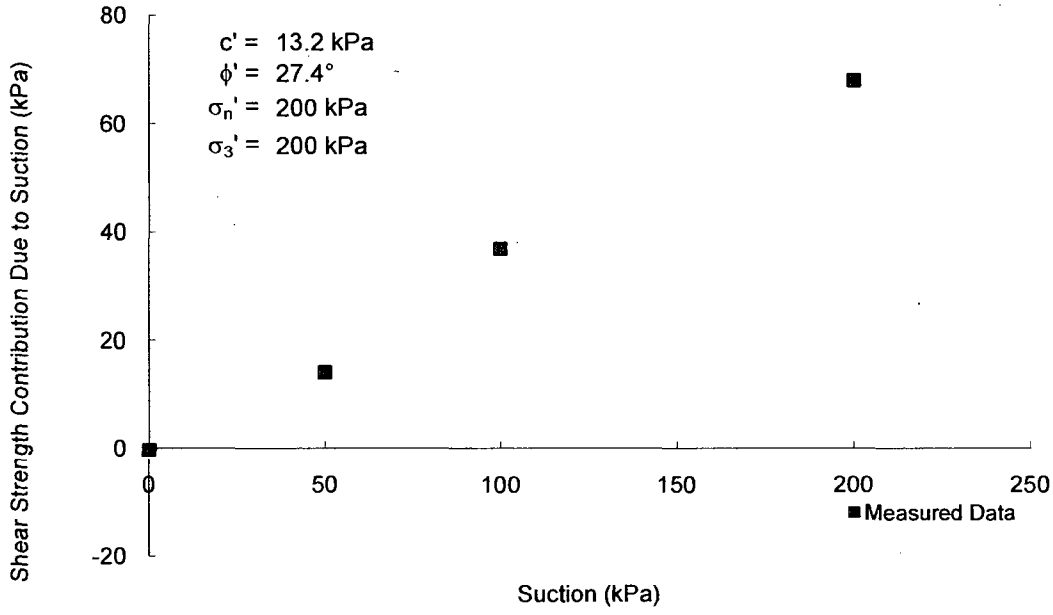

SWRC

Test Method: Pressure plate, filter paper

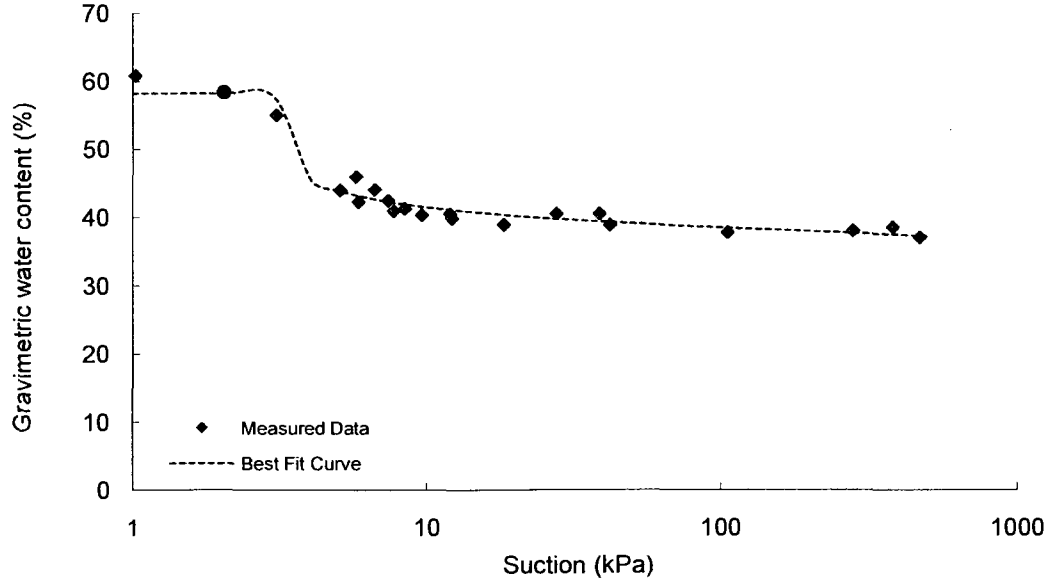

Soil No. 26d

RO colluvium

Feuerharmel, Pereira, Gehling and Bica, 2006

Undisturbed Soil Specimens

Sand = 13%, Silt = 34%, Clay = 53%; Liquid Limit = 74, Plasticity Index = 17

Heavy silt, MH

Shear Strength

Test Method: Modified direct shear test

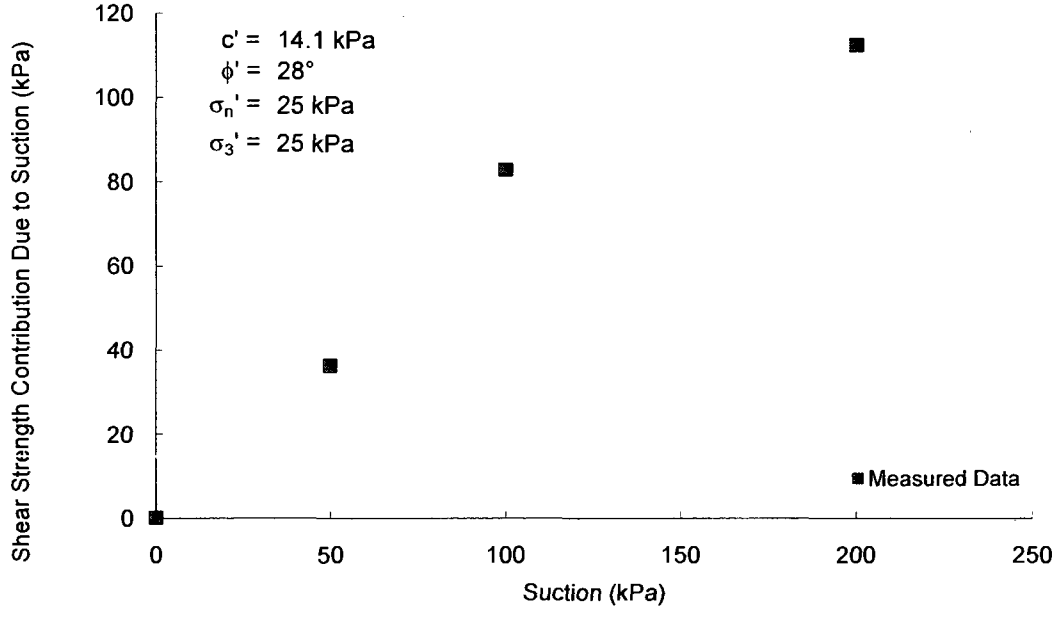

SWRC

Test Method: Pressure plate, filter paper

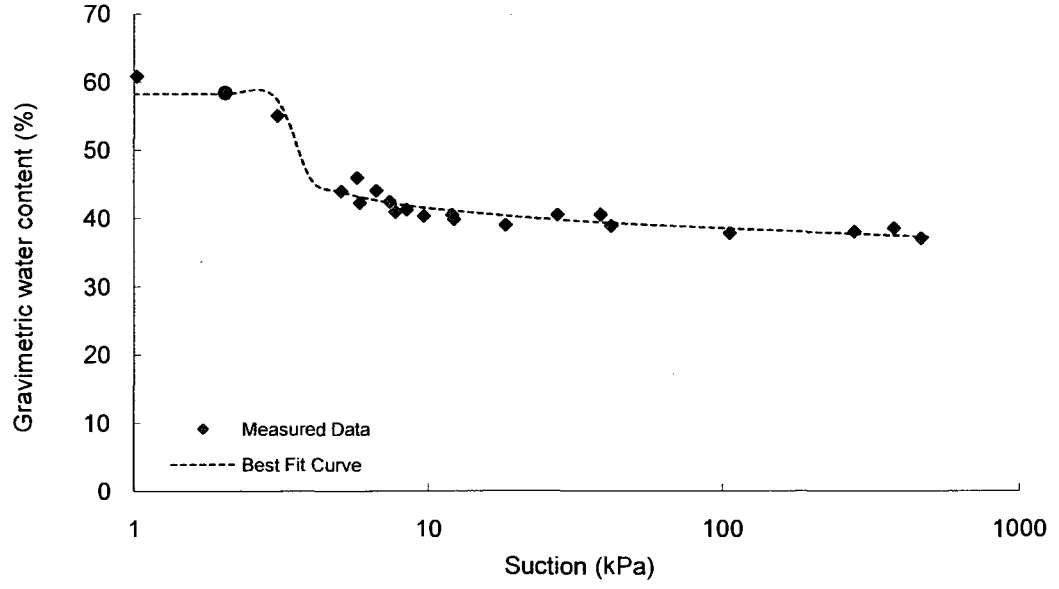

Soil No. 26e

RO colluvium

Feuerharmel, Pereira, Gehling and Bica, 2006

Undisturbed Soil Specimens
Sand = 13%, Silt = 34%, Clay = 53%; Liquid Limit = 74, Plasticity Index = 17
Heavy silt, MH

Shear Strength

Test Method: Modified direct shear test

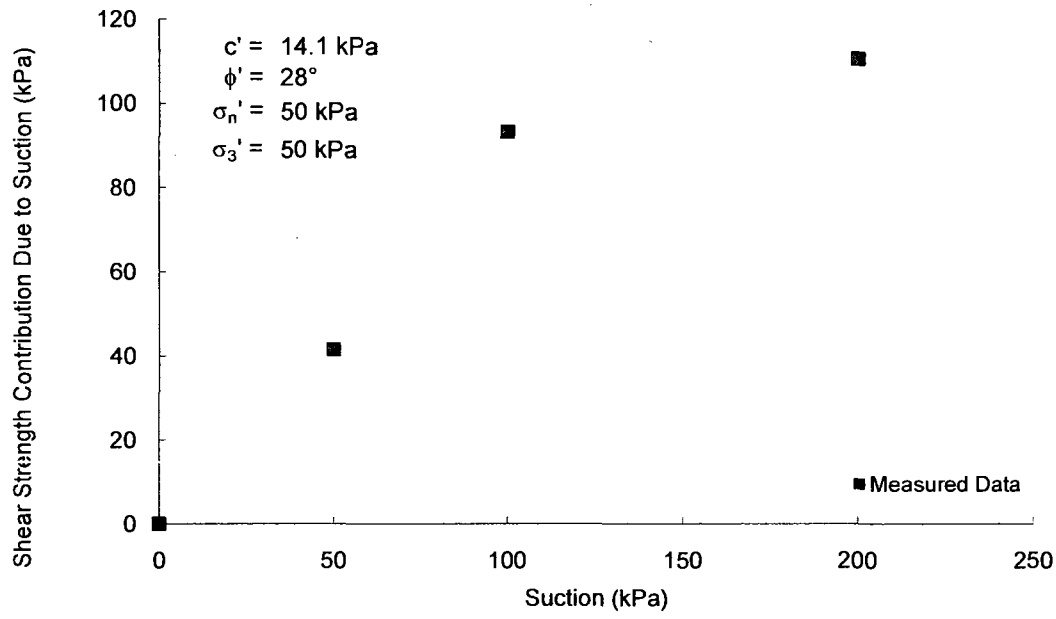

SWRC

Test Method: Pressure plate, filter paper

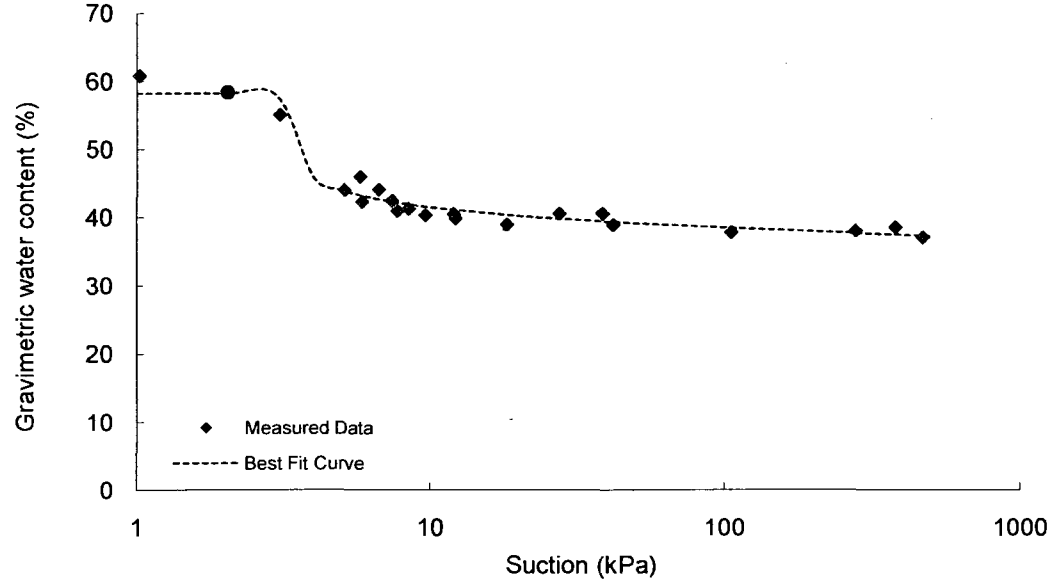

Soil No. 26f **RO colluvium**

Feuerharmel, Pereira, Gehling and Bica, 2006

Undisturbed Soil Specimens
Sand = 13%, Silt = 34%, Clay = 53%; Liquid Limit = 74, Plasticity Index = 17
Heavy silt, MH

Shear Strength Test Method: Modified direct shear test

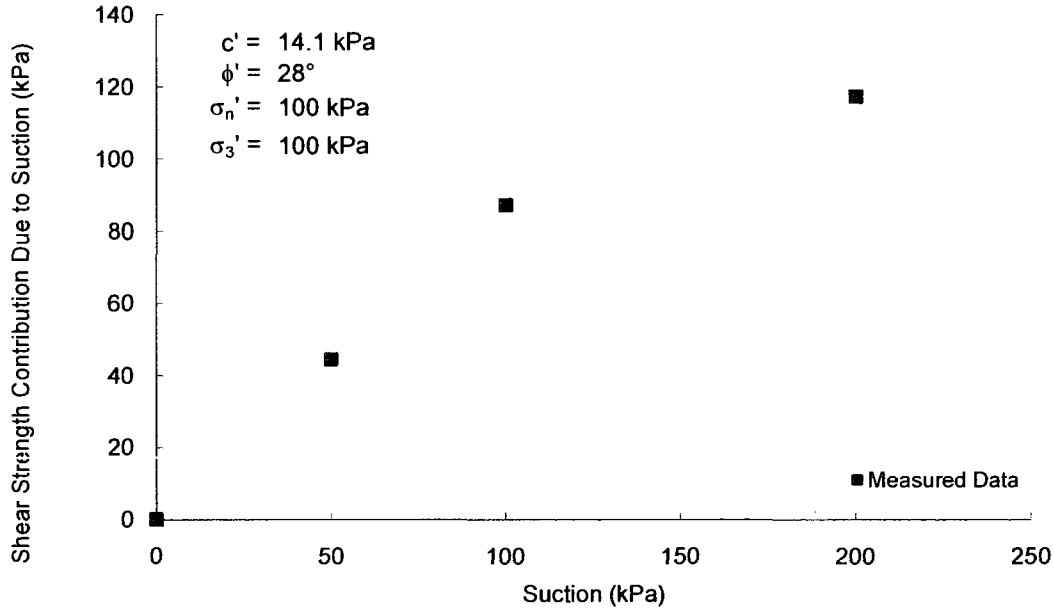

SWRC Test Method: Pressure plate, filter paper

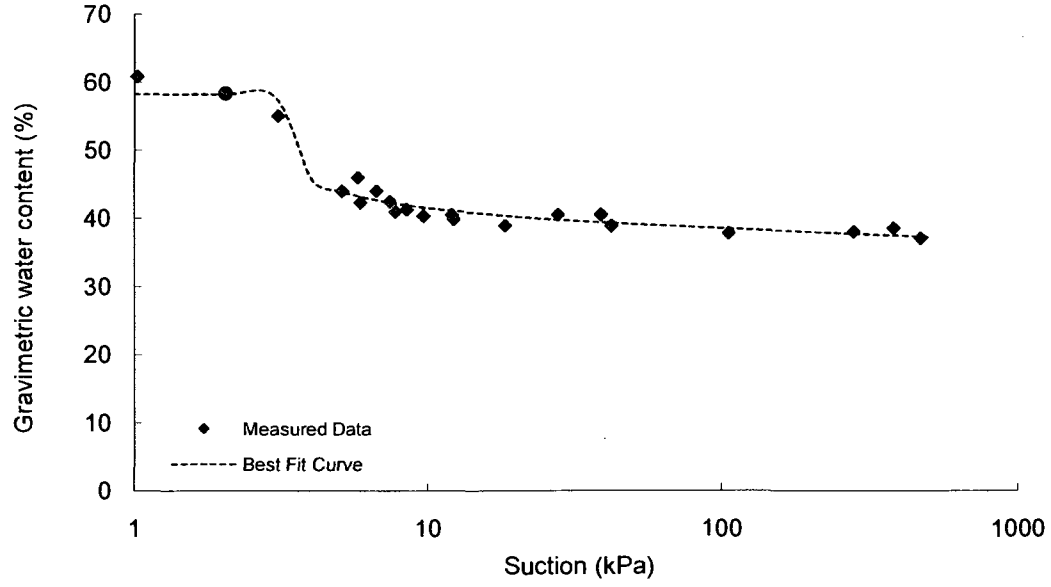

Soil No. 26g

RO colluvium

Feuerharmel, Pereira, Gehling and Bica, 2006

Undisturbed Soil Specimens

Sand = 13%, Silt = 34%, Clay = 53%; Liquid Limit = 74, Plasticity Index = 17

Heavy silt, MH

Shear Strength

Test Method: Modified direct shear test

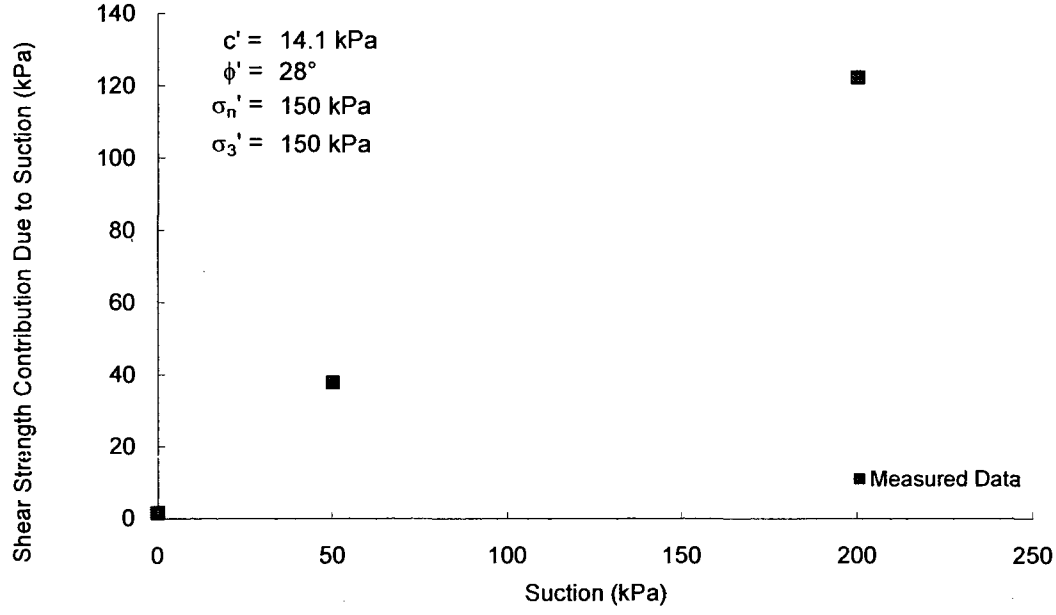

SWRC

Test Method: Pressure plate, filter paper

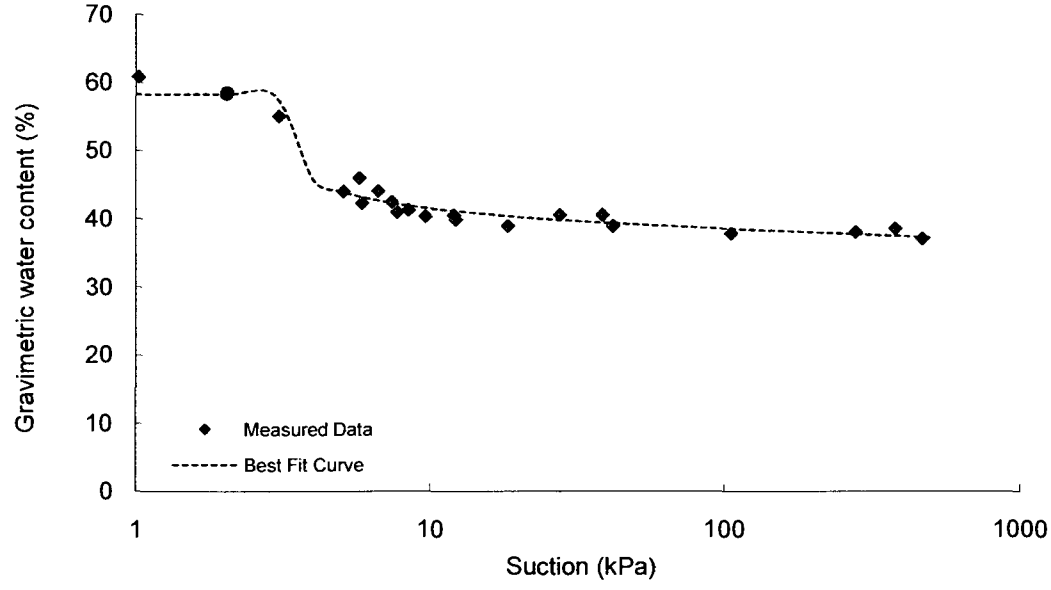

Soil No. 26h **RO colluvium**

Feuerharmel, Pereira, Gehling and Bica, 2006

Undisturbed Soil Specimens
Sand = 13%, Silt = 34%, Clay = 53%; Liquid Limit = 74, Plasticity Index = 17
Heavy silt, MH

Shear Strength Test Method: Modified triaxial test

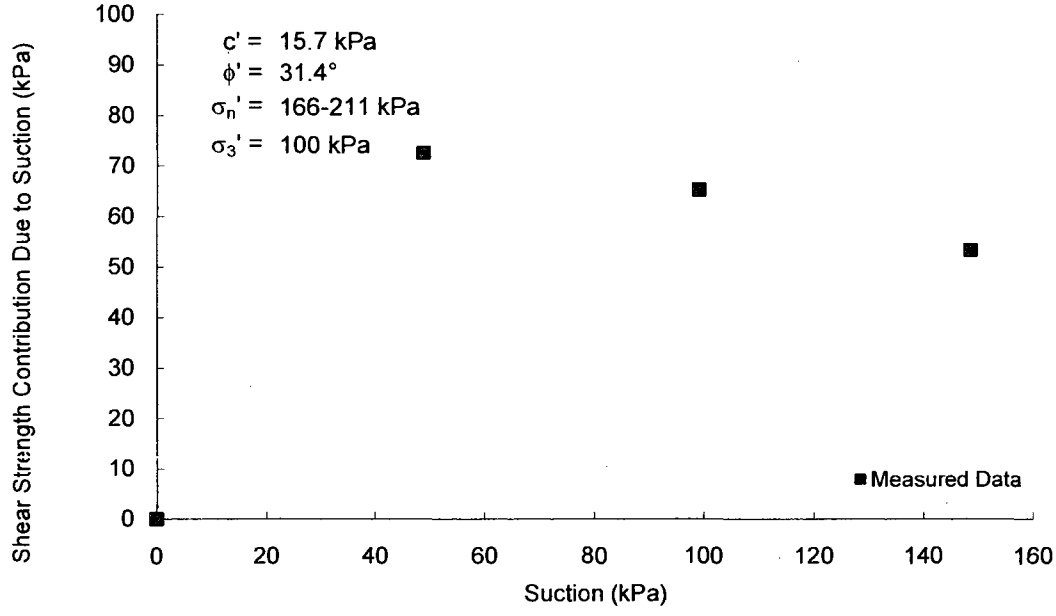

SWRC Test Method: Pressure plate, filter paper

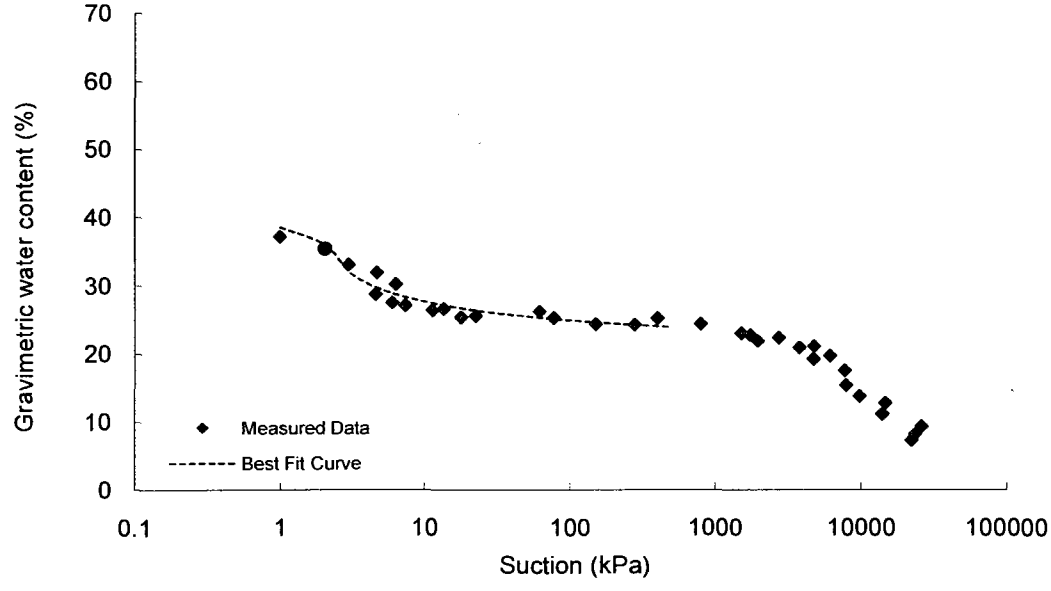

Soil No. 27a **CRDB silt**

Cunningham, Ridley, Dineen and Burland, 2003

Sample Prepared by reconstituting from slurry
Sand = 22%, Silt = 52%, Clay = 26%; Liquid Limit = 28, Plasticity Index = 18
Lean clay, CL

Shear Strength Test Method: Modified triaxial test

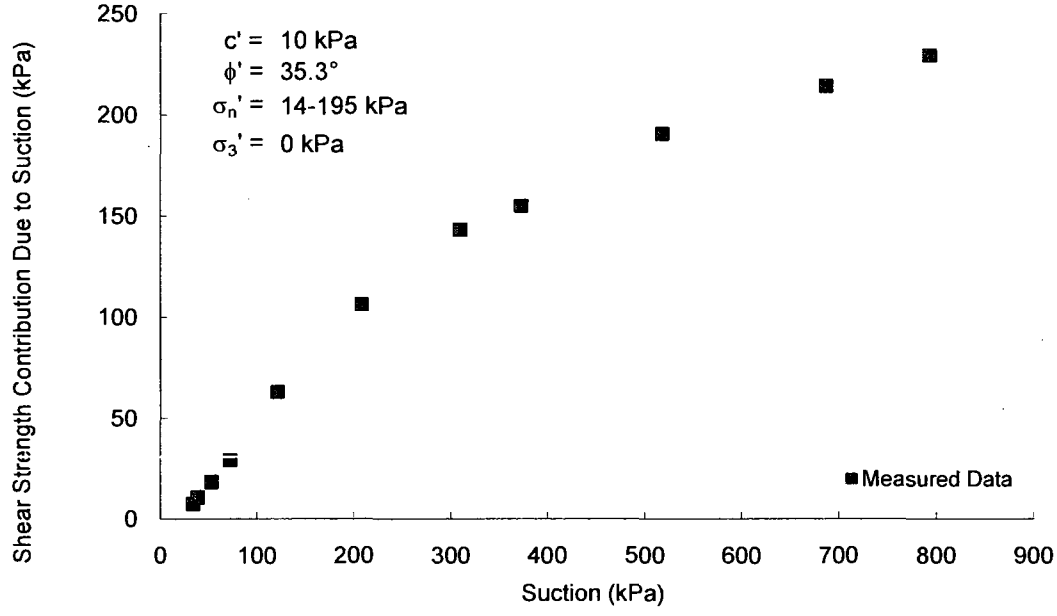

SWRC Test Method: Filter paper

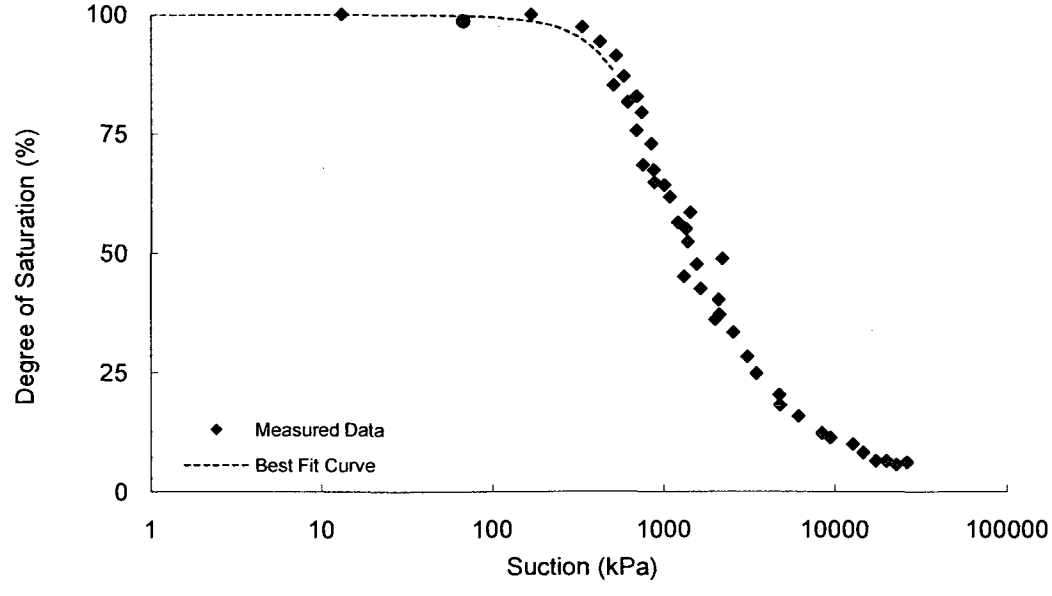

**Gradation curve available in Appendix B

Soil No. 27b **CRDB silt**

Cunningham, Ridley, Dineen and Burland, 2003

Sample Prepared by reconstituting from slurry
Sand = 22%, Silt = 52%, Clay = 26%; Liquid Limit = 28, Plasticity Index = 18
Lean clay, CL

Shear Strength Test Method: Modified triaxial test

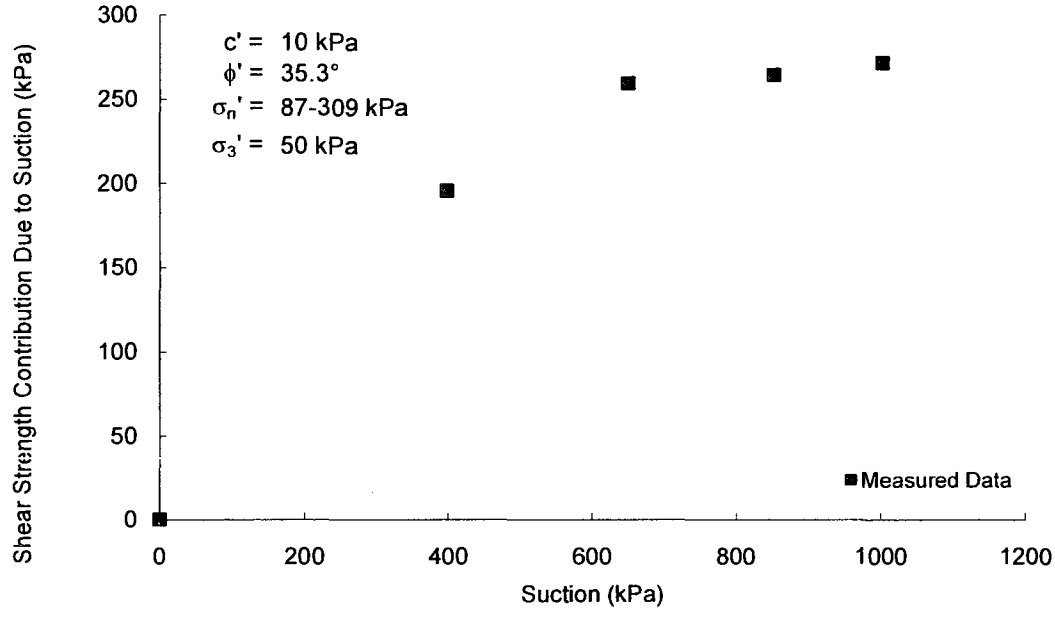

SWRC Test Method: Filter paper

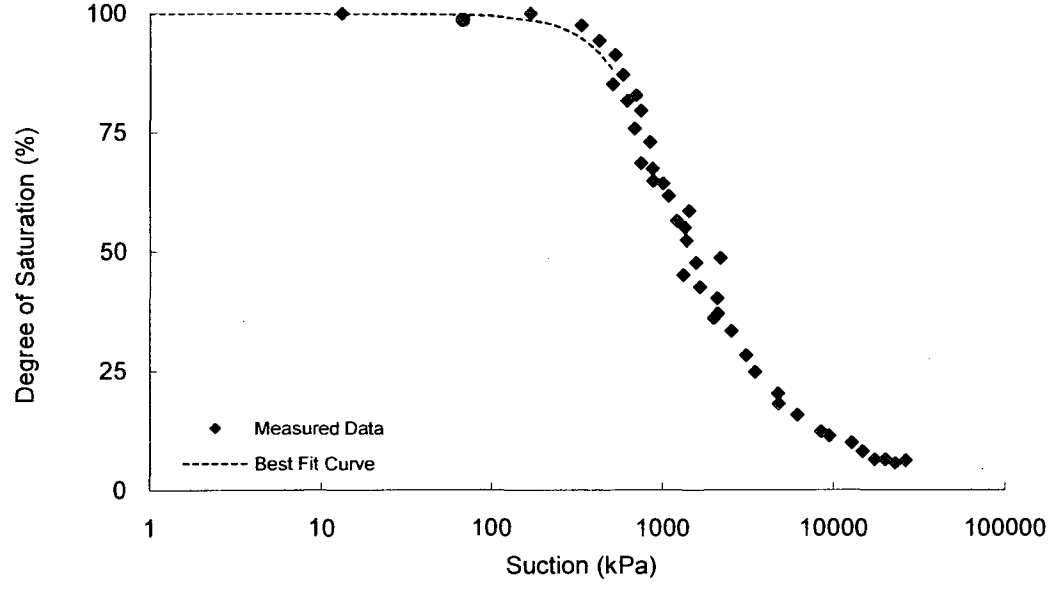

**Gradation curve available in Appendix B

Soil No. 27c **CRDB silt**

Cunningham, Ridley, Dineen and Burland, 2003

Sample Prepared by reconstituting from slurry Sand = 22%, Silt = 52%, Clay = 26%; Liquid Limit = 28, Plasticity Index = 18 Lean clay, CL

Shear Strength Test Method: Modified triaxial test

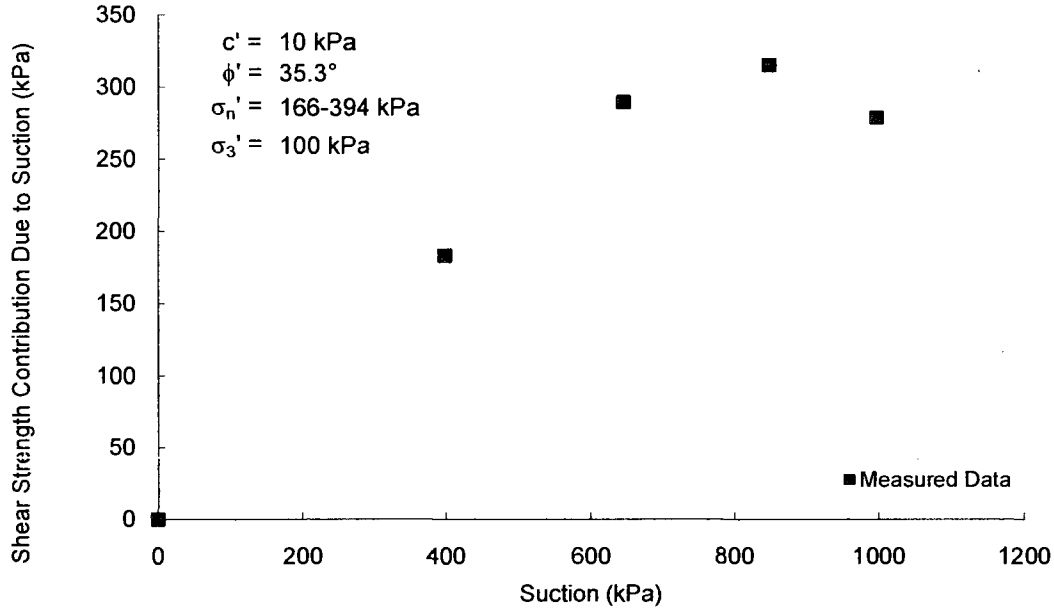

SWRC Test Method: Filter paper

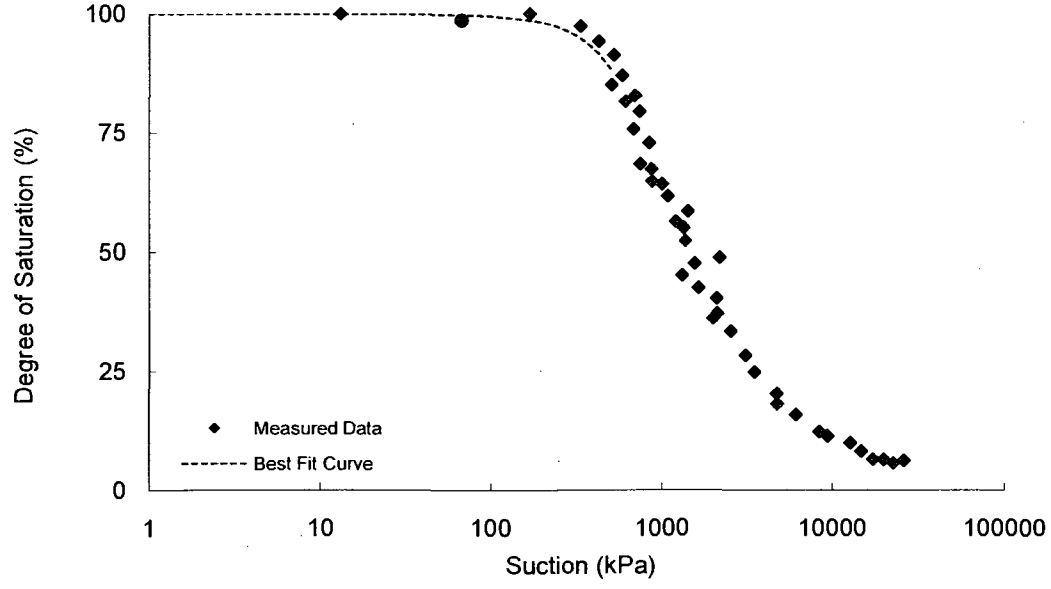

**Gradation curve available in Appendix B

Soil No. 27d **CRDB silt**

Cunningham, Ridley, Dineen and Burland, 2003

Sample Prepared by reconstituting from slurry Sand = 22%, Silt = 52%, Clay = 26%; Liquid Limit = 28, Plasticity Index = 18 Lean clay, CL

Shear Strength Test Method: Modified triaxial test

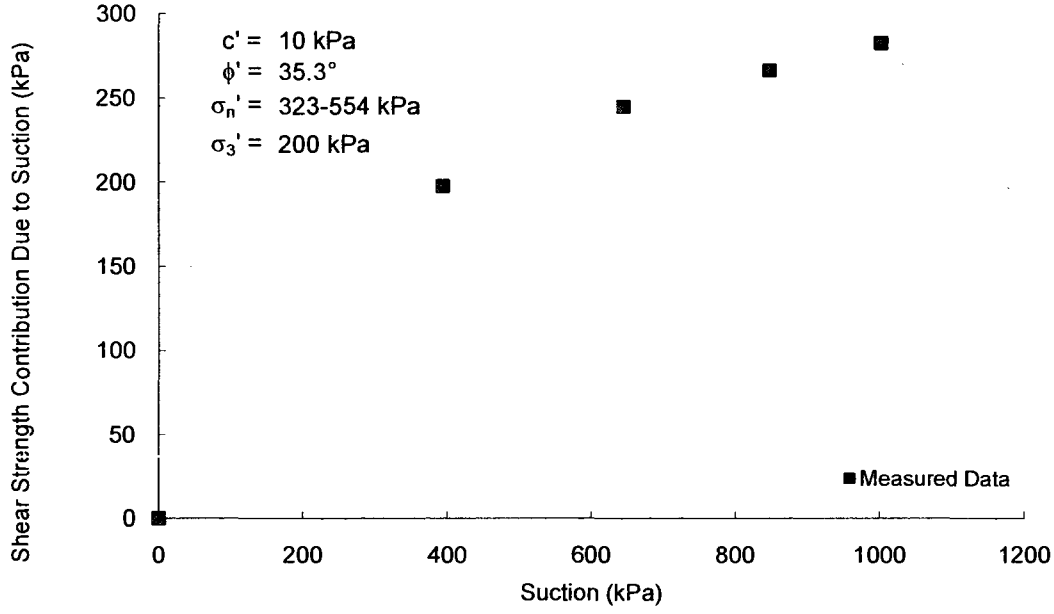

SWRC Test Method: Filter paper

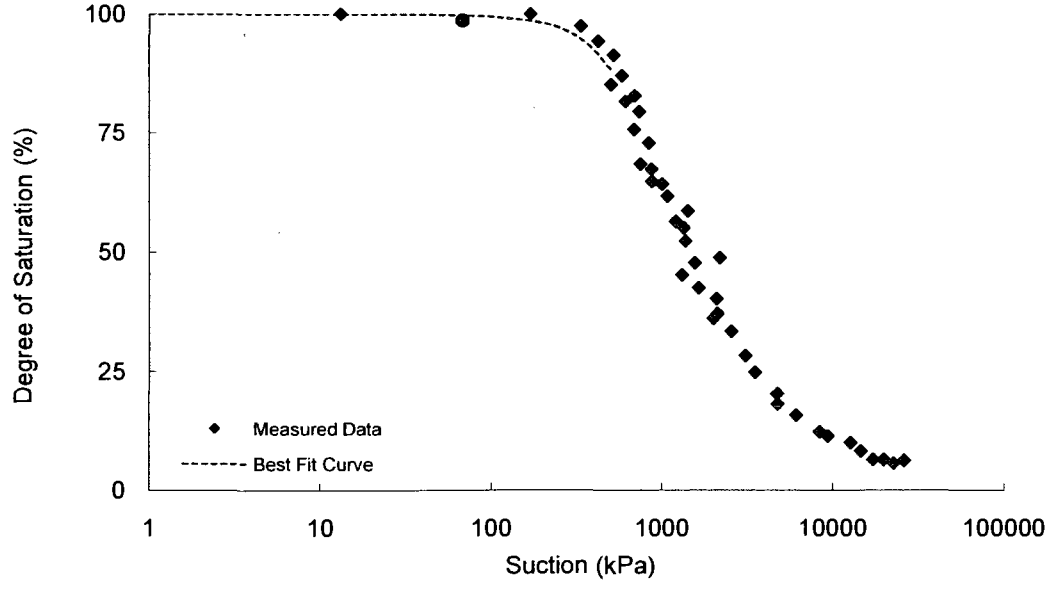

**Gradation curve available in Appendix B

Soil No. 27e **CRDB silt**

Cunningham, Ridley, Dineen and Burland, 2003

Sample Prepared by reconstituting from slurry Sand = 22%, Silt = 52%, Clay = 26%; Liquid Limit = 28, Plasticity Index = 18 Lean clay, CL

Shear Strength Test Method: Modified triaxial test

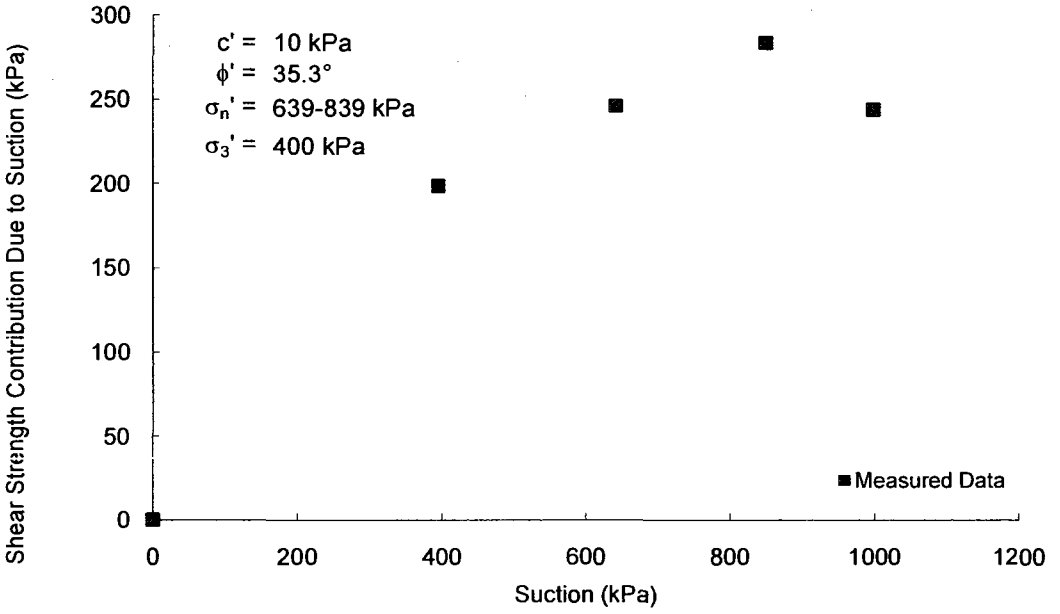

SWRC Test Method: Filter paper

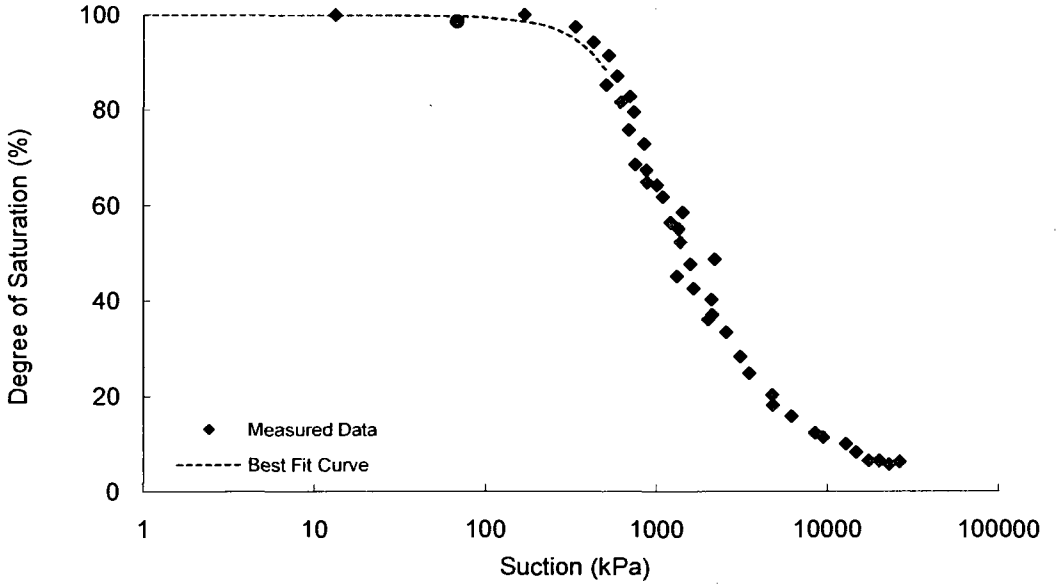

**Gradation curve available in Appendix B

Soil No. 28a

Botkin silt

Oloo and Fredlund, 1996; Oloo, 1994

Compacted Sample
Sand = 52.5%, Silt = 37.5%, Clay = 10%; Liquid Limit = 22, Plasticity Index = 6
Silty clay, CL-ML

Shear Strength

Test Method: Modified triaxial test

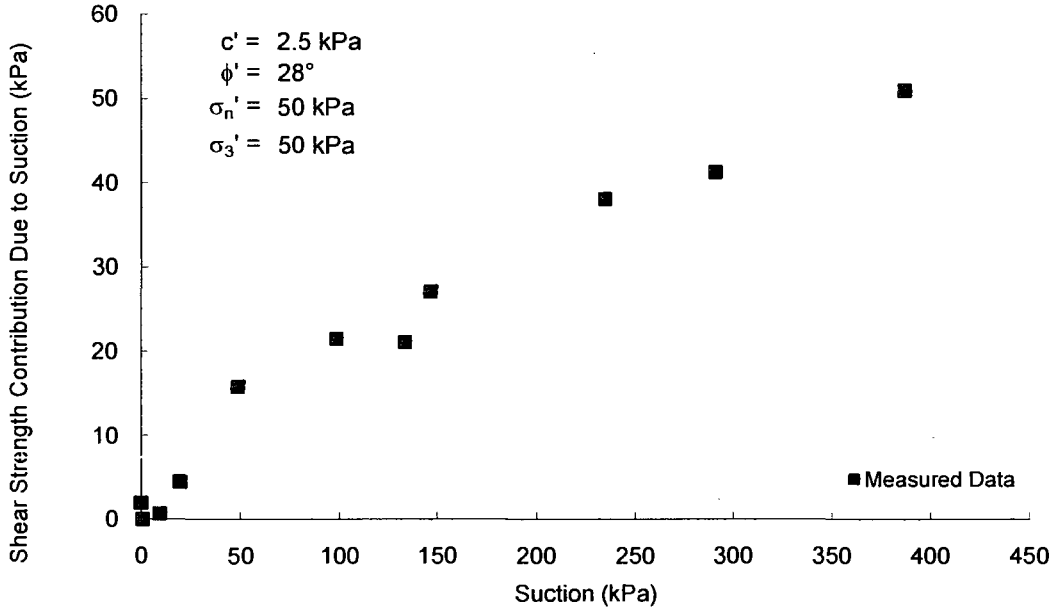

SWRC

Test Method: Pressure plate

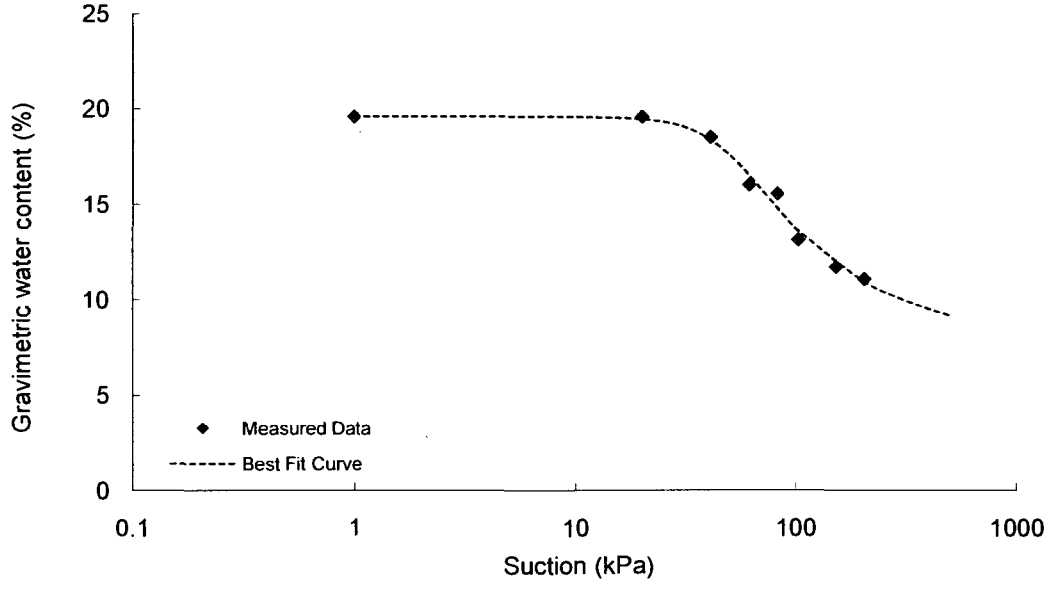

**Gradation curve available in Appendix B

Soil No. 28b **Botkin silt**

Oloo and Fredlund, 1996; Oloo, 1994

Compacted Sample
Sand = 52.5%, Silt = 37.5%, Clay = 10%; Liquid Limit = 22, Plasticity Index = 6
Silty clay, CL-ML

Shear Strength Test Method: Modified triaxial test

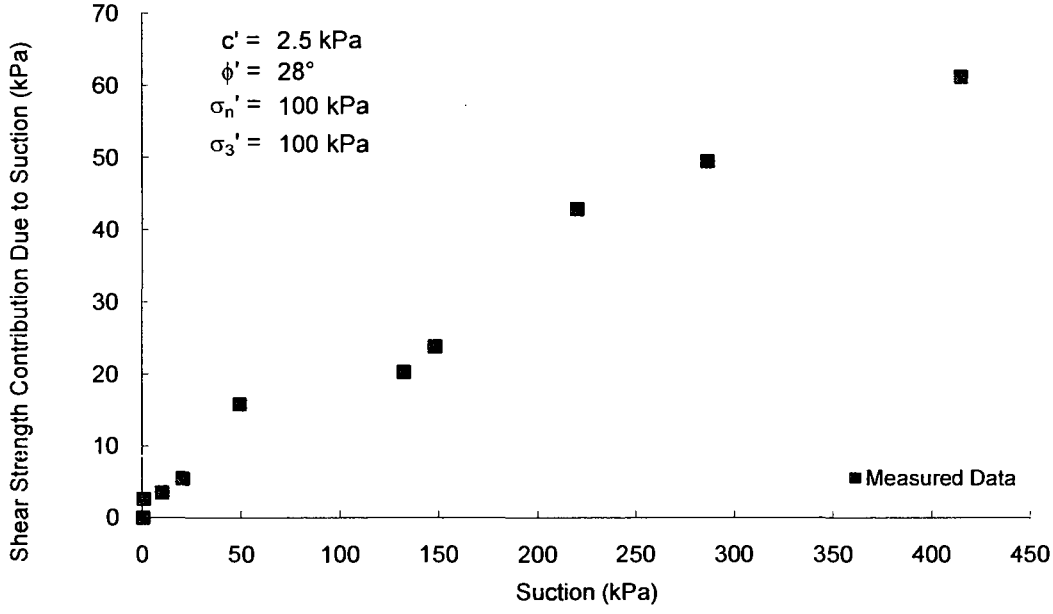

SWRC Test Method: Pressure plate

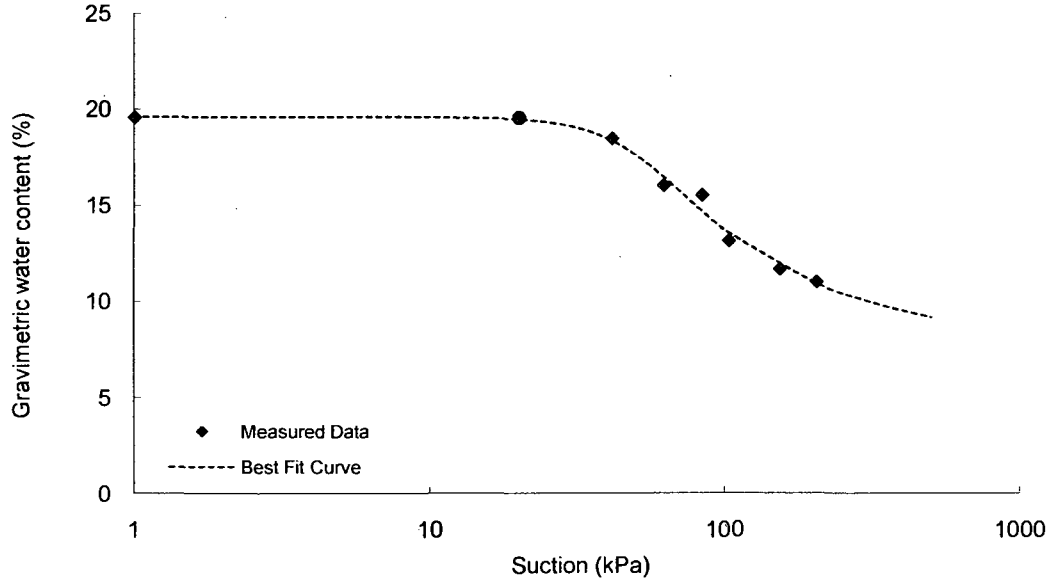

**Gradation curve available in Appendix B

Soil No. 28c

Botkin silt

Oloo and Fredlund, 1996; Oloo, 1994

Compacted Sample
Sand = 52.5%, Silt = 37.5%, Clay = 10%; Liquid Limit = 22, Plasticity Index = 6
Silty clay, CL-ML

Shear Strength

Test Method: Modified triaxial test

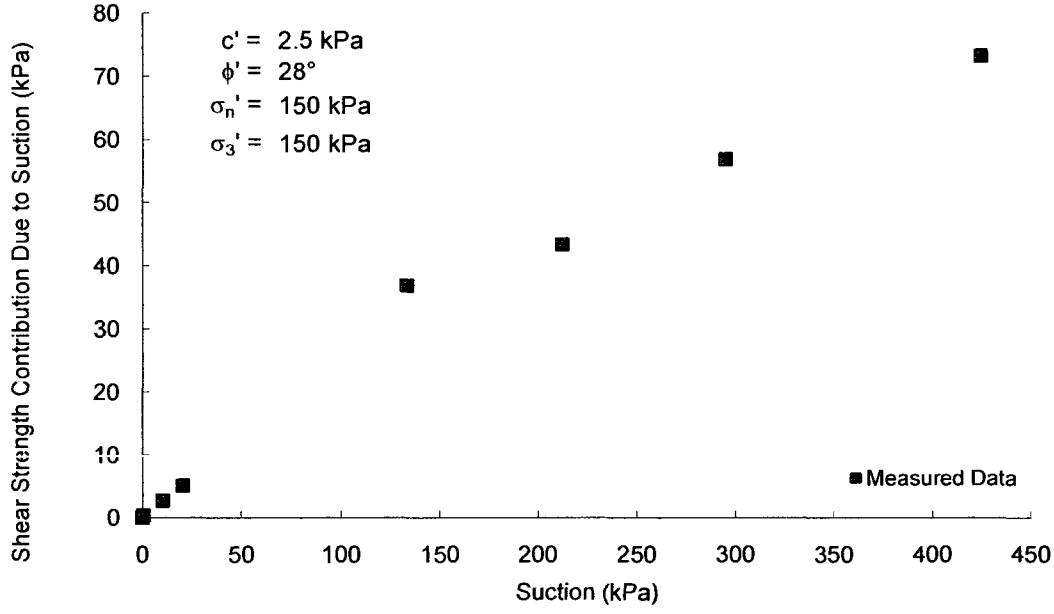

SWRC

Test Method: Pressure plate

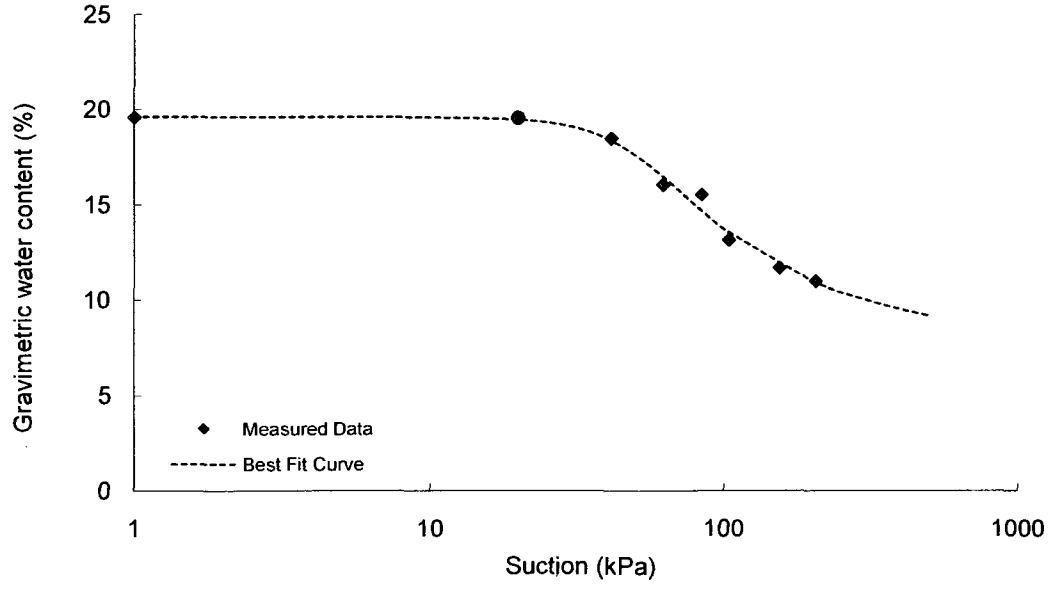

**Gradation curve available in Appendix B

Soil No. 29a

Indian Head till

Oloo and Fredlund, 1996; Oloo, 1994

Compacted Sample
Sand = 28%, Silt = 42%, Clay = 30%; Liquid Limit = 36, Plasticity Index = 19
Lean clay, CL

Shear Strength

Test Method: Modified triaxial test

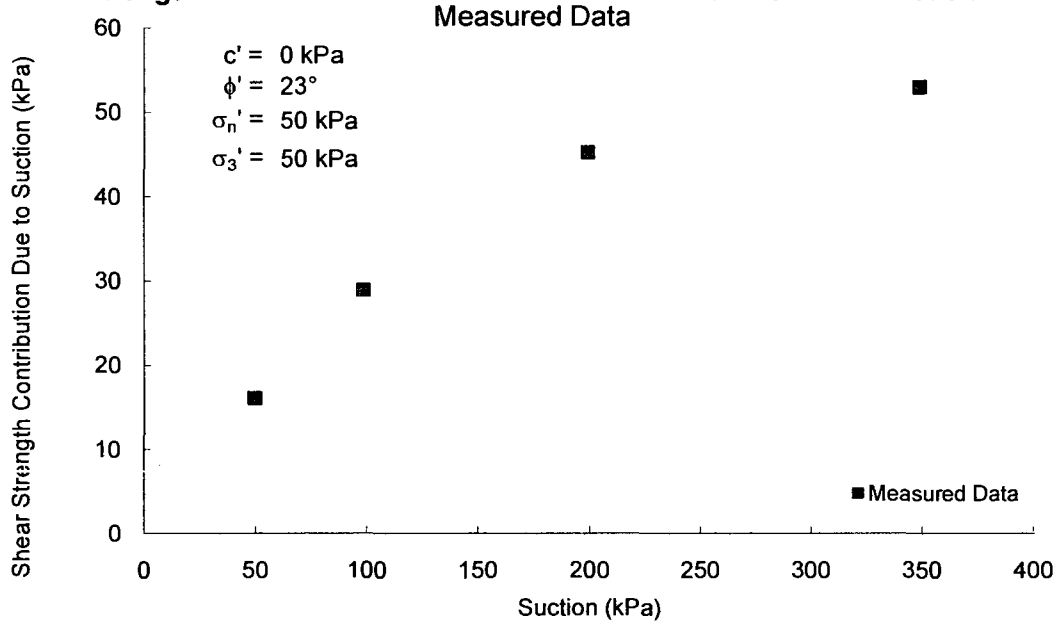

SWRC

Test Method: Pressure plate

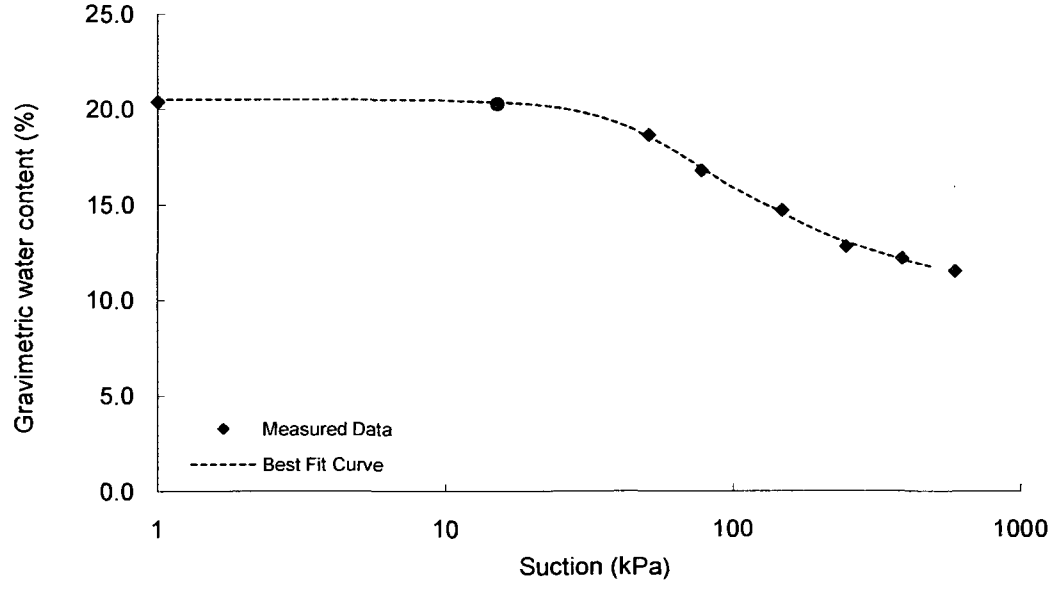

**Gradation curve available in Appendix B

Soil No. 29b

Indian Head till

Oloo and Fredlund, 1996; Oloo, 1994

Compacted Sample
Sand = 28%, Silt = 42%, Clay = 30%; Liquid Limit = 36, Plasticity Index = 19
Lean clay, CL

Shear Strength

Test Method: Modified triaxial test

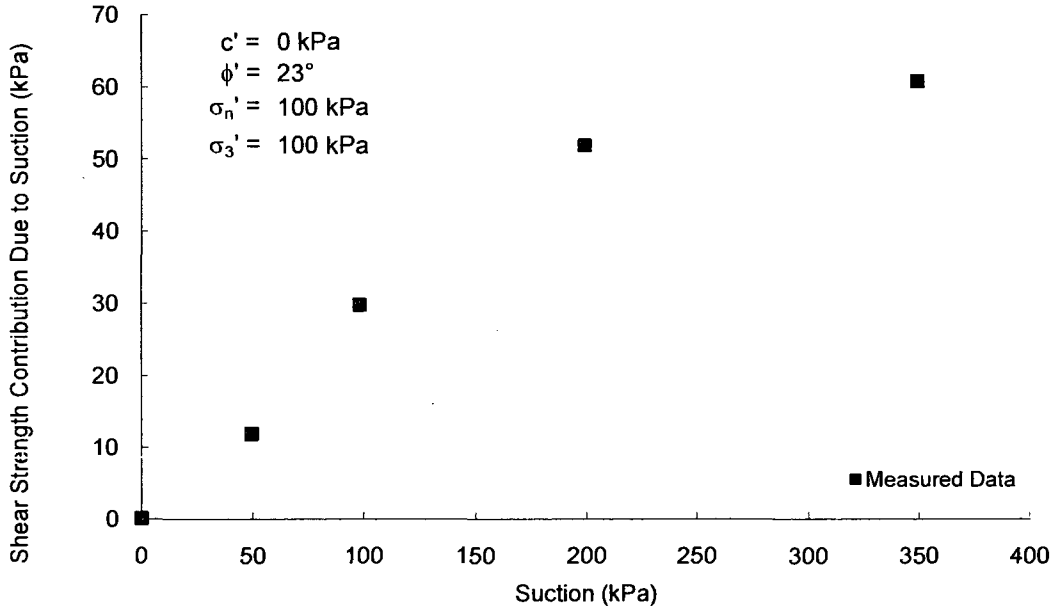

SWRC

Test Method: Pressure plate

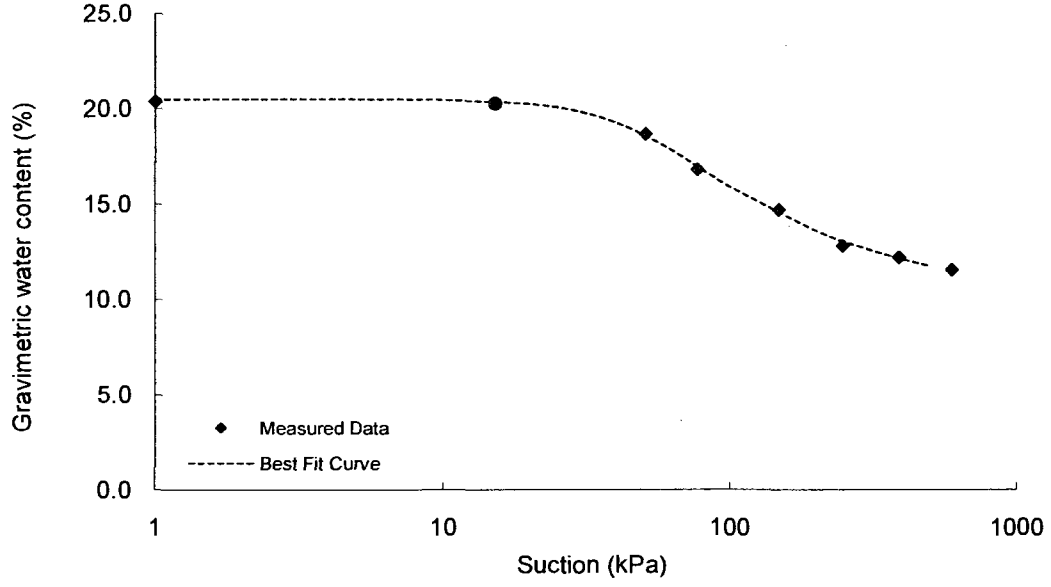

**Gradation curve available in Appendix B

Soil No. 29c

Indian Head till

Oloo and Fredlund, 1996; Oloo, 1994

Compacted Sample

Sand = 28%, Silt = 42%, Clay = 30%; Liquid Limit = 36, Plasticity Index = 19

Lean clay, CL

Shear Strength

Test Method: Modified triaxial test

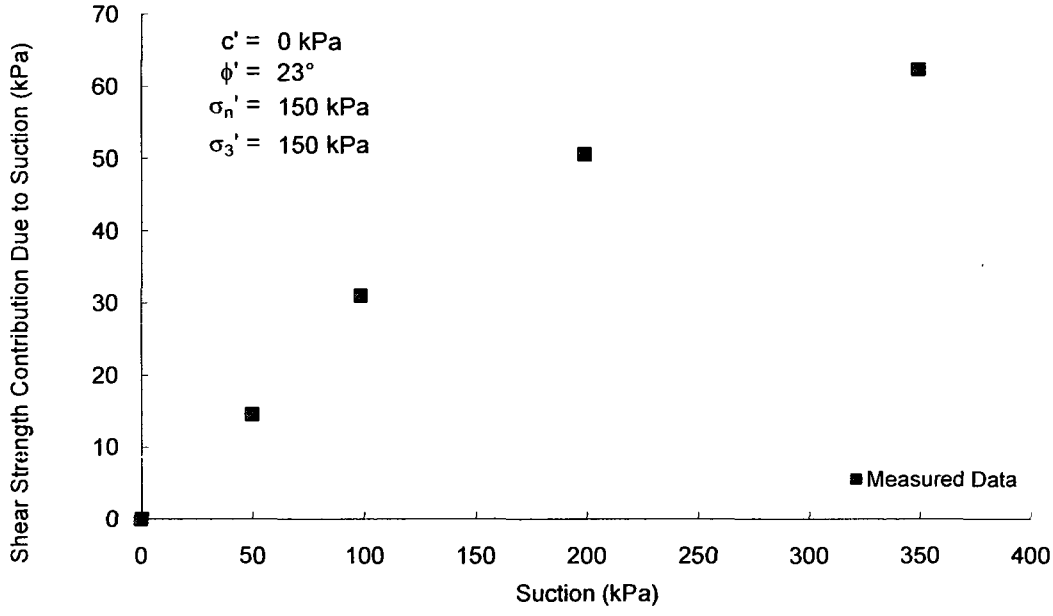

SWRC

Test Method: Pressure plate

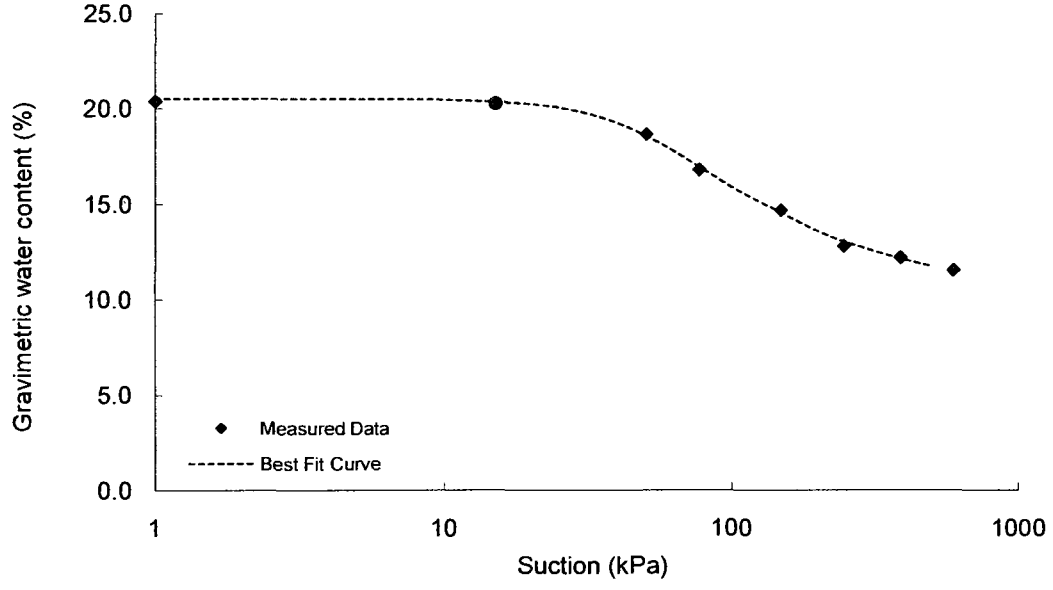

**Gradation curve available in Appendix B

Soil No. 30

Nanyang expansive soil

Miao, Liu and Lai, 2002

Compacted Sample

Sand = 6.7%, Silt = 68.5%, Clay = 24.8%; Liquid Limit = 58, Plasticity Index = 31

Fat clay, CH

Shear Strength

Test Method: Modified triaxial test

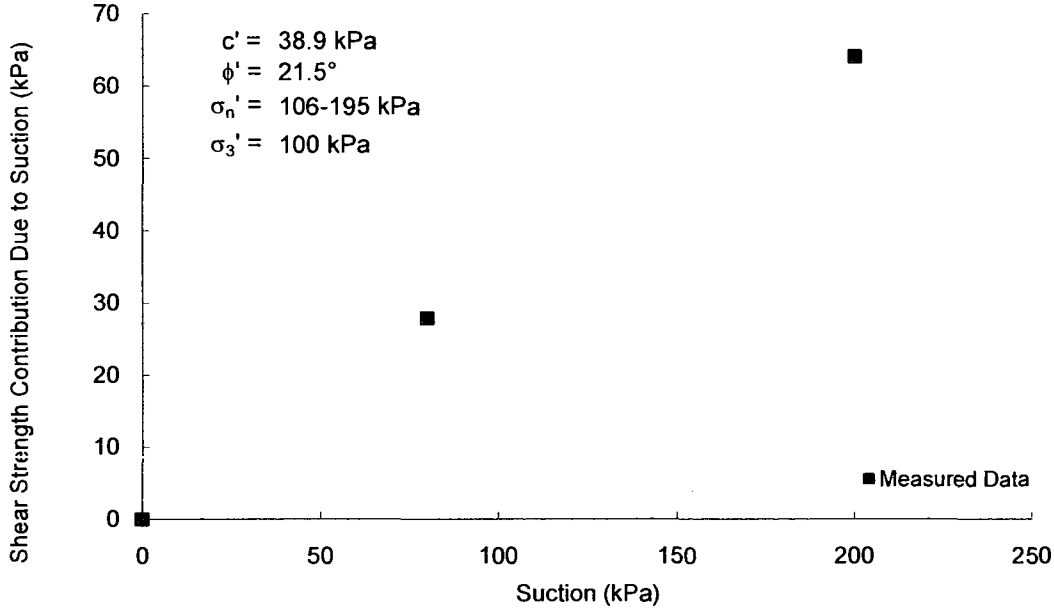

SWRC

Test Method: Pressure plate

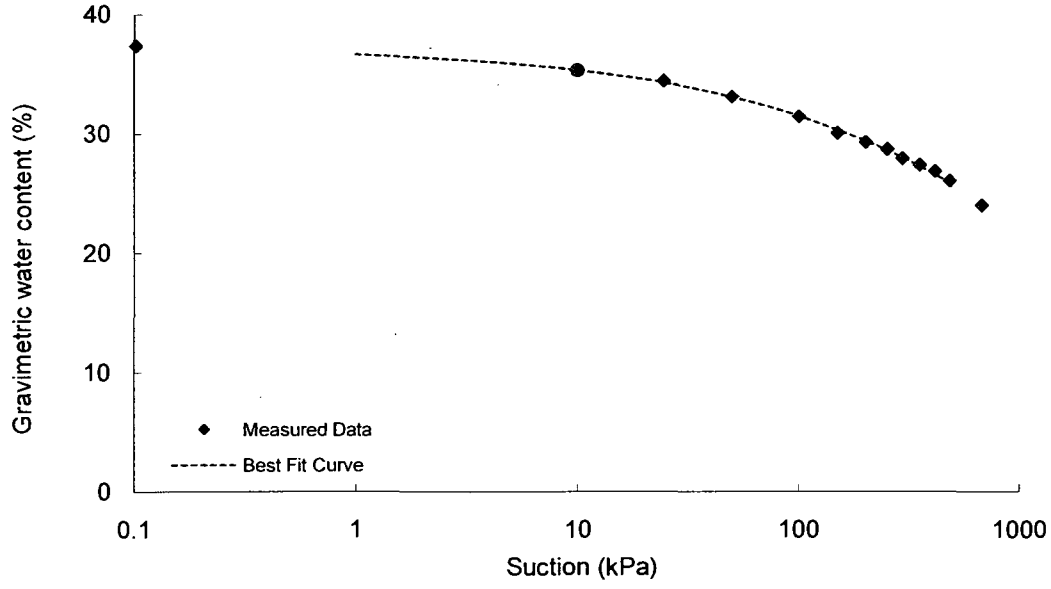

Soil No. 31a

Ouro Preto tropical (1 m)
Futai, Almeida and Lacerda, 2006

Undisturbed Soil Specimens
Sand = 44%, Silt = 9%, Clay = 46%; Liquid Limit = 57, Plasticity Index = 29
Fat clay, CH

Shear Strength

Test Method: Modified triaxial test

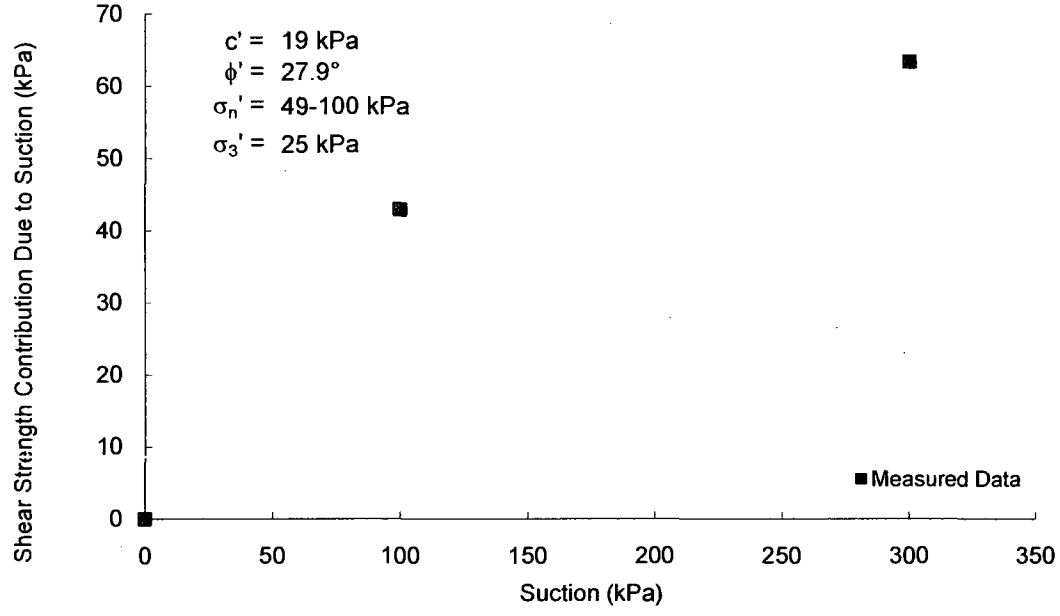

SWRC

Test Method: Pressure plate

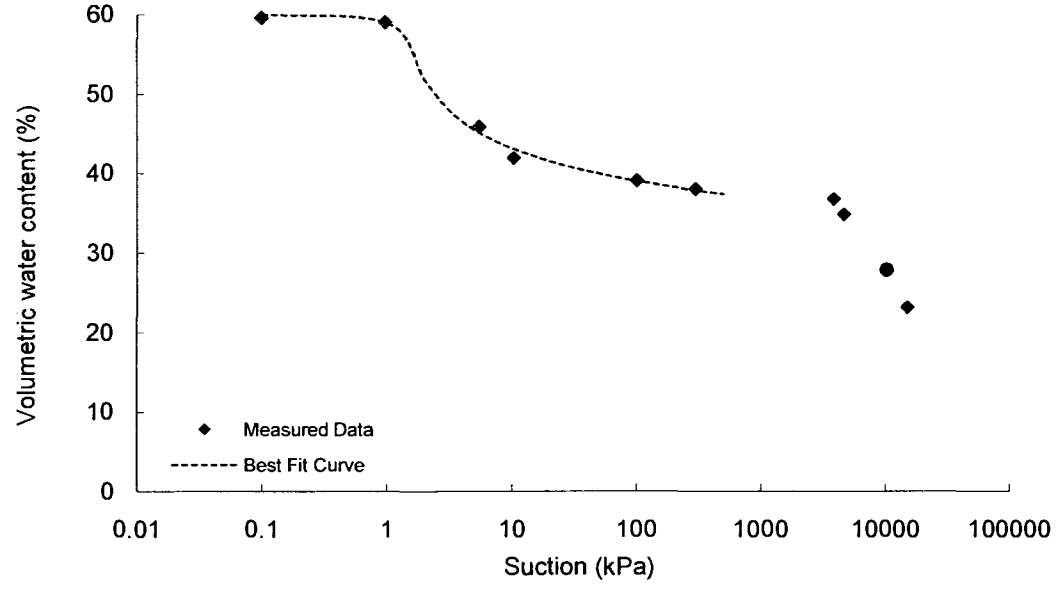

Soil No. 31b

Ouro Preto tropical (1 m)

Futai, Almeida and Lacerda, 2006

Undisturbed Soil Specimens

Sand = 44%, Silt = 9%, Clay = 46%; Liquid Limit = 57, Plasticity Index = 29

Fat clay, CH

Shear Strength

Test Method: Modified triaxial test

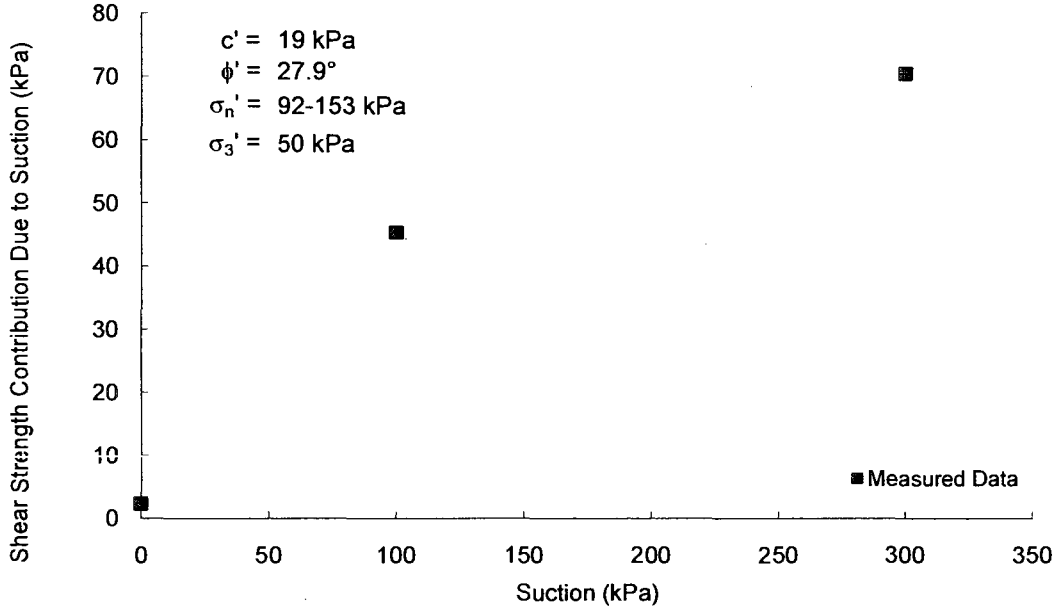

SWRC

Test Method: Pressure plate

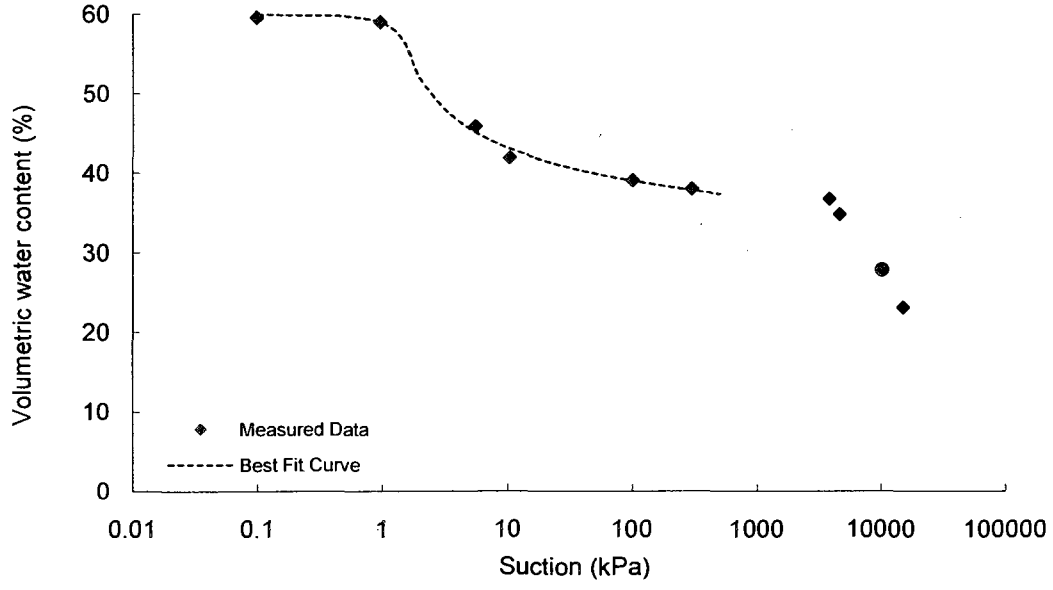

Soil No. 31c

Ouro Preto tropical (1 m)
Futai, Almeida and Lacerda, 2006

Undisturbed Soil Specimens
Sand = 44%, Silt = 9%, Clay = 46%; Liquid Limit = 57, Plasticity Index = 29
Fat clay, CH

Shear Strength

Test Method: Modified triaxial test

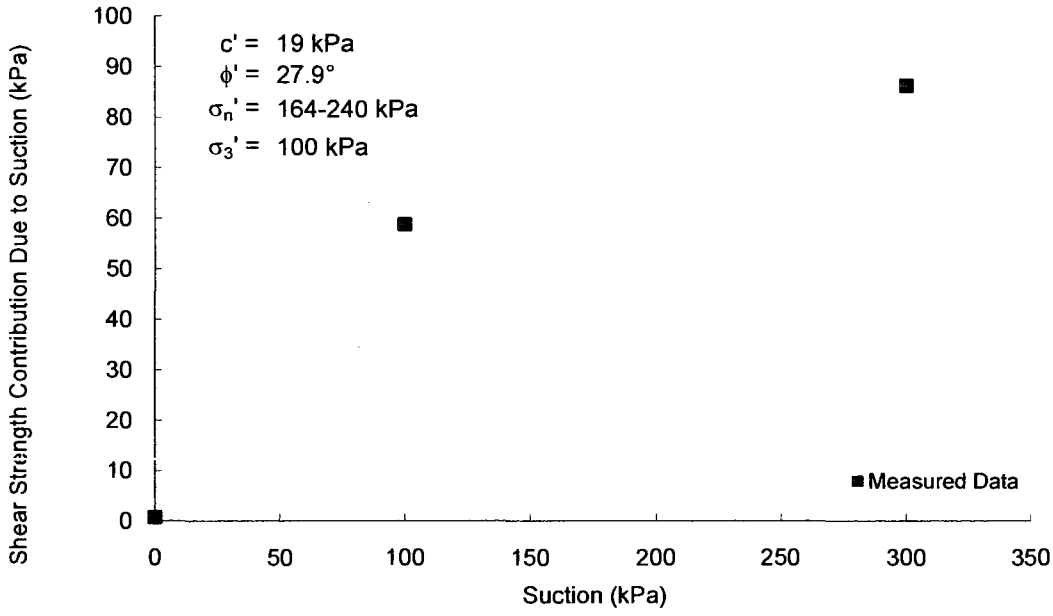

SWRC

Test Method: Pressure plate

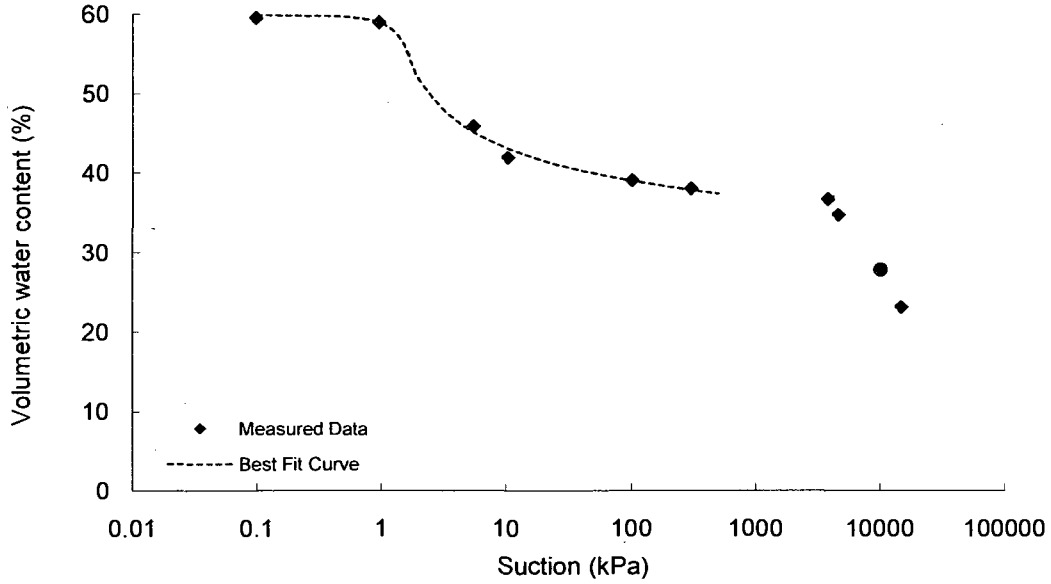

Soil No. 32a

Ouro Preto tropical (5 m)
Futai, Almeida and Lacerda, 2006

Undisturbed Soil Specimens
Sand = 38%, Silt = 54%, Clay = 8%; Liquid Limit = 42, Plasticity Index = 19
Lean clay, CL

Shear Strength

Test Method: Modified triaxial test

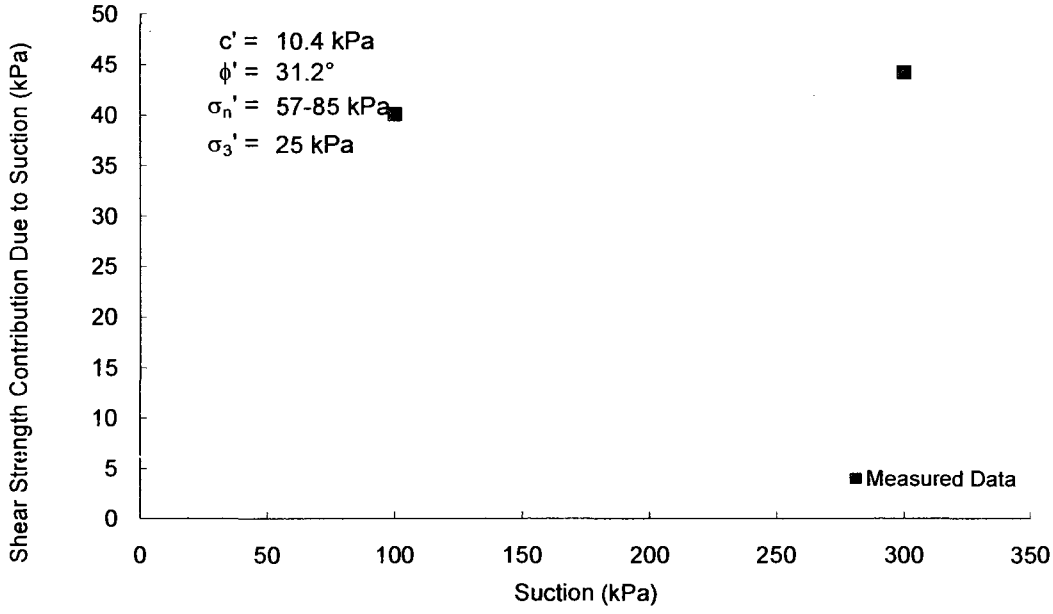

SWRC

Test Method: Pressure plate

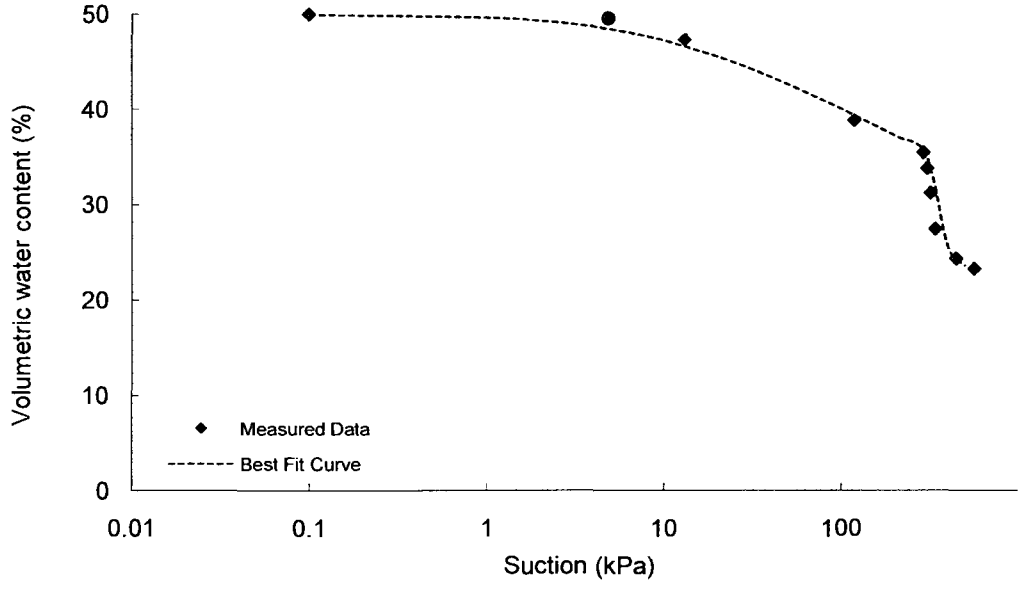

Soil No. 32b

Ouro Preto tropical (5 m)
Futai, Almeida and Lacerda, 2006

Undisturbed Soil Specimens
Sand = 38%, Silt = 54%, Clay = 8%; Liquid Limit = 42, Plasticity Index = 19
Lean clay, CL

Shear Strength

Test Method: Modified triaxial test

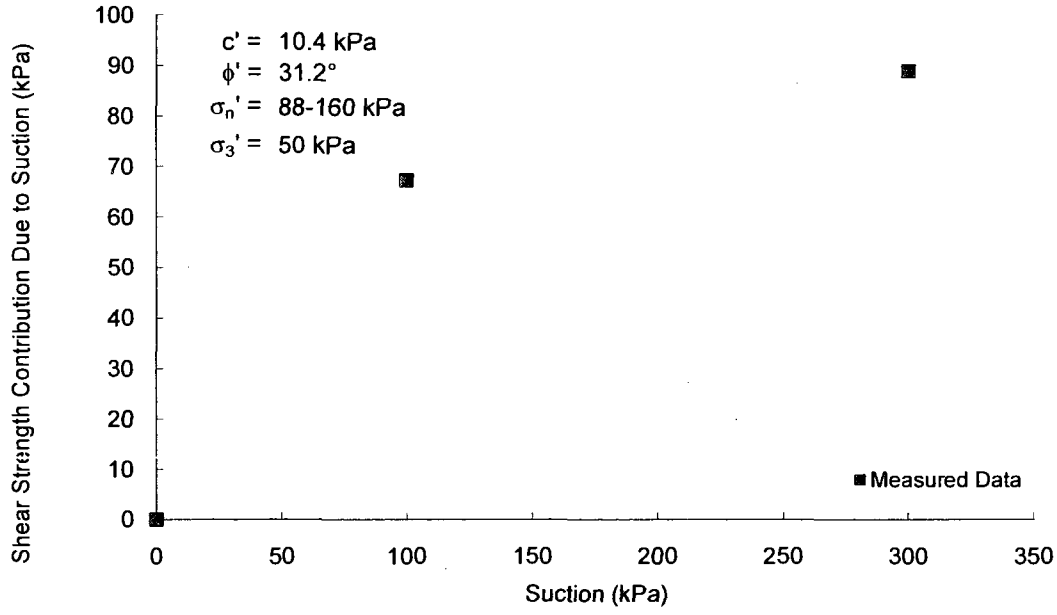

SWRC

Test Method: Pressure plate

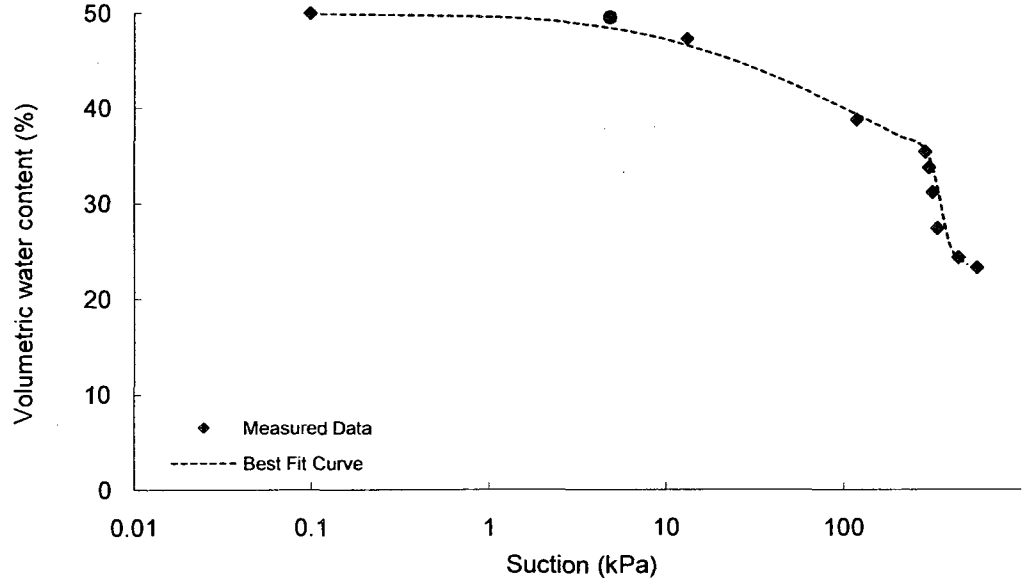

Soil No. 32c

Ouro Preto tropical (5 m)
Futai, Almeida and Lacerda, 2006

Undisturbed Soil Specimens
Sand = 38%, Silt = 54%, Clay = 8%; Liquid Limit = 42, Plasticity Index = 19
Lean clay, CL

Shear Strength

Test Method: Modified triaxial test

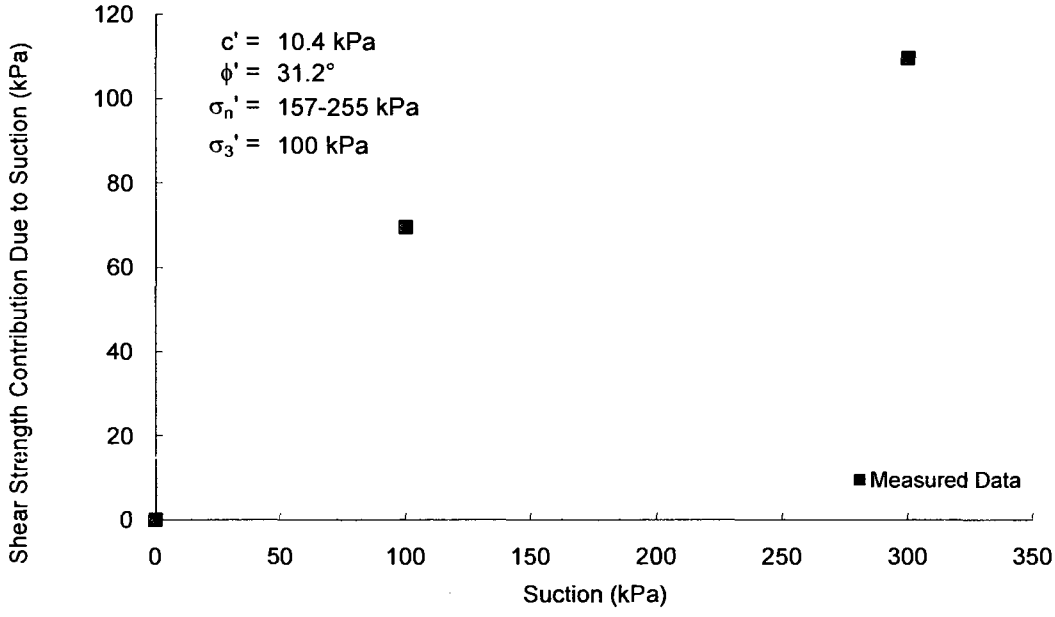

SWRC

Test Method: Pressure plate

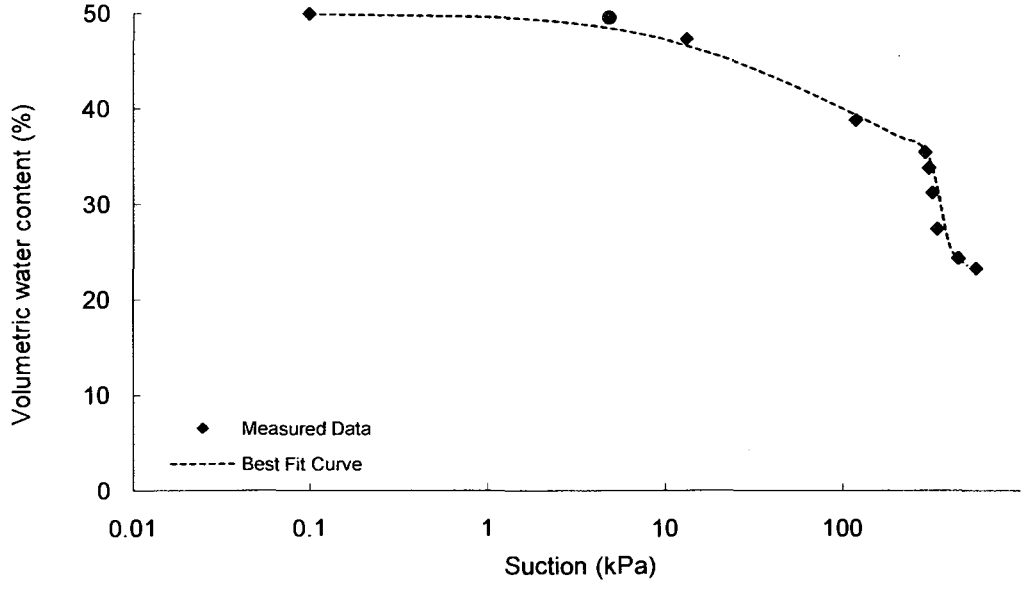

Soil No. 32d

Ouro Preto tropical (5 m)
Futai, Almeida and Lacerda, 2006

Undisturbed Soil Specimens
Sand = 38%, Silt = 54%, Clay = 8%; Liquid Limit = 42, Plasticity Index = 19
Lean clay, CL

Shear Strength

Test Method: Modified triaxial test

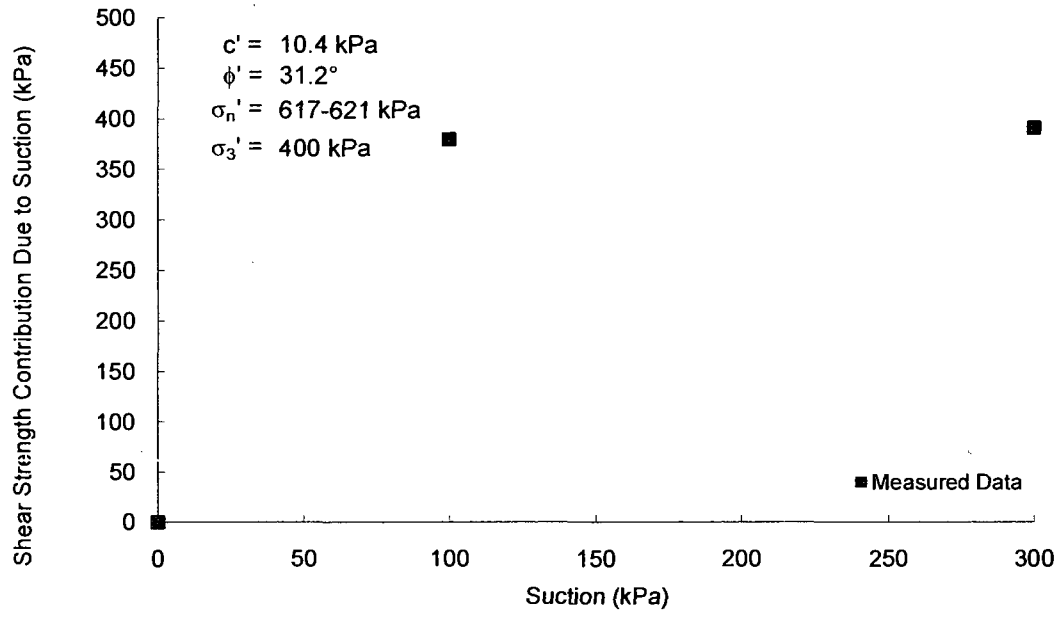

SWRC

Test Method: Pressure plate

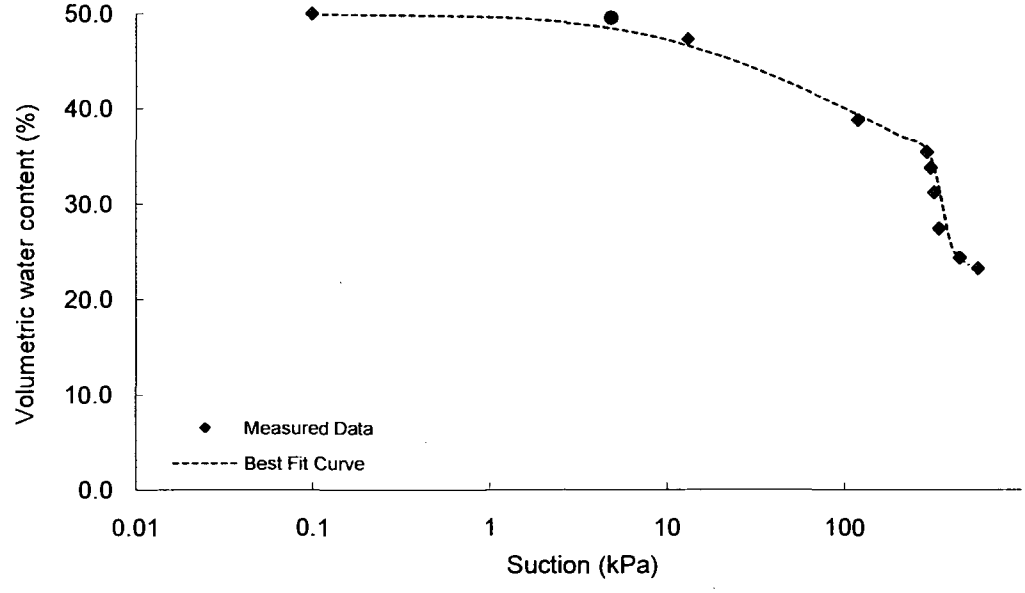

Soil No. 33a **C02**

Li, 1989; Hardcastle, Li and Fragaszy, 1992

Undisturbed Soil Specimens
Sand = 20%, Silt = 78%, Clay = 2%; Liquid Limit = 22, Plasticity Index = 2
Lean silt, ML

Shear Strength Test Method: Modified triaxial test

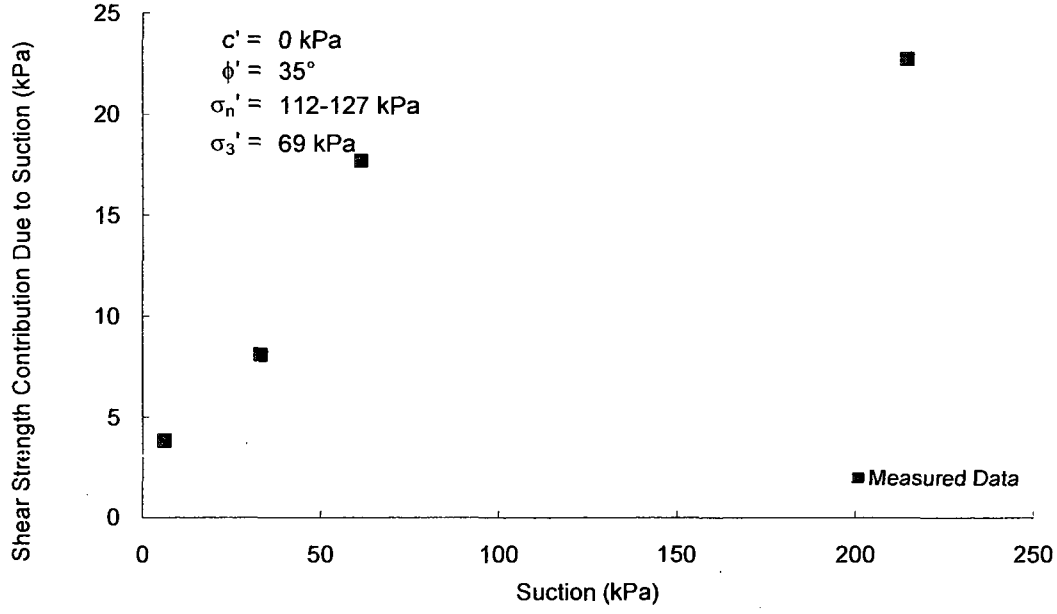

SWRC Test Method: Pressure plate

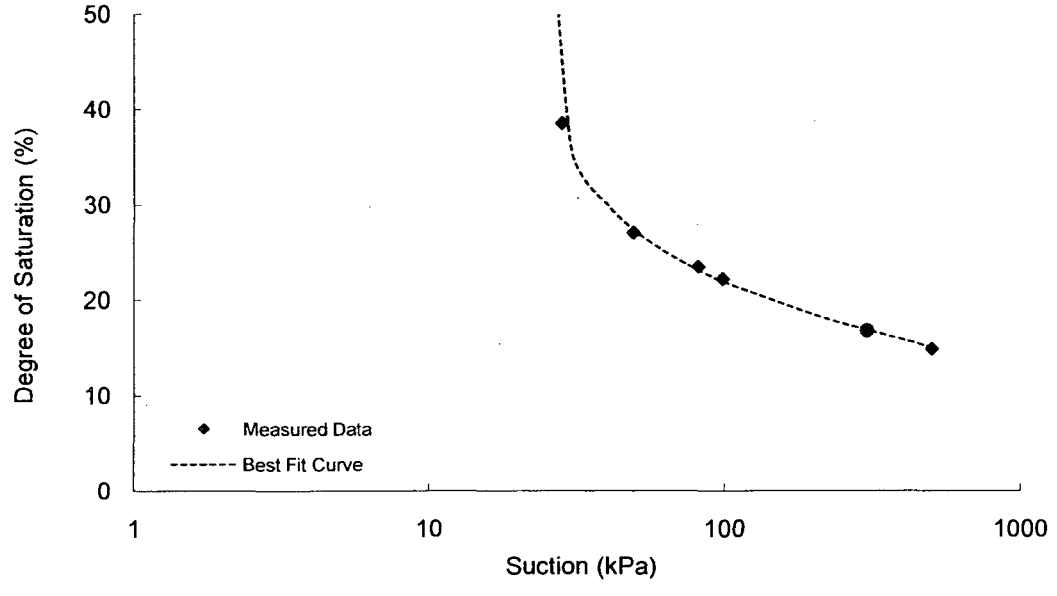

**Gradation curve available in Appendix B

Soil No. 33b **C02**

Li, 1989; Hardcastle, Li and Fragaszy, 1992

Undisturbed Soil Specimens Sand = 20%, Silt = 78%, Clay = 2%; Liquid Limit = 22, Plasticity Index = 2 Lean silt, ML

Shear Strength Test Method: Modified triaxial test

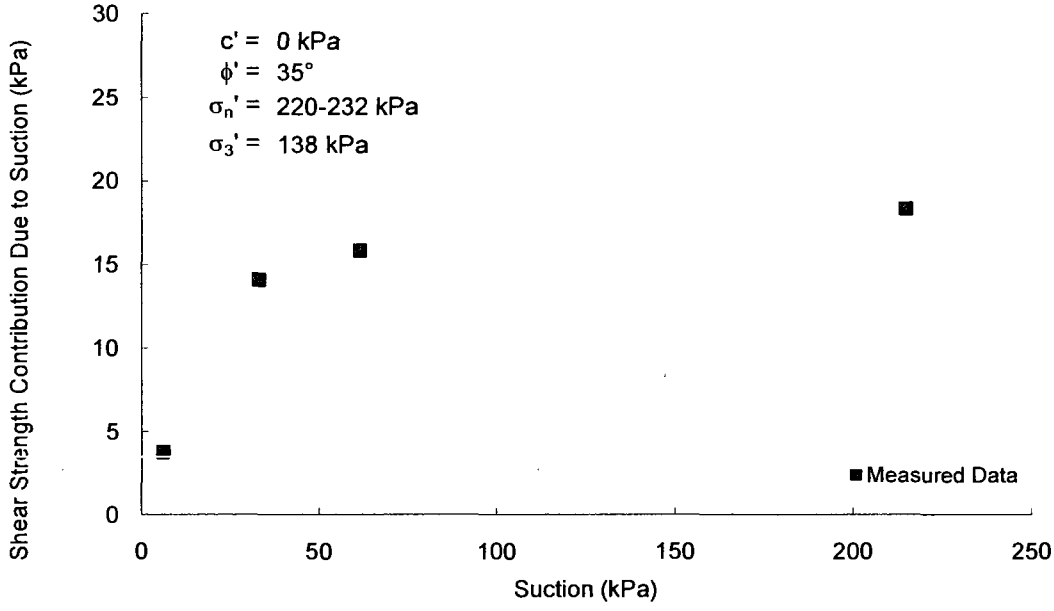

SWRC Test Method: Pressure plate

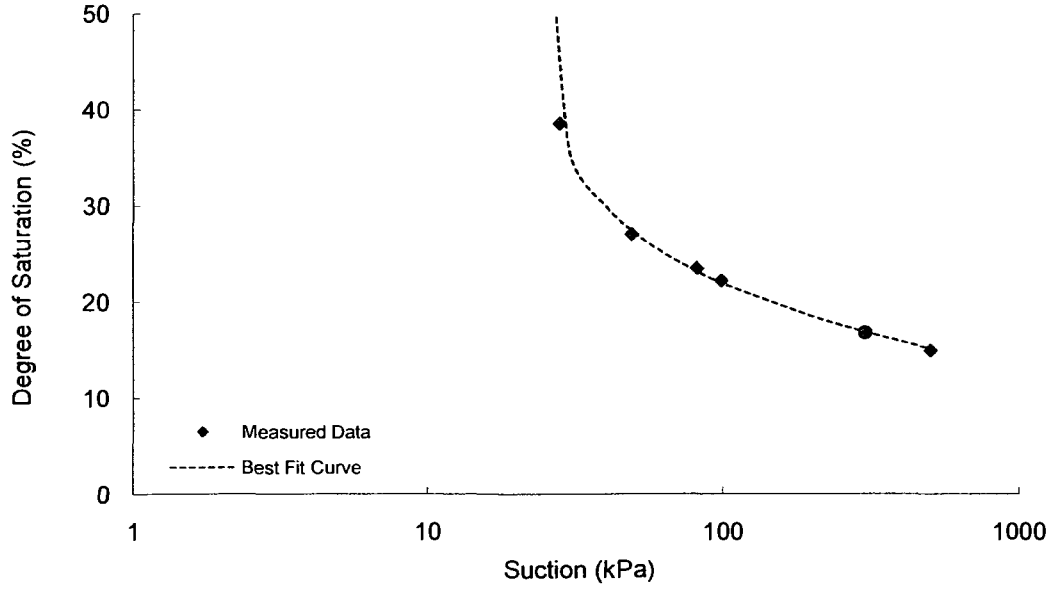

**Gradation curve available in Appendix B

Soil No. 34a **C11**

Li, 1989; Hardcastle, Li and Fragaszy, 1992

Undisturbed Soil Specimens
Sand = 6%, Silt = 83%, Clay = 11%; Liquid Limit = 29, Plasticity Index = 6
Lean silt, ML

Shear Strength

Test Method: Modified triaxial test

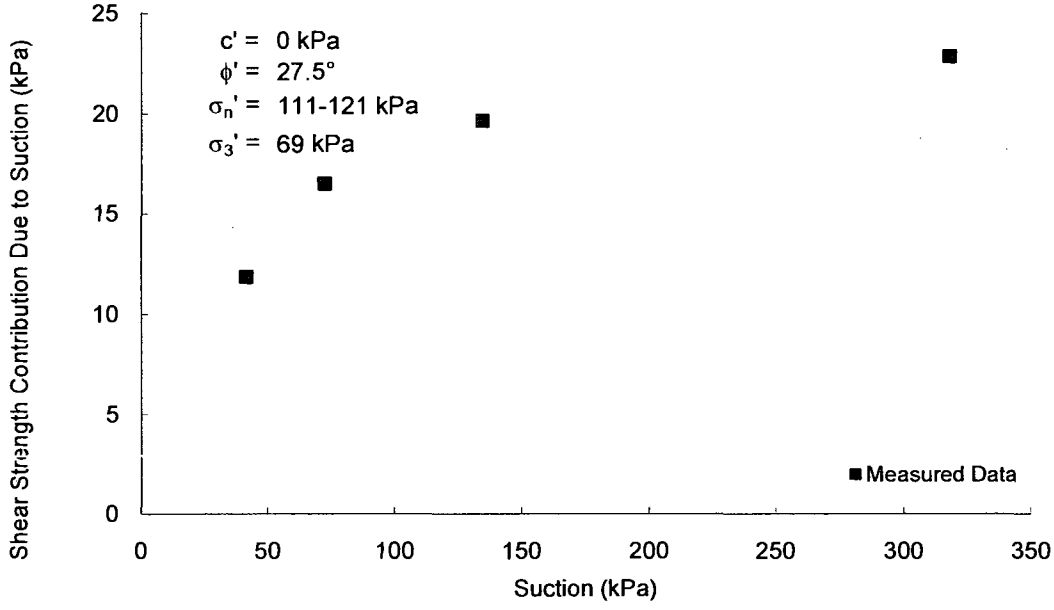

SWRC

Test Method: Pressure plate

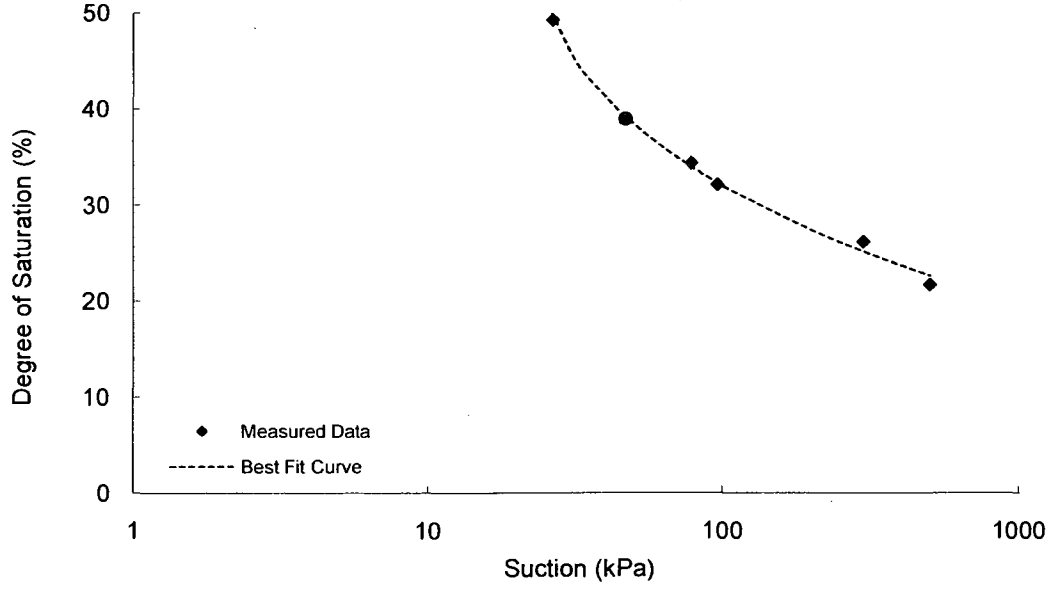

**Gradation curve available in Appendix B

Soil No. 34b **C11**

Li, 1989; Hardcastle, Li and Fragaszy, 1992

Undisturbed Soil Specimens
Sand = 6%, Silt = 83%, Clay = 11%; Liquid Limit = 29, Plasticity Index = 6
Lean silt, ML

Shear Strength

Test Method: Modified triaxial test

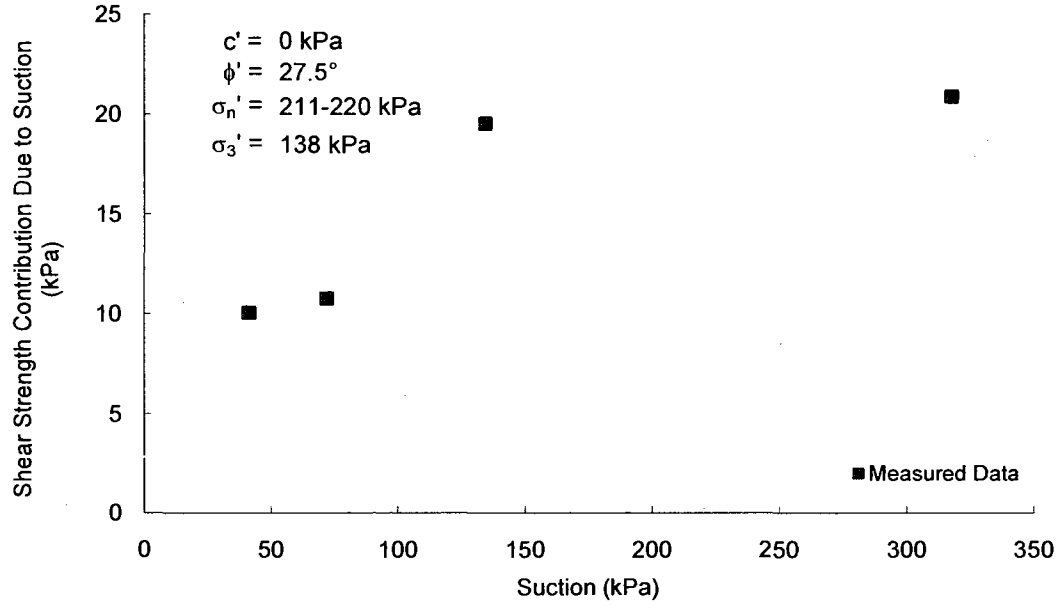

SWRC

Test Method: Pressure plate

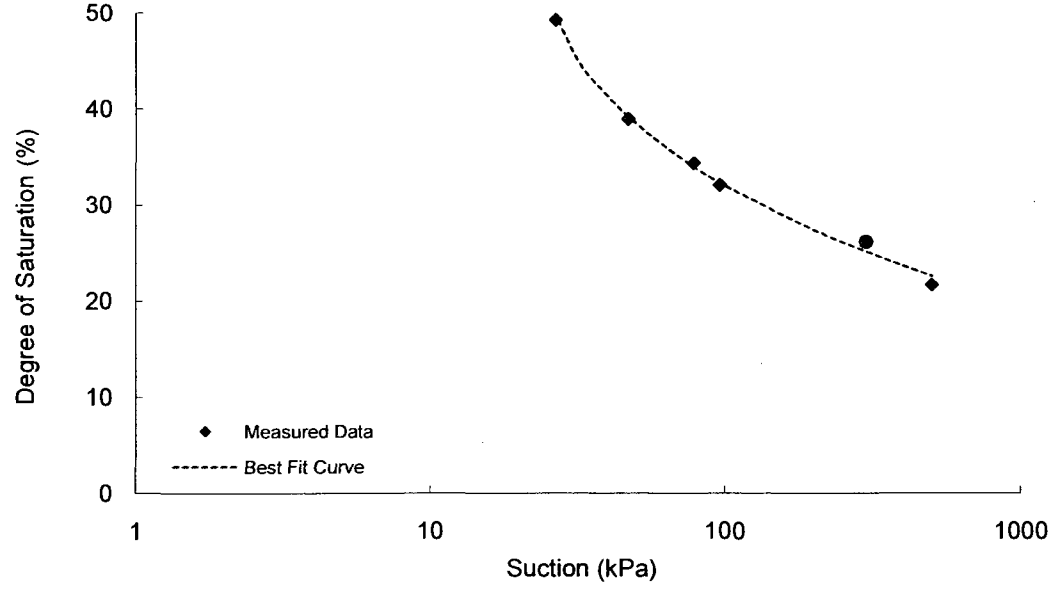

**Gradation curve available in Appendix B

Soil No. 35a **C20**

Li, 1989; Hardcastle, Li and Fragaszy, 1992

Undisturbed Soil Specimens

Sand = 4%, Silt = 76.4%, Clay = 20%; Liquid Limit = 30, Plasticity Index = 12

Lean clay, CL

Shear Strength

Test Method: Modified triaxial test

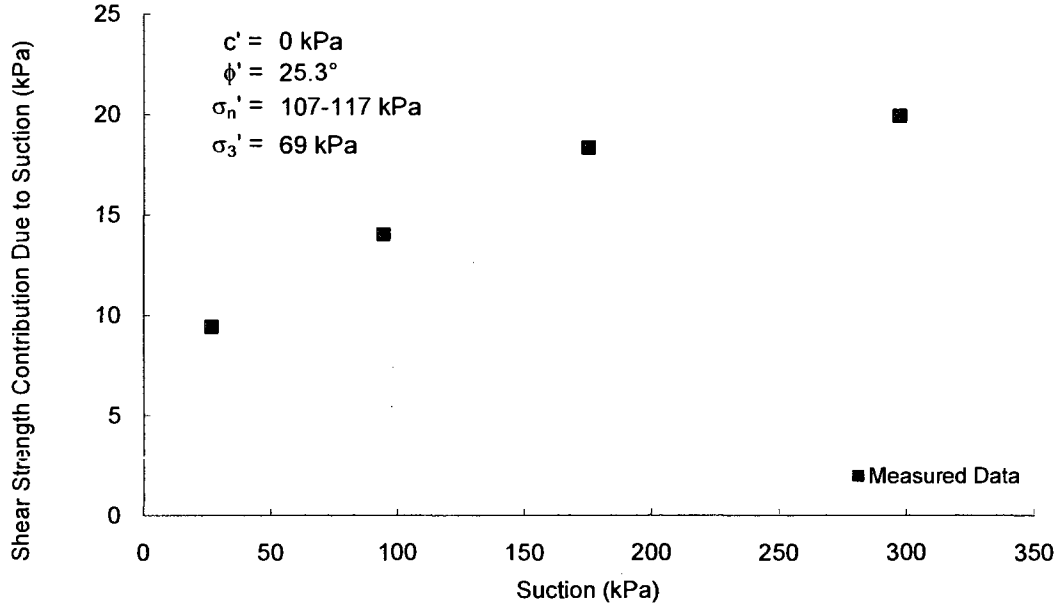

SWRC

Test Method: Pressure plate

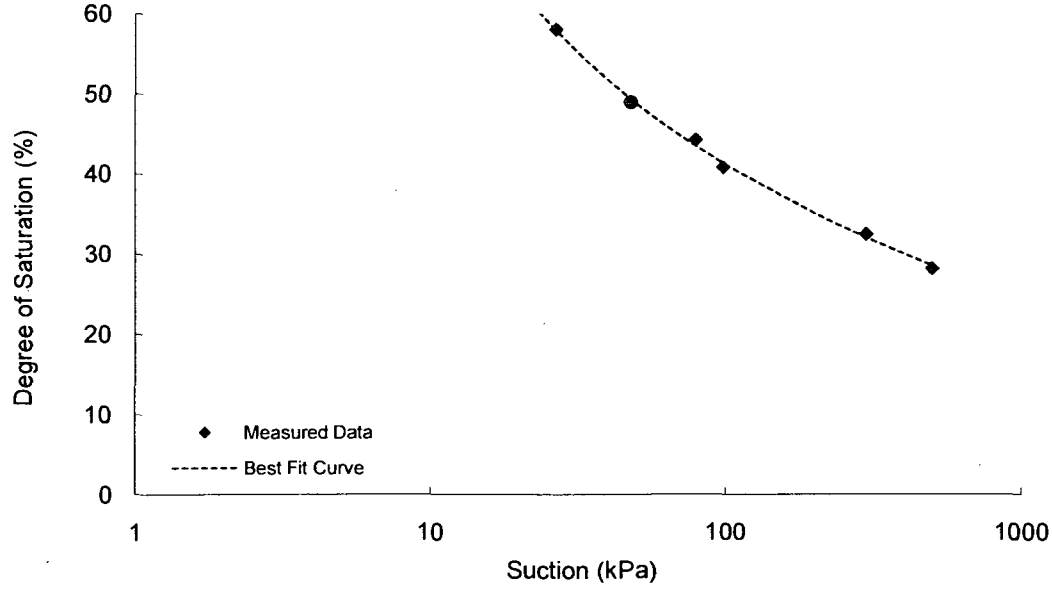

**Gradation curve available in Appendix B

Soil No. 35b **C20**

Li, 1989; Hardcastle, Li and Fragaszy, 1992

Undisturbed Soil Specimens
Sand = 4%, Silt = 76.4%, Clay = 20%; Liquid Limit = 30, Plasticity Index = 12
Lean clay, CL

Shear Strength Test Method: Modified triaxial test

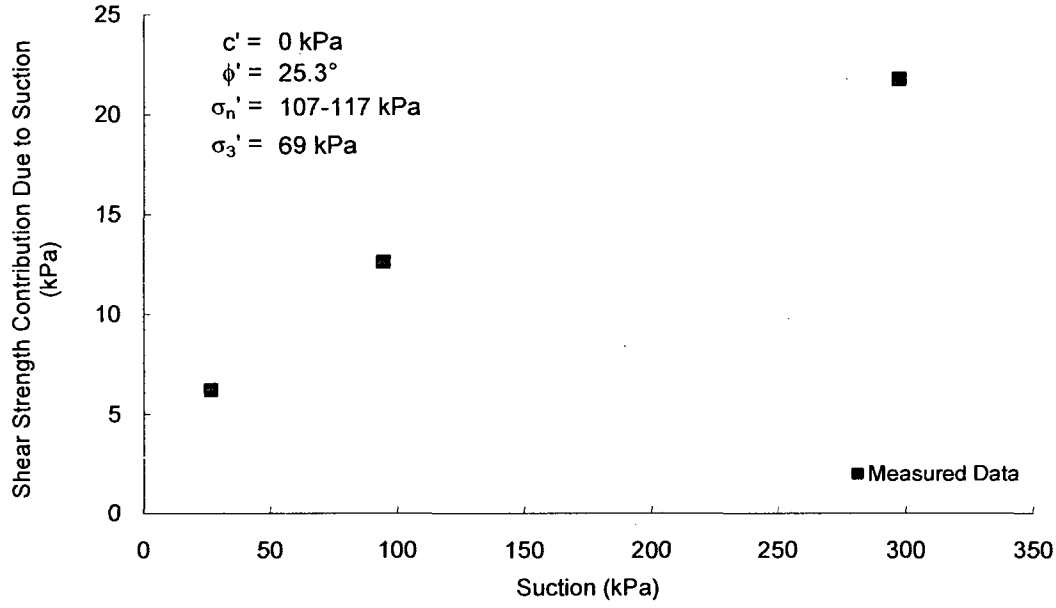

SWRC Test Method: Pressure plate

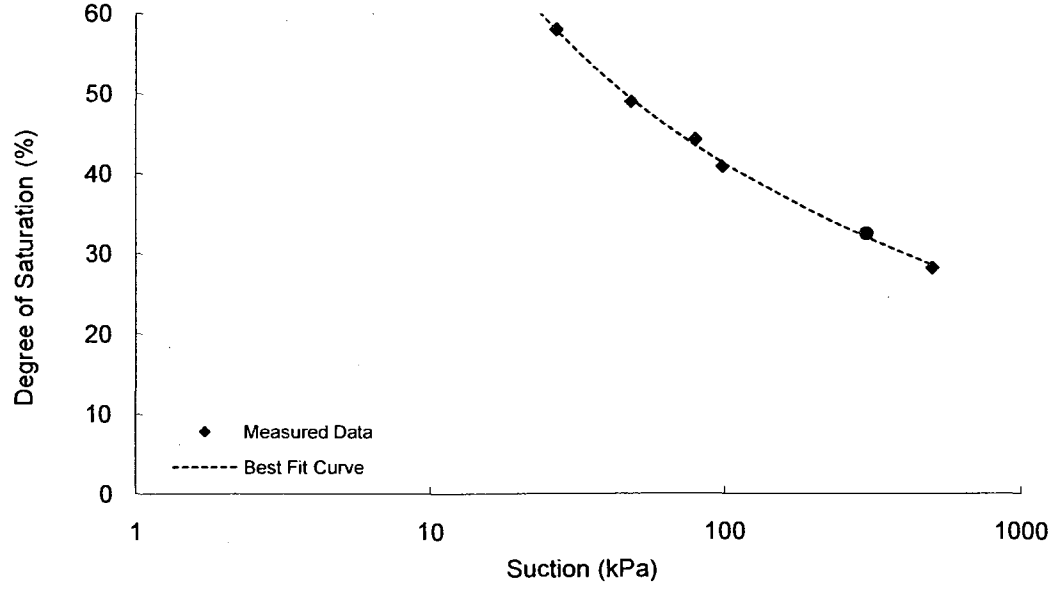

**Gradation curve available in Appendix B

Soil No. 36a **C30**

Li, 1989; Hardcastle, Li and Fragaszy, 1992

Undisturbed Soil Specimens

Sand = 2.2%, Silt = 67.8%, Clay = 30%; Liquid Limit = 38, Plasticity Index = 17

Lean clay, CL

Shear Strength

Test Method: Modified triaxial test

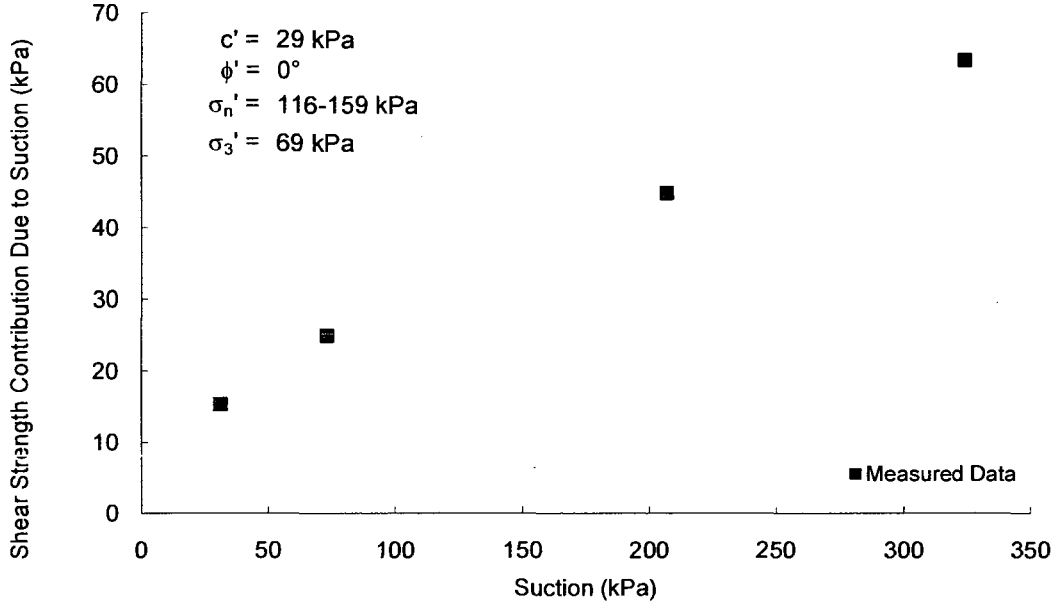

SWRC

Test Method: Pressure plate

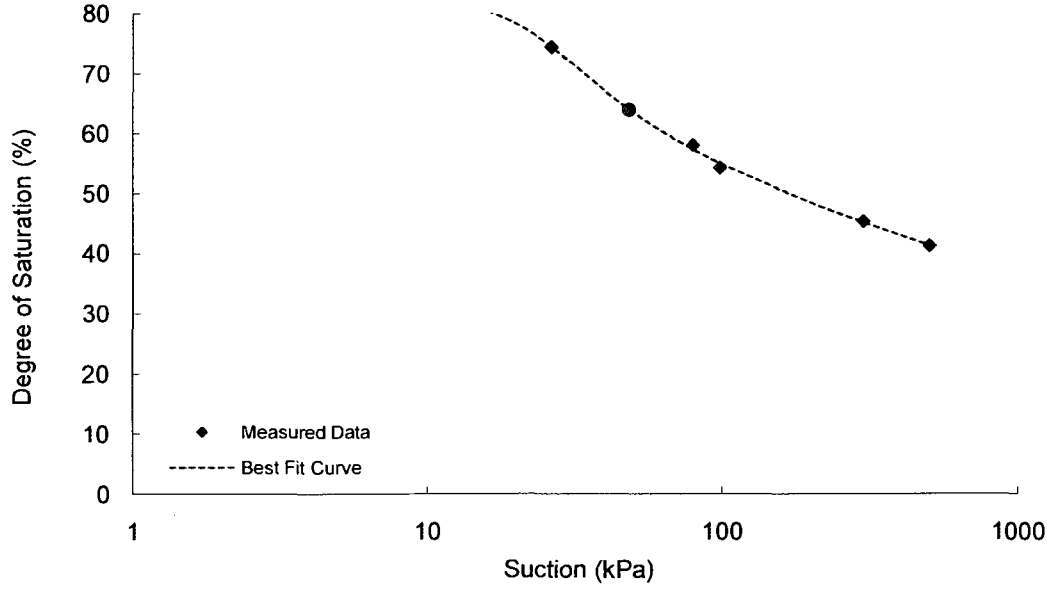

**Gradation curve available in Appendix B

Soil No. 36b **C30**

Li, 1989; Hardcastle, Li and Fragaszy, 1992

Undisturbed Soil Specimens
Sand = 2.2%, Silt = 67.8%, Clay = 30%; Liquid Limit = 38, Plasticity Index = 17
Lean clay, CL

Shear Strength Test Method: Modified triaxial test

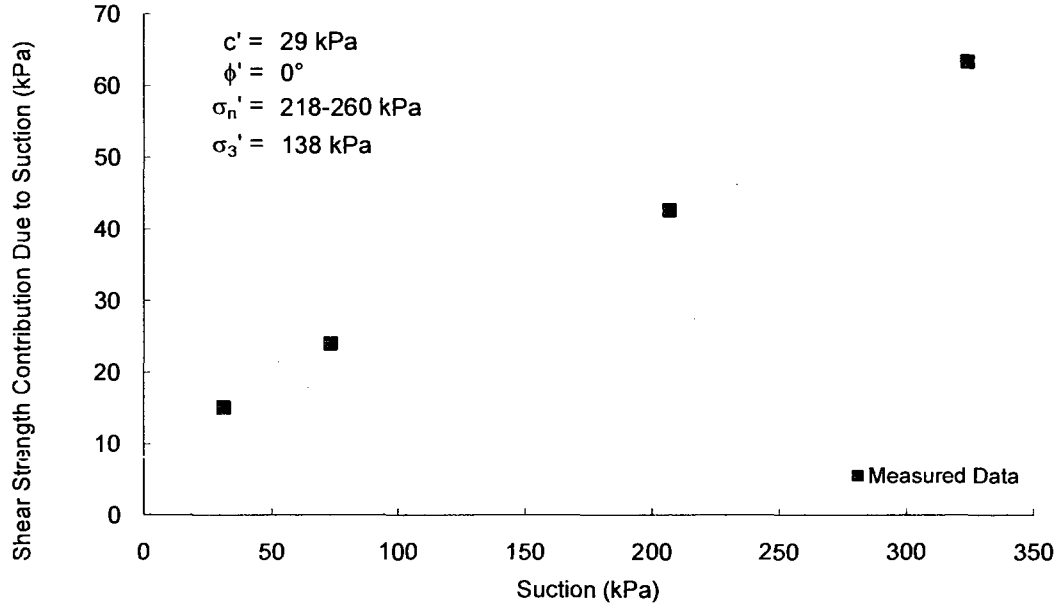

SWRC Test Method: Pressure plate

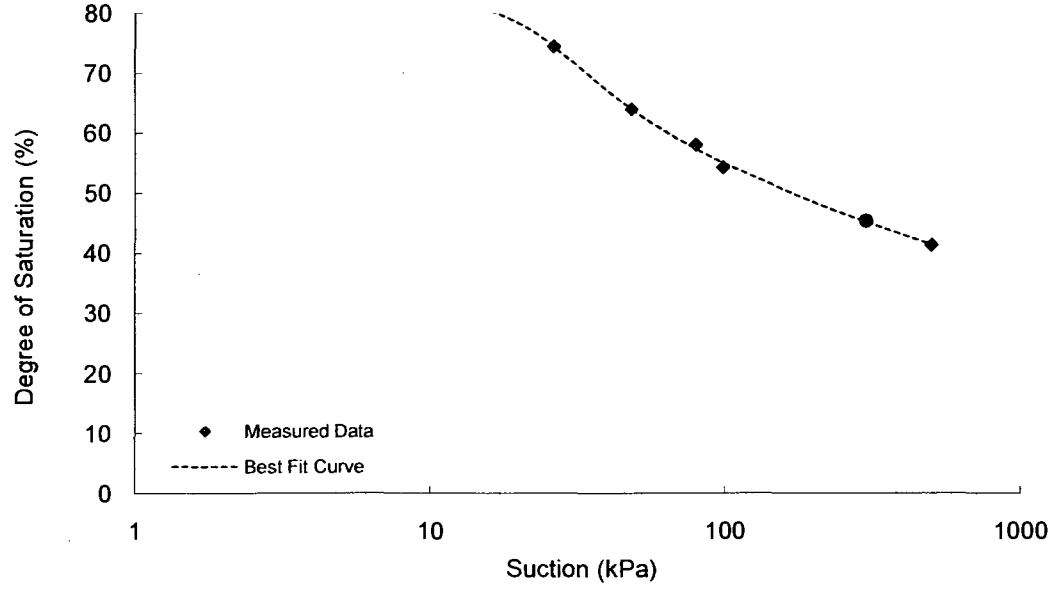

**Gradation curve available in Appendix B

Soil No. 37a

Recife clay

Jucá, Ferreira and Bastos, 1995

Undisturbed Soil Specimens
Sand = 20%, Silt = 21%, Clay = 59%; Liquid Limit = 73, Plasticity Index = 19
Heavy silt, MH

Shear Strength

Test Method: Modified triaxial test

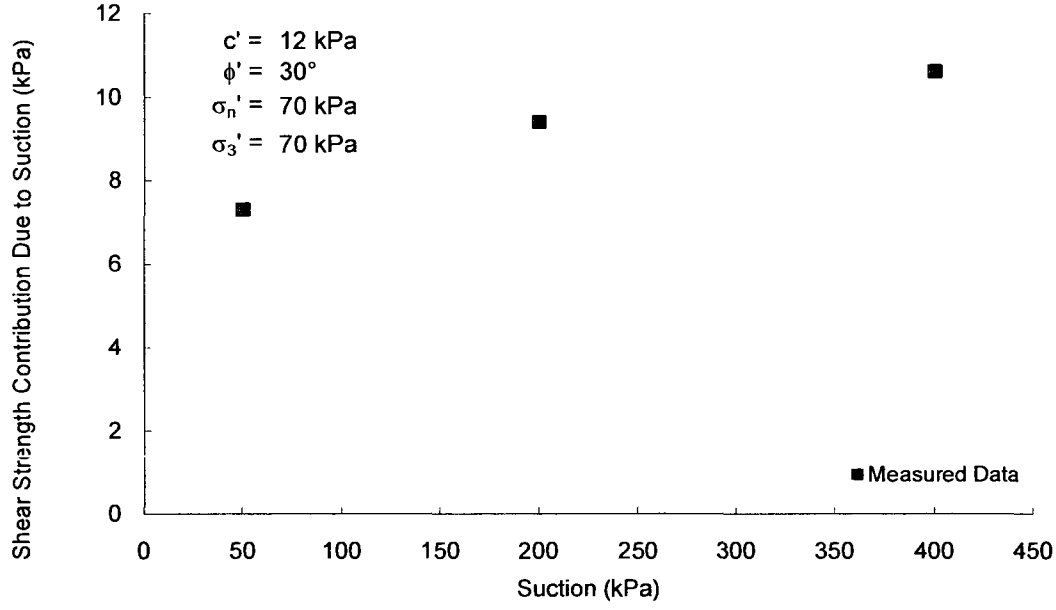

SWRC

Test Method: Pressure plate

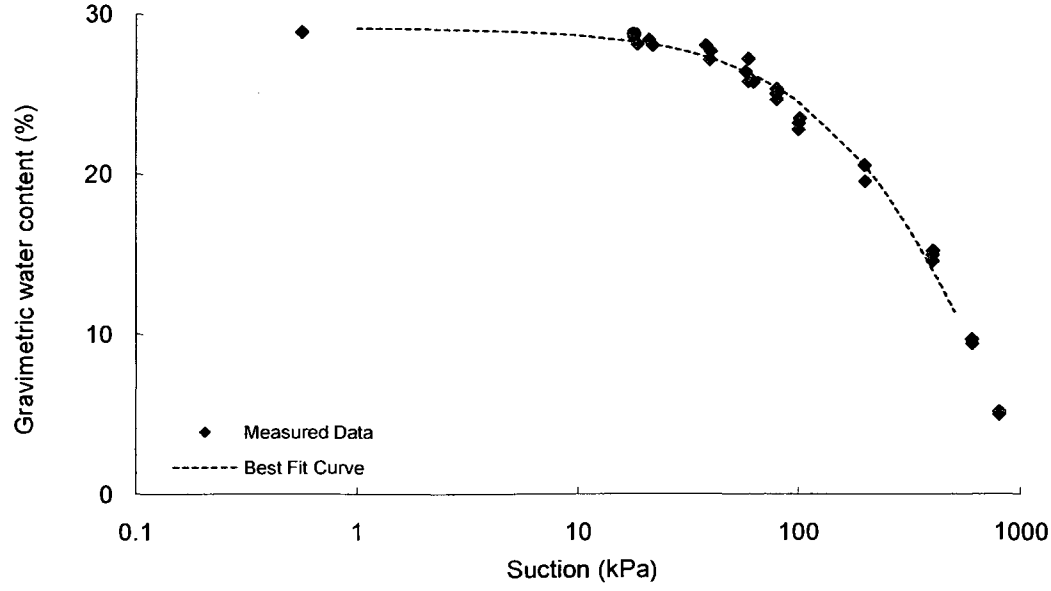

Soil No. 37b

Recife clay

Jucá, Ferreira and Bastos, 1995

Undisturbed Soil Specimens

Sand = 20%, Silt = 21%, Clay = 59%; Liquid Limit = 73, Plasticity Index = 19

Heavy silt, MH

Shear Strength

Test Method: Modified triaxial test

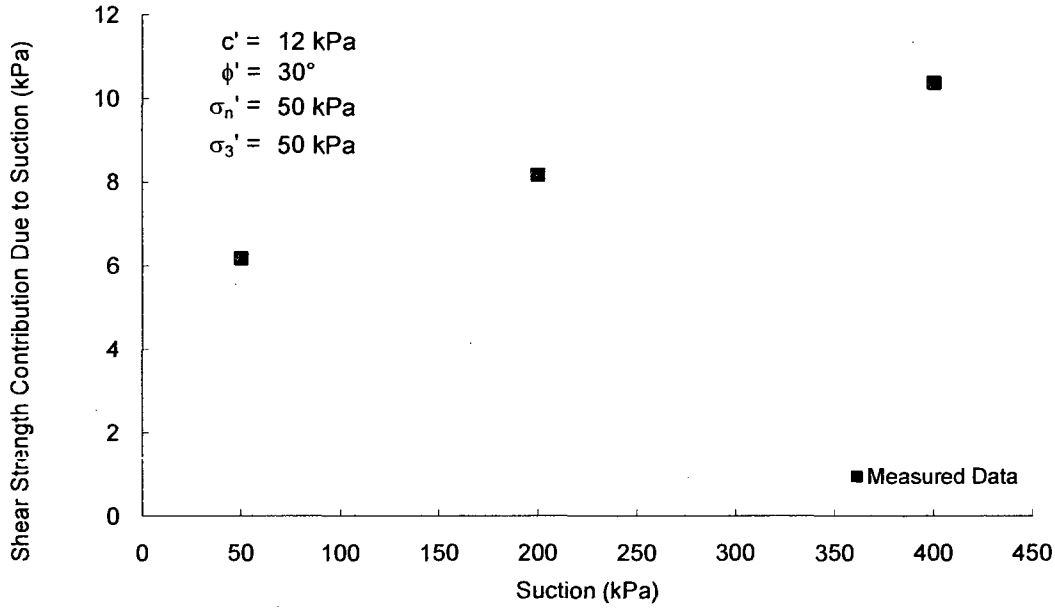

SWRC

Test Method: Pressure plate

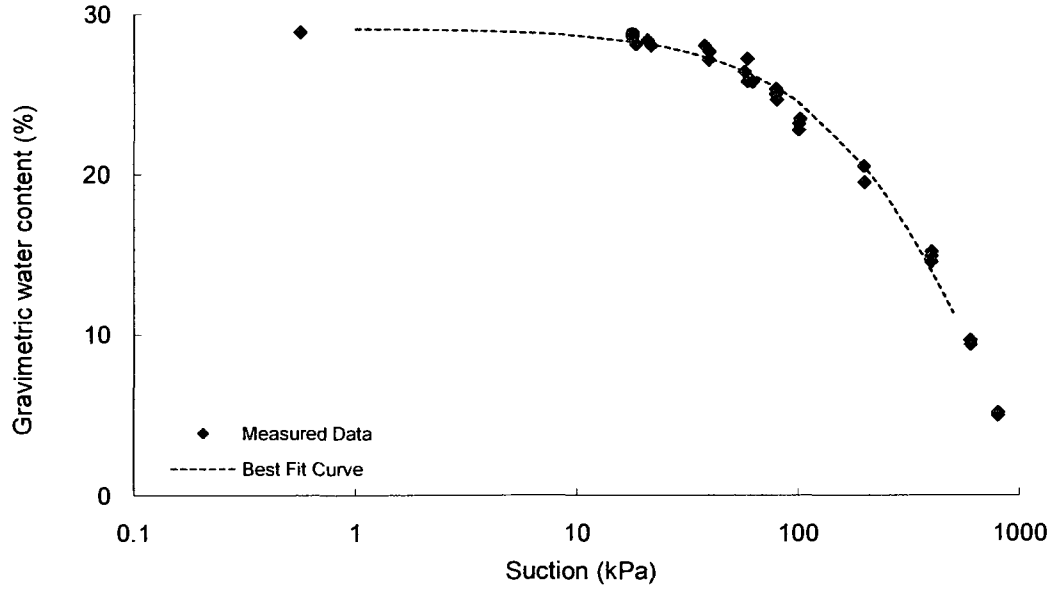

Soil No. 37c

Recife clay

Jucá, Ferreira and Bastos, 1995

Undisturbed Soil Specimens

Sand = 20%, Silt = 21%, Clay = 59%; Liquid Limit = 73, Plasticity Index = 19

Heavy silt, MH

Shear Strength

Test Method: Modified triaxial test

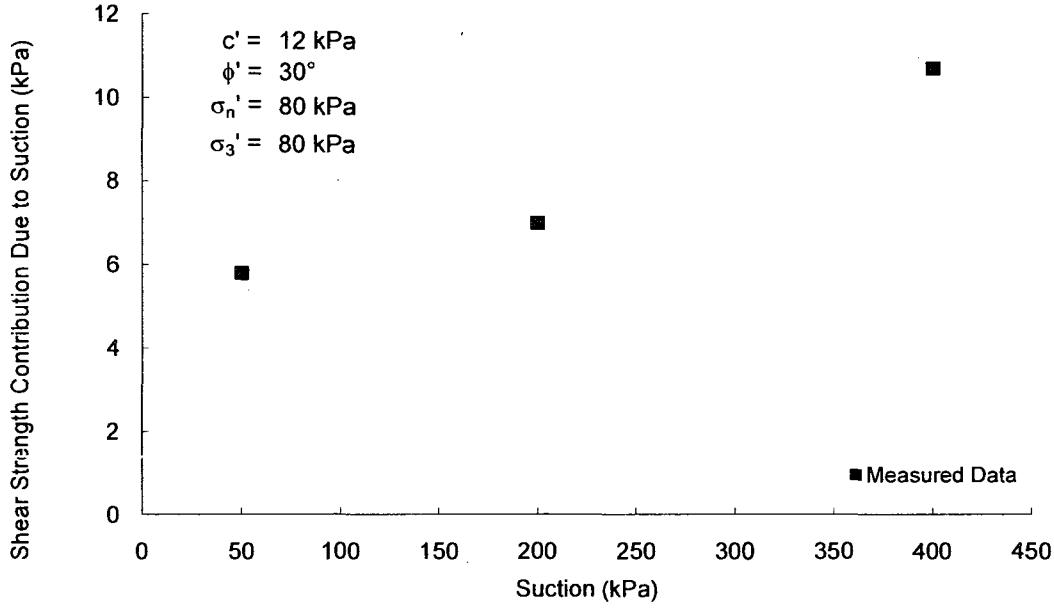

SWRC

Test Method: Pressure plate

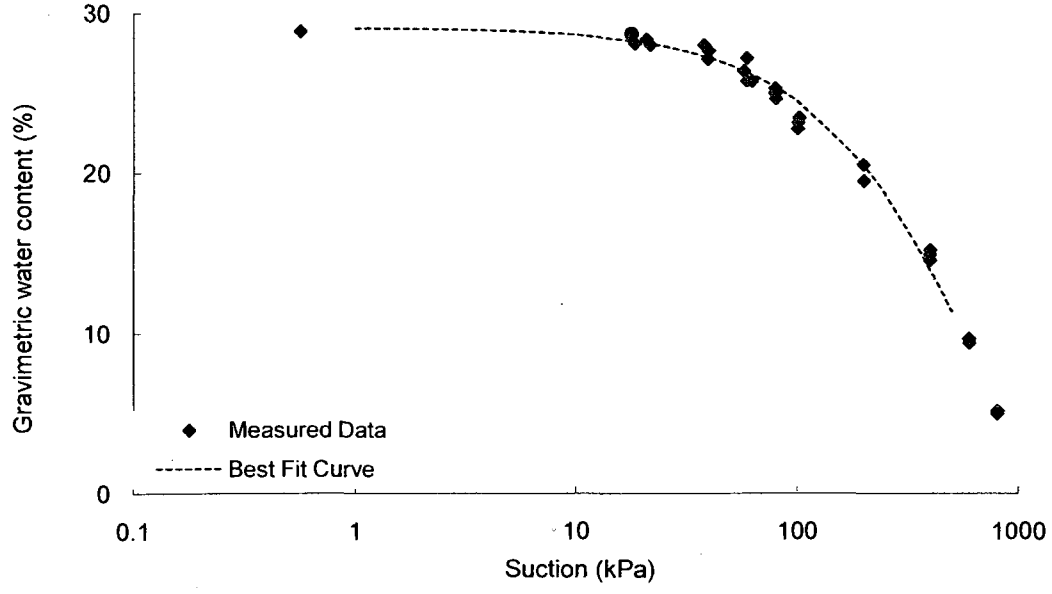

Soil No. 38a

Pacatuba residual sand
Perreira and Fredlund, 1999

Undisturbed Soil Specimens
Sand = 52%, Silt = 35%, Clay = 13%; Liquid Limit = 29, Plasticity Index = 12
Lean clay, CL

Shear Strength

Test Method: Modified direct shear test

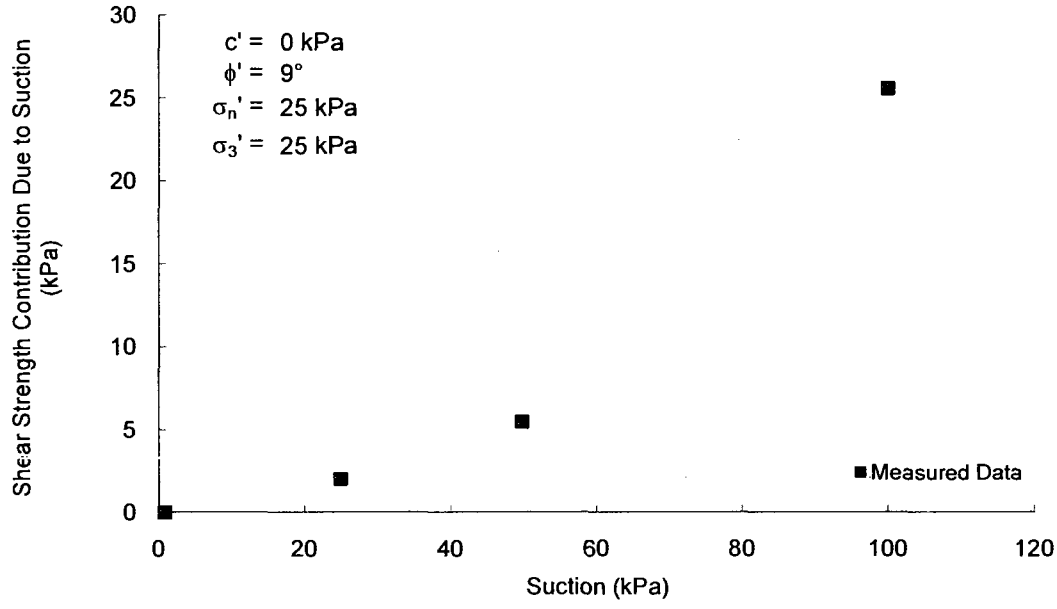

SWRC

Test Method: Tempe cell, pressure plate

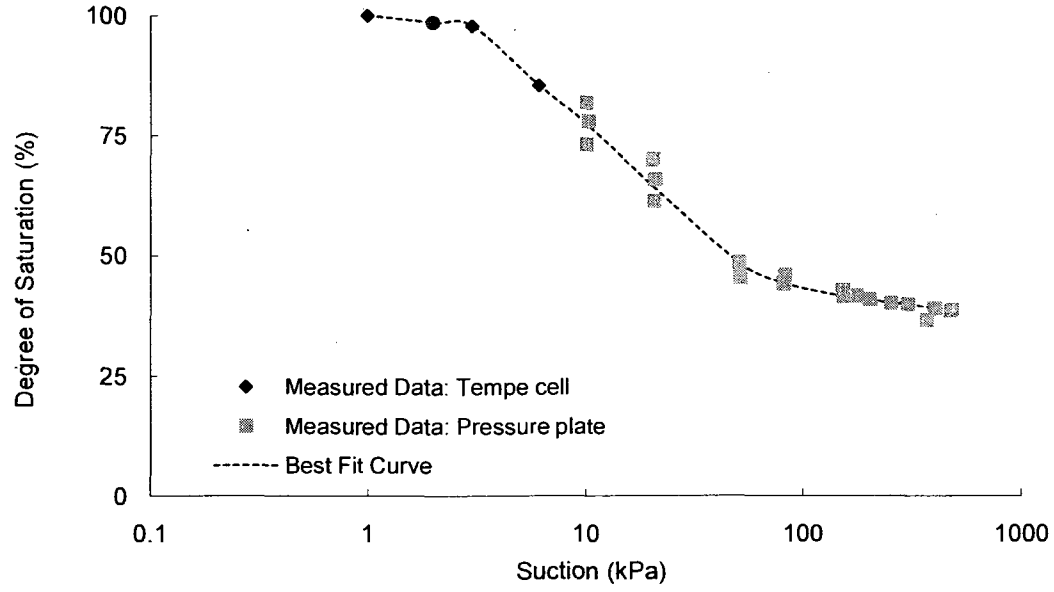

Soil No. 38b

Pacatuba residual sand
Perreira and Fredlund, 1999

Undisturbed Soil Specimens
Sand = 52%, Silt = 35%, Clay = 13%; Liquid Limit = 29, Plasticity Index = 12
Lean clay, CL

Shear Strength

Test Method: Modified direct shear test

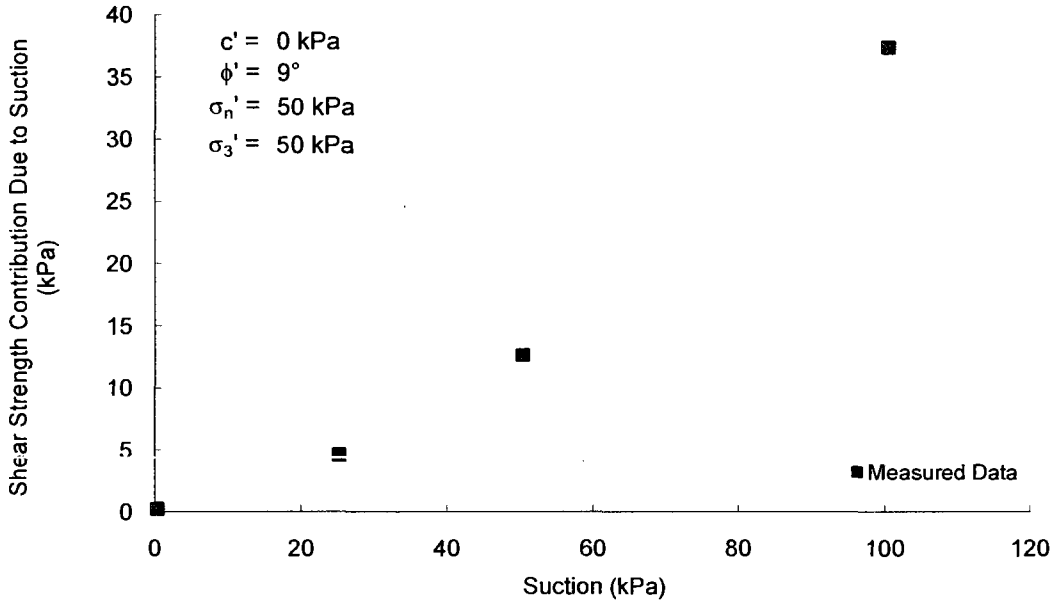

SWRC

Test Method: Tempe cell, pressure plate

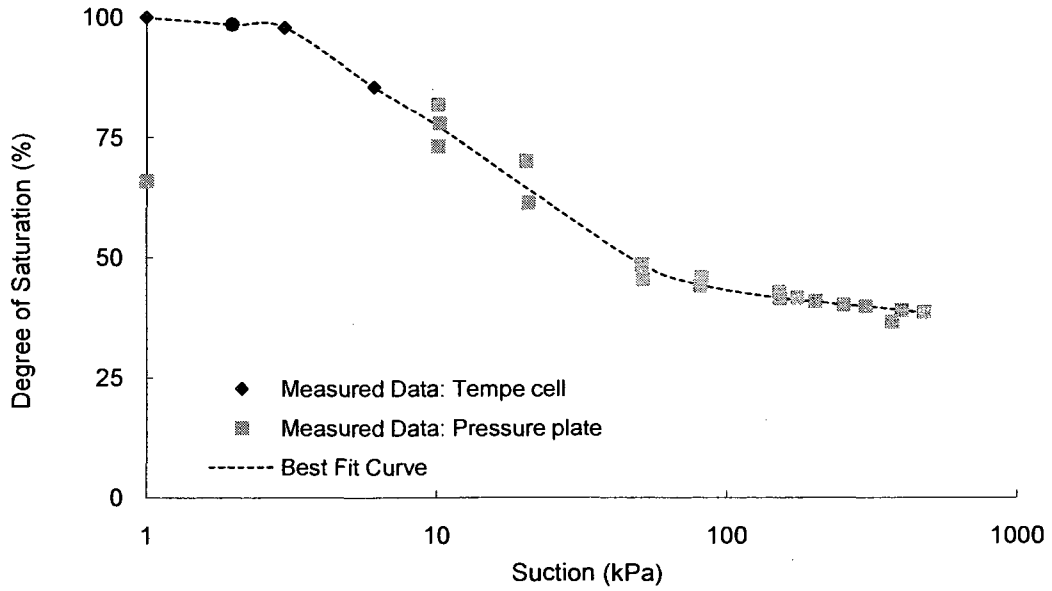

Soil No. 38c

Pacatuba residual sand

Perreira and Fredlund, 1999

Undisturbed Soil Specimens
Sand = 52%, Silt = 35%, Clay = 13%; Liquid Limit = 29, Plasticity Index = 12
Lean clay, CL

Shear Strength

Test Method: Modified direct shear test

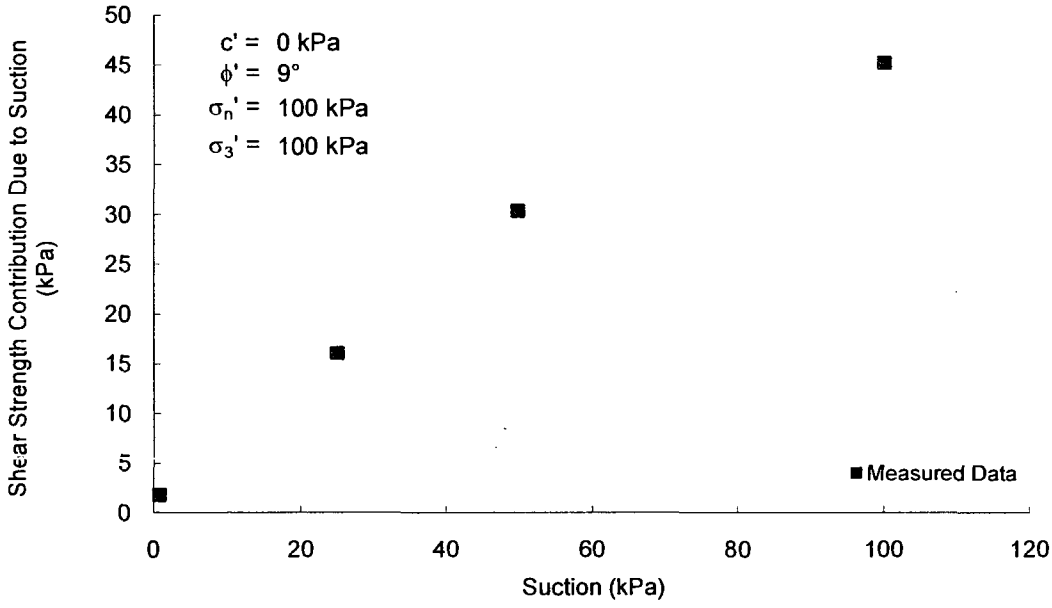

SWRC

Test Method: Tempe cell, pressure plate

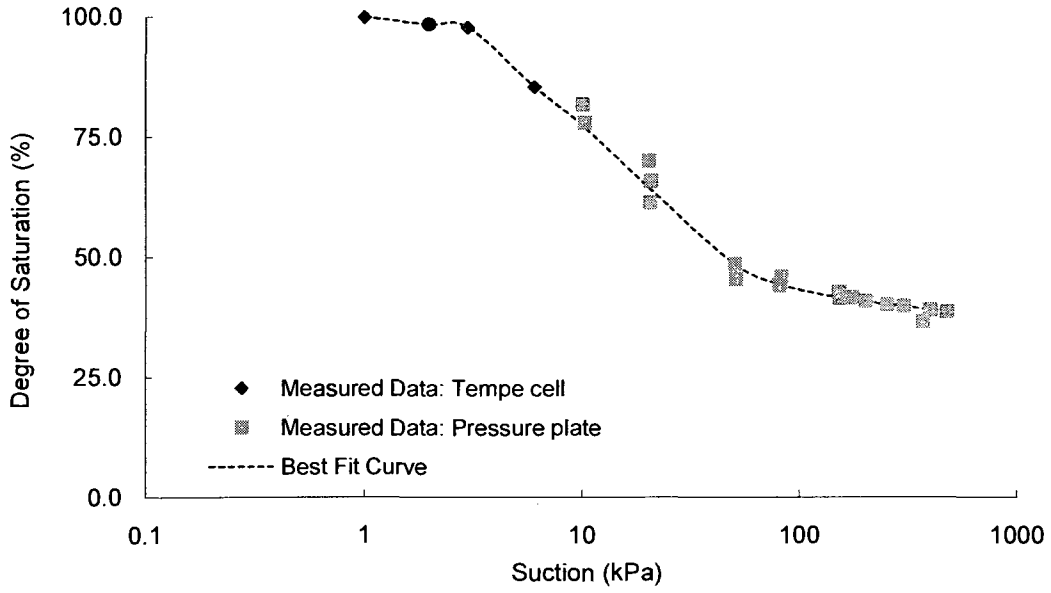

Soil No. 39

Ningxia soil

Xu and Sun, 2001; Xu, 2004

Compacted Sample

Sand = 25%, Silt = 57%, Clay = 18%; Liquid Limit = 51, Plasticity Index = 22

Heavy silt, MH

Shear Strength

Test Method: Modified triaxial test

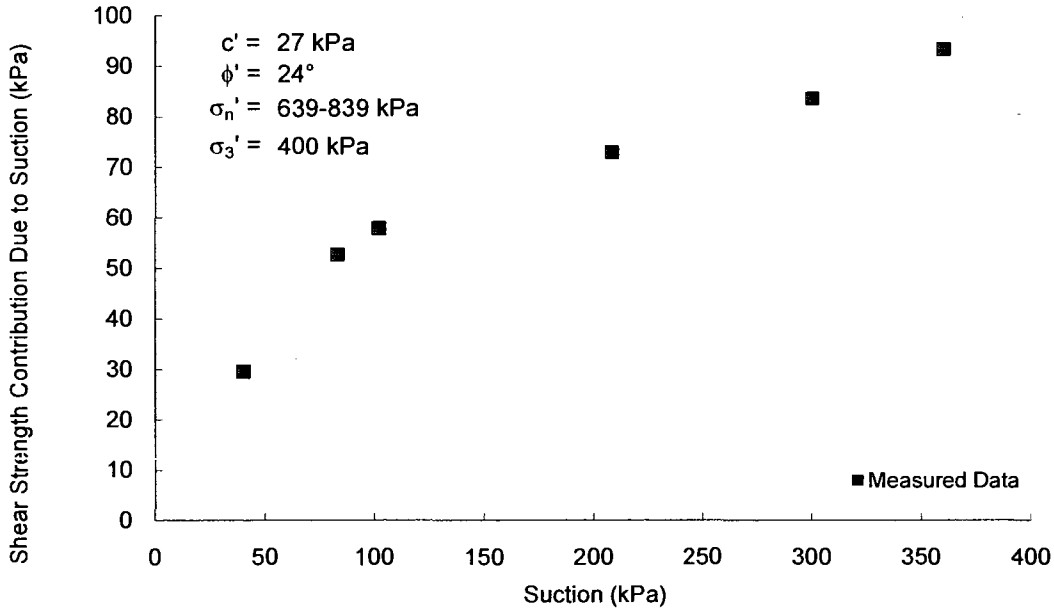

SWRC

Test Method: Pressure plate, tensiometer

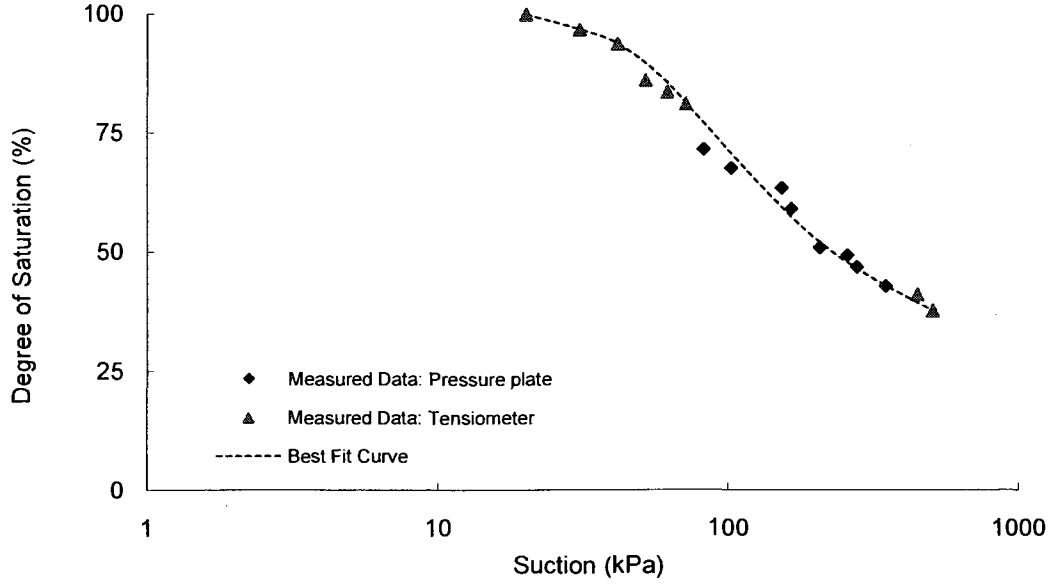

Soil No. 40

Hubei natural soil
Zhan and Ng, 2006

Undisturbed Soil Specimens
Sand = 3%, Silt = 48%, Clay = 39%; Liquid Limit = 51, Plasticity Index = 31
Fat clay, CH

Shear Strength

Test Method: Modified direct shear test

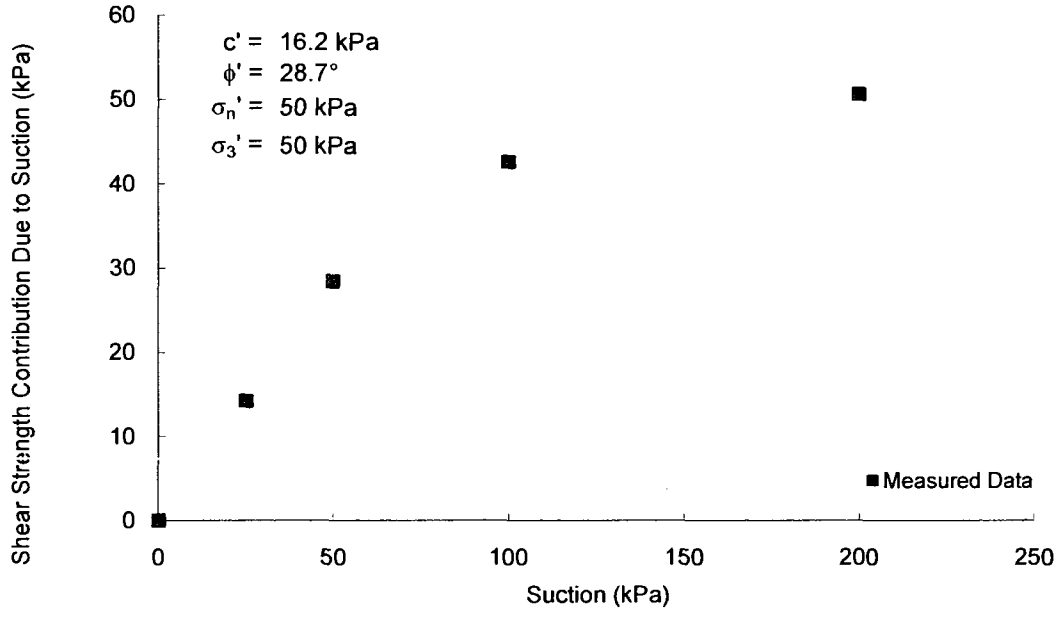

SWRC

Test Method: Pressure plate

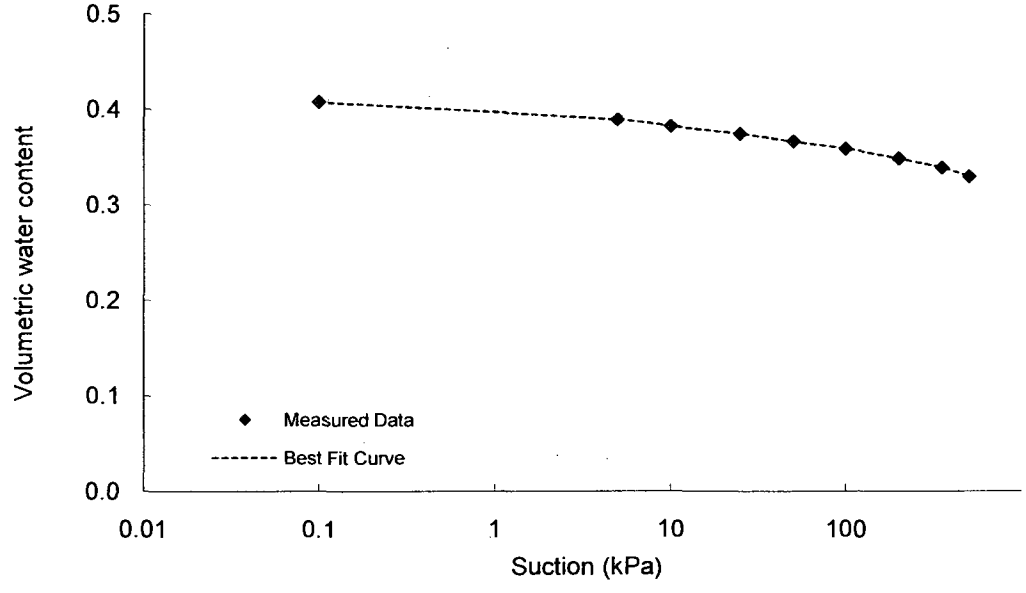

Soil No. 41

Hubei compacted soil

Zhan and Ng, 2006

Undisturbed Soil Specimens

Sand = 3%, Silt = 48%, Clay = 39%; Liquid Limit = 51, Plasticity Index = 31

Fat clay, CH

Shear Strength

Test Method: Modified direct shear test

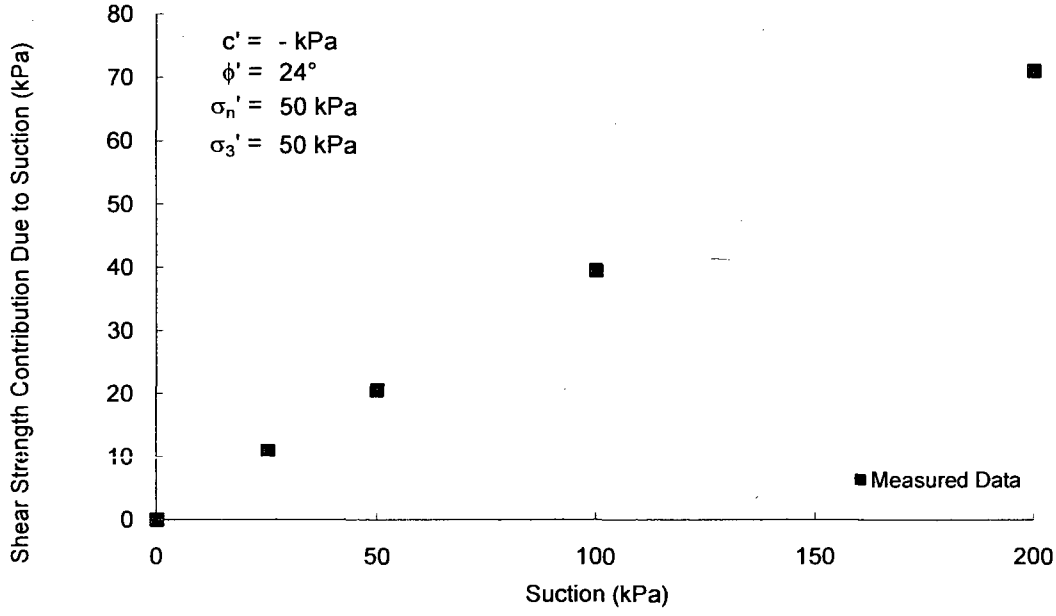

SWRC

Test Method: Pressure plate

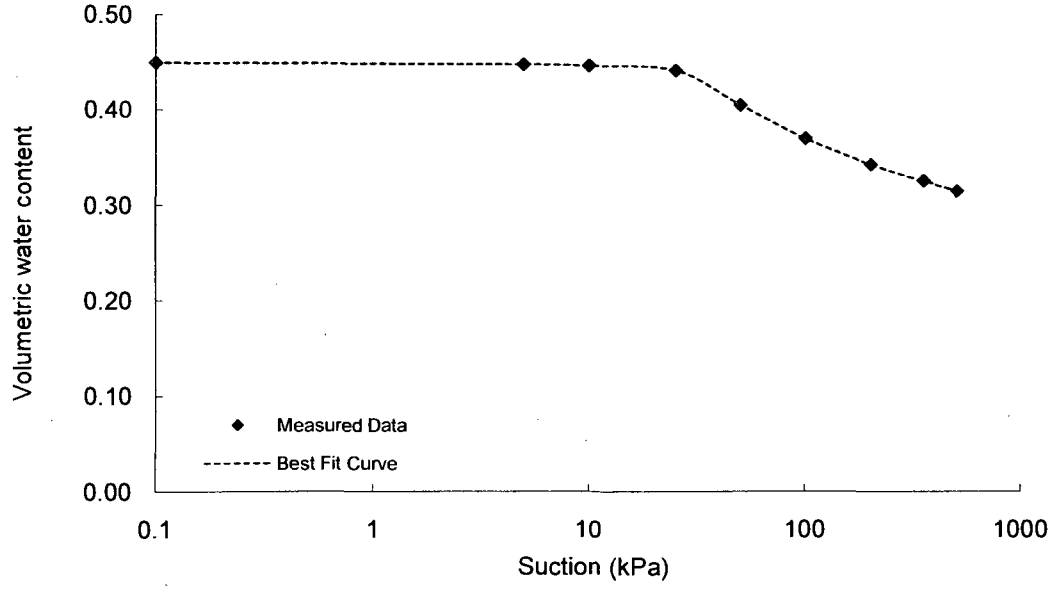

Soil No. 42a

Kuala Lumpur residual
Huat, Ali and Hashim, 2005

Compacted Sample
Sand = 43%, Silt = 9%, Clay = 48%; Liquid Limit = 95, Plasticity Index = 50
Heavy silt, MH

Shear Strength

Test Method: Modified direct shear test

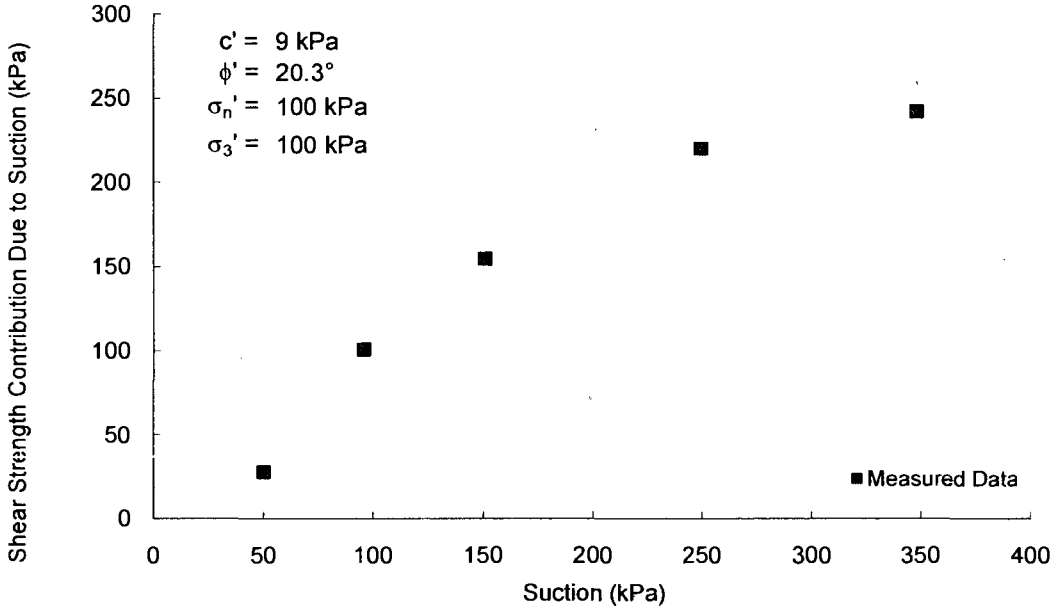

SWRC

Test Method: Pressure plate

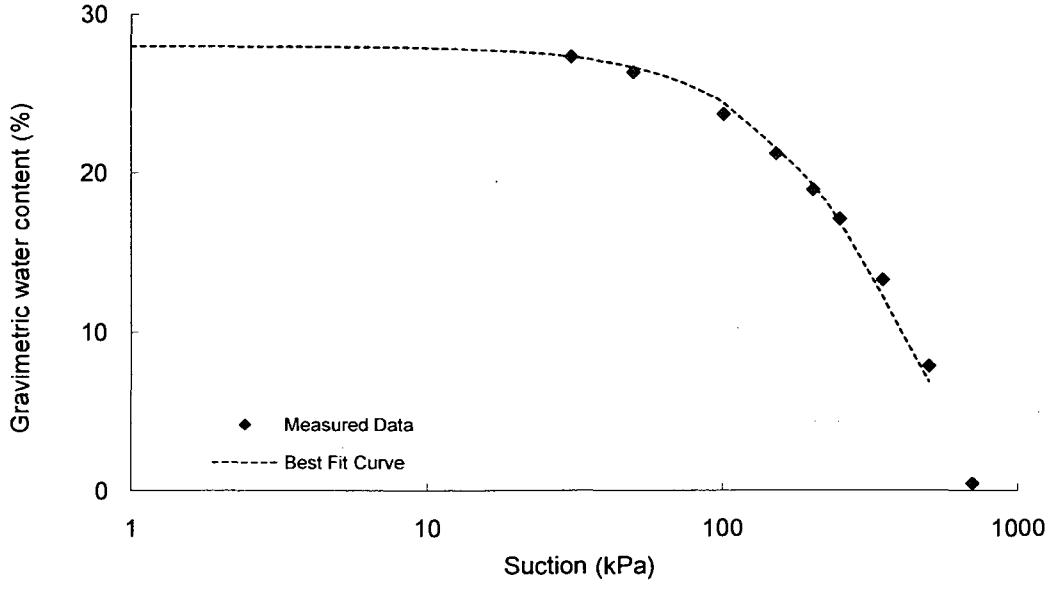

Soil No. 42b

Kuala Lumpur residual
Huat, Ali and Hashim, 2005

Compacted Sample
Sand = 43%, Silt = 9%, Clay = 48%; Liquid Limit = 95, Plasticity Index = 50
Heavy silt, MH

Shear Strength

Test Method: Modified direct shear test

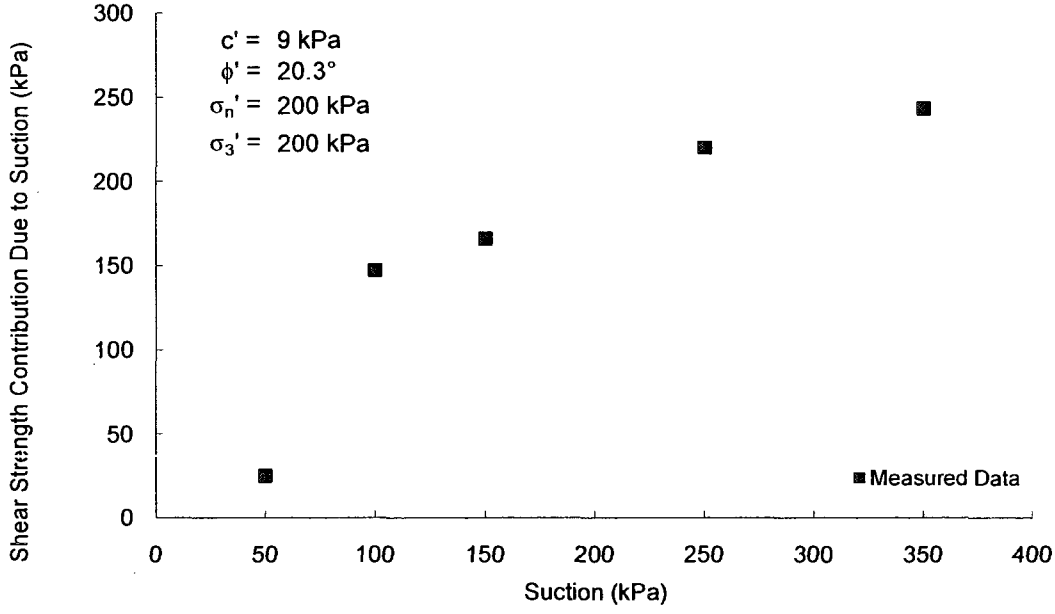

SWRC

Test Method: Pressure plate

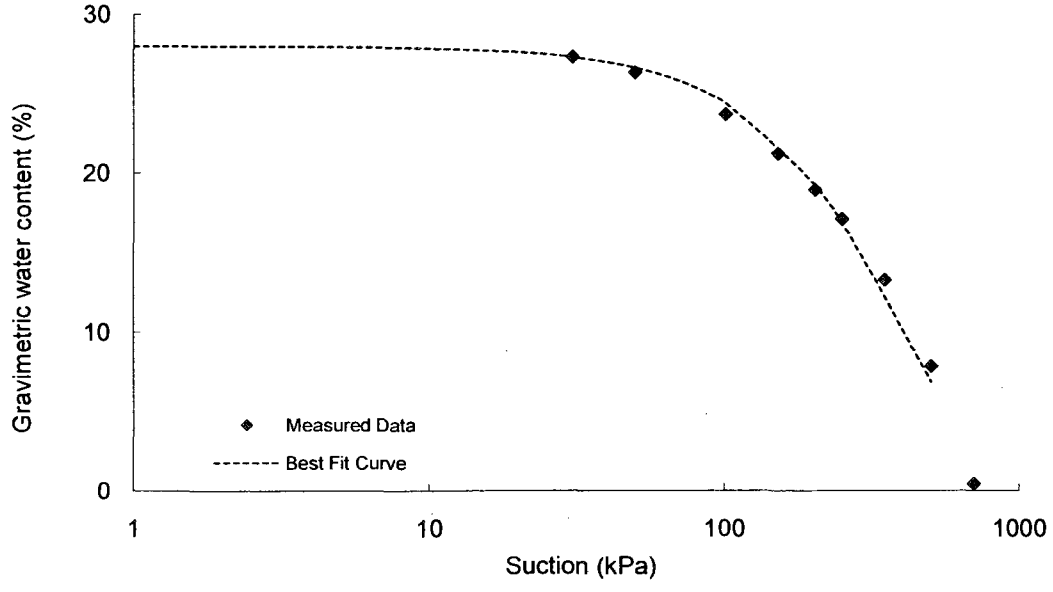

Soil No. 42c

Kuala Lumpur residual
Huat, Ali and Hashim, 2005

Compacted Sample
Sand = 0%, Silt and Clay= 100%; Liquid Limit = 95, Plasticity Index = 50
Heavy silt, MH

Shear Strength

Test Method: Modified direct shear test

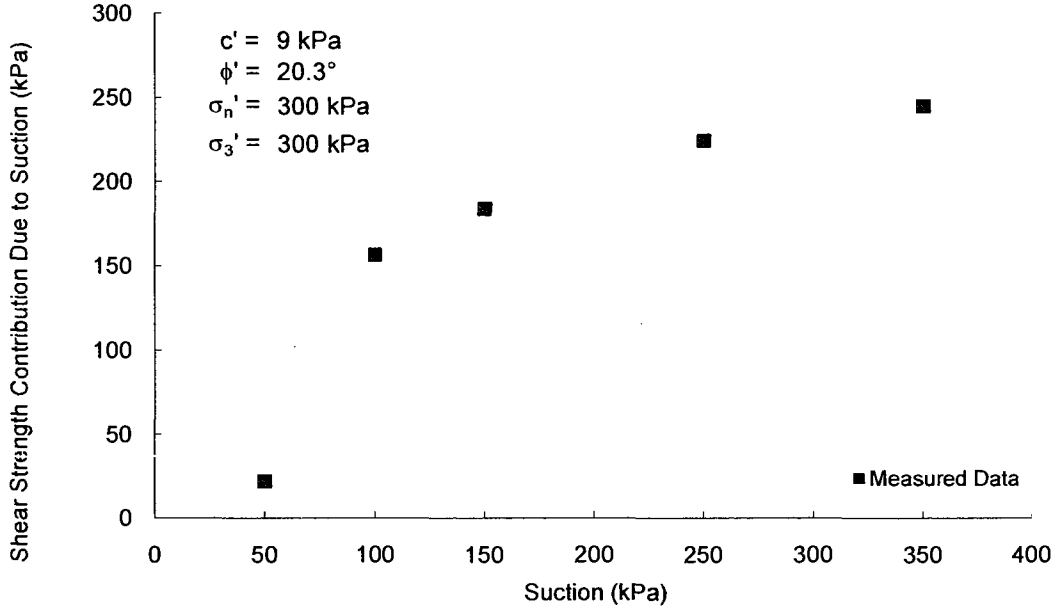

SWRC

Test Method: Pressure plate

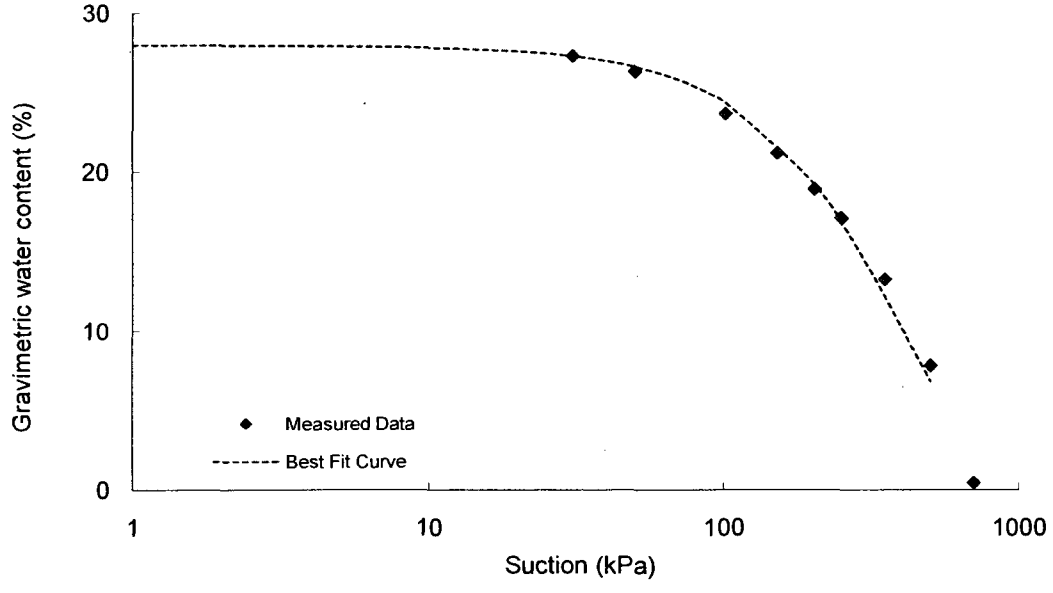

Soil No. 42d

Kuala Lumpur residual
Huat, Ali and Hashim, 2005

Compacted Sample
Sand = 43%, Silt = 9%, Clay = 48%; Liquid Limit = 95, Plasticity Index = 50
Heavy silt, MH

Shear Strength

Test Method: Modified direct shear test

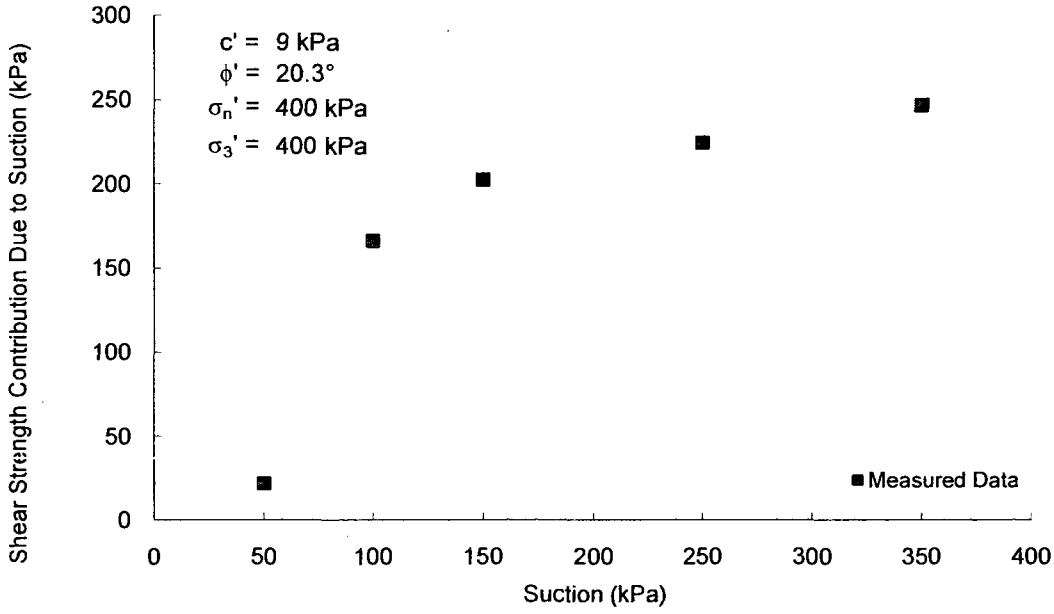

SWRC

Test Method: Pressure plate

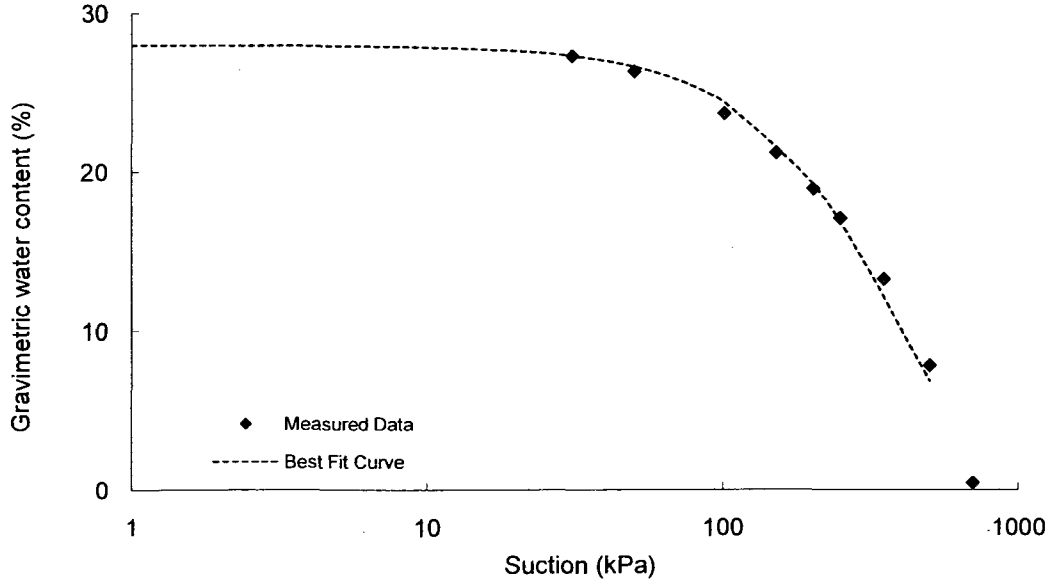

Soil No. 43a

Jovem residual soil
Reis and Vilar, 2005

Compacted Sample
Sand = 50%, Silt = 45%, Clay = 5%; Liquid Limit = 50, Plasticity Index = 39
Lean clay, CL

Shear Strength

Test Method:

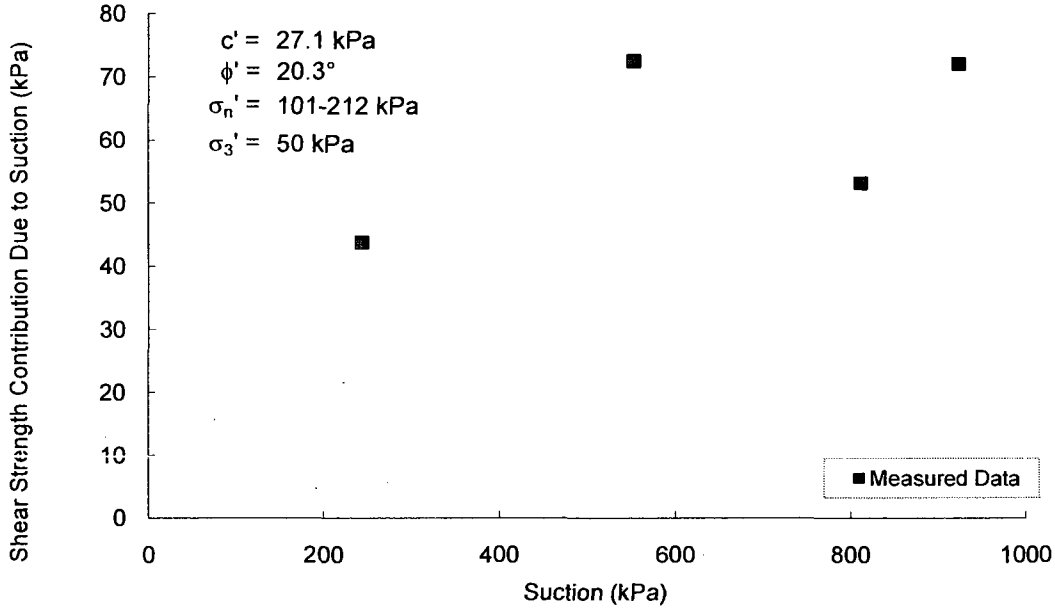

SWRC

Test Method:

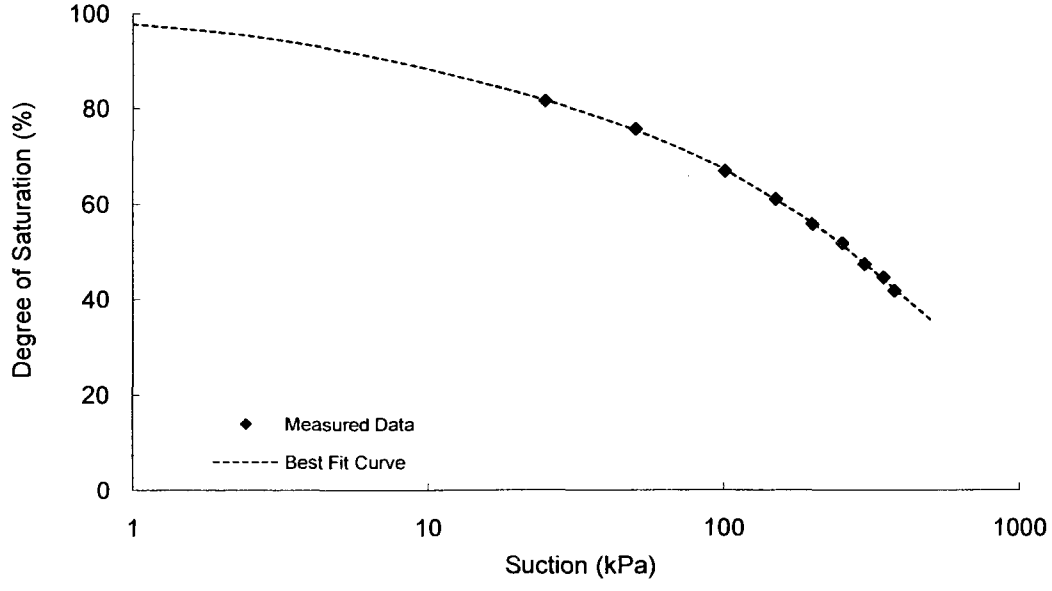

Soil No. 43b

Jovem residual soil
Reis and Vilar, 2005

Compacted Sample
Sand = 50%, Silt = 45%, Clay = 5%; Liquid Limit = 50, Plasticity Index = 39
Lean clay, CL

Shear Strength

Test Method:

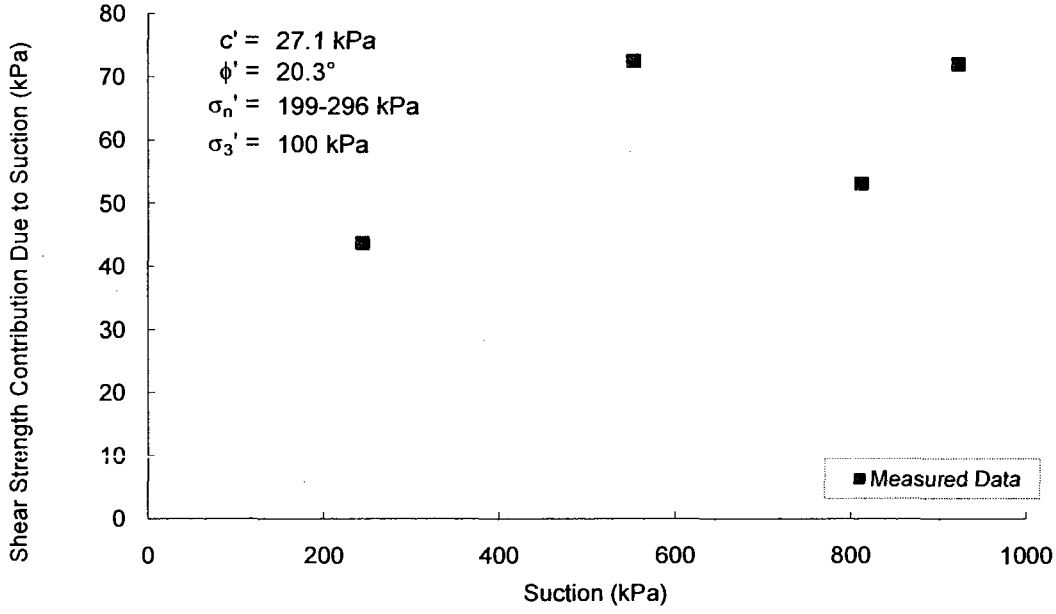

SWRC

Test Method:

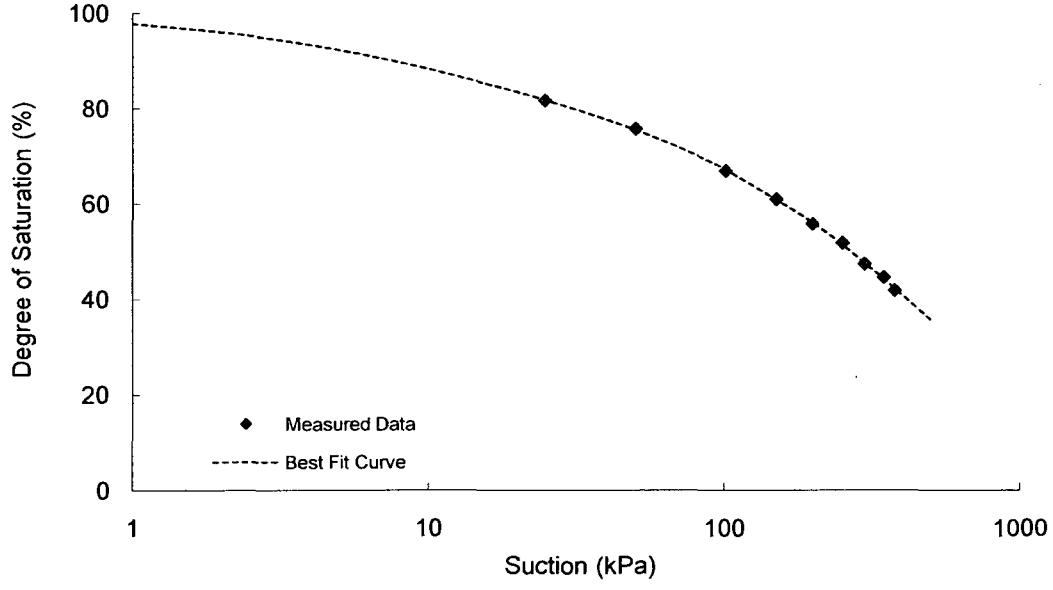

Soil No. 43c

Mature residual soil
Reis and Vilar, 2005

Compacted Sample
Sand = 50%, Silt = 45%, Clay = 5%; Liquid Limit = 50, Plasticity Index = 39
Lean clay, CL

Shear Strength

Test Method:

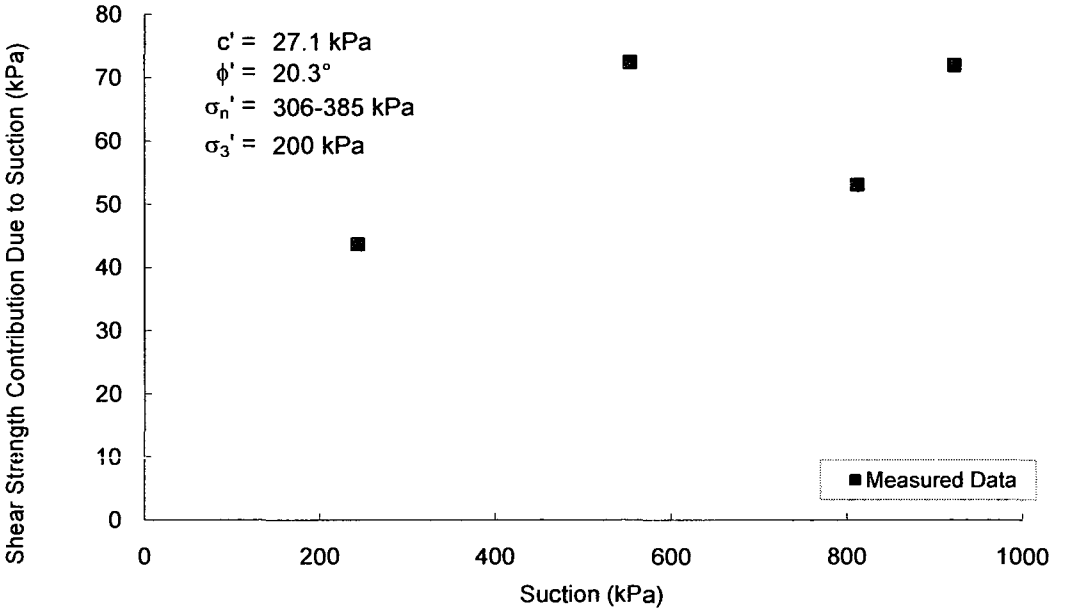

SWRC

Test Method:

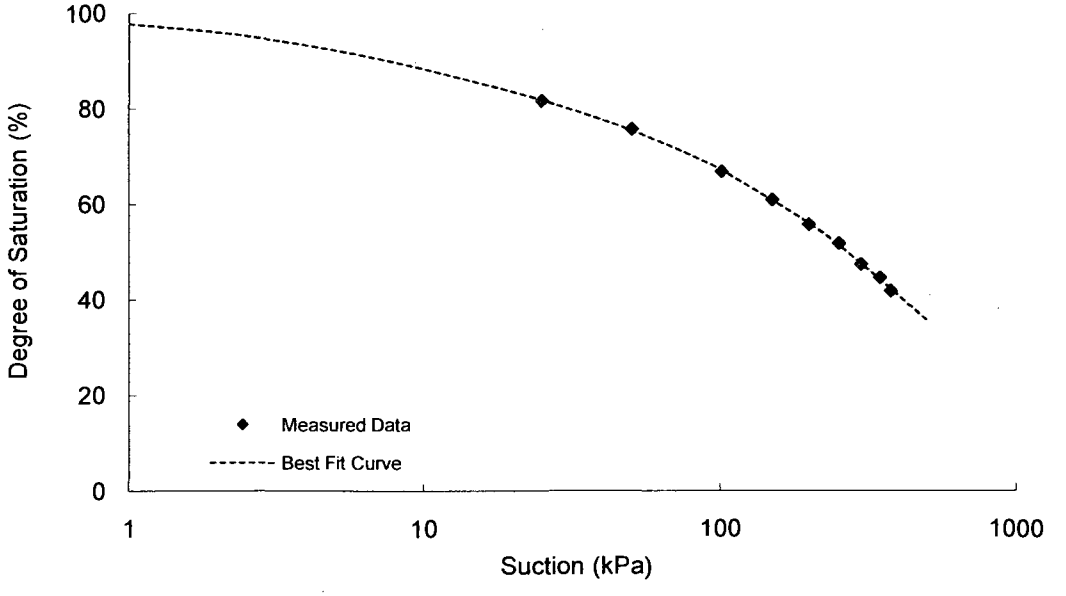

Soil No. 44a

Mature residual soil

Reis and Vilar, 2005

Compacted Sample

Sand = 27%, Silt = 15%, Clay = 58%; Liquid Limit = 73, Plasticity Index = 39

Fat clay, CH

Shear Strength

Test Method:

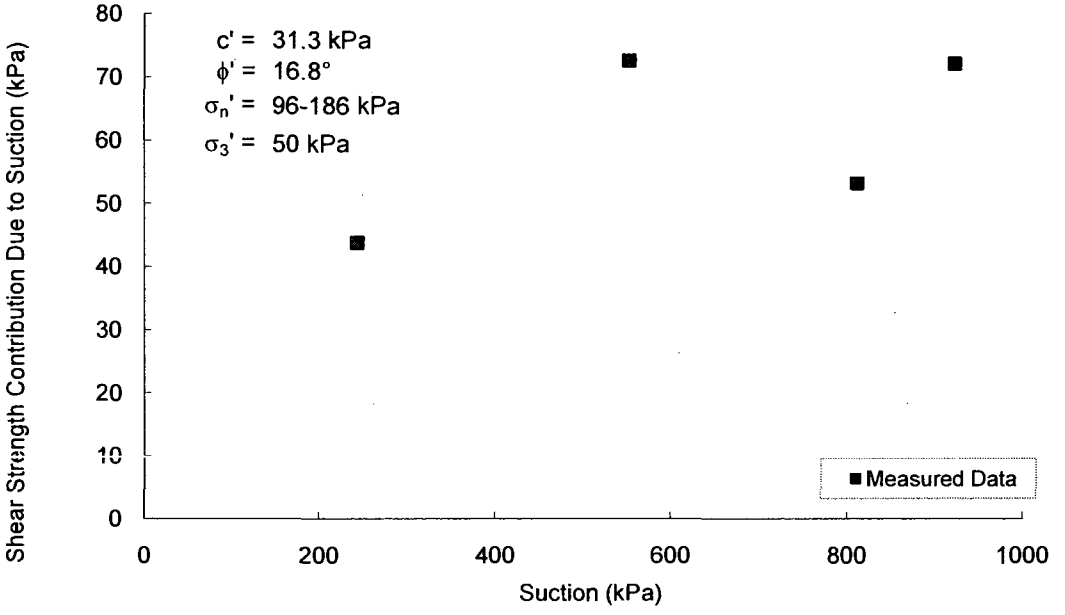

SWRC

Test Method:

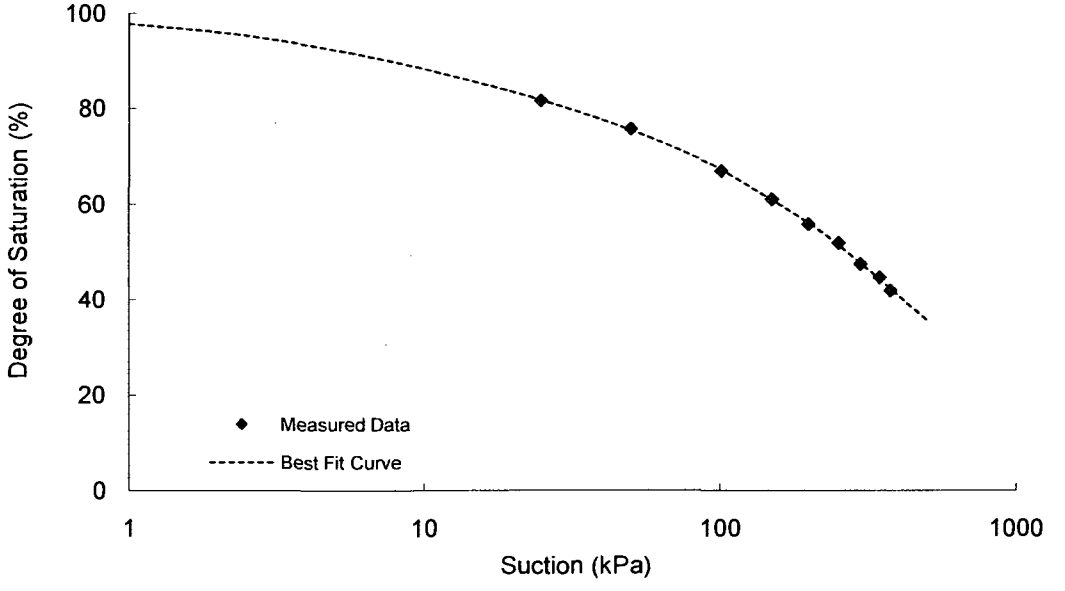

Soil No. 44b

Mature residual soil
Reis and Vilar, 2005

Compacted Sample
Sand = 27%, Silt = 15%, Clay = 58%; Liquid Limit = 73, Plasticity Index = 39
Fat clay, CH

Shear Strength

Test Method:

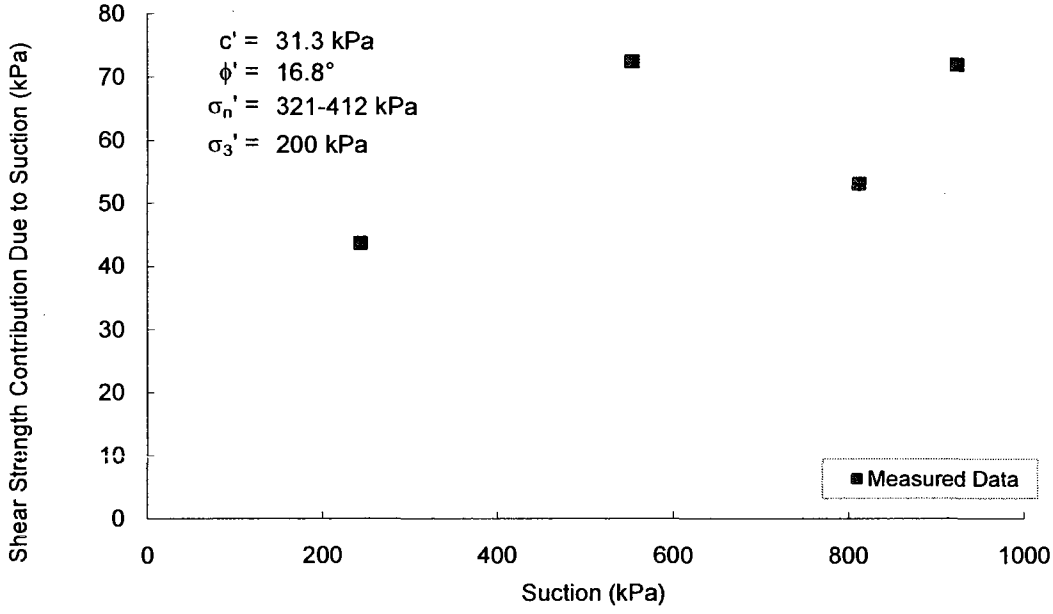

SWRC

Test Method:

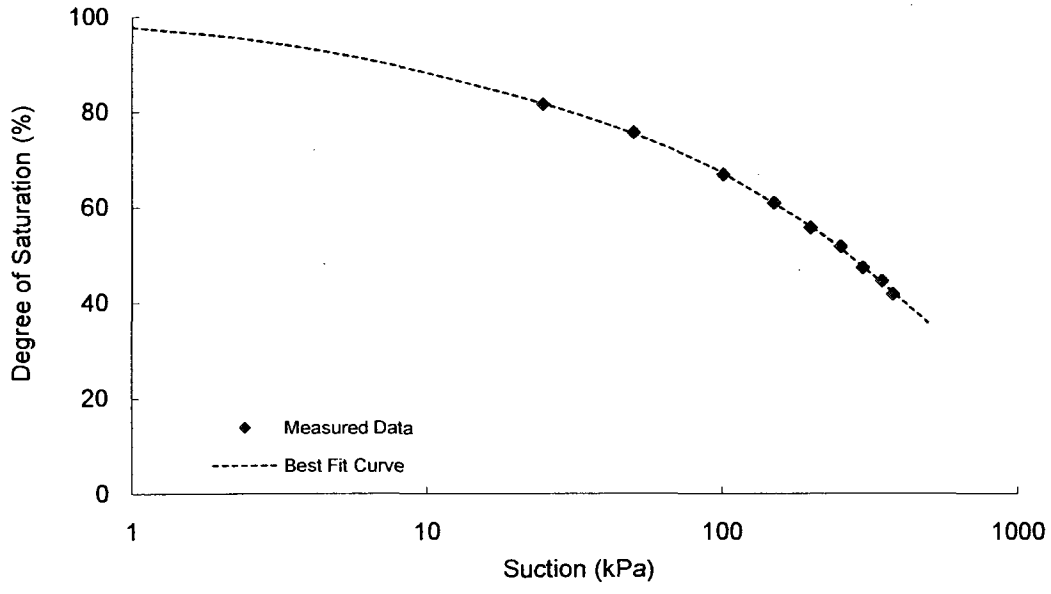

Soil No. 45a **Ashikaga silt**

Nishimura, Fredlund, Gan and Hirabayashi, 1999

Compacted Sample Sand = 0%, Silt = 92%, Clay = 8% Lean silt, ML

Shear Strength Test Method: Modified direct shear test

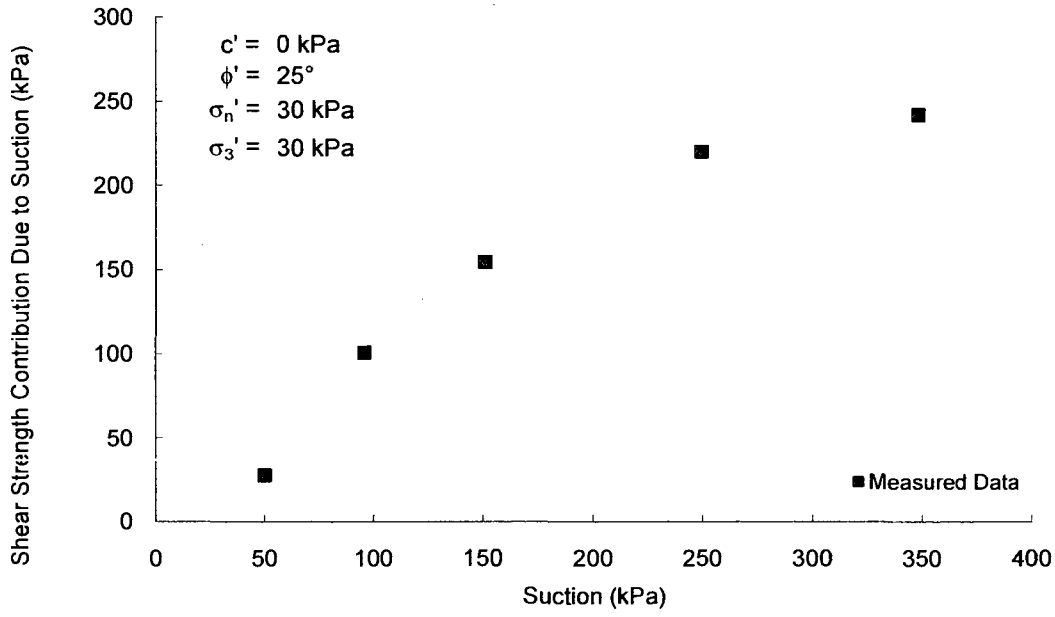

SWRC Test Method: Pressure plate

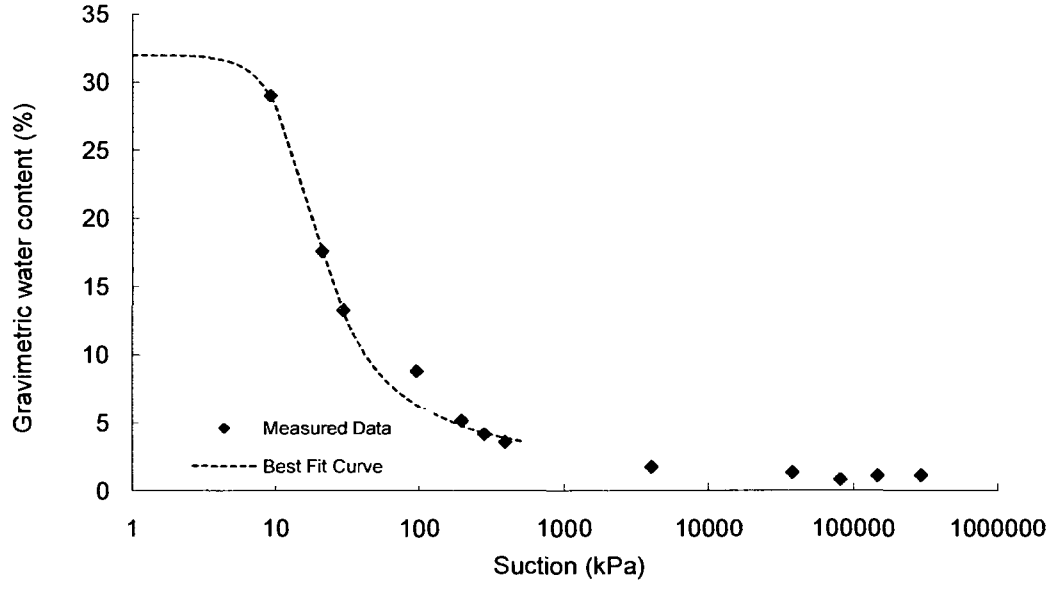

**Gradation curve available in Appendix B

Soil No. 45b

Ashikaga silt

Nishimura, Fredlund, Gan and Hirabayashi, 1999

Compacted Sample Sand = 0%, Silt = 92%, Clay = 8% Lean silt, ML

Shear Strength

Test Method: Modified direct shear test

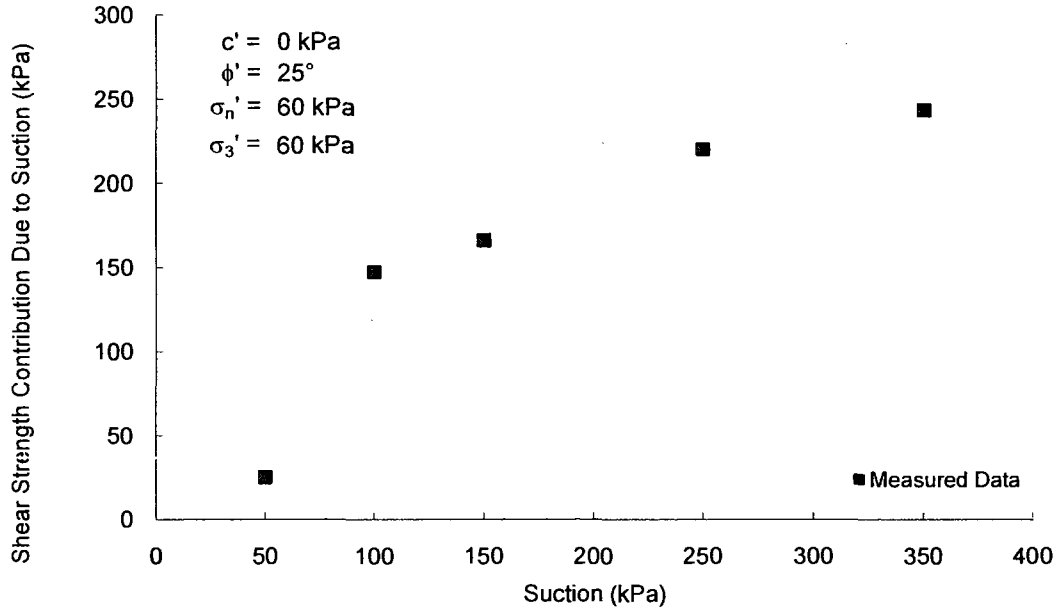

SWRC

Test Method: Pressure plate

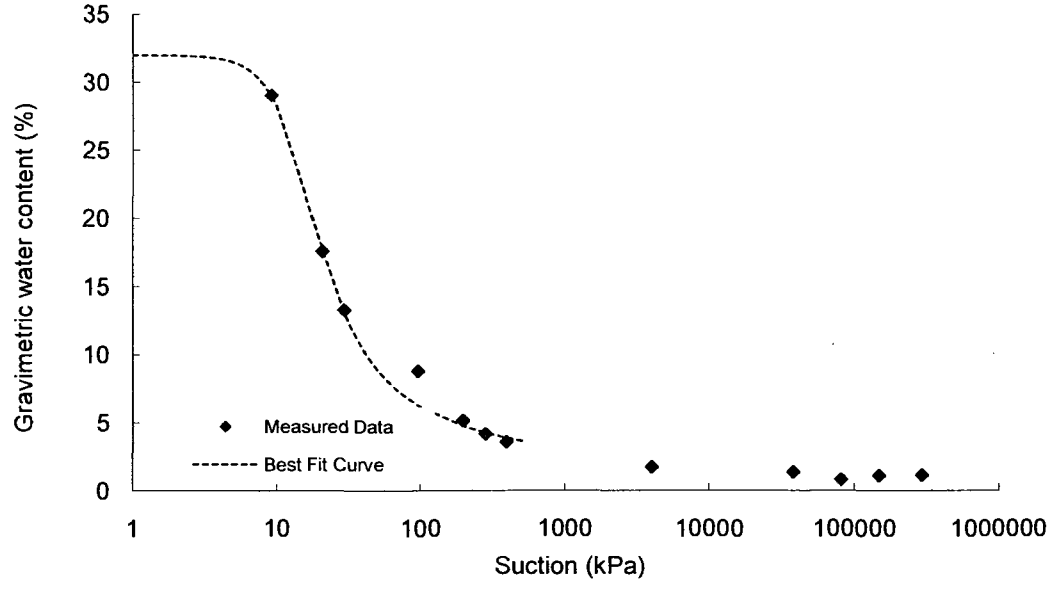

**Gradation curve available in Appendix B

Soil No. 45c

Ashikaga silt

Nishimura, Fredlund, Gan and Hirabayashi, 1999

Compacted Sample
Sand = 0%, Silt = 92%, Clay = 8%
Lean silt, ML

Shear Strength

Test Method: Modified direct shear test

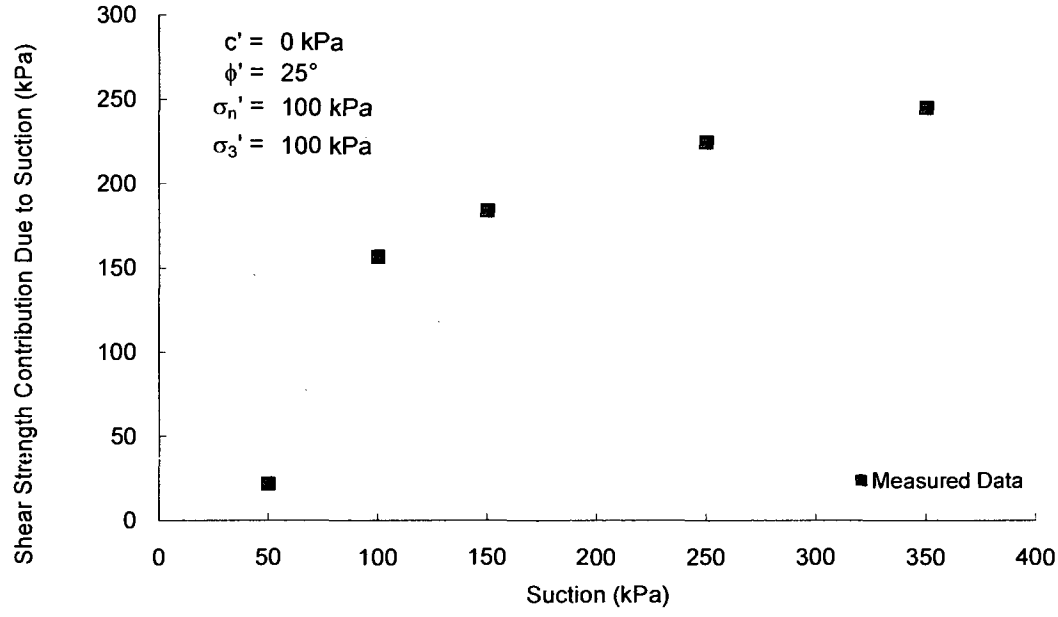

SWRC

Test Method: Pressure plate

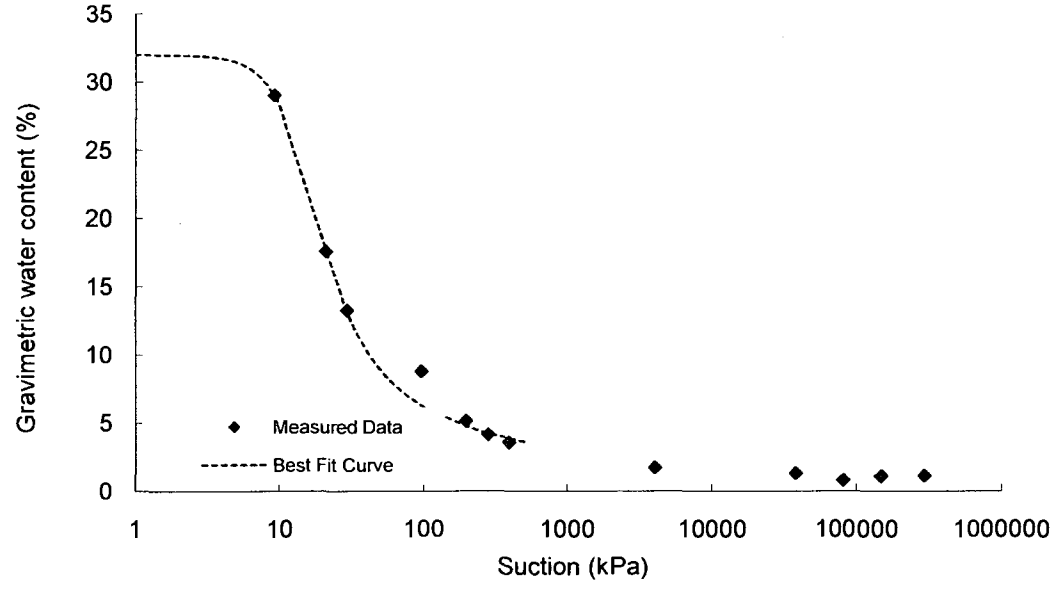

**Gradation curve available in Appendix B

Soil No. 45d

Ashikaga silt

Nishimura, Fredlund, Gan and Hirabayashi, 1999

Compacted Sample Sand = 0%, Silt = 92%, Clay = 8% Lean silt, ML

Shear Strength

Test Method: Modified direct shear test

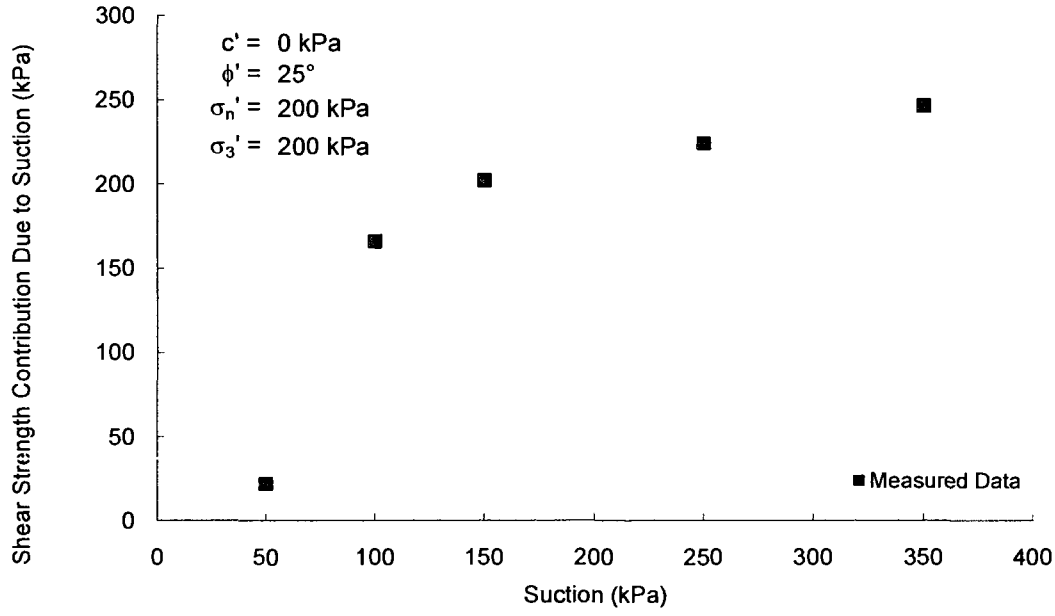

SWRC

Test Method: Pressure plate

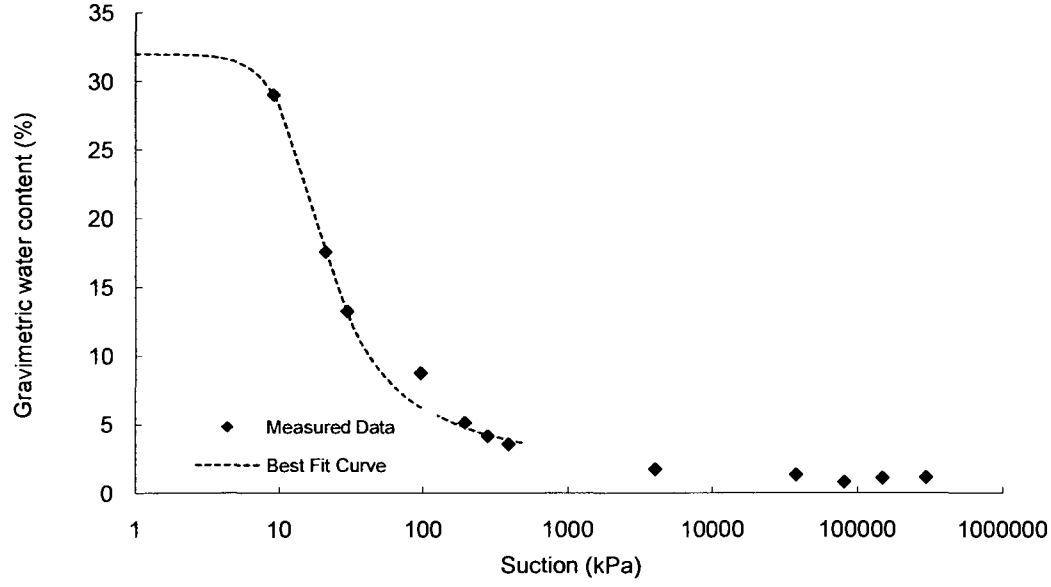

**Gradation curve available in Appendix B

Soil No. 45e

Ashikaga silt

Nishimura and Fredlund, 1999

Compacted Sample
Sand = 0%, Silt = 92%, Clay = 8%
Lean silt, ML

Shear Strength

Test Method: Modified direct shear

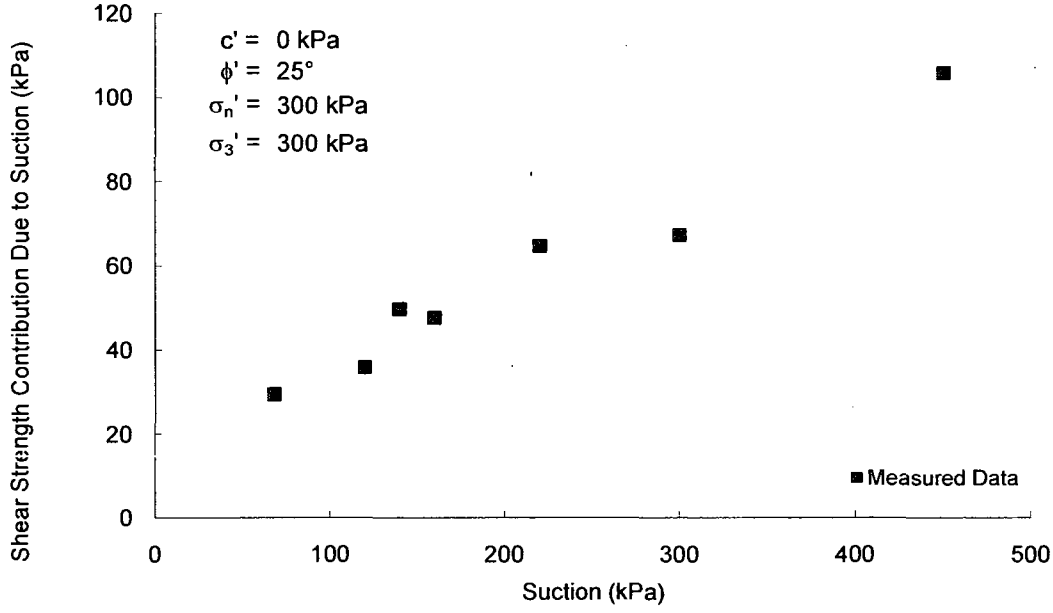

SWRC

Test Method: Pressure plate, osmotic dessicator

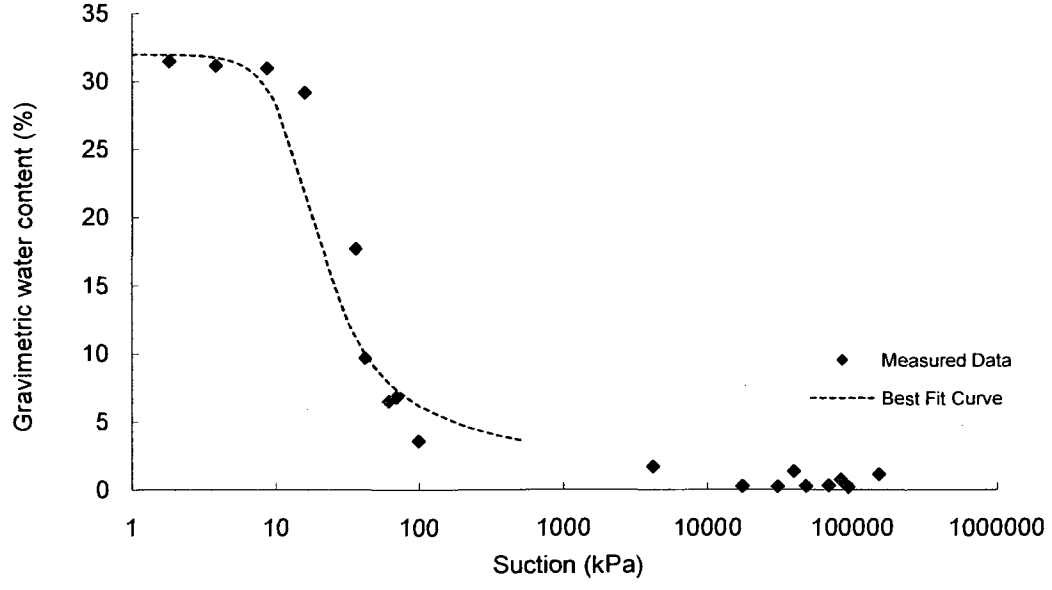

**Gradation curve available in Appendix B

Soil No. 45f

Ashikaga silt
Nishimura and Fredlund, 1999

Compacted Sample
Sand = 0%, Silt = 92%, Clay = 8%
Lean silt, ML

Shear Strength

Test Method: Modified triaxial test

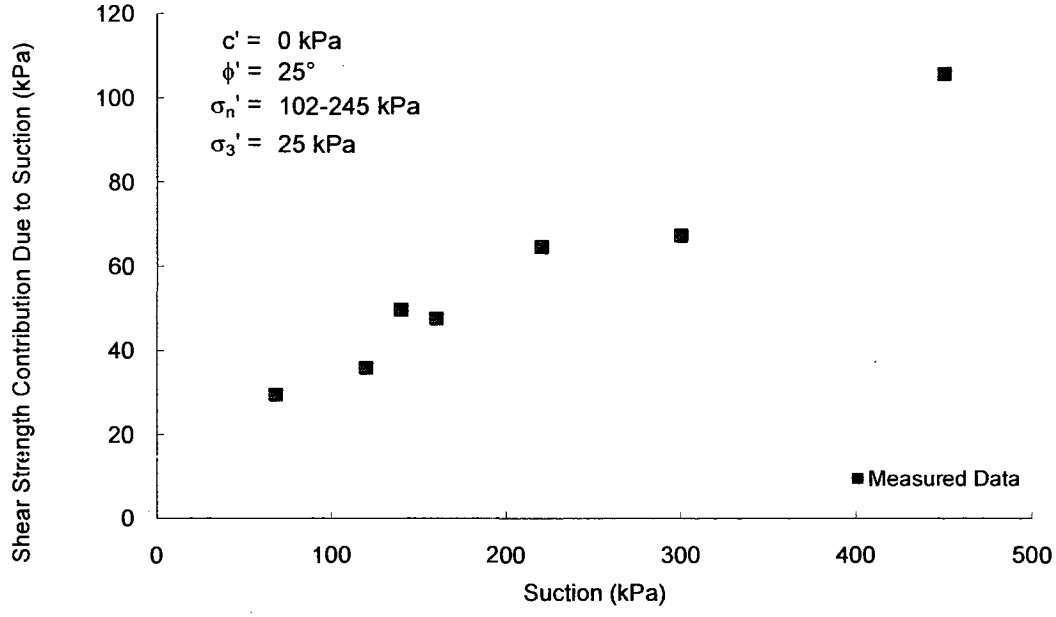

SWRC

Test Method: Pressure plate, osmotic dessicator

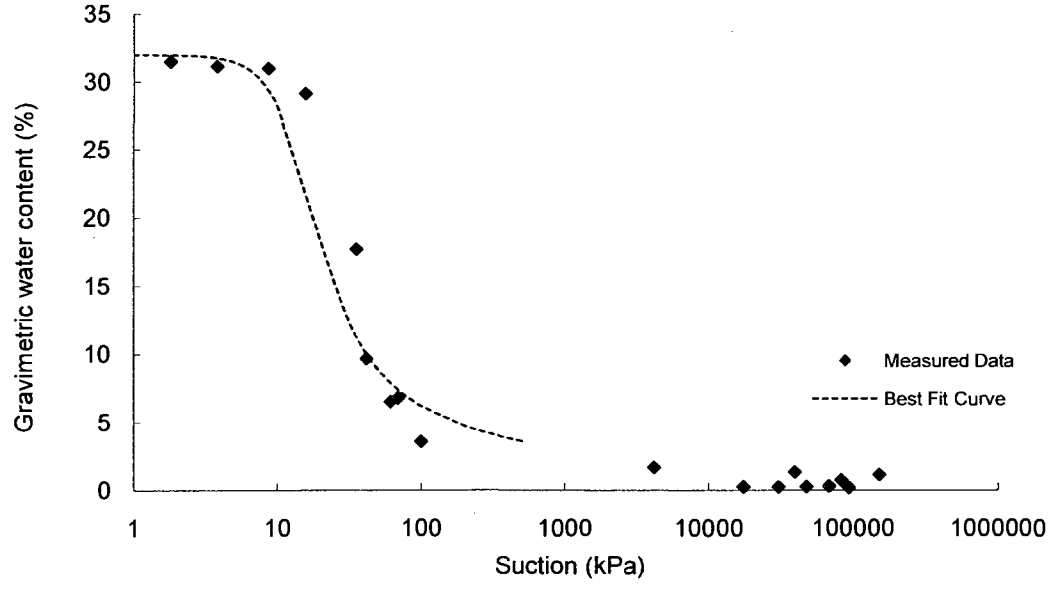

**Gradation curve available in Appendix B

Soil No. 46

Kiunyu gravel
Toll, 1990

Compacted Sample
Sand = 30%, Silt = 7%, Clay = 8%; Liquid Limit = 36.4, Plasticity Index = 14.8
Lean clay, CL

Shear Strength

Test Method: Modified triaxial test

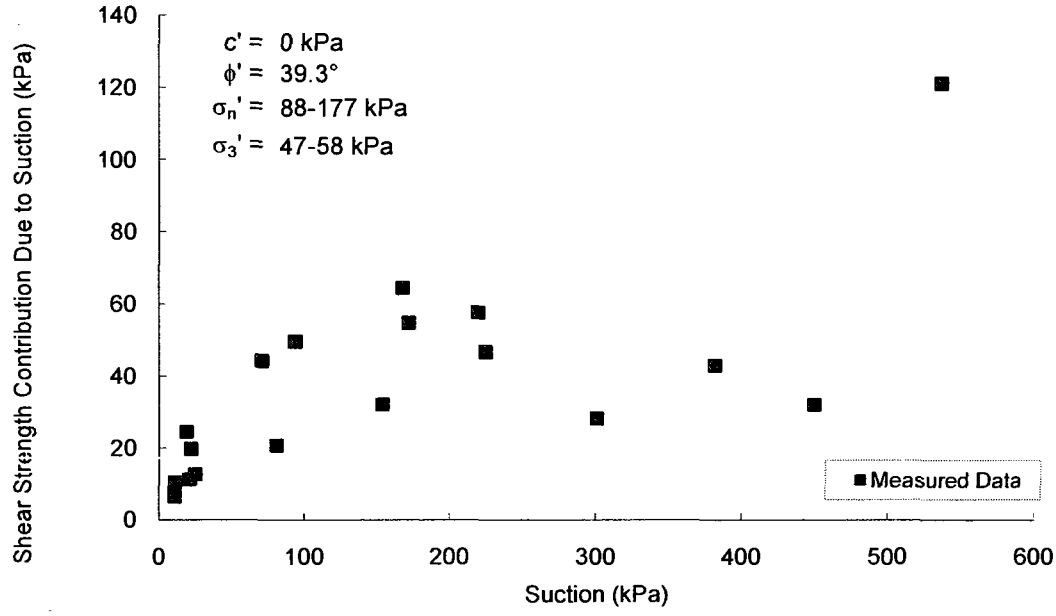

SWRC

Test Method: Pressure plate

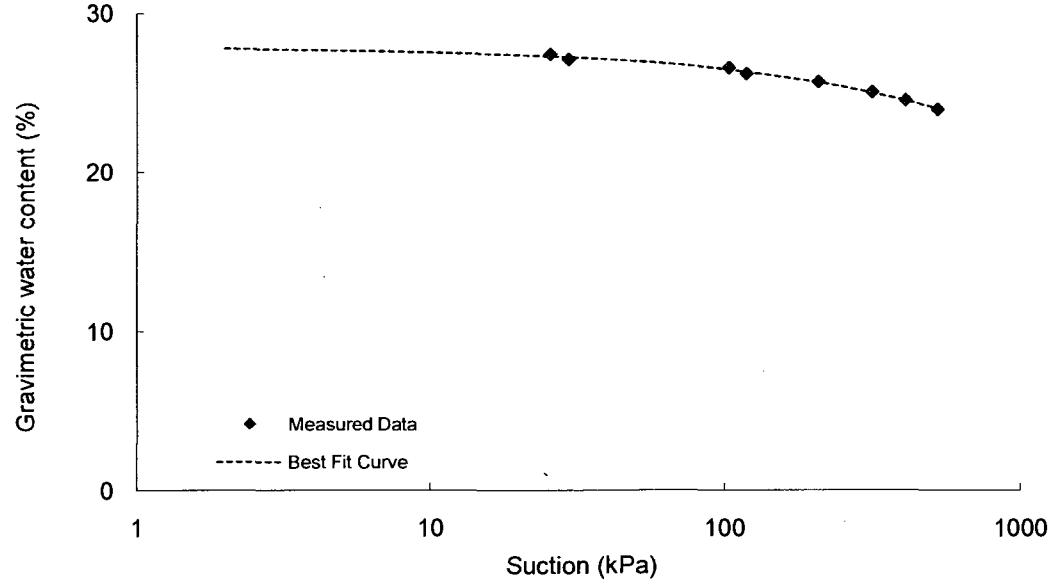

Soil No. 47a

Jossigny silt
Cui and Delage, 1996

Compacted Sample
Sand = 4%, Silt = 62%, Clay = 34%; Liquid Limit = 37, Plasticity Index = 18
Lean clay, CL

Shear Strength

Test Method: Modified triaxial test

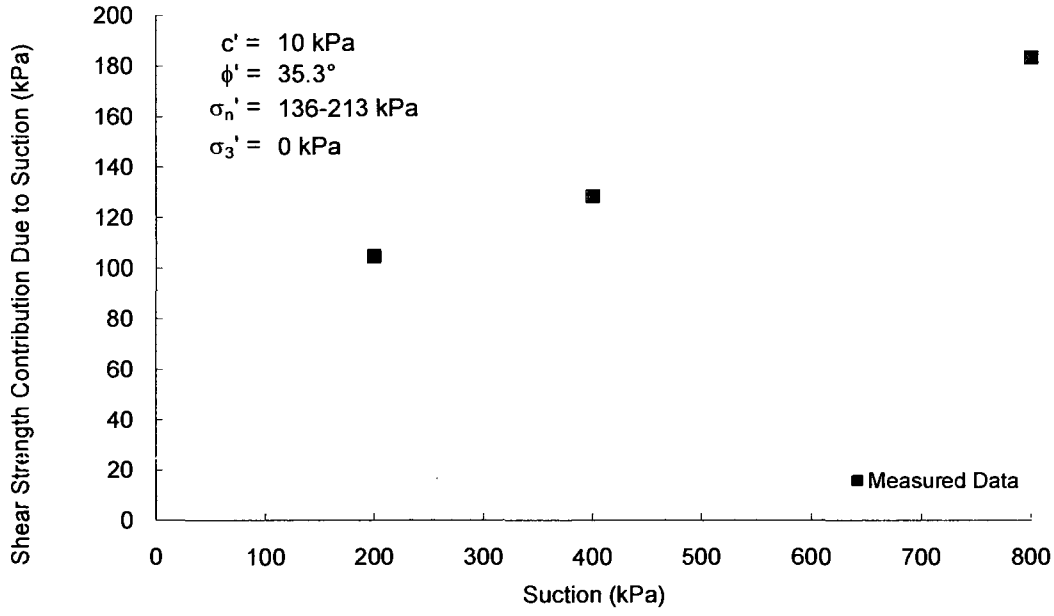

SWRC

Test Method: Indirect

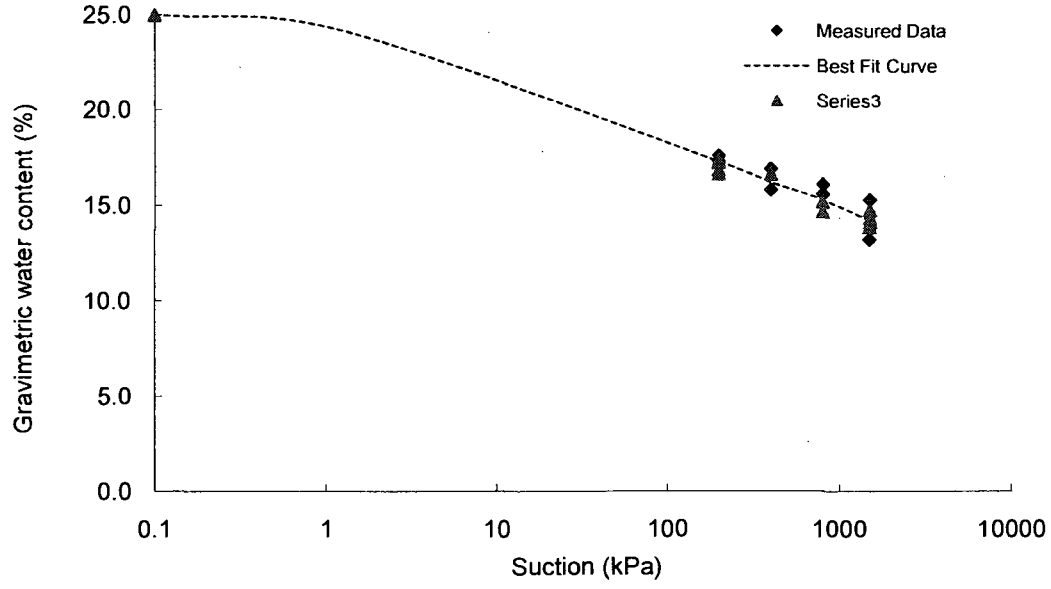

Soil No. 47b

Jossigny silt
Cui and Delage, 1996

Compacted Sample
Sand = 4%, Silt = 62%, Clay = 34%; Liquid Limit = 37, Plasticity Index = 18
Lean clay, CL

Shear Strength

Test Method: Modified triaxial test

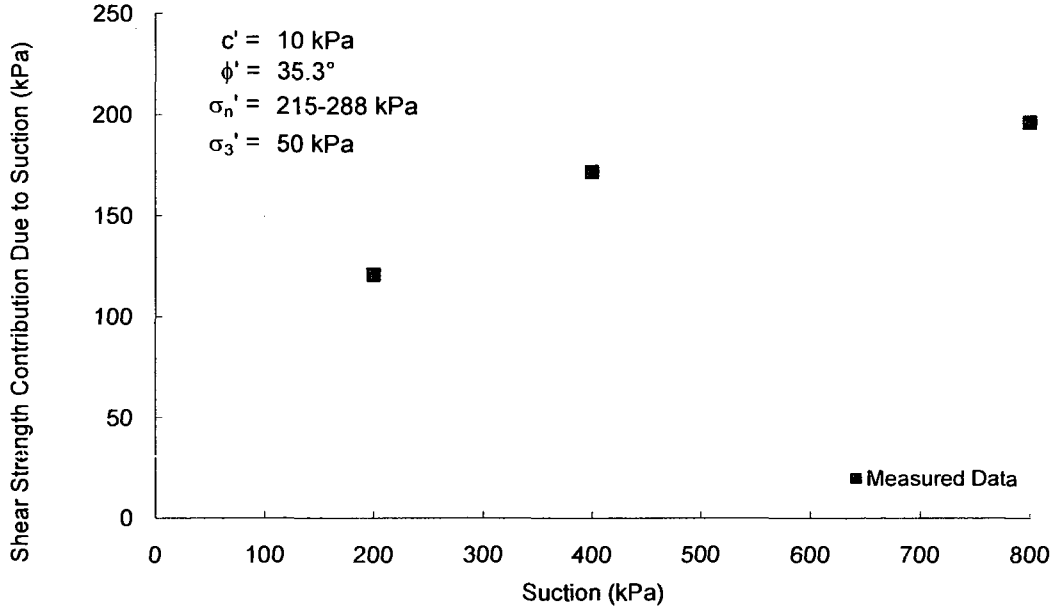

SWRC

Test Method: Indirect

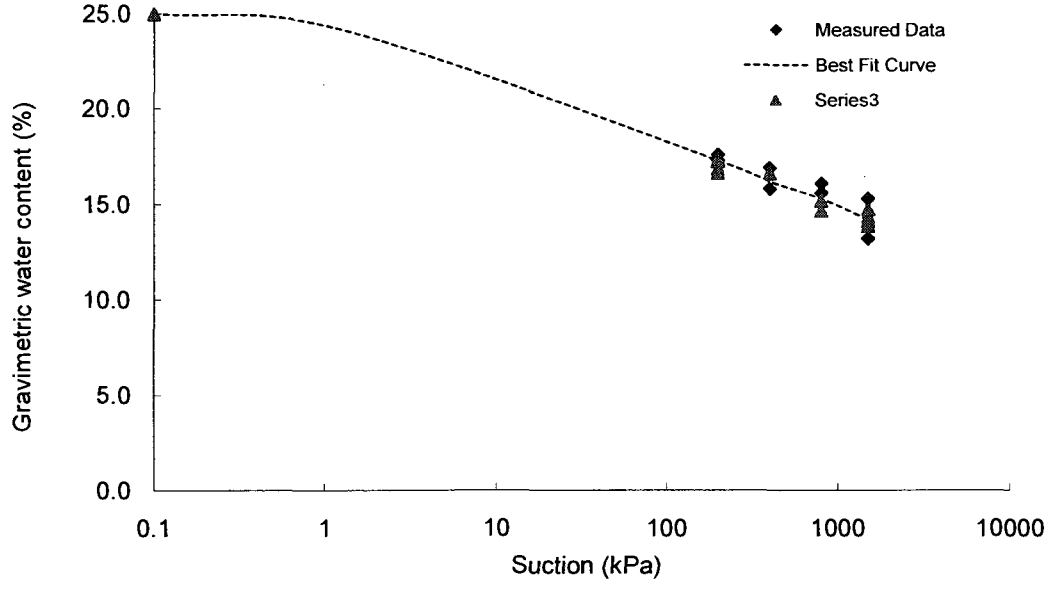

Soil No. 47c

Jossigny silt
Cui and Delage, 1996

Compacted Sample
Sand = 4%, Silt = 62%, Clay = 34%; Liquid Limit = 37, Plasticity Index = 18
Lean clay, CL

Shear Strength

Test Method: Modified triaxial test

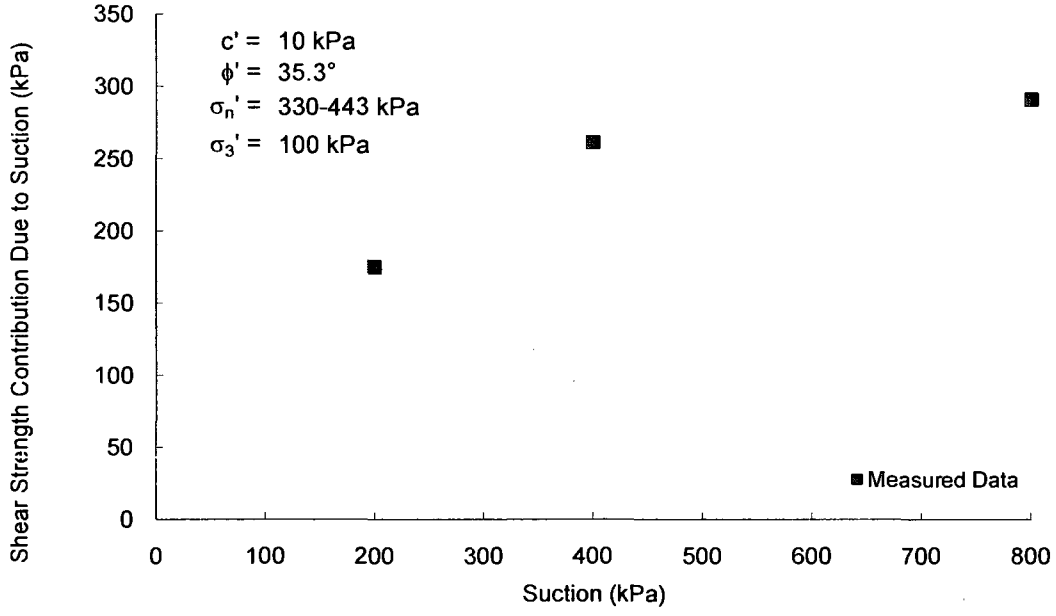

SWRC

Test Method: Indirect

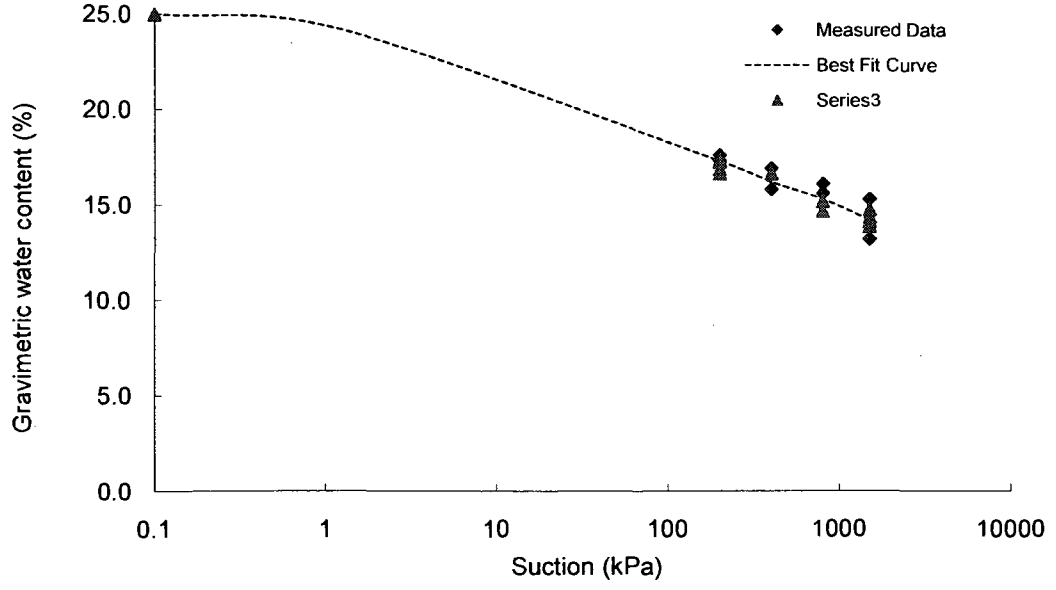

Soil No. 47d

Jossigny silt
Cui and Delage, 1996

Compacted Sample
Sand = 4%, Silt = 62%, Clay = 34%; Liquid Limit = 37, Plasticity Index = 18
Lean clay, CL

Shear Strength

Test Method: Modified triaxial test

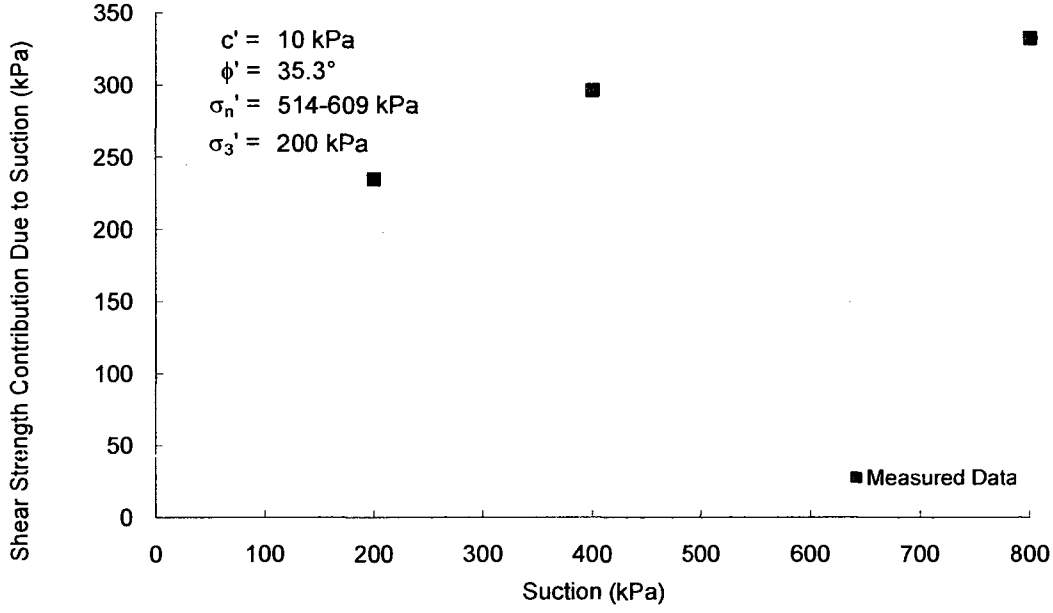

SWRC

Test Method: Indirect

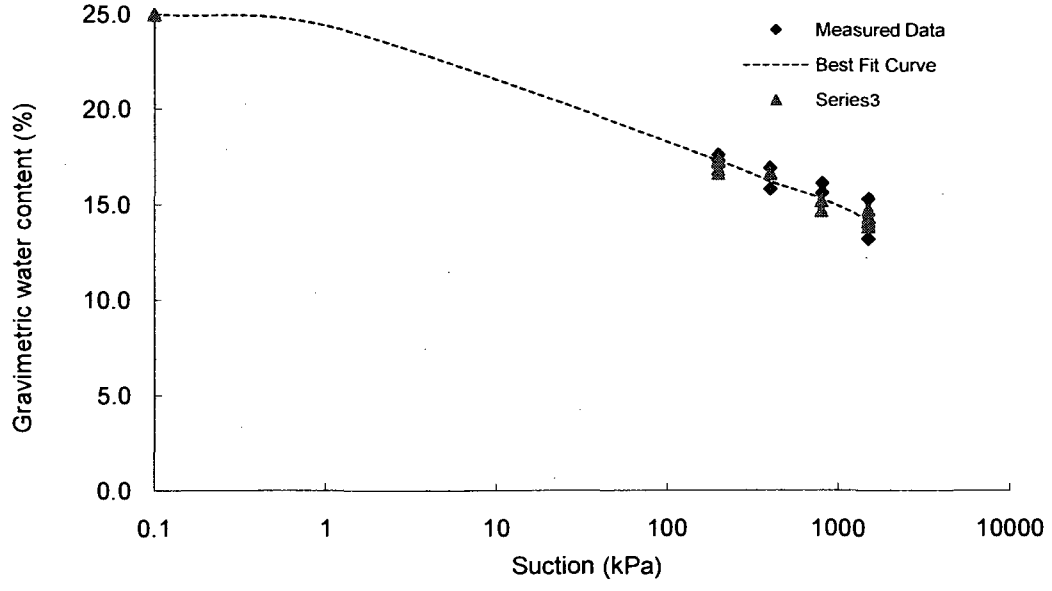

Soil No. 48

Yellow Colluvium
de Campos and Carrillo, 1995

Compacted Sample
Sand = 50.3%, Silt = 4.6%, Clay = 42.5%; Liquid Limit = 46, Plasticity Index = 23
Lean clay, CL

Shear Strength

Test Method: Modified direct shear test

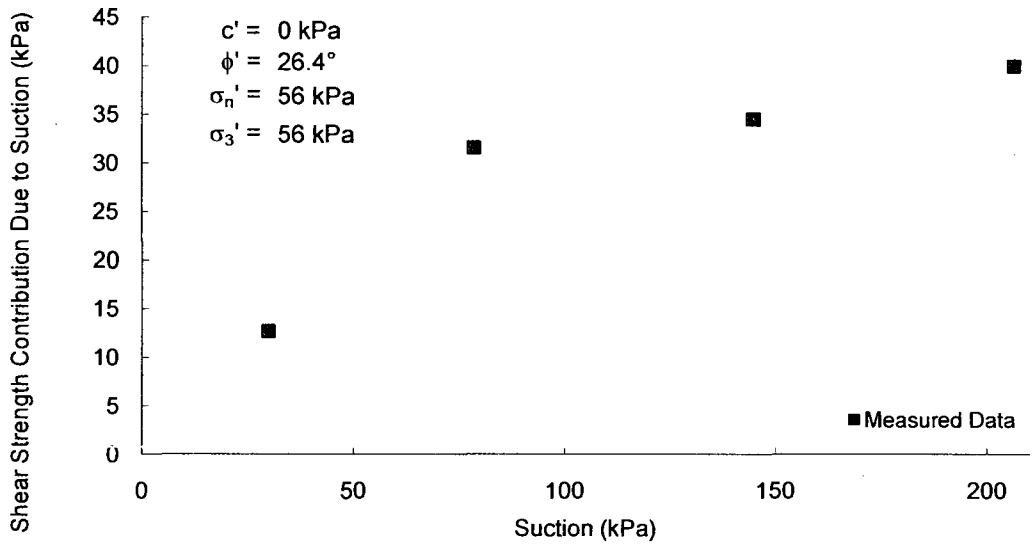

SWRC

Test Method: Tempe cell

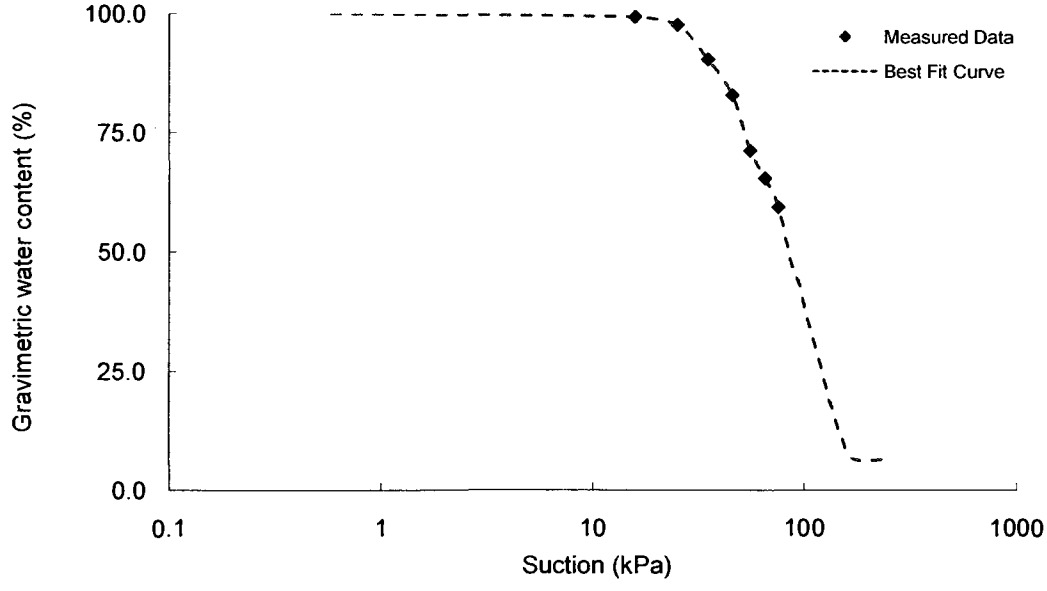

Soil No. 49

Red colluvium
de Campos and Carrillo, 1995

Compacted Sample
Sand = 44.5%, Silt = 5.8%, Clay = 43.2%; Liquid Limit = 60, Plasticity Index = 17
Heavy silt, MH

Shear Strength

Test Method: Modified direct shear test

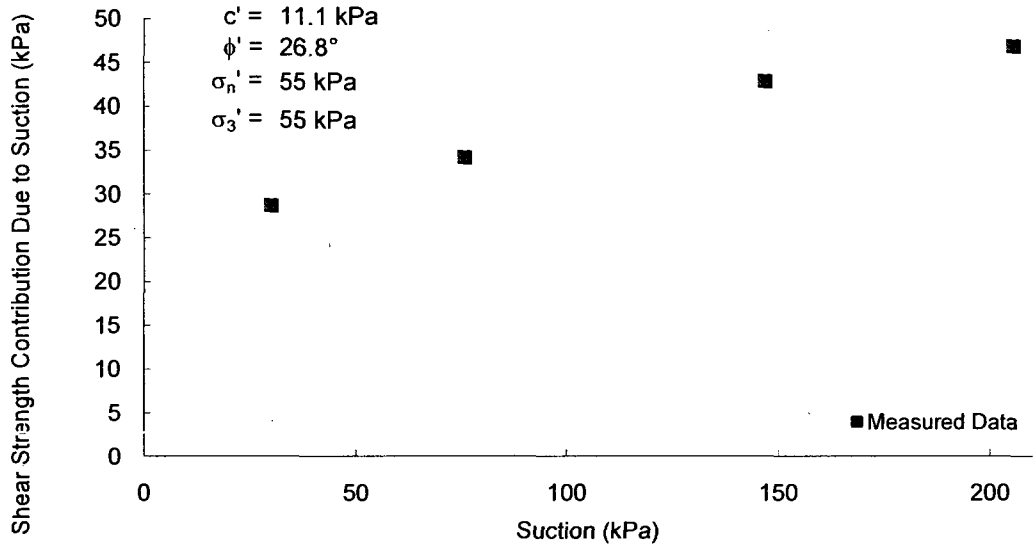

SWRC

Test Method: Tempe cell

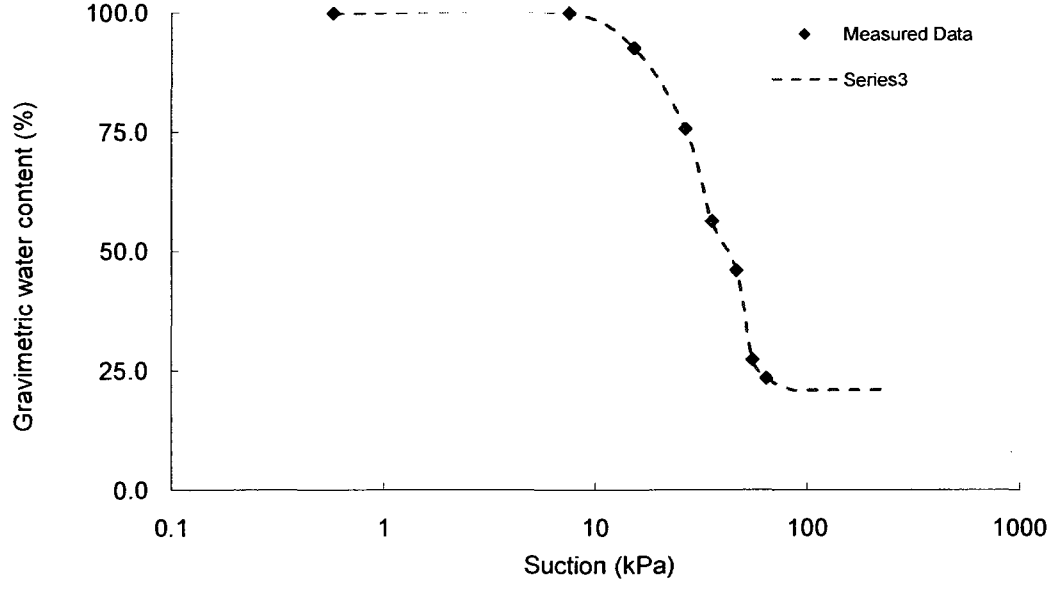

Soil No. 50

Typical Residual
de Campos and Carrillo, 1995

Compacted Sample
Sand = 71.7%, Silt = 12.2%, Clay = 7.6%; Liquid Limit = 30, Plasticity Index = 30
Lean clay, CL

Shear Strength

Test Method: Modified direct shear test

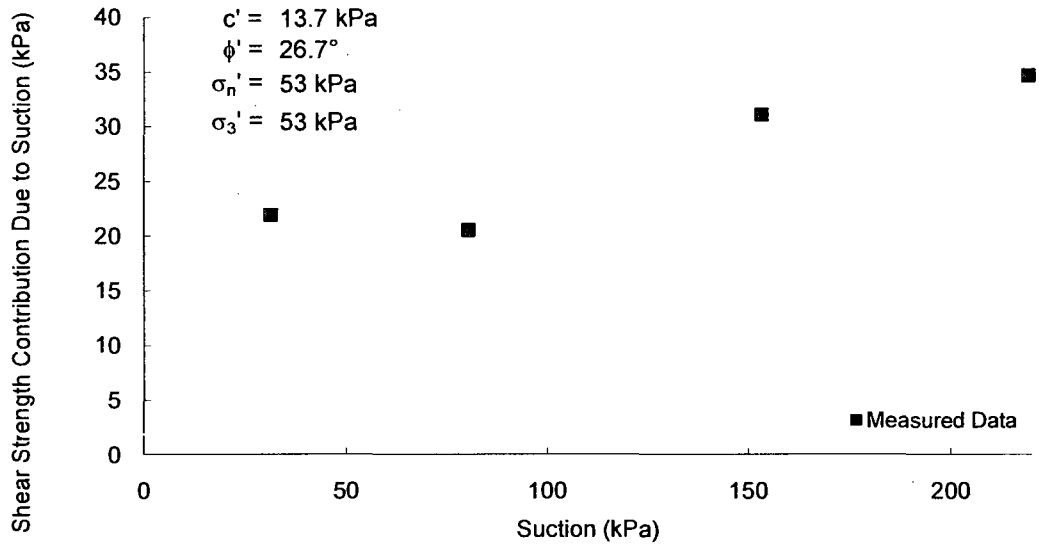

SWRC

Test Method: Tempe cell

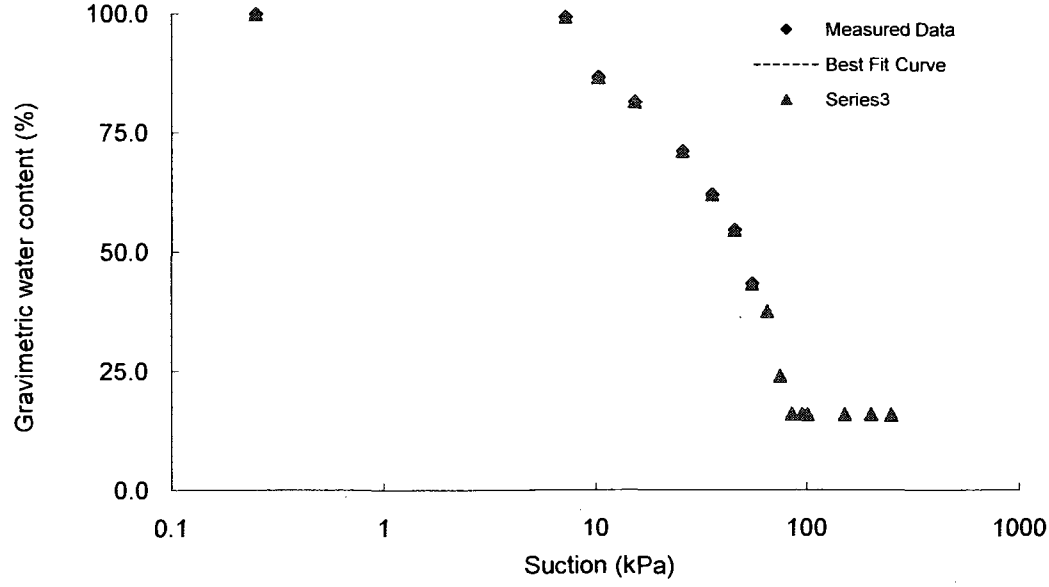

Soil No. 51

Red Residual

de Campos and Carrillo, 1995

Compacted Sample

Sand = 60%, Silt = 6.5%, Clay = 24.4%; Liquid Limit = 51, Plasticity Index = 18

Heavy silt, MH

Shear Strength

Test Method: Modified direct shear test

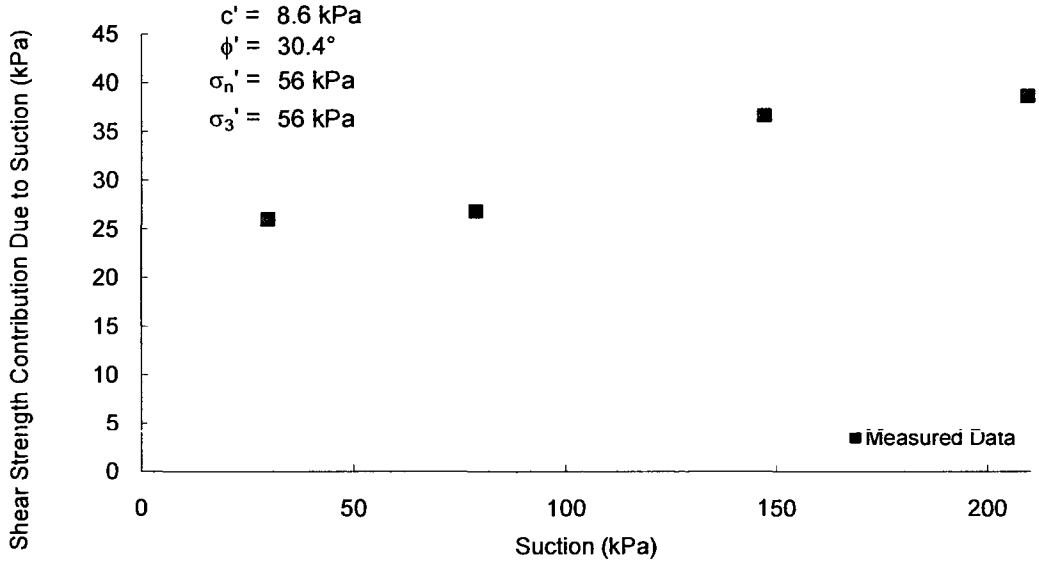

SWRC

Test Method: Tempe cell

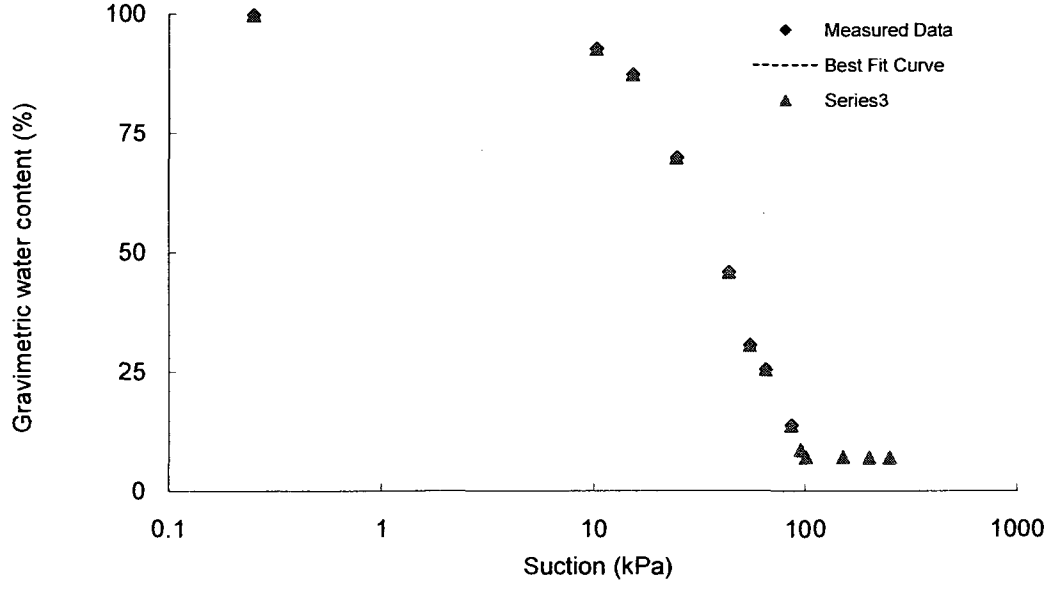

Soil No. 52

Kaolin

Pineda and Colmenares, 2005

Compacted Sample

Sand = 0%, Silt = %, Clay = 24.4%; Liquid Limit = 84, Plasticity Index = 38

Heavy silt, MH

Shear Strength

Test Method: Modified direct shear test

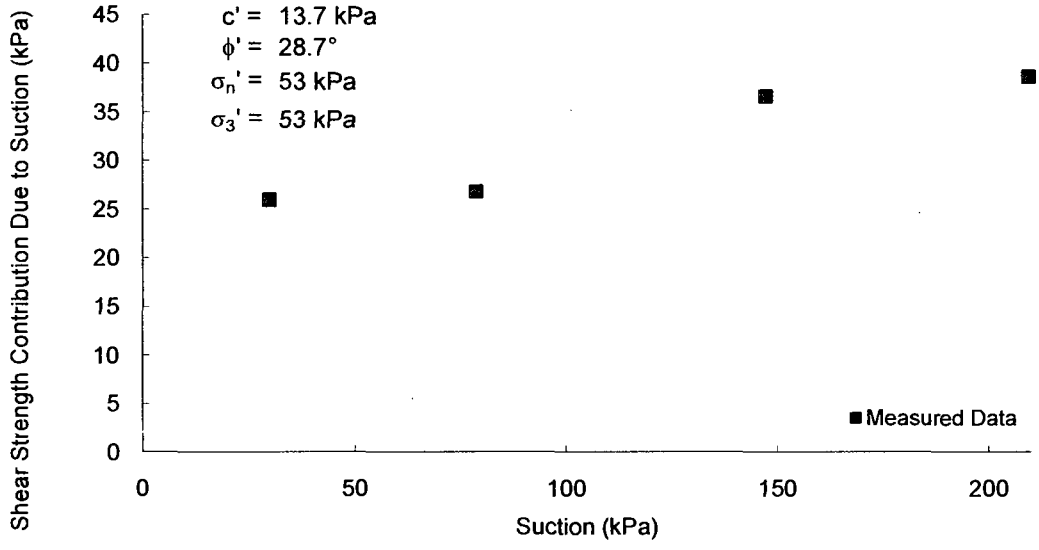

SWRC

Test Method: Tempe cell

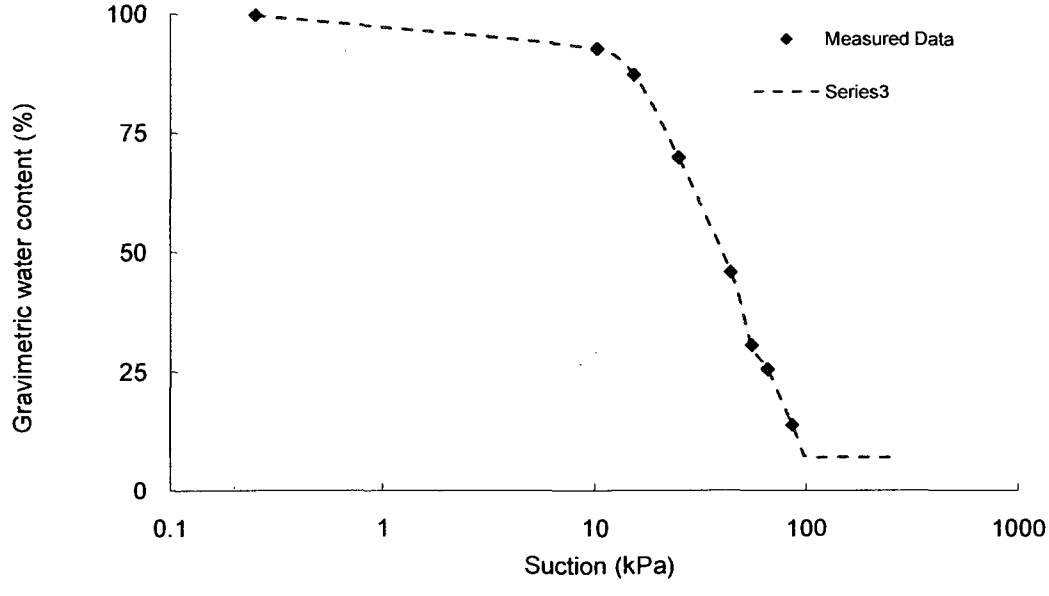

APPENDIX B

PARTICLE SIZE DISTRIBUTIONS

Soil No. 4 **Glacial till**

Vanapalli, Fredlund, Pufahl and Clifton, 1996

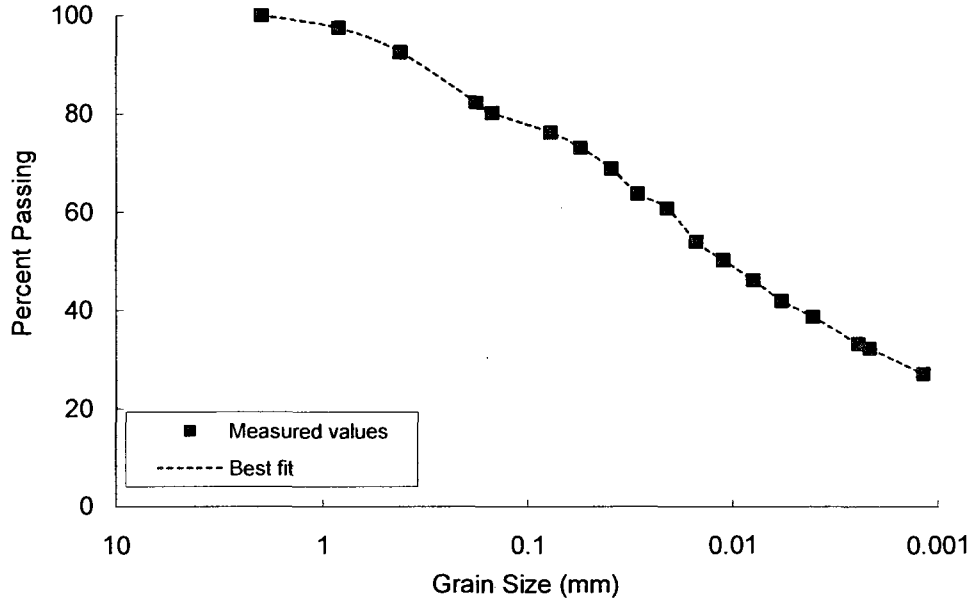

Soil No. 5 **Botkin Silt**

Vanapalli, Wright and Fredlund, 1999

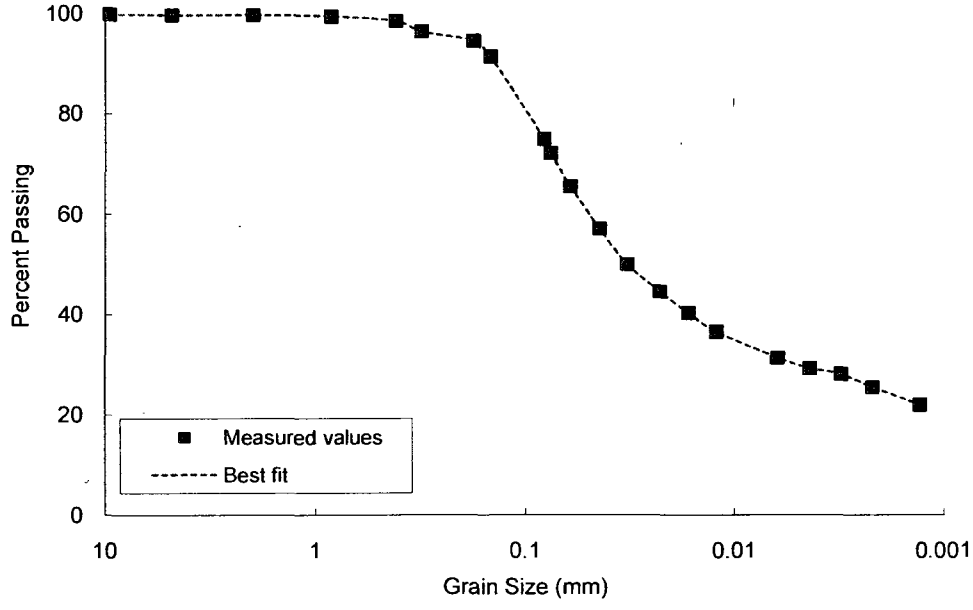

Soil No. 6

Dhanauri Clay
Gulhati and Satija, 1981

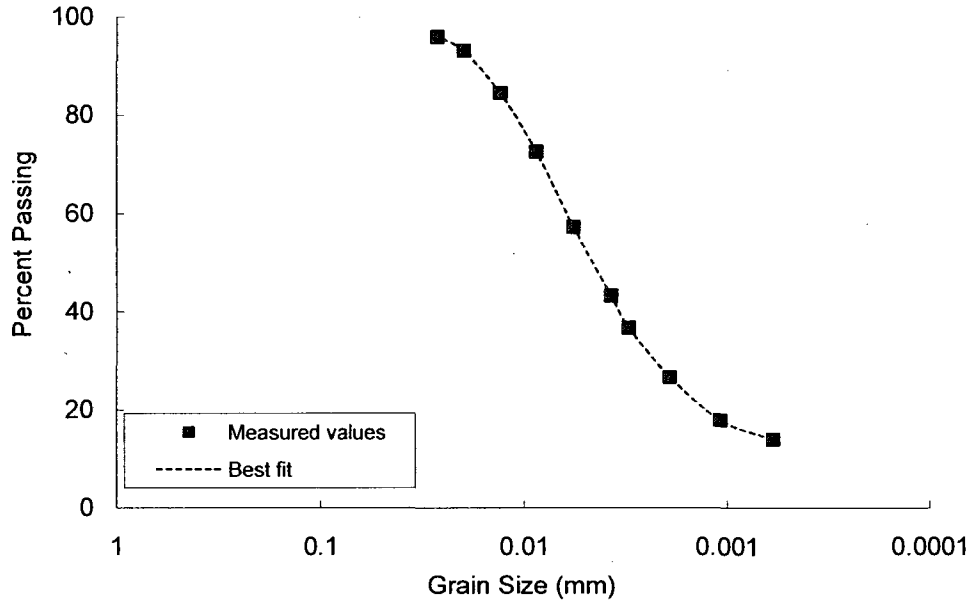

Soil No. 7

Weathered Granite
Lee, Sung and Cho, 2005

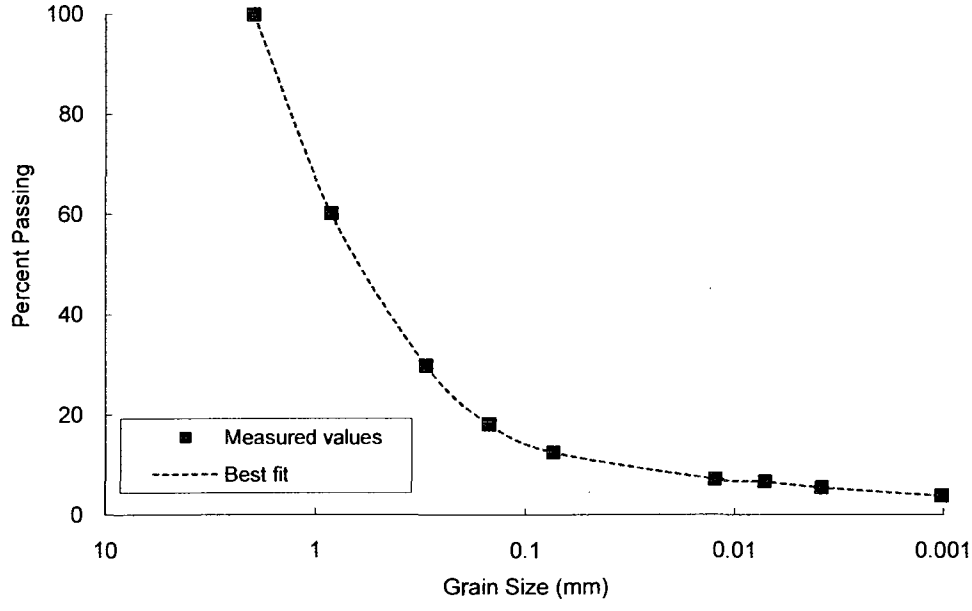

Soil No. 8

Jurong soil

Rahardjo, Heng and Choon, 2004

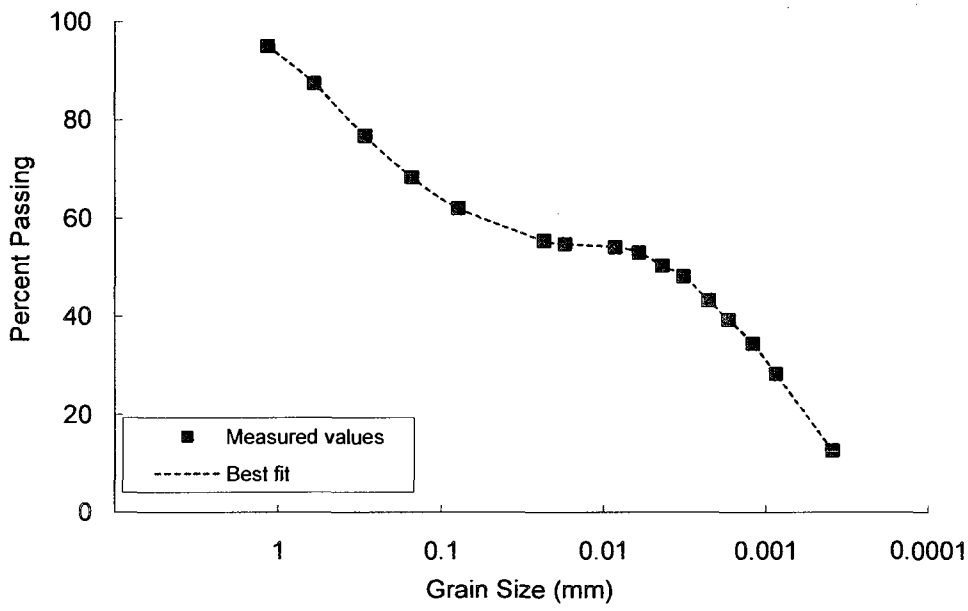

Soil No. 12

SJ10a

Khalili, Geiser and Blight, 2004

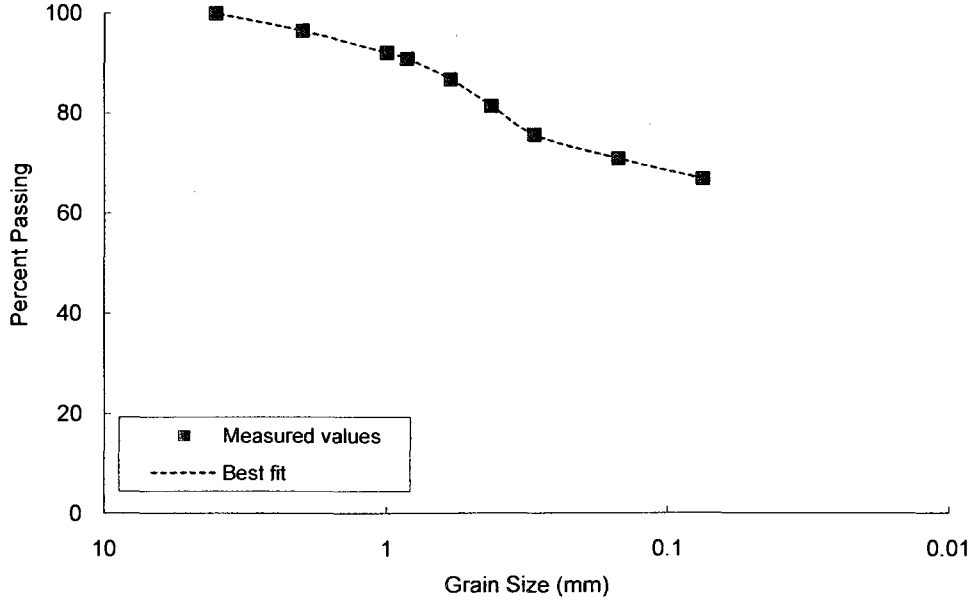

Soil No. 13 **SJ10b**

Khalili, Geiser and Blight, 2004

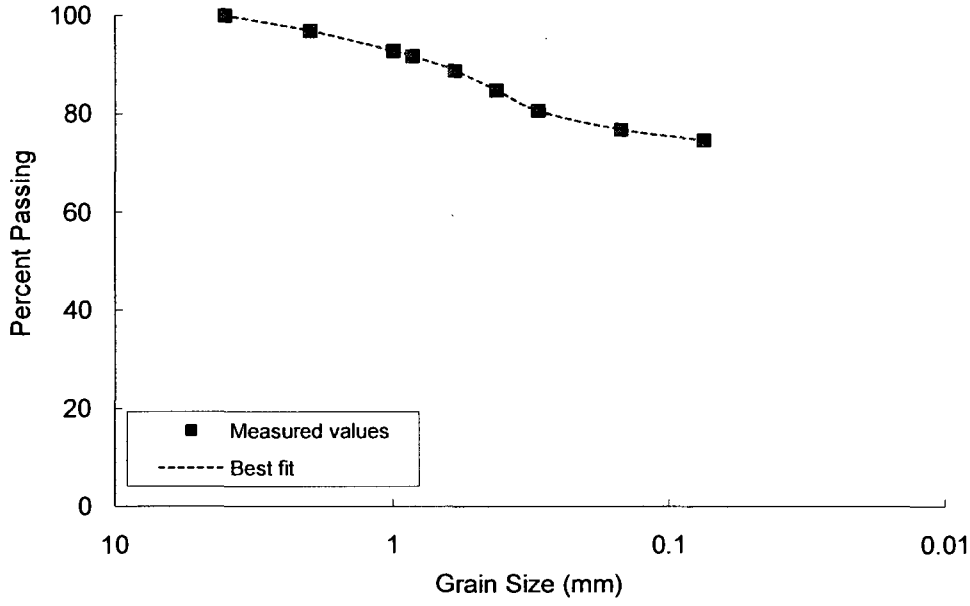

Soil No. 14 **SJ11.**

Khalili, Geiser and Blight, 2004

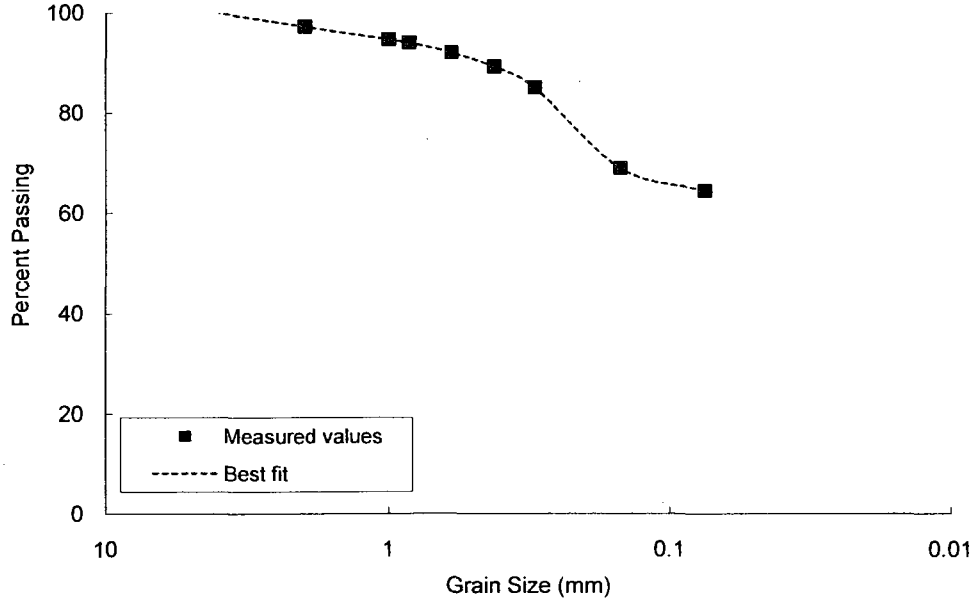

Soil No. 15

Tailings (50 m)
Rassam and Williams, 1999

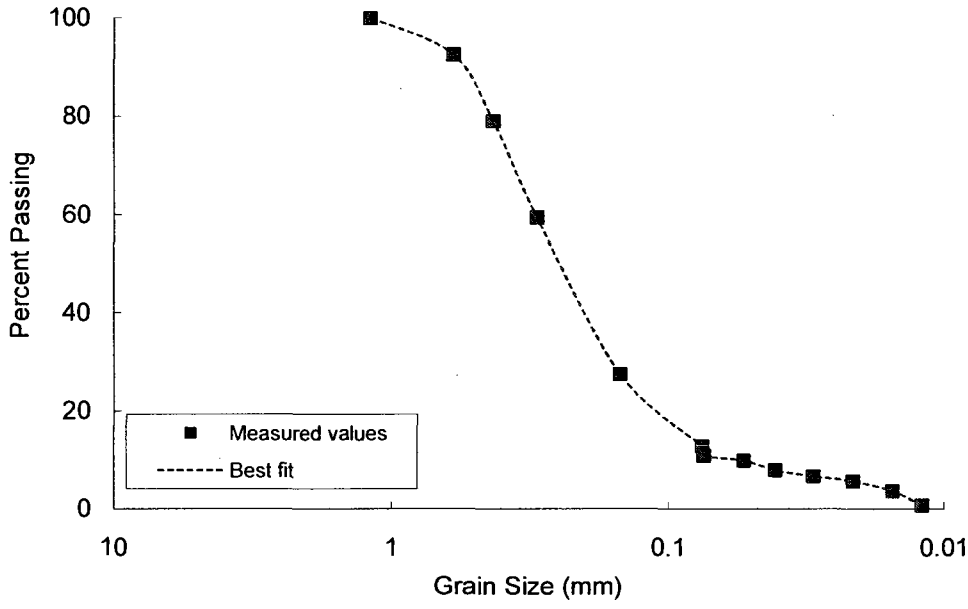

Soil No. 16

Tailings (150 m)
Rassam and Williams, 1999

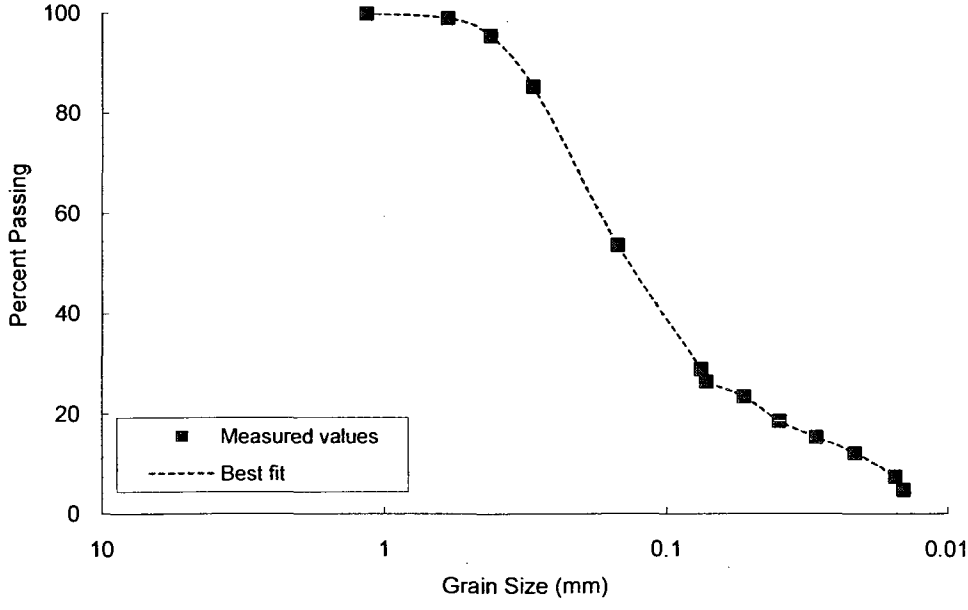

Soil No. 17

Rohm Laterite
Rohm and Vilar, 1995

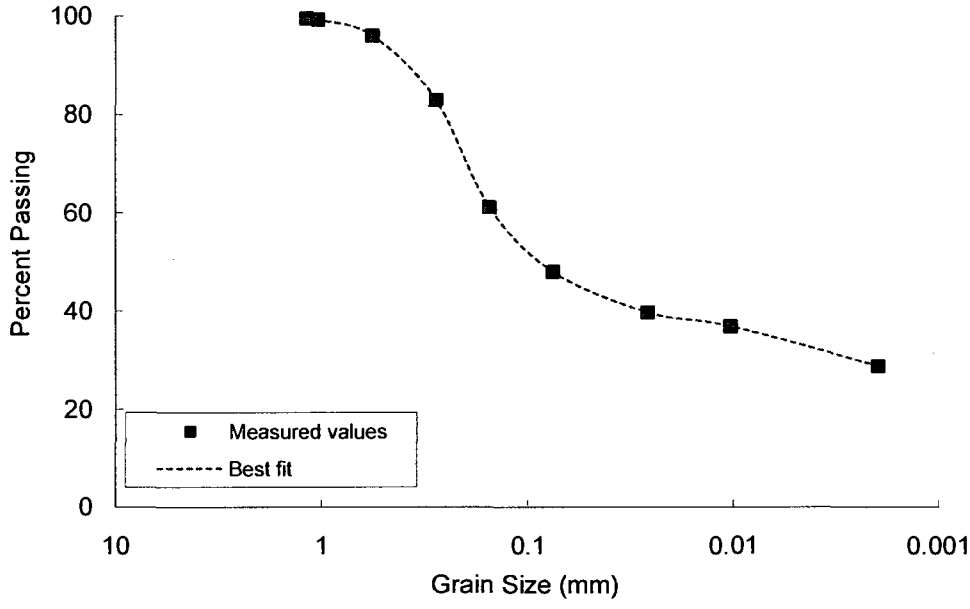

Soil No. 20

Frankston Fine
Donald, 1957

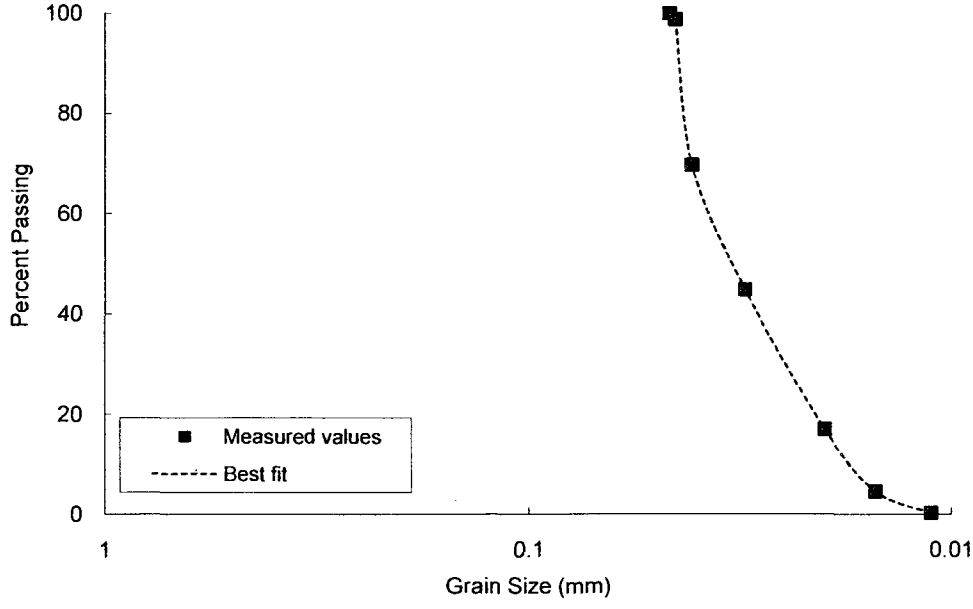

Soil No. 21

Medium Frankston
Donald, 1957

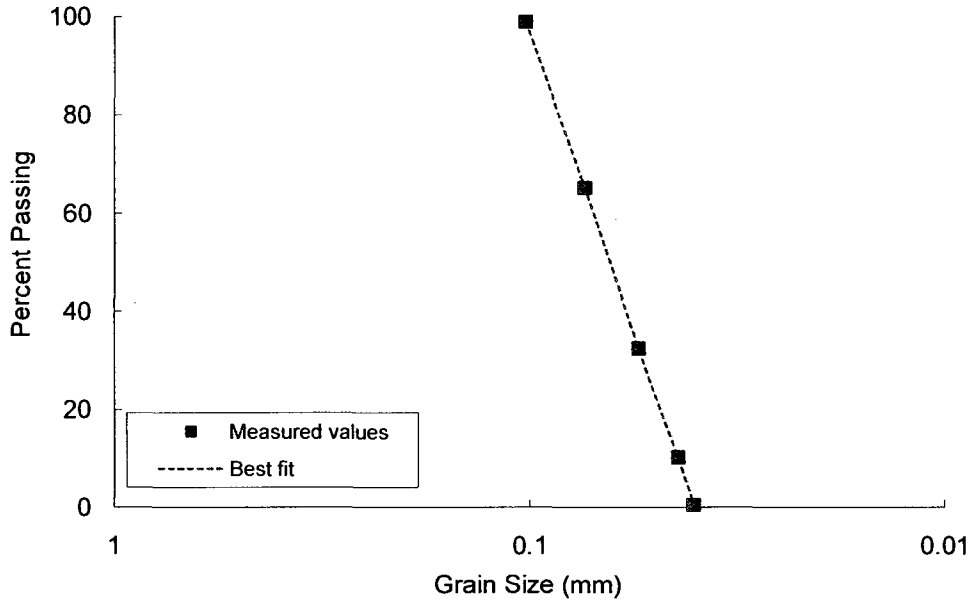

Soil No. 22

Graded Frankston
Donald, 1957

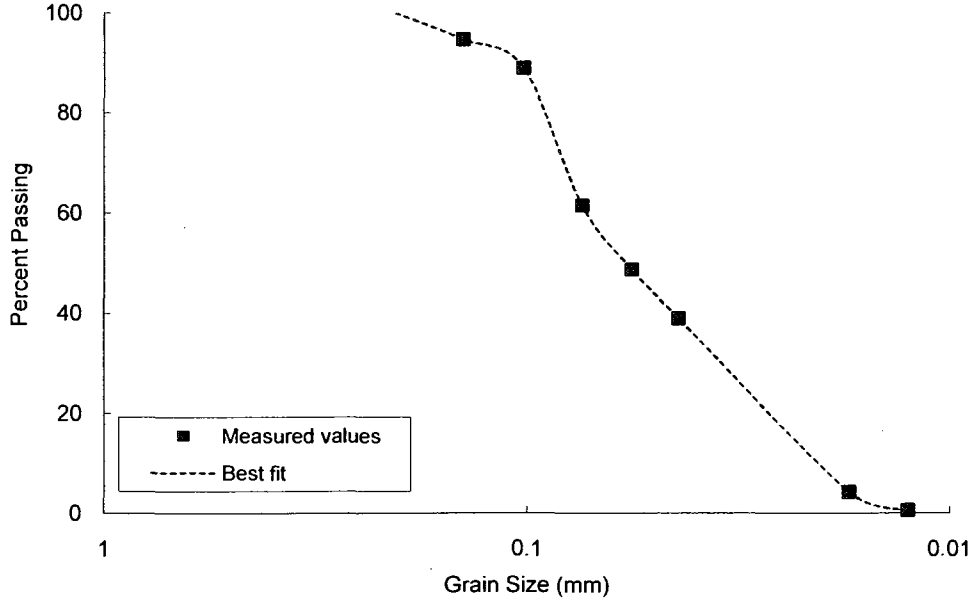

Soil No. 23

Brown sand
Donald, 1957

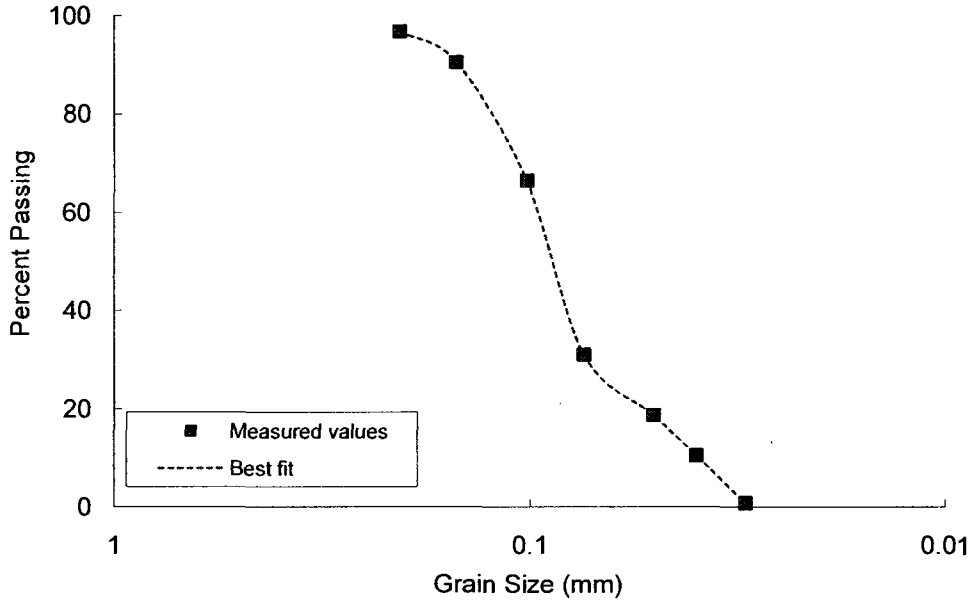

Soil No. 24

Copper tailings
Drumright, 1989

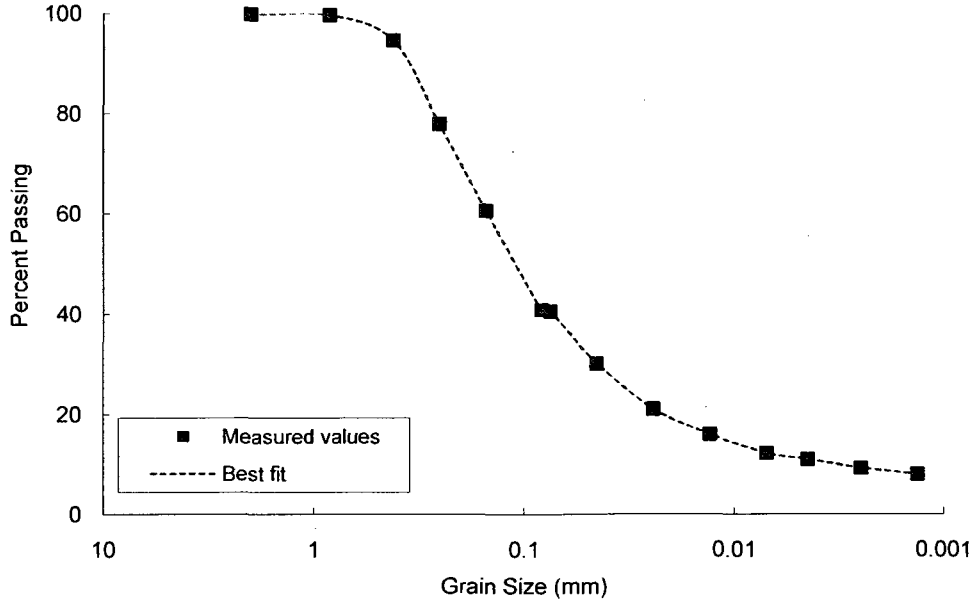

Soil No. 25 **AV colluvium**

Feuerharmel, Bica, Gehling and Flores, 2006

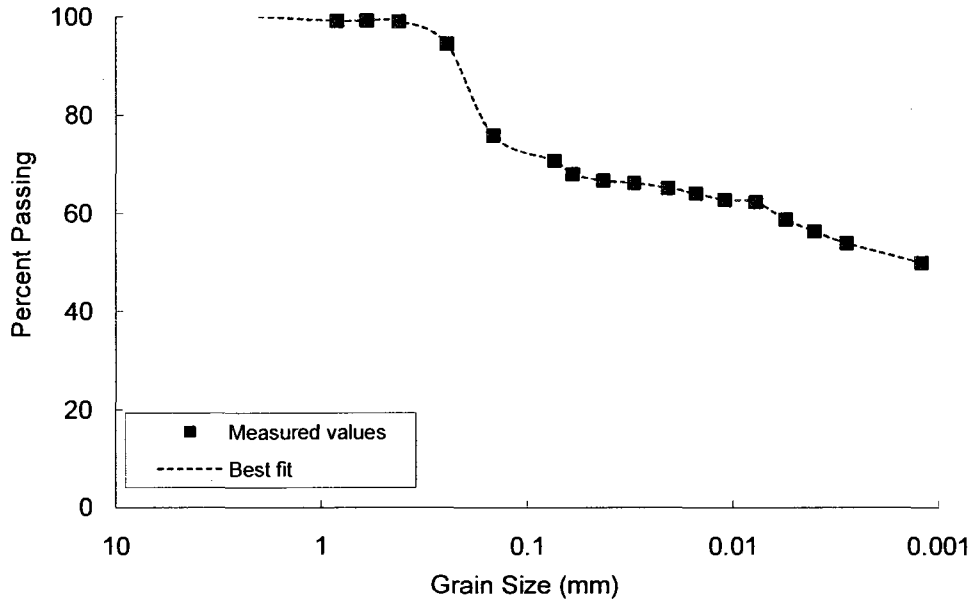

Soil No. 27 **CRDB silt**

Colmenares, Ridley, Dineen and Burland, 2003

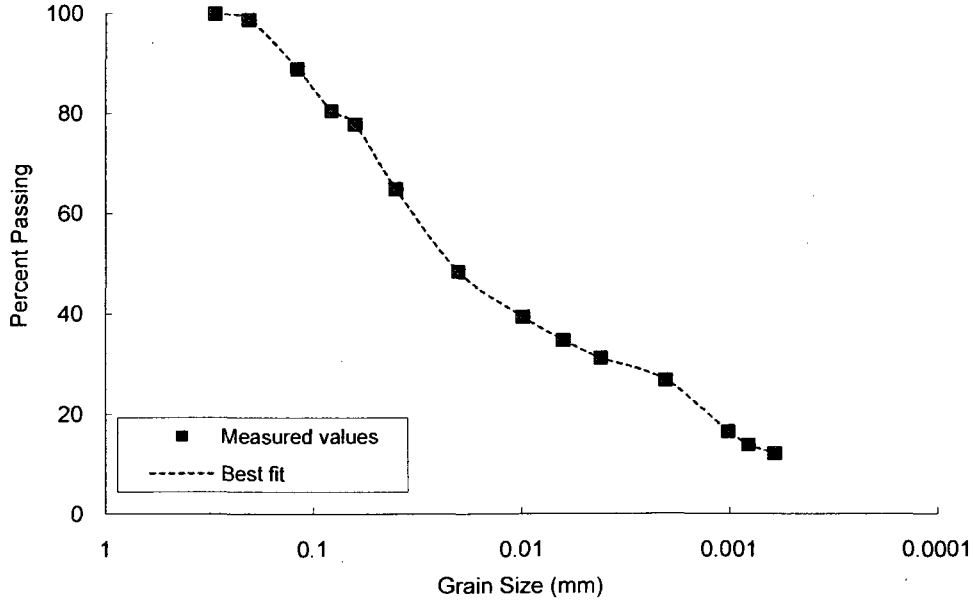

Soil No. 28

Oloo Botkin silt

Oloo and Fredlund, 1996; Oloo, 1994

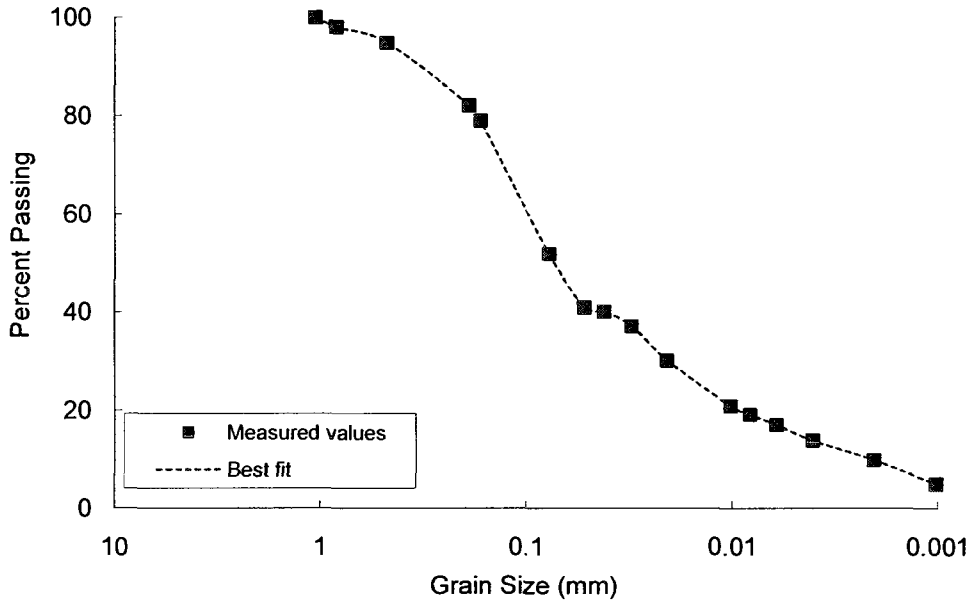

Soil No. 29

Oloo Indian Head till

Oloo and Fredlund, 1996; Oloo, 1994

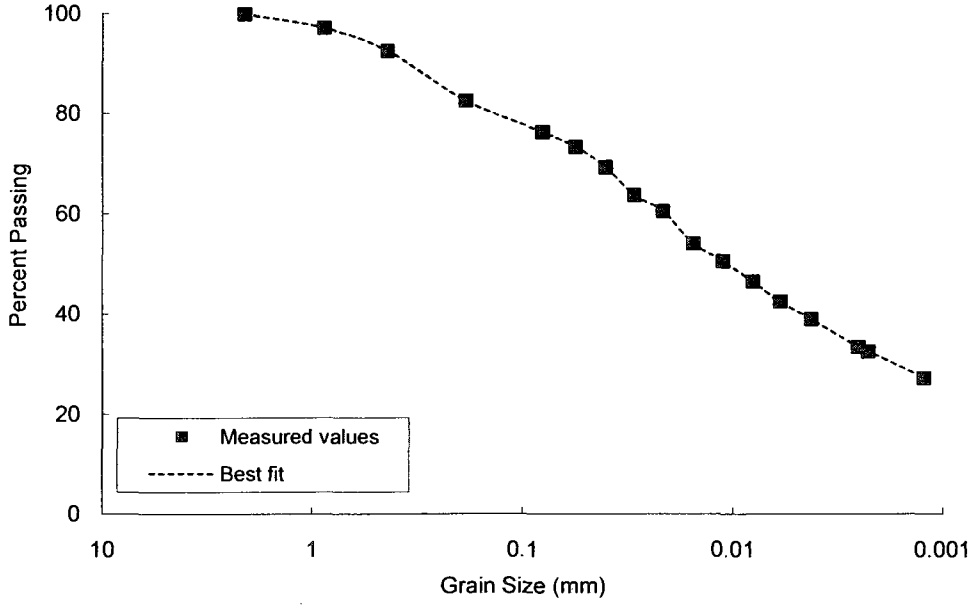

Soil No. 33 **C02**

Li, 1989; Hardcastle, Li and Fragaszy, 1992

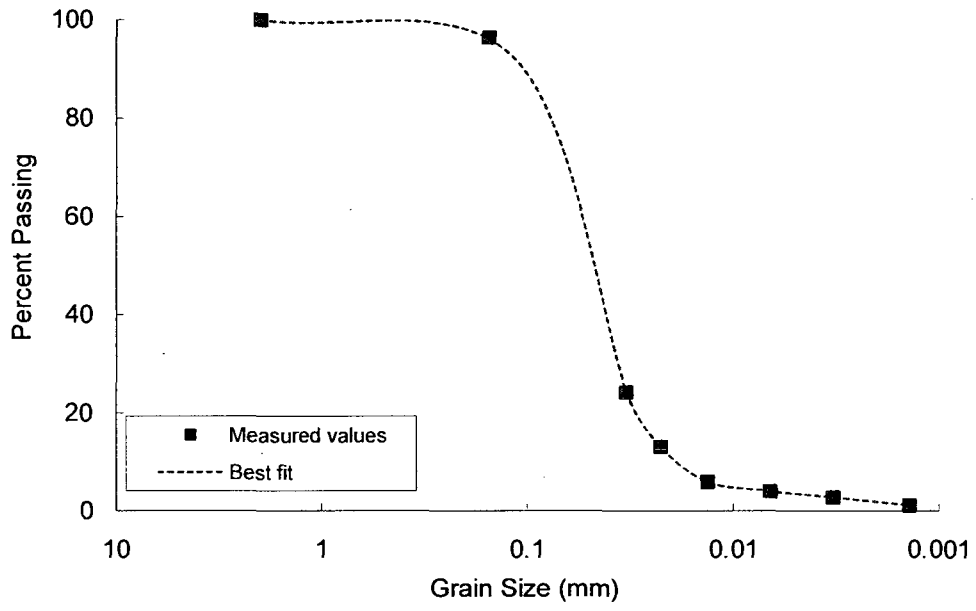

Soil No. 34 **C11**

Li, 1989; Hardcastle, Li and Fragaszy, 1992

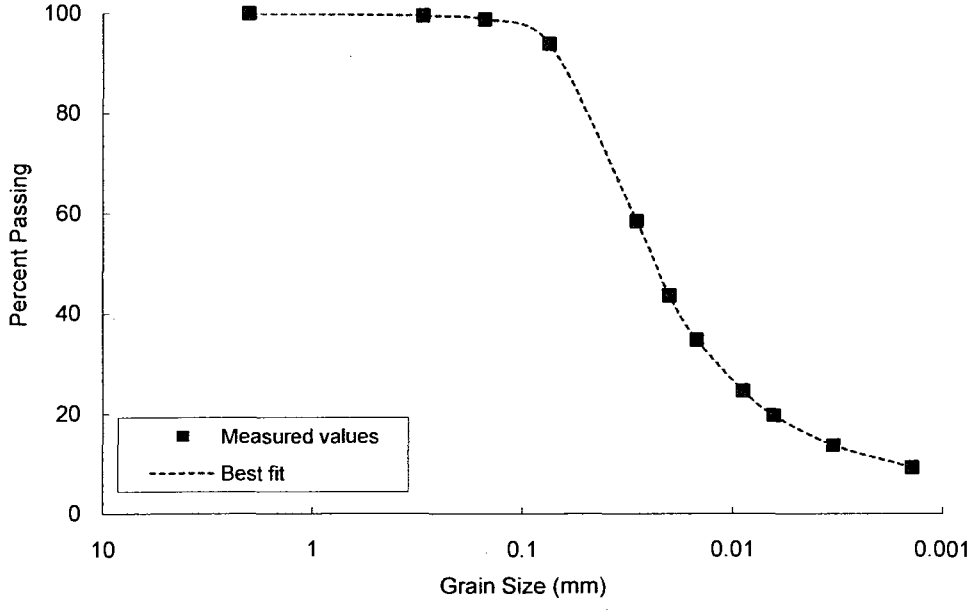

Soil No. 35 **C20**

Li, 1989; Hardcastle, Li and Fragaszy, 1992

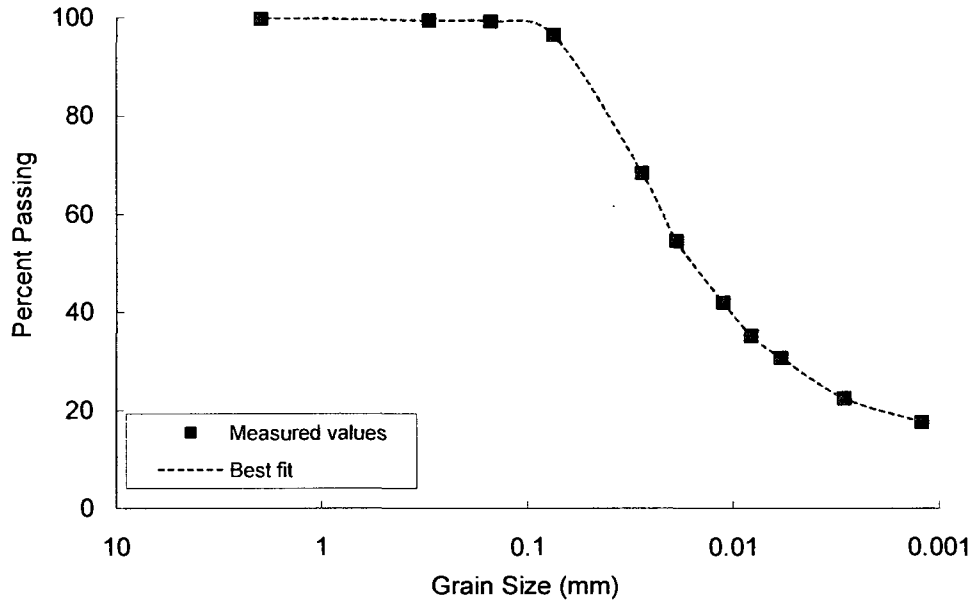

Soil No. 36 **C30**

Li, 1989; Hardcastle, Li and Fragaszy, 1992

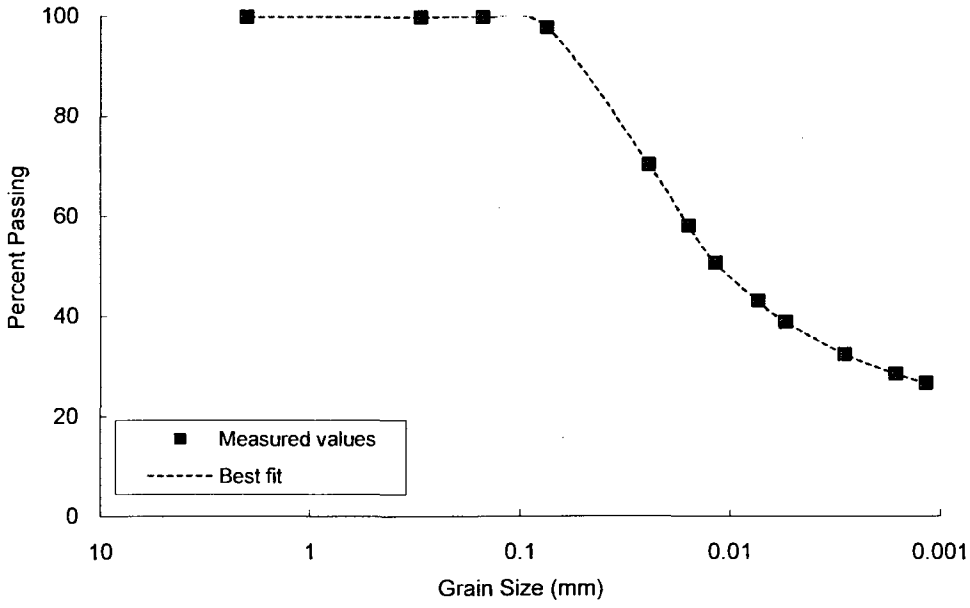

Soil No. 44

Nishimura silt

Nishimura, Fredlund, Gan and Hirabayashi, 1999

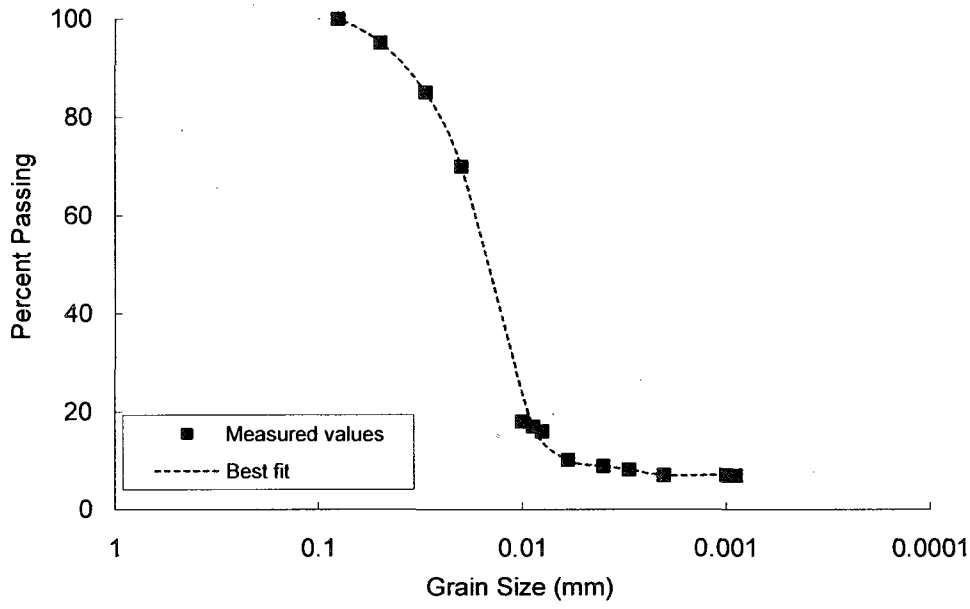

APPENDIX C

MEASURED AND CALCULATED SHEAR STRENGTH VALUES

Soil No. 1a

Red silty clay

Escario and Saez, 1986; Escario and Juca, 1989

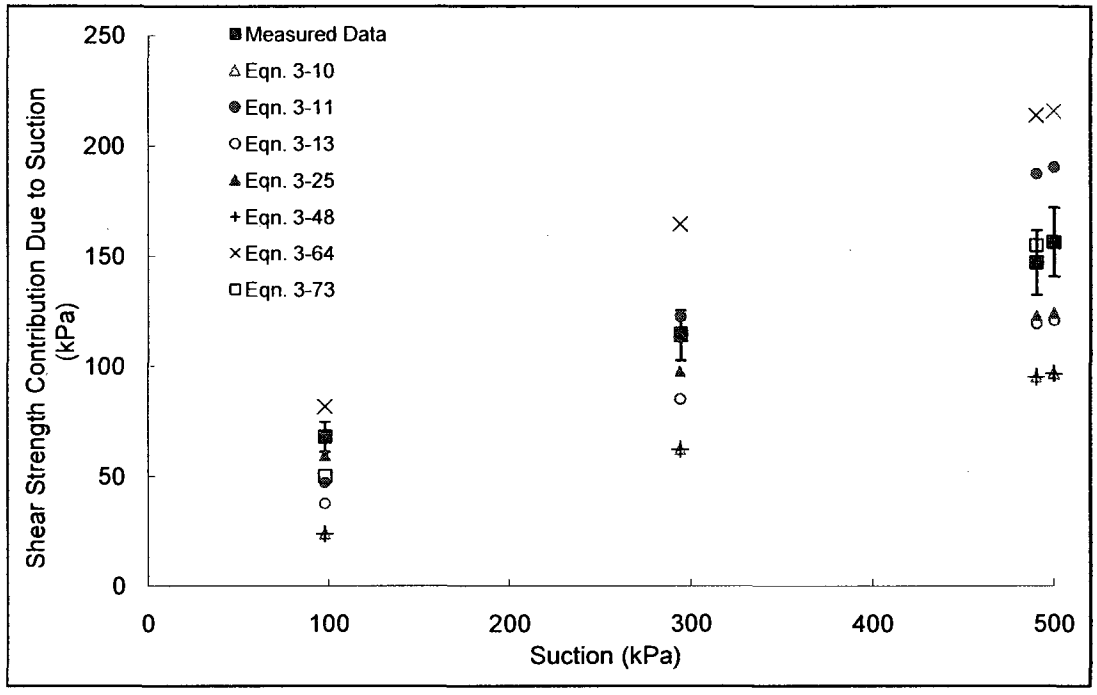

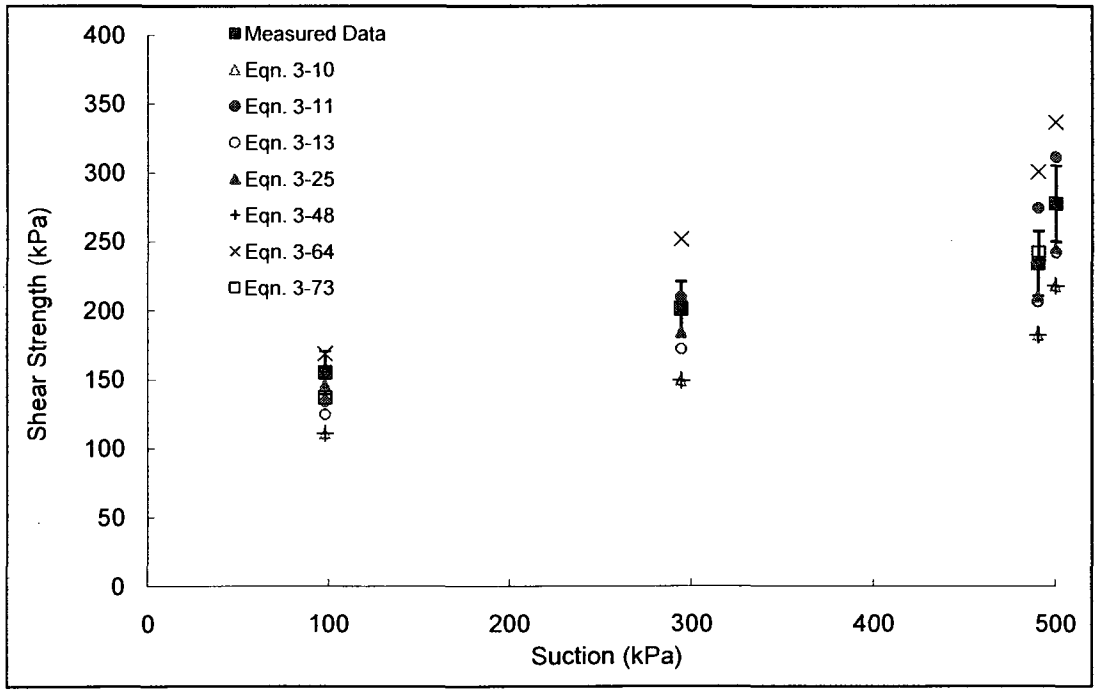

Soil No. 1b

Red silty clay

Escario and Saez, 1986; Escario and Juca, 1989

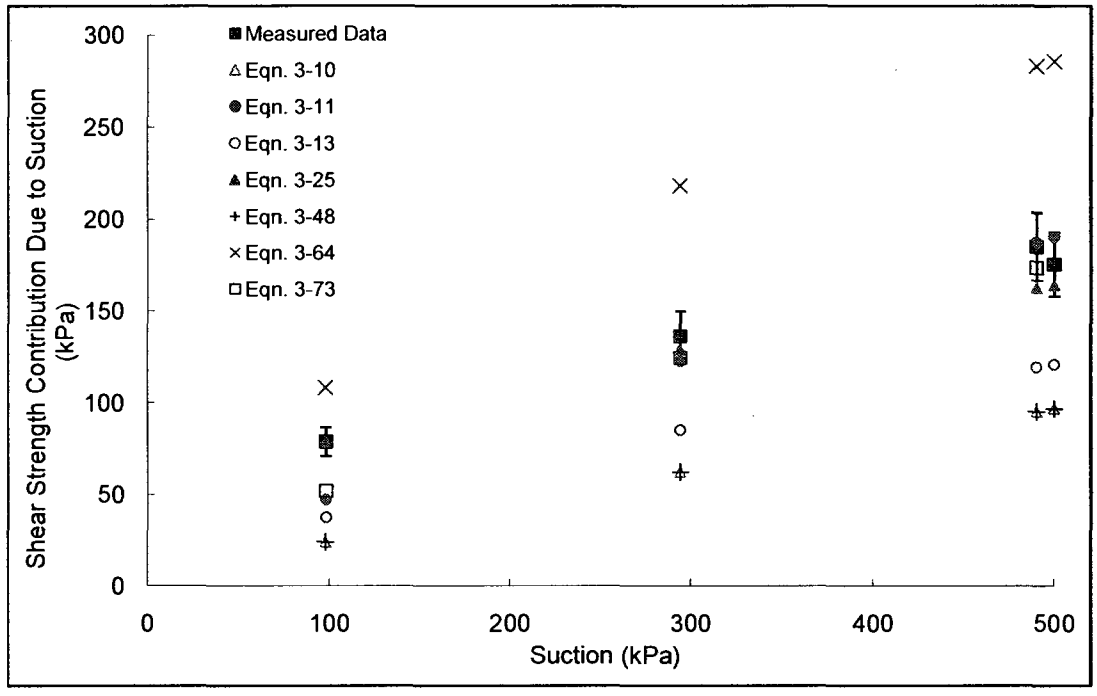

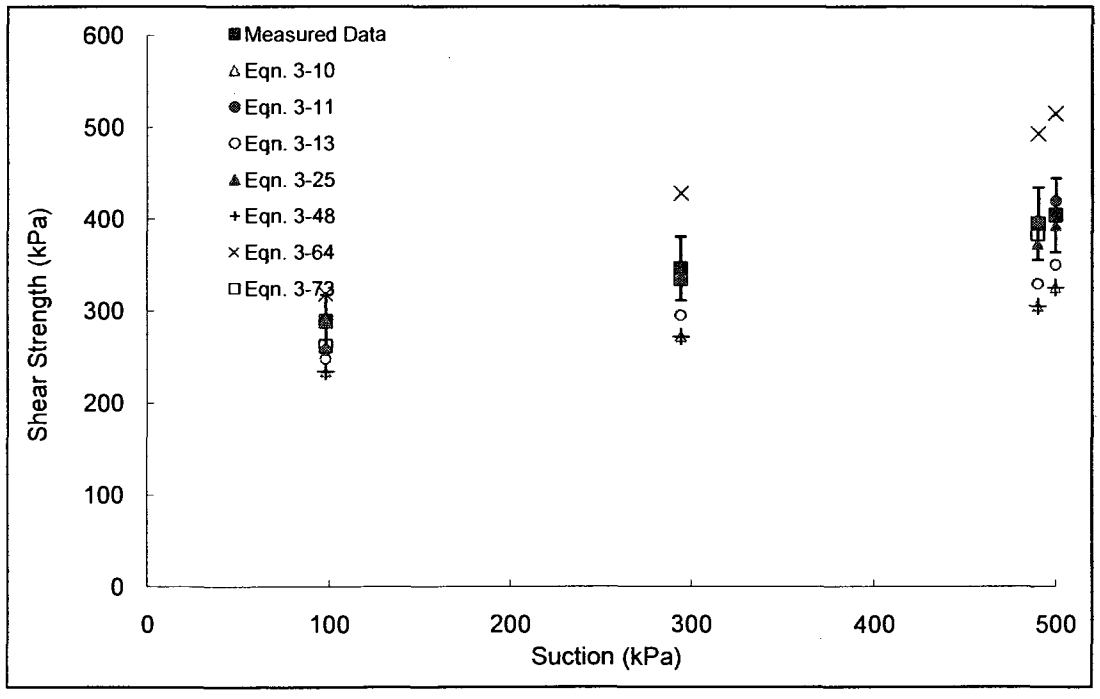

Soil No. 1c

Red silty clay

Escario and Saez, 1986; Escario and Juca, 1989

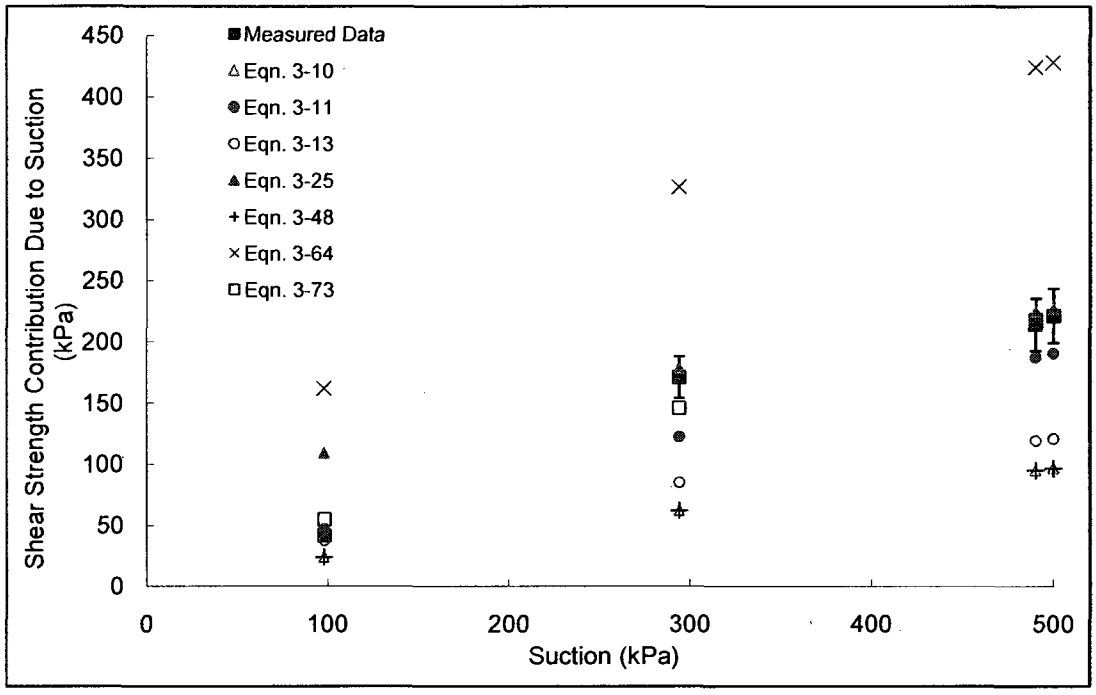

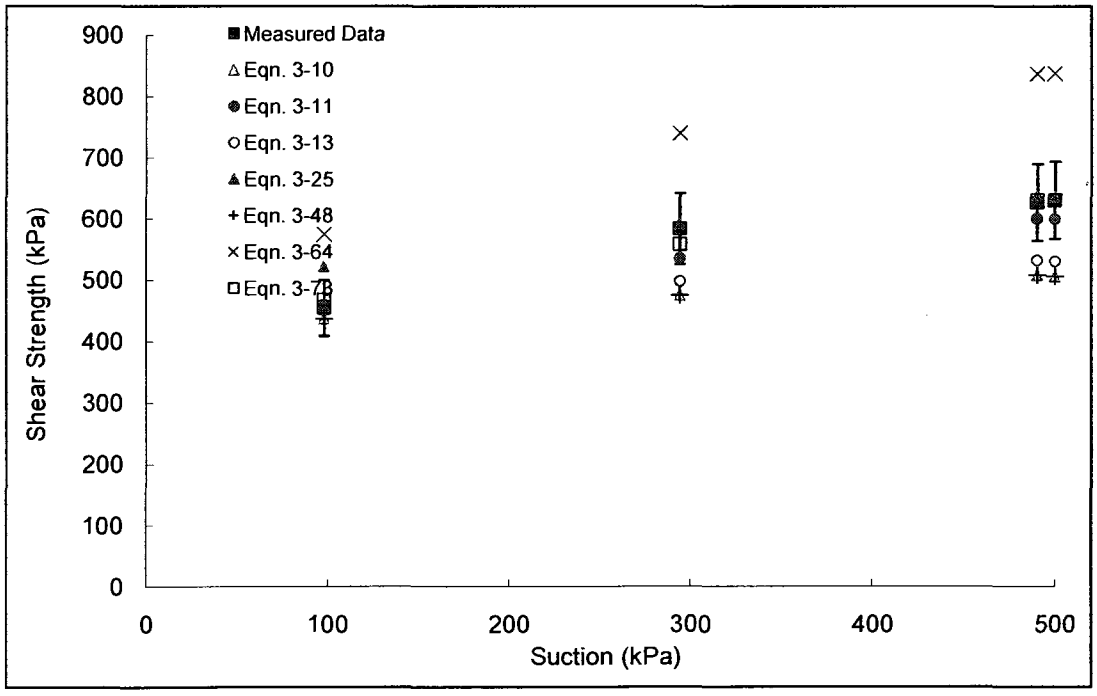

Soil No. 25a

AV colluvium

Feuerharmel, Bica, Gehling and Flores, 2006

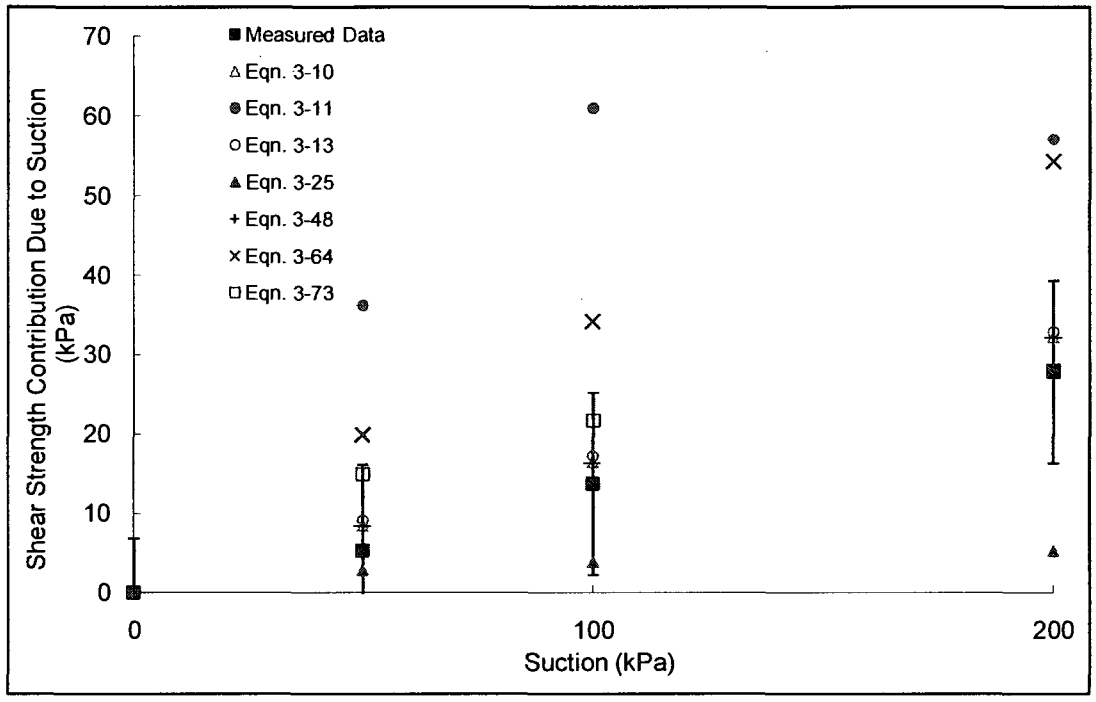

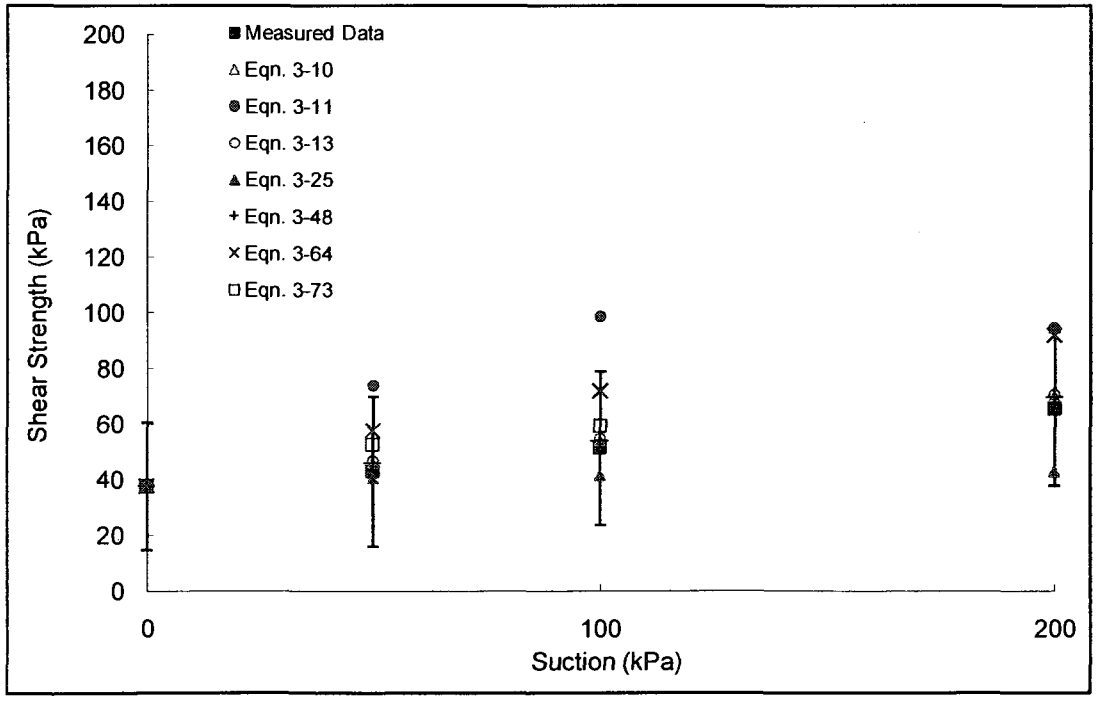

Soil No. 25b

AV colluvium

Feuerharmel, Bica, Gehling and Flores, 2006

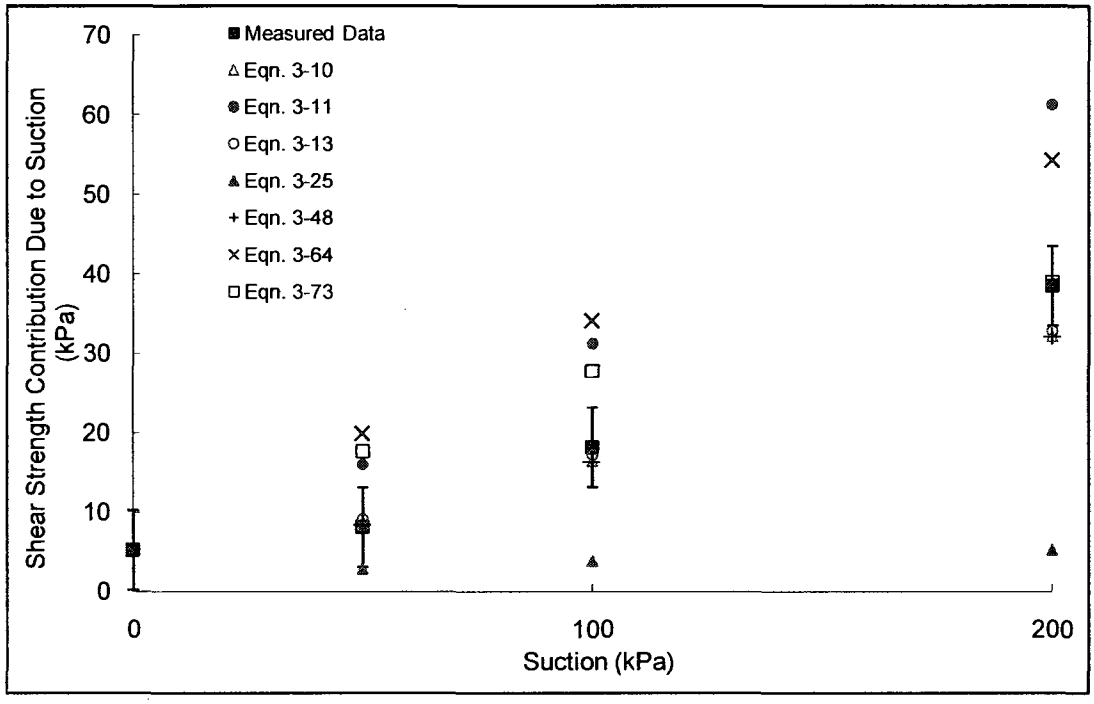

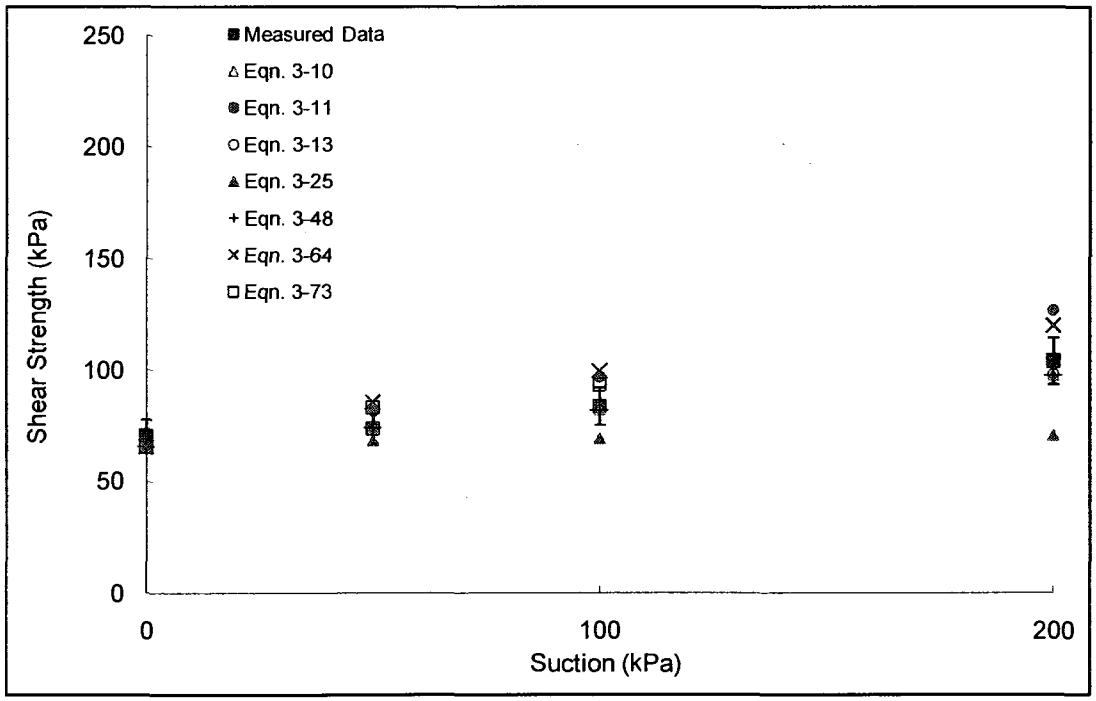

Soil No. 25c

AV colluvium

Feuerharmel, Bica, Gehling and Flores, 2006

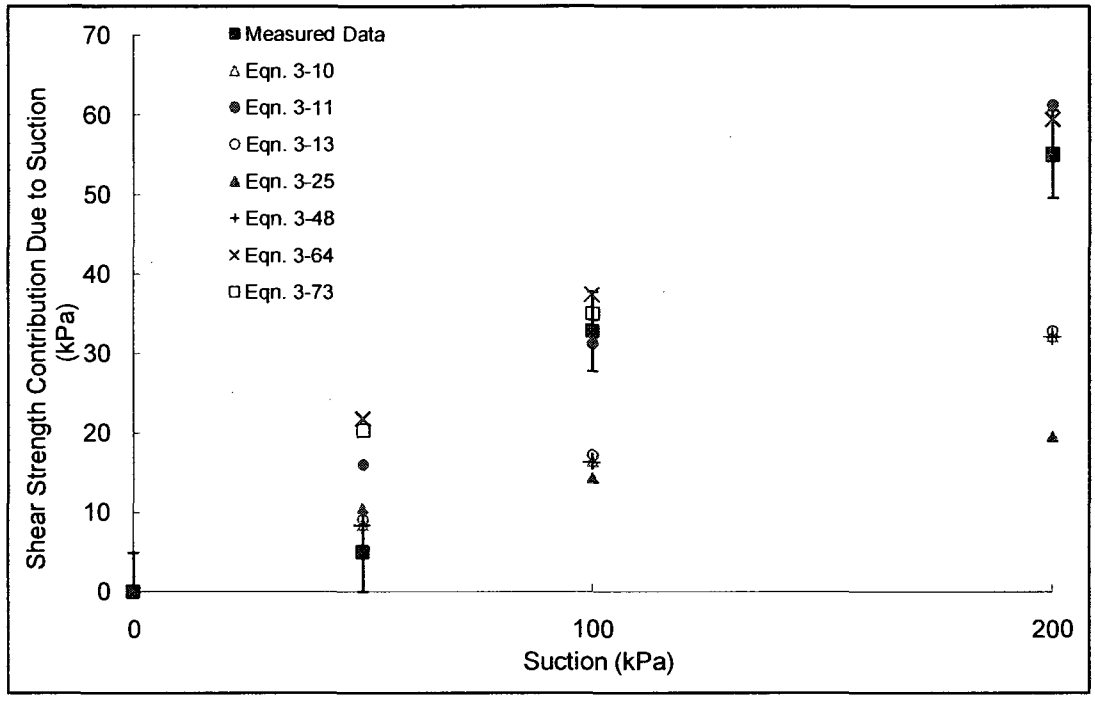

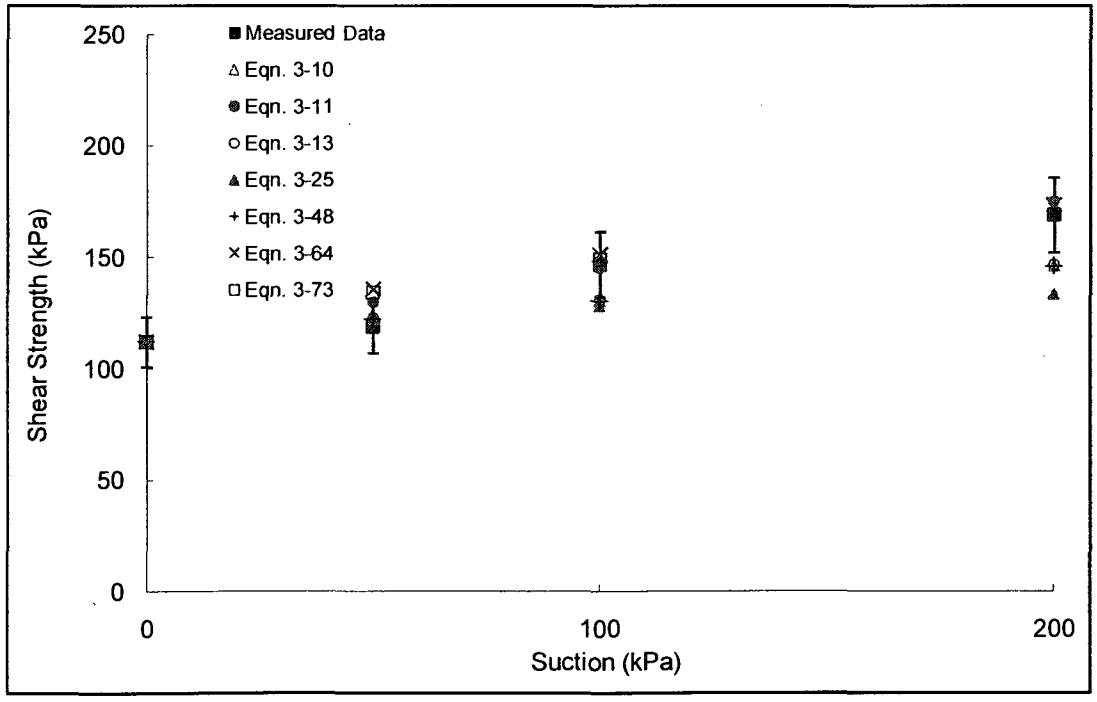

Soil No. 25d

AV colluvium

Feuerharmel, Bica, Gehling and Flores, 2006

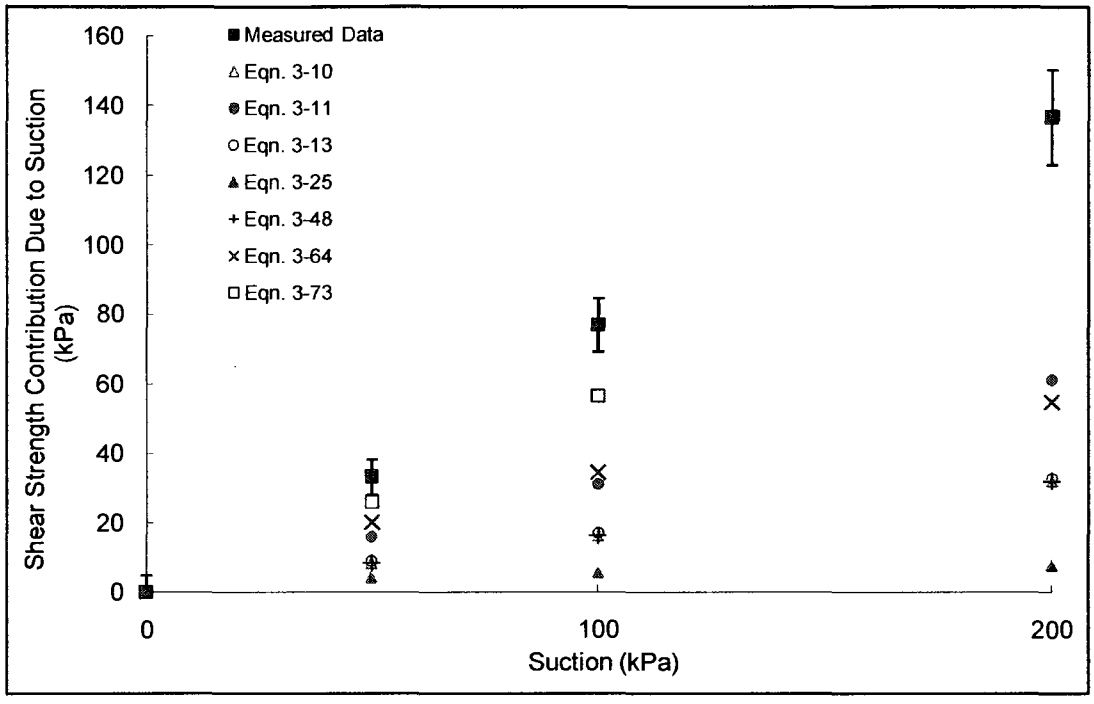

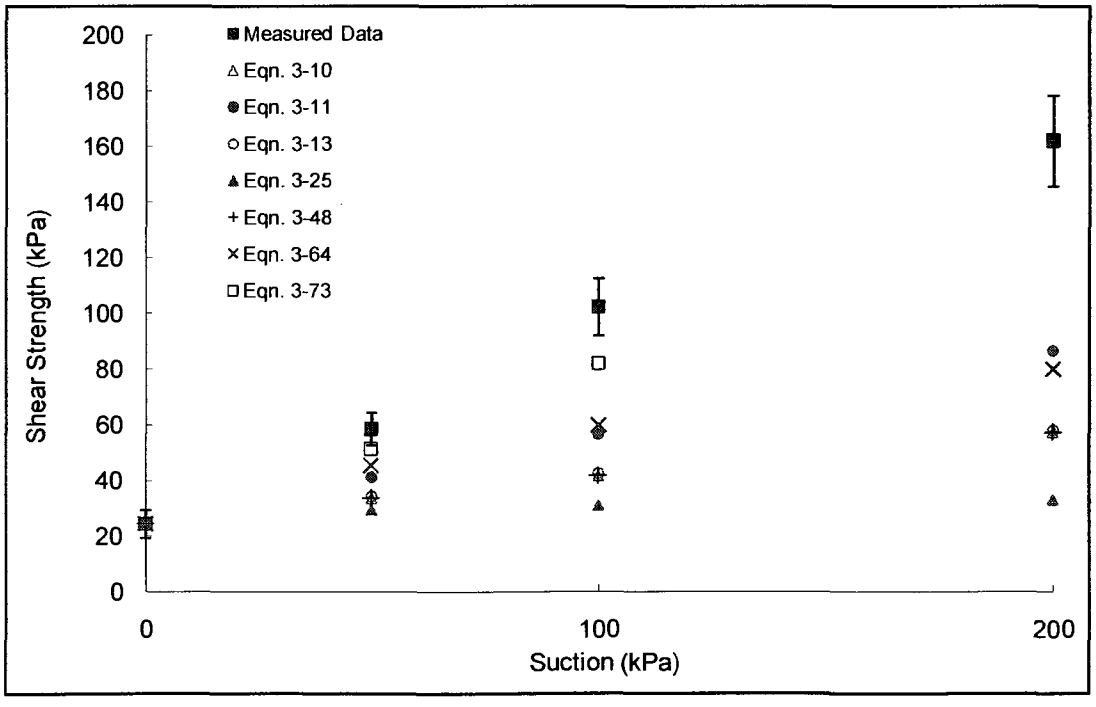

Soil No. 25e

AV colluvium

Feuerharmel, Bica, Gehling and Flores, 2006

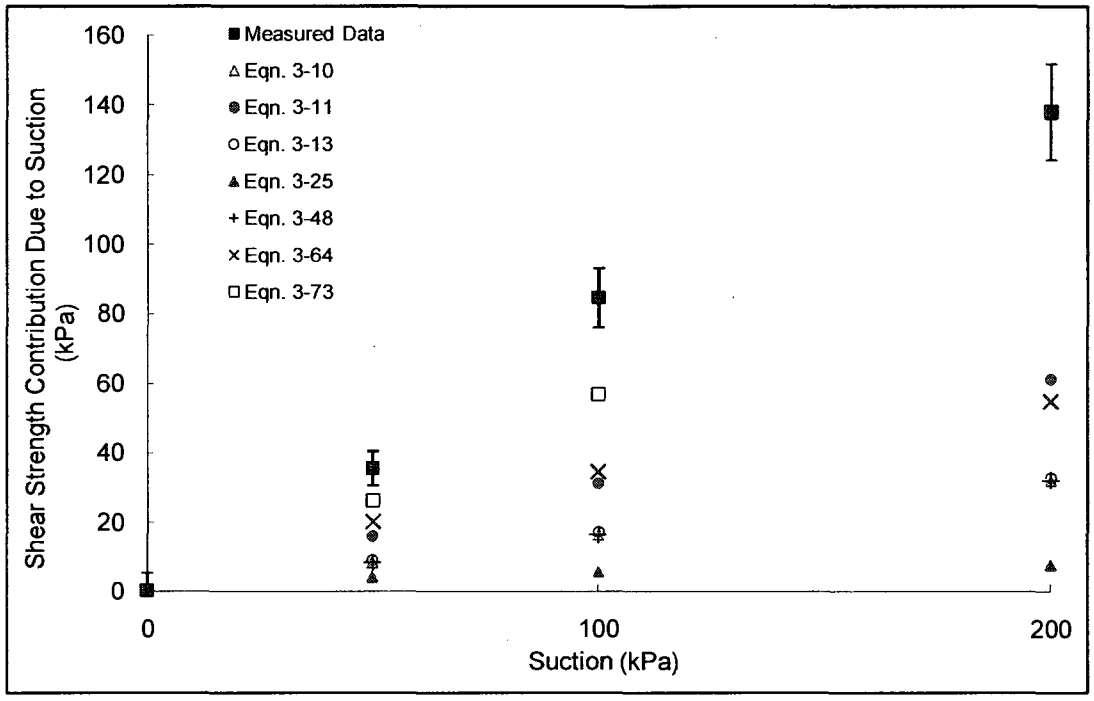

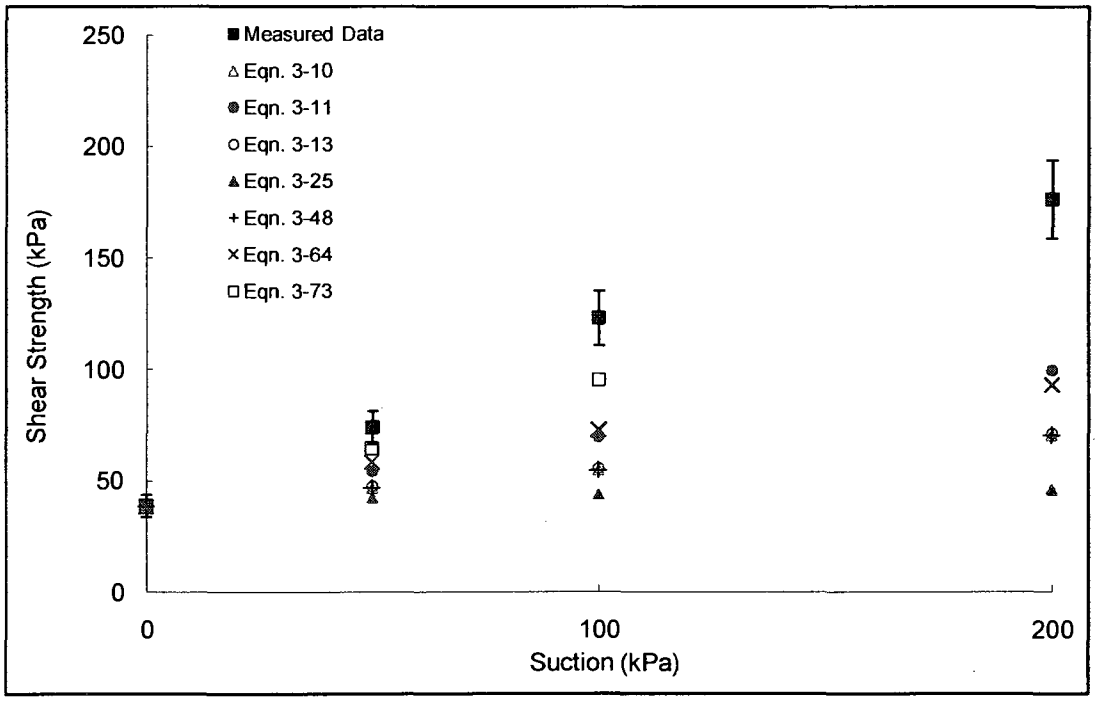

Soil No. 25f

AV colluvium

Feuerharmel, Bica, Gehling and Flores, 2006

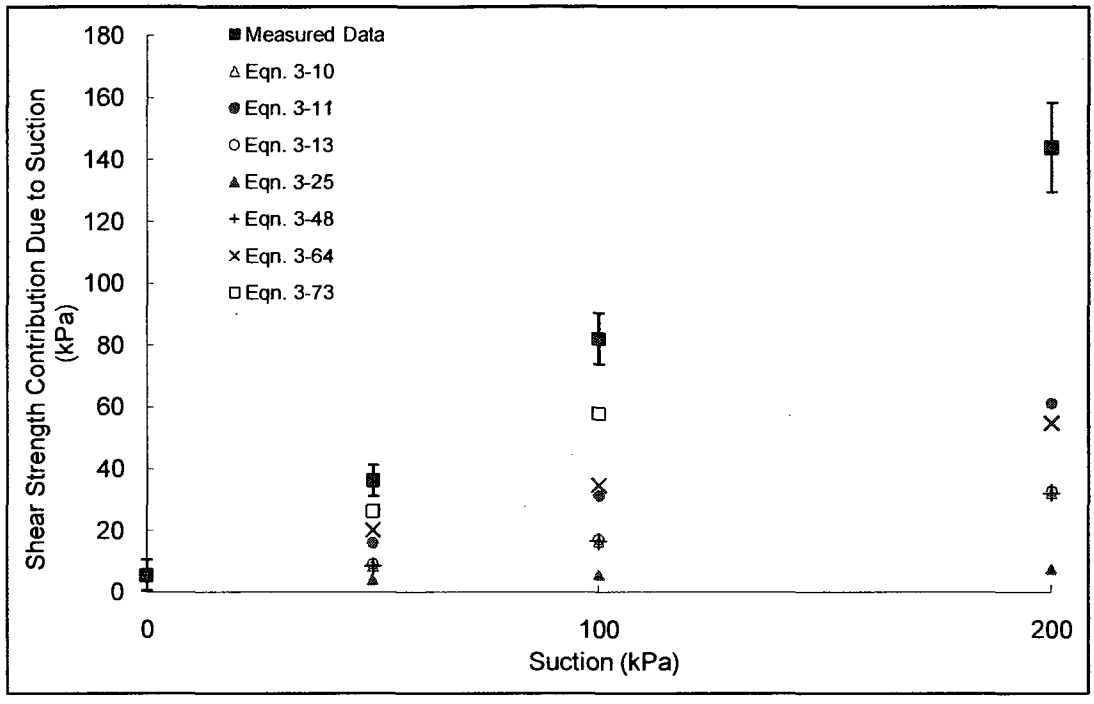

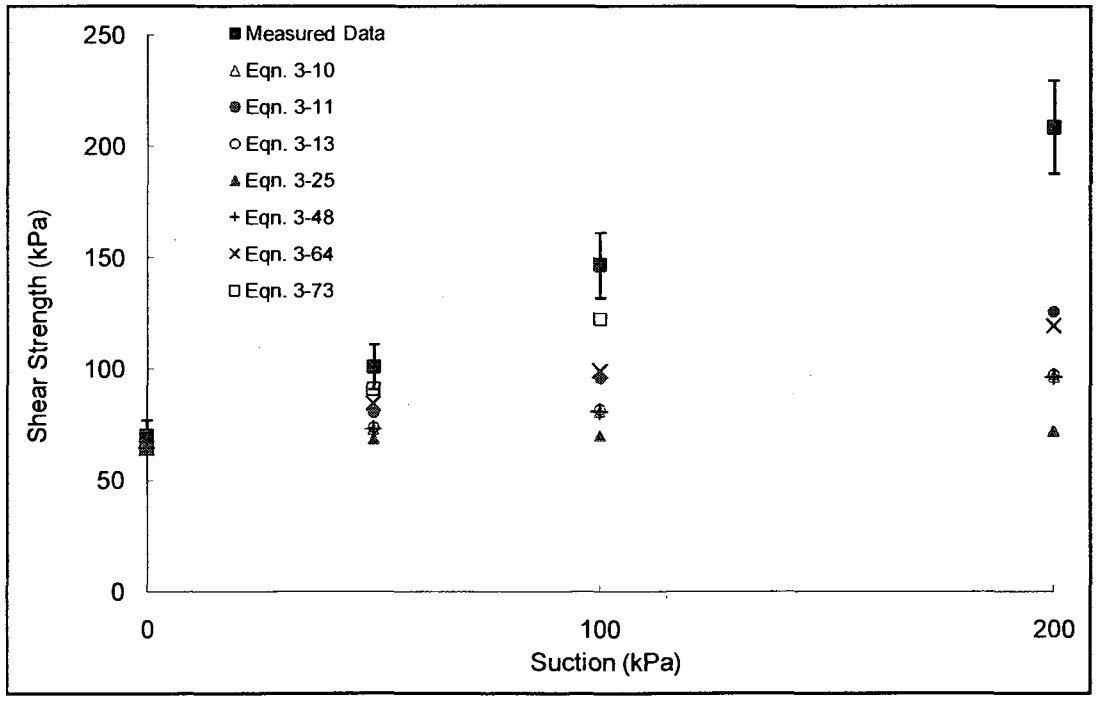

Soil No. 25g

AV colluvium

Feuerharmel, Bica, Gehling and Flores, 2006

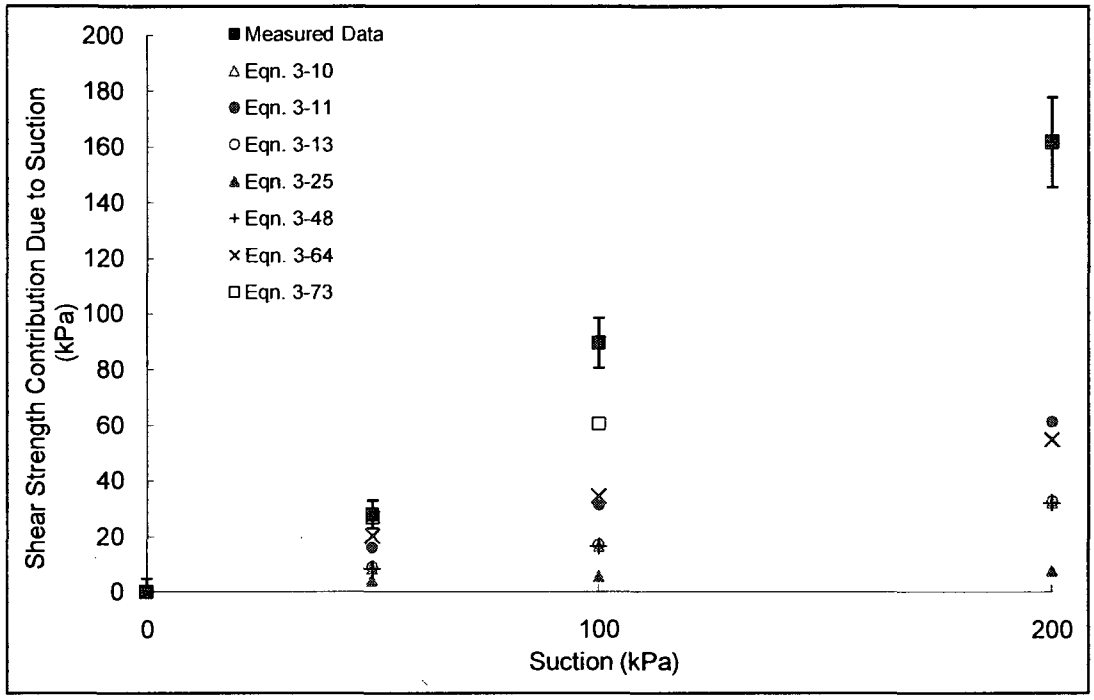

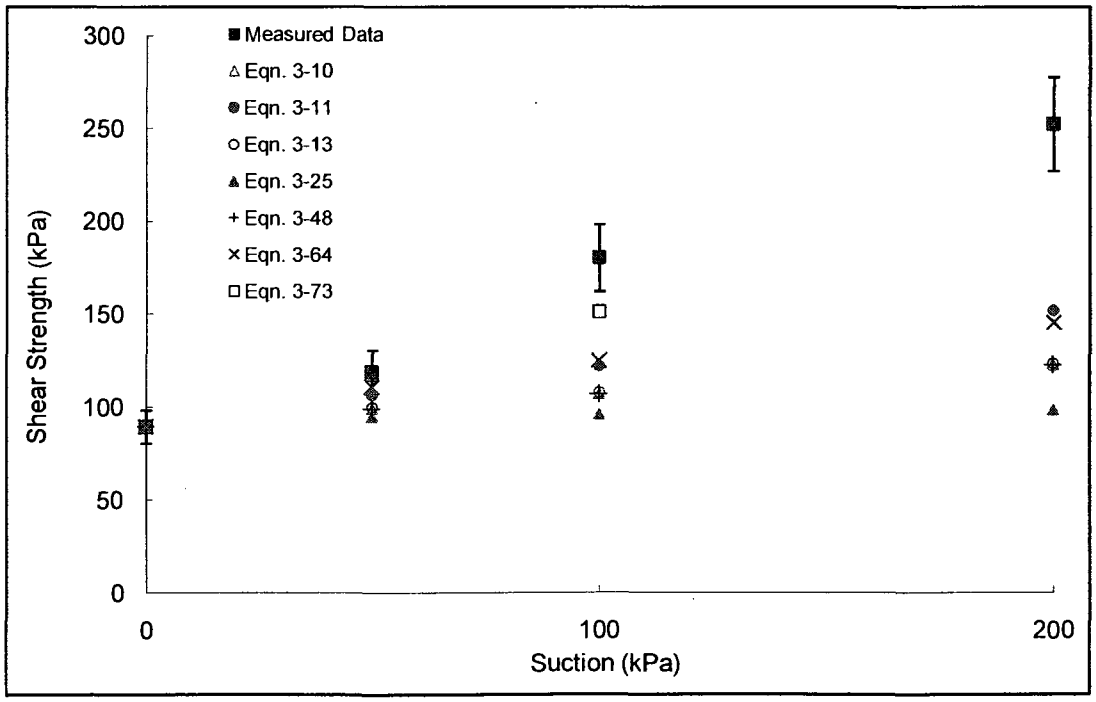

Soil No. 25h

AV colluvium

Feuerharmel, Bica, Gehling and Flores, 2006

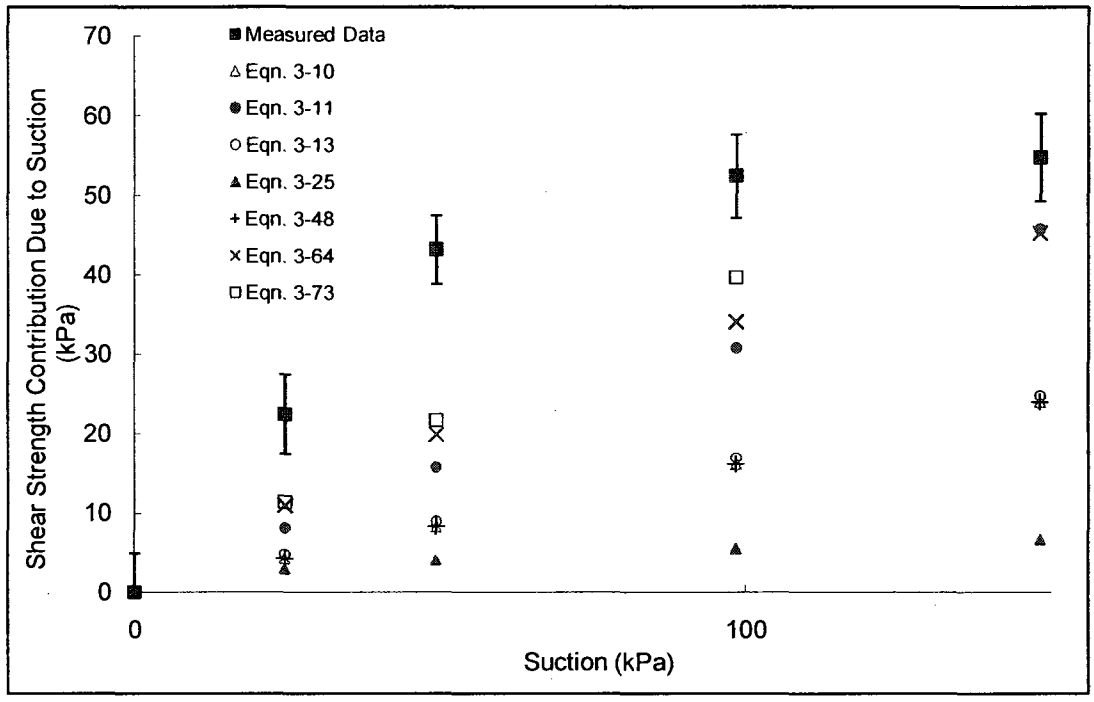

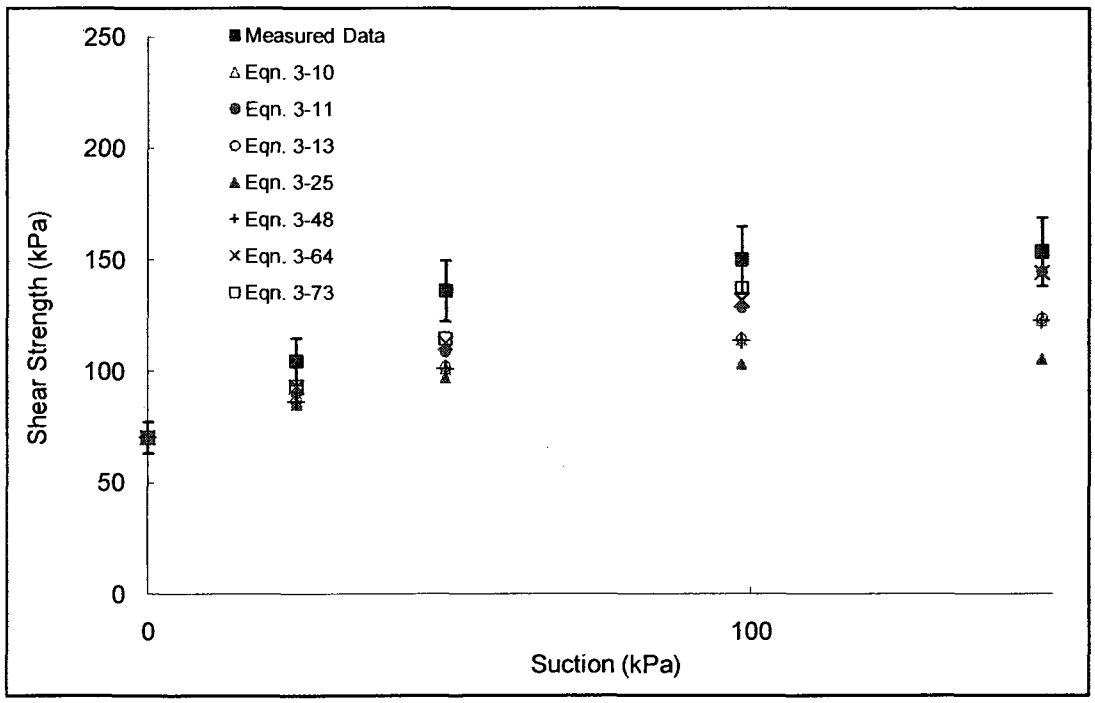

Soil No. 25i

AV colluvium

Feuerharmel, Bica, Gehling and Flores, 2006

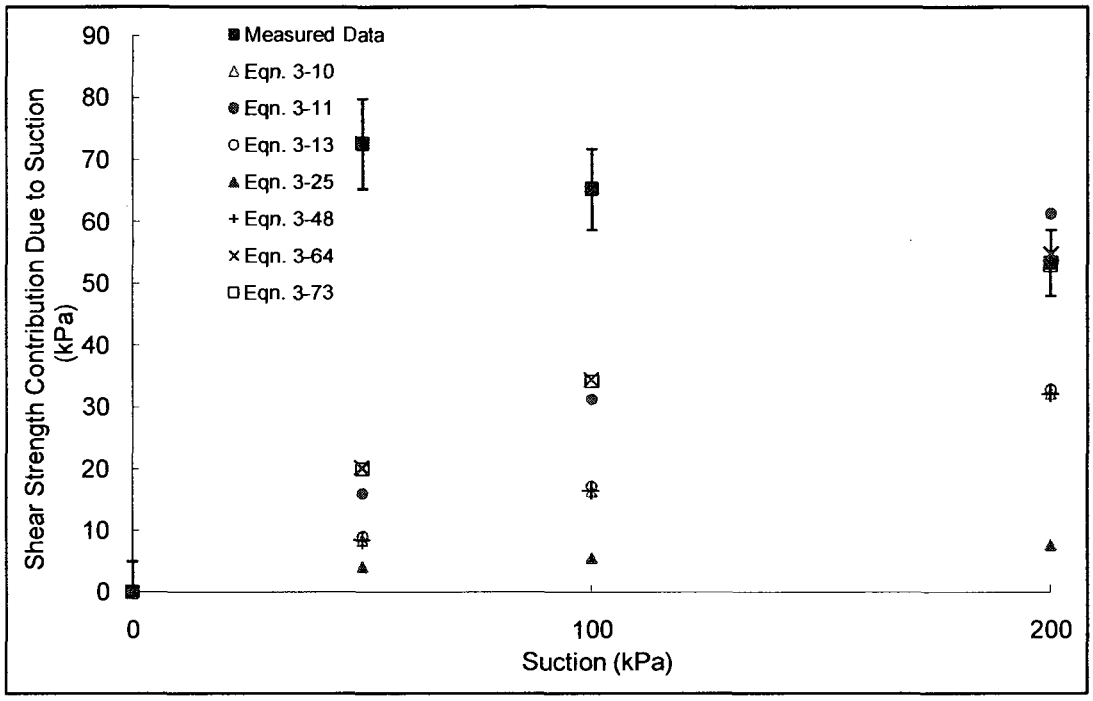

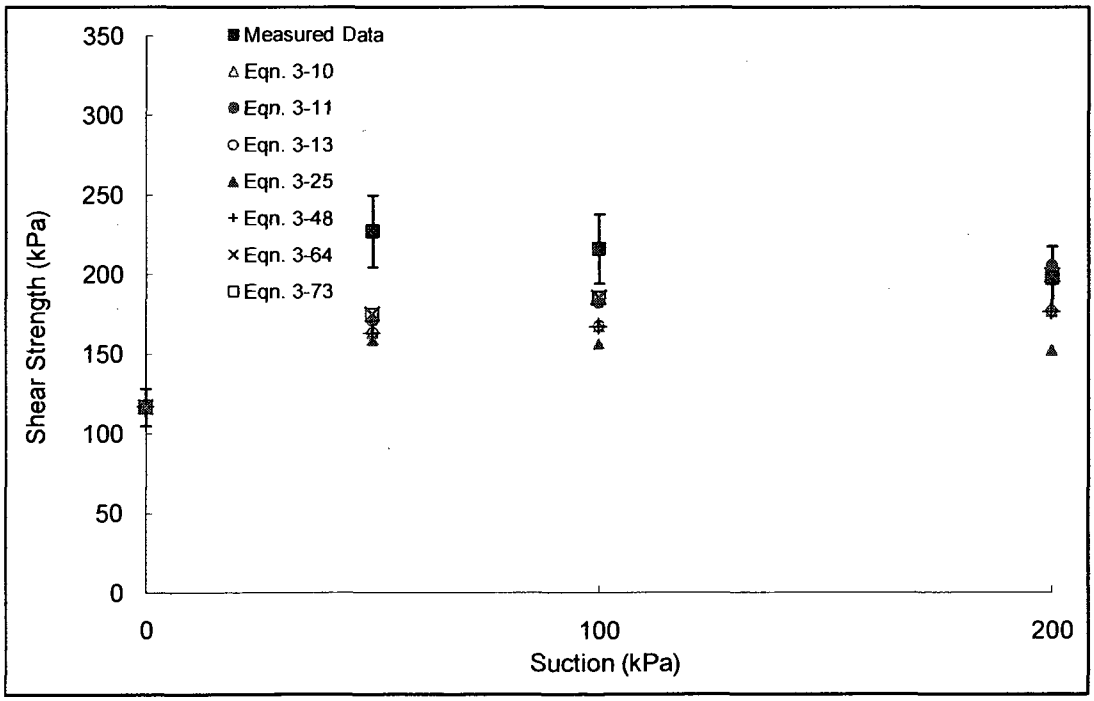

Soil No. 26a

RO colluvium

Feuerharmel, Bica, Gehling and Flores, 2006

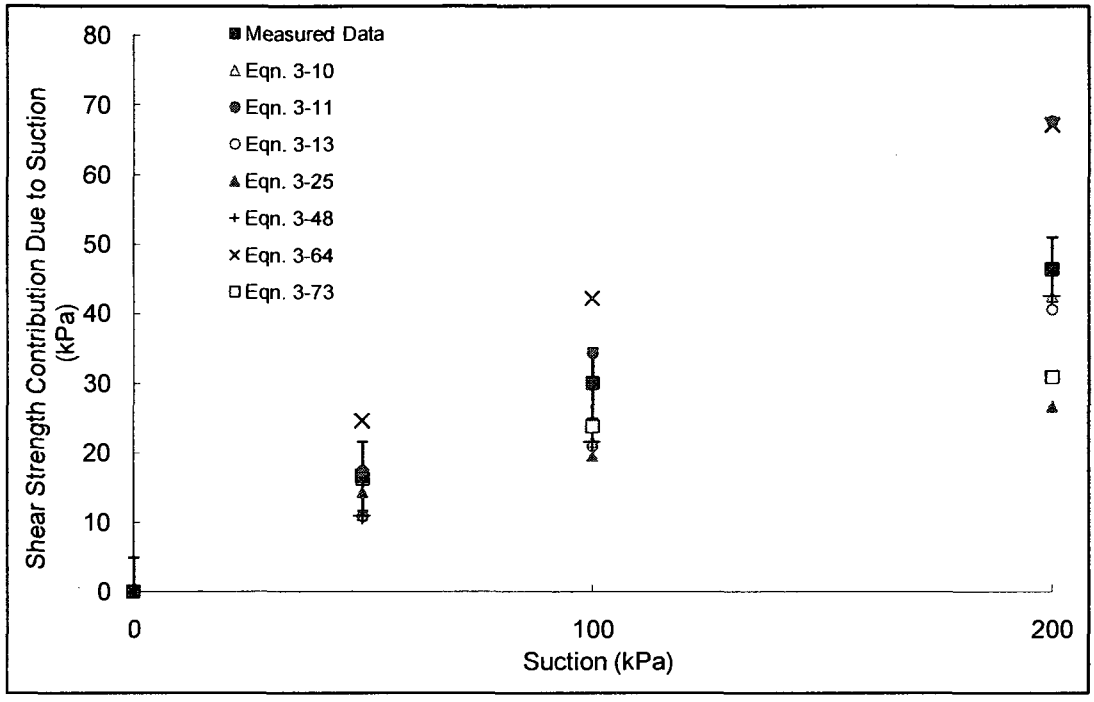

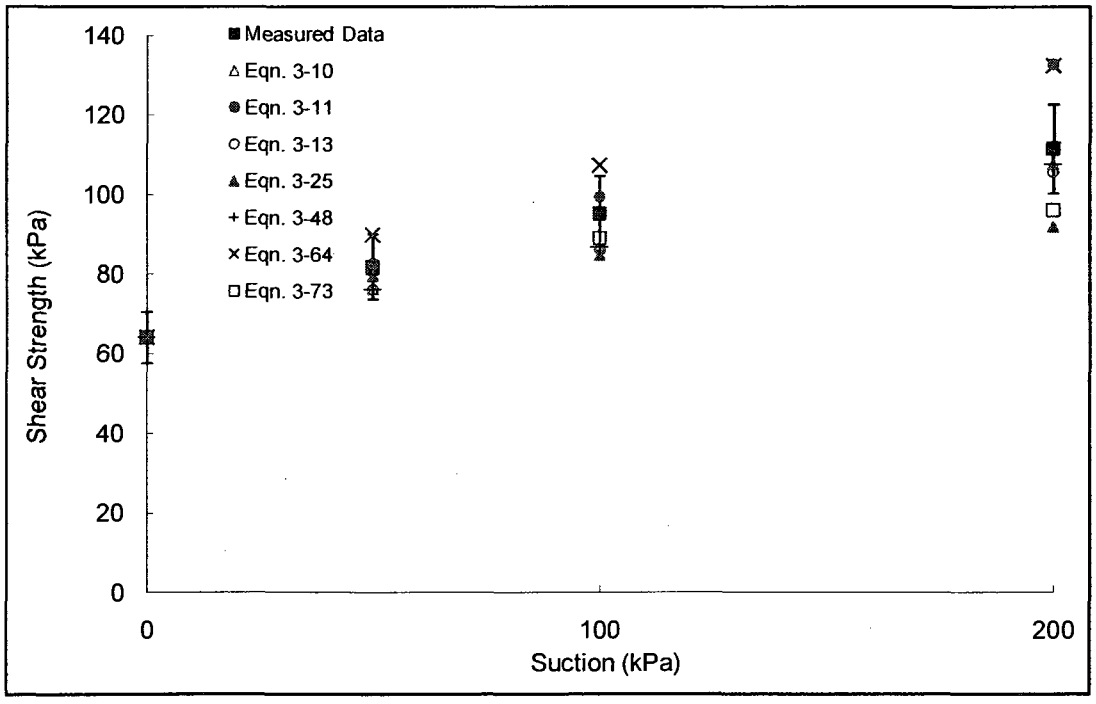

Soil No. 26b

RO colluvium

Feuerharmel, Bica, Gehling and Flores, 2006

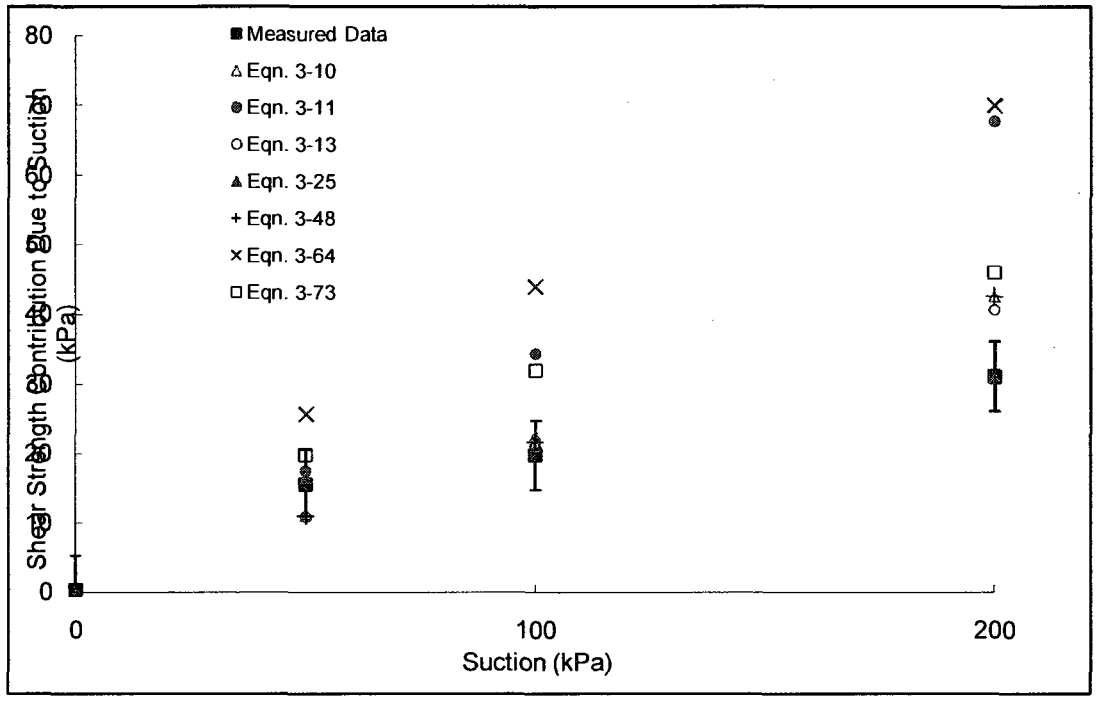

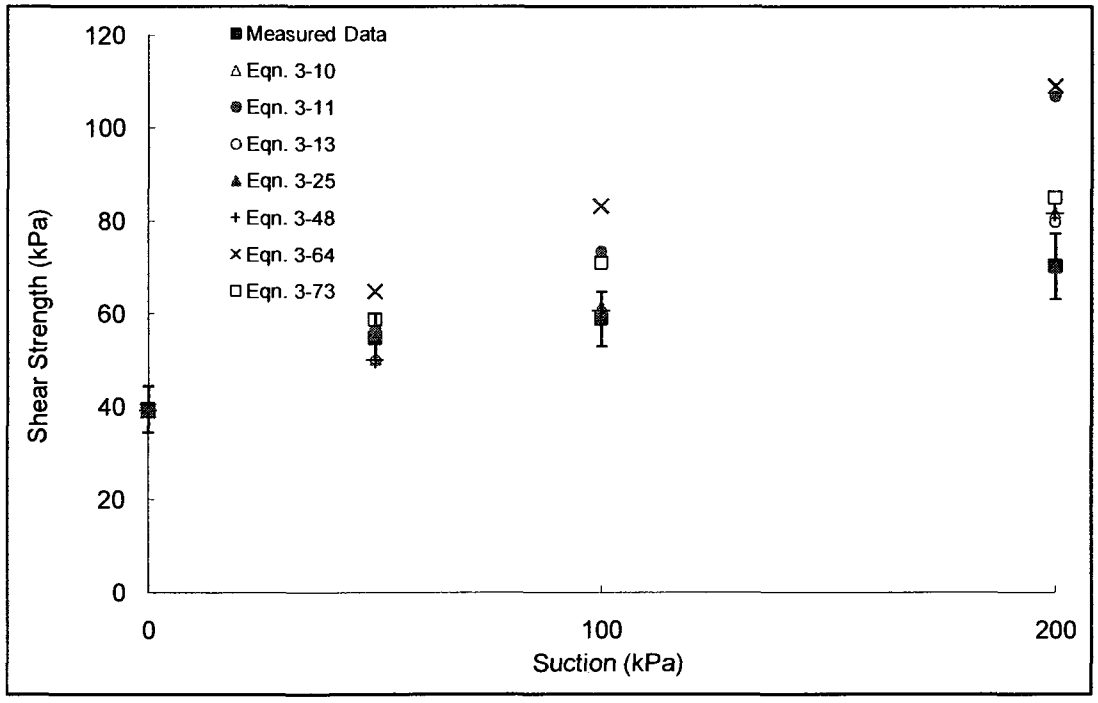

Soil No. 26c

RO colluvium

Feuerharmel, Bica, Gehling and Flores, 2006

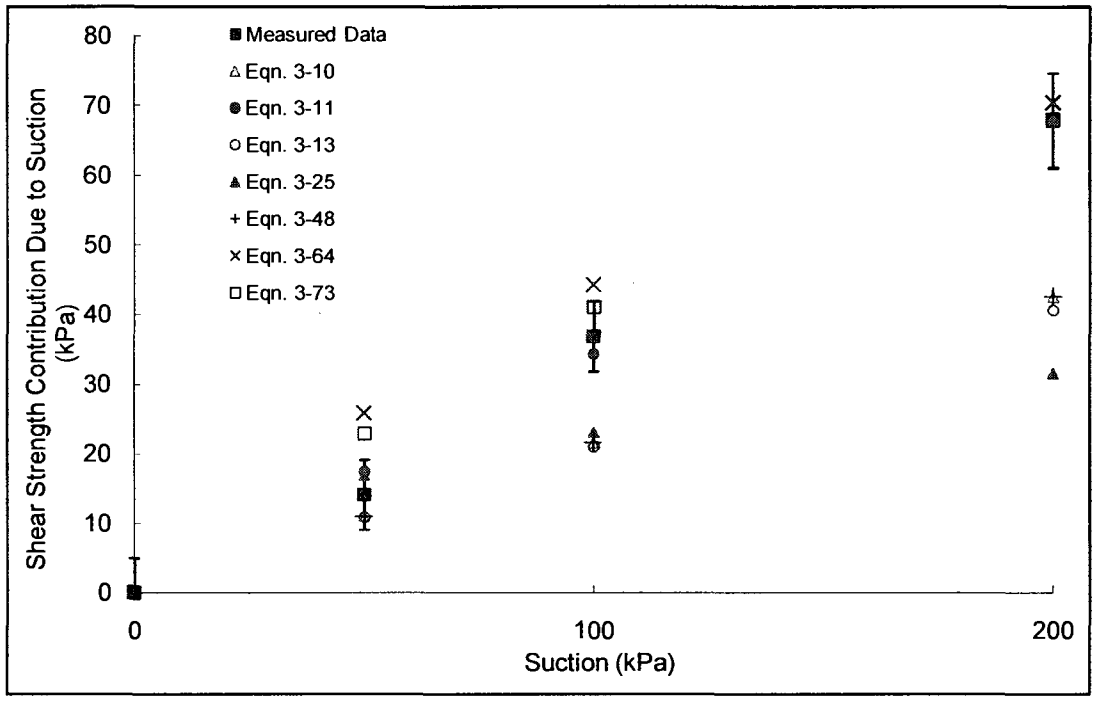

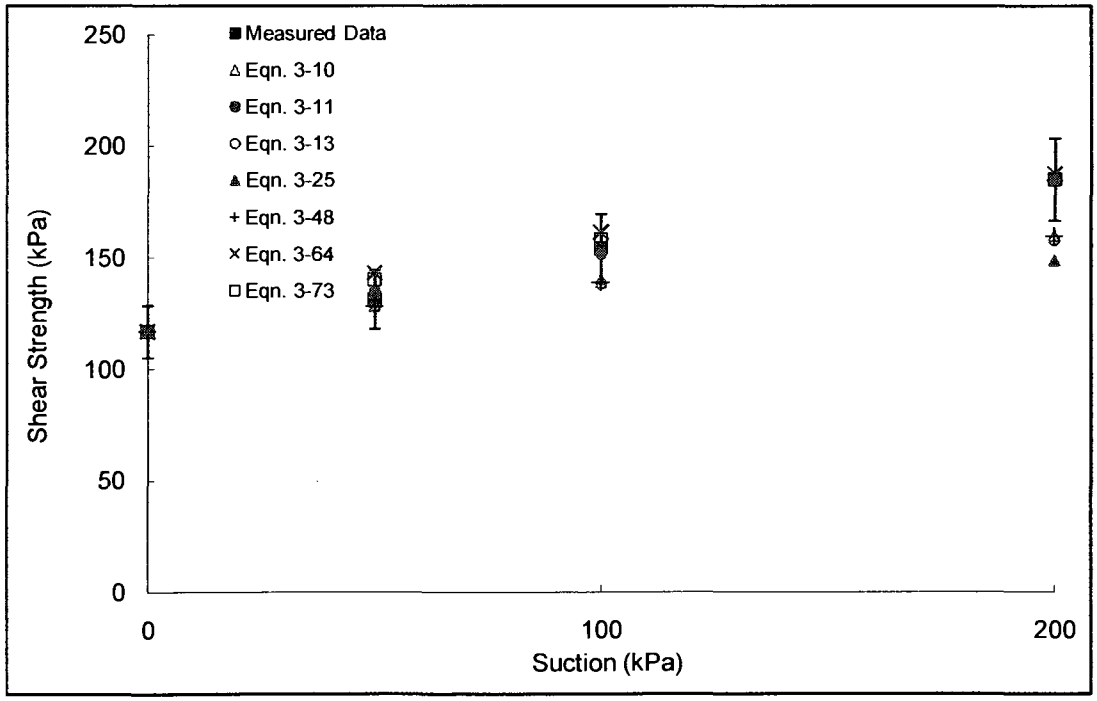

Soil No. 26d

RO colluvium

Feuerharmel, Bica, Gehling and Flores, 2006

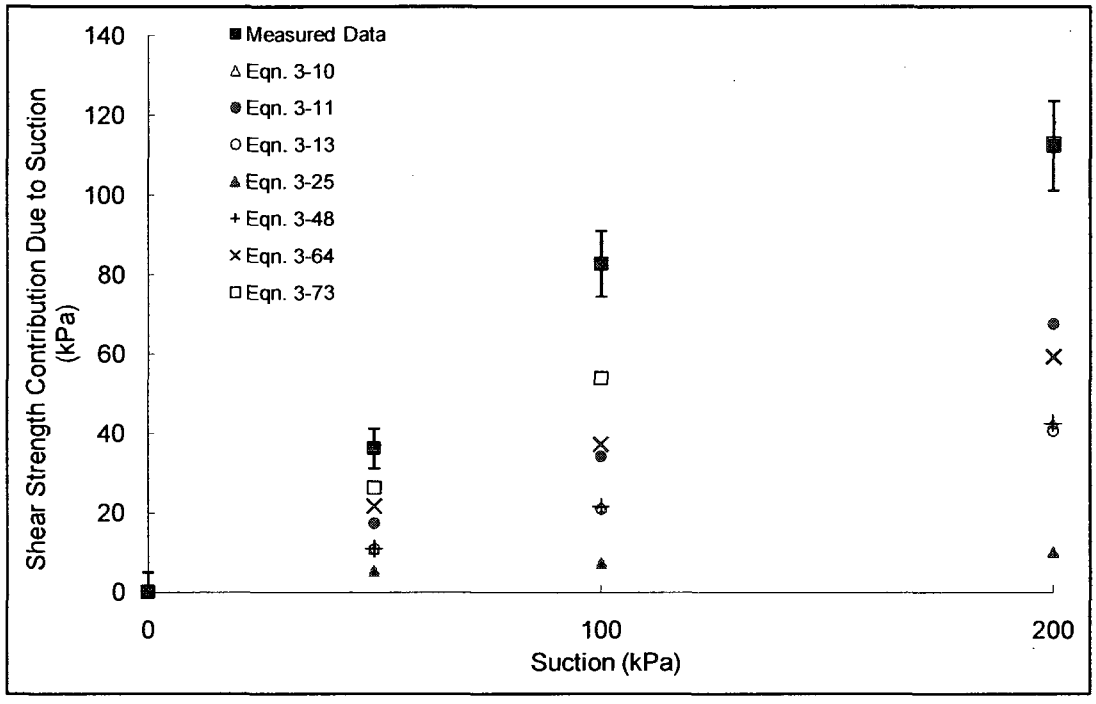

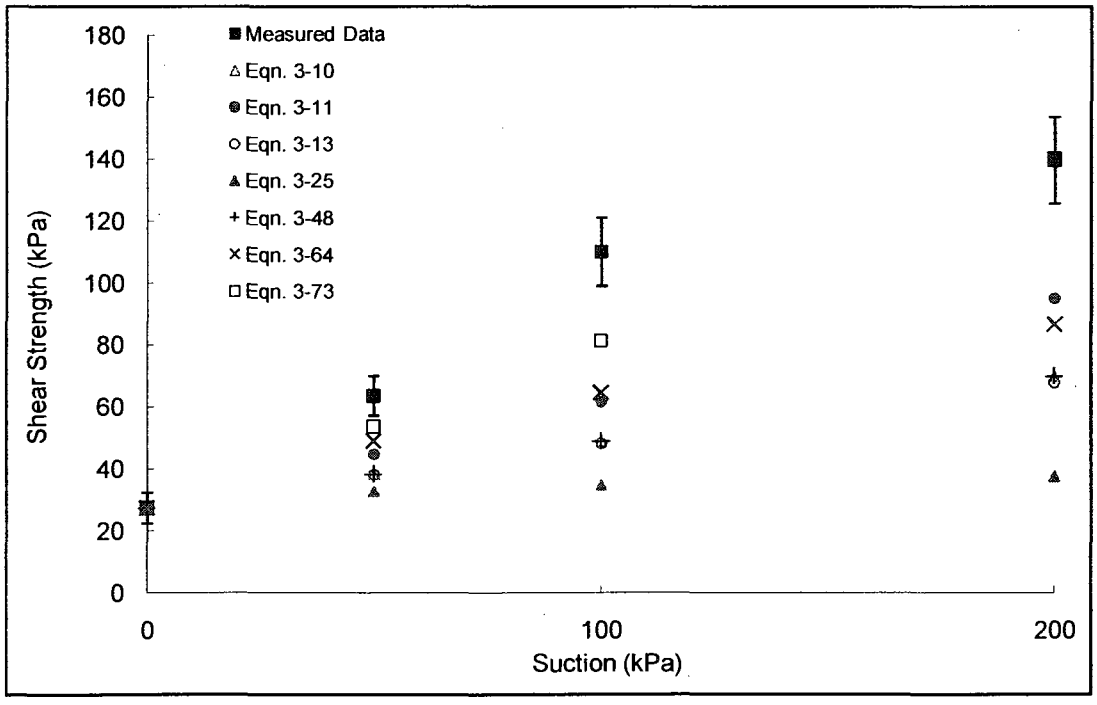

Soil No. 26e

RO colluvium

Feuerharmel, Bica, Gehling and Flores, 2006

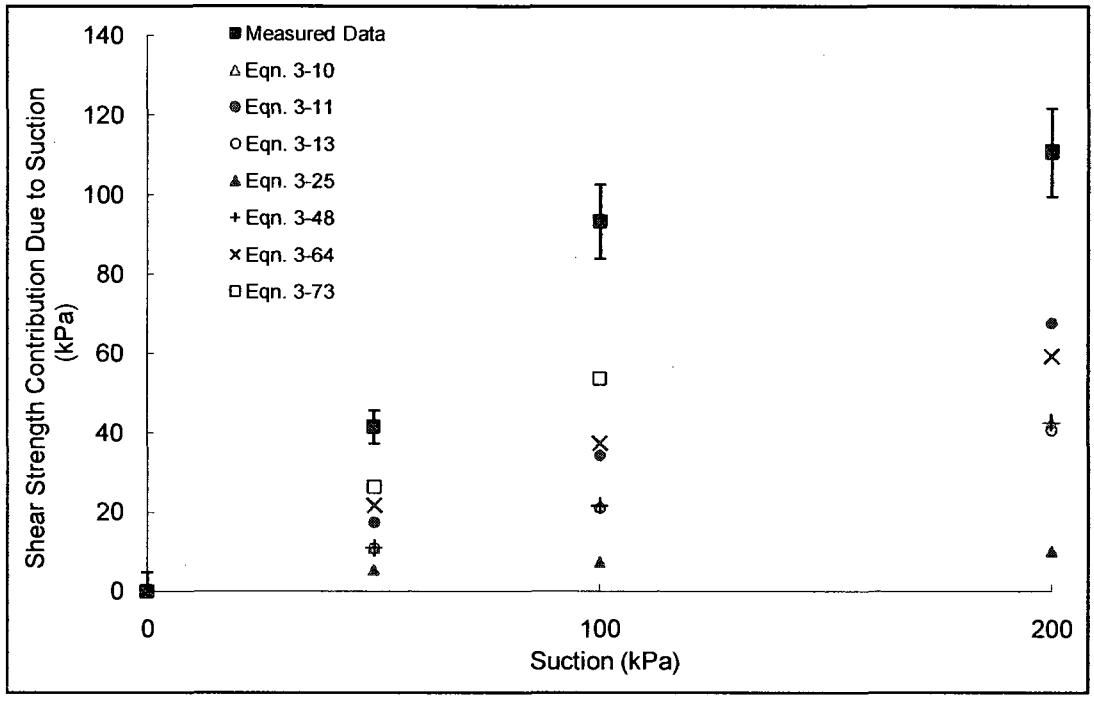

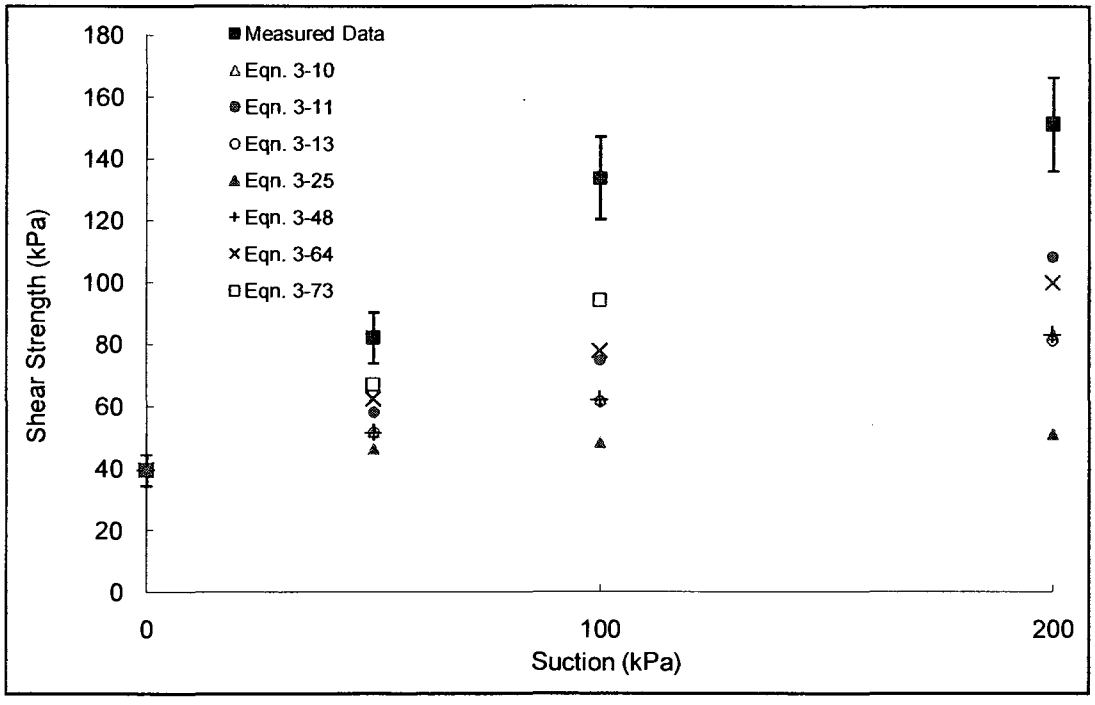

Soil No. 26f **RO colluvium**

Feuerharmel, Bica, Gehling and Flores, 2006

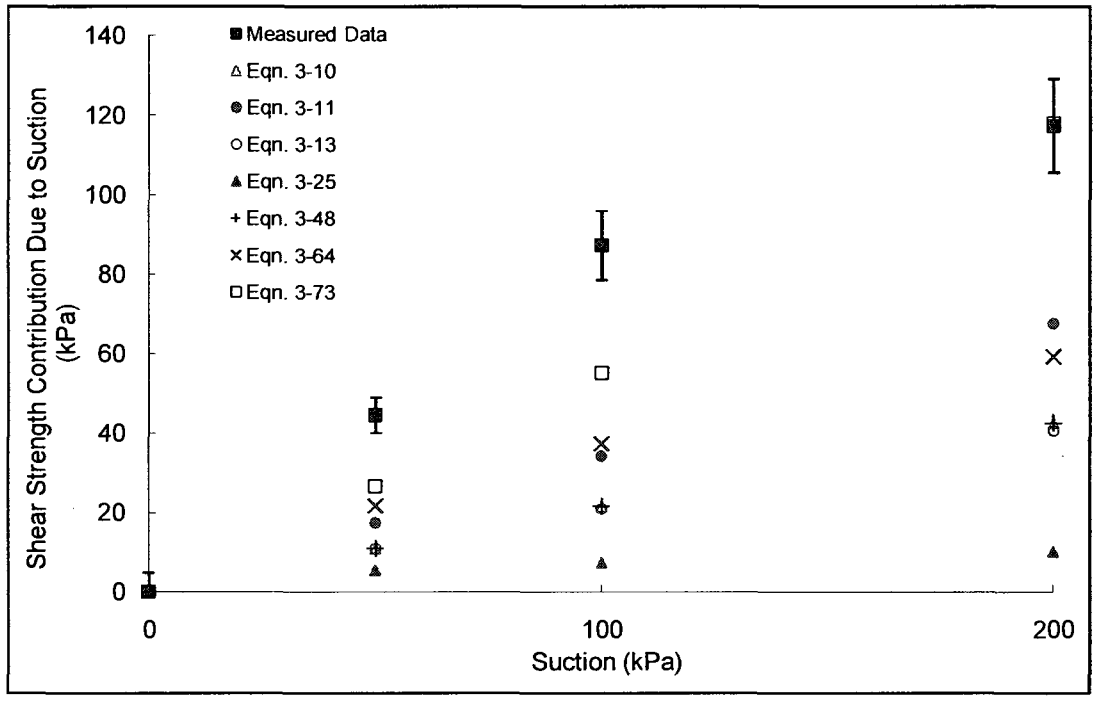

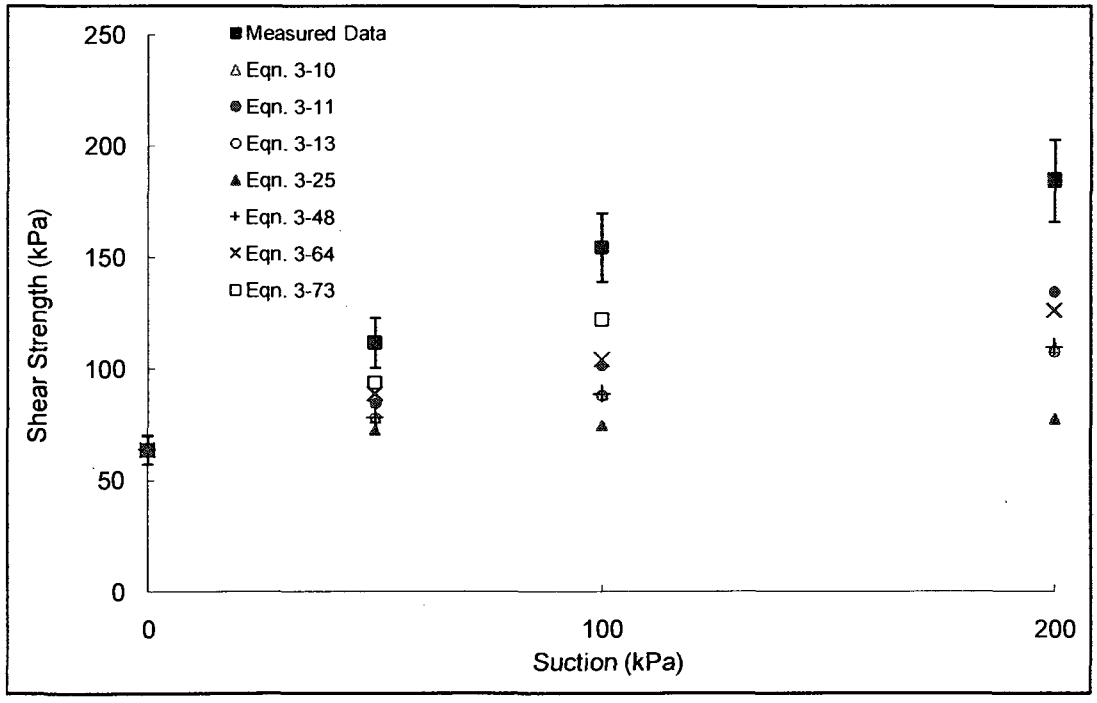

Soil No. 26g

RO colluvium

Feuerharmel, Bica, Gehling and Flores, 2006

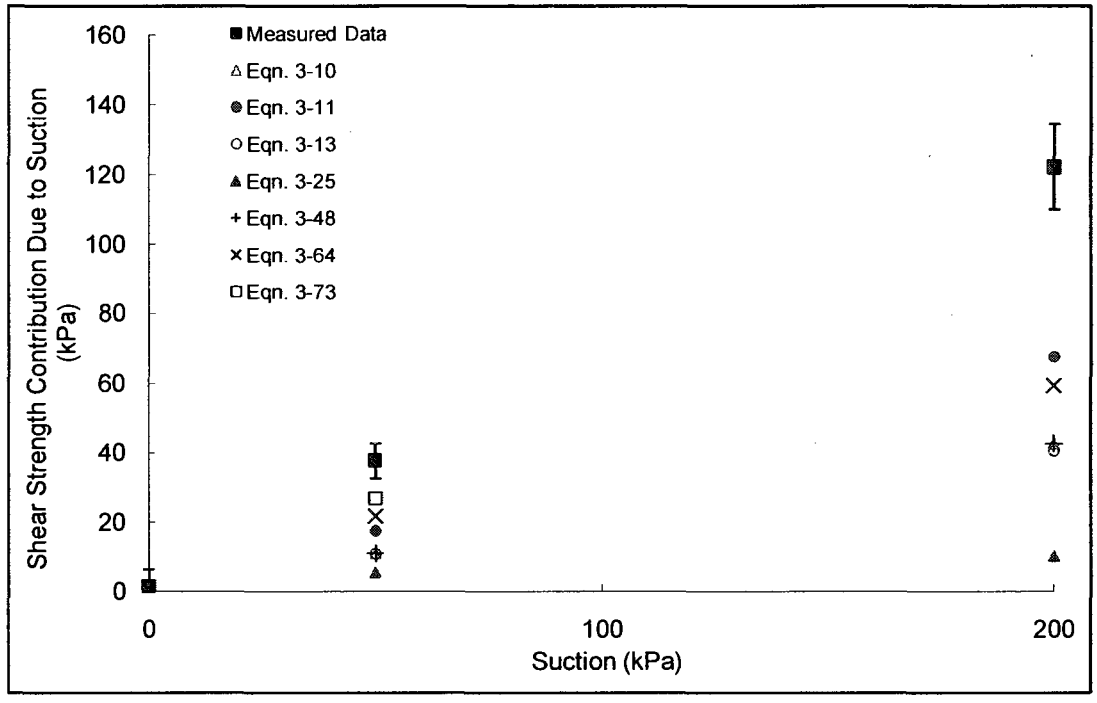

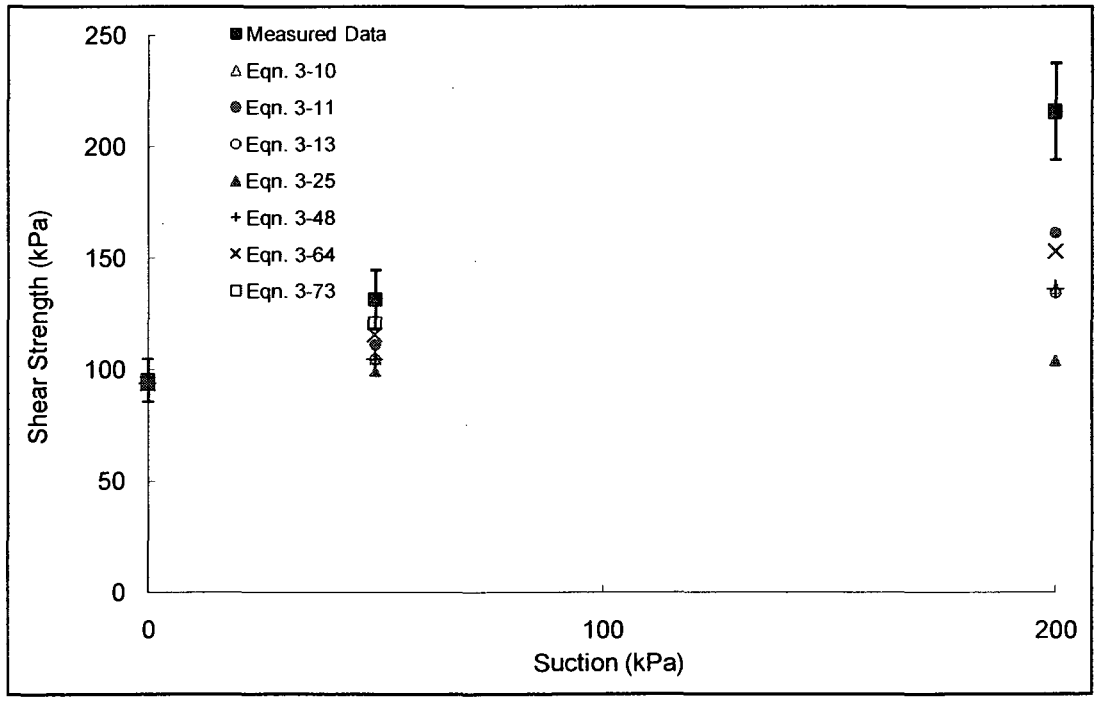

Soil No. 27a **CRDB silt**

Cunningham, Ridley, Dineen and Burland, 2003

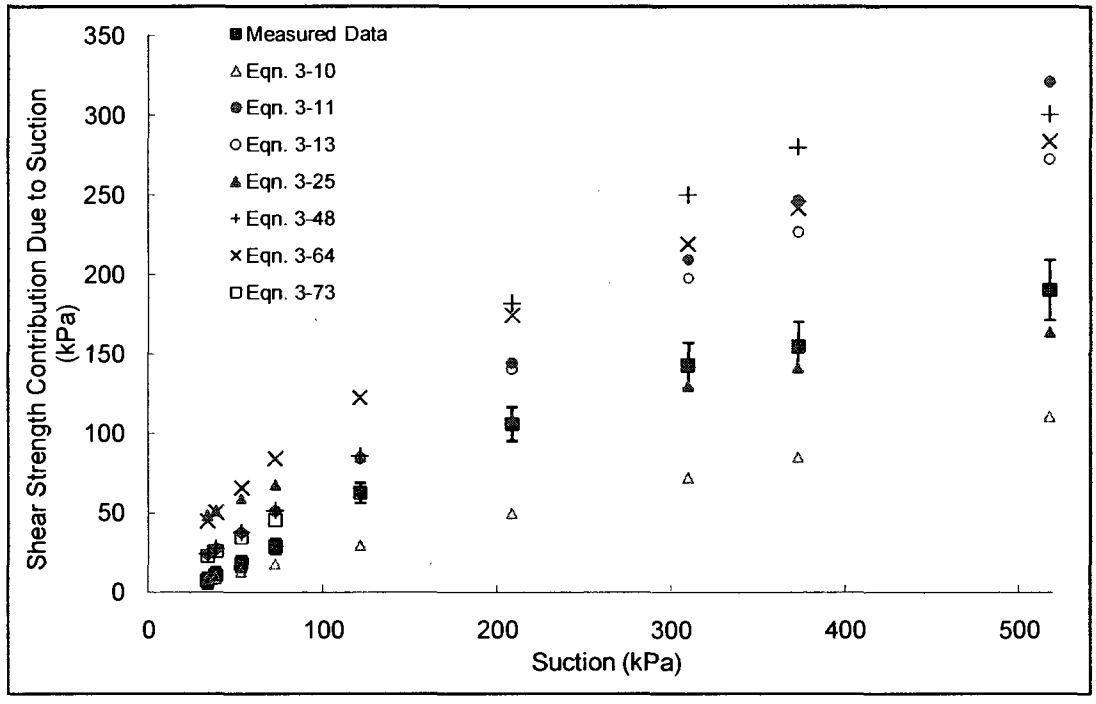

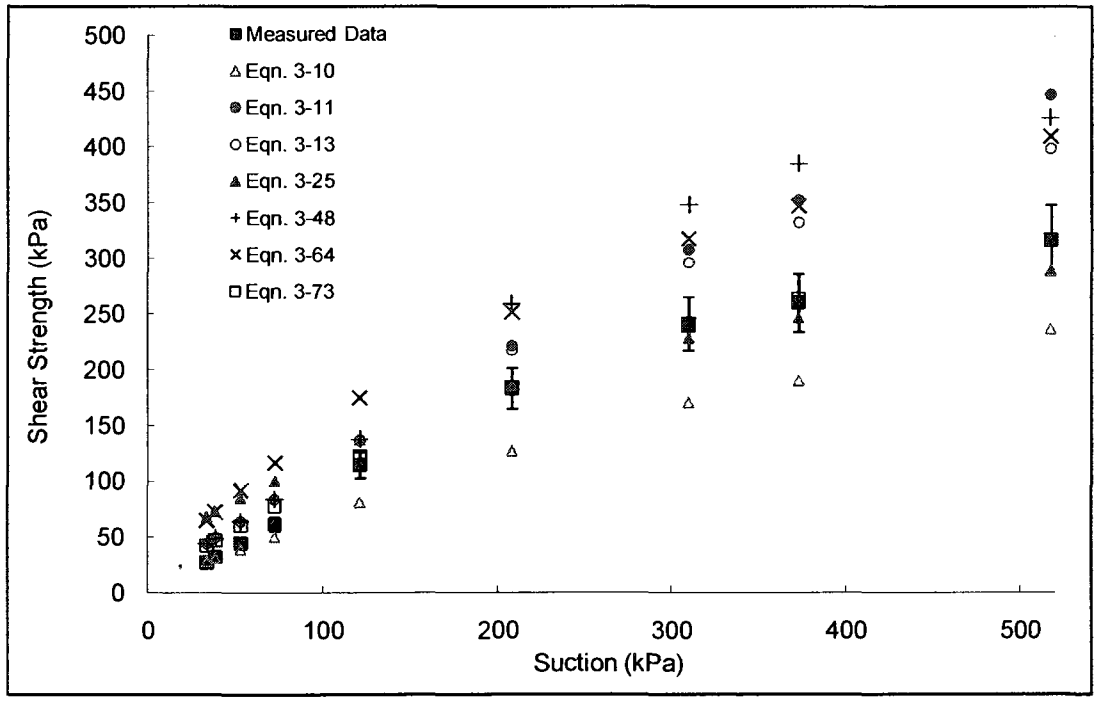

Soil No. 27b **CRDB silt**

Cunningham, Ridley, Dineen and Burland, 2003

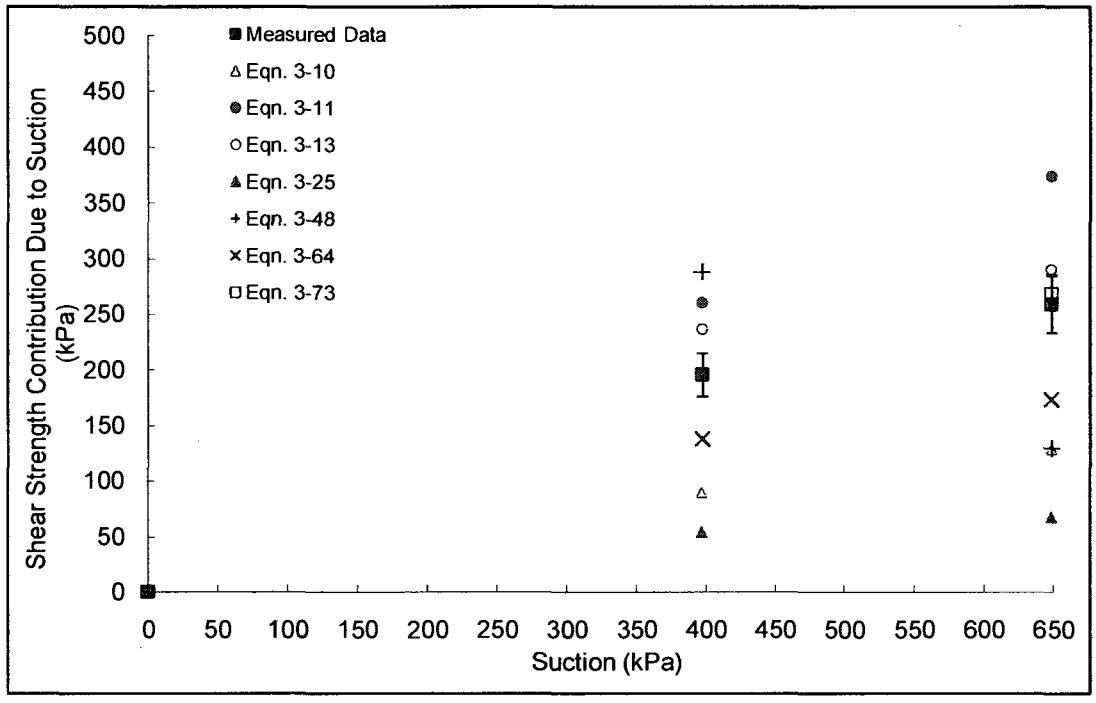

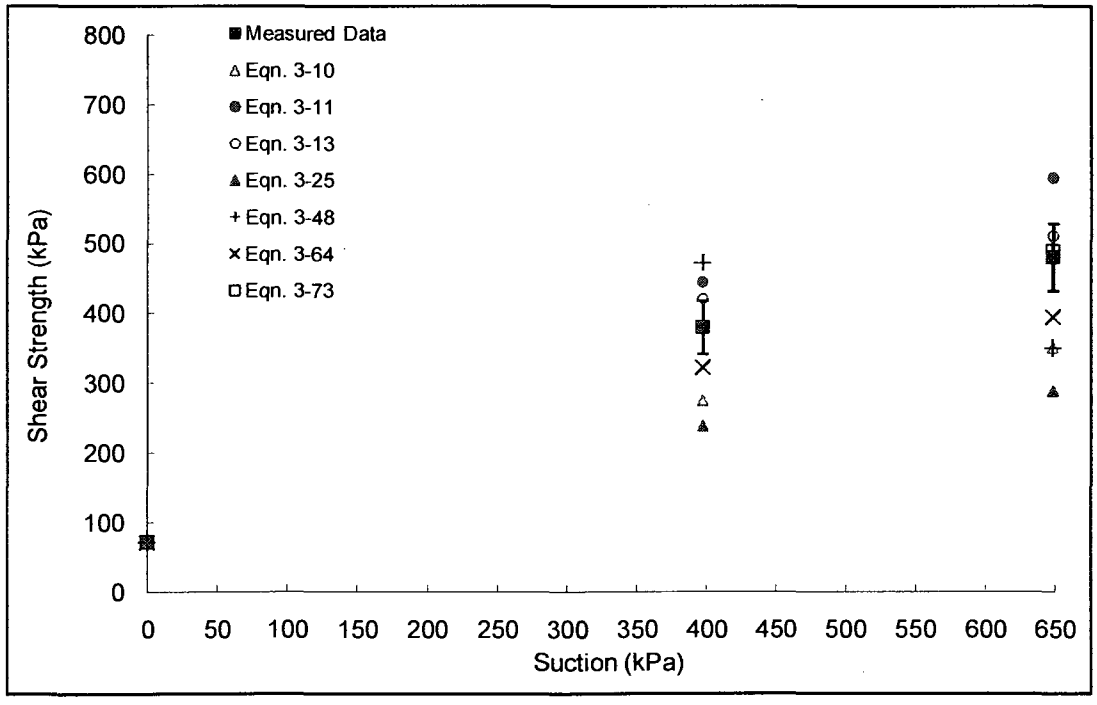

Soil No. 27c **CRDB silt**

Cunningham, Ridley, Dineen and Burland, 2003

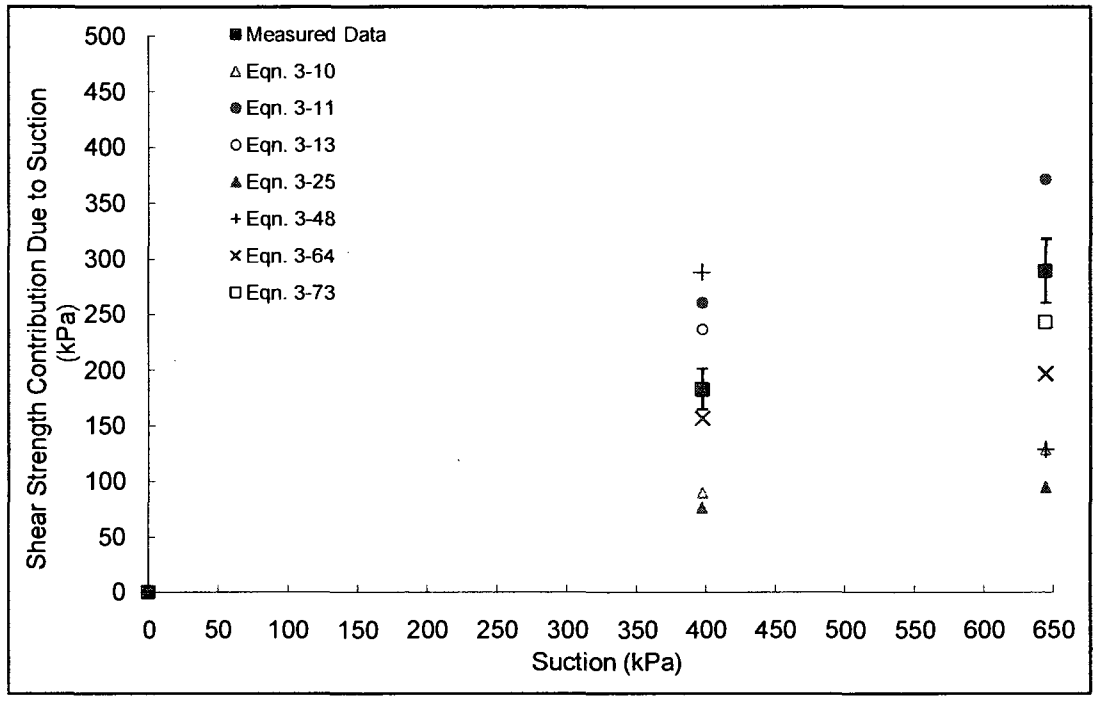

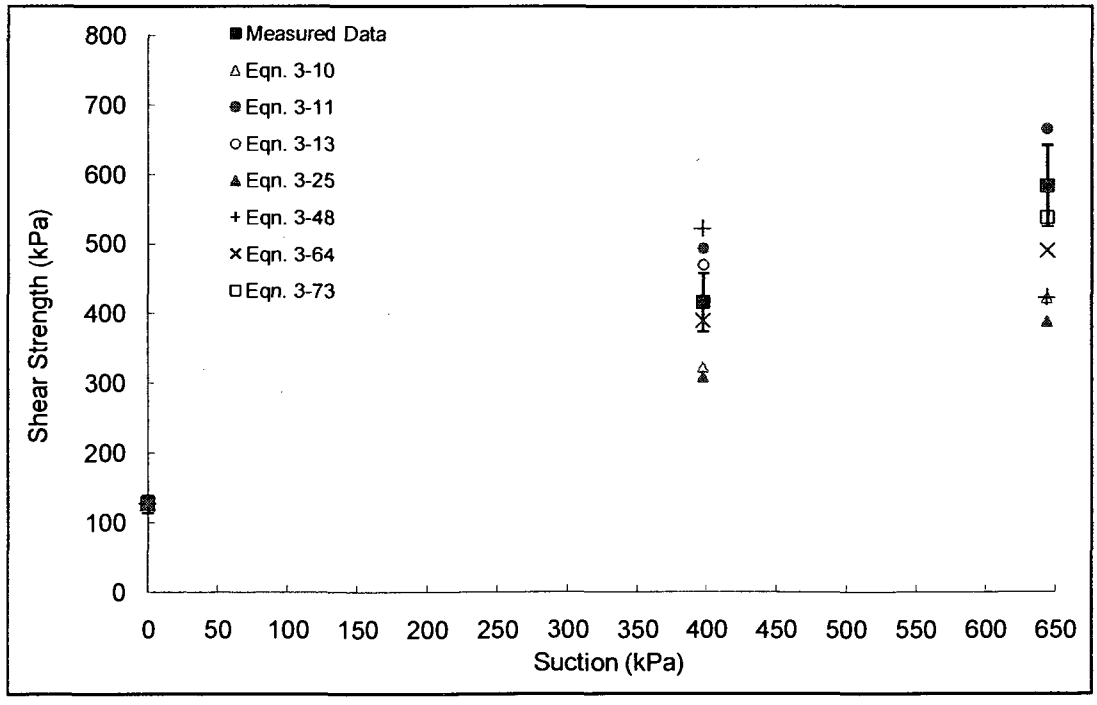

Soil No. 27d **CRDB silt**

Cunningham, Ridley, Dineen and Burland, 2003

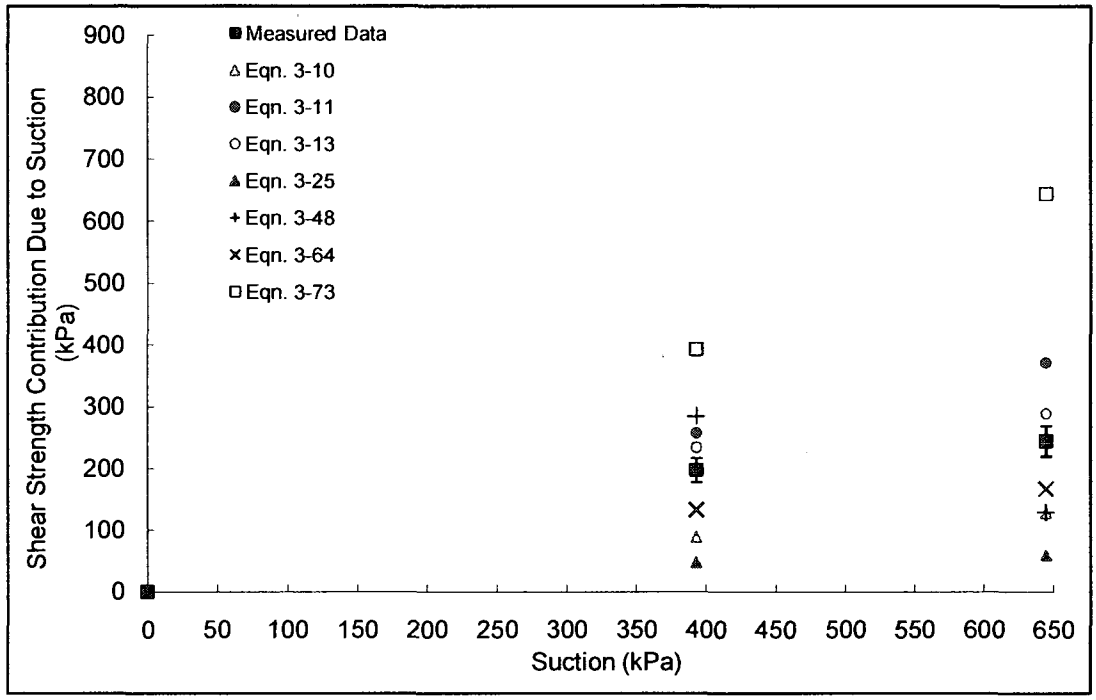

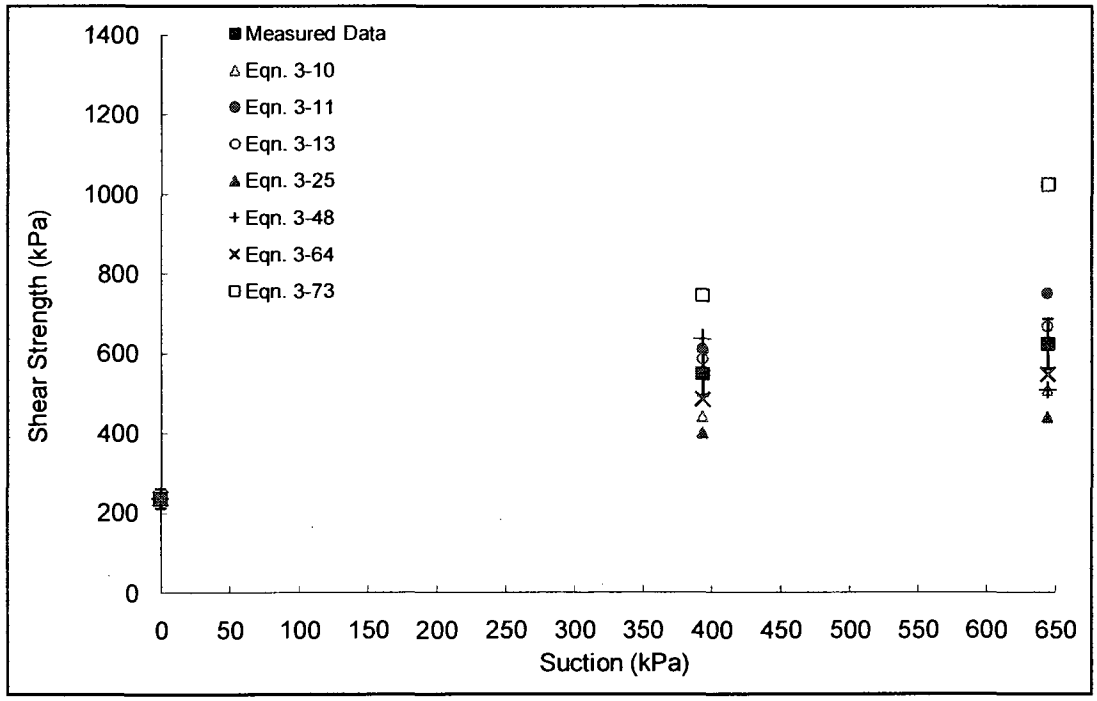

Soil No. 27e

CRDB silt

Cunningham, Ridley, Dineen and Burland, 2003

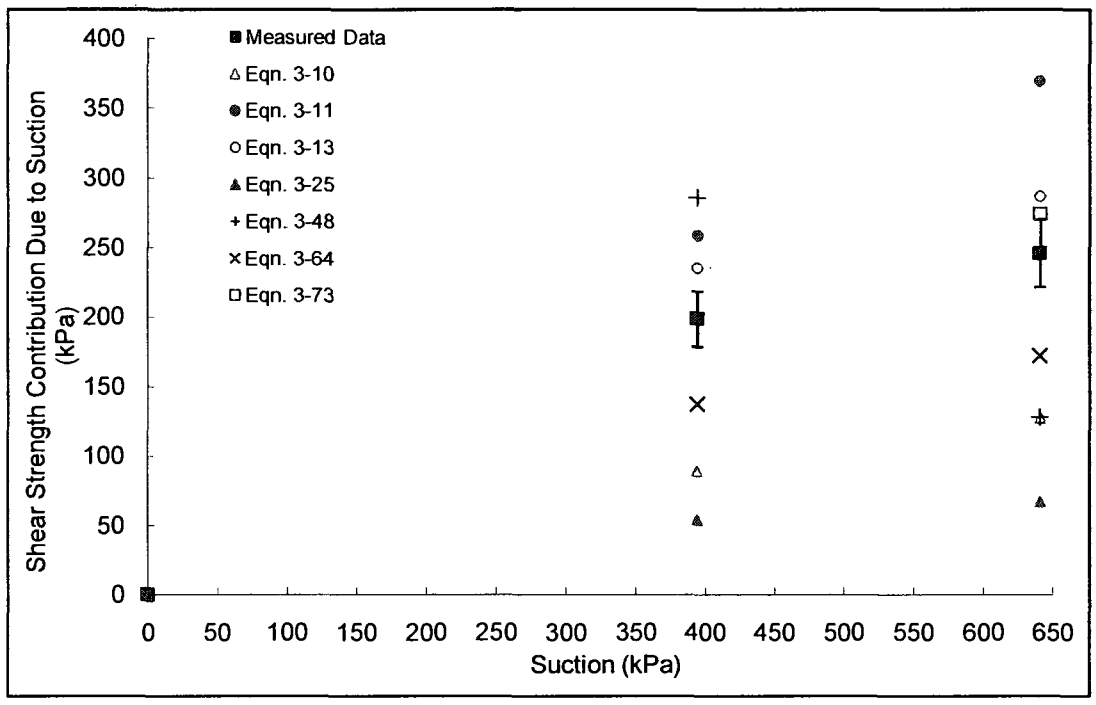

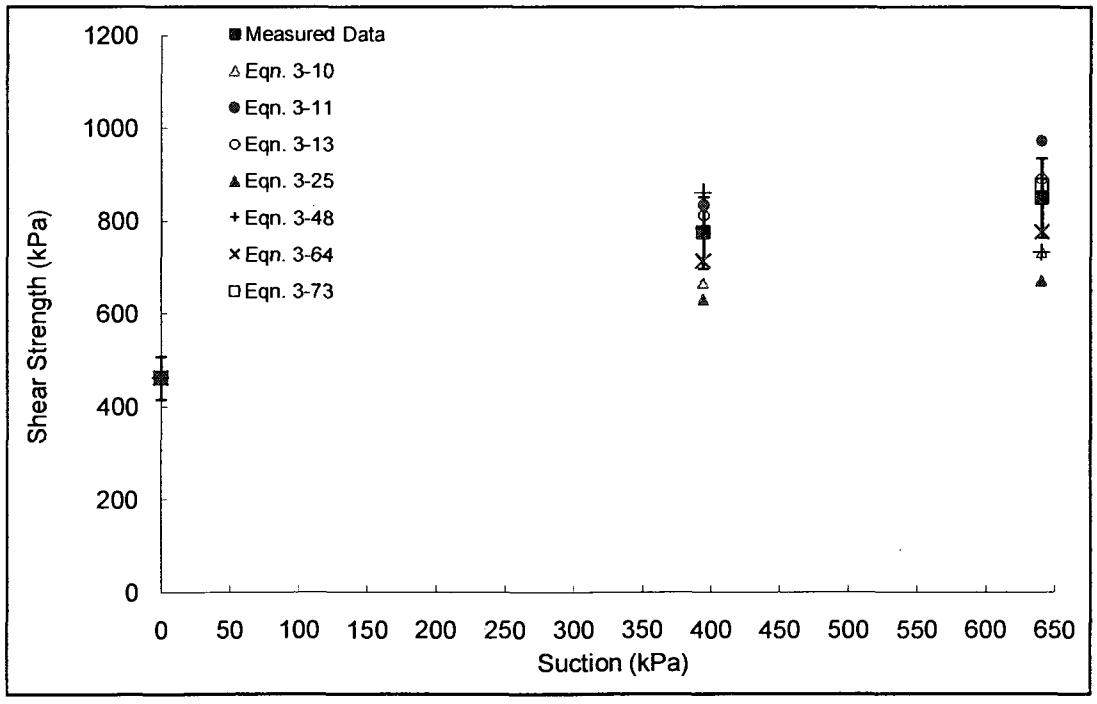

Soil No. 28a

Botkin silt

Oloo and Fredlund, 1996; Oloo, 1994

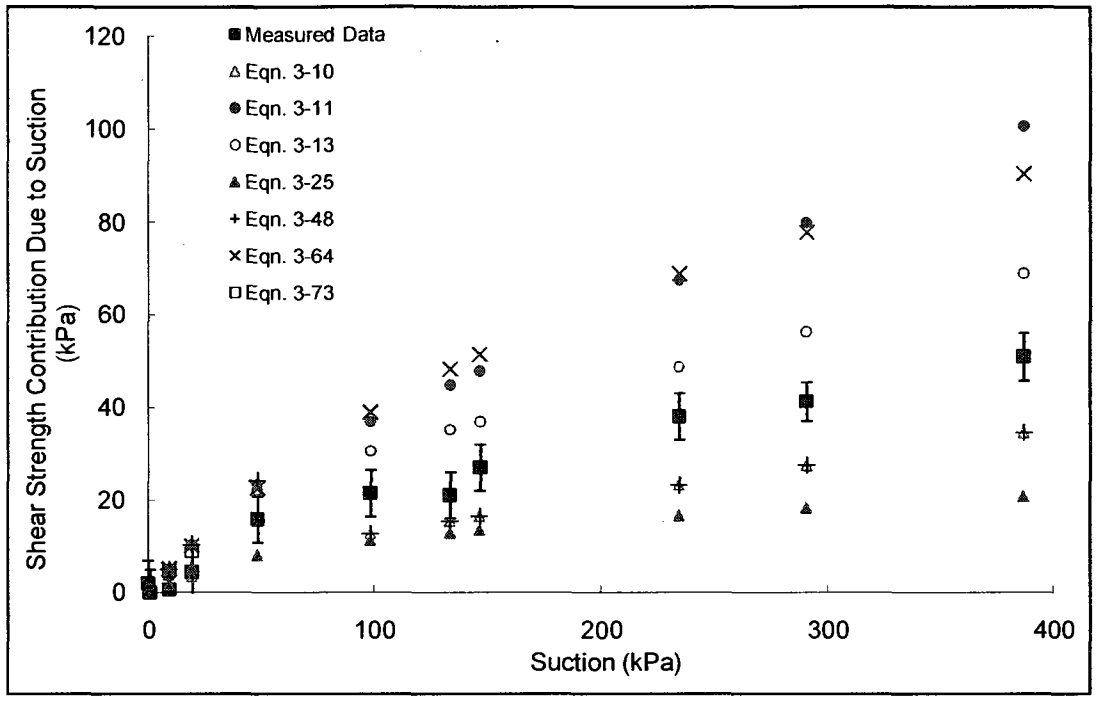

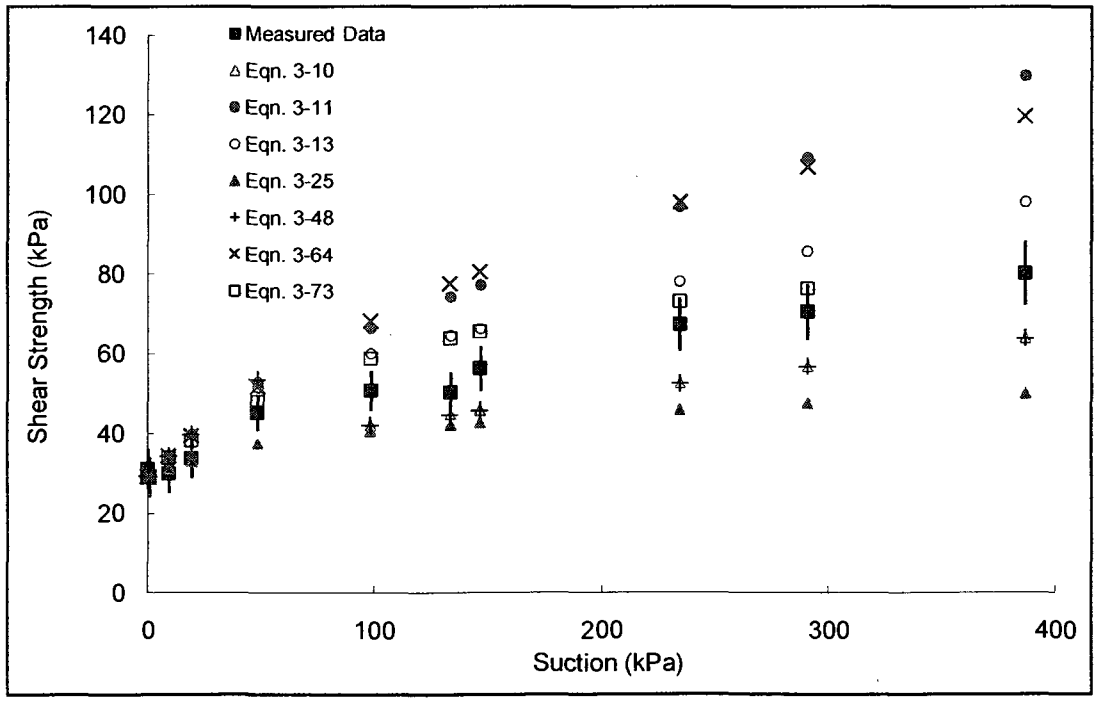

Soil No. 28b

Botkin silt

Oloo and Fredlund, 1996; Oloo, 1994

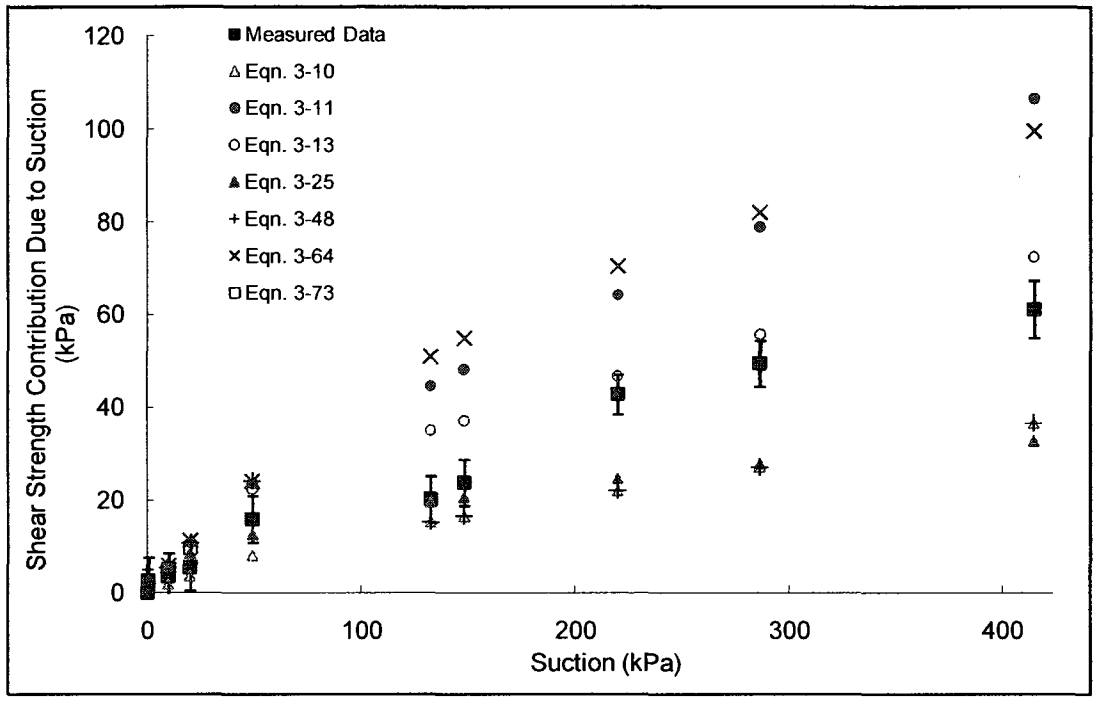

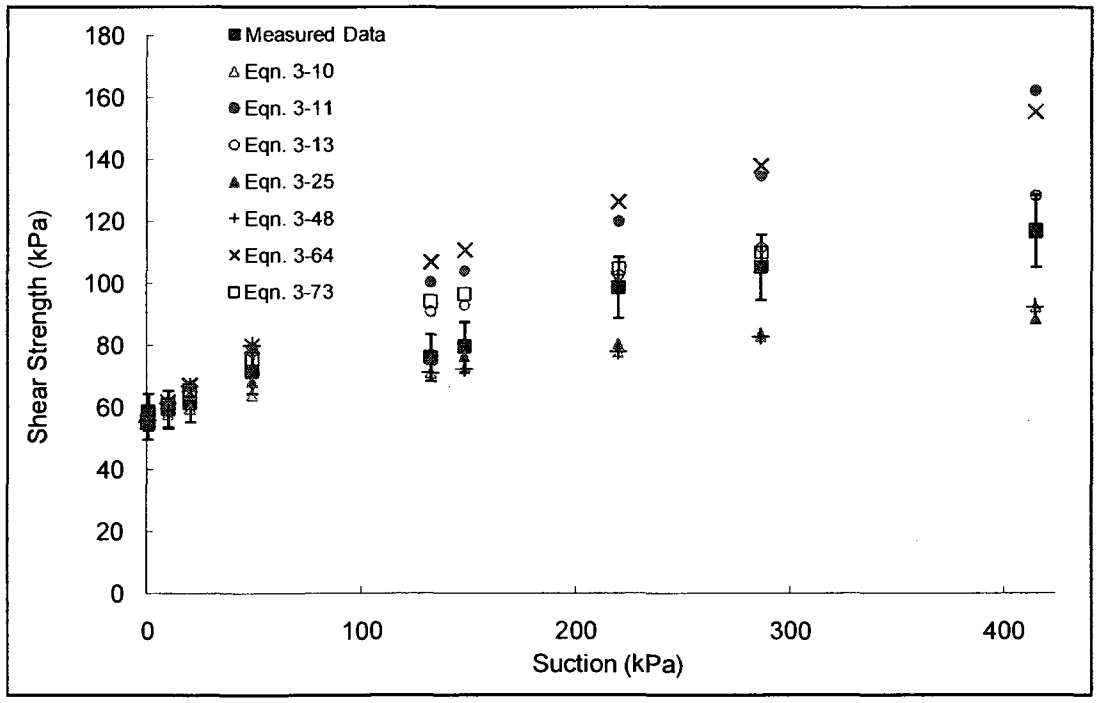

Soil No. 28c

Botkin silt

Oloo and Fredlund, 1996; Oloo, 1994

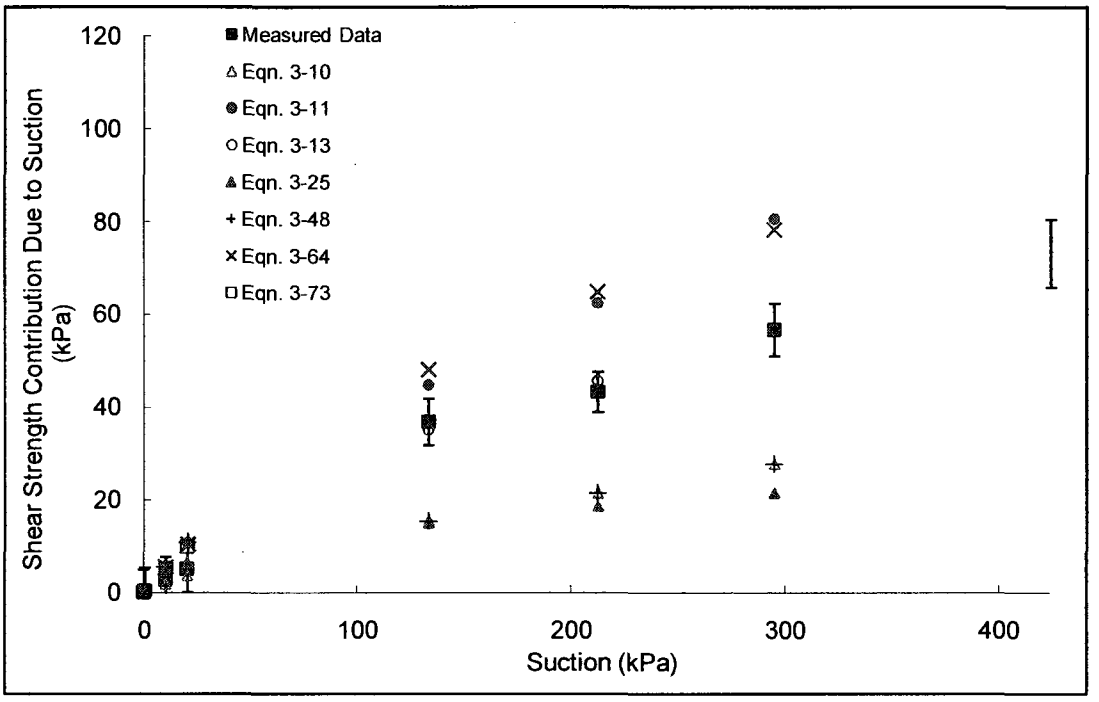

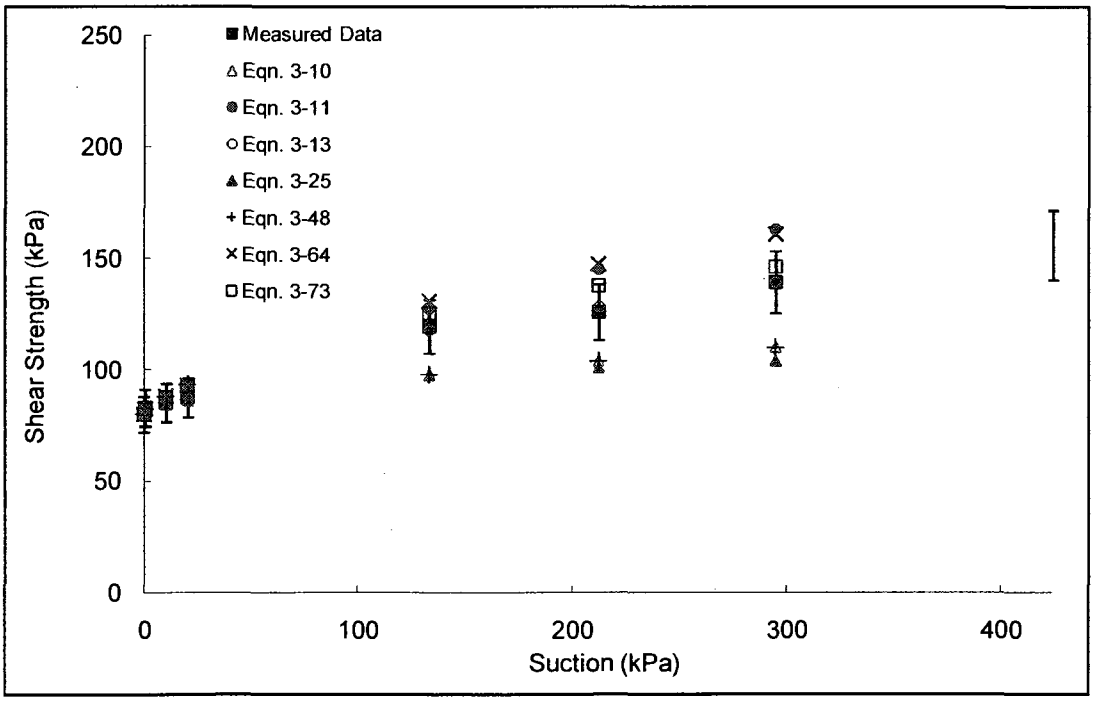

Soil No. 29a

Indian Head till

Oloo and Fredlund, 1996; Oloo, 1994

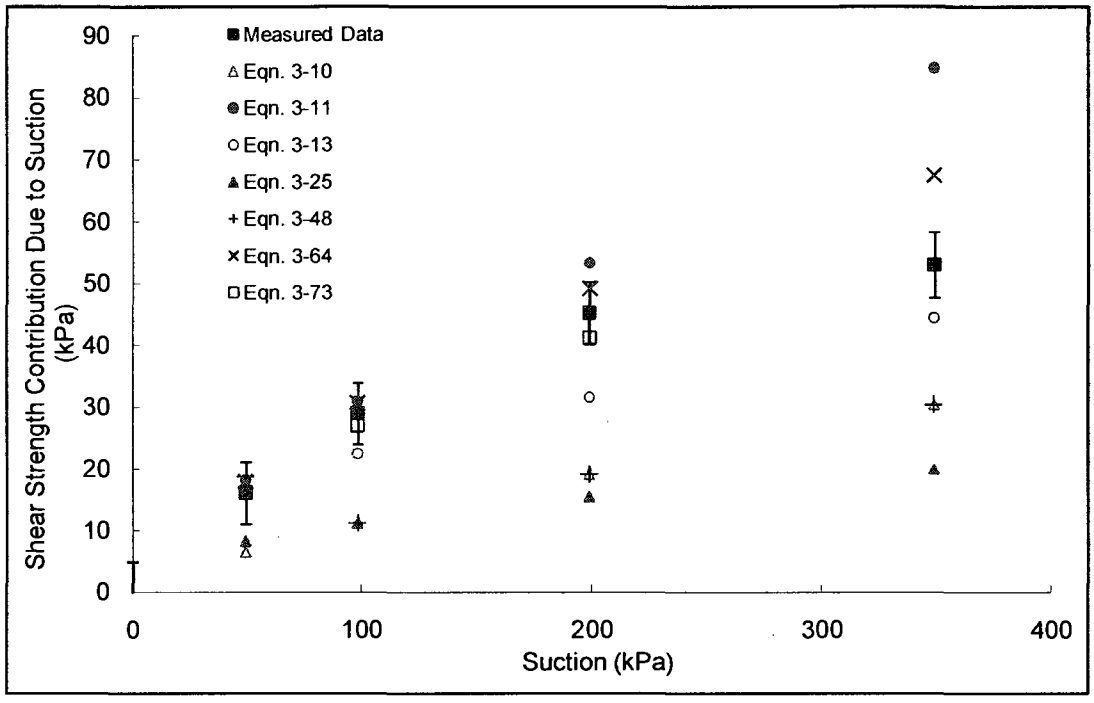

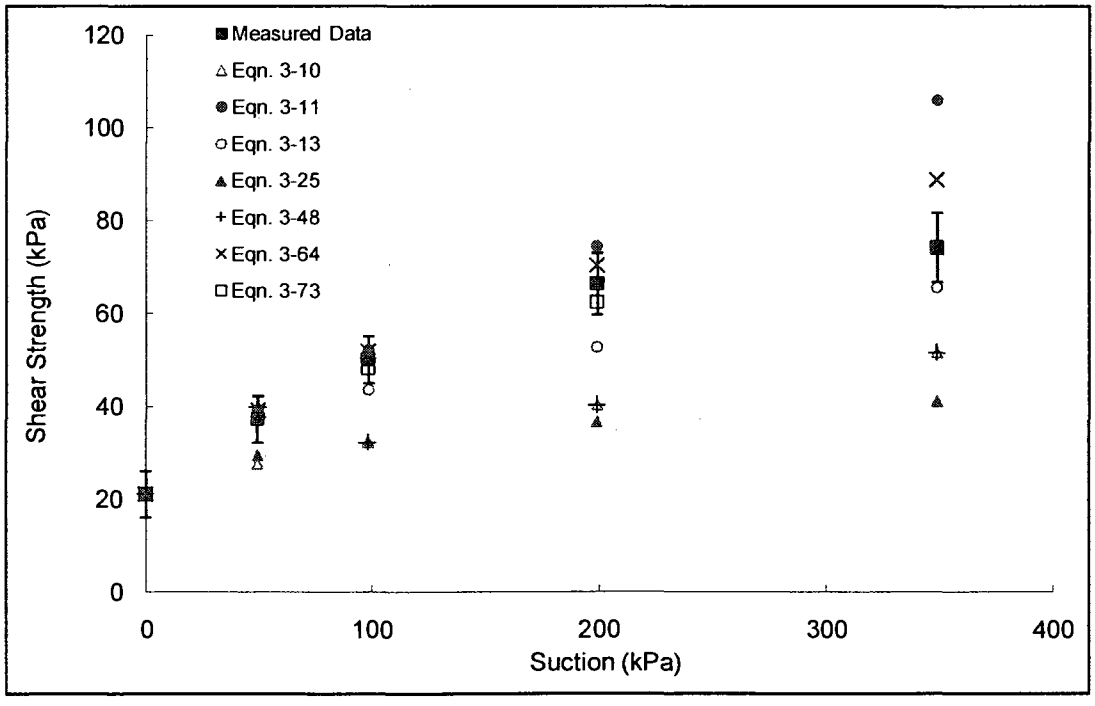

Soil No. 29b

Indian Head till

Oloo and Fredlund, 1996; Oloo, 1994

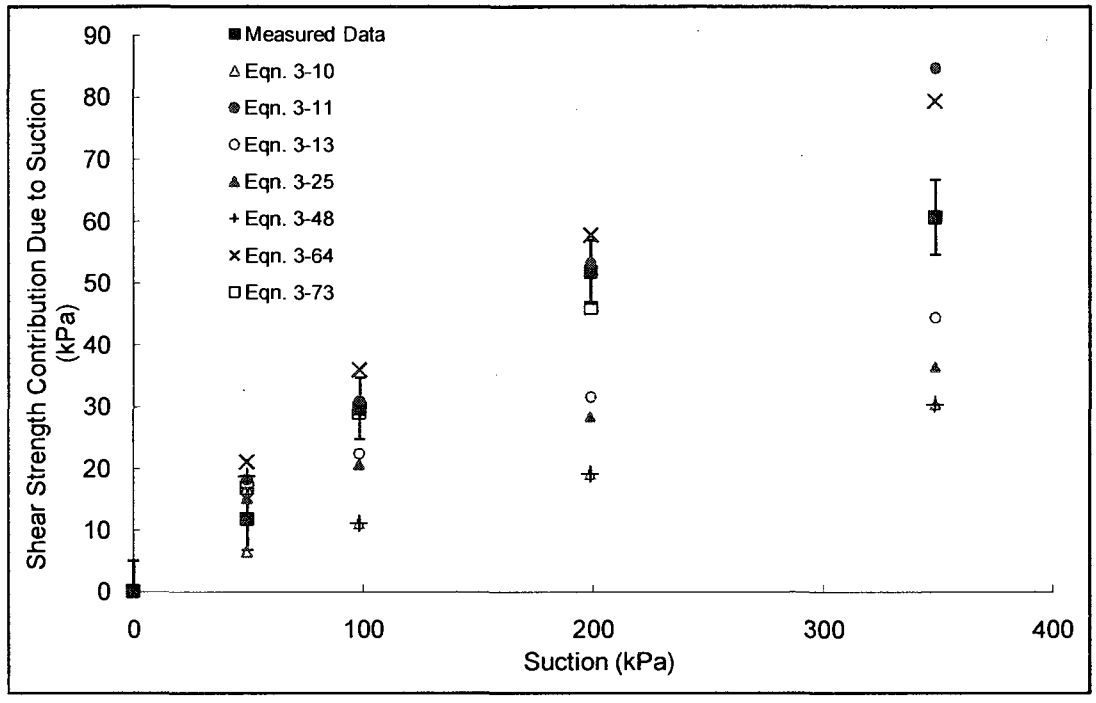

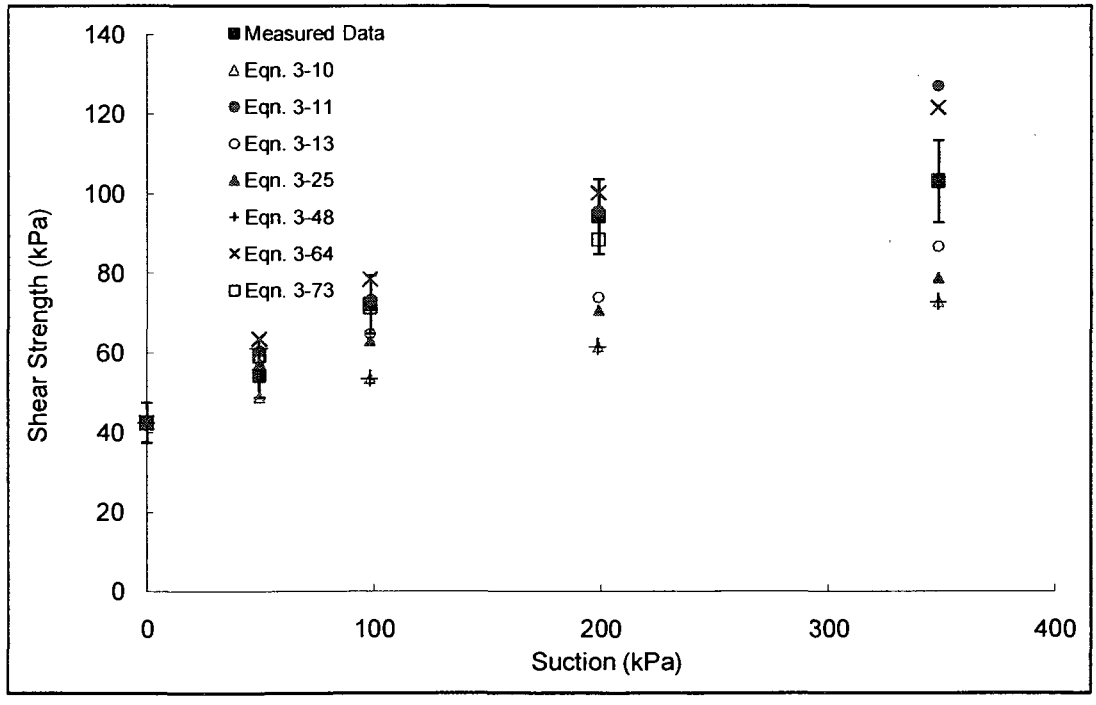

Soil No. 29c

Indian Head till

Oloo and Fredlund, 1996; Oloo, 1994

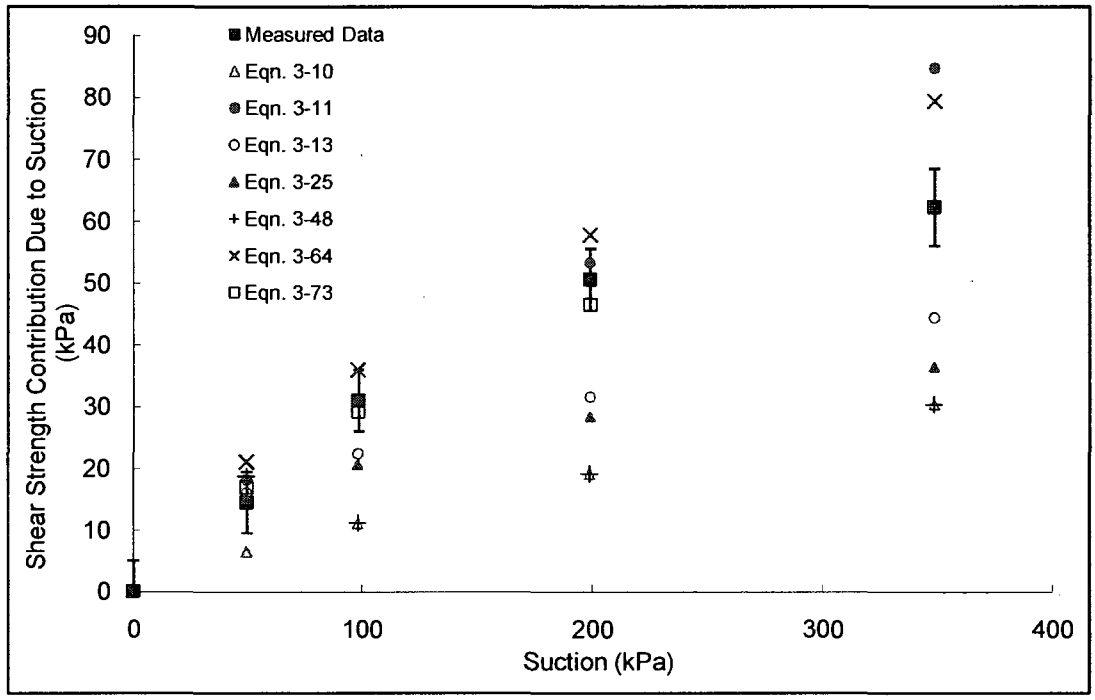

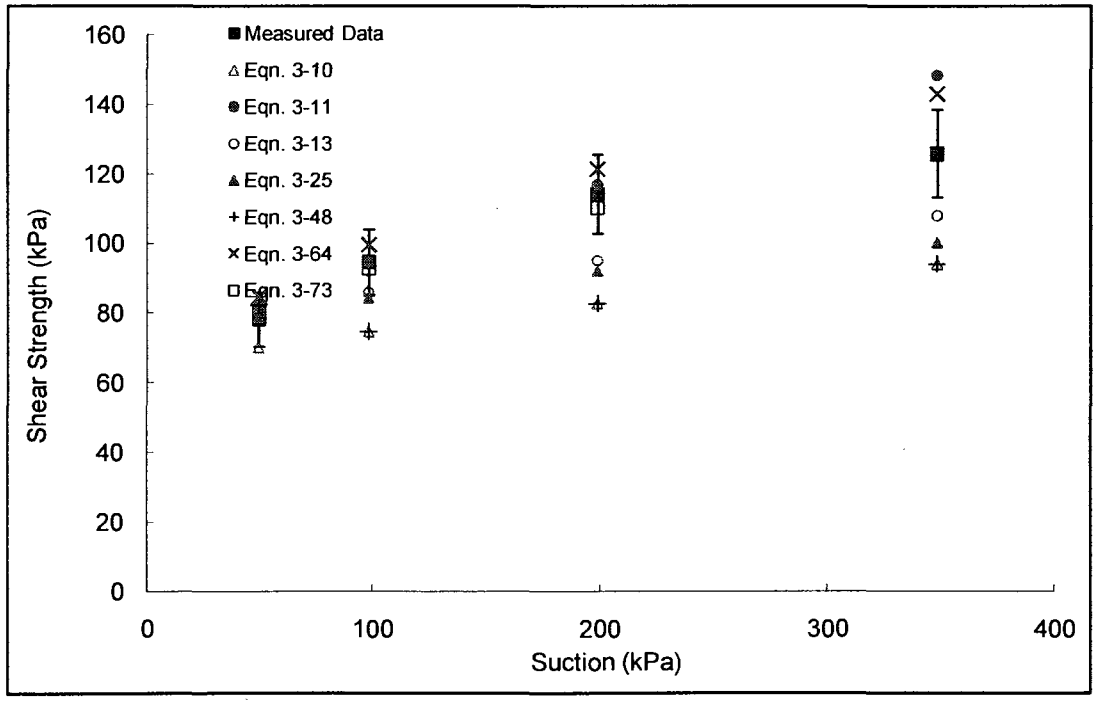

Soil No. 30

Nanyang expansive soil

Miao, Liu and Lai, 2002

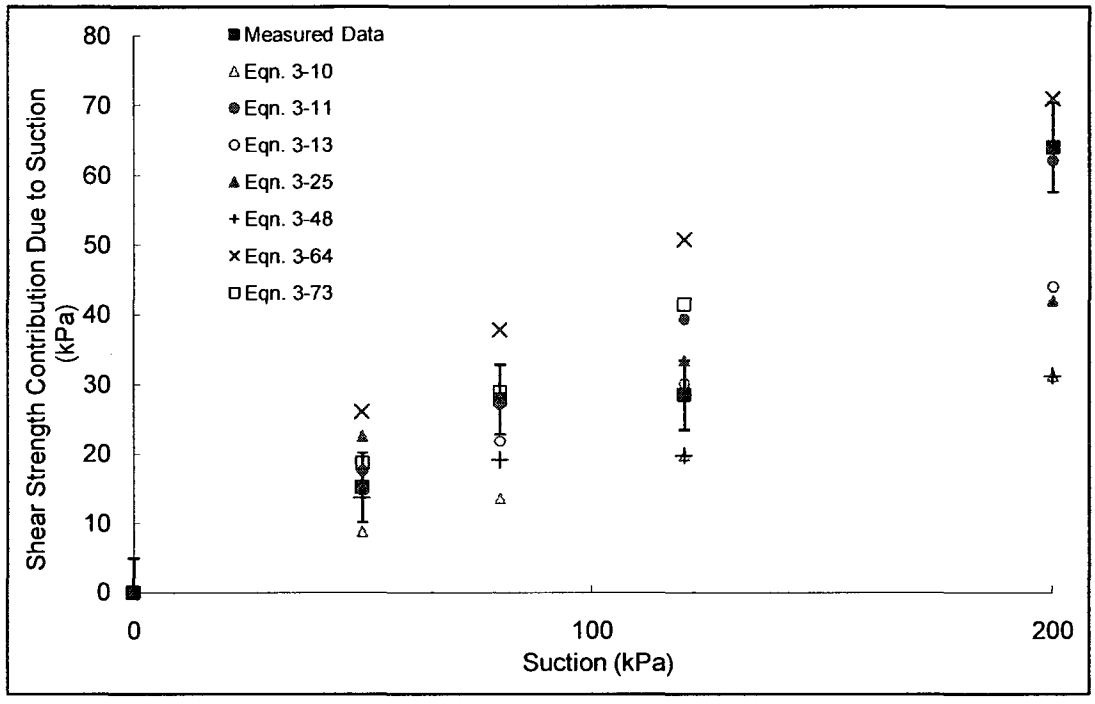

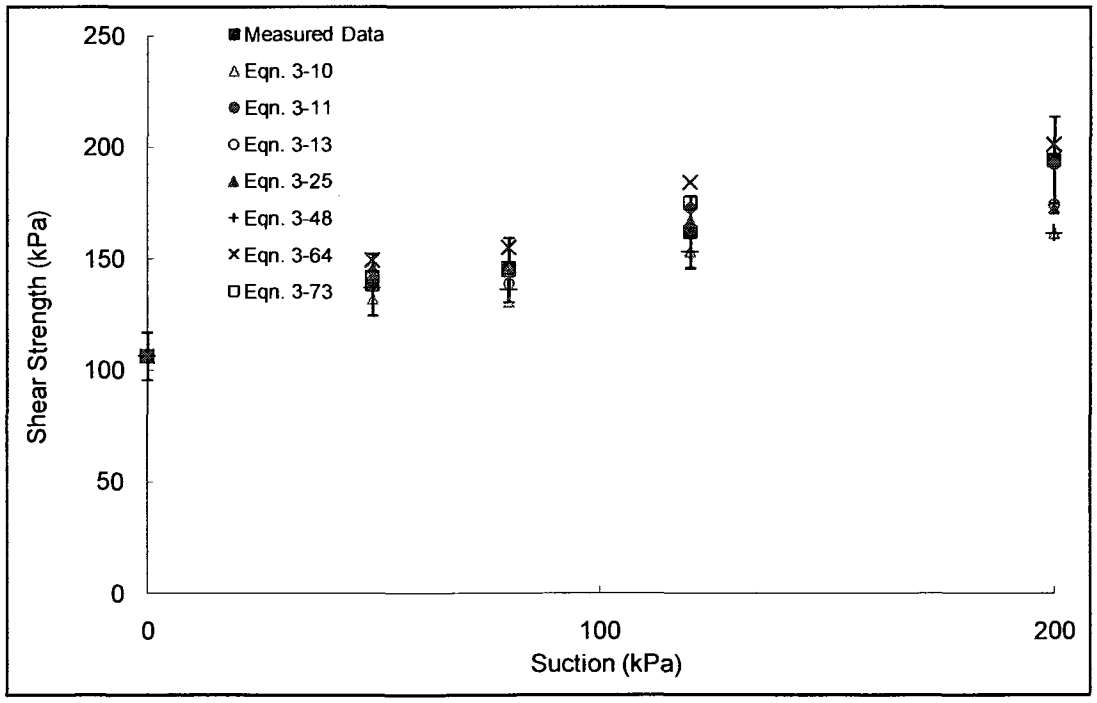

Soil No. 31a

Ouro Preto tropical (1 m)

Futai, Almeida and Lacerda, 2006

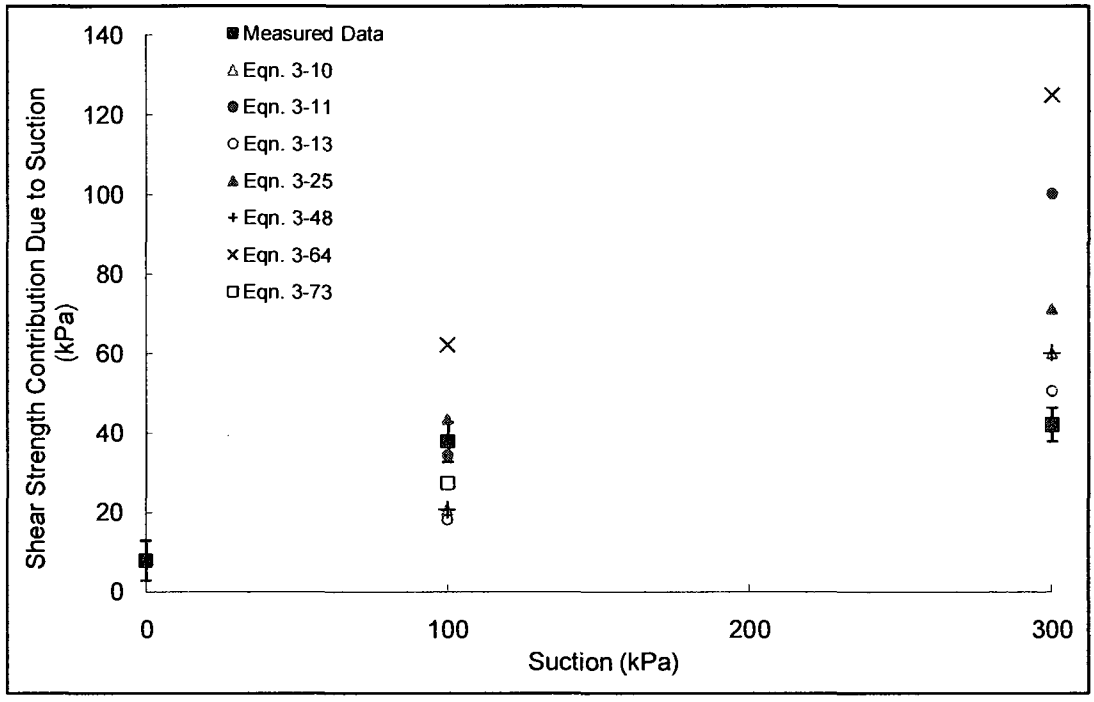

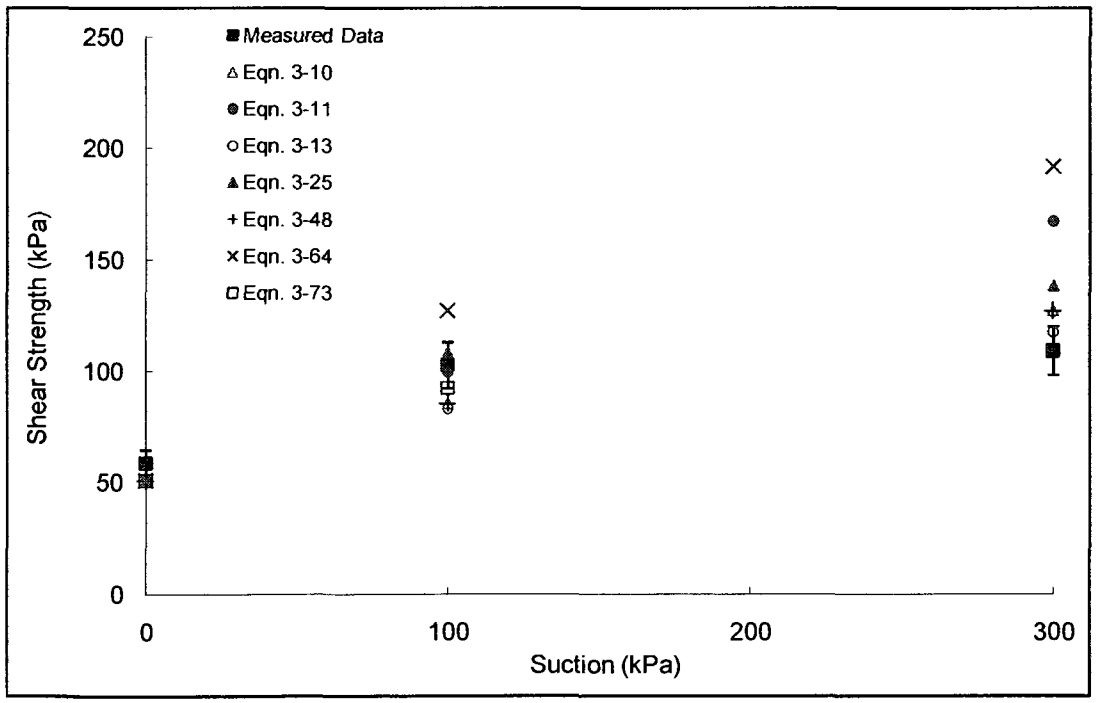

Soil No. 31b

Ouro Preto tropical (1 m)

Futai, Almeida and Lacerda, 2006

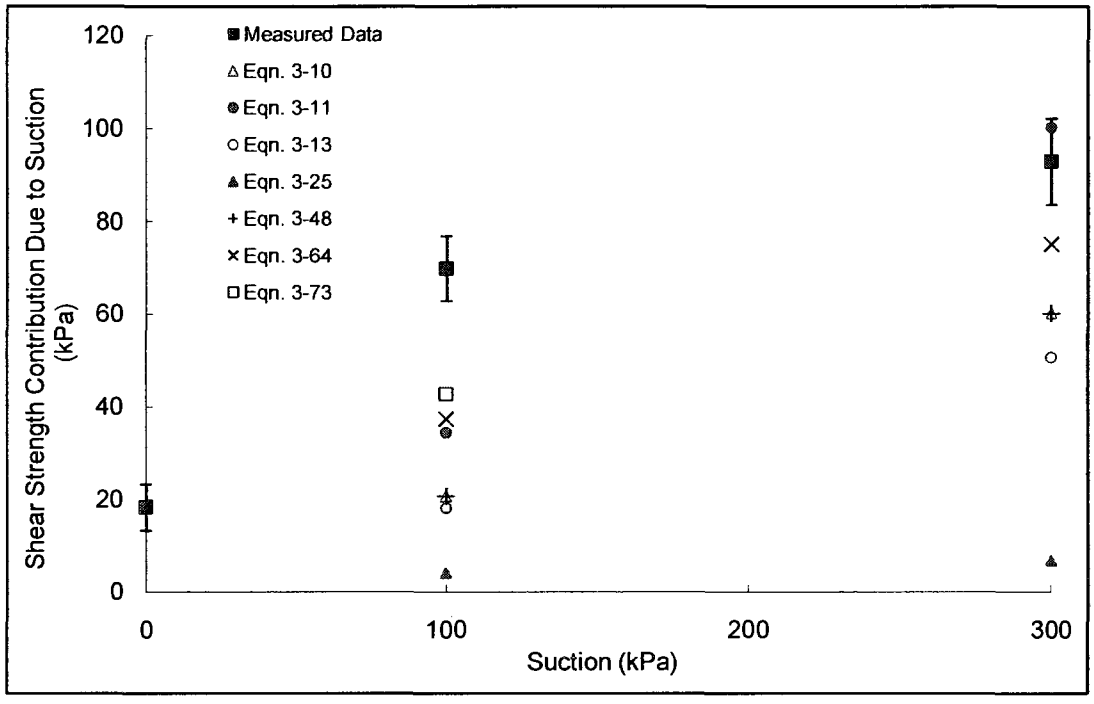

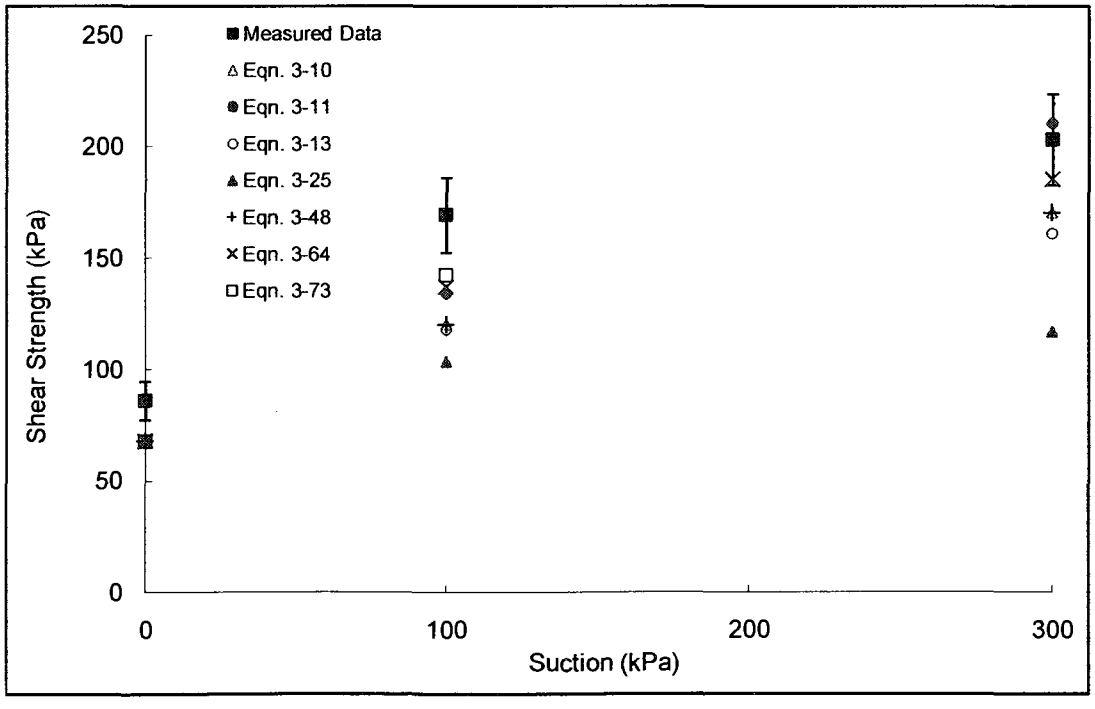

Soil No. 31c

Ouro Preto tropical (1 m)
Futai, Almeida and Lacerda, 2006

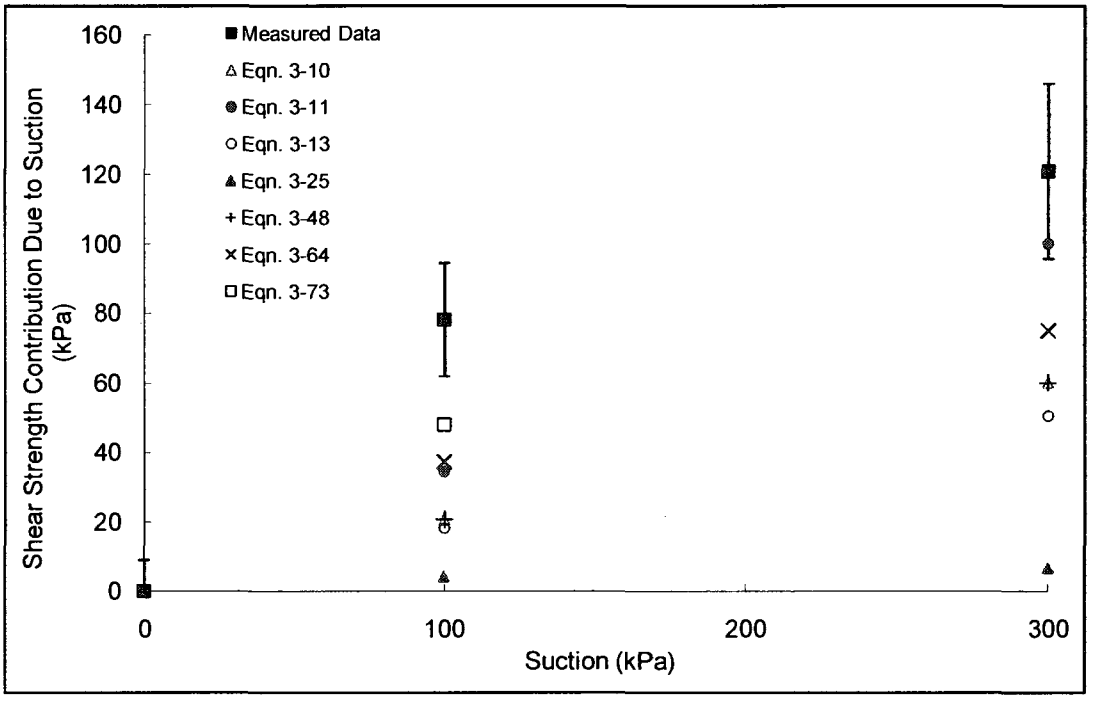

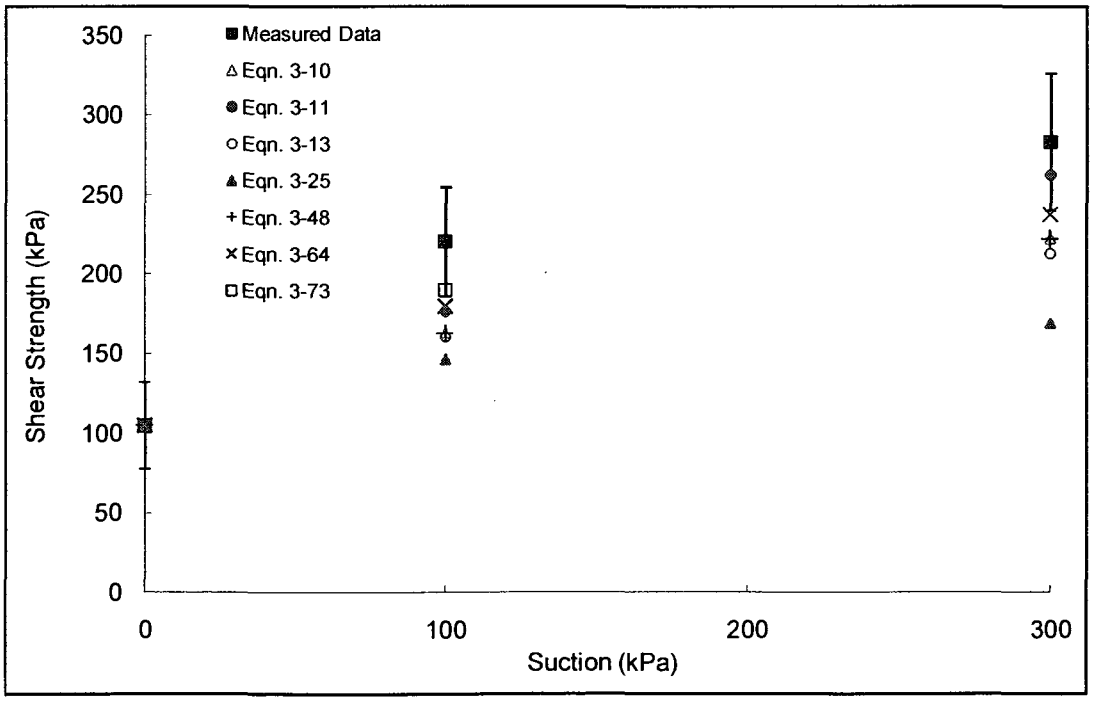

Soil No. 32a

Ouro Preto tropical (5 m)

Futai, Almeida and Lacerda, 2006

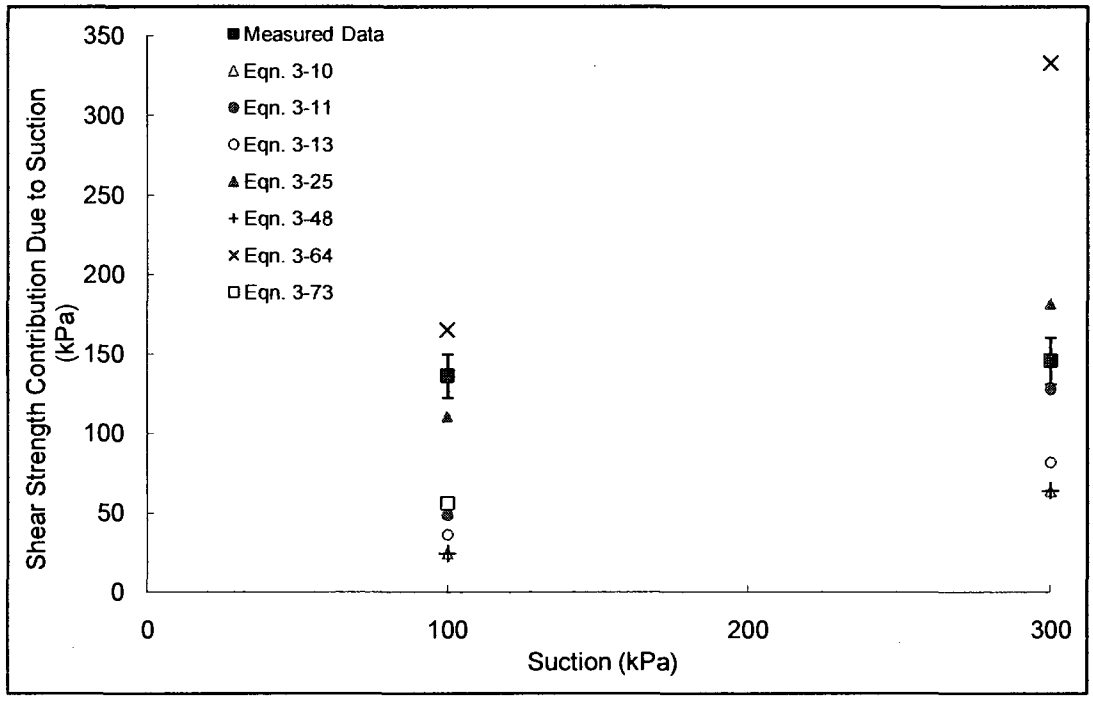

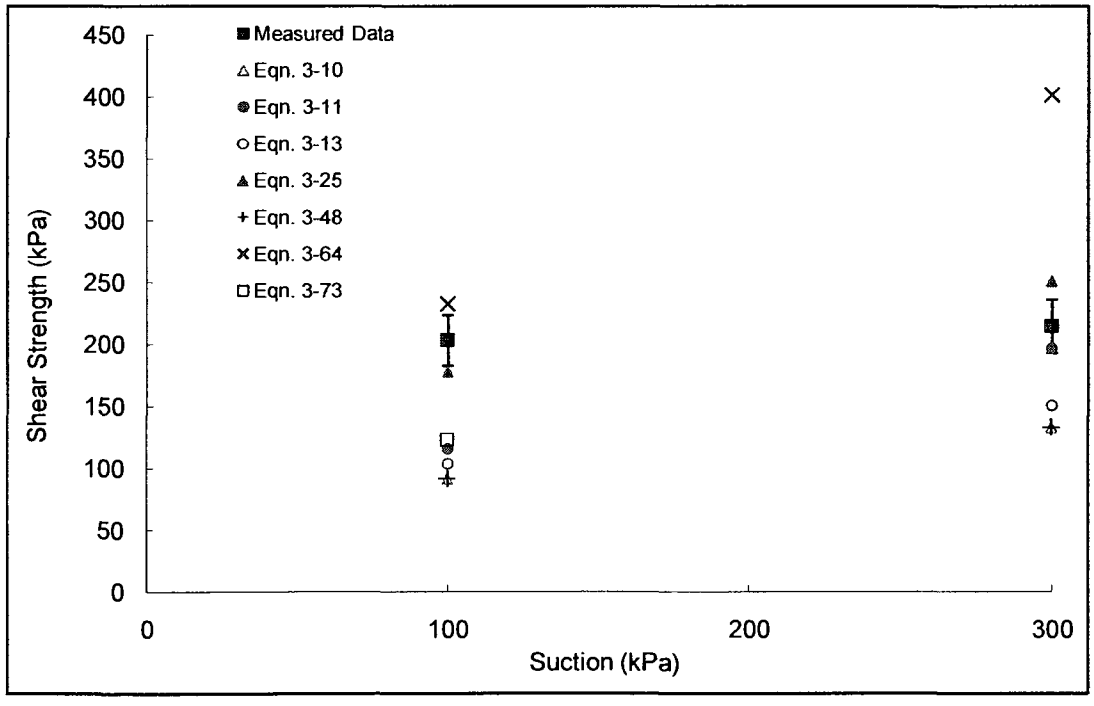

Soil No. 32b

Ouro Preto tropical (5 m)

Futai, Almeida and Lacerda, 2006

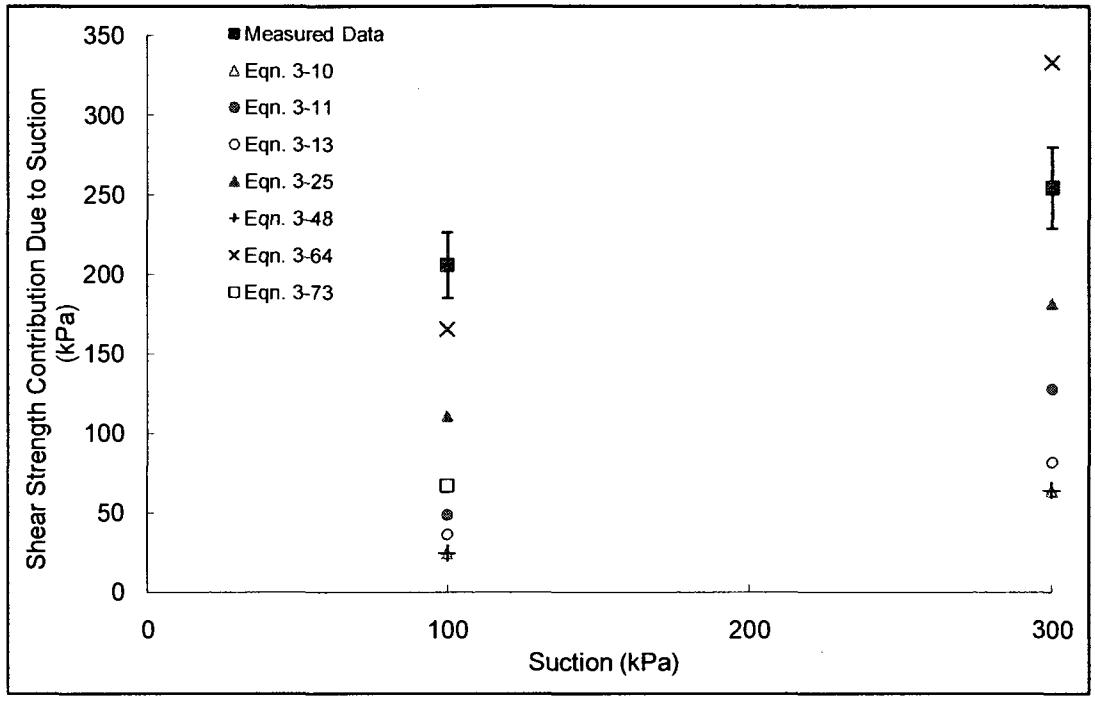

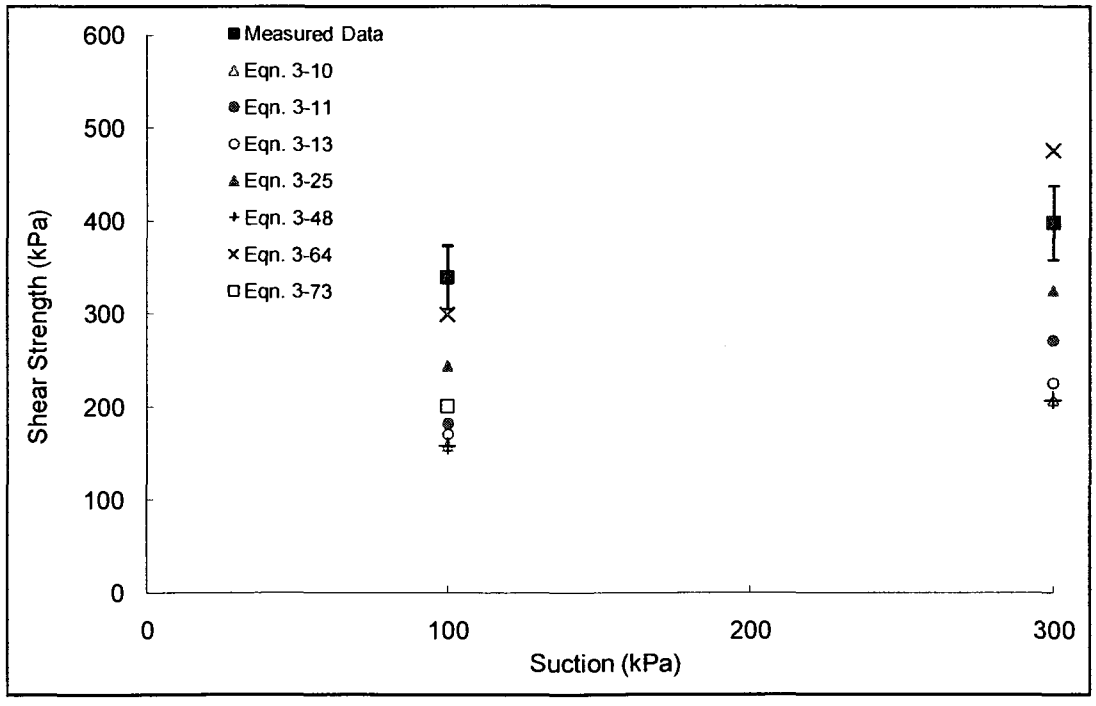

Soil No. 32c

Ouro Preto tropical (5 m)
Futai, Almeida and Lacerda, 2006

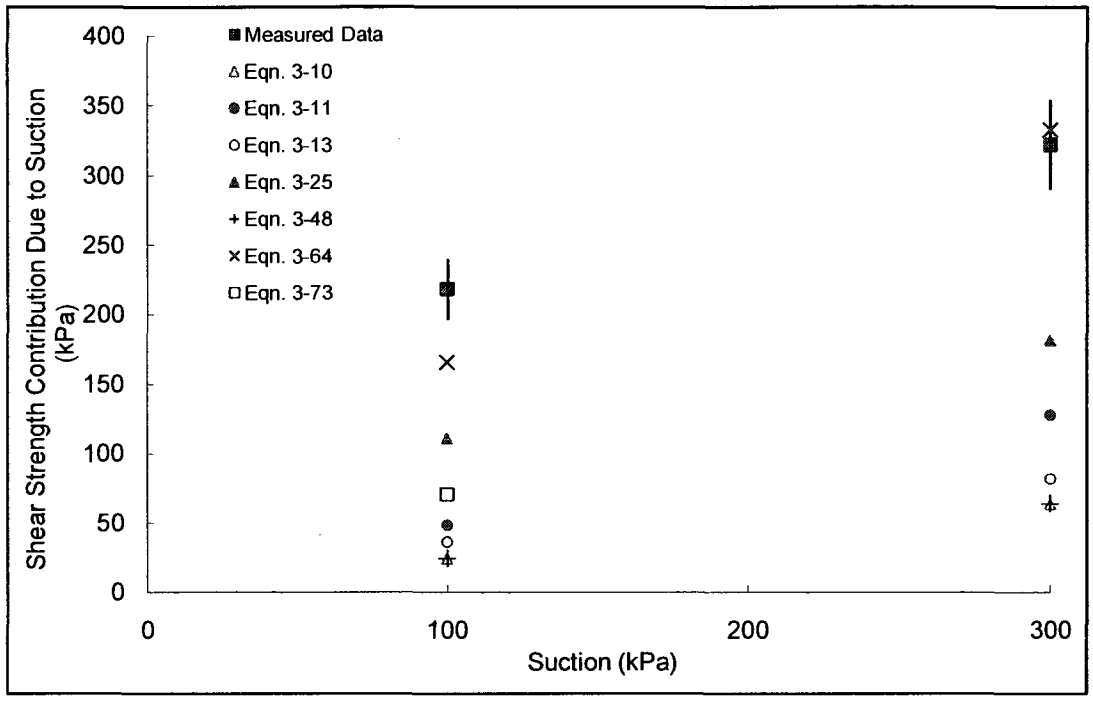

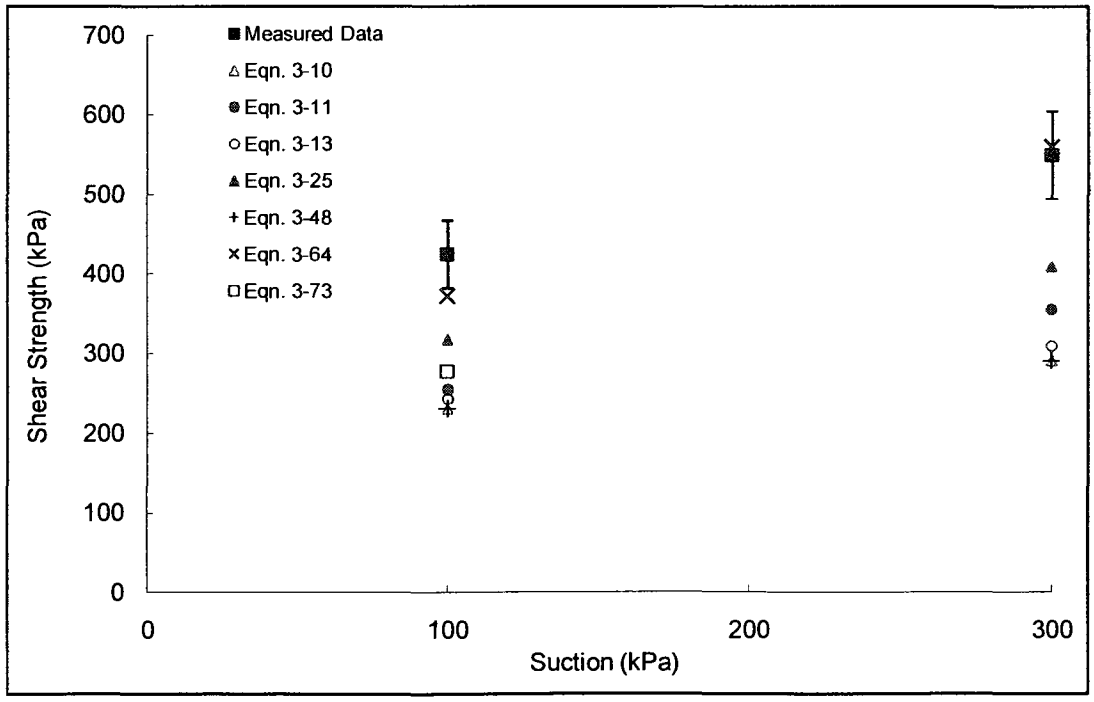

Soil No. 32d

Ouro Preto tropical (5 m)
Futai, Almeida and Lacerda, 2006

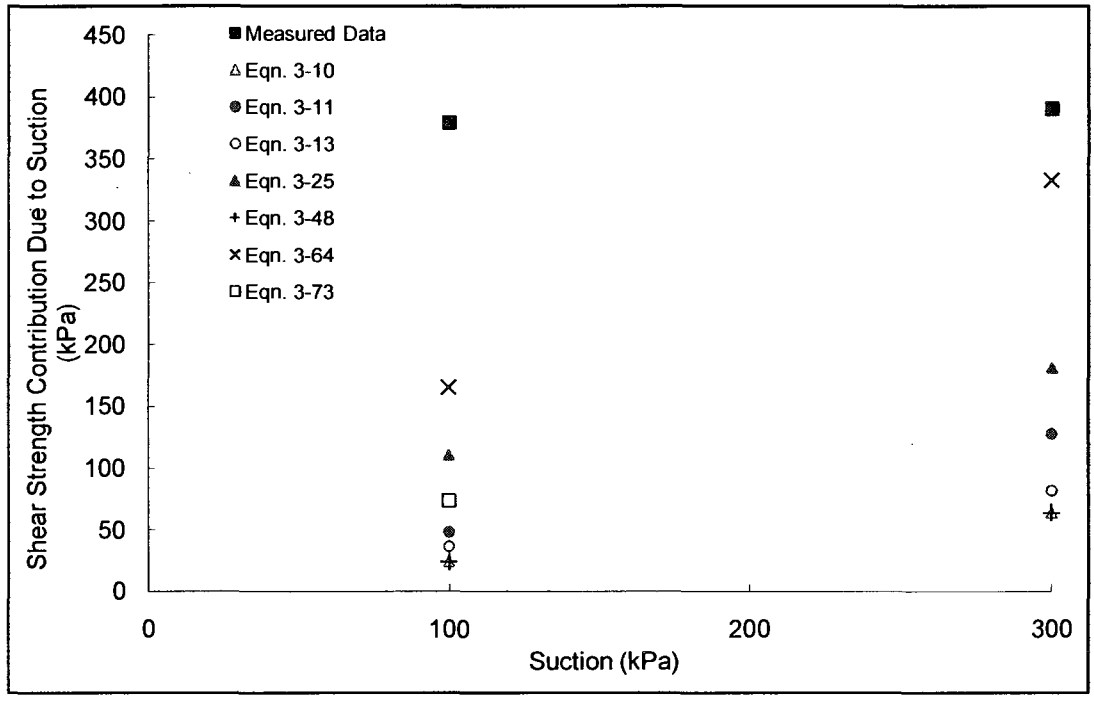

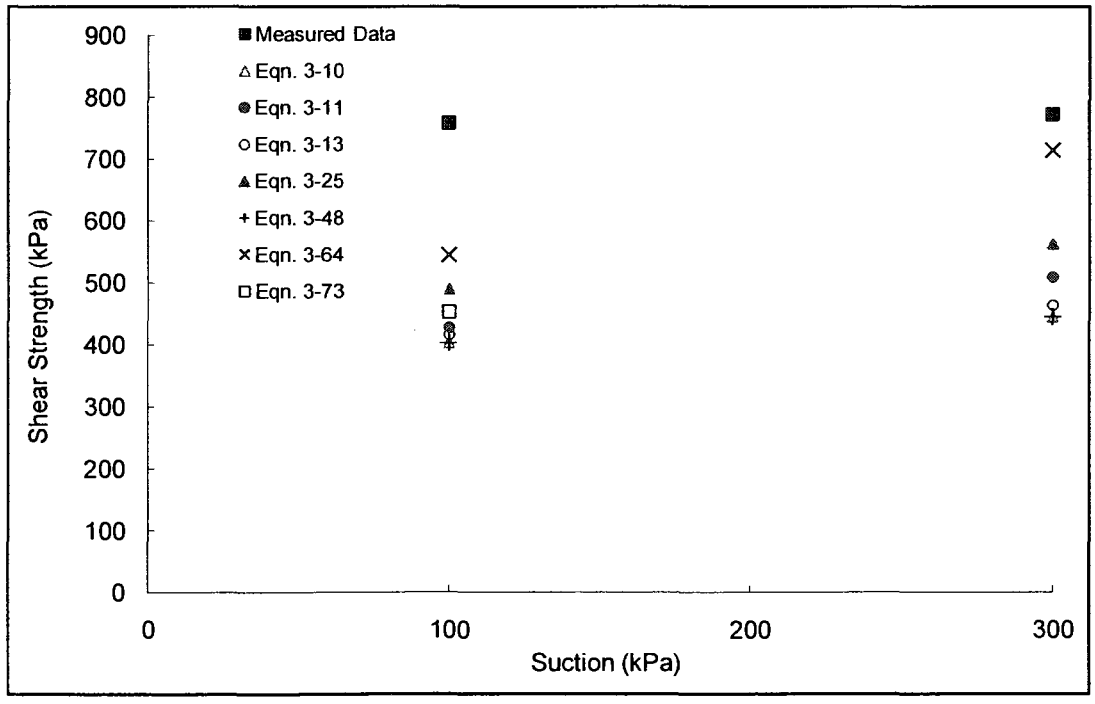

Soil No. 33a **C02**

Li, 1989; Hardcastle, Li and Fragaszy, 1992

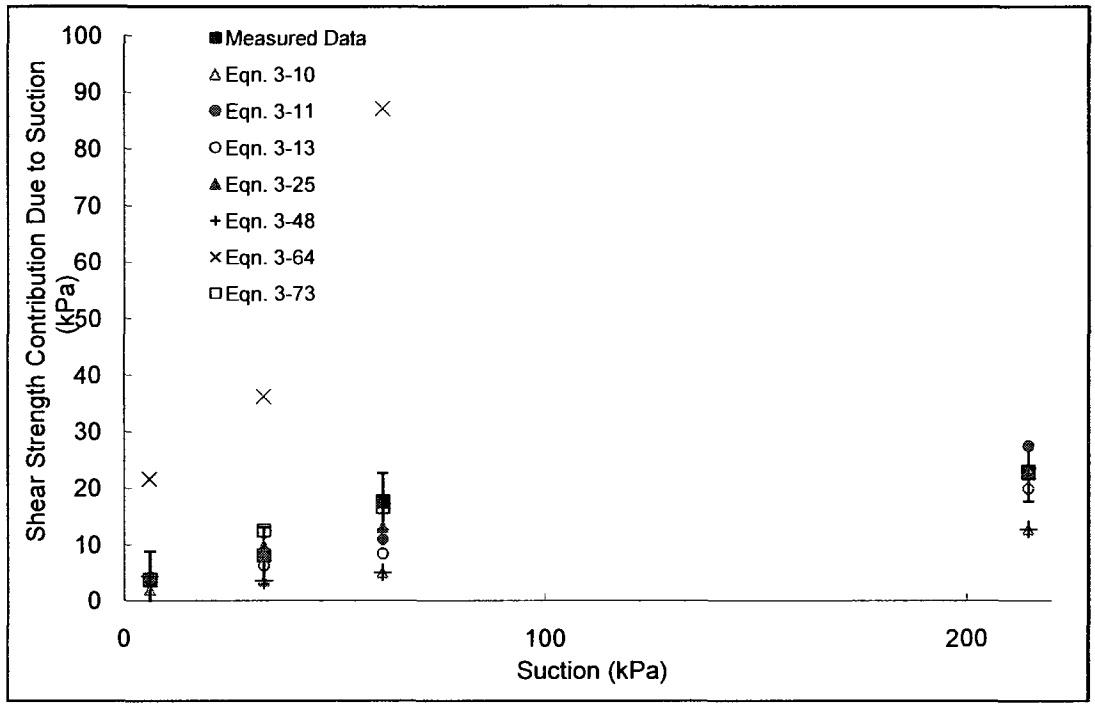

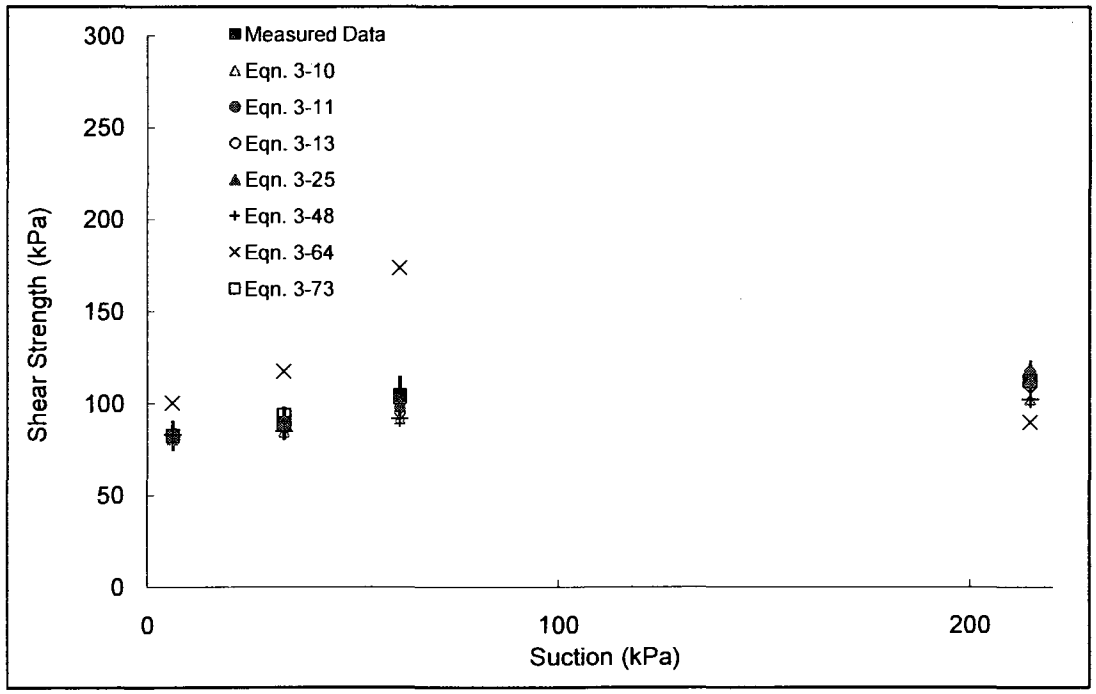

Soil No. 33b **C02**

Li, 1989; Hardcastle, Li and Fragaszy, 1992

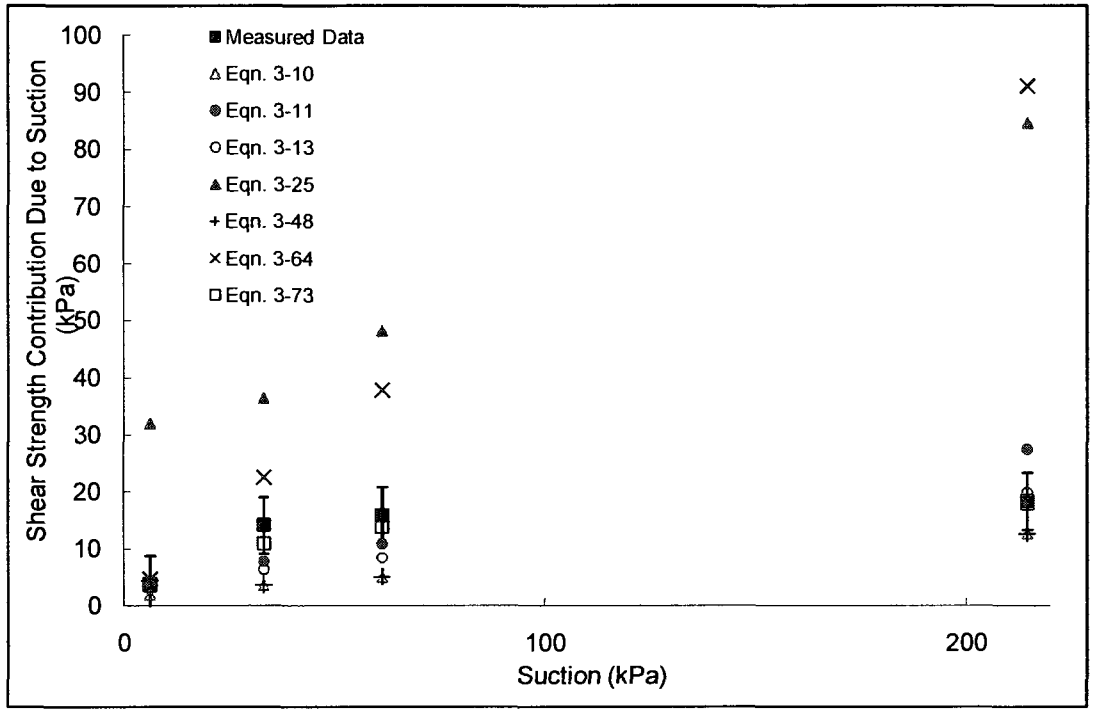

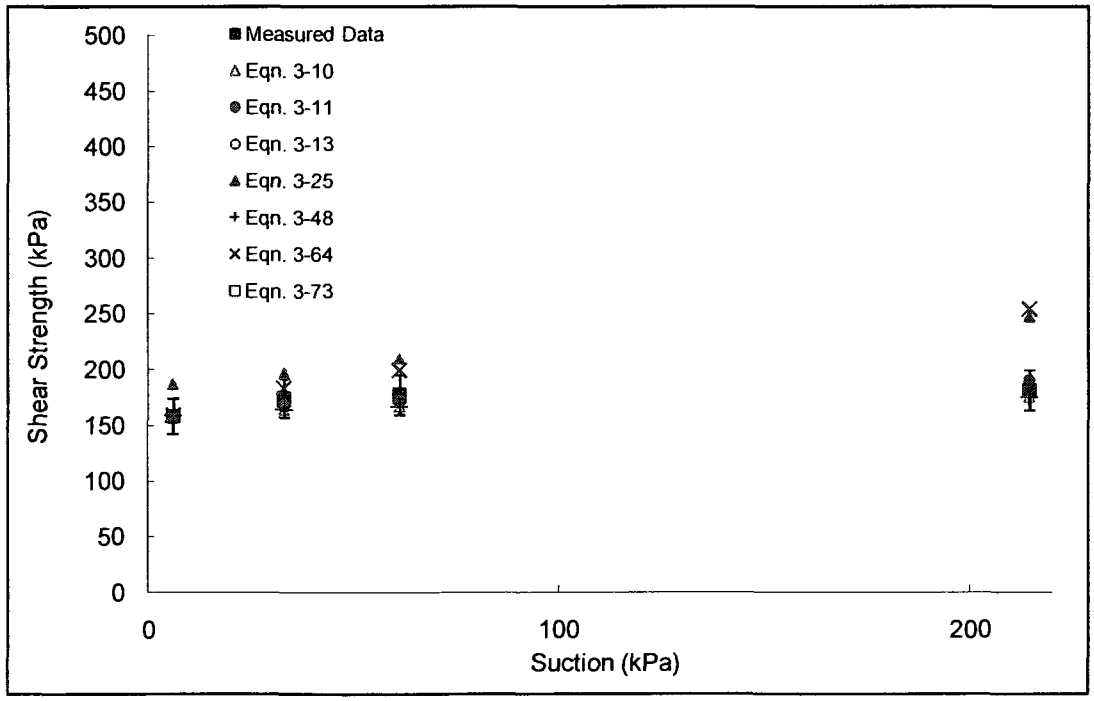

Soil No. 34a **C11**

Li, 1989; Hardcastle, Li and Fragaszy, 1992

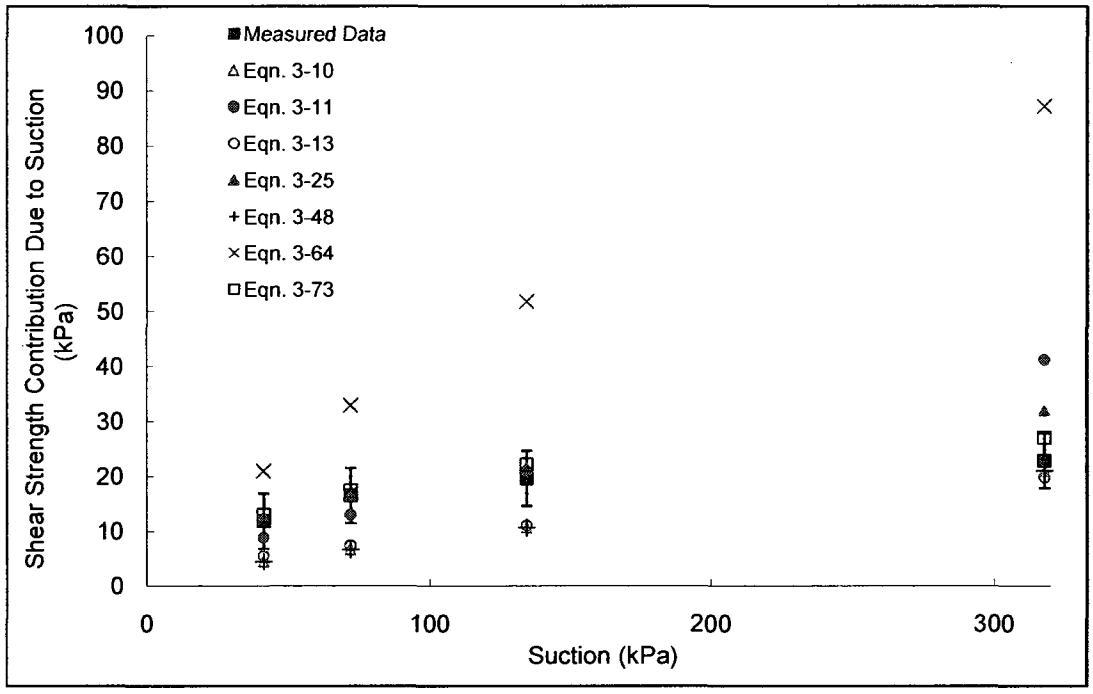

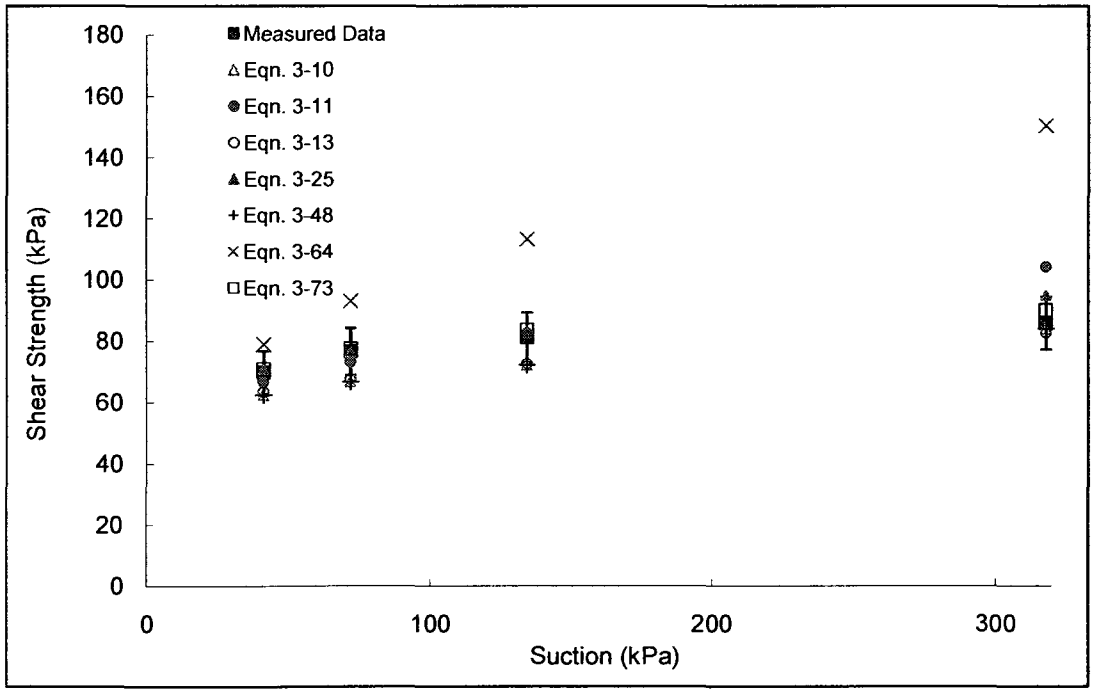

Soil No. 34b **C11**

Li, 1989; Hardcastle, Li and Fragaszy, 1992

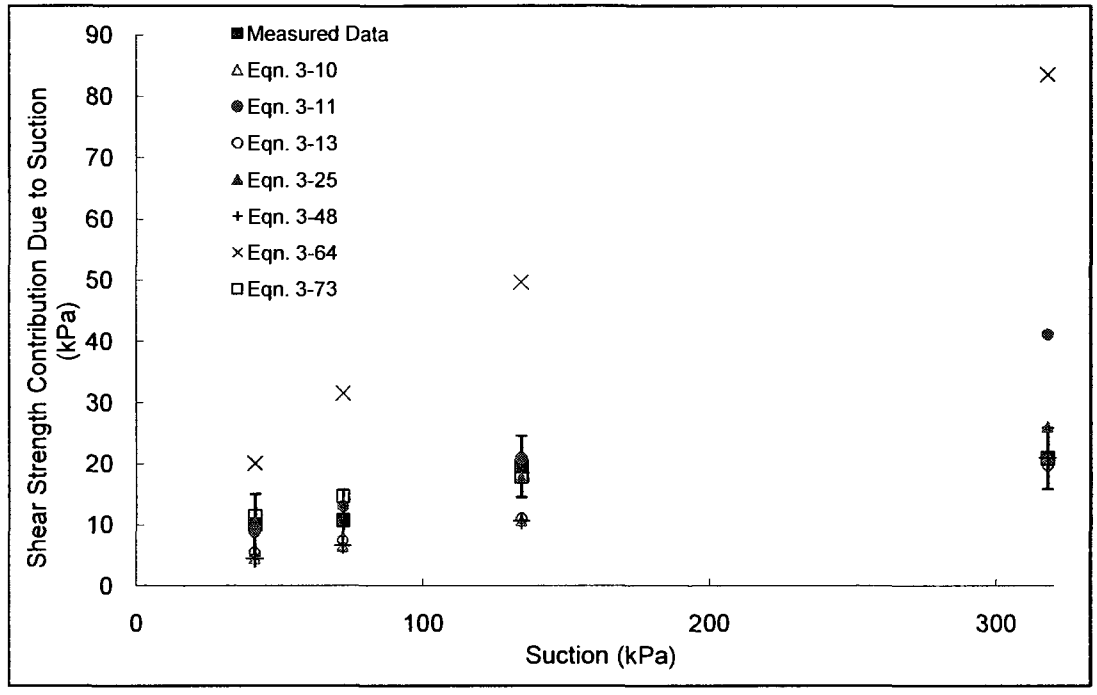

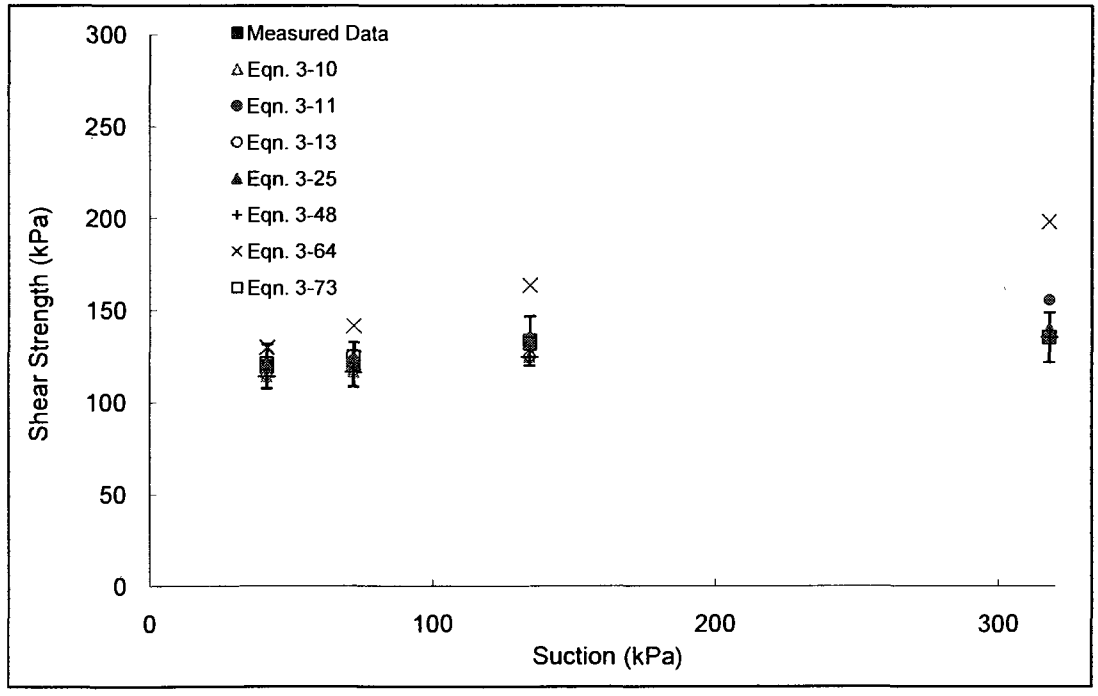

Soil No. 35a **C20**

Li, 1989; Hardcastle, Li and Fragaszy, 1992

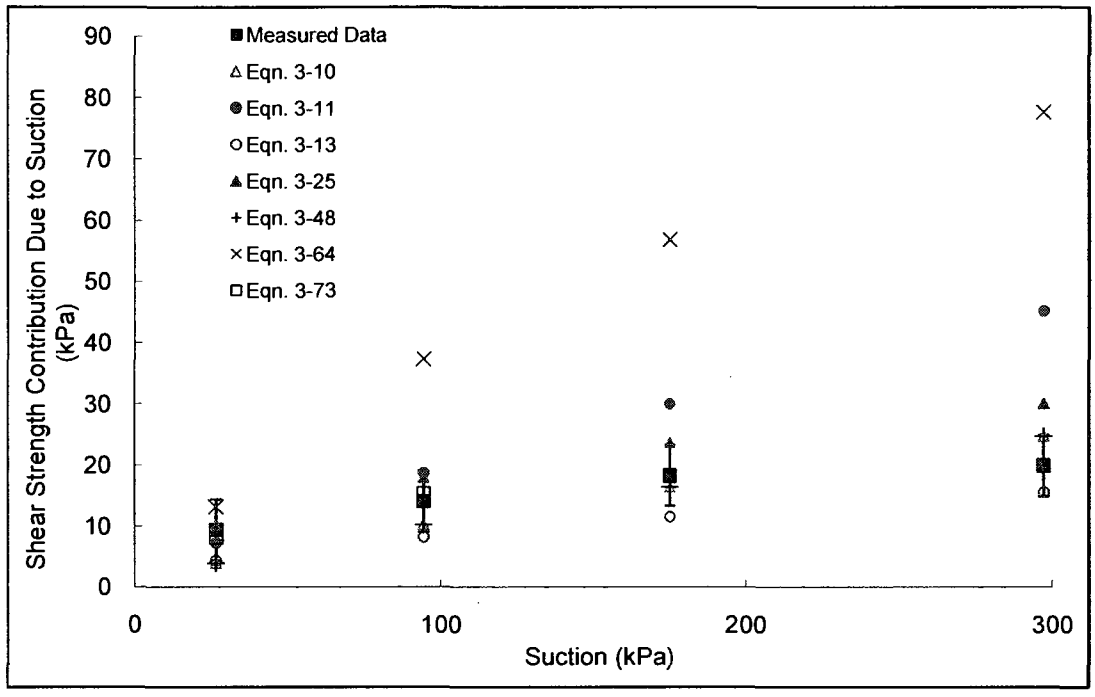

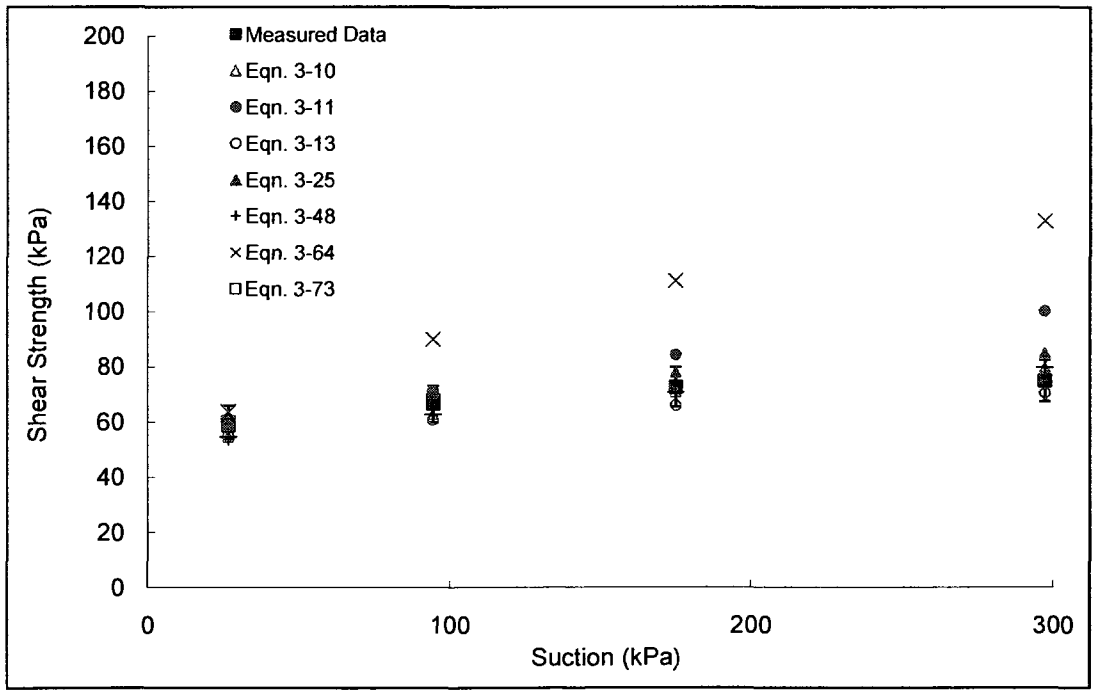

Soil No. 35b **C20**

Li, 1989; Hardcastle, Li and Fragaszy, 1992

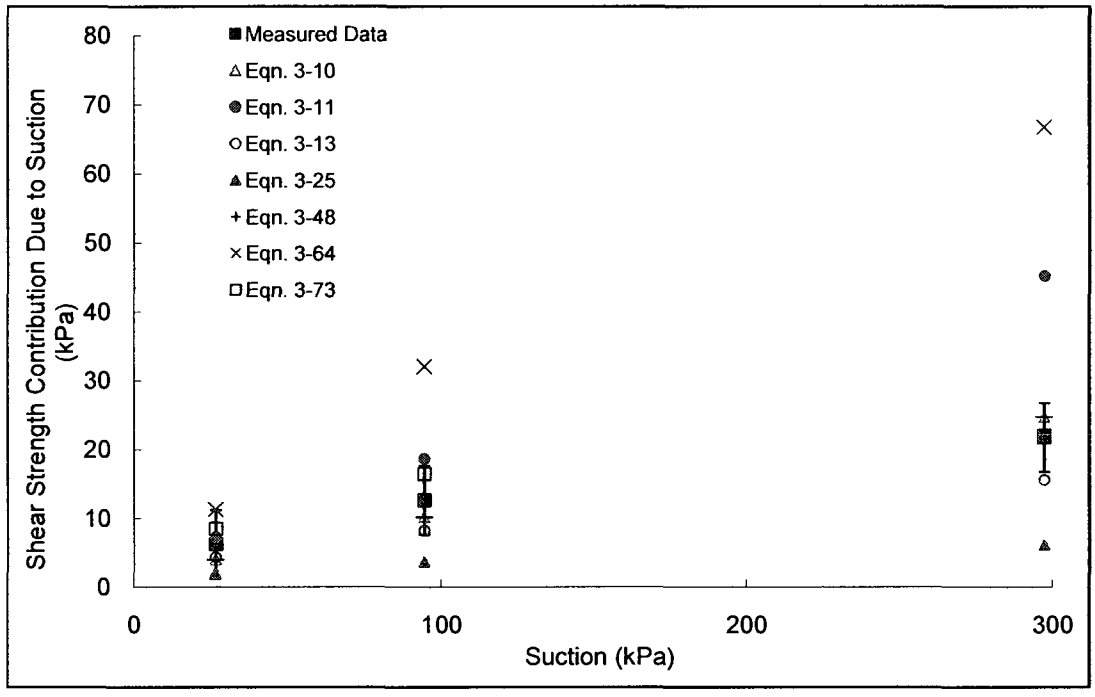

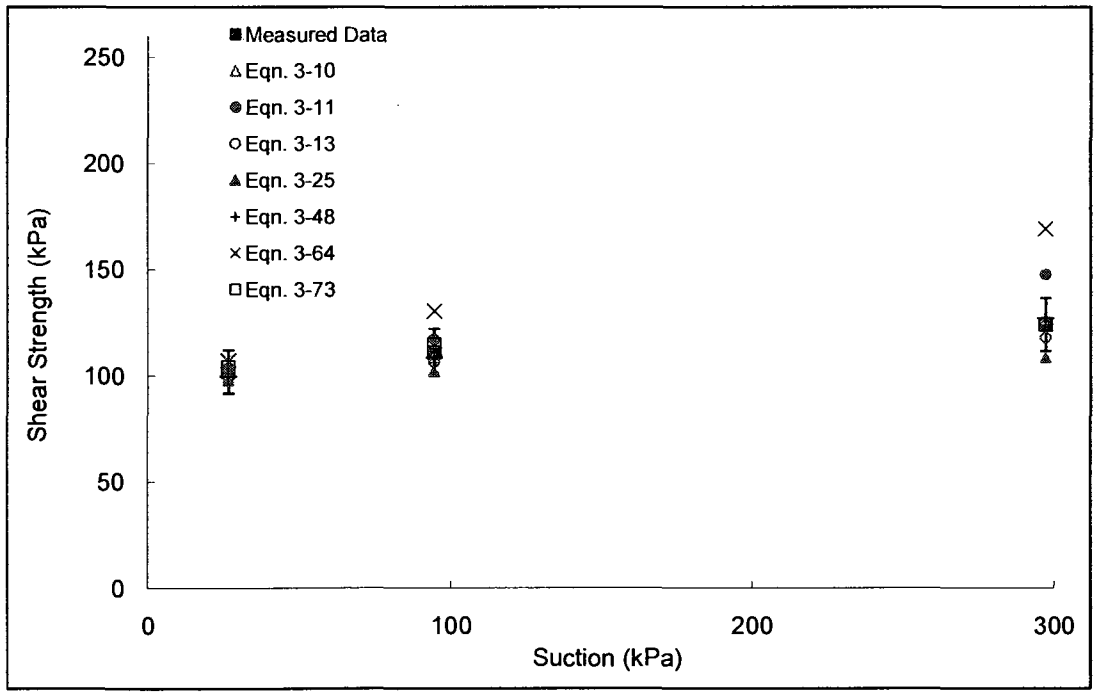

Soil No. 36a **C30**

Li, 1989; Hardcastle, Li and Fragaszy, 1992

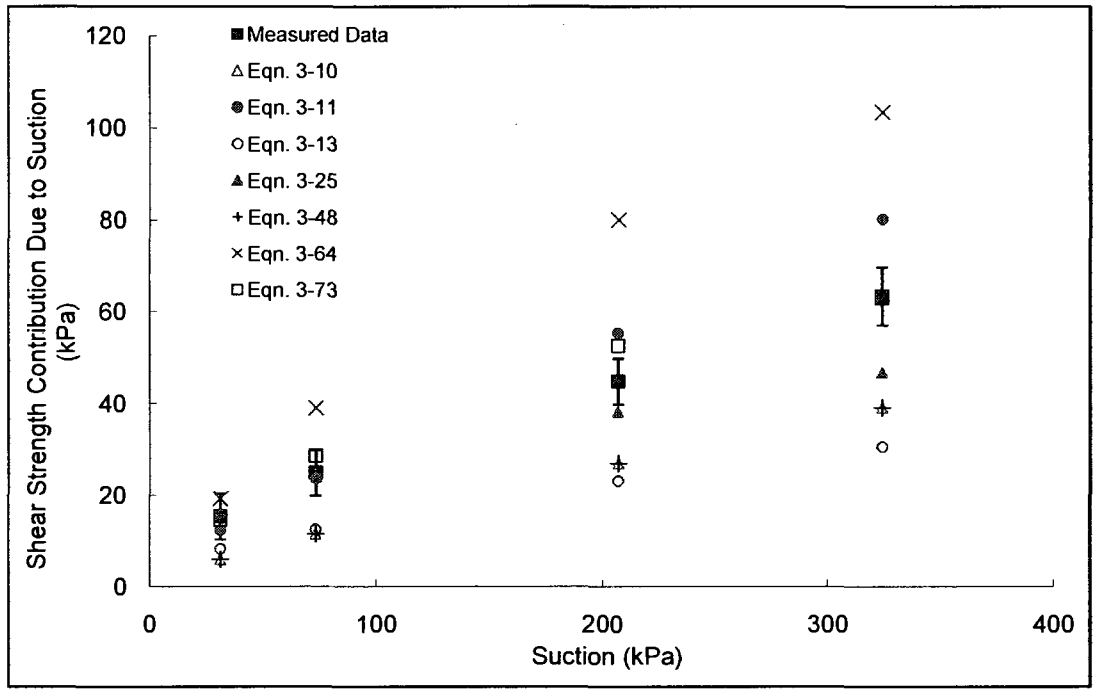

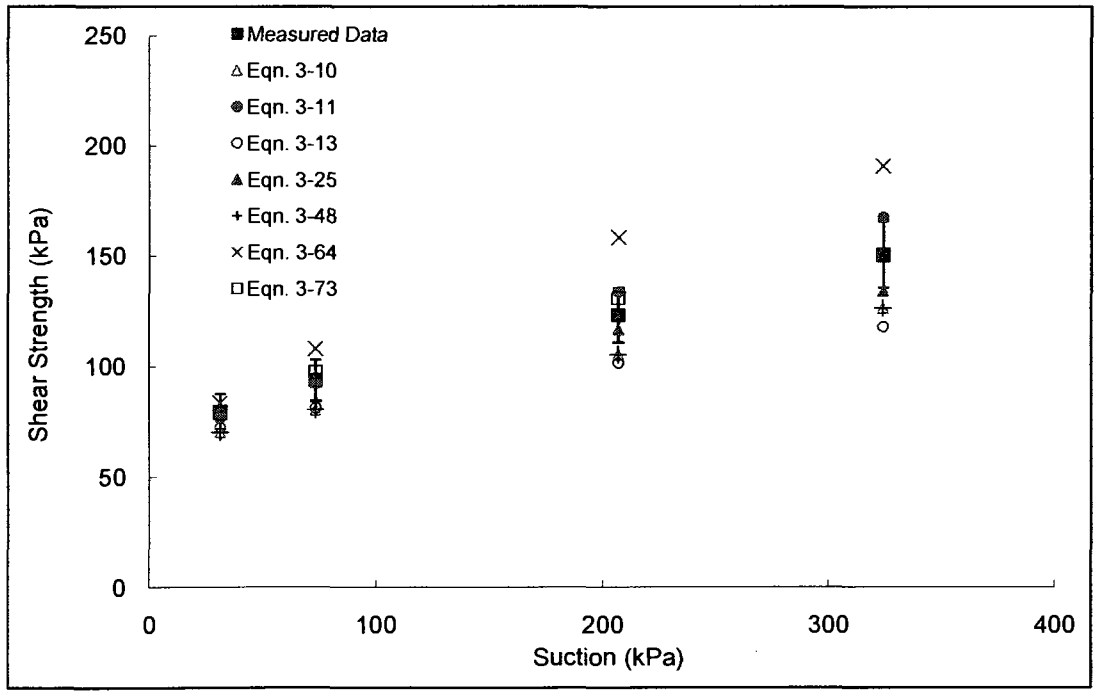

Soil No. 36b **C30**

Li, 1989; Hardcastle, Li and Fragaszy, 1992

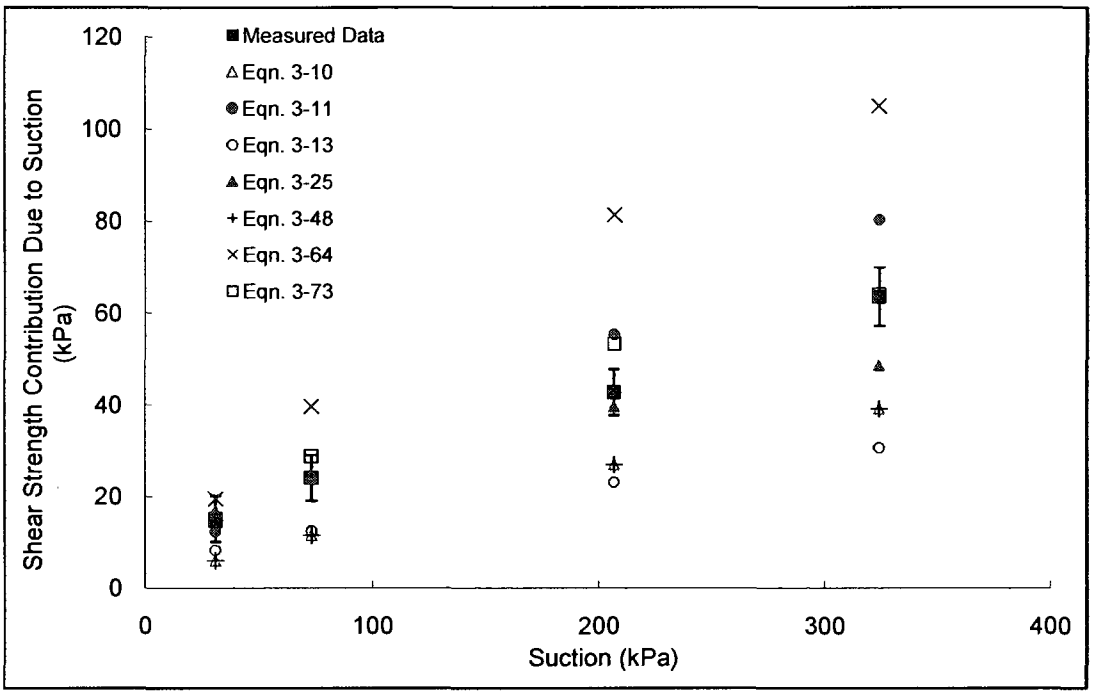

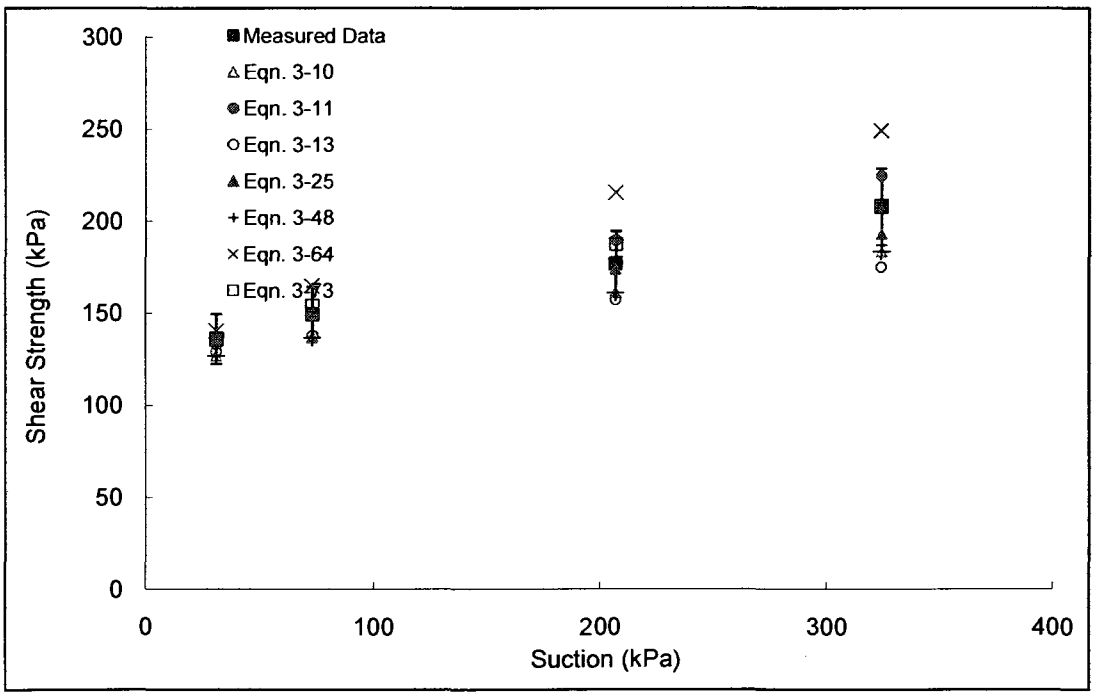

Soil No. 37a

Recife clay

Jucá, Ferreira and Bastos, 1995

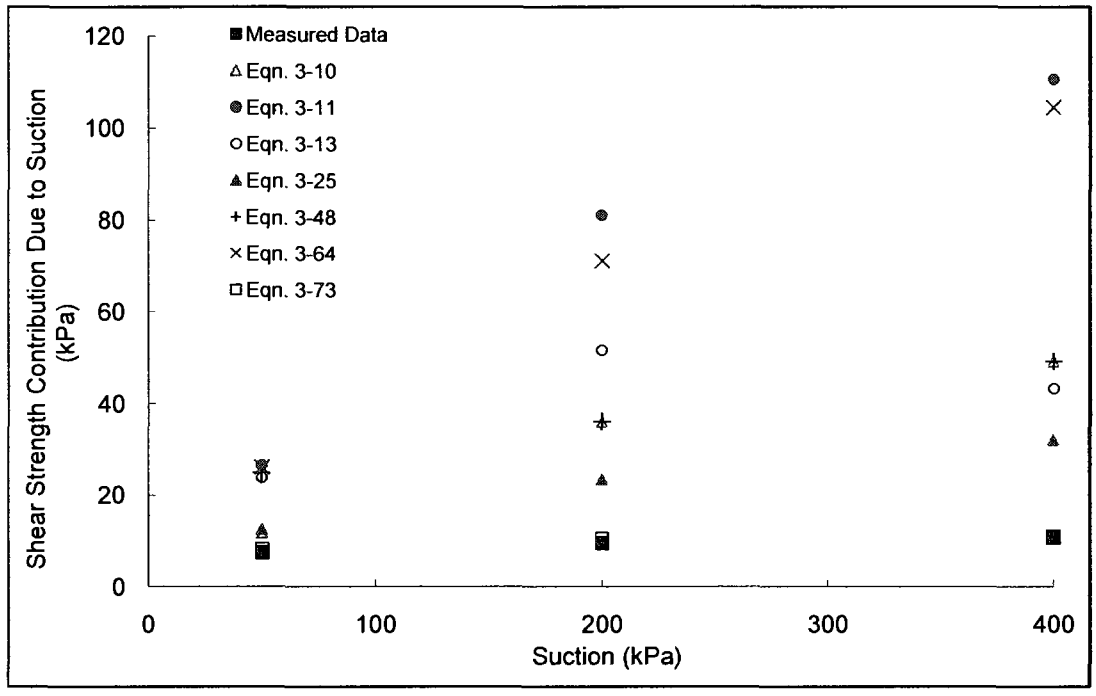

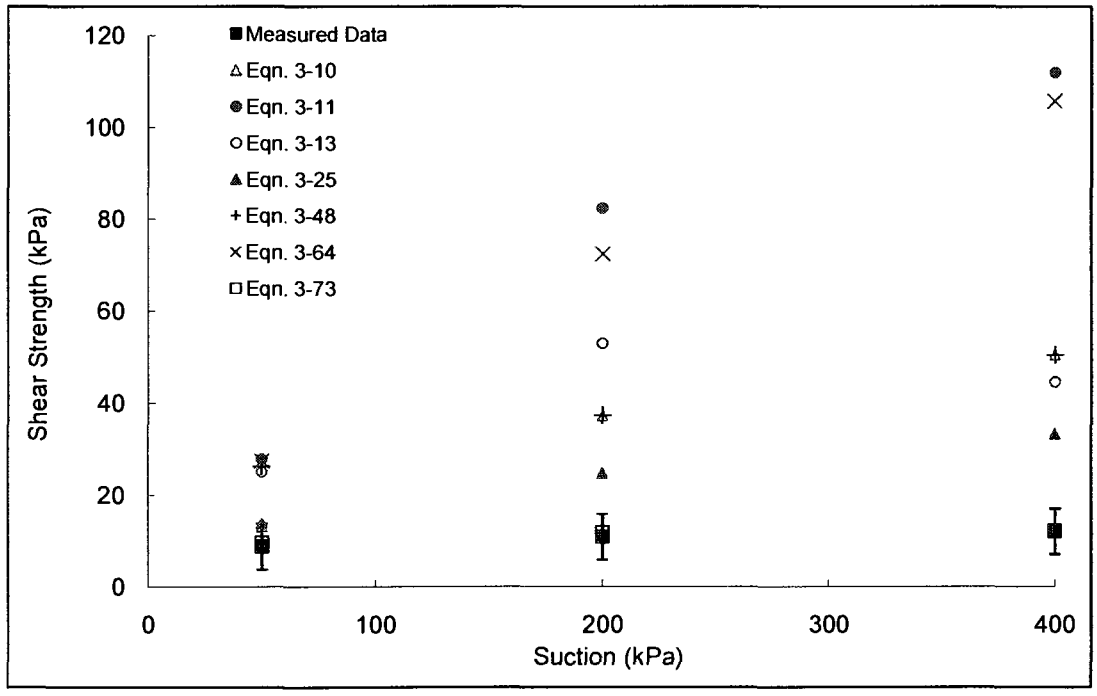

Soil No. 37b

Recife clay

Jucá, Ferreira and Bastos, 1995

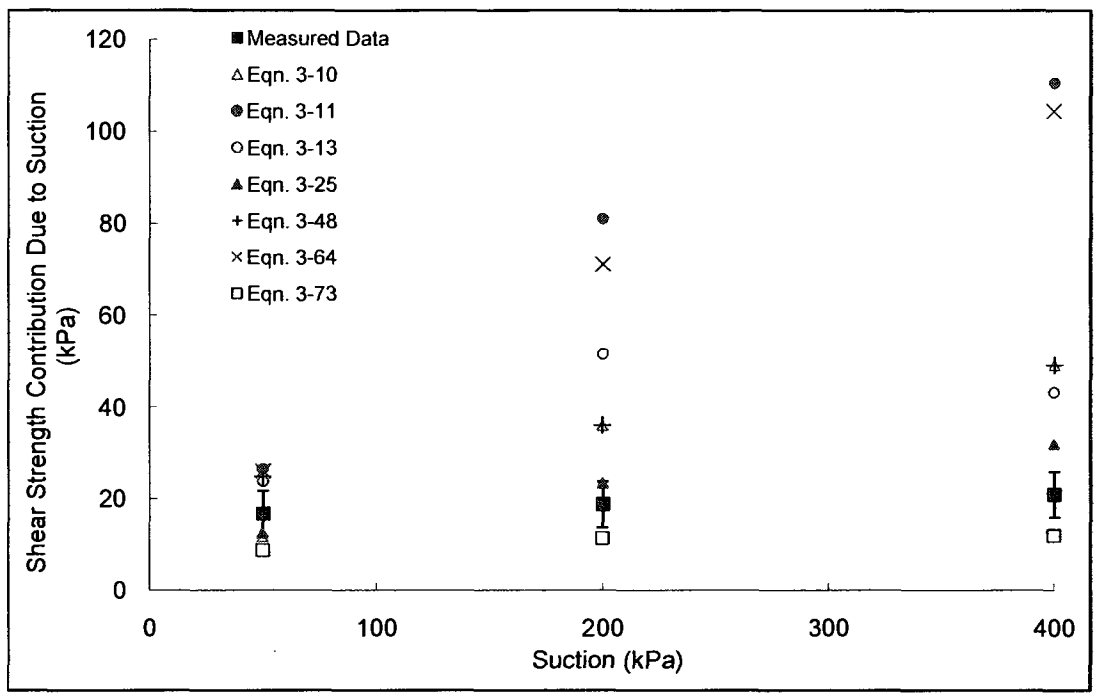

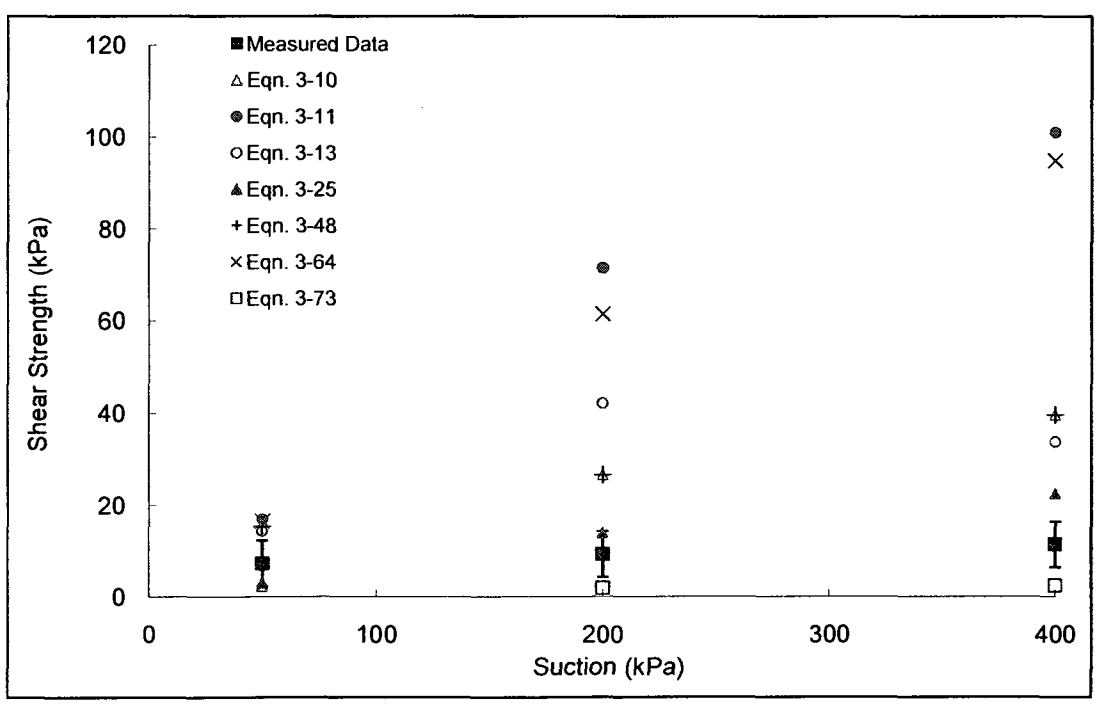

Soil No. 37c

Recife clay

Jucá, Ferreira and Bastos, 1995

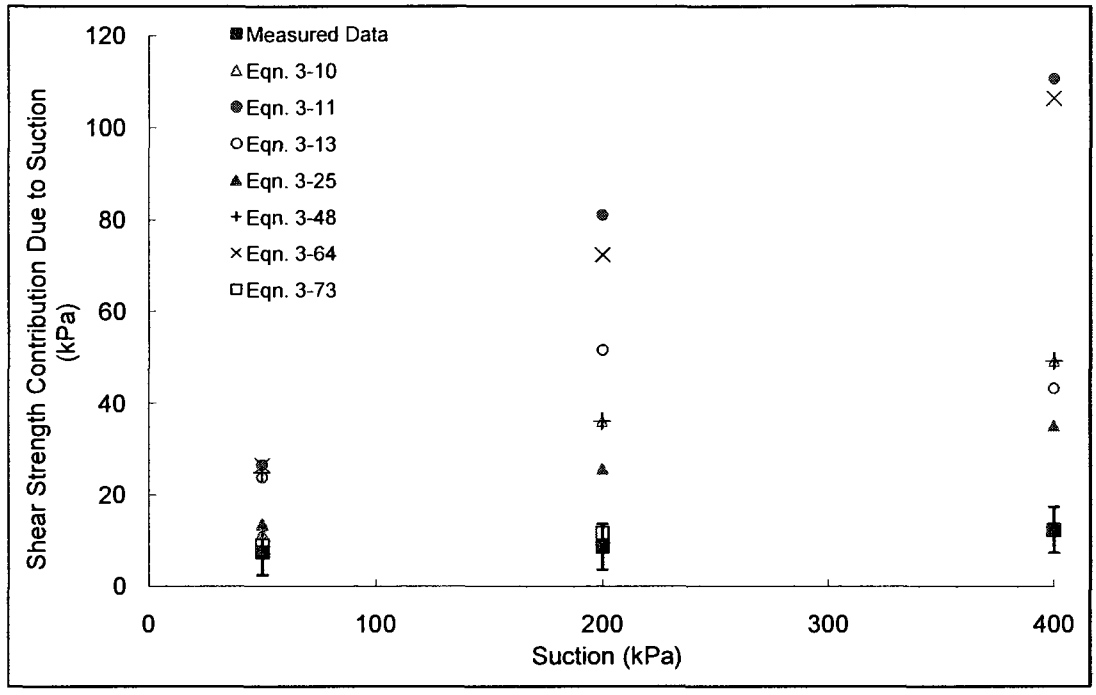

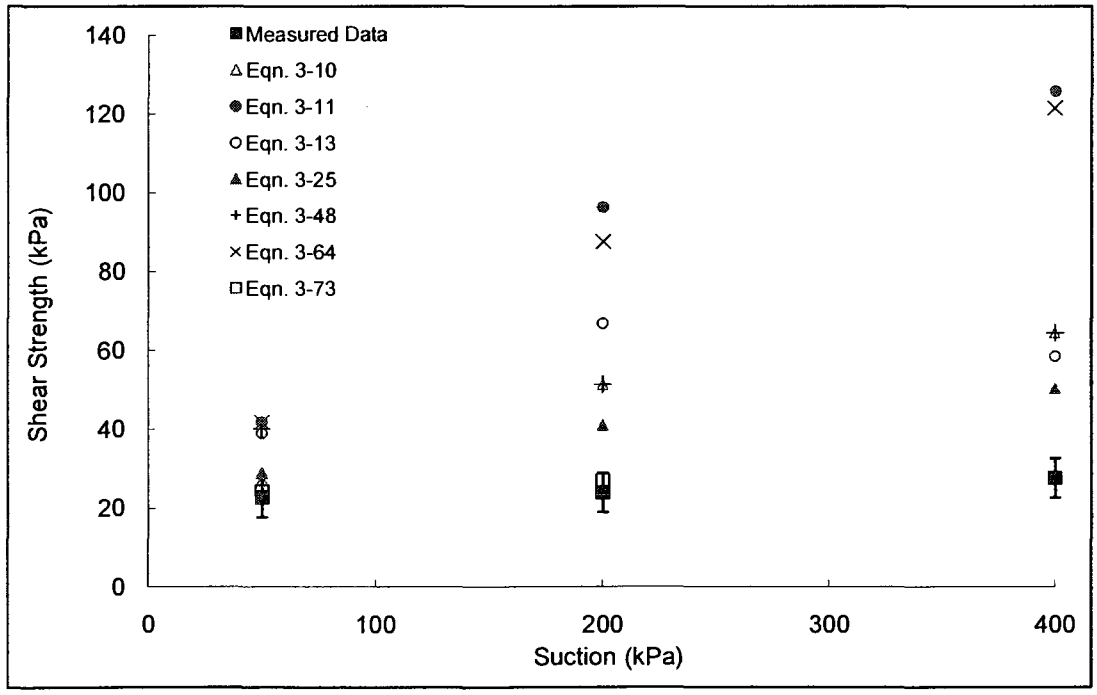

Soil No. 38a

Pacatuba residual sand

Perreira and Fredlund, 1999

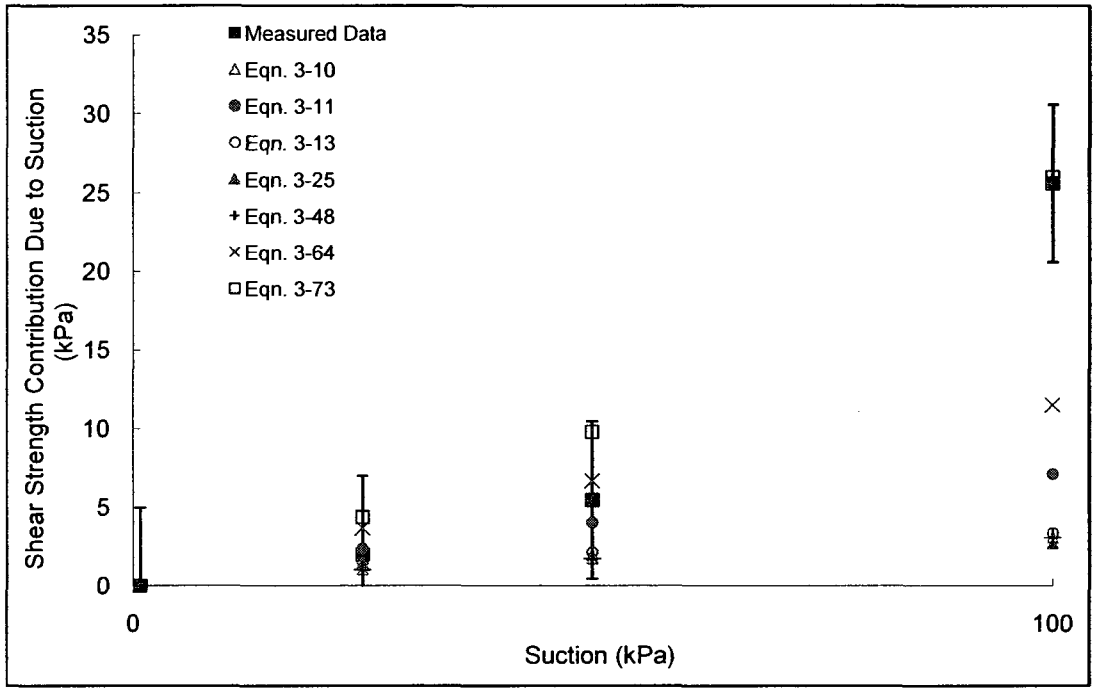

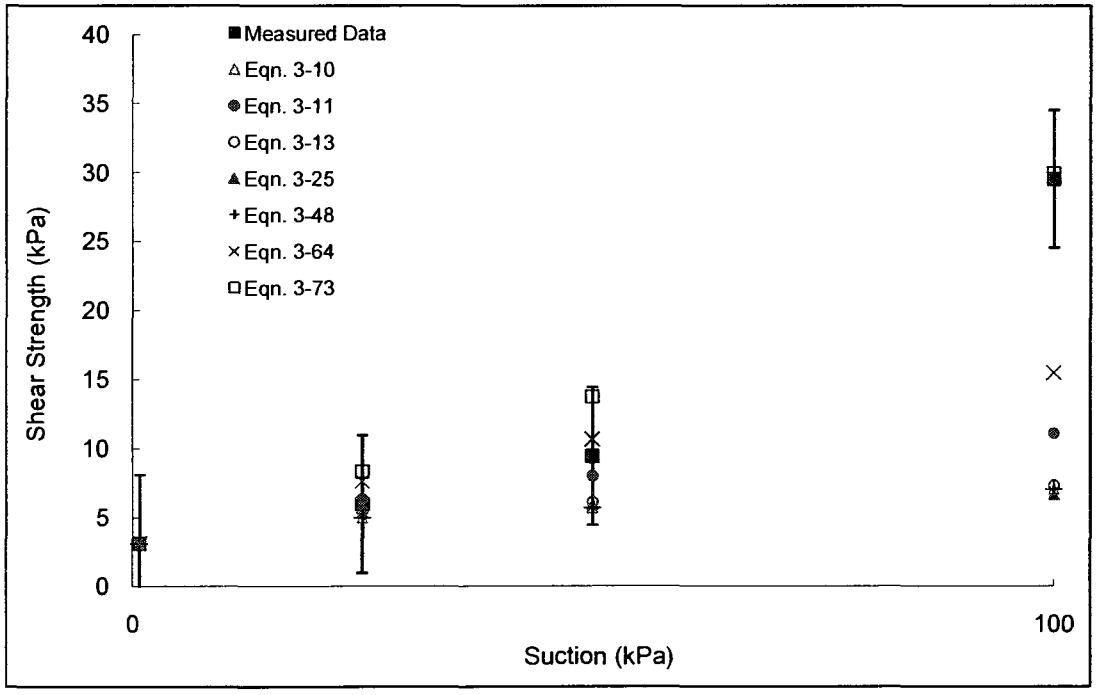

Soil No. 38b

Pacatuba residual sand

Perreira and Fredlund, 1999

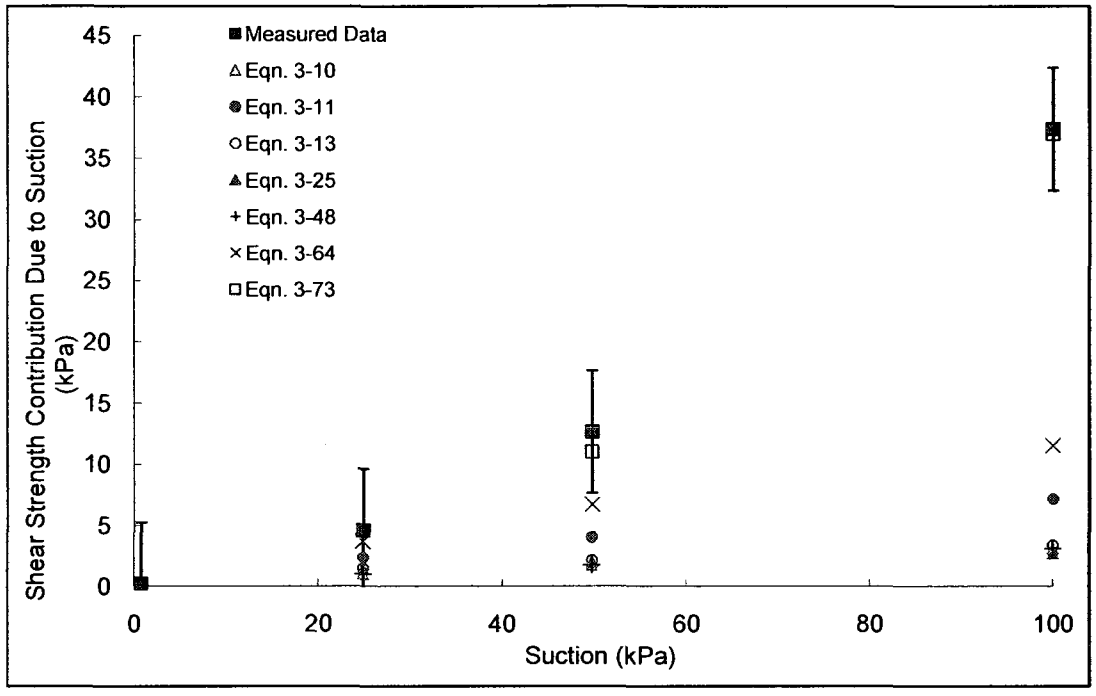

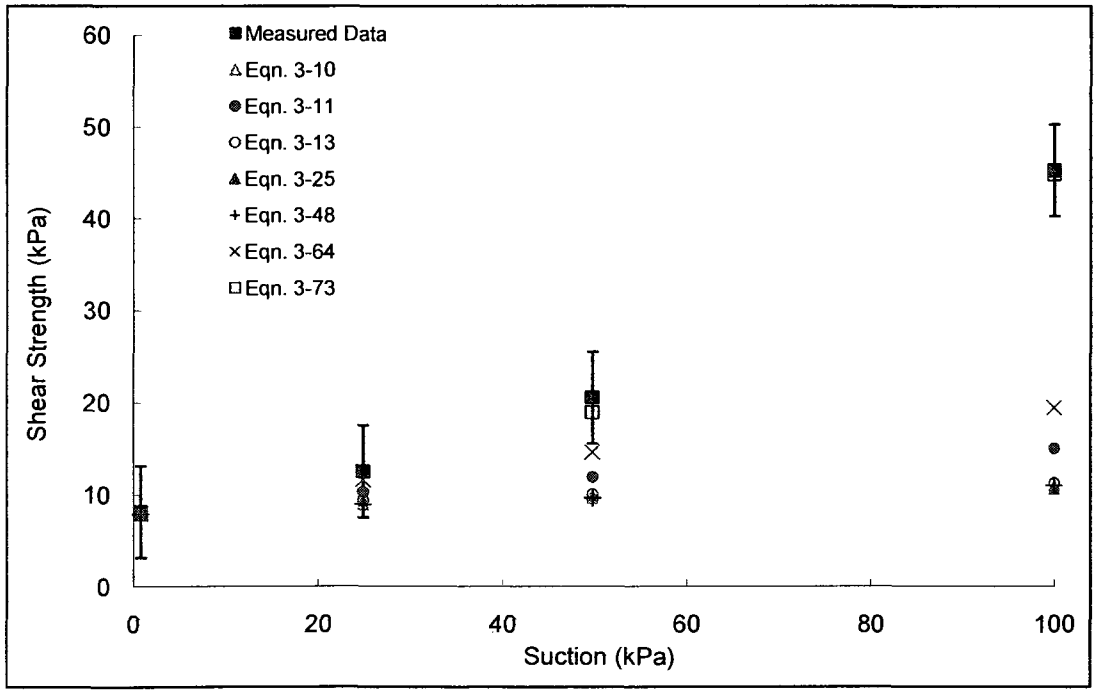

Soil No. 38c

Pacatuba residual sand

Perreira and Fredlund, 1999

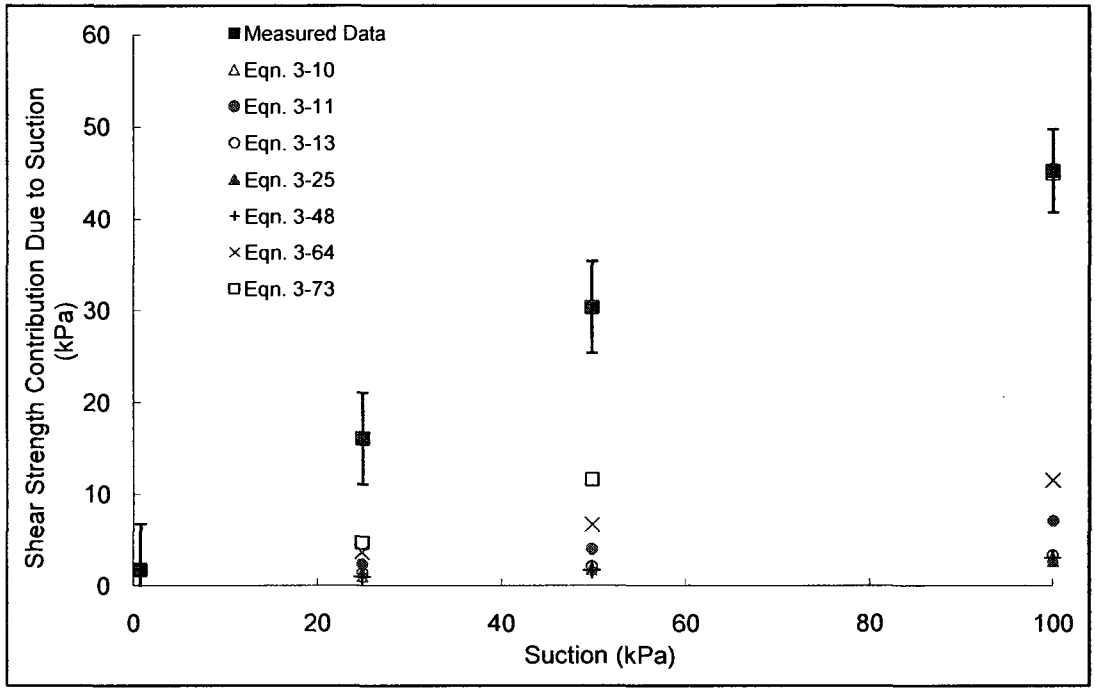

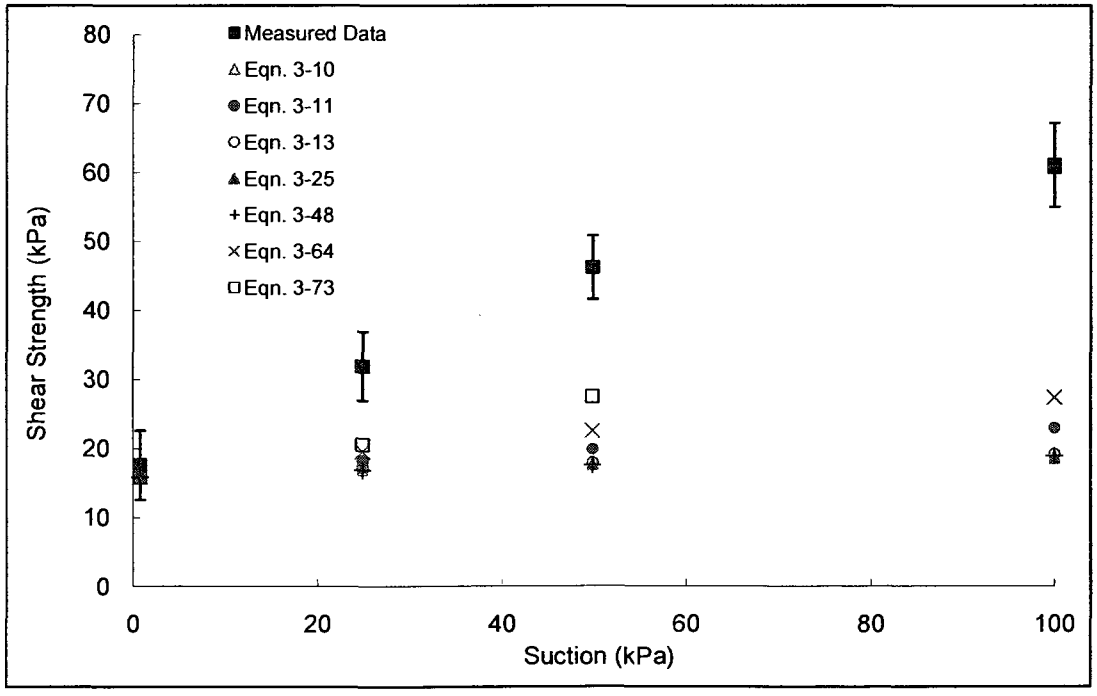

Soil No. 39

Ningxia soil

Xu and Sun, 2001; Xu, 2004

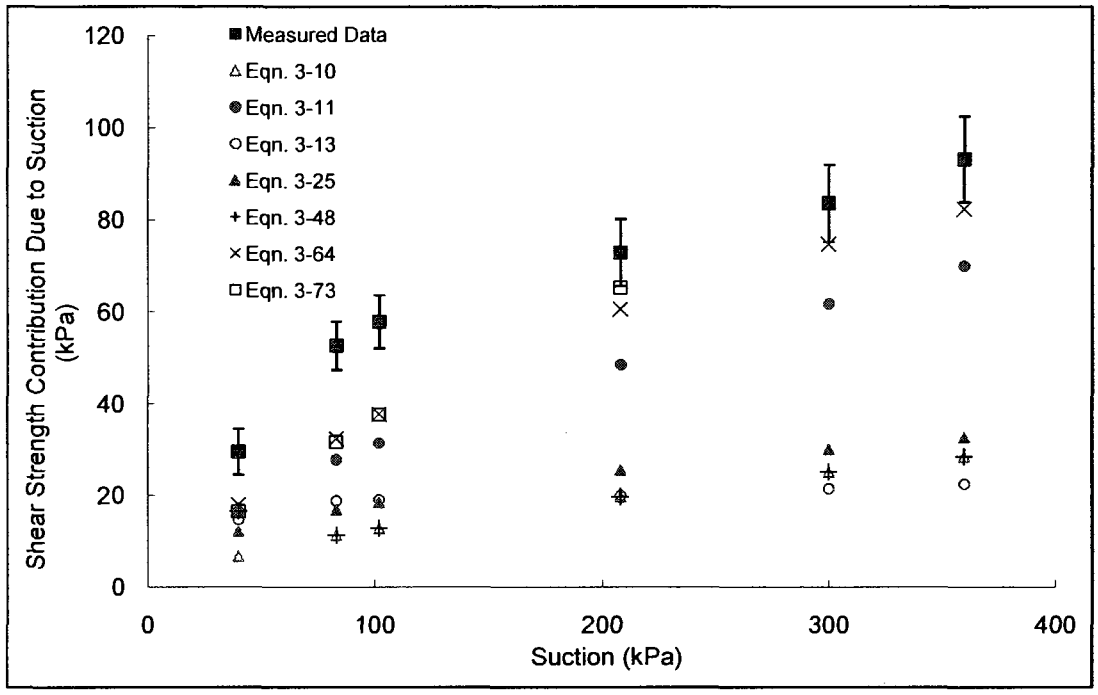

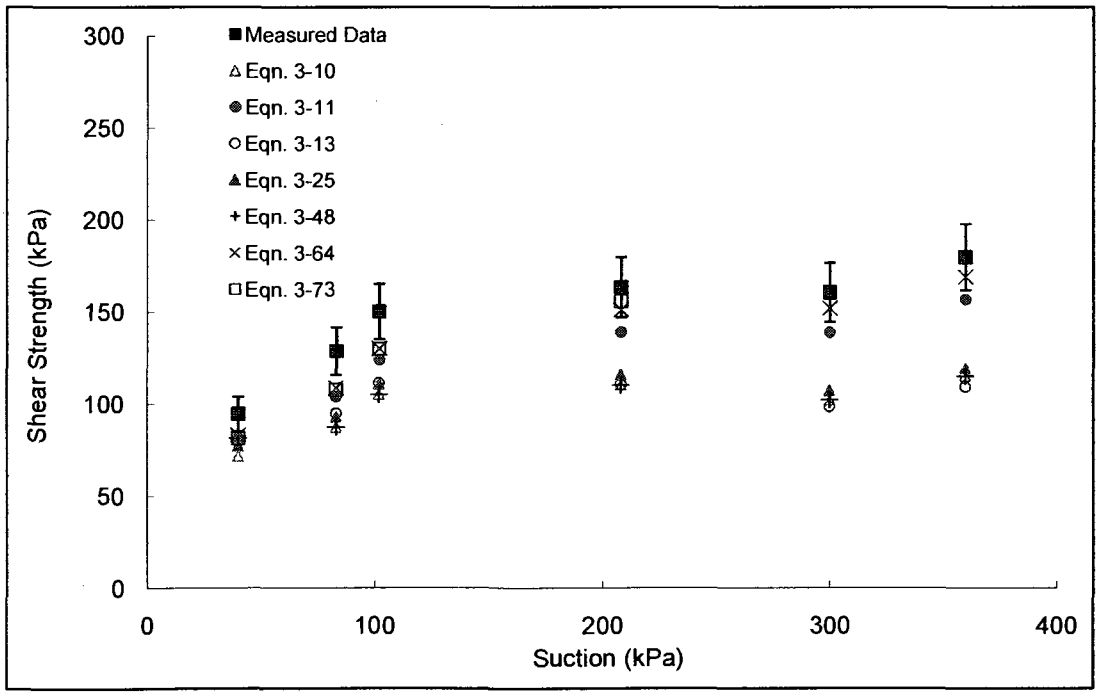

Soil No. 2

Madrid grey clay

Escario and Saez, 1986; Escario and Juca, 1989

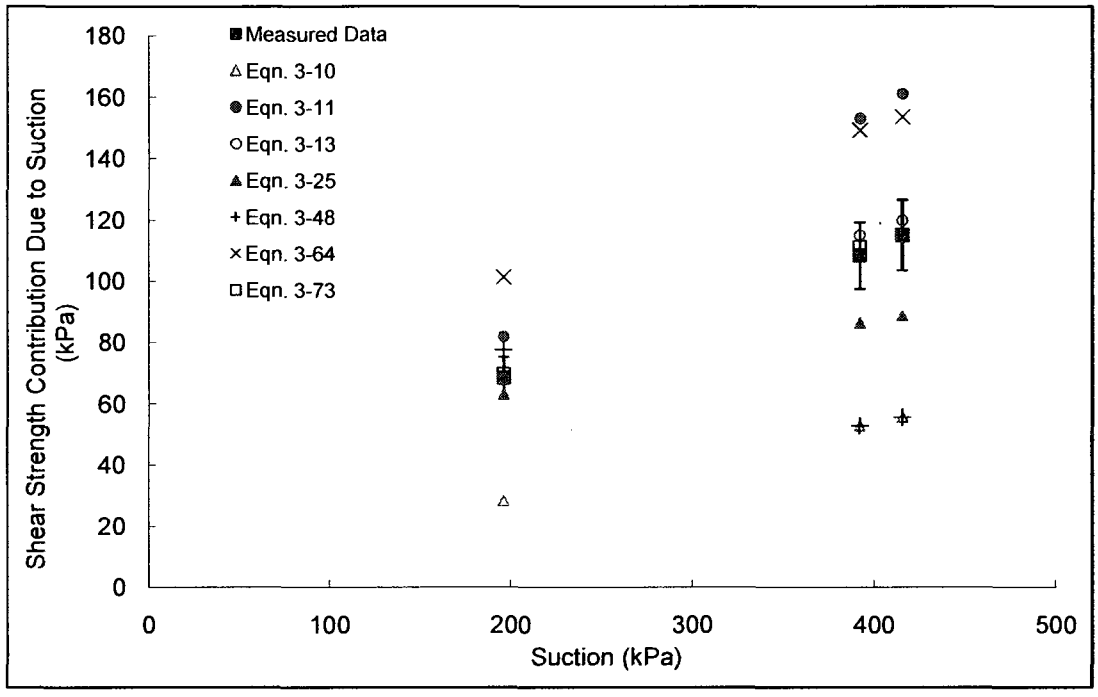

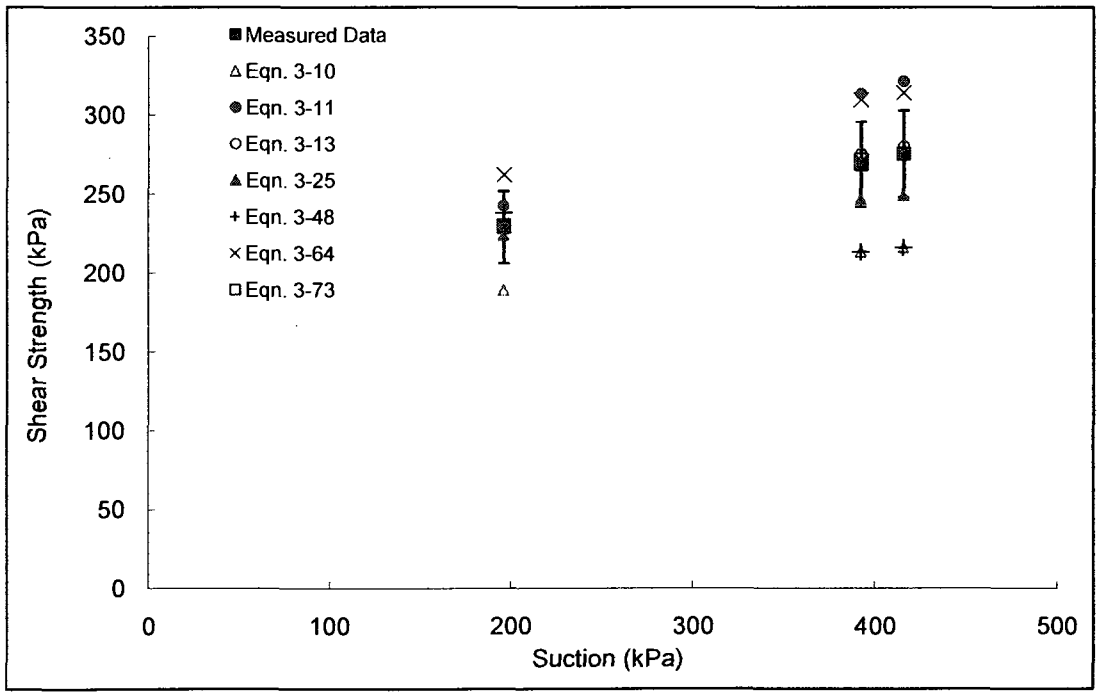

Soil No. 3a

Grey clay sand

Escario and Saez, 1986; Escario and Juca, 1989

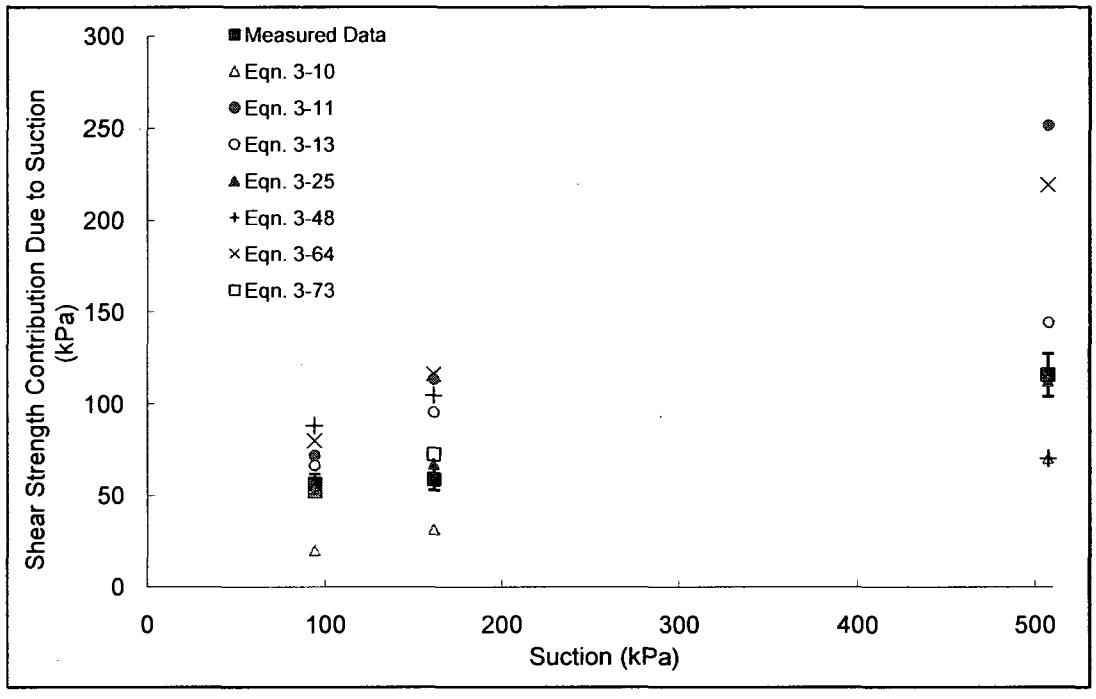

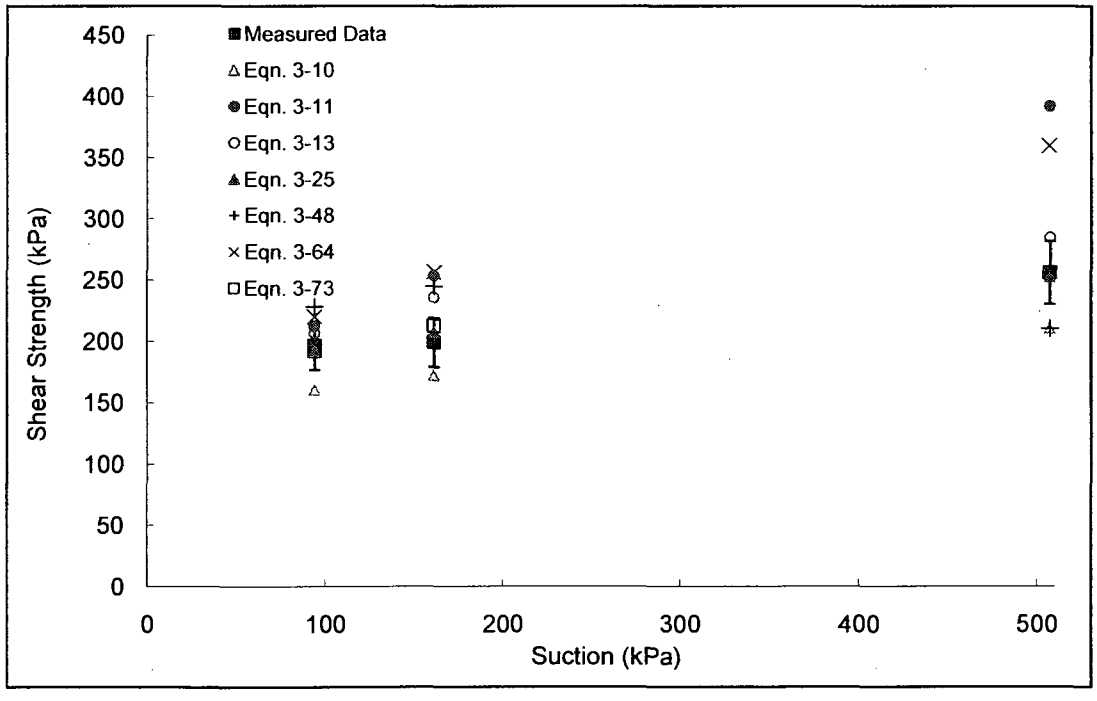

Soil No. 3b

Grey clay sand

Escario and Saez, 1986; Escario and Juca, 1989

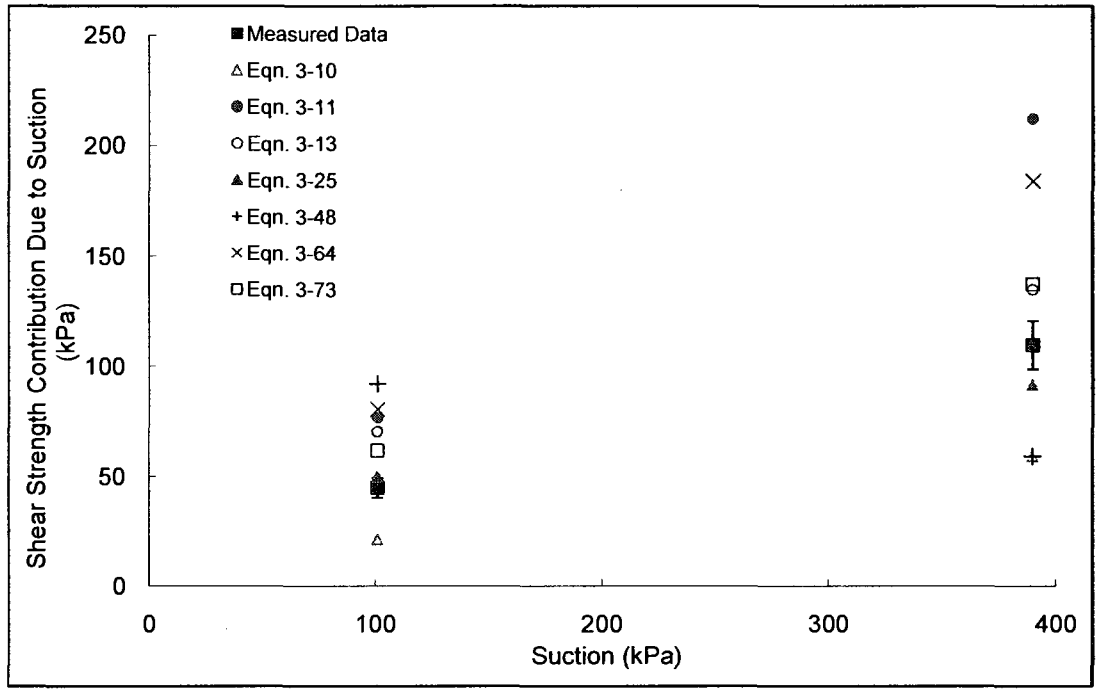

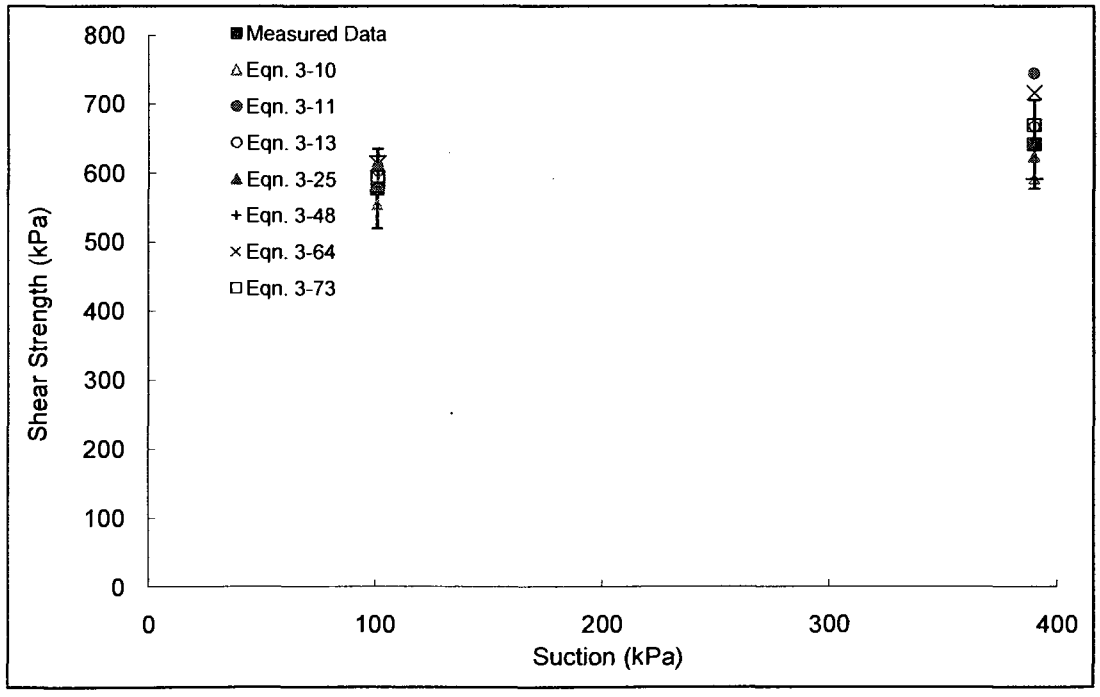

Soil No. 4a

Glacial till, optimum

Vanapalli, Fredlund, Pufahl and Clifton, 1996

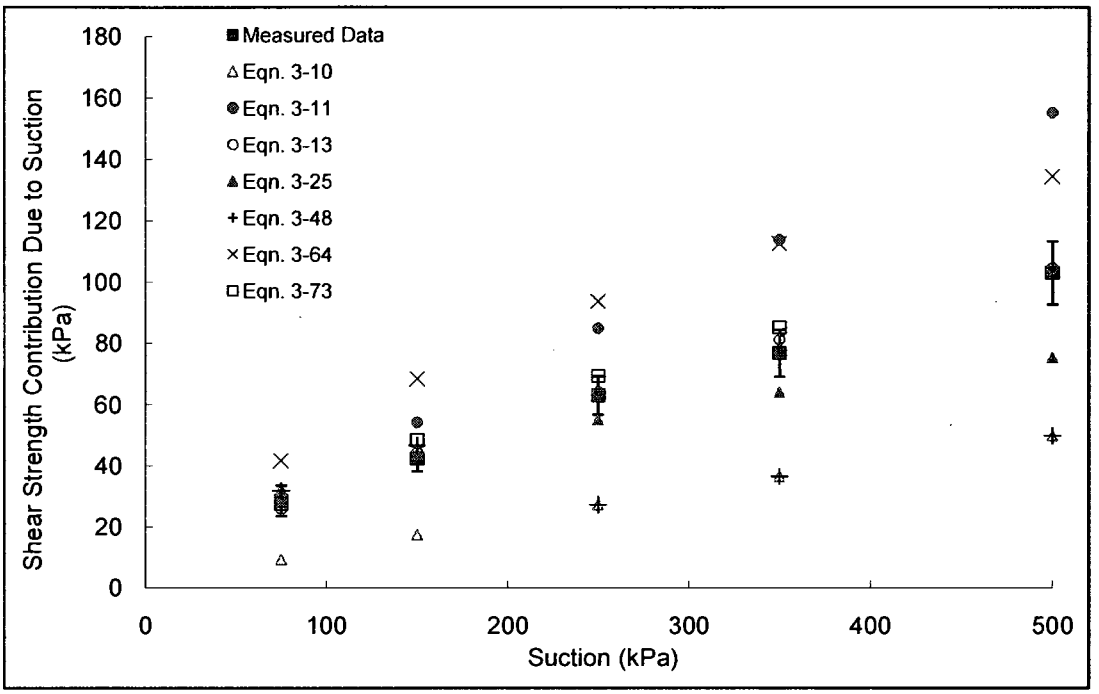

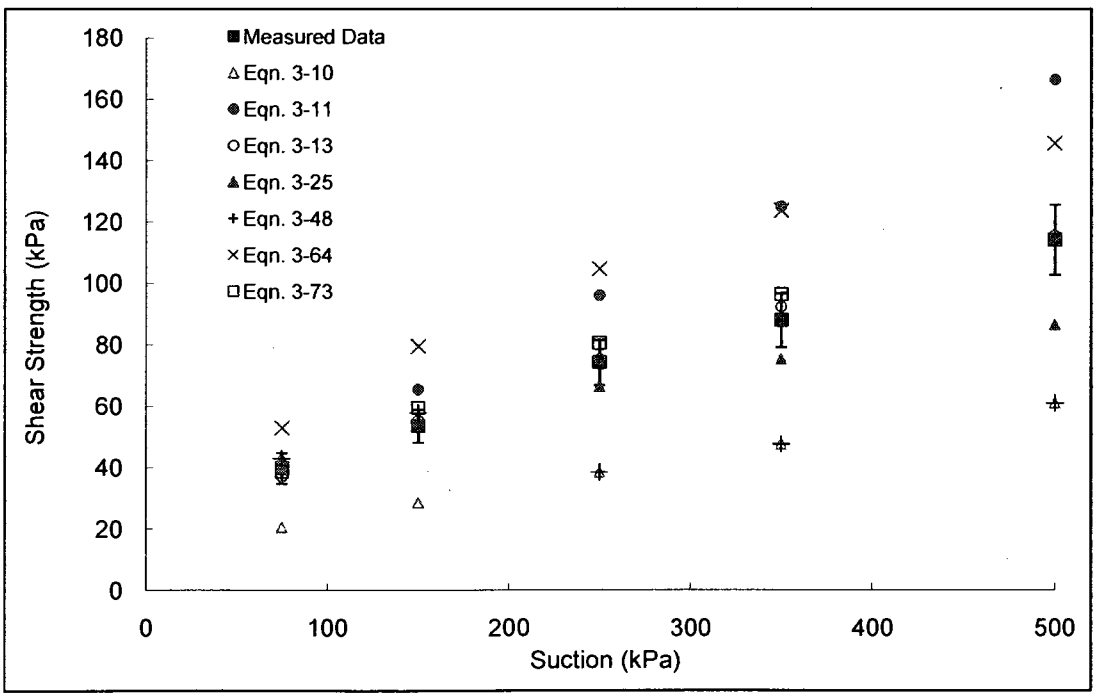

Soil No. 4b

Glacial till,optimum

Vanapalli, Fredlund, Pufahl and Clifton, 1996

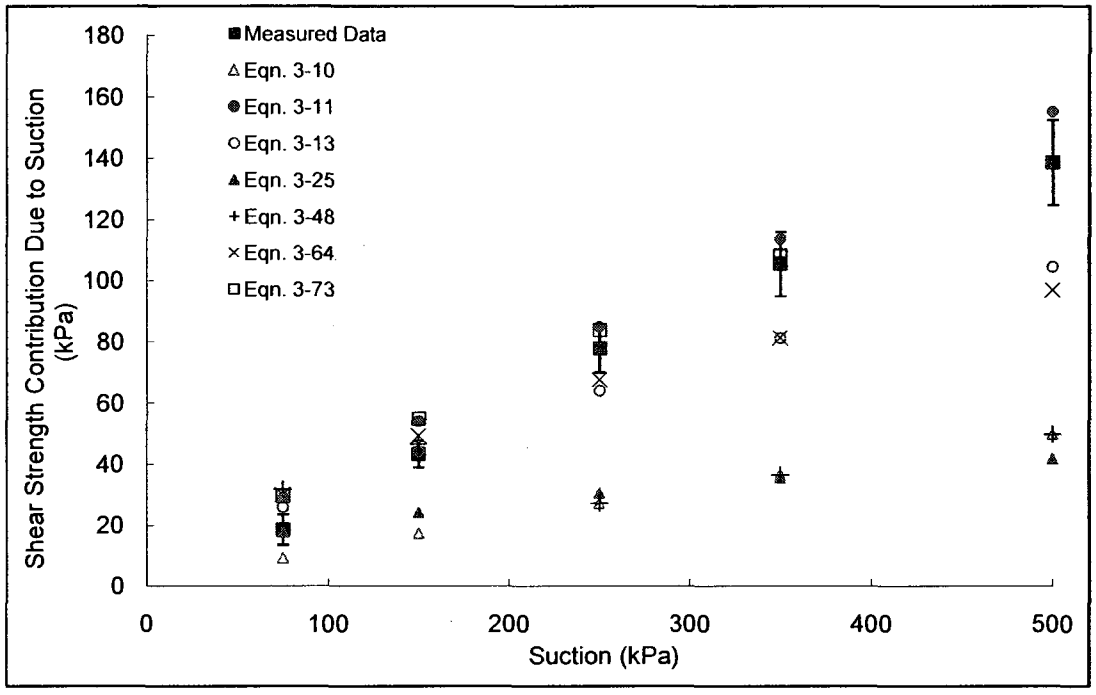

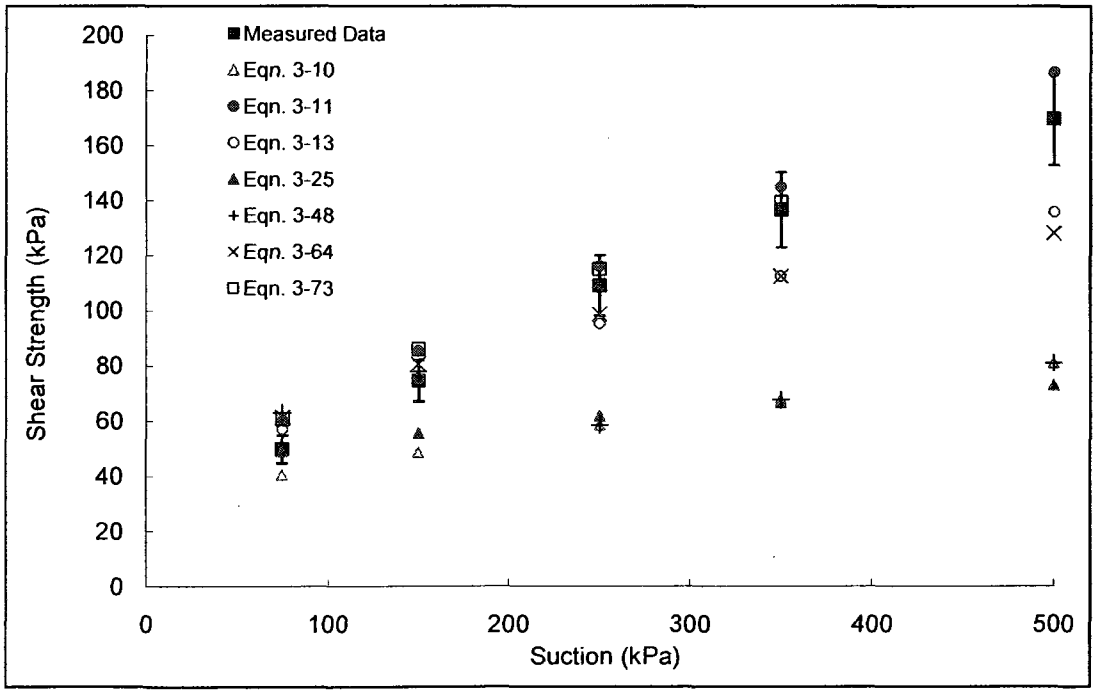

Soil No. 4c

Glacial till,optimum

Vanapalli, Fredlund, Pufahl and Clifton, 1996

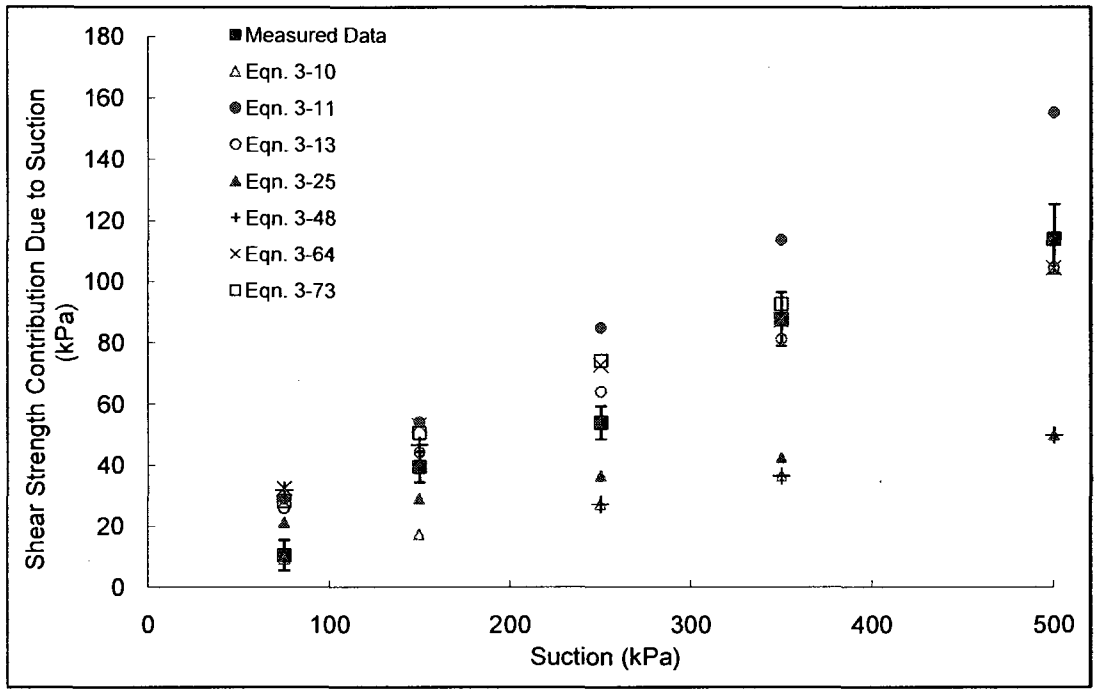

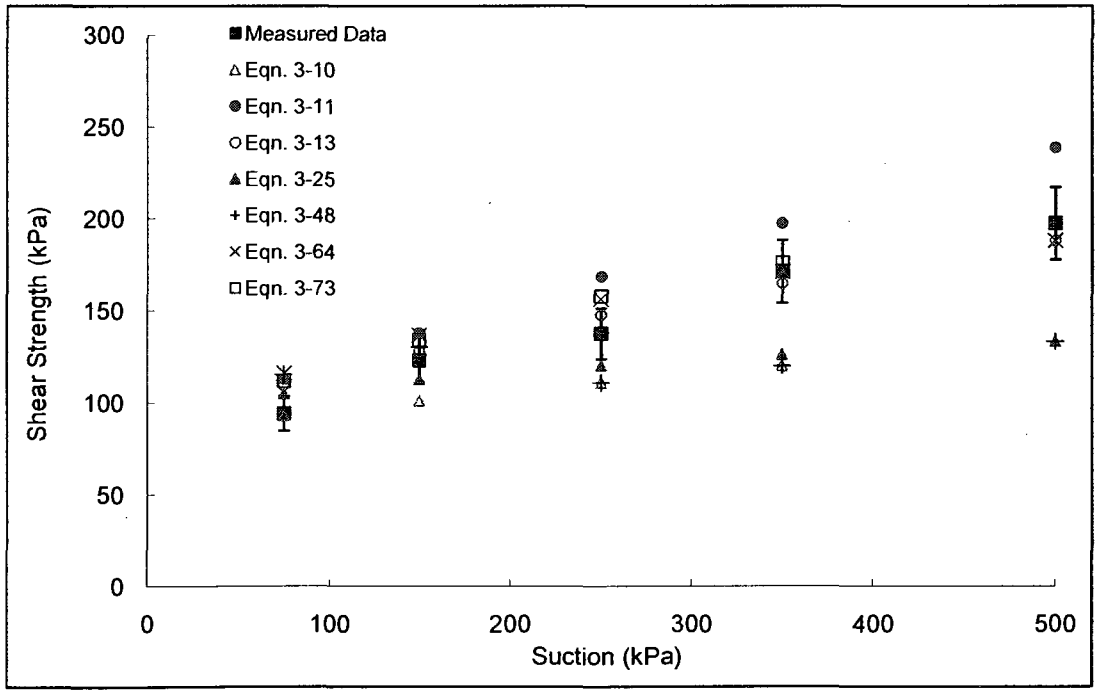

Soil No. 5

Botkin Silt

Vanapalli, Wright and Fredlund, 1999

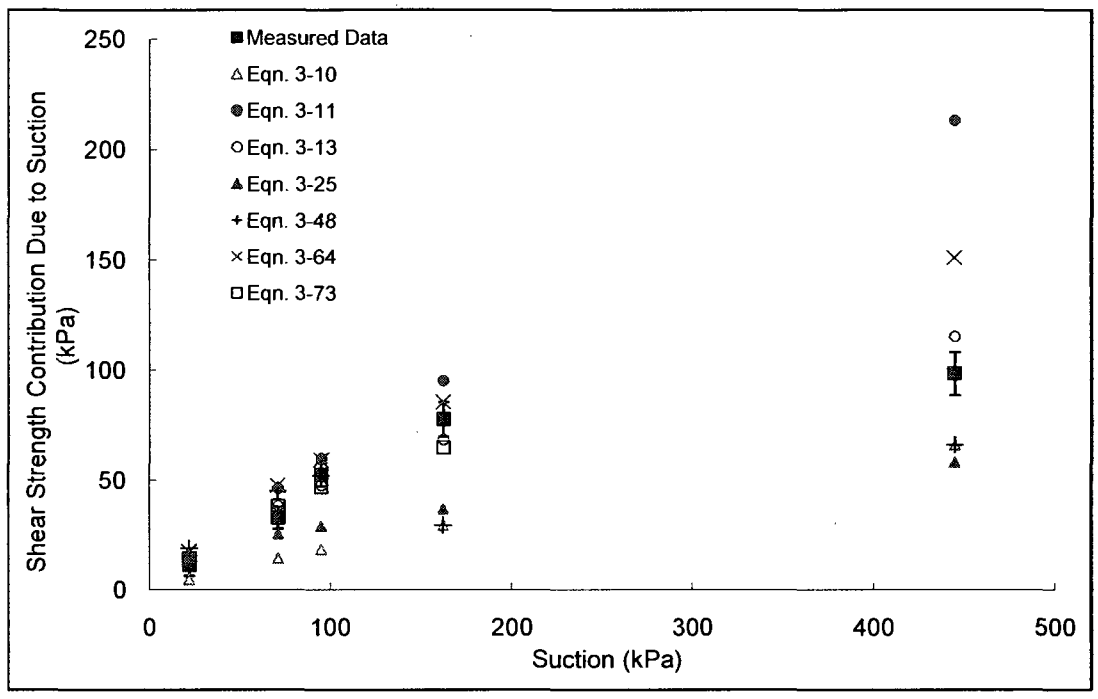

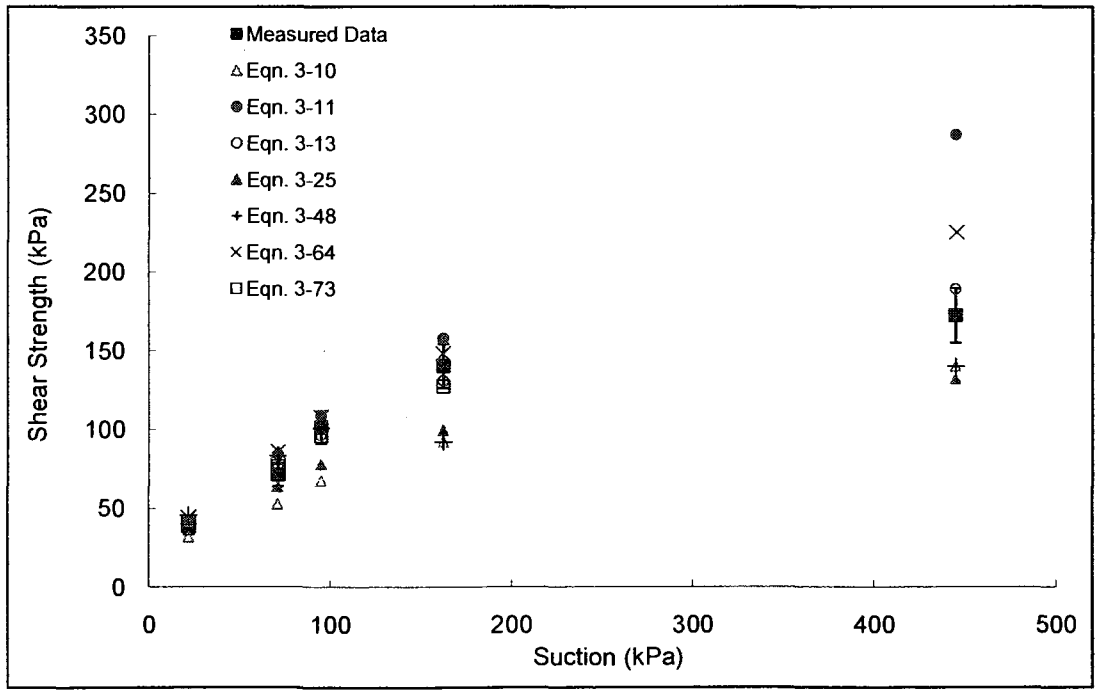

Soil No. 6a

Low-density Dhanauri clay

Satija, 1978

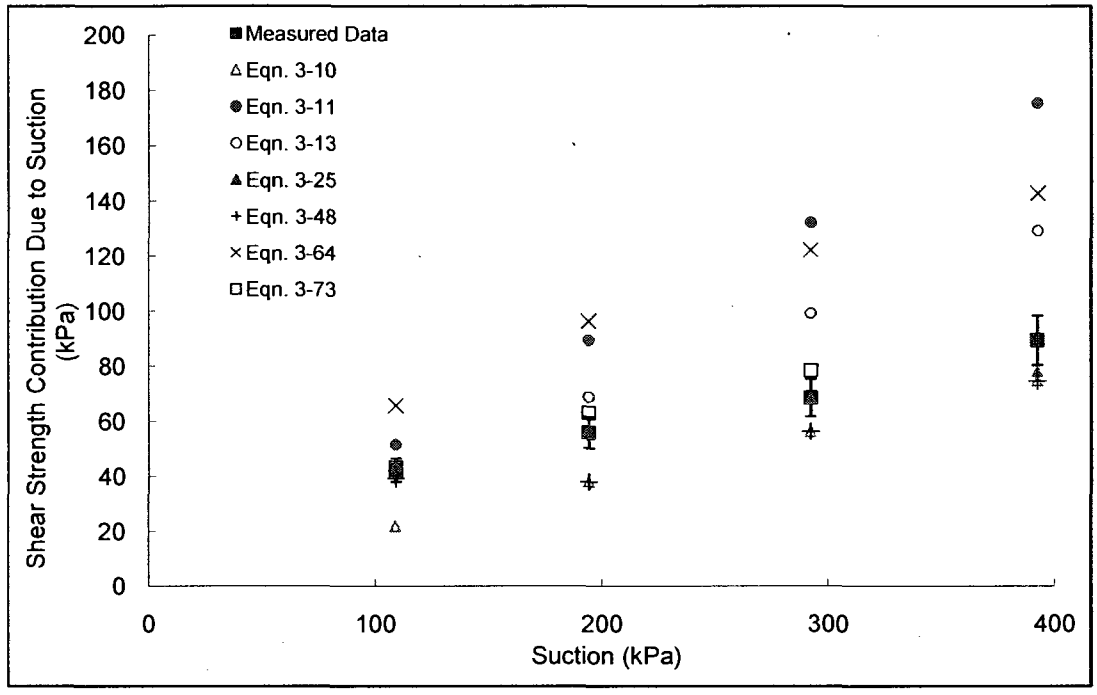

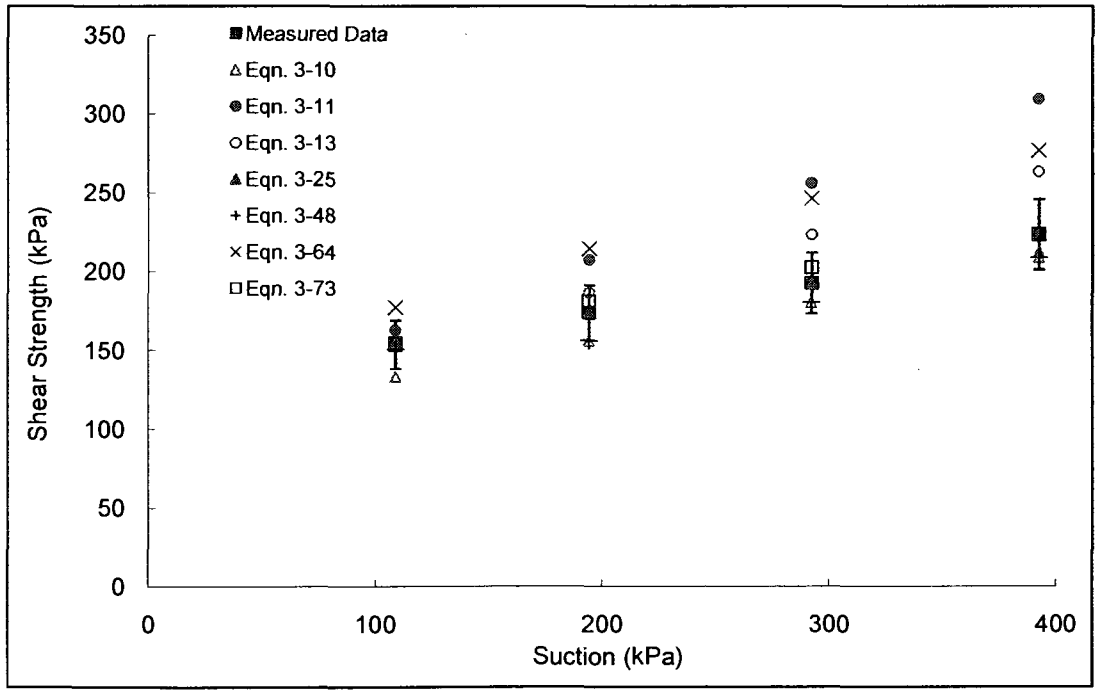

Soil No. 6b

Low-density Dhanauri clay

Satija, 1978

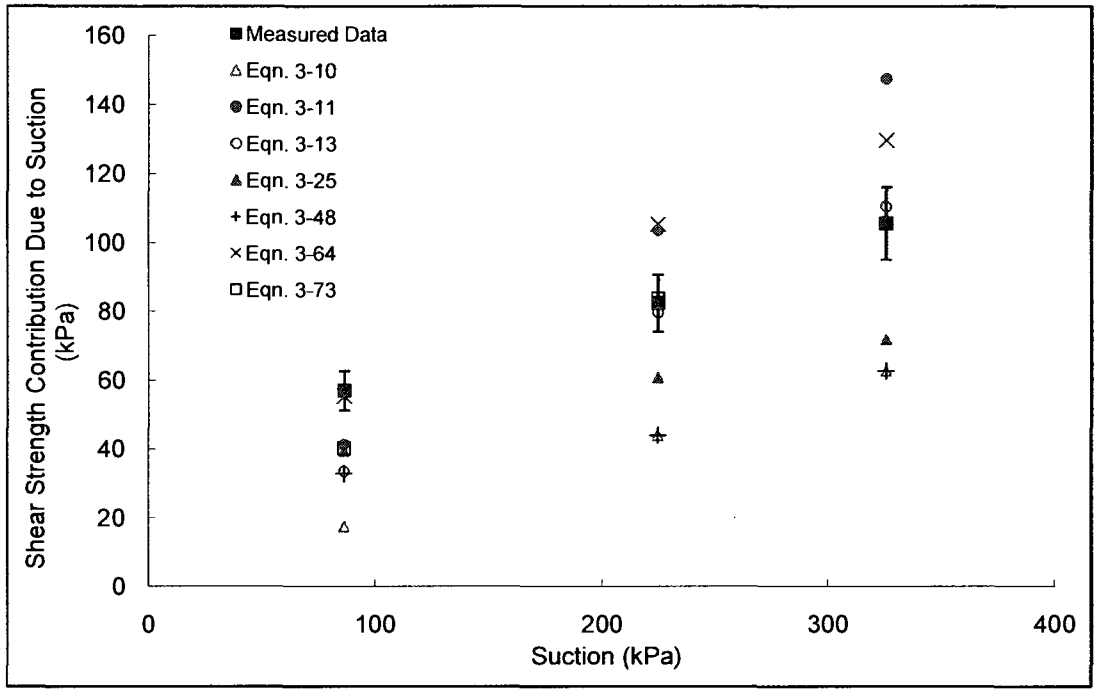

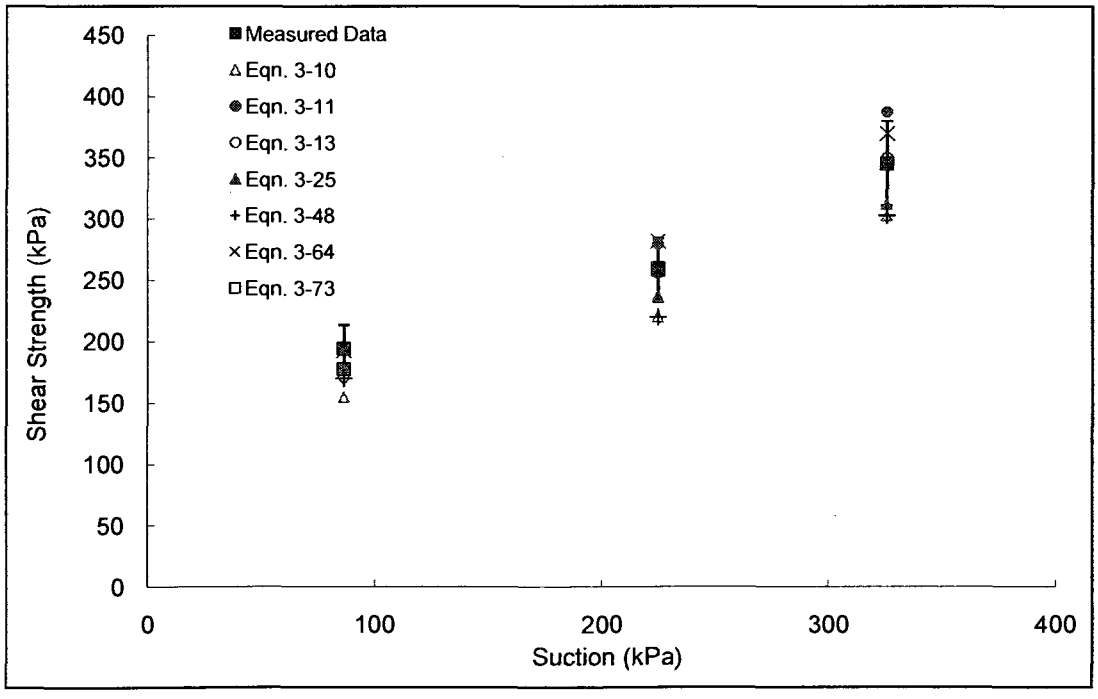

Soil No. 6c

Low-density Dhanauri clay

Satija, 1978

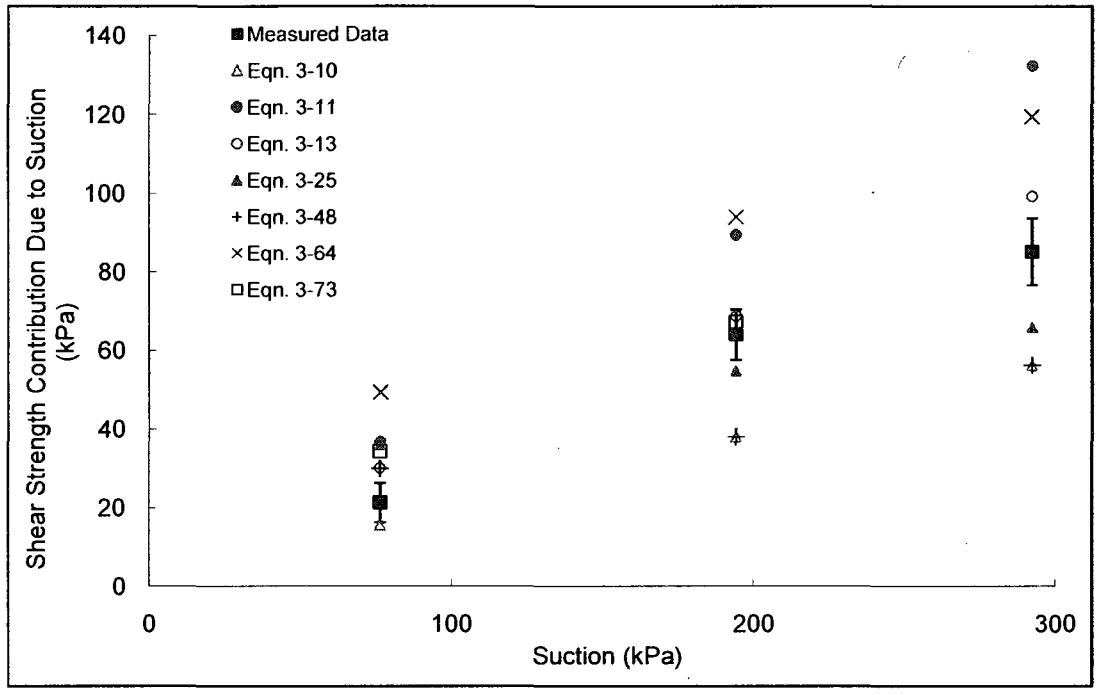

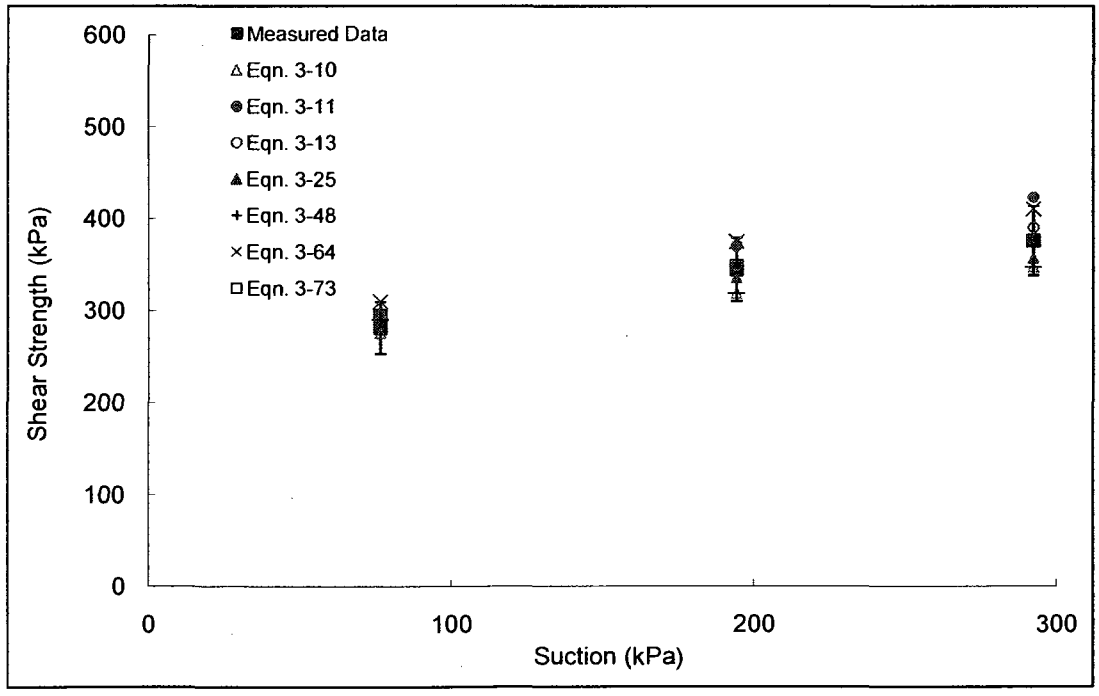

Soil No. 6d

Low-density Dhanauri clay

Satija, 1978

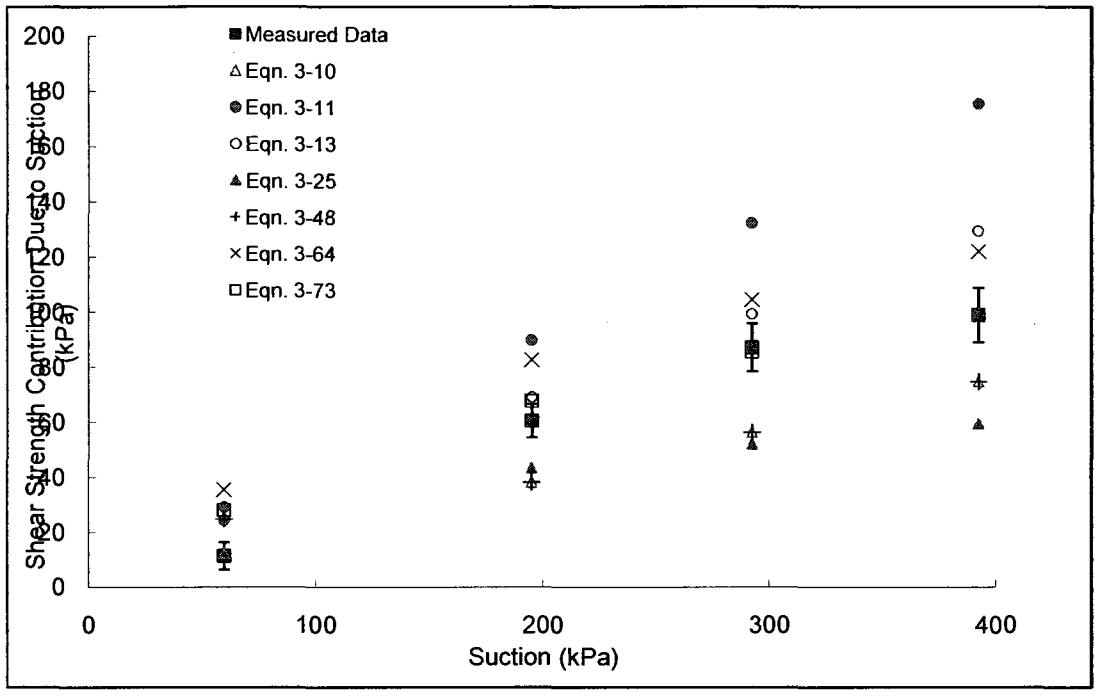

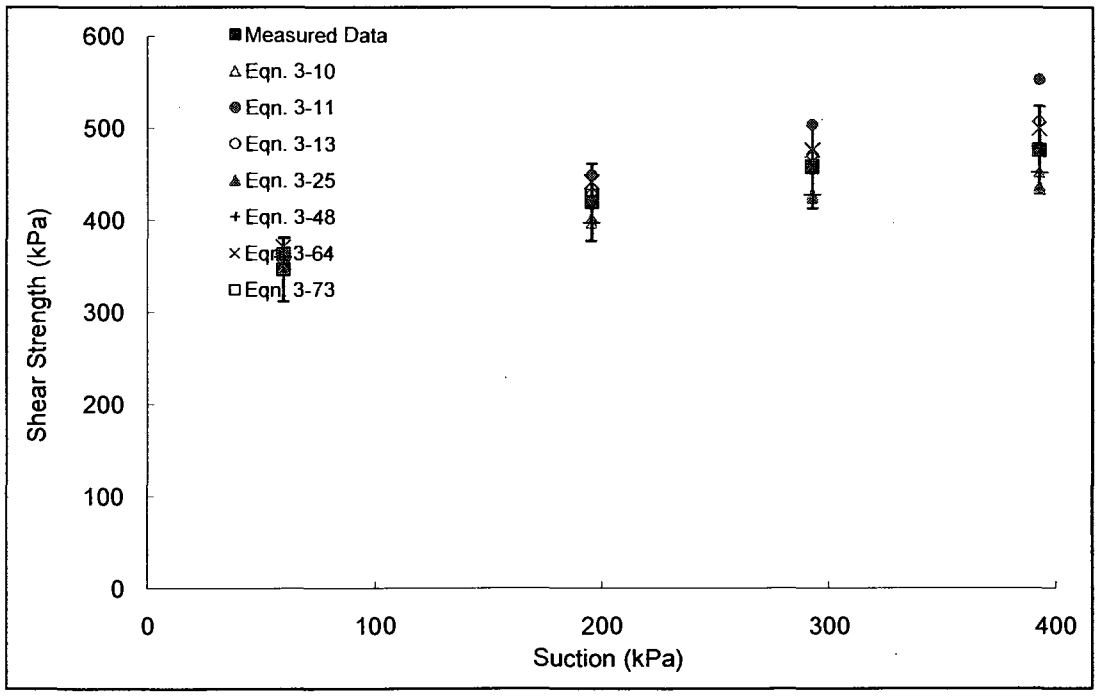

Soil No. 6e

High-density Dhanauri clay

Satija, 1978

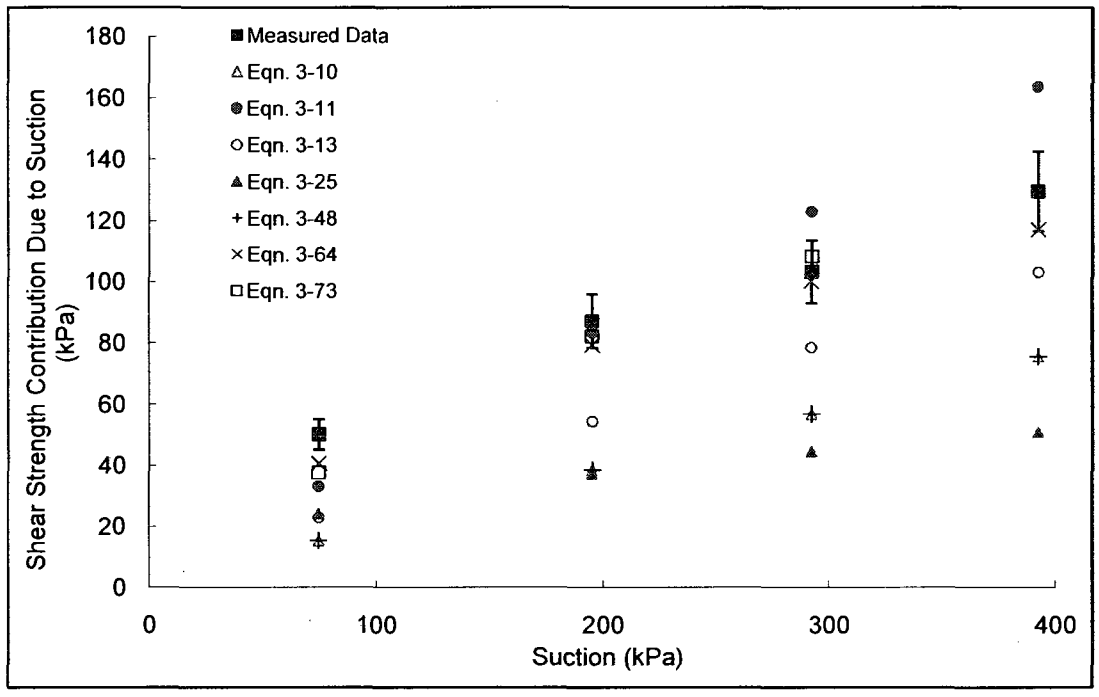

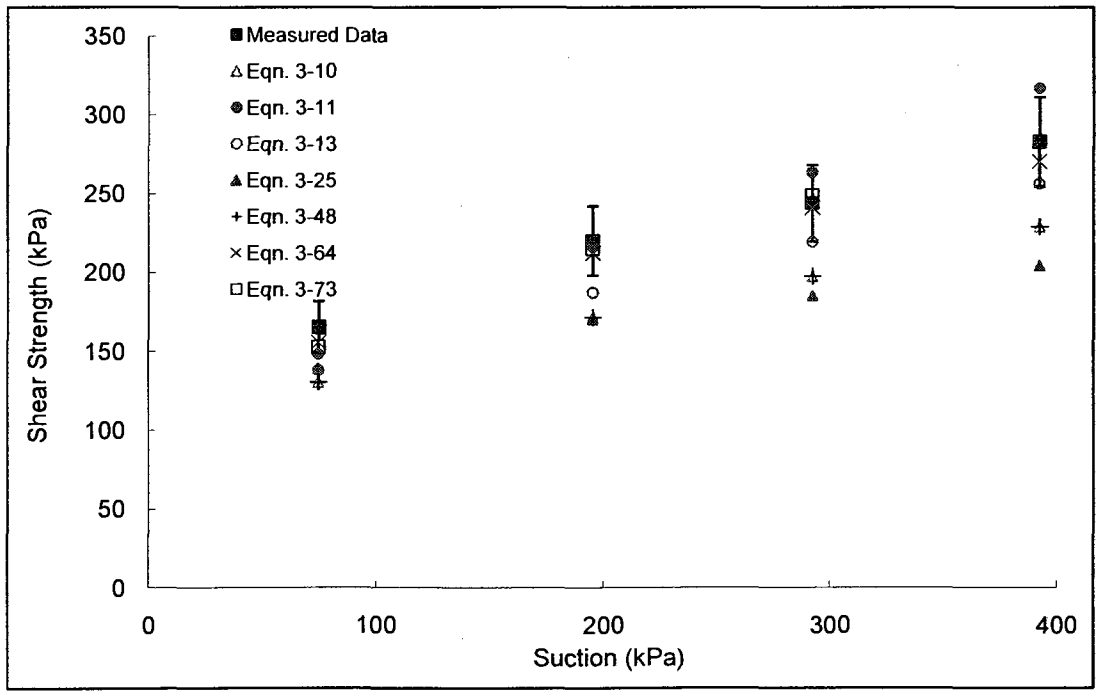

Soil No. 6f

High-density Dhanauri clay

Satija, 1978

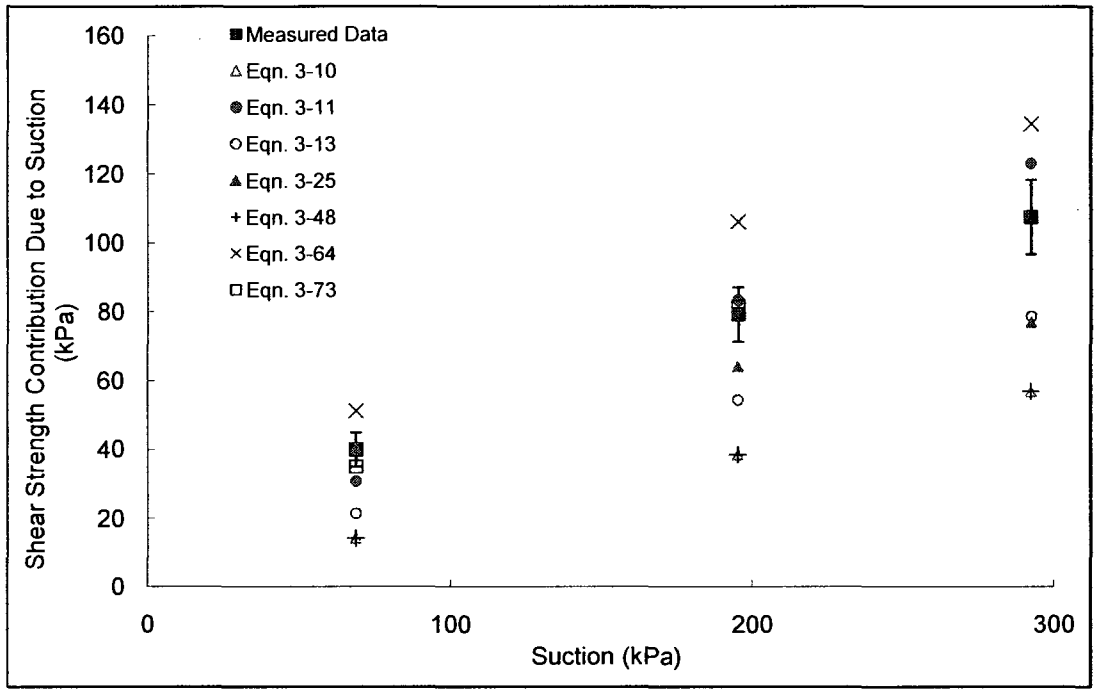

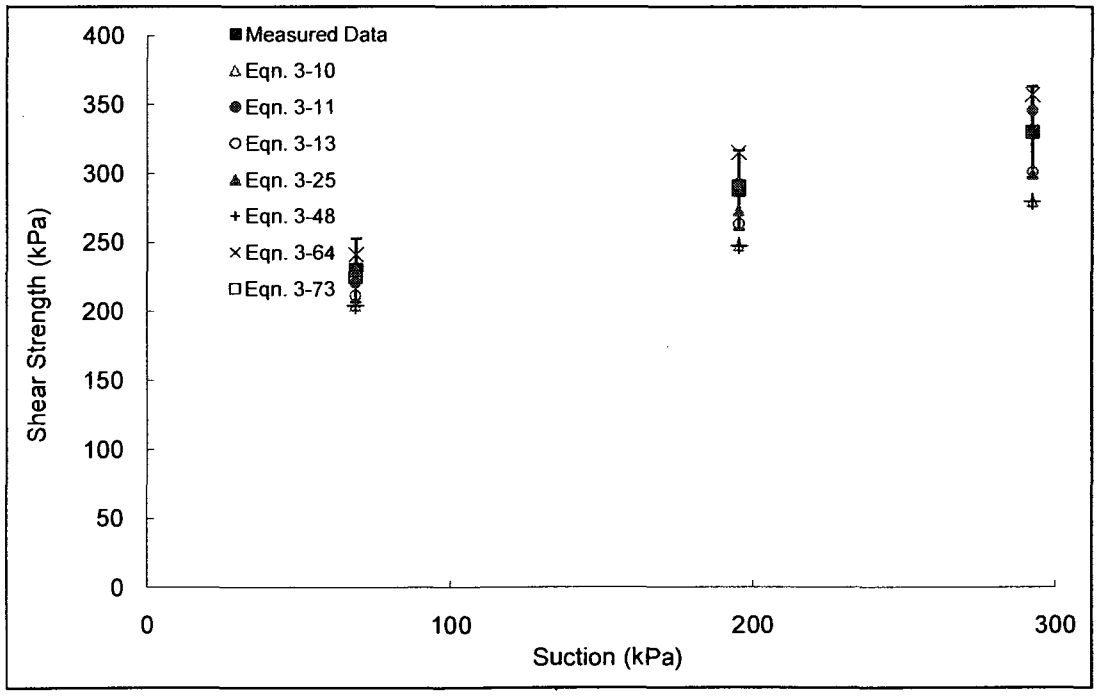

Soil No. 6g

High-density Dhanauri clay

Satija, 1978

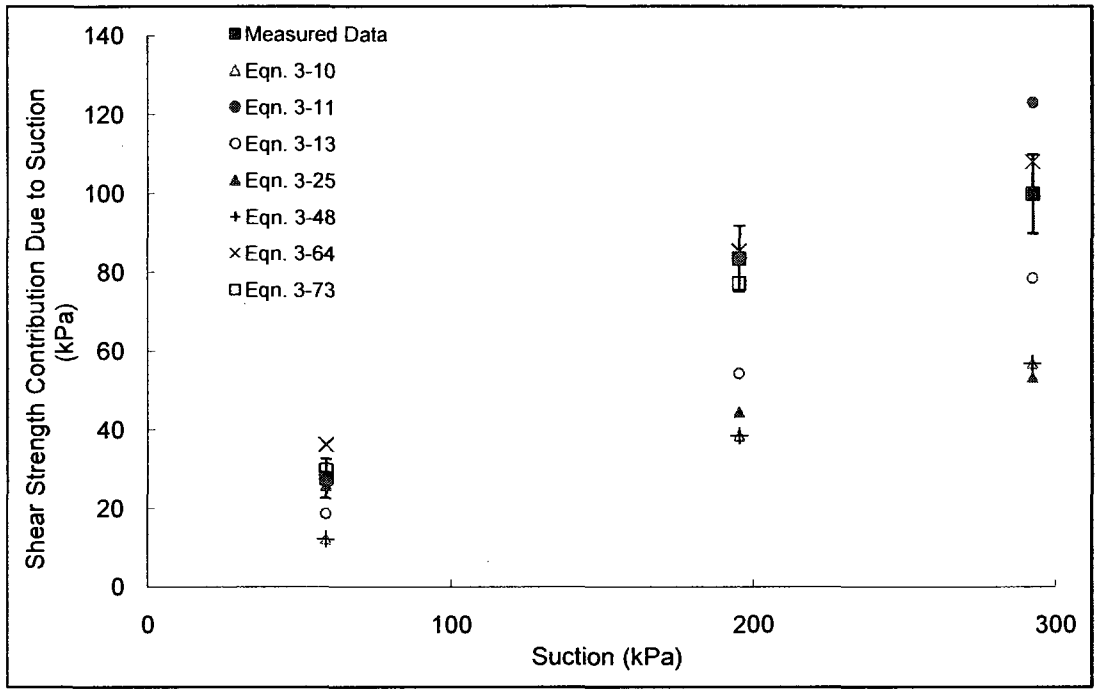

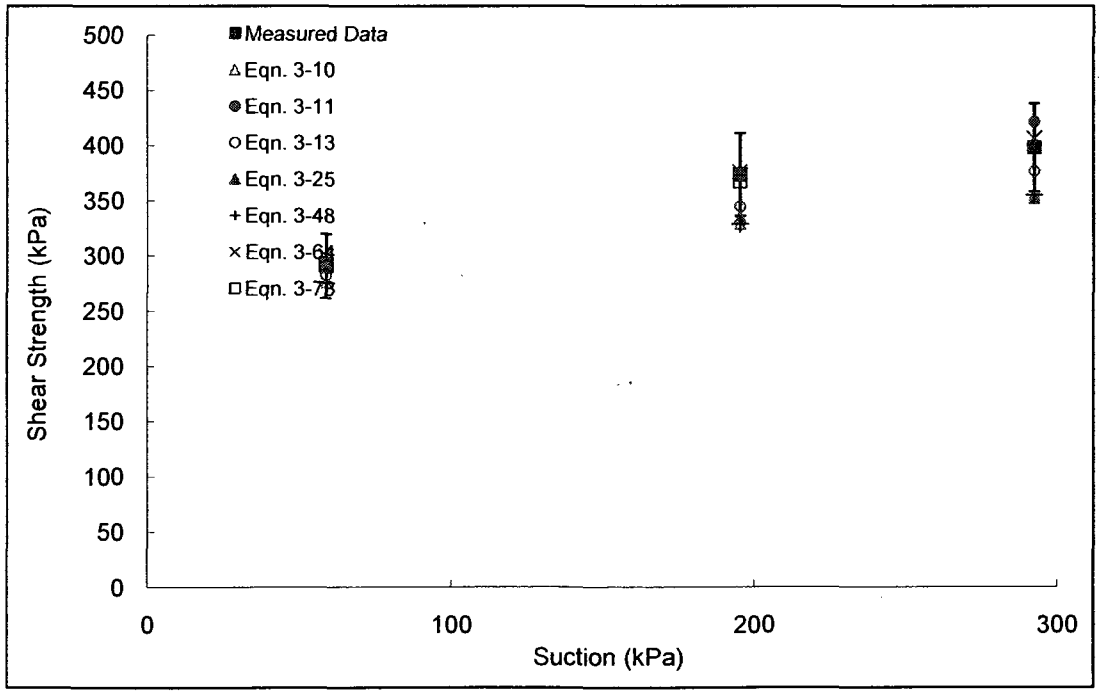

Soil No. 6h

High-density Dhanauri clay

Satija, 1978

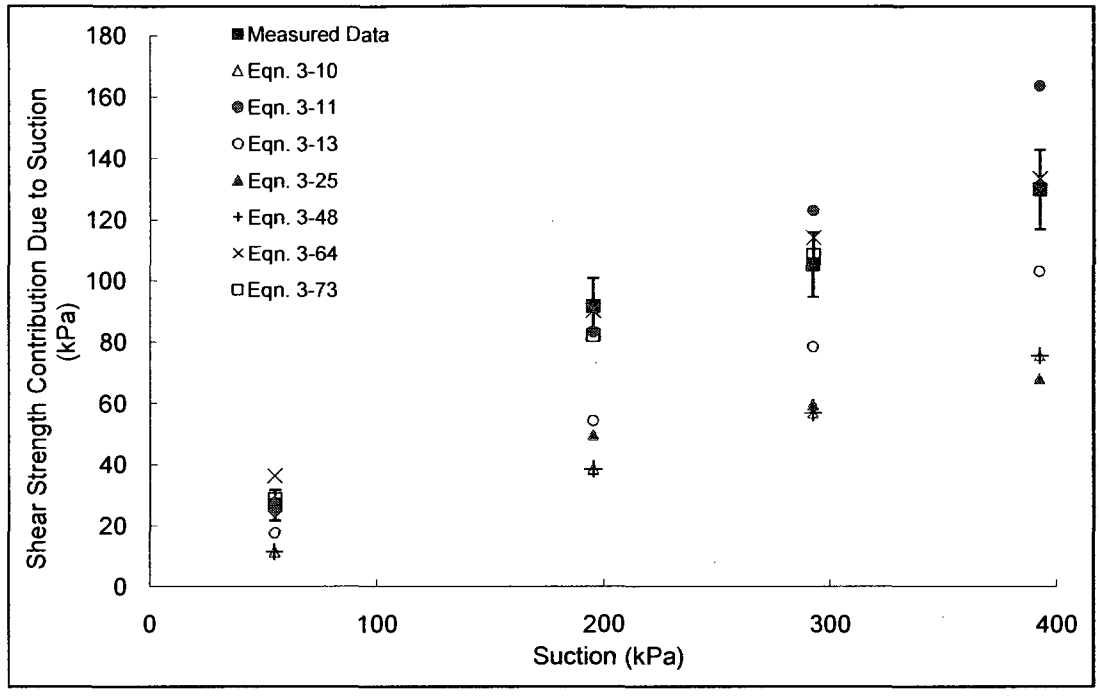

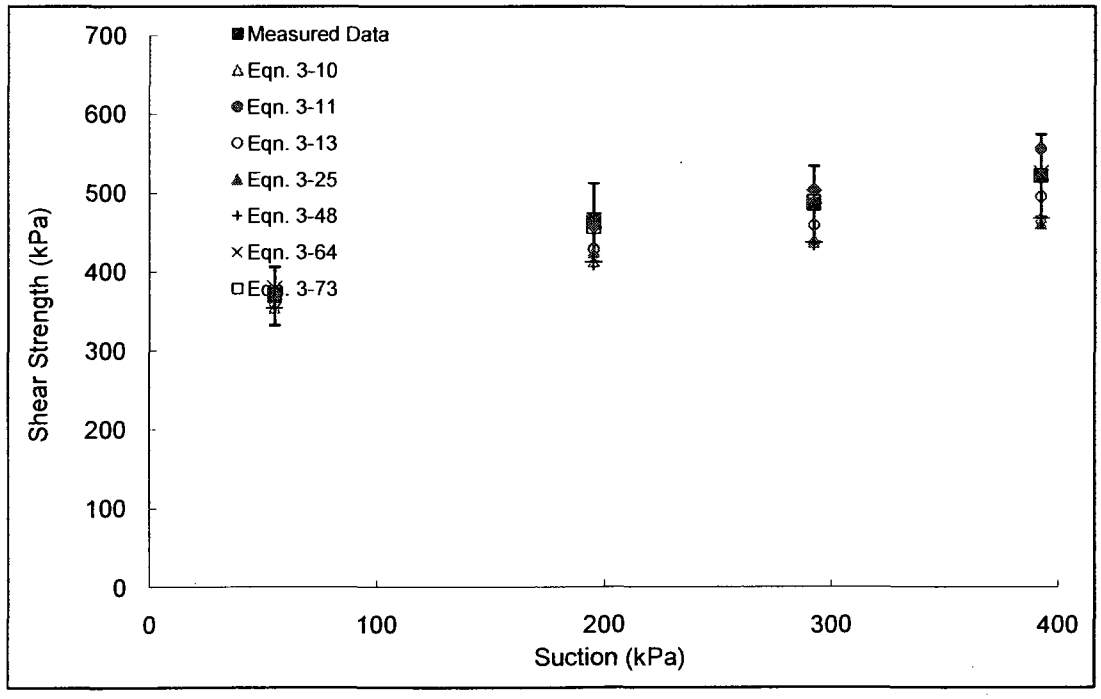

Soil No. 7a

Weathered Granite

Lee, Sung and Cho, 2005

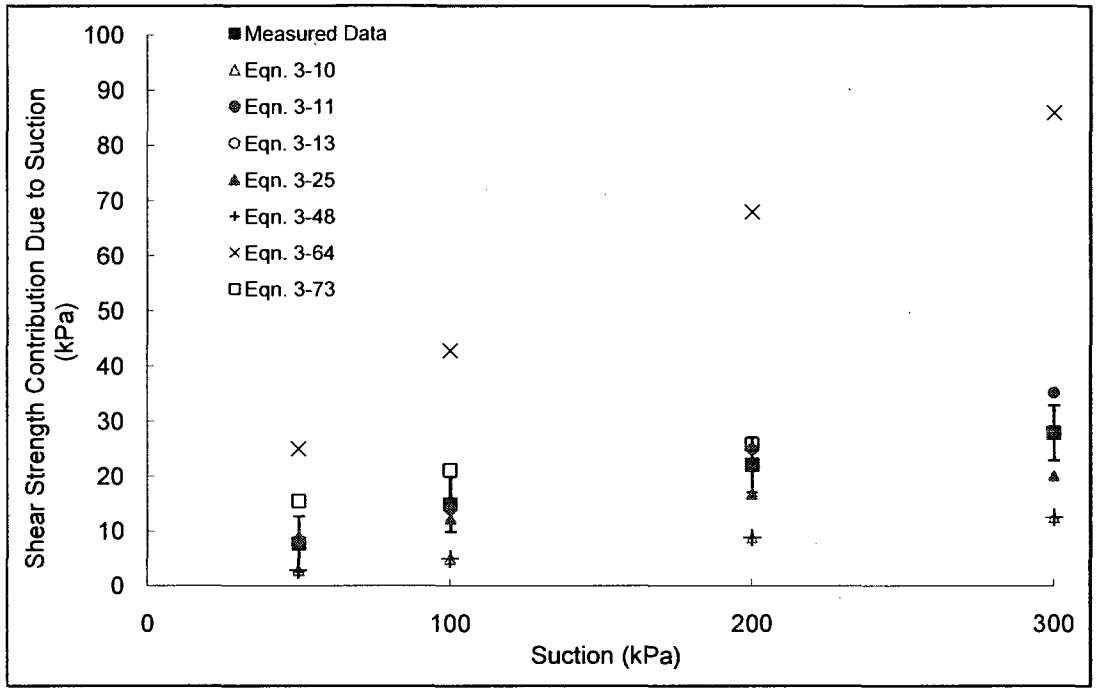

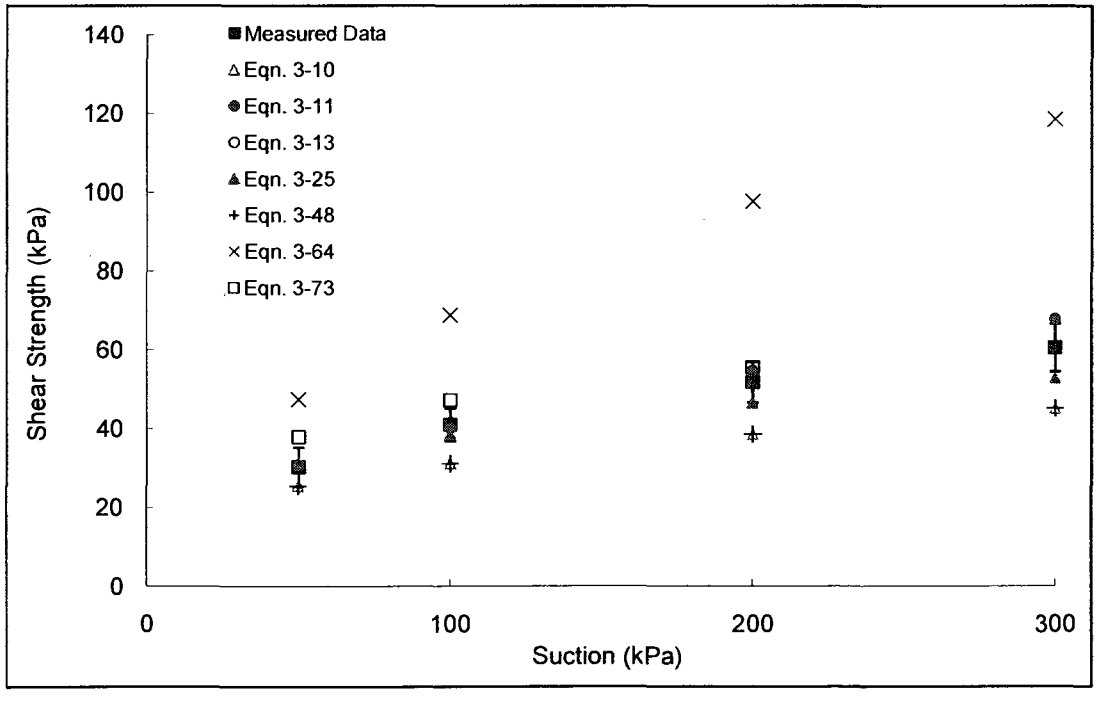

Soil No. 7b

Weathered Granite

Lee, Sung and Cho, 2005

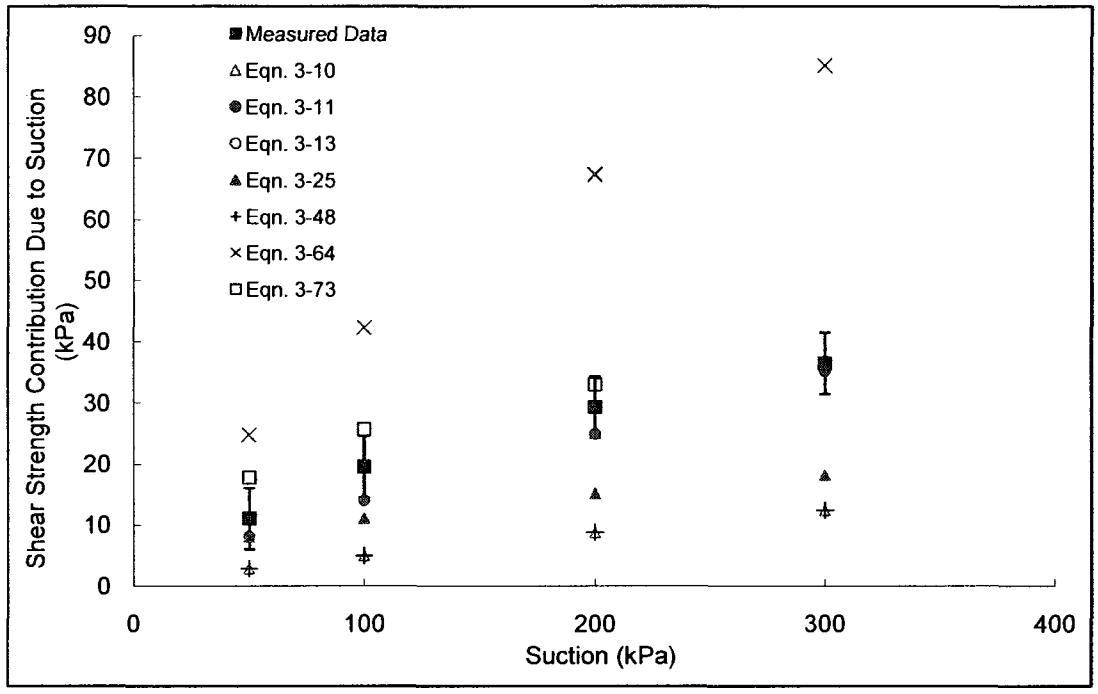

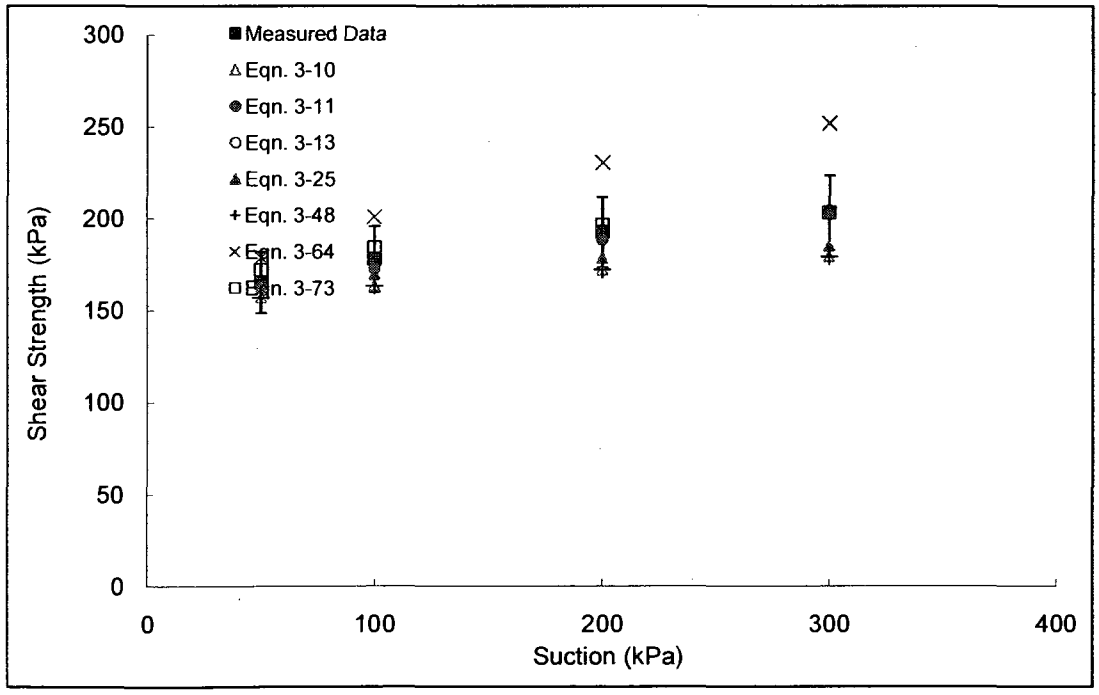

Soil No. 7c

Weathered Granite

Lee, Sung and Cho, 2005

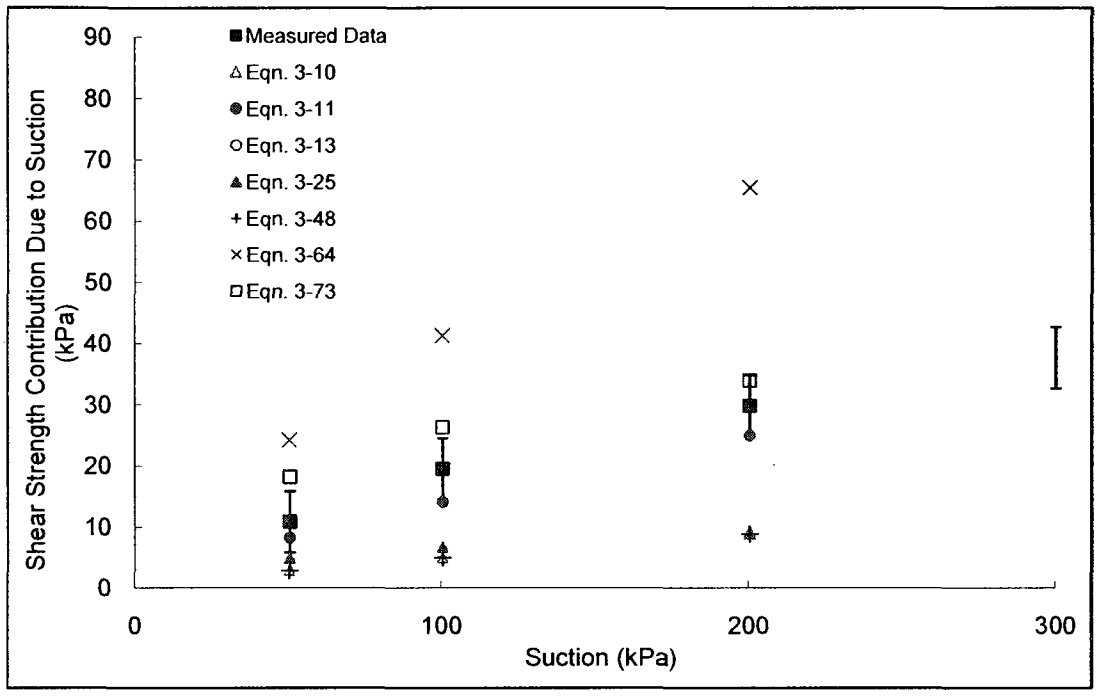

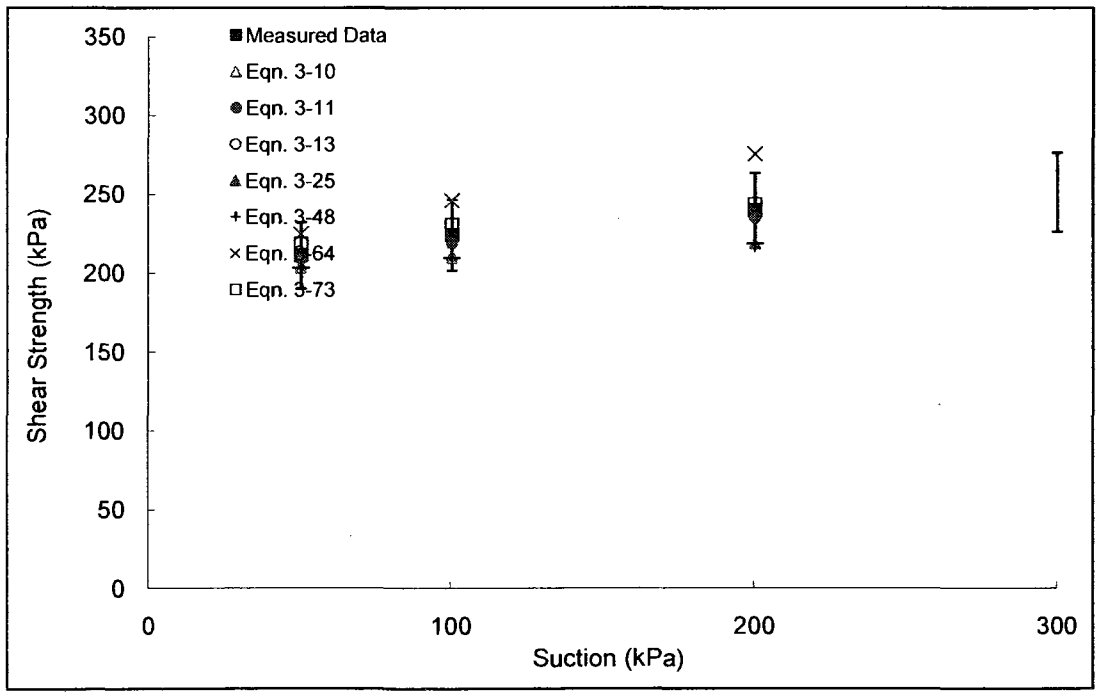

Soil No. 7d

Weathered Granite

Lee, Sung and Cho, 2005

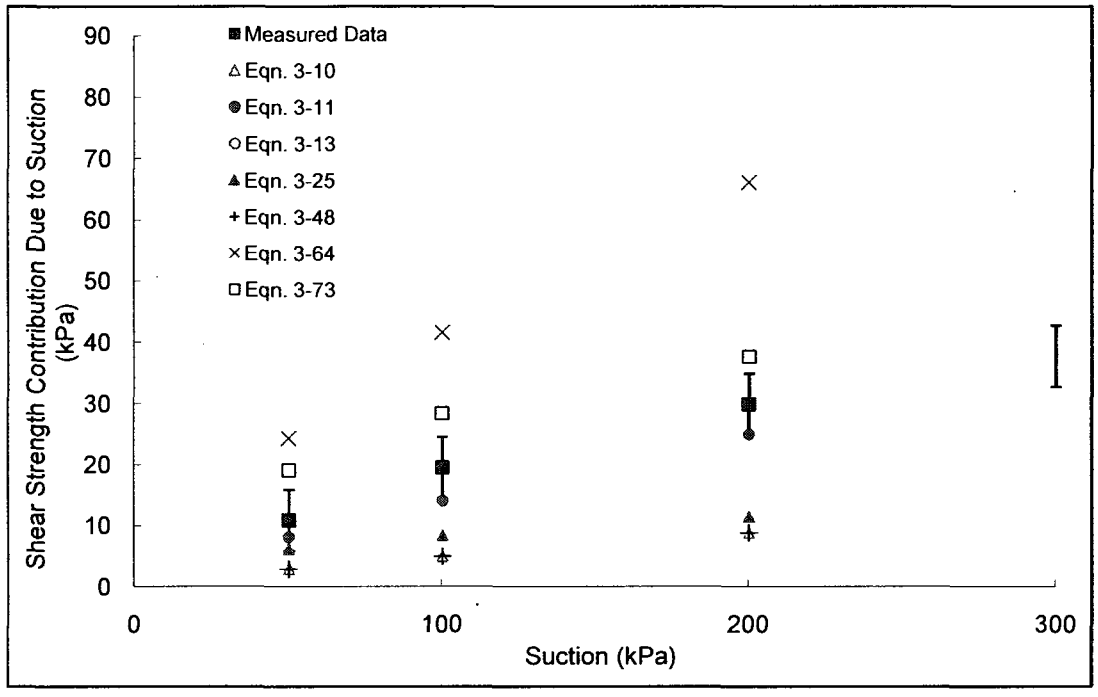

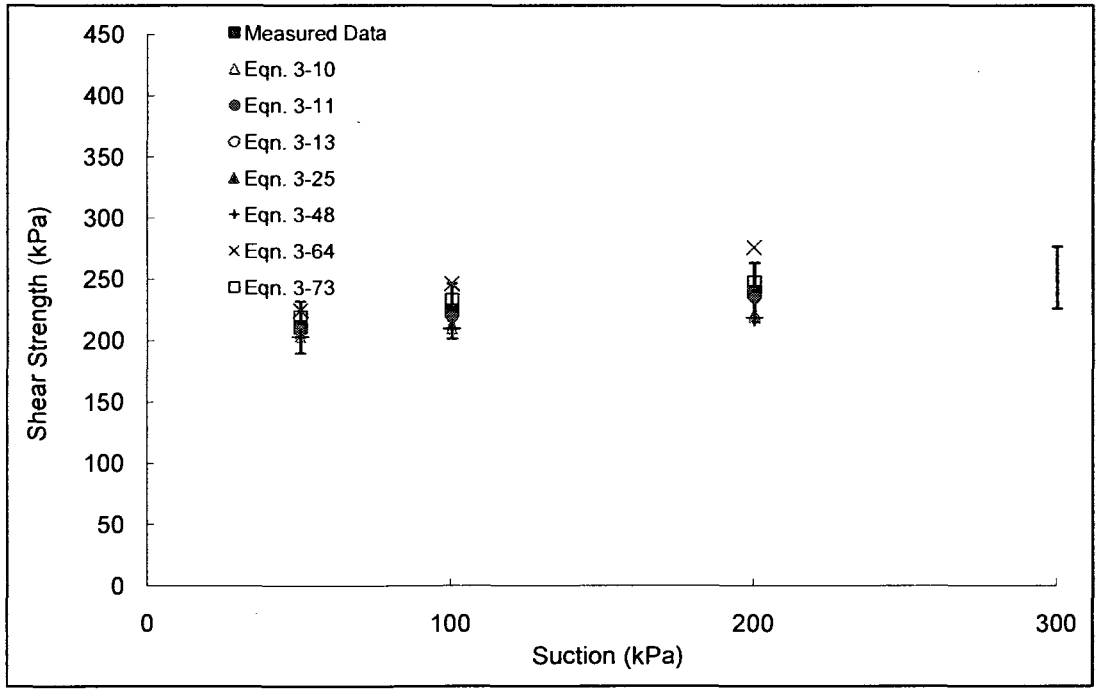

Soil No. 8a

Jurong soil

Rahardjo, Heng and Choon, 2004

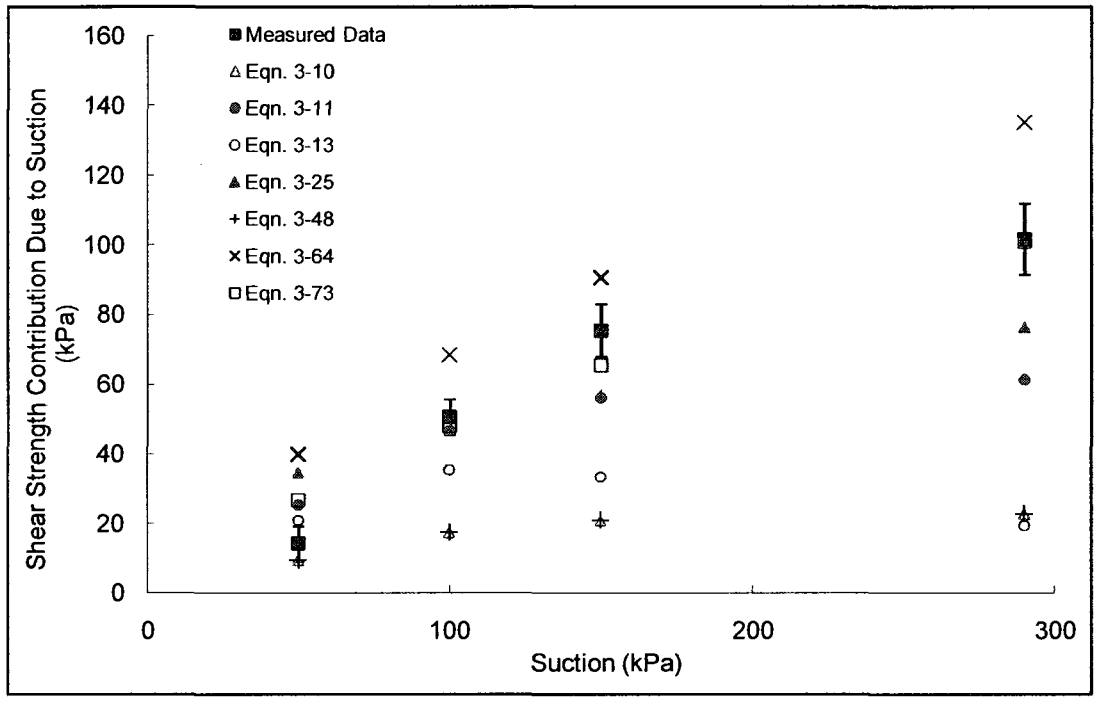

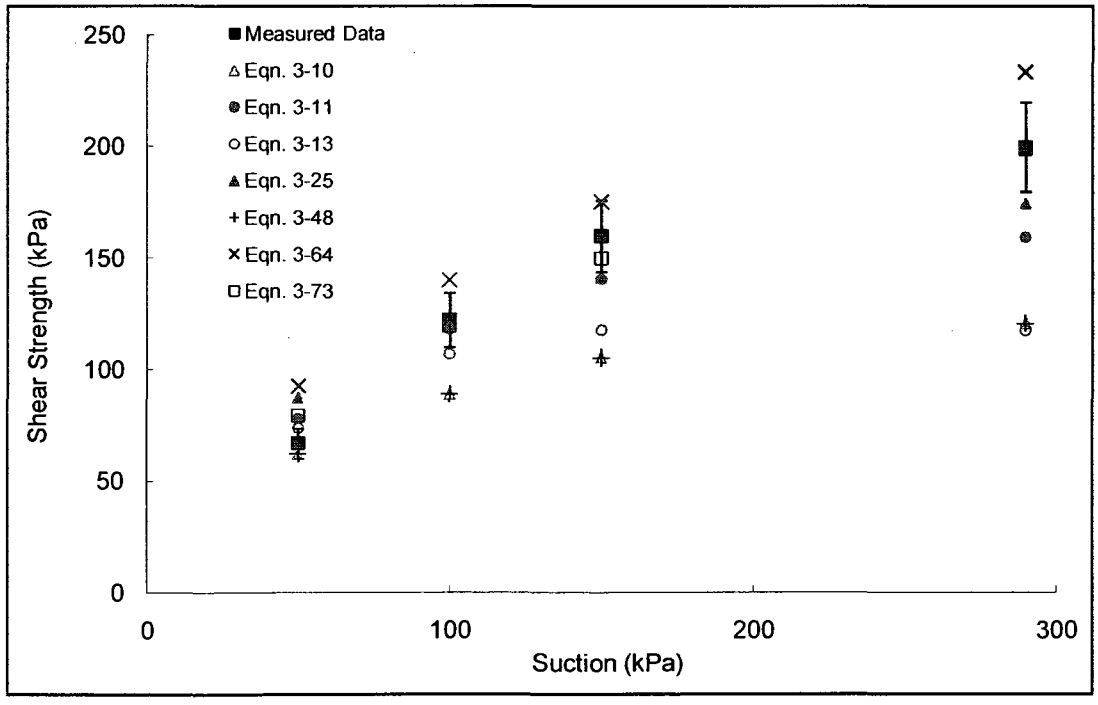

Soil No. 8b

Jurong soil

Rahardjo, Heng and Choon, 2004

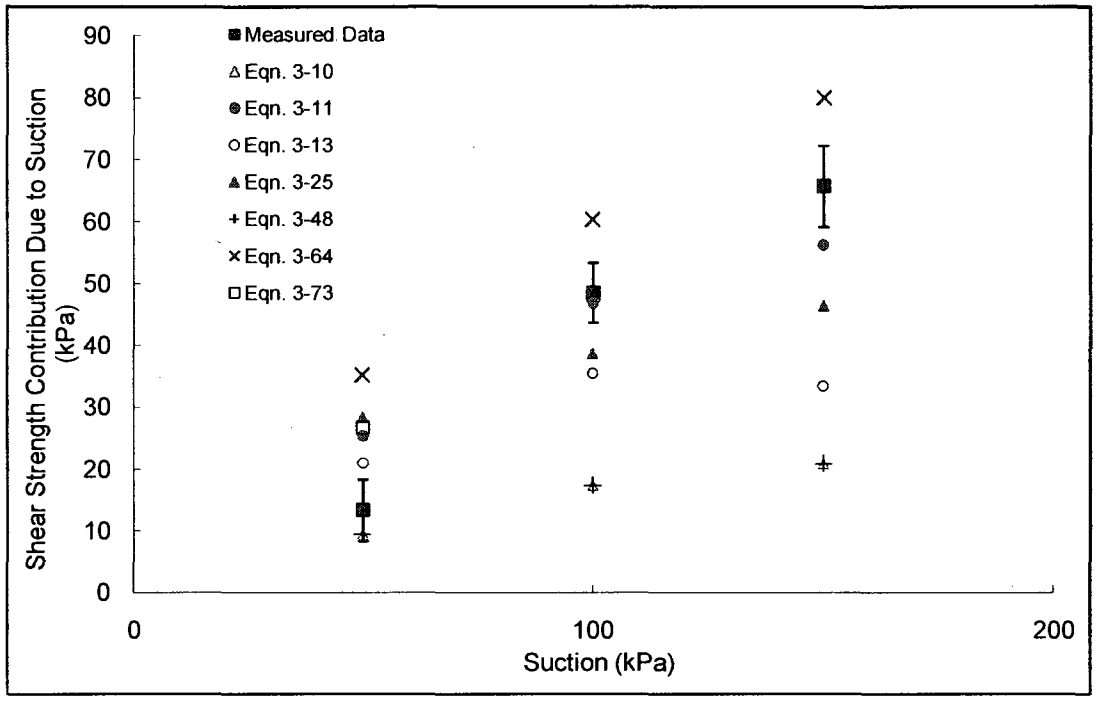

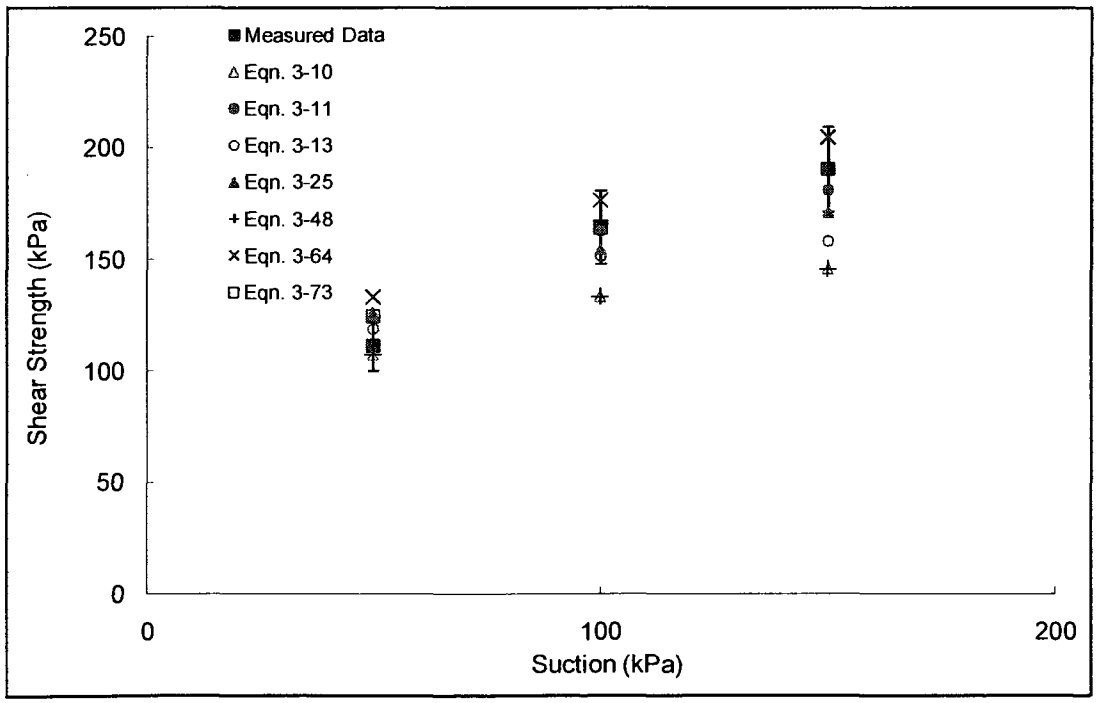

Soil No. 8c

Jurong soil

Rahardjo, Heng and Choon, 2004

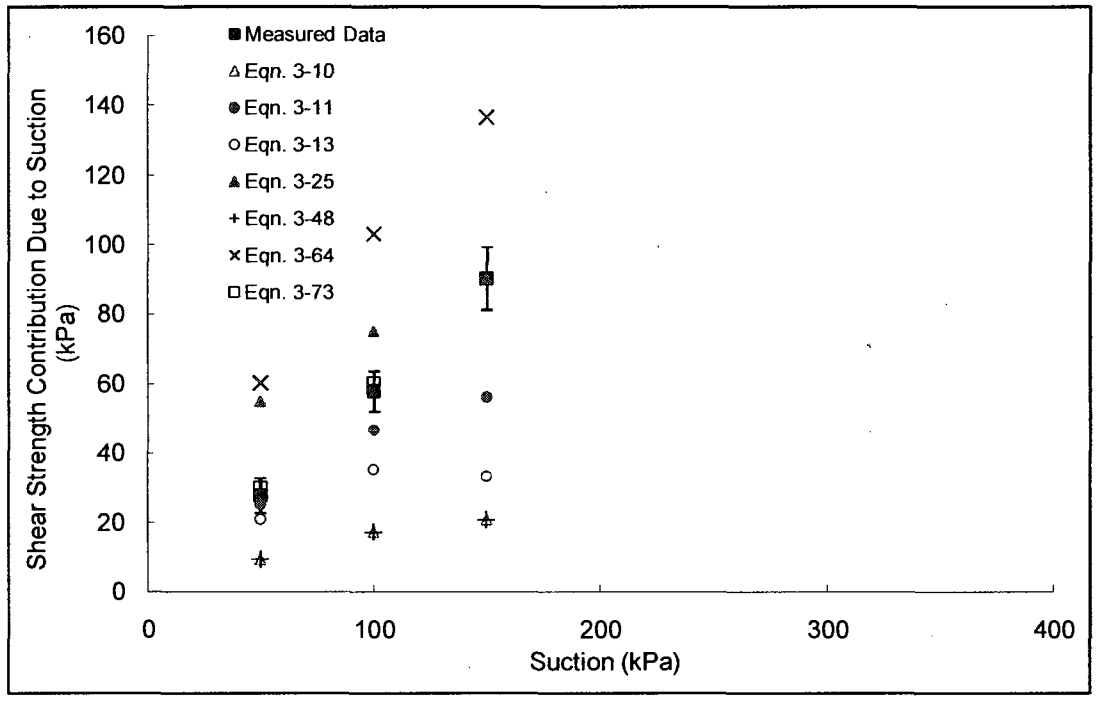

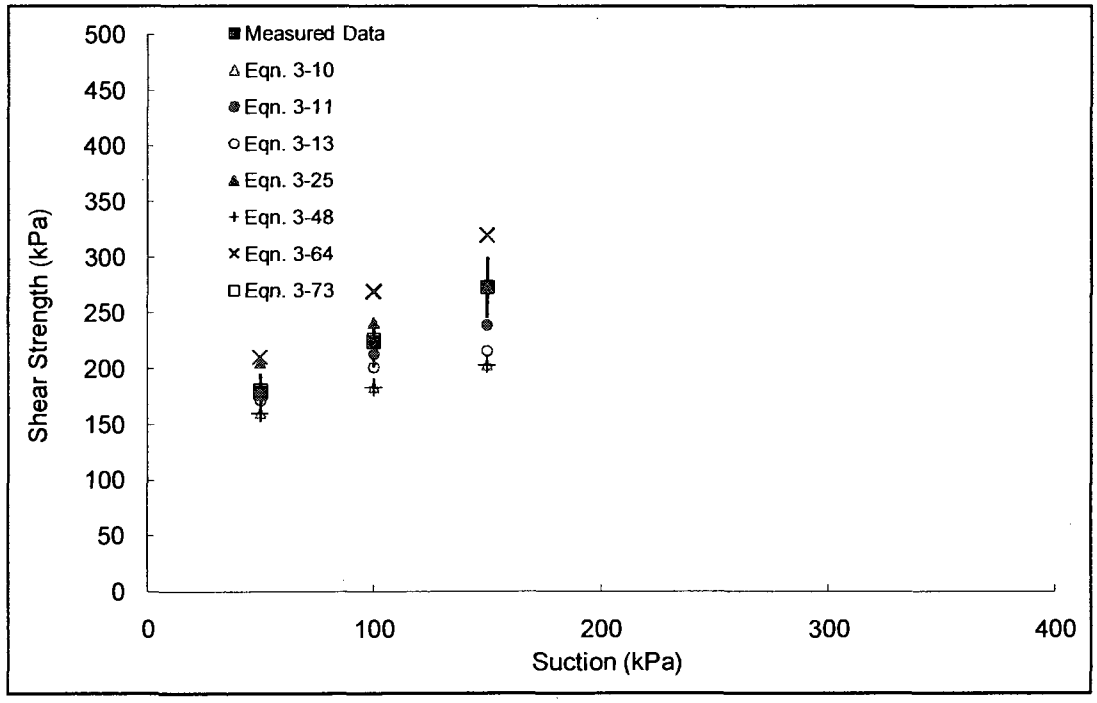

Soil No. 9

Nanyang undisturbed clay

Bao, Gong and Zhan, 1998

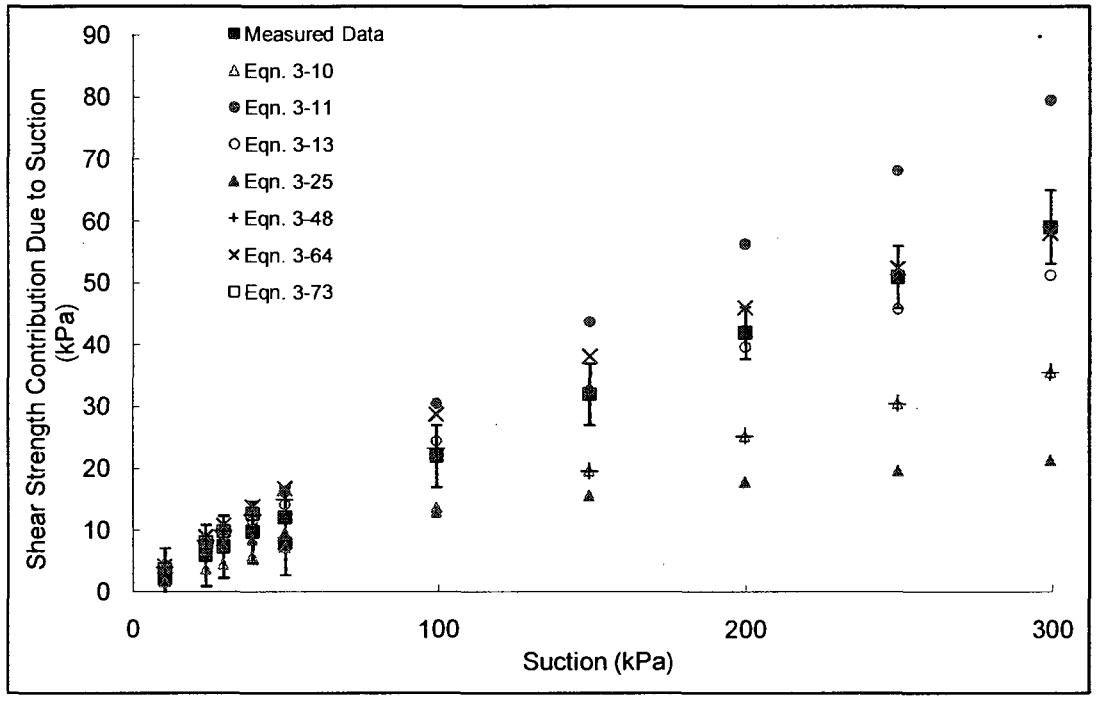

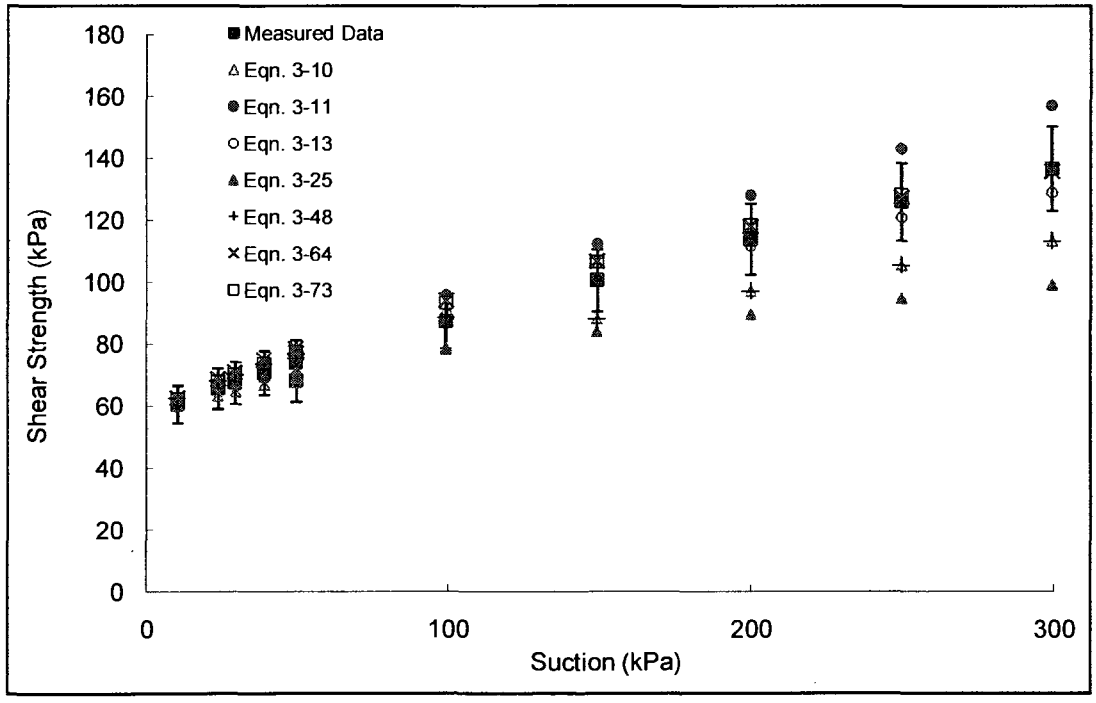

Soil No. 10

Nanyang compacted clay

Bao, Gong and Zhan, 1998

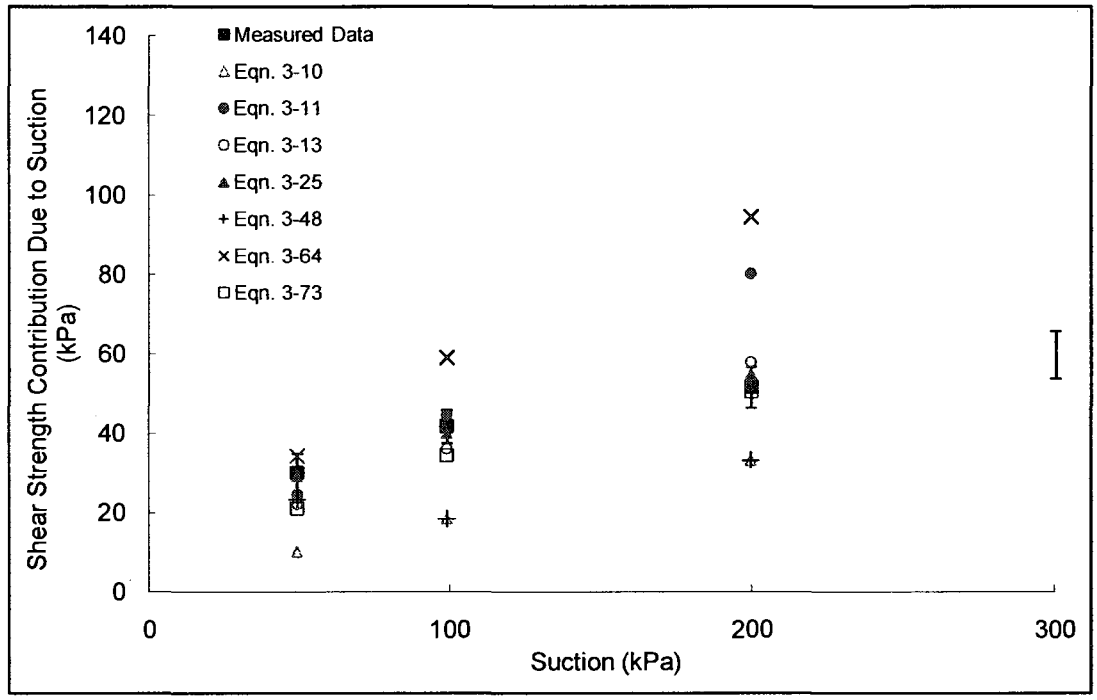

Soil No. 11a

Speswhite kaolin

Tarantino and Tombolato, 2005

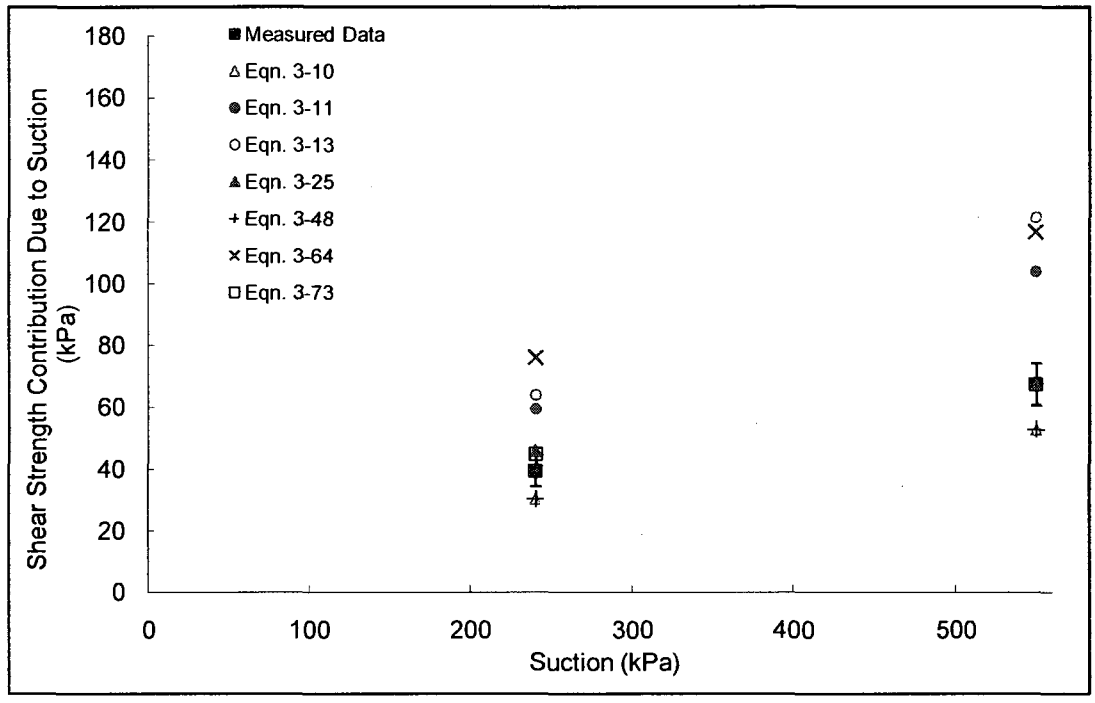

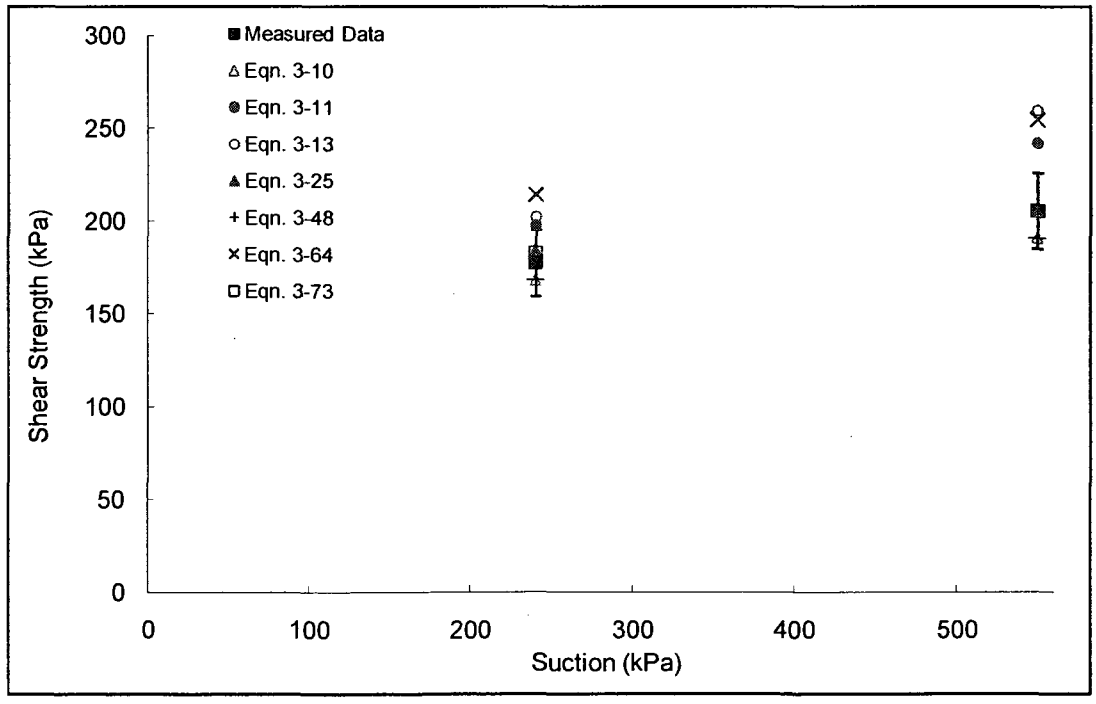

Soil No. 11b

Speswhite kaolin

Tarantino and Tombolato, 2005

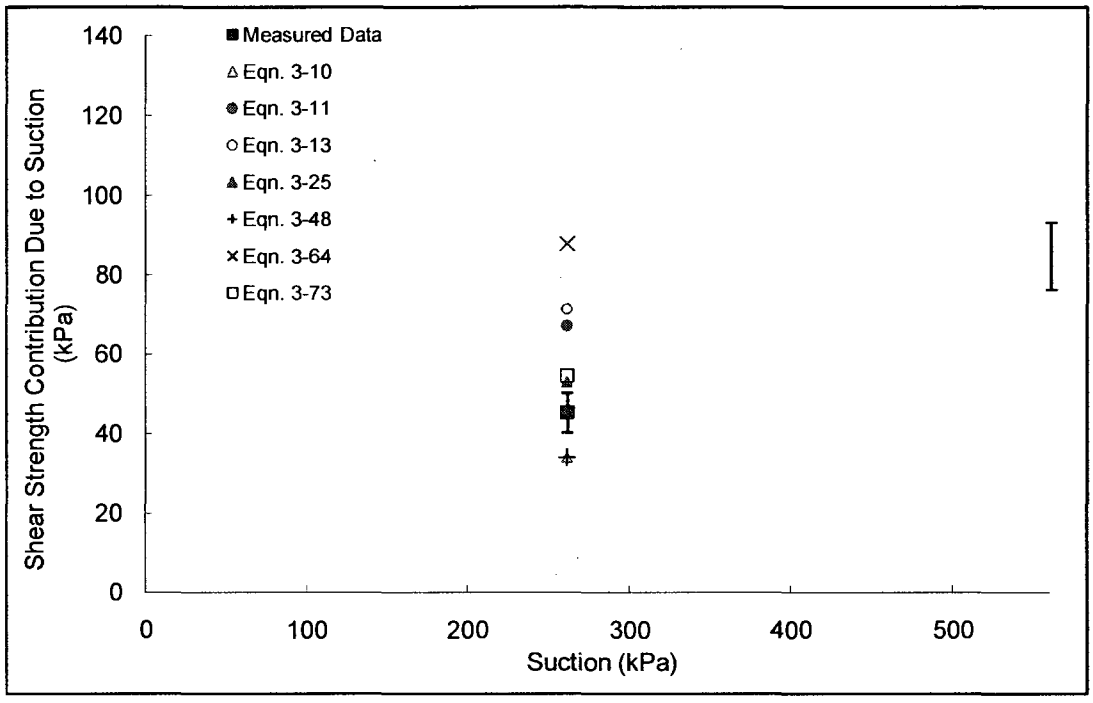

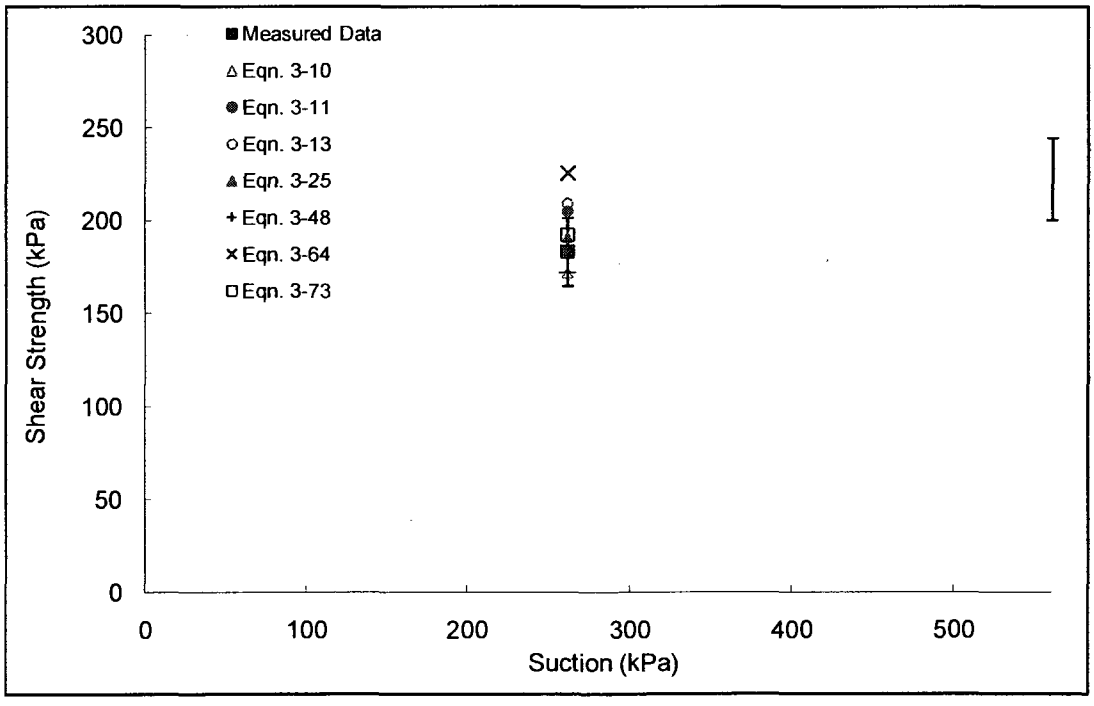

Soil No. 11c

Speswhite kaolin

Tarantino and Tombolato, 2005

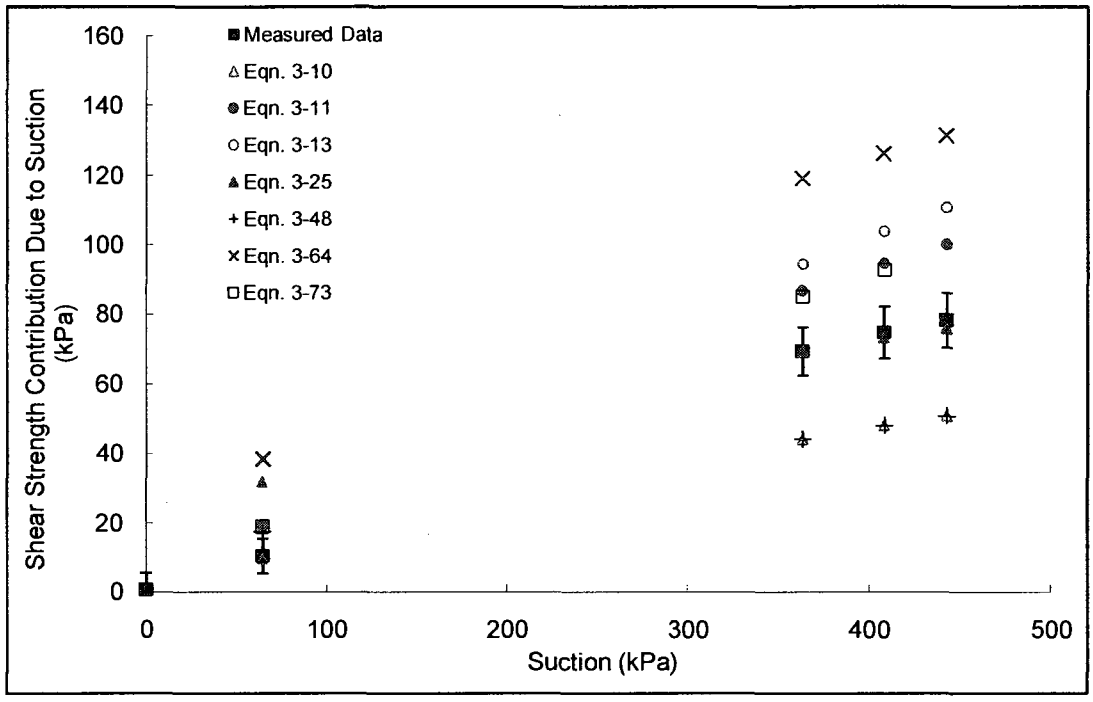

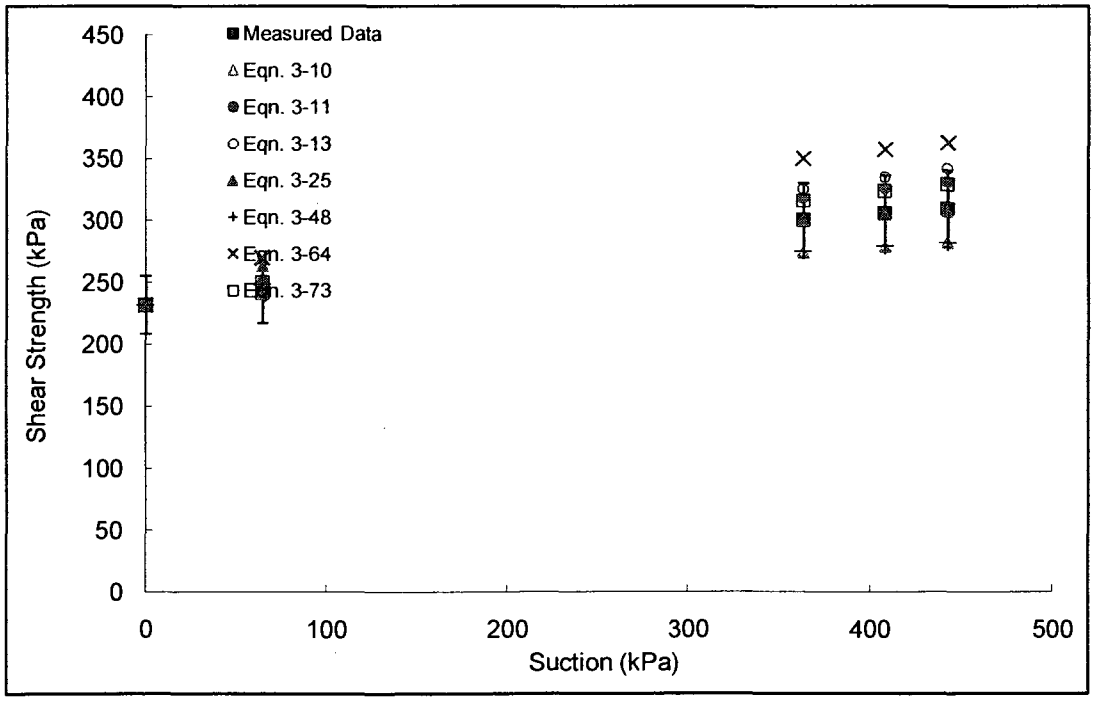

Soil No. 11d

Speswhite kaolin

Tarantino and Tombolato, 2005

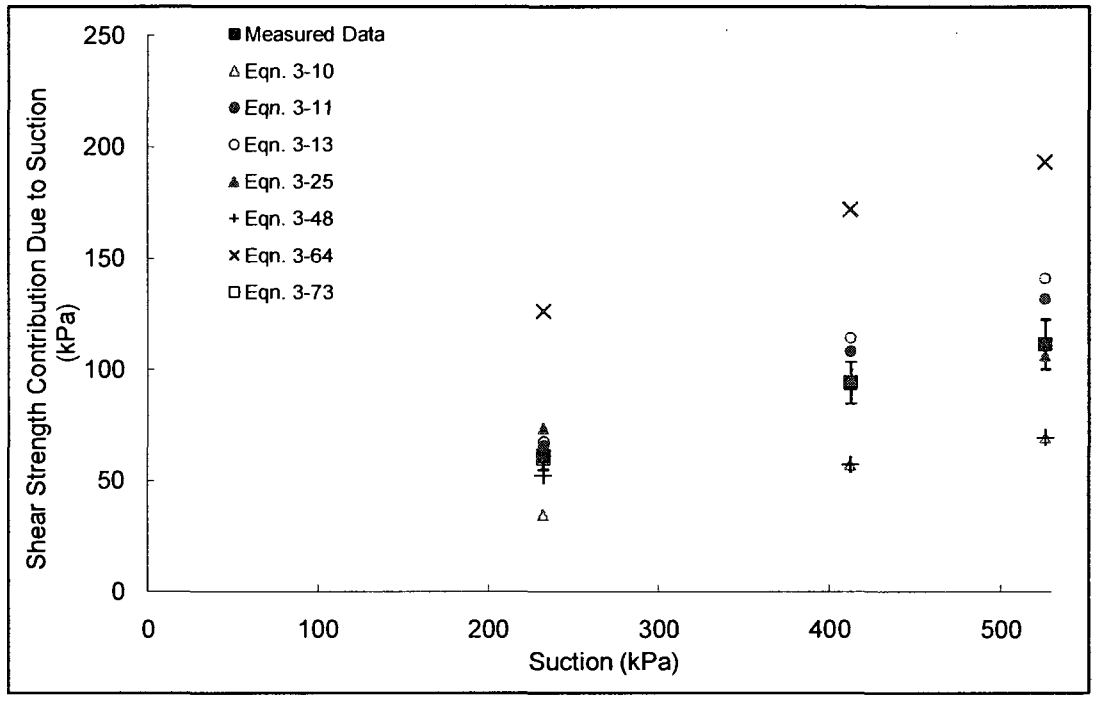

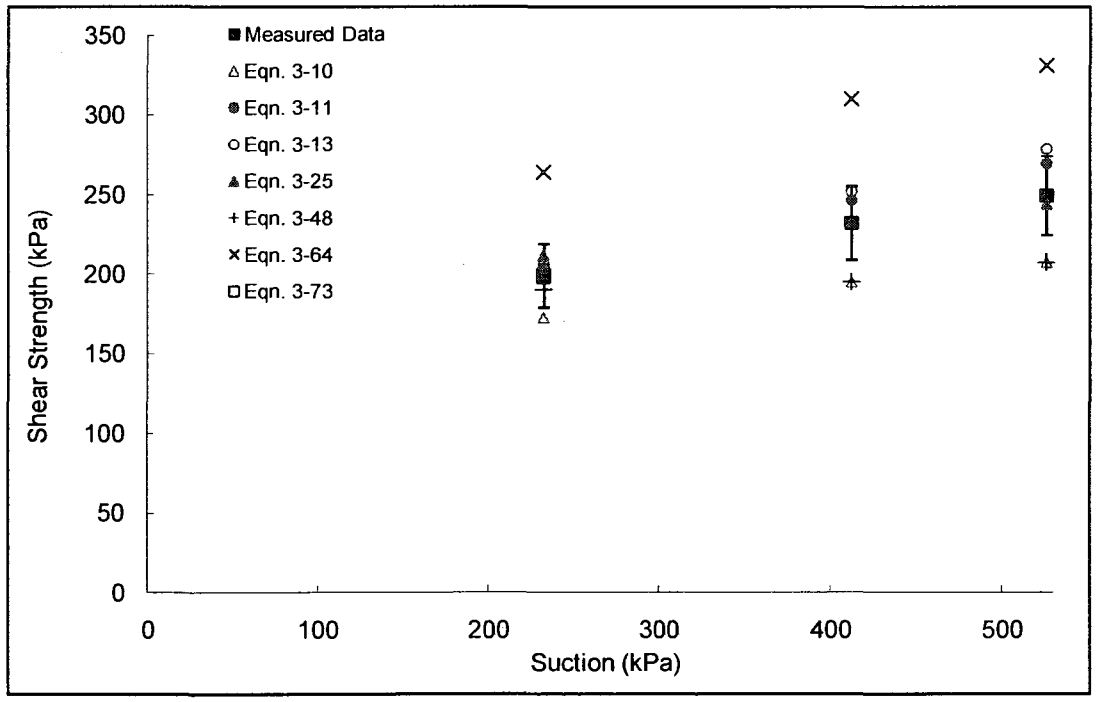

Soil No. 12 **SJ10a**

Khalili, Geiser and Blight, 2004

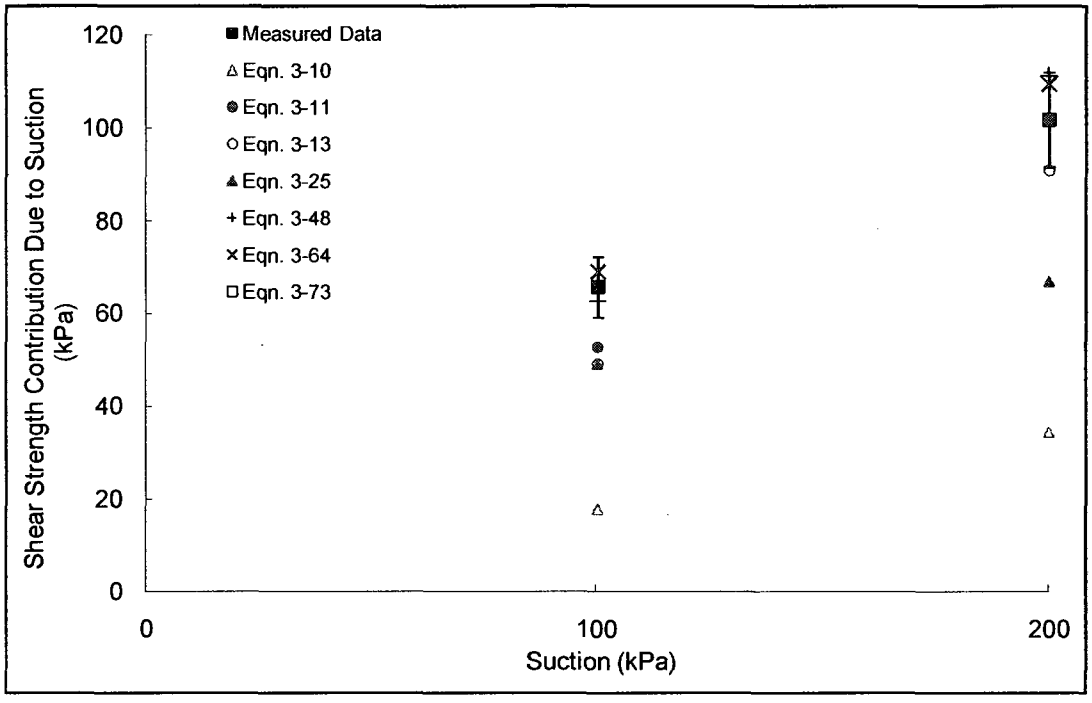

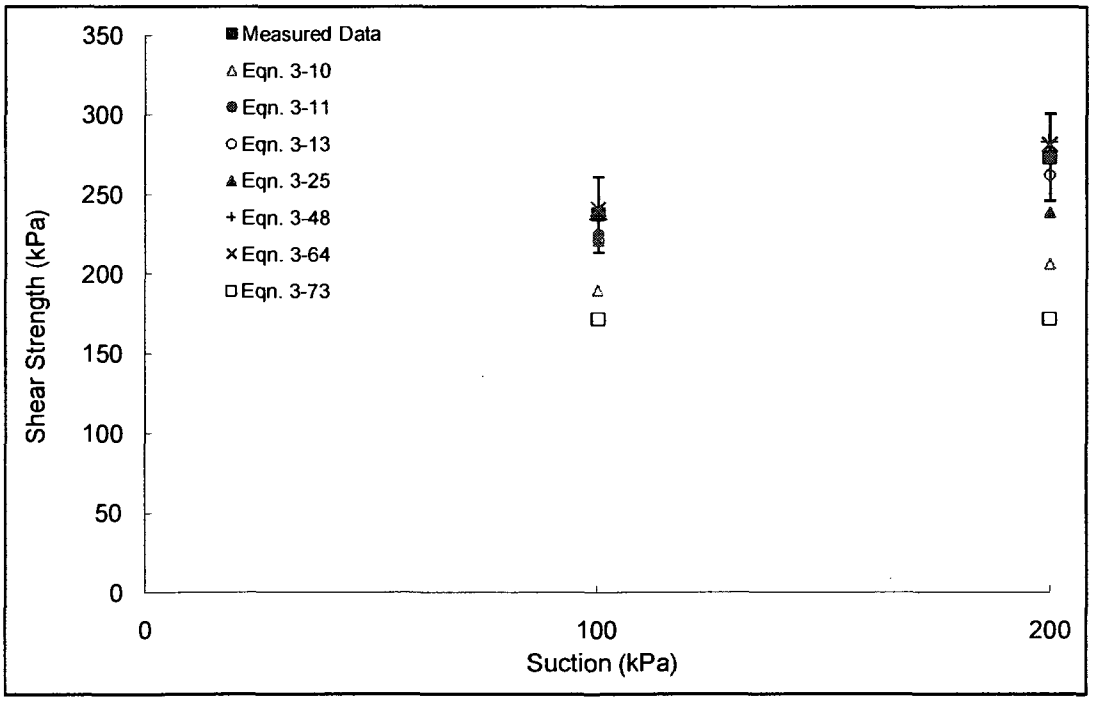

Soil No. 13 **SJ10b**

Khalili, Geiser and Blight, 2004

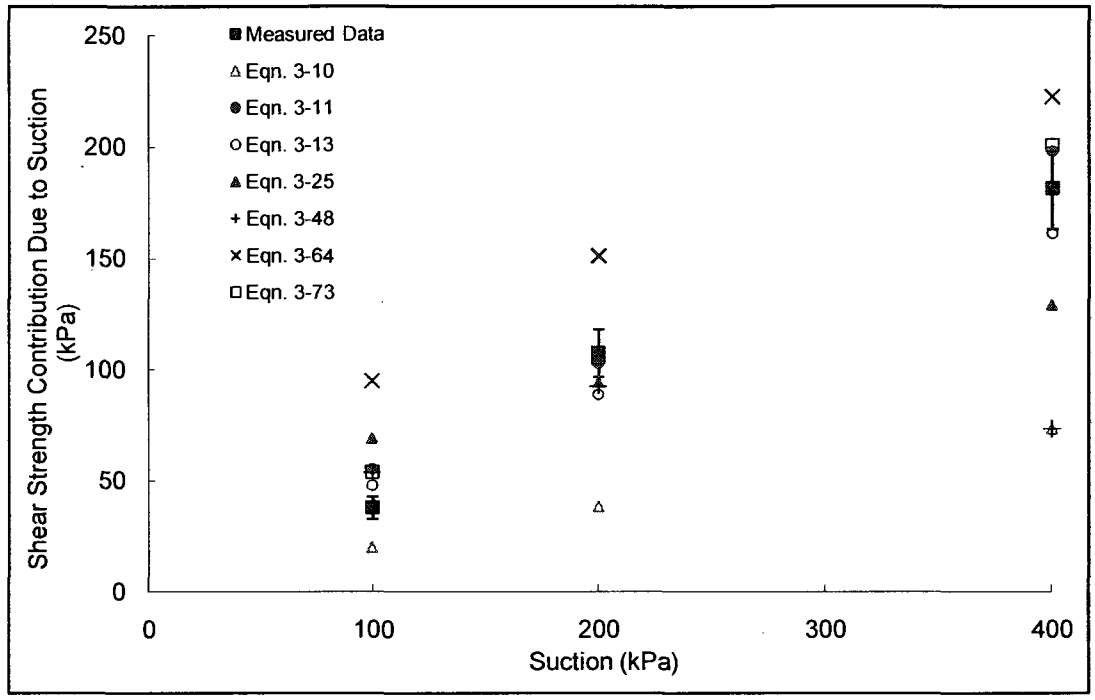

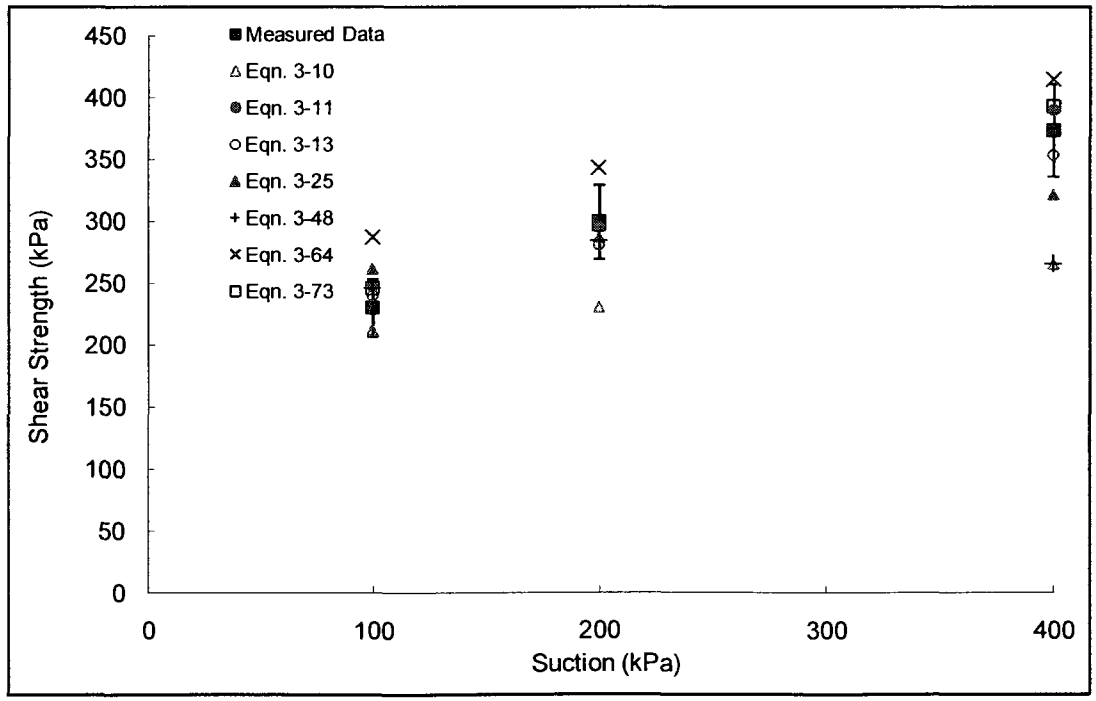

Soil No. 14 **SJ1**

Khalili, Geiser and Blight, 2004

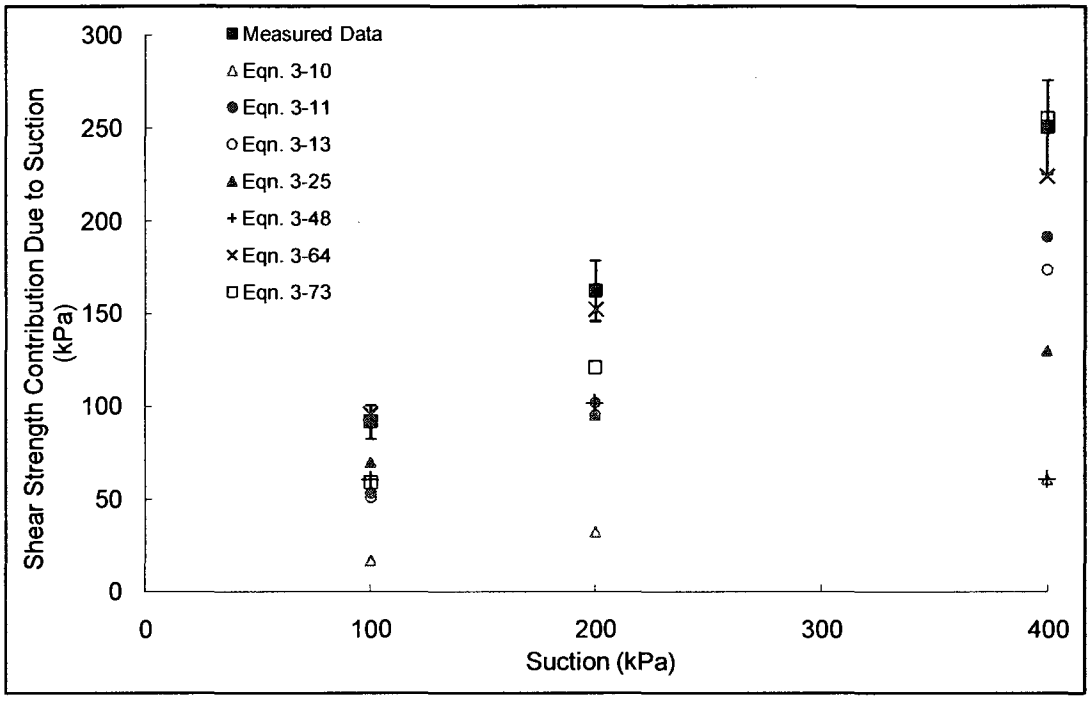

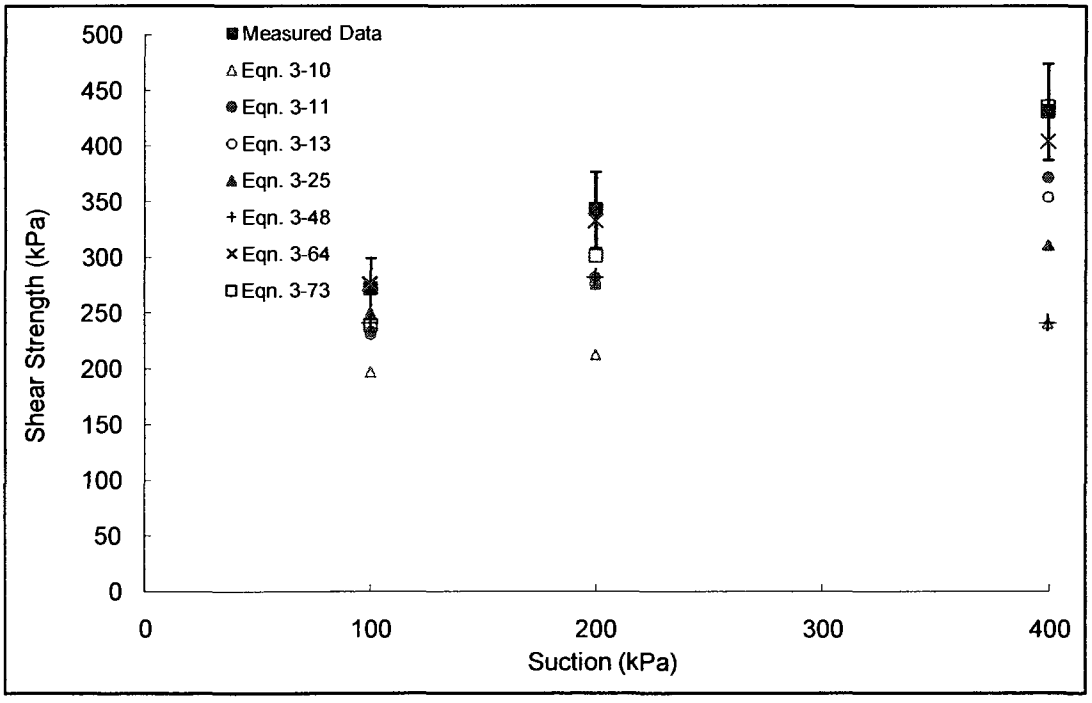

Soil No. 15a

Tailings (50 m)

Rassam and Williams, 1999

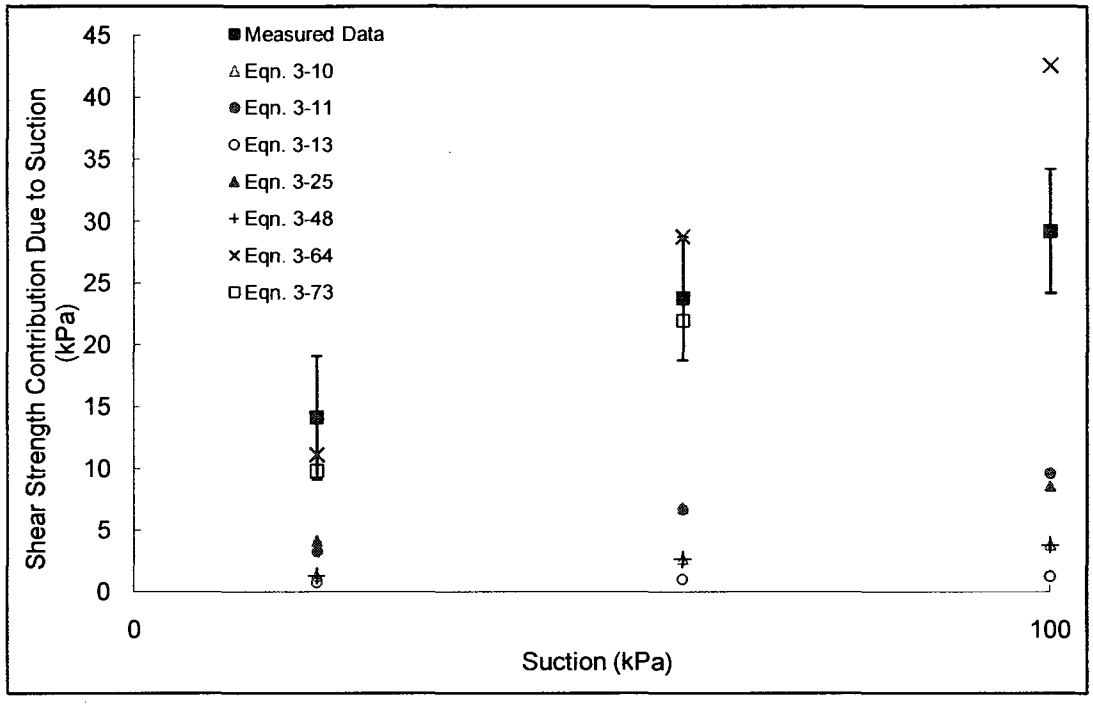

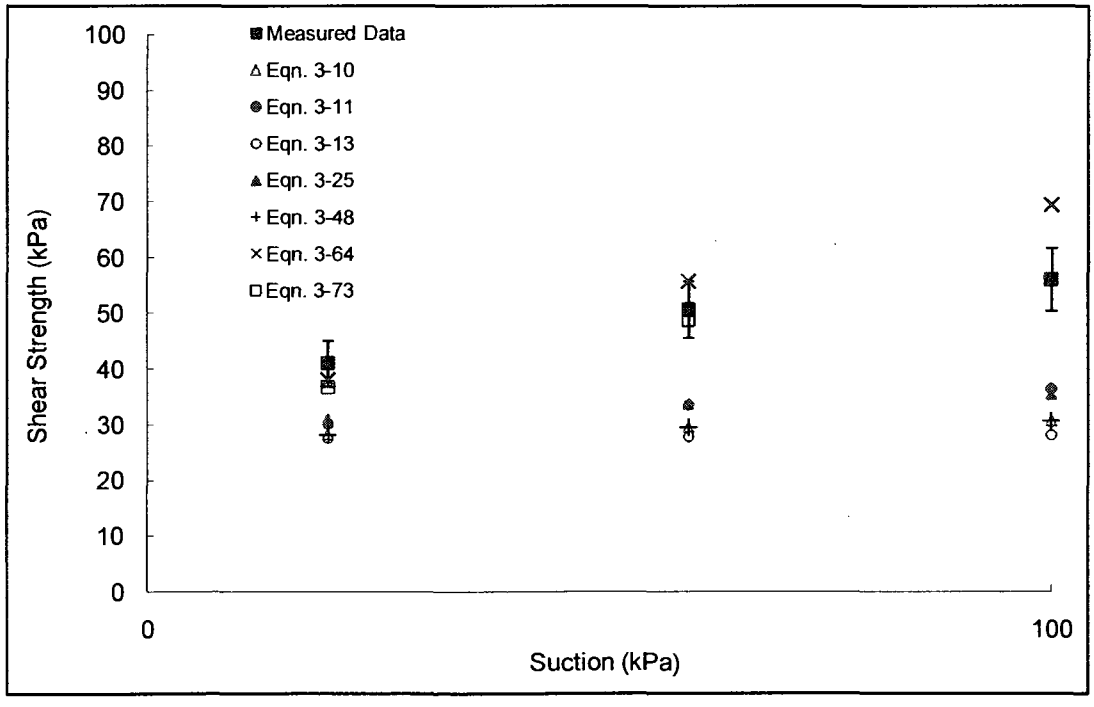

Soil No. 15b

Tailings (50 m)

Rassam and Williams, 1999

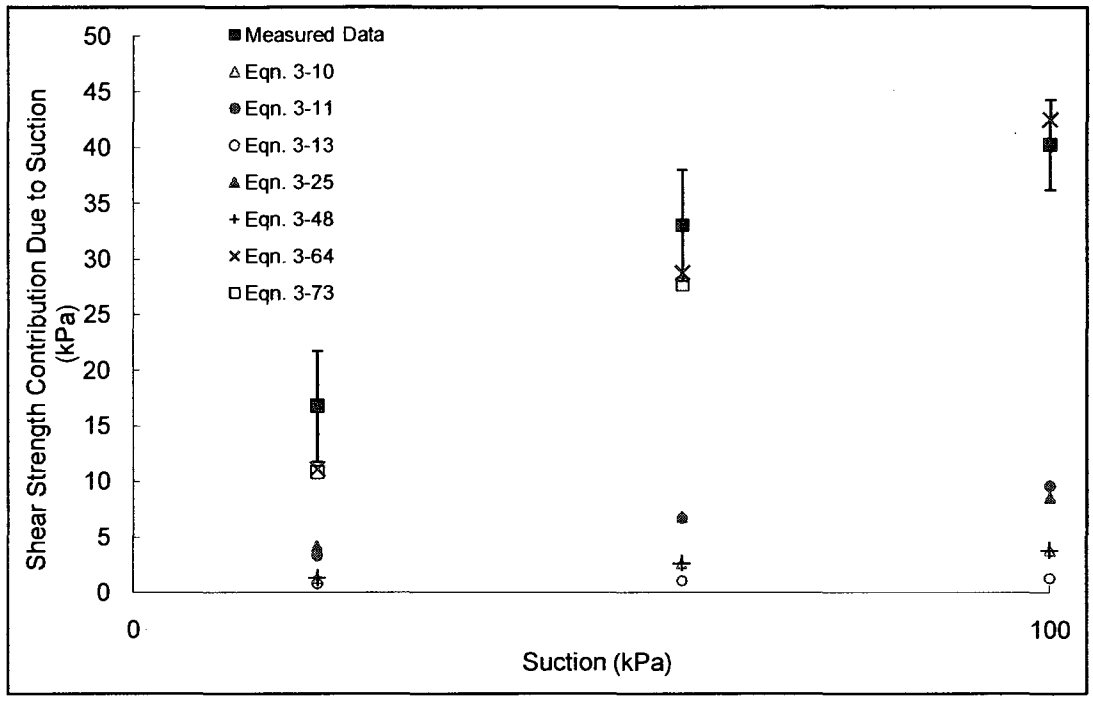

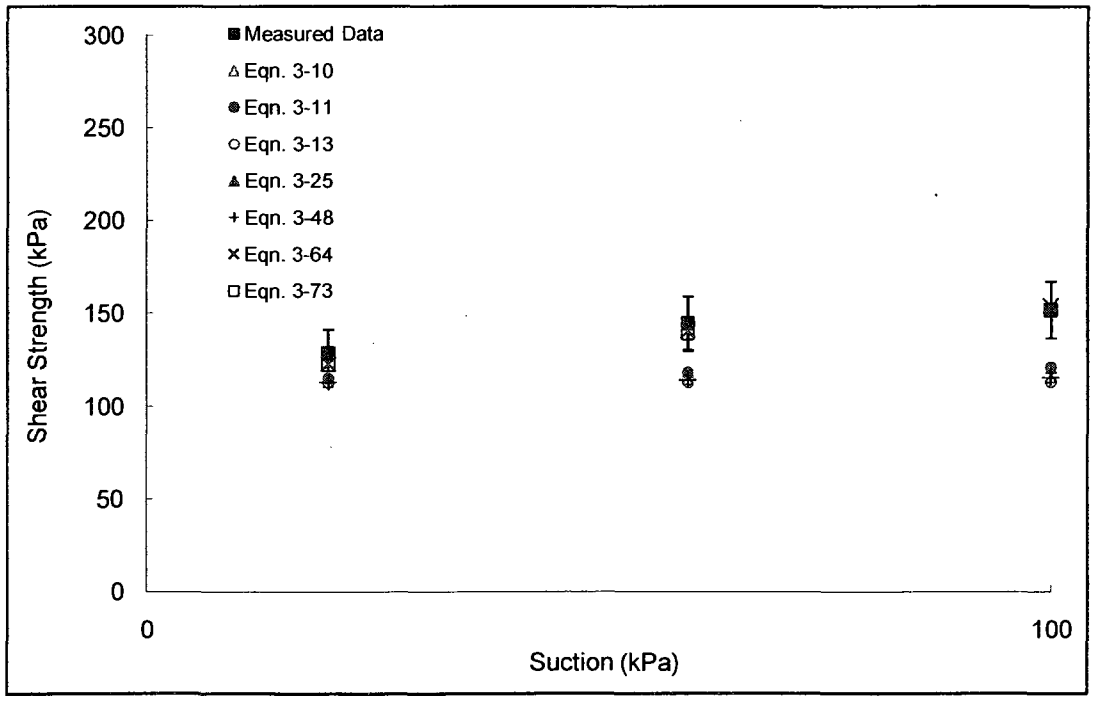

Soil No. 15c

Tailings (50 m)

Rassam and Williams, 1999

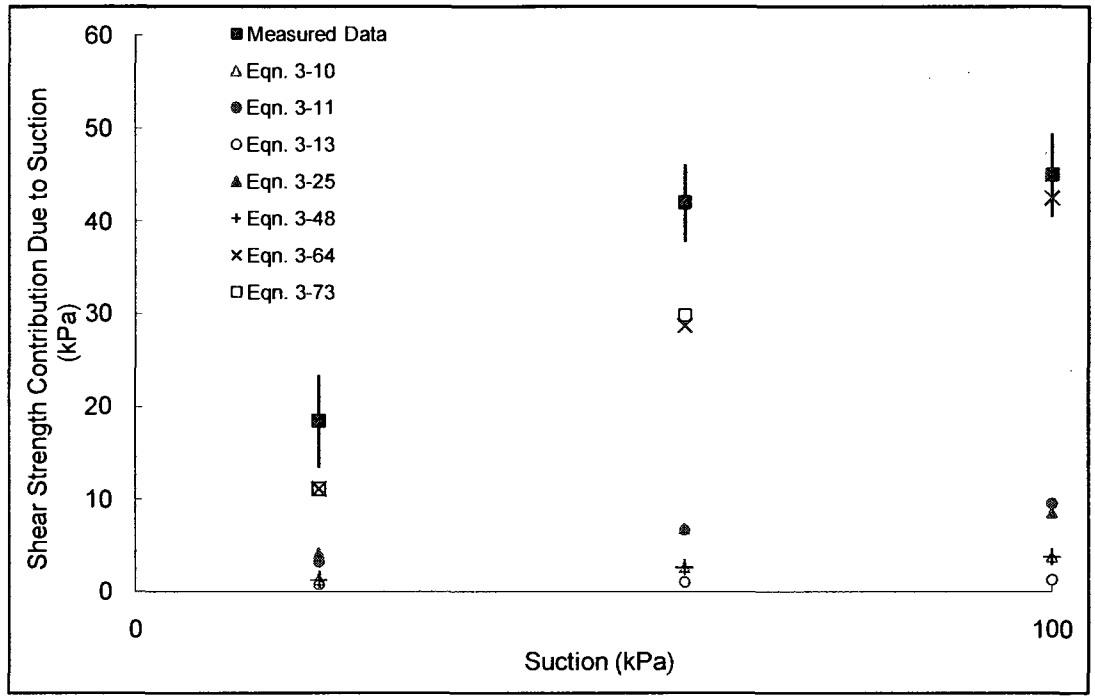

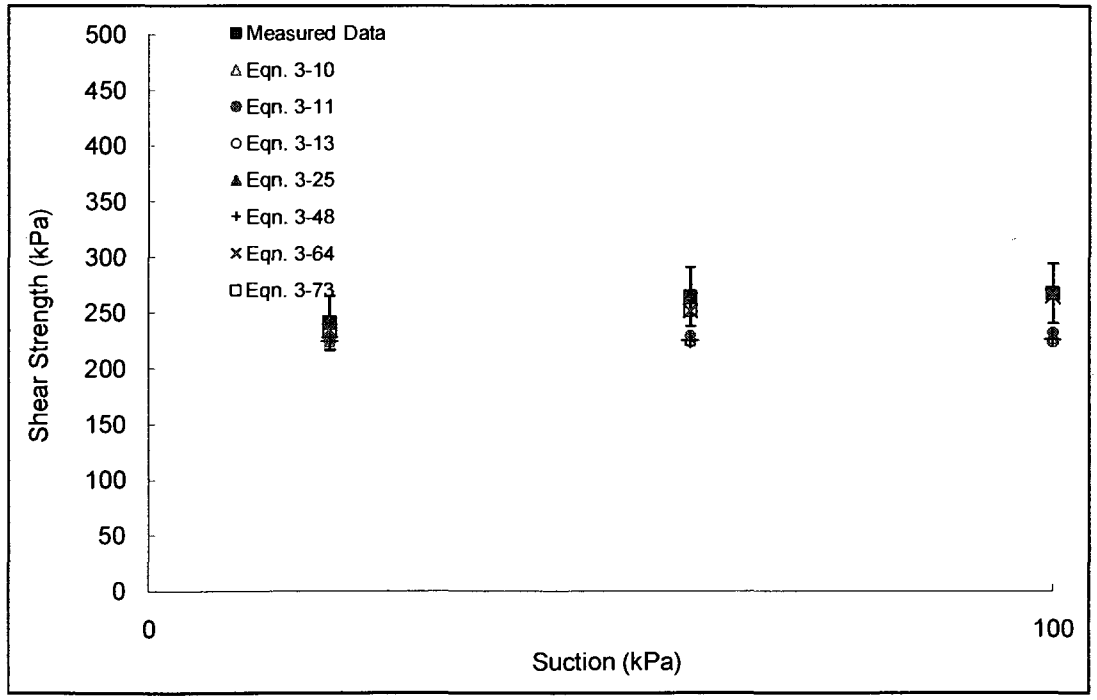

Soil No. 16a

Tailings (150 m)
Rassam and Williams, 1999

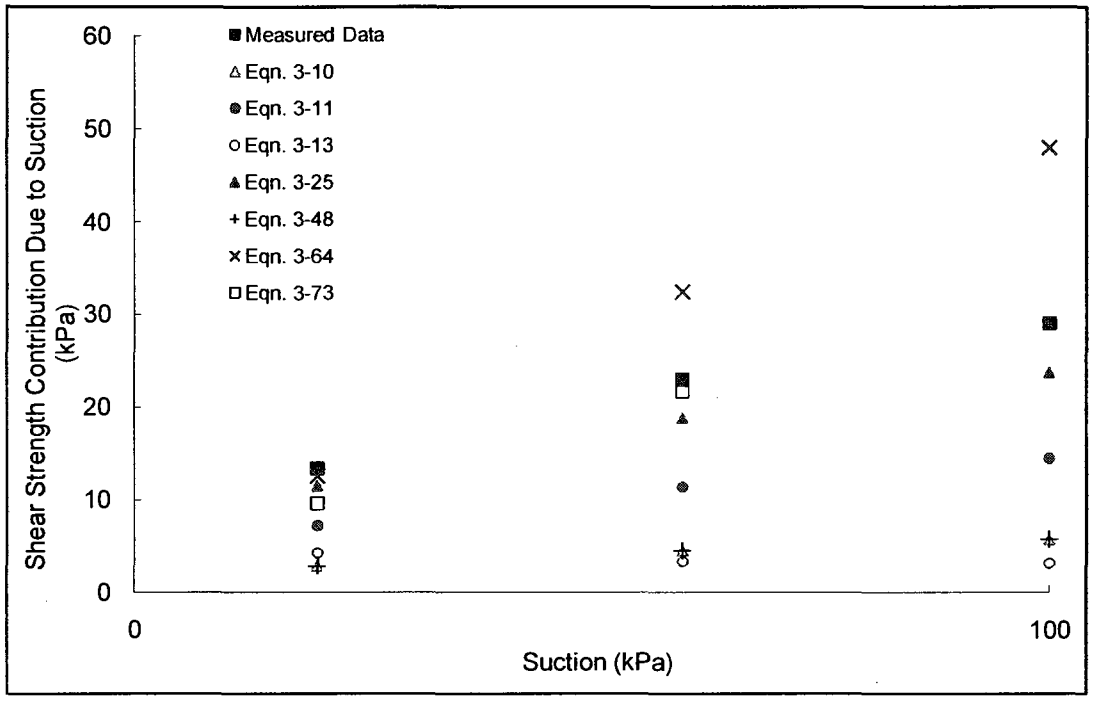

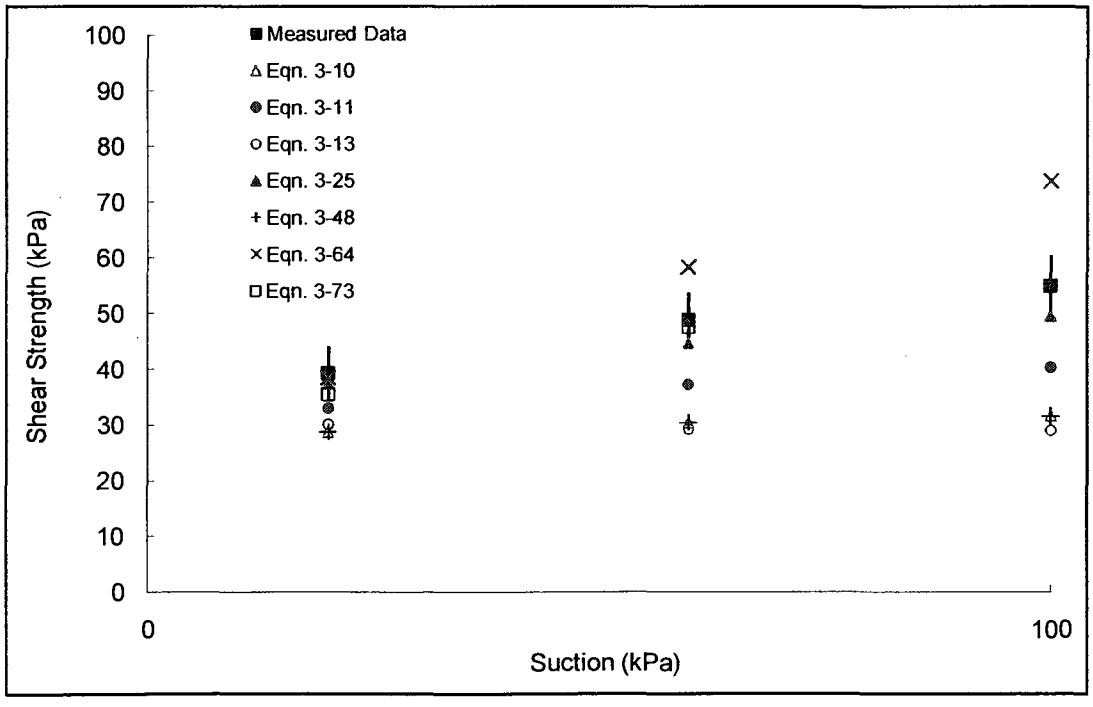

Soil No. 16b

Tailings (150 m)
Rassam and Williams, 1999

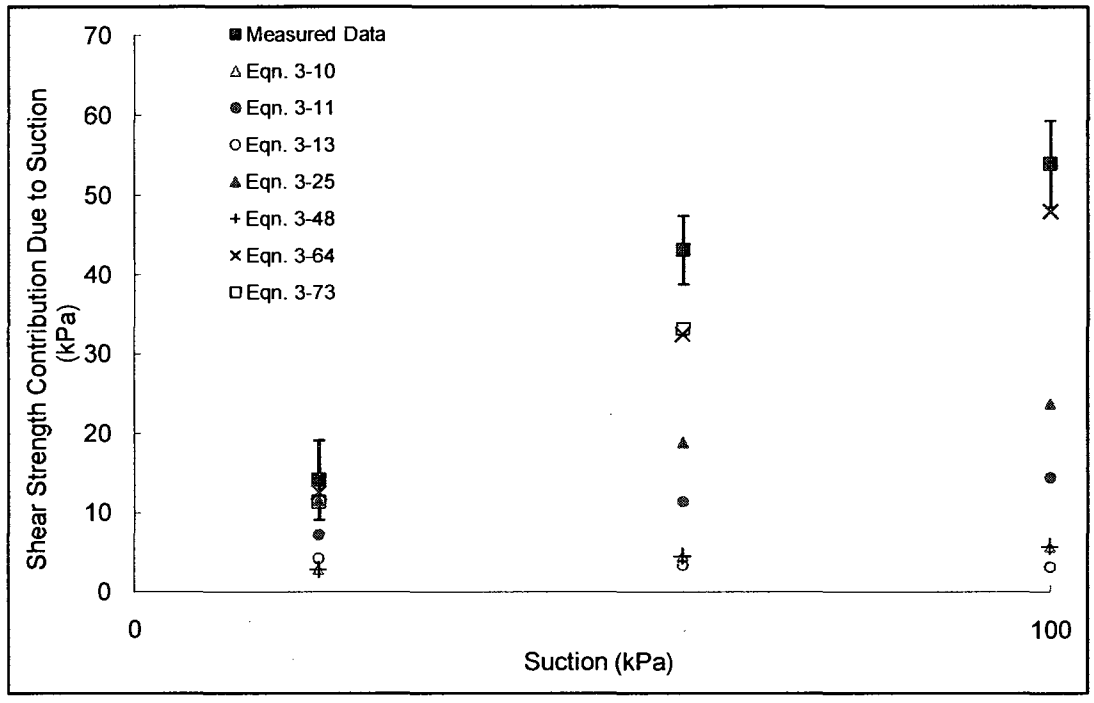

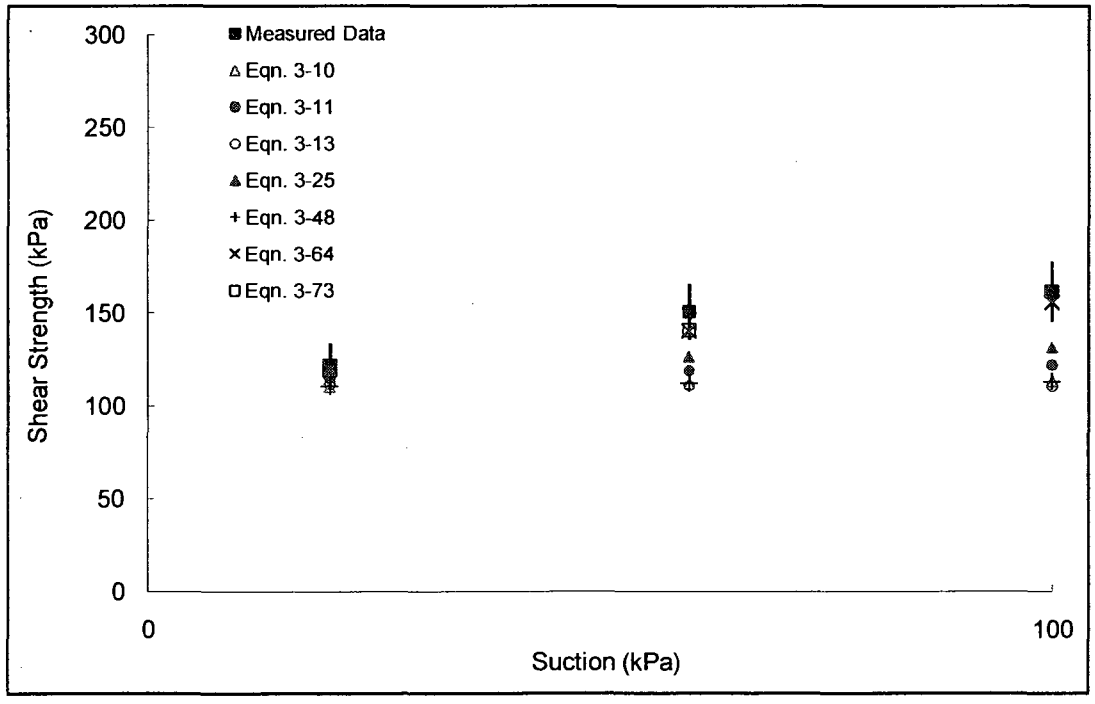

Soil No. 16c

Tailings (150 m)

Rassam and Williams, 1999

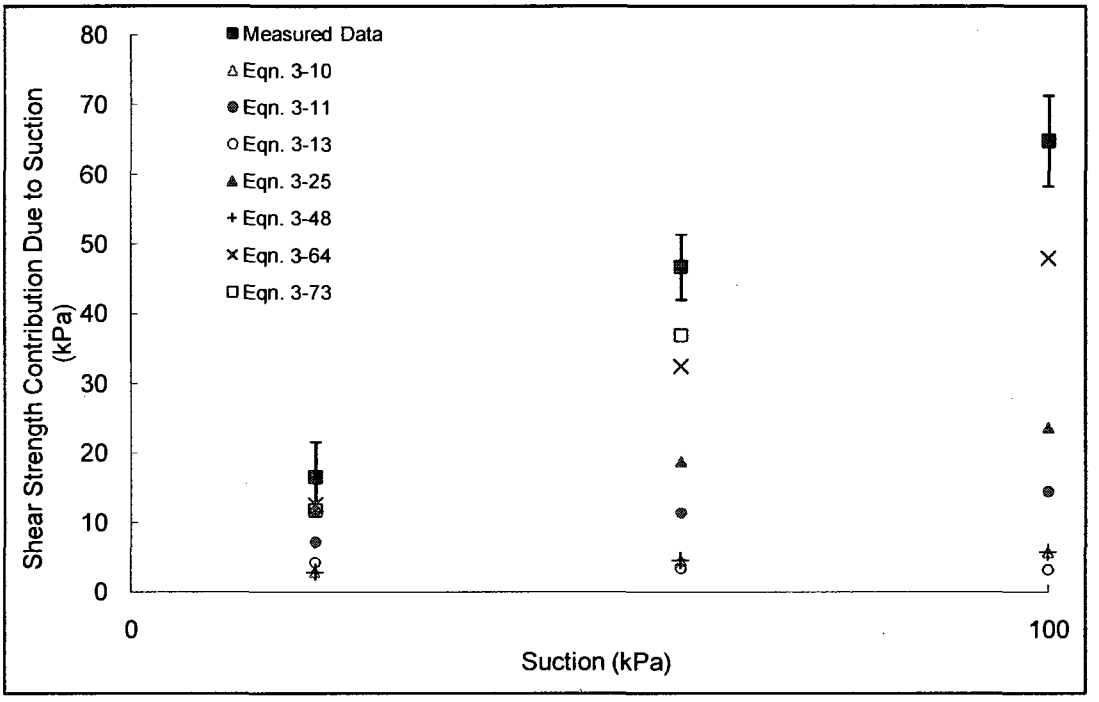

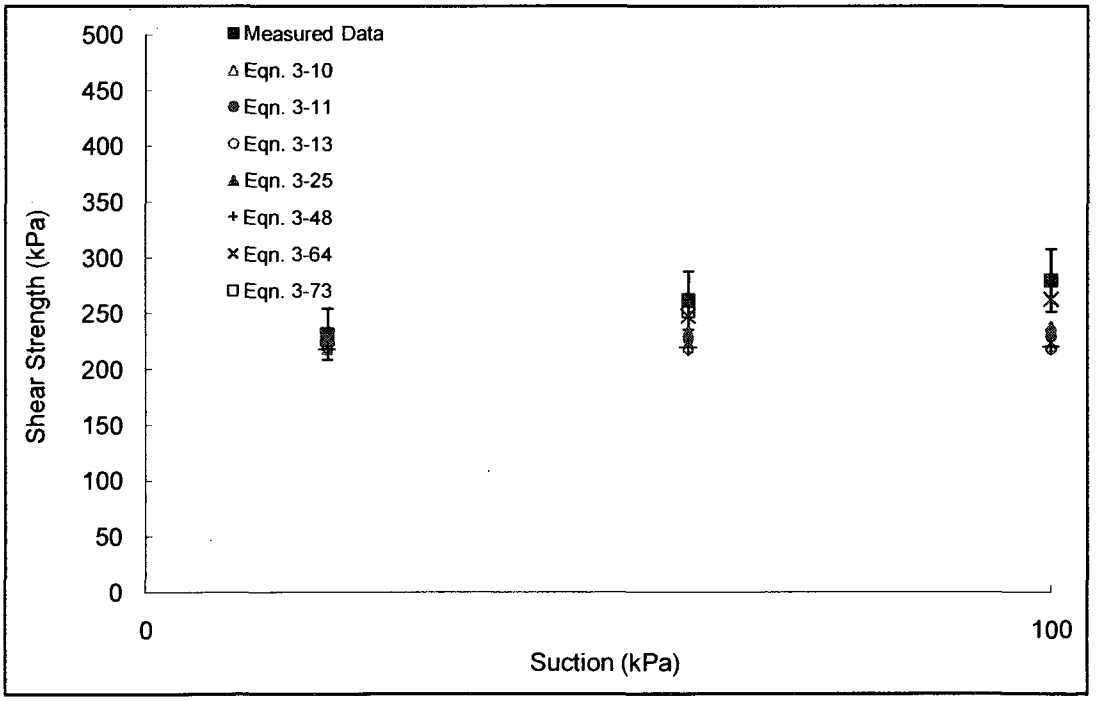

Soil No. 17a

Brazilian laterite

Rohm and Vilar, 1995

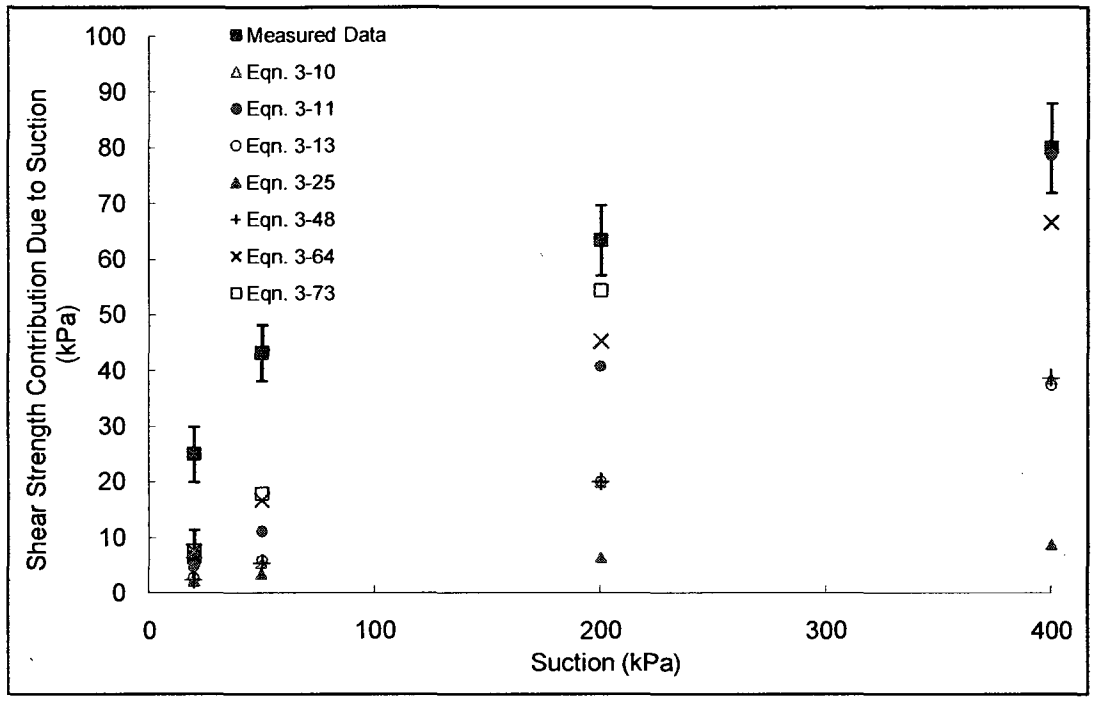

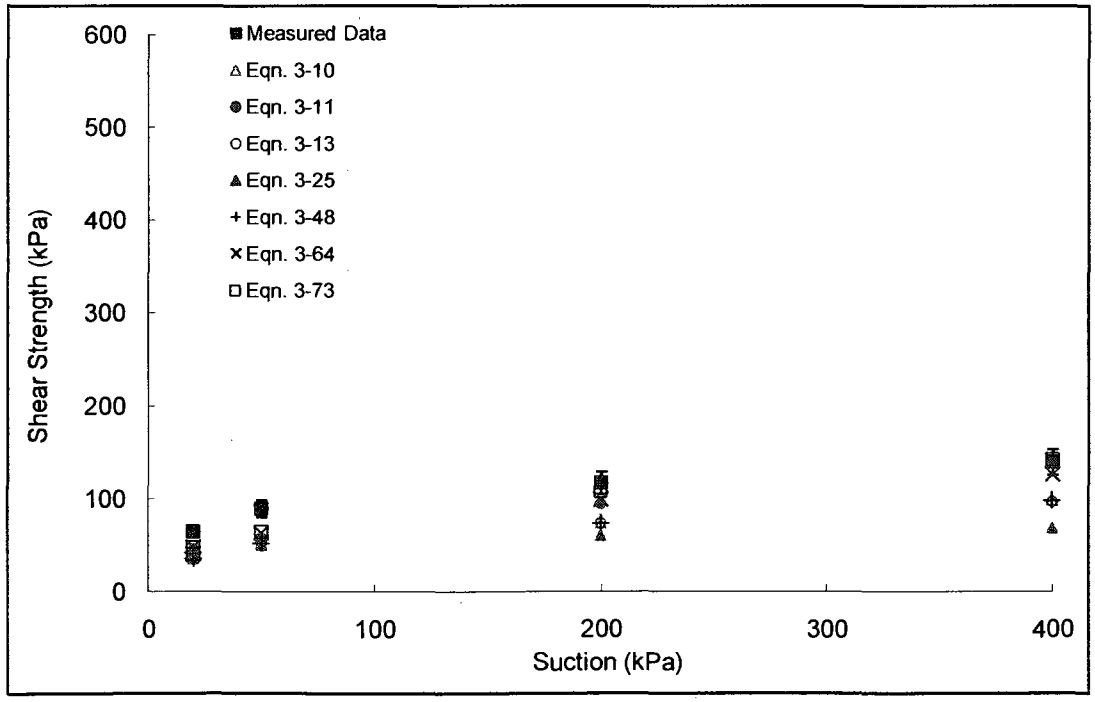

Soil No. 17b

Brazilian laterite

Rohm and Vilar, 1995

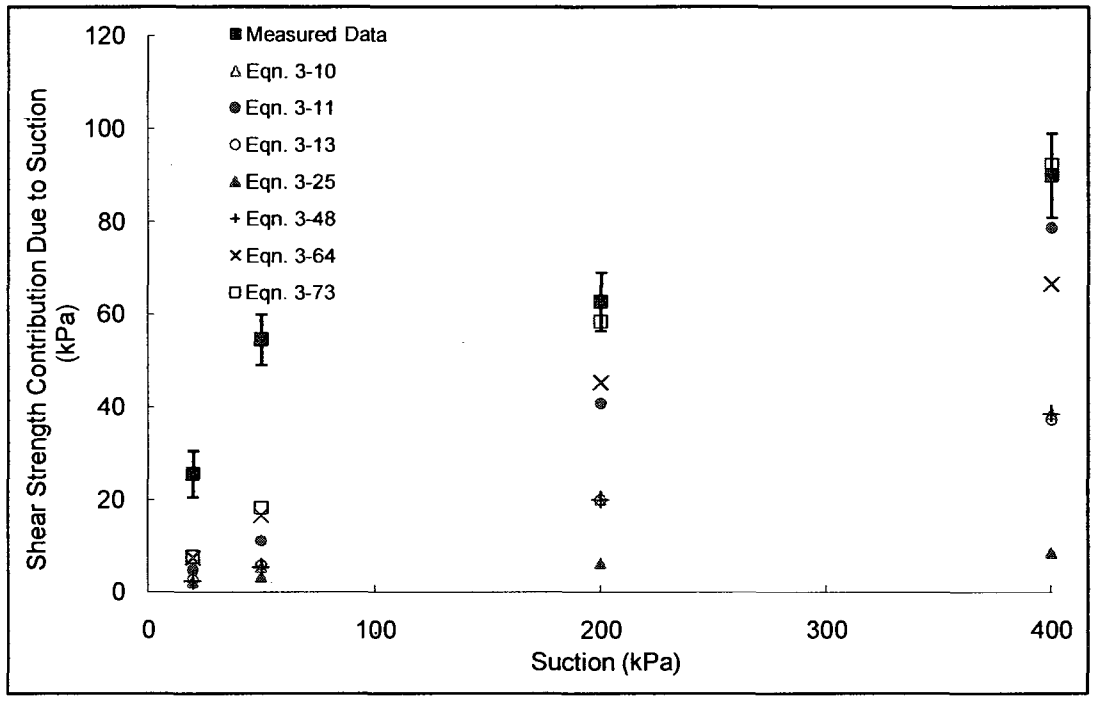

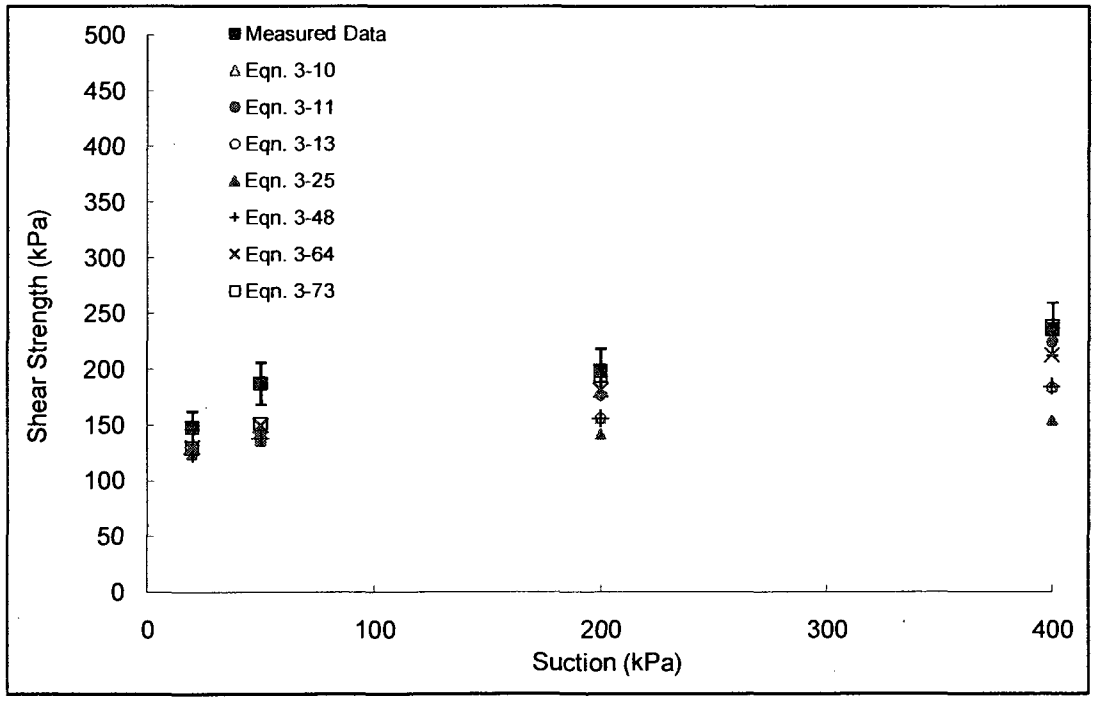

Soil No. 17c

Brazilian laterite

Rohm and Vilar, 1995

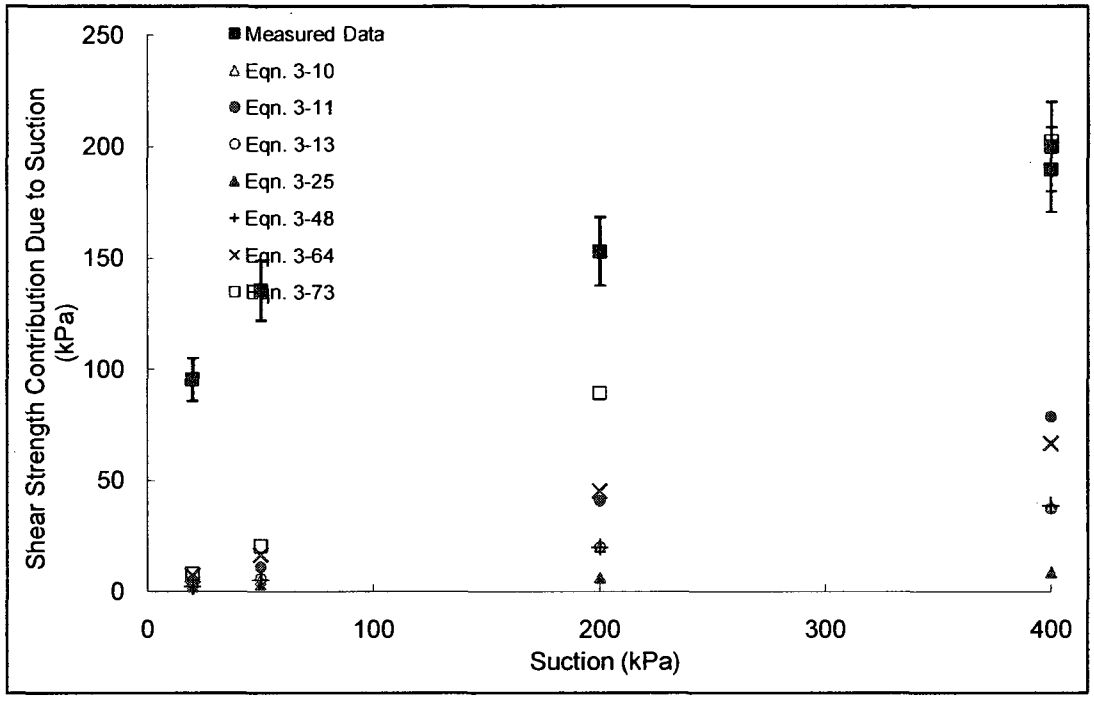

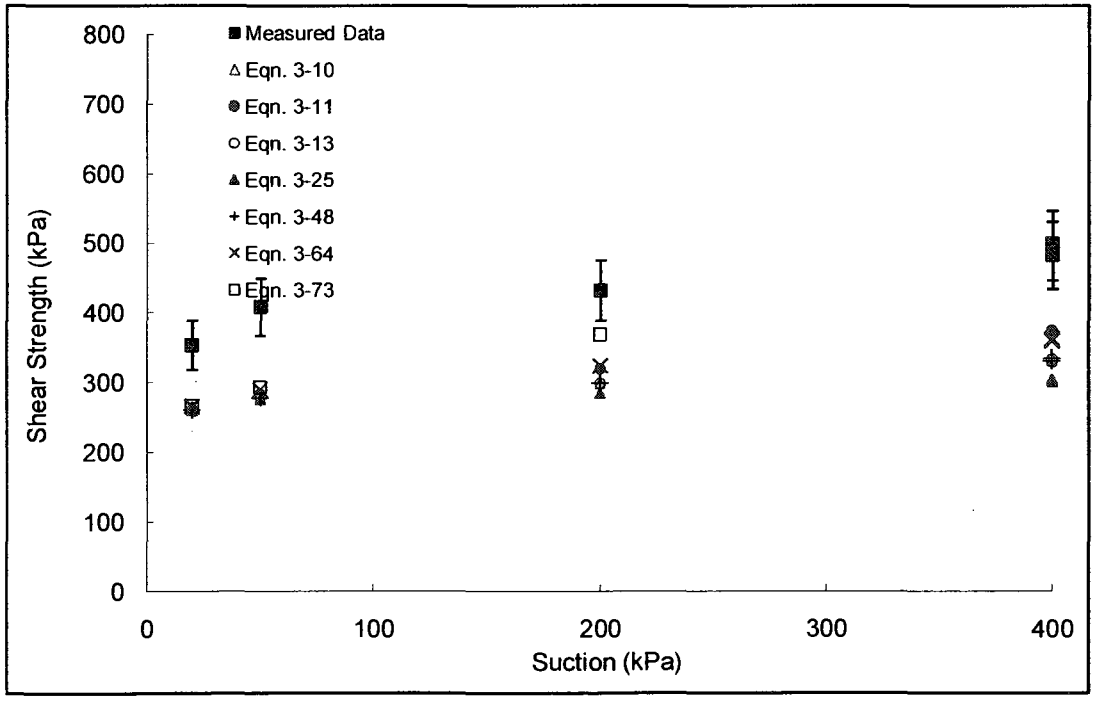

Soil No. 18

Serro do Mar soil

Abramento and Carvalho, 1989

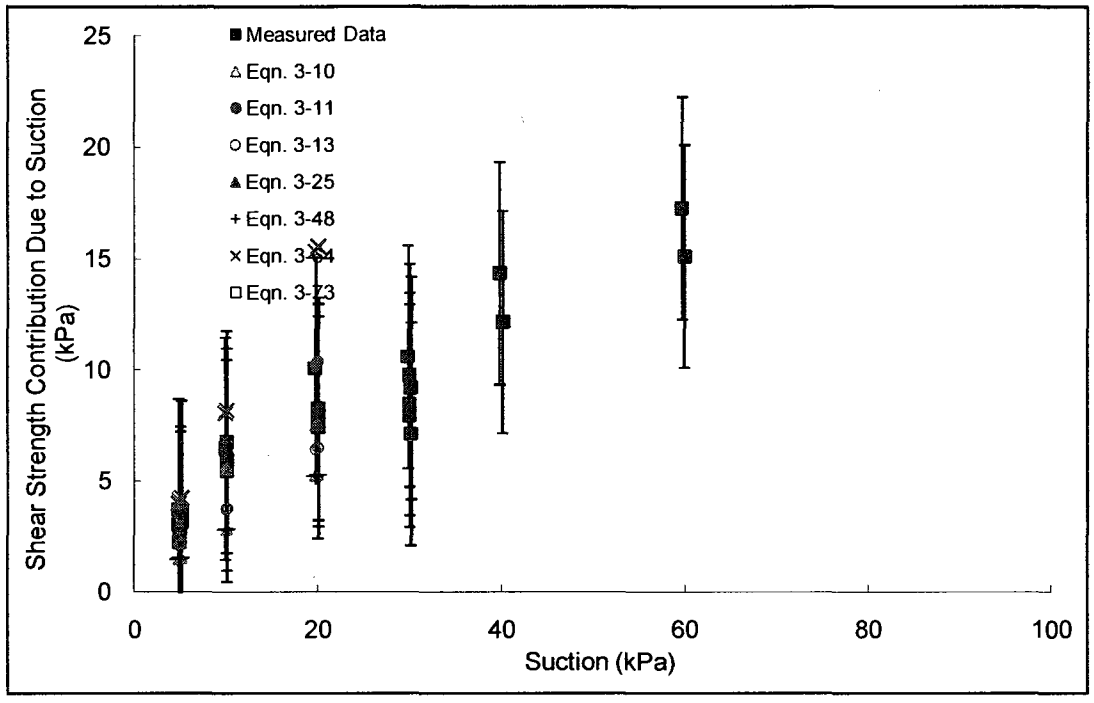

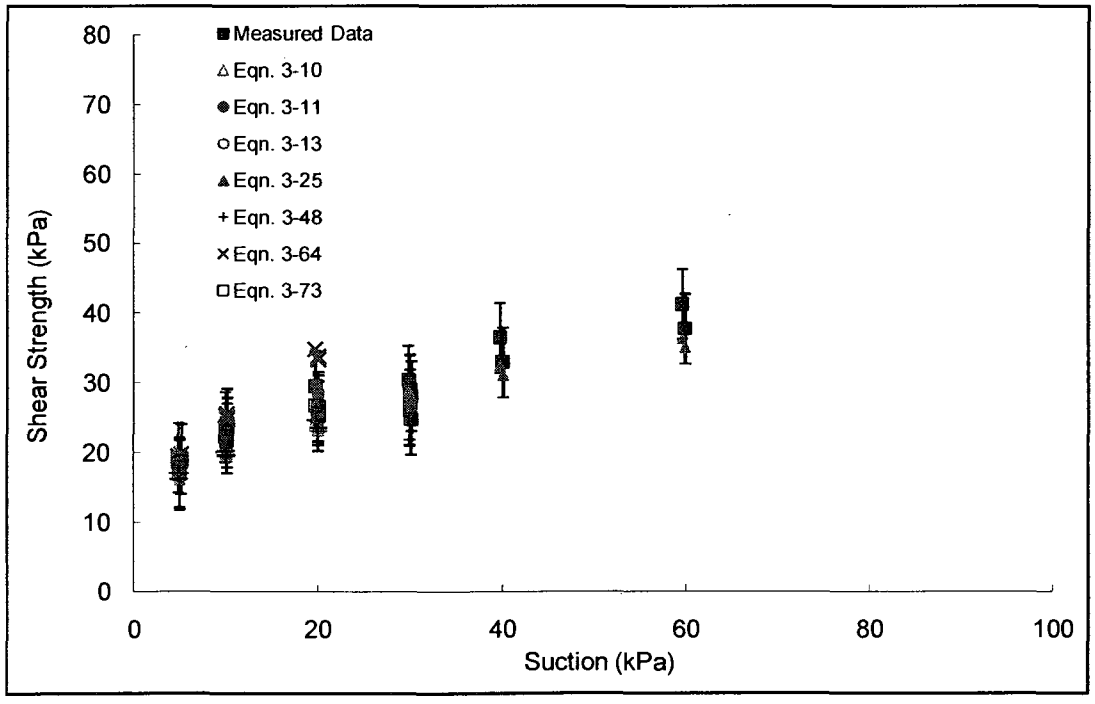

Soil No. 19

Sandy clay loam

Adams, 1996

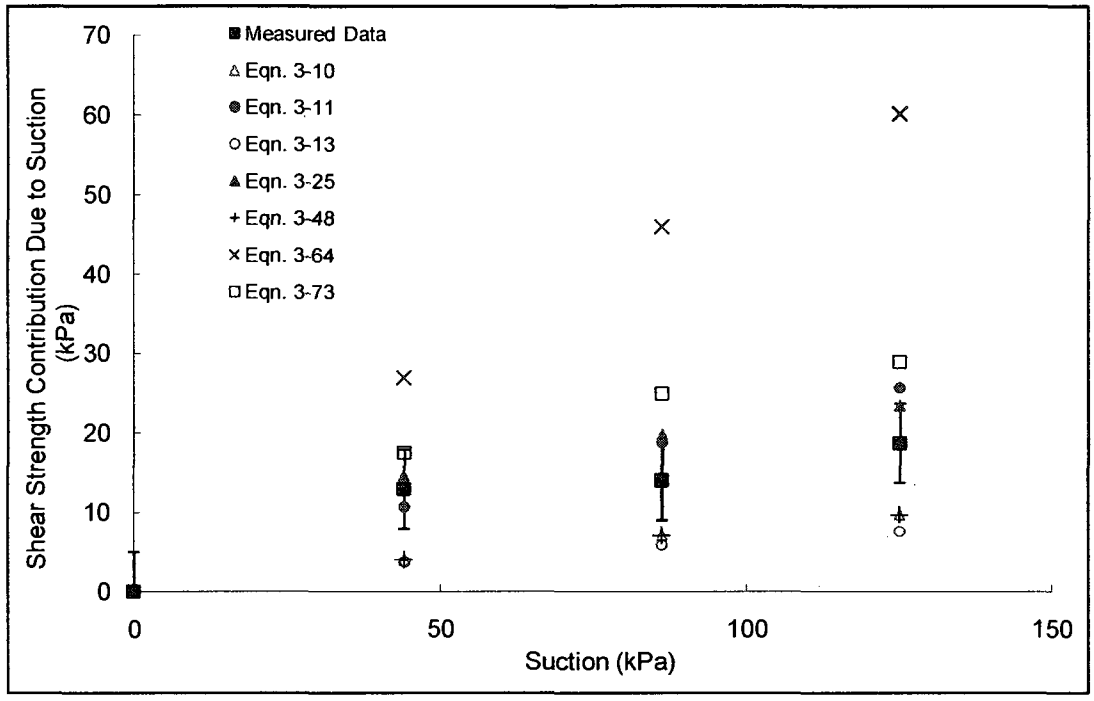

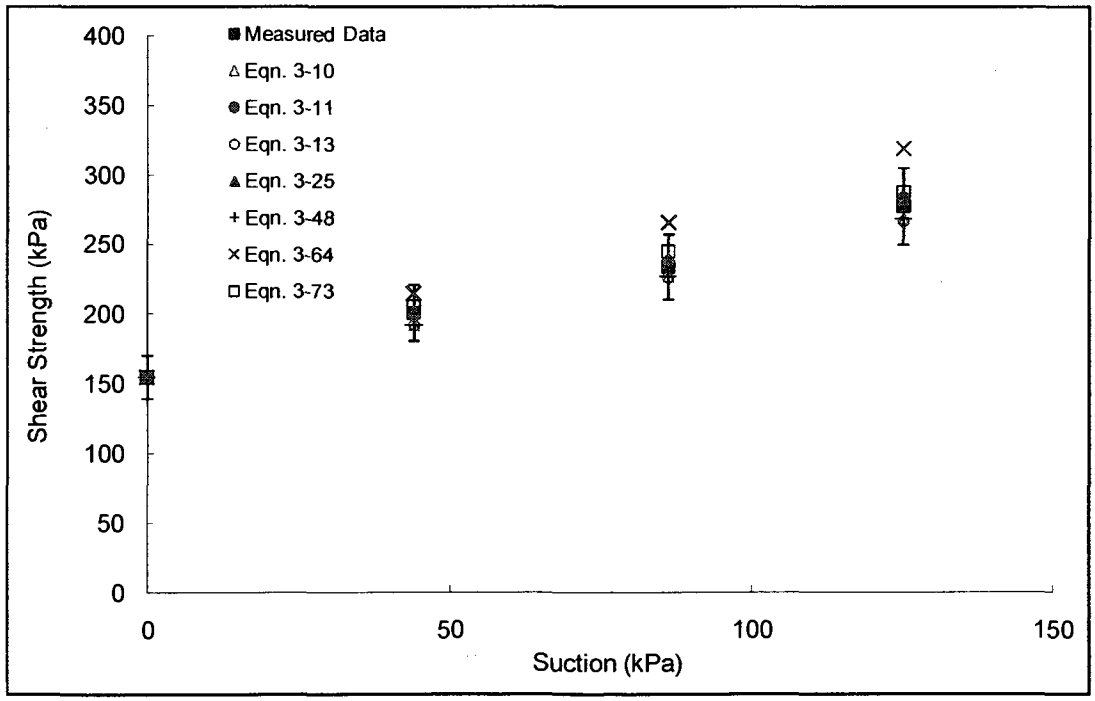

Soil No. 20

Frankston Fine
Donald, 1957

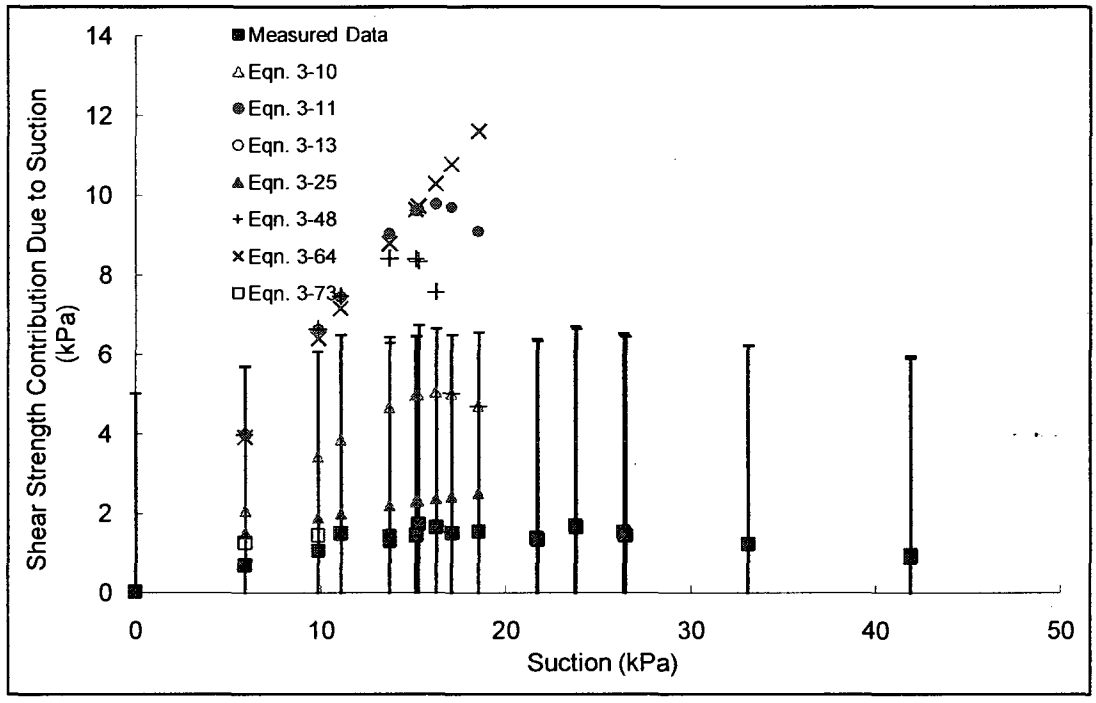

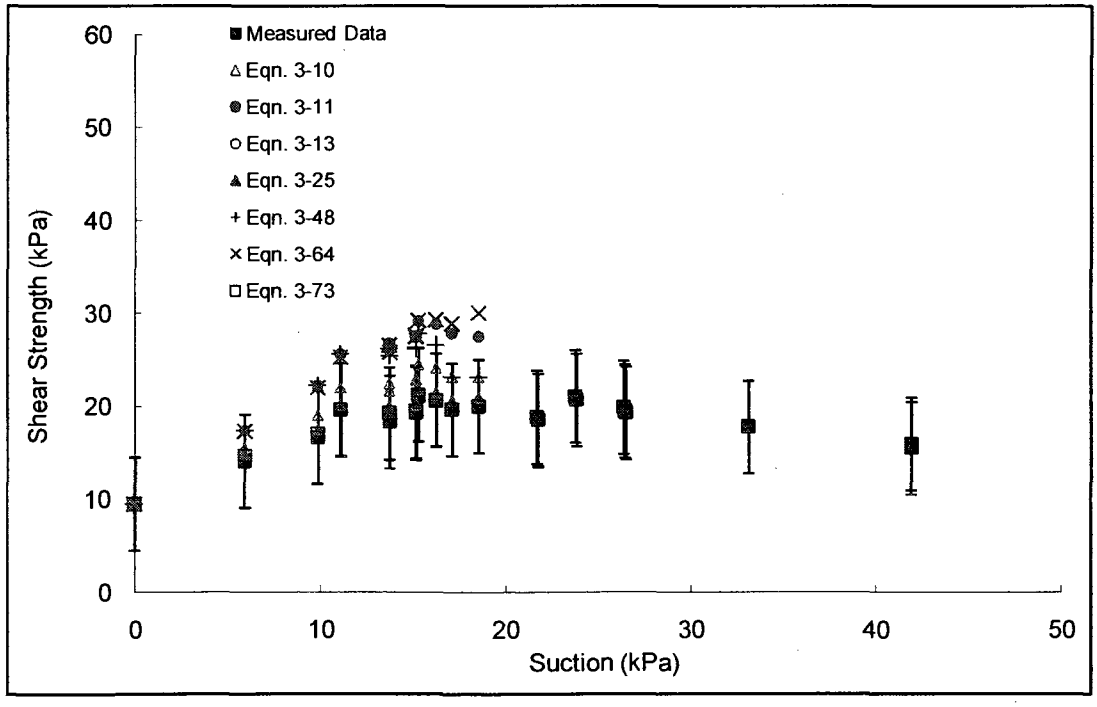

Soil No. 21

Medium Frankston
Donald, 1957

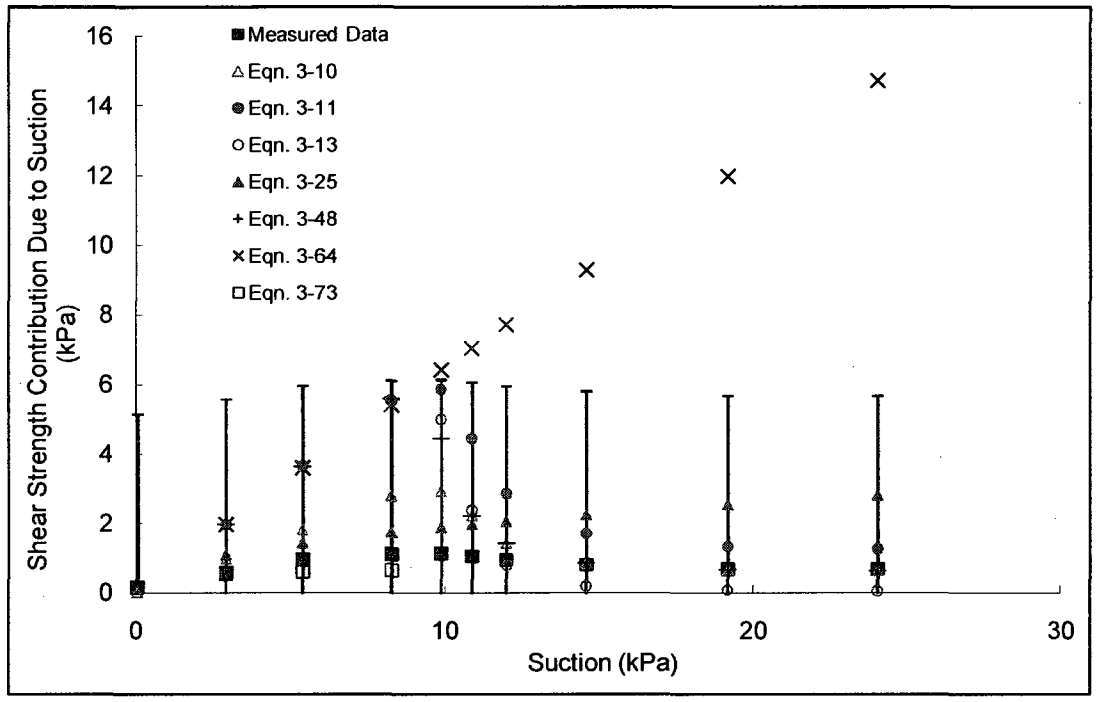

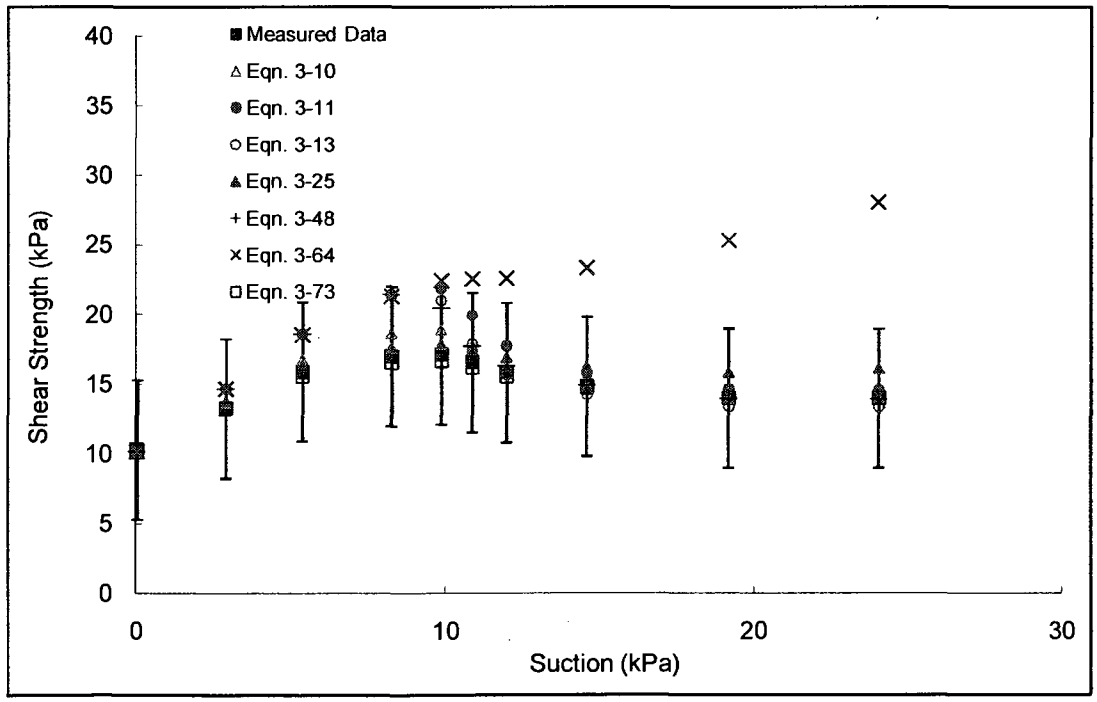

Soil No. 22

Graded Frankston
Donald, 1957

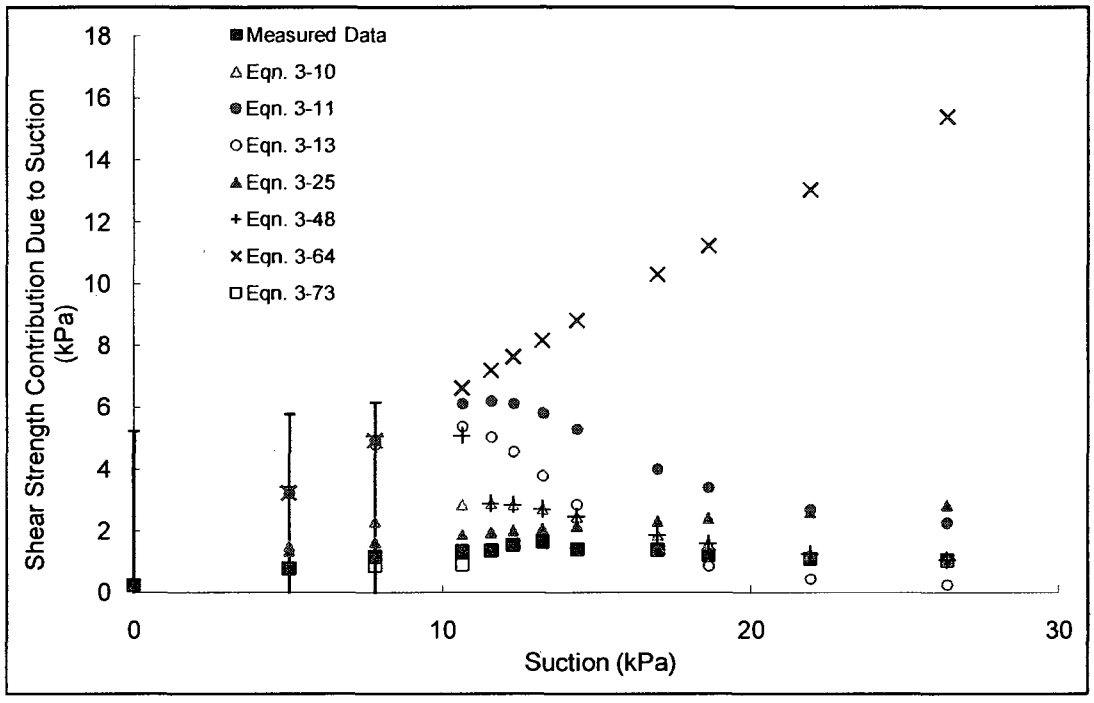

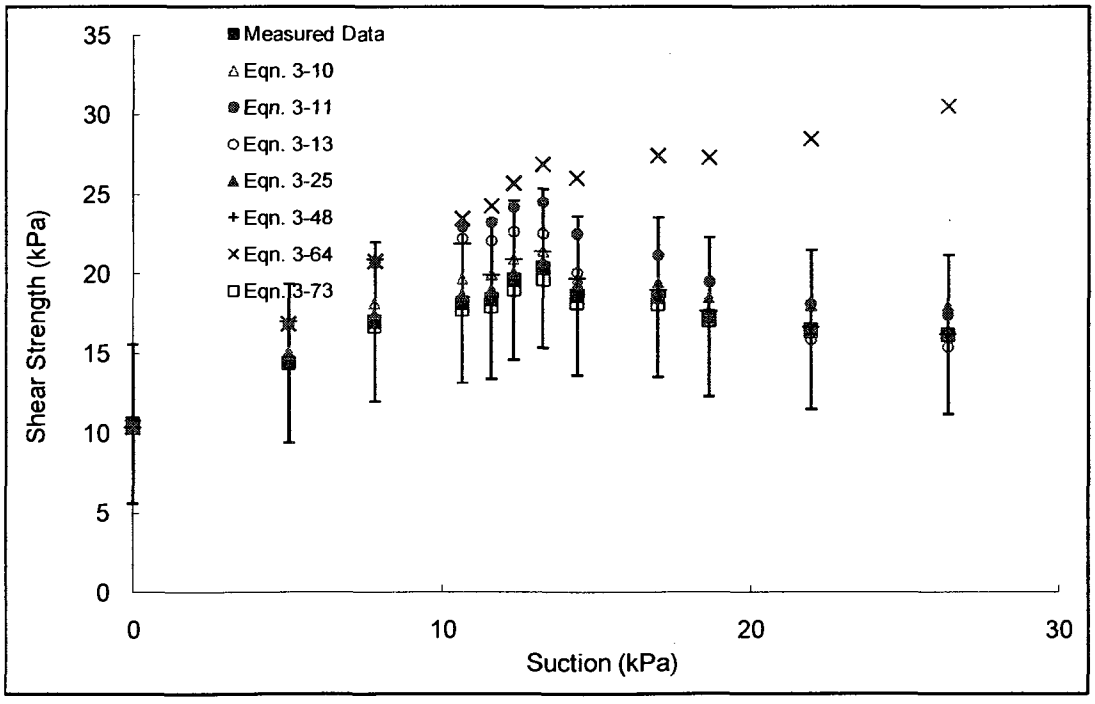

Soil No. 23

Brown sand

Donald, 1957

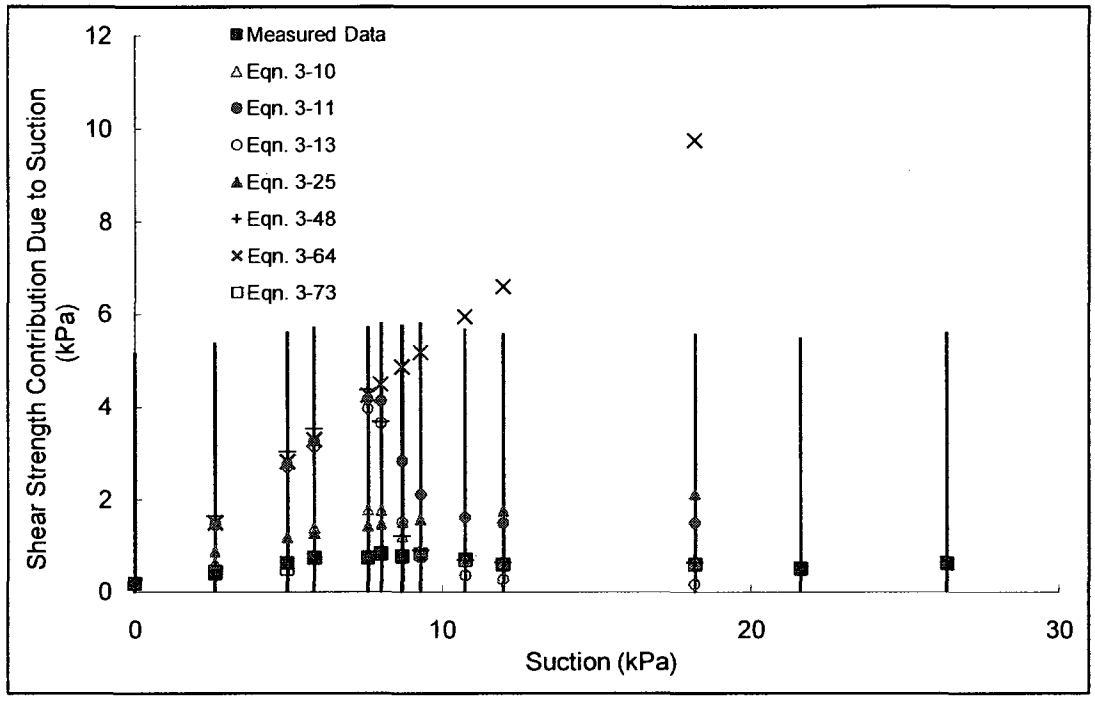

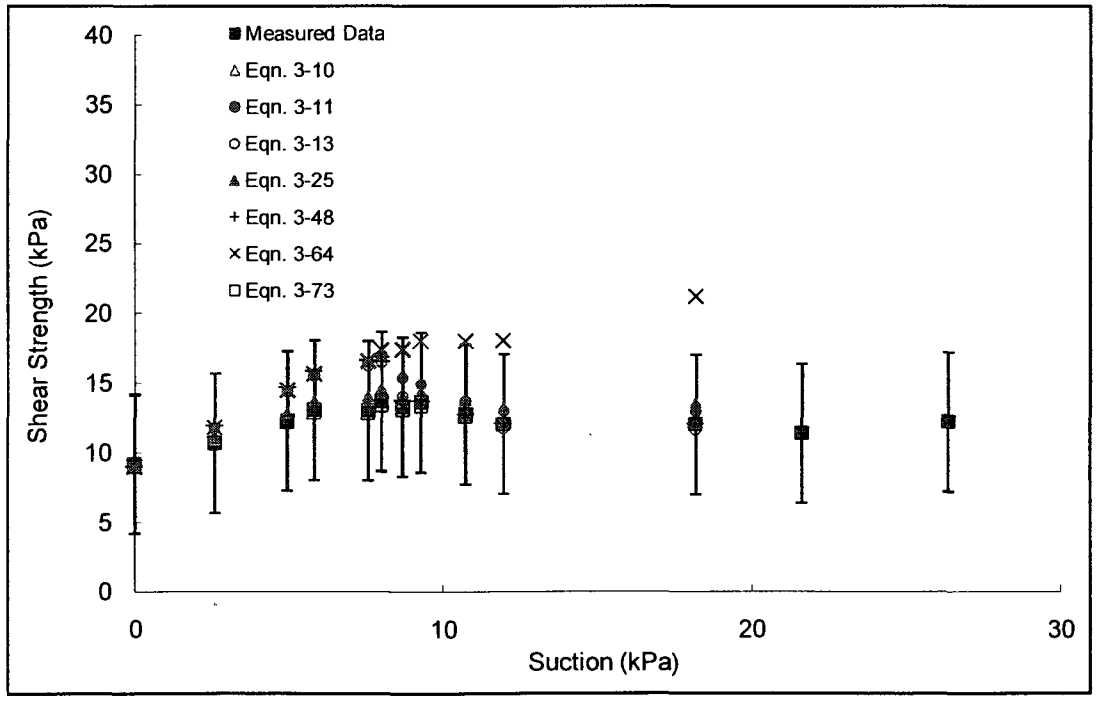

Soil No. 24a

Copper tailings

Drumright and Nelson, 1995; Drumright, 1989

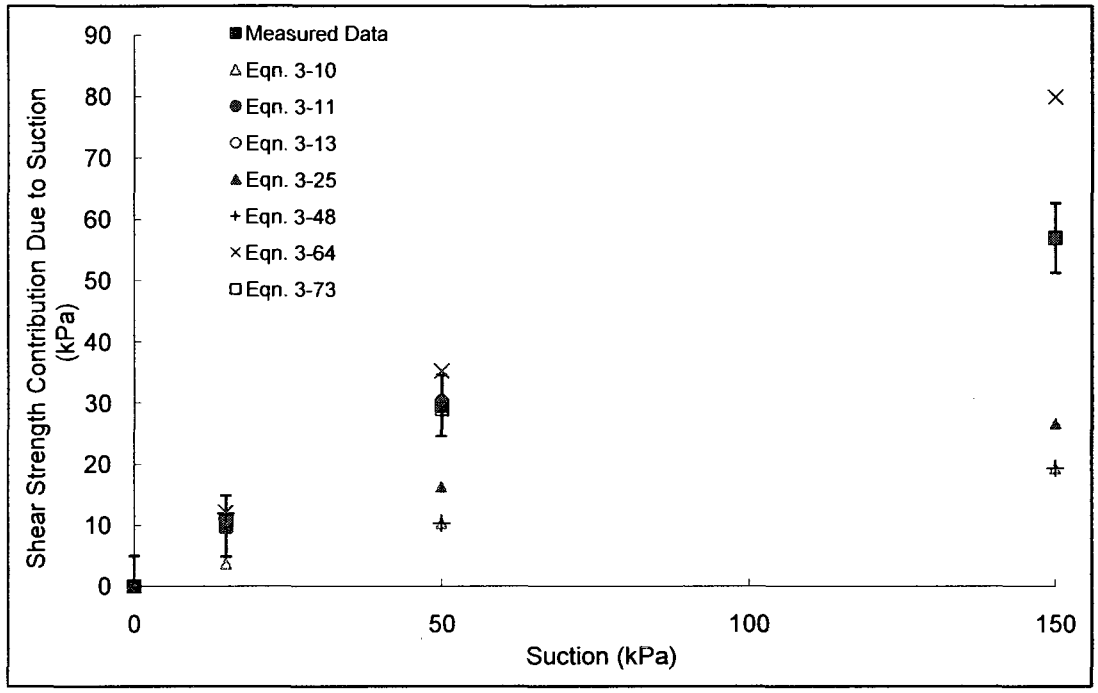

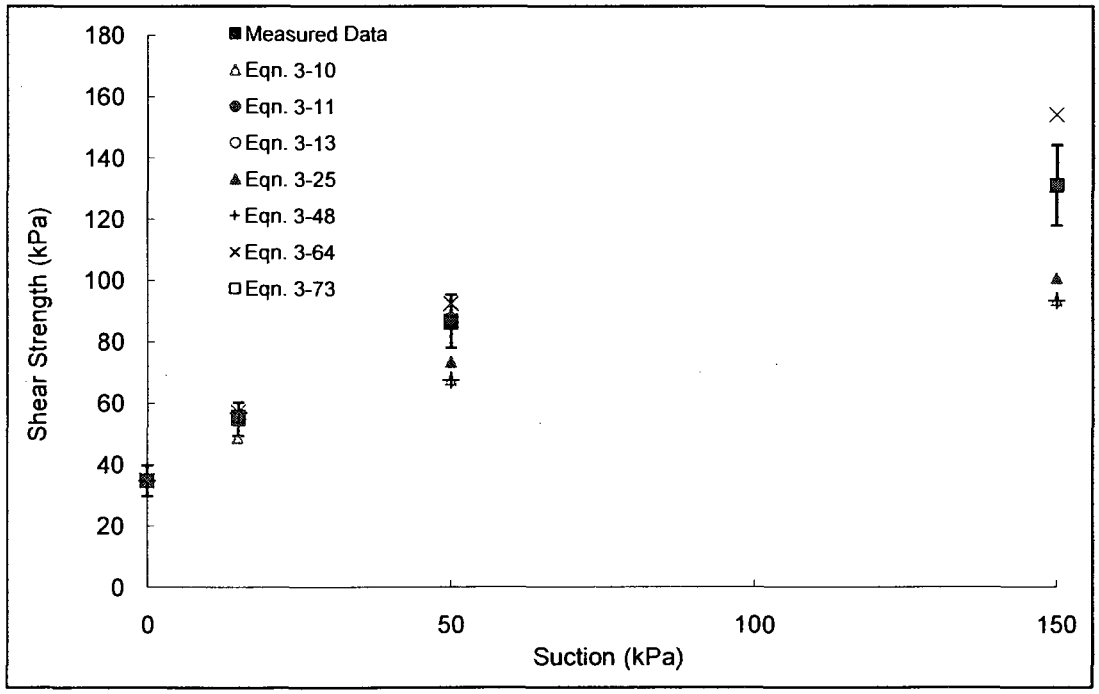

Soil No. 24b

Copper tailings

Drumright and Nelson, 1995; Drumright, 1989

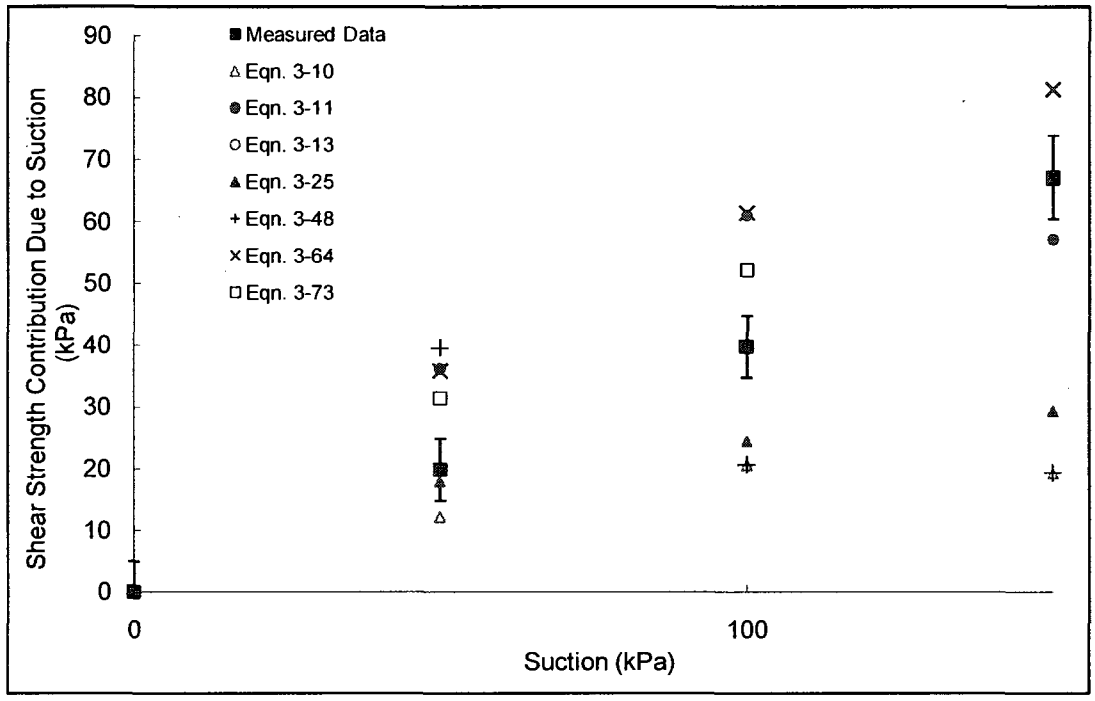

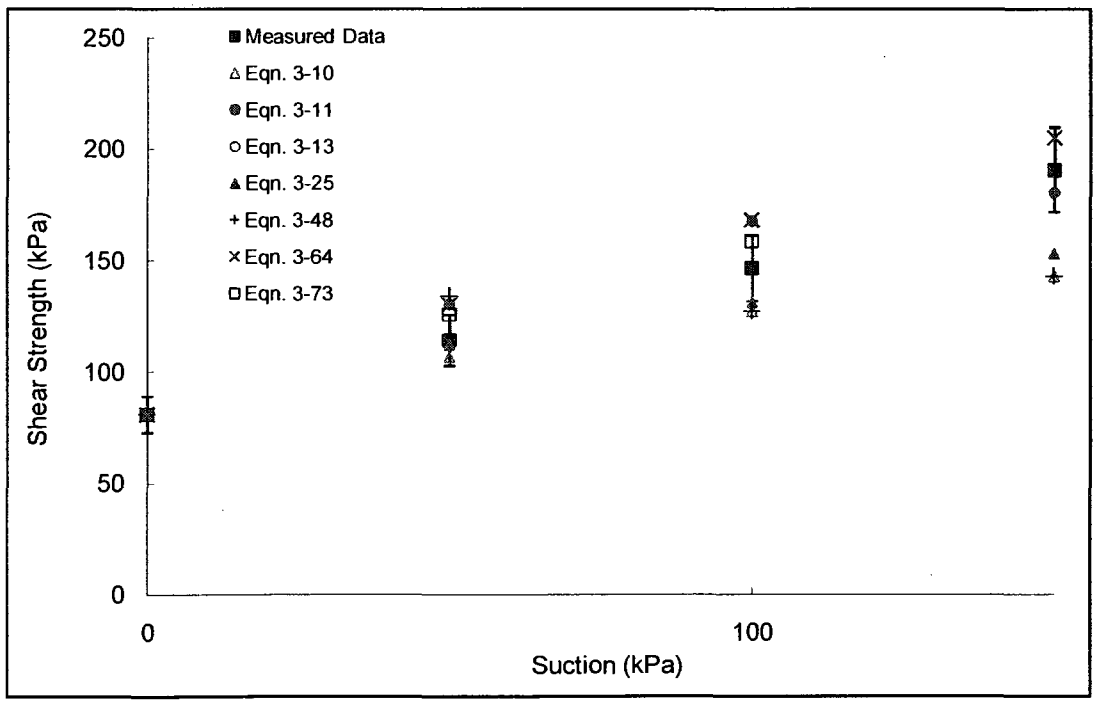

Soil No. 24c

Copper tailings

Drumright and Nelson, 1995; Drumright, 1989

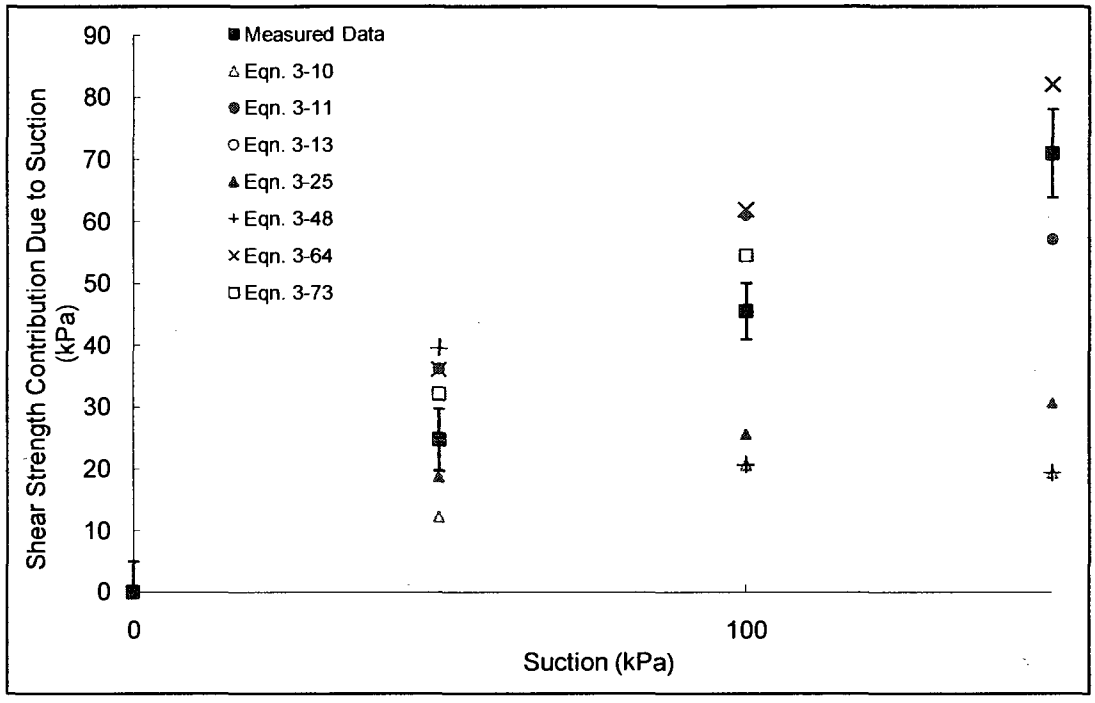

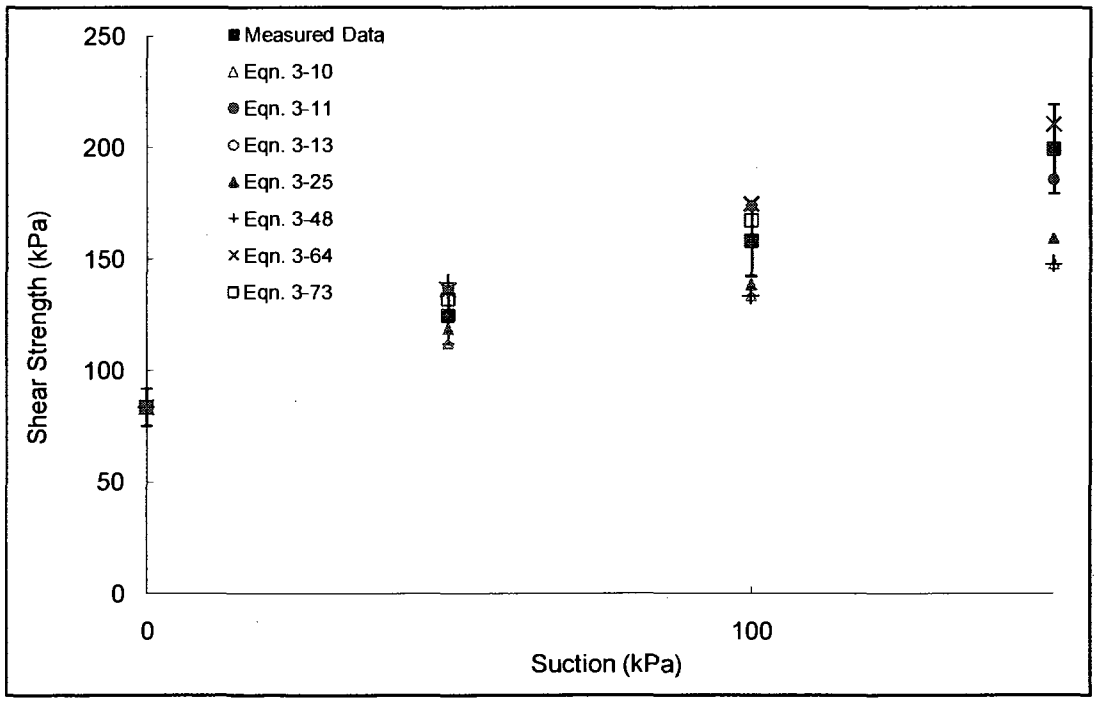

Soil No. 24d

Copper tailings

Drumright and Nelson, 1995; Drumright, 1989

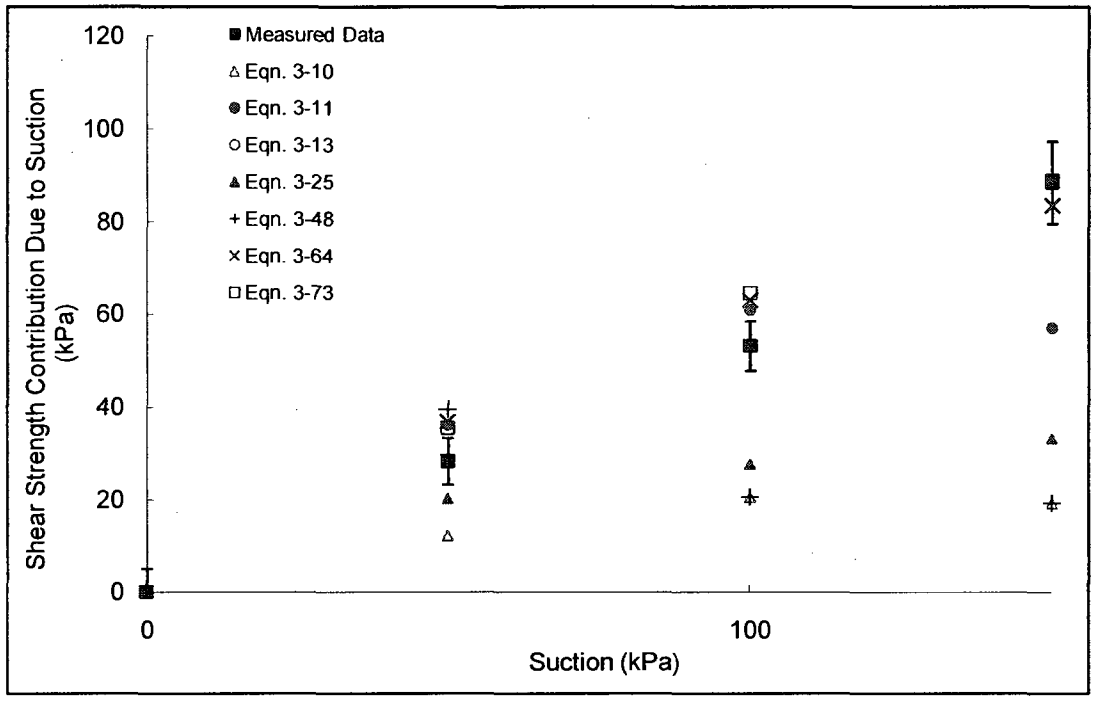

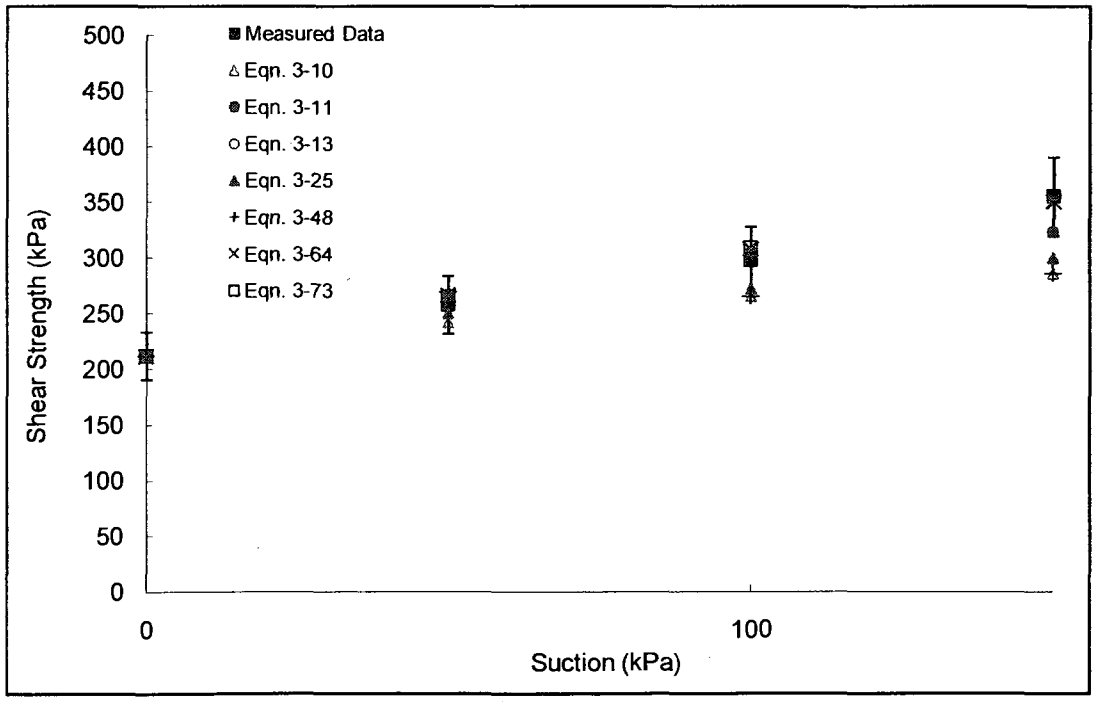

Soil No. 40

Hubei natural soil

Zhan and Ng, 2006

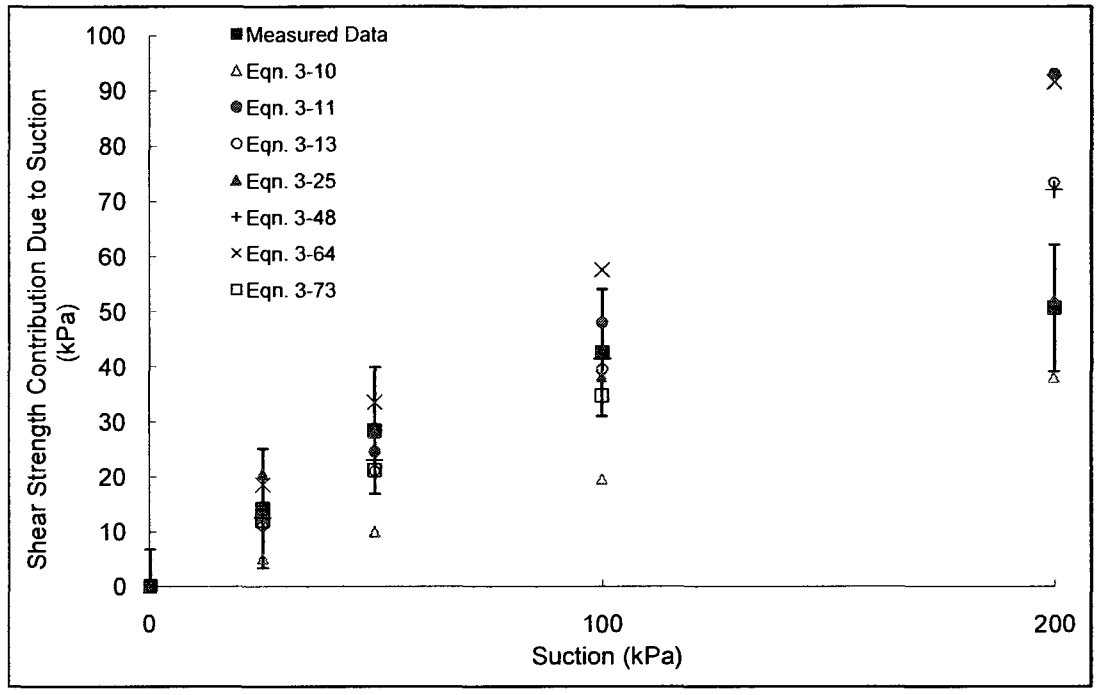

Soil No. 41

Hubei natural soil

Zhan and Ng, 2006

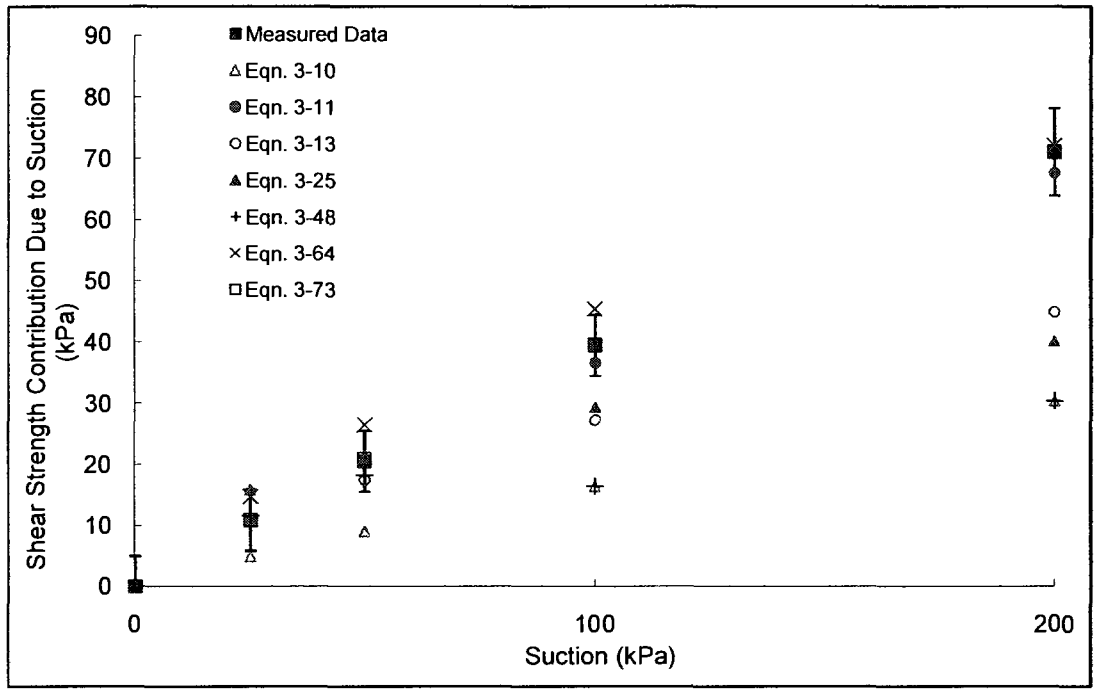

Soil No. 42a

Kuala Lumpur residual

Huat, Ali and Hashim, 2005

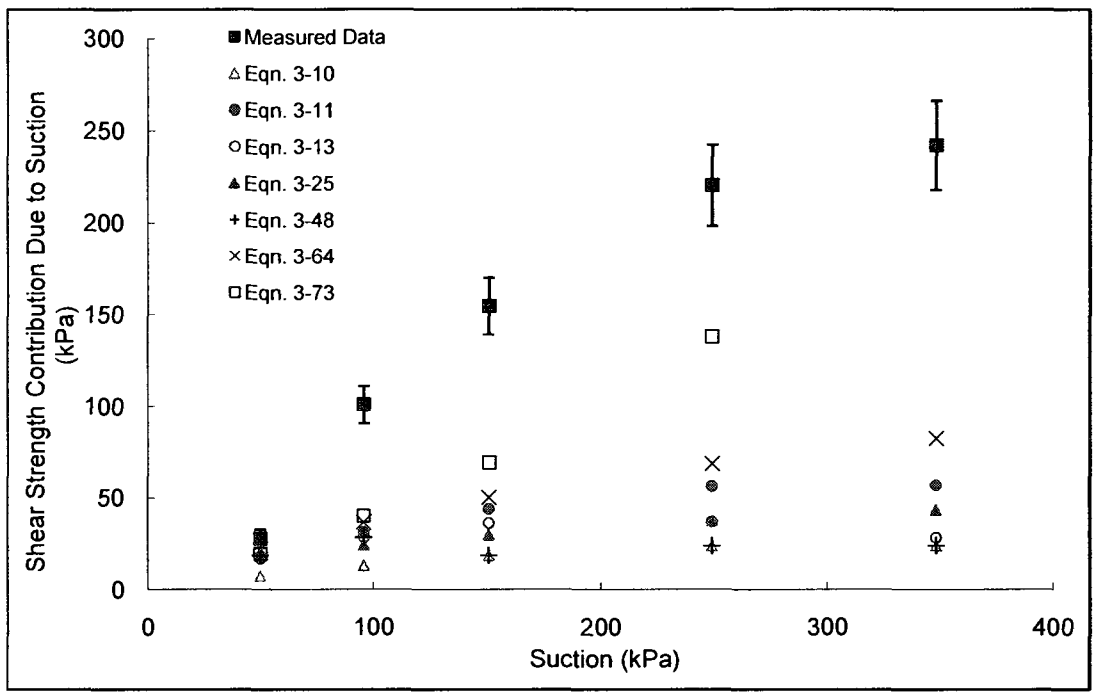

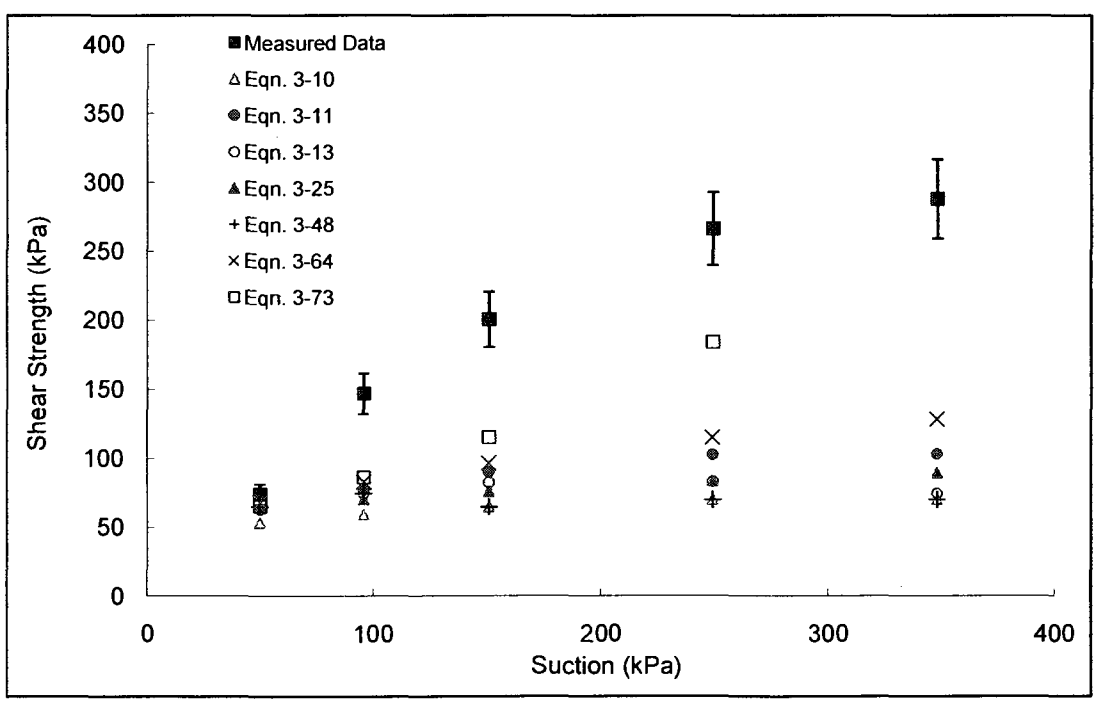

Soil No. 42b

Kuala Lumpur residual

Huat, Ali and Hashim, 2005

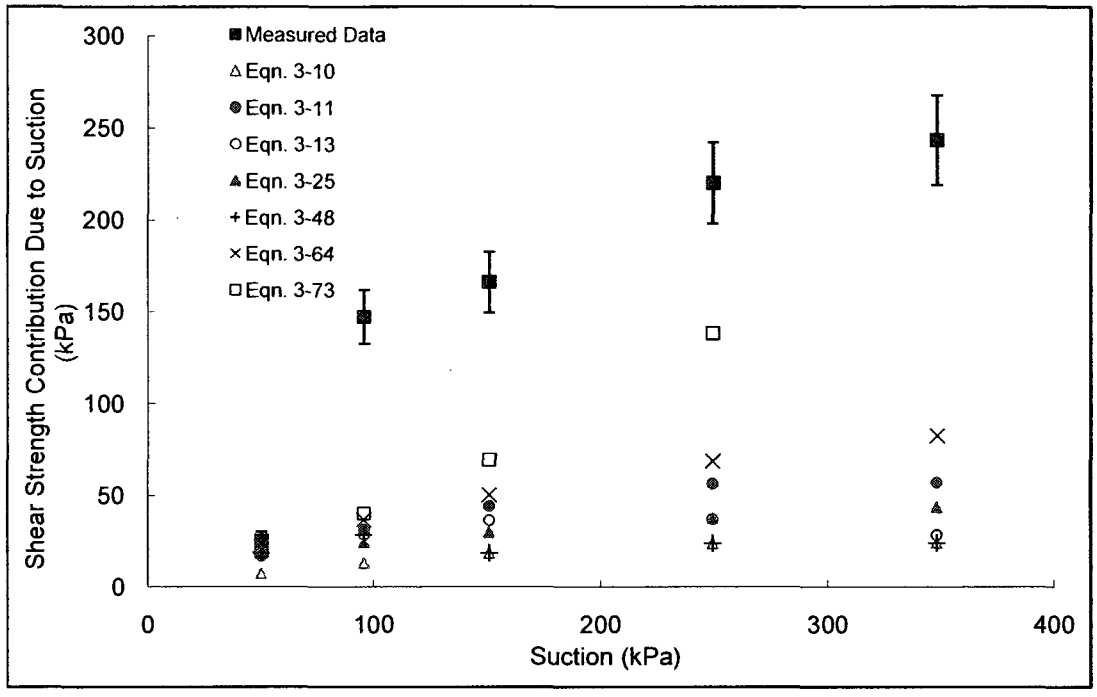

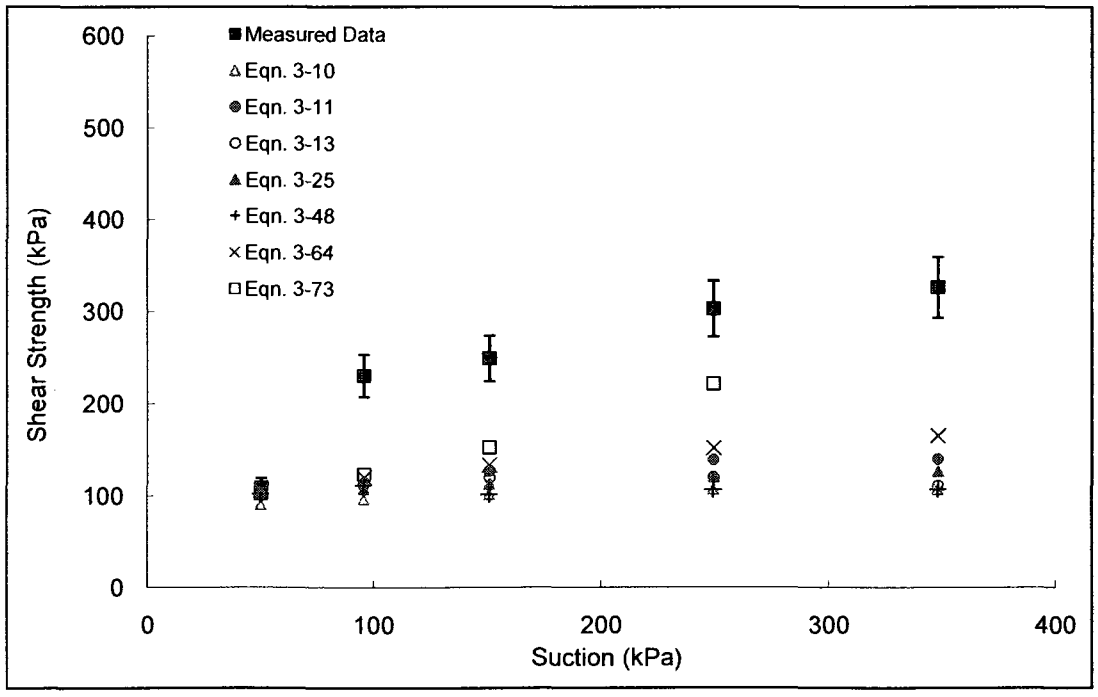

Soil No. 42c

Kuala Lumpur residual

Huat, Ali and Hashim, 2005

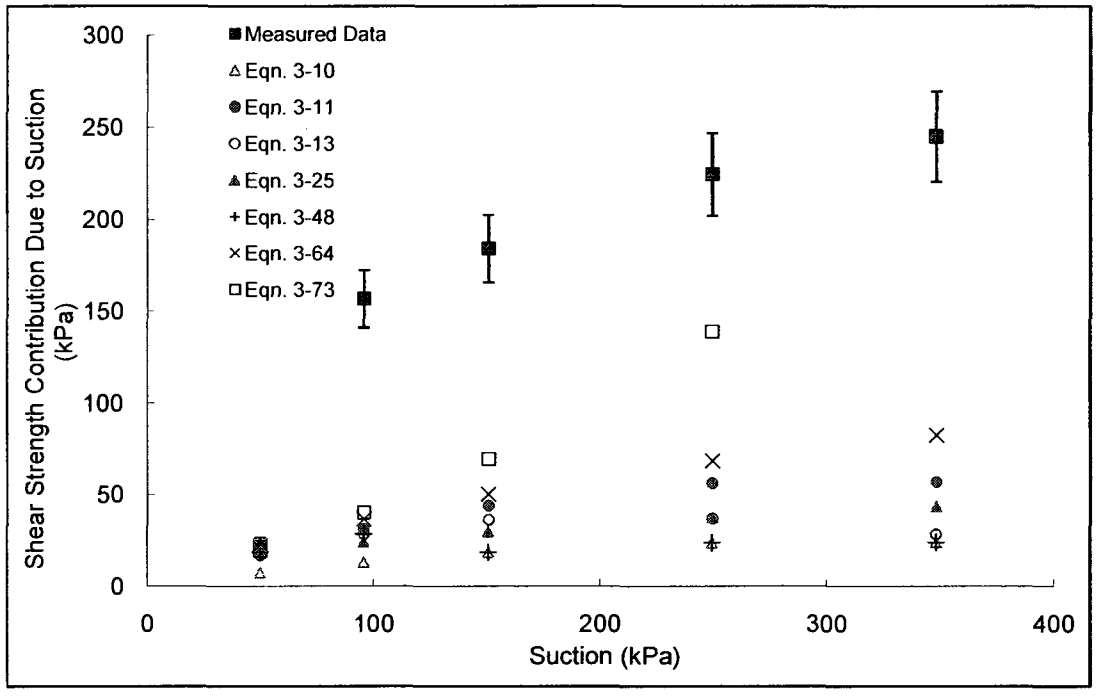

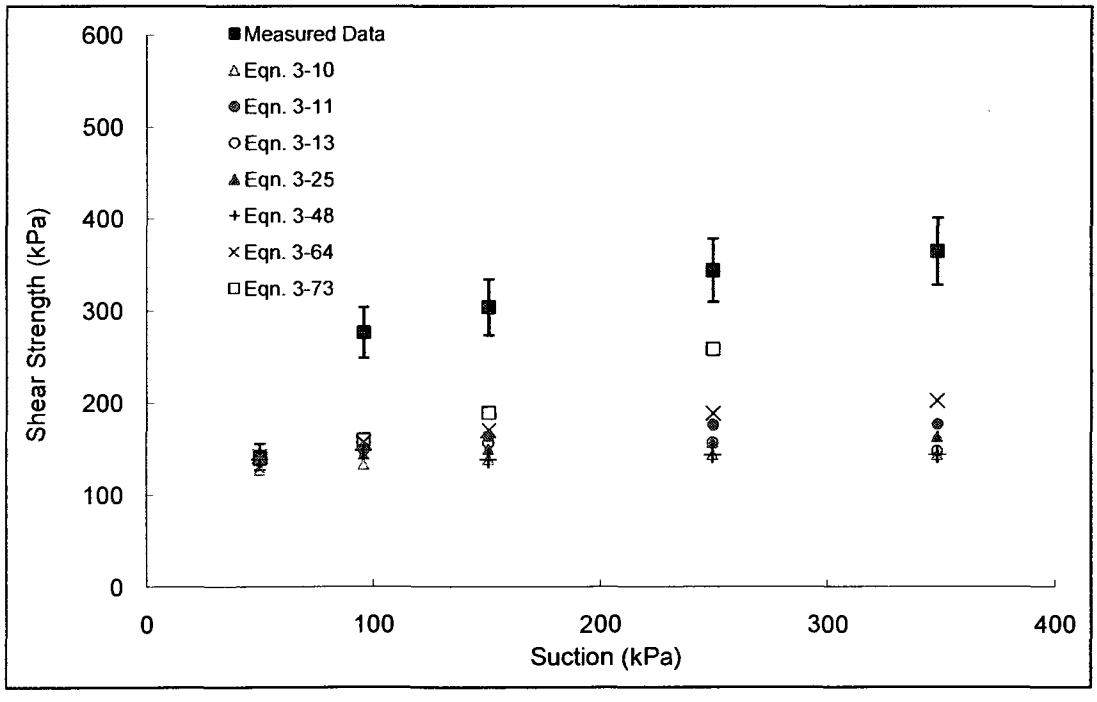

Soil No. 42d

Kuala Lumpur residual

Huat, Ali and Hashim, 2005

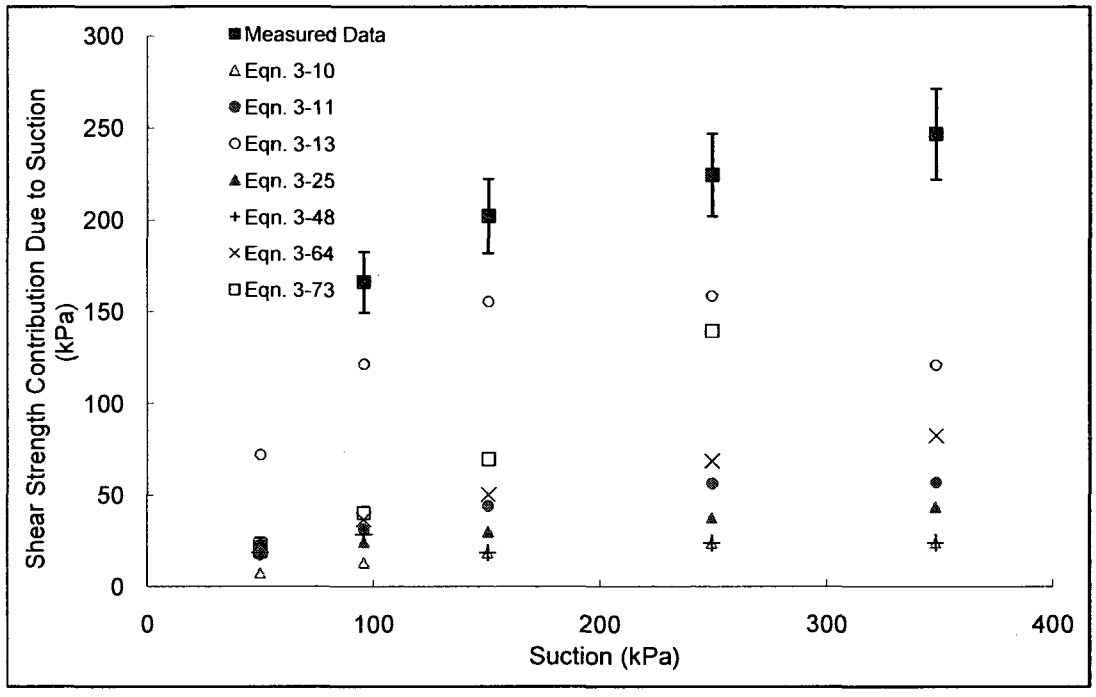

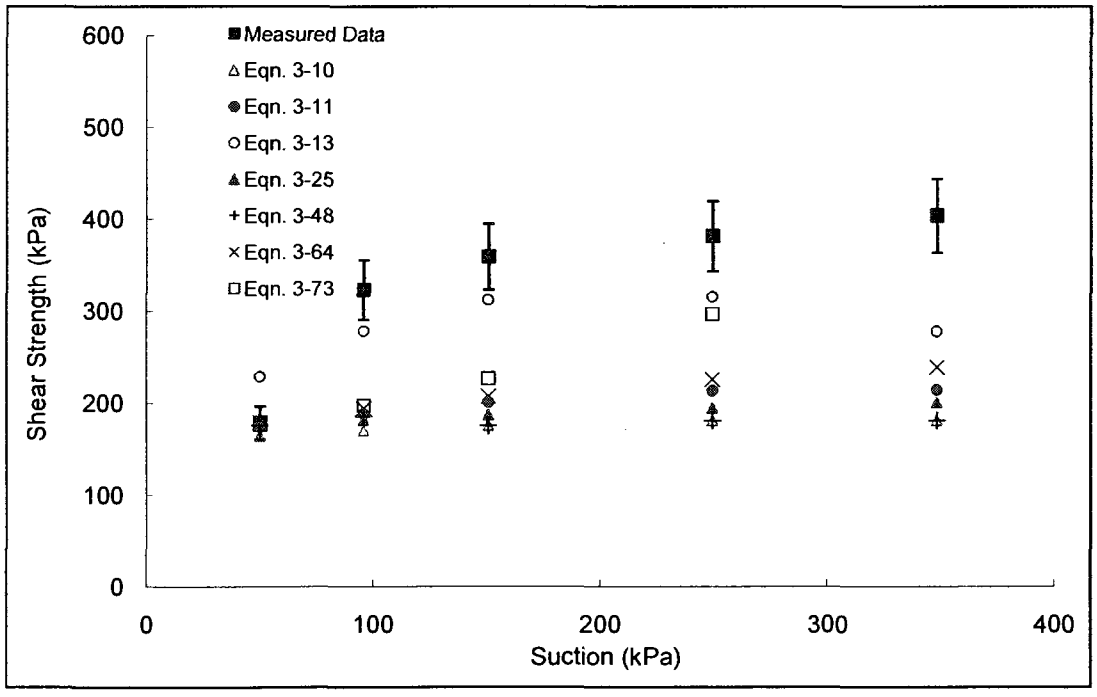

Soil No. 43a

Jovem

Reis and Vilar, 2005

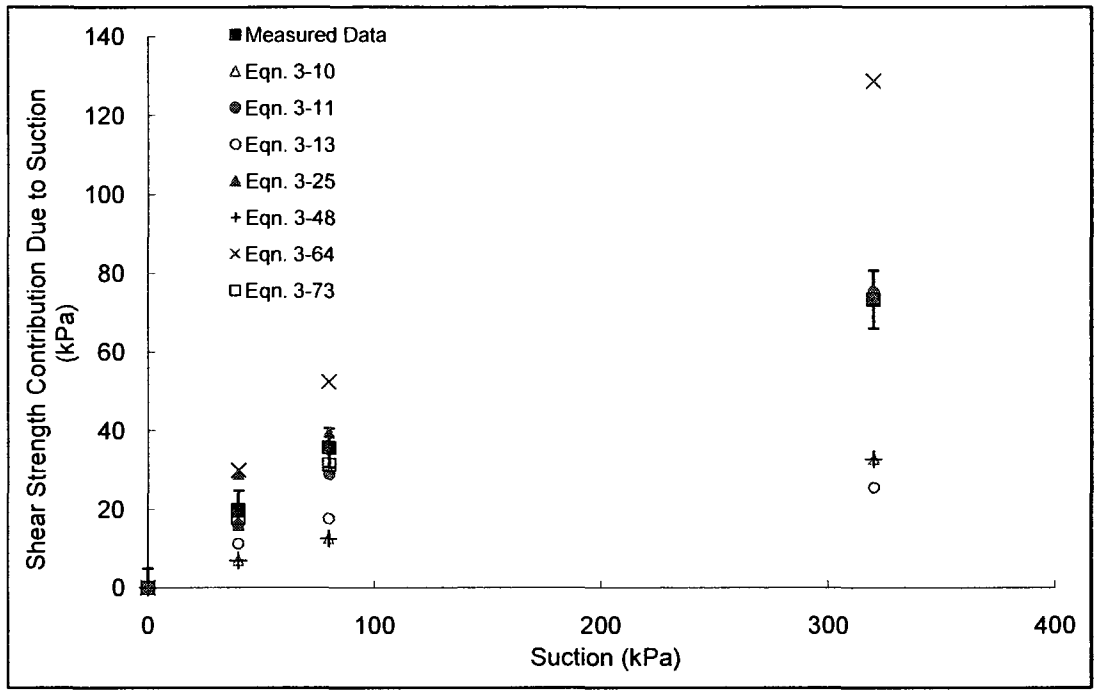

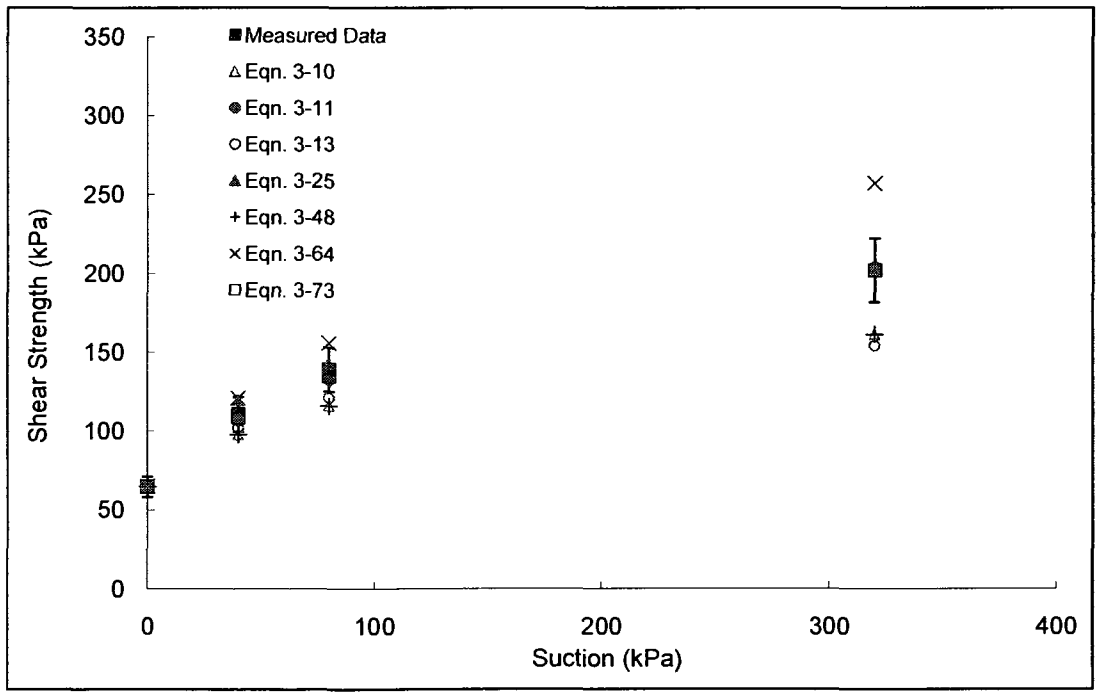

Soil No. 43b

Jovem

Reis and Vilar, 2005

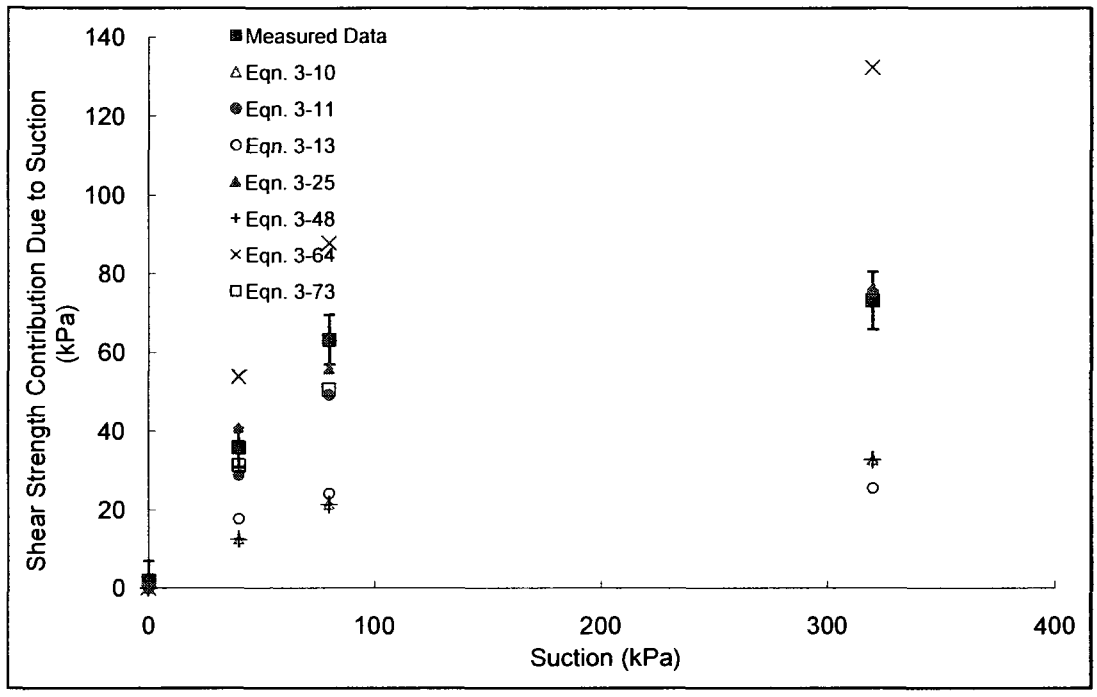

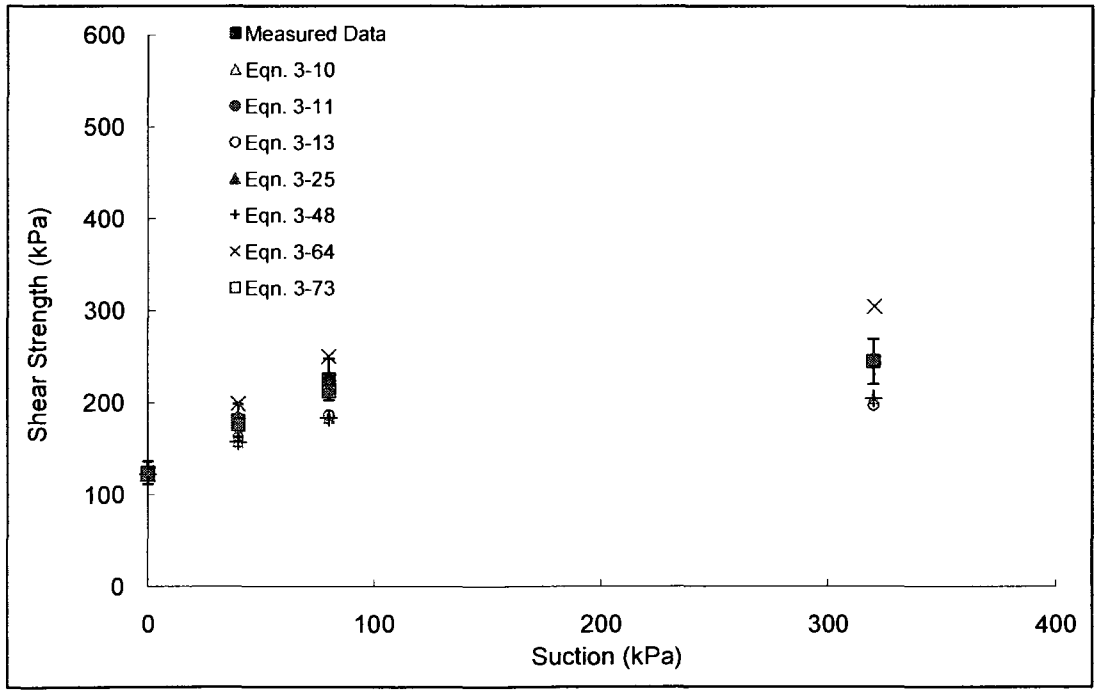

Soil No. 43c

Jovem

Reis and Vilar, 2005

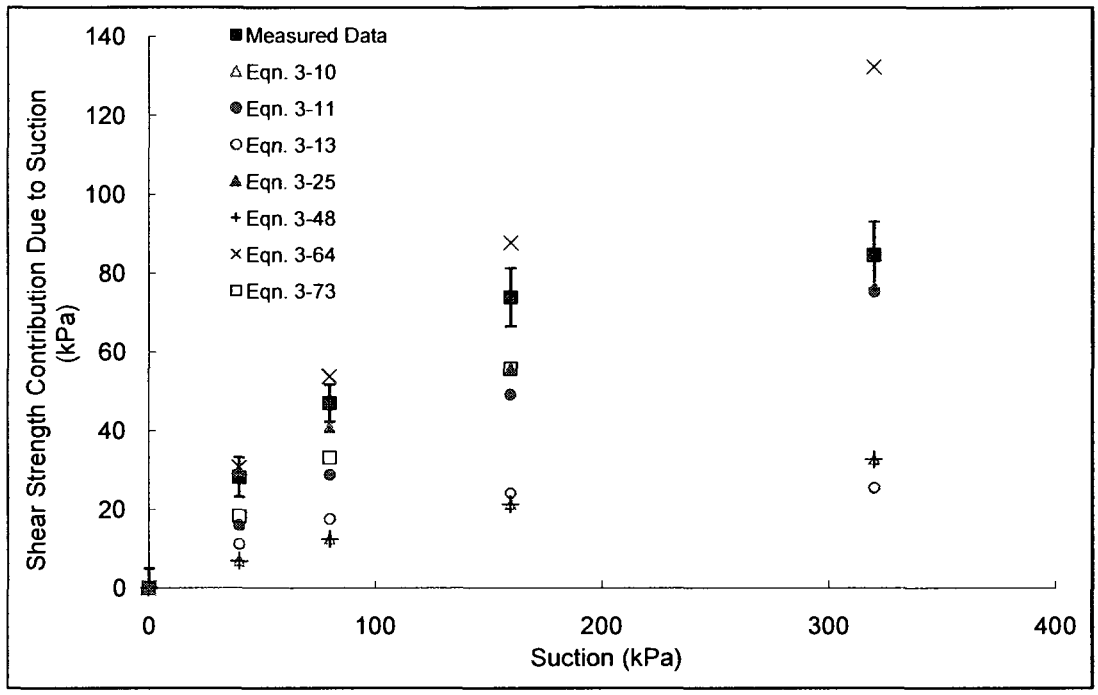

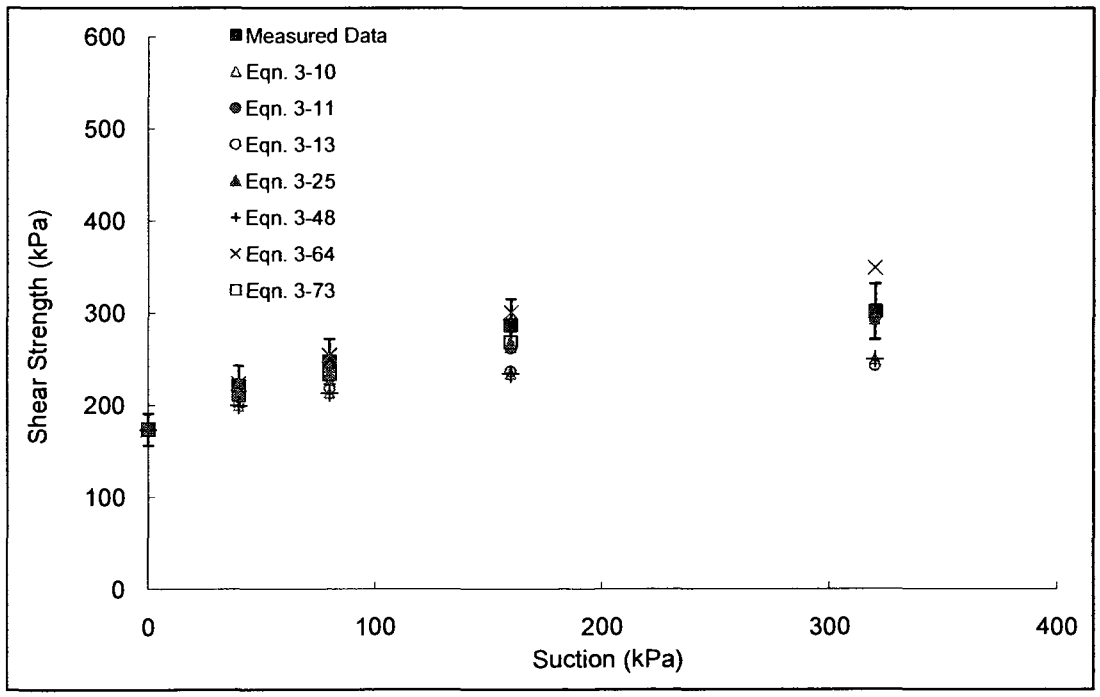

Soil No. 44a

Maduro

Reis and Vilar, 2005

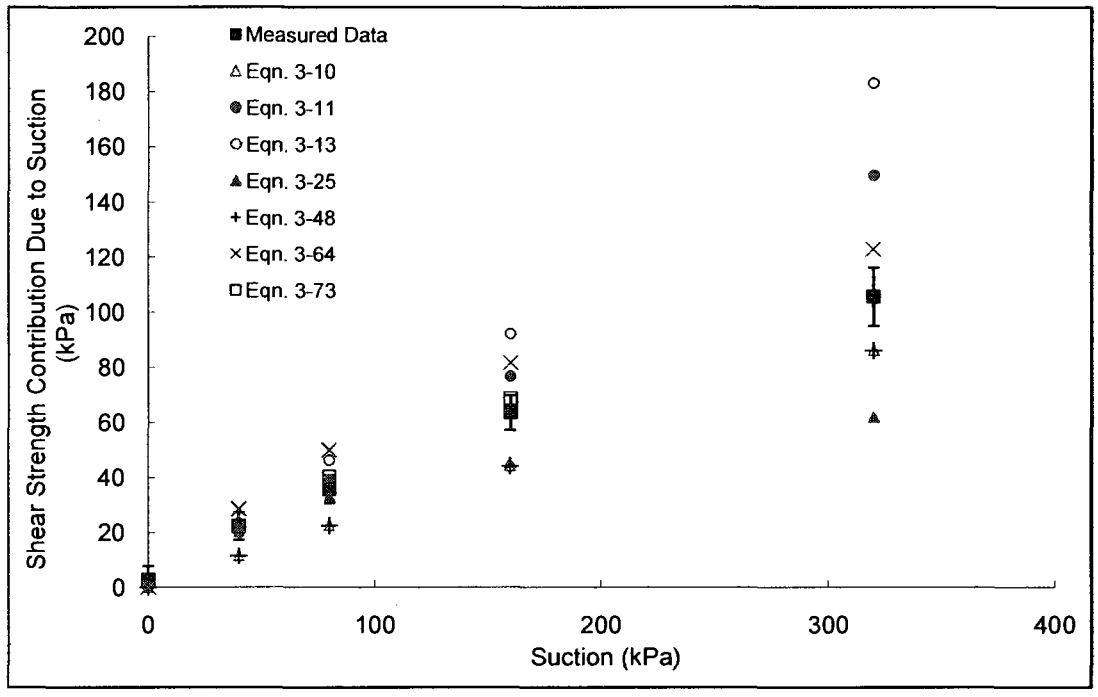

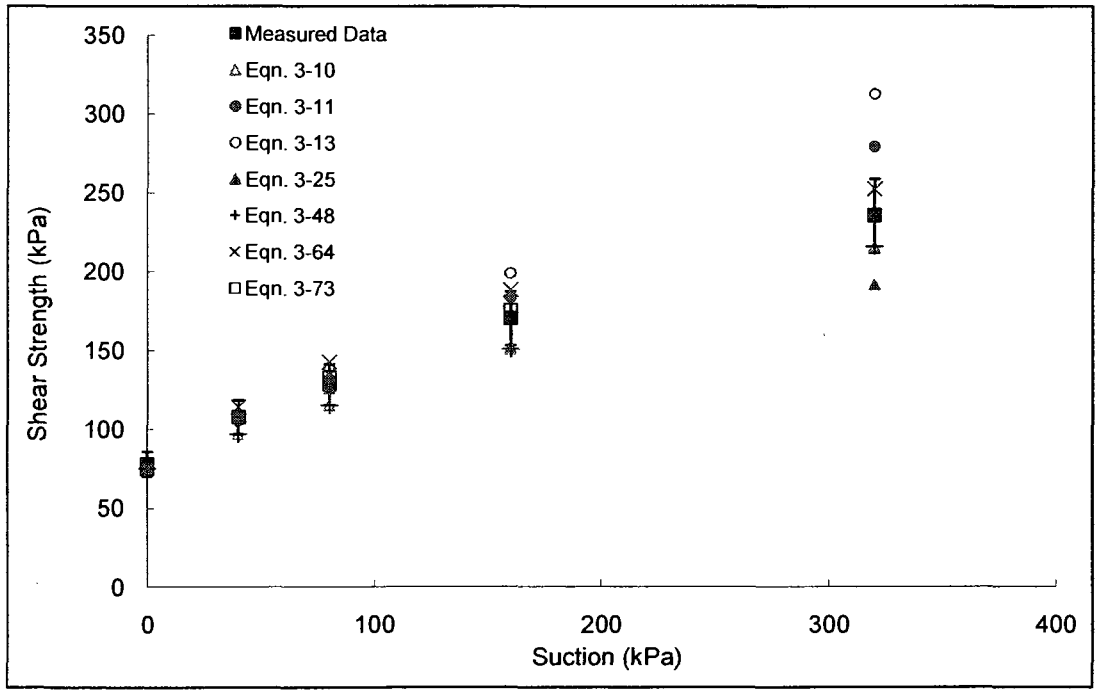

Soil No. 44b

Maduro

Reis and Vilar, 2005

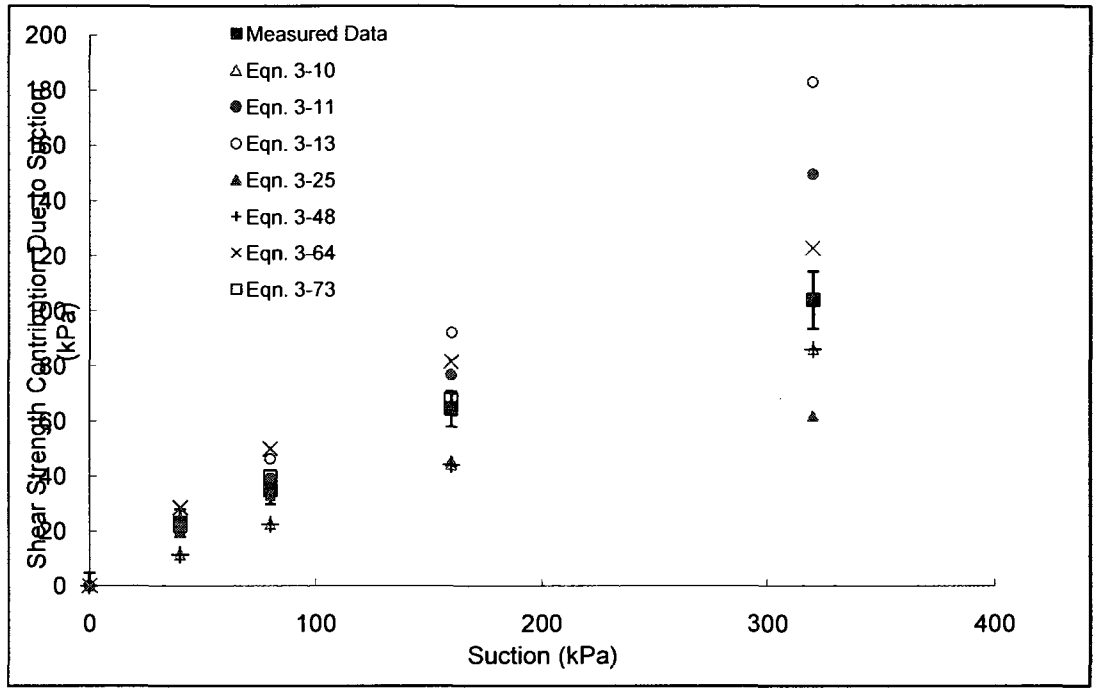

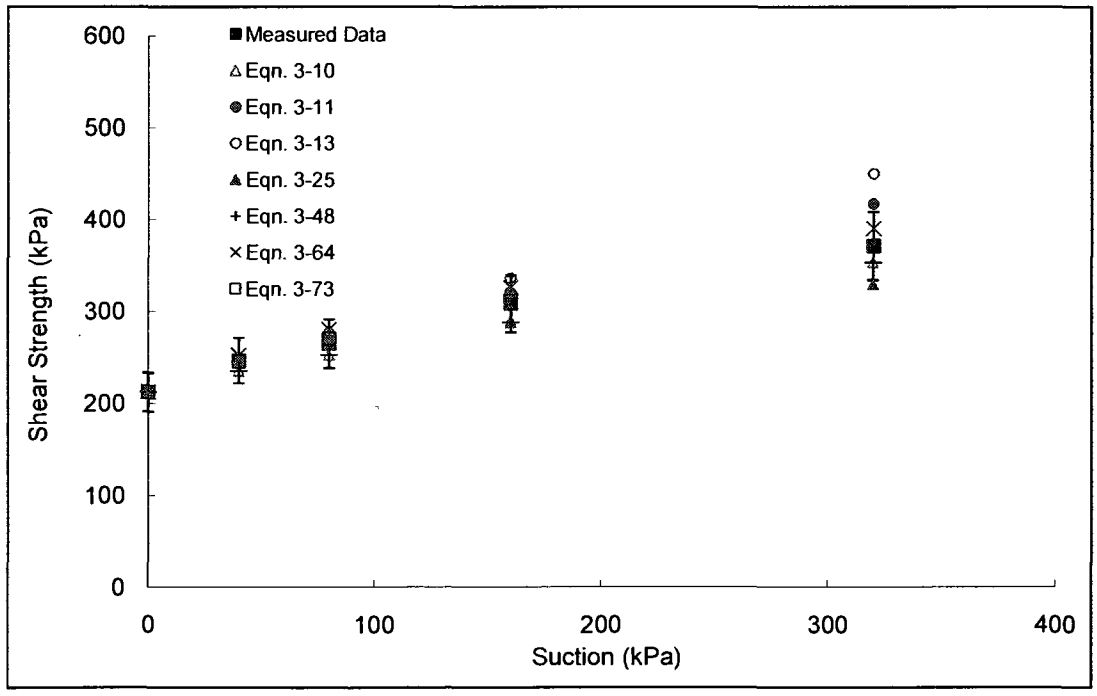

Soil No. 45a

Ashikaga silt

Nishimura, Fredlund, Gan and Hirabayashi, 1999

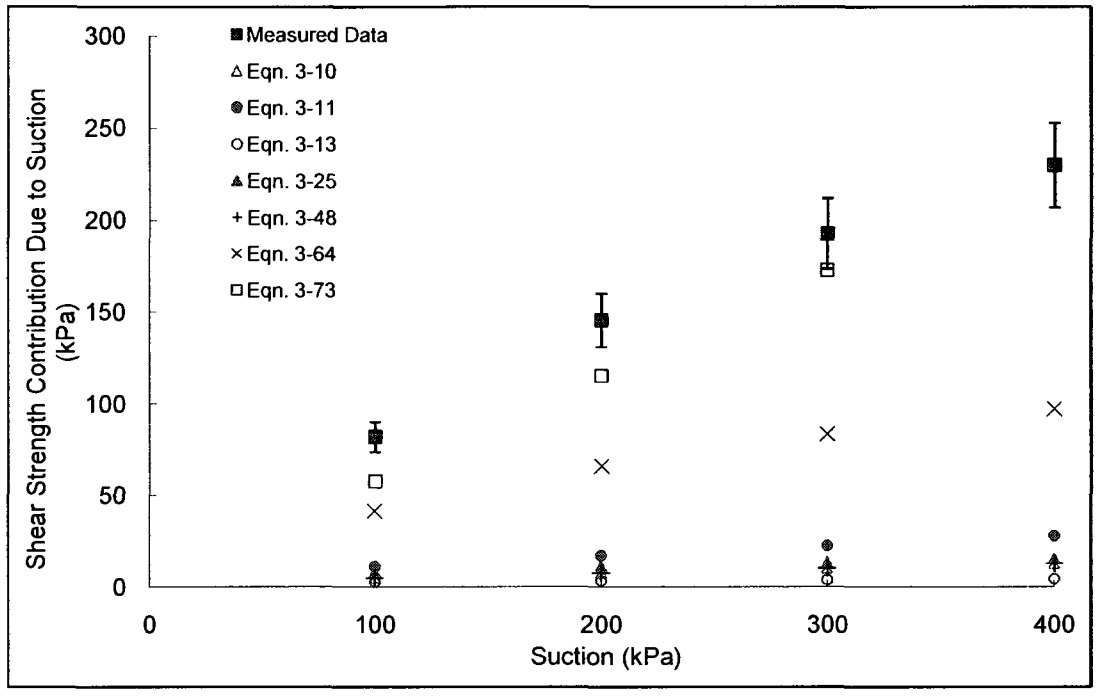

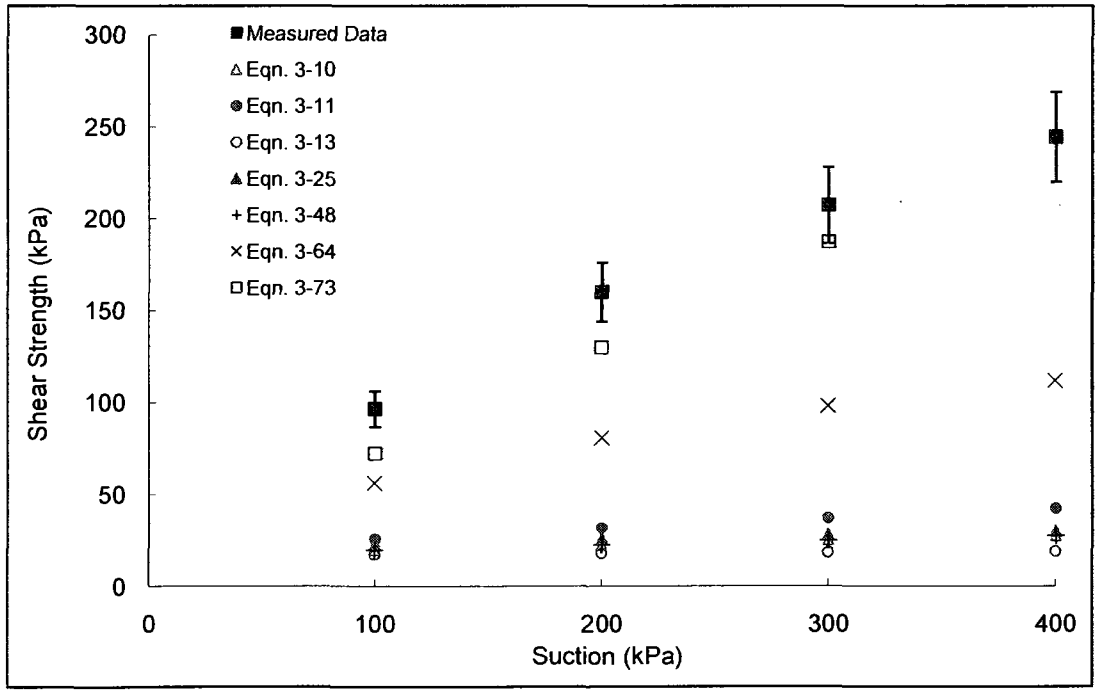

Soil No. 45b **Ashikaga silt**

Nishimura, Fredlund, Gan and Hirabayashi, 1999

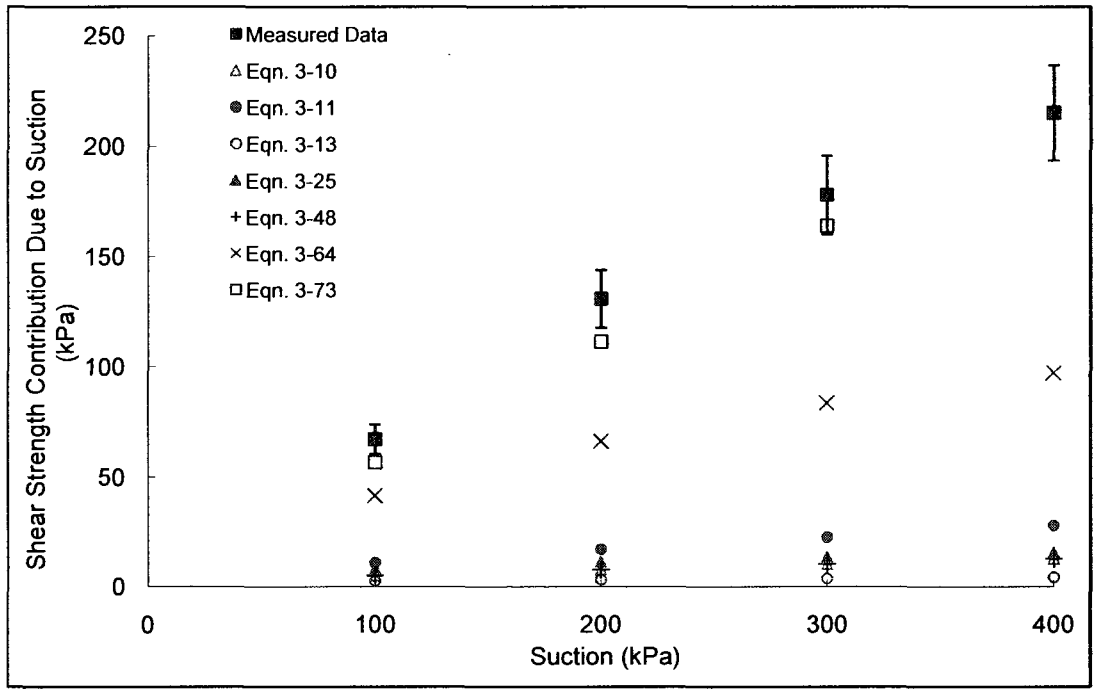

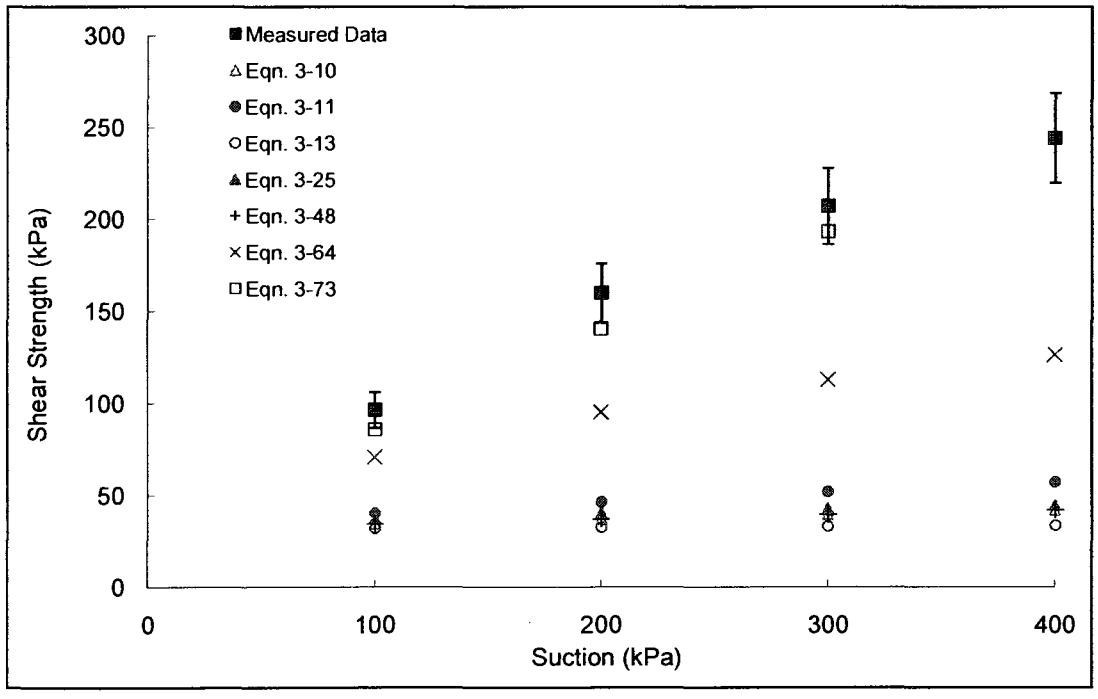

Soil No. 45c

Ashikaga silt

Nishimura, Fredlund, Gan and Hirabayashi, 1999

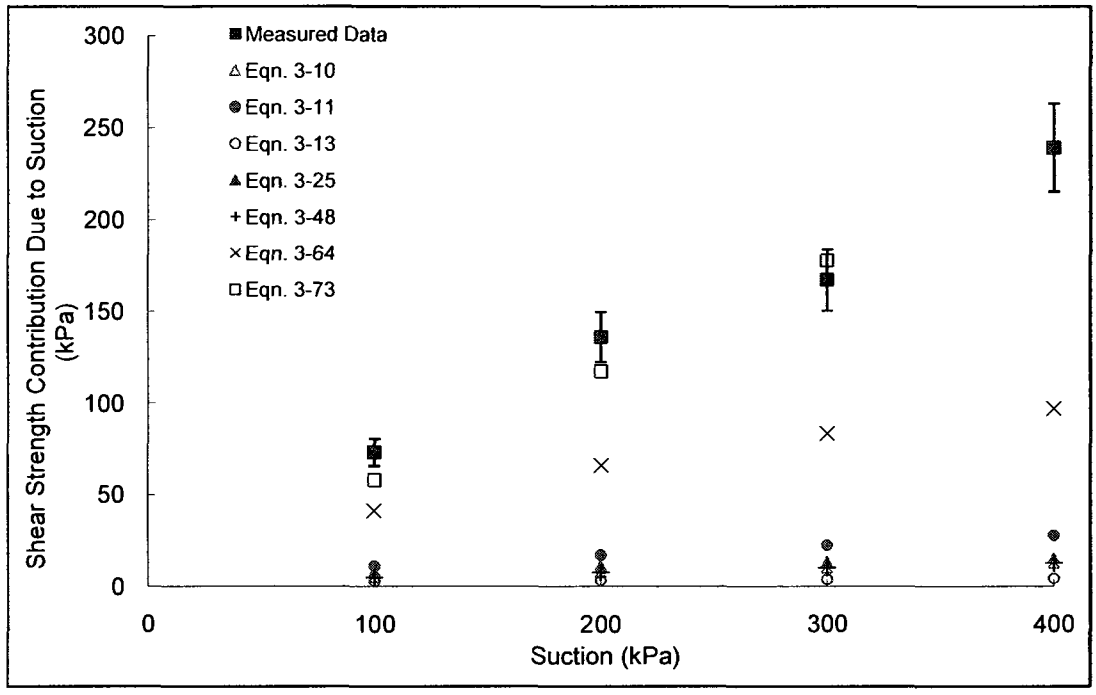

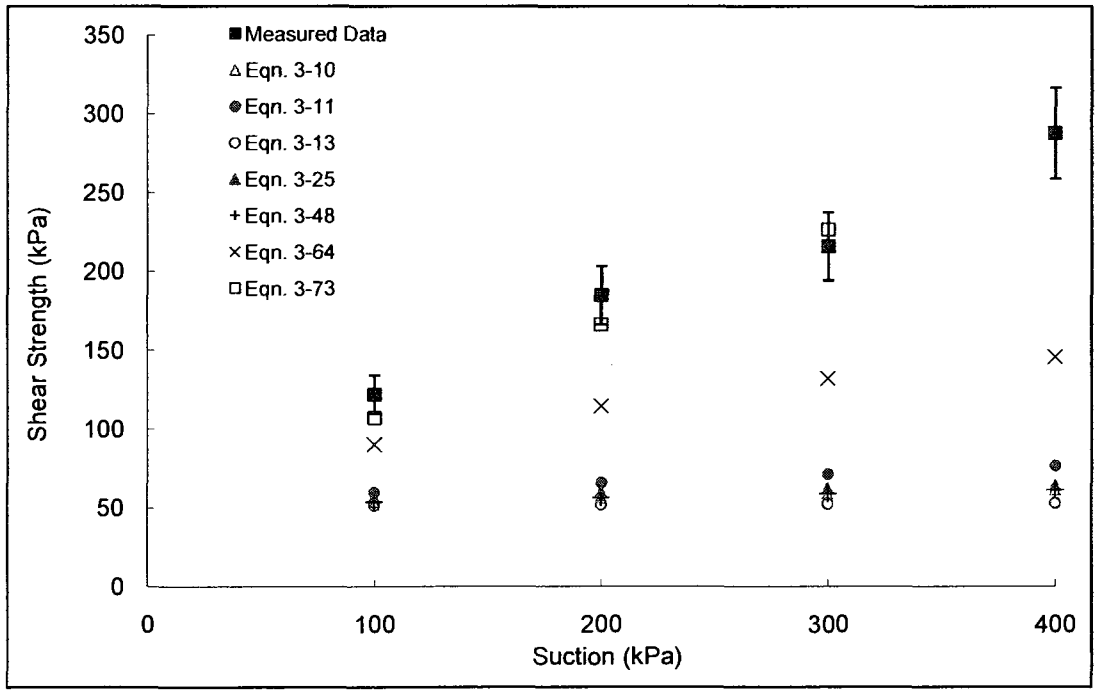

Soil No. 45d

Ashikaga silt

Nishimura, Fredlund, Gan and Hirabayashi, 1999

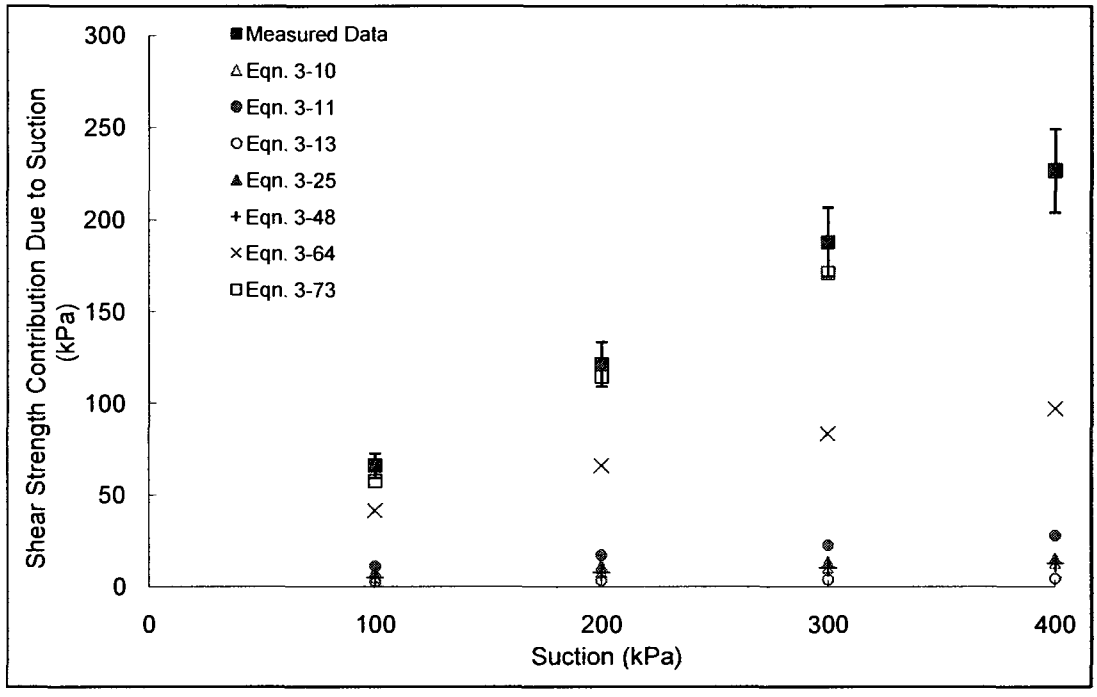

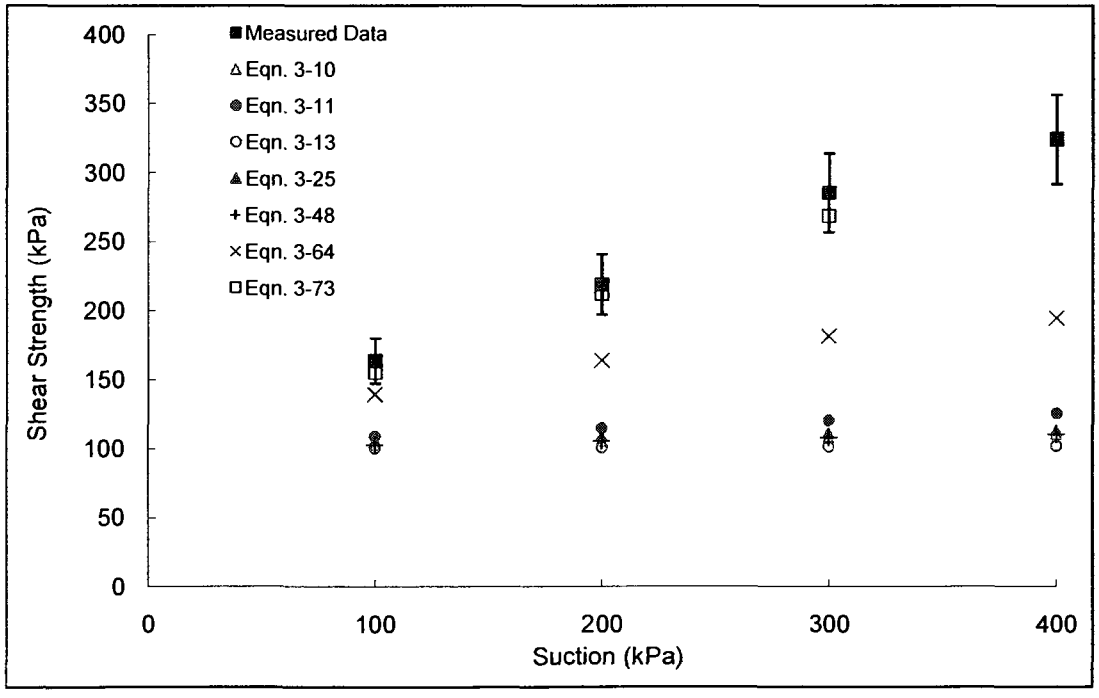

Soil No. 45e **Ashikaga silt**

Nishimura, Fredlund, Gan and Hirabayashi, 1999

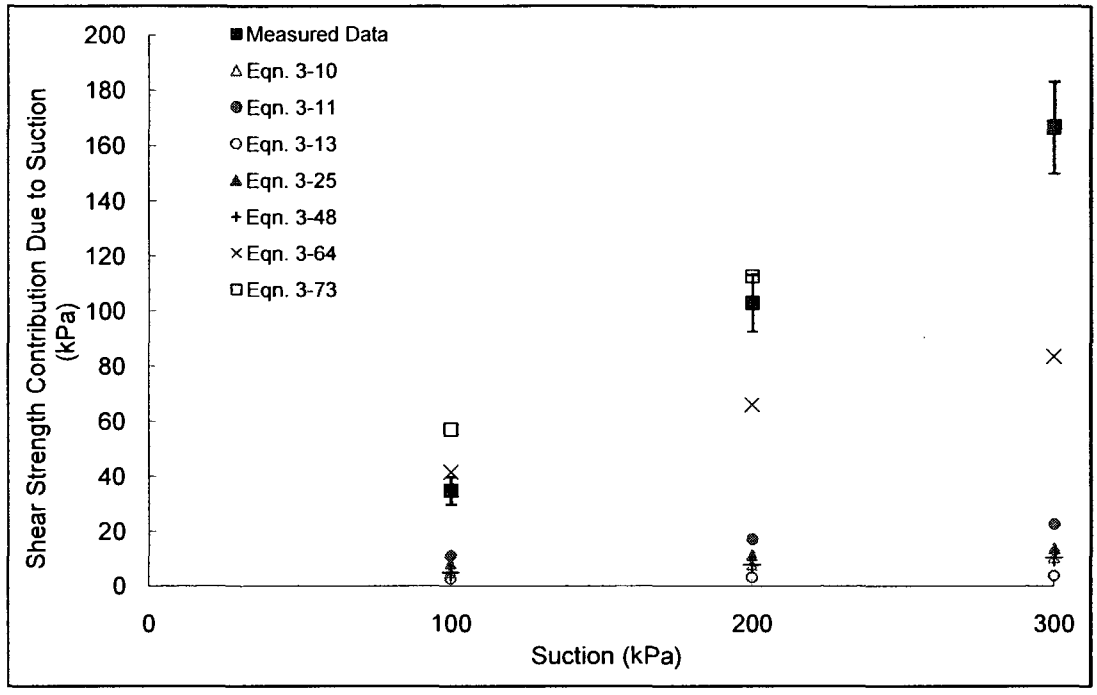

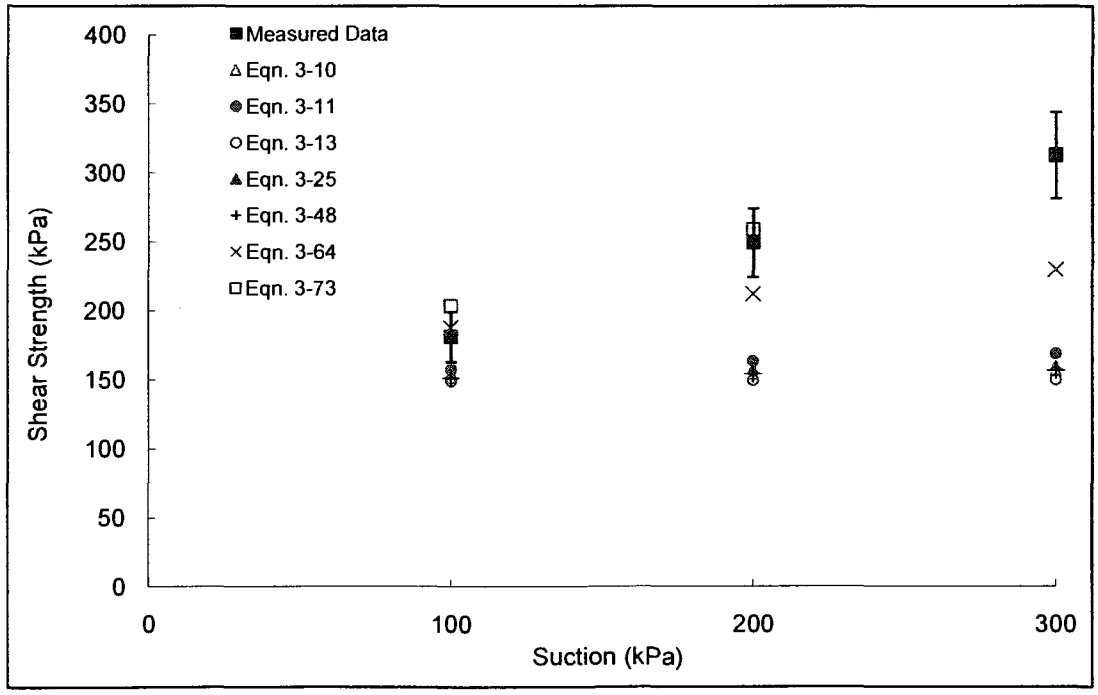

Soil No. 45f **Ashikaga silt**

Nishimura, Fredlund, Gan and Hirabayashi, 1999

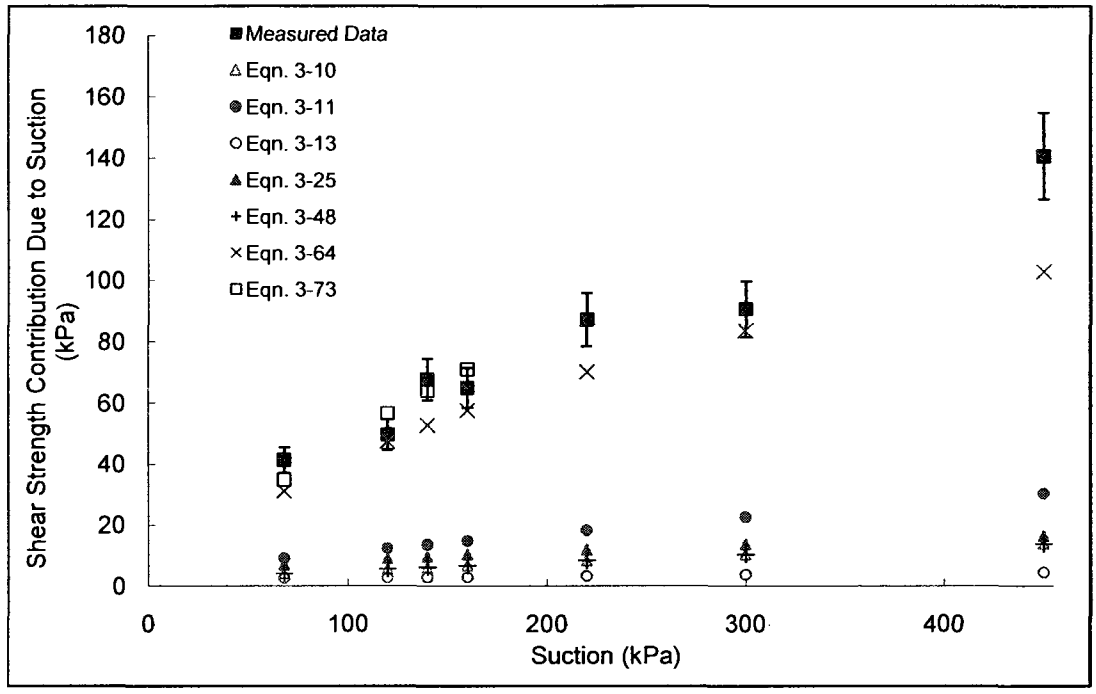

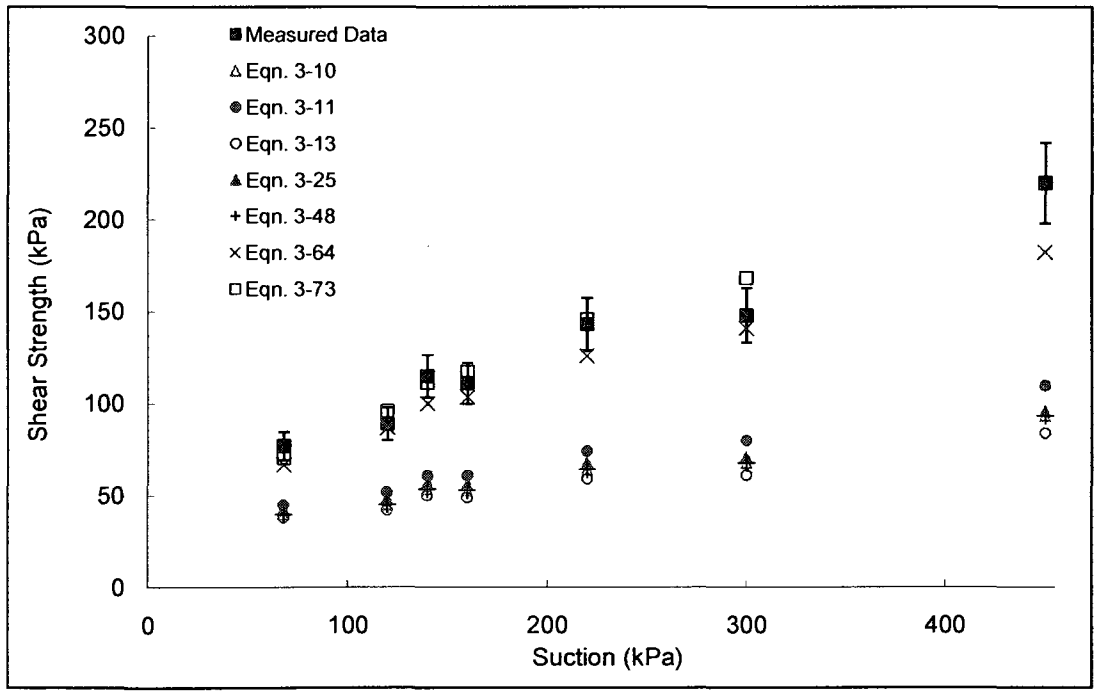

Soil No. 46

Kiunyu gravel
Toll, 1990

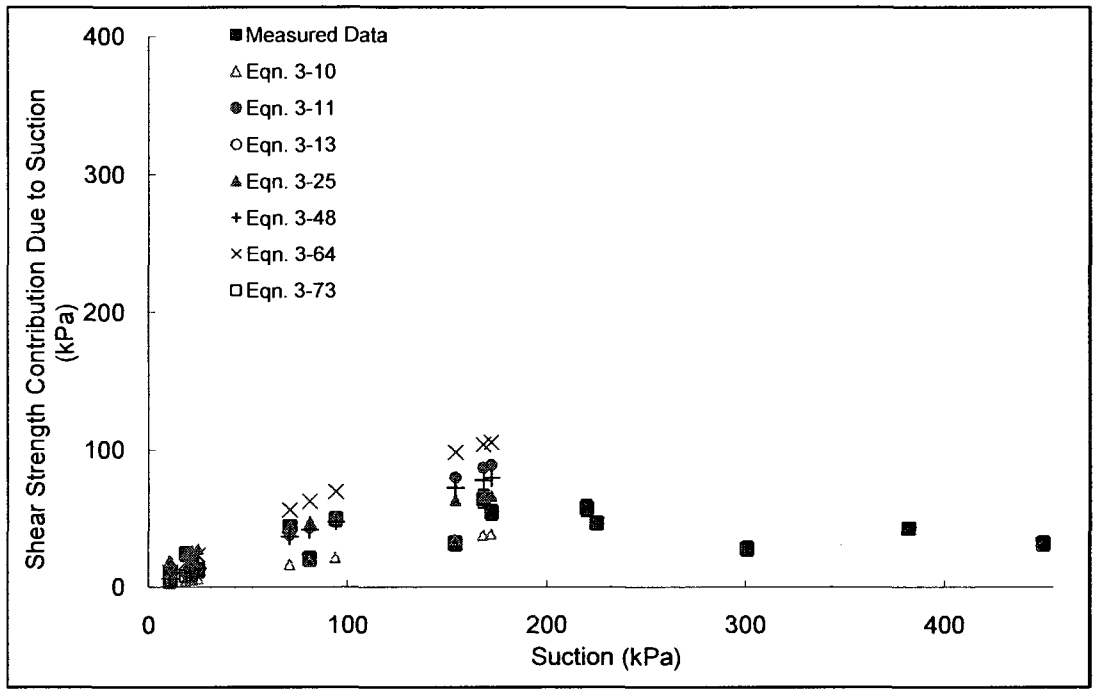

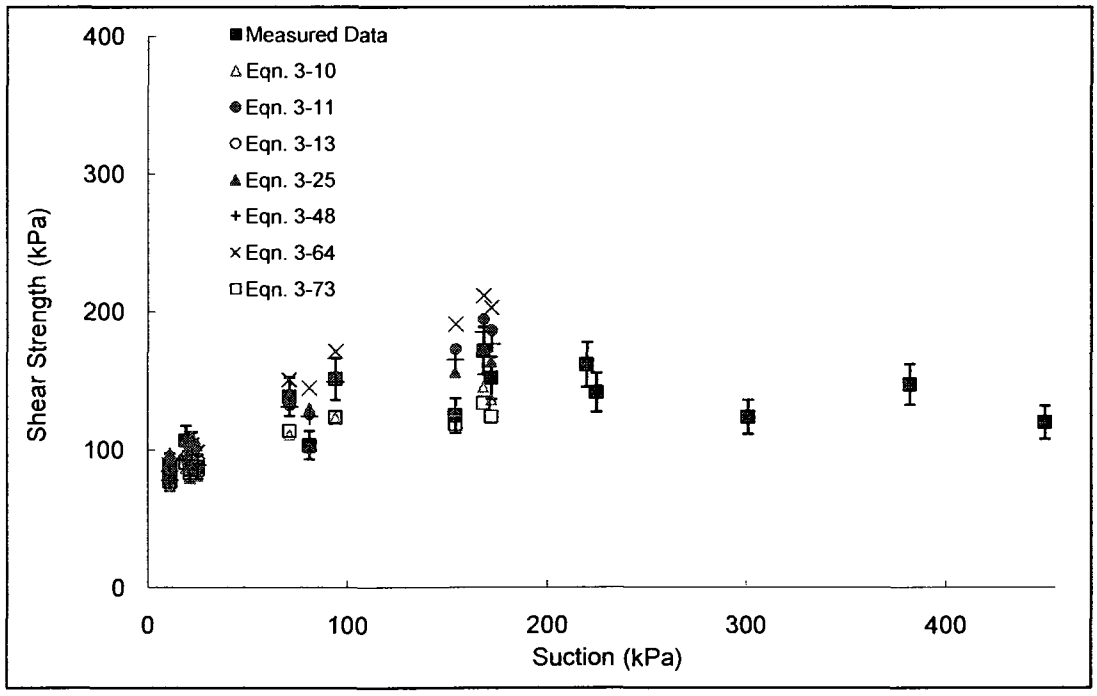

Soil No. 47a

Jossigny silt

Cui and Delage, 1993

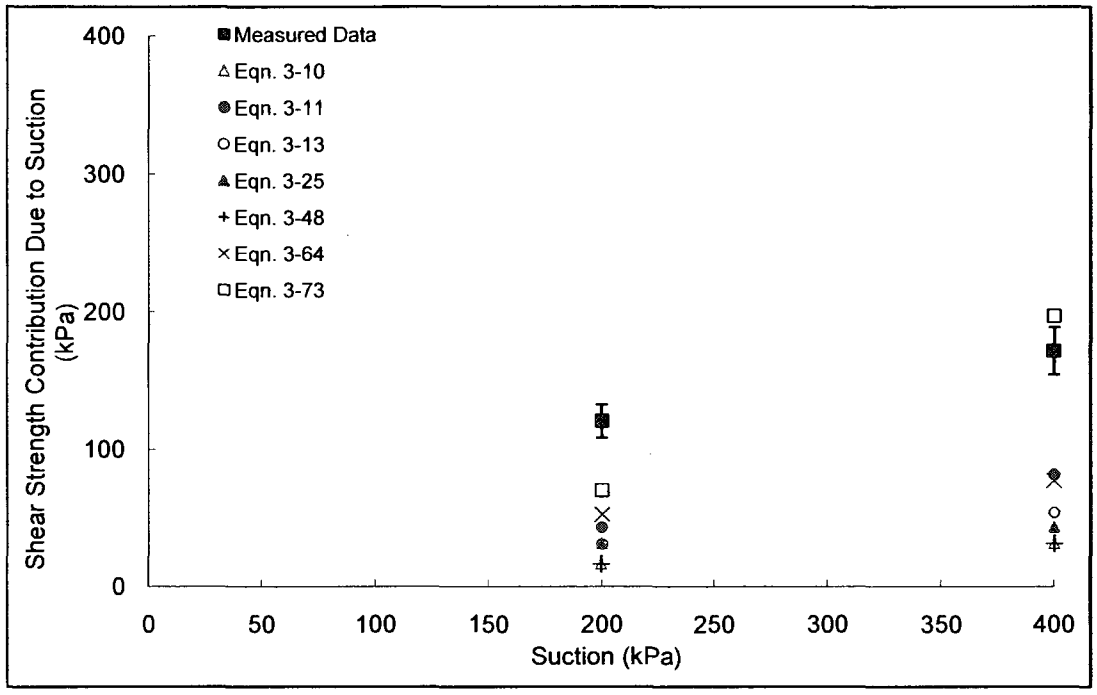

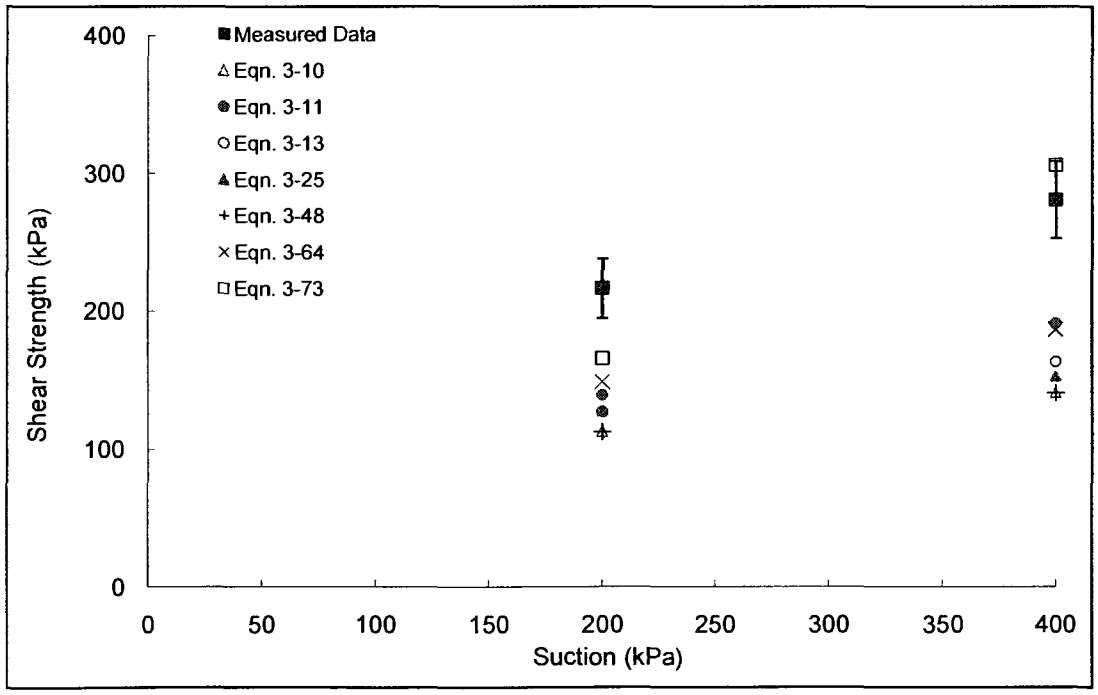

Soil No. 47b

Jossigny silt

Cui and Delage, 1993

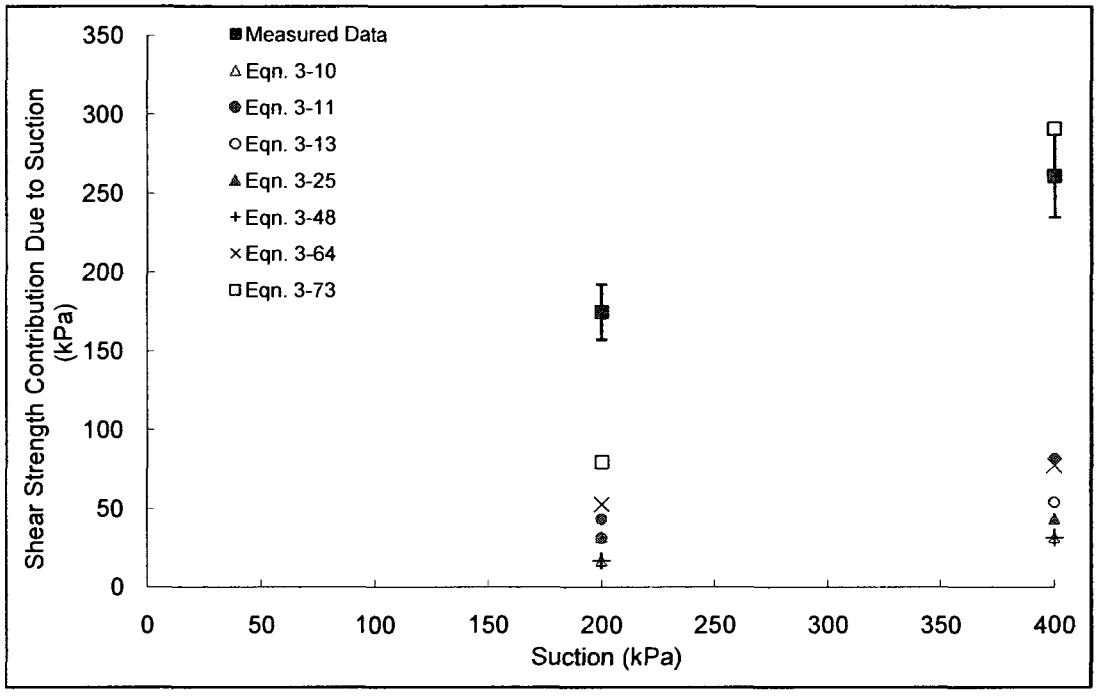

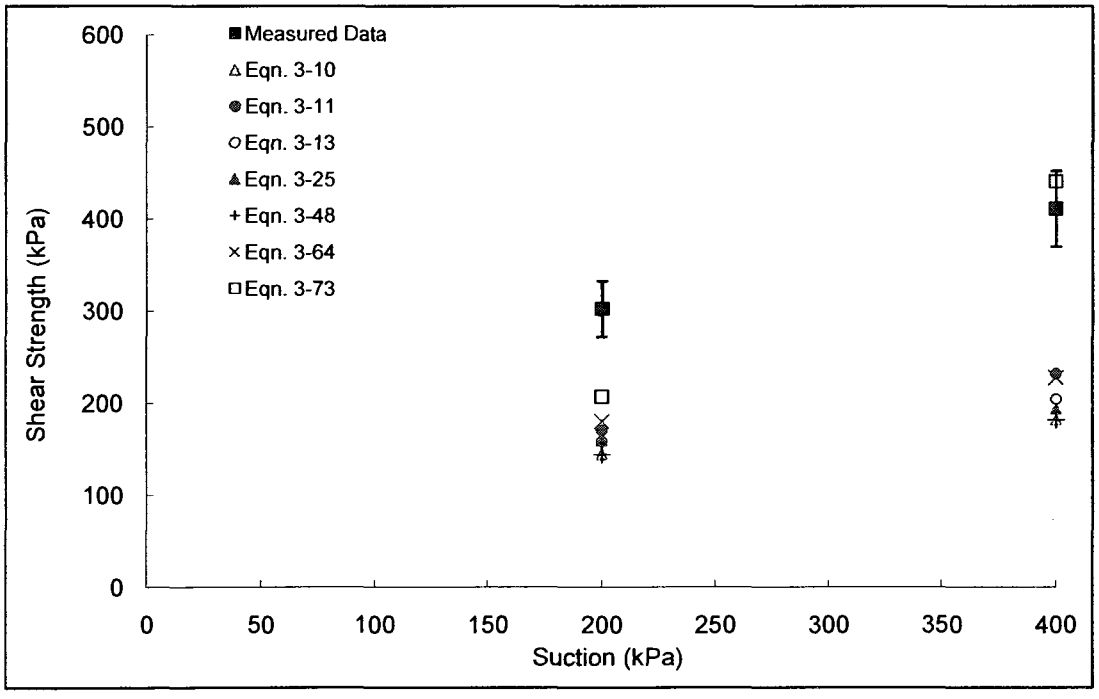

Soil No. 47c

Jossigny silt

Cui and Delage, 1993

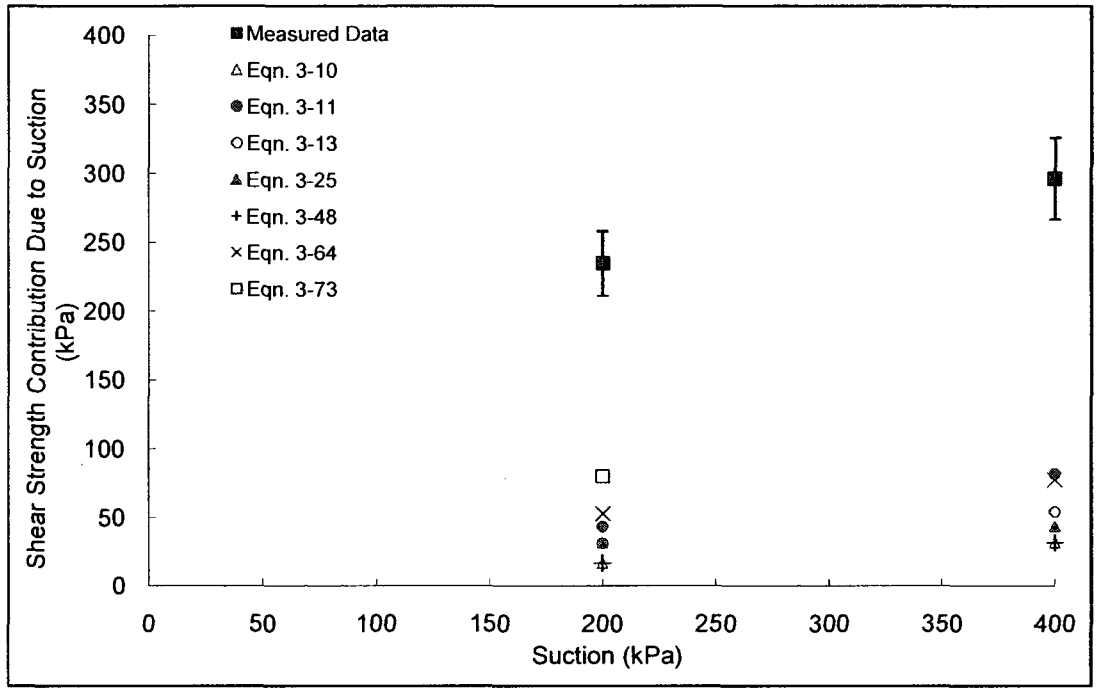

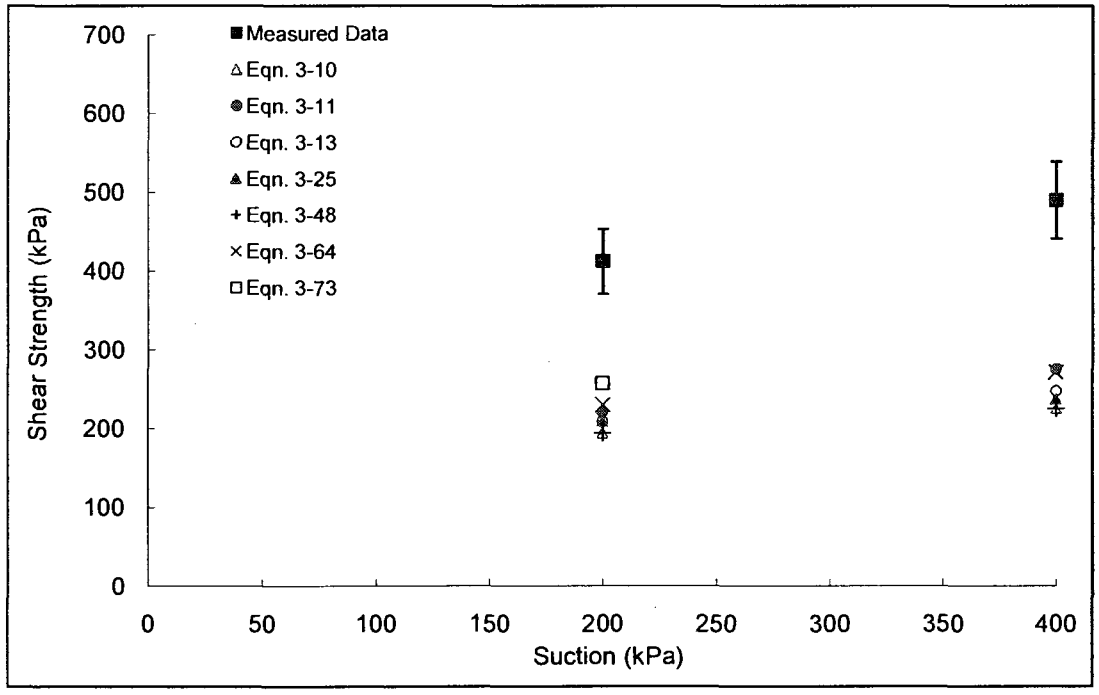

Soil No. 48

Yellow colluvium

de Campos and Carrillo, 1995

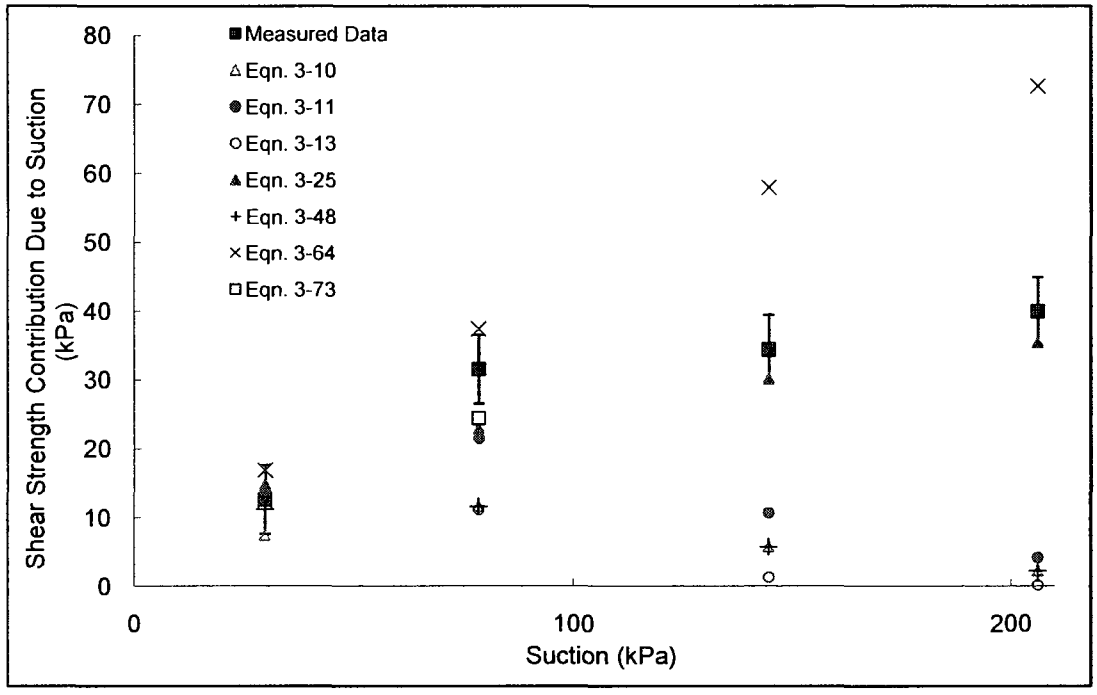

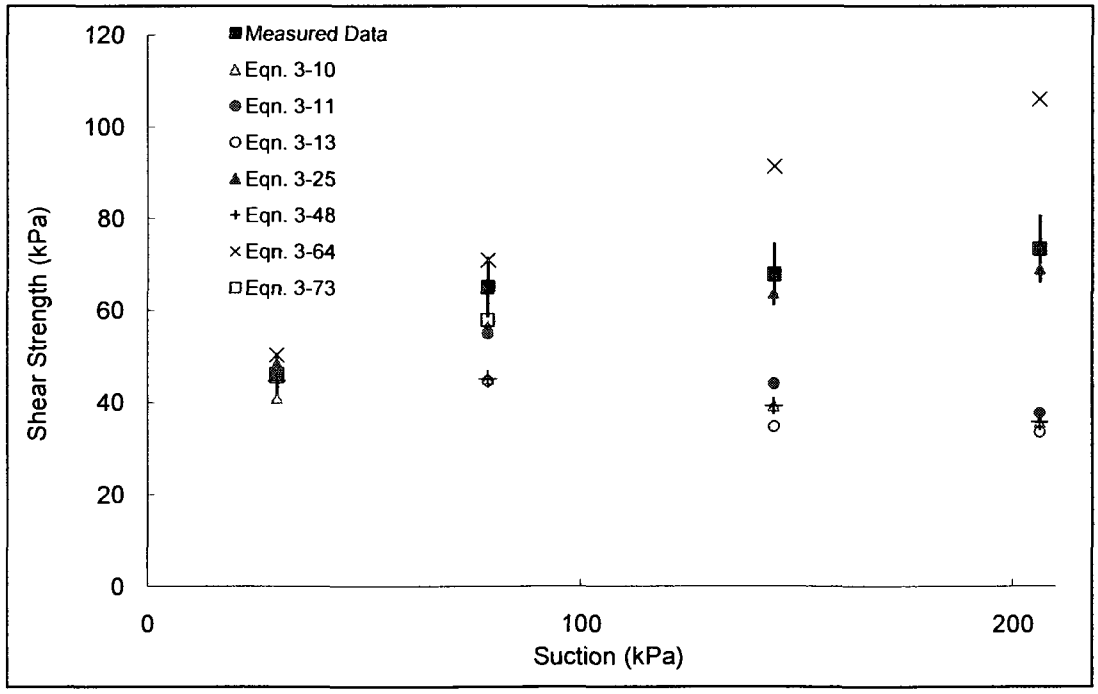

Soil No. 49

Red colluvium

de Campos and Carrillo, 1995

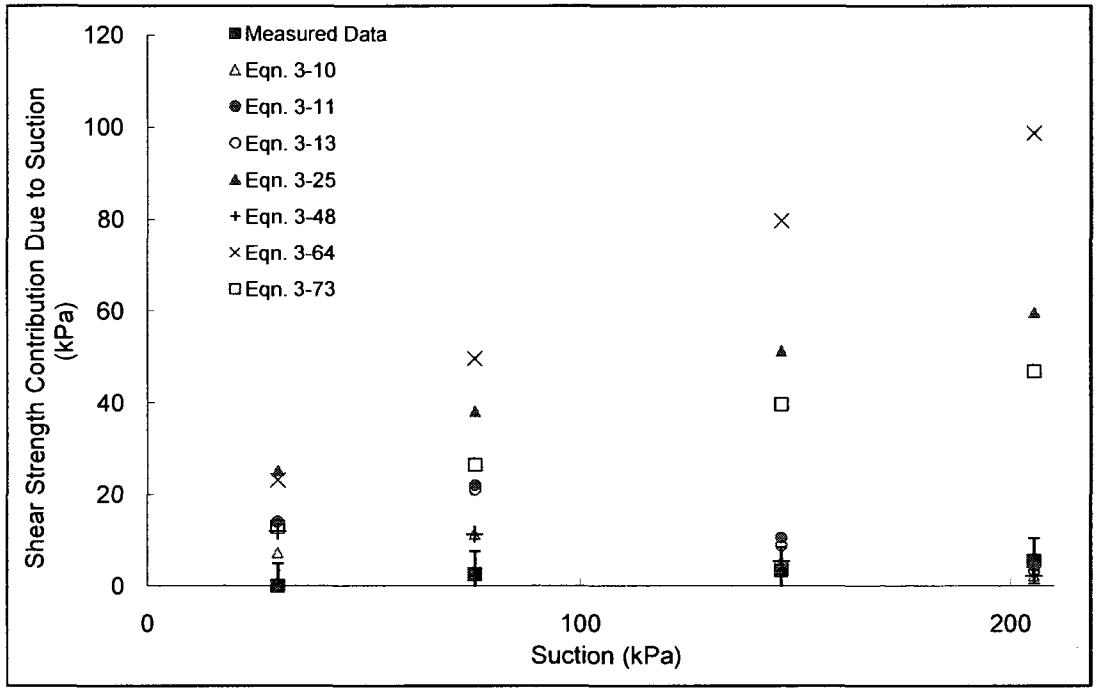

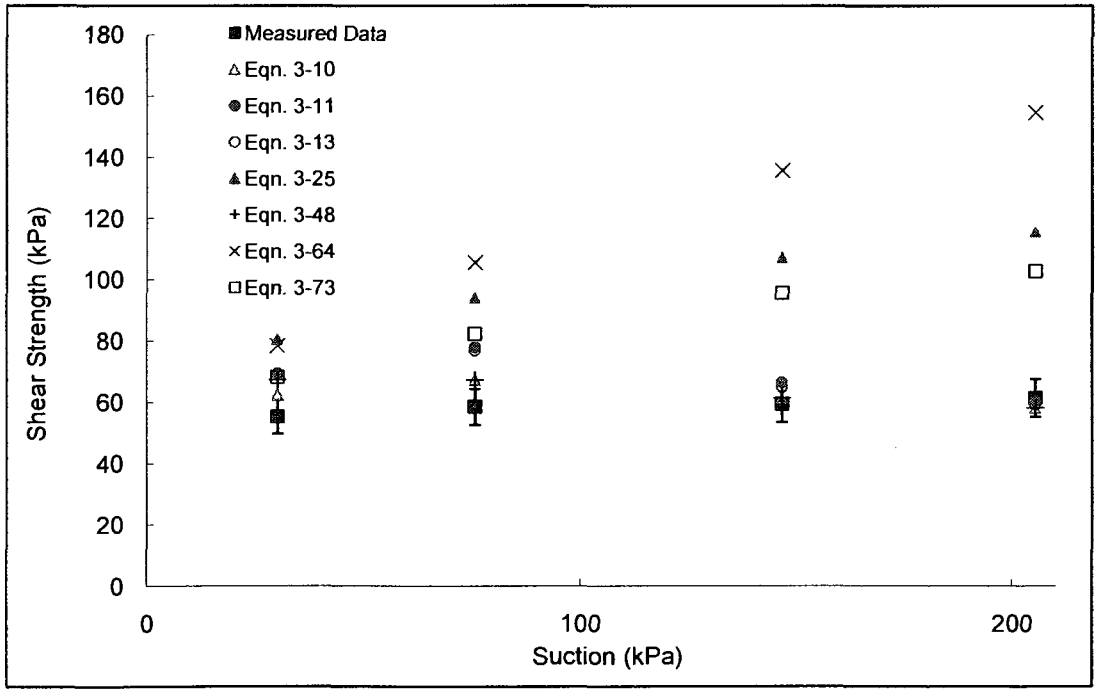

Soil No. 50

Typical residual

de Campos and Carrillo, 1995

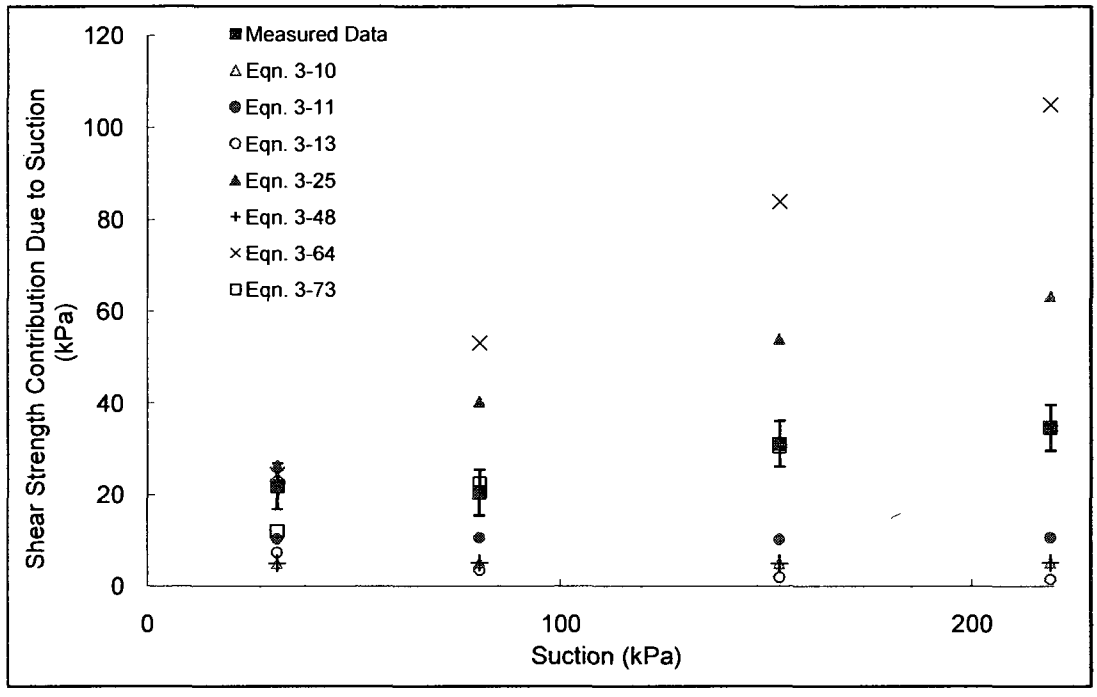

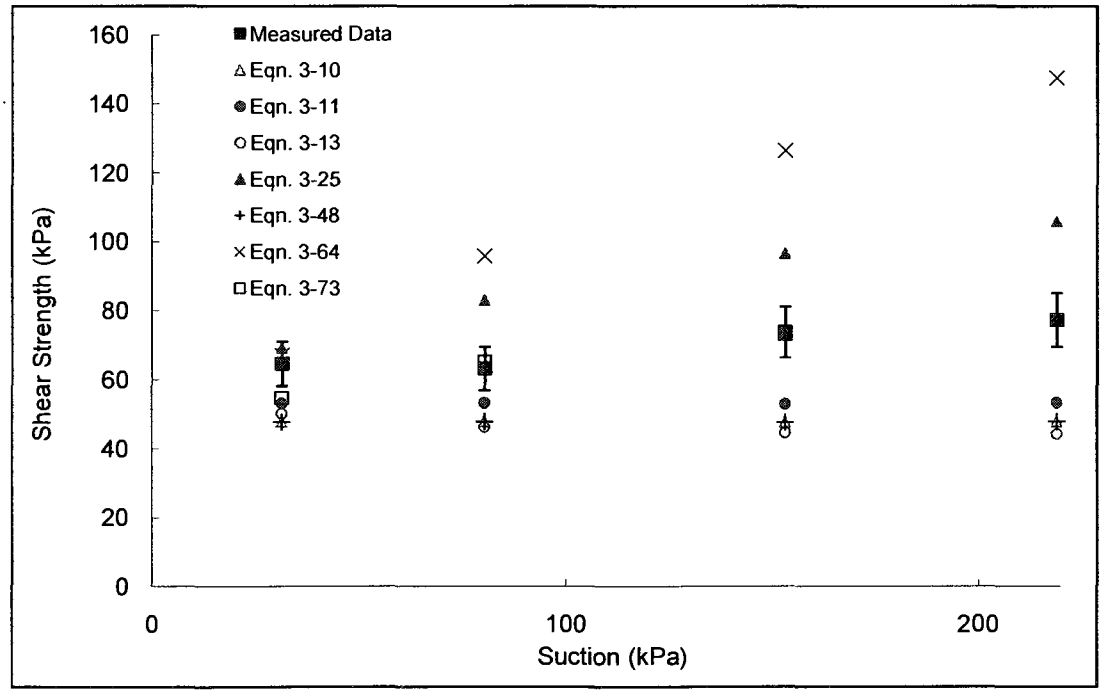

Soil No. 51

Red residual

de Campos and Carrillo, 1995

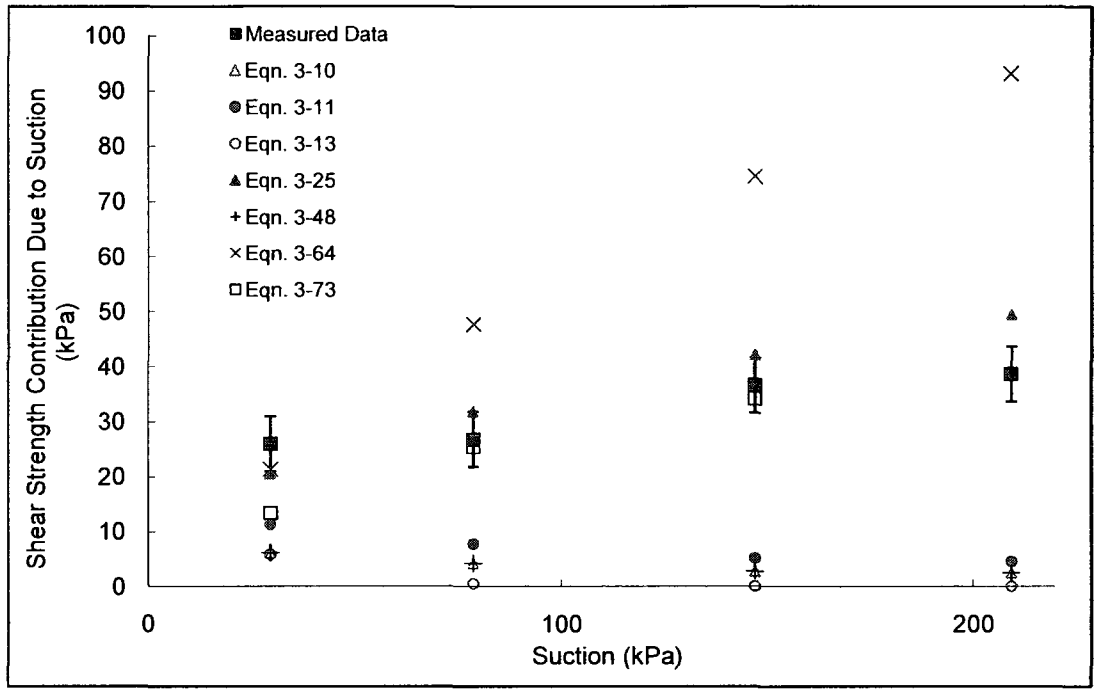

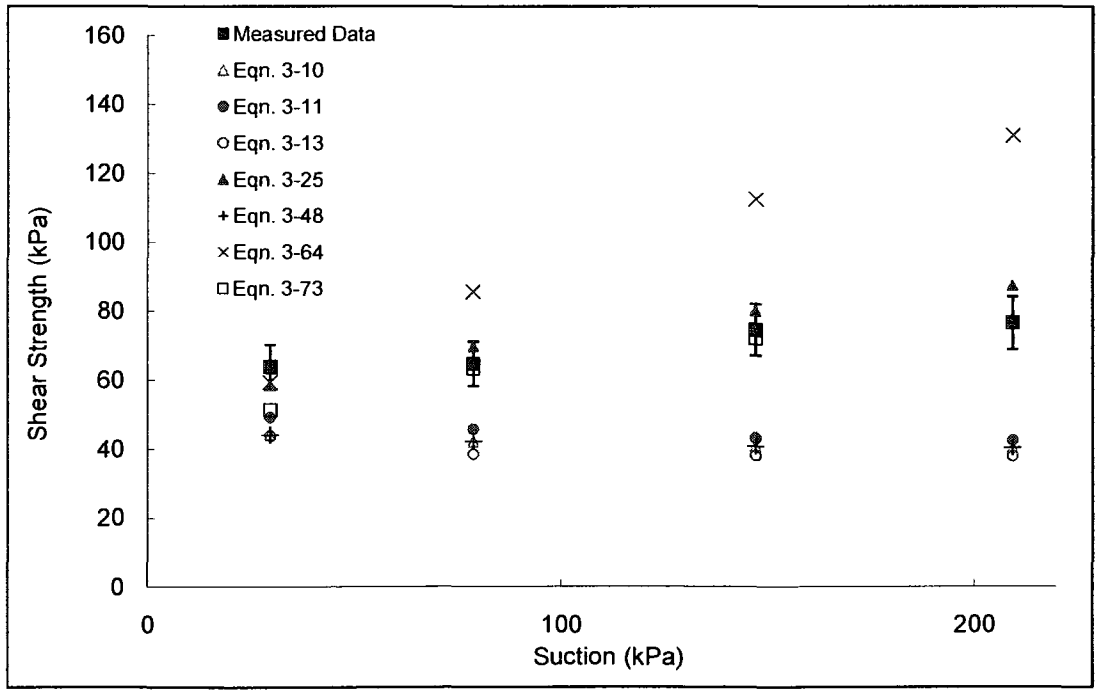

Soil No. 52

Kaolin

Pineda and Colmenares, 2006